

JOURNAL *of* CHROMATOGRAPHY

INTERNATIONAL JOURNAL ON CHROMATOGRAPHY,
ELECTROPHORESIS AND RELATED METHODS

EDITOR

MICHAEL LEDERER (Rome)

ASSOCIATE EDITOR

K. MACEK (Prague)

EDITORIAL BOARD

P. Boulanger (Lille), I. E. Bush (Plainview, N.Y.), G. P. Cartoni (Rome),
C. B. Coulson (Weybridge, Surrey), G. Duyckaerts (Liège), J. E. Falk
(Canberra), L. Fishbein (Research Triangle Park, N. C.), C. W. Gehrke
(Columbia, Mo.), I. M. Hais (Hradec Králové), E. Heftmann (Albany, Calif.),
E. C. Horning (Houston, Texas), A. T. James (Sharnbrook, Beds.), J. Janák
(Brno), A. I. M. Keulemans (Eindhoven), K. A. Kraus (Oak Ridge, Tenn.),
E. Lederer (Gif-sur-Yvette, S. et O.), A. Liberti (Rome), H. M. McNair
(Blacksburg, Va.), G. B. Marini-Bettolo (Rome), R. Neher (Basel), J. Schubert
(Pittsburgh, Pa.), G.-M. Schwab (Munich), L. R. Snyder (Brea, Calif.),
A. Tiselius (Uppsala), H. Tuppy (Vienna), O. Westphal (Freiburg-Zähringen),
H. H. Woltz (Boston, Mass.)

EDITORS, BIBLIOGRAPHY SECTION

K. Macek (Prague), J. Janák (Brno), Z. Deyl (Prague)

EDITOR, BOOK REVIEW SECTION

S. G. Perry (Abingdon, Berks.)

EDITOR, NEWS SECTION

G. Nickless (Bristol)

COORDINATING EDITOR, DATA SECTION

J. Gasparič (Pardubice)

VOL. 53

1970



ห้องสมุด กรมวิทยาศาสตร์
8 เม.ย. 2514

SPECIAL ISSUE

**8th INTERNATIONAL GEL PERMEATION AND
LIQUID CHROMATOGRAPHY SEMINAR**

Prague (Czechoslovakia), July 1-3, 1970

Edited by:

K. MACEK
(Prague)

B. SEDLÁČEK
(Prague)

M. LEDERER
(Rome)

CONTENTS

8th INTERNATIONAL GEL PERMEATION AND LIQUID CHROMATOGRAPHY SEMINAR, HELD IN PRAGUE (CZECHOSLOVAKIA), JULY 1-3, 1970

Preface	I
B. G. BELENKII AND E. S. GANKINA, Thin-layer chromatography of polymers. Introductory lecture	3
K. J. BOMBAUGH, Recent developments in gel permeation chromatography: High speed and high resolution. Introductory lecture	27
W. HEITZ, Syntheses and properties of gel chromatography materials	37
B. BÖMER, W. HEITZ AND W. KERN, Preparation of monodisperse polyethylene oxides by gel permeation chromatography of discontinuous polymer-homologous series	51
D. BEREK, I. NOVÁK, Z. GRUBISIC-GALLOT AND H. BENOIT, Surface area and volume of pores as characteristics of silica supports for gel permeation chromatography	55
D. RANDAU UND H. BAYER, Anwendungen von Vinylacetatgelen	63
J. CHURÁČEK AND P. JANDERA, The separation of the coloured derivatives of some organic compounds using liquid chromatography in small-bore columns packed with ion-exchange resins	69
S. P. ZHDANOV, E. V. KOROMALDI, R. G. VINOGRADOVA, M. B. GANETSKII, O. M. GOLYNKO, N. E. ZHILZOVA, B. G. BELENKY, L. Z. VILENCHIK AND P. P. NEFEDOV, Application of porous glasses for gel chromatography of polymers	77
A. CERVENKA AND T. W. BATES, Characterisation of polydisperse branched polymers by means of gel permeation chromatography	85
A. HOLMSTRÖM AND E. SÖRVIK, Thermal degradation of polyethylene in a nitrogen atmosphere of low oxygen content. I. Changes in molecular weight distribution	95
V. V. EVREINOV, A. K. ROMANOV AND S. G. ENTELIS, Calculation of the weight and number functions of molecular weight distribution for oligomers from the gel permeation chromatography data	109
D. D. NOVIKOV, N. G. TAGANOV, G. V. KOROVINA AND S. G. ENTELIS, Shape of the chromatographic band for individual species and its influence on gel permeation chromatographic results	117

PREFACE

The Eighth International Gel Permeation and Liquid Chromatography Seminar took place in Prague, from July 1 to 3, 1970. Its programme included, apart from six main lectures, seventeen communications and three panel discussions. Of these lectures and communications twelve are published in the present volume and further ones will appear in later issues of this journal.

The Prague Seminar is the eighth of a series of meetings which have become an international forum, surveying annually the progress in gel permeation chromatography, not only regarding its methods and instrumentation, but also its theory and applications.

The seminars, although sponsored by an American firm and a Czech agency (Waters Associates and Rapid), do not have a narrow, commercially oriented character. They are, first and foremost, a good opportunity for an international exchange of new ideas and for obtaining information on the latest development in gel permeation chromatography.

It was the main aim of the Czechoslovak organizers in preparing the Seminar to intensify the interdisciplinary and international exchange of scientific information. They wanted, moreover, to stimulate interest in the new methods of gel permeation chromatography in both their own and other socialist countries. Since gel permeation chromatography is, in fact, a highly progressive and efficient technique, which has been successfully applied in many branches of science and industry, and particularly in macromolecular research.

The organizers would like to avail themselves of this opportunity and to express their gratitude to the publishers and editors, who by editing the papers delivered will further the sense and intentions of the Seminar.

CHROM. 4964

THIN-LAYER CHROMATOGRAPHY OF POLYMERS

INTRODUCTORY LECTURE

B. G. BELENKII AND E. S. GANKINA

Institute of High Molecular Compounds, Academy of Sciences of the U.S.S.R., Leningrad (U.S.S.R.)

SUMMARY

1. Principal peculiarities of thin-layer chromatography (TLC) of polymers on porous adsorbents have been considered on the basis of the concept that macromolecules are adsorbed as a flexible polymer chain. A dependence relating R_F of the polymer to its molecular weight has been suggested.

2. A method for TLC of homopolymers has been used with separation according to the molecular weight and using systems with low and high resolution on silica gels of various porosity. A method for determining the molecular weight distribution of polymers has been worked out. It takes into account chromatographic spreading of polymer fractions by comparison of one- and two-dimensional TLC in one solvent system.

3. A method of TLC of copolymers according to their composition has been suggested. It may be used for determining their homogeneity. The effect of the molecular weight on the chromatographic distribution of copolymers on plates has been investigated. This effect was found to decrease when silica gel with small pores was used.

4. The concentration dependences in TLC of homopolymers and copolymers have been studied. They were shown to be of the nature of adsorption in the lower part of the plate. In its upper part these dependences are characteristic for gel chromatography when the rate of the movement of macromolecules decreases with the increase in concentration.

5. A method has been worked out for determining homopolymer admixtures in the block and graft copolymers by two-dimensional TLC. Block and graft copolymers were diagnosed by comparing their chromatographic mobility with that of the corresponding homopolymers of equal molecular weight.

INTRODUCTION

At the present time, chromatographic methods are widely used for the investigation of macromolecules. Gel permeation chromatography (GPC) is used for determining molecular weight distribution (MWD) and for fractionating polymers^{1,2}. Precipitation chromatography³ has been adopted as a method for fractionating large

amounts of polymer. Adsorption chromatography is much less developed, nevertheless this method is worth consideration as a method in connection with the various specific peculiarities of macromolecules which become apparent in their adsorption.

Despite the fact that there are many reports dealing with the TLC of oligomers⁴⁻⁸ and investigations on gel TLC of polymers have also been carried out^{9,10}, the study of adsorption TLC for polymers began comparatively recently. At present work is being developed in two laboratories: Prof. INAGAKI's laboratory in Kyoto University¹¹⁻¹⁵ and in our laboratory in the Institute of High Molecular Compounds of the Academy of Sciences of the U.S.S.R. in Leningrad¹⁶⁻¹⁹.

INAGAKI's publications deal with the possibilities of using adsorption TLC for the study of the compositional homogeneity of copolymers¹¹, their structural properties¹² and stereoregularity and stereocomplexes of poly(methyl methacrylate)^{13,14}.

The possibility of applying TLC to the molecular-weight study of homopolymers is also mentioned¹⁵. Our work on the TLC of polymers also commenced with the investigation of statistical copolymers¹⁶⁻¹⁸. Later we studied the use of TLC for investigating homopolymers and their MWD determination¹⁹.

In addition we have examined the possibilities of TLC for determining the purity and structural peculiarities of block and graft copolymers. Our work deals with these questions.

EXPERIMENTAL

Characteristics of the sorbents

For the chromatography of polymers we used silica gels with the properties described in Table I and with the pore size distribution shown in Fig. 1.

TABLE I
PROPERTIES OF SILICA GELS

<i>Silica Gel</i>	<i>Apparent density (g/cm³)</i>	<i>True density (g/cm³)</i>	<i>Specific surface area (m²/g)</i>	<i>The total pore volume (cm³/g)</i>	<i>Porometric pore volume (cm³/g)</i>	<i>Pore volume with radii 2.9-31 Å</i>
Microporous Silica Gel KSM-5	1.050	2.195	715	0.497	0.079	0.41
Silica Gel KSK with large pores	0.727	2.176	350	0.916	0.870	0.046
Macroporous Silica Gel MSA-1	0.997	2.186	25	0.646	0.521	0.025

Fig. 1 also shows the distribution coefficients of polystyrenes (K_d) obtained from TLC data as functions of their unperturbed size, $(h_0^2)^{1/2}$, size in θ -solvent, corresponding to MW of polystyrene samples. It is noteworthy that strong adsorption of polystyrenes with a MW $> 4 \times 10^5$ takes place despite the fact that Silica Gel KSK pores are practically inaccessible to them.

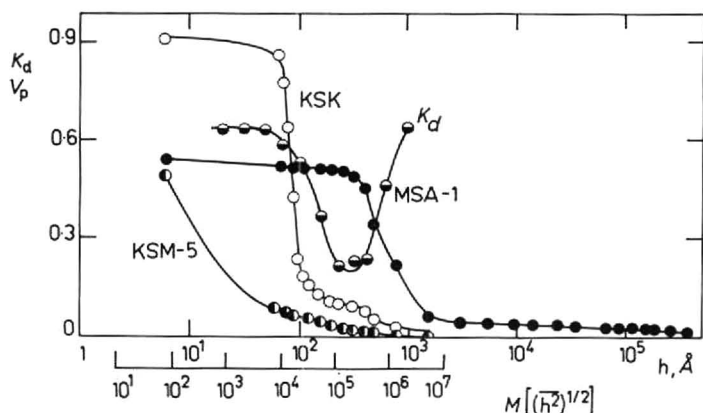


Fig. 1. Pore size distribution of Silica Gels KSM-5, KSK and MSA-1 determined by means of mercury porosimetry. K_d distribution coefficient of PS in Silica Gel KSK.

Chromatographic procedure

Glass plates, measuring 6×6 , 6×9 and 6×12 cm were used for the TLC of the polymers. They were prepared by pouring a suspension of silica gel with the particle size $20\text{--}30\ \mu$.

Before applying the samples the thin-layer plates were heated for 30 min at 120° . Chromatographic solvent systems were used only once and were prepared from freshly rectified solvents. Homopolymers: polystyrene (PS); poly(methyl methacrylate) (PMMA) and polyethylene oxide (PEO) as well as graft and block copolymers were subjected to chromatography in the usual way. Sandwich chambers (S-chambers) were used for chromatographing statistical copolymers; they were obtained by covering a chromatographic plate from above with glass at $0.8\text{--}1$ mm distance from the silica gel layer. By placing the S-chambers in a vessel with a solvent it is possible to create the conditions for gradient chromatography owing to the gradual evaporation of the solvent into the air space in the S-chamber when the solvent moves along the sorbent layer. The presence of gradient conditions in S-chambers may be easily detected if the starting points of styrene (St) and methyl methacrylate (MMA) copolymers are placed diagonally on the plate. Fig. 2 shows that under these conditions the finishing points are arranged in a straight line which is parallel to the immersion line of the plate irrespective of the position of the starting points. This fact indicates the presence of a gradient on the plate. After the chromatography had been completed, the plates were placed in a thermostat for $10\text{--}30$ min at 20° in order to remove traces of solvents. For solvent systems see Table III.

Detection and photographic registration of thin-layer chromatograms

For detection of the polymers the plates were sprayed with a 3% solution of KMnO_4 in concentrated H_2SO_4 and heated in an oven for $15\text{--}30$ min at 150° .

The spots of polymers acquire a black colour which stands out against the light background of a plate.

The sensitivity of detection for PS was $0.5\text{--}1\ \mu\text{g}$. Chromatographic plates were photographed by means of a contact-print method on reflex photo-paper or film. After developing in the usual manner the negative prints of thin-layer chromatograms

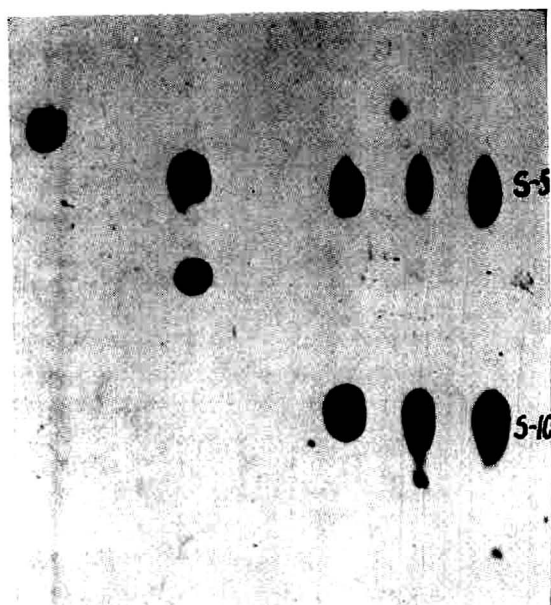


Fig. 2. TLC of the copolymers St-MMA, S-5 and S-10 in an S-chamber with Silica Gel KSK and an acetone- CHCl_3 system (1:2:12) with the points of sample application placed diagonally on the plate. Positive print.

were obtained as white spots against black background*. For the detection of block copolymers of styrene (ST) and ethylene oxide (EO) a modified Dragendorff reagent⁴ was used.

This reagent visualised the PEO in the form of reddish-orange spots against the yellow background of the chromatographic plate.

Subsequent spraying of the plate with a 3% solution of KMnO_4 in concentrated H_2SO_4 led to the disappearance of the yellow colour and development became more contrasting. Sensitivity of detection was 0.1–0.5 μg PEO. If the plate was heated at 140–150°, black spots appeared instead of reddish PEO spots, but sensitivity of detection diminished to 1–2 μg .

RESULTS AND DISCUSSION

Chromatography of polystyrenes

Narrow fractions of polystyrene (PS) were used, their properties are presented in Table II. PS samples were applied to the plate from benzene solution at a concentration of 5 mg/ml.

Chromatography of polystyrene on silica gels with different porosity. Three types of silica gels (macroporous, microporous and with large pores) were examined in order to study the influence of the pore size distribution on the TLC of polystyrenes. The chromatographic behaviour of PS with molecular weights from 50×10^3 to 2×10^6 was investigated. In Fig. 3 chromatograms obtained under conditions of maximum resolution according to molecular weight (MW) are presented; chromatography was carried out in the system cyclohexane–benzene–acetone (C–B–A). Fig. 3 shows an

* The photographs are negatives unless otherwise indicated.

TABLE II

MOLECULAR WEIGHT AND POLYDISPERSION INDEX FOR POLYSTYRENES INVESTIGATED BY MEANS OF TLC
PS-I + PS-2 — Pressure Chemical Co. (Japan); PS-3 to PS-11 — Waters Associates (U.S.A.).

Samples	PS-1	PS-2	PS-3	PS-4	PS-5	PS-6	PS-7	PS-8	PS-9	PS-10	PS-11
$M_w \times 10^{-3}$	0.9	2.03	5	10.3	19.85	51	98.2	173	411	867	2145
$M_n \times 10^{-3}$			4.6	9.7	19.65	49	96.2	164	392	773	1730
M_w/M_n			1.10	1.09	1.01	1.04	1.02	1.055	1.05	1.12	1.2

TABLE III

R_F VALUES FOR CHROMATOGRAPHY OF POLYSTYRENES I-11 ON SILICA GEL KSK WITH LARGE PORES IN VARIOUS SOLVENT SYSTEMS

No.	Composition of the solvent system (with saturation for 30 min) C-B-A	PS-1	PS-2	PS-3	PS-4	PS-5	PS-6	PS-7	PS-8	PS-9	PS-10	PS-11
1	13:3:0.1	0.90	0.80	0.61	0.10	0	0	0	0	0	0	0
2	12:4:0.4	0.96	0.96	0.94	0.85	0.76	0.33	0.14	0.05	0	0	0
3	12:4:0.7	0.97	0.97	0.97	0.87	0.78	0.58	0.46	0.37	0.27	0.22	0.20
4	12:4:1	0.98	0.98	0.98	0.91	0.86	0.74	0.66	0.62	0.58	0.58	0.58
5	12:4:2	0.98	0.98	0.98	0.98	0.98	0.98	0.98	0.98	0.98	0.98	0.98
6	12:4:0.2	0.63	0.63	0.63	0.65	0.67	0.74	0.83	0.82	0.82	0.70	0.63

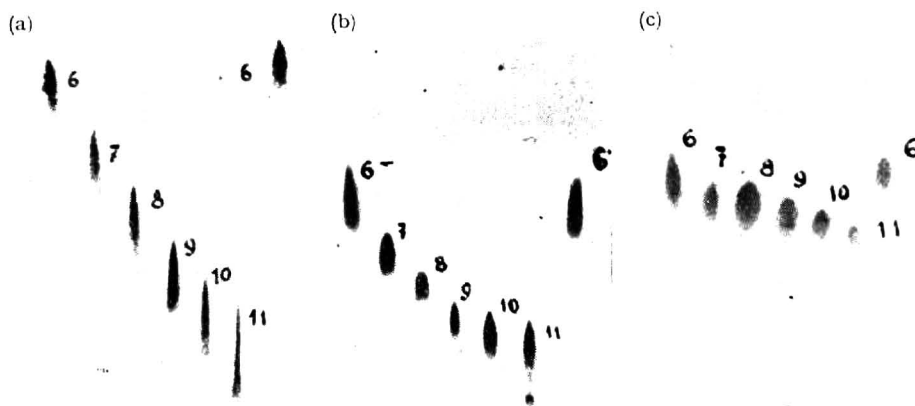


Fig. 3. TLC of polystyrenes 6 to 11 on silica gels. (a) MSA-1 in the system C-B-A (13:3:1.1); (b) KSK in the C-B-A system (12:4:0.6); (c) KSM-5 in the C-B-A system (12:4:0.8). Positive prints.

almost linear dependence of R_F on MW for the MSA-1 silica gel, whereas for the Silica Gel KSK and an MW close to 4×10^5 , as well as for the Silica Gel KSM-5 and an MW close to 5×10^4 , this dependence becomes less marked. This is due to the molecular-sieve (gel) effect on PS adsorption.

Chromatography of polystyrenes on Silica Gel KSK with large pores in different solvent systems. The 9×12 cm plates were used for studying the chromatographic behaviour of PS 1-11 in various solvent systems on Silica Gel KSK with large pores. The experimental results are summarised in Table III and illustrated in Fig. 4. In system I containing a minimum of acetone — 0.66% (Fig. 4a) — only the lowest molecular weight PS (MW up to 5×10^3) were observed to move.

When the acetone content is increased to 2.5% (Fig. 4b) PS with an MW not exceeding 5×10^3 moved with the front, PS with MW's between 5×10^3 and 9.7×10^4 are distributed along the plate and those with MW 1.73×10^5 remain on start. When the acetone content increases to 4.2% (Fig. 4c), PS with MW lower than 5×10^3 move with the front whereas PS with MW between 10^4 and 2×10^5 are distributed along the plate. A still greater increase in the acetone content to 5.9% (Fig. 4d) produces an increase in the R_F of high molecular weight PS to 0.6, the dependence of R_F on MW being weakened. If the acetone content is increased to 11%, the polymers move with the front of the solvent. Under these conditions when the adsorption

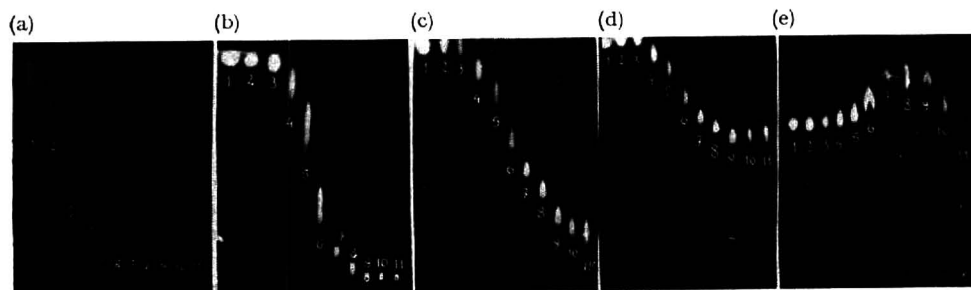


Fig. 4. TLC of polystyrenes 1 to 11 on Silica Gel KSK in the C-B-A systems: (a) 13:3:0.1; (b) 12:4:0.4; (c) 12:4:0.7; (d) 12:4:1.0; (e) 12:4:2 (with saturation).

of PS is completely suppressed, the gel effect should take place and large macromolecules move faster than small ones. However, to have it noticeably displayed, the TLC must be conducted with the plates saturated with the solvent vapour. The fact is that chromatography on dry (unsaturated) plates involves the consumption of solvent for filling not only canals between the particles of adsorbent but the pores as well. Under these conditions velocity of the solvent front movement is lower than the flow rate and corresponds to the velocity of movement for any non-adsorbing macromolecules for which all pores of adsorbent are entirely accessible.

When the plate is saturated by the solvent vapour, the silica gel pores are filled with the solvent and the velocity of movement of the solvent front is in accordance with the flow rate of the mobile phase. It makes the macromolecules, for which the adsorbent pores are accessible, move slower than the solvent front.

Under these conditions (Fig. 4e) the gel effect becomes apparent. PS with MW of not over 10^4 move to a certain distance from the solvent front. When the MW is higher than 2×10^4 , the PS velocity increases owing to partial exclusion of macromolecules from the silica gel pores.

In the range of $MW > 4 \times 10^5$ the velocity of the macromolecules decreases again owing to their adsorption in large pores and on the surface of the silica gel grains. Fig. 4 shows a continuous transition from strong adsorption of macromolecules to weak adsorption and finally to the gel effect. These peculiarities of TLC permit one to choose special conditions of chromatography for the PS samples of every MW range to obtain maximum resolution according to MW. Similar results of chromatographic separation according to MW have been obtained with the TLC of polyethylene oxide and poly(methyl methacrylate).

Concentration dependence of R_F for polystyrenes with different molecular weight on Silica Gel KSK with large pores. For studying dependence of R_F values on the concentration of the PS, samples with 5, 10, 15, 20 and 40 μg of PS were applied to the plate and the solvent systems permitting the observation of PS spots in the lower, middle and upper parts of the plate were used. Results for PS-5 and PS-9 are shown in Fig. 5.

It can be seen that with increased concentrations the PS spots in the lower part of a plate are stretched upwards, this effect is characteristic of the Langmuir (convex) adsorption isotherm.

In the upper part of the plate, the centre of a spot is displaced downwards with increasing concentration. This effect is associated with a concave adsorption isotherm which is the result of the gel effect from the adsorbent pores owing to reduction of their size. In the middle part of the plate where the gel and the adsorption effects oppose each other, a linear adsorption isotherm occurs producing the minimum concentration dependence. Furthermore we find that the gel effects of concentration become stronger with increasing MW of PS, because in this case the increase in the accessibility of the silica gel pores for PS with concentration is much higher. When the PS concentration is small (*i.e.* in the absence of the concentration effects), there is maximum stretching of the chromatographic spots and hence the best chromatographic resolution according to MW occurs in the middle part of the plate.

Determination of the molecular weight distribution of polystyrene. In order to determine the MWD of polymers by means of TLC it is necessary to eliminate chromatographic spreading due to the polymer distribution on the plate. For this purpose

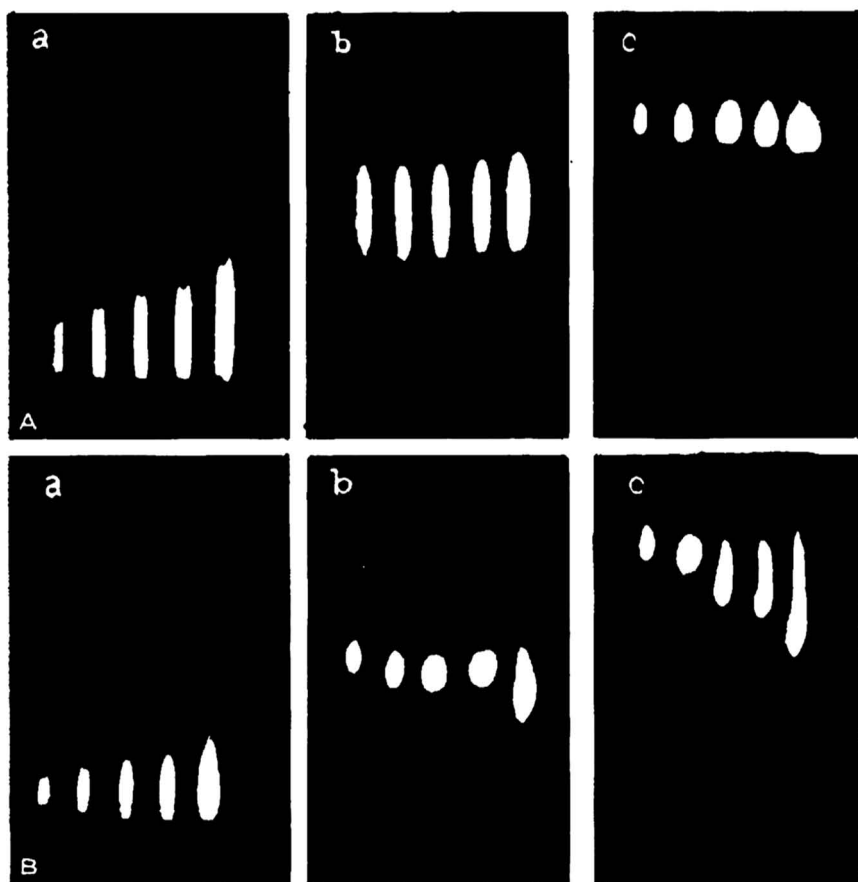


Fig. 5. Concentration effects in TLC of PS on Silica Gel KSK. (A) for PS-5 in the C-B-A systems: (a) 12:4:0.25; (b) 12:4:0.5; (c) 12:4:1; (B) for PS-9 in the C-B-A systems: (a) 12:4:0.5; (b) 12:4:1; (c) 12:4:1.3; 5, 10, 15, 20 and 40 μ g of PS were applied.

a method is proposed (Fig. 6) which is based on two-dimensional chromatography of a polymer in the directions A and B, and a comparison of the width of the chromatographic spots arranged diagonally on the plate with the width of a spot obtained for a single chromatographic run in direction B in the same solvent system. If the starting spots of two samples both have the same size, and are applied at equal distances from the immersion line and the solvent run is the same for both directions, then under these conditions a spot of sample 1 can be treated as the starting zone for sample 2 when it is subjected to chromatography in the B direction.

If we carry out densitometry of both spots along the line B'B'' which is parallel to B, we can obtain the dispersion of a chromatographic sample (1) in the form of difference between the dispersions of concentration distributions in the spots (1) and (2) along the line B'B'',

$$\sigma^2 = \sigma_1^2 - \sigma_2^2. \quad (1)$$

It is noteworthy that this method for determining chromatographic dispersion of a polymer does not distort the shape of the distribution curve for polymer homologues which is characteristic for example of the reverse elution method of TUNG *et al.*²⁰. For determining the MWD of PS-5 with a MW 19870 two samples of this polymer (1, 2) were applied to the plate 6×9 cm at the points shown in Fig. 6.

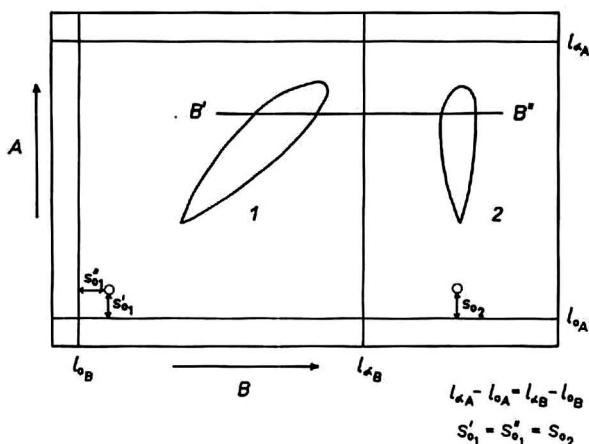


Fig. 6. Determination of chromatographic spreading in TLC of polymers by means of two-dimensional chromatography.

For studying concentration effects some samples of this PS-5 in increasing quantities (3-5) were also applied together with PS of MW 500, 10000 and 50000 (6-8) in order to graduate the chromatographic plate according to MW. After two-dimensional chromatography in the C-B-A system (12:4:4.5) a chromatogram was obtained (Fig. 7a). By means of a densitometer with a slit width of 0.1 mm, densitograms of samples 2-8 in the A direction and of the samples 1, 2 in the B direction were obtained (Fig. 7b). These results permitted one to ascertain the absence of concentration effects upon the densitogram shape and to obtain the graduation curve MW- R_F value shown in Fig. 7b.

These data together with the data on chromatographic spreading calculated by means of formula (1) or with the help of TUNG's method²¹ make elimination of spreading possible by means of the MWD curve for PS-5 which is shown in Fig. 7b. The value of polydispersity for PS, $M_w/M_n = 1.02$, is in good agreement with data in the table for this PS sample ($M_w/M_n < 1.06$) and its MWD coincides well with TUNG's results obtained with the help of GPC²². As a PS sample with narrow MWD was examined in these experiments, detection of increments of it was assumed to be constant. For the samples with a broader MWD the changes in the optical density increment with increasing MW should be taken into account. It is worth noting that not only PS samples with narrow MW distribution can be used for graduating the plate but also a polymer with broader MWD as was done in GPC²³. Fig. 8 illustrates the comparative efficiency of GPC²⁴ and TLC for the same PS samples.

The separation of these samples on a thin-layer plate (6 cm in length) is much more efficient than the separation by means of 4 columns of a GPC. The HETP of TLC is 300 times smaller than in the case of GPC. The above data show that determination of the MWD of polymers by means of TLC requires a 1000–10000 times smaller quantity of the substance with a considerably better separation than a determination by means of GPC and it is carried out 5–10 times faster. Another advantage of TLC is the possibility of simultaneous chromatography of several samples on a single plate.

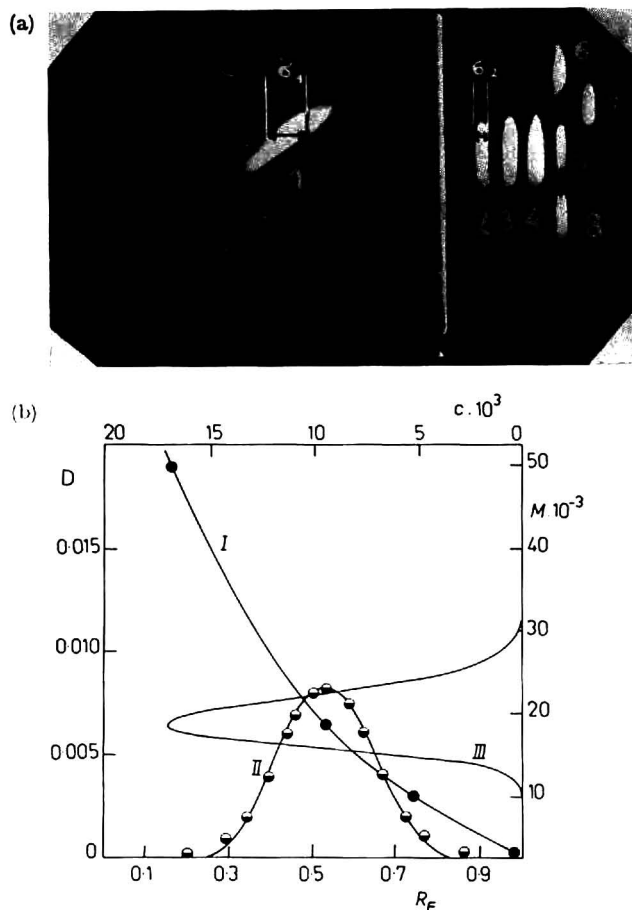


Fig. 7. Determination of the MWD for PS-5 by means of TLC on Silica Gel KSK: (a) Two-dimensional chromatogram of sample (1) and one-dimensional chromatogram of samples (2) and (3) in the C-B-A system (12:4:4.5); (b) graduating curve R_F -MW (I), densitogram of sample (2) in direction A (II) and MWD of PS-5 (III).

Chromatography of statistical copolymers of styrene and methyl methacrylate

TLC of statistical copolymers synthesised by LITMANOVITCH and coworkers²⁵ and characterised in Table IV was investigated. The composition of the copolymers was determined by elementary analysis with the help of pyrolytic gas chromatography¹⁶ and by means of the refraction index increment in 3–4 solvents. Molecular weight

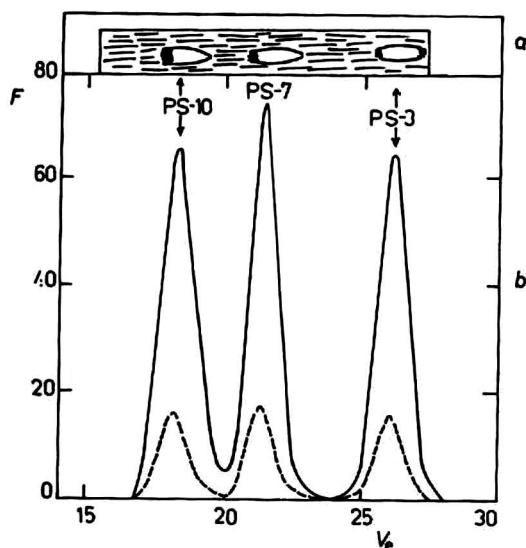


Fig. 8. TLC and GPC of polystyrenes 3, 7, and 10. (a) TLC on Silica Gel KSK in the C-B-A system (12:4:0.7); (b) GPC²⁴ with the concentration of the sample: (—) 0.1 g/100 ml; (---) 0.025 g/100 ml.

was examined by means of the light scattering method²⁵. TLC of copolymers was carried out on chromatographic plates 6 × 6 cm with layers of Silica Gel KSK with large pores.

The copolymer samples, in amounts of 1–5 g, were applied to the plate from a dichloroethane solution with a concentration of 5 mg/ml and subjected to chromatography in the solvents listed in Table V. These solvents can be divided into two classes: (a) solvents containing oxygen which forms hydrogen bonds with the silanol hydroxyl groups of the silica gel²⁶ ("displacers") and (b) true solvents (chlorinated hydrocarbons).

The above solvents may be arranged in the following eluotropic series according to the R_F values of the copolymers containing 31 and 54 % of styrene:

A: diethyl ether < methyl ethyl ketone < acetone < tetrahydrofuran < dioxane

B: dichlorobenzene < dichloroethane < chloroform.

It is obvious that these series depend both on the displacement power of the solvents and on their solvation ability with respect to the copolymers. Thus separation systems of low or high resolution for separating copolymers according to their composition, can be obtained with different mixtures of A and B type solvents.

Chromatography with low resolution. Strong "displacers" in small quantities (THF, dioxane, acetone) or weak "displacers" (diethyl ether, MEK) in large quantities allow chromatographic systems to be devised for the separation of copolymers which differ greatly in their composition. Fig. 9 illustrates TLC of copolymers with 22, 31, 53 and 80% of styrene, respectively, and shows that the R_F value of a copolymer increases with the St content. As in the case of homopolymers, there is also a concentration dependence of R_F values for the copolymers (Fig. 10), in the lower part of the plate it is characteristic of the Langmuir's adsorption isotherm and in the upper part it corresponds to the concave isotherm characteristic of GPC. Owing to high

TABLE IV
PROPERTIES OF STYRENE-METHYL METHACRYLATE COPOLYMERS SAMPLES EXAMINED BY MEANS OF TLC

Samples	S-1	S-2	S-3	S-4	S-5	S-6	S-7	S-8	S-9	S-10	S-11	S-12	S-13	S-14
Composition (mol % of styrene)	80	80	80	54	54	54	54	54	31	31	31	31	32	22
$M_w \times 10^{-3}$	120	—	—	73	80	130	160	260	50	88	160	180	260	230

TABLE V

R_F VALUES FOR COPOLYMERS OF STYRENE AND METHYL METHACRYLATE WITH 31 % (S-10) AND 54 % (S-5) OF STYRENE IN SYSTEMS CONTAINING 10 % OF THE "DISPLACER"

Solvents	Displacer											
	Ether		Methyl ethyl ketone (MEK)		Acetone		Tetrahydrofuran (THF)		Dioxan			
	S-10	S-5	S-10	S-5	S-10	S-5	S-10	S-5	S-10	S-5	S-10	S-5
Dichlorobenzene (DCB)	0	0	0	0	0	0	0	0.52	0	0.71	0	0.83
Dichloroethane (DCE)	0	0	0	0	0	0	0.69	0.70	0.92	0.92	0.77	0.92
Chloroform (CHCl ₃)	0	0.17	0	0.32	0.49	0.85	0.70	0.90	0.90	0.83	0.83	0.95

sensitivity of detection, however, the experiments can be carried out in the range where the R_F -concentration dependence is absent.

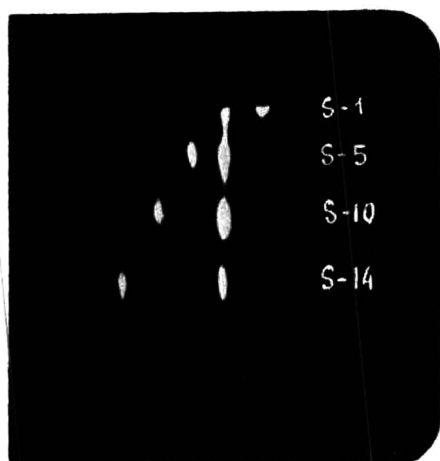


Fig. 9. Low resolution TLC on KSK Silica Gel of statistical copolymers St-MMA with 80, 54, 31 and 22% of St (S-1, S-5, S-10 and S-14) in the CHCl_3 -acetone system (12:2.4).

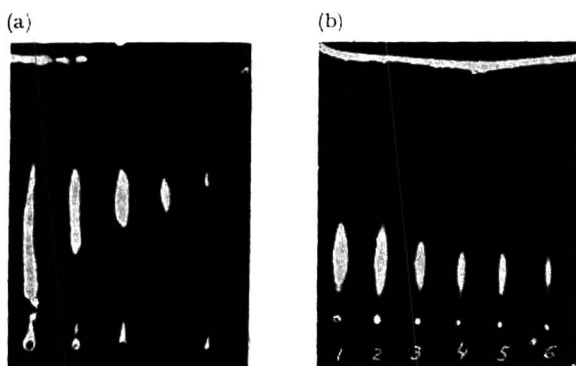


Fig. 10. Concentration effects for the copolymer S-5 with 54% of St on Silica Gel KSK in the CHCl_3 -MEK systems: (a) (12:2.4); (b) (12:1.2); 1, 2, 4, 8, 16, and 32 μg of sample was applied.

The effect of the MW of a copolymer on its behaviour during TLC. Fig. 11 shows TLC of copolymers with different MW containing 3% and 54% of styrene. Comparatively strong dependence of the R_F value on MW is noticeable when the MW does not exceed 10^5 . In the range of MW higher than 1.0 – 1.5×10^5 this dependence weakens and the chromatographic distribution of the copolymers on the plate becomes governed mainly by their composition. It would also be possible to reduce the dependence of the R_F of the copolymer on MW, in the range of $\text{MW} > 10^5$, if the microporous Silica Gel KSM-S, with pores inaccessible for macromolecules with a $\text{MW} > 40 \times 10^5$, is used instead of Silica Gel KSK with large pores. Chromatograms of copolymers on Silica Gel KSK and KSM-5 are presented for comparison in Fig. 12. These silica gels differ little in their sensitivity to the composition of the copolymers.

However, the dependence of the R_F value on MW for Silica Gel KSM is considerably less pronounced than for Silica Gel KSK. It is evident that the use of the micro-

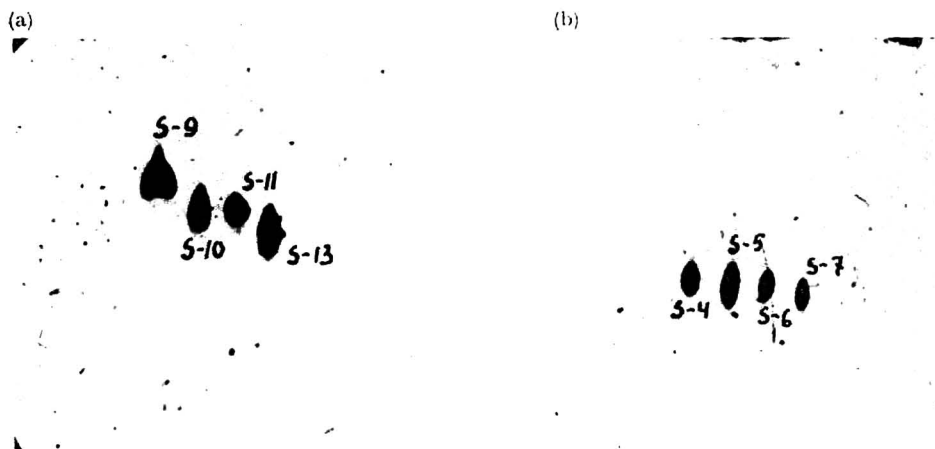


Fig. 11. Effect of the MW on the chromatographic behaviour of statistical copolymers St-MMA on Silica-Gel KSK. (a) Copolymers with 31% of St and MW 2.6×10^5 , 8.8×10^4 and 5×10^4 (S-13, S-11, S-10, S-9) in a CHCl_3 -acetone system (12:2.2); (b) copolymers with 54% of St and MW 1.6×10^5 , 1.3×10^5 , 8×10^4 , 7.3×10^4 (S-7, S-6, S-5, S-4) in the CHCl_3 -MEK system (12:1.6). Positive prints.

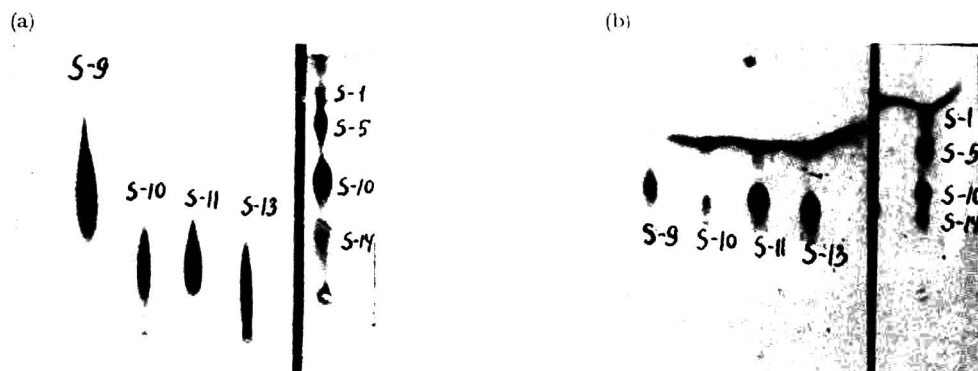


Fig. 12. TLC of statistical copolymers St-MMA on various silica gels. (a) Copolymers with 31% of St and MW 2.6×10^5 , 1.6×10^5 , 8.8×10^4 , 5×10^4 (S-13, S-11, S-10, S-9) on KSK in the CHCl_3 -acetone system (12:2.2); (b) copolymers with 80, 54, 31 and 22% of St (S-1, S-5, S-10, S-14) on KSK in the CHCl_3 -acetone system (12:2.4); (c) copolymers with 31% of St and MW 2.6×10^5 , 1.6×10^5 , 3.8×10^4 (S-13, S-11, S-10, S-9) on KSM-5 in the CHCl_3 -acetone system (12:3.2); (d) copolymers with 30, 54, 31 and 22% of St (S-1, S-5, S-10, S-14) on KSM-5 in the CHCl_3 -acetone system (12:3.4). Positive prints.

porous Silica Gel KSM-5 is advisable for TLC of copolymers with a MW not over 10^5 , whereas for copolymers of higher MW Silica Gel KSK with large pores should be used.

TLC of copolymers with high resolution. Using weak "displacers" (diethyl ether, MEK), one can obtain chromatographic systems of high resolution for the separation of copolymers slightly differing in composition. Fig. 13a illustrates the TLC separation of copolymers having similar composition — 80% St according to elementary analysis and refraction index increment data. In this case, despite the gradient conditions of chromatography, the chromatographic spots may be found to be connected by a narrow path of bi-modal distribution.

In order to distinguish this phenomena from tailing, two-dimensional chroma-

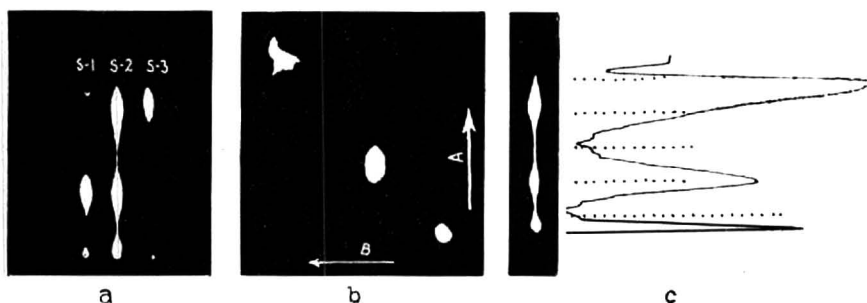


Fig. 13. TLC with high resolution. (a) The copolymers St-MMA with 80% of St (S-1, S-2, S-3) in the CHCl_3 -MEK system (12:0.6); (b) two-dimensional chromatogram S-2; (c) one-dimensional chromatogram and densitogram of S-2.

tography in a single system of solvents was used. Fig. 13b represents a two-dimensional chromatogram of the copolymer S-2 which is separated into three isolated spots positioned diagonally on the plate. This fact indicates that they are individual components. A densitogram of this copolymer is shown in Figure 14b. The resolution of this method of TLC is so high that it permits the detection of inhomogeneity of copolymers of azeotropic composition with the increase in the conversion. As shown in Fig. 14a, the extent of the stretching of the spots of 54% St copolymers becomes higher with increasing conversion. A two-dimensional chromatogram of S-5 confirms that these results are not due to the formation of chromatographic artifacts. When the S-chamber is used, it must be taken into account that the "displacer" gradient only extends for a short distance on the plate near the front. The chromatographic spots are compact and occur near each other in this zone.

The other copolymers (with a lower St content), for which the concentration of the "displacer" is not sufficient, are found either on the start or move in the non-gradient zone of solvent and form wide bands as shown in Fig. 9. Apparently, the gradient zone corresponds to conditions of low resolution whereas the non-gradient zone moving next gives high resolution.

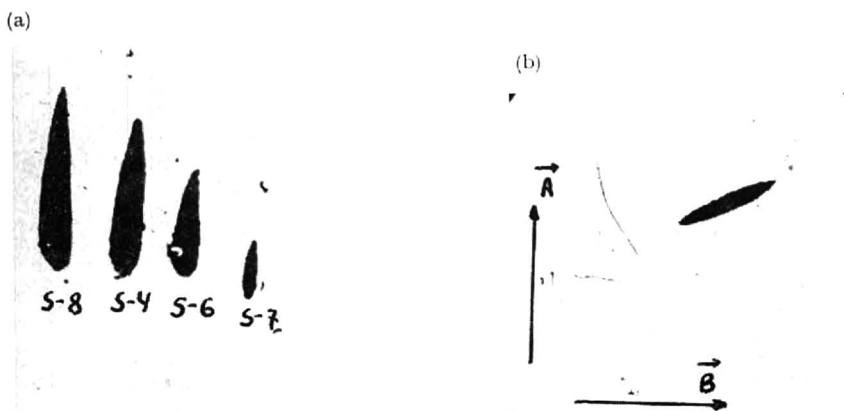


Fig. 14. TLC of azeotropic copolymers St-MMA with 54% of St. (a) Copolymers with different conversion: S-7 (0.5%), S-6 (11.7%), S-4 (3.3%), S-8 (70.6%) on Silica Gel KSK in the CHCl_3 -diethyl ether system (12:4.2); (b) two-dimensional chromatogram of S-4. Positive prints.

Thin-layer chromatography of block and graft copolymers

The two main tasks for TLC of block and graft copolymers are to determine homopolymer admixtures in the copolymer and to diagnose block and graft copolymers. The first problem is solved by means of two-dimensional TLC in two solvent systems where the two homopolymers are moved in different directions, while the block (graft) copolymer remains on start. In the case when the copolymer moves in one of the solvent systems, one of the homopolymers moves with it in the same solvent system. Then after two-dimensional chromatography with a suitable second solvent system the copolymer and the homopolymers mixed with it will be moved so that they are positioned in different corners of the plate.

The problem of diagnostics of block and graft copolymers may be solved in two ways. The first is to compare the mobilities of the copolymer and the homopolymers which are known to be of much higher MW. A second approach (which is more reliable) is possible if we succeed in finding two solvent systems, the first of which keeps one of the homopolymers at the start making the copolymer move, while in the second system the copolymers move with the front as before but the homopolymers exchange their places. For differentiating graft copolymers and in general branched linear macromolecules, a highly specific method can be used; it is based on the difference in their thermodynamic rigidity which determines the number of adsorbed segments and hence the stability of the adsorption bond. As a result, the R_F value of a graft copolymer corresponds to the R_F value of the linear homopolymer with the same composition as that of the side branches of the graft copolymer but with a considerably lower MW.

Investigation of graft copolymers of styrene and methyl methacrylate. TLC was used for graft copolymers whose backbone consisted of poly(methyl methacrylate) (PMMA) with a MW of 5×10^3 , and have side branches of St with a MW of 2×10^3 . The ratio St/MMA was 1/10, hence the MW of the graft copolymer obtained was 1.5×10^6 . Fig. 15a presents the two-dimensional chromatogram of a graft copolymer on a Silica Gel KSK plate with dimensions of 6×6 cm. The graft copolymer was applied in the amounts of 50–100 μ g from a chloroform solution. Chromatography in the first direction was carried out with a solvent system in which PMMA of any MW and low molecular weight PS move with the front and the graft copolymer remains at the start. When chromatography was carried out in the other direction, we used a solvent system in which PMMA did not move whereas PS of any MW (and hence the graft copolymer, as well) moved with the front. As a result all the components of the graft copolymer were found in different corners of the plate. Moreover a substance of unascertained nature was found at the start (apparently it was a product of further cross-linking of the graft copolymer).

When another pair of solvents was used (Fig. 15b), graft copolymer and PS moved in the first direction while PS and PMMA moved in the second one. In this case PS and PMMA was found in the upper and lower left hand corners of the plate, respectively, whereas the graft copolymer was placed above the starting spot (see Fig. 15b).

Fig. 15c also shows that the graft copolymer with a MW of 1.5×10^6 , being more rigid than linear PS, moves on the level of PS with a MW of 1.7×10^5 .

Thin-layer chromatography of block copolymers. Block copolymers of ethylene oxide (EO) and styrene in the ratio 1:1 were investigated. TLC was carried out on

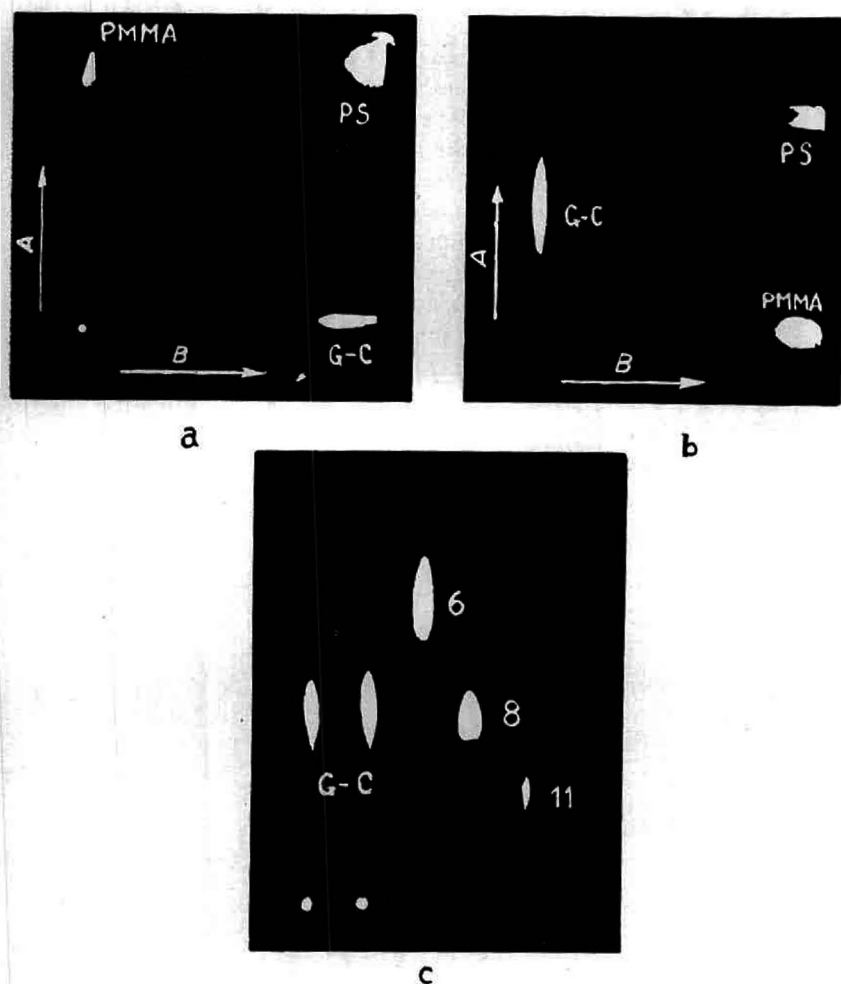


Fig. 15. TLC of graft-copolymer PMMA-PS (G-C). (a) Chromatogram in the acetone-acetic acid system (12:2) in direction A and in the CHCl_3 -MEK system (12:2) in direction B; (b) two-dimensional chromatogram in the C-B-A system (12:4:0.7) in direction A and in the acetone-acetic acid system (12:2) in direction B; (c) one-dimensional chromatogram of the graft-copolymer PMMA-PS and of polystyrenes 6, 8, and 11 in the C-B-A system (12 + 4 + 0.7) on KSK Silica Gel.

the plates 6×6 cm with the Silica Gel KSK. Block copolymer samples were applied in the amount of 50–100 μg from a chloroform solution. After the chromatographic process the polymer spots were detected with the help of a 3% KMnO_4 solution or Dragendorff's reagent. Fig. 16 illustrates a two-dimensional chromatogram of the block copolymer ST-EO. The chromatographic systems used were selected so that PS (MW 3×10^6) and PEO (MW $> 10^6$) moved with the front. The block copolymer was found at the start and the colour of its spot was developed with both reagents. The chromatogram shows that free PS moving in the C-B-A system was present in the block copolymer sample together with a small quantity of PEO moving in the pyridine-water system. Unfortunately, owing to a great difference in polarity between PEO and PS, we failed to find a solvent system which would force the block copolymer

under investigation to move, as well. Such a system was, however, successfully selected for the block copolymer of St with the less polar monomer MMA (50:50). In the system containing acetone the block copolymer ST-MMA moved on the same level as the PS while the PMMA remained on start and the statistical copolymer of the same composition was in the middle of the plate. In another system containing methanol the block copolymer also moved with the front together with PMMA whereas PS remained on start. As in the first case, the statistical copolymer was placed in the centre of the plate. These results show that in these solvent systems one of the copolymer blocks, either PMMA (in the first case) or PS (in the second case), collapses and the chromatographic behaviour of these copolymers resembles that of PS or PMMA, respectively. Similar changes in the conformation of block copolymers in different solvents are described in literature²⁷.

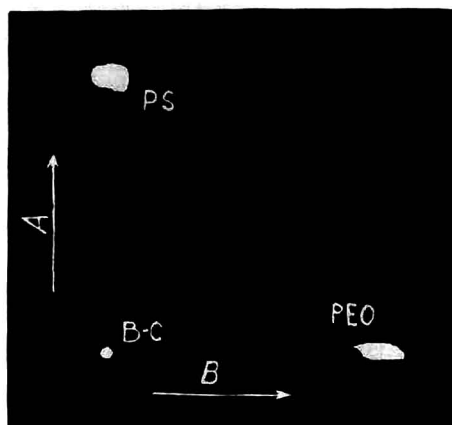


Fig. 16. Two-dimensional TLC of block-copolymer (B-C) St-EO (50:50) in the systems: C-B-A (12:4:2) in direction A and pyridine-water (3:7) in direction B.

CONCLUSIONS

The results of the TLC of polymers (copolymers) reported above show this method to be effective for the investigation, with high resolution, of such properties of macromolecules as MW and MWD, and the composition of homopolymers and structural properties of copolymers. This method also permits diagnosis of block and graft copolymers and the determination of the homopolymer admixtures in them. Using the microporous adsorbent KSM-5, it is possible to eliminate, to a considerable extent, the influence of MW on TLC of copolymers. Two-dimensional TLC permits one to distinguish between the chromatographic phenomena on the plate, *viz.* which causes the formation of a stretched spot and which causes tailing. This method also enables us to determine the homopolymer admixtures in graft and block copolymers. Finally, two-dimensional TLC permits one to take into account chromatographic spreading when MWD of homopolymers is to be determined by means of TLC. The concentration dependences were established for the TLC of polymers; the adsorption isotherms were of the gel type in the upper part of the plate and of the adsorption type in the lower one. It should be noted that INAGAKI paid no attention in his work¹¹ to the dependence of the R_F values of polymers on the concentration and the MW of

copolymers. This dependence does not follow from the diad model he used^{12,15} for interpreting the peculiarities of TLC of polymers.

We shall examine the mechanism of the polymer movement along the thin-layer plate. During the elution movement in the adsorbent layer, the polymers are distributed between the mobile and the stationary phases. The mobile phase is homogeneous in structure and has a section β , while the stationary phase is subdivided into two zones: firstly a film with a section α' accessible for macromolecules of all sizes which covers the surface of the adsorbent grains and fills the spaces between these particles, and secondly the space of adsorbent pores which is accessible only for macromolecules smaller than the pore entrance diameter. The section of such pores (we shall designate it as α_N^{acc}) according to MOORE's relation²⁸ can be expressed as $\alpha_N^{\text{acc}} = \alpha(1 - \log N / \log N_m)$, where α is the overall section of the porous part of adsorbent, N is the number of macromolecular units (the degree of polymerisation), N_m represents the maximum size of macromolecules for which the largest of the adsorbent pores

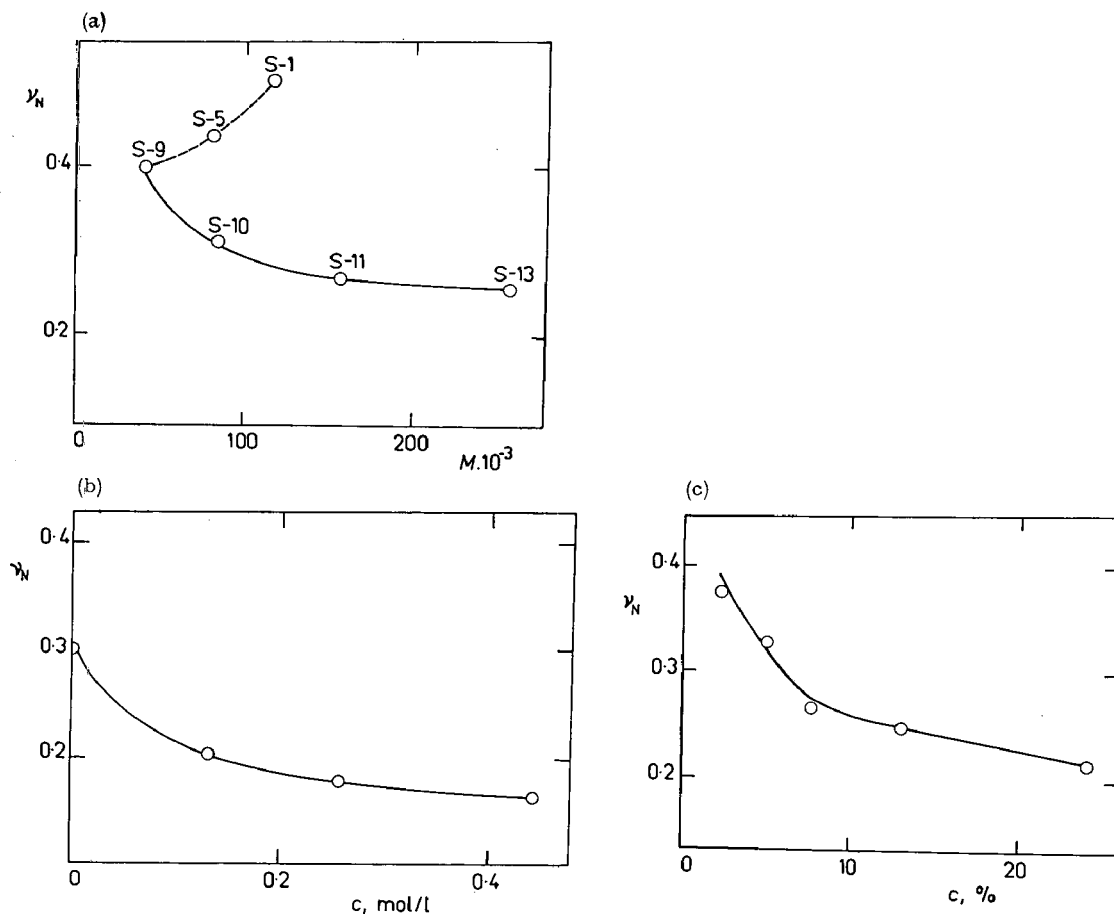


Fig. 17. Dependence of ν_N for statistical copolymers St-MMA during the adsorption on aerosil with the specific surface $150 \text{ m}^2/\text{g}$ on: (a) MW of copolymers with 31% of St (S-9, S-10, S-11, S-13) and the content of St in copolymers (S-1, S-5, S-9); (b) the concentration of displacer (dioxan in moles/l) for copolymers with 24% of St; (c) concentration (%) of the solution of copolymer with 24% of St.

are accessible. As shown in reference 29, when the energies of interaction with the adsorbent are not very high, the macromolecules represent slightly deformed random coils and come into contact with the adsorbent only by some fraction, ν_N , of their units, and on the whole are located above the adsorbent surface having the shape of loops. The number of the adsorbed units ν_N can be determined experimentally by means of infrared spectroscopy, for example, for the MMA units it is calculated from the shift of the carbonyl adsorption band from $\nu = 1732 \text{ cm}^{-1}$ to $\nu = 1710 \text{ cm}^{-1}$. Fig. 17a shows the percentage of the adsorbed units (ν_N) determined by this method for a copolymer St-MMA as a function of its composition, MW, the composition of the solvent and the concentration of the solution. This figure shows that ν_N decreases with increasing MW and with decreasing percentage of the St units. The latter fact is probably due to a decreasing probability of contact between the adsorbent and the MMA units when these units are arranged sufficiently close to each other in the copolymer loops (Fig. 17a) and when the displacing power of the solvent (per cent of dioxan) is increased (Fig. 17b). The increase in the polymer concentration (Fig. 17c) leads to a decrease in ν_N produced by a deformation of the coils in the direction tangential to the adsorbent surface. This fact explains why an adsorption isotherm having the LANGMUIR characteristics for macromolecules is distinctly seen in the TLC of polymers (see Figs. 5 and 10).

With adsorption of the macromolecules, its entropy diminishes owing to a deformation of the coil. The loss of entropy is compensated by the energy of interaction of macromolecular units with the active centres of adsorbent, $\theta = \varepsilon/KT$. Here ε is the mean energy of mutual exchange in the adsorption of a single unit from the solution, $\varepsilon = \omega(\varphi_{23} + \varphi_{11} - \varphi_{12} - \varphi_{13})$, where ω is the coordination number, φ is the energy of intermolecular interaction (indices 1, 2 and 3 refer to the solvent, the polymer and the adsorbent, respectively). During the adsorption the configurational entropy ΔS_c in the solution also changes owing to the formation of a macromolecular adsorption layer in the large pores and to the separation of the solvent from the macromolecular solution in the small pores. Since the stratification of the polymer solution takes place in the whole pore volume, ΔS_c must only slightly depend on the porous structure of the adsorbent and the MW of the polymer. If we examine the free energy change in the macromolecular solution during adsorption according to the conceptions of FLORY-HUGGINS³⁰, we can write for the adsorption coefficient of macromolecules:

$$K = P \exp (N\nu_N\theta) \quad (2)$$

where $P = \exp (\Delta S_c/K)$. Since ν_N decreases with increasing N and increases with increasing θ (Figs. 18a and 18b) ($\nu_N = \xi N^{-a}\theta^b$), where ξ , a and b are dimensionless parameters, the distribution coefficient for macromolecules can be expressed as follows:

$$K_d = P \exp [\xi N^{1-a}\theta^{1+b}] \quad (3)$$

From this equation the expression for the R_F value can be derived:

$$\begin{aligned} R_F &= \left(1 + \frac{\alpha'}{\beta} + \frac{\alpha_N^{\text{acc}}}{\beta} K_d\right)^{-1} = \left[1 + \frac{\alpha'}{\beta} + \frac{\alpha_N^{\text{acc}}}{\beta} P \exp (N\nu_N\theta)\right]^{-1} = \\ &= \left[1 + \frac{\alpha'}{\beta} + \frac{\alpha}{\beta} (1 - \log N / \log N_m) P \exp (\xi N^{1-a}\theta^{1+b})\right]^{-1} \end{aligned} \quad (4)$$

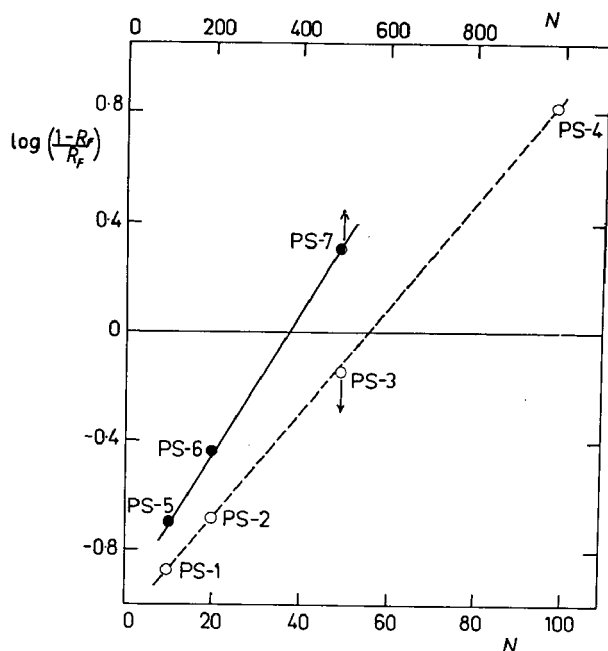


Fig. 18. Dependence of $\log(1 - R_F)/R_F$ on $MW(N)$: for PS 1, 2, 3, 4 in the C-B-A-system (13:3:0.1); for PS 5, 6, 7 in the C-B-A system (12:4:0.4) on the Silica Gel KSK.

We shall examine this expression for the case when $\alpha_N^{\text{acc}} = \alpha$. Then eqn. 4 can be written:

$$R_F = \left(1 + \frac{\alpha'}{\beta} + \frac{\alpha}{\beta} P \exp [N\nu_N\theta]\right)^{-1} = \left[1 + \frac{\alpha'}{\beta} + \frac{\alpha}{\beta} P \exp (\xi N^{1-a_\theta 1+b})\right]^{-1} \quad (5)$$

The term α'/β in eqn. 5 can be omitted (which is permissible for plates with a well prepared adsorption layer) and the resulting equation then becomes linear:

$$\log [(1 - R_F)/R_F] = -\log (\beta/\alpha P) + \nu_N\theta N \quad (6)$$

Fig. 18 shows that this equation is correct. In fact, we find a linear dependence of $\log [(1 - R_F)/R_F]$ on $MW(N)$ for PS 1-4 and PS 5-7 on the Silica Gel KSK; this shows that it is correct to describe TLC of polymers by means of eqn. 4. It must be noted that the slope of the lines in Fig. 18 is equal to $\nu_N\theta$, i.e., it is connected with the energy of interaction between the polymer unit and the adsorbent.

It is interesting that for low molecular weight PS this slope is steeper and, hence, for TLC of such polymers the interaction energy between the polymer and the adsorbent must be increased (for example, by decreasing the displacer content in the eluent). We shall determine the sensitivity of TLC to $MW(N)$ and to the composition (θ); differentiating eqn. 5 we obtain

$$\frac{\partial R_F}{\partial N} = \frac{\frac{\alpha'}{\beta} P \exp (\xi N^{1-a_\theta 1+b})}{\left[1 + \frac{\alpha'}{\beta} + \frac{\alpha}{\beta} P \exp (\xi N^{1-a_\theta 1+b})\right]^2} \times (1 - \alpha) N^{-a_\theta 1+b} \quad (7)$$

and

$$\frac{\partial R_F}{\partial \theta} = \frac{\frac{\alpha'}{\beta} P \exp(\xi N^{1-a_\theta 1+b})}{\left[1 + \frac{\alpha'}{\beta} + \frac{\alpha}{\beta} P \exp(\xi N^{1-a_\theta 1+b})\right]^2} \times (1+b) N^{1-a_\theta b} \quad (8)$$

Examination of eqns. 7 and 8 permits the following conclusions to be drawn.

(1) Since the maximum value of $x/(a+x)^2$ is attained when $x = a$, it follows that $\partial R_F/\partial N$ and $\partial R_F/\partial \theta$ have maximum values when

$$\frac{\alpha'}{\beta} P \exp(\xi N^{1-a_\theta 1+b}) \approx 1 + \frac{\alpha'}{\beta},$$

i.e. with $R_F \leq 0.5$; this is clear from Fig. 5.

(2) The sensitivity of the analysis to MW (i.e., the quotient $\partial R_F/\partial N$) increases and its sensitivity to composition ($\partial R_F/\partial \theta$) decreases with MW; this is also in good agreement with experimental results (Fig. 4).

(3) The presence of the term v_N in the exponential of eqn. 4 permits one to connect R_F with the thermodynamic rigidity of macromolecules. It follows from our studies that the R_F of graft-copolymers and other branched macromolecules with increased rigidity must be higher than R_F for linear polymers of the same MW.

In conclusion, the advisability of combining the TLC and GPC methods must be noted. GPC can be used for obtaining standard samples of known MW which are necessary for the calibration of TLC plates. In addition, the relation between the volumes of macromolecules determined by GPC and their adsorption determined by TLC can be used for studying the structural peculiarities of the polymer samples including the diagnostics of graft-copolymers.

REFERENCES

- 1 B. G. BELENKII, L. S. VILENCHIK AND D. D. NOVIKOV, in *Novoe v metodach issledovaniya polimerov*, Mir, Moscow, 1968, p. 81.
- 2 *Analytical Gel Permeation Chromatography*, J. Polymer Sci., C-21 (1968).
- 3 R. M. SREATON, in *Noveishie metody issledovaniya polimerov*, Mir, Moscow 1966, p. 361.
- 4 K. BURGER, *Z. Anal. Chem.*, 224 (1967) 421.
- 5 L. FAVRETTO, G. PERTOLDI MARIETTA AND L. FAVRETTO GABRIELLI, *J. Chromatog.*, 46 (1970) 255.
- 6 M. T. BRIK, A. S. SHEVLYAKOV AND O. B. KRESUB, *Vysokomol. Soedin.*, 10B (1968) 893.
- 7 M. S. Y. DALLAS AND M. F. STEWART, *Analyst*, 92 (1967) 634.
- 8 V. A. DORMAN-SMITH, *J. Chromatog.*, 29 (1967) 265.
- 9 H. HALPAAP AND K. KLATYK, *J. Chromatog.*, 33 (1968) 80.
- 10 N. HEITZ, K. KLATYK, F. KRAFCZYK, K. PFITZNER, D. RANDAU AND E. MERK, in *Seventh Intern. Gel Permeation Chromatog. Seminar*, Monte Carlo, 1969, p. 217.
- 11 H. INAGAKI, H. MATSUDA AND F. KAMIYAMA, *Macromolecules*, 1 (1968) 520.
- 12 F. KAMIYAMA, H. MATSUDA AND H. INAGAKI, *Makromol. Chem.*, 125 (1969) 286.
- 13 H. INAGAKI, T. MIYAMOTO AND F. KAMIYAMA, *Polymer Letters*, 7 (1969) 329.
- 14 H. INAGAKI AND T. MIYAMOTO, *Macromolecules*, in press.
- 15 H. INAGAKI, *Bull. Inst. Chem. Res. Kyoto Univ.*, 47 (1969) 196.
- 16 B. G. BELENKII, E. S. GANKINA AND L. D. TURKOVA, in *Lektsii 2-oi shkoly po metodam ochistki i ozenki chistoty monomerov i polimerov*, Chernogolovka, 1968, p. 216.
- 17 I. A. BARANOVSKAYA, B. G. BELENKII, E. S. GANKINA AND V. E. ESKIN, in *Sintez, struktura i svoistva polimerov*, Trudy XV nauchn. konfer. Instituta Vysokomolekulyarnykh Soedinenii Acad. Nauk S.S.S.R. (April 1967), Nauka, Leningrad, 1970, p. 77.

- 18 B. G. BELENKII AND E. S. GANKINA, *Dokl. Akad. Nauk S.S.S.R.*, 186 (1969) 857.
- 19 B. G. BELENKII AND E. S. GANKINA, *Dokl. Akad. Nauk S.S.S.R.*, in press.
- 20 L. H. TUNG, J. C. MOORE AND G. W. KNIGHT, *J. Appl. Polymer Sci.*, 10 (1966) 1261.
- 21 L. H. TUNG, *J. Appl. Polymer Sci.*, 10 (1966) 375.
- 22 L. H. TUNG AND J. R. RUNYON, *J. Appl. Polymer Sci.*, 13 (1969) 2397.
- 23 M. CANTOW, R. S. PORTER AND J. F. JOHNSON, *J. Polymer Sci.*, A-1 5 (1967) 1391.
- 24 J. E. HAZELL, L. A. PRINCE AND H. E. STAPELFELDT, *J. Polymer Sci.*, C-21 (1968) 43.
- 25 I. A. BARANOVSKAYA, A. D. LITMANOVICH, M. S. PROTASOVA AND V. E. ESKIN, *Vysokomol. Soedin.*, 7 (1965) 509.
- 26 A. B. KISELEV AND YA. I. YASHIN, *Gas-adsorbtsionnaya chromatografiya*, Nauka, Moscow, 1967.
- 27 E. G. ERENBURG, G. G. KAZTASHEVA, M. A. EREMINA AND I. YA. PODDUBNYI, *Vysokomol. Soedin.*, A-9 (1967) 2709.
- 28 I. E. MOORE, *J. Polymer Sci.*, A-2 (1964) 835.
- 29 R. R. STROMBERG, in P. WEISS AND G. D. CHEEVER (Editors), *Interface conversion for polymer coating*, Elsevier, New York, 1968, p. 321.
- 30 P. J. FLORY, *Principles of Polymer Chemistry*, Cornell Univ. Press, Ithaca, 1953.

J. Chromatog., 53 (1970) 3-25

CHROM. 4965

RECENT DEVELOPMENTS IN GEL PERMEATION CHROMATOGRAPHY:
HIGH SPEED AND HIGH RESOLUTION

INTRODUCTORY LECTURE

K. J. BOMBAUGH

Waters Associates Inc., Framingham, Mass. (U.S.A.)

SUMMARY

High resolution, high speed and heavy load are each attainable by gel permeation chromatography each at the expense of the other two. However, by use of appropriate compromises any two may be increased without significant loss. For example, flow rate and load may be increased to gain throughput by recycling to increase column length. Further flow rate and column length or flow rate and temperature may be increased to increase speed. However, when highest resolution is desired, load, flow rate, and temperature must all be optimized.

INTRODUCTION

The chromatographer is confronted with a choice between three interdependent factors, *i.e.*, resolution, speed and load, which can be represented by an equilateral triangle with one factor at each apex¹. In this triangular system an increase in one factor is gained at the expense of the other two. It is the purpose of this presentation to summarize recent development in gel permeation chromatography (GPC) in terms of this interdependence and to demonstrate some useful compromises.

During the past two years several major accomplishments have occurred in gel permeation chromatography which have resulted in new developments in techniques and equipment. Increased understanding of chromatographic principles led to increased speed through increased flow rates and increased temperature. Simultaneously, developments in instrument technology led to increased resolution at increased load through the use of recycle.

RESOLUTION IN GPC

First consideration is given to resolution since GPC is primarily a separation process. Numerous workers have contributed to the advances which led to high-resolution GPC. Particular attention is given to the work of ČOUPEK AND HEITZ², who clearly showed the value of both increased capacity ratio (KV_s/V_0) and optimized

solvent velocity in obtaining high resolution. The high capacity ratio was obtained by use of highly swollen, lightly cross-linked gels. The benefit of increasing capacity ratio (K') through increased pore volume is discernible in the expanded resolution equation³, which describes resolution in terms of selectivity, capacity and efficiency,

$$R = \frac{1}{4} \left(\frac{K_2}{K_1} - 1 \right) \left(\frac{K'}{1 + K'} \right) \sqrt{n} = \frac{1}{4} \left(\frac{K_2}{K_1} - 1 \right) \sqrt{N} \quad (1)$$

where $N = 16\{(V_e - V_0)/W\}^2$ represents the number of effective plates, n the number of theoretical plates, K the distribution coefficient, $K' = KV_s/V_0$ the capacity ratio, and W the peak width.

Plate number n , widely used to evaluate the resolving power of a GPC column, can be misleading since resolution is related to the number of effective plates, N , where correction is made for column void volume. Since K_2/K_1 is related to molecular size, the selectivity term is generally fixed in GPC. The capacity term, however, must be considered when choosing a GPC column packing since the phase ratios (V_s/V_0) of commercial gels range from 0.5 to 2. (A column packed with a $V_s/V_0 = 0.5$ gel would require four times the plate number, *i.e.* four times the length, to provide equal resolution equal to a column with $V_s/V_0 = 1$.)

While highly swollen gels offer the advantage of high phase ratio they are subject to compaction when exposed to high solvent velocities. This is particularly true with macroporous gels. Consequently rigid gels⁴⁻⁷ have found virtually universal acceptance in instrumented GPC. The phase ratios of most commonly used rigid gels range between 0.8 and 1.2, with a nominal value of 1.

With the capacity term of the resolution equation limited by the phase ratio of rigid gels to values between 1 and 2 increased resolution must be attained by an increase in the number of effective plates of the column, N (*cf.* ref. 8), which is accomplished by increasing column length⁸. Increased column length is accompanied by a proportional increase in both pressure drop and cost.

An alternative to long columns as a means of increasing N is to recycle the solute through the columns^{9,10}. The approach is particularly reasonable in GPC since K values do not exceed unity and maximum elution volume is fixed by the volume of the columns in the systems. Late peaks common to sorption chromatography need not be considered.

Peak width in recycle chromatography

Peak width (W) of a single species in recycle chromatography relates to cycle number (ν) by the relationship

$$W_\nu = V_\nu \left(\frac{16H}{L_\nu} \right)^{1/2} \quad (2)$$

Since $V_\nu = \nu V_0$ and $L_\nu = \nu L_0$ peak width of the ν -th cycle is

$$W_\nu = W_0 \sqrt{\nu}.$$

For W_0 to be valid it must include the contribution to spreading of the entire system,

i.e. postdetector and pump. When injection is by means of a valve after the pump $\Delta W/\text{cycle}$ must be determined and W_0 obtained by extrapolation.

High resolution with recycle

The distance between peaks in recycle chromatography increases as a function of the number of cycles. Resolution with recycle is therefore described by the expression

$$R_v = \frac{vV_2 - vV_1}{W_v} = \frac{v(V_2 - V_1)}{W_0\sqrt{v}} = \frac{\sqrt{v}(V_2 - V_1)}{W_0} = \sqrt{v}R_0. \quad (3)$$

Actual distribution of a polydispersed solute at maximum resolution may be defined¹¹ by eqn. 4

$$(W_T/v)^2 = W_c^2/v + W_s^2 \quad (4)$$

where W_T is the total width of a distribution, W_c = width due to random dispersion, and W_s = width due to separation. A plot of $(W_T/v)^2$ versus $1/v$ yields a straight line which, when extrapolated to $1/v = 0$, defines W_s^2 at infinite cycles. By this technique WATERS¹¹ extrapolated a 16-cycle separation of a narrow fraction polystyrene with a molecular weight of 173 000 to $D = 1.0025$.

THE PRACTICE OF RECYCLE CHROMATOGRAPHY

Recycle chromatography, first considered in gas chromatography¹², was introduced in gel filtration by PORATH AND BENNICH¹³ using a peristaltic pump at low pressure and low velocity. In our work¹⁰ a small volume reciprocating pump (Milton Roy) used in commercially available GPC equipment was shown to be capable of recycle operation with minimal band spreading^{10,14}. In our original work the outlet to the detector was connected to the suction of the pump with a minimum amount of small-diameter tubing. During recycle the inlet from the solvent tank was left

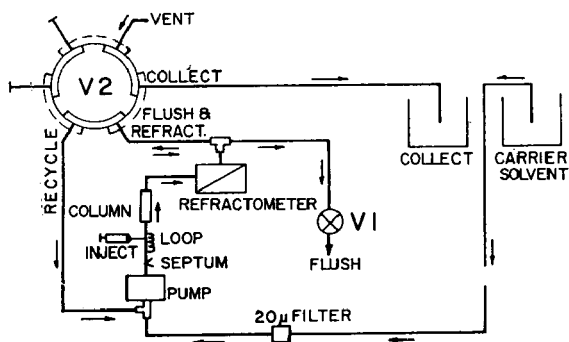


Fig. 1. Schematic diagram of recycle operation. Method of operation: (a) Recycle to collect sequence (V_2 in recycle position). (1) Turn pump and recorder off. (2) Flush with approximately 15 ml of solvent by opening and closing V_1 . (3) Turn V_2 to "collect" position. (4) Turn pump and recorder on. (b) Collect to recycle sequence (V_2 in collect position). (1) Turn pump and recorder off. (2) Turn V_2 to "recycle" position. (3) Flush as "recycle to collect" sequence. (4) Turn pump and recorder on.

open to prevent cavitation. The system was changed from recycle to collect modes by means of needle valve.

High-performance recycle equipment

For simplified operation a system was designed around a 6-port valve as shown in Fig. 1. The valve was designed into a Waters Associates GPC/ALC Model 301 using minimal lengths of small-diameter transport tubing. The system operates at flow rates up to 3 ml/min and pressures up to 1000 p.s.i.

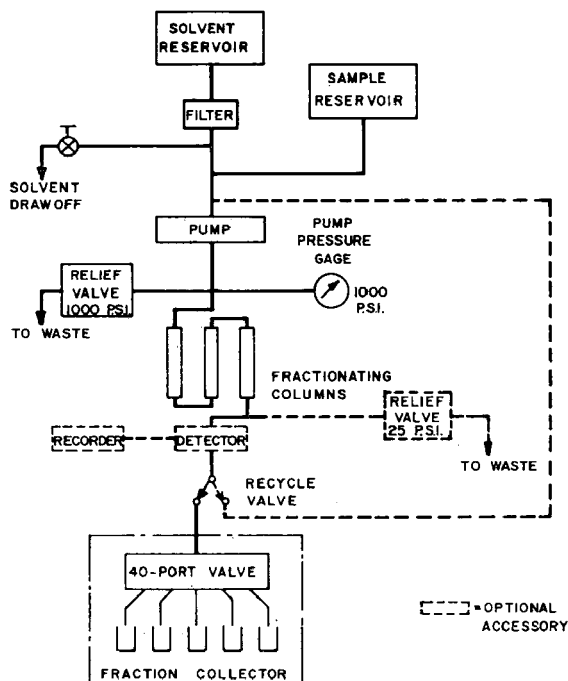


Fig. 2. Schematic diagram of Chromato-Prep.

The method of operation shown in the caption is vital to successful use of recycle since it includes a procedure to draw off the sides of the distribution to prevent peak overlap¹⁴ and also provides a method of flushing the solvent inlet Tee to prevent spurious peaks caused by reinjection of any solute which may have migrated into the inlet line during recycle operation. The recycle system shown is usable with columns ranging between 0.303 in. and 1 in. in I.D.

Large-scale GPC, using recycle and heavy load

A large-scale preparative apparatus, the "Chromato-Prep", shown schematically in Fig. 2, was developed to fractionate, in the recycle mode, gram quantities of material using columns up to 2.24 in. I.D. by 4 ft. in length. The "Chromato-Prep" is equipped with a constant displacement piston-type pump operable to 1000 p.s.i. at flow rates between 10 and 100 ml/min. Sample is injected through the pump by

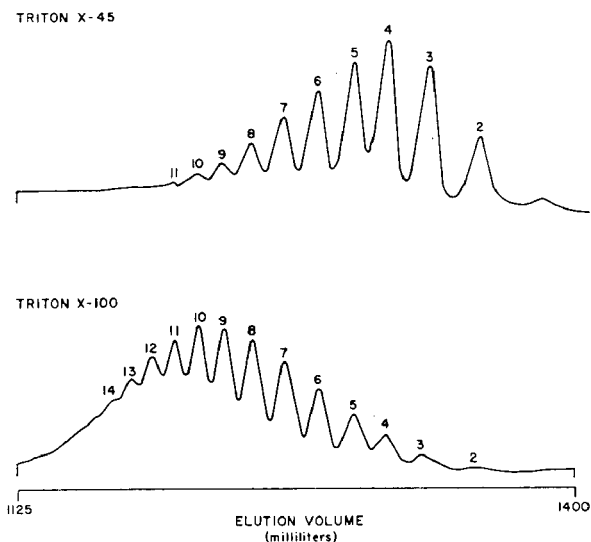


Fig. 3. High-resolution GPC separation of surfactants (nonylphenol-ethylene oxide adducts). Analytical/operating conditions: columns, 160 ft. \times 3/8 in. O.D. 500 Å gel; flow rate, 0.4 ml/min. The numbers 2 through 14 represent moles of ethylene oxide per molecule of nonylphenol.

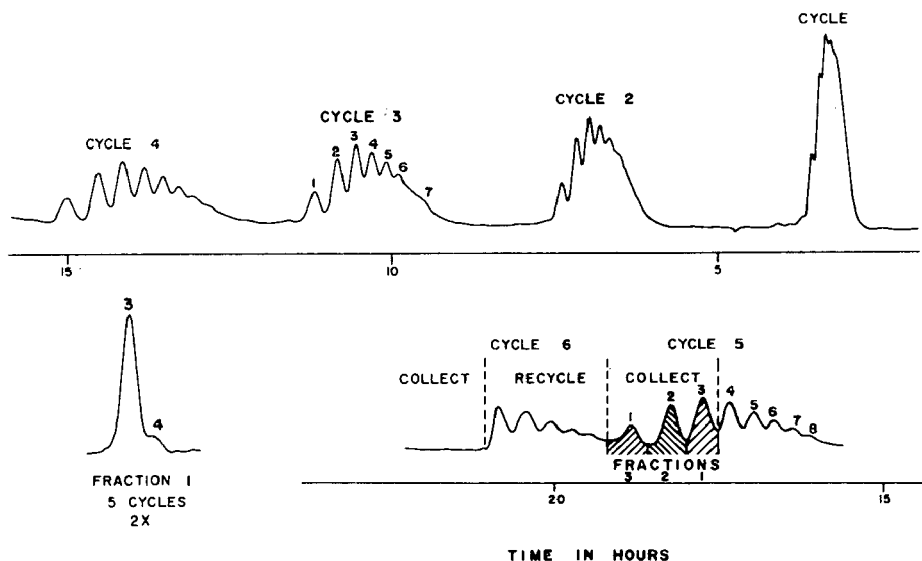


Fig. 4. Effect of cycle number on resolution. Sample, Triton X-45; concentration, 50%; injection volume, 30 μ l; solvent, THF; flow rate, 0.48 ml/min; columns, Styragel 60 Å (15 ft.).

means of remotely operated electrical controls mounted on a graphic panel on the front of the instrument. The instrument can accommodate up to four columns 4 ft. in length by 2.24 in. I.D. The columns are mounted vertically in a recess in the sides of the enclosure. Columns are of stainless steel construction designed to withstand

pressures up to 1500 p.s.i. Nominal pressure drop for 2.24 in. columns, packed with Styragel is 200 p.s.i. for toluene at a flow rate of 100 ml/min at room temperature. Provision is made for both refractive index and UV detector. The refractive index detector is equipped with a 28° cell to provide an increase in linear range at heavy sample load. A detector is essential to recycle operation since the operator must see when resolution is adequate to collect fractions or when peak sides must be drawn off to prevent overlap.

EVALUATION OF RECYCLE OPERATION

Recycle operation may be compared with single-pass chromatography by use of Figs. 3 and 4. The Triton X-45 resolved by a 160-ft. column on a single pass was also resolved by a column 15 ft. in length after six cycles. Peaks 1, 2, and 3, removed after the fifth cycle to prevent overlap, were collected as individual fractions. Peak 3 evaluated separately shows only minor contamination by peak 4. To resolve oligomers it is desirable to provide enough system capacity to obtain the desired resolution before peak overlap occurs. This is illustrated in Fig. 5. At the high flow rate six cycles were completed in 4 h, but peak overlap resulted before discrete peaks were observed. At the lower flow rate individual peaks are resolved after the second cycle and four cycles (19 h) are completed before overlap occurs. By increasing column length from 20 to 32 ft. and operating at an intermediate flow rate discrete peaks were resolved before overlap occurred¹⁴.

Load versus resolution

The deleterious effect of increased load on resolution is evident from Tables I and II (*cf.* ref. 14). Also evident is the effect of increased column capacity gained by recycle; Fig. 6 shows chromatograms of a 3.5-g load after three cycles.

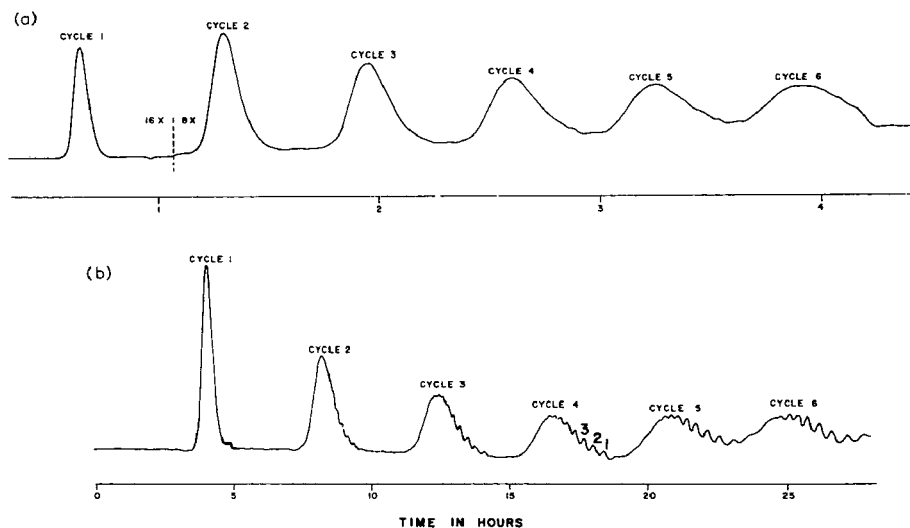


Fig. 5. Effect of flow rate on capacity requirement. Sample, Triton X-100; concentration, 50%; injection volumes, (a) 50 μ l and (b) 70 μ l; solvent, THF; flow rates, (a) 3.1 ml/min and (b) 0.5 ml/min; columns, Styragel 100 Å (8 ft.) and 60 Å (12 ft.).

TABLE I

RESOLUTION AT VARIOUS SAMPLE LOADS USING CONSTANT VOLUME (100 ml)

Sample load (g)	Concentration (mg/ml)	Resolution		
		Cycle 1	Cycle 2	Cycle 3
1.0	10	1.06	1.31	1.47
2.0	20	0.59	1.13	1.29
3.5	35	0.34	0.77	1.14
5.0	50	0.25	0.54	0.92

TABLE II

RESOLUTION AT VARIOUS SAMPLE LOADS USING CONSTANT CONCENTRATION (10 mg/ml)

Sample load (g)	Volume (ml)	Resolution		
		Cycle 1	Cycle 2	Cycle 3
1.0	100	1.06	1.31	1.47
2.2	220	0.70	1.20	1.34
3.5	350	0.39	0.91	1.14

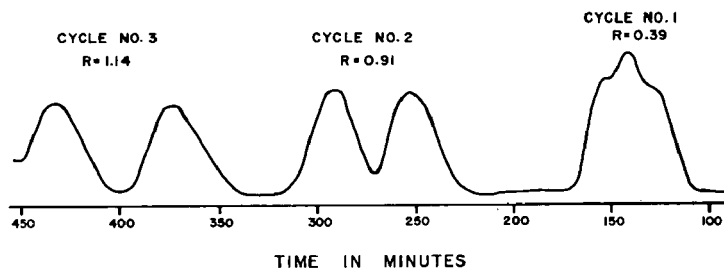


Fig. 6. Effect of recycle on resolution at heavy load. Sample, polystyrene mixture 51 *K* + 10.3 *K* (1-1); load, 3.5 g; concentration, 10 mg/ml; injection volume, 350 ml; solvent, toluene; flow rate, 14.4 ml/min; column, 2.5×10^4 Å Styragel (4 ft.).

Resolution is greatest at the low molecular weight (high *K'*) end of the distribution. When a heavy load is applied to the column with recycle, the resolved end may be drawn off first, thereby increasing column efficiency for the more difficult end of the distribution. In this way column length is programmed according to the need of the problem and throughput is optimized.

Flow rate versus resolution at high speed

In GPC as in other forms of liquid chromatography retention time t_r may be described by equation

$$t_r = \frac{V_r}{F} = \frac{V_0 + KV_s}{F} = \frac{KV_s}{F} \left(\frac{1 + K'}{K'} \right) \quad (5)$$

In GPC as discussed earlier K , K' , and V_s are limited. Increased speed demands an increase in flow rate F . Increased flow rate increases peak widths (W). The relationship between F and W is best described in terms of solvent velocity (U) and plate height (H) by the empirical expression¹⁵:

$$H = aU^n$$

At velocities up to 2 cm/sec n values were found to be 0.3 for Styragel^{16,17} and 0.6 for Porasil¹⁵. Elution volume was shown to be invariant with flow velocity up to 2 cm/sec (*cf.* refs. 16–18). Flow rate dependence reported by some workers was seen only when large particles were used¹⁹. The large voids between the particles introduced large distances to be traversed by macromolecules, introducing non-equilibrium. With well packed columns of small uniform spherical particles steric exclusion prevails. Further, equal peak widths for all values of K' show virtually no resistance to mass transfer in the stationary phase³. Consequently increased speed is obtained by increased flow rate provided a moderate increase is made in column length to offset the efficiency loss accompanying the increase in velocity.

Resolution per unit time may therefore be increased by increasing both column length and flow rate simultaneously. This may be accomplished by recycle without increasing column head pressure. Fig. 6 shows the effect of flow rate on resolution at one, two, and three cycles. The resolution obtained in the third cycle at 121 ml/min was superior to that of the first cycle at 14.4 ml/min.

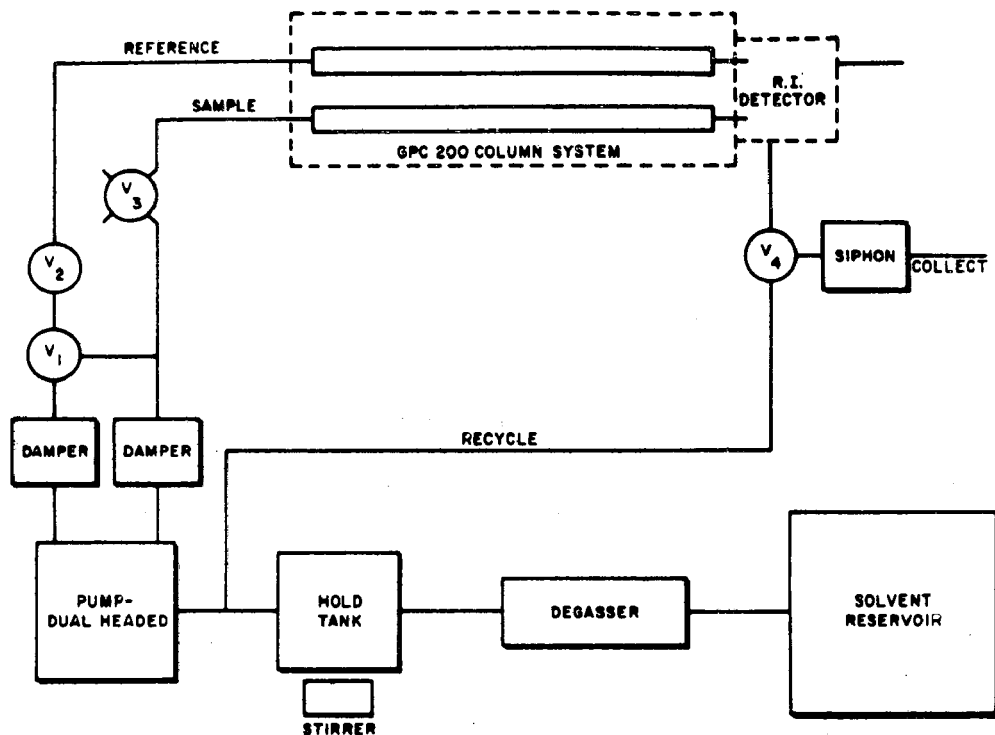


Fig. 7. High flow solvent supply system for GPC.

EQUIPMENT FOR HIGH-SPEED GPC

High-speed GPC requires equipment which affords the high pressures needed to produce high flow velocity as well as elevated column temperature to reduce solvent viscosity and increase diffusion. Two systems are described, *viz.* high-pressure and high-temperature.

High-pressure system

A high-pressure auxiliary pumping system is used with the Waters Associates GPC Model 200. A schematic diagram of the system is shown in Fig. 7. The unitized system may be used externally in place of the original pumping system. The dual-piston system affords pressures up to 1000 p.s.i. at flow rates between 0.4 and 7.0 ml/min as a dual-column system or up to 14 ml/min when flows are combined. The system injection valve is mounted outside the oven for high-pressure operation.

High-temperature system

The second system is a high-temperature oven for use with the Waters Associates GPC/ALC Model 301, which already has the high-pressure capability. The oven, designed to fit into the present column compartment, is temperature controlled to $\pm 0.1^\circ$ over a range of 35° to 200° . The oven accepts columns 2 ft. in length. Our work has shown that two such columns coupled by a short U-tube of 0.009 I.D. affords efficiencies equal to a single 4-ft. length of column.

REFERENCES

- 1 R. SCOTT, *Proc. Intern. Symp. Chromatog.*, Sixth, New York, 1967.
- 2 J. ČOUPEK AND W. HEITZ, *Makromol. Chem.*, **112** (1968) 296.
- 3 L. R. SNYDER, *J. Chromatog. Sci.*, **7** (1969) 352.
- 4 J. C. MOORE, *J. Polymer Sci.*, **A2**, **2** (1964) 835.
- 5 A. J. DE VRIES, M. LE PAGE, R. BEAU AND C. L. GUILLEMIN, *Anal. Chem.*, **39** (1967) 935.
- 6 W. HALLER, *Nature*, **206** (1965) 693.
- 7 W. HEITZ, B. BOMER AND H. ULLNER, *Makromol. Chem.*, **121** (1969) 102.
- 8 K. J. BOMBAUGH, W. A. DARK AND R. F. LEVANGIE, *Separation Sci.*, **3** (1968) 375.
- 9 J. PORATH AND P. FLODIN, *Nature*, **183** (1959) 1657.
- 10 K. J. BOMBAUGH, W. A. DARK AND R. F. LEVANGIE, *J. Chromatog. Sci.*, **7** (1969) 42.
- 11 J. L. WATERS, *J. Polymer Sci.*, **A2**, **8** (1970) 411.
- 12 A. J. P. MARTIN, in V. J. COATES, H. J. NOEBELS AND I. S. FAGERSON (Editors), *Gas Chromatography*, Academic Press, New York, 1958, p. 237.
- 13 J. PORATH AND H. BENNICHI, *Arch. Biochem. Biophys.*, *Suppl.*, **1** (1962) 152.
- 14 K. J. BOMBAUGH AND R. F. LEVANGIE, *Separation Sci.*, **5** (1970) 751.
- 15 J. L. WATERS, J. N. LITTLE AND D. F. HORGAN, *J. Chromatog. Sci.*, **7** (1969) 293.
- 16 K. J. BOMBAUGH AND R. F. LEVANGIE, *Anal. Chem.*, **41** (1969) 1357.
- 17 J. N. LITTLE, J. L. WATERS, K. J. BOMBAUGH AND W. J. PAUPLIS, *Separation Sci.*, **5** (1970) 765.
- 18 J. N. LITTLE, J. L. WATERS, K. J. BOMBAUGH AND W. J. PAUPLIS, *J. Polymer Sci.*, **A2**, **7** (1969) 1775.
- 19 J. N. LITTLE AND W. J. PAUPLIS, *Separation Sci.*, **7** (1969) 513.

CHROM. 4966

SYNTHESES AND PROPERTIES OF GEL CHROMATOGRAPHY MATERIALS

WALTER HEITZ

Organisch-Chemisches Institut der Universität Mainz (G.F.R.)

(Received August 11th, 1970)

SUMMARY

The effect of the mode of synthesis on the characteristics of cross-linked polymers is examined for cross-linked copolymers of ethylvinylbenzene-divinylbenzene and vinyl acetate-divinyl adipate. For homogeneously cross-linked gels the amount of cross-linking agent determines the "pore size" of these gels in the swollen state. Decreasing the amount of the divinyl component results in gels with an increase in the excluded molecular weight. The mechanical stability sets the experimental limit of their usage, so this type of gel is mostly suited for the separation of oligomers; polymers, however, may be separated by use of heterogeneously cross-linked gels. The latter type of gel is prepared by using high amounts of cross-linking agent and polymerising in the presence of an inert compound. It is demonstrated that in case of a heterogeneously cross-linking polymerisation the heterogeneity of the copolymers increases while at the same time the solvating ability of the inert component decreases; this leads simultaneously to an increase in the excluded molecular weight.

A decrease in the quality of the solvent using a non-polar non-solvent may result in gels having a dense shell. Gels with such balloon-like structures separate over a narrow range of molecular weights. As to be expected by theory, substances which are totally excluded ($V_e = V_0$) and substances which can easily penetrate these gels give sharp peaks, whereas substances in the separation range give broad peaks.

INTRODUCTION

Gel chromatography is a method, whereby the separation of a mixture takes place due to differences in molecular weight. Like any other chromatographic procedure gel chromatography may be defined as a method where a mixture of substances suspended in a mobile phase passes over a stationary phase and an exchange of matter is effected. In gel chromatography the stationary phase is a porous material. The pore size and particle size distribution must match any function of molecular size.

The aim of this paper is to elucidate some points which are important for the optimal construction of these polymer networks. On eluting a mixture of substances on a column filled with swollen gel particles the first substances to appear in the eluate are those substances having molecular sizes which prevent them entering into the gel.

They are eluted in a volume of eluate, corresponding to the volume between the gel particles which we will call V_0 . With decreasing molecular weight the accessible volume increases, that is, the substances are eluted in the sequence of their decreasing molecular weight. Neglecting specific interactions with the gel for the moment, the last substance will appear at the end of the column after an additional volume V_i , corresponding to the volume of the solvent in the gel particles, has passed through the column. If we plot the logarithm of the molecular weight against elution volume we get, over a fairly large range, a linear relationship within the given limits V_0 and $V_0 + V_i$. The gels may be characterised by their excluded molecular weight which is obtained by definition when extrapolating this straight line to V_0 .

The separation efficiency obtainable in gel chromatography is greatly restricted by the limited volume in which the separation occurs. For example the peak at V_0 corresponds to the air peak in gas chromatography. The total volume of the column V_t may be divided into three parts. V_0 which, if we assume a statistical arrangement of spheres, is equal to $0.35 V_t$, V_i and V_p the volume of the polymer network. V_p is found experimentally to be in the range of 0.1 to 0.3 V_t , that is, in a column of 100 ml total volume the separation occurs in 35 to 55 ml. And without any experimental work we can say that the smaller V_p is, the better the separation would be. That is, gels which can be highly swelled should be used; then not very much cross-linked copolymer is needed for packing the column. However, we have another experimental requirement: the gels must be mechanically stable. As the mechanical stability decreases with increasing pore volume within the gel we have to find the optimal conditions by experiment.

PRINCIPLES OF PREPARATION

It is a common practice to use the gels as spherical particles as they are obtained in this form by suspension polymerisation. In principle there are three ways of obtaining gels which fit gel chromatography requirements. The first possibility is to cross-link a linear polymer. The first gel to be used for a separation according to molecular size was of this type¹. It was a cross-linked dextran now available under the trade mark Sephadex. These gels are prepared by cross-linking dextran with epichlorohydrin. The pore size of these gels is controlled by the concentration and the molecular weight of the linear polymer and the amount of cross-linking agent. This type of preparation has the disadvantage that gels with high excluded molecular weights swell to extreme limits.

The second mode of synthesis consists in starting with the pure monomers. Copolymerising a monovinyl compound with a certain amount of cross-linking agent results in a cross-linked copolymer where only the amount of cross-linking agent determines the mesh size of the network. This is only true if the polymerisation is performed in absence of solvent. In the dry state these copolymers have no porosity. On swelling these cross-linked copolymers, the single polymer chains become solvated and form a loose statistical network, the porosity is only present in the swollen state and is called the swelling porosity. The mean working range of these gels corresponds, within an order of magnitude, to the mean mesh size of the network as calculated from the amount of cross-linking agent. Thus we may conclude that these gels are — in a statistical sense, of course — homogeneously cross-linked. This statement is

questionable, but some results which might bring us to better criteria will be discussed later.

With decreasing amount of cross-linking agent the excluded molecular weight rises. Nevertheless these gels can only be used for the separation of oligomers; as already pointed out with a decreasing amount of cross-linking agent the swelling is greater and they do not have good mechanical stability. Similar problems existed in the preparation of ion exchangers accessible to large ions. This problem was solved by the process of heterogeneous cross-linking polymerisation. The first patent dealing with ion exchangers of this type came from CORTE in 1957². MOORE first published results of the successful use of this type of copolymer in 1964³ in gel chromatography. The basic principle of this method is the polymerisation of a monomer mixture which could be cross-linked in presence of an inert and soluble compound. This inert compound should have the following qualities: it must be soluble in the monomer mixture and should not be chemically bound to the network during polymerisation. After the polymerisation it should be easily removable from the polymer.

As suspension polymerisation is the main mode of synthesis the inert compound may not be miscible with water. Many organic liquids fulfill these conditions, acting as a solvent or non-solvent for the polymer being produced. Even the use of polymers has been described⁴.

When polymerising a mixture of a monovinyl and a divinyl compound the growing polymer has only a limited swelling capacity. So a phase separation must occur assuming that the system is in a thermodynamic equilibrium. It is obvious that this phase separation is the more pronounced the higher the amount of cross-linking agent and the lower the solvating power of the solvent.

In the extreme case we have a process like a precipitation polymerisation in each polymerising droplet and the microgel particles which are formed within these droplets at an early stage of the polymerisation gradually grow together.

After removing the inert compound, *e.g.* by steam distillation, we get a cross-linked polymer which is in most cases porous even in the dry state. This porosity will be called permanent porosity, but besides this permanent porosity these copolymers have a swelling porosity. Because of the heterogeneous structure of these copolymers we will call this method heterogeneous cross-linking polymerisation. The main factors governing the heterogeneity are the amount of cross-linking agent as well as the kind and amount of the inert compound. The heterogeneity of these cross-linked copolymers may be easily seen under a normal microscope⁵ and with an electron microscope⁶.

Gels prepared in the presence of increasing amounts of inert substance in which they are insoluble show an increasing turbidity when observed by microscopy. The electron microscope allows one to see the pores directly and to measure the pore size distribution. Much more detail is obtained by scanning electron microscopy^{7,8}. Here the steric arrangement of the pores is visualised much more clearly.

Homogeneously cross-linked gels

Fig. 1 shows the elution behaviour of homogeneously cross-linked poly(vinyl acetate) gels with different amounts of divinyl adipate as cross-linking compound. The same substances were tested with all gels in tetrahydrofuran. $\log M$ is plotted against V_e . Over their linear part, the curves always have approximately the same slope, that is, from a given difference in molecular weight the same difference in elution

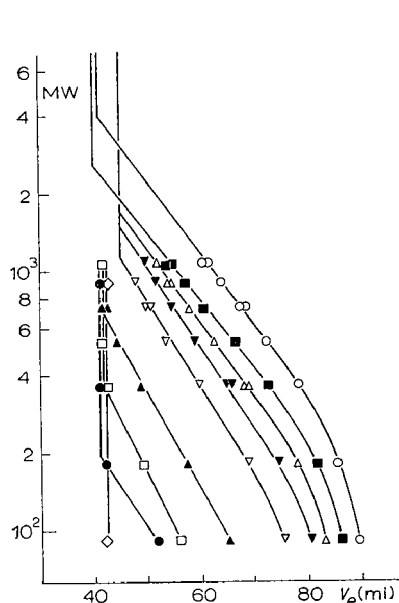


Fig. 1. Elution behaviour of homogenously cross-linked gels in dependence of the amount of cross-linking agent. \circ , 0.5; \blacksquare , 1; \triangle , 2; \blacktriangledown , 3; ∇ , 5; \blacktriangle , 10; \square , 20; \bullet , 30; \diamond , 63.

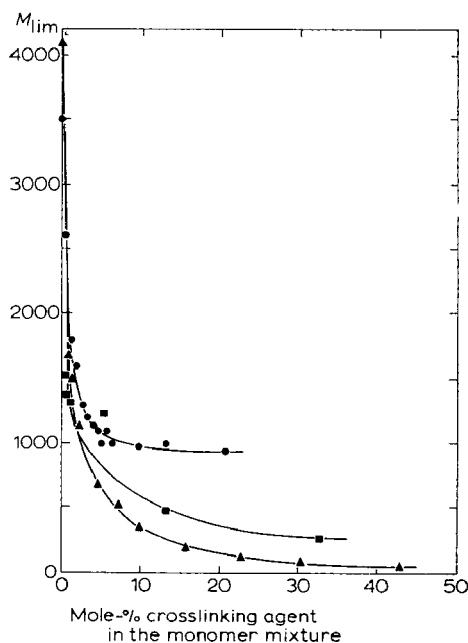


Fig. 2. Excluded molecular weight of homogenously cross-linked gels in dependence of the amount of cross-linking agent. \bullet , vinyl acetate-butenediol divinylether; \triangle , vinyl acetate-divinyl adipate; \blacksquare , methyl methacrylate-ethyleneglycol dimethacrylate.

volume results. With decreasing amount of cross-linking agent the excluded molecular weight gets larger but the mechanical stability decreases due to larger amount of swelling in these gels. The limit of practical use is in the range of 1 % cross-linking agent and the corresponding excluded molecular weight is approximately 3000. With 63 % divinyl adipate the cross-linking density is so high that even toluene cannot enter the pores of this network, toluene is eluted with V_0 . The results of plotting the excluded molecular weight *versus* the amount of cross-linking agent are shown in Fig. 2.

Values for vinyl acetate gels cross-linked with butanedioldivinylether and with divinyl adipate, respectively, as well as methyl methacrylate gels are given. Each kind of gel gives a different curve. Obviously the copolymerisation behaviour of the cross-linking compound has a marked influence. Vinyl ethers have a poor tendency to copolymerise with vinyl acetate, that is, the cross-linking density is not very high even with high amounts of divinyl ether. The porosity of the homogeneously cross-linked gels is effected by the swelling. The specific gel bed volume is a measure of the swelling.

Plotting the excluded molecular weight *versus* the gel bed volume results in an approximately linear relationship. Values for 2 types of polyvinyl acetate gels, polymethyl methacrylate gels and polystyrene gels are on the same curve. The fact that the two types of polyvinyl acetate gels have the same dependence is remarkable but due to their chemical similarity this conclusion is fairly safe.

Using these homogeneously cross-linked gels a number of oligomers could be separated⁹. Only typical examples are given here. Fig. 4 shows a separation of a low molecular weight polystyrene, prepared with butyl lithium. The figures at the peaks

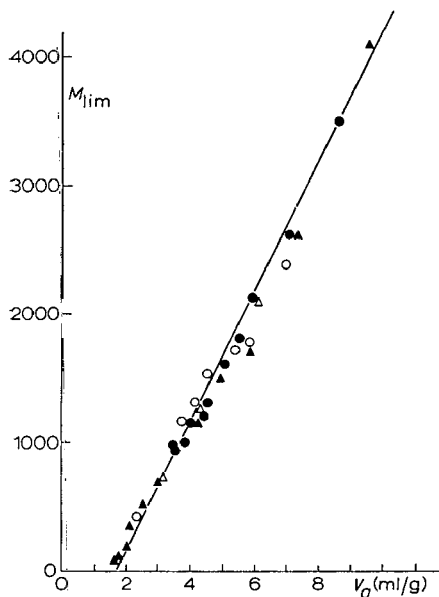


Fig. 3. Excluded molecular weight vs. gel bed volume for homogeneously cross-linked gels. ●, vinyl acetate-butenediol divinyl ether; ▲, vinyl acetate-divinyl adipate; △, methyl methacrylate-ethylene glycol dimethacrylate; ○, styrene-divinylbenzene.

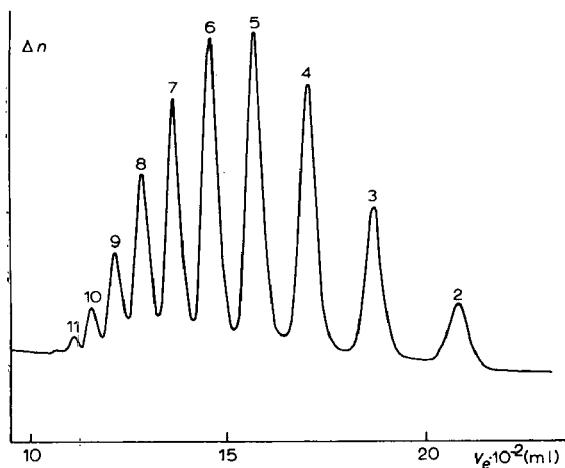
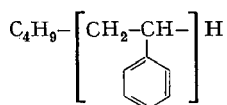


Fig. 4. Gel chromatogram of



($M_n = 580$). Experimental conditions: polystyrene gel cross-linked with 2% divinylbenzene, column: 200 × 5 cm, eluent: tetrahydrofuran.

correspond to the degree of polymerisation. Integration of the peak area gives an \bar{M}_n -value of 580 in good agreement with value of 583 obtained by vapour phase osmometry. Fig. 5 shows a separation of a polyethylene oxide. The lower curve shows the separation of a polyethylene oxide with $\bar{M}_n \approx 600$. Here again the figures at the peaks correspond to the degree of polymerisation. To obtain curve b, polymerisation degrees of 9 and 15 were added together resulting in an enlargement of these peaks. In Fig. 6 the limits of separation can be seen. Although we are well below the excluded molecular weight the high molecular weight end of this distribution is not resolved.

Similar separations can be obtained with tensides (Fig. 7) and epoxides (Fig. 8).

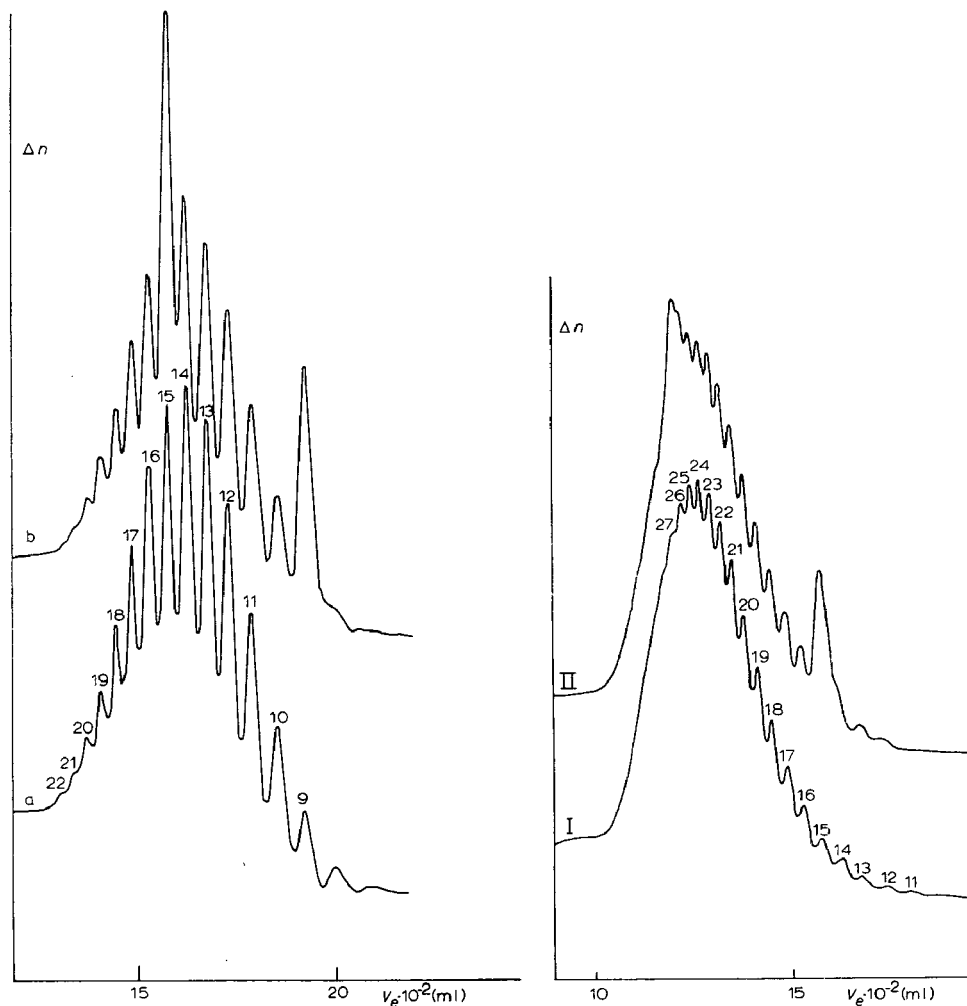


Fig. 5. Gel chromatogram of $\text{HO}(\text{CH}_2\text{CH}_2\text{O})_n\text{H}$. Curve a: $\bar{M}_n \approx 600$; curve b: $\bar{M}_n \approx 600 + n = 9$ and 15.

Fig. 6. Gel chromatogram of $\text{HO}(\text{CH}_2\text{CH}_2\text{O})_n\text{H}$. Curve I: $\bar{M}_n \approx 1000$; curve II: $\bar{M}_n \approx 1000 + n = 15$ and 27.

The separation of the epoxides (Fig. 8) shows that 2 series of oligomers are present, their peaks are differing in size and in alternating sequence.

The examples given show that a separation of the low members of a polymeric

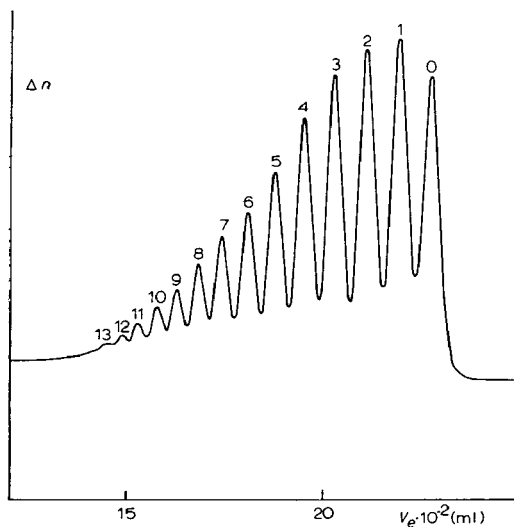


Fig. 7. Gel chromatogram of a tenside $R-O(CH_2CH_2O)_nH$.

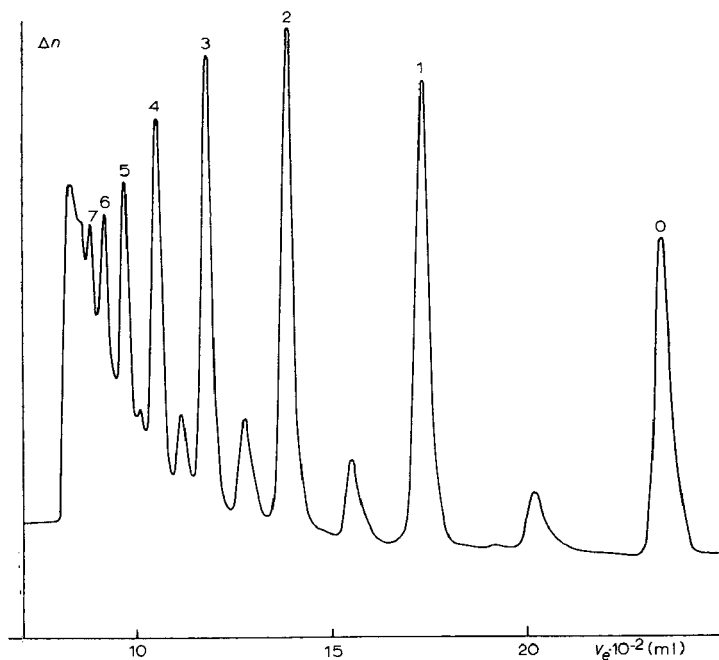
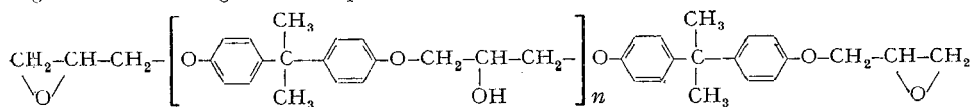


Fig. 8. Gel chromatogram of an epoxide resin



homologous series is possible. However, due to the limited volume there is no way of extending this range very much. An unresolved peak is obtained which consists of a dense sequence of overlapped peaks. Furthermore with homogeneously cross-linked gels the excluded molecular weights attained are too low. The method of heterogeneously cross-linking polymerisation must therefore be used to prepare suitable gels.

Heterogeneously cross-linked gels

The most important factors governing the heterogeneity of the network are the kind and the amount of inert compound as well as the cross-linking density. The copolymerisation of vinyl acetate with divinyl adipate was investigated with butyl acetate as a good solvent and *n*-octane as a non-solvent. Fig. 9 shows the influence of the amount of inert compound on the apparent density. The apparent density is the density of the copolymer plus the air in the pores. Independent of the amount of butyl acetate the apparent density of the copolymers from vinyl acetate and 40 % divinyl adipate is constant although the excluded molecular weight rises sharply between 40 and 50 % butyl acetate. This change in heterogeneity causes no change of the apparent density, that is, they have no permanent porosity. The effect of *n*-octane is completely different. Copolymers prepared in presence of more than 20% *n*-octane show permanent porosity as can be seen from the change in apparent density. The gel chromatographic properties of these gels are discussed later.

The influence of the concentration of the cross-linking compound using a good solvent as the inert compound is shown in Figs. 10 and 11. Between 40 and 50 % divinyl adipate the apparent density changes sharply, but this change amounts to about 10 %, although during polymerisation about 2/3 of the organic phase consisted of butyl acetate, that is, the permanent porosity is only a small fraction of this amount. The uptake of an organic liquid by a cross-linked copolymer is called solvent regain.

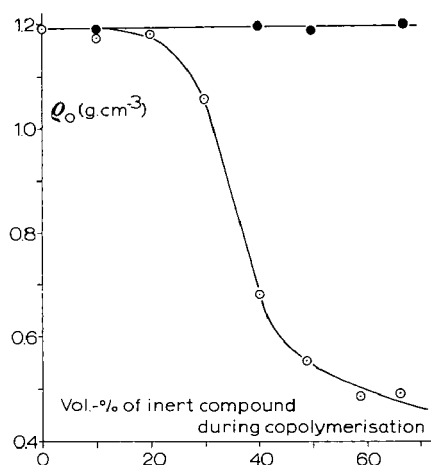


Fig. 9. Apparent density ρ_0 of heterogeneously cross-linked polyvinyl acetate gels ○, *n*-octane, 20 wt.-% divinyl adipate; ●, *n*-butyl acetate, 40 wt.-% divinyl adipate.

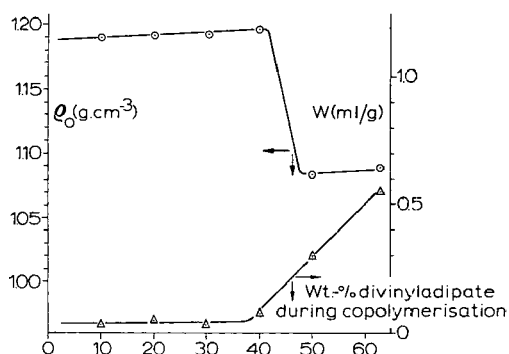


Fig. 10. ○, Apparent density ρ_0 and △, *n*-heptane regain *W* for copolymers of vinyl acetate-divinyl adipate, polymerised in the presence of 67 vol.-% *n*-butyl acetate.

When a polymer with permanent porosity is brought into contact with a non-solvent this can only enter the permanent pores, that is, the solvent regain for the non-solvent also characterises the heterogeneity of a gel structure. The lower curve shows the solvent regain obtained with *n*-heptane. Only if the amount of cross-linking compound is greater than 40% do we get appreciable *n*-heptane regain. But this *n*-heptane regain is higher than expected from the apparent density. This means that even the non-solvent *n*-heptane is able to swell this cross-linked copolymer of vinyl acetate.

The volume swelling was determined by the volume ratio of the gel in the swollen and unswollen state. With increasing amount of divinyl adipate the volume swelling decreases but at about 30% we get a sudden break in this dependence. Assuming a homogeneous distribution of the network density the excluded molecular weight should decrease with increasing amount of cross-linking compound. But this curve shows that the excluded molecular weight increases with increasing amount of cross-linking agent and this clearly shows that heterogeneity increases. Even using a good solvent such as butyl acetate the excluded molecular weight obtainable is only in the range of about 100000. If higher excluded molecular weights are required non-solvents must be used as inert compounds.

Using higher amounts of *n*-octane the gels have permanent porosity, as shown by lower values for the apparent density. The copolymers show permanent porosity if more than 20% *n*-octane is added. But the conclusion that these gels have high excluded molecular weights is rejected by Fig. 12. In both cases curves with maxima are obtained. These maxima agree with the onset of permanent porosity. This maximum is found if a non-polar non-solvent is used as an inert compound. Similar behaviour has been found by MOORE with polystyrene gels³. If the hydrophobic properties of the inert compound are higher than those of the copolymer, the microgel particles which form at an early stage of polymerisation tend to accumulate in the phase boundary. The assumption that these gels have a dense shell is supported by their behaviour in gel chromatography. Fig. 13 shows the behaviour of such a gel

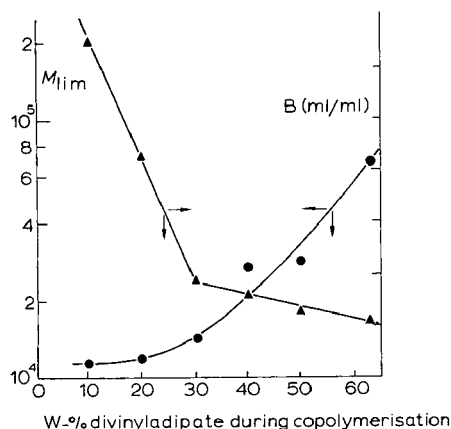


Fig. 11. ●, Excluded molecular weight M_{lim} and ▲, volume swelling B of copolymers of vinyl acetate-divinyl adipate, polymerised in presence of 67 vol.-% *n*-butyl acetate.

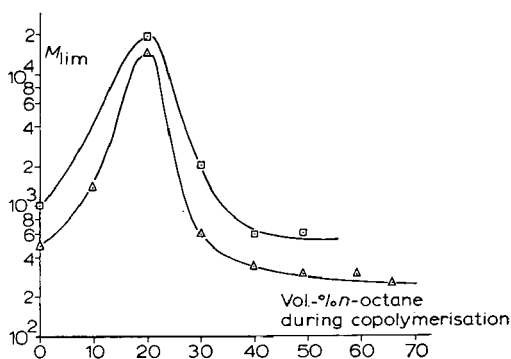


Fig. 12. Excluded molecular weight M_{lim} of copoly(vinyl acetates) prepared in presence of □, 10 and △, 20 wt.-% divinyl adipate.

together with the corresponding peak forms. From the elution volume of a low molecular weight substance one might extrapolate to an excluded molecular weight of $2 \cdot 10^4$. But substances with molecular weights higher than 800 are all eluted with V_0 . The broad and unsymmetrical shape of the curves show that these gels have a kinetically controlled behaviour. Such behaviour is to be expected if the gels have the proposed structure. All gels on the right hand side of the maximum in Fig. 12 show a similar behaviour. Furthermore these gels are brittle and are easily ground to a powder. If polar non-solvents such as *n*-heptanol are used this effect is not observed. In this case excluded molecular weights of 10^7 and higher are obtainable. These gels have a good mechanical stability and separation characteristics for polymers.

Fig. 14 shows a separation in the medium molecular weight range using a column length of 25 cm. Analysis time is less than 1 h. The gel has an excluded molecular weight of 11000. The peaks are symmetrical. This separation was done as a preliminary experiment in order to optimise analysis time.

In accordance with the theory of van Deemter and Giddings a normalised presentation of separation efficiency is obtained if reduced quantities are used¹⁰. Due to the small diffusion coefficient of the polymers the values for the reduced velocity v ($v = vd_p/D$; $h = H/d_p$; h = reduced plate height, v = linear velocity; H/d_p ; H = HETP, d_p = mean particle diameter; D = diffusion coefficient of the solute in the mobile phase) are high. This allows this dependence to be approximately represented by a straight line through the origin ($h \sim d_p$). So we have $H \sim d_p^2$.

If we decrease the particle size by a factor of two we can reduce the column

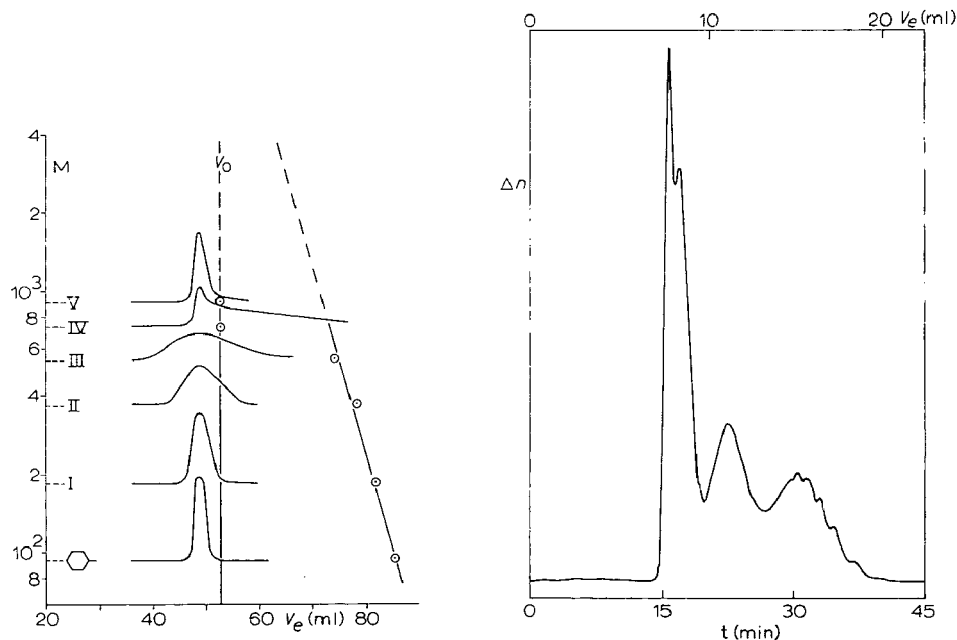


Fig. 13. Elution behaviour of copoly(vinyl acetates) prepared with 40 vol.-% *n*-octane in the organic phase and 10 wt.-% divinyl adipate in the monomer mixture.

Fig. 14. Separation of polystyrenes $\overline{M}_n = 173000; 10300; 2000; 600$. Column length 25 cm.

length by a factor of 4. Using the same linear elution velocity the analysis time is also reduced to 1/4. As the pressure drop $\Delta p \sim l/d_p^2$, l = column length, we get no increase in pressure. These two effects cancel out.

Homogeneously cross-linked gels show a linear dependence between excluded molecular weight and the specific gel bed volume. For heterogeneously cross-linked gels the swelling and therefore the specific gel bed volume is not so characteristic. The relative increase in volume is a more characteristic quantity. This increase in volume can be determined by the ratio of the gel bed volume in the swollen and unswollen state. We will call this quantity volume swelling.

This quantity can never be smaller than 1 and furthermore characteristic behaviour should be expected for the volume swelling if the network density is very homogeneous.

Fig. 15 shows the dependence of $\log M_{lim}$ resulting from volume swelling for poly(vinyl acetate) gels. Curve I represents the homogeneously cross-linked gels; the experimental points are omitted here. The deviation from curve I is a measure of the heterogeneity of the gel structure. A variation in the concentration of the inert compound results in the curves II, III and IV. With increasing amount of inert compound we are approaching area *d*. A variation in the concentration of the cross-linking compound results in the curves V and VI. With increasing amount of cross-linking compound we go onto these curves from the right to the left. The dotted line VII marks the boundary between copolymers with permanent porosity and swelling porosity. Copolymers with permanent porosity are marked by a big circle. The lowest possible value for volume swelling is 1, that is, no values can be found in field *a*, furthermore no values were found in field *b*. If any one succeeds in preparing gels with uniform mesh size of the network they would belong to area *b*. This shows a difficulty

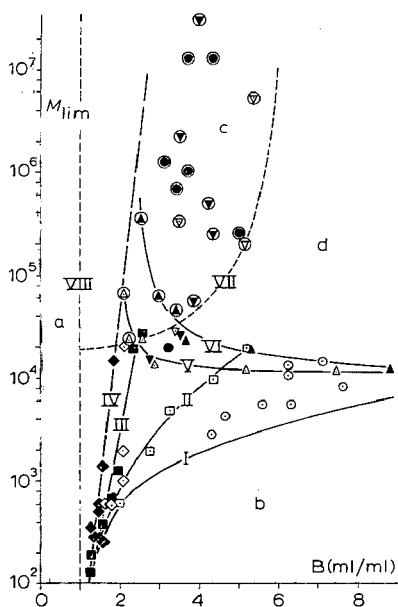


Fig. 15. Excluded molecular weight M_{lim} vs. gel bed volume B for copoly(vinyl acetates). For explanation see text.

necessarily connected with this problem: The gels should have a large swelling capacity if appreciable excluded molecular weights are wanted. In area *d*, limited by curves VI and VII we also found no values. Too large a dilution of the monomer mixture either results in the formation of microgels or we get syneresis; that is the inert compound is expelled with contraction of the gel.

From different points of view it is of interest to investigate gels where the swelling porosity is negligible, that is, gels which occupy the same volume in the swollen and unswollen state. Styrene homogeneously cross-linked with 55 % divinylbenzene has practically no swelling capacity. For this reason the corresponding heterogeneously cross-linked copolymers were investigated. Fig. 16 shows some data obtained with heterogeneously cross-linked polystyrenes using 55 % of divinylbenzene. The monomer mixture was composed of 400 ml mixture of monomers and the amount of inert compound is given as the abscissa. On the left of the double line the values of the homogeneously cross-linked copolymer are given. In all the other cases the ratio of monomer/inert compound was 1:2. The inert compound consisted of amyl alcohol and toluene. Increasing the amount of amyl alcohol means a decrease in the solvent power.

The homogeneously cross-linked gel has an apparent density of 1.16. All copolymers prepared in presence of inert compounds have a low apparent density, but only in this range does the decrease in density agree with the amount of inert compound. As a ratio of monomer to inert compound of 1:2 was used the apparent density should be reduced to 1/3 of the value of the homogeneously cross-linked copolymer if the inert compound is decisive for the pore volume.

The values of the inner surface were determined by the BET-method. The homogeneously cross-linked gel has a surface area lower than 1 m²/g. That is the surface of the compact spheres. With decreasing solvent power the inner surface increases to values higher than 500 m²/g and then it decreases. This behaviour is just as would be expected. With increasing pore size we need less pores for the same volume, that is, the inner surface becomes smaller. The decrease observed when using toluene alone

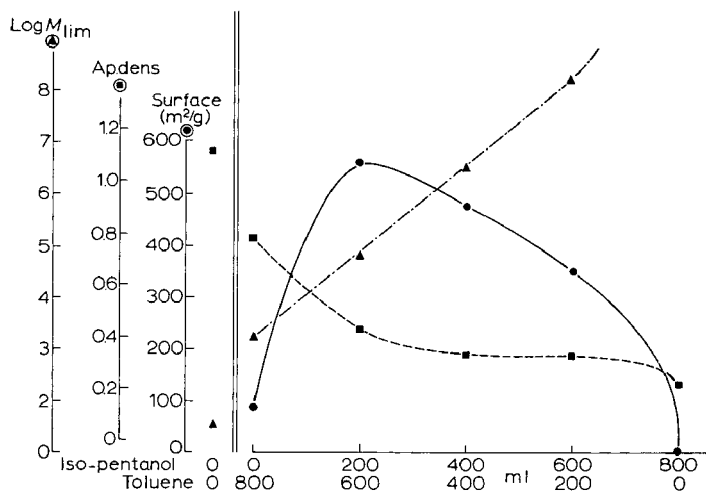


Fig. 16. Properties of heterogeneously cross-linked polystyrenes (55 % divinylbenzene). Each run composed of 400 ml monomer mixture and the amount of inert compound *cf.* abscissa.

is caused by a lower pore volume as the lower apparent density shows. The excluded molecular weight increases with decreasing solvent power to values of 10^6 , 10^8 and finally to a value which cannot be extrapolated.

REFERENCES

- 1 P. FLODIN AND K. GRANATH, *Symposium über Makromoleküle, Wiesbaden, 1959*.
- 2 H. CORTE, *Ger. Pat.*, 1021 166 (1957).
- 3 J. C. MOORE, *J. Polymer Sci.*, A2 (1964) 835.
- 4 J. SEIDL, J. MALINSKÝ, K. DUŠEK AND W. HEITZ, *Adv. Polymer Sci.*, 5 (1967) 113.
- 5 W. HEITZ AND K. L. PLATT, *Makromol. Chem.*, 127 (1969) 113.
- 6 J. R. MILLAR, D. G. SMITH, W. E. MARR AND T. R. E. KRESSMANN, *J. Chem. Soc.*, (1963) 218.
- 7 F. K. AZZOLA AND E. SCHMIDT, *Angew. Makromol. Chem.*, 10 (1970) 203.
- 8 M. DE METS AND A. LAGASSE, *J. Chromatog.*, 47 (1970) 487.
- 9 W. HEITZ, B. BÖMER AND H. ULLNER, *Makromol. Chem.*, 121 (1969) 102.
- 10 W. HEITZ AND J. ČOUPEK, *J. Chromatog.*, 36 (1968) 290.

J. Chromatog., 53 (1970) 37-49

CHROM 4967

PREPARATION OF MONODISPERSE POLYETHYLENE OXIDES BY GEL PERMEATION CHROMATOGRAPHY OF DISCONTINUOUS POLYMER-HOMOLOGOUS SERIES

B. BOMER, W. HEITZ AND W. KERN

Institute of Organic Chemistry, University of Mainz (G.F.R.)

SUMMARY

Starting from triethylene glycol, monodisperse polyethylene oxides of a molecular weight (MW) up to 2000 (degree of polymerisation (DP) ≤ 45) were synthesised in a two-step process.

During the first step the ditosylate of triethylene glycol is reacted with the sodium alkoxide of the same diol at room temperature. The condensation product (polymer homologues of triethylene glycol) was separated by molecular distillation and yielded the pure oligomers nonaethylene glycol (DP = 9, MW = 414) and pentadecaethylene glycol (DP = 15, MW = 678), as proved by gel chromatography.

During the next step the polymer homologues of nonaethylene glycol were synthesised in a similar way. The pure oligomers heptecosa (DP = 27, MW = 1207) and pentatetracontaethylene glycol (DP = 45, MW = 2000) were isolated by preparative gel permeation chromatography on a polystyrene gel cross-linked with 2% divinylbenzene. Using a column, 200 \times 5 cm, samples of up to 5 g could be separated.

The separation of technical polyethylene oxides prepared by polymerisation indicated that up to a DP of approximately 27 adjacent oligomers are still resolved.

INTRODUCTION

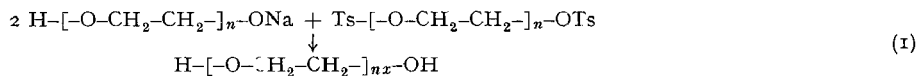
Oligomers have hitherto been prepared mainly either by separation of polymers of low molecular weight with the aid of efficient separation methods or by specific syntheses. In order to prepare monodisperse polyethylene oxides we have combined these two methods and have thus been able to obtain in a few stages absolutely uniform products of relatively high molecular weight.

We have chosen the Williamson ether synthesis for the construction of the polymer chain. This reaction has the advantage that both condensation components (ditosylate and sodium alcoholate) can be prepared from the corresponding diol under conditions where the ether bonds are fully stable. After termination of the condensation the unconverted reactive groups may easily be hydrolysed back to the hydroxyl groups, so that a reaction mixture with only one type of the end group is obtained.

In each stage of the synthesis, the alcoholate of an oligoethylene glycol reacts with the ditosylate of the same oligomer. Because of the influence of the dialcoholate

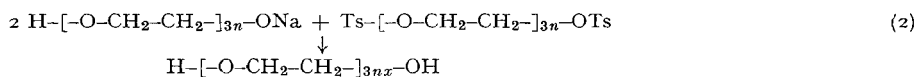
molecules, present in the equilibrium, the polymer homologues of the original oligomer are obtained after hydrolysis of the unreacted tosylate groups.

The synthesis can be written thus:



Ts = tosyl group

$n = 1, 2, 3, 4, 5 \dots$



$n = 1, 2, 3, 4, 5 \dots$

Using gel chromatography, which provides a method of separation according to molecular size, it should be possible to separate completely at least the first members of such a discontinuous polymer homologous series. By using an excess of diol, the main reaction product is the oligomer with a DP three times higher, which can be used as the starting material for the next synthesis stage.

We suggest the name "triplication process" for this type of synthesis.

It is especially important to have high purity triethylene glycol as the starting material. It can be shown by gas chromatography of the bis-(trimethylsilyl) ethers that the triethylene glycol used for the synthesis contains less than 0.1 % each of neighbouring oligomers, di- and tetraethylene glycol.

In the first stage we let sodium alcoholate of triethylene glycol react with the ditosylate of the same compound in an excess of triethylene glycol, in the dark and in a nitrogen atmosphere. After 50 days at room temperature over 90 % of the alcoholate had reacted. The sodium tosylate formed, in aqueous solution, was removed by ion-exchange chromatography and the excess triethylene glycol was distilled off under vacuum.

From the remaining mixture of polymer homologues of triethylene glycol, the oligomers nonaethylene glycol ($n = 9$) and pentadecaethylene glycol ($n = 15$) were isolated by repeated molecular distillations, and can be shown to be pure by gel chromatography. The crude yield of the condensation products was 74 % based on the ditosylate.

In the next triplication step the polymer homologues of nonaethylene glycol were prepared. The oily ditosylate of nonaethylene glycol was purified by column chromatography over silica gel and was obtained in a 72 % yield. The condensation was carried out in toluene and, after 8 days reaction at room temperature, 90 % of the alcoholate had been used. In order to hydrolyse unreacted tosylate groups, water was added and the reaction mixture refluxed. The excess nonaethylene glycol was removed by molecular distillation. The yield of condensation products was 81 % of the theoretical.

The mixture of polymer homologues of nonaethylene glycol, obtained in this way, was separated by gel chromatography on a polystyrene gel cross-linked with 2 % divinyl benzene. Tetrahydrofuran (THF) was used as eluant. The column dimensions were 200×5 cm which corresponds to a total volume of 3.9 l. We have already des-

described a reproducible method for filling a column of these dimensions¹. The average particle diameter of the swollen gel is about $65\ \mu\text{m}$ and a theoretical plate count of 13,500 is obtained for benzene at an elution rate of 200 ml/h.

Fig. 1 shows an analytical gel chromatogram of polymer homologues of nonaethylene glycol. Although the molar ratio of diol to sodium was 2:1, a considerable amount of higher condensation products is formed. These are resolved up to $n = 63$.

Samples of up to 5 g in 50 ml THF could be roughly separated. The fractions thus obtained were then rechromatographed in amounts of 0.5–1 g and thus monodisperse substances were obtained.

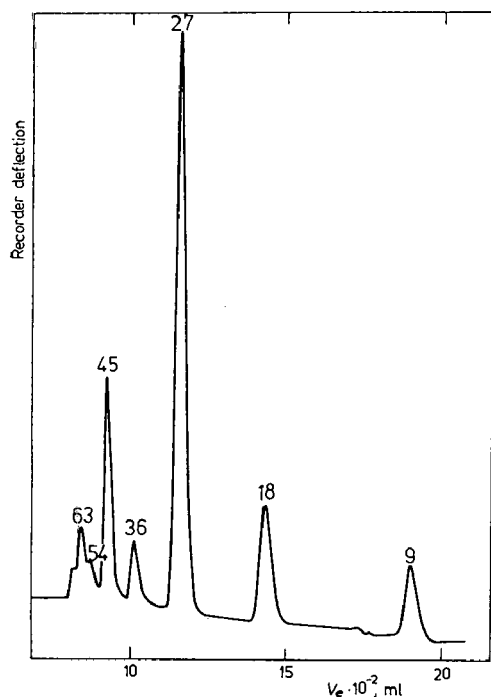


Fig. 1. Analytical gel chromatogram of a discontinuous polymer homologous series of oligoethylene glycols. $\text{HO}-(\text{CH}_2-\text{CH}_2-\text{O})_n-\text{H}$ ($n = 9x$; $x = 1, 2, 3 \dots$). The numbers above the peaks correspond to the degree of polymerisation n .

Since the uniformity of the molecular weight was tested by gel chromatography, it was important to know the resolving efficiency under the separation conditions used. For this purpose we separated commercial polyethylene oxides prepared by polymerisation and forming a continuous polymer homologous series². In this way it was found that the resolving efficiency was adequate up to about $n = 27$ when comparable amounts of the homologues are present.

Alongside the dispersivity test by gel chromatography, molecular weight determinations were also carried out by vapour pressure osmometry. The values obtained agree very well with the formula weights.

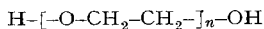
Table I shows a comparison of the melting points of oligoethylene glycols. We determined the melting points in a thermostated vessel, the temperature of which was

raised about 0.2° every 10 min. The melting points of our oligomers lie significantly above the literature values.

From the theoretical considerations of the possibility of the formation of side products and of the ease with which they may be removed, it follows that only the products which are formed by linking an even number of units can include side prod-

TABLE I

MELTING POINTS OF OLIGOETHYLENE GLYCOLS



<i>n</i>	<i>M.p.</i> ($^\circ\text{C}$) <i>our values</i>	<i>M.p.</i> ($^\circ\text{C}$) <i>lit. values</i>
9	29.8–30.0	only b.p.
14	—	29.5
15	38.6–38.8	—
18	32.0–32.4	24 35
27	44.6–44.8	—
30	—	38.6
36	43.0–43.4	—
42	—	33.8
45	49.9–50.1	—
90	—	40.6
186	—	44.1

ucts, formed by elimination or cyclisation in appreciable amounts. In agreement with this the polyethylene oxides with $n = 18$ (2×9) and $n = 36$ (4×9) show relatively lower melting points and broader melting ranges than the absolutely pure substances with $n = 9, 15, 27$ and 45 .

Polyethylene oxides of higher molecular weight are not very soluble in THF. Preparative scale separations of the polymer homologues of heptecosaethylene glycol ($n = 27$) may be carried out on Merckogel OR 20000, a poly(vinyl acetate) gel, with methanol as solvent. We filled two columns each 100×2.4 cm (total volume of each 450 ml) with a quantity of this gel with a narrow particle size distribution, methanol being used as eluant. At an average particle diameter of $24 \mu\text{m}$ in the swollen state we obtained for diethylene glycol a theoretical plate count of 20000 for a 2 m column length at an elution rate of about 40 ml/h. In methanol this gel has a M_{lim} for polyethylene oxides of about 9000. This arrangement allows a good separation of the polymer homologues of nonaethylene glycol up to $\text{DP} = 72$.

The reaction mixture of a preliminary condensation of heptecosaethylene glycol ($n = 27$) was resolved up to $\text{DP} = 135$ (5×27), corresponding to a molecular weight of about 6000.

REFERENCES

1. W. HEITZ AND H. ULLNER, *Makromol. Chem.*, **120** (1968) 58.
2. W. HEITZ, B. BÖMER AND H. ULLNER, *Makromol. Chem.*, **121** (1969) 102.

J. Chromatog., **53** (1970) 51–54

CHROM. 4968

SURFACE AREA AND VOLUME OF PORES AS CHARACTERISTICS OF SILICA SUPPORTS FOR GEL PERMEATION CHROMATOGRAPHY

D. BEREK

Polymer Institute of the SAV, Bratislava 9 (Czechoslovakia),

I. NOVÁK

Institute of Inorganic Chemistry of the SAV, Bratislava 9 (Czechoslovakia)

AND

Z. GRUBISIC-GALLOT AND H. BENOIT

Centre de Recherches sur les Macromolécules, 67 Strasbourg (France)

SUMMARY

A comparison of porous silica gels of different origin was made. It was shown that there is no simple correlation between the mercury porosimetry curve and the corresponding chromatographic data.

The pore surface area was found to be an important parameter reflecting both the size and the shape of the pores. A linear dependence was established between $\log M_{\text{infl}}$ and $\log V/SA$, where M_{infl} is the molecular weight at the inflection point of the chromatographic calibration curve, V is the total pore volume and SA the total pore surface area.

INTRODUCTION

One of the advantages of inorganic support materials for gel permeation chromatography (GPC) is their dimensional stability, resulting in the ability to characterise them by means of porosity data. The quantitative description of the separation (fractionation) ability of the gel in terms of both the shape and dimensions of its pores might permit the preparation of suitable gel mixtures which would be most effective over the given range of the molecular weights for polymer fractionation. Furthermore, such a description might lead to a universal calibration method for gel permeation chromatography, which — provided that the interaction of the solute with the support material is negligible — would include not only the parameters of the dissolved macromolecules, but also the characteristics of the gels. The establishment of a relationship between the size and shape of the gel pores and its fractionation ability may also be interesting from a theoretical point of view.

Several authors¹⁻³ have attempted to correlate the pore volume determined by mercury porosimetry with corresponding chromatographic data. Their results show a good agreement, at least qualitatively, between theory and experiments. However, they have to make assumptions about the shape of the pores, which means that the parameters obtained from simple mercury porosimetry data are not the only ones that

govern chromatographic separation. An important role may also be played by the surface of the pores, even if one assumes that there is no adsorption. In this work, it will be shown by comparing gels from different sources that mercury intrusion porosimetry is not the only method for characterising the separation ability of the columns and that a very simple parameter, the volume over surface area of the pores, can, at least in our case, describe the chromatographic behaviour of the columns.

EXPERIMENTAL

The silica beads studied were either products of Péchiney-Saint-Gobain, distributed under the name Sphérosil, or samples prepared at the Institute of Inorganic Chemistry of the SAV, Bratislava. (The letters A to F refer to the Sphérosil samples, HA and HC to the samples made in Bratislava.) The calibration curves, *i.e.*, the curves obtained by plotting the logarithm of polymer molecular weight (M) as function of elution volume (V_e), were determined on a Waters Model 200 gel permeation chromatograph under the following conditions:

Temperature: $20 \pm 1^\circ\text{C}$

Column: length 120 cm, diameter 3/8 in.

Solvent: tetrahydrofuran

Polymer: Waters' and Pressure Chemical Co. "monodisperse" polystyrene samples and samples prepared and characterised in Strasbourg

Concentration: 2 mg/cc

Injection time: 2 min

Elution rate: 1 cc/min

The total surface area and the pore volume were measured for all the gels, the former being determined from argon adsorption at 77.3 °K by the BET method⁴, the latter by means of either the Carlo Erba mercury intrusion porosimeter Model AG 65 or the differences between mercury and benzene pycnometry data.

RESULTS AND DISCUSSION

The calibration curves of the gels C, HA and HC are shown in Fig. 1. Instead of plotting the classical calibration curves which are difficult to compare due to slight chan-

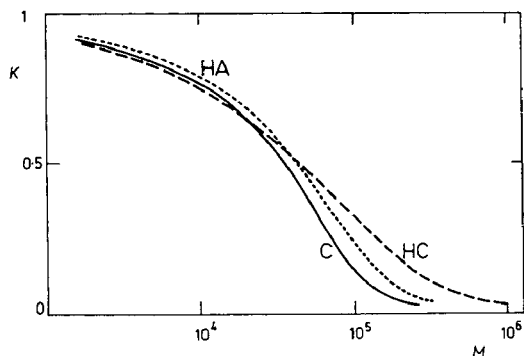


Fig. 1. The calibration curve for gels: Sphérosil C, HA and HC.

ges in total column volumes, the partition coefficients, $K = (V_e - V_0)/(V_i - V_0)$, were plotted as a function of $\log M$. In this expression, V_e is the elution volume of the polymer, V_0 and V_i are respectively the interstitial volume (dead volume) and the total volume of the eluent, *i.e.* the elution volume of benzene. The cumulative pore size distribution obtained from mercury porosimetry is shown in Fig. 2.

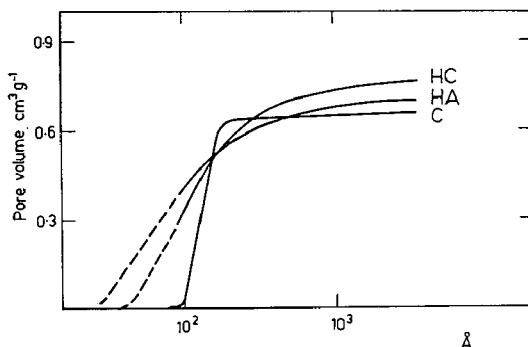


Fig. 2. The porosimetry curves for gels: Sphérosil C, HA and HC.

It is important to note that, despite the similarity of calibration curves for gels HA and C, their porosimetric curves do differ appreciably.

On the other hand, the HA and HC gels, whose partition coefficients behave differently as reflected by the slope of the "linear" part of the calibration curve, possess more similar porosimetric curves. These results show that there is no simple relation between the porosimetric curves and calibration curves. This is not surprising since there is no reason to assume that gels of different origins having the same pore size distribution will also have the same pore shape.

From an experimental point of view, it should also be stated that extremely high pressures (> 1000 atm) are necessary for the determination of the volumes of pores with effective radii less than 75 Å. Due to this difficulty, the total pore volumes for HA and HC gels were calculated from the pycnometric data and the dashed portions of the porosimetric curves in Fig. 2 show the assumed courses. However, this fact does not affect the above-mentioned conclusion.

In addition to the pore size distribution, the surface area, SA , is also an important characteristic of the porous silica beads. The SA reflects the shape and the size of the pores (the bigger the pores, the smaller is the SA and *vice versa*) and is independent of the texture of the porous gel particles (their shape, irregularity etc...). Thus, the silica beads can be evaluated by a single parameter depending only on their pore structure. The pore surface also plays an important role in the presence of specific interaction forces between gel and solute molecules and governs the adsorption effects. The relative simplicity of the surface area determination is a further advantage of using this parameter. Since this factor is closely related to the nature of the gel, it was interesting to see whether or not it would be possible to establish a correlation between surface area and the chromatographic properties of these gels.

The calibration curve, V_e vs. $\log M$, is a direct picture of the fractionation ability of a given gel. If one is interested only in the range of molecular weight in which the

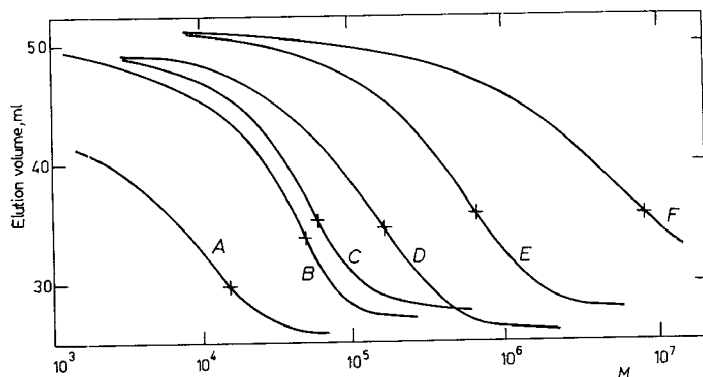


Fig. 3. The calibration curves for the series of Sphérosil gels.

TABLE I

PARAMETERS AT THE INFLECTION POINTS OF THE CALIBRATION CURVES GIVEN IN Fig. 4

Silica beads	Total surface area (m^2g^{-1})	Total pore volume (cm^3g^{-1})	M_{infl}
A	277.8	1.05 ^a	1.5×10^4
B	155.0	1.14 ^a	4.5×10^4
C	88.2	0.67	5.5×10^4
D	31.0	0.60	1.5×10^5
E	17.6	0.70	6.0×10^5
F	3.51	0.50	8.0×10^6
HA	91.2	0.70 ^a	6.1×10^4
HC	76.5	0.79 ^a	9.5×10^4

^a Data calculated from the difference between mercury and benzene pycnometry determinations.

column is efficient, the value of the molecular weight at the inflection point is a very interesting parameter. As shown by our experiments, this parameter is insensitive to different practical aspects of the preparation of the columns (such as the dead volumes, the amount of gel in the column and the method of its filling etc. . .) and to the size and shape of the gel particles. In Fig. 3, the calibration curves V_e vs. $\log M$ are shown for the different Sphérosils. The corresponding inflection points, evaluated by means of auxiliary curves $\Delta V_e / \Delta \log M = f(\log M)$ are marked. Such a determination is not very accurate owing to the shape of the calibration curves and to experimental errors. It can be used as a first approximation only. In order to determine M_{infl} more accurately, an analytical expression describing the calibration curves should be used.

The values of total surface area, total volume of pores and molecular weights at the inflection points of the calibration curves are summarised in Table I. The total volume of the pores (V) for individual gels changes only slightly. On the other hand, there is a good correlation between SA and M_{infl} . More precisely, if one plots $\log SA$ as function of $\log M_{infl}$, the points lie on a straight line, regardless of the method of preparation of the gels. (See Fig. 4.)

The V/SA ratio seems to be a good parameter to describe the chromatographic behaviour of the gel; the straight line in Fig. 5 obeys the following equation:

$$M_{\text{infl}} = 1.61 \times 10^8 \left(\frac{V}{SA} \right)^{5/3}$$

Physically, the ratio V/SA represents an effective pore radius averaged over all the pores of different shapes and sizes. It is evident that the larger this value, the bigger the molecules which can enter into the gel. Since the V/SA ratio has the dimensions of length, it can be related to the diameters of molecules penetrating into the gel.

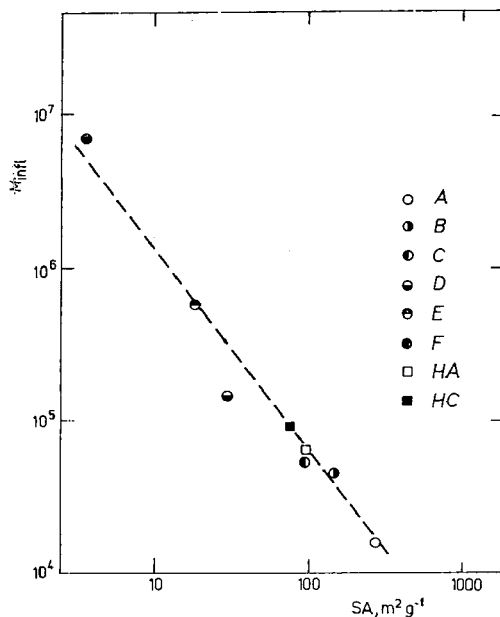


Fig. 4. The dependence of M_{infl} on the total pore surface area.

The corresponding results are to be found in Fig. 6. Values of the hydrodynamic diameters $2R\eta$ of the macromolecules were calculated from the M_{infl} data according to the relation

$$2R\eta = 2 \left[\frac{[\eta]M}{\Phi_0 6^{3/2}} \right]^{1/3}$$

where $[\eta]$ is the limiting viscosity number, M the average molecular weight of polymer and Φ_0 Flory's universal constant. The limiting viscosity numbers were calculated for the M_{infl} values from the relation⁵:

$$[\eta] = 1.41 \times 10^{-2} M^{0.70}$$

From Fig. 6, where the $2R\eta$ values are plotted as a function of V/SA , it can be seen that there is a good correlation between these two quantities. More precisely, $2R\eta$ and V/SA are almost directly proportional and the $2R\eta$ values are numerically close to the values of the "effective pore size".

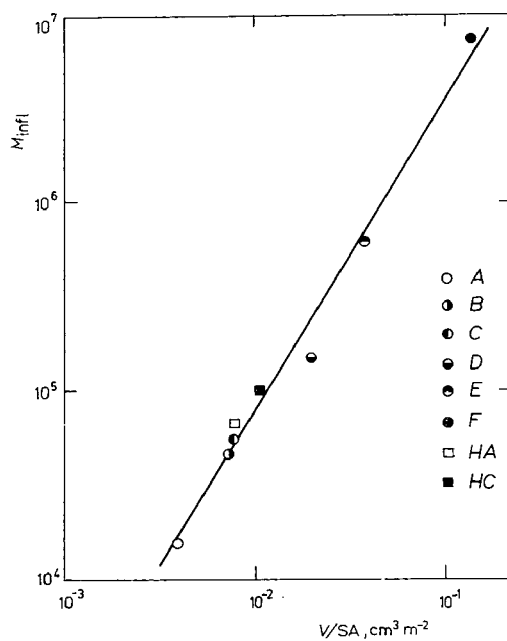


Fig. 5. The dependence of M_{infl} on the ratio: total pore volume (V) over total pore surface area (SA).

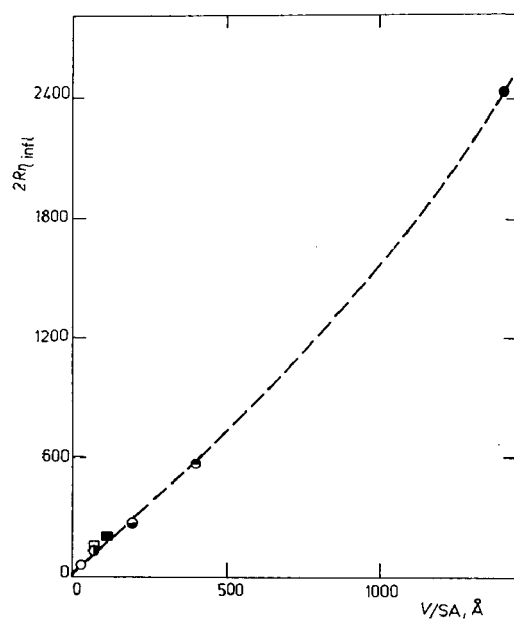


Fig. 6. The dependence of the hydrodynamic coil diameter, $2R_{\text{infl}}$, on the ratio V/SA .

CONCLUSIONS

In this paper we have tried to compare porous silica gels from different sources for their use in gel permeation chromatography. We have shown that there is no simple correlation between the mercury intrusion porosimetry data and the GPC calibration curve. This fact can be explained by differences in the shape of pores and also by the limitation of the mercury porosimeter technique.

Further, we have tried to characterise a given gel by the range of molecular weights in which it is efficient. For this purpose, we have used the molecular weight M_{infl} for which the calibration curve exhibits an inflection point.

It is remarkable that the logarithm of M_{infl} depends linearly on the logarithm of the volume over surface ratio of the pores. If it can be shown that this law, already verified on two different kinds of gel, is general, it would be very helpful in the selection of an appropriate gel for studying a given polymeric material. Some work still in progress is attempting to extend these results and to show that the slope of the inflectional tangent, *i.e.*, the selectivity of the column, can also be related directly to cumulative variation of volume and surface of the pores.

ACKNOWLEDGEMENT

We wish to thank Péchiney-Saint-Gobain for providing us with samples of Sphérosil gels.

REFERENCES

- 1 M. J. R. CANTOW AND J. F. JOHNSON, *J. Polymer Sci., A-1*, 5 (1967) 2835.
- 2 R. BEAU, M. LE PAGE AND A. J. DE VRIES, *Appl. Polymer Symp.*, 8 (1969) 137.
- 3 Z. GRUBISIC-GALLOT AND H. BENOIT, *Intern. Seminar GPC, Monte Carlo, 1969*.
- 4 S. BRUNAUER, P. EMMETT AND E. TELLER, *J. Am. Chem. Soc.*, 60 (1938) 309.
- 5 H. BENOIT, Z. GRUBISIC-GALLOT, P. REMPP, D. DECKER AND J. ZILLIOX, *J. Chim. Phys.*, 63 (1966) 1507.

J. Chromatog., 53 (1970) 55-61

CHROM. 4969

ANWENDUNGEN VON VINYLACETATGELEN

D. RANDAU UND H. BAYER

E. Merck, Darmstadt (B.R.D.)

SUMMARY

Application of vinyl acetate gels

Cross-linked copolymers of vinylacetate have been used for gel chromatographic separations of polystyrenes^{1,2}. In the search for new applications of these gels we have investigated the separations of a number of polar compounds by using different eluents. Resins of conifers, lignins, lipids, tobacco smoke condensate, aldehydes and polyvinylacetate were separated.

EINLEITUNG

Bei allen chromatographischen Hilfsmitteln ist es wichtig, ihre Anwendungsbreite aufzuzeigen. In der Gelchromatographie von organophilen Polymeren haben sich bisher als Träger verschieden hoch vernetzte Polystyrole, aber auch vernetzte Copolymere des Vinylacetats bewährt^{1,2}. Im Unterschied zu den Polystyrolgelen weisen die Vinylacetatgele* in ihrem chemischen Aufbau polare C=O-Gruppierungen auf, und es war daher zu erwarten, dass sich Substanzen mit polaren Gruppierungen an Vinylacetatgelen trennen lassen müssen. Ausserdem sollten auch polar aufgebaute Fliessmittel, wie Methanol oder Essigsäure, geeignet sein. In diesem Sinne wurden die im folgenden beschriebenen Versuche durchgeführt. Die dabei erhaltenen Ergebnisse konnten von uns nur teilweise interpretiert werden; wir halten es aber trotzdem für richtig, sie schon jetzt zur Diskussion zu stellen.

APPARATIVES

Bei den Versuchen wurden Glassäulen von 1 m Länge und 1.4 cm Innendurchmesser verwendet. Die Packung der Säule geschah durch einfaches Sedimentieren der im jeweiligen Laufmittel ausgequollenen Gele. Die Detektion erfolgte differentialrefraktometrisch. Die Substanzgemische wurden mit Hilfe einer Pipette vorsichtig aufgetragen.

ERGEBNISSE UND DISKUSSION

Die natürlichen Harze von Nadelbäumen setzen sich zur Hauptsache aus Harzsäuren der Summenformel $C_{20}H_{30}O_2$ (MG 302.44) zusammen.

* Im Handel erhältlich als Merckogel® OR der Firma E. Merck, Darmstadt, B.R.D.

In Fig. 1 sind die Gelchromatogramme verschiedener Harze wiedergegeben. Man sieht, dass Kiefern- und Fichtenharz sowie Kanadabalsam und Kolophonium eine Komponente mit Molekulargewicht > 500 enthalten, während das Harz der Douglastanne keinen derartigen Anteil enthält. Der Vorteil der Gelchromatographie von derartigen Harzen liegt darin, dass durch schonende Auftrennung die bei Terpenen häufig auftretenden Umlagerungen ausgeschaltet werden.

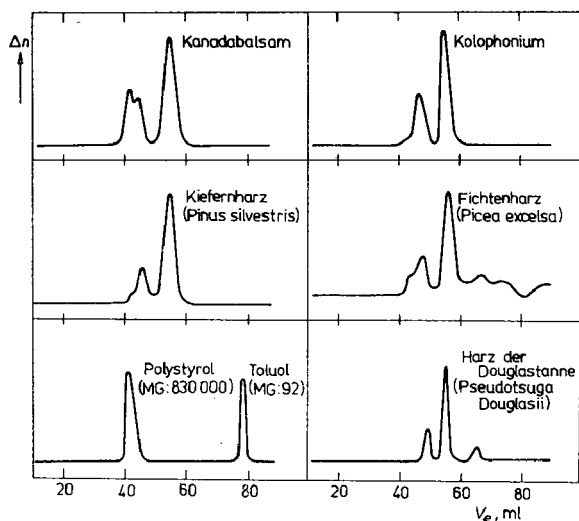


Fig. 1. Trennung von natürlichen Harzen an Merckogel® OR 500. Laufmittel, THF; Säule, 1 m \times 1.4 cm.

Fig. 2 zeigt die Auftrennung eines aus Fichtenholz gewonnenen³ Ligningemisches. Während bei den Harzsäuren Stoffe mit Carboxylfunktion getrennt wurden, sind es hier vornehmlich Stoffe mit phenolischen OH-Gruppen, die sich an einem Vinylacetatgel trennen ließen.

Es war zu erwarten, dass auch Ester an Vinylacetatgelen ein normales gelchromatographisches Verhalten zeigen würden. In dem oberen Teil von Fig. 3 ist als Beispiel eine Trennung von Fettsäureestern zu sehen. Enthalten allerdings die Ester ionische Gruppierungen, wie es bei Lecithinen der Fall ist, so tritt eine beträchtliche

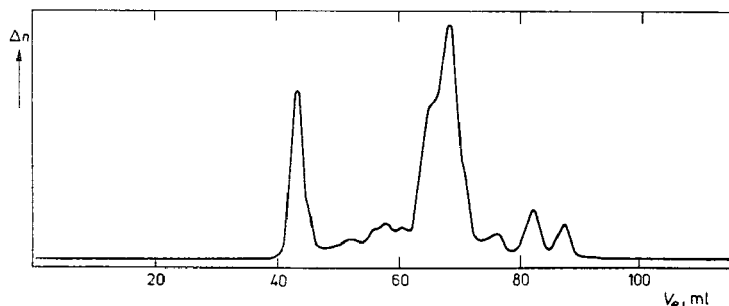


Fig. 2. Trennung von Ligninen an Merckogel® OR 500. Laufmittel, THF; Säule, 1 m \times 1.4 cm.

Verschiebung zu höheren Elutionsvolumina auf, die mit der linearen Beziehung zwischen $\log M$ und V_e nicht mehr in Einklang zu bringen ist.

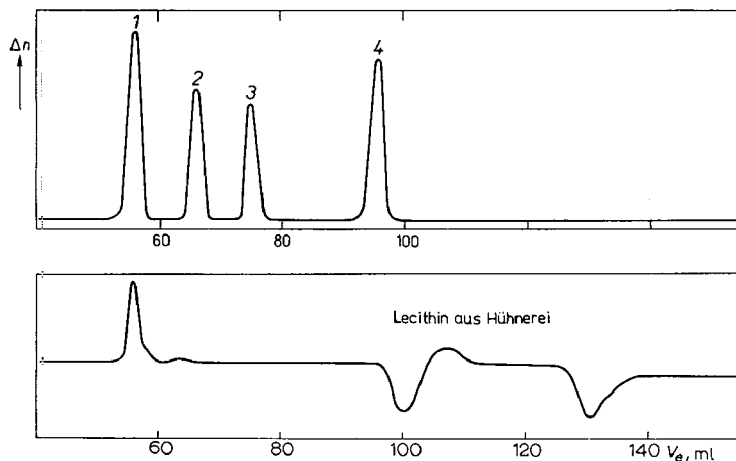


Fig. 3. Trennung von Lipiden an Merckogel® OR 500. 1 = Glycerintripalmitat (MG: 807.4); 2 = Palmitinsäuremethylester (MG: 250.5); 3 = Caprinsäuremethylester (MG: 186.3); 4 = Toluol (MG: 92). Laufmittel, THF; Säule, 1 m × 1.4 cm.

Fig. 4 zeigt die Auftrennung eines Tabakrauchkondensats, aus der ersichtlich ist, dass in dem Gemisch Substanzen bis zum Molekulargewicht 2000 enthalten sind, die gaschromatographisch nicht erfasst werden können.

Bei Paraformaldehyd erwarteten wir Polymere mit Molekulargewichten bis 3000. Mit Eisessig als Laufmittel erhielten wir aber zwei Peaks, die auf Molekulargewichte um 100 hindeuten (Fig. 5). Überraschend war auch die Gelchromatographie des Paraldehyds. Statt eines für das Trimere erwarteten Peaks traten zwei Peaks auf.

Ähnlich ungewöhnlich verlief die Trennung von Polyvinylacetaten mit Methanol als Laufmittel an einem Vinylacetatgel mit dem Ausschlussmolekulargewicht 1000000 (Fig. 6). Mowilith® 30 mit einem nach Viskositätsmessungen ermittelten Molekulargewicht von 61000 wird gelchromatographisch aufgetrennt; Mowilith® 70

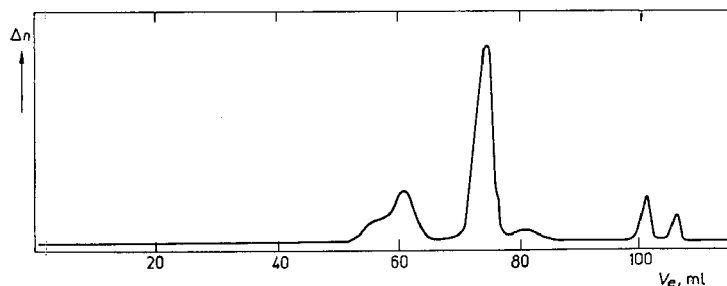


Fig. 4. Auftrennung eines Tabakrauchkondensats an Merckogel® OR 2000. Laufmittel, THF; Säule, 1 m × 1.4 cm.

dagegen, das ein durchschnittliches Molekulargewicht von 690000 haben soll, wird praktisch vollkommen ausgeschlossen.

Die beiden letzten Beispiele, die mit den Laufmitteln Eisessig bzw. Methanol durchgeführt wurden, lassen uns vermuten, dass nicht nur gelchromatographische, sondern auch verteilungschromatographische Vorgänge an Vinylacetatgelen auftreten, sobald das Laufmittel stark polar ist und eine hohe Dielektrizitätskonstante aufweist.

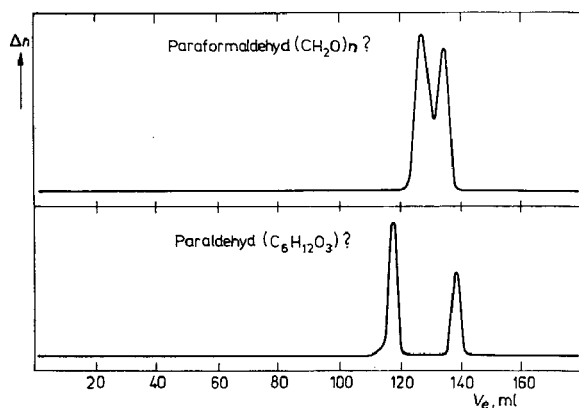


Fig. 5. Trennung von Aldehyden an Merckogel® OR 20000. Laufmittel, Eisessig; Säule, 1 m × 1.4 cm.

In der Flüssigkeitschromatographie kann man einen Trend nach schnellen Trennungen in dünnen Säulen unter hohen Drucken beobachten. In Fig. 7 ist eine in knapp 20 min abgeschlossene Trennung von Polystyrolen an Merckogel® OR 500 ($< 30 \mu$) unter einem Druck von 10 atm in einer 2-mm-dicken Säule gezeigt. Unter Verwendung eines enger klassierten Korngrößenbereichs, Verwendung längerer Säulen und Erhöhung des Drucks dürften sich derartige Trennungen noch verbessern lassen.

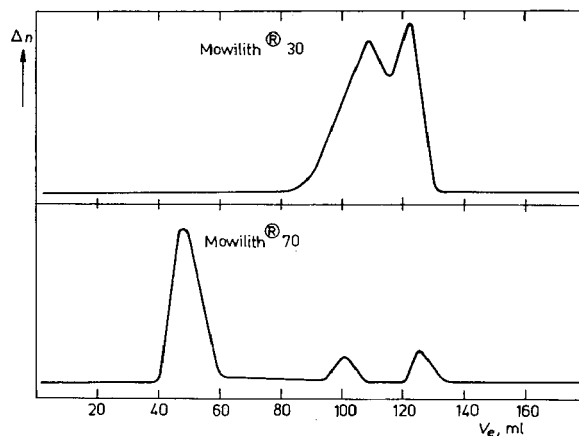


Fig. 6. Trennung von Polyvinylacetaten an Merckogel® Typ OR 1·10⁶. Laufmittel, Methanol; Säule, 1 m × 1.4 cm.

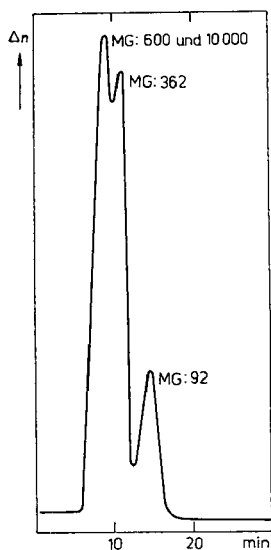


Fig. 7. Trennung von Polystyrolen an Merckogel® OR 500. Laufmittel, THF; Säule, 50 cm × 2 mm; Durchfluss, 5 ml/Std.; Druck, 10 atm.

ZUSAMMENFASSUNG

Vernetzte Copolymere des Vinylacetats haben sich bei der gelchromatographischen Auftrennung von Polystyrolen bewährt. Auf der Suche nach weiteren Anwendungsmöglichkeiten der Vinylacetatgele haben wir unter einfachen Laborbedingungen eine Reihe von polaren Substanzen unter Benutzung verschiedener Laufmittel untersucht. Dabei liessen sich Harze von Nadelbäumen, Lignine, Lipide, Tabakrauchkondensat, Aldehyde und Polyvinylacetate auftrennen. Die bei diesen Trennungen auftretenden Erscheinungen werden diskutiert.

LITERATUR

- 1 W. HEITZ, F. KRAFFCZYK, K. PFITZNER UND D. RANDAU, *Chimia (Aarau), Suppl.*, (1970) 126.
- 2 W. HEITZ, K. KLATYK, F. KRAFFCZYK, K. PFITZNER UND D. RANDAU, *Intern. Seminar GPC, 7th, Monte Carlo, Okt. 1969*, S. 214.
- 3 H. NIMZ, *Chem. Ber.*, 102 (1969) 799.

CHROM. 4970

THE SEPARATION OF THE COLOURED DERIVATIVES OF SOME ORGANIC COMPOUNDS USING LIQUID CHROMATOGRAPHY IN SMALL-BORE COLUMNS PACKED WITH ION-EXCHANGE RESINS

J. CHURÁČEK AND P. JANDERA

Department of Analytical Chemistry, Institute of Chemical Technology, Pardubice (Czechoslovakia)

SUMMARY

A possibility of applying liquid chromatography to the separation of coloured homologous N,N-dimethyl-*p*-aminobenzeneazobenzoyl esters and amides has been studied using apparatus consisting of a pulse-free plunger feeding pump, a narrow bore column, a spectrophotometer with a flow-through measuring cell of our own design, and a recorder. These compounds can be sorbed on sulphonated styrene-divinylbenzene cation-exchange resins with a low degree of cross-linking and separated by elution with hydrochloric acid solutions in aqueous-organic solvents. The influence of the eluent composition, the molecular size of the solute and functional groups upon chromatographic behaviour have been studied. Good resolution can also be achieved by adsorption chromatography on silica columns.

INTRODUCTION

Liquid column chromatography has become an invaluable tool in biochemical research, namely in the analysis of amino acids, proteins, enzymes, hormones, nucleosides, sugars and carboxylic acids. Gel chromatography, closely related to the above method, is now the most convenient technique for the determination of the molecular weight distribution of synthetic and natural polymers. Recently a few fundamental papers have appeared dealing with increasing the speed and efficiency of liquid chromatography¹⁻⁸, which may stimulate its application to the separation of other classes of compounds. We have tried to combine the outstanding properties of N,N-dimethyl-*p*-aminobenzeneazobenzoyl derivatives with the advantages of liquid chromatography.

N,N-dimethyl-*p*-aminobenzeneazobenzoyl esters and amides have proved their outstanding qualities for the separation and identification of aliphatic alcohols, glycols and amines by means of paper and thin-layer chromatography⁹⁻¹². N,N-dimethyl-*p*-aminobenzeneazobenzoyl chloride, which is used for their preparation, is very stable and highly reactive. The preparation is very simple and rapid. Coloured derivatives of phenols, mercaptans and possibly other compounds may also be prepared. Detection of these derivatives is possible without any addition of a colour-developing agent, and has a high sensitivity.

Liquid chromatography of *N,N*-dimethyl-*p*-aminobenzeneazobenzoyl derivatives would have some special advantages: a wide range of organic compounds can react with this single reagent forming coloured products differing in polarities (basicities), which makes it possible, in principle, for both ion-exchange and adsorption chromatographic separations to be carried out in conjunction with continuous spectrophotometric effluent monitoring which would yield a record of the elution pattern. In addition to its better accuracy in comparison with paper and thin-layer chromatography, this method is easy to automate. An apparatus for the column liquid chromatography of microgram quantities of these coloured compounds was designed using available laboratory instruments, in order to investigate the liquid chromatography of these derivatives.

MATERIALS AND METHODS

Liquid chromatography system

Straight glass columns of narrow bore (0.8–3 mm in diameter, 10–100 cm long, jacketed) are used. Their lower end is fixed into a polyethylene tube reduced to capillary size (0.5 mm I.D.) connecting the column to a flow-through detector measuring

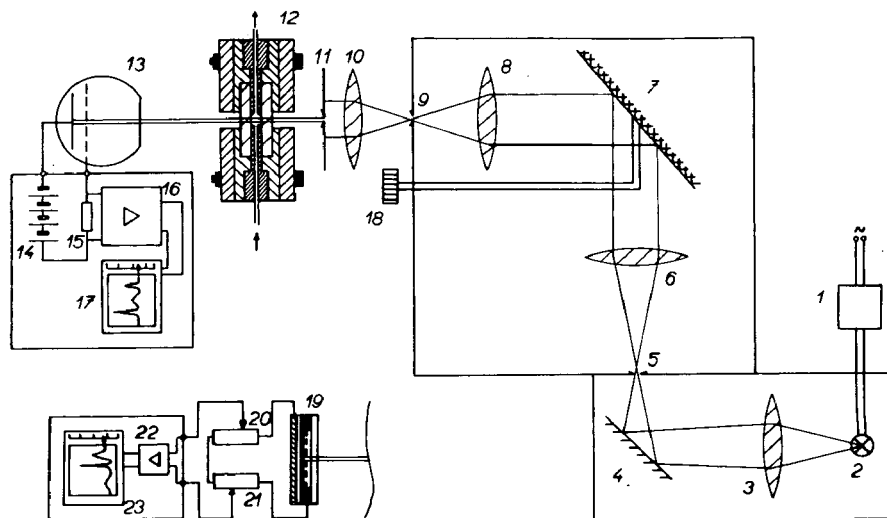


Fig. 1. Diagram of the photometric detector. A spectrophotometer Spekol (Zeiss, Jena) serves as a monochromatic light source. Light from a lamp (2) with a stabilised direct current power supply (1) is focused by the optical system (3), (4) on the monochromator entrance slit (5). A narrow monochromatic beam of light is selected by a slit (9) from spectrum reflected by a dispersion grating (7) and enters an adaptor of our own design screwed on to the Spekol housing. A lens (10) and a screen (11) of the objective fixed in the adaptor cap direct the light beam into the centre of a flow-through cell (12) which is fixed on the adaptor cover and can be removed with it from the duralumin adaptor cap. The light emerging from the cell falls on a photoelectric element connected to the adaptor cap. A gas filled phototube (13) can be used in conjunction with a compensation recorder G1B1 (Zeiss, Jena) (17) having its own phototube potential source (14) and amplifier (16). A selenium cell (19) can also be used, its potential being recorded (23) after sensitivity reduction by resistors. (20), (21) and amplification (22) by an EZ 3 or EZ 4 recorder (Laboratory Instruments, Prague). The wavelength required can be adjusted by a micrometric screw (18) controlling the dispersion grating position.

ing cell. The eluent is delivered at a constant, reproducible flow rate by a pulse-free pump (Linear proportioner, ZSNP, Žiar n. Hronom) with a constant speed motor driving a plunger by means of an adjustable gear system. The plunger pushes the eluting liquid out from a precision graduated glass syringe (10 or 20 ml capacity) through a polyethylene capillary (1 mm I.D.) connected to the upper end of the column.

A photometric detector to give continuous effluent stream monitoring was designed. A single-beam spectrophotometer Spekol (Zeiss, Jena) is used to provide a monochromatic light source. A narrow monochromatic beam of light selected by a slit from the spectrum reflected by a dispersion grating is focussed into the centre of a flow-through cell of our own design, placed in an adaptor screwed on to the Spekol housing. The light emerging from the cell falls on the photoelectric element. A gas filled phototube can be used in conjunction with a compensation recorder G1 B1 (Zeiss, Jena) having its own phototube potential source and amplifier. A selenium cell potential recording by an EZ 3 or EZ 4 recorder (Laboratory Instruments, Prague) has also given satisfactory results.

The flow-through measuring microcell is made out of a small teflon cylinder which has been bored through the centre. The channel forming the optical path is sealed at both ends perpendicularly to the optical path by glass windows (2 mm thick). Liquid enters the channel from a teflon capillary (0.5 mm I.D.), at the bottom end and flows through the channel, leaving it at the other end to flow out through another teflon capillary. The cell is placed between two metal sheets and screwed tight by means of four bolts. Plastic gaskets bored in the centre are inserted between the teflon cylinder and the glass windows making the cell leak tight. Two bored rubber pieces inserted between the metal sheets and the windows protect the windows from cracking.

The cell is resistant to corrosive agents (only teflon and glass come in contact with liquid) and easy to take apart and clean.

The cell has been designed in two sizes for measuring at different sensitivities — one 20 μ l volume (with feeding capillary), 1.5 mm optical path length, 2 mm I.D., the other 35 μ l volume, 10 mm path length and 1 mm I.D.

The base-line shift during an 8 h run did not exceed 1.5 %, the recorder scale corresponding to the full absorbance value range. A tenfold absorbance scale expansion is possible (in the range from 450 to 550 nm).

The linear relationship between the peak areas evaluated as peak widths at their half peak heights multiplied by the corresponding absorbance values and the amount of coloured compound was determined experimentally for both inert and retarded components (Ponceau 6R and *n*-amyl ester of *N,N*-dimethyl-*p*-aminobenzeneazo-benzoic acid) on a Dowex 50W-X2 column. The random error of peak area measurement was about 3–5 % rel. An increase in the eluent flow rate causes a slight increase in the peak areas, whereas the response (peak height) falls off exponentially.

Separations by liquid chromatography

A strongly acidic sulphonated styrene-divinylbenzene cation-exchange resin, Dowex 50W-X2 (H⁺ form) was used for the separation of the coloured derivatives. Their protonised forms are distributed between the external solution (eluent) and the solution in the resin particles in accordance with the basicities of the non-ionic forms.

The equilibrium depends on the H^+ ion activity in the external solution and in the resin particles.

Because of the negligible solubility of these compounds in aqueous-acid solutions, it is necessary to employ mixed aqueous-organic media. The amount of the organic solvent present obviously affects the distribution equilibrium by its solubility and solvation effects, and also by the dielectric constant effect.

Cation-exchange resin with a low degree of cross linking (X2) was used in the separation in order to improve the accessibility of the ion-exchange phase to the rather large molecules of the derivatives and to accelerate the diffusion rate in the resin.

The quantitative sorption of coloured esters and amides on Dowex 50W-X2 (H^+ form), 200–400 mesh, from mixed aqueous-organic solutions (80 % ethanol; 80 % methanol) has been established. Sorbed compounds can be eluted by aqueous-ethanolic or aqueous-methanolic solutions of hydrochloric acid. The effect of the eluent composition on the chromatographic behaviour of some homologous esters and amides has been studied, and the volume distribution coefficients D_v have been determined by the dynamic method¹³. Both homologous esters and amides are eluted in order of increasing basicities; *i.e.*, in order of decreasing molecular weights. Amides with a higher basicity have a higher distribution coefficient than esters, whose basicity is lower. Secondary amides are sorbed more strongly than the less basic primary ones, their elution curves showing greater broadening than those of the esters.

The contribution of the CH_2 -group to the logarithm of the distribution coefficient has proved to be about the same for the homologous esters of aliphatic alcohols and primary aliphatic amides. It increases to some extent with decreasing hydrocarbon chain length. Secondary amides have shown greater changes corresponding to the same molecular weight contribution. D_v values of iso-derivatives are slightly lower compared with the normal ones. Multiple bond contribution to D_v values does not seem to be significant (Table I).

The hydrochloric acid concentration in the eluent influences the equilibrium

TABLE I

VOLUME DISTRIBUTION COEFFICIENTS D_v OF SOME DERIVATIVES OF N,N-DIMETHYL-*p*-AMINO-BENZENEAZOBENZOIC ACID ON CATION EXCHANGER DOWEX 50W-X2 IN 0.925 *M* HYDROCHLORIC ACID SOLUTION IN 80.5 % ETHANOL

D_v has been defined as a ratio of the amount of compound in a unit volume of the ion-exchanger phase to the same volume of external solution.

<i>Derivative</i>	D_v	<i>Derivative</i>	D_v
Methyl ester	6.3	Methyl amide	8.6
Ethyl ester	5.2	Ethyl amide	7.4
<i>n</i> -Propyl ester	4.5	<i>n</i> -Propyl amide	6.5
<i>n</i> -Butyl ester	3.9	<i>n</i> -Butyl amide	5.6
<i>n</i> -Amyl ester	3.5	<i>n</i> -Hexyl amide	4.7
<i>n</i> -Hexyl ester	3.0	Allyl amide	6.4
<i>n</i> -Octyl ester	2.3	Dimethyl amide	9.9
<i>n</i> -Nonyl ester	2.1	Diethyl amide	6.6
<i>n</i> -Decyl ester	1.9	Di-(<i>n</i> -propyl) amide	4.7
Isopropyl ester	4.3	Di-(<i>n</i> -butyl) amide	3.5
Isobutyl ester	3.6		

between the protonised and non-ionic form of these compounds. A higher concentration decreases the volume distribution coefficients of the compounds under study and the corresponding retention volumes (and also their differences). This effect becomes more significant at lower hydrochloric acid concentrations (Fig. 2).

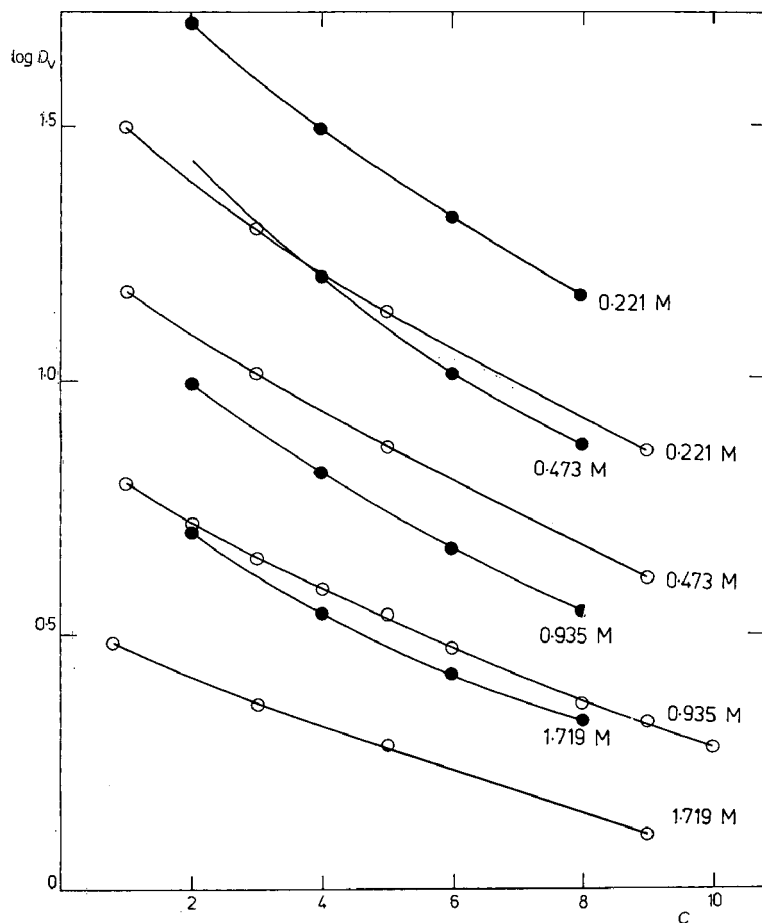


Fig. 2. The effect of the hydrochloric acid concentration in the eluent. Volume distribution coefficients D_v for esters and amides are plotted *versus* the number C of carbon atoms in a primary aliphatic alcohol or secondary amine molecule. Ethanol concentration in eluent, 80.5 % by weight. ○, Esters of homologous primary aliphatic n -alcohols. ●, Amides of homologous secondary aliphatic n -amines.

Ethanol or methanol concentration has a similar influence (Fig. 3). In solutions with an alcohol concentration ≤ 50 % these derivatives are sorbed too strongly by the ion-exchanger, with only small differences in D_v values. A higher concentration enhances solubility in the external solution, especially that of the higher homologous esters and amides. The distribution coefficients decrease and their differences increase. The external alcoholic solutions have an optimum composition at about 80–90 wt. %. The differences in the distribution coefficients of homologous derivatives reach a

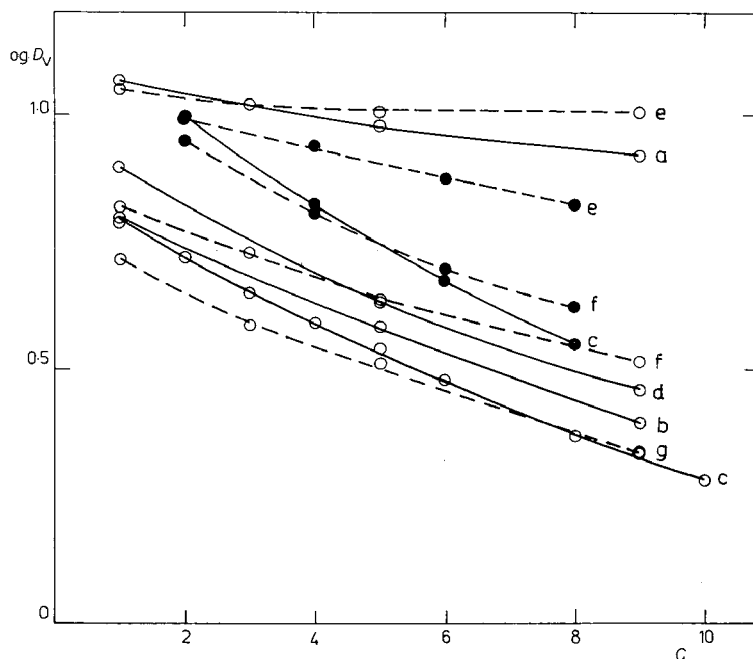


Fig. 3. The effect of the alcohol concentration in eluent. Solid lines — ethanol; broken lines — methanol. Hydrochloric acid concentration in eluent — 0.935 *M*. Other symbols have the same meaning as in Fig. 2. Ethanol concentration: (a) 47.0% by weight; (b) 63.1%; (c) 80.5%; (d) 91.0%; methanol concentration: (e) 58.5% by weight; (f) 74.9%; (g) 88.0%.

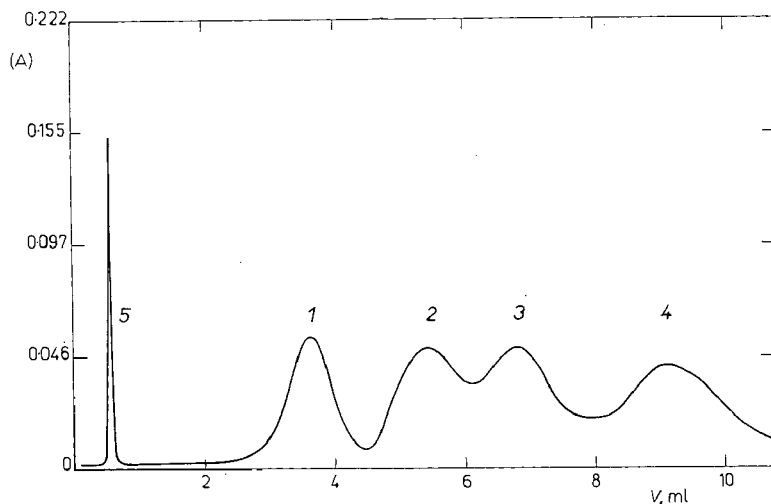


Fig. 4. Chromatographic separation of some primary aliphatic esters of *N,N*-dimethyl-*p*-amino-benzeneazobenzoic acid. (A) absorbance. Column 240 × 2.7 mm, Dowex 50W-X2 (200-400 mesh) H^+ form. Sample volume 20 μ l. Eluent — 0.925 *M* HCl in 80.5% ethanol. Flow rate 0.016 ml/min, 10 mm optical path length cell, $\lambda = 510$ nm. (1) 0.5 μ g of *n*-nonyl ester; (2) 0.5 μ g of *n*-amyl ester; (3) 0.5 μ g of *n*-propyl ester; (4) 0.5 μ g of methyl ester; (5) inert compound (Ponceau 6R).

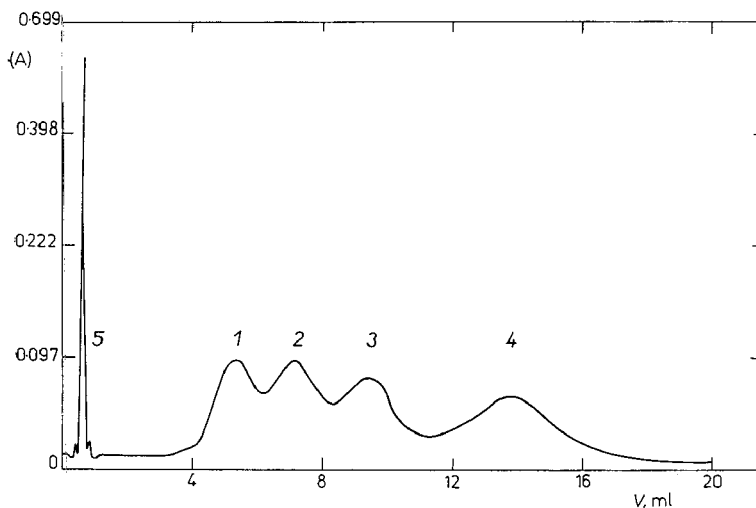


Fig. 5. Chromatographic separation of some secondary aliphatic amides of *N,N*-dimethyl-*p*-amino-benzeneazobenzoic acid. (A) absorbance. Flow rate 0.032 ml/min; sample volume = 60 μ l, other conditions as in ester separation. (1) 1.5 μ g of di-(*n*-butyl) amide; (2) 1.5 μ g of di-(*n*-propyl) amide; (3) 1.5 μ g of diethyl amide; (4) 1.5 μ g of dimethyl amide; (5) inert compound (Ponceau 6R).

maximum in these solutions whereas the D_v values are minimal; solvation and dielectric properties controlled by the alcohol ratio in both phases are obviously most advantageous for chromatographic separation.

In these experiments the hydrochloric acid concentration was kept constant at 0.925 *M*.

An example of the separation of esters of lower aliphatic alcohols on a Dowex 50W-X2 column by elution with aqueous-ethanolic hydrochloric acid solution is shown in Fig. 4; Fig. 5 illustrates the chromatographic separation of some lower secondary amides under similar conditions.

Further improvement of separation efficiency and time can be expected from elution with a hydrochloric acid gradient, which is the subject of our investigations now.

Good resolution of coloured derivatives was also achieved by adsorption chromatography on Silica CH (5–40 μ m) columns. Some homologous amides and esters can be resolved by elution with cyclohexane-ethyl acetate mixtures in the order of increasing polarities.

REFERENCES

- 1 T. W. SMUTS, F. A. NIEKERK AND V. PRETORIUS, *J. Gas. Chromatog.*, 5 (1967), 190.
- 2 C. G. HORVATH, B. A. PREISS AND S. R. LIPSKY, *Anal. Chem.*, 39 (1967) 1422.
- 3 C. G. HORVATH AND S. R. LIPSKY, *J. Chromatog. Sci.*, 7 (1969) 109.
- 4 J. J. KIRKLAND, *J. Chromatog. Sci.*, 7 (1969) 361.
- 5 J. H. KNOX AND M. SALEEM, *J. Chromatog. Sci.*, 7 (1969) 745.
- 6 L. R. SNYDER, *J. Chromatog. Sci.*, 7 (1969) 352.
- 7 I. HALÁSZ AND P. WALKLING, *J. Chromatog. Sci.*, 7 (1969) 129.
- 8 J. F. K. HUBER, *J. Chromatog. Sci.*, 7 (1969) 85.
- 9 J. CHURÁČEK, J. ŘÍHA AND M. JUREČEK, *Z. Anal. Chem.*, 249 (1970) 120.
- 10 J. CHURÁČEK, *J. Chromatog.*, 48 (1970) 241.
- 11 J. CHURÁČEK, AND H. PECHOVÁ, *J. Chromatog.*, 48 (1970) 250.
- 12 J. CHURÁČEK, M. HUŠKOVÁ, H. PECHOVÁ AND J. ŘÍHA, *J. Chromatog.*, 49 (1970) 511.
- 13 O. SAMUELSON, *Ion Exchange Separation in Analytical Chemistry*, Wiley, New York, 1963.

CHROM. 497I

APPLICATION OF POROUS GLASSES FOR GEL CHROMATOGRAPHY OF POLYMERS

S. P. ZHDANOV AND E. V. KOROMALDI

Institute of Silicate Chemistry, Academy of Sciences of the U.S.S.R., Leningrad (U.S.S.R.),

R. G. VINOGRADOVA, M. B. GANETSKII, O. M. GOLYNKO AND N. E. ZHILZOVA

Special Design Bureau of Analytical Instruments, Academy of Sciences of the (U.S.S.R.), Leningrad (U.S.S.R.),

B. G. BELENKY, L. Z. VILENCHIK AND P. P. NEFEDOV

Institute of High Molecular Compounds, Academy of Sciences of the (U.S.S.R.) Leningrad (U.S.S.R.)

SUMMARY

The basic principles of obtaining and controlling porous structure of glasses with large pores were formulated and the possibility of using these glasses for gel chromatography of polymers was demonstrated.

It was established that the curve of polystyrene elution does not correspond to the curve of the pore distribution in glass. Moreover, a part of porometrically accessible pores does not participate in the separation of the macromolecules, the pores whose size corresponds to the radius of gyration of macromolecules in this solvent being inaccessible to these macromolecules.

Porous glasses are very promising materials for gel chromatography of polymers¹. This paper deals with the basic principles of formation and control of the porous structure of glasses with large pores. Relationships between their structural parameters and the size and elution characteristics of macromolecules have also been investigated.

The products known as "porous glasses" are usually obtained by treating sodium borosilicate glasses capable of opalescence with acid solutions. The development of opalescence in these glasses when they are kept within a certain temperature range is due to their separation into two microphases of different composition. One of them is rich in silica and the other one mainly consists of borate. The exact composition of each phase is regulated by the composition of the glass and the temperature at which it is maintained in the opalescence zone. Since borates and B_2O_3 are soluble in acids, these components of the borate phase (under conditions of its steric continuity) are removed selectively from the glass by treatment with acids leaving a system of canals and pores in the leached glass. That is the reason why the pore size and volume depend on the amount of B_2O_3 and Na_2O passing from the glass into solution during the acid treatment. These amounts, in their turn, depend on the composition of the respective phases of the glass and on the peculiarities of its phase distribution.

Usually, the pore diameters in porous glasses obtained by a simple acid treatment vary approximately from 15 to 100 Å and the pore volumes vary from 0.10 to 0.25

cm³/g. The structural characteristics of a porous glass can be controlled by varying the composition of the glass and the conditions of heat treatment within these limits. Sodium borosilicate glasses capable of forming a porous glass contain only a limited amount of acid-soluble material (B₂O₃ and Na₂O). Owing to this fact, attempts to obtain porous glasses with large pores by acid treatment have failed. The possibility of preparing such porous glasses has been reported earlier², it consisted of a supplementary treatment of the porous glass with solutions of 0.5 N KOH or NaOH at room temperature.

It was shown² that this treatment resulted in a considerable increase in both the pore volume and the pore size. The changes observed in the structure of porous glasses are quite different for initially transparent and opalescent sodium borosilicate glasses. In both cases alkali treatment produced an approximately equal (a 4–5-fold) increase in the pore volume but for opalescent glass the increase in the pore size was much greater than for the transparent one. Typical differences in the structure of porous glasses after alkali treatment of transparent and opalescent glass are illustrated by adsorption isotherms and curves of the pore volume distribution (by radii) (see Fig. 1).

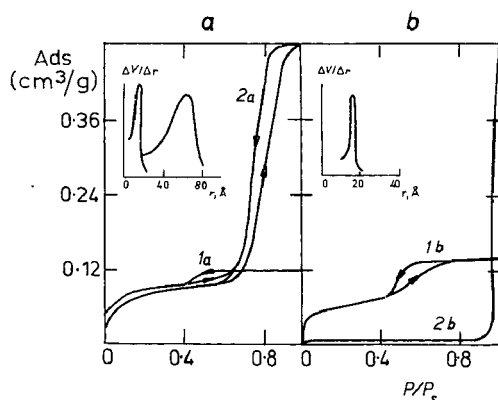


Fig. 1. Adsorption isotherms of C₂H₅OH on porous glasses obtained from transparent (a) and opalescent (b) glasses before (1a and 1b) and after (2a and 2b) their alkali treatment. In the insets, curves of the pore radii distribution are shown.

Particular changes in the structure of porous glasses after alkali treatment were accounted for² by assuming that the skeleton of the porous glass had a bidisperse structure. It is formed by a silica framework (skeleton) with large pores and relatively thick walls. Within these pores is situated a considerable amount of silica with a fine network structure forming the actual thin pore structure. In porous glasses obtained by the treatment of the original sodium borosilicate glasses with acids the adsorption measurements only reveal the fine pore structure while the structure of the large pore framework remains masked. However, by careful treatment with alkali one can dissolve the fine silica network of porous glass and destroy the fine structure formed within the framework without affecting the framework itself. The structure of the silica framework is directly revealed in the glass with the large pores obtained in this manner.

The conception of the bidisperse structure of porous glasses suggested earlier² was later confirmed by the small-angle X-ray scattering^{3,4} and electron microscopy⁵.

The nature of the finely dispersed silica in porous glasses and the bidisperse structure of their framework find a comprehensive explanation in terms of metastable liquation or of the immiscibility in sodium borosilicate glasses⁶⁻¹⁰. In accordance with the theory of metastable liquation, the borate phase of the inhomogeneous sodium borosilicate glasses should always contain not only B_2O_3 and Na_2O but also some SiO_2 . Its quantity in this phase depends on the composition of glass and the conditions of its heat treatment. This silica forms the fine pore structure within the main silica framework. The amount of this silica in the borate phase determines a possible increase in the pore volume in the porous glass after alkali treatment. The pore size after this treatment will depend on the size of the "particles" of the borate phase or on the state of phase separation in the glass. The composition of the phases in the inhomogeneous glass and the size of the borate bodies are determined by the temperature and duration of the heat treatment of the glass in the region of metastable liquation. Consequently variation of the conditions of the heat treatment is a very efficient method for regulating not only the structure of glasses with small pores, obtained by acid treatment, but also the structure of glasses with large pores obtained by the alkali treatment of the porous glasses.

The porograms in Fig. 2 and the curves of the pore volume distribution *vs.* logarithms of their radii in Fig. 3 demonstrate the possibility of controlling the porous structure of glasses with large pores just by varying the conditions of the heat treatment of the sodium borosilicate glass. This method enables us to obtain, with good reproducibility, porous glasses with large, small and intermediate pore sizes and volumes.

The wide possibilities of being able to control the structure of porous glasses, their stability in various solvents and the absence of swelling make the use of such

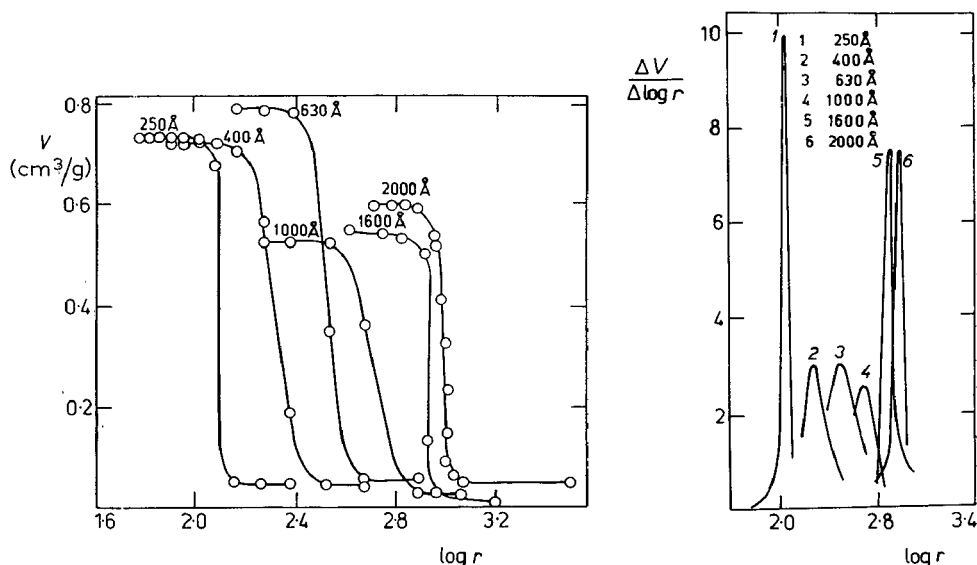


Fig. 2. Porograms of samples of glasses with large pores.

Fig. 3. Differential curves of pore distribution *vs.* the logarithm of their radii (according to Fig. 2). Å values in Figs. 2 and 3 are the pore diameters.

TABLE I

CHARACTERISTICS OF POLYSTYRENES USED

The perturbed dimensions of PS molecules in toluene were calculated from PRTSYN-EIZNER's equation¹³ using experimental data for PS in toluene found in ref. 16.

Polystyrenes	$M_w \times 10^{-4}$	$M_n \times 10^{-4}$	$M_{peak} \times 10^{-4}$	M_w/M_n	$(\overline{h_0^2})^{1/2}$ Å (cf. ref. 12)	$(\overline{h^2})^{1/2}$ Å (cf. ref. 12)	$(\overline{R^2})^{1/2}$ Å (cf. ref. 13)	(\overline{H}) Å (cf. ref. 14)	(\overline{Q}) Å (cf. ref. 15)
Styrene	—	0.0106	—	—	—	—	—	5.5	—
ST-25169	0.50	0.46	0.48	1.09	48.2	56.2	22.9	78.5	39.4
ST-25171	1.03	0.97	1.00	1.07	69.7	85.3	34.8	119.5	59.7
ST-25168	1.985	1.965	1.975	1.02	97.8	126	51.4	176	88.2
ST-25170	5.10	4.90	5.00	1.05	156	214	87.4	300	150
ST-41995	9.82	9.62	9.72	1.03	215	324	132	453	227
ST-41984	17.3	16.4	17.1	1.06	288	437	178	611	306
ST-25166	41.1	39.2	40.2	1.05	442	725	296	1015	508
ST-25167	86.7	77.3	83.0	1.13	635	1100	449	1540	770
ST-61970	214.5	178.0	198.7	1.2	978	1780	726	2490	1250
PS-No. 1 fr. 2	1100	—	—	—	2310	4900	2000	6850	3430
PS-No. 1 fr. 1	1600	—	—	—	2860	6020	2460	8410	4220

porous glasses very promising in liquid chromatography for separating mixtures of substances with molecules of different size. We have used macroporous glasses successfully for fractionating polymer mixtures with respect to their molecular weight.

Experiments have been carried out with a liquid chromatograph ChL-1302 (U.S.S.R.) with a refractometer detector. Porous glasses were placed in chromatographic glass columns 120 cm in length and 8 mm in internal diameter. The columns were filled by the method recommended in ref.11. Experiments were carried out in toluene at 20° and the elution rate was 50 ml/h. The sample volume was 1 ml of a polymer solution at a concentration of 0.5 g/100 ml. Standard samples of polystyrenes (Waters Associates) and two samples of high molecular weight polystyrene were used. Their characteristics are given in Table I.

The porous glasses described proved to be quite suitable for the gel chromatography of polymers. This can be seen from Fig. 4 which shows the results of chromatographing a polystyrene mixture using four columns with porous glasses Zh-130, Zh-250, Zh-700 and Zh-1600, their mean pore diameter is 130, 250, 700 and 1600 Å, respectively. We obtained a relationship between the reduced volumes and the size of the macromolecules, for each porous glass.

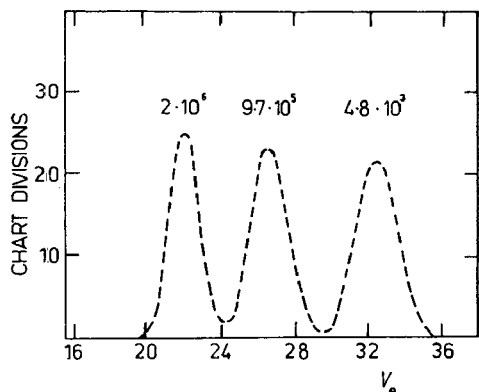


Fig. 4. Gel chromatogram of standard polystyrenes with molecular weights 4.8×10^3 ; 9.7×10^5 and 2.0×10^6 on four columns with porous glasses Zh-130, Zh-250, Zh-700, Zh-1600. Solvent: toluene; elution rate: 50 ml/h, temperature: +20°; sample volume: 1 ml at a concentration of 0.2 %.

This relationship is shown in Fig. 5 together with the respective porometric curves*. The calibration curves in this figure were obtained by subtracting from the reduced volume (V_e) the free volume (V_0) of the column which was assumed to be equal to the reduced volume of polystyrene with a MW = 1.6×10^7 . The porometric curves are given without the lower flat part which refers to the spaces between the sorbent particles, *i.e.* to V_0 . Thus, Fig. 5 permits the evaluation of the ratios of the reduced volume to the porometric pore size distribution.

One of the main problems in GPC is the ratio of the size of macromolecules to the gel pores. It is generally assumed¹⁷ that those pores whose size exceeds the mean square end-to-end distance of the chain by not less than twofold are accessible.

This relationship was not confirmed in our experiments. In columns with the

* Similar results have been obtained with silica gels²².

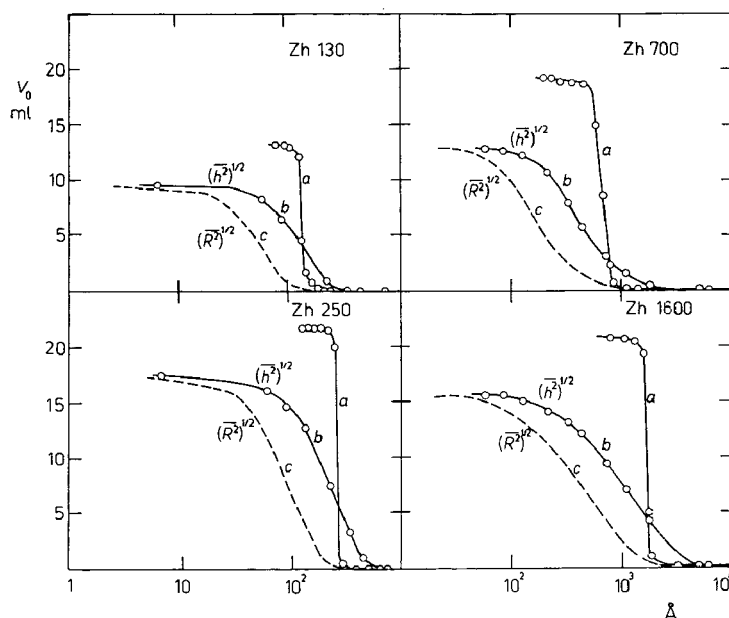


Fig. 5. Porometric curves (a) for glasses with large pores Zh-130, Zh-250, Zh-700, Zh-1600 in the amounts of 54.9, 30.9, 42.2, and 38.2 g in columns 1.2 m in length and 0.8 cm in diameter and of the corresponding elution curves of PS with different MW, characterised by mean square end-to-end distance (b) and mean square radius of gyration (c). Solvent: toluene; elution rate: 50 ml/h; temperature: 20°.

glasses: Zh-130, Zh-250, Zh-700 and Zh-1600, the pore whose size is commensurable with the radius of gyration of a macromolecule* does not participate; this finding may be interpreted in two ways. Either the macromolecules in pores are greatly deformed (they have changed their size by several times) or on approaching the pores they are oriented in such a way that their least mean size P is placed in front of the narrowest part of the corresponding pore.

A comparison of our results with porometric data shows that not all the accessible pores take part in the chromatographic process.

Moreover, the number of accessible pores which do not take part in the process increases with the size of the macromolecules. It is reasonable to assume that these pores are the deep ones, *i.e.*, that they are located relatively far from the surface of the sorbent particles.

The porous glasses with a narrow pore size distribution which were used in our work permitted us to establish the fact that the molecular sieve effect does not play a major part in the chromatographic separation of macromolecules since it is possible to separate macromolecules for which the porous glasses have the same size of accessi-

* Polystyrene molecules in solution are known to be bean-shaped and are characterised in three mutually perpendicular dimensions by sizes $(\bar{h}^2)^{1/2}$; $(\bar{g}^2)^{1/2}$; $(\bar{p}^2)^{1/2}$ (ref. 18) which are interconnected by the ratio $(\bar{h}^2)^{1/2} : (\bar{g}^2)^{1/2} : (\bar{p}^2)^{1/2} = 2\sqrt{6} : 2 : 1$. Moreover, the mean maximum size of the coil is determined by $\bar{H} = 1.4(\bar{h}^2)^{1/2}$, the mean maximum transverse size — by $\bar{Q} = 0.7(\bar{h}^2)^{1/2}$ (ref. 15). The radius of gyration of macromolecules is $(\bar{R}^2)^{1/2} = 1/\sqrt{6}(\bar{h}^2)^{1/2}$ (ref. 14), this is close to the mean maximum transverse size in the third direction \bar{P} .

ble pores. This separation can proceed only owing to the diffusion factor which was taken into account in refs. 19 and 20 as well as in another paper²¹ read at this seminar. In this paper²¹, the diffusion effect was determined by two factors $\exp [-u^2 r^2 / \zeta D^2]$ and $[1 - (u^2 \tau^2 / \sigma^2)]$ where u is the elution rate, D is the coefficient of translational diffusion of the macromolecules, r is the mean radius of the canals between the sorbent particles, σ is the dispersion of the chromatographic peak, τ is the value characterising the non-equilibrium of the process. The first of these factors is responsible for diffusion effects in the mobile phase, the second one also includes diffusion effects in the stationary phase, since the value τ is a function of the diffusion coefficient D' of macromolecules in the sorbent phase:

$$\tau = B \times a^2 / D'$$

where a is the depth of penetration of the macromolecules into the sorbent grains, and B is a certain geometrical constant.

REFERENCES

- 1 I. H. ROSS AND M. E. CASTO, *J. Polymer Sci. C*, **21** (1968) 143.
- 2 S. P. ZHDANOV, *Dokl. Akad. Nauk SSSR*, **82** (1952) 281.
- 3 S. P. ZHDANOV, E. A. PORAI-KOSHITS AND D. I. LEVIN, *Izv. Akad. Nauk SSSR, Otd. Khim. Nauk*, No. 1 (1955) 31; No. 2 (1955) 197; and No. 3 (1955) 395.
- 4 S. P. ZHDANOV AND E. A. PORAI-KOSHITS, *Metody Issledovaniya struktury vysokodispersnykh i poristykh tel*, Ed. Akad. Nauk SSSR (1958).
- 5 W. SCATULLA, W. VOGEL AND H. WESSEL, *Silikat Techn.*, **9** (1954) 51.
- 6 F. YA. GALAKHOV, *Izv. Akad. Nauk SSSR, Otd. Khim. Nauk*, No. 5 (1962) 743.
- 7 J. W. CAHN, *J. Chem. Phys.*, **42** (1965) 93.
- 8 J. W. CAHN AND R. J. CHARLES, *Phys. Chem. Glasses*, **6** (1965) 181.
- 9 W. HALLER, *J. Chem. Phys.*, **42** (1965) 686.
- 10 F. YA. GALAKHOV AND O. S. ALEKSEEVA, *Likvatsionnye yavleniya v stekle*, Izdatelstvo Nauka, Leningrad, 1969.
- 11 M. LE PAGE, R. BEAU, AND A. I. DE VRIES, *J. Polymer Sci. C*, **21** (1968) 119.
- 12 V. N. TSVETKOV, V. E. ESKIN, AND S. YA FRENKEL, *Struktura makromolekul v rastvorakh*, Izdatelstvo Nauka, Moscow, 1964.
- 13 O. B. PTITSYN AND YU. W. ELZNER, *Zh. Tekhn. Fiz.*, **29** (1959) 1117.
- 14 P. DEBYE, *J. Chem. Phys.*, **14** (1946) 636.
- 15 W. KUHN, *Experientia*, **1** (1945) 28.
- 16 P. QUTER, C. CARR AND B. ZIMM, *J. Chem. Phys.*, **18** (1950) 830.
- 17 M. I. R. CANTON AND I. F. JOHNSON, *Polymer*, **8**, 9 (1967) 487.
- 18 M. V. VOLKENSTEIN, *Konfiguratsionnaya statistika polimernykh tsepei*, Moscow, Leningrad.
- 19 W. W. YOU AND C. P. MALONE, *J. Polymer Sci. B*, **5** (1967) 663.
- 20 W. W. YOU, C. P. MALONE AND S. W. FLEMING, *J. Polymer Sci. B*, **6** (1968) 803.
- 21 L. Z. VILENCHIK AND B. G. BELENKII, *8th Intern. Gel Permeation and liquid Chromatog. Seminar, Prague, July 1-3, 1970*, preprints, B65-B75.
- 22 A. J. DE VRIES, M. LE PAGE, R. BEAU AND C. L. GUILLEMIN, *Anal. Chem.*, **39** (1967) 935.

CHROM. 4972

CHARACTERISATION OF POLYDISPERSE BRANCHED POLYMERS
BY MEANS OF GEL PERMEATION CHROMATOGRAPHY

A. CERVENKA AND T. W. BATES

Shell Research Limited, Carrington Plastics Laboratory, Urmston, Manchester (Great Britain)

SUMMARY

Theoretical gel permeation chromatography curves have been derived for model polydisperse polymers having chosen molecular weight averages and a given degree of random trifunctional branching. Gel permeation chromatography traces had been treated on a computer using the method proposed by DROTT, and the molecular weight averages and a branching characteristic obtained were compared with those following directly from the model used (the STOCKMAYER type of distribution). The basic assumption of DROTT (the ratio of the number of branch points to the molecular weight being constant) is discussed.

INTRODUCTION

Gel permeation chromatography provides an extremely convenient and rapid method for determination of the molecular weight distribution of polydisperse linear polymers. With polydisperse branched polymers, on the other hand, interpretation of the gel permeation chromatography (GPC) traces in terms of molecular weight averages and branching densities is considerably complicated by a distribution, not only of molecular weights, but of branch points. Two attempts¹⁻⁴ have been made to analyse gel permeation chromatograms of polydisperse branched polymers. Both methods assume, *a priori*, a branching distribution. Thus DROTT *et al.*¹⁻³ assume that the number of branch points, n_M , per molecule is proportional to the molecular weight, M , while SHULTZ⁴ assigns a definite distribution of both branch points and molecular weights to the branched polymer.

The branching model assumed by DROTT is likely to be in error, particularly at low molecular weights, for most real polymers. It is, however, difficult to predict how seriously this assumption affects the calculated molecular parameters. The validity of DROTT's method has been checked by calculating theoretical gel permeation chromatograms for a polydisperse branched polymer conforming to a distribution of n and M first derived by STOCKMAYER⁵ and for which n_M is not proportional to M over the whole molecular weight range. The theoretical GPC traces were analysed according to the method of DROTT and the molecular parameters obtained compared with those used to calculate the GPC trace.

THEORETICAL GEL PERMEATION CHROMATOGRAMS

A gel permeation chromatogram is, in effect, a plot of the weight fraction W_v of polymer having an elution volume V against V . On the other hand, the molecular weight distribution of a polydisperse branched polymer is usually^{4,6-8} more conveniently expressed in terms of the differential weight fraction W_z of polymer having a relative molecular weight Z and having an average number n_z of branch points. Here Z is a reduced variable defined as $Z = M/\bar{Y}_n$, where \bar{Y}_n is the number average molecular weight of the "primary" chains, *i.e.* the number average molecular weight which would be obtained if all the branches were severed. In order therefore to construct a theoretical GPC trace for a polydisperse branched polymer, W_v must be written in terms of W_z , and the elution volume V corresponding to each Z -mer calculated.

The latter calculation requires knowledge of the "universal" calibration curve for the particular GPC column set under its operating condition, *i.e.* the constants A , B , C , etc. in the equation

$$\log [\eta]M = A + BV + CV^2 + \dots \quad (1)$$

must be known. ($[\eta]$ is the intrinsic viscosity.) As shown by SHULTZ⁴, the elution volume for each Z -mer is given by

$$\log ([\eta]Z) = A' + B'V + C'V^2 + \dots = \log K' + \left(\frac{1}{2}\right) \log g_z + (1 + a) \log Z \quad (2)$$

The constants a and K' occur in the intrinsic viscosity-molecular weight relationship for the monodisperse linear polymer in the GPC solvent at its operating temperature, *i.e.*

$$[\eta]_L = KM^a = K'Z^a \quad (3)$$

The branching parameter g_z in eqn. 2 is a function of n_z , being related to the intrinsic viscosities of the branched and linear chains of the same molecular weight by⁹

$$g_z^{1/2} = f(n_z) \simeq [\eta]_B/[\eta]_L \quad (4)$$

Expressions relating g_z to n_z have been calculated¹⁰⁻¹² for various branching topologies. If the dependence of n_z on Z is known, the relationship between g_z and Z can be calculated; hence V can be obtained for each Z -mer from eqn. 2.

It follows from eqn. 1 that W_v corresponds to the weight fraction $W_{\log[\eta]Z}$ of polymer having logarithm of the product intrinsic viscosity and molecular weight $\log [\eta]Z$. It is readily shown that

$$W_v = W_{\log[\eta]Z} [d \log [\eta]Z / dV] \quad (5)$$

Combining this equation with the relationship between $W_{\log[\eta]Z}$ and W_z derived by SHULTZ for a branched polymer (eqn. 7 of ref. 4) yields the desired dependence of W_v on W_z , namely

$$W_v = g_z^{1/2} Z^{1+a} \left[\frac{d(g_z^{1/2} Z^{1+a})}{dZ} \right]^{-1} \left[\frac{d \log ([\eta]Z)}{dV} \right] W_z \quad (6)$$

Construction of a theoretical gel permeation chromatogram from eqns. 2 and 6 requires knowledge of the functions W_z and g_z . A model polydisperse polymer with trifunctional branch points distributed randomly was used for this purpose. The differential weight fraction distribution functions for such a polymer were first derived by STOCKMAYER⁵; they apply to polymers formed by polycondensation of monomers of the type $XA_2 + YA_3 + ZB_2$ (where A reacts only with B and *vice versa*, and all reacting groups have the same reactivity). We use the slightly modified distribution function of SHULTZ^{4,8}:

$$W_{nz} = [\gamma Z^2/n(n+2)]W_{n-1,z}, \quad n \geq 1 \quad (7)$$

$$W_{0z} = Z e^{-Z(\gamma+1)}$$

and

$$W_z = \sum_{n=0}^{\infty} W_{nz}$$

Here γ is a branching index, being zero for a linear chain and unity at the point of incipient gelation; γ is related to the weight average number \bar{n}_w of branch points per molecule and to the polydispersity factor $\bar{M}_w/\bar{M}_n = Q$ by^{4,5}

$$\gamma = \bar{n}_w/(2 + \bar{n}_w) = 3(Q-2)/(3Q-2) \quad (8)$$

For this model polymer, ZIMM AND STOCKMAYER¹⁰ calculated g_z as a function of n_z :

$$g_z \simeq \{[1 + (n_z/7)]^{1/2} + 4n_z/9\pi\}^{-1/2} \quad (9)$$

where

$$n_z = \sum_{n=0}^{\infty} nW_{nz} / \sum_{n=0}^{\infty} W_{nz}$$

SHULTZ⁸ has tabulated W_z and n_z for various values of Z and for different values of γ . Using these tabulated results and the simplified expressions⁸ for g_z and W_z at large (>120) Z allows the gel permeation chromatography trace to be constructed from eqns. 1, 2, 6 and 9. An actual (non-linear) universal calibration curve was used for this purpose (Fig. 1). This curve was obtained with column combinations of 3×10^5 , 3×10^4 , 3×10^3 and 60 Å using polystyrene fractions in 1,2,4-trichlorobenzene at 135° with a flow rate of 1 ml/sec. The constants K and a in eqn. 2 were given values of 9.54×10^{-4} dl/g and 0.64, respectively; these values were obtained in this laboratory for fractions of linear polyethylene in trichlorobenzene at 135°.

Fig. 2 shows theoretically calculated curves of W_v versus V for polymers having a constant weight-average molecular weight \bar{M}_w of 2×10^5 but with different values of the branching index γ (0, 0.6 and 0.9). Obviously the molecular weight distribution width increases with increasing degree of branching. Of more interest is Fig. 3, which shows the effect on the shape of the gel permeation chromatography trace of changing molecular weight at constant degree of branching ($\gamma = 0.9$, $\bar{n}_w = 18$) and hence constant polydispersity Q . Despite the fact that the distribution of M and n is identical

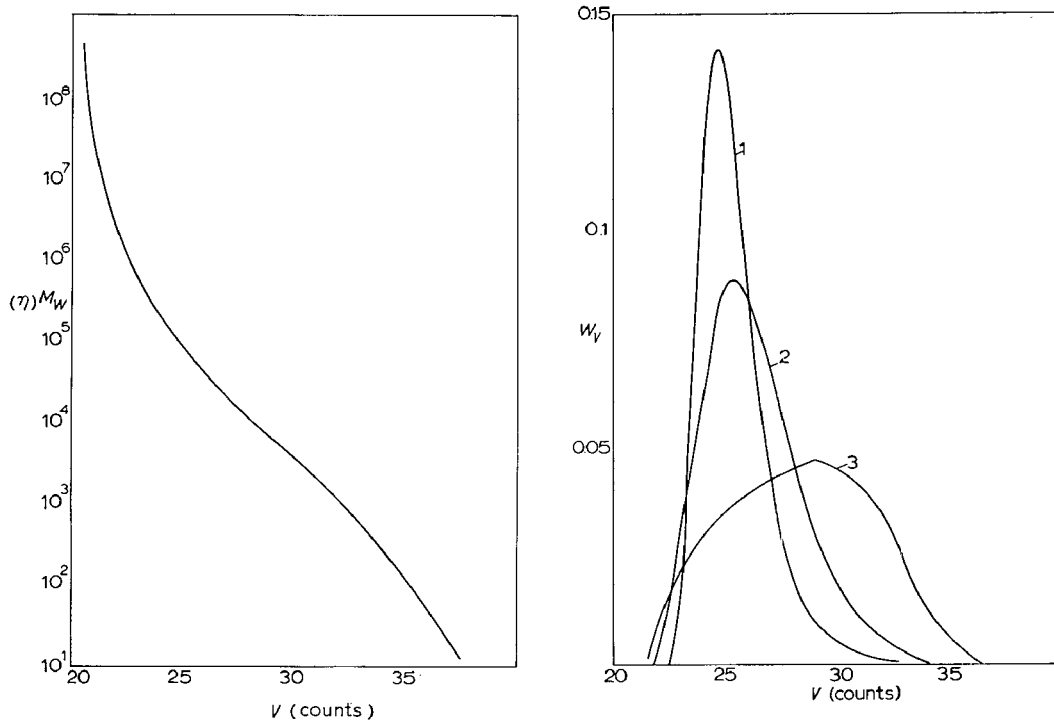


Fig. 1. The universal calibration established experimentally and used throughout all calculations.

Fig. 2. GPC curves for polydisperse branched polymers with $\bar{M}_w = 2 \times 10^5$ and different degrees of branching. (1) $\gamma = 0.0$; (2) $\gamma = 0.6$; (3) $\gamma = 0.9$.

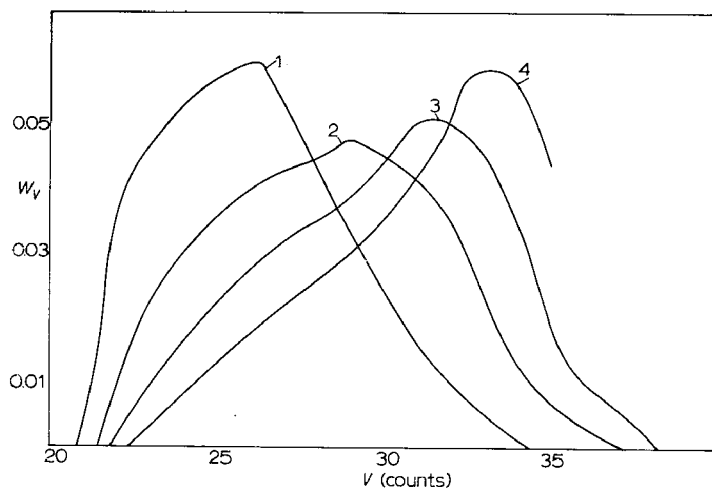


Fig. 3. GPC curves for polydisperse branched polymers with the degree of branching $\gamma = 0.9$ and different molecular weights. (1) $\bar{M}_w = 6 \times 10^5$; (2) $\bar{M}_w = 2 \times 10^5$; (3) $\bar{M}_w = 1.0 \times 10^5$; (4) $\bar{M}_w = 0.5 \times 10^5$.

for each of these curves, there are significant differences in the shapes of the GPC traces for the different \bar{M}_w . In particular, the appearance of shoulders at varying elution volumes is noteworthy. The actual differential distribution curves of W_z versus Z (Fig. 4) do not show such shoulders. In the GPC traces, the latter arise from the use of a non-linear universal calibration curve. For such a curve, the slope $d \log ([\eta]Z)/dV$ appearing in eqn. 6 is not a constant; this fact alone accounts for the appearance of shoulders and the different shapes of the curves in Fig. 3. Similar effects were found by YAU *et al.*¹³. This result has an important practical consequence: qualitative conclusions about the molecular weight distribution (such as association of shoulders with an excess of a certain molecular weight species) drawn from visual observation of a gel permeation chromatography trace can be misleading, particularly when a broad molecular weight distribution polymer (branched or linear) is combined with a non-linear calibration curve.

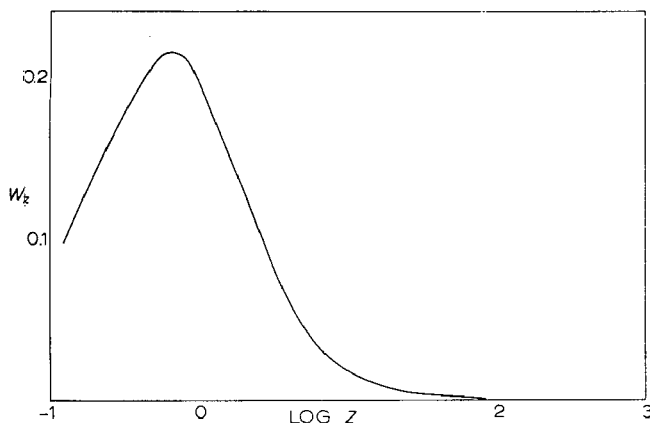


Fig. 4. Differential molecular weight distribution function of STOCKMAYER's type of branched polymers ($\gamma = 0.9$, Z is the reduced molecular weight).

The validity of the calculated gel permeation chromatograms was checked by assuming the polymers were linear and analysing the gel permeation chromatography trace in the usual manner for a linear polymer. The molecular weights $(\bar{M}_n)_{app}$, $(\bar{M}_w)_{app}$ and $(\bar{M}_z)_{app}$ so obtained are of course apparent values only. However, in a recent paper, SHULTZ⁴ calculated the ratios of the actual to apparent molecular weights and of the actual to apparent Q 's for the same trifunctionally branched polydisperse model polymer used here (Tables I and III of ref. 4). Table I shows the results for three polymers, each having an actual \bar{M}_w of 2×10^5 but with $\gamma = 0.9$ ($\bar{n}_w = 18.0$), 0.6 ($\bar{n}_w = 3.0$) and zero ($\bar{n}_w = 0$). The calculated molecular weights and Q values are in general within 10% of the actual values. These differences are considered to be within the error (arising mainly from determination of slopes required in eqn. 6) of calculating the theoretical gel permeation chromatography traces.

ANALYSIS OF THE THEORETICAL GEL PERMEATION CHROMATOGRAPHY TRACES BY THE METHOD OF DROTT

Average molecular weights and the weight average number \bar{n}_w of branch points per molecule were determined from the theoretical gel permeation chromatograms

TABLE I

ANALYSIS OF THE THEORETICAL GPC TRACES FOR POLYDISPERSE TRIFUNCTIONALLY BRANCHED POLYMERS BY THE METHOD OF SHULTZ^a

γ	Q	$10^{-4} \bar{M}_n$		$10^{-5} \bar{M}_w$		$10^{-6} \bar{M}_z$		\bar{n}_w	
		Actual	Apparent Calc. ^a	Actual	Apparent Calc. ^a	Actual	Apparent Calc. ^a	Actual	Calc. ^b
0.90	14.00	9.98	14.51	1.40	1.70	1.73	1.89	2.10	1.61
0.60	4.00	3.23	3.64	5.00	5.40	5.46	1.74	0.60	0.58
0	2.00	1.83	1.83	10.0	10.8	10.8	1.98	0.30	0.29

^a From the apparent values using the correction factors in Tables I and III of ref. 4 (for $a = 0.66$).^b Calculated from $\bar{n}_w = (3Q_{\text{calc.}} - 6)/2$ (see eqn. 8).

TABLE II

COMPARISON OF ACTUAL MOLECULAR WEIGHTS AND \bar{n}_w 'S WITH THOSE CALCULATED BY THE DROTT PROCEDURE UNDER THE ASSUMPTION THAT $\lambda_1 = \eta/M = \text{CONSTANT}$

γ	$10^{-4} \bar{Y}_n$	$[\eta]_D/[\eta]_L^a$	$[\eta]_L^b$ (dl/g)	$[\eta]_B$ (dl/g)	$10^{-4} \bar{M}_n$	$10^{-5} \bar{M}_w$	$10^{-6} \bar{M}_z$	Q	$10^4 \lambda_1$	\bar{n}_w	$10^4 \lambda_2$
Actual	0.90	1.0	0.4618	2.238	1.034	2.00	2.10	14.0	—	18.0	0.95
Calc. ^d	—	—	—	—	1.033	1.89	1.50	14.4	0.97	18.3 ^e	—
Calc. ^e	—	—	—	—	1.034	1.91	1.52	14.6	—	—	1.04
Actual	0.60	4.0	0.7778	2.238	1.741	2.00	0.600	4.00	—	3.0	0.19
Calc. ^d	—	—	—	—	1.745	1.97	0.549	3.58	0.15	2.96 ^e	—
Calc. ^e	—	—	—	—	1.740	1.97	0.561	3.61	—	—	0.18
Actual	0	10.0	1	2.238	10.00	2.00	0.300	2.00	—	0	0
Calc. ^d	—	—	—	—	11.00	2.04	0.304	1.85	—0.09	0	0

^a From Table I of ref. 14 with $a = 0.66$ and $b = 0.50$.^b Calculated from eqn. 12 with $\bar{M}_w = 2 \times 10^6$.^c Calculated from $\bar{n}_w = \lambda_1 \bar{M}_w$.^d Calculation assuming $\eta_M/M = \text{constant} = \lambda_1$.^e Calculation using $\eta_M = (1 + \lambda_2^2 M^2)^{1/2} - 1$.

by a method proposed by DROTT¹⁻³ for polydisperse branched polymers. In this method, the various molecular weight averages and the branching density are calculated from the measured intrinsic viscosity $\langle[\eta]_B\rangle$ of the whole branched polymer and the observed GPC trace by an iterative procedure. Such a procedure requires an *a priori* assumption about branch distribution function. DROTT assumes a model in which the number of branch points, n_M , is proportional to the molecular weight of the chain, *i.e.*

$$n_M/M = \text{constant} = \lambda_1 \quad (10)$$

With this assumption and using an initial trial value of the branching parameter λ_1 , the GPC trace is used to compute the intrinsic viscosity of the whole polymer by use of the equation

$$\langle[\eta]_B\rangle = K \sum_M g_M \lambda_1^{1/2} M^{1+a} W_M \quad (11)$$

The procedure is repeated by incrementing or decrementing λ_1 until the calculated intrinsic viscosity agrees with the measured value.

Since the various molecular weight averages and the weight average number \bar{n}_w of branch points per molecule are known for the theoretically calculated GPC traces, comparison of the actual values with those calculated by the DROTT procedure allows the validity of the assumption that λ_1 is constant and independent of M to be checked.

In the analysis of the theoretical GPC traces by this method, the value of $g_M \lambda_1$ required in eqn. 11 was calculated from eqn. 9 by replacing n_z by $M \lambda_1$. The intrinsic viscosities of the whole polymers are required as input to DROTT's programme. These viscosities were computed from the ratios $\langle[\eta]_B\rangle/\langle[\eta]_L\rangle$ calculated by BERGER AND SHULTZ¹⁴ for the same model polymer as employed here. $\langle[\eta]_L\rangle$ is the intrinsic viscosity of a linear chain having the same \bar{M}_w as the branched polymer but having the most probable molecular weight distribution (for which $Q = 2$). The value of $\langle[\eta]_L\rangle$ was computed by correcting the constant K in eqn. 3 for the effect of the polydispersity (since eqn. 3 applies to a monodisperse polymer). It can readily be shown for the most probable distribution that

$$\langle[\eta]_L\rangle = 0.946 K \bar{M}_w^a \quad (12)$$

where $K = 9.54 \times 10^{-4}$ dl/g and $a = 0.64$, as used for calculating the theoretical gel permeation chromatography traces. This value of $\langle[\eta]_L\rangle$ was used to calculate $\langle[\eta]_B\rangle$ from the ratios $\langle[\eta]_B\rangle/\langle[\eta]_L\rangle$, the latter being obtained from Table I of ref. 14 with $a = 0.66$ and $b = 0.50$.

Table II shows the actual molecular weight averages and those calculated by the DROTT procedure for three polymers having the same \bar{M}_w (2×10^5) but with different degrees of branching, γ values being between 0 (*i.e.* linear chain) and 0.90. The difference between the actual and calculated values is considered to be within the error involved in constructing the theoretical GPC traces. Also shown in Table II are the calculated values for λ_1 . With the linear polymer ($\gamma = 0$), a negative value for λ_1 is obtained. Since the iterative procedure ceases as soon as a negative value of

λ_1 is obtained, such a value indicates a linear chain. The final column of Table II shows the weight average number, \bar{n}_w , of branch points, the actual values being calculated from γ via eqn. 8 and the calculated values from the product of λ_1 and the calculated \bar{M}_w . Good agreement is obtained between the actual and calculated values of \bar{n}_w .

We conclude therefore, that the DROTT procedure for analysing polydisperse branched polymers provides a reliable measurement of both molecular weight averages and of \bar{n}_w , at least for polymers conforming to the STOCKMAYER distribution of molecular weights and branch points. At first sight, such a conclusion may seem surprising since the assumption that $\lambda_1 = n_M/M$ is constant applies only approximately to the STOCKMAYER distribution. Fig. 5 shows a plot of n_z/Z against $Z = M/\bar{Y}_n$ for different values of γ . Although at higher values of molecular weight, constancy of n_z/Z is observed, it decreases with decreasing molecular weight at low molecular weights.

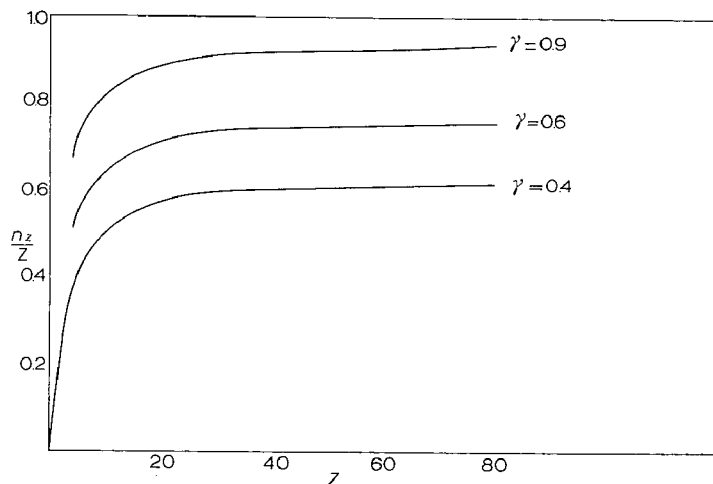


Fig. 5. Plot of the ratio n_z/Z (the average number of branch points per Z -mer to the reduced molecular weight) versus Z for three different degrees of branching.

However, the DROTT procedure for determining molecular parameters is based on the use of eqn. 11 for $\langle [\eta]_B \rangle$; this equation involves a weight averaging and consequently is relatively insensitive to the characteristics of low molecular weight species. As a result, the calculated value of λ_1 is determined mainly by the high molecular weight chains for which λ_1 is constant for the STOCKMAYER distribution. This latter conclusion was confirmed by modifying the DROTT method by replacing eqn. 10 by an equation which more accurately represents the dependence of n on M for the STOCKMAYER distribution. The equation used was⁴

$$n_M = (1 + \lambda_2^2 M^2)^{1/2} - 1 \quad (13)$$

where λ_2^2 is a constant equal to γ/\bar{Y}_n^2 . Thus λ_2 is now the branching index (in place of λ_1 in DROTT's original method) which is determined by the iterative procedure. No significant difference in the calculated average molecular weights and \bar{n}_w 's was obtained by using the more accurate eqn. 13 in place of the approximate eqn. 10 (see Table II).

Thus we may conclude that the DROTT procedure for characterising polydisperse branched polymers is fairly insensitive to the characteristics of the low molecular weight chains; reliable molecular weights and branching densities will be obtained provided that the distribution of branch points in the real polymer is such that λ_1 is constant at the higher molecular weights.

REFERENCES

- 1 E. E. DROTT, *Intern. Seminar Gel Permeation Chromatog.*, 4th, Miami, 1967.
- 2 E. E. DROTT AND R. A. MENDELSON, *Intern. Seminar Gel Permeation Chromatog.*, 5th, London, 1968.
- 3 E. E. DROTT, *Intern. Seminar Gel Permeation Chromatog.*, 6th, Miami, 1968.
- 4 A. R. SHULTZ, *European Polymer J.*, 6 (1970) 69.
- 5 W. H. STOCKMAYER, *J. Chem. Phys.*, 11 (1943) 45; *ibid.*, 12 (1944) 125.
- 6 C. D. THURMOND AND B. H. ZIMM, *J. Polymer Sci.*, 8 (1952) 477.
- 7 R. W. KILB, *J. Polymer Sci.*, 38 (1959) 403.
- 8 A. R. SHULTZ, *J. Polymer Sci.*, A3, (1965) 4199.
- 9 B. H. ZIMM AND R. W. KILB, *J. Polymer Sci.*, 37 (1959) 19.
- 10 B. H. ZIMM AND W. H. STOCKMAYER, *J. Chem. Phys.*, 17 (1949) 1301.
- 11 K. KURATA AND M. FUKATSU, *J. Chem. Phys.*, 41 (1964) 2434.
- 12 T. OROFINO, *Polymer (London)*, 2 (1961) 295, 305.
- 13 W. W. YAU, H. L. SUCHAN, C. P. MALONE AND J. W. FLEMING, *Intern. Seminar Gel Permeation Chromatog.*, 5th, London, 1968.
- 14 H. L. BERGER AND A. R. SHULTZ, *J. Polymer Sci.*, A2, (1965) 3643.

J. Chromatog., 53 (1970) 85-93

CHROM. 4973

THERMAL DEGRADATION OF POLYETHYLENE IN A NITROGEN ATMOSPHERE OF LOW OXYGEN CONTENT

I. CHANGES IN MOLECULAR WEIGHT DISTRIBUTION

A. HOLMSTRÖM AND E. SÖRVIK

The Polymer Group, Department of Organic Chemistry, Chalmers University of Technology, Gothenburg (Sweden)

SUMMARY

Unstabilised samples of low-density polyethylene were heated in nitrogen containing small amounts of oxygen. The changes in molecular weight distribution were followed by gel permeation chromatography and intrinsic viscosity. A threshold temperature was found at 315° and a threshold oxygen concentration in the range 410–1000 p.p.m.

In accordance with the theory of random scission, degradation caused a shift of the peak position towards lower molecular weights and an increasing skewness of the molecular weight distributions within the original molecular weight limits. No drastic drop of \bar{M}_w/\bar{M}_n was observed.

A simplified method for the construction of gel permeation chromatography calibrations for low- and high-density polyethylene, from measurements on polystyrene standards, is demonstrated. The method is based on the concept of "universal calibration".

INTRODUCTION

Since 1949, when OAKS AND RICHARDS published their work¹, little has been published on the structural changes of low-density polyethylene (LDPE) when heated between 200 and 400°. Work has been done, however, at temperatures below 200°, mostly in air or other oxygen rich atmospheres. In most of these studies the aim has been to investigate the oxidative changes of polyethylene when heated at temperatures in the neighbourhood of its melting point. These studies are of value when evaluating degradation at ordinary processing conditions. A survey of such studies was recently published by REICH AND STIVALA².

In order to elucidate the decomposition mechanism a few studies^{3–7} have been carried out in high vacuum at 400° or above.

OAKS AND RICHARDS¹ performed their experiments on LDPE in vacuum at temperatures from 295 to 360°. They followed the changes in molecular weight by viscosity measurements, and in addition they analysed the chemical structure by infrared spectroscopy and iodine number. The decomposition of LDPE has also been

followed by ordinary non-isothermal thermogravimetric (TGA) measurements. ANDERSON AND FREEMAN⁸ carried out their experiments in a vacuum and IGARASHI AND KAMBE⁹ operated in nitrogen and air whereby activation energies were calculated.

The temperature range between 200 and 400° is of practical importance because modern extruders work in this high temperature range. Moreover, the polymer melt is kept at this high temperature in the reactor during the high-pressure polymerisation process.

Structural changes in HDPE, when heated between 300 and 400°, have been the subject of two important investigations published in 1966. QUACKENBOS¹⁰ treated the HDPE in nitrogen and nitrogen containing 0.34 % oxygen and followed the changes in intrinsic viscosity and carbonyl content.

ARNETT AND STACY¹¹ heated HDPE in a vacuum and measured the changes in molecular weight by intrinsic viscosity and ebullioscopy. They treated their data kinetically and established that the hypothesis of a constant probability of bond scission per unit time (random scission) fits the observed decrease in molecular weight with heating time, if the decrease in bonds breaking is taken into account.

Our work concerns structural changes occurring in LDPE when heated to temperatures between 280 and 360° in atmospheres containing 0.3 % oxygen and less. The results of gel permeation chromatography (GPC) measurements and intrinsic viscosity determinations are reported in this paper.

EXPERIMENTAL

Samples

Nine narrow-distribution standards of polystyrene (PS), \bar{M}_w : $5 \cdot 10^3$ – $2145 \cdot 10^3$, supplied by Waters Associates and four narrow-distribution hydrogenated polybutadienes, supplied by Phillips Chemical Co. were used. The LDPE resin (sample A) was an ordinary quality high pressure resin, free from additives. It was kindly supplied by Unifos Kemi AB (Stenungsund, Sweden):

Density: 0.9210 (g/cm³)

Melt index: 0.24 (g/10 min)

\bar{M}_w : $164 \cdot 10^3$ (from GPC)

\bar{M}_w/\bar{M}_n : 6.8 (from GPC)

$[\eta]_{p\text{-xyl}}^{105^\circ}$: 0.93 (dl/g).

A 0.3 mm thick film was moulded, from which samples 22 × 45 mm were cut for the degradation experiments. The samples were degassed and stored in a vacuum desiccator.

Solvents

1,2,4-Trichlorobenzene (TCB), purum grade, obtained from Th. Schuchardt, (München, G.F.R.), was distilled and the fraction 213–215° was used. 0.45 g/l Santonox-R was added as antioxidant.

p-Xylene, puriss grade, from Fluka AG (Switzerland) was used without further purification.

Nitrogen-oxygen mixtures

Nitrogen-oxygen mixtures containing 22, 63, 410, 1000, 1900 and 2800 p.p.m. oxygen were supplied by Nordiska Syrgasverken AB (Uddevalla, Sweden). The latter also determined the oxygen concentrations.

Heating device

The tubular oven used was similar to that described by QUACKENBOS¹⁰ (Fig. 1).

This construction met the following requirements: (1) Heating and cooling of sample to the desired temperature within 30 sec; (2) temperature constancy to $\pm 1^\circ$ during the experiment; (3) large sample area; and (4) high gas flow.

The samples were placed on 0.1 mm microscopic cover glasses. Before use, the glasses were washed with chromic acid, distilled water and ethanol, and after that dried and stored in a vacuum-desiccator. The mounted sample was kept in the cold part of the oven for at least 20 min before heating. The gas flow was 90 l/h and heating times ranged from 2 to 90 min.

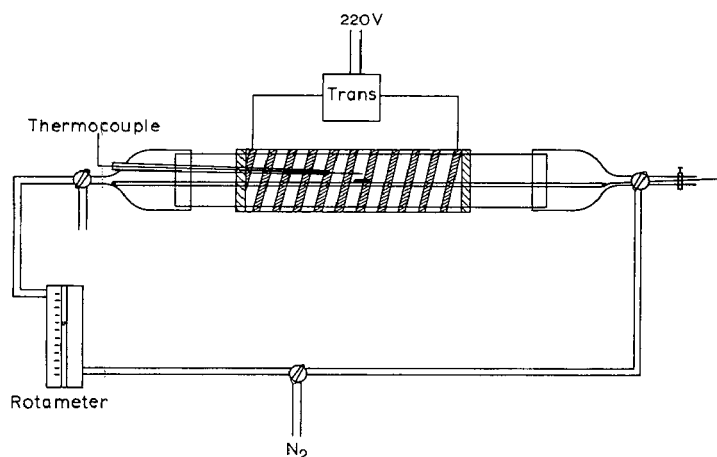


Fig. 1. Heating device.

Thermogravimetric measurements

Thermogravimetric analyses (TGA) were performed with a Mettler thermo-analyser No. 71. Sample size was 6 mg.

Gel permeation chromatography

Waters Associates GPC Model 200 was used. The GPC was equipped with an automatic injection system, a dual-headed pump and an all stainless steel solvent system.

All samples were filtered before injection and all injections were done by the automatic injection system. The experimental conditions were as follows:

Solvent: TCB

Temperature: 135°

Columns: 10⁷, 10⁶, 10⁵, 10⁴, 10³ Å

Plate count: 1060 plates/ft.

Flow rate: 1.0 ml/min

Sample conc.: 1–4 mg/ml

Injection time: 5 min

Sensitivity: 8×.

Usually GPC determinations of PS-standards and PE-samples were duplicated. As a precaution the only slightly degraded PE-samples were run three times and the undegraded PE-sample A six times. Every second day a control test was done, using a mixture of three completely resolved PS-standards ($\bar{M}_w = 5 \cdot 10^3$, $51 \cdot 10^3$ and $411 \cdot 10^3$).

The baseline-timedrift was small and constant, the noise level *ca.* 1 mm and the reproducibility of \bar{M}_w within $\pm 5\%$.

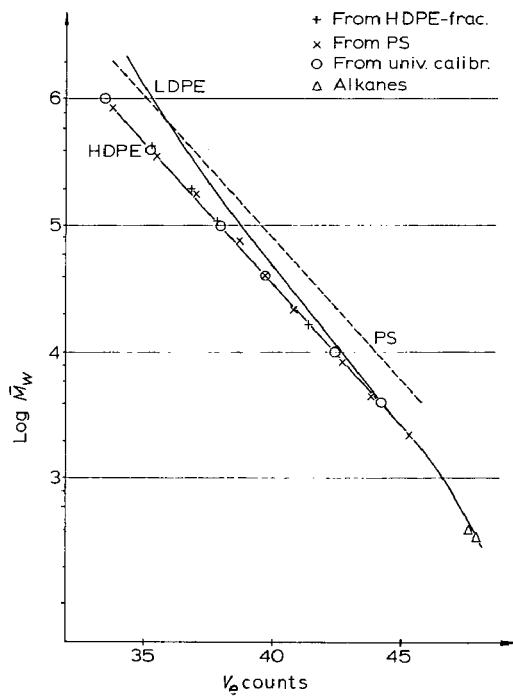


Fig. 2. Calibration curves.

Viscosity

Measurements on intrinsic viscosity for LDPE were carried out in TCB at $135 \pm 0.01^\circ$ and in *p*-xylene at $105 \pm 0.01^\circ$. Like Drott¹³, we found that the solvent systems gave the same result.

Ubbelohde dilution viscometers with flow times of pure solvent greater than 110 sec were used (capillary diam. 0.5 mm). In order to avoid problems caused by transferring hot solutions, the samples were dissolved directly in the viscometers. Viscosity determinations on the PS-standards were carried out in TCB at $135 \pm 0.01^\circ$.

Calibration

Calibration curves for PS, LDPE and HDPE are shown in Fig. 2. The calibration curve for PS was determined in the usual way by plotting elution volume at peak maximum (V_e) against $\log \bar{M}_w$. The calibration curves for LDPE and HDPE were

not determined in this manner but were computed directly from the PS calibration curve in combination with published PE-data, by using the methods described below. These calculations are based on the concept of using hydrodynamic volume as the key parameter in constructing a "universal calibration curve". BENOIT and co-workers¹² first proposed this concept, using $\log ([\eta] \cdot \bar{M})$ as a measure of the hydrodynamic volume. They showed that by plotting $\log ([\eta] \cdot \bar{M})$ against V_e a single curve is given for a variety of polymers (PMMA, polybutadiene, PVC and branched and linear PS). DROTT¹³ and others¹⁴⁻¹⁸ found that this relation is also valid for LDPE and HDPE.

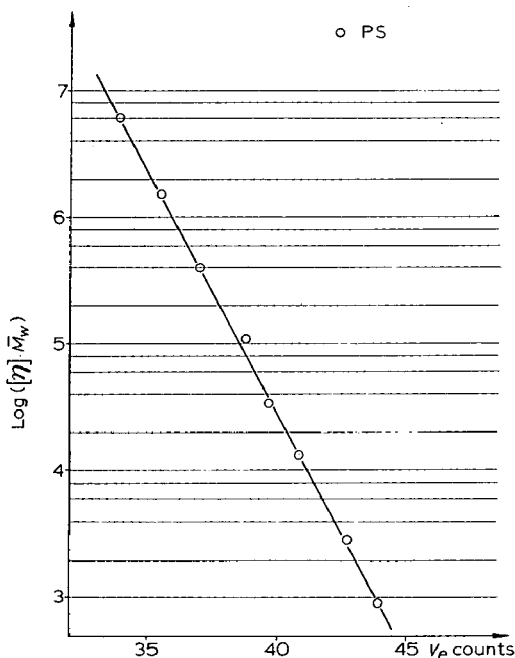


Fig. 3. Universal calibration curve.

By combining data from GPC and viscosity measurements on the PS-standards and using their stated molecular weights, a universal calibration curve has been constructed, (Fig. 3) giving the relation between $[\eta] \cdot \bar{M}$ and V_e .

As this relation should also be valid for PE^{14,18}, the relation between \bar{M}_{PE} and V_e can be calculated if $[\eta]_{PE} \cdot \bar{M}_{PE}$ is known for different values of \bar{M}_{PE} .

For HDPE a Mark-Houwink relationship exists between $[\eta]$ and \bar{M}_w in TCB at 135°. We have used that given by CROUZET¹⁹ *et al.* $[\eta] = 5.23 \cdot 10^{-4} \cdot \bar{M}_w^{0.70}$ to calculate $[\eta]$ and $[\eta] \cdot \bar{M}_w$ for different chosen values of \bar{M}_w . The points thus obtained are shown by \circ in Fig. 2.

Approaching the problem in another way WILLIAMS AND WARD²⁰ found a simple means of constructing a HDPE calibration curve from a known PS-calibration: for every single V_e , $\bar{M}_{PS} = 2.317 \cdot \bar{M}_{HDPE}$. In Fig. 2 such calculations for PS-standards are marked by \times . These points show excellent agreement with the HDPE calibration curve obtained by the method mentioned above. Further confirmation

was obtained by plotting data from the measurements on HDPE-standards (hydrogenated polybutadiene) (Fig. 2. (+)).

So far no mathematical expression for the relationship between \bar{M} and $[\eta]$ has been found for the LDPE. DROTT¹³, PANARIS AND PRECHNER¹⁸ and CROUZET *et al.*¹⁹ have published viscosity and light scattering measurements on LDPE-fractions, using TCB-solutions at 135° for the viscosity measurements. We have utilised these values to construct a $\log \bar{M}_w$ - $\log [\eta]$ relationship (Fig. 4). From this plot it is possible to obtain $[\eta]$ and subsequently calculate $[\eta] \cdot \bar{M}_w$ for different values of \bar{M}_w .

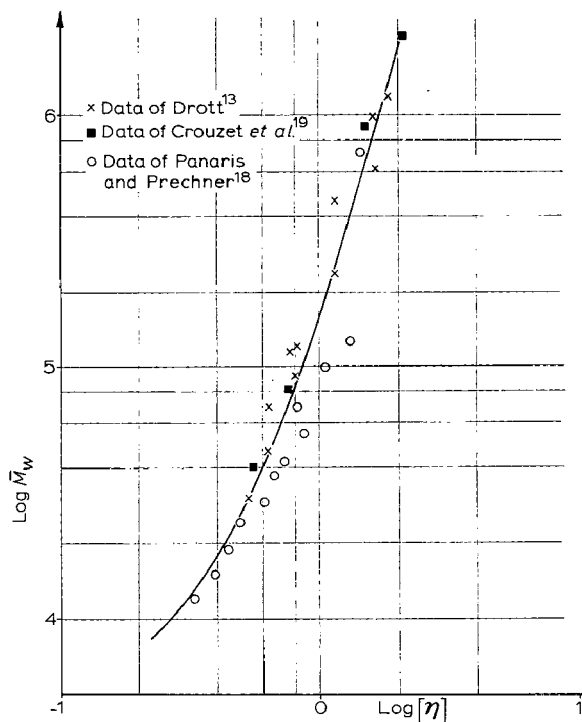


Fig. 4. Relationship between $\log [\eta]$ and $\log \bar{M}_w$ for LDPE.

Using the same calculating procedure as mentioned previously the calibration curve for LDPE (Fig. 2) is obtained *via* the universal calibration curve (Fig. 3). CROUZET *et al.*¹⁹ has published similar calculations starting with data on HDPE and LDPE fractions. The resulting calibration curve for LDPE has the same general appearance and position in relation to the HDPE curve as our LDPE calibration curve.

Treatment of GPC data

Calculation of average molecular weights and plots of weight fraction against $\log M$ (molecular weight distribution (MWD)) from the GPC-curves was carried out by the computer program devised by DROTT AND MENDELSON²¹.

RESULTS AND DISCUSSION

The samples became successively more and more brittle during heat treatment, even at the lowest oxygen levels. The sample treated at the highest temperature, for the longest time in the most oxygen-rich atmosphere acquired a thin brown surface layer. No other sample was discoloured.

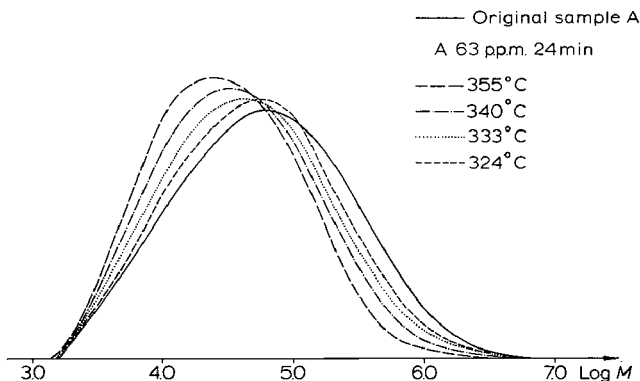


Fig. 5. Weight fraction plotted against $\log M$ (MWD) for sample A, heated for 24 min in 63 p.p.m. oxygen.

None of the samples contained insoluble matter, showing that no (extensive) crosslinking occurred. On the contrary, the heat treatment caused chain scission, clearly demonstrated by a drop in molecular weight (MW), and minor weight losses. The latter effect was followed by TGA-measurements.

In the following paragraphs the effect of temperature, heating time and oxygen content on chain scission is discussed. The experimental work to elucidate time-temperature effects was conducted in 63 p.p.m. oxygen as this low oxygen content gave the same result as oxygen-free nitrogen²².

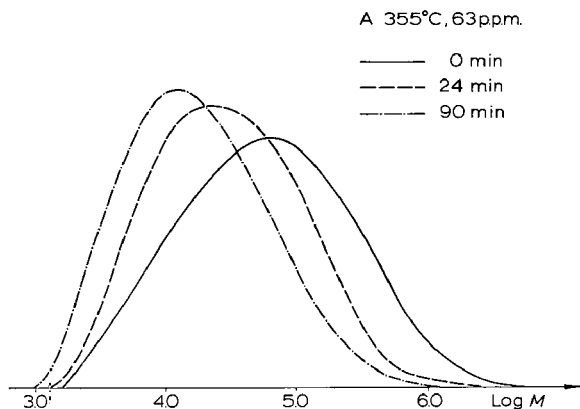


Fig. 6. Weight fraction plotted against $\log M$ (MWD) for sample A, heated at 355° in 63 p.p.m. oxygen.

Effect of temperature and heating time in a nitrogen atmosphere

A series of experiments was conducted in "nitrogen" (63 p.p.m. oxygen). The following time and temperature levels were used (Figs. 5-9 and 13): 2, 6, 12, 24, 90 min; and 284, 315, 324, 333, 340, 355°. Figs. 5 and 6 demonstrate the pronounced effect of temperature and heating time on MWD. The quantity of high molecular weight material diminishes. The highest M -value noticed drops by a factor of two in

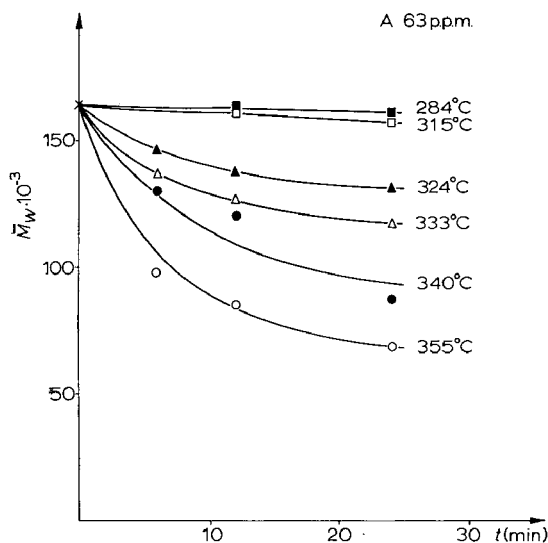


Fig. 7. Change of \bar{M}_w with heating time for sample A heated in 63 p.p.m. oxygen.

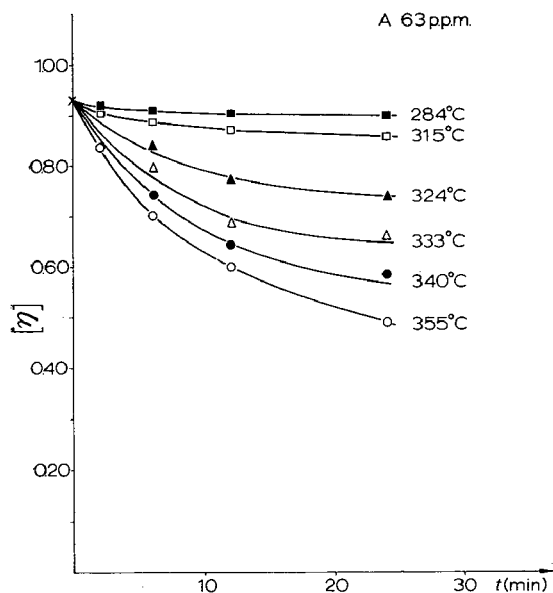


Fig. 8. Change of $[\eta]$ with heating time for sample A heated in 63 p.p.m. oxygen.

each step 0–24–90 min at 355°. However, even after 90 min at 355° material of an M in the order of 10^6 is present.

The low molecular weight end of the MWD is much steeper and does not shift to any appreciable extent up to 24 min at 355°. When the heating time is increased to 90 min, the low molecular weight end drops by a factor of about two. The peak position is moved from $65 \cdot 10^3$ to $12 \cdot 10^3$ and the width of the MWD at 50 % peak height is getting smaller.

The TGA-measurements showed the following values:

Time (min)	Temperature (°C)	Weight loss (%)
24	315°	1
24	355°	6
90	355°	17

Fig. 5 shows that a rise in temperature affects the MWD in the same general way as described above for increase in the heating time. The observed changes with time and temperature can be explained qualitatively by the theory of random scission. The high molecular weight end should not vanish completely as the amount of material is small. Thus the MWD is not growing narrower due to the disappearance of the high molecular weight molecules as reported for HDPE¹⁰. According to the random scission

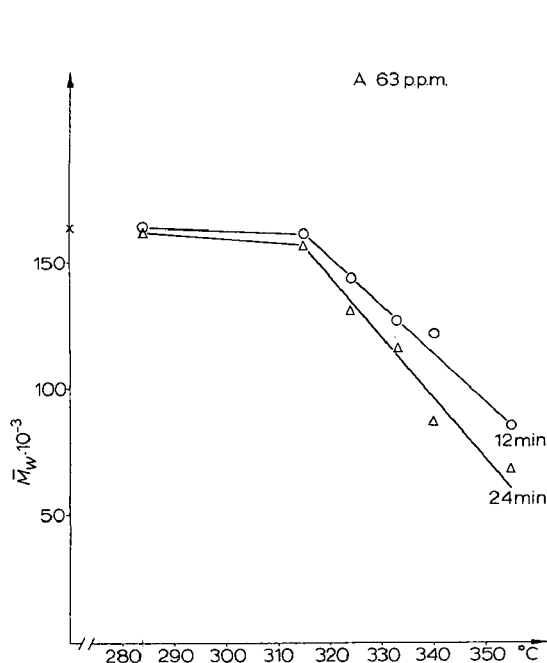


Fig. 9. Change of \bar{M}_w with temperature. Sample A, 63 p.p.m. oxygen.

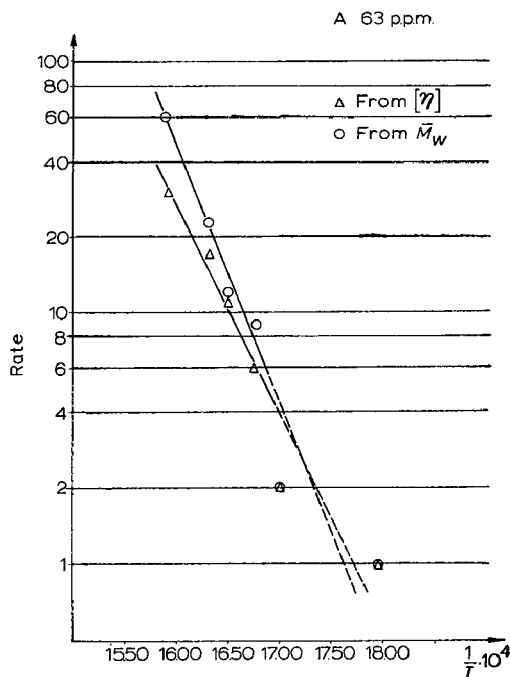


Fig. 10. Arrhenius plot for sample A at 63 p.p.m. oxygen. Data from GPC and viscosity measurements.

theory the main changes will appear in the central part of the MWD, as is observed. The very small changes in the low end and the steepness of the curve is a result of the low statistical probability of bond breaking in a fraction containing small and few molecules.

The fairly large amount of volatile material obtained is not inconsistent with the above reasoning. TSUCHIYA AND SUMI⁷ showed that intramolecular transfer of radicals results in the formation of C₃, C₂, C₄ and C₆ fragments mainly. Thus volatile material is not formed mainly from the low molecular weight tail of the MWD, as proposed by QUACKENBOS¹⁰, but from the whole MWD.

For a more quantitative discussion of the degradation process the \bar{M}_w was calculated. It was supplemented with a determination of $[\eta]$, which also afforded the opportunity of comparison with previously published results. The results are given in Figs. 7 and 8, respectively. Hardly any changes in \bar{M}_w or $[\eta]$ are observed at 284 and 315°. At the higher temperatures the curves are characterised by an initial rapid drop, succeeded by a slower change. Such a degradation course is to be expected for LDPE when being subjected to random scission. This is in accordance with previously published data^{1, 10, 11}. To find the threshold temperature, above which changes are fast, the data were rearranged according to Fig. 9. This plot gave a threshold temperature of 315°, which is in close agreement with data reported for HDPE. (TABAR in ref. 10). The decrease in \bar{M}_w on each side of the threshold temperature follows linear relationships. Like QUACKENBOS¹⁰, who worked with HDPE, we have found that the curves in Figs. 7 and 8 may be super-imposed by sliding the time axis. This time scale can be used as a measure of rate. If the rate is unity at 284° we obtain the following values:

Temperature (°C)	Rate ([η])	Rate (\bar{M}_w)
284	1	1
315	2	2
324	6	9
333	11	12
340	17	23
355	30	60

These values have been used in the Arrhenius plot (Fig. 10). Activation energies have been calculated from this plot and we found 64 kcal/mole from $[\eta]$ and 69 kcal per mole from \bar{M}_w . These values are in good accordance with the value of 67 ± 5 kcal/mole given by ANDERSON AND FREEMAN⁸ and also with the values of IGARASHI AND KAMBE⁹ who reported 61 and 74 kcal/mole for a LDPE, from TGA measurements. This means that the activation energy is approximately the same for weight loss and MW-decrease in nitrogen as it is in a vacuum for a LDPE resin. According to our previous discussion on the effect of random scission on changes in MWD, this is a further indication that TSUCHIYA AND SUMI's theory⁷ on intramolecular transfer of radicals is valid. The highest probability, by far, is in the medium molecular weight range. Thus the scission of the molecules in this part of the MWD causes both the bulk of the changes in \bar{M}_w and $[\eta]$ as well as the bulk of the formation of volatile material.

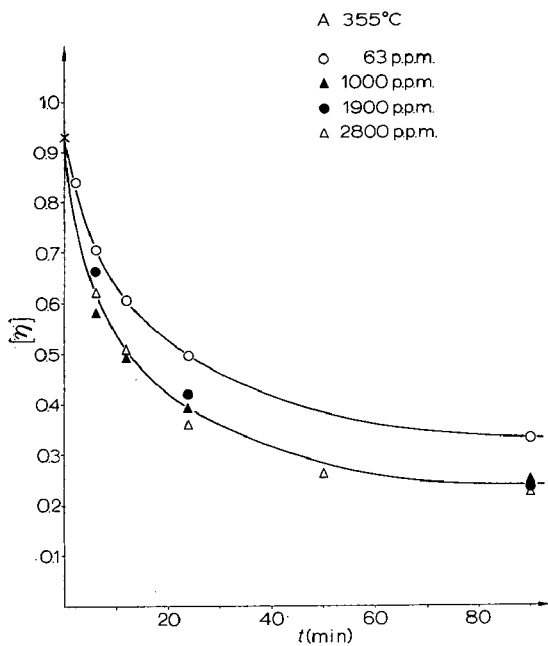


Fig. 11. Change of $[\eta]$ with heating time for sample A heated at 355°

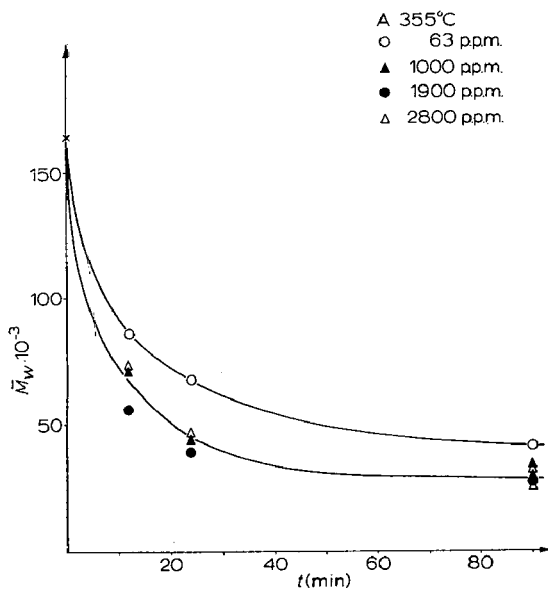


Fig. 12. Change of \bar{M}_w with heating time for sample A heated at 355°.

Effect of oxygen

It is known that the combination of heat and oxygen causes discolouration and formation of odoriferous material while the mechanical and electrical properties of the PE's are declining. In air at temperatures above 250° these changes are very rapid. The present investigation concerns oxygen concentrations below 3000 p.p.m. Changes in MW and MWD will be discussed below, while the changes in chemical structure and crystallinity will be reported elsewhere.

To study the influence of oxygen a series of experiments was conducted at 355°. Heating times were 2, 6, 12, 24 and 90 min and nitrogen containing the following oxygen concentrations was used: 22, 63, 410, 1000, 1900 and 2800 p.p.m. The results are given in Figs. 11-13. Within the range of oxygen concentrations studied an increase in the degradation velocity was observed, but no simple relationship was found. During the investigation we soon found that increasing the oxygen content from 22 to 410 p.p.m. had no effect on the relationship between \bar{M}_w respectively $[\eta]$ and heating time²². Therefore only data from experiments on 63 p.p.m. are given. Furthermore, a similar lack of response was observed on increasing the oxygen content from 1000 to 2800 p.p.m. (Figs. 11 and 12). This means that the experimental results can be summarised in two curves as is shown in Figs. 11 and 12.

The same remarkable tendency was observed when the MWD's were compared with each other. The changes could be summarised in two series covering the two ranges of oxygen concentration (22-410 and 1000-2800 p.p.m.).

Changes in MWD's are shown in Fig. 13. High oxygen content causes a gradually increasing skewness which is pronounced after 90 min. The high molecular weight

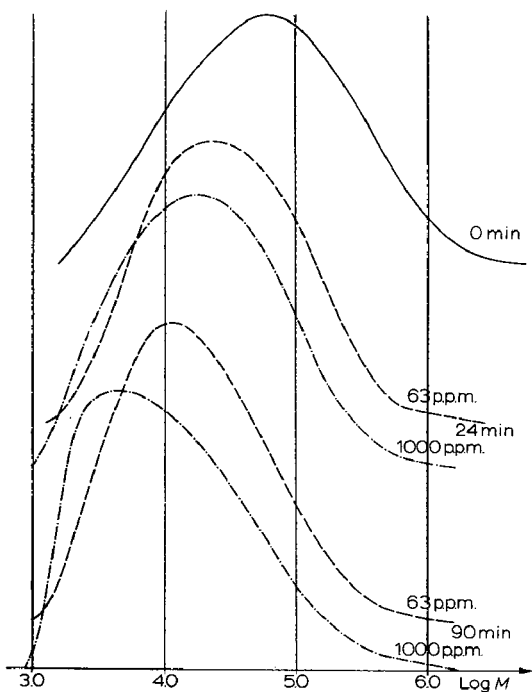


Fig. 13. Weight fraction plotted against $\log M$ (MWD) for sample A heated at 355°.

tail is still in the region of 10^6 and the low end of the MWD remains at about 10^3 . The MWD is very steep at the lower end and the peak position has moved from $\sim 10^4$ to $\sim 5 \cdot 10^3$ ($C_{700}-C_{350}$).

The reason for the difference in degradation rate between low and high oxygen concentrations is not clearly understood. A reaction that involves equilibrium conditions between oxygen and active sites for chain scission in the polymer, could be an explanation. If this is true the oxygen concentration at 410 p.p.m. should be too low for reaction whereas at 1000 p.p.m. reaction occurs. Furthermore at 1000 p.p.m. all active sites ought to be reactive and a further increase in oxygen concentration to 1900 p.p.m. should not cause any further chain scission. Work on elucidating the influence of oxygen on the chain scission is going on in our laboratory.

The curves in Figs. 11 and 12 cannot be super-imposed by sliding the time axis. Therefore it was not possible to construct an Arrhenius plot. The increase in rate at the high oxygen concentrations is 2-4 times, the lower value corresponding to the shortest heating times.

\bar{M}_w/\bar{M}_n and \bar{M}_z/\bar{M}_w values were calculated from GPC data and plotted against heating time at different oxygen levels (Fig. 14).

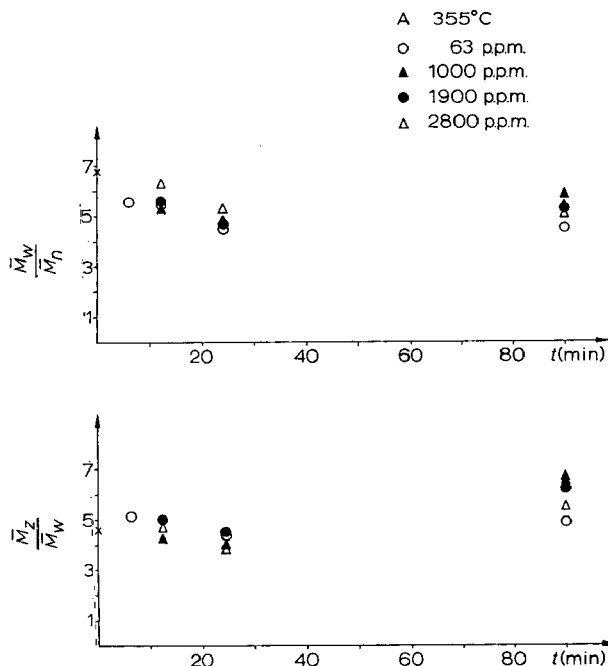


Fig. 14. \bar{M}_w/\bar{M}_n and \bar{M}_z/\bar{M}_w values for sample A, heated at 355°.

The \bar{M}_w/\bar{M}_n and \bar{M}_z/\bar{M}_w values are remarkably constant and not consistent with the drastic drop in \bar{M}_w/\bar{M}_n reported earlier, *e.g.*, by ARNETT AND STACY¹¹, for a HDPE resin. Our plots indicate a shallow minimum in the order of 4 and no continuous decrease of \bar{M}_w/\bar{M}_n approaching a value of 2, which should be expected from current theories of random scission.

ACKNOWLEDGEMENTS

This work was financially supported by the Swedish Board of Technical Development (STU).

The authors wish to thank Dr. L. BINDER, Unifos Kemi AB, for supplying LDPE-resin and for valuable discussions in the course of the work, Dr. E. DROTT, Monsanto, for sending his computer program, Ing. C. LARSSON and Ing. G. HEDLUND for GPC and viscosity measurements and Ing. B. JOHANSSON for technical assistance.

REFERENCES

- 1 W. G. OAKS AND R. B. RICHARDS, *J. Chem. Soc.*, (1949) 2929.
- 2 L. REICH AND S. S. STIVALA, *Rev. Macromol. Chem.*, 1 (1966) 249.
- 3 L. A. WALL, *J. Res. Natl. Bur. Std.*, 41 (1948) 315.
- 4 H. H. G. JELLINEK, *J. Polymer Sci.*, 4 (1949) 1.
- 5 S. L. MADORSKY, *Science*, 111 (1950) 360.
- 6 P. P. LUFF AND M. WHITE, *Vacuum*, 18 (1968) 437.
- 7 Y. TSUCHIYA AND K. SUMI, *J. Polymer Sci., A-1*, 6 (1968) 415.
- 8 D. A. ANDERSON AND E. S. FREEMAN, *J. Polymer Sci.*, 54 (1961) 253.
- 9 S. IGARASHI AND H. KAMBE, *Bull. Chem. Soc. Japan*, 37 (1964) 176.
- 10 H. M. QUACKENBOS, *Polymer Eng. Sci.*, 6 (1966) 117.
- 11 R. L. ARNETT AND C. J. STACY, *Polymer Eng. Sci.*, 6 (1966) 295.
- 12 Z. GRUBISIC, P. REMPP AND H. BENOIT, *J. Polymer Sci., B*, 5 (1967) 753.
- 13 E. E. DROTT, *Reprints, 4th Intern. Seminar on Gel Permeation Chromatography, Miami Beach, May 1966*.
- 14 L. WILD AND R. GULIANA, *J. Polymer Sci., A-2*, 5 (1967) 1087 and *Seminar Proceedings, 6th Intern. Seminar on Gel Permeation Chromatography, Miami Beach, October 1968*.
- 15 K. A. BONI, F. A. SLIEMERS AND P. B. STICKNEY, *J. Polymer Sci., A-2*, 6 (1968) 1567, 1579.
- 16 D. J. POLLOCK AND R. F. KRATZ, *Seminar Proceedings, 6th Intern. Seminar on Gel Permeation Chromatography, Miami Beach, October 1968*.
- 17 H. COLL AND D. K. GILDING, *Seminar Proceedings, 7th Intern. Seminar on Gel Permeation Chromatography, Monte Carlo, October 1969*.
- 18 R. PANARIS AND R. PRECHNER, Paper presented at 7th Intern. Seminar on Gel Permeation Chromatography, Monte Carlo, October 1969.
- 19 P. CROUZET, A. MARTENS AND P. MANGIN, *Seminar Proceedings, 7th Intern. Seminar on Gel Permeation Chromatography, Monte Carlo, October 1969*.
- 20 T. WILLIAMS AND I. M. WARD, *J. Polymer Sci., B*, 6 (1968) 621.
- 21 E. E. DROTT AND R. A. MENDELSON, *Seminar Proceedings, 6th Intern. Seminar on Gel Permeation Chromatography, Miami Beach, October 1968*.
- 22 T. ENGEL, *Diploma work*, Chalmers University of Technology, Gothenburg, Sweden, 1969.

CHROM. 4974

CALCULATION OF THE WEIGHT AND NUMBER FUNCTIONS OF MOLECULAR WEIGHT DISTRIBUTION FOR OLIGOMERS FROM THE GEL PERMEATION CHROMATOGRAPHY DATA

V. V. EVREINOV, A. K. ROMANOV AND S. G. ENTELIS

Institute of Chemical Physics, Academy of Sciences, Moscow (U.S.S.R.)

SUMMARY

A method is developed to calculate the weight and number functions of molecular weight distribution for oligomers. The influence of the shape of the chromatographic bands of the individual substances on the molecular weight distribution function is discussed, both as the influence on the instrumental spreading and as the change of the refraction index with the molecular weight. The weight, number functions, M_n and M_w were obtained for the condensation oligomers of poly(diethylene glycol adipinates) with molecular weight 400–1200.

Gel permeation chromatography (GPC) is a convenient fast method for determining the molecular weight distribution (MWD) of oligomers. However, it is a complicated problem to obtain weight and number MWD functions from the GPC data. TUNG¹ suggested two methods of calculation of the MWD function for polymers: solving the integral equation of a gel chromatogram by the least-squares method, and by the method of "polynomial expansion". These methods, especially in the resolution chromatogram range, are difficult to apply to oligomers. There are practically no literature data on calculations of the MWD function for oligomers.

A method of calculation of the weight and number MWD functions from the GPC data for oligomers has been outlined in the present paper. The influence of shape of the individual substance chromatographic band (SCBIS) and of the changes in instrumental spreading and refraction index with molecular weight on the distribution is discussed.

Let us write the equation of a gel chromatogram $F(v)$, when (SCBIS) is given by a Gaussian function, whose half-width does not depend on eluent volume:

$$F(v) = \sum_{i=1}^n A(v_i) e^{-h(v-v_i)^2} \quad (1)$$

In eqn. 1 v_i is the eluent volume at maximum of Gaussian curve, $A(v_i)$ is a function which characterizes the weight concentration of substance, h is the resolution factor. The interpretation of gel chromatogram $F(v)$ consists in determining the dependence $A(v_i) = f(M_i)$, i.e. in calculating the weight function distribution $w(M)$, if the calibration curve $\log M$ vs. v is known.

Let us compare, at the point v_k , the values $F(v_k)$ on the gel chromatogram with the maximum value of Gaussian curve $A(v_k)$ which characterizes the oligomer weight fraction of the given chain length*. Let us expand the function $A(v_i)$ to the left and right from the point v_k , and find the value $F(v_k)$, assuming that the function $A(v_i)$ is rather smooth:

$$F(v_k) = \sum_{i=1}^n \sum_{j=0}^{\infty} A^{(j)}(v_k) \frac{(v_i - v_k)^j}{j!} e^{-h(v_i - v_k)^2} \quad (2)$$

Having considered $F(v_k)$ for $m + 1$ of the range members of the decomposition function $A(v_i)$ at the point v_k , we obtain

$$F(v_k) = \sum_{i=1}^n \sum_{j=0}^m A^{(j)}(v_k) \frac{(v_i - v_k)^j}{j!} e^{-h(v_i - v_k)^2}. \quad (3)$$

On differentiating eqn. 3 we get the derivative:

$$F^{(s)}(v_k) = \sum_{i=1}^n \sum_{j=0}^m \sum_{p=0}^s C_s^p A^{(j+s-p)}(v_k) \left[\frac{(v_i - v_k)^j}{j!} e^{-h(v_i - v_k)^2} \right]^{(p)} \quad (4)$$

Denoting $j + s - p = t$ and expanding $F^{(s)}(v_k)$ with respect to $A^{(t)}$ we have

$$F^{(s)}(v_k) = \sum_{t=0}^{m+s} A^{(t)}(v_k) \sum_{\substack{i=1 \\ p=0}}^m \sum_{\substack{p=s-t \text{ for } 0 \leq t < s \\ \text{for } t \geq s}}^s C_s^p \left[\frac{(v_i - v_k)^{t-s+p}}{(t-s+p)!} e^{-h(v_i - v_k)^2} \right]^{(p)} \quad (5)$$

If we neglect the terms $A^{(t)}$ having $t > m$, we shall obtain a system of $m + 1$ linear equations with respect to $A^{(t)}$. The derivatives $F^{(s)}(v_k)$ are calculated from the experimental data, i.e. from the gel chromatogram.

Finding of the height of the Gaussian curve in the basic point is reduced to the solving of a system of $m + 1$ linear equations with respect to $A(v_k)$.

In this case the whole solution is:

$$A = \frac{\det \|D_{ts}\|}{\det \|B_{ts}\|}$$

where

$$B_{ts} = \sum_{i=0}^n \sum_{\substack{p=s-t \text{ for } 0 \leq t < s \\ \text{for } t \geq s}}^s C_s^p \left[\frac{(v_i - v_k)^{t-s+p}}{(t-s+p)!} e^{-h(v_i - v_k)^2} \right]^{(p)} \quad (6)$$

and the matrix $\|D_{ts}\|$ is obtained on substitution of the column B_{0s} for the column $F^{(s)}(v_k)$ in matrix $\|B_{ts}\|$.

Zero approximation:

$$F^{(0)}(v_k) = \sum_{i=1}^n A^{(0)}(v_k) e^{-h(v_i - v_k)^2}; \quad (7)$$

thus:

$$A(v_k) = \frac{F(v_k)}{\sum_{i=1}^n e^{-h(v_i - v_k)^2}} \quad (8)$$

*The basic point v_k corresponds to the real value of molecular weight of the oligomer $M_0 K$, where M_0 is the weight of the segments, and K is the degree of polymerization.

From eqn. 8 it follows that the contribution of neighbour Gaussian curves at the point v_k is realized with the height equal to a Gaussian curve with maximum at the point v_k . It influences the accuracy of determination of $A(v_k)$ at sufficient densities of overlapping functions and large values of $A^{(1)}$.

Linear approximation: $m = 1$, $S_{\max} = 1$:

$$F^{(0)}(v_k) = A^{(0)}(v_k) \sum_{i=1}^n e^{-h(v_i-v_k)^2} + A^{(1)}(v_k) \sum_{i=1}^n (v_i - v_k) e^{-h(v_i-v_k)^2} \quad (9)$$

$$F^{(1)}(v_k) = A^{(0)}(v_k) \sum_{i=1}^n 2h(v_i - v_k) e^{-h(v_i-v_k)^2} + A^{(1)}(v_k) \sum_{i=1}^n 2h(v_i - v_k)^2 e^{-h(v_i-v_k)^2} \quad (10)$$

In $F^{(1)}(v_k)$ the term containing $A^{(2)}$ is neglected. Consequently, matrixes $\|B_{ts}\|$ and $\|D_{ts}\|$ are:

$$B_{ts} = \begin{pmatrix} \sum_{i=1}^n e^{-h(v_i-v_k)^2} & \sum_{i=1}^n (v_i - v_k) e^{-h(v_i-v_k)^2} \\ \sum_{i=1}^n 2h(v_i - v_k) e^{-h(v_i-v_k)^2} & \sum_{i=1}^n 2h(v_i - v_k)^2 e^{-h(v_i-v_k)^2} \end{pmatrix} \quad (11)$$

$$D_{ts} = \begin{pmatrix} F^{(0)} & \sum_{i=1}^n (v_i - v_k) e^{-h(v_i-v_k)^2} \\ F^{(1)} & \sum_{i=1}^n 2h(v_i - v_k)^2 e^{-h(v_i-v_k)^2} \end{pmatrix} \quad (12)$$

and the solution will be:

$$A(v_k) = \frac{F^{(0)}(v_k) - F^{(1)}(v_k) \frac{\sum_{i=1}^n (v_i - v_k) e^{-h(v_i-v_k)^2}}{\sum_{i=1}^n 2h(v_i - v_k)^2 e^{-h(v_i-v_k)^2}}}{\sum_{i=1}^n e^{-h(v_i-v_k)^2} - \frac{2h \left[\sum_{i=1}^n (v_i - v_k) e^{-h(v_i-v_k)^2} \right]^2}{\sum_{i=1}^n 2h(v_i - v_k)^2 e^{-h(v_i-v_k)^2}}} \quad (13)$$

The expression for quadratic and higher approximations can be obtained in a similar manner.

In practice, the suggested method of calculation of MWD functions for oligomers is reduced to a calculation of $A(v_k)$ by means of a computer.

The accuracy of the suggested method of calculation of the weight function $w(M)$ can be seen from Fig. 1. For an arbitrarily fixed $w(M)$ (full lines), gel chromatograms were computed by superposition of Gaussian curves in the basic points of the calibration curves (Fig. 2)*. From these gel chromatograms, using zero, linear, and quadratic approximations, the function $w(M)$ was calculated, which in the case of correct assumptions must coincide with the initial one. As it is seen from Fig. 1a, for

* Half-width 0.7 count.

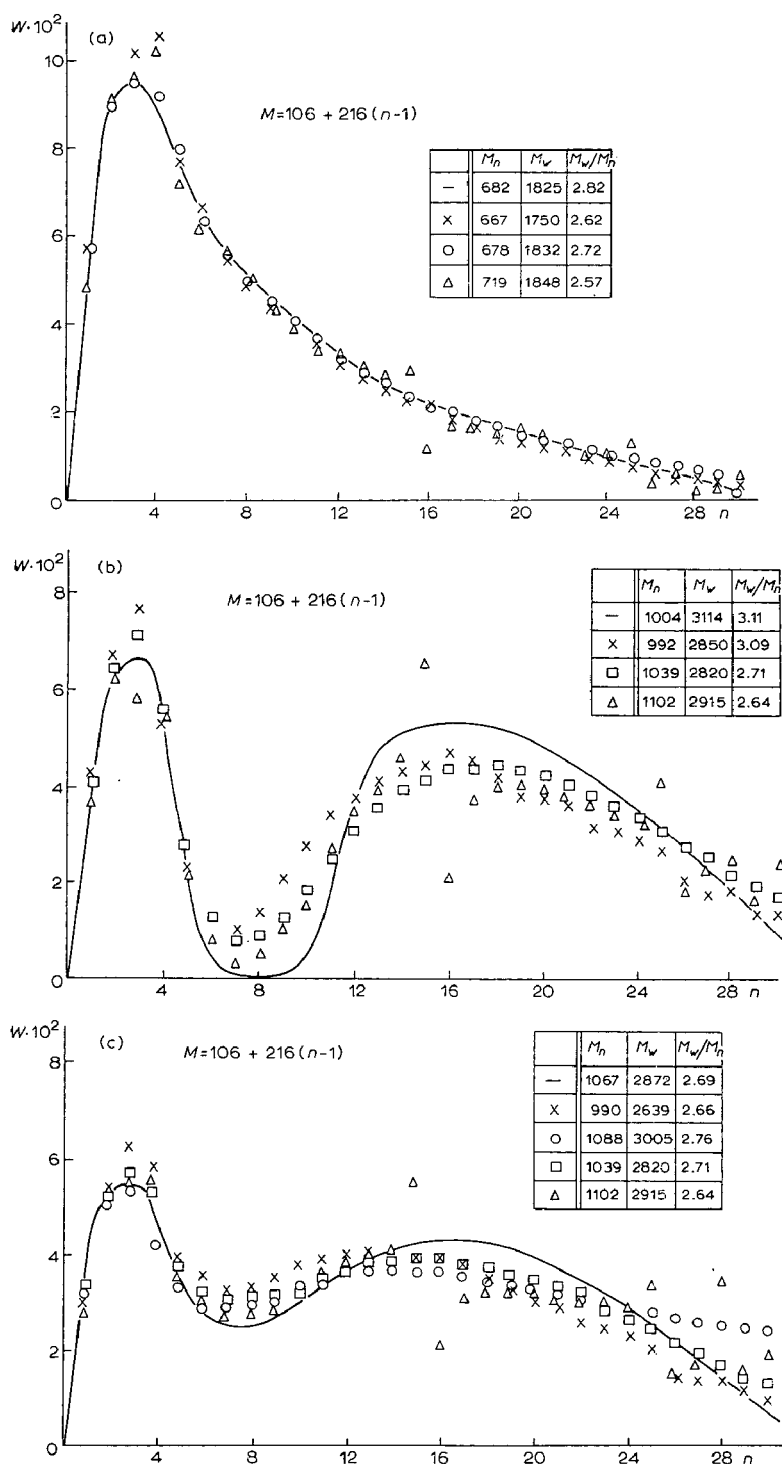


Fig. 1. (a, b, c). The weight functions of oligomer distribution. —, theoretical curves; x, calculated by means of eqns. 15 and 16; ○, zero approximations; □, linear approximations; △, quadratic approximations.

unimodal MWD function, the zero approximation gives a good agreement between the obtained $w(M)$ and the fixed one. The linear approximation for bimodal distribution describes the fixed function $w(M)$ (Fig. 1a and c) better than the zero approximation.

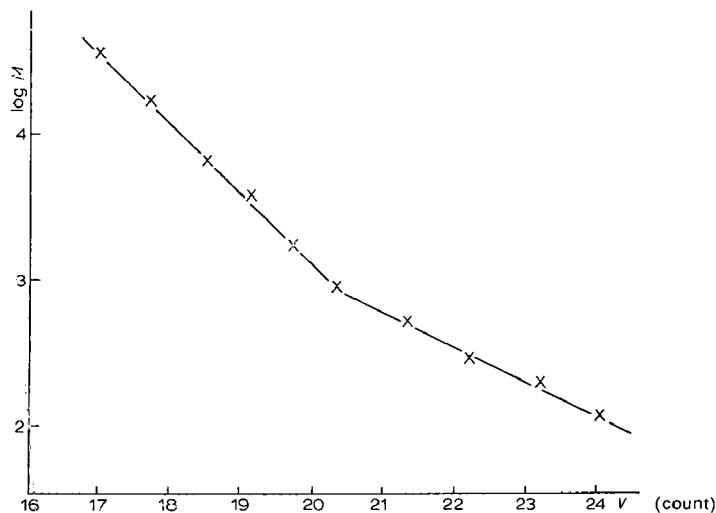


Fig. 2. The calibration curve for (PDEGA).

In calculation by means of the quadratic approximation, oscillations occur due to higher sensitivity to errors. With respect to the half-widths of Gaussian curves and the density of their overlapping, the oscillations may occur in higher approximations.

To estimate the weight and number MWD functions of oligomers, a simpler method has been suggested.

For the unresolved part of a gel chromatogram of a polydispersed sample, the weight concentration of the individual substance is:

$$A(v_k) = \frac{F(v_k)(v_{k+1} - v_{k-1})}{a \times 2} \quad (14)$$

If the area under the Gaussian curve is $S = A\sqrt{\pi/h}$, and a is the half-width, we shall have

$$S = A \frac{a}{2} \sqrt{\frac{\pi}{\ln 2}} \simeq A \times a, \quad (15)$$

and for the linear part of the calibration curve $\log M = C_1 - C_2 v$ we get:

$$A(v_k) = \frac{F(v_k)}{2aC_2} \log \frac{M_{k+1}}{M_{k-1}} \quad (16)$$

For the resolution range of the chromatogram the value $A(v_k)$ is found by using eqn. 15.

For the cases considered previously, the function $w(M)$ calculated using eqns. 15 and 16 is shown in Fig. 1.

Figs. 3 and 4 represent the weight and number MWD functions obtained by

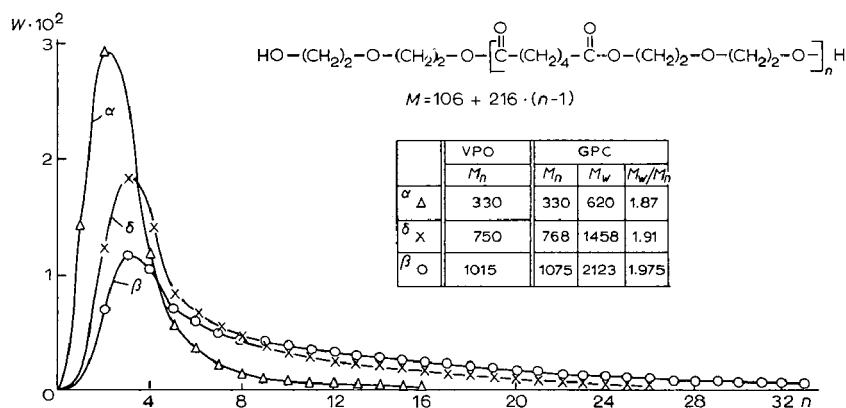


Fig. 3. The weight functions of MWD. α, $M_n = 330$; δ, $M_n = 750$; β, $M_n = 1015$.

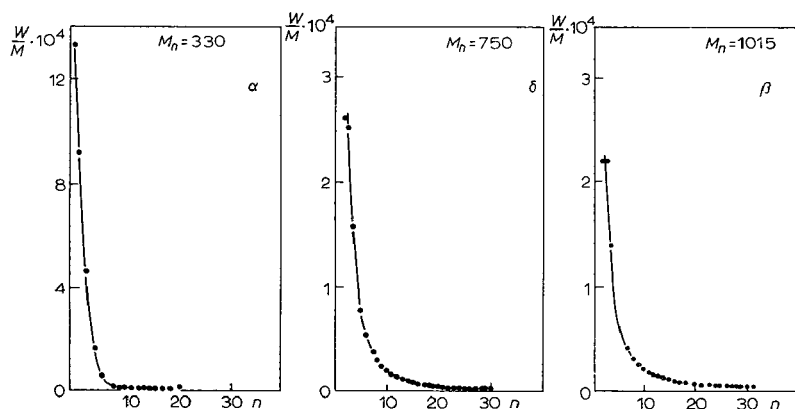


Fig. 4. The number functions of MWD for (PDEGA). α, $M_n = 330$; δ, $M_n = 750$; β, $M_n = 1015$.

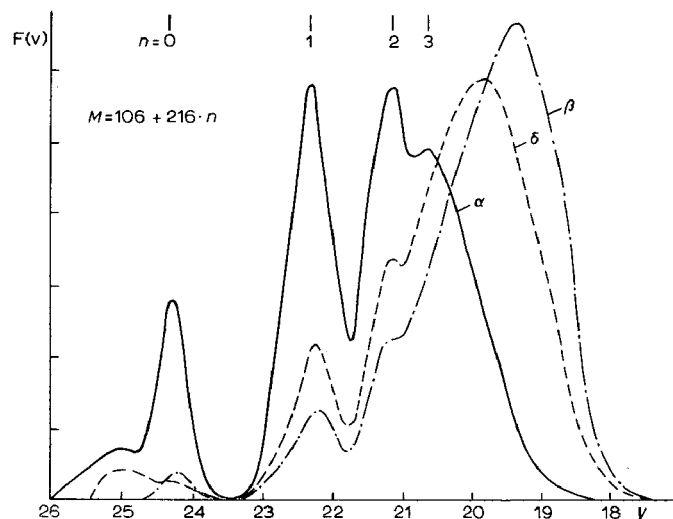


Fig. 5. Gel chromatograms of (PDEGA). Waters G 200 column 1-60 Å, 10³ Å, 10⁴ Å styrogel; solvent, tetrahydrofuran; eluent flow rate, 1 ml/min.

means of eqns. 15 and 16 for poly(diethylene glycol adipate) (PDEGA) oligomers. The examples of chromatograms obtained with a Waters G-200 unit are shown in Fig. 5, and the calibration curve $\log M$ vs. v is in Fig. 2. A good agreement has been obtained between M_n calculated from the determined MWD function and M_n measured by an independent method.

In the previous cases it was assumed that the instrumental spreading (h) and refraction index $C(v_i)$ do not depend on molecular weight, and that (SCBIS) has a Gaussian shape. However, there are cases when these assumptions may lead to considerable errors in determining MWD. The suggested method allows the determination of $w(M)$ if the (SCBIS), $f(v)$ and the dependence of h and $C(v_i)$ on M are known.

In this case, eqns. 3, 5 and 6 will be:

$$F(v_k) = \sum_{i=1}^n \sum_{j=0}^m A^{(j)}(v_k) \frac{(v_i - v_k)^j}{j!} C(v_i) f(v_i - v_k), \quad (17)$$

$$F^{(s)}(v_k) = \sum_{t=0}^{m+s} A^{(t)}(v_k) \sum_{i=1}^n \sum_{\substack{p=s-t \text{ for } 0 \leq t < s \\ p=0 \text{ for } t \geq s}}^s C_s^p \left[\frac{(v_i - v_k)^{t-s+p}}{(t-s+p)!} C(v_i) f(v_i - v_k) \right]^{(p)} \quad (18)$$

$$B_{ts} = \sum_{i=1}^n \sum_{\substack{p=s-t \text{ for } 0 \leq t < s \\ p=0 \text{ for } t \geq s}}^s C_s^p \left[\frac{(v_i - v_k)^{t-s+p}}{(t-s+p)!} C(v_i) f(v_i - v_k) \right]^{(p)} \quad (19)$$

To our mind, for the description of (SCBIS) $f(v)$, it is more convenient to use the function of the type:

$$\begin{cases} f(v) = \frac{\rho(\rho v)^{\alpha-1} e^{-\rho v}}{\Gamma(\alpha)} & (v > 0) \\ f(v) = 0 & (v < 0) \end{cases} \quad (20)$$

where ρ and α are parameters, and $\Gamma(\alpha)$ is gamma function. By varying the parameters ρ and α the shape of the line may be changed.

Finally, it should be noted that the suggested method of calculation of the MWD function for a system of oligomers can be applied to the determination of the weight function of polymers.

In a common case, the choice of the number of basic points v_k in which $A(v_k)$ is calculated depends on the function $w(M)$.

The estimation of the possibilities of the suggested method will be the subject of further investigations.

REFERENCE

I. L. H. TUNG, *J. Appl. Polymer Sci.*, **10** (1966) 375.

J. Chromatog., **53** (1970) 109-115

CHROM. 5041

SHAPE OF THE CHROMATOGRAPHIC BAND FOR INDIVIDUAL SPECIES AND ITS INFLUENCE ON GEL PERMEATION CHROMATOGRAPHIC RESULTS

D. D. NOVIKOV, N. G. TAGANOV, G. V. KOROVINA AND S. G. ENTELIS

Institute of Chemical Physics, Academy of Sciences, Moscow (U.S.S.R.)

SUMMARY

The determination of the real differential molecular weight distribution requires that the instrumental spreading of the chromatographic band should be taken into account accurately. In other words, the dependence of the instrumental spreading function for an individual substance on the eluent volume should be known under experimental conditions.

Current methods of calculations do not deal with a continuous change in the shape of the chromatographic band for individual species (SCBIS) due to the molecular weight. This may be due to inaccurate differential DMWD results.

The methods of calculating MWD data from GPC involving the continuous change in SCBIS are presented in this work.

In gel permeation chromatography (GPC) the correlation between the raw chromatogram, $f(v)$, and the chromatogram after correction for instrumental spreading, $w(y)$, is given by the integral eqn. 1 which was first suggested by TUNG¹.

$$f(v) = \int_{-\infty}^{\infty} w(y) G(v-y) dy \quad (1)$$

v and y are interchangeable and are used to indicate the eluent volume; y is used mainly to indicate the eluent volume as a variable under the integral sign. $G(v-y)$ is a function which determines all types of instrumental spreading.

The real chromatogram represents a superposition of the resulting curves of a finite number of the individual species. It is assumed for the simplicity of calculations that the chromatogram of the individual species is described by a Gaussian function². However, the discrepancy between the average molecular weights calculated upon that assumption and obtained by independent methods indicates the necessity of accounting for the deviation of shape of the chromatographic band for individual species (SCBIS) from the Gaussian curve³⁻⁵.

PROVDER AND ROSEN⁴ suggest the following expression to describe the SCBIS:

$$G(v-y) = \Phi(v-y) + \sum_{n=3}^{\infty} (-1)^n \frac{A_n}{n!} \frac{\Phi^{(n)}(v-y)}{(\sqrt{2h})^n} \quad (2)$$

where the first member $\Phi(v-y) = (h/\pi)^{1/2} \exp [-h(v-y)^2]$ is a Gaussian function and the second member takes into account the correction on symmetric and asymmetric deviation from Gaussian shape.

Three parameters (h , A_3 and A_4) have been used which can be determined with calibration standards with three known molecular weight distribution (MWD) characteristics, e.g., M_n , M_w , M_η (M_n is number-average, M_w is weight-average and M_η is viscosity-average molecular weight). Using the experimentally obtained dependences of h , A_3 and A_4 on eluent volume, and the refined HAMIELEC formulas⁶, one can obtain average molecular weight for any other polymer sample under the given conditions (viz. columns, temperature, solvent, etc.).

It should be noted that this method gives good results for M_n and M_w but does not guarantee the correct values for M_z , M_{z+1} nor the distribution function. This may be due to the fact that linear calibration was assumed as well as the fact that continuous SCBIS change is not taken into account in the range of interest.

In this paper we tried to take into account the continuous change of SCBIS. The following expression is assumed:

$$G(v,y) = \frac{1 + \sum_{i=0}^{\infty} a_i(y) (v-y)^i}{1 + \sum_{i=0}^{\infty} a_{2i}(y) \frac{(2i-1)!!}{(2h)^i}} \Phi(v-y) \quad (3)$$

where $\Phi(v-y) = (h/\pi)^{1/2} \exp [-h(v-y)^2]$, y is eluent volume corresponding to maximum on the chromatogram of individual species, v is the chromatogram abscissa, expressed in the eluent volume and $a_i(y)$ is a function characterising the change in SCBIS with the molecular weight of individual species. The expression (3) contains members which depend only on y , that permit variation of the effective half-width and deviation from Gaussian shape according to the experimental conditions.

With eqn. 3 it is possible to obtain an analytical expression of the dependence of SCBIS on eluent volume. It should be noted that the expression is normalised at any fixed y .

Thus, to find MWD it is necessary to determine h and $a_i(y)$, using the set of well-characterised narrow polymer fractions, i.e. to carry out the SCBIS calibration under the given experimental conditions.

The SCBIS calibration proceeds in two stages:

(1) By any method described in refs. 3, 5, 7-9, the resolution factor h is obtained for any standard. For further calculation h is taken as constant and equal to the arithmetic mean.

(2) Assuming that in the range of narrow polymer fractions which are used as standards, $a_i(y)$ is constant, $a_i(y)$ can be determined for every standard.

Therefore, formulas from HAMIELEC AND RAY expressions for average molecular weights should be used¹⁰:

$$M_k(t) = M_k(\infty) \frac{\left(1 + \sum_{i=1}^{i_0} a_i (-1)^i \frac{d^{(i)}}{ds^i}\right) e^{s^2/4h} \Big|_{s=(k-2)D_2}}{\left(1 + \sum_{i=1}^{i_0} a_i (-1)^i \frac{d^{(i)}}{ds^i}\right) e^{s^2/4h} \Big|_{s=(k-1)D_2}} \quad (4)$$

where $M_k(t)$ are average molecular weights, $(k=1)$ corresponds to M_n ($k=2$ to M_w , etc.), and

$$M_k(\infty) = D_1 \frac{\int_{-\infty}^{\infty} f(v) e^{(1-k)D_2 v} \cdot dv}{\int_{-\infty}^{\infty} f(v) e^{(2-k)D_2 v} \cdot dv} \quad (5)$$

D_1 and D_2 are parameters of calibration curve

$$M = D_1 e^{-D_2 v}.$$

i_0 is the number of known average molecular weights (it determines the number of terms in eqn. 3).

Having solved the system (4) with respect to a_i ($i=1, 2, \dots, m$) for all of the available standards, we obtain the dependence of a_i on eluent volume. This dependence may be approximated for convenience by polynomials of k_0 degree.

Thus,

$$a_i(y) = \sum_{k=0}^{k_0} a_{i,k} y^k. \quad (6)$$

After calibrating SCBIS we may introduce the correction for the instrumental spreading of the polymer chromatogram of any unknown distribution. Thus, we solve eqn. 7, which represents by itself eqn. 1, accounting for eqns. 3 and 6.

$$f(v) = \int_{-\infty}^{\infty} w(y) \frac{1 + \sum_{i=1}^{i_0} \sum_{k=0}^{k_0} a_{i,k} y^k (v-y)^i}{1 + \sum_{i=1}^I \sum_{k=0}^{k_0} a_{2i,k} y^k \frac{(2i-1)!!}{(2h)^i}} \Phi(v-y) dy \quad (7)$$

where

$$I = \begin{cases} i_0/2, & \text{if } i_0 \text{ is even} \\ (i_0-1)/2, & \text{if } i_0 \text{ is odd.} \end{cases}$$

The solution of eqn. 7 may be realised by the following scheme: Let us denote

$$H(y) = \frac{w(y)}{1 + \sum_{i=1}^I \sum_{k=0}^{k_0} a_{2i,k} y^k \frac{(2i-1)!!}{(2h)^i}}.$$

Represented in eqn. 7

$$\Phi(v-y) = (h/\pi)^{1/2} \sum_{m=0}^{m_0} \frac{(-h)^m}{m!} (v-y)^{2m}$$

and regrouping the members we obtain eqn. 8.

$$f(v) = \sum_{j=0}^{2m_0+i_0} v^j \sum_{m=\alpha}^{m_0} \sum_{i=\beta}^{i_0} \sum_{k=0}^{k_0} \sqrt{\frac{h}{\pi}} a_{ik} \frac{(-h)^m (2m+i)! (-1)^{2m+i-j}}{m! j!(2m+i-j)!} \int_{-\infty}^{\infty} y^{2m+i+k-j} H(y) dy \quad (8)$$

where

$$\alpha = \begin{cases} \max. \left(0, \frac{j-i_0}{2} \right), & \text{if } j-i_0 \text{ is even} \\ \max. \left(0, \frac{j-i_0-1}{2} \right), & \text{if } j-i_0 \text{ is odd,} \end{cases}$$

and

$$\beta = \max. (0, j-2m), \quad \begin{aligned} a_{00} &= 1, \\ a_{0k} &= 0 \text{ for } k = 1, 2, \dots, k_0. \end{aligned}$$

It should be noted that the right hand part of eqn. 8 is the expansion of $f(v)$ of v degrees. Let $f(v)$ be $\sum_{j=0}^{2m_0+i_0} C_j v^j$, and equating coefficients of the same power, we obtain the system of linear algebraic eqn. 9 for the determination:

$$\int_{-\infty}^{\infty} y^n H(y) dy; \\ C_j = \sum_{n=0}^{2m_0+i_0+k_0-j} \sum_{m=\gamma_1}^{\gamma_2} \sum_{i=\eta_1}^{\eta_2} a_{i, n+j-2m-i} (h/\pi)^{1/2} \frac{h^m (2m+i)! (-1)^{m+i-j}}{m! j!(2m+i-j)!} \int_{-\infty}^{\infty} y^n H(y) dy \quad (9)$$

where

$$\gamma_1 = \begin{cases} \max. \left(\alpha, \frac{n+j-i_0-k_0}{2} \right), & \text{if } n+j-i_0-k_0 \text{ is even,} \\ \max. \left(\alpha, \frac{n+j-i_0-k_0-1}{2} \right), & \text{if } n+j-i_0-k_0 \text{ is odd,} \end{cases}$$

$$\gamma_2 = \begin{cases} \min. \left(m_0, \frac{n+j}{2} \right), & \text{if } n+j \text{ is even,} \\ \min. \left(m_0, \frac{n+j-1}{2} \right), & \text{if } n+j \text{ is odd;} \end{cases}$$

$$\eta_1 = \max. (\beta, n+j-2m-k_0),$$

$$\eta_2 = \min. (i_0, n+j-2m).$$

In eqn. 9 the coefficients at integrals sufficiently decrease with increasing n . It allows one to neglect the integrals with $n > 2m_0 + i_0$.

Thus, we have the system of equations,

$$\int_{-\infty}^{\infty} H(y) y^n dy = A_n, \quad n = 0, 1, 2, \dots, 2m_0 + i_0 \quad (10)$$

representing $H(y)$ in the range of Sin

$$H(y) = \sum_{j=1}^{j_0} b_j \sin \left[j \frac{\pi}{y_k - y_0} (y - y_0) \right] \quad (11)$$

where y_0 and y_k are the beginning and termination of the carrier $w(y)$, respectively.

Substituting (11) into (10) and integrating, we obtain the following system of equations for determining b_j :

$$A_n = \sum_{j=1}^{j_0} b_j \sum_{m=0}^n y_0^{n-m} \frac{(y_k - y_0)}{\pi m} \frac{n!}{m!(n-m)!} \times$$

$$\left[\sum_{k=0}^m \frac{m!}{(m-k)!} \frac{\pi^{m-k}}{j^{k+1}} \cos \left(j + \frac{i}{2} k \right) \pi - \frac{m!}{j^{m+1}} \cos \frac{\pi m}{2} \right] \quad n = 0, 1, 2, \dots, j. \quad (12)$$

Now, we solve that system for b_j :

$$w(y) = \left(1 - \sum_{i=1}^I \sum_{k=0}^{k_0} a_{2i,k} y^k \frac{(2i-1)!!}{(2k)^i} \right) \sum_{j=1}^{j_0} b_j \sin \left(j \pi \frac{y - y_0}{y_k - y_0} \right) \quad (13)$$

For the linear calibration ($v = c_1 + c_2 \ln M$) an analytical solution of TUNG's equation can be obtained, taking into account the dependence of SCBIS on molecular weight. For this purpose, the following expression for SCBIS can be employed:

$$G(v, y) = \Phi(v - y) + \sum_{i=3}^{\infty} a_i(y) \Phi^{(i)}(v - y) \quad (14)$$

where $\Phi(v - y) = \sqrt{h/\pi} \exp [-h(v - y)^2]$, $\Phi^{(i)}(v)$ is the i -th derivative of $\Phi(v)$; $a_i(y)$ and h have the same meaning as in eqn. 3.

The calibration of SCBIS is carried out according to the scheme suggested above. Only eqn. 4 is replaced by the following equation:

$$\frac{M_k(t)}{M_k(\infty)} = \frac{1 + \sum_{i=3}^{\infty} a_i (k-2)^i D_2^i}{1 + \sum_{i=3}^{\infty} a_i (k-1)^i D_2^i} \exp \left[(3-2k) \frac{D_2^2}{4h} \right] \quad (15)$$

To make the calculations easier, let us represent $a_i(y)$ in the form of a cubic polynomial

$$a_i(y) = \sum_{k=0}^3 d_{ik} y^k \quad (16)$$

By substituting eqns. 14 and 16 into TUNG's equation, we obtain:

$$f(v) = \int_{-\infty}^{\infty} w(y) \Phi(v-y) dy + \sum_{i=3}^{i_0} \sum_{k=0}^3 a_{ik} \int_{-\infty}^{\infty} y^k w(y) \Phi^{(i)}(v-y) dy. \quad (17)$$

(i_0 is the number of known molecular weight averages of the samples used in the calibration of SCBIS plus three).

To solve the above equation we shall use the two-sided Laplace transformation, as suggested by HAMIELEC AND RAY¹⁰.

$$\bar{F}(s) = \bar{w}(s) e^{s^2/4h} + \sum_{i=3}^{i_0} \sum_{k=0}^3 a_{ik} (-1)^k \bar{w}^{(k)}(s) s^i e^{s^2/4h} \quad (18)$$

or

$$\bar{w}(s) + \sum_{i=3}^{i_0} \sum_{k=0}^3 a_{ik} (-1)^k \bar{w}^{(k)}(s) s^i = \bar{F}(s) e^{-s^2/4h}, \quad (19)$$

where

$$F(s) = \int_{-\infty}^{\infty} f(v) e^{-sv} dv; \quad w(s) = \int_{-\infty}^{\infty} w(v) e^{-sv} dv.$$

Here, $\bar{w}^{(k)}(s)$ is the k -th derivative of $\bar{w}(s)$; s is, generally speaking, a complex variable, but from the standpoint of using the formulae obtained we can limit ourselves only to real values of s . Since $w(y)$ is unambiguously determined from the moments (Q_k) of DMWD, and

$$Q(k) = \int_{-\infty}^{\infty} w(y) D_1^{k-1} \exp[(1-k)D_2 y] dy \equiv D_1^{k-1} \bar{w}[(k-1)D_2] \quad (20)$$

the problem of determining $w(y)$ is reduced to the solution of the differential eqn. 18.

Let us represent $\bar{F}(s)$ in the form of a series

$$\bar{F}(s) = \sum_{n=0}^{\infty} b_n s^n \quad (21)$$

b_n in eqn. 21 can be determined from the experimental data using the expression

$$b_n = \frac{(-1)^n}{n!} \int_{-\infty}^{\infty} v^n f(v) dv \quad (22)$$

Since $f(v)$ is bounded in $(-\infty, +\infty)$ and is different from zero in the final interval $[a, b]$, it can be shown using eqn. 22 that the series converges uniformly to $\bar{F}(s)$.

The expansion of $e^{-s^2/4h}$ into a polynomial in s has the form

$$e^{-s^2/4h} = \sum_{m=0}^{\infty} \frac{(-1)^m}{m!(4h)^m} s^{2m} \quad (23)$$

and converges uniformly to $\exp(-s^2/4h)$.

Thus, the solution to eqn. 19 can be represented as a series

$$\bar{w}(s) = \sum_{j=0}^{\infty} x_j s^j \quad (24)$$

and converges to $\bar{w}(s)$.

Substituting eqns. 21, 23 and 24 into eqn. 19 and equating terms having the same power of s , we obtain

$$\begin{aligned} x_n &= \sum_{m=0}^{\gamma} \frac{(-1)^m}{m!(4h)^m} b_{n-2m} \quad (\text{for } n = 0, 1, 2) \\ x_n + \sum_{j=\alpha}^n x_j \sum_{i=\beta_1}^{\beta_2} (-1)^{i+j-n} a_{i,i+j-n} \frac{j!}{(n-i)!} &= \sum_{m=0}^{\gamma} \frac{(-1)^m}{m!(4h)^m} b_{n-2m} \quad (25) \\ (\text{for } n = 3, 4 \text{ etc.}) \end{aligned}$$

where

$$\begin{aligned} \alpha &= \max. (0, n-i_0); \\ \beta_1 &= \max. (3, n-j); \\ \beta_2 &= \min. (i_0, n, n+3-j); \\ \gamma &= \begin{cases} n/2, & \text{if } n \text{ is even,} \\ (n-1)/2, & \text{if } n \text{ is odd,} \end{cases} \end{aligned}$$

or

$$\begin{aligned} x_0 &= b_0; \\ x_1 &= b_1; \\ x_2 &= b_2 - \frac{1}{4h} b_0; \\ x_n &= \frac{1}{\left(1 - a_{33} \frac{n!}{(n-3)!}\right)} \times \\ &\quad \left\{ \sum_{m=0}^{\gamma} \frac{(-1)^m b_{n-2m}}{m!(4h)^m} - \sum_{j=\alpha}^{n-1} x_j \sum_{i=\beta_1}^{\beta_2} (-1)^{i+j-n} a_{i,i+j-n} \frac{j!}{(n-i)!} \right\} \quad (\text{for } n = 3, 4, 5 \text{ etc.}) \quad (26) \end{aligned}$$

Let us note that for physical reasons $w(y)$ is bounded and different from zero in the final interval $[c, d]$; since $x_n = [(-1)^n/n!] \int_{-\infty}^{\infty} y^n w(y) dy$, the series $\sum_{n=0}^{\infty} x_n s^n$ converges uniformly to $\bar{w}(s)$.

The determination of $w(y)$ is thus reduced to the determination of the coefficients b_i according to expression 22 and to the solution of system (26) with respect to x_n .

In the same way, expressions for average molecular weights (M_k) can also be obtained:

$$M_k = D_1 \frac{\sum_{n=0}^{\infty} x_n (k-1)^n D_2^n}{\sum_{n=0}^{\infty} x_n (k-2)^n D_2^n} \quad (27)$$

REFERENCES

- 1 L. H. TUNG, *J. Appl. Polymer Sci.*, **10** (1966) 375.
- 2 J. C. GIDDINGS, *Dynamics of Chromatography*, Marcel Dekker, New York, 1965.
- 3 M. HESS AND R. F. KRATZ, *J. Polymer Sci.*, **A2**, **4** (1966) 731.
- 4 T. PROVIDER AND E. M. ROSEN, *Am. Chem. Soc. Preprints*, Houston, U.S.A., 1970.
- 5 S. T. BALKE AND A. E. HAMIELEC, *J. Appl. Polymer Sci.*, **13** (1969) 1381.
- 6 A. E. HAMIELEC, *J. Appl. Polymer Sci.*, to be published.
- 7 H. E. PICKETT, M. J. R. CANTOW AND J. F. JOHNSON, *J. Polymer Sci.*, **C-21** (1968) 67.
- 8 L. H. TUNG, J. C. MOORE AND G. W. KNIGHT, *J. Appl. Polymer Sci.*, **10** (1966) 1261.
- 9 L. H. TUNG AND J. R. RUNYON, *J. Appl. Polymer Sci.*, **13** (1969) 2397.
- 10 A. E. HAMIELEC AND W. H. RAY, *J. Appl. Polymer Sci.*, **13** (1969) 1319.

J. Chromatog., **53** (1970) 117-124

CHROM. 5018

A MULTIPLE COLUMN GAS CHROMATOGRAPH

W. R. LANDIS AND T. D. PERRINE

National Institute of Arthritis and Metabolic Diseases, Bethesda, Md. 20014 (U.S.A.)

AND

GEORGE THOMAS

Division of Research Services, National Institutes of Health, Bethesda, Md. 20014 (U.S.A.)

(Received July 28th, 1970)

SUMMARY

In this article, we present the results of our study on the design, construction and use of a multiple column exploratory gas chromatograph. This device has a single oven and a single hydrogen flame detector, but has five valves, injection ports and columns in parallel, so that any one of the columns may be connected to the detector by switching its valve. Our purpose in developing this device was to provide a compact and inexpensive arrangement whereby a number of packings could be held immediately available in standby condition for a quick qualitative evaluation in the separation at hand. The design has also proved useful for preparative chromatography on a small scale.

One of the most time-consuming aspects of gas chromatography is the installation and conditioning of columns. Where a variety of columns are in intermittent use, considerable time is lost in making interchanges. We have tested a design in which five columns can be held at operating temperature with a normal carrier gas flow, and valved into operation as desired. Over a period of several years, we have found this method of operation to give satisfactory results.

Practical design considerations dictated that valving should take place at the low pressure, or at the detector end of the column. This implies that each column must have its own injection port, but that one detector system will suffice for all the columns in a single oven. If several columns are to be connected to a single detector, it may be desirable to provide a positive gas flow which will minimize dead spots and carry residual gases to the detector after a valve is closed. This is easy to do if a hydrogen flame detector is used, since column effluents can be valved into the hydrogen stream through very short connecting tubes.

The design adopted is shown schematically in Fig. 1. A pillar is used which contains five valves, injection and exhaust ports, connections to the individual columns, and a single detector mounted at the top of the pillar. Axial ducts in the pillar supply

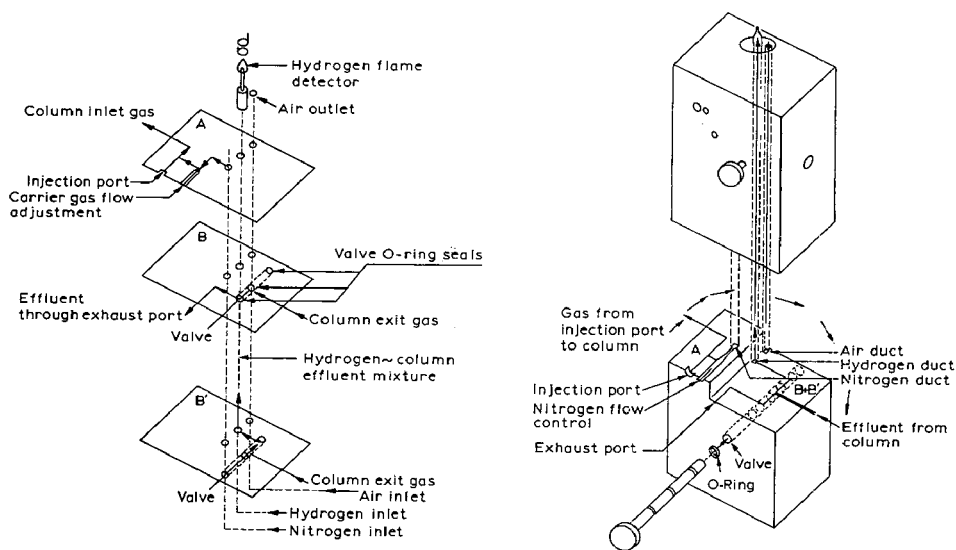


Fig. 1. A is a plane section through the column which contains the inlet port. B is a similar section through the exhaust port with the valve in closed position (*i.e.*, open to the exhaust port). B' is the same section, but with the valve open to the hydrogen (detector) duct. For each column in the chromatograph there is a plane A and plane B. The spacing between planes A and B is $\frac{3}{4}$ in., and between the adjacent A planes, $1\frac{1}{2}$ in. In order to provide proper heat circulation to the bottom column, the bottom A plane should be at least 3 in. from the floor of the oven.

hydrogen and air for the detector as well as carrier gas for the columns. Effluent from a column flows through its O-ring sealed valve and thence either to the exhaust port or to the hydrogen duct, where it mixes with the hydrogen and is carried directly to the detector.

The valve itself, which is built into the pillar, is a very simple arrangement of three ports and three O-rings, and is shown in Fig. 2*. This arrangement has been satisfactory for continuous operation at temperatures up to 150° , using silicone rubber or fluorocarbon O-rings (Parker compound Nos. S 455-7, S 318-6 and 77-545 (Viton) have proven satisfactory).

Above 150° , O-rings take a set and develop leaks. Therefore, for temperatures above this point we use a flat rotating graphite** disc to replace the O-ring valve. This has proved very satisfactory although its construction is a little more complicated than the O-ring type. Fig. 3a shows this type of valve and also outlines the arrangement of column connections, the mechanism for adjusting carrier gas flow and a simplified arrangement for conducting the carrier gas and the hydrogen streams.

The chief simplifications in construction involve the replacement of the dif-

* The hole for the valve is finished by forcing an oversized hardened steel ball through it. This not only burnishes the hole to a high finish, but slightly relieves the edges of the ports, and minimizes the tendency to cut the O-rings. The O-rings need only press very lightly against the bore of the tube, since the pressure at the valve is very small.

** Teflon is not suited to this application. Above 250° it begins to deteriorate rapidly, and corrodes the ambient metal. Moreover, contact of the column gas stream with Teflon is deleterious (see ref. 1). While we expected that graphite might show adsorption of column effluents, in fact, we have not noticed this effect.

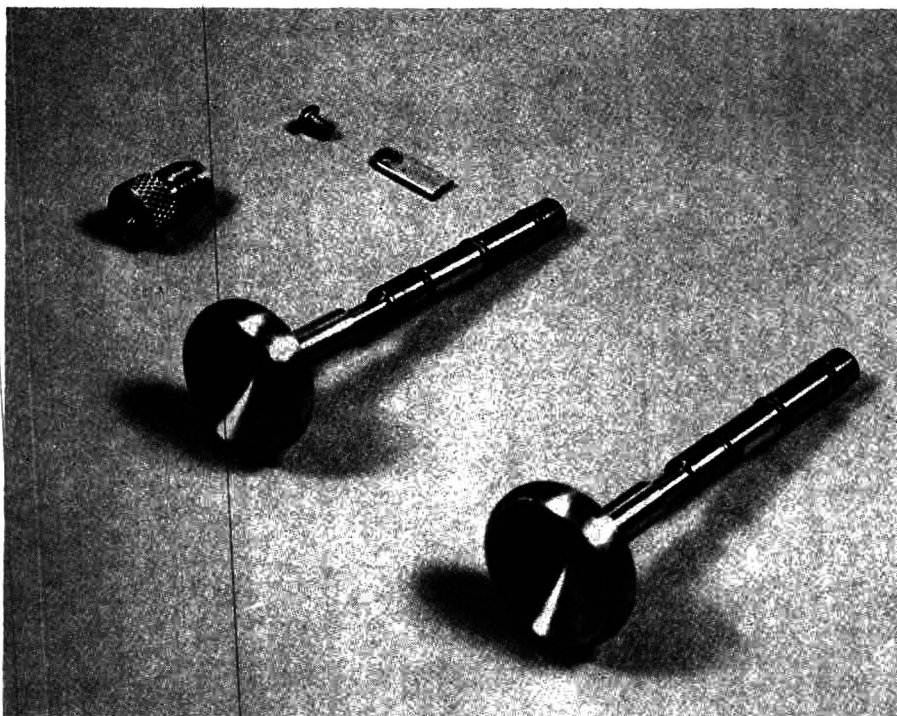


Fig. 2. Valves with O-rings for lower temperature application. The valve stems are $\frac{1}{4}$ in. diameter, relieved 0.010 in. between the O-rings. Movement of the valve is limited by the stop-tab shown. A septum retaining screw is also shown at the top of this figure. Although the valve handles shown here are of metal, they should actually be made of heat-insulating material.

difficult-to-make axial gas passages in the column by corresponding tubes fastened exterior to the pillar (E and F, Fig. 3a). It is feasible to furnace braze these carrier gas and hydrogen tubes to the back side of the column, and to drill into them at right angles to tap off for the various gas ports*. A second modification was introduced to overcome a problem with individual needle valves (D, Fig. 3a) which regulate the carrier gas flow for each column.

We have found it particularly unsatisfactory to attempt to regulate the carrier gas flow with a tapered needle which screws into the chromatograph pillar. Aside from the difficulty of getting the required finish in the hole, the needles tend to seize and break off—probably because when the column is heated there may be a lack of perfect concentricity of the needle stem threads with the carrier gas passage. The use of a steel ball in a tapered gas passage has been found to give far better results. This construction is detailed in the insert of Fig. 3b. If the ball N becomes wedged in the taper due to injudicious tightening of the screw, plug M can be removed and the ball tapped out with a punch.

Fig. 4 shows the appearance of a pillar for five low temperature ($\leq 150^\circ$)

* Faulty brazing which leads to internal leaks between the ports in the individual tubes is not of consequence, although large pockets of trapped gas between the valve and the hydrogen stream could lead to peak tailing. We have not observed such an effect.

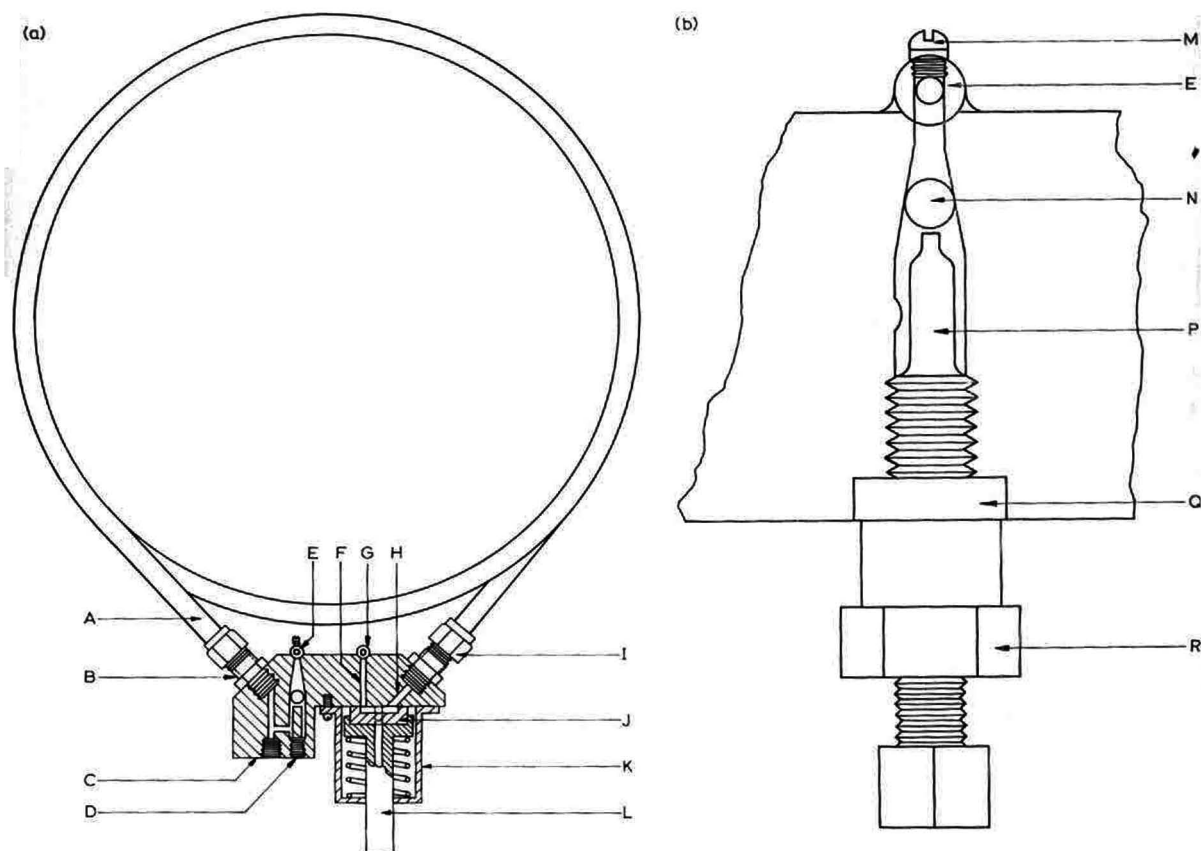


Fig. 3. (a) A valve for higher temperature application and the arrangement to the column. A = the circular column, B = column inlet, C = injection port, D = carrier gas flow control assembly, E = carrier gas supply tube, F = connecting passage, G = hydrogen supply tube (to detector), H = connecting passage, I = column outlet, J = carbon valve disc (showing valve in a position to connect column to detector), K = valve guide, L = valve stem. (b) Enlarged view of carrier gas flow regulator assembly. M = plug, E = carrier gas supply tube, N = ball, P = adjusting screw, Q = packing, R = gland nut.

columns. The valve for column 4 is in position to direct the column effluent to the detector. Fig. 5 is a corresponding view of a high temperature (150–300°) pillar utilizing an earlier version of the graphite valve shown in Fig. 3. In this type, the valve is essentially the same as the later version except that it is encased within the pillar rather than being on surface with the moving parts exposed. While this construction is quite satisfactory, it is very difficult to get a good finish on the bottom of the hole which forms the valve face, and the valve spring tends to lose its temper because of the high ambient temperature. The version shown in Fig. 3 represents a considerable simplification in construction and improvement in performance. Fig. 6 is a photograph of the component parts of this valve. Note the stainless steel stand-offs which insulate the valve guide from the pillar and help to minimize heat loss from the pillar. The valve stem is made of stainless steel for the same reason.

Inasmuch as the pillar contains the inlet and exhaust ports for each column,

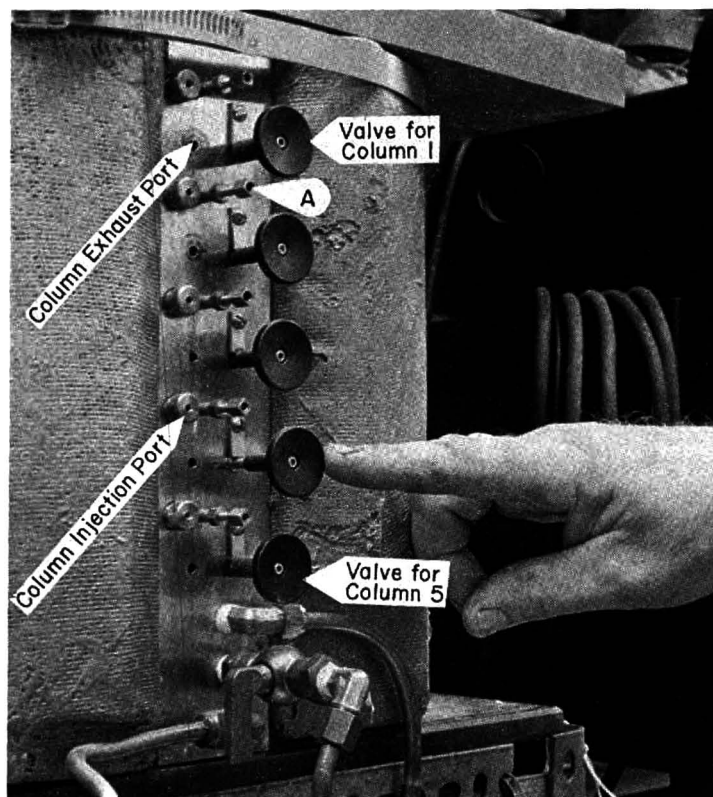


Fig. 4. Pillar for O-ring type valves for use at temperatures not exceeding 150°.

it needs to be heated somewhat above the ambient temperature for the columns. This is accomplished by means of small cartridge heaters placed immediately adjacent to each injection port. The top four ports use 65 W heaters, while a 130 W heater is used for the bottom port. These heaters are connected in parallel, and controlled by a single variable transformer. Since stainless steel is a relatively poor heat conductor, the heat loss from the pillar is not prohibitively great, and we have not felt that it is necessary to insulate its exposed face. However, in the external valve model, with more exposed components shown in Fig. 3, we have taken precautions to minimize the heat loss from this source.

In operations at 250 to 300°, septum life is annoyingly short, and we have found it advantageous to use a device for insulating the septum from the heat of the injection port. This is shown in Fig. 7. The device is constructed from very thin stainless steel hypodermic tubing to minimize heat transfer to the septum. Air is drawn through the cooling jacket and chimney by thermal convection, and the septum life is greatly prolonged. This device requires the use of a 3 in. injection needle. We have found Hamilton 2822-gage needles to be suitable for this purpose. Although this device may lead to the loss of a fraction of the material injected because of non-volatilization, in fact, we have not noticed that its use alters our results.

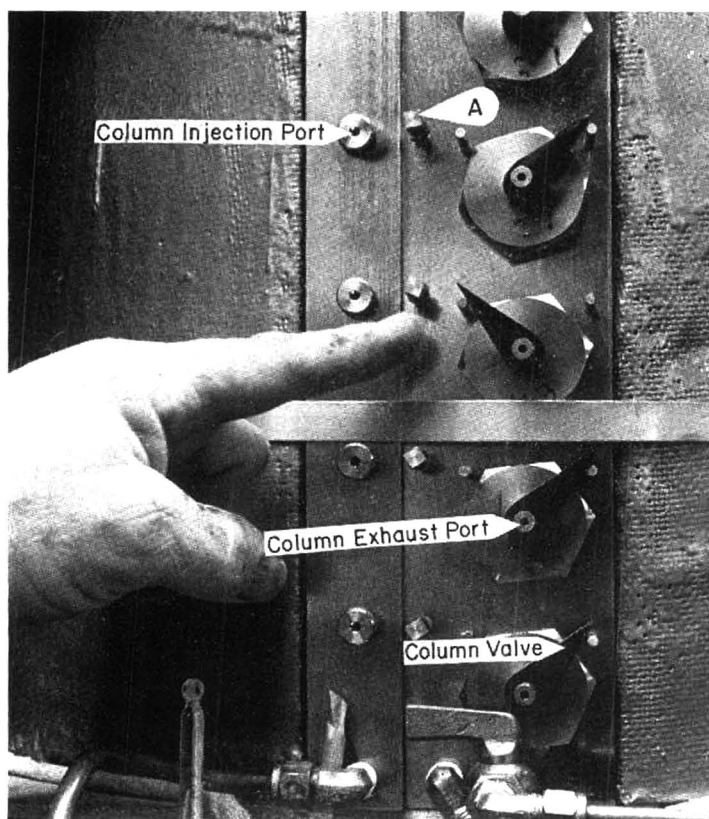


Fig. 5. Front view of a high temperature pillar. The third valve from the bottom is in open position. A is the needle valve for adjusting the carrier gas flow to that individual column. This pillar uses the earlier style internal graphite faced valve.

RESULTS

The aspects of this design which might be expected to affect the results and which require comment are (a) the valve and (b) the variable path length and nature of the passage through the effluent duct in the chromatograph pillar. With regard to the valve, we can see no effect. Retention times, peak shapes and peak yields are comparable to those obtained in a standard chromatograph. The variable gas passage does have a moderate effect on peak yield. Fig. 8 shows chromatograms run on the same column when the column was used at the top position (upper trace) and the bottom position (lower trace) of the chromatograph pillar. There is a moderate, reproducible decrease in peak yield in the bottom position, which varies slightly with the material which is being eluted. The average attenuations in peak (height, area) which we obtained were as follows: ethanol, (14%, 23%); benzene, (9%, 18%); ethyl acetate (14%, 18%); tetrahydrofuran (THF) (15%, 18%). (Since ethyl acetate and THF were not completely resolved, the combined peak area was used in each case.) While for precise quantitative analytical work these differences would be important, we do not regard them as significant in an instrument intended for ex-

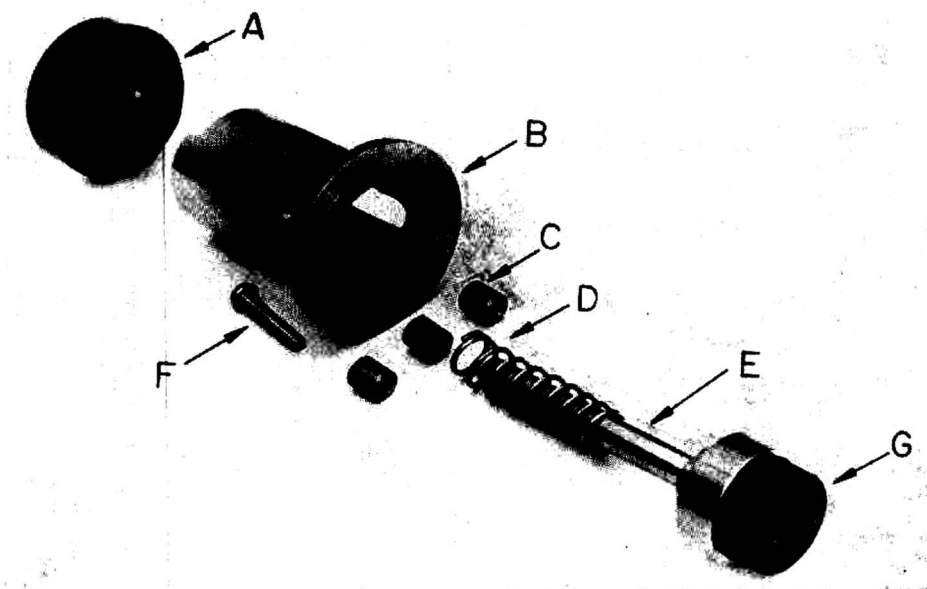


Fig. 6. Exploded view of high-temperature valve assembly. A = valve handle, B = valve guide, C = stand-offs for valve guide (not shown in Fig. 3), D = valve spring, E = valve stem, F = valve graphite disc. The slot in the disc carries gas from column to detector. The round hole near the periphery carries to the hollow stem of guide, E, whence it exhausts to the atmosphere (see exhaust port, Fig. 5).

ploratory work which is the primary objective of this design. Furthermore, these differences are constant and reproducible, so that any one column can be used in a quantitative way, as in the ordinary chromatograph.

At the time this test was made, the instrument had been in use for about two

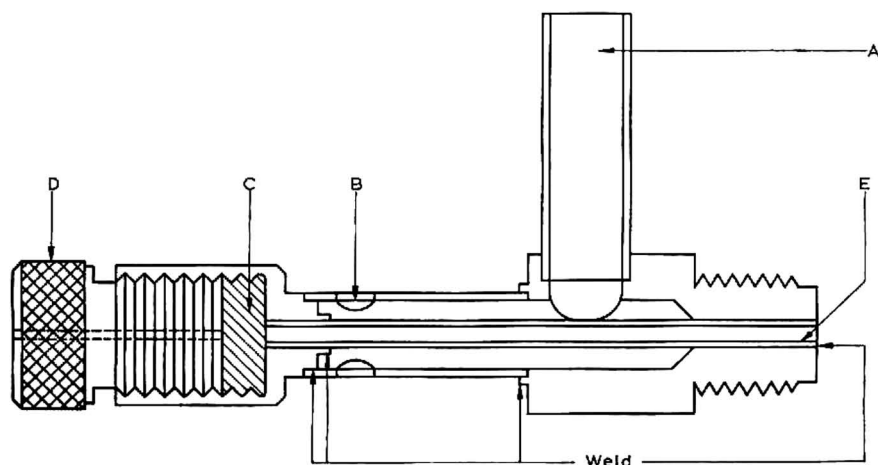


Fig. 7. Septum heat protector. A = chimney, B = air inlet holes, C = septum, D = septum retaining screw, E = injection passage.

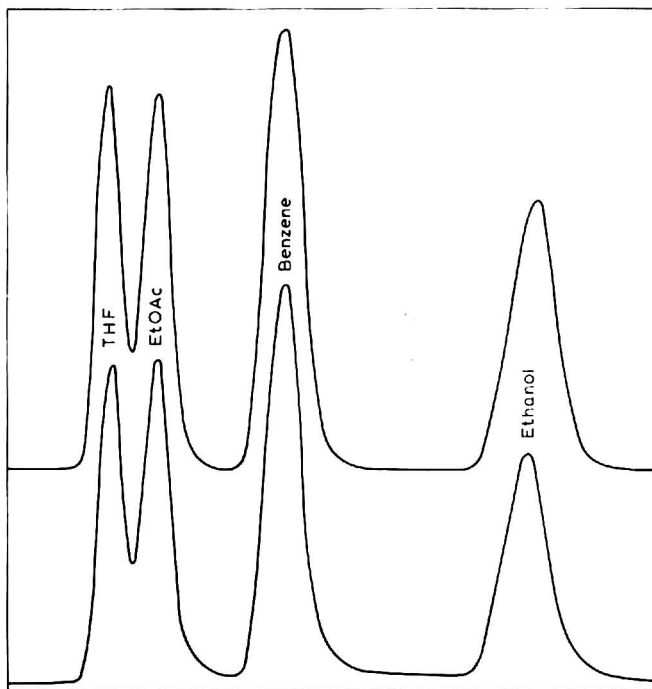


Fig. 8. Chromatogram run on the same column. Upper trace, column was used at the top position, lower trace, column was used at the bottom position.

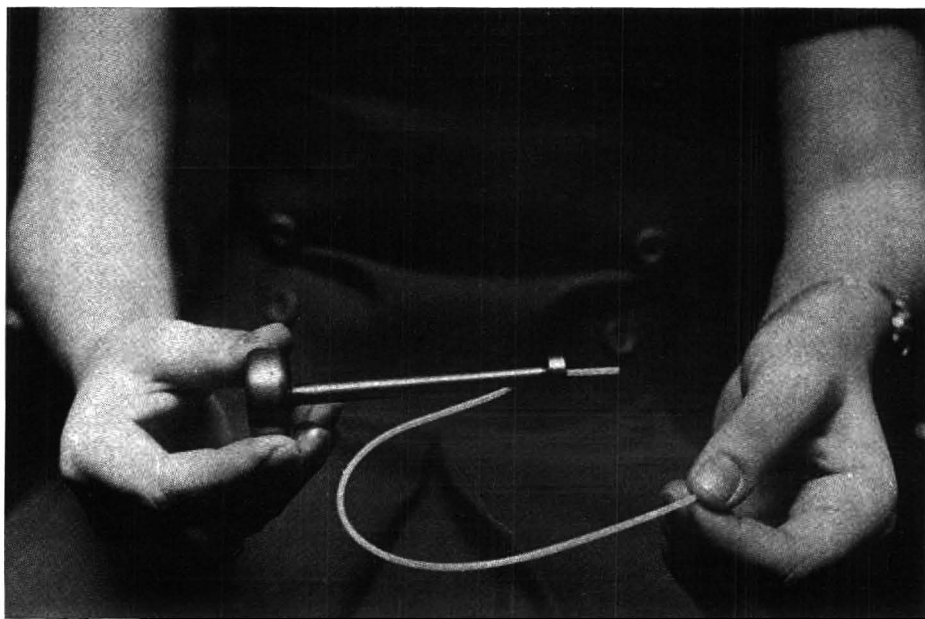


Fig. 9. Device for collecting chromatographed products.

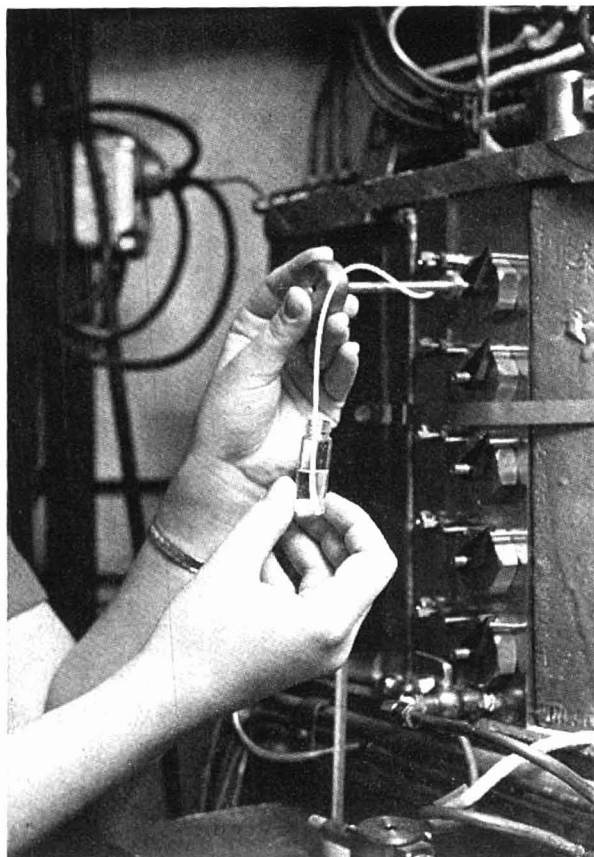


Fig. 10. Sample collection technique.

years, and we suspected that leakage at the valves might account for the attenuations seen. However, when we replaced the O-rings on all the valves in the pillar, the results were identical, indicating that valve leakage is not a significant factor in the operation of the instrument. Since the pillar used in this test was made by milling the gas passages in flat plates and subsequently bolting the plates together, the most likely place for leakage is at the seams between the plates. The brazed design discussed above obviates this source of leakage.

As with other chromatographs which have stainless steel injection ports, steroids occasionally give trouble, although at other times we obtain entirely satisfactory results. This effect, which has been noted by others² may be due to decomposition products in the injection ports left from previous injections, but as of now, we have no clear understanding of the phenomenon. At present, we are experimenting with the possibility of incorporating a glass vaporizing chamber within the pillar.

Use of the valve in preparative gas chromatography

The column effluent, when not directed to the detector, comes out of the front of the pillar, as illustrated in Figs. 4 and 5. It is a simple matter to collect manually

condensable materials at this point using the device illustrated in Fig. 9. The small Teflon tube is inserted into the exhaust port of the column. The holder has a flat silicone-rubber gasket (not shown) made from a $\frac{3}{8}$ in. diameter flat septum, which tightly surrounds the teflon tube and permits a tight seal to the exhaust port.

A normal chromatogram is run and the width of the desired peak determined. The injection is then repeated, and when the desired peak begins to appear, the valve is turned to shift the column effluent to the exhaust port. The effluent is collected by bubbling the gas stream through solvent as illustrated in Fig. 10. We have also made use of a sintered glass bubbler to help break up the aerosol. At a time when the peak material would be expected to be 90% eluted, the valve can be returned to the detector position, so that the correctness of the peak collection can be affirmed. It is also possible to collect portions of peaks where the homogeneity of the effluent is in question. A single collection is usually ample for a mass spectrum determination, while for NMR determinations, twenty or more repetitive collections may be required.

REFERENCES

- 1 J. F. ARNOLD AND H. M. FALES, *J. Gas Chromatog.*, 3 (1965) 131.
 - 2 *Handbook of Silation*, Pierce Chemical Co., Rockford, Ill., 1970, p. 7.
- J. Chromatog.*, 53 (1970) 125-134

CHROM. 4928

THE USE OF HIGH EFFICIENCY PACKED COLUMNS FOR GAS-SOLID CHROMATOGRAPHY

III. SEPARATION OF DEUTERIUM SUBSTITUTED COMPOUNDS

ANTONIO DI CORCIA, DÈNES FRITZ AND FABRIZIO BRUNER

Istituto di Chimica Analitica, Università di Roma, 00185, Roma (Italy)

(Received July 14th, 1970)

SUMMARY

Gas-solid chromatography with packed columns is used for the separation of some polar and nonpolar isotopic pairs.

The technique involves the use of graphitized carbon black modified with proper amounts of suitable liquid phases. A comparison with capillary columns shows that in many cases these can be conveniently substituted by packed columns. The technique is useful either for the study of isotope effects or for analytical uses.

The gas chromatography of isotopically substituted molecules is of interest both as an analytical tool and as a method for investigating isotope effects.

There are several reports in the literature concerning the separation of various isotopic mixtures by exploiting isotope effects either in gas-liquid (GLC) or in gas-solid (GSC) systems using capillary or packed columns¹⁻⁴.

The use of capillary columns involves a rather sophisticated technique and the chemist is often discouraged by the operative difficulties encountered in preparing high resolution capillary columns with particular liquid phases.

Our efforts have recently been directed to the exploitation of high resolution packed columns, so that gas chromatography can be used as a routine method of analysis of isotopic mixtures as well as a simple technique for the study of isotope effects.

The exploitation of the gas chromatographic properties of Graphon⁵, which is a graphitized carbon black with a surface area of about 100 m²/g, has made it possible to extend the use of gas-liquid-solid chromatography (GLSC) to the elution of polar and H-bonding compounds. This macroporous adsorbent, whose surface properties are the same⁶ as those of the other graphitized carbon blacks with lower surface areas, like FT or MT, exhibits a higher mechanical resistance, so that packing of long columns with relatively high permeability is possible.

This paper reports the separation of some polar isotopic pairs (CH₃OH-CD₃OH; C₂H₅OH-C₂D₅OH; CH₃CN-CD₃CN) obtained by GLSC employing Graphon partially coated with 1.5% w/w of TEPA.

The separation of C_2H_6 - $C_2H_3D_3$ - C_2D_6 and C_2H_4 - C_2D_4 isotopic molecules has also been achieved with a 15-m column packed with Graphon deactivated with only 0.1% w/w of glycerol.

Furthermore, the analysis of all deuterated isotopic methanes is reported; they are eluted at -78° by means of a 120-m column packed with Graphon deactivated by 0.1% of squalane.

EXPERIMENTAL

Experiments, as far as polar isotopic pairs are concerned, have been carried out using a commercial gas chromatograph (Carlo Erba ATC/f, model C) equipped with a thermal conductivity detector. The separations were performed in a temperature range between $+50^\circ$ and $+90^\circ$, with an accuracy of $\pm 0.3^\circ$.

After some preliminary experiments to eliminate severe tailing of the peaks of the compounds considered, due to some hydrophilic sites on the Graphon, the adsorbent was partially coated with 1.5% w/w of TEPA (tetraethylenepentamine), which provided a surface coverage of about 5%. This addition of liquid phase, due to specific lateral interactions between the functional groups of the liquid phase and the eluate, increased the retention times and separation factors, so that elution of the isotopic mixtures at temperatures above room temperature was possible.

A 15 m \times 4 mm I.D. stainless steel tube packed with Graphon (40-60 mesh) was chosen. The column had a theoretical plate value of 16,000 referred to CH_3CN and 13,000 referred to CH_3OH . Hydrogen was used as carrier gas. The pressure drop did not exceed 3 kg/cm².

Separations of C_2H_6 - $C_2H_3D_3$ - C_2D_6 and C_2H_4 - C_2D_4 were performed in the temperature range between $+37.5^\circ$ and -41.5° , with an accuracy of $\pm 0.2^\circ$. Low-temperature measurements were carried out using a methanol-dry ice cryostat (Lauda, G.F.R.) which refrigerated the thermostatic bath, in which the column was immersed. The gas chromatograph was slightly modified so that it would bear inlet pressures of 10-12 atm and operate at a low temperature, as previously described⁴.

The 15 m long, 2 mm I.D. column was packed with Graphon 60-80 mesh coated with glycerol 0.1% w/w, which provided a surface coverage of about 3%. In this way, tailing of the ethylene peak, still present when squalane is used as deactivant, is fully eliminated. The column had a theoretical plate value of 26,000 referred to C_2H_6 and 21,000 referred to C_2H_4 . In this case the pressure drop was 8-12 kg/cm².

The analysis of isotopic methanes was carried out on a special gas chromatograph equipped with a thermostatic bath at -78° (acetone-dry ice). Particular attention has been devoted to the detector. The effluent from the column, about 250 ml/min, was split and about 5% of it was sent to a flame ionization detector. An additional flow of hydrogen was used at the splitting point as scavenging gas so that dead volumes were avoided. In this way, a double advantage is obtained. Firstly, most of the sample remains intact, which is useful if preparative chromatography is being considered; secondly, the sensitivity of the thermal conductivity detector is much lower than that of the flame ionization detector, and furthermore, the sensitivity of the former would be lowered by using such high flow rates. A detection limit about 1000 times lower is attained, even though 95% of the sample injected is not passing through the detector.

All the compounds were from commercial sources, but the mixture of deuterated methanes was prepared according to a procedure previously described².

RESULTS AND DISCUSSION

Fig. 1 shows the plot of the logarithm of the ratio of the retention volumes of hydrogen and the deuterated species *vs.* $1/T$. As can be seen, all the isotopic mixtures eluted show an abnormal isotope effect (*i.e.* the heavier species is eluted first) and a relationship of the type $\ln(V_R)_H/(V_R)_D = B/T + C$ describes the variation of the separation factor with the temperature.

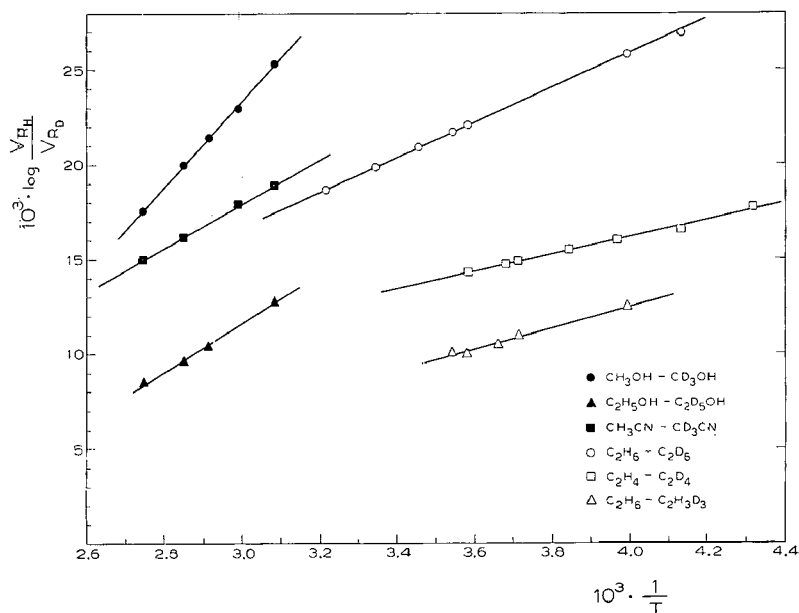


Fig. 1. Plot of the logarithms of ratios of the retention volumes *vs.* $1/T$.

As far as polar isotopic mixtures are concerned, it is interesting to note that the highest isotope effect is shown by the isotopic pair $\text{CH}_3\text{OH}-\text{CD}_3\text{OH}$.

The relative differences in polarizability ($\Delta\alpha/\alpha$), shown in Table I, can partially account for the higher isotope effect shown by the $\text{CH}_3\text{OH}-\text{CD}_3\text{OH}$ isotopic system with respect to the isotopic pair $\text{CH}_3\text{CN}-\text{CD}_3\text{CN}$, but this difference does not justify the lower isotope effect for the isotopic pair, $\text{C}_2\text{H}_5\text{OH}-\text{C}_2\text{D}_5\text{OH}$. Tentatively, the above disagreement can be explained if it is assumed that the substitution of protium for deuterium atoms in the methyl group slightly decreases the strength of the hydrogen bond between the alcoholic and the amino group of TEPA, introducing an isotope effect of the second order. In this hypothesis, the isotope effect on the OH group works in the same direction as the differences in polarizability and the two effects cannot be easily divorced.

As would be expected from the differences in polarizability, the separation of

TABLE I

NUMERICAL VALUES FOR THE ISOTOPE EFFECT FOR THE PAIRS INVESTIGATED

Isotopic pair	$Q_H - Q_D$ (cal/mole) ^a	$B \cdot 10^3$ (K)	$C \cdot 10^3$	$\Delta a/a \cdot 10^2$
CH ₃ OH-CD ₃ OH	105	52.5	-105	0.85
C ₂ H ₅ OH-C ₂ D ₅ OH	58	29.0	-61	0.92
CH ₃ CN-CD ₃ CN	51	25.5	-35.5	0.55
C ₂ H ₆ -C ₂ D ₆	43	21.5	-25.0	1.2
C ₂ H ₆ -C ₂ H ₃ D ₃	~23	11.5	-18.0	0.60
C ₂ H ₄ -C ₂ D ₄	21	10.5	-5.0	0.85

^a Differences of chromatographic molar heats.

C₂H₆ and C₂D₆ is better than that between C₂H₄ and C₂D₄. It is noteworthy that the values of the B and C terms on Graphon, shown in Table I, are approximately equal to those obtained on FT (ref. 7), a graphitized carbon black with a surface area of about 15 m²/g. This confirms the experimental results obtained by KISELEV⁶, that the surface properties of these carbon blacks are the same in spite of the differences in the surface

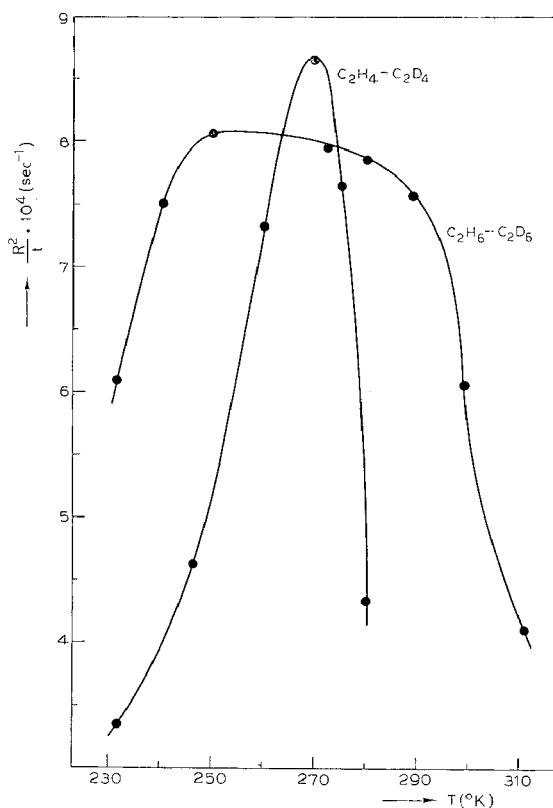


Fig. 2. Graph showing the ratio R^2/t vs. temperature for the pairs ethane-ethane-D₆, ethylene-ethylene-D₄.

area. Furthermore, the above results show that glycerol at such low coverages ($\theta = 3 \cdot 10^{-2}$) acts as a deactivant only, and it does not modify the surface properties of Graphon substantially.

Fig. 2 shows the behavior of the factor R^2/t vs. temperature, t being the elution time and R the resolution of the isotopic pair according to the definition $R = \Delta t/w$, where Δt is the difference in retention time of the two species and w the width of the peak at the base expressed in the same units as t . As already reported², the factor R^2/t is important for determining the experimental conditions required to get the best separation for a given pair in the minimum time. As can be seen, this factor shows a sharp maximum in the case of $C_2H_4-C_2D_4$, while the range of temperature for which optimum conditions for the separation are obtained in the case of the isotopic pair, $C_2H_6-C_2D_6$, is rather extended. This is due to the fact that the separation factor of the latter increases steeply inversely with temperature, so that the two counteracting terms balance each other over a wide range. In the case of ethylene, the separation factor increases to a smaller extent, so that an "optimum" of temperature exists for the best separation. The same figures are not reported for the other isotopic pairs examined, since the temperature is much less critical for their R^2/t factor.

Fig. 3 illustrates the best separations obtained for the pairs investigated. A better separation is obtained for methanol, with respect to methanol- D_3 , than that obtained on capillary columns and reported previously⁸. The same can be said for the separation $C_2H_6-C_2H_3D_3-C_2D_6$. Separations of this kind by packed columns have already been reported in the literature³, but our results represent a large improvement in analysis time, temperature and resolution. Moreover, a comparison of analysis time and resolution of the isotopic pair $C_2H_6-C_2D_6$ shows that Graphon is a better

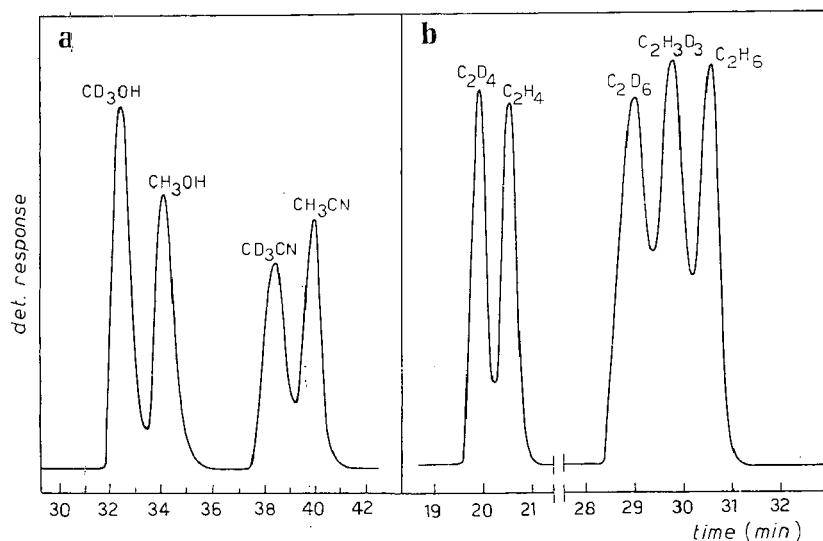


Fig. 3. Separations of methanol-methanol- D_3 , methylcyanide-methylcyanide- D_3 , ethylene-ethylene- D_4 , ethane-ethane- D_3 -ethane- D_6 . Columns: (a) 15 m \times 4 mm I.D. stainless steel column packed with Graphon 40-60 mesh, coated with TEPA 1.5% w/w; temperature, 63°; flow rate, 120 ml/min; inlet pressure, 3 kg/cm². (b) 15 m \times 2 mm I.D. column packed with Graphon 60-80 mesh coated with 0.1% glycerol w/w; temperature, -22.5°; flow rate, 72 ml/min; inlet pressure, 11 kg/cm².

medium than Porapak⁹ since in our case the R^2/t ratio is more than doubled at the same temperature.

The separation of ethylene-ethylene- D_4 is not as good as that reported in literature¹⁰. However, we wish to point out that this separation was carried out in order to get further information about the isotope effect on physical adsorption, and not for analytical use.

Lastly, the separation of all deuterated methanes is shown in Fig. 4. This separation has often been reported in the literature¹¹. However, it was obtained by means of capillary columns at liquid nitrogen temperature and using a mixture of nitrogen and helium as carrier gas. The technique used in this work is much simpler and does

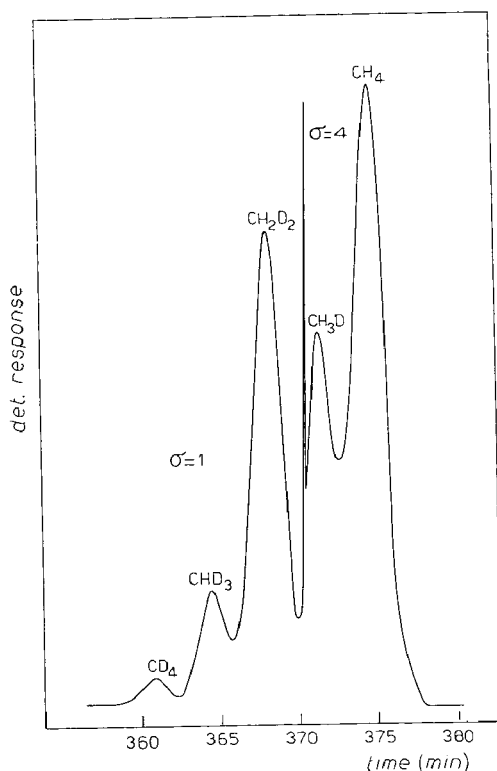


Fig. 4. Chromatogram showing the separation of deuterated methanes. Column: 120 m \times 4 mm I.D. copper column packed with Graphon 40-60 mesh coated with 0.1% squalane w/w; temperature, -78° ; flow rate, 250 ml/min; inlet pressure, 13.5 kg/cm².

not require any special equipment. Furthermore, the detection limit for trace components is about ten times lower with the present technique.

The results of this investigation show that high efficiency packed columns can be competitive and, in some cases, better than capillary columns as regards resolution and analysis time.

The technique of gas-liquid-solid chromatography with packed columns is useful for the investigation of the isotope effect, and offers a very simple method of

analysis for isotopic mixtures, at the same time allowing isotopic separations at more convenient temperatures.

ACKNOWLEDGEMENTS

The technical assistance of E. BRANCALEONI and C. CANULLI is gratefully acknowledged.

This work was supported by the Consiglio Nazionale delle Ricerche.

REFERENCES

- 1 A. LIBERTI, G. P. CARTONI AND F. BRUNER, in A. GOLDUP (Editor), *Gas Chromatography, 1964*, Inst. Petrol., London, 1965, p. 301, and references therein.
- 2 F. BRUNER, G. P. CARTONI AND A. LIBERTI, *Anal. Chem.*, 38 (1966) 298 and references therein.
- 3 W. A. VAN HOOK AND M. E. KELLY, *Anal. Chem.*, 37 (1965) 509 and references therein.
- 4 A. DI CORCIA AND F. BRUNER, *J. Chromatog.*, 49 (1970) 139.
- 5 A. DI CORCIA, D. FRITZ AND F. BRUNER, *Anal. Chem.*, 42 (1970) in press.
- 6 A. V. KISELEV, *Advan. Chromatog.*, (1967) 113.
- 7 A. DI CORCIA AND A. LIBERTI, *Trans. Faraday Soc.*, 66 (1970) 967.
- 8 G. P. CARTONI, A. LIBERTI AND A. PELA, *Anal. Chem.*, 39 (1967) 1618.
- 9 M. POSSANZINI, A. PELA, A. LIBERTI AND G. P. CARTONI, *J. Chromatog.*, 38 (1968) 492.
- 10 J. G. ATKINSON, A. A. RUSSEL AND R. S. STUART, *Can. J. Chem.*, 45 (1967) 1963.
- 11 F. BRUNER, G. P. CARTONI AND M. POSSANZINI, *Anal. Chem.*, 41 (1969) 1122 and references therein.

J. Chromatog., 53 (1970) 135-141

CHROM. 4985

GAS-LIQUID CHROMATOGRAPHY OF DISUBSTITUTED BENZENE ISOMERS

I. SEPARATION AND STUDY OF THE DICHLOROBENZENES

ALBERTINE E. HABBOUSH AND ADNAN H. TAMEESH

College of Science, University of Baghdad (Iraq)

(Received June 10th, 1970)

SUMMARY

Dichlorobenzene isomers were separated on squalane, silicone oil, polyethyleneglycol, polyoxyethylenesorbitan monostearate and polyethyleneglycol succinate. Types of interactions and forces which affected the specific retention volumes and elution orders were discussed. Thermodynamic quantities were calculated and studied on squalane and polyethyleneglycol. Polyesters were selective for the separation of these isomers.

INTRODUCTION

Dichlorobenzenes were studied by COWAN AND HARTWELL¹ on Bentone 34, MORTIMER AND GENT² on Bentone 34 modified with silicone oil, and HABBOUSH AND NORMAN³ on Apiezon L, dinonyl phthalate, polyethyleneglycol-stearic acid, tritolyl phosphate, 2,4,7-trinitrofluorenone and silicone gum rubber. The mechanism of separations was not available. LANGER AND PURNELL⁴ calculated thermodynamic quantities for dichlorobenzenes on benzyl diphenyl and 7,8-benzquinoline.

In the present work, quantitative separations for dichlorobenzene isomers were studied on squalane (SQ), silicone oil (SO), polyethyleneglycol 1500 (PEG), polyethyleneglycol succinate (PEGS) and polyoxyethylenesorbitan monostearate (PA). The specific retention volumes, separation factors and fractional band impurities were calculated. The solute-solvent interactions affecting the retention volumes and elution orders were discussed. Thermodynamic quantities were also calculated and discussed on SQ and PEG.

EXPERIMENTAL AND RESULTS

Apparatus

A Perkin-Elmer Model 451 Fractometer equipped with a thermistor-type thermal conductivity detector was used. The recorder was a 2.5 mV Honeywell Brown

TABLE I

THE CHEMICAL COMPOSITION OF THE LIQUID PHASES USED^a

<i>Chemical Name</i>	<i>Formula</i>	<i>D</i> ^b	<i>Mol. wt.</i>	<i>MOT</i> ^c (°C)
Polyethyleneglycol (PEG)	$(\text{CH}_2)_4(\text{OH})_2\text{O}(\text{OCH}_2\text{CH}_2)_n$	1.152	1500	225
Polyethyleneglycol succinate (PEGS)	$[\text{O}(\text{CH}_2\text{CH}_2\text{O})_2\text{COCH}_2\text{CH}_2\text{CO}]_n$	—	$(188.2)_n$	225
Polyoxyethylenesorbitan monostearate (PA)	—	—	—	160
2,6,10,15,19,23-Hexamethyl-tetracosane (squalane) (SQ)	$\text{C}_{30}\text{H}_{62}$	0.829	422.5	160
Silicone oil (MS 200/50) (SO)	$(\text{CH}_3)_3\text{Si}[\text{OSi}(\text{CH}_3)_2]_n\text{O-Si}(\text{CH}_3)_3$	0.971	—	200

^a G. W. HINE, Perkin-Elmer Ltd., Beaconsfield, Bucks, Great Britain, private communication.

^b Density at 20° in g/ml.

^c Maximum operating temperature when columns were packed.

Electronic unit. Nitrogen was used as the carrier gas. The average column temperature was controlled to within $\pm 0.2^\circ$. Columns were specially ordered from Perkin-Elmer, Great Britain. They were stainless-steel tubing (2 m long and $\frac{1}{8}$ in. O.D.) bent into a U-shape and surrounded by asbestos sleeves to ensure uniform heating. The chemical composition of the liquid phases used is shown in Table I. Packing specifications of all columns used were identical. The weight of pure liquid phase per column was 3.40 g and the liquid on the support was 20% (w/w). These were certified in this laboratory using a solvent extraction technique. The solid support was 60–80 mesh Chromosorb P.

TABLE II

SPECIFIC RETENTION VOLUMES, V_g^0 (ml/g), FOR DICHLOROBENZENE ISOMERS ON DIFFERENT LIQUID PHASES AND AT DIFFERENT COLUMN TEMPERATURES

<i>Phase</i>	<i>Temp.</i> (°C)	<i>Dichlorobenzene isomer</i>		
		<i>Ortho</i>	<i>Meta</i>	<i>Para</i>
PEGS	80	662	450	511
	100	335	233	264
	120	184	132	147
	180	59.0	46.0	50.0
PA	100	303	212	235
	120	174	124	136
SO	120	397	345	345
	140	257	226	226
	180	107	95.0	95.0
SQ	120	412	294	320
	130	297	214	233
	140	225	163	176
	100	88.0	75.1	75.1
PEG (1500)	120	57.8	50.8	50.8
	140	40.5	35.7	35.7
	160	31.0	27.0	27.0

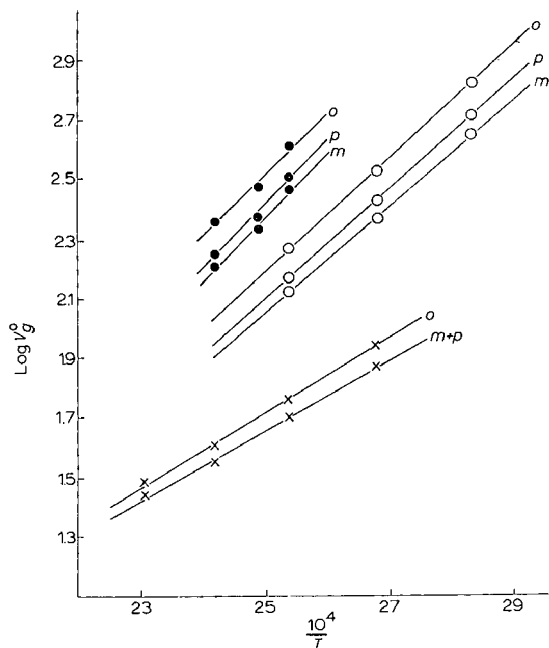


Fig. 1. Variation of $\log V_g^0$ with $1/T$ for dichlorobenzene isomers on the following liquid phases: ●, squalane; ○, polyethyleneglycol succinate; ×, polyethyleneglycol.

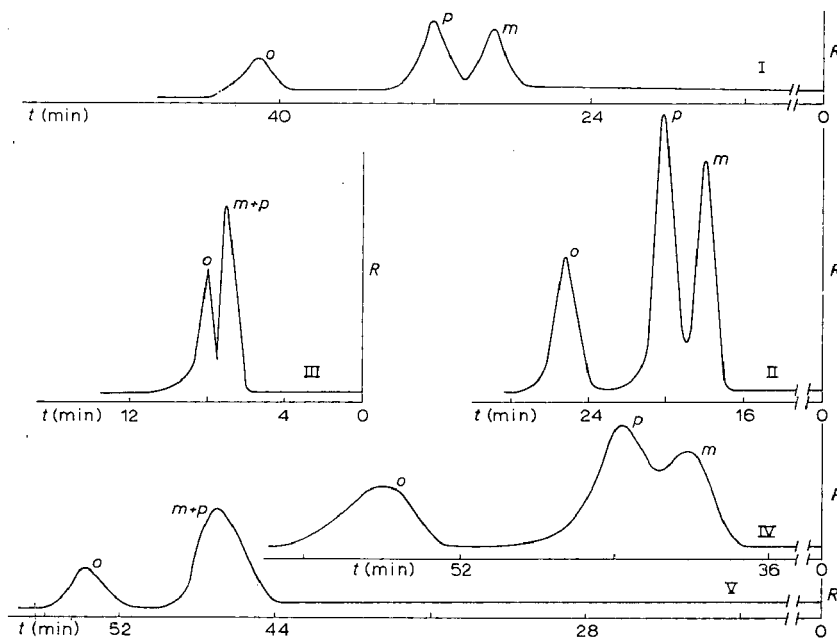


Fig. 2. Chromatograms showing the separation of dichlorobenzene isomers at 120° on: (I) PA; (II) PEGS; (III) PEG; (IV) SQ; and (V) SO. t is the time in minutes and R is the recorder deflection.

Materials

Pure *o*-, *m*-, and *p*-dichlorobenzenes were obtained from Hopkin and Williams Ltd., Great Britain.

Sampling

Equal weights of the isomers were blended in a cylindrical Pyrex cell, having a 3 ml capacity, made in this laboratory. Sample sizes ranged from 0.5 to 1 μ l. The injections were made using a 10- μ l Hamilton 1-in. fixed needle syringe. An optimum flow rate of 20 ml/min at NTP was encountered throughout the investigations. The average inlet pressure was 6 ± 1 p.s.i. The outlet pressure was atmospheric.

The specific retention volumes, V_g^0 , were calculated following the well-known procedure given by LITTLEWOOD *et al.*⁵ The retention volume for the air peak was taken to be zero. Specific retention volumes for dichlorobenzene isomers at different column temperatures on the liquid phases examined are listed in Table II.

Variation of $\log V_g^0$ with $1/T$ is linear (see Fig. 1). Fig. 2 shows the separation of dichlorobenzenes on the liquid phases examined.

The number of theoretical plates, n , was calculated as recommended by JOHNSON AND STROSS⁶. Table III gives the number of theoretical plates, separation factors and fractional band impurities for the isomers.

Electron polarizabilities per unit volume, α_e^v , were calculated using the Clausius-Mosotti equation:

$$\alpha_e^v = \frac{n^2 - 1}{n^2 + 2} \cdot \frac{3}{4\pi N} \quad (1)$$

where n is the refractive index and N is the Avogadro number. Refractive indices of

TABLE III

NUMBER OF THEORETICAL PLATES, n , SEPARATION FACTORS, α , AND FRACTIONAL BAND IMPURITIES, η , FOR DICHLOROBENZENES ON DIFFERENT LIQUID PHASES AND COLUMN TEMPERATURES^a

Dichloro- benzene isomer	Phase (°C)	n	α	η
<i>Meta</i>	PEGS	1860		
<i>Para</i>	(80°)	1860	1.14	$2 \cdot 10^{-3}$
<i>Ortho</i>		2000	1.29	$5 \cdot 10^{-8}$
<i>Meta</i>	PA	2100		
<i>Para</i>	(100°)	2930	1.11	$4 \cdot 10^{-3}$
<i>Ortho</i>		2470	1.29	$1 \cdot 10^{-12}$
<i>Meta</i>	PEG	475	1.0	
<i>Para</i>	(100°)	475		
<i>Ortho</i>		550	1.17	$5 \cdot 10^{-2}$
<i>Meta</i>	SO	3220		
<i>Para</i>	(120°)	3220	1.0	
<i>Ortho</i>		4250	1.15	$3 \cdot 10^{-6}$
<i>Meta</i>	SQ	752		
<i>Para</i>	(120°)	890	1.08	$1 \cdot 10^{-1}$
<i>Ortho</i>		1088	1.28	$5 \cdot 10^{-5}$

^a Where a set of isomers was examined at more than one temperature, values of n , α , and η are recorded for the temperature at which resolution was more satisfactory.

TABLE IV

DIPOLE MOMENTS, REFRACTIVE INDICES, ELECTRON POLARIZABILITIES AND BOILING POINTS OF DICHLOROBENZENE ISOMERS

<i>Dichloro- benzene isomer</i>	<i>D</i>	<i>n_D⁵⁵⁰</i>	<i>E. P.</i> (<i>cm</i> ³ × 10 ²⁶)	<i>B. P.</i> (°C)
<i>Ortho</i>	2.69	1.5335	12.306	179
<i>Meta</i>	1.55	1.5288	12.215	173
<i>Para</i>	0.0	1.5305	12.248	173

dichlorobenzene isomers at 55° were measured in this laboratory using an Ape refractometer.

Dipole moments were calculated as given by SMITH⁷. Dipole moments and other physical constants are tabulated in Table IV.

The activity coefficients at infinite dilution, γ_2^0 , were calculated on SQ and PEG from the following equation⁸:

$$\gamma_2^0 = \frac{17.04 \times 10^6}{M_1 \cdot P^0 \cdot V_g^0} \quad (2)$$

γ_2^0 measures the non-ideal behavior in both the gas phase and solution. Activity coefficients for dichlorobenzenes on SO, PEGS and PA could not be determined due to their undetermined molecular weights (M_1). Table V gives data on vapor pressures and activity coefficients.

The excess partial molar free energy, $\Delta\bar{G}_e^0$, the partial molar excess entropy, $\Delta\bar{S}_e^0$, and the partial molar excess enthalpy $\Delta\bar{H}_e^0$, of mixing at infinite dilutions were calculated as given by LANGER AND PURNELL⁴. These data are shown in Table VI.

Dichlorobenzene isomers were selectively resolved on PEGS and PA (as shown in Table III and Fig. 2). SO and PEG failed to resolve *m*- and *p*-isomers.

TABLE V

VAPOR PRESSURES^a, *P* (mm Hg), AND ACTIVITY COEFFICIENTS AT VARIOUS TEMPERATURES

<i>Data</i>	<i>Temp.</i> (°C)	<i>Dichlorobenzene isomer</i>		
		<i>Ortho</i>	<i>Meta</i>	<i>Para</i>
Vapor pressure	106	62.55	81.20	77.70
	110	91.57	117.4	112.6
	120	130.9	165.7	159.3
	130	183.1	229.2	220.9
	140	251.0	311.0	300.4
Activity coefficient γ_2^0 (on PEG)	100	2.064	1.863	1.947
	120	1.501	1.349	1.404
	140	1.117	1.023	1.059
Activity coefficient γ_2^0 (on SQ)	120	0.748	0.828	0.791
	130	0.742	0.822	0.784
	140	0.714	0.796	0.763

^a These were calculated using Antoine's equations and constants (see ref. 9).

TABLE VI

THERMODYNAMIC DATA ON DIFFERENT PHASES

Phase	Dichloro- benzene isomer	Temp. (°C)	Thermodynamic data		
			$\Delta\bar{G}_e^0$ (cal/mole)	$\Delta\bar{H}_e^0$ (kcal/mole)	$\Delta\bar{S}_e^0$ e.u.
PEG	<i>ortho</i>	100	536.6		
		120	317.1	3.870	+9.040
		140	90.6		
	<i>meta</i>	100	460.7		
		120	233.7	3.933	+9.414
		140	18.5		
	<i>para</i>	100	493.3		
		120	264.2	4.007	+9.524
		140	47.1		
SQ	<i>ortho</i>	120	-226.8	-0.530	-0.771
		130	-239.2		
		140	-276.2		
	<i>meta</i>	120	-147.4	-0.552	-1.030
		130	-156.6		
		140	-187.5		
	<i>para</i>	120	-183.1	-0.485	-0.768
		130	-195.1		
		140	-222.1		

DISCUSSION

The different values of activity coefficients, γ_2^0 , of Table V could be explained using the two terms, $\Delta\bar{H}_e^0$ and $\Delta\bar{S}_e^0$, of the following equation⁸:

$$\ln \gamma_2^0 = \frac{\Delta\bar{H}_e^0}{RT} - \frac{\Delta\bar{S}_e^0}{R} \quad (3)$$

$\Delta\bar{H}_e^0$ is related to the disparities in the intermolecular forces and $\Delta\bar{S}_e^0$ to the inequalities in the volumes of solute and solvent molecules. The following approximation is also valid:

$$\Delta\bar{H}_e^0 \doteq z\Delta W = z(\tfrac{1}{2}W_{11} + \tfrac{1}{2}W_{22} - W_{12}) \quad (4)$$

where z is the number of nearest neighbors, ΔW the molar interaction change energy, and W_{11} , W_{22} , W_{12} are the pairwise potential energies of interaction, respectively, for two solvent molecules, two solute molecules and between a solute and a solvent molecule.

The inequalities in the volumes of solute and solvent molecules means that the "packing" of molecules of different sizes is less orderly. It appears that in PEG, W_{11} and W_{22} are higher than W_{12} . This might be due to internal association through intermolecular hydrogen bonding that such a relatively polar phase may exert. This would lead to a higher value of $\Delta\bar{H}_e^0$ and consequently to a higher value of γ_2^0 . Although the $\Delta\bar{S}_e^0$ term may give a large contribution, the overall value results in a higher value than unity for γ_2^0 and leads to a positive deviation from Raoult's law.

In SQ, which is not polar, solvent-solvent interaction is much weaker than in PEG. The W_{12} contribution might be small due to the induction or London forces.

Moreover, SQ which has a branched methyl group in its structure, may give a small positive contribution to the partial excess entropy term. This might explain the lower than unity values of γ_2^0 which would yield a negative deviation from Raoult's law. The values of γ_2^0 and $\Delta\bar{H}_e^0$ in PEG and SQ are in agreement with the above argument.

Any interaction in GLC has to be associated with interaction energy and entropy (configurational) requirements. Each one of these factors would predominate, if it has a larger value than the other, and characterize the overall interaction. Table VI shows that the difference between $\Delta\bar{S}_e^0$ and $\Delta\bar{H}_e^0$ values for *m*- and *p*-isomers in PEG are not large enough to cause one of the parameters to predominate and cause separation, while in SQ, although the $\Delta\bar{H}_e^0$ values of the *m*-isomer are higher than that of the *p*-isomer, it is associated with a higher entropy requirement which would predominate and cause the *m*-isomer to be eluted before the *p*-isomer.

The calculation of thermodynamic quantities are susceptible to many errors⁴ especially in the calculations of $\Delta\bar{G}_e^0$ and $\Delta\bar{H}_e^0$, and hence $\Delta\bar{S}_e^0$. The calculated thermodynamic quantities for the present work are good as far as they have been used for comparison.

The observed order of elution of the isomers was *meta*-, *para*- and then *ortho*. This is in disagreement with the order of calculated dipole moments of the isomers (see Table IV). *p*-Dichlorobenzene may undergo polarization by the influence of the dipoles or the induced dipoles of the stationary phase. The values of electron polarizabilities support the above mechanism. Therefore, the order of elution of dichlorobenzene isomers follows their order of increasing electron polarizabilities.

REFERENCES

- 1 C. Y. COWAN AND J. M. HARTWELL, *Nature*, 190 (1961) 712.
- 2 J. V. MORTIMER AND P. L. GENT, *Anal. Chem.*, 36 (1964) 754.
- 3 A. E. HABBOUSH AND R. O. C. NORMAN, *J. Chromatog.*, 7 (1962) 438.
- 4 S. H. LANGER AND J. H. PURNELL, *J. Phys. Chem.*, 67 (1963) 263.
- 5 A. B. LITTLEWOOD, C. S. G. PHILLIPS AND D. T. PRICE, *J. Chem. Soc.*, (1955) 1480.
- 6 H. W. JOHNSON AND F. H. STROSS, *Anal. Chem.*, 30 (1958) 1586.
- 7 J. W. SMITH (Editor), *Electrical Dipole Moments*, Butterworths, London, 1955, p. 96.
- 8 D. E. MARTIRE AND L. Z. POLLARA, *Advan. Chromatog.*, (1965) 335.
- 9 R. R. DREIBACH, *Physical Properties of Chemical Compounds (Advances in Chemical Series)*, American Chemical Society, Washington, D.C., No. 15.

J. Chromatog., 53 (1970) 143-149

CHROM. 4986

GAS-LIQUID CHROMATOGRAPHY OF DISUBSTITUTED BENZENE ISOMERS

II. SEPARATION AND STUDY OF THE HALONITROBENZENES, ANISOLES AND TOLUENES

ALBERTINE E. HABBOUSH AND ADNAN H. TAMEESH

College of Science, University of Baghdad (Iraq)

(Received June 10th, 1970)

SUMMARY

Quantitative separation of halonitrobenzenes, anisoles and toluenes was studied on polyethyleneglycol, polyethyleneglycol succinate, polyoxyethylenesorbitan monostearate, silicone oil and squalane as liquid phases. The interactions and forces that affected the separation of the isomers and their elution sequences were discussed. It was found that polyethyleneglycol succinate and polyoxyethylenesorbitan monostearate could selectively separate all the isomers studied.

INTRODUCTION

The separation and study of the dichlorobenzene isomers were presented in Part I (ref. 1). The present work concerns the study of fluoro-, chloro-, and bromonitrobenzenes, fluoro-, chloro-, bromo-, and nitroanisoles, and fluoro-, chloro-, bromo-, iodo-, cyano-, and nitrotoluenes. HABBOUSH AND NORMAN² recorded the retention data for nineteen sets of *o*-, *m*-, and *p*-isomers on Apiezon L, dinonyl phthalate, polyethyleneglycol-stearic acid, tritolyl phosphate, 2,4,7-trinitrofluorenone and silicone gum rubber. Nitrotoluenes were resolved by NORMAN³ on 2,4,7-trinitrofluorenone, by COURTIER *et al.*⁴ on cyanated silicone oil, and by PARSON *et al.*⁵ using Apiezon L. BOMBAUGH⁶ examined chloronitrobenzene on Carbowax (1000) and other liquid phases. RATUSKY AND BASTER⁷ studied chloronitrobenzenes, nitroanisoles and other solutes on 1,2,3,4-tetrakis(2-cyanoethoxy)butane.

Most of the reported work did not discuss mechanisms for the separations and interactions involved, but few suggestions for the efficiencies of some systems were given. General quantitative separations and mechanisms of interactions for the isomers dealt with in this study are not available.

The selectivity of stationary liquid phases was studied by several workers⁸⁻¹³, and others¹⁴⁻²⁶ discussed the role of stationary phases in gas-liquid chromatography (GLC), aiming to evaluate quantitatively the interactions of the solutes with liquid

TABLE I
SPECIFIC RETENTION VOLUMES, V_g^0 (ml/g), FOR DISUBSTITUTED BENZENE ISOMERS AT DIFFERENT COLUMN TEMPERATURES

Isomer	PEGS ^a	PA	PEG	SO	SQ
<i>Temperature (°C)</i>	(140)	(120)	(120)	(140)	(140)
<i>o</i> -Fluoronitrobenzene	931	1017	319	538	1174
<i>m</i> -Fluoronitrobenzene	483	509	168	384	617
<i>p</i> -Fluoronitrobenzene	615	644	213	423	760
<i>Temperature (°C)</i>	(160)	(140)	(140)	(120)	(140)
<i>o</i> -Chloronitrobenzene	944	758	283	NR ^b	NE ^c
<i>m</i> -Chloronitrobenzene	673	538	210	NR	NE
<i>p</i> -Chloronitrobenzene	778	612	228	NR	NE
<i>Temperature (°C)</i>	(160)	(140)	(140)	(120)	(140)
<i>o</i> -Bromonitrobenzene	1564	1038	405	NR	NE
<i>m</i> -Bromonitrobenzene	1119	754	302	NR	NE
<i>p</i> -Bromonitrobenzene	1305	850	328	NR	NE
<i>Temperature (°C)</i>	(80)	(100)	(100)	(120)	(120)
<i>o</i> -Fluoroanisole	658	184	58	32	276
<i>m</i> -Fluoroanisole	462	135	46	27	215
<i>p</i> -Fluoroanisole	509	150	49	29	233
<i>Temperature (°C)</i>	(120)	(100)	(100)	(140)	(140)
<i>o</i> -Chloroanisole	516	682	157	73	1001
<i>m</i> -Chloroanisole	348	450	111	54	508
<i>p</i> -Chloroanisole	400	523	128	61	372
<i>Temperature (°C)</i>	(120)	(140)	(100)	(120)	(140)
<i>o</i> -Bromoanisole	905	580	263	113	812
<i>m</i> -Bromoanisole	629	415	193	86	706
<i>p</i> -Bromoanisole	727	482	226	99	424
<i>Temperature (°C)</i>	(160)	(150)	(140)	(180)	(140)
<i>o</i> -Nitroanisole	2622	1328	456	237	NE
<i>m</i> -Nitroanisole	1438	703	214	119	NE
<i>p</i> -Nitroanisole	2859	1473	502	260	NE

TABLE II

COLUMN EFFICIENCIES FOR DISUBSTITUTED BENZENE ISOMERS AT DIFFERENT COLUMN TEMPERATURES

Where a set of isomers was examined at more than one temperature, values of n , a , and η are recorded for the temperature at which resolution was more satisfactory.

Isomer	PEGS			PA			PEG			SO			SQ		
	n	a	η	n	a	η	n	a	η	n	a	η	n	a	η
<i>Temperature (°C)</i>															
<i>m</i> -Fluoronitrobenzene	(140) 2560	1.27	$1 \cdot 10^{-10}$	(120) 2270	1.26	$1 \cdot 10^{-9}$	(120) 352	1.27	$2 \cdot 10^{-3}$	(120) 6050	1.1	$5 \cdot 10^{-5}$	(140) 1550	1.23	10^{-6}
<i>p</i> -Fluoronitrobenzene	2670	1.51	$\ll 10^{-11}$	2800	1.58	$\ll 10^{-14}$	600	1.5	$8 \cdot 10^{-8}$	6550	1.27	$< 10^{-14}$	2050	1.55	$< 10^{-14}$
<i>o</i> -Fluoronitrobenzene	3800			2500			380			5100			1710		
<i>Temperature (°C)</i>															
<i>m</i> -Chloronitrobenzene	(160) 1600	1.15	$4 \cdot 10^{-4}$	(140) 1950	1.14	$1 \cdot 10^{-3}$	(140) 175	1.09	$> 10^{-1}$	NR ^a			NE ^b		
<i>p</i> -Chloronitrobenzene	2210	1.22	$6 \cdot 10^{-6}$	2200	1.24	$7 \cdot 10^{-7}$	270	1.24	$5 \cdot 10^{-2}$	NR			NE		
<i>o</i> -Chloronitrobenzene	2510			2530			600			NR			NE		
<i>Temperature (°C)</i>															
<i>m</i> -Bromonitrobenzene	(160) 2650	1.16	$6 \cdot 10^{-5}$	(140) 2240	1.13	$5 \cdot 10^{-4}$	(140) 435	1.08	$> 10^{-1}$	NR			NE		
<i>p</i> -Bromonitrobenzene	2380	1.2	$8 \cdot 10^{-6}$	3000	1.22	$5 \cdot 10^{-8}$	890	1.24	$5 \cdot 10^{-4}$	NR			NE		
<i>o</i> -Bromonitrobenzene	4000			4100			970			NR			NE		
<i>Temperature (°C)</i>															
<i>m</i> -Fluoroanisole	(80) 1870	1.13	$1 \cdot 10^{-3}$	(100) 1520	1.1	$3 \cdot 10^{-2}$	(100) 1025	1.07	$> 10^{-1}$	(120) 2150	1.0		(120) 1380	1.08	$> 10^{-1}$
<i>p</i> -Fluoroanisole	2140	1.29	10^{-8}	1580	1.23	$5 \cdot 10^{-5}$	700	1.16	$3 \cdot 10^{-2}$	2150	1.07	10^{-2}	960	1.18	$5 \cdot 10^{-3}$
<i>o</i> -Fluoroanisole	3200			2070			1600			3840			1250		
<i>Temperature (°C)</i>															
<i>m</i> -Chloroanisole	(120) 2720	1.15	$5 \cdot 10^{-6}$	(100) 1970	1.16	$2 \cdot 10^{-3}$	(100) 455	1.16	10^{-2}	(120) 3060	1.06	$2 \cdot 10^{-3}$	(120) 1210	1.15	$1 \cdot 10^{-3}$

<i>p</i> -Chloroanisole	3040	1.29	10^{-12}	1000	1.3	$5 \cdot 10^{-8}$	815	1.22	$2 \cdot 10^{-3}$	4070	1.06	$2 \cdot 10^{-2}$	1800	1.23	$5 \cdot 10^{-6}$
<i>o</i> -Chloroanisole	3100			1700			1160			6070			1650		
Temperature (°C)	(120)			(120)			(100)			(120)			(140)		
<i>m</i> -Bromoanisole	2660		$2 \cdot 10^{-4}$	2000		$6 \cdot 10^{-4}$	364		$3 \cdot 10^{-2}$	1490	1.0		1530	1.15	$3 \cdot 10^{-3}$
<i>p</i> -Bromoanisole	2620	1.15	10^{-8}	1820	1.16	$5 \cdot 10^{-5}$	675	1.17	$4 \cdot 10^{-2}$	1490	1.1	$3 \cdot 10^{-2}$	1760	1.15	$5 \cdot 10^{-4}$
<i>o</i> -Bromoanisole	3900	1.25		1740	1.2		1120	1.16		1520			2340		
Temperature (°C)	(160)			(150)			(140)			(140)					
<i>m</i> -Nitroanisole	3470		$\ll 10^{-14}$	2660		$\ll 10^{-14}$	424	2.12	10^{-11}	3170	1.15	$5 \cdot 10^{-7}$	NE		
<i>o</i> -Nitroanisole	6750	1.82	$2 \cdot 10^{-4}$	2320	1.89	$7 \cdot 10^{-3}$	342	1.1	$> 10^{-1}$	4900	1.29	$< 10^{-14}$	NE		
<i>p</i> -Nitroanisole	9750	1.09		3600	1.11		468			4080			NE		
Temperature (°C)	(80)														
<i>o</i> -Fluorotoluene	1710	1.09	$7 \cdot 10^{-2}$	NR			NR			NR			NR		
<i>m</i> -Fluorotoluene	1025			NR			NR			NR			NR		
<i>p</i> -Fluorotoluene	1025	1.0		NR			NR			NR			NR		
Temperature (°C)	(80)			(80)			(100)						(120)		
<i>o</i> -Chlorotoluene	1370	1.12	$8 \cdot 10^{-3}$	2239	1.11	$6 \cdot 10^{-3}$	675	1.15	$3 \cdot 10^{-2}$	NR			2610	1.09	$7 \cdot 10^{-2}$
<i>m</i> -Chlorotoluene	1760			2250			710			NR			1300	1.0	
<i>p</i> -Chlorotoluene	1760	1.0		2250	1.0		710	1.0		NR			1300		
Temperature (°C)	(100)			(120)			(100)						(120)		
<i>o</i> -Bromotoluene	2045	1.1	10^{-2}	1670	1.1	10^{-2}	975	1.11	$> 10^{-1}$	NR			3070	1.07	$6 \cdot 10^{-3}$

(continued on p. 156)

TABLE II (continued)

Isomer	PEGS			PA			PEG			SO			SQ		
	n	a	η	n	a	η	n	a	η	n	a	η	n	a	η
<i>m</i> -Bromotoluene	2070	1.0		2070	1.0		304	1.11	$>10^{-1}$	NR			5250	1.03	$>10^{-1}$
<i>p</i> -Bromotoluene	2070			2070			375			NR			1110		
Temperature (°C)	(120)			(100)			(100)						NR		
<i>o</i> -Iodotoluene	1870	1.05	$>10^{-1}$	1250	1.08	$>10^{-1}$	448	1.1	$>10^{-1}$	NR			NR		
<i>m</i> -Iodotoluene	1600			825			225	1.11	$>10^{-1}$	NR			NR		
<i>p</i> -Iodotoluene	1600	1.0		825	1.0		520			NR			NR		
Temperature (°C)	(140)			(120)			(120)			(140)			(140)		
<i>o</i> -Nitrotoluene	3450	1.28	$5 \cdot 10^{-14}$	3660	1.33	$<10^{-14}$	260	1.4	10^{-3}	4000	1.24	10^{-11}	1920	1.33	$<10^{-14}$
<i>m</i> -Nitrotoluene	3520	1.18	$5 \cdot 10^{-7}$	3300	1.18	10^{-6}	320	1.16	$8 \cdot 10^{-3}$	4250	1.09	10^{-3}	3200	1.16	10^{-8}
<i>p</i> -Nitrotoluene	6650			4550			640			6300			3270		
Temperature (°C)	(140)			(120)			(100)			(120)			(140)		
<i>o</i> -Tolunitrile	2100	1.23	$5 \cdot 10^{-8}$	1720	1.27	$5 \cdot 10^{-8}$	940	1.32	$5 \cdot 10^{-7}$	6250	1.14	10^{-10}	1200	1.22	10^{-6}
<i>m</i> -Tolunitrile	2700	1.15	$2 \cdot 10^{-4}$	1900	1.16	$4 \cdot 10^{-4}$	1220	1.15	$8 \cdot 10^{-3}$	7420	1.08	10^{-4}	2240	1.13	10^{-3}
<i>p</i> -Tolunitrile	3770			2300			1680			11750			1700		

^a NR = not resolved.^b NE = not eluted.

TABLE III

SOME PHYSICAL CONSTANTS FOR DISUBSTITUTED BENZENES

<i>Isomer</i>	n_D^T	<i>T</i> (°C)	<i>E.P.</i> ($cm^3 \times 10^{26}$)	<i>B.p.</i> ^c (°C)	<i>D.M.</i> ^d (Debye)
<i>o</i> -Fluoronitrobenzene	1.5278 ^a	31	12.196	214.6	4.86
<i>m</i> -Fluoronitrobenzene	1.5212 ^a	31	12.068	205.0	3.49
<i>p</i> -Fluoronitrobenzene	1.5269 ^a	31	12.179	205.0	2.53
<i>o</i> -Chloronitrobenzene	1.5330 ^a	85	12.296	245.7	5.01
<i>m</i> -Chloronitrobenzene	1.5385 ^a	85	12.402	235.6	3.47
<i>p</i> -Chloronitrobenzene	1.5501 ^a	85	12.622	242.0	2.43
<i>o</i> -Bromonitrobenzene				261.0	4.97
<i>m</i> -Bromonitrobenzene				256.5	3.48
<i>p</i> -Bromonitrobenzene				256.0	2.45
<i>o</i> -Fluoroanisole	1.4940 ^a	30.5	11.534	155.0	2.32
<i>m</i> -Fluoroanisole	1.4859 ^a	30.5	11.373		1.35
<i>p</i> -Fluoroanisole	1.4830 ^a	30.5	11.313	157.0	0.18
<i>o</i> -Chloroanisole	1.5478 ^b	12.0	12.581	195.0	2.43
<i>m</i> -Chloroanisole	1.5378 ^b	12.0	12.390	194.0	1.65
<i>p</i> -Chloroanisole	1.5401 ^b	12.0	12.434	198.0	0.28
<i>o</i> -Bromoanisole	1.5691 ^a	29.0	12.982	210.0	2.41
<i>m</i> -Bromoanisole	1.5591 ^a	29.0	12.794	211.0	1.41
<i>p</i> -Bromoanisole	1.5596 ^a	29.0	12.802	215.0	0.26
<i>o</i> -Nitroanisole	1.5428 ^a	59	12.483	277.0	4.73
<i>m</i> -Nitroanisole	1.5410 ^a	59	12.446	258.0	3.53
<i>p</i> -Nitroanisole	1.5698 ^a	59	12.994	260.0	2.71
<i>o</i> -Fluorotoluene	1.4703 ^a	20	11.062	114.0	1.28
<i>m</i> -Fluorotoluene	1.4691 ^a	20	11.034	116.0	1.66
<i>p</i> -Fluorotoluene	1.4699 ^a	20	11.054	117.0	1.85
<i>o</i> -Chlorotoluene	1.528 ^b	20	12.200	159.4	1.34
<i>m</i> -Chlorotoluene	1.523 ^b	20	12.106	162.4	1.74
<i>p</i> -Chlorotoluene	1.521 ^b	20	12.064	162.5	1.96
<i>o</i> -Bromotoluene				181.8	1.31
<i>m</i> -Bromotoluene				183.7	1.71
<i>p</i> -Bromotoluene				183.6	1.93
<i>o</i> -Iodotoluene				211.0	1.15
<i>m</i> -Iodotoluene				204.0	1.54
<i>p</i> -Iodotoluene				211.5	1.77
<i>o</i> -Nitrotoluene	1.5488 ^b	15	12.600	222.3	3.83
<i>m</i> -Nitrotoluene	1.5491 ^b	15	12.606	231.0	4.18
<i>p</i> -Nitrotoluene	1.5384 ^b	15	12.401	238.0	4.38
<i>o</i> -Tolunitrile				204.0	3.82
<i>m</i> -Tolunitrile				214.0	4.22
<i>p</i> -Tolunitrile				217.0	4.42

^a Measured in this laboratory.^b Ref. 28 and 29.^c Ref. 30 and 31.^d Calculated as given by SMITH³².

phases. However, separations of complex mixtures of various chemical compositions were given in the literature, but investigations of their mechanisms of separation were rather rare.

EXPERIMENTAL AND RESULTS

The apparatus, columns and experimental conditions were the same as given in Part I (ref. 1).

Materials

Pure *o*-, *m*- and *p*-fluorotoluenes, chloroanisoles and chlorotoluenes, iodotoluenes, fluoroanisoles and bromoanisoles were obtained from T. J. Sas and Son Ltd., Great Britain. Pure bromotoluenes, nitrotoluenes, tolunitriles, nitroanisoles, *p*-fluoronitrobenzene, chloronitrobenzenes and bromonitrobenzenes were from Hopkin and Williams Ltd., Great Britain. Pure *o*- and *m*-fluoronitrobenzenes were from L. Light and Co. Ltd., Great Britain.

Sampling for liquid isomers was the same as in the previous work, but for solid isomers a 10% (w/w) acetone or ether solution of the isomers was used. Sample sizes ranged from 1–3 μ l.

Specific retention volumes, v_g^0 , for all the isomers on the liquid phases studied were calculated as given by LITTLEWOOD *et al.*²⁷ and are listed in Table I. From the results obtained, the number of theoretical plates, n , relative peak separation, α , and the fractional band impurity, η , were calculated as in Part I. The values of n , α , and η are listed in Table II.

Refractive indices for some isomers were not available; therefore, they were determined in this laboratory in order to calculate the electron polarizabilities per unit volume, α_v'' , as in Part I. An Ape Refractometer fitted with a Colara K0930 ultra-thermostat was used for this purpose. Table III gives some important physical constants (refractive indices, electron polarizabilities, boiling points and dipole moments) for the disubstituted benzene isomers to be utilized in the discussion.

DISCUSSION

The elution order of halonitrobenzenes and of anisoles was always *m*-, *p*- and *o*-. For nitroanisoles, it was *m*-, *o*- and *p*-. These orders are not the order of the increase of the calculated dipole moments of these isomers. The calculated electron polarizabilities per unit volume for these isomers show that the polarization of the *p*-isomers is higher than that of the corresponding *m*-isomer. In fact, *p*-isomers would exert higher polarity than the calculated polarity, this being due to the polarizing effect of the solvent (as shown in Table III).

Toluenes, namely fluoro-, chloro-, bromo-, iodo-, nitro- and cyanotoluenes were eluted in the order: *o*-, *m*- and *p*-. They seem to follow the same order of their calculated dipole moments (as seen in Table III and Fig. 1).

In general, the explanation of the orders can be simplified if one considers the large dipole moment of *p*-isomers, other than toluenes, and the steric effects of the *ortho*-derivatives. The consistently stronger retention of the *p*- versus *m*-isomers seems most likely to be due to an intramolecular electronic effect, as by resonance-

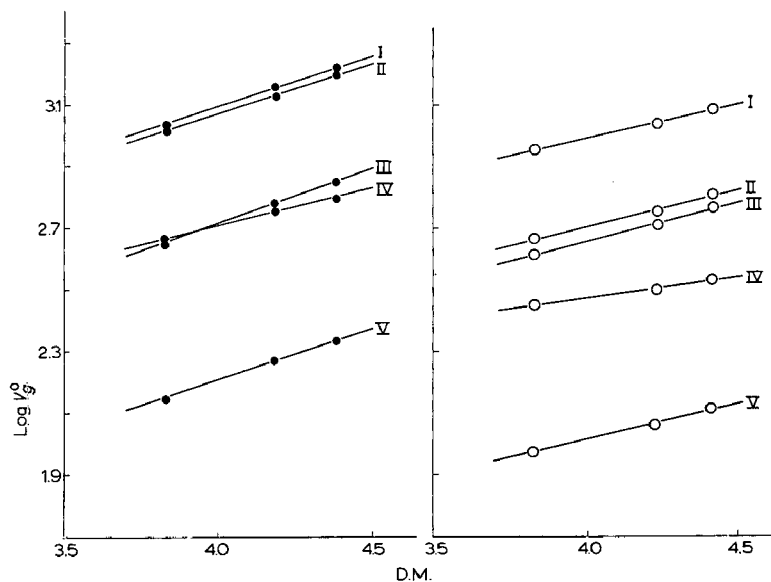


Fig. 1. Variation of $\log V_g^0$ with dipole moment for nitrotoluenes (●) and tolunitriles (○) at 140° and on the following liquid phases: I, Squalane; II, polyethyleneglycol succinate; III, polyoxyethylenesorbitan monostearate; IV, silicone oil; and V, polyethyleneglycol.

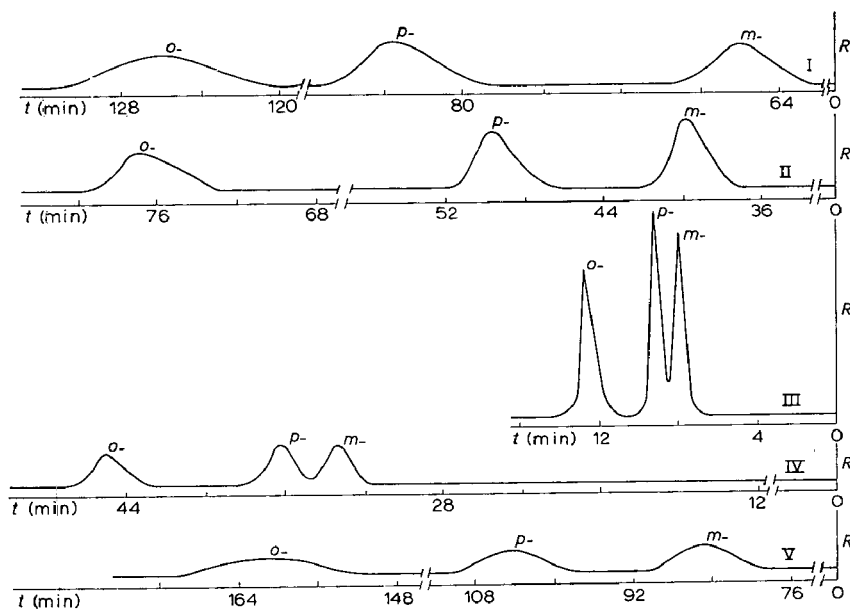


Fig. 2. Chromatograms showing the separation of fluoronitrobenzene isomers on I, polyethyleneglycol succinate at 140°; II, polyoxyethylenesorbitan monostearate at 140°; III, polyethyleneglycol at 160°; IV, silicone oil at 140°; and V, squalane at 140°. R is the recorder deflection and t is the retention time in min.

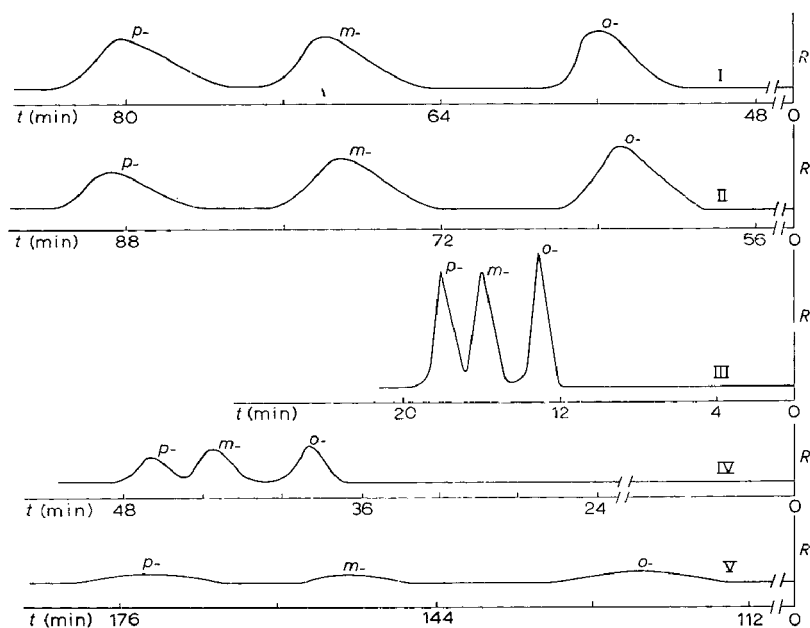


Fig. 3. Chromatograms showing the separation of tolunitriles at 140° on I, polyoxyethylene-sorbitan monostearate; II, polyethyleneglycol succinate; III, polyethyleneglycol; IV, silicone oil; V, squalane. R is the recorder deflection and t is the retention time in min.

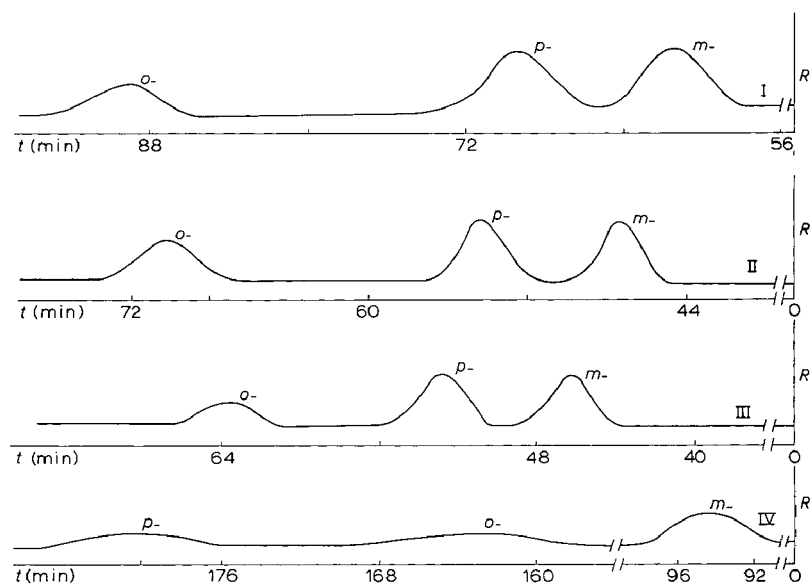


Fig. 4. Chromatograms showing the separation of anisoles on polyethyleneglycol succinate. The chromatograms are represented as follows: I, fluoroanisoles at 80°; II, chloroanisoles at 120°; III, bromoanisoles at 140°; IV, nitroanisoles at 180°. R is the recorder deflection and t is the retention time in min.

induced electron transfer to one of the ring substituents when it is under the influence of a solvent dipole. For toluenes, it seems fairly clear that the steric effects in the *ortho*-derivatives are the main differences. For other derivatives (chloromethoxy, bromo-nitrobenzene, etc.) the *ortho*-derivatives have an effectively larger dipole moment, leading to stronger interactions with the solvent. In the toluenes this effect is missing (alkyl group dipole moments are small) and steric hindrance to solvent interactions with the dipole by the methyl becomes dominant, leading to lesser interaction of the *o*-toluene isomers.

The most selective liquid phases for separation and quantitative determination in this work are the polyesters, *i.e.* PEGS and PA (as seen in Table II, and Figs. 2-4). The substitution of a hydrogen atom in a glycol-type liquid phase by an ester group (succinate or stearate) seems to enhance greatly the selectivity. Carbonyl groups of esters may act as a good polarizing group and would then yield a better resolution of polar solutes.

In SO and SQ, the selectivity was lower than in other liquid phases. They gave wide peaks but were accompanied with larger retention volumes. PEG gave sharp peaks but with a wide base; therefore, the number of theoretical plates was the lowest among the other solvents. In PEG, the specific retention volumes are the smallest among the other liquid phases. This may be caused by the thinner film of the liquid on the solid support due to the higher density of this liquid relative to the other liquids (as in Part I, Table I). In addition, the high molecular weight of PEG and the presence of intermolecular hydrogen bonds would also decrease the retentions of the isomers on this liquid phase.

ACKNOWLEDGEMENTS

The authors are thankful to the Head of the Chemistry Department, College of Science, and to the University of Baghdad for providing every facility to accomplish this work.

REFERENCES

1. A. E. HABBOUSH AND A. H. TAMEESH, *J. Chromatog.*, 53 (1970) 143.
2. A. E. HABBOUSH AND R. O. C. NORMAN, *J. Chromatog.*, 7 (1962) 438.
3. R. O. C. NORMAN, *Proc. Chem. Soc.*, (1958) 151.
4. J. C. COURTIER, L. ETIENNE, J. TRANCHANT AND S. VERTALIER, *Bull. Soc. Chim. France*, (1965) 3181.
5. J. S. PARSONS, S. M. TSANG, M. P. DIGIAIMO, R. FEINLAND AND R. A. PAYLOR, *Anal. Chem.*, 33 (1961) 1858.
6. K. BOMBAUGH, *Anal. Chem.*, 33 (1961) 29.
7. J. RATUSKY AND L. BASTER, *Chem. Ind. (London)*, (1964) 579.
8. T. ARAKI, *Bull. Chem. Soc. Japan*, 36 (1963) 879.
9. A. N. KOROL, *Teoreticheskaya i Eksperimental'naya Khimiya*, 1, No. 6 (1965) 769.
10. A. N. KOROL, *Teoreticheskaya i Eksperimental'naya Khimiya*, 2, No. 1 (1966) 79.
11. A. I. M. KEULEMANS, in C. G. VERVER (Editor), *Gas Chromatography*, Reinhold, New York, 1959, p. 166.
12. L. ROHRSCHEIDER, *Z. Anal. Chem.*, 211 (1965) 18.
13. S. H. LANGER, *Anal. Chem.*, 39 (1967) 524.
14. H. M. MCNAIR AND T. M. DEVRIES, *Anal. Chem.*, 33 (1961) 806.
15. I. BROWN, *J. Chromatog.*, 10 (1963) 284.
16. S. H. LANGER AND J. H. PURNELL, *J. Phys. Chem.*, 67 (1963) 263.
17. P. CHOVIN, *Bull. Soc. Chim. France*, (1964) 1800.
18. L. ROHRSCHEIDER, *J. Chromatog.*, 22 (1966) 6.
19. A. N. KOROL, *Ukr. Khim. Zh.*, 32 (1966) 329.

- 20 A. R. COOPER, C. W. P. CROWNE AND P. G. FARRELL, *J. Chromatog.*, 27 (1967) 362.
 - 21 A. O. S. MACZEK AND C. S. G. PHILLIPS, *J. Chromatog.*, 29 (1967) 15.
 - 22 A. R. COOPER, C. W. P. CROWNE AND P. G. FARRELL, *J. Chromatog.*, 29 (1967) 1.
 - 23 C. BIGHI, A. BETTI AND G. SAGLIETTO, *Bull. Soc. Chim. France*, (1967) 4637.
 - 24 S. H. LANGER, C. ZAHN AND G. PANTAZOPLOS, *J. Chromatog.*, 3 (1960) 154.
 - 25 J. JANÁK AND M. HRIVNÁČ, *J. Chromatog.*, 3 (1960) 297.
 - 26 D. E. MARTIRE, in A. B. LITTLEWOOD (Editor), *Gas Chromatography*, 1966, Inst. Petrol., London, 1967. p. 21.
 - 27 A. B. LITTLEWOOD, C. S. G. PHILLIPS AND D. T. PRICE, *J. Chem. Soc.*, (1955) 1480.
 - 28 E. H. HUNTRESS, *Organic Chlorine Compounds*, J. Wiley & Sons, New York, 1948.
 - 29 J. TIMMERMANS, *Physico-Chemical Constants of Pure Organic Compounds*, Vol. I, Elsevier, Amsterdam, London, New York, 1950.
 - 30 E. W. WASHBURN, *International Critical Tables*, Vols. I and VII, McGraw-Hill Co., New York, 1926.
 - 31 C. D. HODGMAN (Editor), *Hand Book of Chemistry and Physics*, 42th Ed., 1960-1961, The Chemical Rubber Publishing Co., Ohio, 1960-1961.
 - 32 J. W. SMITH (Editor), *Electrical Dipole Moments*, Butterworths, London, 1955, p. 96.
- J. Chromatog.*, 53 (1970) 151-162

CHROM. 4984

RELATIVE RETENTION TIME CHANGES WITH TEMPERATURE FOR THE GAS CHROMATOGRAPHIC IDENTIFICATION OF VOLATILE OIL COMPONENTS

P. N. BRECKLER AND T. J. BETTS

Department of Pharmacy, Western Australian Institute of Technology, Bentley 6102, Western Australia (Australia)

(Received July 13th, 1970)

SUMMARY

Changes in relative retention times of volatile oil components with change in column temperature appear to relate to polarity matches of the substance concerned with the stationary phase used. Usually relative retention times to linalol decrease with increase in temperature, but this is not always so. Such observations, on three different types of stationary phase, seem to be of value in indicating the class of oil constituents.

INTRODUCTION

Discussing gas chromatographic relative retention times, CRAMERS AND KEULEMANS¹ have observed that these are affected "only slightly by the column temperature" and that their dependence on temperature "is complicated, no general rules can be given". In the course of a study of constituents of volatile oils, we have observed general patterns of relative retention times which should prove of value in identifying the class of an unknown oil constituent.

EXPERIMENTAL

A Beckman "GC-M Research" gas chromatograph with FID, and Sargent recorder was used. Nitrogen or helium was used as mobile phase, supplied at 60 ml/min, with hydrogen supplied to the detector at 92.5 ml/min to give maximum sensitivity. Three different stainless steel columns were used, each 2 m long \times 5 mm I.D., packed by the manufacturer with 15% stationary phase on 42/60 Chromosorb W. Stationary phases used were the non-polar dimethyl polysiloxane (SE-30), the increasingly polar diethylene glycol succinate (DEGS), and the polyethyleneglycol Carbowax 20M. Reference volatile oil constituents and oils were obtained from various commercial sources, including some kindly presented by Plaimar Ltd. of Perth, W.A. Relative retention times were observed against linalol as standard on several different occasions

TABLE I

RELATIVE RETENTION TIMES OF SUBSTANCES TO LINALOL ON GIVEN STATIONARY PHASES AT VARIOUS TEMPERATURES

Stationary phase	Column temperature (isothermal)				
	160°	175°	190°	205°	220°
<i>Citronellyl acetate (A₁)</i>					
DEGS	1.00	1.00	1.00	1.00	1.00
20 M	1.24	1.20	1.18	1.17	1.11
SE-30	2.73	2.54	2.31	2.20	2.08
<i>Geranyl acetate (A₁)</i>					
DEGS	1.58	1.57	1.55	1.50	
20 M	1.83	1.74	1.71	1.64	1.56
SE-30	3.05	2.79	2.61	2.38	2.21
<i>Linalyl acetate (A₁)</i>					
DEGS	1.08	1.04	1.00	1.00	1.00
20 M	1.14	1.15	1.13	1.13	1.12
SE-30	1.98	1.87	1.78	1.73	1.65
<i>Menthyl acetate (A₁)</i>					
DEGS	1.15	1.14	1.14	1.13	1.12
20 M	1.31	1.33	1.35	1.35	1.35
SE-30	2.52	2.33	2.22	2.10	2.00
<i>Terpinyl acetate (A₁)</i>					
DEGS	2.05	2.00	1.91	1.88	1.83
20 M	2.14	2.15	2.15	2.13	2.13
SE-30	3.20	2.90	2.83	2.60	2.43
<i>Cineole (A₂)</i>					
DEGS	0.26	0.31	0.32	0.33	0.38
20 M	0.31	0.36	0.39	0.47	0.42
SE-30	0.86	0.86	0.90	0.91	0.91
<i>Isomenthone (A₂)</i>					
20 M	0.97	1.03	1.07	1.09	1.13
DEGS	1.00	1.07	1.09	1.14	1.17
SE-30	1.39	1.38	1.39	1.39	1.39
} note!					
<i>Limonene (A₂)</i>					
DEGS	0.21	0.24	0.26	0.28	0.33
20 M	0.25	0.31	0.33	0.35	0.40
SE-30	0.76	0.80	0.85	0.87	0.82
<i>Myrcene (A₂)</i>					
DEGS	0.21	0.23	0.24	0.25	0.33
20 M	0.21	0.24	0.27	0.30	0.30
SE-30	0.55	0.56	0.56	0.57	0.54
<i>β-Pinene (A₂)</i>					
DEGS	0.16	0.17	0.18	0.24	0.25
20 M	0.18	0.23	0.25	0.27	0.31
SE-30	0.65	0.68	0.73	0.73	0.70
<i>Citronellol (B₁)</i>					
SE-30	1.79	1.71	1.67	1.56	1.47
DEGS	2.16	2.06	2.00	1.88	1.83
20 M	2.58	2.48	2.24	2.17	1.94
<i>Geraniol (B₁)</i>					
SE-30	2.01	1.93	1.83	1.76	1.65
DEGS	3.21	3.06	2.91	2.63	2.49
20 M	3.62	3.35	3.10	2.91	2.72

TABLE I (continued)

Stationary phase	Column temperature (isothermal)				
	160°	175°	190°	205°	220°
<i>Isoborneol (B1)</i>					
SE-30	1.50	1.50	1.49	1.47	1.47
DEGS	1.83	1.85	1.80	1.73	
20 M	1.90	1.91	1.89	1.91	1.88
<i>Menthol (B1)</i>					
SE-30	1.54	1.48	1.45	1.43	1.40
DEGS	1.48	1.50	1.48	1.47	1.50
20 M	1.63	1.64	1.63	1.64	1.63
<i>Anethole (B2)</i>					
SE-30	2.28	2.17	2.12	2.03	1.95
20 M	3.53	3.44	3.26	3.17	
DEGS	4.02	3.75	3.55	3.38	3.17
<i>Cinnamaldehyde (B2)</i>					
SE-30	2.29	2.24	2.15	2.03	1.92
20 M			6.9	6.4	5.9
DEGS		10.00	9.35	8.65	8.0
<i>Estragole (B2)</i>					
SE-30	1.61	1.55	1.52	1.47	1.45
20 M	2.00	1.94	1.92	1.92	1.89
DEGS	2.25	2.15	2.11	2.05	2.00
<i>Eugenol (B2)</i>					
SE-30	3.29	3.09	2.83	2.67	2.51
20 M			9.8	9.0	7.6
DEGS		12.5	11.3	10.3	
<i>Safrole (B2)</i>					
SE-30	2.25	2.19	2.13	2.04	
20 M	4.21	4.04	3.94	3.82	3.59
DEGS		4.88	4.65	4.25	
<i>Camphor (B3)</i>					
20 M	1.24	1.31	1.35	1.36	1.38
SE-30	1.39	1.41	1.41	1.41	1.39
DEGS	1.47	1.55	1.61	1.63	1.66
<i>Carvone (B3)</i>					
SE-30	2.05	2.00	1.90	1.83	1.73
20 M	2.67	2.65	2.55	2.54	2.38
DEGS	3.22	3.13	3.09	2.93	
<i>Citral (B3)</i>					
SE-30	2.21	2.07	1.97	1.86	1.73
20 M	2.46	2.42	2.31	2.26	2.16
DEGS	2.89	2.79	2.75	2.63	
<i>Piperitone (B3)</i>					
SE-30	2.12	2.04	1.97	1.93	1.86
20 M	2.62	2.63	2.63	2.64	2.63
DEGS	3.11	3.03	3.00	2.87	
<i>Pulegone (B3)</i>					
SE-30	1.95	1.87	1.88	1.86	1.77
20 M	1.95	2.00	2.00	2.00	2.00
DEGS	2.17	2.16	2.20	2.19	2.17
<i>Terpineol (B3—anomalous)</i>					
SE-30	1.62	1.58	1.56	1.53	1.50
20 M	2.11	2.06	2.00	1.95	1.89
DEGS	2.16	2.13	2.10	2.07	2.00

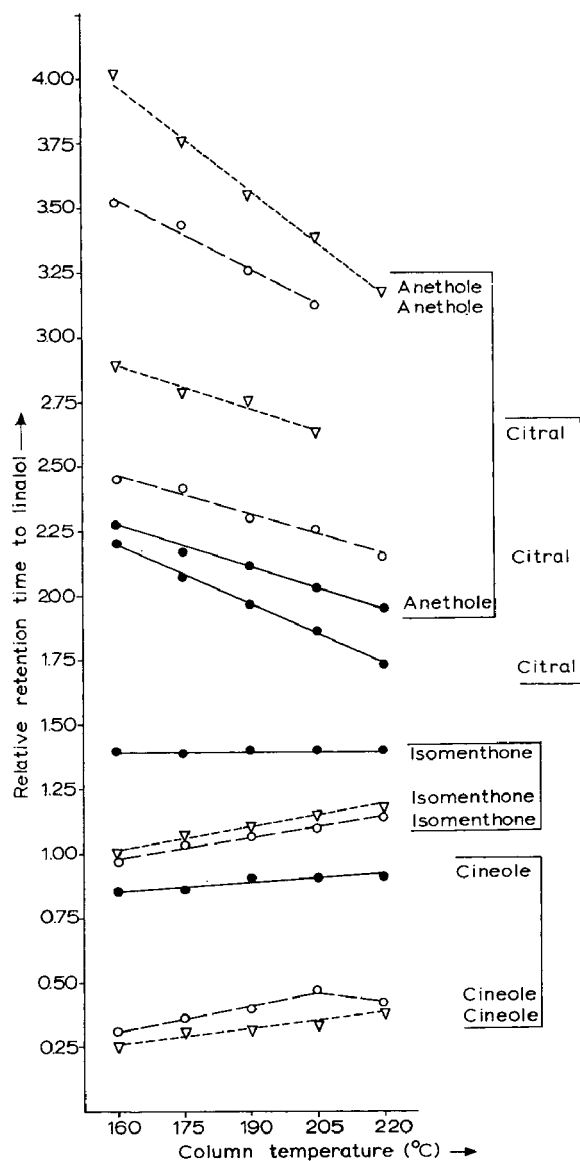


Fig. 1. Relative retention times to linalol on three columns at different column temperatures. ▽—▽, on DEGS; ○—○, on 20 M; ●—●, on SE-30.

for the various oil constituents, at a series of isothermal temperatures 15° apart, the oven temperature being checked by thermistor. The upper temperature limit was the limitation of the column stationary phase material, and the lower limit, the reasonable time for obtaining peaks.

RESULTS AND DISCUSSION

Relative rather than absolute retention times were used for this work, to offset

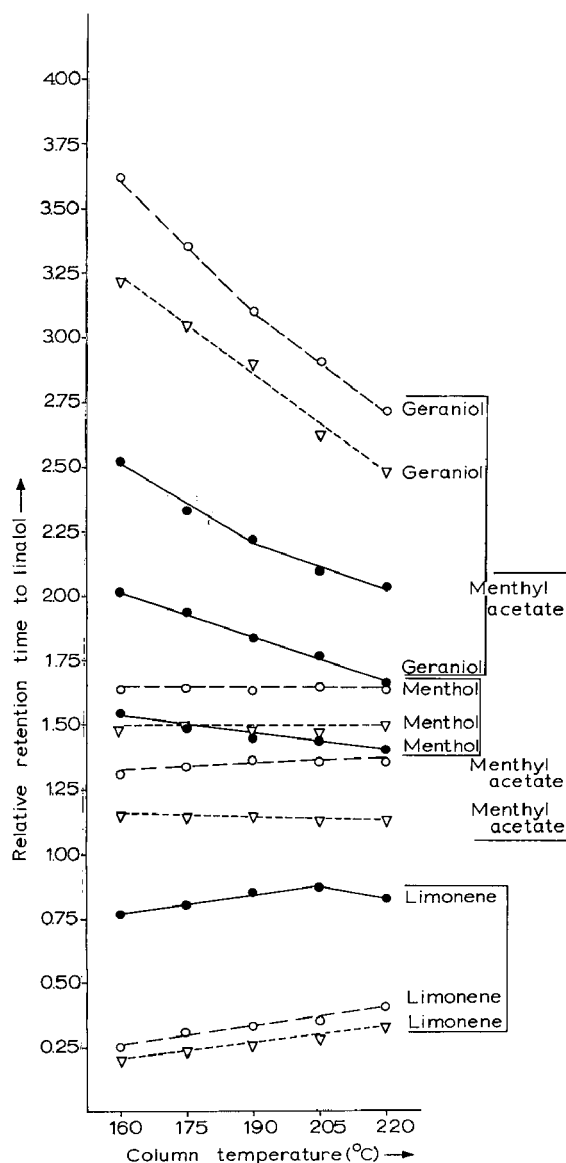


Fig. 2. Relative retention times to linalol on the three columns indicated, at different column temperatures. ▽— — ▽, on DEGS; ○— — ○, on 20 M; ●— — ●, on SE-30.

any slight day-to-day changes in mobile phase flow rate. They were calculated from chart distances measured in millimeters. Linalol was chosen as the standard as it has a fairly short retention time (between 0.9 min on Carbowax 20M at 220°, and 6.0 min at 145°) intermediate between those of the non-polar terpene hydrocarbons such as limonene, and the slightly polar oxygenated terpenoids such as carvone, which represent the most frequently occurring components of many volatile oils.

Results are arranged according to polarity in Table I in five groups, which are explained below, and some results are plotted in Figs. 1 and 2 to illustrate graphically

TABLE II

RELATIVE RETENTION TIMES OF SOME SUBSTANCES TO LINALOL ON GIVEN STATIONARY PHASES AT 205° WITH DIFFERENT MOBILE PHASES

Mobile phase	Stationary phase		
	SE-30	20 M	DEGS
	<i>Menthol</i>		
Helium	1.43	1.66	1.43
Nitrogen	1.44	1.63	1.50
	<i>Piperitone</i>		
Helium	1.93	2.66	2.86
Nitrogen	1.94	2.63	2.88

the patterns characteristic of the groups, which serve to identify members of each of them. Change of mobile phase produced very little change in relative retention time (see Tables II and III) unless high temperatures, near the limit for the stationary phase, were used. Thus results obtained with the nitrogen and helium are averaged in Table I. Whilst the range of stationary phases available for columns is very great, those used represent the three main types, namely non-polar (SE-30), slightly polar electron-donor (DEGS), and more polar electron-acceptor (20M), and so should indicate the style of result which would be obtained using other columns of these types. For all substances examined, of course, the actual retention time decreased with increase in temperature of the column. When measured against the standard linalol, a relatively polar substance, the relative retention times also decreased with increase in temperature, except in the case of some non-polar compounds.

For most slightly polar substances, the relative retention times to linalol are greatest on DEGS, of the three stationary phases used. This includes terpenoid carbonyls such as citral and substituted aromatics such as anethole (see Fig. 1). Their limited polarity thus appears to be best matched by the limited polarity of DEGS. The only exception to this is that for most terpenoid alcohols such as geraniol, the relative retention times shown on 20M are slightly greater than those shown on DEGS, indicating the higher polarity of these alcohols, best matched by the 20M glycol

TABLE III

RELATIVE RETENTION TIMES OF SOME SUBSTANCES TO LINALOL ON CARBOWAX 20 M GLYCOL AT VARIOUS TEMPERATURES WITH DIFFERENT MOBILE PHASES

Mobile phase	Column temperature (isothermal)				
	160°	175°	190°	205°	220°
	<i>Piperitone</i>				
Helium	2.63	2.63	2.59	2.66	2.56
Nitrogen	2.61	2.63	2.63	2.63	2.63
	<i>Safrole</i>				
Helium	4.21	4.00	3.94	3.83	3.56
Nitrogen	4.22	4.08	3.94	3.82	3.63

groups (see Fig. 2). Nevertheless, in almost all cases where the solute can be said to be slightly polar (as in the B group of Table I) relative retention times are lowest on the non-polar SE-30 column at a given temperature.

The lowering of the polarity of terpenoid alcohols upon esterification (*e.g.* menthol to menthyl acetate) is clearly indicated by the results obtained (placing them in Group A of Table I) in which an inversion of response to polar and non-polar stationary phases is observed, although their polar "origin" is perhaps indicated by the slope of these plots, when compared with other non-polar substances, such as limonene (see Fig. 2). In contrast to the slightly polar substances, the non-polar volatile oil components exhibit their highest relative retention times on SE-30 (usually with the lowest values on DEGS). These non-polar substances fall into two groups, the terpenoid esters, in which relative retention time, as usual, decreases with rise in column temperature, and the terpene hydrocarbons (*e.g.* limonene), in which it increases slightly or remains constant.

To summarise the information for identifying the chemical class of an unknown component of a volatile oil using its relative retention times to linalol:

A. Non-polar substances with relative retention times on SE-30 greater than those on both the other two columns: (1) Relative retention times decrease rapidly on SE-30 as temperature rises—terpenoid ester. (2) Relative retention times are low and increase slightly as temperature rises—terpene hydrocarbon or non-polar terpenoid.

B. Slightly polar substances with relative retention times on SE-30 below those on the other two columns, or at least not greater than both: (1) Relative retention times greatest on 20M—terpenoid alcohol. (2) Relative retention times greater on DEGS than on 20M, but with the results on these two polar columns fairly close, converging as temperature rises, and both well-separated from those on SE-30—substituted aromatic. (3) Relative retention times greater on DEGS than on 20M, with those on 20M roughly equally spaced between the other two—terpenoid carbonyl.

The results given for limonene are typical for group A₂ substances such as β -pinene, cineole and myrcene as well. Thus the low polarity of the terpenoid ether cineole is comparable to that of terpene hydrocarbons. The non-polar column (SE-30) is clearly best for distinguishing between these substances. The saturated terpenoid carbonyl isomenthone is also sufficiently low in polarity to fall in this group, although its relative retention time to linalol is approximately 1.40. Typically for this group A₂, the relative retention times for isomenthone on the two polar columns increase with rising temperature (Fig. 1), so isomenthone changes from emerging ahead of linalol to being behind it on the column.

Menthol, in contrast to isomenthone, is sufficiently polar to fall with other terpenoid alcohols into group B₁, with results for SE-30 and DEGS close together, and, in fact, crossing, being just less than those on 20M. The slopes of the results for isomenthone, which in two cases increase with temperature rise, are again unlike those of menthol (Figs. 1 and 2). Isoborneol shows similar behaviour to menthol. The acyclic terpenoid alcohols geraniol and citronellol exhibit distinctly higher relative retention times than menthol and isoborneol, especially on the polar columns, and show rapid decrease in values as temperature increases. The only terpenoid alcohol not appearing with the others in group B₁ is terpineol, for although terpineol results on polar columns are distinctly greater than those on SE-30, the values on 20M are not quite above

those for DEGS. Other terpenoid alcohols examined all show highest relative retention times on the 20M glycol column, unlike all other substances examined here, including the phenolic alcohol eugenol.

Camphor, whilst showing similar relative retention times on SE-30 to isomenthone, menthol and isoborneol, falls satisfactorily into the appropriate group B₃ of carbonyl terpenoids. Camphor is the only substance examined for which values on SE-30 come between those on DEGS (greatest) and 20M, and the rising slope of the results obtained on polar columns suggests an affinity with the low-polarity substances such as cineole. At higher temperatures than those possible here, it appears from extrapolation that the more usual situation would occur with results on SE-30 being the lowest.

Results obtained with menthyl acetate are typical of those for all the other terpenoid acetate esters—perhaps surprisingly in the case of terpinyl acetate in view of the anomalous behaviour of terpineol. Values for citronellyl and linalyl acetates on DEGS are very close to unity.

The terpenoid carbonyls in group B₃ such as citral give distinctive results in that plots of the relative retention times show 20M in the middle with DEGS results approximately as far above as those on SE-30 are below the 20M figures. From this distribution the carbonyls are thus less polar than the terpenoid alcohols but more polar than the esters. Carvone and piperitone are normally difficult to distinguish by gas chromatography, but piperitone, unlike carvone, hardly alters in relative retention time to linalol on 20M, as the temperature is changed.

The substituted aromatics of group B₂ are also distinct because of the converging tendency of their values on the two polar columns as the temperature rises, these normally being widely separated from the non-polar column results. The distribution of these results, however, suggests that they are only comparable in polarity with the carbonyls of group B₃. Substances such as apiole, which fall in group B₂, exhibit relative retention times of up to 18 times that of linalol on DEGS, and such values tend to be inconvenient and unreliable for identification work. Thus, although on grounds of matching polarity DEGS or 20M columns give the best separation of substituted aromatics, for speedy results the non-polar SE-30 column is to be preferred. These high retention times on polar columns do not, however, mean that the group B₂ compounds are more polar than those of group B₁, for the results on DEGS and 20M suggest the reverse.

From the polarity match principle, indicated by a substance exhibiting greatest relative retention times on the column stationary phase most closely resembling it in polarity, terpene hydrocarbon and terpenoid ester oils should be chromatographed on non-polar columns, terpenoid alcohol oils on polar glycol columns, and oils with terpenoid carbonyls or aromatics (not too highly substituted) on slightly polar ester columns. However, as volatile oils are complex mixtures in many cases, one type of column is likely to be inadequate for best separation of all the oil components.

REFERENCE

- 1 C. A. M. G. CRAMERS AND A. I. M. KEULEMANS, in J. KRUGERS (Editor), *Instrumentation in Gas Chromatography*, Centrex, Eindhoven, 1968.

CHROM. 4992

GAS-LIQUID CHROMATOGRAPHY OF AMINO ACIDS IN BIOLOGICAL SUBSTANCES*

ROBERT W. ZUMWALT**, DON ROACH*** AND CHARLES W. GEHRKE§

University of Missouri, Columbia, Mo. 65201 (U.S.A.)

(Received August 12th, 1970)

SUMMARY

The development of a gas-liquid chromatographic (GLC) method for the quantitative analysis of amino acids in complex biological substances, specifically blood plasma and urine, has been achieved. The amino acids present in these physiological fluids were quantitatively isolated by ion-exchange methods and retained on the ion-exchange resin while the substances which interfere with the GLC analysis passed through the column and were discarded. The amino acids were then eluted from the column, derivatized to their N-trifluoroacetyl (N-TFA) *n*-butyl esters and analyzed by GLC. Quantitative recovery of the amino acids from the cation and anion-exchange clean-up columns, and amino acids in blood and urine were successfully carried out.

Also, techniques for the analysis of amino acids over a wide range of concentrations were developed. Analyses were made on aliquots of human blood plasma containing only 200 μg of total amino acids, and the results obtained at this level of concentration were both accurate and precise. Further, quantitative data were obtained with samples containing only 20 μg of total amino acids, and semiquantitative analyses were performed on samples containing 2 μg of total amino acids. The data obtained by the GLC method were in excellent agreement with results by classical ion exchange.

Investigations on acylation of the amino acid *n*-butyl esters have shown that the optimum molar ratio of TFAA/amino acids is 50:1 with regard to reproducibility of acylation, stability of the derivative, and maintenance of a small sample volume ($> 75 \mu\text{l}$).

Experiments involving concentration of the derivatized samples have shown

* Contribution from the Missouri Agricultural Experiment Station, Journal Series No. 6056. Approved by the Director. Supported in part by grants from the National Aeronautics and Space Administration (NGR 26-004-011), the National Science Foundation (GB 7182) and the United States Department of Agriculture (12-14-100-8468 (34)).

** Experimental data taken in part from doctoral research, University of Missouri, NSF predoctoral research fellow.

*** Experimental data taken in part from doctoral research, University of Missouri, William Henry Hatch predoctoral research fellow. Now professor of Chemistry, Miami Dade Junior College, Miami, Florida.

§ Professor, Experiment Station Chemical Laboratories.

that the N-TFA *n*-butyl esters have a significant advantage over the N-TFA methyl esters in that evaporative losses do not occur on concentration of the sample at room temperature; whereas serious losses result when the N-TFA methyl esters of the amino acids are concentrated to a smaller volume.

INTRODUCTION

In recent years, many investigations have been conducted to develop and refine techniques for quantitatively determining the amino acids in biological materials. These studies have been of intense interest in the fields of biochemistry, nutrition, medical science, bacteriology, and many other areas. The increasingly wide interest in amino acids and proteins has brought with it the need, and indeed, demand, for accurate, sensitive and rapid amino acid analyses.

Investigations by Drs. MOORE, STEIN, HAMILTON, PIEZ, and others have resulted in accurate and precise methods for amino acid analysis by classical ion-exchange chromatographic techniques. However, over the past eight years, gas-liquid chromatographic (GLC) methods have also reached great refinement, with GLC techniques being widely used for the analysis of lipids, carbohydrates, steroids, various metabolites, pesticides, and many drugs. Similar methods for the routine analysis of amino acids have only recently been reported, since the period 1966 through 1970.

For satisfactory analysis of amino acids by GLC, a complete derivatization of these molecules is essential. Due to the variations in chemical structure and reactivity of the twenty amino acids commonly found in proteins, and other biologically important non-protein amino acids, the quantitative derivatization of all the functional groups under one set of reaction conditions has posed many problems.

Earlier reviews of this area by BLAU¹ and WEINSTEIN² discussed in detail various derivatization and chromatographic techniques for the GLC analysis of amino acids. However, prior to 1968, a complete general GLC procedure for the quantitative analysis of the twenty protein amino acids had not been reported.

Extensive research investigations, led by Professor CHARLES W. GEHRKE, resulted in the development of a GLC technique for quantitatively analyzing the twenty protein amino acids as their N-trifluoroacetyl (N-TFA) *n*-butyl ester derivatives. The reaction conditions for quantitatively preparing the amino acid N-TFA *n*-butyl esters of the twenty protein amino acids have been determined³⁻⁷.

Further, complete GLC resolution on a single column of the protein amino acid derivatives has also been extremely difficult to achieve. GEHRKE AND SHAHROKHI⁷ reported in 1966 a mixed polyester liquid phase for the separation of the N-TFA *n*-butyl esters of the twenty amino acids, but reproducible elution of arginine, histidine, and cystine was not achieved using this column. STEFANOVIC AND WALKER⁸ investigated the use of ethylene glycol adipate (EGA) as a stationary phase for separation of the twenty amino acid N-TFA *n*-butyl ester derivatives, but these workers also did not achieve quantitative elution of arginine, histidine, and cystine.

Investigations were also conducted by MCBRIDE AND KLINGMAN⁹ to find a single column which would separate the amino acid N-TFA *n*-butyl esters, and data were reported for all the protein amino acids with the exception of arginine, histidine, and cystine. Studies on the derivatization and chromatography of the amino acid

N-TFA methyl esters were made by DARBRE, BLAU AND ISLAM^{10,11}. In their investigations using different mixed siloxane liquid phases, quantitative elution of histidine was not obtained.

In 1968, GEHRKE *et al.*¹² reported on a dual-column chromatographic system, using stabilized ethylene glycol adipate and OV-17 as the liquid phases, from which all twenty of the protein amino acids were quantitatively eluted and separated as their N-TFA *n*-butyl esters. Further, a recent monograph by GEHRKE *et al.*¹³ presents in considerable detail macro-semimicro, and micro methods, reagents, sample preparation, instrumental and chromatographic requirements, and sample ion-exchange cleanup for the quantitative GLC analysis of the protein amino acids as their N-TFA *n*-butyl esters.

Refinements of the GLC method have been reported by ROACH *et al.*¹⁴ with regard to the quantitative analysis of histidine, and by ROACH AND GEHRKE¹⁵ on improved performance and reliability of the EGA column of the dual-column system. Conversion of monoacyl histidine to the diacyl derivative on the chromatographic column by injection of trifluoroacetic anhydride has obviated the need for the previously reported *n*-butanol injection. Present studies have shown that histidine (diacyl) can be completely separated from Asp and Phe on the siloxane column of the dual-column system. Further, these investigators have reported that columns containing 0.65 w/w% of stabilized EGA coated on 80/100 mesh AW Chromosorb W, dried at 140° for 12 h, is generally superior to 80/100 mesh AW heat-treated Chromosorb G in terms of resolution, reliability, and ease of preparation¹⁵.

WATERFIELD AND DEL FAVERO¹⁶ reported on the use of silica gel column chromatography for purification of the amino acid N-TFA *n*-butyl esters. After derivatization of the amino acids to the N-TFA *n*-butyl esters, the samples were applied to a silicic acid column, then the amino acids were eluted with diethyl ether. However, for quantitative analyses, difficulties might be expected to be encountered with regard to hydrolysis of the amino acid derivatives during the clean-up procedure.

Recently, the N-trimethylsilyl (TMS) esters of the protein amino acids were extensively investigated by GEHRKE, NAKAMOTO *et al.*¹⁷⁻¹⁹. This technique offers certain advantages in that trimethylsilylation of the twenty protein amino acids is completed in a single reaction medium, and can be separated on a single chromatographic column. Although this latest method has not yet reached the level of sophistication that has been attained by the N-TFA *n*-butyl ester technique, these researchers have shown that the TMS amino acid derivatives hold great promise as a general and complementary method for routine GLC analysis.

Investigations have also been carried out by GEHRKE and co-workers on the experimental conditions for silylation and GLC analysis of some biologically important groups of molecules: nucleic acid components^{20,21}, iodo-containing amino acids²², sulfur-containing amino acids²³, and N-acetylneuraminic acid²⁴. An extensive series of studies was made on the exact reaction conditions required for quantitative silylation of each organic class. Detailed methods are presented and data reported on the precision, accuracy, recovery, and application of the methods.

It was the purpose of this investigation to establish the applicability of the developed GLC technique to the quantitative analysis of amino acids as their N-TFA *n*-butyl esters in complex physiological materials, specifically blood plasma and urine. Successful extension of the GLC method into these areas would greatly enhance the

utility of the technique. To this end, ion-exchange methods for cleanup of these complex materials prior to derivatization were studied.

Further, experiments were made to determine the quantitation of the GLC procedure over a wide range of amino acid concentrations, with emphasis on the development of techniques for accurately analyzing microgram and submicrogram amounts of amino acids in physiological substances.

Also, further refinement of the general procedure was studied with regard to the evaluation of various molar excesses of trifluoroacetic anhydride as the acylating reagent. Studies on evaporative losses due to concentration of the N-TFA methyl esters and N-TFA *n*-butyl ester derivatives were also carried out.

These reported GLC methods, developed in the Missouri laboratories were used by the present authors for the analysis of amino acids in the Apollo 11 and 12 returned lunar samples. The authors served as co-investigator and scientists of the NASA-Ames Consortium of principal and co-investigators under the direction of Dr. CYRIL PON-NAMPERUMA, senior scientist, of the Ames Research Center, National Aeronautics and Space Administration, Moffett Field, Calif.

EXPERIMENTAL

I. Apparatus

(a) General

A Micro-Tek Model 220 dual hydrogen flame detector gas chromatograph equipped with a Varian Model 30 recorder, and a Varian Aerograph Model 2100 gas chromatograph equipped with a Varian Model 20 recorder were used. A Packard Instrument Co. 7300 Series dual-column gas chromatograph with hydrogen flame detectors and equipped with a Honeywell Elektronik 16 strip chart recorder was also used. A digital readout integrator, Infotronics Model CRS 104 was used for determining the peak areas.

Filters for the hydrogen, air, and nitrogen carrier gas to the chromatographs were obtained from the Packard Instrument Co. and contained Linde 5-A molecular sieve and CaSO_4 .

Solvents were removed from the samples with a CaLab rotary evaporator, "cold finger" condenser, and a Welch Duo-Seal vacuum pump, or the samples were taken just to dryness with a stream of dry, purified nitrogen gas in a 100° constant-temperature sand bath.

Filters containing activated charcoal and CaSO_4 were used for purification of the nitrogen gas.

Pyrex 16 × 75 mm glass screw-cap culture tubes with Teflon lined caps (Corning No. 9826) were used as the reaction vessel for the acylation reaction in the macro method and throughout the entire semimicro method.

(b) Macro method

The esterification and interesterification of the amino acids were done in 125-ml § flat-bottom flasks. For the interesterification, the samples were heated in a 100° constant-temperature oil bath supported by a magnetic hot plate stirrer.

The oil bath used for closed-tube acylation of the amino acid *n*-butyl esters consisted of a 3½ in. × 4 in. × 6 in. aluminum pan supported on a magnetic stirrer to

maintain uniform temperature of the oil. Two 100-W heaters controlled by a Variac were used to maintain the temperature at 150°.

The acylation bath was placed in a hood behind a safety shield (Instruments for Research and Industry-IR²) to provide protection for accidental breakage of the acylation tube.

Automatic repipets (Scientific Products Co.) were attached to 950-ml amber bottles for dispensing $\text{CH}_3\text{OH} \cdot \text{HCl}$, $\text{BuOH} \cdot \text{HCl}$, and CH_2Cl_2 . The top portion of the metal plunger was coated with a silicone to prevent metal contamination.

(c) *Micro method*

The complete chemical derivatization by the micro technique was carried out in the special micro reaction vials with teflon-lined screw caps (Fig. 1) (Analytical Biochemistry Laboratories, Columbia, Mo.).

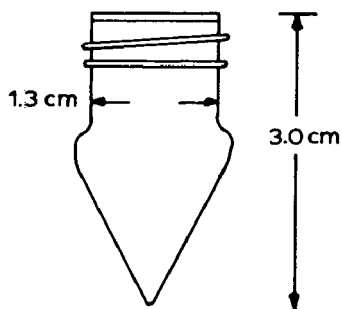


Fig. 1. Reaction vial for the micro method.

The micro samples were heated in a 100° constant temperature sand bath during interesterification.

The solvents were evaporated from the micro samples by placing the sample vials in the sand bath at 100° and directing a stream of dry, purified nitrogen gas into the mouth of the vial, and taking just to dryness.

A Varian Aerograph ultrasonic cleaner was used for mixing of the micro samples.

(d) *Ion-exchange cleanup*

Amberlite IRA-410 or Dowex 2 (50/100 mesh) resin in the chloride form was used for the removal of picrate from the deproteinized blood plasma.

Amberlite CG-120-H or Dowex 50 (80/100 and 100/200 mesh) resin in the hydrogen form were used to exchange the amino acids present in the physiological samples. These resins can also be used to exchange the amino acids in the presence of picrate from deproteinized samples and to allow the picrate to pass through the column.

Amberlite IRA-410 or Dowex 1 X2 (80/100 and 100/200 mesh) anion-exchange resins in the acetate form were also used for the separation of amino acids from interfering substances present in physiological fluids.

Fischer-Porter pyrex glass columns (Fischer-Porter Co., Warminster, Pa.), 0.9 × 15 cm and 1.5 × 15 cm with sintered glass filters, were packed with the various exchange resins for isolation of the amino acids from interfering materials and picrate.

II. Reagents and materials

(a) General

All of the amino acids used in this study were obtained from Mann Research Laboratories, Inc., New York, N.Y., or Nutritional Biochemicals Corp., Cleveland, Ohio, and were chromatographically pure. Ribonuclease (Lot No. 26B-1370) was obtained from Sigma Chemical Company, St. Louis, Mo.

Methanol and *n*-butanol were "Baker Analyzed" reagents. The trifluoroacetic anhydride was obtained from Distillation Products Industries, and was an "Eastman Grade" chemical. Acetonitrile, a "Baker Analyzed" reagent of "Nanograde" purity, was stored over drierite in a bottle with a ground glass stopper. Anhydrous HCl, 99.0% minimum purity, was obtained from the Matheson Company, Joliet, Ill.

The methanol, *n*-butanol, and methylene chloride were redistilled from an all-glass system and stored in all-glass inverted top bottles to protect from atmospheric moisture. The methanol was first refluxed over magnesium turnings, and the methylene chloride and *n*-butanol over calcium chloride before distillation. The anhydrous HCl gas was passed through a H₂SO₄ drying tower before bubbling into the *n*-butanol or methanol.

Silanized spun glass, obtained from Analabs, North Haven, Conn., was stored in a desiccator over P₂O₅.

For the ion-exchange cleanup procedures, the following reagents were prepared: 0.02 *N* HCl, 0.01 *N* HCl, 3 *N* HCl, 3 *N* CH₃COOH, 1% picric acid, 3 *N* NH₄OH, 0.1 *N* KOH, and 3 *N* KOH.

(b) Standard stock solutions

Standard amino acid solution. This solution consisted of an aqueous solution (0.1 *N* HCl) containing the twenty protein amino acids at individual concentrations of 2.5 mmol/L.

n-Butyl stearate internal standard solution (I.S.). This solution contained 2.5 mmol/L.

(c) GLC columns

Stabilized grade ethylene glycol adipate (EGA) was obtained from Analabs, Inc., North Haven, Conn., and coated on 80/100 mesh Chromosorb G which had been heat-treated as described by GEHRKE *et al.*^{12,13}. The EGA column material was packed into 1.5 m × 4 mm I.D. U-shaped glass columns. The recommended packing is described in ref. 15.

The OV-22 siloxane substrate was purchased from Supelco, Inc., Bellefonte, Pa. The support material for the OV-22 column was 80/100 mesh high-performance (HP) Chromosorb G, and the column packing was placed in 1.0 m × 4 mm I.D. U-shaped glass columns.

The column packing was prepared by first adding a known amount of the support material to a 500-ml ribbed round-bottom flask, then adding the solvent used to dissolve the stationary phase until the liquid level was about $\frac{1}{4}$ in. above the support material. The stationary phase was weighed into a small erlenmeyer flask, dissolved in the appropriate solvent (CH₃CN or CH₂Cl₂ for EGA, and CH₂Cl₂ for OV-17 and OV-22) and then transferred to the flask containing the support. The flask containing the support and stationary phase was placed in a 60° water bath, and the solvent was

removed slowly over a period of 45 min with the rotary evaporator under a partial vacuum. The column material was then packed in clean, dry glass columns with gentle tapping to ensure uniform distribution. A plug of silanized spun glass was then placed in each end of the column to hold the column packing in place. The columns were then conditioned as described by GEHRKE *et al.*^{12,13}.

III. Sample preparation of proteins and biological fluids

(a) Protein hydrolysate

Fifty milligrams of ribonuclease (dried over P_2O_5 at room temperature to a constant weight) were hydrolyzed with 50 ml of constant boiling HCl (6 *N*) for 20 h at 110° in a closed tube under a nitrogen atmosphere. The sample was then dried at room temperature on a rotary evaporator, and the residue transferred to a 50-ml volumetric flask and brought to volume with 0.1 *N* HCl.

(b) Removal of proteins from blood plasma with picrate

Five milliliters of the blood plasma to be deproteinized were placed in a 125-ml erlenmeyer flask, 25 ml of a 1% aqueous picric acid solution were added, and the solution was swirled or stirred with a magnetic stirrer for 5 min. The protein suspension was then centrifuged for 10 min at 3500 r.p.m. and the clear supernatant liquid containing the free amino acids and excess picrate removed by decantation.

(c) Method I—Removal of picrate by anion-exchange chromatography

To remove the picrate, a 25 ml aliquot of the protein-free supernatant from IIIb was passed through a 1.5 × 5 cm column of Amberlite IRA-410 or Dowex 2 (50/100 mesh) resin in the chloride form at the rate of 1 to 2 ml/min. The resin was then washed with two 5-ml portions of 0.02 *N* HCl at a similar rate. Then, the resin was washed with three additional 10-ml portions of 0.02 *N* HCl with the column stopcock completely open. The effluent and washings were collected in a 125-ml § flat-bottom flask and evaporated to dryness on a rotary evaporator with the flask immersed in a 60° constant-temperature water bath. The residue was then redissolved in 5 ml of 0.1 *N* HCl and placed on a cation-exchange column for exchange separation of the amino acids from interfering materials in the sample.

(d) Preparation of the cation-exchange column

In the following ion-exchange procedures, a 60-fold or greater excess of resin capacity to exchangeable ions placed on the column was maintained.

The resin (Amberlite CG-120-H) was placed in a 500-ml beaker. *Ca.* 3 g of dry resin (14-mequiv. capacity) were required for each 0.9 × 15 cm column. The resin was then covered with 3 *N* NH_4OH , swirled for 30 to 60 min, and allowed to settle. The NH_4OH was then removed from the resin by decantation. The process was repeated twice, then washed with d.d. H_2O until approximately neutral.

The resin was regenerated with 3 *N* HCl (three times) as described above, then washed with d.d. H_2O until neutral.

The Fischer and Porter columns were then filled *ca.* half full with the wet resin (*ca.* 3 g dry weight of resin), avoiding any channeling in the column. The column was partially filled with d.d. H_2O and the wet resin was added. The column was washed and drained so that the liquid level was at the resin surface. The sample was then added as follows.

(e) *Method II—Cation-exchange cleanup of protein-free blood plasma and urine*

The protein- and picrate-free blood plasma which had been dissolved in 5 ml of 0.1 *N* HCl, as described earlier, was carefully placed on the resin and allowed to pass slowly through the column (*ca.* 20 drops/min). The effluent containing the interfering substances was discarded. For cation-exchange cleanup of urine, a 5-ml aliquot of urine was taken to near dryness on a rotary evaporator at 60° with a constant-temperature water bath. The residue was then dissolved in 5 ml of 0.1 *N* HCl, and carefully placed on the resin. The flask was washed three times with 2-ml portions of 0.1 *N* HCl, and these washings were placed on the resin. The solution was then allowed to pass through the column at *ca.* 20 drops/min, and the effluent was discarded. *Caution:* The level of the liquid in the column must not be allowed to fall below the surface of the resin.

Five 5- to 10-ml portions of d.d. H₂O were passed through the column (3 to 5 ml/min) and the washings were discarded.

Five separate 2-ml portions of 3 *N* NH₄OH at *ca.* 1 ml/min, followed by five 5-ml portions of d.d. H₂O, were passed through the column at *ca.* 3 ml/min. The eluate containing the amino acids was collected in a 125-ml flat-bottom flask with § 24/40 ground glass top. The sample was then taken to dryness at 60° in a constant-temperature water bath by use of a rotary evaporator and stored under refrigeration until analyzed. (Also, the sample may be shell frozen and lyophilized.) Alternatively, the eluate may be collected in a 16 × 75 mm glass culture tube (8-ml volume) which is placed in a 100° constant-temperature sand bath, while directing a stream of dry, purified nitrogen into the tube during elution to aid evaporation.

(f) *Method III—Isolation of amino acids from deproteinized samples containing picrate and other interferences*

For biological samples to be analyzed by GLC, the amino acids can be exchanged from both picrate and interfering substances in the following single cation-exchange cleanup procedure:

A 0.9 × 7 cm column of Amberlite CG-120-H or Dowex 50 (80/100 or 100/200 mesh) resin in the hydrogen form was prepared.

A 25-ml aliquot of the protein-free supernatant from IIIb was passed through the column at a rate of 1 to 2 ml/min.

Five 5- to 10-ml portions of distilled water were used to wash the resin, and the effluent and washings containing picrate and interfering materials were discarded.

The amino acids were eluted from the resin with five separate 2-ml portions of 3 *N* NH₄OH at 1 to 2 ml/min, followed by five 5-ml portions of distilled water at 3 ml/min.

The alkaline effluent was collected in a 125-ml § flat-bottom flask and evaporated to dryness as described in IIIc. The sample was then ready for derivatization and analysis by GLC.

For classical ion-exchange chromatographic analysis of the sample, the residue was redissolved in 5.0 ml of 0.1 *N* HCl, transferred to a screw top culture tube with a teflon-lined cap, tightly sealed, and refrigerated until analysis.

(g) *Preparation of the anion-exchange column*

The resin (Dowex 1 X2) was placed in a 500-ml beaker. *Ca.* 3 g of dry resin

(10 mequiv. capacity) are required for each 0.9×15 cm column. The resin was covered with 3 *N* KOH, swirled for 30 to 60 min, and allowed to settle. The KOH was removed from the resin by decantation, and the process was repeated two times. The resin was then washed with d.d. H_2O until approximately neutral.

The resin was regenerated to the acetate form with 3 *N* CH_3COOH as described above, then washed with d.d. H_2O until neutral.

The Fischer and Porter columns were filled *ca.* half full with the wet resin (*ca.* 3 g dry weight of resin), avoiding any channeling in the column. The column was first partially filled with d.d. H_2O , then the wet resin was added. The column was then washed and drained so that the liquid level was at the resin surface. The cation-exchange cleaned urine sample was added to the resin column as follows.

(h) Anion-exchange cleanup of urine

The urine sample cleaned by cation-exchange (procedure IIIe) which had been taken to dryness and redissolved in 5 ml of 0.1 *N* KOH was carefully placed on the resin and allowed to pass slowly through the column at *ca.* 20 drops/min. The effluent was discarded. *Caution:* The level of the liquid in the column must not be allowed to fall below the surface of the resin.

Fifteen 10-ml portions of d.d. H_2O were then passed through the column (3 to 5 ml/min) and the effluent was discarded. (150–250 ml of d.d. H_2O may be required to clean the urine samples, *i.e.* removal of all urea.)

Five separate 3-ml portions of 3 *N* CH_3COOH at *ca.* 20 drops/min, followed by five 5-ml portions of d.d. H_2O , were passed through the column at 3 ml/min. The effluent containing the amino acids was collected in a 125-ml § flat-bottom flask and taken to dryness with a rotary evaporator at 60° in a water bath. The sample was then ready for derivatization and subsequent analysis by GLC.

(i) Recovery studies of the ion-exchange cleanup procedures

To establish the quantitation of the cation- and anion-exchange cleanup procedures for separation of amino acids from interfering materials, known amounts of the protein amino acids were placed on the columns and taken through the described methods. After elution of the amino acids from the cation or anion resin column, an exact amount of ornithine was added as an internal standard, and the amino acids were derivatized to their N-TFA *n*-butyl esters.

Standard samples of amino acids which had not passed through the ion-exchange columns but which contained identical amounts of amino acids and internal standard were also converted to the N-TFA *n*-butyl esters. The percent recovery of each of the protein amino acids taken through exchange columns was then determined by comparison of the GLC analyses of the ion-exchange cleaned samples with the standard samples not passed through the ion-exchange cleanup methods.

To confirm the recovery of the amino acids from physiological materials, known amounts of each of the protein amino acids were added to a stock solution of human urine. The urine solution had previously been analyzed both by GLC and the classical ion-exchange methods. Aliquots of the "spiked" urine solution were then taken through both cation- and anion-exchange cleanup and the amino acids were analyzed by GLC as their N-TFA *n*-butyl esters. *n*-Butyl stearate was used as the internal

standard. Since the amino acid composition of the stock urine solution was known, it was possible to determine the recovery of the added amino acids.

IV. Derivatization of the ion-exchange cleaned physiological fluids

(a) Macro method (5 to 50 mg total)

The effluent from the ion-exchange cleanup procedures containing the amino acids was taken to dryness with the aid of a rotary evaporator and 60° water bath.

To form the methyl esters of the amino acids, 10 ml of methanol·HCl were added to the flasks, stoppered, and stirred at room temperature for 30 min with a magnetic stirrer. The samples were again evaporated to dryness via the rotary evaporator and 60° water bath.

Then, 10 ml of *n*-butanol·HCl were added, along with an appropriate exact aliquot of the *n*-butyl stearate internal standard solution, a drying tube containing CaSO₄ was attached to the mouth of the flask, and the flasks were placed in a 100° constant-temperature oil bath and stirred magnetically for 2½ h. The samples were then evaporated to dryness on the rotary evaporator with the aid of a 60° water bath.

The amino acid *n*-butyl esters were then acylated by adding 7 ml of methylene chloride and 1 ml of trifluoroacetic anhydride for each *ca.* 10 mg of amino acids in the sample. The samples were then stirred at room temperature for 15 min.

To complete the acylation, a *ca.* 4 ml aliquot of the solution from the above step was placed in a Corning No. 9826 culture tube. The tube was closed securely with a teflon-lined screw cap, and heated at 150° for 5 min in a constant-temperature oil bath behind a safety shield.

After allowing to cool to room temperature, the samples were then analyzed on the dual-column EGA-OV 17 chromatographic system as described by GEHRKE *et al.*^{12,13}. The recommended chromatographic method now used is described in ref. 15.

(b) Semimicro method (0.1 mg to 10 mg total)

An aqueous aliquot of cation-exchange cleaned blood plasma or amino acid mixture containing 0.1 to 10 mg of total amino acids was placed in a Corning No. 9826 glass culture tube, and the samples were evaporated just to dryness by placing the tube in a 100° sand bath while directing a stream of dry, purified nitrogen gas into the heated tube. To ensure complete removal of water from the sample, 0.5 ml of CH₂Cl₂ was then added and evaporated in the same manner.

To form the amino acid methyl esters, 2.0 ml of methanol·HCl were added, the tubes were capped with a teflon-lined screw cap, and mixed by manual inversion and ultrasonic mixing for 15 to 30 sec, then allowed to stand 30 min at room temperature.

The excess methanol·HCl was then evaporated at 100° with nitrogen gas as described above.

The interesterification to form the amino acid *n*-butyl esters was performed by adding 2.0 ml of *n*-butanol·HCl, mixing as described above and the tightly capped samples were then heated at 100° for 2½ h in the sand bath.

The excess *n*-butanol·HCl was then evaporated from the sample with the 100° sand bath and nitrogen gas as described above.

The amino acid *n*-butyl esters were acylated by adding 0.8 ml of CH₂Cl₂ and 0.2 ml of TFAA, the tube was then securely capped, and the solution was mixed by manual inversion and ultrasonic mixing. To complete the acylation, the tubes were

placed in a 150° constant temperature oil bath for 5 minutes. After allowing to cool, the samples were then analyzed by the dual-column EGA-OV-17 chromatographic system.

(c) *Micro method (2 µg to 200 µg total)*

An aqueous aliquot of an amino acid mixture containing 2 µg of total amino acids was placed in the special screw cap reaction vial (Fig. 1), and evaporated just to dryness using the 100° sand bath and a stream of dry, purified N₂ gas as described in the previous section. Azeotropic removal of water was completed by adding 100 µl of CH₂Cl₂ and evaporating just to dryness in the above manner. To ensure complete removal of water, this step was repeated.

The amino acid methyl esters were formed by addition of 100 µl of methanol·HCl to the reaction vial. The vial was capped with a teflon-lined screw cap, then the sample was mixed ultrasonically for 15 to 30 sec and allowed to esterify at room temperature for 30 min with mixing at 10-min intervals.

The methanol·HCl was evaporated at 100° with nitrogen gas as described above.

For interesterification to the *n*-butyl esters, 100 µl of *n*-butanol·HCl were added to the reaction vial, and mixed ultrasonically. The solution was then heated at 100° for 2½ h in the sand bath, with ultrasonic mixing at 30-min intervals.

The *n*-butanol·HCl was then evaporated at 100° with a sand bath and nitrogen gas as described above.

The amino acid *n*-butyl esters were acylated by addition of 60 µl of CH₂Cl₂ and 20 µl of TFAA, ultrasonic mixing, and acylation at 150° for 5 min in an oil bath. The samples were then ready for GLC analysis.

V. *TFAA molar excess*

During chromatography of the amino acid N-TFA *n*-butyl esters on a polyester liquid phase (EGA), it had previously been noted that the chromatographic peak due to trifluoroacetic acid interfered with the quantitation of the most volatile amino acid derivatives (alanine, glycine). Therefore, experiments were conducted to determine the optimum molar ratio of TFAA/amino acids that would result in the most accurate and precise analysis of the twenty protein amino acids.

Equal aliquots of the standard amino acid solution were derivatized to their N-TFA *n*-butyl esters as described in section IVc and acylated at 150° for 5 min using 4, 10, 20, 50, and 100 molar excess of TFAA/amino acids. This experiment was repeated twice independently, with duplicate GLC analyses being made on each sample.

VI. *Loss of derivatives on evaporation*

To study the comparative losses during evaporation of the N-TFA methyl esters and N-TFA *n*-butyl esters of the protein amino acids, the following procedures were used.

(a) *N-TFA methyl esters*

A 1-ml aliquot of the 2.5 mM standard amino acid solution was placed in a 16 × 75 mm glass culture tube and dried at 100° in a sand bath with a stream of dry, purified nitrogen gas directed into the mouth of the tube.

To form the amino acid methyl esters, 1 ml of methanol·HCl was added to the

culture tube, closed, and heated at 100° in the sand bath for 1 h. The sample was then dried with nitrogen gas and the 100° sand bath as described above.

The N-trifluoroacetyl methyl esters were then formed by adding 1.8 ml of CH₂Cl₂ and 0.2 ml of TFAA (50 molar excess) and heating the tightly capped tubes for 5 min at 150° in an oil bath.

The derivatized sample was then analyzed by GLC in triplicate.

The remaining derivatized sample was then divided into two equal parts and taken to dryness with nitrogen gas, one at 100° and the other at 25° to observe the effect of evaporation temperature on loss of the amino acid N-TFA methyl esters.

Both samples were again reacylated as in VIa, and duplicate chromatographic analyses were made on each sample.

(b) N-TFA n-butyl esters

A 1-ml aliquot of the 2.5 mM standard amino acid solution was placed in a 16 × 75 mm glass culture tube and dried at 100° in the sand bath under a stream of nitrogen gas.

The amino acid methyl esters were formed as in VIa of the preceding section and again dried with the aid of nitrogen gas and the 100° sand bath.

One milliliter of *n*-butanol·HCl was then added to the tube and the tightly capped tube was heated at 100° for 2½ h in the sand bath. The sample was then taken to dryness on the 100° sand bath with nitrogen gas as previously described.

To acylate the amino acid *n*-butyl esters, 1.8 ml of CH₂Cl₂ and 0.2 ml of TFAA (50 molar excess) were added, and the tube was heated at 150° for 5 min in a constant-temperature oil bath.

Duplicate chromatographic analyses were then made on the derivatized sample.

The remaining derivatized sample was then taken to dryness at 100° on the sand bath with nitrogen gas, reacylated as above, and again duplicate chromatographic analyses were performed.

The above sample was then dried under nitrogen gas at 25°, reacylated again as above, and again two chromatographic analyses were made.

RESULTS AND DISCUSSION

Concentration of N-TFA amino acid esters

The effect of concentrating the amino acid N-TFA *n*-butyl esters at various temperatures with regard to loss of the amino acid derivatives was studied. Also, a similar study was carried out with the N-TFA methyl esters. The acylated samples were concentrated under dry, purified nitrogen gas at temperatures of 25° and 100°. Table I presents the relative response factor data obtained from the GLC analysis of the N-TFA methyl ester derivatives. No attempt was made to identify the chromatographic peaks in this case, and a relative response factor for each peak was calculated relative to the thirteenth peak, which was arbitrarily assigned a value of unity. It is seen from these data that losses of up to 100% of the N-TFA methyl ester derivatives occurred during evaporation at 25°. Table II presents the corresponding data for the N-TFA *n*-butyl derivatives. It is apparent from these data that the N-TFA *n*-butyl esters sustain only minor losses when evaporated at 100° and even lower relative losses when dried at 25°.

TABLE I

EFFECT OF EVAPORATION ON THE N-TFA METHYL ESTER DERIVATIVES^a

Peak No.	Relative response factors ^b								
	Original ^c		Av.		25° evaporation		Av.		Relative loss (%)
1	— ^d	— ^d	— ^d	— ^d	—	—	—	—	
2	— ^d	— ^d	— ^d	— ^d	—	—	—	—	
3	0.15	0.16	0.16	0.16	—	—	—	—	100
4	0.45	0.45	0.43	0.44	0.15	0.15	0.15	0.15	66
5	0.64	0.65	0.63	0.64	0.32	0.32	0.32	0.32	50
6	0.55	0.53	0.53	0.54	0.31	0.31	0.31	0.31	43
7	0.47	0.47	0.49	0.48	0.25	0.25	0.25	0.25	48
8	0.35	0.35	0.37	0.36	0.24	0.24	0.24	0.24	33
9	0.40	0.41	0.40	0.40	0.33	0.33	0.33	0.33	17
10	0.64	0.64	0.68	0.65	0.54	0.53	0.54	0.54	17
11	0.42	0.43	0.43	0.43	0.44	0.44	0.44	0.44	0
12	1.18	1.18	1.13	1.16	1.13	1.13	1.13	1.13	0
13	1.00	1.00	1.00	1.00	1.00	1.00	1.00	1.00	0
14	0.63	0.63	0.63	0.63	0.58	0.58	0.58	0.58	9
15	0.50	0.51	0.52	0.51	0.40	0.39	0.40	0.40	—

^a Evaporated just to dryness under nitrogen gas.^b Calculated relative to peak No. 13, which was assigned the value of unity.^c Analyzed before evaporation.^d Not resolved.

TABLE II

EFFECT OF EVAPORATION ON THE N-TFA *n*-BUTYL ESTER DERIVATIVES^a

Amino acid	Relative response factors ^b										
	Original ^c		Av.		100° evaporation		Av.		Relative loss (%)		
Alanine	0.45	0.44	0.45	0.41	0.40	0.41	9	0.37	0.37	0.37	10
Valine	0.51	0.51	0.51	0.46	0.46	0.46	10	0.42	0.42	0.42	9
Glycine	0.41	0.40	0.41	0.37	0.37	0.37	10	0.34	0.35	0.35	5
Isoleucine	0.62	0.61	0.62	0.58	0.57	0.58	6	0.53	0.53	0.53	9
Leucine	0.64	0.63	0.64	0.59	0.59	0.59	8	0.59	0.58	0.59	0
Proline	0.70	0.70	0.70	0.67	0.68	0.68	3	0.67	0.66	0.67	1
Threonine	0.58	0.58	0.58	0.54	0.54	0.54	7	0.54	0.52	0.53	2
Serine	0.58	0.57	0.58	0.54	0.53	0.54	7	0.56	0.53	0.55	0
Methionine	0.12	0.11	0.12	0.09	0.07	0.08	34	0.12	0.08	0.10	0
Hydroxyproline	0.76	0.75	0.76	0.75	0.75	0.75	1	0.75	0.73	0.74	1
Phenylalanine	1.11	1.11	1.11	1.10	1.10	1.10	1	1.10	1.11	1.11	0
Aspartic acid	0.83	0.83	0.83	0.83	0.82	0.83	0	0.85	0.83	0.84	0
Glutamic acid	1.00	1.00	1.00	1.00	1.00	1.00	0	1.00	1.00	1.00	0
Tyrosine	0.94	0.95	0.95	0.94	0.94	0.94	1	0.94	0.93	0.94	0
Ornithine	0.78	0.76	0.77	0.76	0.76	0.76	1	0.74	0.75	0.75	1
Lysine	0.88	0.87	0.88	0.84	0.84	0.84	5	0.83	0.83	0.83	1

^a Evaporated just to dryness under nitrogen gas.^b Calculated relative to glutamic acid, which was assigned the value of unity.^c Analyzed before evaporation.

TFAA molar excess

To refine further the developed GLC technique for the quantitative analysis of amino acids, various molar ratios of TFAA/total amino acids were evaluated. Molar ratios of 4, 10, 20, 50, and 100 of TFAA/total amino acids during the acylation step were used.

Two independent samples were prepared at each of the TFAA concentrations, and duplicate GLC analyses were made on each sample. Table III presents the data

TABLE III

THE INFLUENCE OF EXCESS TFAA ON THE RMR VALUES FOR THE TAB DERIVATIVES OF THE AMINO ACIDS^a

<i>Amino acid</i>	<i>4-molar^b excess</i>	<i>10-molar^b excess</i>	<i>20-molar^b excess</i>	<i>50-molar^b excess</i>	<i>100-molar^b excess</i>
Alanine	0.44	0.45	0.49	0.48	0.49
Valine	0.52	0.54	0.61	0.63	0.62
Glycine	0.39	0.40	0.39	0.41	0.40
Isoleucine	0.63	0.68	0.74	0.73	0.74
Leucine	0.78	0.77	0.78	0.74	0.75
Proline	0.70	0.72	0.68	0.69	0.70
Threonine	0.54	0.59	0.61	0.63	0.65
Serine	0.56	0.55	0.54	0.56	0.55
Methionine	0.64	0.59	0.63	0.63	0.62
Hydroxyproline	0.64	0.75	0.76	0.73	0.75
Phenylalanine	1.08	1.12	1.14	1.11	1.12
Aspartic acid	0.85	0.84	0.86	0.83	0.84
Glutamic acid	1.00	1.00	1.00	1.00	1.00
Tyrosine	0.35	0.97	0.94	0.96	0.99
Ornithine	0.73	0.76	0.74	0.73	0.72
Lysine	0.78	0.85	0.84	0.86	0.87

^a Absolute molar excess in each case.

^b Each of these values represent the average of duplicate analyses of two independent samples.

obtained from these experiments. A 50-molar or greater excess of TFAA/total amino acids was found to be best with regard to accuracy, precision, and stability of the acylated samples. A larger excess of TFAA created problems with regard to sample volume especially in samples analyzed at the micro method level; thus molar ratios larger than 50:1 of TFAA/total amino acids were not used.

GLC analysis of microgram and submicrogram amounts of amino acids

To determine the applicability of the developed GLC technique for the analysis of microgram and submicrogram amounts of amino acids in physiological fluids or proteins, aliquots of the standard amino acid solution containing microgram quantities of each amino acid were derivatized according to the micro method and analyzed. In these experiments, the micro reaction vials were used, with reaction volumes of *ca.* 80 μ l. In all cases it was necessary to maintain solubility of the sample by retaining a liquid phase during acylation.

A typical chromatogram obtained from the derivatization and GLC analysis of 2.5 μ g of each amino acid is presented in Fig. 2, with each peak representing *ca.* 150 ng of amino acid injected. Fig. 3 presents the chromatogram obtained from the analysis

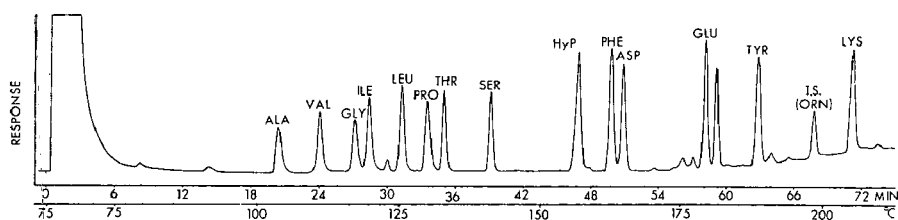


Fig. 2. Chromatogram obtained on GLC of 2.5 μg of each of the amino acid N-TFA *n*-butyl esters. Conditions: Varian Aerograph 2100; column, 0.325 w/w% EGA on 80/100 mesh AW heat-treated Chromosorb G, 1.5 m \times 4 mm I.D., glass; nitrogen flow rate, 70 ml/min; temperature, programmed at a rate of 2°/min, initial temperature 75°. Sample, 80 μl . Each peak represents *ca.* 150 ng. Internal standard, ornithine.

of a sample containing only 1 μg of each amino acid, or 20 μg of total amino acids, with each chromatographic peak corresponding to *ca.* 60 ng. The relative standard deviation was found to be in the range of 2 to 10%. Fig. 4 presents data on a submicrogram analysis of amino acids. In this experiment only 0.1 μg of each amino acid was derivatized, with each peak representing *ca.* 6 ng of amino acid. By concentrating the

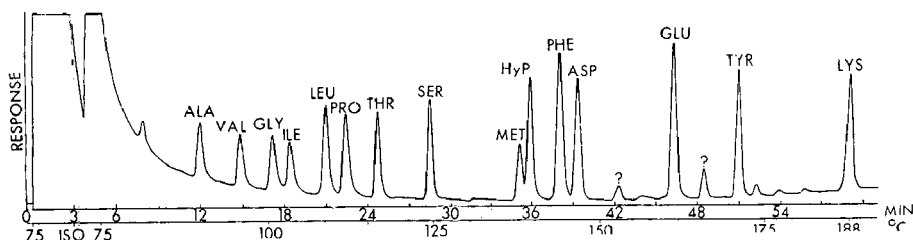


Fig. 3. Chromatogram obtained on GLC of 1 μg of each of the amino acid N-TFA *n*-butyl esters. Temperature, programmed at a rate of 2°/min up to 195°, initial temperature, 75°. For further conditions, see the legend to Fig. 2. Sample, 80 μl . Volume injected, 5 μl . Each peak represents *ca.* 60 ng. Sensitivity, 1×2 .

final 80 μl of acylation solution to 20 μl , and injecting 8 μl , the amount of starting material could be reduced to 10 ng or less of each amino acid and a semiquantitative analysis could still be achieved.

Analysis of human blood plasma

GLC analyses of deproteinized human blood plasma indicated that further

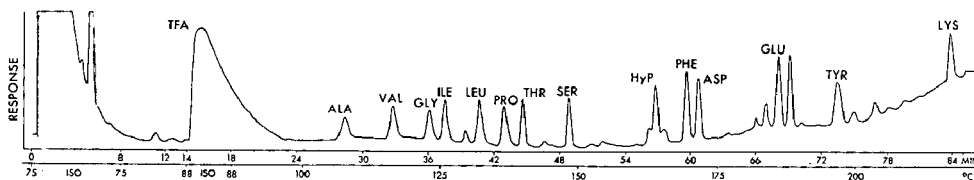


Fig. 4. Chromatogram obtained on GLC of submicrogram amounts of the amino acid N-TFA *n*-butyl esters. Temperature, programmed at a rate of 2°/min, initial temperature 75°. For further conditions, see the legend to Fig. 2. Sample, 0.1 μg of each amino acid in 80 μl . Volume injected, 5 μl . Each peak represents *ca.* 6 ng. Sensitivity, 0.1×2 .

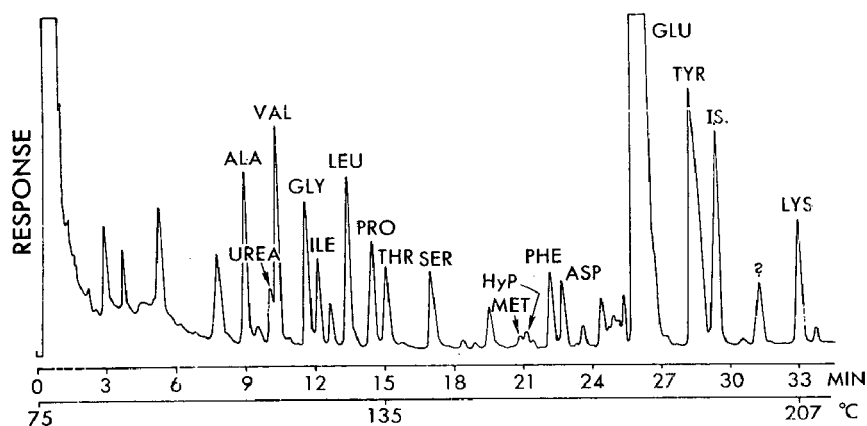


Fig. 5. Chromatogram obtained on GLC of human blood plasma amino acid N-TFA *n*-butyl esters not cleaned by cation exchange. Temperature, programmed at a rate of 4°/min, initial temperature 75°. For further conditions, see the legend to Fig. 2. Sample, *ca.* 6 ml of plasma in a final volume of 2.5 ml. Volume injected, 5 μ l (*ca.* 3.5 μ g total amino acids). Internal standard, *n*-butyl stearate. Final temperature, 210°.

TABLE IV

AMINO ACID ANALYSIS OF HUMAN BLOOD PLASMA

Amino acid	Mg per 100 ml of plasma				Ion-exchange chromatography		Average		
	Gas-liquid chromatography ^{a,†}								
	Macro		Micro				Macro	Micro	IE
Alanine	3.12	3.12	2.92	2.97	3.45	3.39	3.12	2.95	3.42
Valine	3.24	3.48	3.21	3.51	3.25	3.24	3.36	3.36	3.25
Glycine	2.58	2.72	2.54	2.88	2.68	2.69	2.65	2.71	2.69
Isoleucine ^b	1.41	1.38	1.67	1.55	1.19	1.24	1.40	1.61	1.22
Leucine	2.49	2.68	2.65	2.15	2.73	2.56	2.59	2.40	2.65
Proline ^c	2.69	2.63	2.99	2.84	2.92	2.10	2.66	2.92	2.51
Threonine	2.07	2.02	2.20	2.22	1.50	1.60	2.05	2.21	1.55
Serine	1.80	1.76	1.74	1.81	1.42	1.46	1.78	1.78	1.44
Methionine	0.61	0.62	0.75	0.71	0.37	0.32	0.62	0.73	0.35
Phenylalanine	0.92	0.92	0.97	0.86	0.98	0.95	0.92	0.92	0.97
Aspartic acid ^d	1.29	1.30	1.29	1.23	0.70	0.66	1.30 ^d	1.26	0.68
Glutamic acid ^d	3.35	3.34	3.22	3.30	2.12	2.08	3.35 ^d	3.26	2.10
Tyrosine	0.98	0.98	0.94	0.99	0.93	0.86	0.98	0.97	0.90
Ornithine	2.01	2.05	2.30	2.19	1.74	1.72	2.03	2.25	1.73
Lysine	3.43	3.60	3.38	3.21	3.62	3.60	3.52	3.30	3.61
Arginine	1.20	1.32	1.26	1.17	1.58	1.61	1.27	1.22	1.60
Histidine ^e	1.01	1.32	1.19	1.09	1.93	1.93	1.17	1.14	1.93 ^e
Tryptophan ^e	0.63	0.57	0.66	0.69			0.60	0.68	
Cystine	0.45	0.43	0.49	0.54	T	T	0.44	0.52	T
							35.81	36.19	32.10

^a Cleaned by cation exchange prior to derivatization.

^b GLC values include *allo*-isoleucine.

^c The lack of ion-exchange precision is due to poor separation of Pro and Cit.

^d GLC values include Asp(NH₂) and Glu(NH₂).

^e His and Trp not separated by ion-exchange.

^f N-TFA *n*-butyl esters.

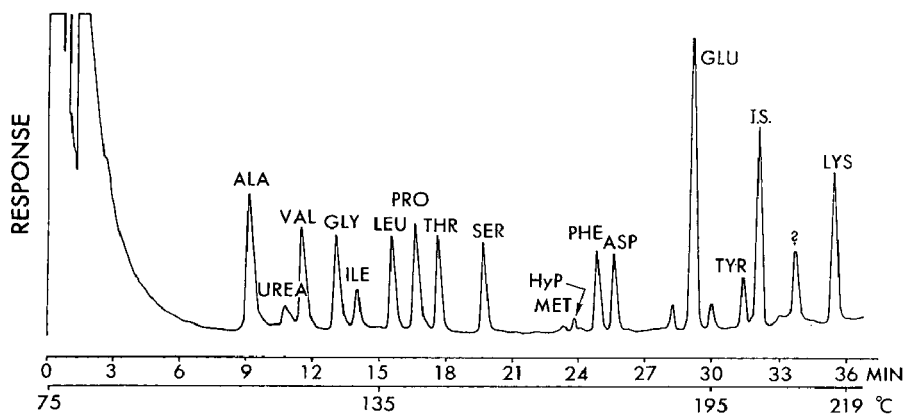


Fig. 6. Chromatogram obtained on GLC of human blood plasma amino acid N-TFA *n*-butyl esters cleaned by cation exchange. For further information, see the legend to Fig. 5. Final temperature, 220°.

sample cleanup was necessary to achieve quantitative amino acid analysis. Fig. 5 shows a typical chromatogram for amino acids in an uncleaned deproteinized blood plasma on an EGA column. In order to remove the extraneous substances in blood plasma which interfere with GLC analysis, the cation-exchange cleanup procedure

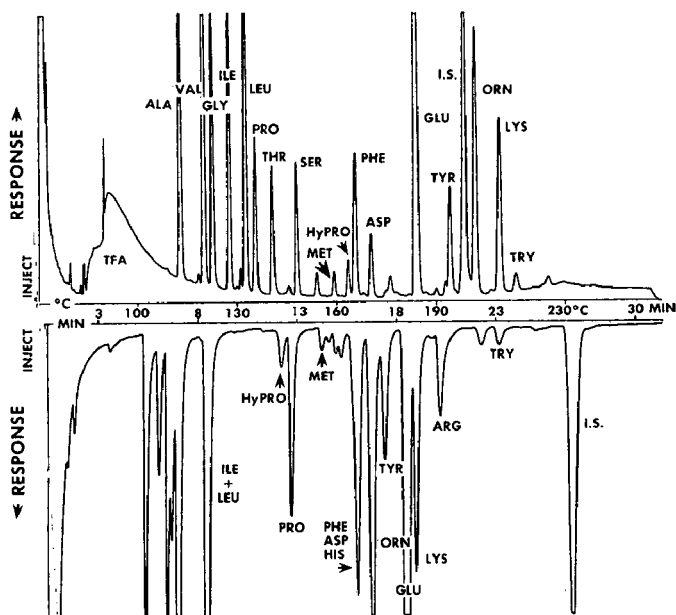


Fig. 7. GLC analysis of bovine blood plasma. 10.0 ml of plasma deproteinized with 40 ml of 1% picric acid, cation-exchange-cleaned. Final acylation volume, 2 ml; injected, 5 μ l; ca. 5 μ g total amino acid injected. Attenuation, 8×10^{-10} AFS; initial temperature, 70°; program rate, 6°/min; final temperature, 230°. Upper part: Column, 0.65 w/w% EGA on 80/100 mesh A.W. Chromosorb W, 1.5 m \times 4 mm I.D. glass. Lower part: column, 1.0 w/w% OV-17 on 80/100 mesh H.P. Chromosorb G, 1.0 m \times 4 mm I.D. glass. Internal standard, *n*-butyl stearate.

was studied. After passing the deproteinized plasma through a small cation-exchange column, the sample was again chromatographed on an EGA column and found to be suitable for quantitative analysis by GLC (Fig. 6). Fig. 7 shows a complete amino acid analysis of cation-exchange cleaned blood plasma on both EGA and OV-17 columns.

To investigate the quantitation of the micro method for the analysis of biological samples, duplicate aliquots of a stock solution of deproteinized human blood plasma were analyzed by GLC at both the macro and micro levels, and also by the classical ion-exchange technique. The samples analyzed by GLC were cleaned by cation exchange prior to derivatization to the N-TFA *n*-butyl esters. The classical ion-exchange analyses were made without prior cleanup. The data obtained from each of these experiments are presented in Table IV and give comparisons for the macro analyses (*ca.* 4 mg of total amino acids), micro analyses (*ca.* 200 μ g of total amino acids), and classical ion-exchange analyses. All of the data were in good agreement. Also, it is noted from this table that quantitative recovery of the amino acids from the cation-exchange cleanup column was achieved.

Recovery from the cation-exchange cleanup column

To establish further the quantitation of the cation-exchange cleanup technique, the recovery of each of the protein amino acids from the column was established by taking known amounts of each of the amino acids through the cation cleanup pro-

TABLE V

RECOVERY OF AMINO ACIDS FROM CATION-EXCHANGE CLEANUP

<i>Amino acid</i>	<i>Milligrams of amino acids</i>			<i>Recovery (%)</i>
	<i>Added</i>	<i>Found^{a,b,c}</i>	<i>Av.</i>	
Alanine	2.23	2.21	2.23	99.6
Valine	2.93	2.90	2.81	97.3
Glycine	1.88	1.88	1.95	102.1
Isoleucine	3.28	3.23	3.11	96.6
Leucine	3.28	3.22	3.31	99.4
Proline	2.88	2.83	2.91	99.7
Threonine	2.98	2.95	2.84	97.0
Serine	2.63	2.57	2.63	98.9
Methionine	3.73	3.80	3.87	102.9
Hydroxyproline	3.27	3.21	3.27	99.1
Phenylalanine	4.13	4.08	3.89	96.4
Aspartic acid	3.32	3.27	3.32	99.4
Glutamic acid	3.68	3.63	3.63	98.6
Tyrosine	4.53	4.46	4.46	98.5
Lysine	3.66	3.60	3.66	98.6
Arginine	4.36	4.10	4.24	95.6
Tryptophan	5.10	4.86	4.99	96.7
Histidine ^d	3.88	3.74	3.71	96.1
Cystine	6.01	5.84	5.89	98.0
	67.76		66.58	Av. 98.5

^a Analyses by GLC as the N-TFA *n*-butyl esters.

^b Ornithine as internal standard.

^c Each value represents an independent analysis.

^d Analyzed as the diacyl derivative after injection of 4 μ l of TFAA¹⁴.

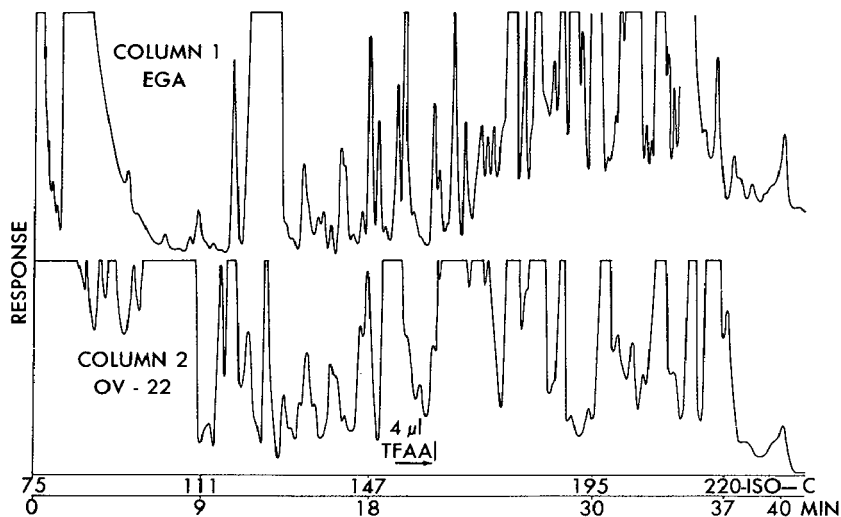


Fig. 8. Chromatogram obtained on GLC of human urine amino acid N-TFA *n*-butyl esters. Not cleaned by cation exchange on two different columns. Conditions: Column 1—0.65 w/w% EGA on 80/100 mesh dried (140°, for 12 h) AW Chromosorb W, 1.5 m × 4 mm I.D., glass. Column 2—1.5 w/w% OV-22 on 80/100 mesh HP Chromosorb G, 1.0 m × 4 mm I.D., glass. Temperature, programmed at a rate of 4°/min up to 220°, initial temperature 75°. Sample, 4 ml (ca. 4 mg amino acids in 2.5 ml final acylation volume). Volume injected, 8 μ l (ca. 13 μ g total amino acids).

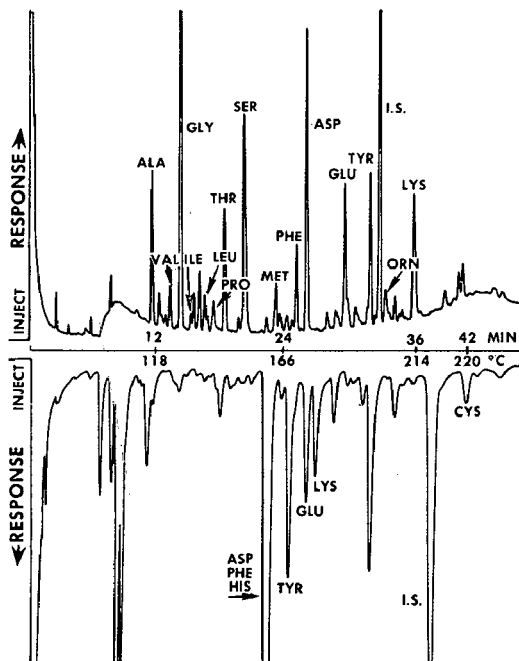


Fig. 9. GLC analysis of human urine. 4.5 ml of human urine hydrolyzed with 1 N HCl at 110° for 2 h. Final acylation volume, 2 ml; injected, 5 μ l, ca. 2 μ g of total amino acid injected. Initial temperature, 70°; program rate, 4°/min; final temperature, 220°; attenuation, 8×10^{-10} AFS. Upper part: column, 0.65 w/w% EGA on 80/100 mesh A.W. Chromosorb G, 1.5 m × 4 mm I.D. glass. Lower part: column, 1.0 w/w% OV-17 on 80/100 mesh H.P. Chromosorb G, 1 m × 4 mm I.D. glass. Internal standard, *n*-butyl stearate.

cedure. The eluates from the columns were derivatized and analyzed by GLC. Also, identical samples which had not been passed through the cleanup columns were analyzed in the same manner, and the per cent recovery of each amino acid through the cation-exchange column was determined by comparison of these analyses. These data are presented in Table V, and indicate that no losses occurred during cation-exchange cleanup of biological samples.

GLC analysis of human urine

Initial GLC analyses of uncleaned human urine revealed that an efficient method of removing extraneous substances was essential. A chromatogram of the N-TFA *n*-butyl derivatives of uncleaned human urine is shown in Fig. 8.

Aliquots of a stock urine solution, cleaned by both the cation- and anion-exchange procedures, were analyzed by GLC and the classical ion-exchange techniques. A GLC chromatogram of the cleaned urine is shown in Fig. 9. Also, classical ion-exchange analyses were made on aliquots of unhydrolyzed stock solution and on

TABLE VI

AMINO ACID ANALYSIS OF HUMAN URINE^a

Amino acid	Mg per 100 ml of urine				Ion-exchange chromatography ^d				Average		RSD ^c (%)	
	Gas-liquid chromatography ^b				Non-hydrolyzed				GLC		IE	
Alanine	2.82	2.64	2.78		2.39	2.75	2.52	2.58	2.75	2.56	2.79	5.00
Valine	0.66	0.67	0.59		0.60	0.60	0.78	0.75	0.64	0.68	5.40	12.40
Glycine	16.52	16.58	16.64		17.18	17.19	17.78	17.53	16.58	17.42	0.03	1.40
Isoleucine	T ^f	0.18	0.24		0.23	0.28	0.24	0.22	0.21	0.24		9.20
Leucine	0.78	0.68	0.82		—	0.70	0.77	0.76	0.76	0.74	7.70	4.10
Proline	T	T	T		T	T	T	T	T	T		
Threonine	3.02	2.98	3.08		2.64	2.88	3.07	2.51	3.03	2.78	1.40	7.70
Serine	5.56	5.62	5.60		5.39	5.28	5.28	5.43	5.59	5.35	0.40	1.80
Methionine	0.20	0.47	0.50		0.41	0.34	0.31	—	0.39	0.35		
Hydroxyproline	0.00	T	T		0.00	0.00	0.00	0.00	T	0.00		
Cysteine	0.00	0.00	T		T	T	T	T	T	T		
Phenylalanine	1.63	1.71	1.66		1.68	1.81	1.92	1.77	1.67	1.80	3.70	4.70
Aspartic acid	5.88	5.74	5.62		0.52	0.71	5.00	5.30	5.74	5.15	1.40	7.20
Glutamic acid	10.31	10.20	10.16		0.68	0.72	10.15	9.69	10.22	9.92	0.60	3.60
Tyrosine	3.68	3.80	3.76		3.41	3.45	3.31	3.44	3.75	3.40	0.13	1.20
Lysine	3.98	4.20	4.12		—	—	3.92	4.50	4.10	4.21	2.20	4.60
Arginine	0.21	0.25	0.16		0.11	0.14	0.20	0.26	0.21	0.18		
Histidine	26.51	25.46	27.30		27.91	26.65	29.11	—	26.42	27.89	0.78	3.70
Tryptophan	5.62	5.49	5.68		g	g	g	g	5.60	g	1.40	
Cystine	0.08	0.13	0.09		0.11	0.14			0.10	0.13		
									87.76	86.91	2.15 ^h	5.12 ^h

^a Cleaned by cation and anion exchange prior to analysis.

^b Each an independent analysis.

^c Relative standard deviation, %.

^d Each an independent analysis, norleucine as internal standard.

^e Hydrolyzed 2 h at 110° under nitrogen gas in 1 N HCl.

^f Trace.

^g Not resolved from histidine.

^h Average RSD, %. Note conversion of Asp(NH₂) and Glu(NH₂) to Asp and Glu on hydrolysis.

aliquots subjected to a mild hydrolysis. The data from these analyses are presented in Table VI and the results are seen to be in good agreement. If the concentrations of the amino acids in urine samples are usually divergent then two analyses of a sample should be made using internal standards at high and low concentrations approximating that of the amino acids in the sample. In this way, the precision and accuracy of the analysis will be greatly improved.

To establish the quantitation of the anion-exchange cleanup method, known amounts of each of the protein amino acids were taken through the anion-exchange cleanup procedure as described earlier, and the percent recovery of each determined. These data are presented in Table VII, and the recovery was quantitative. To confirm

TABLE VII

RECOVERY OF AMINO ACIDS FROM ANION-EXCHANGE CLEANUP

<i>Amino acid</i>	<i>Milligrams of amino acids</i>					<i>Recovery (%)</i>	<i>RSD (%)</i>
	<i>Added</i>	<i>Found^{a,b,c}</i>			<i>Av.</i>		
Alanine	0.891	0.917	0.911	0.913	0.914	102.6	1.07
Valine	1.171	1.210	1.203	1.191	1.201	102.6	0.80
Glycine	0.751	0.738	0.746	0.741	0.742	98.9	0.55
Isoleucine	1.312	1.281	1.326	1.423	1.343	102.4	5.40
Leucine	1.312	1.278	1.285	1.293	1.285	97.9	0.58
Proline	1.151	1.126	1.113	1.213	1.151	100.0	4.72
Threonine	1.191	1.190	1.241	1.238	1.223	102.7	2.34
Serine	1.051	1.091	1.073	1.071	1.078	102.6	1.02
Methionine	1.492	1.436	1.451	1.479	1.455	97.5	1.50
Hydroxyproline	1.312	1.343	1.351	1.336	1.343	102.4	0.56
Phenylalanine	1.652	1.692	1.691	1.621	1.668	101.0	2.44
Aspartic acid	1.331	1.374	1.362	1.371	1.369	102.8	0.46
Glutamic acid	1.470	1.491	1.498	1.499	1.496	101.8	0.29
Tyrosine	1.612	1.642	1.651	1.648	1.647	102.2	0.28
Lysine	1.462	1.497	1.492	1.501	1.497	102.4	0.30
Arginine	1.742	1.745	1.773	1.786	1.768	101.5	1.19
Tryptophan	2.042	2.091	2.084	2.080	2.085	102.1	0.27
Histidine	1.552	1.501	1.496	1.510	1.502	96.8	0.47
Cystine	2.403	2.381	2.380	2.369	2.377	98.9	0.28
	26.900				27.140	Av 101.0	Av 1.29

^a Analyses by GLC as the N-TFA *n*-butyl esters.

^b Ornithine as internal standard.

^c Each value represents an independent analysis.

further the quantitation of the entire cleanup procedure through both cation- and anion-exchange columns known amounts of each of the protein amino acids were added to the "stock" urine solution. Then, aliquots of this solution were taken through both the cation- and anion-exchange cleanup, and analyzed by GLC. The recovery of the amino acids from the urine is given in Table VIII, and was quantitative.

COMMENTS ON THE GLC METHOD

The injection port should be maintained at 200°; the detector at 250°.

Moisture must be excluded from both the sample during derivatization and the chromatographic column.

TABLE VIII

RECOVERY OF AMINO ACIDS FROM URINE

Amino acid	Milligrams of amino acids					Recovery (%)	RSD (%)
	Added ^a	Found ^{b,c}			Av.		
Alanine	2.23	2.17	2.27	2.30	2.25	100.9	3.03
Valine	2.93	2.99	2.81	2.84	2.88	98.3	3.37
Glycine	1.88	1.79	1.94	1.99	1.91	101.6	5.47
Isoleucine	3.28	3.35	3.39	3.42	3.39	103.4	1.06
Leucine	3.28	3.10	3.19	3.20	3.16	96.3	1.76
Proline	2.88	2.74	2.76	2.80	2.77	96.1	1.11
Threonine	2.98	2.91	2.94	2.95	2.93	98.3	0.72
Serine	2.63	2.65	2.67	2.69	2.67	101.5	0.75
Methionine	3.73	3.90	3.89	3.85	3.88	104.0	0.68
Hydroxyproline	3.28	3.41	3.47	3.48	3.45	105.2	1.10
Phenylalanine	4.13	4.10	4.06	4.04	4.06	98.3	0.78
Aspartic acid	3.33	3.17	3.11	3.19	3.42	94.8	1.22
Glutamic acid	3.68	3.60	3.59	3.62	3.60	97.8	0.44
Tyrosine	4.53	4.37	4.39	4.36	4.37	96.5	0.36
Lysine	3.66	3.69	3.74	3.75	3.73	101.9	0.87
Histidine	3.88	3.78	3.69	3.85	3.77	97.2	2.13
Arginine	4.36	4.30	4.51	4.48	4.43	101.6	2.56
Tryptophan	5.11	4.70	4.78	4.64	4.71	92.2	1.49
Cystine	6.01	6.18	6.20	6.29	6.22	103.5	0.94
	67.79				66.60	Av. 99.44	Av. 1.57

^a Known amounts were added to a stock sample of human urine, then cleaned by cation- and anion-exchange chromatography. N-TFA *n*-butyl esters.

^b *n*-Butyl stearate as internal standard.

^c Each value represents an independent analysis.

When drying the samples on the 100° sand bath with filtered gas, it is essential that the nitrogen gas is pure, and that the samples are taken just to dryness. Prolonged heating results in some breakdown of the samples.

A 50-molar excess or greater of TFAA/total amino acids should be used in the acylation medium, with the ratio of TFAA/CH₂Cl₂ being dependent on the sample concentration.

The chromatographic columns should be prepared and well conditioned as reported by GEHRKE *et al.*^{13,15}

Performance blanks on all reagents should be made to check the purity of all reagents. It is especially important to check the purity of the TFAA to make certain it has not hydrolyzed on standing to TFA.

Iron must be carefully excluded during use of the rotary evaporator and magnetic stirring to obtain accurate and reproducible values for methionine. It is recommended that the samples be analyzed shortly after acylation to prevent any reduction in the chromatographic peak for methionine.

In some instances, especially with microgram samples, the TFA peak tails into the chromatogram, resulting in incorrect values for the first few amino acid peaks. To overcome this problem, hold the temperature program at the TFA peak, allow the TFA peak to be eluted, then resume the temperature program.

Direct on-column injection or the use of glass-lined injection ports eliminate

thermal decomposition of threonine and arginine which was observed when all-metal flask heaters were used.

CONCLUSIONS

It is concluded that quantitative GLC analyses of amino acids can be performed accurately and precisely on the most complex physiological substances if the samples are properly cleaned prior to derivatization and analysis.

Ion-exchange techniques were found to be well suited for cleanup of biological samples with regard to the removal of substances which interfere with the GLC analysis of the protein amino acids.

Also, quantitative analysis of amino acids by GLC can be made on biological samples containing microgram amounts of amino acids or protein. Good results can be obtained on samples containing 1 to 20 μg of total amino acids or protein, and by concentrating the final 100 μl of acylation solution to 20 μl , and injecting 8 μl , the amount of starting material can be reduced to about 50 to 100 ng of each amino acid and still achieve a semiquantitative analysis. With very careful techniques, ultra pure reagents and exclusion of all moisture, analyses can be made at the 1 to 10 ng level.

The applicability of GLC analysis of biological materials at the semimicro and micro levels was further demonstrated with the analysis of ribonuclease and lysozyme isolated from human milk. These analyses were made in joint investigations with Dr. SHAHANI, B. DALALY, and R. EITENMILLER of the University of Nebraska, Lincoln.

It is also concluded that the amino acid N-TFA *n*-butyl ester derivative possesses a distinct advantage over the N-TFA methyl esters in that the *n*-butyl derivatives are not lost to any appreciable extent on concentration of the final acylated sample. Sample loss of the methyl esters becomes even more critical when analyses are performed on microgram and submicrogram amounts of amino acids, where concentration of the derivatized sample is necessary.

Manuscripts recently published in the *Journal of Chromatography* by ROACH AND GEHRKE describe in detail a new approach to chromatography¹⁵, and a "direct esterification" method for forming the amino acid *n*-butyl ester derivatives directly from the amino acids²⁵, thus eliminating the formation of the amino acid methyl esters and the interesterification reaction steps. These advancements greatly enhance the overall speed and simplicity of sample preparation and GLC analysis of the amino acids.

REFERENCES

- 1 K. BLAU, *Biomedical Applications of Gas Chromatography*, Vol. 2, Plenum Press, New York, 1968.
- 2 B. WEINSTEIN, *Methods Biochem. Anal.*, 16 (1966) 203.
- 3 C. W. GEHRKE AND D. L. STALLING, *Separation Sci.*, 2 (1967) 101.
- 4 W. M. LAMKIN AND C. W. GEHRKE, *Anal. Chem.*, 37 (1965) 383.
- 5 C. W. GEHRKE, W. M. LAMKIN, C. L. STALLING AND F. SHAHROKHI, *Biochem. Biophys. Res. Commun.*, 13 (1965) 328.
- 6 D. L. STALLING AND C. W. GEHRKE, *Biochem. Biophys. Res. Commun.*, 22 (1966) 329.
- 7 C. W. GEHRKE AND F. SHAHROKHI, *Anal. Biochem.*, 15 (1966) 97.
- 8 M. STEFANOVIC AND B. L. WALKER, *Anal. Chem.*, 39 (1967) 710.

- 9 W. J. MCBRIDE, JR. AND J. D. KLINGMAN, *Anal. Biochem.*, 25 (1968) 109.
- 10 A. DARBRE AND K. BLAU, *J. Chromatog.*, 29 (1967) 49.
- 11 A. DARBRE AND A. ISLAM, *Biochem. J.*, 106 (1968) 923.
- 12 C. W. GEHRKE, R. W. ZUMWALT AND L. L. WALL, *J. Chromatog.*, 37 (1968) 398.
- 13 C. W. GEHRKE, D. ROACH, R. W. ZUMWALT, D. L. STALLING AND L. L. WALL, *Quantitative Gas-Liquid Chromatography of Amino Acids in Proteins and Biological Substances*, Analytical Biochemistry Laboratories, Inc., P.O. Box 1097, Columbia, Mo., 1968.
- 14 D. ROACH, C. W. GEHRKE AND R. W. ZUMWALT, *J. Chromatog.*, 43 (1969) 311.
- 15 D. ROACH AND C. W. GEHRKE, *J. Chromatog.*, 43 (1969) 303.
- 16 M. D. WATERFIELD AND A. DEL FAVERO, *J. Chromatog.*, 40 (1969) 294.
- 17 C. W. GEHRKE, D. L. STALLING AND R. W. ZUMWALT, *Biochem. Biophys. Res. Commun.*, 31 (1968) 616.
- 18 C. W. GEHRKE, H. NAKAMOTO AND R. W. ZUMWALT, *J. Chromatog.*, 45 (1969) 24.
- 19 H. NAKAMOTO, *Master's Thesis*, University of Missouri, June, 1969.
- 20 C. W. GEHRKE, D. L. STALLING AND C. D. RUYLE, *Biochem. Biophys. Res. Commun.*, 28 (1967) 869.
- 21 C. W. GEHRKE AND C. D. RUYLE, *J. Chromatog.*, 38 (1968) 473.
- 22 F. SHAHROKHI AND C. W. GEHRKE, *Anal. Biochem.*, 24 (1968) 281.
- 23 F. SHAHROKHI AND C. W. GEHRKE, *J. Chromatog.*, 36 (1968) 31.
- 24 D. CRAVEN AND C. W. GEHRKE, *J. Chromatog.*, 37 (1968) 414.
- 25 D. ROACH AND C. W. GEHRKE, *J. Chromatog.*, 44 (1969) 269.

J. Chromatog., 53 (1971) 171-194

CHROM. 4994

THE EFFECT OF SALTS ON THE DERIVATIZATION AND CHROMATOGRAPHY OF AMINO ACIDS*

CHARLES W. GEHRKE** AND KENNETH LEIMER***

University of Missouri, Columbia, Mo. 65201 (U.S.A.)

(Received August 14th, 1970)

SUMMARY

This study was made to determine the effects of inorganic salts on the derivatization and chromatography of the N-TFA *n*-butyl esters of the amino acids. In general, the presence of an equal weight of inorganic salts to total weight of amino acids (or $W_{\text{salt}}/W_{\text{a.a.}}$ of 20 for each amino acid) on the derivatization and chromatography is not serious for qualitative work, but in certain cases can be significant in quantitative work. The following ions cause problems: oxalate, manganese(II), cobalt(II), nickel, zinc, tin(II), lead(II), chromium(III), and iron(III). When a 1:1 ratio of salts to total amino acid is present in the sample, it is suggested that they be removed by the use of ion-exchange chromatography. However, the following ions at a $W_{\text{salt}}/W_{\text{a.a.}}$ ratio of about 20 are not considered of significance: sodium, potassium, copper(I), silver, magnesium, calcium, barium, mercury(II), aluminum, chloride, bromide, acetate, nitrate, sulfate, and phosphate. The repeated injection of a sample containing salt, such as sodium chloride, results in reduced response for all long retention time amino acids and for the internal standard, butyl stearate. However, the column is not harmed by the repeated injections, for when the injection port end of the column is cleaned, good quantitative results are again obtained.

INTRODUCTION

Gas-liquid chromatographic (GLC) methods have proved to be useful for the analysis of amino acids in biological substances because of their speed and sensitivity. Since the low volatility of the amino acids has prevented their direct analysis by GLC, suitable derivatives of the amino acids must be prepared. ZOMZELY *et al.*¹ investigated the N-trifluoroacetyl (N-TFA) *n*-butyl esters as a possible derivative. LAMKIN AND GEHRKE² reported that the most suitable derivative with respect to volatility and

* Contribution from the Missouri Agricultural Experiment Station, Journal Series No. 6043. Approved by the Director. Supported in part by grants from the National Aeronautics and Space Administration (NGR 26-004-011) and the National Science Foundation (GB 7182).

** Professor. Experiment Station Chemical Laboratories.

*** Experimental data taken in part from master's research, University of Missouri.

chromatography for the GLC analysis of the natural protein amino acids is the N-TFA *n*-butyl ester. GEHRKE AND STALLING³ reported detailed experimental conditions for quantitative derivatization and chromatographic separation, and in 1968 GEHRKE *et al.*⁴ wrote a monograph covering macro, semimicro, and micro methods, reagents, sample preparation, instrumental and chromatographic requirements and sample ion-exchange cleanup for the quantitative GLC analysis of the twenty protein amino acids in biological substances. ROACH AND GEHRKE⁵ have reported on the use of acid-washed Chromosorb W in place of the heat-treated HP Chromosorb G used in the earlier work. Also, ROACH AND GEHRKE⁶ reported an esterification procedure with *n*-butanol · 3 *N* HCl with heating at 100° (15–30 min), which allows one to form the butyl ester derivatives by “direct esterification” rather than by interesterification from the methyl ester. These reports considerably simplified the chromatography and derivatization of the amino acids.

In the analysis of amino acids in sea water, soil, and some biological samples by GLC, one is aware of the presence of cations and anions without knowledge of their effect on the analysis. This study was undertaken to investigate the effects of cations and anions on the derivatization and chromatography of seventeen protein amino acids as the N-TFA *n*-butyl esters.

EXPERIMENTAL

Apparatus

A Micro-Tek MT 220 gas chromatograph with a four-column oven bath, four flame ionization detectors, two dual differential electrometers, and equipped with a Varian Model 30 dual-pen recorder, was used for this study. A digital readout integrator (Hewlett-Packard Model 3370A) was used for determining peak areas.

Pyrex 16 × 75 mm glass screw top culture tubes with teflon-lined caps (Corning No. 9826) were used as the reaction vessel for the acylation reaction. A 1/32-in. hole was drilled in the center of the caps. This hole was covered with a silicone septum and a teflon liner for entering with a syringe without opening and exposure of the sample to the moisture and air.

A CaLab rotary evaporator, “cold finger” condenser, and a Welch Duo-Seal vacuum pump were used for the removal of solvents in the preparation of column packing.

Reagents

All amino acids used in this study were obtained from Mann Research Laboratories, Inc., New York, N.Y. and were chromatographically pure.

n-Butanol was “Baker Analyzed” reagent. The trifluoroacetic anhydride was obtained from Distillation Products Industries, Rochester, N.Y. 14603, and was an “Eastman Grade” chemical. Acetonitrile, a “Baker Analyzed” reagent of high purity was stored over drierite in a bottle with a ground glass stopper. Anhydrous HCl was generated by the slow addition of 250 ml of reagent grade HCl to 500 ml of concentrated H₂SO₄. The HCl gas was passed through two H₂SO₄ drying towers and then bubbled into the *n*-butanol.

The *n*-butanol and methylene chloride were redistilled from an all-glass system and stored in an all-glass inverted top bottle to protect from atmospheric moisture.

The methylene chloride and *n*-butanol were refluxed over calcium chloride before distillation.

Chromatographic column

Stabilized grade ethylene glycol adipate (EGA) was obtained from Analabs, Inc., Hamden, Conn. 06518, and coated on 80/100 mesh acid-washed (AW) Chromosorb W which had not been heated at 140° for 12 h. The EGA column material was packed in a 1.5 m × 4 mm I.D. glass column.

The column packing was prepared by first adding 30.00 g of 80/100 mesh AW Chromosorb W to a 500-ml ribbed round-bottom flask. Acetonitrile was added until the liquid level was about 1/4 in. above the support material. 0.20 g of EGA were weighed into a small erlenmeyer flask, dissolved in 20 ml acetonitrile, and transferred to the flask containing the support. The flask containing the support and substrate was placed in a 60° water bath, and the solvent slowly removed with a rotary evaporator over a period of 1 h under a partial vacuum.

Derivatization

Two milliliters of a stock solution of the seventeen amino acids containing 0.1 mg/ml of each amino acid in 0.1 *N* hydrochloric acid were pipetted into a 16 × 75 mm culture tube. The water was evaporated under a stream of filtered dry nitrogen at 70°. Two milliliters of a solution of 0.1 mg/ml of stearic acid (internal standard, I.S.) in *n*-butanol 3 *M* in HCl were added to the tube. Five milliliters of butanol 3 *M* in HCl were added for each 1.0 mg of total amino acids. The solution was heated at 100° for 45 min to esterify the amino acids, then the butanol was removed with a stream of filtered nitrogen at 70°. One milliliter of a 1:1 solution of chloroform to trifluoroacetic anhydride (TFAA) solution was added, then acylated at 150° for 5 min.

In derivatization of samples containing added salt, the salt was weighed into the reaction tube before the addition of the amino acid solution and the above procedure followed.

Chromatography

For the chromatography and quantitative analysis of the samples, 5.0 μ l of the derivatized sample were injected. The first injection on each day was a standard followed by a salt-containing sample, then the standard was reinjected. If the response values for the second standard failed to agree with those for the first standard, the glass wool and top 1/2 in. of column packing were replaced and the above injections repeated. It was necessary to precede and follow each salt-containing sample with chromatography of standards to prove that the chromatographic column would still give the required separation and quantitation.

The same concentration of each amino acid and internal standard was used in all experiments, and the same known volume was injected each time into the chromatography column. Thus, for the standard, the peak area was obtained in such a manner that the same area should be obtained for each amino acid derivative in the sample containing salt. By doing the experiments in this way, one was able to note whether the experimental areas for the amino acids, or internal standard was enhanced or reduced by the added salt.

TABLE I

THE EFFECT OF SALTS ON THE N-TFA *n*-BUTYL ESTER AMINO ACID DERIVATIVES—NON-INTERFERING^aExperiments were performed with 4 mg of salt and 4 mg of total amino acid mixture; $W_{\text{salt}}/W_{\text{a.a.}} = 20$.

Amino acid	$RWR_{\text{a.a.}/\text{stearic acid}}^b$											
	Std. ^c	NaCl	KCl	CuCl	AgNO ₃	MgSO ₄	CaCl ₂	BaCl ₂ ^d	HgBr ₂	AlCl ₃	Na ₃ PO ₄	NaNO ₃
Alanine	1.14	1.14	1.07	1.09	1.16	1.16	1.21	1.05	1.08	1.15	1.16	1.13
Valine	1.14	1.23	1.07	1.07	1.21	1.15	1.16	1.02	1.08	1.15	1.16	1.16
Glycine	1.04	1.09	1.08	1.05	1.06	1.06	1.02	1.01	1.03	1.06	1.02	1.08
Isoleucine	1.17	1.14	1.08	1.09	1.16	1.18	1.19	1.06	1.09	1.17	1.16	1.17
Leucine	1.11	1.17	1.13	1.12	1.13	1.13	1.14	1.11	1.05	1.13	1.11	1.14
Proline	1.20	1.19	1.15	1.19	1.19	1.28	1.19	1.14	1.17	1.12	1.20	1.18
Threonine	0.93	0.96	0.96	0.94	0.95	0.90	0.94	0.92	0.92	0.95	0.96	0.94
Serine	0.99	0.98	0.96	0.99	0.97	1.05	1.04	0.93	0.98	1.00	0.97	0.97
Cysteine	0.57	0.58	0.59	0.47	0.55	0.60	0.54	0.56	0.53	0.56	0.59	0.60
Methionine	0.73	0.76	0.73	0.74	0.73	0.75	0.82	0.70	0.75	0.67	0.71	0.72
Hydroxyproline	0.97	0.99	0.96	0.97	0.99	0.94	0.93	0.96	0.98	0.99	0.96	0.93
Phenylalanine	1.23	1.21	1.17	1.24	1.22	1.31	1.29	1.16	1.19	1.19	1.21	1.22
Aspartic acid	1.14	1.21	1.18	1.16	1.15	1.13	1.10	1.14	1.16	1.16	1.14	1.10
Glutamic acid	1.22	1.18	1.16	1.22	1.20	1.15	1.13	1.14	1.18	1.24	1.22	1.20
Tyrosine	0.93	0.94	0.91	0.92	0.92	0.94	0.93	0.83	0.93	0.89	0.93	0.94
Lysine	1.04	1.07	1.03	1.05	1.05	1.00	1.01	0.99	1.05	1.11	1.04	1.07
Tryptophan	0.45	0.44	0.43	0.43	0.45	0.47	0.47	0.38	0.45	0.40	0.45	0.45

^a A salt was classified as non-interfering if the RWR's varied by less than $\pm 10\%$ from the standard values.

$$^b RWR_{\text{a.a.}/\text{stearic acid (I.S.)}} = \frac{A_{\text{a.a.}}/g_{\text{a.a.}}}{A_{\text{I.S.}}/g_{\text{I.S.}}}$$

^c Average of three independent analyses.^d Two waters of hydration.

RESULTS AND DISCUSSION

The data for salts which are classified as non-interfering are listed in Table I. A salt was classified as non-interfering if the relative weight response, $RWR_{\text{a.a.}/\text{I.S.}}$, did not deviate from the value of the standards by more than $\pm 10\%$. The following ions were found to be non-interfering: potassium, copper(I), silver, magnesium, calcium, barium, sodium, mercury(II), and aluminum as cations; and chlorides, bromides, nitrates, sulfates, and phosphates as anions.

A salt was listed as interfering if the relative weight response, $RWR_{\text{a.a.}/\text{I.S.}}$, deviated from the value of the standards by more than $\pm 10\%$. The ions classified as interfering are listed in Table II and were manganese(II), cobalt(II), nickel, zinc, tin(II), lead(II), chromium(III), and iron(III), as cations, and oxalate as an anion.

Three explanations can be offered for the observed results given in Table II. These are: (1) reduced volatilization of the internal standard, (2) reduced volatilization of the amino acids, and (3) reduced response due to chelation of the amino acid by the cation.

A reduced volatilization of the internal standard results in a reduced response for the internal standard and thus an apparent increase in the $RWR_{\text{a.a.}/\text{I.S.}}$ for the amino acids. It should be noted that no enhancement of response for any amino acids was observed as the result of the presence of a salt. All relative weight response values

TABLE II

THE EFFECT OF SALTS ON THE N-TFA *n*-BUTYL ESTER AMINO ACID DERIVATIVES—INTERFERING^aExperiments were performed with 4 mg of salt and 4 mg of total amino acid mixture; $W_{\text{salt}}/W_{\text{a.a.}} = 20$.

Amino acid	$RWR_{\text{a.a./stearic acid}}^b$									
	Std. ^c	$K_2C_2O_4$	$MnCl_2$	$CoCl_2$	$NiCl_2$	$ZnCl_2$	$SnCl_2$	$Pb(C_2H_3O_2)_2$	$CrCl_3^d$	$FeCl_3$
Alanine	1.14	1.06	3.14	1.61	2.18	1.40	1.33	1.28	1.71	1.54
Valine	1.14	— ^e	3.02	1.68	2.23	1.43	1.52	1.29	1.74	1.61
Glycine	1.04	— ^e	1.96	1.53	1.76	1.34	1.24	1.25	1.87	1.40
Isoleucine	1.17	— ^e	2.91	1.65	2.19	1.71	1.59	1.37	1.77	1.63
Leucine	1.11	— ^e	2.32	1.67	2.14	1.42	1.27	1.25	1.74	1.43
Proline	1.20	1.26	3.01	1.65	2.31	1.45	1.40	1.59	1.86	1.60
Threonine	0.93	0.94	1.67	1.14	1.76	1.64	1.24	1.18	1.31	1.32
Serine	0.99	0.98	2.46	1.38	1.10	1.20	1.37	1.19	0.91	1.33
Cysteine	0.57	0.58	0.24	0.28	0.36	0.37	0.59	0.60	0.45	0.47
Methionine	0.73	0.74	1.64	0.98	1.20	0.36	0.64	0.91	1.08	0.54
Hydroxyproline	0.97	0.97	1.68	1.64	1.96	1.44	0.76	1.18	1.35	1.36
Phenylalanine	1.23	1.24	2.90	1.68	2.15	1.50	1.47	1.63	1.88	1.63
Aspartic acid	1.14	1.15	1.19	1.43	2.31	1.74	0.91	1.47	1.15	1.52
Glutamic acid	1.22	1.30	0.98	1.17	1.18	0.92	0.93	1.58	1.25	1.11
Tyrosine	0.93	0.92	1.57	0.85	0.02	2.61	0.58	0.93	0.03	1.15
Lysine	1.04	1.03	0.28	0.86	0.36	0.92	1.02	1.09	0.56	0.78
Tryptophan	0.45	0.46	0.39	0.11	0.11	0.88	0.11	0.50	0.09	0.36

^a A salt was classified as interfering if the RWR's varied by more than $\pm 10\%$ from the standard values.^b $RWR_{\text{a.a./stearic acid (I.S.)}} = \frac{A_{\text{a.a./g a.a.}}}{A_{\text{I.S./g I.S.}}}$ ^c Average of three independent analyses.^d Six waters of hydration.^e Interference due to di-*n*-butyl oxalate.

TABLE III

THE EFFECT OF NaCl ON THE N-TFA *n*-BUTYL ESTER AMINO ACID DERIVATIVESExperiments were performed with 20 mg NaCl and 10 mg of total amino acid mixture; $W_{\text{salt}}/W_{\text{a.a.}} = 20$.

Amino acid	$RWR_{\text{a.a./stearic acid and injection number}}^a$					
	1	4	6	7	10	11 ^b
Alanine	1.131	1.136	1.149	1.224	1.362	1.139
Glycine	1.044	1.043	1.059	1.137	1.271	1.046
Leucine	1.116	1.124	1.176	1.258	1.361	1.109
Threonine	0.941	0.946	0.957	1.036	1.147	0.946
Cysteine	0.562	0.566	0.573	0.611	0.742	0.568
Hydroxyproline	0.981	0.987	0.994	1.107	1.112	0.991
Aspartic acid	1.138	1.142	1.127	1.068	0.987	1.144
Tyrosine	0.941	0.947	0.910	0.763	0.646	0.946
Lysine	1.002	1.001	0.968	0.641	0.463	1.005
Tryptophan	0.457	0.452	0.396	0.246	0.216	0.459

^a $RWR_{\text{a.a./stearic acid (I.S.)}} = \frac{A_{\text{a.a./g a.a.}}}{A_{\text{I.S./g I.S.}}}$ ^b The glass wool and the top 1/2 in. of column packing were replaced, then the column was inserted into the same injection port.

larger than those for the standards occurred as the result of a reduced response for the internal standard, not as a result of an enhancement of the response for an amino acid. The second explanation results in a reduced response of the amino acid. This would be expected to have a greater effect on the less volatile amino acids and indeed this trend was observed. The third explanation, again, would result in a reduced response for the amino acids.

A reasonable explanation of all the experimental observations and data in the tables is that the changed RWR values are a result of reduced volatilization of internal standard, amino acid, and perhaps chelation of the amino acids.

In this study, it was often noted that a decrease in the response of the long retention time amino acids occurred and little change was observed in the response for the short retention time amino acids. In many cases this problem was obviated on replacement of the glass wool plug and top $\frac{1}{2}$ in. of column packing. This observation resulted in a study of the effect of sodium chloride at a 20:1 (w/w) level to each amino acid in a sample upon repeated injection into a chromatographic column. The results of this experiment are given in Table III. As a build-up occurred of sodium chloride deposits in the injection port the volatilization of the less volatile amino acids decreased. When the glass wool plug was replaced and the first $\frac{1}{2}$ in. of column packing was removed, response values were again obtained comparable to the original values. This proves that there has not been a destruction of the column packing, but an interference in the volatilization of the internal standard and amino acids due to deposits of sodium chloride.

REFERENCES

- 1 C. ZOMZELY, G. MARCO AND E. EMERY, *Anal. Chem.*, **34** (1962) 1414.
- 2 W. M. LAMKIN AND C. W. GEHRKE, *Anal. Chem.*, **37** (1965) 383.
- 3 C. W. GEHRKE AND D. L. STALLING, *Separation Sci.*, **2** (1967) 101.
- 4 C. W. GEHRKE, D. ROACH, R. W. ZUMWALT, D. L. STALLING AND L. L. WALL, *Quantitative Gas-Liquid Chromatography of Amino Acids in Proteins and Biological Substances*, Analytical Biochemistry Laboratories, Columbia, Mo., 1968.
- 5 D. ROACH AND C. W. GEHRKE, *J. Chromatog.*, **44** (1969) 269.
- 6 D. ROACH AND C. W. GEHRKE, *J. Chromatog.*, **43** (1969) 303.

J. Chromatog., **53** (1970) 195-200

CHROM. 4995

TRIMETHYLSILYLATION OF AMINO ACIDS*

EFFECT OF SOLVENTS ON DERIVATIZATION USING
BIS(TRIMETHYLSILYL)TRIFLUOROACETAMIDE

CHARLES W. GEHRKE** AND KENNETH LEIMER***

University of Missouri, Columbia, Mo. 65201 (U.S.A.)

(Received August 17th, 1970)

SUMMARY

The number of chromatographic peaks for the TMS derivatives of glycine and arginine are determined by the polarity of the solvent. With hexane, methylene chloride, chloroform, and 1,2-dichloroethane, one peak is obtained for glycine (GLY₂), and two peaks (GLY₂ and GLY₃) in six other more polar solvents. Arginine gives no peak in the four less polar solvents studied and one peak in the other six more polar solvents.

Preliminary work is reported on chromatography using a 6 m × 2 mm I.D. glass column of 10 w/w% OV-11 on 100/120 mesh Supelcoport of which good resolution was obtained for the TMS derivatives of nineteen of the protein amino acids. More detailed chromatographic studies will be the subject of a separate paper.

INTRODUCTION

Since the introduction of the trimethylsilyl (TMS) derivatives of the amino acids by RÜHLMANN AND GIESECKE¹, efforts have been made by several groups of researchers in attempts to use these derivatives for the quantitative gas-liquid chromatographic (GLC) analysis of the twenty protein amino acids. The primary interest in the TMS derivative is the one-step derivatization procedure, whereas almost all other derivatives are formed by two or more reaction steps. RÜHLMANN AND GIESECKE used hexamethyldisilazane and trimethylchlorosilane (TMCS) to obtain derivatives for most of the protein amino acids. SMITH *et al.*^{2,3} made a study of the optimum silylation conditions for leucine, serine, and aspartic acid. They concluded that trimethylsilyldiethylamine with some kind of catalyst was the best silylation reagent. Trimethylsilyldimethylamine recently has been claimed to be more volatile

* Contribution from the Missouri Agricultural Experiment Station, Journal Series No. 6061. Approved by the Director. Supported in part by grants from the National Aeronautics and Space Administration (NGR 26-004-011) and the National Science Foundation (GB 7182).

** Professor, Experiment Station Chemical Laboratories.

*** Experimental data taken in part from master's research, University of Missouri.

and was recommended for these reasons⁴. N-Trimethylsilyl-N-methyl-acetamide has been recommended by BIRKOFER AND DONIKE⁵. KLEBE *et al.*⁶ used bis(trimethylsilyl)acetamide (BSA) to obtain sharp single peaks for all the protein amino acids except arginine, which showed indications of decomposition on the column. However, they were unable to separate the derivatives of glycine and alanine from BSA on an SE-30 column. The introduction of bis(trimethylsilyl)trifluoroacetamide (BSTFA) by STALLING *et al.*⁷ has solved the problem of separation of the TMS derivatives of glycine and alanine from the reagents and reaction products. Then, GEHRKE *et al.*^{8,9} published a comprehensive method for the GLC analysis of all twenty protein amino acids as their TMS derivatives using BSTFA as the silylating agent, but they reported that problems still existed in the analysis of biological fluids such as urine.

BERGSTRÖM *et al.*¹⁰ recently reported on the trimethylsilylation of amino acids. These workers used BSTFA with and without solvent at 125° for 15 min to obtain chromatographic peaks for eighteen amino acids. They also reported on the mass spectra of the two derivatives of glycine and lysine. The results of the mass spectra are in agreement with the structural assignment given by GEHRKE and coworkers^{8,9}.

GEHRKE and coworkers report that urine samples containing large amounts of glycine presented difficulties in obtaining a single peak for glycine. Both the di-trimethylsilyl (GLY₂) derivative and the tri-trimethylsilyl (GLY₃, *ca.* 10%) derivatives were obtained when the samples were derivatized at 135° for both 10 and 15 min. Because of the large quantity of glycine in the urine samples, the GLY₃ peak interfered with the resolution of TMS isoleucine and TMS proline. In preliminary work on the TMS derivative of glycine by the present authors, it was observed that only the first peak for glycine (GLY₂) was obtained when using methylene chloride as a solvent instead of acetonitrile. This study was undertaken to investigate the effect of different solvents on silylation and reports on improvements in the chromatographic separation, thus permitting the analysis of biological fluids such as urine.

EXPERIMENTAL

Reagents and materials

Acetonitrile, hexane, and chloroform were obtained from Mallinkrodt Chemical Works, St. Louis, Mo., and were of "Nanograde" purity. Methylene chloride was obtained from Mallinckrodt Chemical Works, St. Louis, Mo., and was analytical reagent grade. Pyridine, 1,2-dichloroethane, dimethylformamide, tetrahydrofuran, and triethylamine were obtained from Distillation Products Industries, Rochester 3, N.Y. All solvents were dried over calcium chloride and redistilled before use.

The BSTFA (Regisil) was obtained from Regis Chemical Company, Chicago, Ill.

The OV-7, OV-11, and OV-22 liquid phases and solid support, Supelcoport, 100/120 mesh, were obtained from Supelco, Inc., Bellefonte, Pa.

The amino acids were obtained from Mann Research Laboratories, New York, N.Y., and were "Mann Assayed".

Equipment

A Micro-Tek Model MT-220 gas chromatograph with a four-column oven bath, two dual-channel electrometers and four flame ionization detectors were used in this study. A Varian Model 30 recorder was used for the chart presentation.

Chromatographic column

The chromatography column was a mixed phase consisting of 3 w/w% OV-22 and 6 w/w% OV-7 on 100/120 mesh Supelcoport in a 2 m \times 4 mm I.D. glass column. Also used was 10% OV-11 on Supelcoport in a glass column 6 m \times 2 mm I.D.

Derivatization method

Two milliliters of a stock solution containing 0.1 mg/ml of each amino acid were pipetted into a Corning No. 9826 1.6 cm \times 7.5 cm reaction tube and dried under a stream of dry filtered nitrogen at 75°. One milliliter of methylene chloride was added and evaporated under nitrogen to azeotrope any remaining water. Then 1 ml of BSTFA and 1 ml of acetonitrile were added to the tube. The sample tube was closed with a teflon-lined cap and heated at different temperatures and times in a constant-temperature oil bath. For the solvent study, the only change made was to substitute the appropriate solvent for acetonitrile. Also, in some experiments, 1% TMCS in BSTFA was substituted for the BSTFA.

RESULTS

Table I presents a summary of the solvents used in this research and their results. No quantitation was attempted using these solvents. In these experiments,

TABLE I

SOLVENT EFFECTS ON TMS DERIVATIZATION OF PROTEIN AMINO ACIDS

<i>Solvent</i>	<i>No. of glycine peaks</i>	<i>No. of arginine peaks</i>
Acetonitrile	2	1
Dimethylformamide	2	1
Pyridine	2	1
Triethylamine	2	1
Tetrahydrofuran	2	1
10% acetonitrile in methylene chloride	1	0
5% acetonitrile in methylene chloride	1	0
Hexane	1	0
Methylene chloride	1	0
Chloroform	1	0
1,2-Dichloroethane	1	0

essentially the same results were obtained on a qualitative basis as reported by GEHRKE *et al.*⁸, as illustrated in Figs. 1 and 2. GEHRKE and coworkers reported two peaks for glycine and one peak for arginine using acetonitrile as solvent. In this study, using methylene chloride, hexane, chloroform, and 1,2-dichloroethane, it was observed that glycine produced only one peak, as illustrated in Figs. 3 and 4, whereas two peaks were formed in acetonitrile, dimethylformamide, pyridine, triethylamine, and tetrahydrofuran. The number of peaks for glycine derivatized in the non-polar solvents was not affected by the time or temperature, as times from 15 min to 6 h, and temperatures from 50° to 150° were used. Also, arginine under the same experimental conditions is either not derivatized, or decomposed, as no peak was obtained. In these

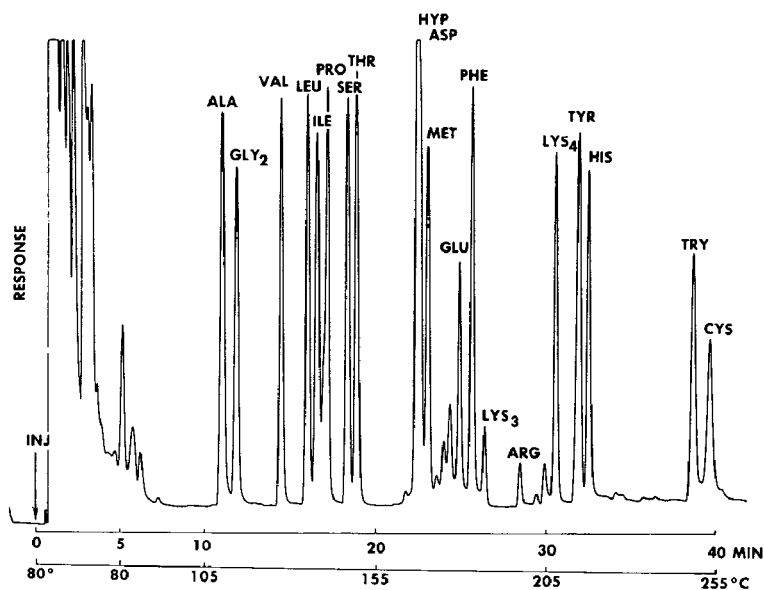


Fig. 1. Chromatogram obtained on GLC of 0.2 mg of each amino acid in 2.0 ml CH_3CN -BSTFA (1:1) after closed-tube silylation at 135° for 15 min. Conditions: Column, mixed liquid phase 6.0 w/w% OV-7 and 3.0 w/w% OV-22 on 100/120 mesh Supelcoport, 2 m \times 4 mm I.D., glass. Temperature, programmed, initial temperature 80° , 5 min hold, then $5^\circ/\text{min}$. Volume injected, 5 μl .

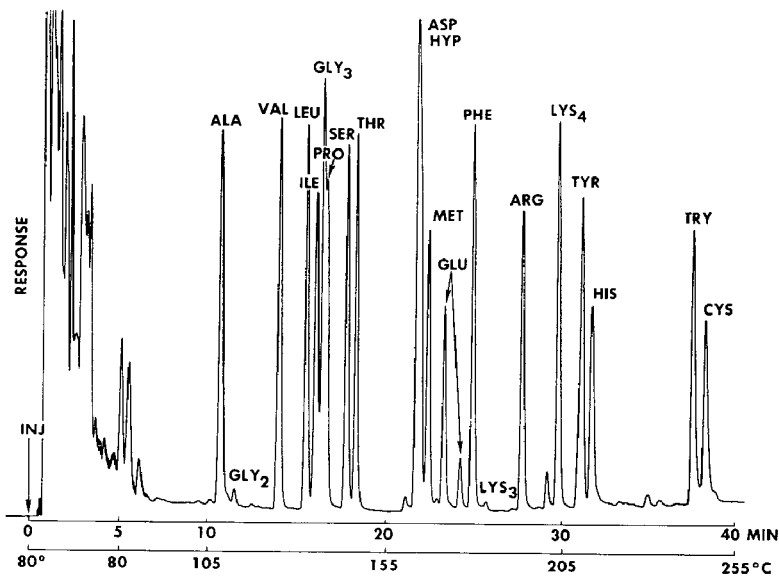


Fig. 2. Chromatogram obtained on GLC of 0.2 mg of each amino acid in 2.0 ml CH_3CN -BSTFA (1:1) after closed-tube silylation at 135° for 4 h. Conditions, see the legend to Fig. 1.

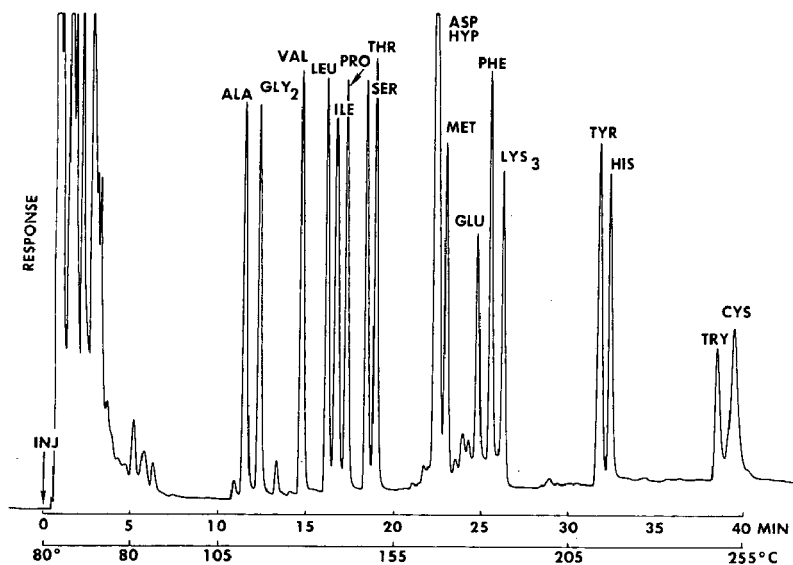


Fig. 3. Chromatogram obtained on GLC of 0.2 mg of each amino acid in 2.0 ml CH_2Cl_2 -BSTFA (1:1) after closed-tube silylation at 135° for 15 min. Conditions, see the legend to Fig. 1.

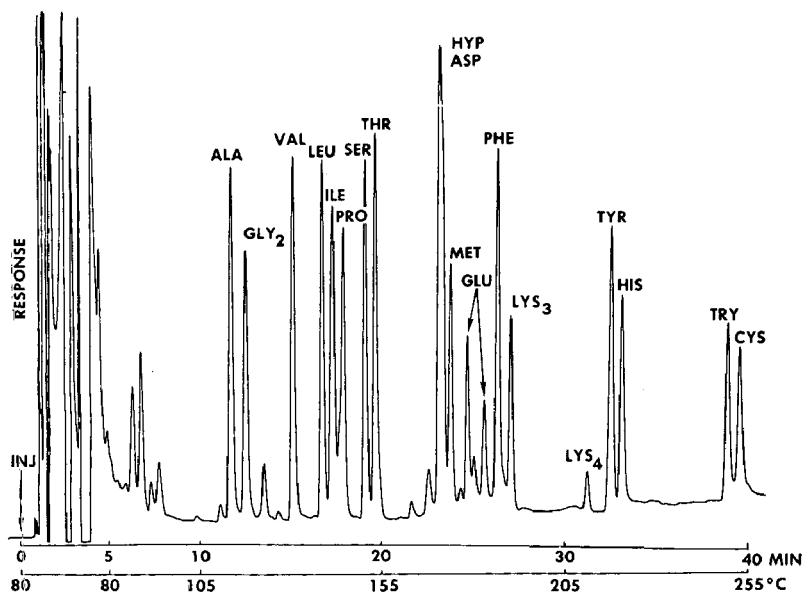


Fig. 4. Chromatogram obtained on GLC of 0.2 mg of each amino acid in 2.0 ml CH_2Cl_2 -BSTFA (1:1) after closed-tube silylation at 135° for 4 h. Conditions, see the legend to Fig. 1. Each peak represents *ca.* 500 ng.

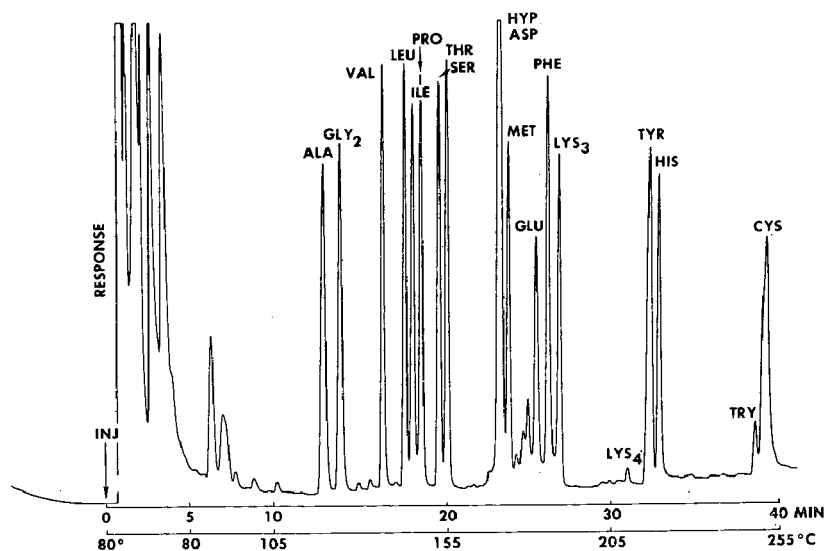


Fig. 5. Chromatogram obtained on GLC of 0.2 mg of each amino acid in 2.0 ml CH_2Cl_2 -1% TMCS in BSTFA (1:1) after closed-tube silylation at 135° for 15 min. Conditions, see the legend to Fig. 1.

non-polar solvents, one notes two peaks for glutamic acid, mostly LYS_3 instead of LYS_4 , no peak for arginine, and nearly all GLY_2 .

CHAMBAZ *et al.*¹¹⁻¹³ has recently reported that the use of 1% TMCS has a catalytic effect on the silylation of steroids using BSA. Regis Chemical Company¹⁴ has suggested

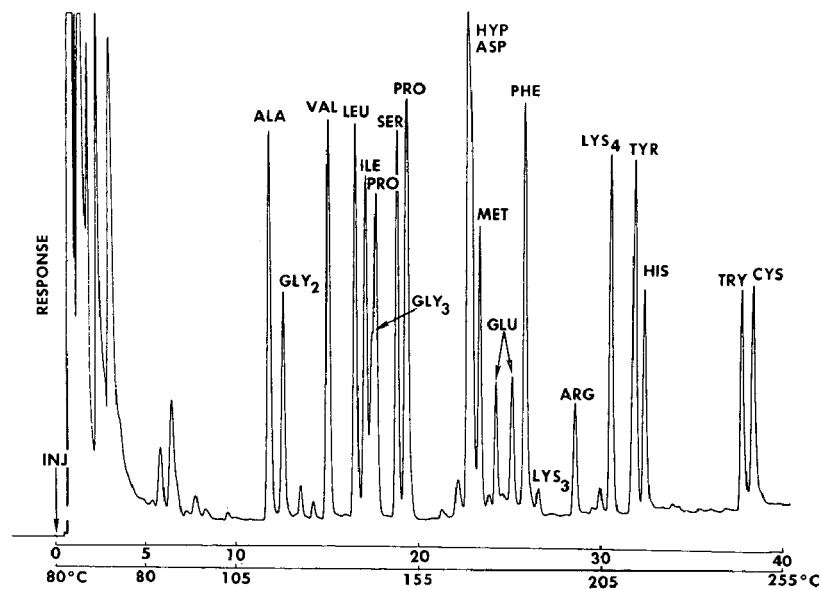


Fig. 6. Chromatogram obtained on GLC of 0.2 mg of each amino acid in 2.0 ml CH_2Cl_2 -1% TMCS in BSTFA (1:1) after closed-tube silylation at 135° for 4 h. Conditions, see the legend to Fig. 1.

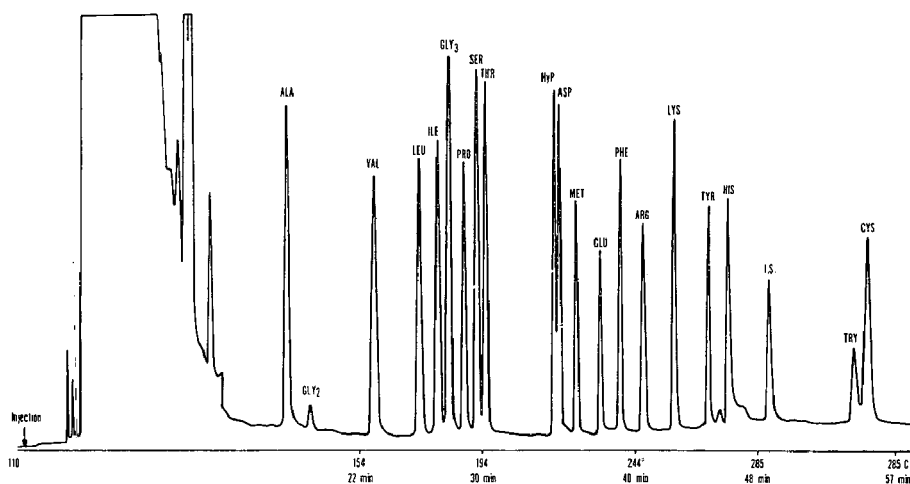


Fig. 7. Chromatogram obtained on GLC of 1.0 μ g of each amino acid (2.0 mg total amino acids) in 1.0 ml BSTFA-CH₃CN (1:1) after closed-tube silylation at 150° for 2.5 h. Conditions: Column, 10% OV-11 on Supelcoport 100/120 mesh, 6 m \times 2 mm I.D., glass. Injector temperature, 275°. Detector temperature, 300°. Column temperature, programmed, initial temperature 110°, 2°/min for 22 min, then 5°/min up to 285°. Nitrogen flow rate, 20 ml/min. Internal standard, phenanthrene.

the use of 1% TMCS with BSTFA. Figs. 5 and 6 show the effect of the use of 1% TMCS with BSTFA in methylene chloride. The use of 1% TMCS as a catalyst results in a more powerful silylating agent as there is a larger amount of GLY₃, LYS₄, and an arginine peak on silylation at 135° for 4 h (Fig. 6). As shown in Fig. 5, silylation under these conditions for 15 min is incomplete. No differences were noted with 1% TMCS as catalyst in a polar solvent, acetonitrile, from the use of BSTFA in acetonitrile.

It appears that the derivatization of glycine, arginine, lysine, and glutamic acid involves the polarity of the solvent, with polar solvents giving two peaks for glycine and one peak for arginine. In non-polar solvents only the first chromatographic peak for glycine and no peaks for arginine were obtained. The explanation for not obtaining a peak for arginine is probably due to solubility of arginine in the solvent, or a difference in the silylating strength of BSTFA in various polarity solvents.

There is a need to expand the earlier work of GEHRKE and coworkers, especially in the area of chromatographic resolution. The results of preliminary studies are given in Fig. 7. This chromatogram shows excellent resolution for nineteen amino acids. Further work is in progress to investigate the chromatography on this column, a 6 m \times 2 mm I.D. 10 w/w% OV-11 on 100/120 mesh Supelcoport.

In the analysis of biological fluids containing large amounts of glycine it may be necessary to derivatize the sample with two different solvents to avoid interference of the GLY₃ peak with isoleucine and proline.

REFERENCES

- 1 K. RÜHLMANN AND W. GIESECKE, *Angew. Chem.*, 73 (1961) 113.
- 2 E. D. SMITH AND H. SHEPPARD, JR., *Nature*, 208 (1965) 878.
- 3 P. S. MASON AND E. D. SMITH, *J. Gas Chromatog.*, 4 (1966) 398.
- 4 *Chromatography/Lipids*, Supelco, Inc., Bellefonte, Pa., 1 (1967) 3.

- 5 L. BIRKOFER AND M. DONIKE, *J. Chromatog.*, 26 (1967) 270.
- 6 J. KLEBE, H. FINKBEINER AND D. WHITE, *J. Am. Chem. Soc.*, 88 (1966) 3390.
- 7 D. L. STALLING, C. W. GEHRKE AND R. W. ZUMWALT, *Biochem. Biophys. Res. Commun.*, 31 (1968) 616.
- 8 C. W. GEHRKE, H. NAKAMOTO AND R. W. ZUMWALT, *J. Chromatog.*, 45 (1969) 24.
- 9 H. NAKAMOTO, *Master's Thesis*, University of Missouri, June, 1969.
- 10 K. BERGSTRÖM, J. GÜRTLER AND R. BLOMSTRAND, *Anal. Biochem.*, 34 (1970) 74.
- 11 E. CHAMBAZ AND E. C. HORNING, *Anal. Letters*, 1 (1967) 201.
- 12 E. CHAMBAZ AND E. C. HORNING, *Anal. Biochem.*, 30 (1967) 7.
- 13 E. CHAMBAZ, G. MARME AND E. C. HORNING, *Anal. Letters*, 1 (1968) 749.
- 14 *Gas Chromatography Catalog*, Regis Chemical Company, Chicago, Ill., 1970, p. 21.

J. Chromatog., 53 (1970) 201-208

CHROM. 5021

GAS CHROMATOGRAPHIC ANALYSIS OF FECAL POLLUTION STEROLS
ON A SINGLE COMBINED PACKED COLUMN

L. TAN, M. CLEMENCE AND J. GASS

Biochemistry Laboratories, Department of Nuclear Medicine and Radiobiology, Centre Hospitalier Universitaire, Sherbrooke, Quebec (Canada)

(Received August 31st, 1970)

SUMMARY

1. The separation of cholesterol from coprostanol and coprostanone on a single column, consisting of a combination of selective and non-selective coated supports, packed in series, is described.

2. The resolution on this combined column is better than when either phase was used alone.

3. Various functional derivatives and isomers of progesterone are also well resolved by our column, which should find general application for the gas chromatographic analysis of mixtures of steroidal compounds of similar structure.

INTRODUCTION

Recently, the possible use of coprostanol (5β -cholestane- 3β -ol) as a molecular tracer for the detection of fecal water pollution has been suggested^{1,2}. Since this sterol is known to be produced only by the action of the intestinal flora of higher animals by stereospecific reduction of the double bond of cholesterol³⁻¹⁰, a reliable and simple analysis for its unambiguous detection in natural waters would indeed provide a desirable complement to the classical method of bacterial Coliform counting. Unfortunately, coprostanol is always excreted together with its precursor cholesterol, and because the two sterols differ in their molecular structure merely by the presence of a double bond, their successful separation based on chromatographic mobilities would require a high degree of efficiency. Furthermore, coprostanol dispersed or dissolved for extended periods in oxygen saturated surface waters, may easily undergo oxidation to coprostanone (5β -cholestane-3-one). Thus, adequate separation of the three C_{27} -steroids coprostanol, cholesterol and coprostanone must be accomplished before coprostanol may be proposed as a suitable reference index for the chemical measurement of fecal water pollution.

We have found that in thin-layer chromatography (TLC) using different solvent systems, and including complexing of the unsaturated bond of cholesterol with silver nitrate, coprostanol consistently showed similar mobilities as its companion cholesterol

so that its positive identification by this method alone is not possible. We had expected gas-liquid chromatography (GLC) with its inherent much higher resolution capability to yield more satisfactory results. However, we discovered that on a non-polar phase such as OV-1, cholesterol was not at all separated from coprostanone, whereas on the selective phase QF-1, considerable overlap of the coprostanol and cholesterol peaks were observed.

In this paper, we report the complete gas chromatographic separation of the three fecal steroids by means of a single combined column, packed alternately with a polar and a non-polar liquid phase.

EXPERIMENTAL

Materials and methods

Reference coprostanol, coprostanone and 5 α -cholestane were purchased from Sigma Chemical Company, Mo. All solvents were reagent grade and distilled before use. TLC was conducted as described previously¹¹. GLC was performed on a Model 402 Hewlett Packard gas chromatograph, equipped with dual hydrogen flame ionization detectors operated in the twin-mode. Unless otherwise indicated operating conditions were: oven temperature 230°, injection port and detector temperatures 265°, nitrogen carrier gas flow 33 ml/min at 40 p.s.i.

Preparation of trimethylsilyl (TMS) derivatives

Two milligrams of steroid was dissolved in 2 drops of anhydrous pyridine, 4 drops of Trisyl reagent (Pierce Chemical Company, Rockford, Ill.) were added and the mixture stored under nitrogen for 30 min at 45°. After evaporation of the solvents with a stream of nitrogen, the residue was dissolved in hexane and the clear supernatant used immediately for the GLC analysis.

Preparation of the combination column

A 180 \times 0.3 cm (I.D.) U-type glass column was packed simultaneously from either end with two layers of 100-120 mesh Gas-Chrom Q (Applied Science Laboratories, State College, Penn.) each coated with 3% OV-1 and 3% QF-1, in such a way that each column half contained approximately equal amounts of the two types of coated support. The firmly packed column was then conditioned overnight at 250° until a stable base line was obtained.

For preparation of standard curves, the peak areas were quantitated either by triangulation or by means of a mechanical Disc integrator and the addition of 5 α -cholestane as an internal standard.

Analysis of fecal sterols from surface waters

A water sample (12 l) from a lake in the area was extracted twice with 2 l of distilled hexane in a wide mouth 20 l glass bottle by stirring vigorously with a mechanically driven stainless steel propeller for a period of 30 min. Other than glass and steel, no other material was used for the extraction apparatus, so that no contamination from hexane-soluble lipid components, other than from the water sample itself, could have been introduced. After stirring, the hexane fractions were siphoned off, pooled, dried over anhydrous sodium sulfate, and evaporated to dryness. The usually colored

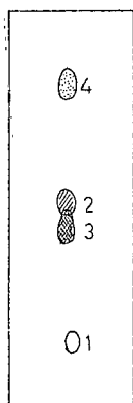


Fig. 1. Thin-layer chromatogram of 5 α -cholestane (1), coprostanol (2), cholesterol (3) and coprostanone (4). Solvent system: chloroform-ether (9:1).

residue thus obtained was dissolved in dioxane and either analyzed directly, or further purified by preparative TLC on 20 \times 20 cm, with 0.1 cm of Silica Gel HF₂₅₄ (Merck, Darmstadt) coated glass plates, by means of a mechanical streaker (Rodder Instruments Corp., Los Altos, Calif.). After irrigation with a mixture of chloroform and ether (9:1), and visualization of a 1.5 cm end-strip of the chromatoplate by spraying with 50% sulfuric acid, the bands containing the suspected sterol fractions were scraped off, eluted with methanol, filtered, concentrated in vacuum, and used for the GLC analysis.

RESULTS AND DISCUSSION

On thin-layer chromatograms, coprostanol is not well separated from cholesterol, although coprostanone is (Fig. 1). Eluted with a mixture of chloroform-ether (9:1), cholesterol could not be readily defined from coprostanol. Other solvent systems such as chloroform-methanol (9:1), hexane-ethyl acetate (1:1), benzene-acetone (4:1), and the use of silver nitrate impregnated silica gel, gave similar unresolved spots. Since both compounds do not absorb in the UV, positive identification by TLC alone remains doubtful. Separation of these two sterols in the gaseous state on OV-1 and QF-1 as stationary phases, was better (Figs. 2 and 3).

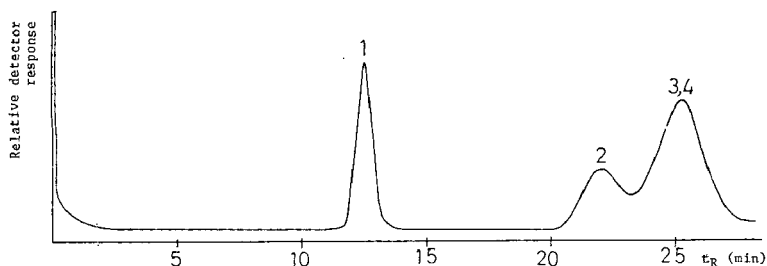


Fig. 2. Gas chromatograms of 5 α -cholestane (1), coprostanol (2), cholesterol (3), and coprostanone (4) on a 3% OV-1 column. Conditions: 180 \times 0.3 cm glass, oven temperature 230°, injection port and detector temperatures 265°, nitrogen carrier gas flow 33 ml/min at 40 p.s.i.

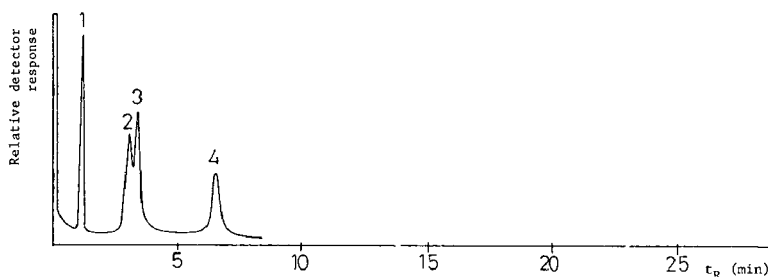


Fig. 3. Gas chromatograms of 5 α -cholestane (1), coprostanol (2), cholesterol (3), and coprostanone (4) on a 3% QF-1 column. For conditions see Fig. 2.

However, although on the non-selective phase OV-1, acceptable resolution between coprostanol and cholesterol was readily achieved, cholesterol could not be distinguished from coprostanone on this column, as both compounds exhibited identical retention times. In contrast, on the selective QF-1 column, cholesterol and coprostanone were well resolved, but not cholesterol from coprostanol. Due to the high background noise of actual water sample extracts, the latter two sterols cannot therefore be readily differentiated on a QF-1 phase alone.

We have thought to combine the desirable separation properties of both phases OV-1 and QF-1 on a single column, and indeed, with our combination column coprostanone was well separated both from cholesterol and coprostanol. At the same time, almost complete resolution between coprostanol and cholesterol was achieved (Fig. 4). The practical utility of this novel column for the analysis of an actual water sample is illustrated in Fig. 5. Despite the high background noise generated by the sample, coprostanol can now easily be distinguished from cholesterol.

The identity of peaks 2, 3 and 4 of the water sample extract was established by consecutive co-injection of the same amount of sample with authentic compound and observation of area enlargement of a single, suspected peak.

That our combination column can be used for the quantitative analysis of fecal sterols is demonstrated in Fig. 6, obtained by plotting known weight ratios of coprostanol and 5 α -cholestane against the ratios of their measured peak areas. As can be seen, good linearity and a zero intercept were observed.

Table I shows the properties of our combination column (C), as compared to the columns containing either only OV-1 (A) or QF-1 (B). For the compounds studied,

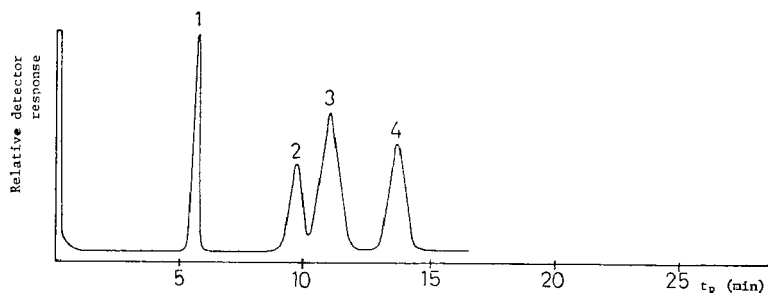


Fig. 4. Gas chromatograms of 5 α -cholestane (1), coprostanol (2), cholesterol (3), and coprostanone (4) on a 3% OV-1, 3% QF-1 combination column. For conditions see Fig. 2.

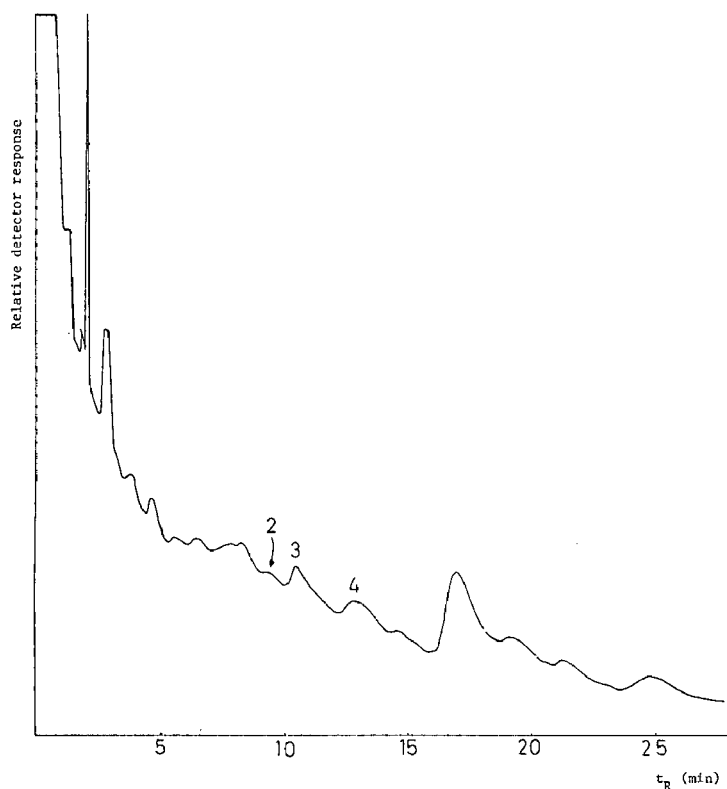


Fig. 5. Gas chromatogram of a water sample from a lake in the Sherbrooke area on the combination column, consisting of 3% OV-1 and 3% QF-1, packed in series. For conditions see Fig. 2.

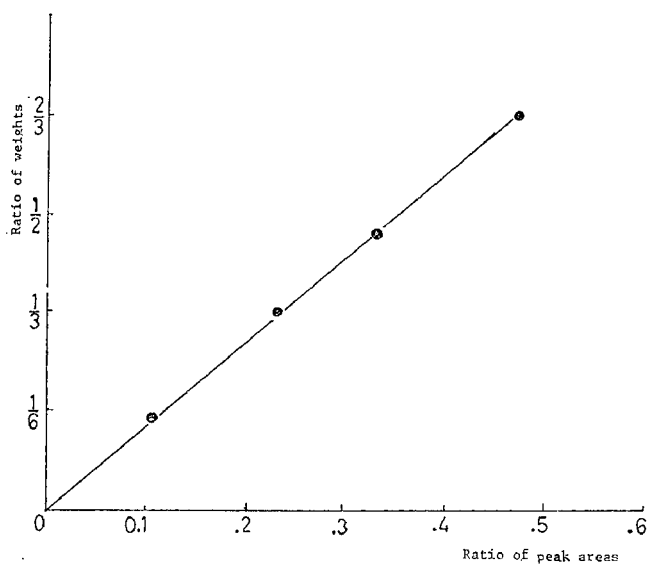


Fig. 6. Known weights of coprostanol and 5 α -cholestane were co-injected on the combination column, and their ratios plotted against the ratios of the peak areas. For conditions see Fig. 2.

the optimal temperature was found to be 230°. At this temperature, our column C showed superior efficiency, as clearly indicated by the higher number of theoretical plates obtained. From these data, we may conclude that our combination column provoked retention times, in between those obtained on columns A and B, while at the same time column C combined the best separation properties of both.

The further advantages of this novel column are obvious, in particular for those chromatographers, who either have only a single column instrument, or a single detector and recorder system at their disposal. Instead of having to inject consecutively the unknown sample at least twice on a selective and non-selective column, in order to avoid identification errors due to identical retention times on one liquid

TABLE I

COMPARATIVE PROPERTIES OF COLUMNS A (3% OV1), B (3% QF1) AND C (3% OV1-QF1) TOWARDS FECAL POLLUTION STEROLS

Oven temperature	Compound	3% OV-1 (A)			3% OF-1 (B)			3% OV-1/QF-1 (C)		
		t_R^a	RRT ^b	Plates ^c	t_R	RRT	Plates	t_R	RRT	Plates
220°	5 α -Cholestane	18.8	1.00	1580	1.81	1.00	435	6.63	1.00	785
	Coprostanol	31.7	1.70	1770	4.42	2.44	380	13.0	1.97	1091
	Cholesterol	36.7	1.97	1650	5.05	2.78	545	14.4	2.17	881
	Coprostanone	36.7	1.97	1720	9.80	5.41	760	18.5	2.79	1380
	Coprostanol-TMS	41.1	2.19	1750	1.77	0.97	188	2.45	0.36	693
	Cholesterol-TMS	51.6	2.74	1680	3.46	1.91	338	18.8	2.83	762
230°	5 α -Cholestane	12.9	1.00	1425	1.26	1.00	463	5.16	1.00	1610
	Coprostanol	22.6	1.75	1290	3.00	2.38	1145	9.64	1.87	1482
	Cholesterol	26.5	2.05	1570	3.44	2.73	660	10.72	2.08	1624
	Coprostanone	26.5	2.05		6.54	5.20	915	13.4	2.60	1505
	Coprostanol-TMS	24.9	1.93	1750-2040	1.89	1.50	370	11.2	2.17	1645
	Cholesterol-TMS	26.5	2.05	1480-1690	2.36	1.88	403	14.1	2.73	2003
240°	5 α -Cholestane	8.50	1.00	1055	0.87	1.00	216	3.70	1.00	982
	Coprostanol	14.3	1.68	1085	2.02	2.32	495	6.90	1.86	1229
	Cholesterol	15.7	1.84	1105	2.20	2.55	385	7.56	2.04	1218
	Coprostanone	15.7	1.84	1360	4.10	4.73	435	9.71	2.62	1680
	Coprostanol-TMS	15.4	1.79	1690	1.26	1.45	880	6.29	1.70	2039
	Cholesterol-TMS	19.2	2.24	1450-1650	1.58	1.82	130	7.80	2.11	1568

^a Absolute retention time in minutes.

^b Retention time, relative to 5 α -cholestane.

^c Number of theoretical plates; average of at least three determinations.

phase, now a single analysis suffices for a positive identification. Indeed, our column should find general application in the analysis of mixtures of steroids with identical functional groups. For instance, the following functional isomers were also found to be easily resolved at 230°: 14 α -hydroxy-4-pregnene-3,20-dione (RRT 13.34) from 21-hydroxy-4-pregnene-3,20-dione (RRT 15.15), and 3-ethoxy-2,4-pregnadien-20-one (RRT 0.61) from 3-ethoxy-3,5-pregnadien-20-one (RRT 0.71).

The gas chromatographic method using a single combination column described

in this paper, has been proven in our laboratory to be of great utility in the rapid and reliable analysis of contamination of natural waters by untreated sewage discharge, whereby as a condition, distinct resolution of the three fecal steroids coprostanol, cholesterol and coprostanone¹² had first to be achieved.

ACKNOWLEDGEMENT

This project (No. 604-7-677) has been supported by a grant-in-aid from the Ministry of Health, Federal Programme for Public Hygiene, which we gratefully acknowledge.

REFERENCES

- 1 J. J. MURTAUGH AND R. L. BUNCH, *J. Water Pollut. Contr. Fed.*, (1966) 404.
- 2 L. L. SMITH AND R. E. GOURON, *Water Res.*, 3 (1969) 141.
- 3 R. S. ROSENFELD, D. K. FUKUSHIMA, L. HELLMAN AND T. F. GALLAGHER, *J. Biol. Chem.*, 211 (1951) 301.
- 4 R. S. ROSENFELD, L. HELLMAN AND T. F. GALLAGHER, *J. Biol. Chem.*, 222 (1956) 321.
- 5 R. S. ROSENFELD AND L. HELLMAN, *J. Biol. Chem.*, 233 (1958) 1089.
- 6 R. S. ROSENFELD, *Arch. Biochem. Biophys.*, 108 (1965) 384.
- 7 K. HELLSTROM, *Acta Physiol. Scand.*, 63 (1965) 21.
- 8 S. CARINI, *Ann. Microbiol. Enzimol.*, 14 (1964) 205.
- 9 J. Å. GUSTAFSSON AND J. SJOVALL, *Acta Chem. Scand.*, 20 (1966) 1827.
- 10 E. EVRARD, E. SACQUET, P. RAIBAUD, H. CHARLIER, R. DICKINSON, H. EYSSSEN AND P. P. HOET, *Ernährungsforschung*, 10 (1965) 257.
- 11 L. TAN, *J. Chromatog.*, 45 (1969) 68.
- 12 P. ENEROTH, K. HELLSTROM AND R. RYHAGE, *J. Lipid Res.*, 5 (1964) 245.

J. Chromatog., 53 (1970) 209-215

CHROM. 5026

ÉTUDE CHROMATOGRAPHIQUE DES STÉRIDES ET DES ESTERS METHYLIQUES DES NOYAUX D'HÉMATIES NUCLÉÉES

G. SOULA, C. SOUILLARD, Y. MAURY ET L. DOUSTE-BLAZY

Laboratoire de Chimie Biologique, UER de Pharmacie, 31 Allées J. Guesde et Laboratoire de Biochimie du Centre Anticancéreux, Hôpital de la Grave, (31) Toulouse (France)

(Reçu le 27 avril 1970, manuscrit modifié reçu le 11 août 1970)

SUMMARY

Chromatographic study of cholesteryl esters and methyl esters in nucleated erythrocytes

Thin-layer chromatography allows the separation of four main fractions of cholesterol esters and also fatty acid methyl esters from nucleated chick erythrocytes.

The fatty acid composition is studied by gas chromatography. Among the cholesterol ester fractions, one contains 88 per 100 saturated fatty acids (mainly palmitic acid and stearic acid) and unsaturated fatty acids are preponderant: 75 per 100 in the three others.

The natural fatty acid methyl esters are mainly palmitate.

INTRODUCTION

Les esters de cholestérol du sérum des mammifères ont été particulièrement étudiés. Séparés par chromatographie sur colonne¹, chromatographie sur papier² ou sur couches minces³⁻⁸ imprégnées ou non de nitrate d'argent, leur étude a montré qu'il existe plusieurs fractions différenciées par le degré d'insaturation de leurs acides gras.

Les hématies des mammifères sont quasiment dépourvues de stérides, par contre les globules rouges d'oiseaux en renferment une plus grande quantité⁹.

Dans le présent travail, nous nous proposons de séparer les stérides d'hématies nucléées de poulet par divers systèmes de chromatographie en couche mince mono- ou bidimensionnelle. Leur composition en acides gras, étudiée par chromatographie en phase gazeuse, est comparée à celle des stérides plasmatiques.

TECHNIQUES

Préparation des hématies et extraction des lipides

Le sang est recueilli sur des animaux âgés de trois à quatre mois* par ponction

* Les prélèvements ont été effectués sur des poulets de race White Leghorn à l'École Vétérinaire de Toulouse, Service de Pathologie des volailles (Prof. J. TOURNUT) par Madame P. MONTLAUR que nous remercions vivement.

à la veine alaire sur une solution de citrate de sodium à 4 pour 100 à 2500 tours/min., le plasma est séparé et après centrifugation les globules rouges lavés à trois reprises au sérum physiologique.

La couche leucocyto-plaquettaire est soigneusement aspirée à chaque lavage, les globules rouges sont prélevés au fond du tube de centrifugation.

Le plasma, les hématies hémolysés par un volume d'eau distillée, ou les noyaux isolés¹⁰, sont additionnés de onze volumes d'alcool isopropylique, agités pendant une heure, puis de sept volumes de chloroforme et agités à nouveau une heure, selon ROSE ET OKLANDER¹¹.

Les solvants sont évaporés à sec sous vide à 37°, l'extrait lipidique est repris par du chloroforme, filtré et conservé à -20°.

Chromatographie sur colonne

Un extrait chloroformique contenant de 100 à 150 mg de lipides totaux de plasma, d'hématies ou de noyaux, est chromatographié sur une colonne d'acide silicique et d'hyfflosupercel (20 g et 10 g). Les stérides et autres lipides non phosphorés sont élués par 500 ml de chloroforme.

Chromatographie en couche mince

Elles sont effectuées sur des plaques 20 × 20 cm de Silica Gel F₂₅₄ Merck (épaisseur: 250 μ) dans plusieurs systèmes de solvants préconisés par NIEMINEN¹²:

(I) *n*-hexane-benzène (5:95), sur 8 cm, puis après séchage de la plaque: *n*-hexane sur 10 cm,

(II) tétrachlorure de carbone sur 9 cm.

De plus, deux sortes de chromatographies ont été réalisées: l'une, monodimensionnelle utilisant le système I, puis après séchage de la plaque le tétrachlorure de carbone sur 16 cm; l'autre, bidimensionnelle utilisant le système I dans la première dimension, le système II dans la seconde.

Les lipides sont révélés par pulvérisation soit d'une solution d'acide phosphomolybdique à 2 g pour 100 dans l'éthanol, soit du réactif de LIEBERMANN suivies d'un chauffage quelques minutes à 110°.

En vue de l'analyse de leurs acides gras, les stérides sont révélés sur plaque par pulvérisation d'une solution éthanolique à 0.2 pour 100 de 2,7-dichlorofluorescéine, examinés en lumière ultraviolette à 254 nm et élués du silica gel par un mélange de chloroforme et d'éther à parties égales.

Hydrolyse et chromatographie en phase gazeuse

Les stérides sont saponifiés par la potasse méthanolique N à reflux au bain-marie bouillant; les acides gras sont extraits par l'éther de pétrole et, après purification, méthylés par le diazométhane dans l'éther ou par le méthylate de sodium 0.1 N dans le méthanol 2 h à 100° (bibl. 6).

Les esters méthyliques d'acides gras sont chromatographiés en phase gazeuse dans l'hexane dans un appareil Aerograph, Modèle 204 B sur colonne de diéthylène-glycol-succinate à 185° sous un débit d'azote de 40 ml/min.

Leurs concentrations molaires, exprimées en pourcentages, sont calculées après planimétrie.

RÉSULTATS

La chromatographie en couche mince dans le tétrachlorure de carbone (Fig. 1) des lipides de globules rouges de poulet et de leurs noyaux, élués par le chloroforme sur colonne d'acide silicique, révèle l'existence de quatre groupes principaux d'esters du cholestérol, accompagnés d'autres fractions en plus faible quantité. L'ensemble de ces taches est coloré en violet par le réactif de LIEBERMAN. Des lipides plasmatiques on isole cinq fractions principales et des fractions mineures.

En réalisant une première chromatographie dans le système I sur 8 cm puis une

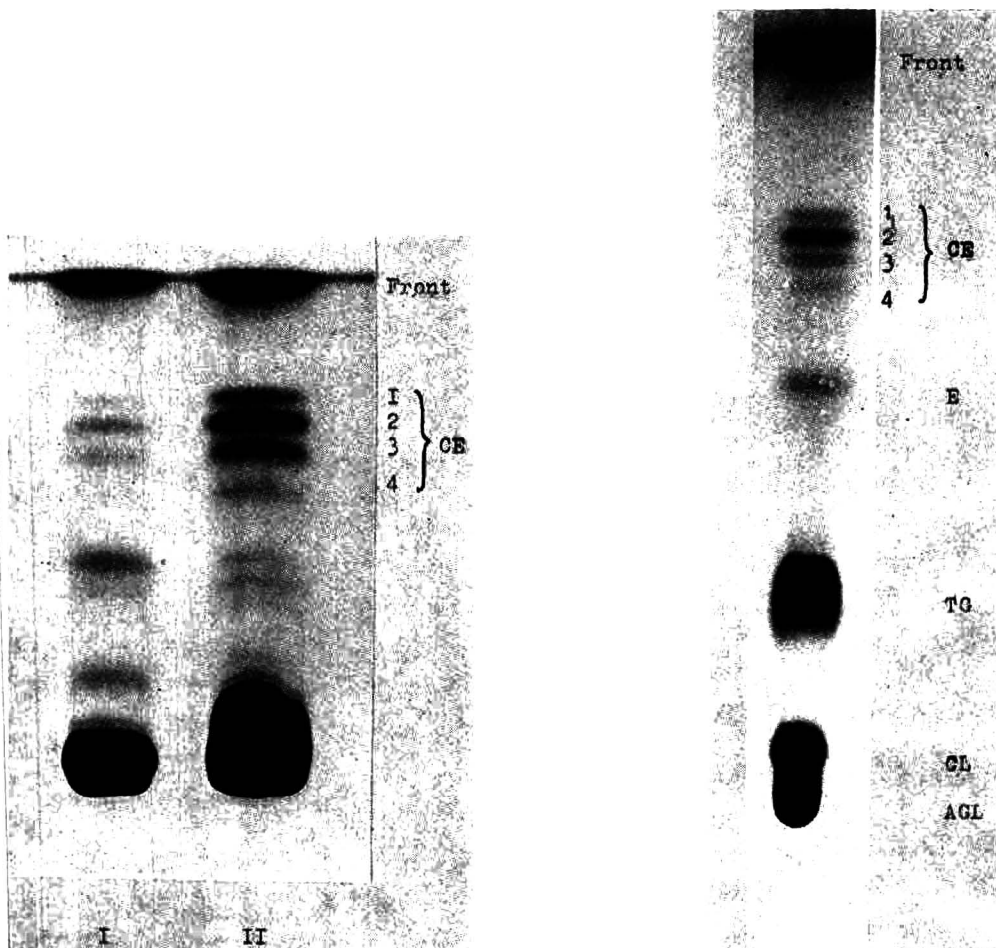


Fig. 1. Chromatographie en couche mince de Silica Gel F₂₅₄ Merck (250 μ) des stérides d'hématies de poulet (I) et de noyaux globulaires de poulet (II) dans le tétrachlorure de carbone (trois passages successifs sur 9 cm). Révélation: solution éthanolique d'acide phosphomolybdique.

Fig. 2. Chromatographie en couche mince de Silica Gel F₂₅₄ des glycérides, stérides et acides gras libres de noyaux d'hématies de poulet. Premier solvant: *n*-hexane-benzène (5:95) sur 8 cm, puis *n*-hexane sur 10 cm. Deuxième solvant: tétrachlorure de carbone sur 16 cm. Révélation: solution éthanolique d'acide phosphomolybdique. CE = cholestérol estérifié, E = esters méthyliques, TG = triglycérides, CL = cholestérol libre, AGL = acides gras libres.

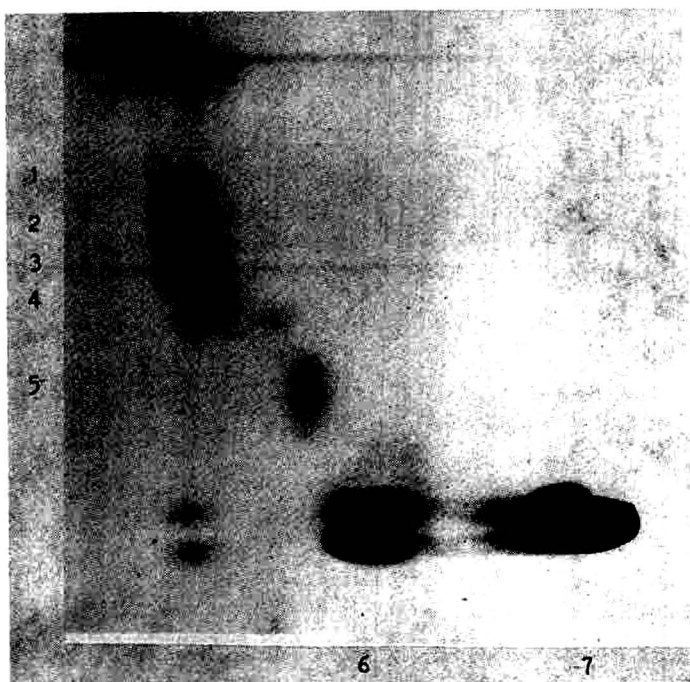


Fig. 3. Chromatographie en couche mince bidimensionnelle sur Silica Gel F₂₅₄ Merck des glycérides, stérides et acides gras libres de noyaux d'hématies de poulet. Première dimension: *n*-hexane-benzène (5:95) sur 8 cm, Deuxième dimension: tétrachlorure de carbone sur 9 cm, Révélation: acide phosphomolybdique à 2% dans l'éthanol 1, 2, 3, 4 = stérides, 5 = esters méthyliques d'acides gras, 6 = triglycérides, 7 = cholestérol libre et acides gras libres.

TABLEAU I

COMPOSITION EN ACIDES GRAS (moles pour 100) DES QUATRE GROUPES DE STÉRIDES ISOLÉS DES NOYAUX DE GLOBULES ROUGES DE POULET

	CE ₁	CE ₂	CE ₃	CE ₄
14:0	8	1	1.2	1.5
15:0	2	0	0	0
16:0	57.0	12.5	12.8	16
16:1	2	14	1	2.5
16:2	0	4	3	3.9
18:0	18	6.5	8	9
18:1	7	46	11	12.1
18:2	2.0	8	53	9
18:3	0	0	1	0
20:0	3	5	3	0
20:3	0	1	2	4
20:4	0	2	3	15
22:5 } et 22:6 }	1	0	1	27
Saturés	88	25	25	26.5
Insaturés	12	75	75	73.5

TABLEAU II

COMPOSITION EN ACIDES GRAS (moles pour 100) DES DIVERS GROUPES DE STÉRIDES PLASMATIQUES DE POULET

	CE ₁	CE ₂	CE ₃	CE ₄	CE ₅
14:0	5	1	0	0	0
16:0	71	8	8	6	6
16:1	1	12	3	2	1
18:0	18	2	0	2	0
18:1	1	76	6	8	4
18:2	0	1	82	2	4
18:3	0	0	1	1	1
20:0	4	0	0	0	0
20:3	0	0	0	4	6
20:4	0	0	0	75	12
22:5	0	0	0	0	66
22:6	0	0	0	0	
<i>Saturés</i>	98	11	8	8	6
<i>Insaturés</i>	2	89	92	92	94

deuxième avec le tétrachlorure de carbone sur 16 cm, on sépare (Fig. 2) les diverses fractions de l'extrait chloroformique: acides gras libres (AGL), cholestérol libre (CL), triglycérides (TG) des esters d'acides gras (E) et quatre fractions de stérides (CE).

Ces deux mêmes systèmes appliqués en chromatographie bidimensionnelle (Fig. 3) réalisent une meilleure séparation des diverses fractions et en particulier des stérides.

Les quatre stérides des noyaux de globules rouges: CE_{1,2,3,4} isolés après chromatographie en couche mince ont été saponifiés et leurs acides gras analysés en phase gazeuse. La composition en acides gras des quatre fractions (Tableau I) se révèle assez différente: la première (CE₁) très riche en acides saturés contient surtout des acides palmitique et stéarique (75 pour 100), les trois autres comportent en majorité des acides insaturés (75 pour 100) avec pour CE₂ surtout de l'acide oléique (46 pour 100),

TABLEAU III

COMPOSITION EN ACIDES GRAS (moles pour 100) DES ESTERS MÉTHYLIQUES DES GLOBULES ROUGES DE POULET

Acides	pour 100	Acides	pour 100
14:0	6	16:1	6
16:0	42	18:1	10
18:0	16	18:2	6
20:0	2	20:1	3
24:0	4	20:4	1
		22:5	4
		22:6	
<i>Saturés</i>	70	<i>Insaturés</i>	30

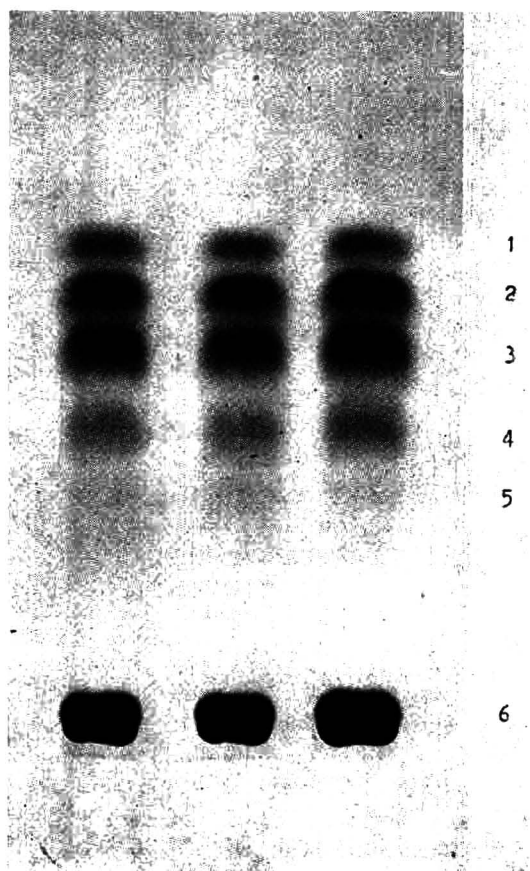


Fig. 4. Chromatographie sur couche mince de Silica Gel G Merck des stérides plasmatiques de poulet. Solvant: tétrachlorure de carbone sur 9 cm (trois migrations). Révélation: pulvérisation du réactif de LIEBERMANN suivie de chauffage 5 min à 110° . 1, 2, 3, 4, 5 = stérides, 6 = cholestérol libre, glycérides et acides gras libres.

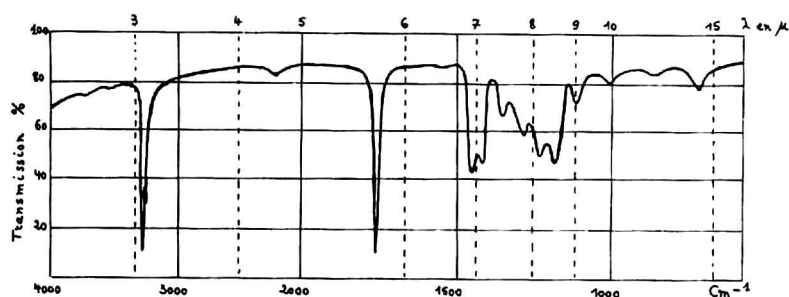


Fig. 5. Spectre infra-rouge des esters d'acides gras isolés de noyaux de globules rouges de poulet. Le spectre a été effectué entre deux lames de chlorure de sodium dans un appareil Perkin-Elmer Modèle 21 entre 4000 et 600 cm^{-1} .

pour CE_3 surtout des acides oléique et linoléique (64 pour 100) et pour CE_4 une forte proportion d'acides gras insaturés en C_{20} et C_{22} .

La composition en acides gras des cinq fractions de stérides plasmatiques (Fig. 4 et Tableau II) montre une plus nette prédominance de l'un d'entre eux: palmitate (71 pour 100) dans la première, oléate (76 pour 100) dans la seconde, linoléate (82 pour 100) dans la troisième, la plus abondante et arachidonate (75 pour 100) dans la quatrième.

Le Tableau III rapporte les proportions d'acides présents dans la tache E, dont l'analyse spectrographique infra-rouge (Fig. 5) montre des bandes d'absorption caractéristiques des groupements ester (1720 cm^{-1}) et carboxyméthylé (triplet de bandes situé entre 1170 et 1260 cm^{-1}). Ces esters qui contiennent 70% d'acides saturés, où prédomine le palmitate (Tableau III), peuvent donc être identifiés à des esters méthyliques.

DISCUSSION

La chromatographie en couche mince mono ou bidimensionnelle des stérides d'hématies de poulet, de leurs noyaux ou du plasma dans divers systèmes de solvants nous a permis de séparer plusieurs groupes d'esters de cholestérol; les plus importants d'entre eux ont été étudiés en chromatographie en phase gazeuse.

Ces résultats sont à rapprocher du fractionnement des esters de cholestérol plasmatique réalisé par PASCAUD^{1,4} sur colonne et sur couche mince d'acide silicique imprégné de nitrate d'argent. Quatre groupes sont ainsi signalés dans le plasma de rat, mais leur composition en acides gras diffère des proportions observées dans les hématies nucléées. En particulier, les stérides d'hématies renferment plus d'acides gras saturés que ceux du plasma.

Par ailleurs, nos résultats se rapprochent de ceux de ALLING *et al.*⁶ pour l'analyse des stérides plasmatiques humains, mais la composition en acides gras des stérides de noyaux globulaires diffère assez nettement de celle-ci ainsi que les proportions relatives des diverses fractions.

On remarquera que plusieurs acides gras différents se retrouvent dans une même fraction, ceci doit être attribué à l'imprécision des méthodes de séparation par chromatographie en couche mince.

Les esters méthyliques présents dans les hématies nucléées sont comparables aux composés signalés dans les extraits lipidiques de tissus animaux^{13,14} ou végétaux¹⁵. Une étude de NIEMINEN¹² démontre leur présence dans le nombreux tissus chez l'homme: cerveau, poumon, rate, coeur, intestin, foie et LEIKOLA *et al.*¹³ attirent l'attention sur leur abondance dans le pancréas.

Pour certains, il s'agirait seulement d'artéfacts formés soit dans le tissu à partir du méthanol libre, la réaction pouvant être catalysée par les bicarbonates^{16,17}, soit au cours de l'extraction par des solvants alcooliques et pendant la concentration de ces extraits¹⁸.

Il est probable que la concentration des extraits à température trop élevée favorise leur formation en provoquant une alcoololyse des triglycérides.

D'autres auteurs au contraire, suggèrent qu'en dehors d'une petite quantité d'artéfacts, ces esters d'acides gras représentent aussi dans les tissus des composés biologiques naturels dont il reste à préciser le mécanisme de biosynthèse.

FISCHER *et al.*¹⁹ démontrent leur existence naturelle dans le foie à côté de méthanol libre, tandis que AXELROD ET DALY²⁰ signalent la présence d'un enzyme hypophysaire hydrolysant la S-adénosylméthionine.

CONCLUSIONS

La chromatographie en couche mince permet de distinguer quatre fractions principales de stérides et des esters méthyliques dans les noyaux d'hématies nucléées de poulet.

Leur composition en acides gras est étudiée par chromatographie en phase gazeuse qui révèle dans les stérides, une fraction contenant 88 pour 100 d'acides gras saturés (essentiellement acide palmitique et acide stéarique) et trois autres fractions renfermant chacune 75 pour 100 d'acides gras insaturés.

Les esters méthyliques naturels sont particulièrement riches en acide palmitique.

BIBLIOGRAPHIE

- 1 M. PASCAUD, *Advan. Tracer Methodol.*, 3 (1966) 181.
 - 2 J. TICHY, *Neurology*, 16 (1966) 1219.
 - 3 L. J. MORRIS, *J. Lipid Res.*, 4 (1963) 357.
 - 4 M. PASCAUD, *Bull. Soc. Chim. Biol.*, 48 (1966) 192.
 - 5 C. ALLING, J. DENCKER, L. SVENNERHOLM ET J. TICHY, *Lancet*, II (1967) 312.
 - 6 C. ALLING, L. SVENNERHOLM, ET J. TICHY, *J. Chromatog.*, 34 (1968) 413.
 - 7 C. MICHALEC, *Naturwissenschaften*, 42 (1955) 509.
 - 8 N. ZOLLNER, G. WOLFRAM ET C. AMIN, *Klin. Wochschr.*, 40 (1962) 273.
 - 9 M. KATES ET A. T. JAMES, *Biochim. Biophys. Acta*, 50 (1961) 478.
 - 10 G. SOULA, Résultats non publiés.
 - 11 H. G. ROSE ET M. OKLANDER, *J. Lipid Res.*, 6 (1965) 428.
 - 12 E. NIEMINEN, *Ann. Acad. Sci. Fennicae*, 118 (1965) 1.
 - 13 E. LEIKOLA, E. NIEMINEN ET E. SALOMAA, *J. Lipid Res.*, 6 (1965) 490.
 - 14 H. P. KAUFMANN ET C. V. VISWANATHAN, *Fette, Seifen, Anstrichmittel*, 65 (1963) 925.
 - 15 A. FATHIPOUR, K. K. SCHLENDER ET H. M. SELL, *Biochim. Biophys. Acta*, 144 (1967) 476.
 - 16 A. K. LOUGH, L. FELINSKI ET G. A. GARTON, *J. Lipid Res.*, 3 (1962) 478.
 - 17 V. P. SKIPSKI, A. F. SMOLOWE, R. C. SULLIVAN ET M. BARCLAY, *Biochim. Biophys. Acta*, 106 (1965) 386.
 - 18 J. FUKUDA, E. MIZUKAMI ET K. IMAICHI, *J. Biochem.*, 61 (1967) 657.
 - 19 G. A. FISCHER, J. J. SAUK ET J. J. KABARA, *Microchem. J.*, 11 (1966) 461.
 - 20 J. AXELROD ET J. DALY, *Science*, 150 (1965) 892.
- J. Chromatog.*, 53 (1970) 217-224

CHROM. 5009

CHROMATOGRAPHY OF ADRENOCORTICAL STEROIDS ON SILICIC ACID COLUMNS

NANCY S. LAMONTAGNE AND DAVID F. JOHNSON

National Institute of Arthritis and Metabolic Diseases, National Institutes of Health, Public Health Service, U.S. Department of Health, Education, and Welfare, Bethesda, Md. 20014 (U.S.A.)

(Received August 24th, 1970)

SUMMARY

The effect of variable parameters, such as water content and activation, on the separation of adrenocortical steroids on silicic acid columns was studied. Screening of nine commercial silicic acid samples, using a standard technique of partition chromatography, showed wide variations in chromatographic behavior. Data is presented on the effects of varying stationary phase (water) and activation on separation and recovery of eight adrenocortical steroids. A standardized technique for preparation of an efficient and reproducible partition column for the separation of steroid mixtures on one of the commercially available silicic acids is described.

INTRODUCTION

A method developed in this laboratory^{1,2} for the separation of adrenocortical steroids by partition chromatography on a silicic acid column utilized Merck silicic acid as the column support. Due to an apparent change in commercial preparation of the silicic acid, the method suffered from poor and inconsistent flow rate, separation, and yield, despite changes in activation and water added as stationary phase. Consequently, nine commercially available silicic acids were screened to find a suitable replacement for the Merck silicic acid. In this initial survey activation and water content were the same as described in the original method². Following the screening process, the effects of changes in the stationary phase (water) and activation (time and temperature) of the silicic acid on peak resolution and recovery of steroids were investigated.

EXPERIMENTAL

Survey of commercial silicic acids

Table I lists the product information, numerical designation, and percent water content of the nine silicic acids obtained commercially. The percent water content was determined by heating 5 + g amounts in an oven for 3 h at 105°, and measuring the weight loss. The values in the fourth column of the table represent the average of

TABLE I

PRODUCT INFORMATION, NUMERICAL DESIGNATION AND WATER CONTENT OF SILICIC ACIDS

<i>Product</i>	<i>Numerical designation</i>	<i>Mesh size</i>	<i>Water (%)</i>
Sigma-SIL-R	1	100	10.14
Bio-Rad-72315	2	200-325	4.78
Bio-Rad-723101	3	100-200	10.30
Nutritional Biochemicals-9606	4	none given	3.00
Mallinckrodt-2847	5	100	5.96
Fisher-A-288	6	none given	2.95
Fisher-A-945	7	325	5.16
Matheson, Coleman and Bell CB-699	8	none given	3.20
Baker-Q324	9	none given	2.36

three such determinations. It can be seen that there is a wide variation in the water content of the silicic acids as originally obtained.

Each silicic acid sample used for preparation of a column was heated in an oven at 105° for five h with frequent stirring to insure uniform activation. The activated silicic acid was immediately transferred to a screw-capped brown bottle, which was taped air tight and stored in a desiccator. For the initial screening procedure, a 40% water impregnated column was used. The column was prepared by adding 20 ml of distilled water in two 10 ml portions to 50 g of the activated silicic acid, while quickly grinding the mixture in a glass mortar. A mobile slurry with water saturated petroleum ether (PE) was prepared and poured into the column in small portions while tamping with moderate pressure to liberate trapped air bubbles. The slurry and column were kept constantly covered with PE to prevent alteration of the 1 to 2.5 ratio by weight of water to silicic acid. The packed column was then washed successively with 200 ml portions of water-saturated dichloromethane (DCM) and PE to insure the removal of impurities with UV absorption at 240 m μ . Ethanol (95%) aliquots containing

TABLE II

SURVEY OF SILICIC ACIDS USING 40% WATER-IMPREGNATED COLUMNS

<i>Silicic acid</i>	<i>Flow rate (min/fraction)</i>	<i>Steroids eluted</i>	<i>Yield</i>	<i>Quality of separation</i>
1	2.5-15.0 erratic	P,Q	P, 50%; Q, 50%	good
2	3.0-7.5	P,Q,A	P and Q, 100%; A, 50%	good
3	3.0-7.0	P,Q,A	P and Q, 100%; A, 50%	poor
4	9.0-12.0	P,Q,A,S,B,E	90% (P,Q,A,S,B,E)	poor
5	5.0-23.0 erratic	P,Q	P and Q, 100%	poor
6	9.0-11.0	P,Q,A	P and Q, 100%	poor
7	51.0-65.0	Silicic acid formed gel; no column		
8	2.0-11.0 erratic	P,Q	P, 100%; Q, 50%	good
9	8.5-10.0	P,Q	P and Q, 50%	poor

300 μg of each steroid standard* were combined in a round-bottomed flask and concentrated *in vacuo* at 40°. The sample mixture was then transferred to a $\frac{1}{2}$ in. diameter filter paper disc with ethanol (95%). The air-dried disc was placed on the column and covered with a $\frac{1}{4}$ in. layer of sea sand. The column was connected to the gradient elution analyzer³ for separation. From previous work² definite percent mixtures had been determined, which were capable of eluting individual steroids in the range between zero and one hundred percent DCM. Each fraction was evaporated *in vacuo*, and the residues dissolved in 5.0 ml of ethanol (95%). The absorbance was read at 240 $\text{m}\mu$ and plotted against tube number for each column. Quantitative amounts were calculated by referring to a linear plot of reference standards, and the peak fractions were pooled separately for identification by thin-layer chromatography⁴.

Table II summarizes the results of the survey using 40% water impregnated columns.

The flow rates of the columns varied considerably (from 2.0–65.0 min), and in some cases were erratic (columns 1, 5, and 8) due to expansion of the silicic acid during chromatography. With all the columns (except 4) only the first two or three steroids in the series (P, Q, and A) were eluted with yields of 50–100%. In fact, the combination of poor separation and low yield (qualitative and quantitative) eliminated silicic acids 3, 5, 6, and 9 from further consideration. Silicic acid 7 was excluded because of its slow flow rate. Of the silicic acids that gave good separations (1, 2, and 8), 2 was selected for further study because it alone of the three eluted 100% of P and Q, and 50% of A. Silicic acid 4 was also selected because it alone eluted six of the eight steroids.

Variation of stationary phase (water)

The weight ratio of stationary phase (water) to support (silicic acid), expressed as the percent water content of the column, was varied in several columns using silicic acid No. 4 in an attempt to improve the quality of the separation and/or the yield. In this series of experiments the fractions were evaporated and read immediately after collection to determine the elution pattern of the steroids, and to enable the subsequent adjustment of the gradient program. Generally, the percent DCM in PE was increased in 5 or 10 percent increments until a steroid peak appeared as an absorbance reading at 240 $\text{m}\mu$. The percent DCM in PE was then dropped by 10% to hold back the next steroid in the series, until the absorbance reading decreased to background. The percent DCM in PE was then increased again to elute the next steroid, or until 100% DCM was attained. With silicic acid No. 4, as with all the others tested, the eight steroids elute in the following sequence: P, Q, A, S, B, E, Aldo and F.

Table III summarizes the results of varying the stationary phase on columns using silicic acid No. 4.

As can be seen by comparing "Water content" and "Steroids eluted", increasing the water content of the column from 40 to 60% did not cause a consistent increase in the number of steroids eluted. Although the increase in water content did allow the elution of B, the fifth steroid in the series, the separation pattern deteriorated so

* Stock solutions of 100 μg per ml of absolute ethanol were prepared from the following steroids: Δ^4 -pregnene-3,20-dione (P), Δ^4 -pregnen-21-ol-3,20-dione (Q), Δ^4 -pregnen-21-ol-3,11,20-trione (A), Δ^4 -pregnene-17 α ,21-diol-3,20-dione (S), Δ^4 -pregnene-11 β ,21-diol-3,20-dione (B), Δ^4 -pregnene-17 α ,21-diol-3,11,20-trione (E), and Δ^4 -pregnene-11 β ,17 α ,21-triol-3,20-dione (F). Pre-weighed 100 μg ampoules from Calbiochem used for Δ^4 -pregnen-18-al-11 β ,21-diol-3,20-dione (Aldo.) solution.

TABLE III

RESULTS OF VARYING STATIONARY PHASE

<i>Water content (%)</i>	<i>Flow rate (min/fraction)</i>	<i>Steroids eluted</i>	<i>Yield^a</i>	<i>Quality of separation</i>
40	6.0 to 9.0	P,Q,A,S,B	93 %	poor
40	22.0	P,Q,A	82 %	good
50	1.5-30.0 erratic	P,Q,A,S,B	86 %	poor
50	2.5-20.0 erratic	P,Q,A,S	90 %	good
50	15.0-20.0	P,Q,A,S	95 %	good
55	9.0-11.0	not determined	not determined	very poor
60	3.0-11.0	P,Q	99 %	very poor
60	9.0-26.0 erratic	not determined	not determined	very poor
47 + 3	5.0-25.0 erratic	P,Q,A,S,B	100 %	very poor

^a The % yield expressed is based on the total μg 's of the steroids eluted.

badly that individual peak identification was impossible. With the 55% and 60% columns the steroids actually eluted in a badly overlapped zone, despite the use of hold back percents. The flow rates varied from 1.5-30.0 min, and were sometimes erratic, because silicic acid No. 4 was difficult to pack consistently. Packing the No. 4 slurry tightly resulted in some improvement in the separating ability of the column, but its flow rate was a slow 15+ min per fraction. The last column in this series was an attempt to improve the separation, and/or yield by using unactivated silicic acid. A 50% water slurry was prepared by adding 23.5 ml of water to the 50 g of silicic acid and 1.5 ml of water already present in the silicic acid (see Table I). The smeared elution pattern obtained indicated that activation of the silicic acid was necessary to improve its separating ability.

Because a 40% water column of silicic acid No. 2 eluted 100% of P and Q, and 50% of A with excellent separation, the percent water was increased by 10% increments in a series of experiments using silicic acid No. 2 to see if the number of steroids eluted would also increase. As with the silicic acid No. 4 study, a variable gradient elution program was used; that is, the % DCM in PE was increased in 5 or 10% increments, and the percent solvent mixture was held constant whenever a steroid was being eluted. The silicic acid No. 2 for these columns was heated for 5 h at 120°. The number of steroids eluted proved to be directly related to the water content used as stationary phase. A 50% water column eluted 90-100% of P, Q, A, S, and B; whereas, a 60% water column eluted 90-100% of P, Q, A, S, B, and E. Both columns gave efficient separation of the peaks. A 70% water column, although yielding 100% of all eight steroids, lacked the resolution of the columns with lower percent water. The 70% silicic acid had apparently reached its physical limit of adsorbed water phase, as evidenced by the marked change in the slurry prepared, and the extremely fast running rate of the column. Consequently, a 65% water column was tried, and did elute 100% of all eight steroids with excellent separation, except for the last two steroids in the series (Aldo and F) which eluted together at 100% DCM. Unfortunately,

the results of this 65% water column could not be reproduced, because the activation parameters (time and temperature) of the silicic acid preparation had been inadvertently altered from 120° for 5 h during the study. This difficulty, coupled with the unactivated silicic acid No. 4 experiment (Table III), suggested that the method of silicic acid activation might be of importance.

A study of the activation parameters was then undertaken with silicic acid No. 2. In these experiments, the percent water content was kept at 65%, the variable gradient elution program was used, and the columns were packed as consistently as possible. Table IV summarizes the results of these experiments.

TABLE IV

RESULTS OF VARYING ACTIVATION PARAMETERS

<i>Activation</i>	<i>Steroids eluted</i>	<i>Quality of separation</i>
5½ h, 130°	P,Q,A,S,B,E	poor
5 h, 124°	?	very poor
7 h, 114°	all	poor
5 h, 114°	?	very poor
5 h, 110°	?	very poor
3 h, 110°	^a A,S,B	good
3½ h, 102°	^a A,S,B	good

^a Only A, S, and B were applied to these columns, since their separation is always the most difficult.

The activation time was varied from 7 h to 3 h, and the temperature from 130° to 102°. The selection of the parameter combinations was random because no relationship between them and the separating quality of the columns was known. The shorter heating time of 3–3½ h did produce the best resolution of peaks, indicating that the longer heating periods, used to insure removal of all the water, undoubtedly alters the structure of the support itself. Despite the varied activation conditions, all the columns had consistent flow rates between 5.0 and 8.0 min per fraction. The yield of the columns, with the exception of the 3 and 3½ h columns, was not determined because the separations were so poor. For the two exceptions, the yield of A, S and B was 100%. In those columns where the separation was very poor, thin-layer identification of the fractions was impractical; hence, the question marks in the "Steroids eluted" column. Of the two procedures that yielded good resolution and recovery, the activation for 3½ h at 102° was selected because A, S, and B were eluted at different percents of DCM; whereas, with activation for 3 h at 110°, A and S were eluted at the same percent DCM. When the separation of all eight steroids was tried with this 102°, 3½ h activation, the result was a poor separation pattern similar to the one obtained with the 70% water column (activation assumed to be 120° for 5 h). Apparently the decrease in time (from 5 to 3 h) and temperature (from 120° to 102°) of activation had a decreased drying effect on the silicic acid and thereby increased its inherent water content. Therefore, when the 32.5 ml of water was added to the 50 g of silicic acid, it produced a slurry of greater than the 65% water content expected.

It was then decided to decrease the water content by 1% increments to de-

termine the precise water content that would give the best resolution of peaks. The water added was measured by a burette to insure accuracy. As the percent water added decreased from 64 to 59 the separation gradually improved. A 58% column did give excellent separation of the first six steroids in the series, but did not elute the last two. In fact, its elution pattern was exactly the same as the 60% water column (activation assumed to be 120° for 5 h) in the initial percent water study of silicic acid No. 2. Since that study proved a direct relationship between water content and number of eluted steroids, but an indirect relationship between water content and quality of separation (as the support's water capacity is reached), it was decided that a slight increase in the percent water added (from 58 to 60) to increase the number of eluted steroids, coupled with a slight increase in activation temperature (from 102° to 110°) to avoid overloading the support, might achieve the correct balance. The good separation of A, S, and B achieved with the 65% column (activation 110° for 3 h, Table IV) indicated that this combination might work. Consequently, a column was prepared with silicic acid No. 2, which was activated for 3 h at 110°, and made 60% water by the burette addition of 30.0 ml of water. A variable gradient elution program

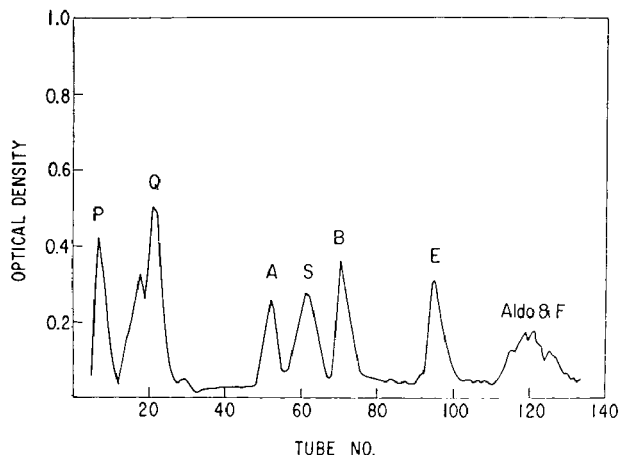


Fig. 1. Separation of eight adrenal steroids on a 60% water-impregnated column of silicic acid No. 2.

was used, and a consistent flow rate of 7.0–8.0 min per fraction was obtained. The eight steroids were eluted with excellent separation, except for Aldo and F which elute together at 100% DCM (Fig. 1). The results of this column were reproducible when the parameters of activation, and the ratio of stationary phase (water) to support (silicic acid) were kept constant.

DISCUSSION

Based on the type of elution peaks obtained from separation of adrenocortical steroids on water-impregnated silicic acid, the method is generally recognized as partition rather than adsorption chromatography^{5,6}. In a similar study, LINFORD⁷ concluded that the properties of silicic acid as an adsorbent can be modified by changing

its free water content. He reported that up to 17% of free water, adsorption at the solid surface predominates; whereas, at 32% of free water, partition effects appear with the steroids used. Our studies further indicate that the performance of a silicic acid column is very dependent, not only on the water content of the support, but also its commercial source and method of activation. Both the recovery of the steroids, and the resolution of the peaks can be adjusted by a slight change in one of these variables. It was found that commercial preparations of silicic acid vary considerably in their chromatographic behavior (ease of packing, flow rate, yield, and separating ability), and that the selection of the best silicic acid must be done by trial and error since the catalogue information does not give sufficient data.

Our results also indicate that the method of activation plays an important role in the performance of silicic acid columns. The temperature and time used for activation influence the choice of water content to be used to achieve the best separation and recovery of steroids. It was found that the time of heating should be limited to under 4 h since longer times seem to cause alterations in the structure of the silicic acid. The temperature of activation must then be balanced with the water added to the silicic acid to give the best resulting percent water. For the adrenocortical steroids in these studies, a 60% water column prepared with Bio-Rad 200-325 mesh silicic acid, heated for 3 h at 110° proved to be the best combination. There is no doubt that the choice of these parameters will vary with the type of compound mixtures to be chromatographed.

A direct relationship appears to exist between the percent water of the silicic acid column, the number of steroids eluted, and the quantitative recovery from the column; but an indirect relationship between percent water and resolution of peaks. In practice it was found advisable to run a preliminary separation using an arbitrary water content (40% in these studies), and then to increase the percent water of the column, which results in a corresponding increase in the yield, until the separation pattern begins to smear. The selection of a percent water slightly less than that point will give the best combination of yield and peak resolution.

Although the effect of temperature changes in column performance was not studied, it is known that varying the operating temperature of silicic acid and silica gel columns can also be a parameter affecting the efficiency and resolution of the column^{8,9}. To insure a constant temperature of 19.5° during these studies, a water jacketed column system was used.

Preliminary investigations with the above combination of parameters selected for chromatography of adrenocortical steroids indicate that the ketosteroids may also be separated on the same column. Studies are in progress in the hope of developing a method for separation of adrenocortical steroid and ketosteroid mixtures on a single column. A similar approach to the chromatography of 17-OH-corticosteroids and 17-ketosteroids has been done by SEKI^{10,11}, who used a support of Sephadex LH-20 to separate the 17-OH-corticosteroids from the 17-ketosteroids. The latter were separated into two groups of C₁₉O₂-17-ketosteroids and C₁₉O₃-17-ketosteroids.

REFERENCES

- 1 E. HEFTMANN AND D. JOHNSON, *Anal. Chem.*, 26 (1954) 519.
- 2 D. FRANCOIS, D. JOHNSON AND E. HEFTMANN, *Anal. Chem.*, 35 (1963) 2019.
- 3 Paper in preparation.

- 4 R. D. BENNETT AND E. HEFTMANN, *J. Chromatog.*, 9 (1962) 348.
- 5 I. BUSH, *Brit. Med. Bull.*, 10 (1954) 229.
- 6 S. LIEBERMAN AND K. DOBRINER, *Ann. Rev. Biochem.*, 20 (1951) 227.
- 7 J. LINFORD, *Can. J. Biochem. Phys.*, 34 (1956) 1153.
- 8 L. SCOTT, *J. Chromatog. Sci.*, 7 (1969) 65.
- 9 R. MAGGS, *J. Chromatog. Sci.*, 7 (1969) 145.
- 10 T. SEKI, *J. Chromatog.*, 29 (1967) 246.
- 11 T. SEKI AND T. SUGASE, *J. Chromatog.*, 42 (1969) 503.

J. Chromatog., 53 (1970) 225-232

CHROM. 4945

GRADIENT ELUTION ADSORPTION CHROMATOGRAPHY OF AROMATIC HYDROCARBONS

M. POPL, J. MOSTECKÝ AND Z. HAVEL

Institute of Chemical Technology, Department of Synthetic Fuel and Petroleum, Technická 1905, Prague 6 (Czechoslovakia)

(Received July 21st, 1970)

SUMMARY

Elution adsorption chromatography of higher aromatic substances on alumina was improved by using a programmed gradient of pentane-ether which shortened the time of analysis and increased the sharpness of the separation.

The suitability of the method was demonstrated in a qualitative and quantitative analysis of creosote oils. A sensitive photometric detection method permitted work with sample amounts smaller than 1 mg.

INTRODUCTION

When separating aromatic substances boiling within a wide distillation range by elution adsorption chromatography on high activity adsorbents, the time necessary for eluting the heaviest compounds, for example the tetraaromatic hydrocarbons, is rather long, and the width of the peaks so large that often they disappear in the noise of the base line. When adsorbents with a lower activity are used, the compounds eluted at the beginning are often not completely separated, or are not separated at all and eluted in a single peak.

These difficulties may be overcome by using gradient elution adsorption chromatography (GEAC), for gradually increasing solvent strength significantly shortens the time necessary for eluting the heaviest compounds, and furthermore, the width of the peaks of these compounds is not much different from those eluted at the beginning. This method was theoretically developed by SNYDER¹, with a special view to the linear gradient elution chromatography.

Mixtures of aromatic substances boiling within a wide distillation range are very often present in commercial products (creosote oil, wash oils, anthracene oil), and it is often important to know their composition, especially in the case of the creosote oil and the other oils for wood protection. Some of these aromatic hydrocarbons even have different fungicidal effects and, therefore, it is often important to have more detailed knowledge about the compositions of these oils, not only from the point of view of research but even for their commercial applications.

Until now, the physico-chemical constants of these oils have been mostly used

for their evaluation, but recently, gas chromatography and mass spectrometry have been tried for their analyses.

The applicability of gas chromatography is limited by the presence of high-boiling aromatic hydrocarbons (chrysene and higher). The determination of the latter is difficult and demands a special adjustment² and, furthermore, the sample is exposed to high temperatures for a considerable time which has a deleterious effect upon thermally unstable or easily polymerising substances.

Mass spectrometry can be used for the analysis of mixtures containing tetra-aromatic hydrocarbons such as chrysene, benzanthracene and others, but not more than seven hydrocarbon groups may be determined simultaneously which means that a mixture containing substances from the alkylbenzenes up to the pyrenes and chrysenes has to be preliminarily separated by means of other methods, for example, by distillation, adsorption chromatography etc. The presence of substances containing nitrogen, oxygen, or sulphur considerably complicates the analysis, for example, benzothiophenes have the same nominal value of m/e as alkylbenzenes, and the derivatives of biphenyloxide are identical with the homologues of biphenyl and acenaphthene. It is not possible to differentiate, by the means of mass spectrometry, substances with an identical nominal value of m/e such as fluoranthene-pyrene or chrysene-1,2-benzanthracene-triphenylene-tetracene. It is also necessary, therefore, as in the case of gas chromatography, to use special treatment in mass spectrometry, especially when the sample contains mechanical impurities, deposits and such like.

In this work, GEAC on alumina in combination with UV-spectrometry was found, to be a suitable method for the analysis of higher-boiling aromatic hydrocarbons, and aromatic mixtures with a wide distillation range.

The analysis of creosote oil, which is a mixture of aromatic hydrocarbons from coal tar having boiling points within the range of 200–400° and containing small amounts of nitrogen, oxygen and sulphur compounds, is reported as an example. No preliminary treatment of the sample was given and the aromatic fraction was divided into eight hydrocarbon types which were quantitatively determined.

EXPERIMENTAL

Materials

Alumina Woelm Eschwege Neutral was used as the adsorbent. The surface area of the activated adsorbent was about 100 m²/g. The adsorbent was first activated at 400° for 8 h and then deactivated by addition of 2% water. The standardisation³ was carried out by measuring the equivalent retention volumes of some aromatic hydrocarbons on elution with *n*-pentane. The results of these measurements are shown in Table I.

One meter long glass columns with an inner diameter of 4 mm, possessing a device for introducing the sample were used.

The pump was a programmed gradient pump, Dialagrad Model 190, manufactured by the firm ISCO.

A UV spectrophotometer SP 800 B (Pye-Unicam) with a flow-through quartz cell, 1 mm path length and a volume of 0.13 ml, was used for the detection.

TABLE I

EQUIVALENT RETENTION VOLUMES R^0 OF AROMATIC HYDROCARBONSAdsorbent: alumina-2.0% H_2O . Eluent: *n*-pentane.

Compound	R^0 (ml/g)
Indane	0.51
Naphthalene	1.55
Acenaphthene	2.88
Fluorene	9.80
Phenanthrene	13.40

Procedure

0.5 mg of a mixture of standards (indane, naphthalene, acenaphthene, fluorene, phenanthrene, pyrene, chrysene, and carbazole), dissolved in iso-octane, was introduced into the column containing 16 g of the adsorbent, previously wetted with pure pentane, and then the program of the gradient of pentane-ether, lasting 2 h, was started. The flow rate of the eluents through the column was 45 ml/h. The detection was realised by measuring the extinction, using a constant wavelength of 260 nm. The chromatogram demonstrating the separation of the mixture of standards, and

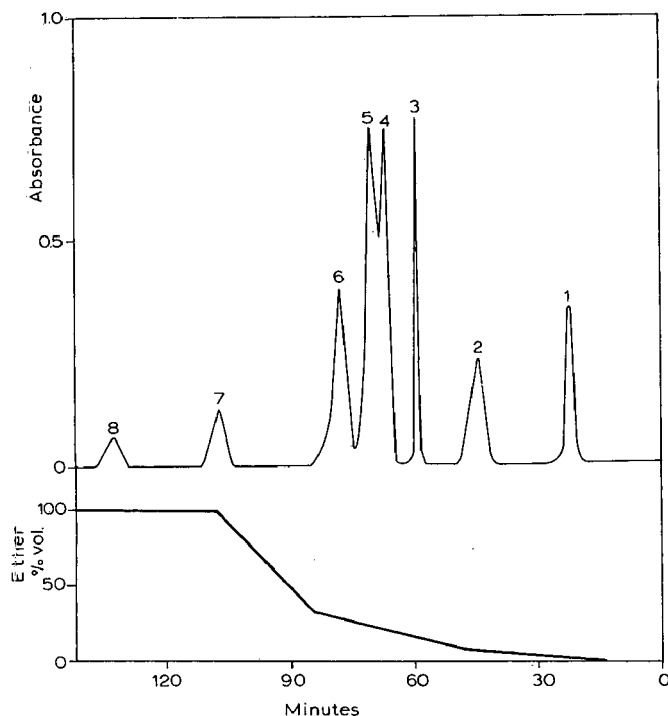


Fig. 1. GEAC separation of the mixture of standards and the course of the gradient. Adsorbent: alumina-2% H_2O . Eluent: Pentane-ether. 1 = Indane; 2 = naphthalene; 3 = acenaphthene; 4 = fluorene; 5 = phenanthrene; 6 = pyrene; 7 = chrysene; 8 = carbazole.

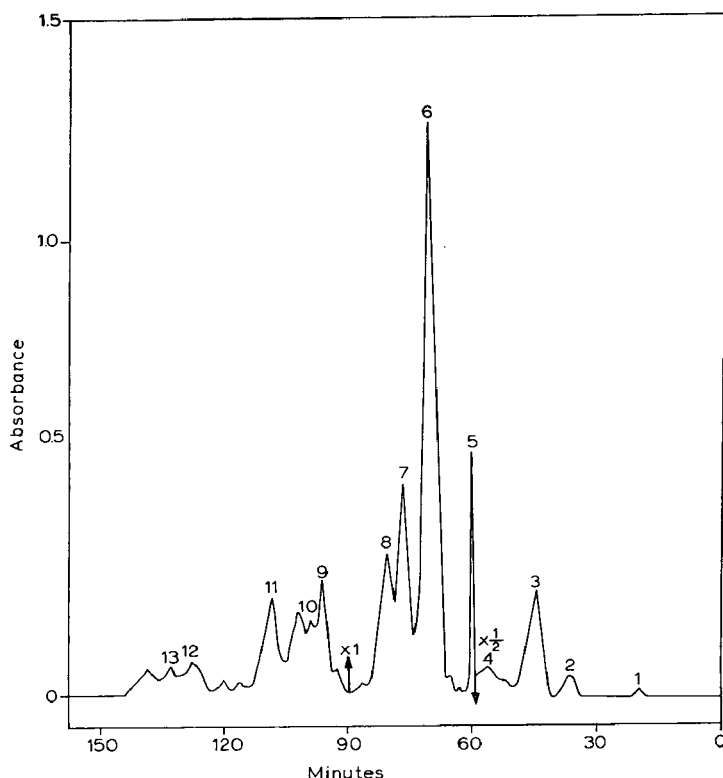


Fig. 2. GEAC separation of creosote oil. Adsorbent: alumina-2% H_2O . Eluent: Pentane-ether. 1 = Alkylbenzenes, indanes, tetralins; 2 = indenenes, dihydronaphthalenes; 3 = naphthalene, benzothiophene; 4 = alkyl-naphthalenes; 5 = acenaphthene, biphenyl; 6 = phenanthrene, anthracene; 7 = pyrene; 8 = fluoranthene; 9 = triphenylene; 10 = 1,2-benzanthracene; 11 = chrysene; 12 = indole; 13 = carbazole.

also the flow of the gradient, are shown on Fig. 1. The analysis of 1 μ l of creosote oil was done under identical conditions, and the chromatogram is shown on Fig. 2.

The qualitative determination of single compounds was carried out by comparing the retention volumes of single peaks of the analysed mixture with those given by the mixture of standards, on one hand, or by adding pure standards directly to the mixture being analysed, on the other hand. In addition, the single eluted compounds were collected, and their UV-spectra were measured and compared with published data.

The quantitative determination of single groups was carried out by measuring the peak areas by means of a planimeter. These groups of substances were then calculated using the following relation:

$$A_j = \frac{P_j \cdot k_j \cdot 100}{\sum_{i=1}^{\infty} P_i \cdot k_i}$$

where A_j represents the percentage weight of compounds of the j -group, P_j is the

TABLE II

GROUPS OF AROMATIC HYDROCARBONS DETERMINED AND THEIR k -FACTORS

Group	Components	k -factor
I	Alkylbenzenes, indanes, tetralins	44.0
II	Indenes, dihydronaphthalenes	6.9
III	Naphthalene, benzothiophene	8.2
IV	Alkyl naphthalenes	12.3
V	Biphenyl, acenaphthene	12.5
VI	Fluorene, phenanthrene, anthracene	1.8
VII	Pyrene, fluoranthene	1.3
VIII	Chrysene, triphenylene, benzanthracene	1.0

peak area of the j -group and k_j is a factor for the said group. The denominator consists of the sum of the products of the peak areas and their k -factors. The partition into groups and k -factors are shown in Table II.

RESULTS AND DISCUSSION

It is necessary, for the successful separation of a mixture of aromatic hydrocarbons, to choose a suitable method of detection. Spectrophotometric detection is suitable for all kinds of aromatic hydrocarbons, especially for polycondensed ones, which are often present in small amounts only. Detection at a constant wavelength 260 nm is very satisfactory, because it permits a reliable determination of these substances even when they are present as only 0.5% of a complicated mixture of aromatic hydrocarbons.

With the regard to the character of a mixture to be separated, another wavelength could be used when measuring the extinction of the eluted compounds. It is not advantageous, however, to work with a wavelength shorter than 230 nm because the gradient itself causes a change of extinction in the eluent.

Interference of saturated hydrocarbons and olefins may be excluded by using a detector measuring the light absorption in the UV-region at a suitable wavelength. The high sensitivity of the detector allows one to work with an extremely small amount of a sample (0.5–1.0 μ l of creosote oil) assuring that the analytical run is in the linear part of the adsorption isotherm. By this means, not only an optimum separation of the mixture, but even good reproducibility, is achieved.

Analysis of creosote oil by the means of elution adsorption chromatography, with a single solvent, *e.g.*, pentane, does not appear to be satisfactory, as the retention volumes of the heaviest compounds are extremely large. As shown in Fig. 2, GEAC not only results in a good separation, but, at the same time, substantially shortens the analysis time. Whilst the analysis of similar mixtures by elution adsorption chromatography took 7–10 h⁴, this time was shortened to about 2.5 h in our case. A very good separation of the basic groups of mono-, di-, tri- and tetraaromatic hydrocarbons was obtained and it was even possible to determine other parts of these groups with good accuracy, for *e.g.* acenaphthene biphenyl; pyrene, fluoranthene; and occasionally some further compounds, such as benzpyrenes, indole, carbazole and others which, in this case, were not taken into consideration and their quantitative evaluation was not provided for.

The reproducibility of the separation achieved, was very good, especially in the region from fluorene onwards. In the part, where naphthalene, alkylnaphthalenes, biphenyl and acenaphthene are eluted, the system is very sensitive to any deviation of the gradient, the purity of the eluent, the room temperature etc. Most of the time this may be obviated by determining the sum of the diaromatic hydrocarbons, *i.e.* groups III, IV and V are determined as a whole. When it is desired to obtain these groups separately, and when accurate conditions cannot be guaranteed, it is better, to carry out a second chromatogram on 2% $\text{H}_2\text{O}-\text{Al}_2\text{O}_3$, eluting the sample with pure pentane and finishing the experiment at the time when acenaphthene and biphenyl are eluted completely. By means of this chromatogram, the distribution of the diaromatic hydrocarbons can easily be determined.

The presence of phenols which are not eluted until after the nitrogen compounds, does not matter, when gradient elution chromatography is used. An advantage of the said method even consists in the possibility of separating the non-basic types of nitrogen substances. In the system Al_2O_3 -pentane the values of the retention volumes for indole and carbazole are approximately the same as those for benzpyrene and dibenzofluorene⁵. With the increase of the solvent strength, the values of retention volumes decrease. This change, however, is not identical as for the nitrogen compounds, as it is for aromatic hydrocarbons. The change of the retention volume caused by a change of the solvent strength, is smaller for the substances containing nitrogen than for the aromatic hydrocarbons⁶ and these nitrogen substances are therefore eluted later than the aromatic hydrocarbons.

Coal tar products are characterised by a small percentage of polyalkylated aromatic hydrocarbons. The greater part of these consist of the parent aromatic hydrocarbons and their monomethyl isomers. This fact facilitates the quantitative evaluation, when no similar mixture with a known composition is available. It is possible, in such case, to prepare a calibration mixture of the basic hydrocarbons and, by evaluating its chromatogram, to determine the appropriate *k*-factors needed. Such measurements just give semi-quantitative results, because, for a more accurate analysis, further data should be known, such as, for example, the relative participation of anthracene and phenanthrene and other information about the composition of the mixture analysed. In our case, we tested several samples of creosote oil, the compositions of which were determined by the means of mass spectrometry. These samples were analysed by the GEAC method and the chromatograms obtained were evaluated. From these samples the *k*-factors, shown in Table II, were calculated. The applicability of the *k*-factors to the quantitative evaluation of the mixture being analysed, is conditioned by the fact that identical conditions of the analysis must be maintained, *e.g.* a constant flow rate of the eluent, a constant wavelength and path length of the cell. It is important, too, to maintain an identical system of gradient concentrations, because it is necessary to achieve a separation for which the *k*-factors have been calculated. It also has to be pointed out that the applicability of the *k*-factors introduced is limited to those coal tar products having an approximately uniform distillation range. When analysis of aromatic hydrocarbons with a considerably different composition is carried out, it is necessary to check up the respective *k*-factors experimentally.

The analyses of two creosote oil samples divided into eight groups (see Table II) are reported in Table III. The results of the mass spectrometry analysis are also shown in the same table for comparison. If a creosote oil sample contains more sulphur, *i.e.*

TABLE III

COMPARISON OF MASS-SPECTROMETRIC (MS) AND GEAC ANALYSES (% WT.) OF CREOSOTE OILS

Group	Sample 1 ^a		Sample 2 ^b	
	MS	GEAC	MS	GEAC
I	9.9	1.3	5.4	3.8
II	2.4	1.1	2.9	2.1
III	26.0	36.5	12.8	14.2
IV	25.9	24.1	17.3	15.3
V	13.3	12.7	14.5	18.1
VI	16.1	12.6	29.6	29.5
VII	5.4	8.1	15.6	12.0
VIII	1.0	3.6	1.9	5.0
Total ^c	100.0	100.0	100.0	100.0

^a Sulphur content 2.1% wt.^b Sulphur content 0.42% wt.^c Aromatic hydrocarbons = 100% wt.

benzothiophene and its homologues are present, then a difference between the analysis by mass spectrometry and by GEAC appears, resulting from the fact that the first method includes benzothiophenes among the alkylbenzenes, while the latter determines it as naphthalene or an alkylnaphthalene. This is illustrated in the case of sample 1 shown in Table III. As is evident from this table, the quantitative analysis of creosote oil by GEAC affords good results, even when the analysed samples have quite different compositions. However, only the relative concentrations of single aromatic hydrocarbon types may be obtained, not the absolute values; furthermore, GEAC gives, in general, higher results for the tetraaromatic hydrocarbons. These higher results are more probable than the lower ones by the mass spectrometry, where some distortion may occur, caused by the preliminary treatment of the sample and by an insufficient evaporation of the heaviest fractions in the evaporator of the mass spectrometer.

REFERENCES

- 1 L. R. SNYDER, *J. Chromatog.*, **13** (1964) 415.
- 2 H. D. SAUERLAND AND M. ZANDER, *Erdöl Kohle*, **19** (1966) 502.
- 3 L. R. SNYDER, *Principles of Adsorption Chromatography*, Marcel Dekker, New York, 1968.
- 4 G. GRIMMER, *Erdöl Kohle*, **19** (1966) 578.
- 5 L. R. SNYDER, *Anal. Chem.*, **36** (1964) 775.
- 6 L. R. SNYDER, *J. Phys. Chem.*, **67** (1963) 2344.

J. Chromatog., **53** (1970) 233-239

CHROM. 4982

DAS GELCHROMATOGRAPHISCHE TRENNVERMÖGEN VON
VINYLACETATGEL FÜR KOHLENWASSERSTOFFE UND MINERALÖLE

H. H. OELERT

*Institut für Chemische Technologie und Brennstofftechnik der Technischen Universität Clausthal,
3392 Clausthal (B.R.D.)*

(Eingegangen am 7. August 1970)

SUMMARY

Gel chromatographic separation characteristics of vinyl acetate gel for hydrocarbons and petroleum

After a discussion on the impact of chemical structure on the separation of small molecules on porous gels, the elution is described of forty hydrocarbons from cyclohexane, methylene chloride and isopropanol on vinyl acetate gel Merckogel OR-500. Different linear relationships of log molecular volume *versus* elution volume are shown to exist for different types of hydrocarbons, depending on the structure of the compounds and the nature of the vehicle. For certain structures the exclusion effect is masked by other effects. Experiments on model compounds indicate that there exists a relationship between the speed of the vehicle and zone broadening. This leads to the conclusion that the speed of the vehicle is dependent on the effects of axial dispersion, mass transfer, eddy diffusion and time dependence of equilibrium. Zone width is shown to increase with sample size. To demonstrate the possibilities of application some crude oils and aromatic parts of vacuum cuts are investigated by means of analysis by liquid chromatography. From the distribution curves recorded petroleum samples may be characterised.

EINLEITUNG

Die als Molekülgrössentrennung für Makromoleküle entwickelte Gel-Permeations-Chromatographie (GPC) wird in neuerer Zeit verstärkt zur Trennung kleinerer Moleküle eingesetzt. Hierfür sind verschiedene Geltypen erhältlich. Während an diesen Gelen für Substanzen einer homologen Reihe in bestimmten Grenzen ein eindeutiger Zusammenhang zwischen dem Molvolumen V_M und dem Elutionsvolumen V_e mit $V_e = a \cdot \log V_M + b$ gegeben ist, bleibt für Substanzreihen unterschiedlicher Struktur der Typ der Beziehung zwar erhalten, jedoch erweist sich die Steigung a oft als klassenspezifisch. Selbst für Klassen geringer Polaritätsunterschiede, wie verschiedene Kohlenwasserstofftypen, sind diese Unterschiede beträchtlich und hängen für ein gegebenes Gel oft auch von der Natur des Elutionsmediums ab. Die Zusammenhänge sind in der neueren Literatur für organophiles Dextrangel¹⁻³, für Polystyrol-

gel⁴⁻⁷ sowie für Glasgele^{8,9} aufgezeigt worden. Jeder Versuch, die GPC für Kohlenwasserstoffgemische und im Mineralölbereich anzuwenden, muss aber diese Unterschiede berücksichtigen, um Fehlinterpretationen zu vermeiden.

Für die seit kurzem verfügbaren Polyvinylacetatgele sind diese Zusammenhänge bisher nicht bekannt. Die vorgelegte Arbeit untersucht das Elutionsverhalten von verschiedenen Kohlenwasserstoffen am Polyvinylacetatgel Merckogel OR-500 aus verschiedenen Elutionsmedien. Die Auswirkungen von Probenmenge und Elutionsgeschwindigkeit auf die Trennleistung werden an einer Modellsubstanz nachgewiesen. Zur Anwendung wird versucht, eine Methode zur schnellen Charakterisierung von Mineralölen auszuarbeiten.

EXPERIMENTELLES

Der Aufbau der für alle Versuche benutzten Apparatur ergibt sich aus dem Weg des Elutionsmediums: Reservoir, Entgaser, Dosierpumpe (Telab Minidos BF 411/200; Telab, Homberg/Ndrh.), Pulsationsdämpfer, Vergleichszelle des Differentialrefraktometers (Modell R-4, Waters, Framingham, Mass.), Probeneingabeventil, Trennsäule, Messzelle des Differentialrefraktometers, Syphon. Der Verlauf der Differenz im Brechungsindex wurde mit einem Kompensationsschreiber registriert. Zugleich wurde das Elutionsvolumen über Kontakte am Syphon mitregistriert.

Mit der Dosierpumpe konnte die Elutionsgeschwindigkeit zwischen 0.08 und 1.2 cc/min eingestellt werden. Die dabei anliegenden Gegendrucke stellten sich zwischen 0 und 4 atm ein.

Entgaser, Dämpfer und Dosierventil sind selbstgefertigt. Das Dosierventil arbeitet als versetzter Vierwegehahn und erlaubt die ein- oder mehrmalige Einspeisung von jeweils 12.5 μ l Probenlösung.

Die Säule ist ein Glasrohr, 60 cm \times 10 mm I.D., mit Gewinde an beiden Enden. Das gemessene Leervolumen beträgt bei einer Effektivlänge von 59.5 cm 46.8 cc. An den Gewindeenden halten Schraubkappen die mit Teflondichtungen eingesetzten Endstücke. Eingelegte 400-mesh Edelstahlsiebe sichern das Gelbett ab. Alle Verbindungen in der Apparatur sind in Edelstahlrohren und Polyäthylenschläuchen mit 1 mm I.D. ausgeführt.

Alle Versuche wurden bei $22 \pm 1^\circ$ für die Gesamtapparatur durchgeführt. Als Elutionsmedien wurden Cyclohexan, Methylenchlorid und Isopropanol verwendet. Das Gel wurde jeweils 24 h im Medium gequollen und in Suspension unter Vibration bei einem Druck von 4 atm in die Säule eingefüllt. Die Säule wurde vor den Messungen mindestens 12 h unter Versuchsbedingungen mit dem jeweiligen Elutionsmedium gespült.

ERGEBNISSE AN KOHLENWASSERSTOFFEN

Modellsubstanzen der Klassen *n*-Paraffine, Polyphenyle, katakondensierte Aromaten, perikondensierte Aromaten sowie einige andere wurden mit jeweils 12.5 μ l in Substanz oder als gesättigte Lösung aufgegeben. Die Elutionsvolumina wurden im Maximum der eluierten Zone gemessen und um die Volumina in der Probeneingabe und im Detektor korrigiert. Die gemessenen Werte gibt Tabelle I. Die mitt-

TABELLE I

ELUTIONSVOLUMINA VON KOHLENWASSERSTOFFEN AN MERCKOGEL ÖR-500 AUS CYCLOHEXAN, METHYLENCHLORID UND ISOPROPANOL

a = Cyclohexan; b = Methylenchlorid; c = Isopropanol.

Substanz	log Mol- volumen	Elutionsvolumen (cc)		
		a	b	c
<i>n</i> -Hexatriacontan	2.79	17.5	7.7	16.8
<i>n</i> -Hexadekan	2.47	19.3	16.2	22.0
<i>n</i> -Dodekan	2.36	19.9	17.6	22.9
<i>n</i> -Heptan	2.17	20.8	21.6	25.0
Squalan	2.72		10.9	19.7
<i>p</i> -Sexiphenyl	2.59		13.1	
<i>m</i> -Quinquephenyl	2.52	19.1	14.8	18.4
<i>p</i> -Quaterphenyl	2.43	19.6	16.8	20.8
<i>p</i> -Terphenyl	2.32	20.5	19.0	22.0
Diphenyl	2.17	20.9	21.4	24.6
Benzol	1.95	22.0	26.3	27.8
Picen	2.37	20.8	20.9	36.3
Chrysen	2.29	21.1	21.8	33.4
Phenanthren	2.21	21.6	22.2	31.6
Naphthalin	2.10	22.8	23.3	29.6
Rubren	2.64	19.0	15.8	
Truxen	2.47		19.1	
Pyren	2.24	19.0	23.6	47.8
Coronen	2.36	29.9	32.8	51.8
Dekacyclen	2.51		45.5	
Cyclohexan	2.03			21.3
Dekalin	2.20	20.7	21.1	22.8
Indan	2.09	21.4		
Tetralin	2.14	21.1	22.9	22.0
Fuoren	2.29		22.7	
Fluoranthren	2.35		22.1	
Dihydrophenanthren	2.26		21.3	25.6
Oktahydrophenanthren	2.26		21.4	26.0
Dihydrotetracen	2.42		21.0	
Diocylbenzol	2.57	18.5	14.5	19.3
Tridecylbenzol	2.48	19.3	15.8	20.0
Diisopropylbenzol	2.28	20.6	19.3	
Äthylbenzol	2.10		22.7	
Dimethylnaphthalin	2.20		22.3	
Trimethylnaphthalin	2.24		21.8	
Methylanthracen	2.25		22.0	
Cholesterylstearat			12.2	
Cholesterylpalmitat			12.6	
Cholesteryllaureat			13.2	
Cholesterin			18.3	

leren Elutionsgeschwindigkeiten betrugen dabei: Cyclohexan 0.2; Methylenchlorid 0.3; Isopropanol 0.1 mm/sec.

Fig. 1 zeigt die Verhältnisse für Paraffine, Polyphenyle und alkylsubstituierte

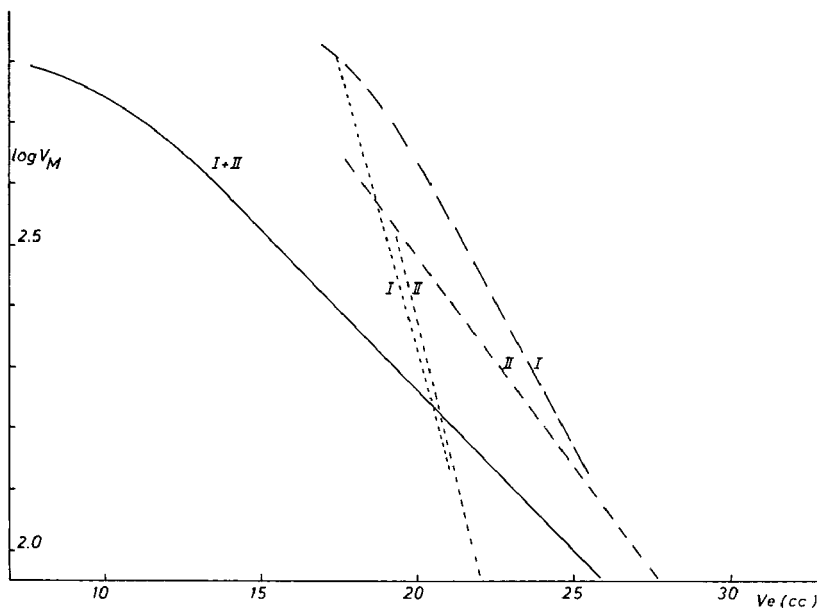


Fig. 1. Logarithmus des Molvolumens (V_M) über dem Elutionsvolumen (V_e) für Paraffine (I) und Polyphenyle (II) aus Cyclohexan (. . .), Methylenchlorid (—) und Isopropanol (---).

Polyphenyle in der Darstellung $\log V_M$ über V_e . Abgesehen von einem geringen Abweichen in der Nähe der Ausschlussgrenze (vom Hersteller des Gels ist hierfür ein Molekulargewicht von 750 angegeben) liegen alle untersuchten Substanzen bei Geraden. Die Lage und Neigung der Geraden sind vom Substanztyp und vom Elutionsmedium abhängig. Alle Geraden haben infolge des eindeutig dominierenden Ausschlusseffektes eine negative Neigung. Für Cyclohexan liegen beide Substanztypen sehr dicht beieinander. Für dieses Elutionsmedium liegt die Raumaufüllung des Gels im gequollenen Zustand aber nur um 0.35 cc/g über dem Schüttvolumen des trockenen Gels. Das erklärt den geringen Winkel gegen die Ordinate und das damit sehr schlechte Auflösungsvermögen. Beim Methylenchlorid fallen die Substanzen beider Typen in einer Geraden zusammen, die die Ordinate unter etwa 45° schneidet. Damit ist aber eine brauchbare Auflösungserwartung gegeben. Für Methylenchlorid liegt die Raumaufüllung des Gels im gequollenen Zustand um 2.1 cc/g über dem Schüttvolumen des trockenen Gels. Für Isopropanol ergibt sich eine deutliche Differenzierung des Elutionsverlaufes bei beiden Typen. Demnach sollte bei gleichem Molvolumen ein Polyphenyl vor dem entsprechenden Paraffin eluieren. Dieser Befund steht im Gegensatz zu allen bisher bei solchen Untersuchungen gemachten Erfahrungen^{2,6,9}. Für Isopropanol liegt die Raumaufüllung des gequollenen Gels um 0.7 cc/g über dem Schüttvolumen im trockenen Zustand. Wertet man die Neigungen der Geraden für Paraffine als Differentialquotienten dV_e/dV_M so sind diese dem Volumenzuwachs bei der Quellung in den verschiedenen Elutionsmedien annähernd proportional. Demnach bewirkt aber ein geringerer Quellungsgrad nicht etwa eine Verschiebung des Arbeitsbereiches, sondern lediglich eine Veränderung des Differentialquotienten im Sinne einer Erniedrigung des Auflösungsvermögens. Wenn die in der Darstellung angegebenen effektiven Arbeitsbereiche für V_e um das Volumen der mobilen Phase korrigiert, d.h.

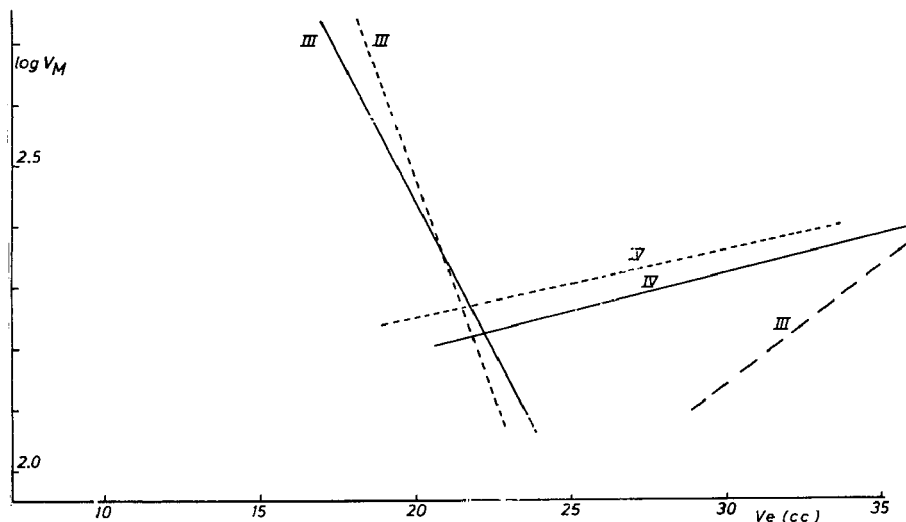


Fig. 2. Logarithmus des Molvolumens (V_M) über dem Elutionsvolumen (V_e) für katakondensierte Aromaten (III) und perikondensierte Aromaten (IV) aus Cyclohexan (. . .), Methylenchlorid (—) und Isopropanol (— — —).

linksverschoben, werden, so schneiden sich die Geraden im Bereich der Ausschlussgrenze. Damit ergibt sich mit Ausnahme der Polyphenyle in Isopropanol insgesamt übereinstimmendes Verhalten und die beobachteten Unterschiede beruhen lediglich auf mechanischen Effekten des Zusammenwirkens von Gel und Quellungsmittel.

In Fig. 2 sind die Verhältnisse für kata- und perikondensierte Aromaten dargestellt. Alle untersuchten Substanzen liegen wiederum dicht bei Geraden. Die Verhältnisse für katakondensierte Substanzen sind in Cyclohexan und Methylenchlorid ähnlich. Im Vergleich zu Fig. 1 sind damit die Unterschiede beim Cyclohexan insgesamt gering. Für Mischungen von Kohlenwasserstoffen verschiedenster Typen darf daher ein annähernd einheitliches Trennverhalten nach der Molekülgrösse erwartet werden. Das geringe Auflösungsvermögen verbietet jedoch eine praktische Anwendung. Beim Methylenchlorid sind die Unterschiede gegenüber Fig. 1 bereits so gross, dass nur auf Grund der Molekülgrösse kein vergleichbares Trennverhalten erwartet werden darf. Dies zeigt sich besonders deutlich am Beispiel des Rubrens, das mit gleichstarken Strukturanteilen eines katakondensierten Moleküllkerns und anhängender Phenylreste etwa in der Mitte zwischen den Linien II und III liegt. Das entspricht Beobachtungen an Polystyrolgel aus Methylenchlorid^{4,5}. Dagegen lassen die Neigungen der Geraden auf eine brauchbare Trennchance innerhalb der einzelnen Substanzreihen schliessen.

Ganz anders ist das Verhalten der perikondensierten Aromaten. Alle bis hier diskutierten Zusammenhänge zeigen mit der negativen Neigung ein eindeutiges Dominieren des Ausschlusseffektes. Nunmehr wechselt die Neigung ins Positive. Dabei sind die Unterschiede so gross, dass sie nicht aus einem falschen Wert für das Molvolumen erklärt werden können. Auch die unterschiedliche Gestalt der Moleküle reicht zu einer Deutung nicht aus. Offenbar kommen Wechselwirkungen zwischen der Geloberfläche und dem π -Elektronensystem der aromatischen Moleküle ins Spiel,

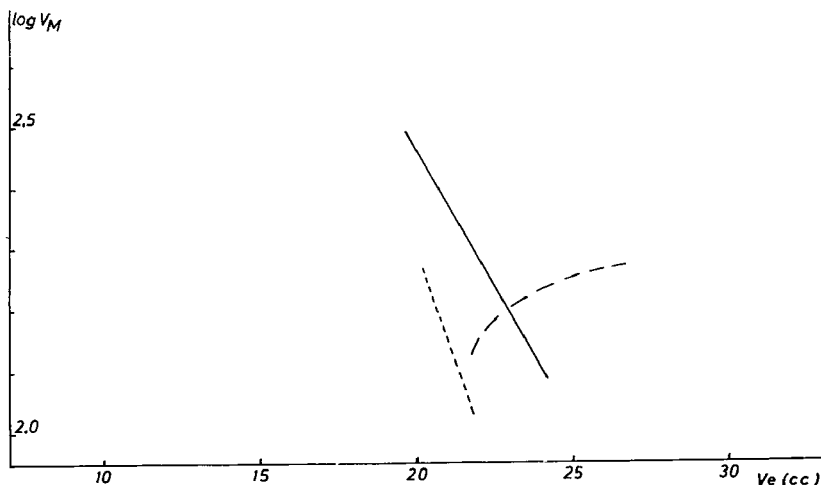


Fig. 3. Logarithmus des Molvolumens (V_M) über dem Elutionsvolumen (V_e) für Naphthene und Naphthenaromaten mit 2 und mehr Ringen aus Cyclohexan (---), Methylenchlorid (—) und Isopropanol (- · - ·).

die sich bei den speziellen Resonanzbedingungen in perikondensierten Aromaten besonders stark im Sinne einer zusätzlichen Retention auswirken. Dass hierbei auch die Wechselwirkung Gel-Elutionsmedium eine Rolle spielen kann, zeigt schon der Verlauf der katakondensierten Aromaten aus Isopropanol. Vermutlich belädt dies stark polare Elutionsmedium die Geloberfläche mit einer Schicht mit erhöhter Wechselwirkungsneigung gegenüber resonanzstabilisierten π -Elektronensystemen. Dieses Verhalten wurde auch an organophilen Dextrangelen beobachtet^{1,3}.

In Fig. 3 sind einige Werte für Naphthene und Naphthenaromaten dargestellt. Die Tendenzen entsprechen im ganzen den in Fig. 2. gezeigten. Vor allem aus Methylenchlorid sind die Unterschiede nicht beträchtlich und es darf ein für katakondensierte Ringsysteme vom Ungesättigtheitsgrad weitgehend unabhängiges Elutionsverhalten erwartet werden. Aus Isopropanol weisen die Ergebnisse insgesamt darauf hin, dass für die praktische Anwendung eine Trennung von Kohlenwasserstoffgemischen erwartet werden darf, bei der die Substanzen in der Reihenfolge: Paraffine, nicht- und alkylsubstituierte Polyphenyle fallender Molekülgröße, und danach alle kondensierten Ringverbindungen in der Reihenfolgen steigender Molekülgröße und zunehmender Ungesättigtheit eluiert werden. Im Molekulargewichtsbereich ab 170 dürfte die Trennung bei nicht zu starker Alkylsubstitution der Ringsysteme eindeutig sein.

DIE AUSWIRKUNG VON OPERATIONSVARIABLEN

Von den für die Versuchsdurchführung in Grenzen frei wählbaren Variablen sind für eine gegebene Trennsäule die Geschwindigkeit und die Probenmenge am wichtigsten. Sie sollen hier am Beispiel des Benzols für das System Merckogel OR-500/ Methylenchlorid in ihrer Auswirkung auf die Trennleistung näher untersucht werden. Hierzu wurden wechselnde Mengen Benzol in einem Probenvolumen von jeweils 12,5 μ l bei verschiedenen Elutionsgeschwindigkeiten untersucht. Aus den registrierten

Elutionsvolumina im Zonenmaximum (V_e) und der Basisbreite der Zone (b) wurde nach $N = (4 V_e/b)^2$ die Zahl der theoretischen Trennstufen formal berechnet und auf die Säulenlänge und die lineare Elutionsgeschwindigkeit bezogen. Einen Teil der Ergebnisse gibt Tabelle II wieder. Für eine gegebene Geschwindigkeit bleiben die Elutionsvolumina mit einer relativen Standardabweichung von etwa $\pm 1\%$ konstant und im untersuchten Bereich unabhängig von der Probenmenge. Mit wachsender Geschwindigkeit nimmt das Elutionsvolumen im Mittel etwas zu und zwar von 0.1 zu 0.8 mm/sec um etwa 7%. Für die Zonenbreite ist keine Konstanz mehr gegeben. Es liegt für jede Geschwindigkeit eine deutliche Zunahme mit der Probenmenge vor. Da die gewählten Probenmengen einander für die drei Geschwindigkeiten entsprechen, dürfen in erster Näherung die Mittelwerte der Zonenbreiten auf die Geschwindigkeiten

TABELLE II

ELUTIONSVOLUMEN, ZONENBREITE UND TRENNSTUFENZAHL FÜR BENZOL AN MERCKOGEL OR-500 AUS METHYLENCHLORID

Abkürzungen: V_e = Elutionsvolumen, in cc; b = Zonenbreite, in cc; N = Trennstufenzahl je min; N' = Trennstufenzahl je sec. Probenvolumen jeweils 12.5 μ l.

Benzol (mg)	$v = 0.10 \text{ mm/sec}$				$v = 0.37 \text{ mm/sec}$				$v = 0.81 \text{ mm/sec}$			
	V_e	b	N	N'	V_e	b	N	N'	V_e	b	N	N'
0.44	24.7	1.8	$5.1 \cdot 10^3$	0.5	26.0	1.5	$8.1 \cdot 10^3$	3.0	26.8	2.2	$4.0 \cdot 10^3$	3.2
0.88	24.9	1.7	5.8	0.6	26.1	1.6	7.2	2.6	26.1	2.1	4.1	3.4
1.76	24.3	1.7	5.2	0.5	26.3	1.7	6.4	2.4	26.3	2.0	4.6	3.8
2.64	24.9	2.2	3.4	0.4	26.3	1.9	5.2	1.9	26.8	2.1	4.4	3.5
3.52	25.0	2.4	2.9	0.3	26.4	2.1	4.3	1.6	26.3	2.2	3.8	3.1
4.40	24.6	2.4	2.8	0.3	26.4	2.1	4.2	1.5	26.1	2.1	3.4	2.7
11.0	24.8	2.7	2.3	0.2	26.5	2.3	3.7	1.4	26.6	2.9	2.3	1.8

bezogen werden. Sie nehmen von 0.1 zu 0.37 mm/sec ab und dann zu 0.8 mm/sec verstärkt zu. Das entspricht aber dem normalen Minimumsverlauf der Trennstufenhöhe über der Geschwindigkeit. So gesehen darf im Bereich bei 0.1 mm/sec noch auf eine Beeinflussung durch axiale Dispersion, bei 0.8 mm/sec aber bereits auf ein Auswirken der Einstellzeit des Austauschgleichgewichtes, des radialen Massentransportes und/oder der Streudiffusion an den Packungsgrenzflächen in der mobilen Phase geschlossen werden. Der Hinweis auf die Einstellzeit wird dabei noch durch ein leichtes Tailing der nachlaufenden Flanke bei höherer Beladung gestützt. Im Bereich von 3 bis 4 mm/sec darf demnach annähernd optimales Arbeiten in Bezug auf die Auflösung angenommen werden. Hier wird bei geringerer Belastung mit etwa 100 μ Trennstufenhöhe ein Wert erreicht, der bereits in der Größenordnung des Durchmessers der gequollenen Gelpartikel liegt. Für höhere Beladungen mit komplexen Gemischen darf aber ein Arbeiten bei etwas niedrigerer Geschwindigkeit als optimal vorausgesetzt werden. Die Zahlen der in der Zeiteinheit angesprochenen Trennstufen (N') sind bei 0.1 mm/sec um nahezu eine Größenordnung niedriger als bei den beiden anderen untersuchten Geschwindigkeiten. Das dürfte sich bei den sehr verschiedenen Einstellzeiten und Diffusionskonstanten der Komponenten eines breiten Gemisches positiv auswirken.

ANWENDUNG

Die Beurteilung der Anwendungsmöglichkeiten soll hier auf den Bereich des Mineralöls beschränkt bleiben. Die GPC wird als Trenn- und Charakterisierungsmethode für höhersiedende Schnitte, Einsatzöle, Bitumina, und auch Rohöle selbst, immer häufiger zitiert. Ohne auf die Literatur im einzelnen eingehen zu können, sei hier auf eine neuere Sammlung von Originalarbeiten verwiesen¹⁰.

Zweifellos kann die hier vorgestellte Methodik auch für bestimmte präparative Trennungen von Nutzen sein. Die Darstellung der in dieser Richtung bereits erzielten Ergebnisse würde aber hier zu weit führen. Es soll dagegen gezeigt werden, wie mit den Mitteln der analytischen Flüssigkeitschromatographie eine reproduzierbare, relativ schnelle Charakterisierung von Mineralölanteilen höheren Molekulargewichtes möglich ist. Ähnliche Bemühungen wurden kürzlich in der Literatur angegeben^{4,11}.

Die folgenden Versuche wurden, wie zuvor angegeben, mit Methylenchlorid als Elutionsmedium durchgeführt. Zunächst war auch für den praktischen Einsatz die Frage des Einflusses von Probenmenge und Geschwindigkeit zu klären. Versuche mit zwischen 10 und 80 mg variiertter Probenmenge eines Rohöls ergaben eine konstante Elutionsbreite der Gesamtverteilung zwischen 11 und 25 cc, die sich lediglich bei 80 mg Öl zu höheren Elutionsvolumina hin verbreiterte. Die Lage des Maximums der Verteilung und das Verteilungsbild blieben aber nur bis zu etwa 35 g Probenmenge konstant. Bei grösserer Menge trat ein vorlaufendes Maximum bei etwa 12 cc auf, das

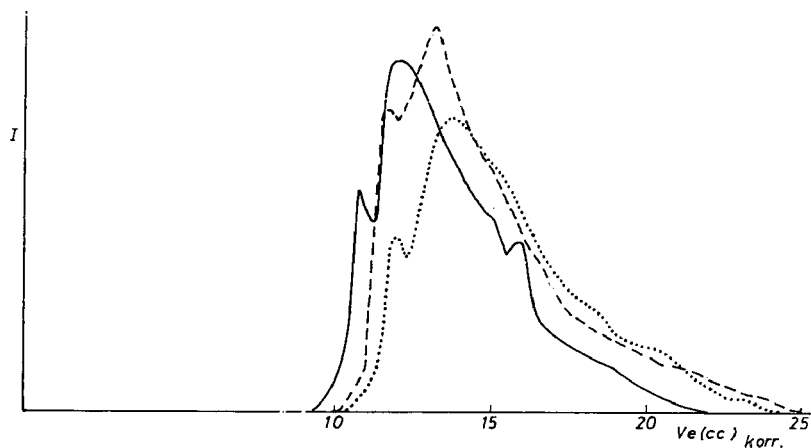


Fig. 4. Relative Änderung des Brechungsindex (I) über dem Elutionsvolumen (V_e) für 30 mg Proben eines Rohöls bei verschiedenen Geschwindigkeiten: —, 0.07 mm/sec; ---, 0.36 mm/sec; . . ., 0.81 mm/sec.

mit wachsender Probenmenge deutlicher hervortrat. Das kann eigentlich nur mit der kürzlich von ALTGELT¹² nachgewiesenen Sekundäre exclusion gedeutet werden. Diese Befunde lassen eine Probenmenge von 30 mg als einen sinnvollen Kompromiss zu. Das entspricht etwa einem Substanzverhältnis von $1 \cdot 10^{-3}$ Probe/Gel. Die in Fig. 4 für ein Rohöl gezeigten Ergebnisse verdeutlichen den Einfluss der Geschwindigkeit. In Übereinstimmung mit den bereits für Benzol diskutierten Befunden ergibt sich für das Hauptmaximum von 0.07 zu 0.81 mm/sec eine Verschiebung um 1.7 cc zu

höheren Elutionsvolumina. Verschiebungen dieser Größenordnung sind aber für Vergleiche und für Umeichungen bereits bedeutungsvoll. Wichtiger ist, dass die Auflösung in dem Verteilungsbild mit zunehmender Geschwindigkeit deutlich schlechter wird. Zwar ergibt die bei der höchsten angegebenen Geschwindigkeit über 17 min laufende Verteilung noch brauchbare Informationen, doch gehen die bei niedrigerer Geschwindigkeit erwartbaren Detailinformationen verloren. Bei der niedrigsten angegebenen Geschwindigkeit läuft die Verteilung allerdings schon über 160 min. Für einmal festgelegte Probenmenge und Geschwindigkeit sind die Verteilungskurven in engen Toleranzen reproduzierbar.

Für eine Charakterisierung von Ölen sind experimentell erhaltene Angaben von Schreiberausschlag und Elutionsvolumen wenig sinnvoll und nur für unmittelbare phänomenologische Vergleiche geeignet. Es wurde daher versucht, die Achsen der Darstellung in sinnvolle Dimensionen umzueichen. Für die Ordinate wurde zunächst durch Messungen an Verdünnungsreihen bekannter Substanzen eine Kalibrierung des Refraktometers vorgenommen. Für die Übertragung dieser Brechungsindexskala in Massenprozent sind aber gewisse Annahmen erforderlich. Es darf angenommen werden, dass die Mehrheit der in einem höhersiedenden Mineralölschnitt vorliegenden Kohlenwasserstoffe prinzipiell als stark alkylsubstituierte Naphthene, Aromaten und Naphthenaromaten aufgebaut sind, und dass andere Strukturtypen daneben nur eine untergeordnete Rolle spielen. Der Verlauf des Brechungsindex dieser Substanztypen ist zwar stark unterschiedlich, nähert sich aber ab einer Molekülgröße von etwa 30 C-Atomen jeweils einem Grenzwert. Für ein gewähltes Molekulargewicht von 450 ergeben sich somit Richtwerte des Brechungsindex von 1.465 für Naphthene und 1.478 für Aromaten. Unter Annahme von Additivität ergeben sich daraus zwei Eichgeraden. Davon wurde die zweite direkt für die Beurteilung von Aromatenkonzentraten herangezogen. Für die Beurteilung gemischter Öle, wie z.B. Rohöle, wurde eine mittlere Eichgerade angenommen. Schreiberausschlag und umgerechnete %-Vol.-Skala sind in den folgenden Figuren gemeinsam angegeben.

Für die Umeichung der Abzisse wurden zunächst die in Fig. 1 und 2 ermittelten Zusammenhänge auf das Molekulargewicht als Bezugsbasis umgestellt und daraus unter der Annahme stark alkylsubstituierter Ringverbindungen in erster Näherung eine Mittelung der für reine Substanzen vorliegenden Verhältnisse vorgenommen, wobei die Ergebnisse an einer Reihe von Cholesterinderivaten mit einbezogen wurden. Die gemittelte Beziehung ergibt sich zu

$$\log M = -0.059 \cdot V_e + 3.525$$

Auf dieser Grundlage sind auf der Abzisse neben den Elutionsvolumina auch Richtwerte des Molekulargewichtes mit angegeben. Eine Bereichsauswertung ist dann angenähert möglich, indem in den Achsen Vol % (cc/cc) über Elutionsvolumen (cc) integriert wird. Die ermittelten Flächenanteile haben dann die Dimension eines Volumens und beziehen sich auf den gewählten Molekulargewichtsbereich. Hierbei wird allerdings die Zonenausbreitung nicht berücksichtigt, und die so ermittelten Angaben bleiben in ihrer Bedeutung eingeschränkt.

Es wurden sechs Rohöle, sechs sorptionschromatographisch aus Vakuumdestillaten abgetrennte Aromatenkonzentrate und ein Dieselöl bei verschiedenen Geschwindigkeiten untersucht. Die bei 0.09 mm/sec erhaltenen Ergebnisse geben die

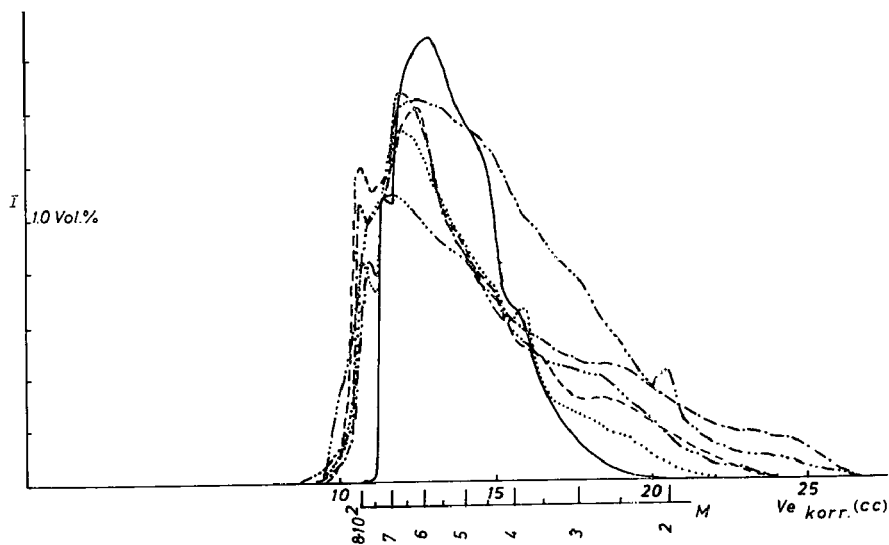


Fig. 5. Relative Änderung des Brechungsindex (I) bzw. Volumenprozent über dem Elutionsvolumen (V_e) bzw. Molekulargewicht (M) für verschiedene Rohöle (30 mg Probe, $v = 0.09$ mm/sec). —, Rohöl I; ---, II; - · - · - ·, III; — · — · — ·, IV; · · · · ·, V; — · — · — ·, VI.

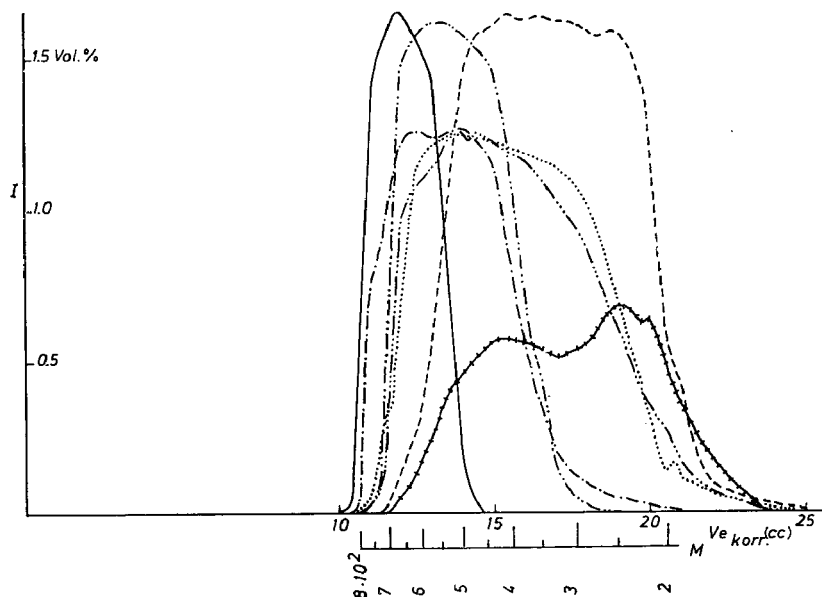


Fig. 6. Relative Änderung des Brechungsindex (I) bzw. Volumenprozent über dem Elutionsvolumen (V_e) bzw. Molekulargewicht (M) für verschiedene Aromatenkonzentrate aus Vakuumschnitten und ein Dieselöl (30 mg Probe, $v = 0.09$ mm/sec). — · — · — ·, Öl Nr. 31; —, 65; — · — · — ·, 66; ---, 68; — · — · — ·, 70; · · · · ·, 85; —|—|—|—|, Dieselöl.

Fig. 5 und 6. Diese und ähnliche Öle wurden auch in anderen Arbeiten von uns untersucht^{13,14}.

In den Verteilungen der Rohöle bestehen deutliche Unterschiede. Es war bisher nicht möglich, eine eindeutige Korrelation der Verteilung mit anderen kennzeichnenden Grössen zu erhalten. Wahrscheinlich sind die Zusammenhänge komplex und können nicht über eine Grösse allein gesehen werden. Kritisch anzumerken ist, dass mit der niedrigen Ausschlussgrenze des Gels die höhermolekularen Anteile nur unzureichend beurteilt werden können. Die Nebenmaxima bei etwa 10.5 cc in den Ölen II, III und V dürfen jedoch als starke Anteile an Asphaltenen gedeutet werden und sind in diesem Sinne auch durch andere Ergebnisse bestätigt¹³. Für diesen Bereich wären die Geltypen OR-1500 oder OR-5000 zweifellos geeigneter. Untersuchungen hierüber wurden inzwischen begonnen.

Ebenfalls stark differenziert sind die Verteilungen der Aromatenkonzentrate. Die gemessenen mittleren Molekulargewichte fallen in der Reihenfolge No. 65, 70, 66, 31, 85, 68, was etwa den Mittellagen der Verteilungskurven entspricht. Auch die Verteilungsbreiten dürften im ganzen zuverlässig beurteilt werden. Lediglich bei den Ölen 85 und 68, deren mittlere Molekulargewichte mit 385 und 345 deutlich niedriger als die der anderen Öle liegen, können gemäss Fig. 2 spezielle Aromatenanteile eine Ausweitung der Verteilung zu höheren Elutionsvolumina bewirken. Wie kritisch die Verhältnisse bei Mischungen niederen Molekulargewichtes beurteilt werden müssen, zeigt der Verlauf für das Dieselöl mit einem gemessenen mittleren Molekulargewicht von 220. Dieser Wert wird nur von dem zweiten Maximum in der Verteilung hinreichend erfüllt. Im ersten Maximum dürfte es sich dagegen vorwiegend um paraffinische Substanzen handeln, die mit der angenommenen Kalibrierungsmethode falsch beurteilt werden. Bezieht man jedoch den Elutionsbereich des ersten Maximums gemäss Fig. 1 allein auf kettenförmige Verbindungen, so ergibt sich unter Beachtung der Dichten ein Molekulargewichtsbereich zwischen 200 und 300 mit dem Maximum bei etwa 240, was wiederum im Einklang mit dem gemessenen Mittelwert steht.

Trotz der diskutierten Einschränkungen sollten dieses hier vorgestellte oder ähnliche Verfahren vor allem für höhermolekulare Mineralölanteile eine relativ schnelle und einfache Möglichkeit zur serienmässigen Charakterisierung bieten. Das gilt natürlich ebenso für andere technische Substanzgemische dieses Molekulargewichtsbereiches. Es wird eines breiteren Erfahrungsmaterials bedürfen, um zuverlässige Korrelationen zu technisch interessierenden Parametern zu finden.

DANK

Der Verfasser dankt der Deutschen Forschungsgemeinschaft, Bad Godesberg, für finanzielle Unterstützung und der Firma Merck AG, Darmstadt, für die Überlassung von Gelmustern.

ZUSAMMENFASSUNG

Nach einer Diskussion der prinzipiellen Struktureinflüsse bei der Trennung niedermolekularer Substanzen an porösen Gelen wird das Elutionsverhalten von vierzig Kohlenwasserstoffen an Vinylacetatgel Merckogel OR-500 aus Cyclohexan, Methylenchlorid und Isopropanol angegeben. Für die verschiedenen Kohlenwasser-

stoffklassen ergeben sich lineare Zusammenhänge von log Molvolumen gegen Elutionsvolumen, die in ihrer Lage durch die Struktur der Substanzen und die Art des Elutionsmediums bestimmt sind. Für gewisse Strukturen wird dabei der Ausschlusseffekt durch andere Effekte überdeckt. Der Einfluss der Probenmenge und der Elutionsgeschwindigkeit an einer Modells substanz untersucht, zeigt eine Abhängigkeit der Zonenausbreitung von der Geschwindigkeit. Dies lässt abhängig von der Geschwindigkeit auf Auswirkungen der axialen Dispersion, des radialen Massentransportes, der Streudiffusion und der Einstellzeit des Austauschgleichgewichtes schliessen. Die Zonenbreite nimmt mit der Beladung zu. Zur Demonstration der Anwendungsmöglichkeiten werden Rohöle sowie die aromatischen Anteile von Vakuumsdestillaten mit den Methoden der analytischen Flüssigkeitschromatographie untersucht. Die registrierten Verteilungen bieten die Möglichkeit zur Charakterisierung von Mineralölproben.

LITERATUR

- 1 M. WILK, J. ROCHLITZ UND H. BENDE, *J. Chromatog.*, 24 (1966) 414.
- 2 B. C. B. HSIEH, R. E. WOOD, L. L. ANDERSON UND G. R. HILL, *Anal. Chem.*, 41 (1969) 1066.
- 3 H. H. OELERT, *Z. Anal. Chem.*, 244 (1969) 91.
- 4 H. H. OELERT, D. R. LATHAM UND W. E. HAINES, *Div. Petrol. Chem., ACS, Preprints*, Vol. 15, No. 2 (1970) A-204.
- 5 H. J. WEBER UND H. H. OELERT, *Div. Petrol. Chem., ACS, Preprints*, Vol. 15, No. 2 (1970) A-212.
- 6 H. H. OELERT UND J. H. WEBER, *Erdöl Kohle*, 23 (1970) 484.
- 7 J. G. BERGMANN UND L. J. DUFFY, *Div. Petrol. Chem., ACS, Preprints*, Vol. 15, No. 2 (1970) A-217.
- 8 *American Petroleum Institute, Res. Proj. 60, Spring Meeting, Bartlesville, Okla., 1970.*
- 9 H. H. OELERT, *Westdeutsche Chemiedozententagung, Köln, 1970, Vortrag A-42.*
- 10 *Div. Petrol. Chem., ACS, Preprints*, Vol. 15, No. 2 (1970) pp. A-1 to A-267.
- 11 J. N. DONNE UND W. K. REID, *Div. Petrol. Chem., ACS, Preprints*, Vol. 15, No. 2 (1970) A-242.
- 12 K. H. ALTGELT, *Div. Petrol. Chem., ACS, Preprints*, Vol. 15, No. 2 (1970) A-115.
- 13 H. H. OELERT, *Erdöl Kohle*, 22 (1969) 19.
- 14 H. H. OELERT, *Erdöl Kohle*, 22 (1969) 536.

J. Chromatog., 53 (1970) 241-252

CHROM. 4954

COLUMN CHROMATOGRAPHY OF THE BROMO-MERCURI-METHOXY ADDUCTS OF FATTY ACID METHYL ESTERS AS A MEANS OF ISOLATING POLYENOIC ACIDS PRESENT IN LOW CONCENTRATIONS

J. D. CRASKE

Unilever Australia Pty. Ltd., Balmain 2041 (Australia)

AND

R. A. EDWARDS

The University of New South Wales, Kensington 2033 (Australia)

(Received July 28th, 1970)

SUMMARY

Due to the extreme complexity of oils such as animal tallows, determination of fatty acid composition by direct gas chromatographic examination of their unfractionated methyl esters is of limited utility. A more detailed analysis of animal fats has been achieved using a silicic acid column chromatographic method to resolve into classes of differing degree of unsaturation, the bromo-mercuri-methoxy adducts of the methyl esters. Methyl esters were recovered from the separated adduct fractions by treatment with acid and analysed by gas chromatography.

This technique should be of general use in those cases where it is necessary to isolate small amounts of dienoic and polyenoic fatty acids from fats, as the required components are protected from autoxidative degradation during the isolation procedure.

INTRODUCTION

As part of an extensive study of animal tallows, a method was required for the determination of fatty acid composition, particular attention being directed towards the amount and nature of the small content of dienoic and more highly unsaturated acids.

Undoubtedly the most commonly used method for determination of the fatty acid composition of fats is gas chromatographic analysis of the methyl esters prepared therefrom. The technique is simple and quick and, in most instances, gives accurate results and excellent resolution of components of the mixture. However, direct analysis is inadequate in certain specialised cases, *e.g.*, determination of trace constituents and analysis of complex fats such as fish oils, animal tallows and hydrogenated oils. In such cases, it is usual first to effect a preliminary fractionation with the aim of enhancing the concentration of the trace components of interest, or

of producing several fractions of composition simpler than that of the starting material, which can then be analysed by gas chromatography. Ideally, the fractions submitted to gas chromatographic analysis should consist either of one unsaturation class (*i.e.*, saturated, monoenes or dienes etc.) or of one chain length.

Traditional methods for separating saturated from unsaturated acids, such as lead soap crystallisation¹ or low-temperature crystallisation of the acids or methyl esters from solvents², can no longer be considered as satisfactory techniques as they do not give clean-cut separations, nor are they easily applicable to small amounts of starting material.

IVERSON *et al.*^{3,4} used urea clathration to fractionate olive and marine oils and to demonstrate the presence of trace concentrations of many acids not readily detectable in the gas chromatogram of the original oil. In a later paper, IVERSON AND WEIK⁵ demonstrated that the ease with which the various methyl esters can form urea adducts depends upon the chain length, the degree of unsaturation and upon the degree of branching. Such methods, then, cannot be expected to effect a clean-cut class separation.

Two methods that do offer a specific separation on the basis of degree of unsaturation are chromatography on silver nitrate impregnated supports⁶ and chromatography of the acetoxy-mercuri-methoxy adducts by paper⁷, column⁸⁻¹² or thin-layer techniques¹³.

For various reasons, these published methods were found to be unsuited to the task of quantitatively isolating the small concentration (2-4%) of polyunsaturated acids present in animal tallow.

Silver nitrate chromatography was abandoned because of autoxidation problems. As the polyunsaturated esters are last to be eluted from the column, as they are only present in small concentrations and, as they are fractionated as the underivatized ester with the double bond unprotected, it was found impracticable to prevent extensive autoxidative deterioration.

Chromatography of the mercury adducts offers the advantage that derivatization temporarily saturates the double bond and so inhibits autoxidation during fractionation. Due to the small content of polyunsaturated acids present in animal tallows, a column chromatographic rather than a paper or a thin-layer technique was indicated as a means of preparing manageable amounts of these minor components. A column technique also permits easy quantitation of the eluted classes. However, the techniques published to date require the use of an acidic solvent for the elution of the highly polar acetoxy adducts of the polyunsaturated esters and thus lead to recovery of the original unsaturated ester rather than the protected derivative.

WHITE¹⁴ and WHITE AND POWELL¹⁵ have shown that conversion of the acetoxy to the bromo derivative leads to an adduct of lower polarity, which is more amenable to separation by thin-layer chromatography. In the present paper it has been demonstrated that the reduced polarity of the bromo derivative can be used to advantage to allow elution of the intact derivative from a silicic acid column and so retain protection from autoxidation pending further analysis.

EXPERIMENTAL

Reagents

Methanol and dioxane were Merck "guaranteed reagents" and were used as received. Diethyl ether, chloroform and petroleum ether b.p. 40–70° were commercial solvents distilled to ensure removal of non-volatile residues. Silicic acid, from Mallinckrodt, SilicAR CC7, 200–235 mesh, was dried overnight at 110°, deactivated by addition of 20% (w/w) water and equilibrated by standing overnight.

Safflower oil was a commercial sample obtained from Unilever Australia Pty. Ltd. (iodine value, 145.0). Mutton tallow was purchased from James Barnes Pty. Ltd. (iodine value, 45.9). Beef perirenal and pericardial tissues were butcher's samples and the lipid was extracted with chloroform-methanol (3:1) (iodine value, 39.3 and 35.2, respectively).

Procedures

The acetoxy-mercuri-methoxy adducts are prepared by boiling, under reflux, methyl esters (weight = 90/iodine value), mercuric acetate (2.25 g) and methanol (15 ml). After cooling, the mixture is diluted with water (160 ml) and extracted five times with ether (35 ml) and twice with chloroform (30 ml). The ether and chloroform extracts are separately pooled. The combined ether extracts are washed three times with water (50 ml) and each water wash is separately re-extracted with

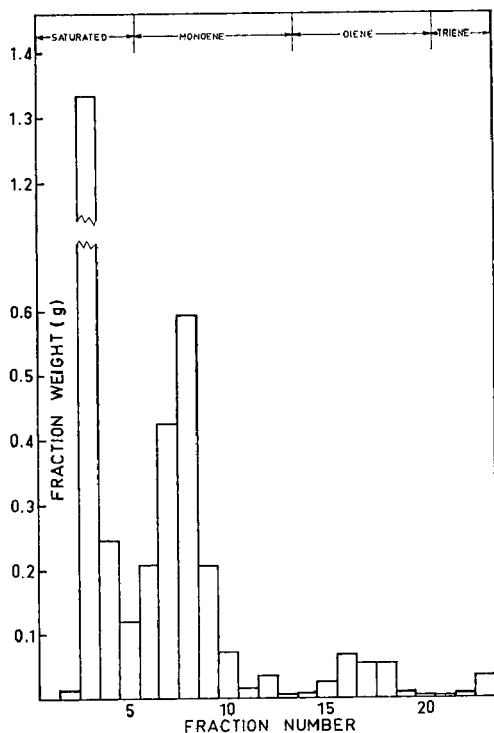


Fig. 1. Histogram showing silica gel chromatographic separation of the bromo-mercuri-methoxy adducts of beef pericardial lipids.

the chloroform extract. The combined ether and chloroform extracts are evaporated dry at low temperature using a rotary evaporator, taken up in chloroform (20 ml) and converted to the bromo derivative by mixing with 5% methanolic solution of sodium bromide (30 ml). The solution of bromo derivatives is diluted with water (60 ml), the chloroform layer removed and the aqueous layer re-extracted with chloroform (20 ml). The combined extracts are washed four times with water (50 ml) and each water wash is re-extracted with chloroform (10 ml). After removal of solvent at low temperature the bromo derivatives are dissolved (if the sample is relatively rich in saturated esters) or dispersed (if highly unsaturated esters predominate) in 1% dioxane in petroleum ether for application to the silicic acid column prepared from 30 g deactivated adsorbent and packed into a 2-cm-diameter column.

The components of the mixture are eluted with petroleum ether containing 1% (saturated), 5% (monoenes), 10% (dienes) and 20% dioxane (trienes) and collected in 25-ml fractions. Appropriate fractions are pooled (Fig. 1) and the esters recovered by boiling under reflux for 5 min with methanol (90 ml) and hydrochloric acid (10 ml), then diluting with water and extracting into petroleum ether. To ensure that all the extract is in the ester form, ethereal diazomethane is added to the ester solution until a permanent yellow colour remains.

RESULTS AND DISCUSSION

Fig. 1 illustrates a typical separation obtained when adducts prepared from beef pericardial lipid were submitted to chromatographic fractionation. In Tables I-IV, results are shown of analyses carried out on samples of safflower oil, mutton tallow and the lipids obtained from beef pericardial and perirenal tissue.

It would not normally be of interest to submit safflower oil or any other oil

TABLE I

ANALYSIS OF SAFFLOWER OIL

	<i>Saturated</i> (<i>Fraction</i> <i>No. 8</i>)	<i>Monoene</i> (<i>Fraction</i> <i>Nos. 9-13</i>)	<i>Diene</i> (<i>Fraction</i> <i>Nos. 14-23</i>)	<i>Safflower oil</i>	
				<i>Calc.^a</i>	<i>Detn.^b</i>
12:0	0.4	1.1	—	0.2	0.3
14:0	1.8	0.9	tr	0.3	0.2
15:0	0.2	tr	—	tr	—
16:0	62.3	14.2	0.2	6.0	6.5
16:1	—	0.8	—	0.1	—
17:0	0.3	—	0.1	0.1	—
18:0	28.8	3.9	0.1	2.5	2.3
18:1	0.4	74.0	2.0	11.0	12.6
18:2	tr	4.0	97.7	79.4	78.1
20:0	3.4	—	—	0.2	—
20:1	—	1.0	—	0.1	—
22:0	2.2	—	—	0.2	—
% recovered	6.7	13.0	82.4	102.1	—

^a Algebraic summation of the compositions of the separated fractions, normalised to 100%.

^b Determined by direct GC analysis of the unfractionated methyl esters.

TABLE II

ANALYSIS OF MUTTON TALLOW

	Relative retention (18:0 = 1)	Saturated (Fraction Nos. 1-4)	Monoene (Fraction Nos. 5-13)	Diene (Fraction Nos. 14-21)	Triene (Fraction Nos. 22 and 23)	Tallow	
						Calc. ^a	Detn. ^b
10:0	0.061	tr	0.1	—	—	0.1	0.1
12:0	0.121	0.1	tr	—	—	0.1	0.1
13:0	0.163	tr	—	—	—	tr	tr
iso-14:0	0.206	0.1	—	—	—	0.1	0.1
14:0	0.242	4.2	1.0	0.1	0.4	2.5	2.6
iso-15:0	0.294	0.5	—	—	—	0.3	0.8
14:1	0.307	—	0.3	—	—	0.1	
anteiso-15:0	0.312	0.5	—	—	—	0.3	0.7
15:0	0.344	1.2	0.3	0.1	0.3	0.7	
15:1	0.392	—	0.2	—	—	0.1	0.3
?	0.414	—	—	0.1	—	tr	
iso-16:0	0.418	0.4	—	—	0.1	0.2	20.4
16:0	0.488	37.8	5.4	0.8	3.1	21.2	
?	0.559	0.3	—	—	—	0.1	2.5
16:1	0.584	—	4.3	0.8	0.9	2.0	
iso-17:0	0.592	1.0	—	—		0.5	0.7
anteiso-17:0	0.628	1.5	—	—	—	0.7	
17:0	0.694	3.4	—	—	0.4	1.7	2.2
16:2	0.70-0.81 ^c	—	—	2.0	0.4	0.1	
iso-17:1?	0.703	—	0.4	—	—	0.2	1.0
17:1	0.817	—	1.4	—	—	0.7	
iso-18:0	0.848	0.3	—	—	—	0.2	24.6
18:0	1.000	47.4	4.4	1.0	3.6	25.5	
18:1	1.14	0.3	80.3	9.3	3.6	37.3	37.7
iso-19:0	1.24	0.1	—	—	—	0.1	4.3
iso-19:1?	1.35	—	1.7	—	—	0.8	
18:2	1.24-1.71 ^d	—	—	68.2	5.8	2.7	0.4
19:0	1.42	0.6	—	—	—	0.3	
19:1	1.60	—	0.2	—	—	0.1	1.5
iso-20:0	1.80	tr	—	—	—	tr	
18:3	1.95	—	—	—	74.0	0.3	0.4
20:0	2.03	0.3	—	—	—	0.2	
19:2?	2.07	—	—	6.7	—	0.3	tr
?	2.27	—	—	1.5	—	0.1	
?	2.52	—	—	7.5	—	0.3	tr
?	2.69	—	—	0.6	4.2	tr	
20:2?	2.89	—	—	0.9		tr	tr
?	3.29	—	—	0.4	2.3	tr	
?	3.73	—	—	—	0.9	tr	—
% recovered		49.4	45.9	3.9	0.4	99.6	—

^a Algebraic summation of the compositions of the separated fractions normalised to 100%.^b Determined by direct GC analysis of the unfractionated methyl esters.^c Unresolved group of peaks containing at least three components.^d Unresolved group of peaks containing at least five components. Probably isomeric C₁₈ dienes.

of simple composition to mercury adduct fractionation. Safflower oil was selected as a simple model mixture to demonstrate the potential of the technique. However, it is of interest to note that a number of acids present in trace concentrations, and not visible in the chromatogram of the original oil, are readily detected in the

TABLE III

ANALYSIS OF BEEF PERICARDIAL TISSUE LIPID

	<i>Relative retention</i> (18:0 = 1)	<i>Saturated</i> (Fraction Nos. 1-5)	<i>Monoene</i> (Fraction Nos. 6-13)	<i>Diene</i> (Fraction Nos. 14-20)	<i>Triene</i> (Fraction Nos. 21-23)	<i>Pericardial lipid</i>	
						<i>Calc.</i> ^a	<i>Detn.</i> ^b
10:0	0.059	0.1	—	—	—	0.1	0.1
12:0	0.120	0.2	—	—	0.3	0.1	0.1
iso-14:0	0.206	0.1	—	—	0.2	0.1	0.1
14:0	0.241	6.1	1.0	0.1	1.4	4.2	4.3
iso-15:0	0.292	0.4	—	—	} 0.8	0.3	} 0.9
14:1	0.307	—	0.6	0.1		0.2	
anteiso-15:0	0.310	0.7	—	—		0.4	
15:0	0.343	1.2	0.1	—	0.5	0.8	0.9
iso-16:0	0.417	0.4	—	—	0.5	0.3	0.3
16:0	0.491	43.5	5.4	0.6	10.4	29.8	30.1
16:1	0.580	—	4.9	1.6	} 1.1	1.7	} 2.1
iso-17:0	0.596	0.7	—	—		0.4	
anteiso-17:0	0.630	1.0	0.2	—		0.8	0.9
17:0	0.695	2.3	—	—	} 0.7	1.5	} 1.6
iso-17:1?	0.700	—	0.1	—		tr	
16:2	0.64-0.80 ^c	—	—	1.9		0.1	} 0.4
?	0.754	0.6	—	—	} 0.7	0.4	
17:1	0.804	—	1.2	—		0.4	
iso-18:0	0.853	0.1	—	—	—	tr	0.4
18:0	1.000	40.8	4.0	0.8	9.5	27.6	27.7
18:1	1.14	1.7	81.5	19.3	10.4	28.0	27.6
iso-19:0	1.22	tr	—	—	—	tr	} 2.1
iso-19:1?	1.34	—	0.9	—	—	0.3	
19:0	1.41	0.1	—	—	—	tr	
18:2	1.29-1.65 ^d	—	—	62.0	11.0	1.9	} 0.4
19:1	1.58	—	0.1	—	—	tr	
18:3	1.94	—	—	—	39.8	0.3	
19:2	2.00	—	—	4.8	—	0.1	} 0.4
20:0	2.01	0.1	—	—	—	0.1	
?	2.18	—	—	2.3	—	tr	—
?	2.44	—	—	4.6	1.2	tr	—
?	2.61	—	—	0.8	1.4	tr	—
20:2?	2.81	—	—	1.0	—	tr	—
?	2.97	—	—	—	1.7	tr	—
?	3.27	—	—	—	5.8	0.1	—
?	3.75	—	—	—	1.9	tr	—
?	4.09	—	—	—	0.4	tr	—
?	4.51	—	—	—	0.2	tr	—
% recovered		64.1	32.2	2.3	0.8	99.4	—

^{a-d} See footnotes to Table II.

chromatograms of the fractions. Thus saturated acids containing 15, 17, 20 and 22 carbon atoms and monoenes of chain lengths 16 and 20 were demonstrated. Whilst the fractions obtained are essentially true to class, they do contain small amounts of atypical acids. In general, there is a more pronounced tendency for components to tail into the following fraction than for the converse phenomenon of leading to occur. It has been found that chromatography of the bromo adducts allows good separation of the monoene from the polyene fraction, but that it is more difficult to effect absolutely clean separation of the saturated acids from the monoenes. The converse situation applies when the acetoxy adducts are submitted

TABLE IV

ANALYSIS OF BEEF PERIRENAL TISSUE LIPID

	Relative retention (18:0 = 1)	Saturated (Fraction Nos. 1-4)	Monoene (Fraction Nos. 5-13)	Diene (Fraction Nos. 14-20)	Triene (Fraction Nos. 21-23)	Perirenal lipid	
						Calc. ^a	Detn. ^b
10:0	0.059	tr	—	—	—	tr	0.1
12:0	0.121	0.6	0.1	—	0.2	0.4	0.4
13:0	0.171	tr	0.1	—	—	0.1	0.1
iso-14:0	0.208	0.3	—	—	—	0.2	0.2
14:0	0.242	12.2	0.7	0.2	1.1	7.3	7.3
iso-15:0	0.293	0.5	—	—	—	0.3	1.5
14:1	0.308	—	1.6	0.3	0.7	0.6	
anteiso-15:0	0.311	1.0	—	—	—	0.6	
15:0	0.343	1.8	0.2	0.1	0.5	1.1	1.1
iso-16:0	0.418	0.6	—	—	—	0.4	0.4
16:0	0.487	44.0	2.1	0.7	11.1	26.3	26.2
16:1	0.580	—	6.6	1.0	1.8	2.6	2.8
iso-17:0	0.597	0.8	—	—	—	0.4	
anteiso-17:0	0.630	1.1	—	—	—	0.6	0.8
17:0	0.695	2.2	—	—	0.6	1.3	1.4
16:2	0.64-0.81 ^c	—	—	2.1	—	0.1	0.1
?	0.765	tr	—	—	—	tr	
17:1	0.818	—	1.2	—	—	0.5	0.4
iso-18:0	0.860	tr	—	—	—	tr	
18:0	1.000	34.20	1.6	1.5	12.0	20.5	20.6
18:1	1.14	0.7	82.0	9.8	13.0	32.4	33.4
iso-19:1?	1.35	—	1.2	—	—	0.5	1.9
19:0	1.42	0.1	—	—	—	tr	
anteiso-19:1?	1.46	—	0.2	—	—	0.1	
18:2	1.26-1.65 ^d	—	—	47.1	11.0	1.6	—
19:1	1.60	—	0.5	—	—	0.2	
?	1.70	—	—	—	1.1	tr	1.5
18:3	1.94	—	—	—	44.8	tr	
19:2	1.97	—	—	22.3	—	0.8	
iso-20:1	2.02	—	0.8	—	—	0.3	0.1
20:0	2.04	tr	—	—	—	tr	
20:1	2.25	—	1.0	—	—	0.4	—
?	2.42	—	—	11.0	2.3	0.4	
20:2?	2.81	—	—	3.0	—	0.1	tr
?	3.19	—	—	0.8	—	tr	—
% recovered		58.0	38.6	3.4	0.04	100.0	—

^{a-d} See footnotes to Table II.

to chromatography, for, in this case, the larger polarity difference between the saturated esters and the monoene adducts leads to facile resolution. The trace concentration of linoleic acid present in the saturated fraction is thought to be due to incomplete reaction or to hydrolysis before chromatographic separation. Cross-contamination from all sources is sufficiently limited to be of no significant consequence.

The results of Tables II-IV illustrate the extreme complexity of animal tallows and demonstrate that a large amount of additional information on their compositions can be obtained following adduct fractionation. This is further illustrated in Fig. 2, where it can be seen that even after isolation of the diene and triene

fractions, their compositions are still too complex to be completely interpreted. This arises from the fact that, in ruminant animals, the lipids in the food ingested are partially hydrogenated in the rumen and give rise to a large number of isomeric acids. The triene fraction is further complicated because 20% dioxane elutes any traces of free acid that might have been present in the original ester. On esterification with diazomethane, this gives rise to a chromatogram of the original fat superimposed on the triene chromatogram. In the case of animal tallow, which contain only a

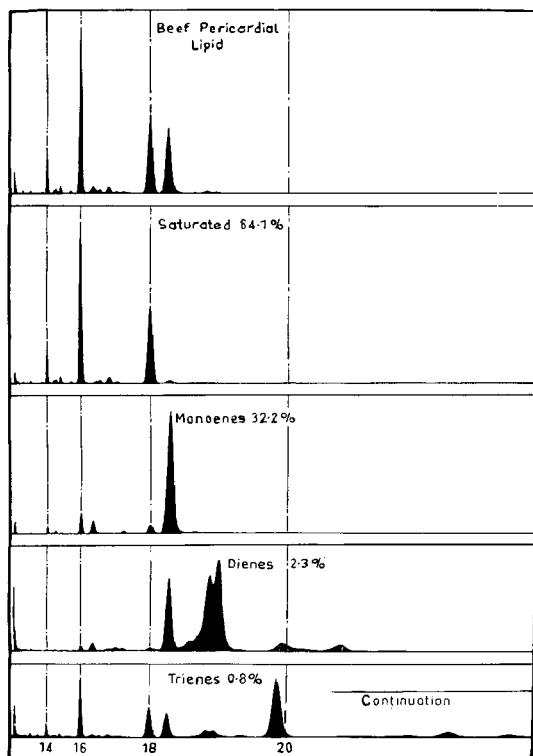


Fig. 2. GLC analysis of beef pericardial lipid methyl esters and of the saturated monoenoic, dienoic and trienoic esters recovered from fractions obtained by silica gel chromatographic fractionation of bromo-mercuri-methoxy adducts. GC parameters: column 5 ft. \times 4 mm I.D.; 15% diethylene glycol succinate on acid-washed Chromosorb W; 30 ml N_2 /min; 160°.

very small amount of trienoic acids, it only needs a minute concentration of free acid in the original sample significantly to distort the triene chromatogram. Interpretation can still be effected, as the trienes of animal tallow elute later than the majority of the peaks of the unfractionated tallow.

It is evident that further fractionation will be necessary to clarify this situation and this work will form the subject of a subsequent publication. However, it is pertinent to note that the method does allow isolation of trienes when present in concentrations below 1%, in a form protected from oxidation and suitable for further analysis.

ACKNOWLEDGEMENT

Technical assistance by Mrs. J. van WEIJE is gratefully acknowledged.

REFERENCES

- 1 T. P. HILDITCH, *The Chemical Constitution of Natural Fats*, 3rd ed., Chapman and Hall, London, 1956, p. 574.
- 2 J. B. BROWN AND D. K. KOLB, in R. T. HOLMAN, W. O. LUNDBERG AND T. MALKIN (Editors), *Progress in the Chemistry of Fats and Other Lipids*, Vol. 3, Pergamon, London, New York, 1955, p. 57.
- 3 J. L. IVERSON, J. EISNER AND D. FIRESTONE, *J. Am. Oil Chemists' Soc.*, 42 (1965) 1065.
- 4 J. L. IVERSON, J. EISNER AND D. FIRESTONE, *J. Assoc. Offic. Agr. Chemists*, 48 (1965) 1191.
- 5 J. L. IVERSON AND R. W. WEIK, *J. Assoc. Offic. Agr. Chemists*, 50 (1967) 1111.
- 6 B. DE VRIES, *J. Am. Oil Chemists' Soc.*, 40 (1963) 184.
- 7 Y. INOUE, M. NODA AND O. HIRAYAMA, *J. Am. Oil Chemists' Soc.*, 32 (1955) 132.
- 8 E. JANTZEN AND H. ANDREAS, *Angew. Chem.*, 70 (1958) 656.
- 9 E. JANTZEN AND H. ANDREAS, *Chem. Ber.*, 92 (1959) 1427.
- 10 E. JANTZEN AND H. ANDREAS, *Chem. Ber.*, 94 (1961) 628.
- 11 E. JANTZEN, H. ANDREAS, K. MORGENSTERN AND W. ROTH, *Fette, Seifen, Anstrichmittel*, 63 (1961) 685.
- 12 D. F. KUEMMEL, *Anal. Chem.*, 34 (1962) 1003.
- 13 H. K. MANGOLD AND R. KAMMERECK, *Chem. Ind. (London)*, (1961) 1032.
- 14 H. B. WHITE, JR., *J. Chromatog.*, 21 (1966) 213.
- 15 H. B. WHITE, JR. AND S. S. POWELL, *J. Chromatog.*, 32 (1968) 451.

J. Chromatog., 53 (1970) 253-261

CHROM. 4993

QUANTITATIVE ANALYSIS OF GLYCERYL NITRATES ON THIN-LAYER CHROMATOGRAMS

COMPARISON OF COLORIMETRY AND DENSITOMETRY

M.-T. ROSSEEL, M. G. BOGAERT AND E. J. MOERMAN

J.F. and C. Heymans Institute of Pharmacology, University of Ghent, Ghent (Belgium)

(First received July 16th, 1970; revised manuscript received August 17th, 1970)

SUMMARY

Densitometry and colorimetry were compared as methods for the quantitative determination of glyceryl nitrates on thin-layer chromatograms. For both methods a linear relationship exists between the amount of nitrate spotted and the results obtained. The reproducibility of densitometry seems acceptable at least for amounts of nitrate larger than 2 μg . As densitometry is much less time consuming than colorimetry after elution, the former method is preferable for our purposes. Application of a correction factor for baseline variation could be useful; correction for plate-to-plate variations is unrewarding, and internal standards have to be used on each plate.

INTRODUCTION

In our study of the metabolism of nitroglycerin, we previously used a quantitative analysis of different organic nitrates (tri-, di- and monoglyceryl nitrates) by separating them on thin-layer chromatograms followed by colorimetric determination of the individual nitrates on material eluted from the chromatograms^{1,2}. Quantitative estimation of the different glyceryl nitrates had been made by CREW AND DiCARLO³ by radioscan on thin-layer plates. In our work with non-radioactive material, the elution and dosage procedure used hitherto is quite time- and effort-consuming. In the last years a number of instruments for direct quantitative spectrophotometry of thin-layer chromatograms were developed (for references see ZÜRCHER *et al.*⁴). In the present work we report our results with the *in situ* spectrophotometric determination of glyceryl nitrates on thin-layer plates, using a "flying spot" scanner, and we compared the results obtained with the results of colorimetric determination after elution from the plates.

MATERIALS AND METHODS

Materials

Glyceryl trinitrate (GTN, nitroglycerin or trinitrine) was available as a commercial 1% solution in ethyl alcohol. Glyceryl 1,3-dinitrate (GDN 1-3), glyceryl 1,2-

dinitrate (GDN 1-2) and glyceryl 1-mononitrate (GMN 1) were prepared from 1,3-dibromohydrine, 1,2-dibromohydrine and 1-chlorohydrine, respectively, according to the method of DUNSTAN *et al.*⁵. The substances obtained were purified and identified as described previously⁶. Appropriate dilutions of the various esters were prepared in ethyl alcohol. For practical purposes the amounts of the different glyceryl nitrates are always expressed in " μg nitrate", *i.e.* their content of nitrate.

Chromatography and detection

One-dimensional TLC of GTN, GDN 1-3, GDN 1-2 and GMN 1 was carried out on 0.25 mm Silica Gel F₂₅₄ plates on glass (Merck). Using a microliter pipet (Haak 10:10), small samples (2–30 μl) of the nitrate solutions were carefully applied to the plates, and ascending chromatograms were run at room temperature. The solvent used for GTN, GDN 1-3 and GDN 1-2 was benzene–ethyl acetate, 4:1 (ref. 7). As solvent for GMN 1 we employed benzene–ethyl acetate, 2:5, with an R_F value for GMN 1 of 0.43. The solvent was allowed to travel 15 cm. The nitrates can be visualised on the thin-layer plate by spraying with a 1% diphenylamine–ethyl alcohol solution (15 ml) followed by irradiation with UV light for 10 min, the nitrate esters appearing as yellow-green spots on a light tan background⁸.

Estimation with densitometry

This estimation is carried out after spraying the plates as described above, using an automatic "flying spot" scanner, the Universal Densitometer Vitatron, type TLD 100. The measuring system is an absorption measurement by means of transmitted light.

Experimental details were provided by the manufacturers (Vitatron N.V., Dieren, The Netherlands). The measurement of the peak area is done automatically by the integrator built into the recorder and is expressed in integration units. This peak area has a linear relation with the total concentration of the spot. Optimal scan conditions were experimentally determined: log (—); level b/5; span 9.60; damping 2; stroke 6 mm; filter 398 m μ .

One of the problems in densitometry is the variability in thickness of the silica gel layer; variations can be seen in one given plate, but even larger differences can be seen from one plate to another. Such variations undoubtedly influence the readings. The manufacturers of the densitometer suggest the use of a correction factor $e^{-2\Delta A_0}$ derived from GOLDMAN AND GOODALL's work on transmission of light through materials such as silica gel layers, with their inherent variability of thickness^{9,10}. This correction factor can be applied for plate (or baseline) correction or for plate-to-plate correction. For plate correction, ΔA_0 is the difference of absorption between a "reference baseline point" and the baseline of each peak. For plate-to-plate correction, ΔA_0 is the difference of absorption between a reference baseline point on each plate and a fixed area of a standard plate.

Estimation with colorimetry after elution

The areas of the thin-layer plates corresponding to the various nitrate esters are scraped off individually; to allow exact localisation of these areas, guide spots of each of the nitrate esters used are applied on the plates, and after completion of the chromatogram these guide spots are colored by spraying with a 1% diphenylamine–

ethyl alcohol solution and by irradiating with UV light (see above). The material scraped off is transferred to glass-stoppered tubes; the nitrates are eluted by adding 3 ml of ethyl alcohol. The tubes are shaken for about 10 min and the silica gel is removed by centrifugation. A similar elution process is followed for a blank sample of the coating material alone. Colorimetric determination of the nitrates is carried out according to the method of LORENZETTI *et al.*¹¹ with an Universal Vitatron Colorimeter at 540 m μ , using 2-cm cells.

For both methods the relative standard deviations (s_{rel}) are calculated from

$$s = \sqrt{\frac{\sum (x - \bar{x})^2}{n - 1}}$$

and used as an index of reproducibility.

RESULTS

Densitometry

Reproducibility of results in one given plate. Different amounts of GTN (2, 5, 10 or 20 μ g of nitrate) were spotted on thin-layer plates; on each plate the same amount of the substance was spotted six times. The results are given in Table I, with the calcu-

TABLE I

REPRODUCIBILITY OF SCANNING OF GTN SPOTTED ON ONE PLATE

Each amount of GTN was spotted 6 times and the mean of the six measurements calculated for each plate. The quantity of GTN spotted is expressed as μ g nitrate. The peak area is given in integration units. Corrected peak area is obtained by multiplying with the plate correction factor (for details see text).

Quantity of GTN spotted	Chromato- gram No.	Peak area		Corrected peak area	
		Mean	s_{rel} .	Mean	s_{rel} .
2	1	25.8	2.7	25.8	3.9
	2	50.4	11.1	50.7	11.1
	3	26.3	8.0	25.7	7.1
5	4	88.7	4.4	89.1	4.5
	5	118.2	3.7	116.3	3.2
10	6	198.6	2.9	196.6	2.2
	7	154.4	3.7	150.6	3.7
	8	139.3	3.2	137.1	2.1
20	9	251.2	4.1	249.6	2.9
	10	215.4	2.4	215.7	2.3

lation of the reproducibility, as expressed by the relative standard deviation. The values for "corrected peak area" are obtained by multiplication of the peak area with $e^{-2\Delta A_0}$ for plate (or baseline) correction.

Reproducibility of results from different plates. Two concentrations of GTN, 10 and 20 μ g nitrate, were spotted on fourteen different plates, and the peak areas, as measured by the densitometer, were compared. Corrected values are also given. They are obtained by multiplying the peak area by the factor $e^{-2\Delta A_0}$, for variations between plates (plate-to-plate correction) (Table II).

Calibration curves for the relationship between concentration of the different glyceryl

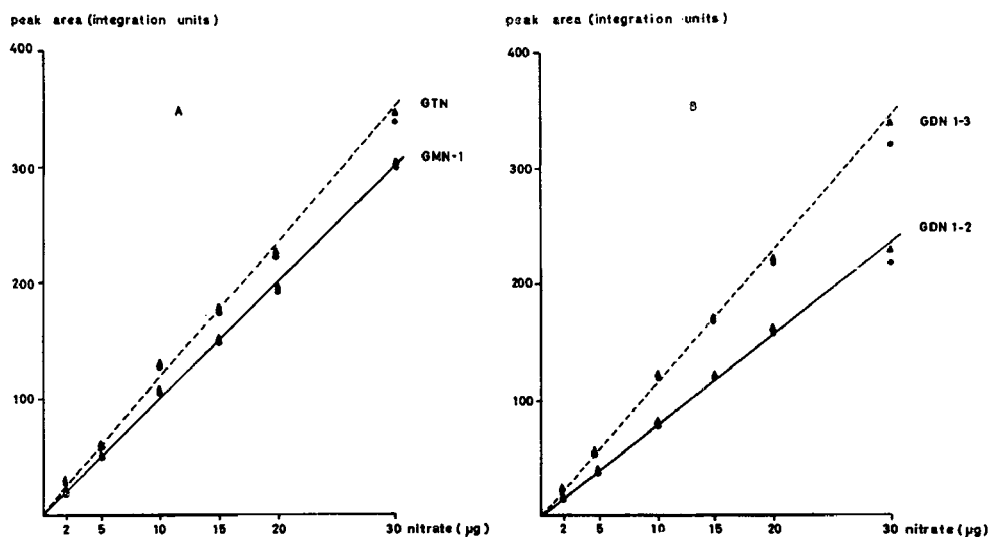


Fig. 1. Relationship between densitometer peak area (expressed in integration units) and amount of four different glyceryl nitrates (expressed as μg nitrate), spotted on thin-layer plates. (A) GTN: glyceryl trinitrate; GMN 1: glyceryl 1-mononitrate. (B) GDN 1-2: glyceryl 1-2-dinitrate; GDN 1-3: glyceryl 1-3-dinitrate. \bullet = uncorrected peak area; \blacktriangle = peak area $\times e^{-2\Delta A_0}$ (plate or baseline correction).

nitrates and the peak area. These curves were obtained by spotting increasing amounts (2–30 μg of nitrate) of one of the glyceryl nitrates used on one plate and by plotting the peak area *versus* the amount spotted. Fig. 1 gives a representative example for each of the four glyceryl nitrates. As the plate-to-plate correction did not prove to be satisfactory (see DISCUSSION), no attempt was made to calculate mean calibration curves (*i.e.* curves calculated from results on different plates). The correction factor for variations in one plate was applied.

Colorimetry

If one measures colorimetrically increasing amounts of inorganic or organic nitrates, a linear relationship between absorbance and nitrate content can be seen, up to 30 μg of nitrate.

To test the reproducibility of the colorimetric determination, the absorbance for six 10- μl samples of GTN, equivalent to 10 μg nitrate each, was measured. For a mean absorbance of 0.289, a relative standard deviation of 4.1% was found. If one spots these small amounts of GTN on a thin-layer plate and elutes them without developing the plate, the material eluted gives an absorbance of 0.272 ($n = 6$), with a relative standard deviation of 7.0%. This absorbance equals 93.2% of the mean absorbance found with colorimetry without spotting (*i.e.* a recovery of 93.2%).

After spotting small quantities of GTN on a plate and developing the plate, the same elution and determination procedure can be followed. For 2 μg of GTN spotted, the mean absorbance ($n = 6$) is 0.054 with a relative standard deviation of 12.6%. The recovery of GTN is 90.0%. For 10 μg of GTN spotted, for six measurements on one plate the mean absorbance was 0.257, with a relative standard deviation of 7.5% and a recovery of 88.9%; for six measurements on another plate, the mean

TABLE II

REPRODUCIBILITY OF SCANNING OF GTN SPOTTED ON FOURTEEN DIFFERENT THIN-LAYER PLATES
10 and 20 μg GTN (expressed as nitrate content) were spotted on each plate. The peak area is given in integration units. Corrected peak area is obtained by multiplying with the plate-to-plate correction factor.

Chromato- gram No.	Peak area		Corrected peak area	
	10 μg	20 μg	10 μg	20 μg
1	101.7	217.0	145.7	311.0
2	135.8	214.1	172.6	272.1
3	148.1	287.4	188.8	366.4
4	135.0	241.2	205.5	367.1
5	119.6	213.4	191.4	341.4
6	136.2	244.1	207.3	371.5
7	141.3	241.0	200.5	342.0
8	123.0	229.4	179.8	335.4
9	121.7	211.0	177.9	308.5
10	115.6	209.0	202.3	365.9
11	165.6	298.0	262.3	472.0
12	180.0	342.2	243.0	461.9
13	128.4	224.0	166.5	290.5
14	192.6	338.5	223.8	393.3
mean	138.9	250.7	197.8	357.1
S _{rel}	18.3	18.6	15.5	16.1

absorbance was 0.251 with a relative standard deviation of 7.9% and a recovery of 86.8%.

DISCUSSION

For quantitative analysis of glyceryl nitrates on thin-layer plates, both colorimetry and densitometry can be used. Indeed the calibration curves indicate a good linear relationship between peak area (densitometry) or absorbance (colorimetry) at one side, and the amount of glyceryl nitrates at the other side, and this up to a nitrate content of 30 μg . For both methods the organic nitrates used (and for that matter inorganic nitrates also) give, for the same content of nitrate, similar results.

Densitometry, with its obvious advantages of simplicity and speed, presents several difficulties. The unequal thickness of a plate provokes irregularities in the baseline. For a nitrate content of 5 to 20 μg , we found a reproducibility, for sets of six measurements, of 2.4 to 4.4% (uncorrected values). These values compare favourably to the results reported, *e.g.* for amino acid determination on thin-layer plates⁴.

For small amounts of nitrates, *e.g.* 2 μg , the relative standard deviation can be as high as 11.1%. Such a variability can be ascribed to the irregular baseline course, making the definition of start and end of the peak area very difficult. Application of the plate correction yields better results in the case of large amounts of nitrate; for 2 μg nitrate this is not true. To us the results of densitometry for 2 μg nitrate look unacceptable.

A second problem in the densitometry is the use of a calibration curve obtained on a set of plates, for quantitation of unknown amounts of nitrates on other plates. For a set of measurements on 14 plates, a relative standard deviation of 18.3% (for

10 μg nitrate) and 18.6% (for 20 μg nitrate) is calculated. Application of the correction for plate-to-plate variation does not improve the results significantly. Although spraying and UV irradiation were rigidly standardised, they probably introduce a variability not correctable by the correction factor used; indeed in the case of dyes, where one can scan on a non-sprayed colourless background, the plate-to-plate correction yields very satisfactory results (non-published results). The lack of reproducibility from plate-to-plate precludes the use of a given calibration curve for measuring the amounts of nitrate on different thin-layer plates. This difficulty can be overcome by using internal standards, *i.e.* by spotting known quantities of the substances used on each plate.

Colorimetry is in itself a reproducible technique, for 10 μg of nitrate six measurements give a relative standard deviation of 4.1%; this variability is due in part to the manipulation of such small volumes (10 μl) and to the inherent variability of colorimetric procedures¹². As expected, the relative standard deviations of measurements after spotting and elution increase. Here a calibration curve obtained once can be used for measurements from other plates. With this method one has to take into account the loss of material during the elution procedure; we usually obtain a recovery of around 90%. As we see no reason why recovery should be different from plate to plate, we think a sensible way of coping with this problem is to control the recovery from known amounts of material at given time intervals.

Concluding we can say that both colorimetry and densitometry can be used for quantitative estimation of glyceryl nitrates on thin-layer plates. An advantage of the colorimetry is that the spot size and uniformity of thickness of the silica gel layer are not important. Densitometry is obviously economical, considering time and effort. The reproducibility of the latter method seems to be at least as good as the reproducibility with colorimetry; it is, however, necessary to use internal standards because of the high plate-to-plate variability. Both methods seem less suitable for quantities of 2 μg of nitrate or less.

REFERENCES

- 1 M. G. BOGAERT, M.-T. ROSSEEL AND A. F. DE SCHAEPRYVER, *Arch. Int. Pharmacodyn.*, 179 (1969) 480.
- 2 M. G. BOGAERT, M.-T. ROSSEEL AND A. F. DE SCHAEPRYVER, *European J. Pharmacol.*, 1a (1970) 224.
- 3 M. C. CREW AND F. J. DICARLO, *J. Chromatog.*, 35 (1968) 506.
- 4 H. ZÜRCHER, G. PATAKI, J. BORKO AND R. W. FREI, *J. Chromatog.*, 43 (1969) 457.
- 5 I. DUNSTAN, J. V. GRIFFITHS AND S. A. HARVEY, *J. Chem. Soc., GB.* (1965) 1319.
- 6 M. G. BOGAERT, M.-T. ROSSEEL AND A. F. DE SCHAEPRYVER, *Arch. Int. Pharmacodyn.*, 176 (1968) 458.
- 7 P. NEEDLEMAN AND J. C. KRANTZ, JR., *Biochem. Pharmacol.*, 14 (1965) 1225.
- 8 L. D. HAYWARD, R. A. KITCHEN, D. J. LIVINGSTONE, *Can. J. Chem.*, 40 (1962) 434.
- 9 J. GOLDMAN AND R. R. GOODALL, *J. Chromatog.*, 32 (1968) 24.
- 10 J. GOLDMAN AND R. R. GOODALL, *J. Chromatog.*, 40 (1969) 345.
- 11 O. J. LORENZETTI, A. TYE AND J. W. NELSON, *J. Pharm. Sci.*, 55 (1966) 105.
- 12 E. J. SHELLARD AND M. Z. ALAM, *J. Chromatog.*, 35 (1968) 72.

J. Chromatog., 53 (1970) 263-268

CHROM. 5010

DÜNNSCHICHTCHROMATOGRAPHISCH-ENZYMATISCHER NACHWEIS
VON CARBAMATENI. NACHWEIS INSEKTIZIDER CARBAMATE MIT
RINDERLEBER-ESTERASE

F. GEIKE

*Biologische Bundesanstalt für Land- und Forstwirtschaft, Institut für Pflanzenschutzmittelforschung,
D 1 Berlin 33 (B.R.D.)*

(Eingegangen am 24. August 1970)

SUMMARY

Thin-layer chromatographic-enzymatic identification of carbamates. I. Identification of carbamate insecticides with bovine liver esterase

The thin-layer chromatographic-enzymatic inhibition technique is used to detect nine carbamate insecticides. The minimum quantities detected under normal conditions were: Minacide 6 ng; Methiocarb 400 ng; Zectran 80 ng; Carbaryl 3 ng; Pyramat 200 ng; Dimetan 80 ng; Isolan 10 ng; Dimetilan 60 ng; and Pyrolan 40 ng. After bromine treatment some carbamates (Carbaryl, Dimetan, and Dimetilan) show stronger inhibition activity against bovine liver esterase while the other show no difference or were weaker inhibitors. After ultraviolet irradiation all carbamates studied lost most of their antiesterase activity.

Unsatisfactory results were obtained when studying the resolution of the carbamates in thirteen solvent systems.

EINLEITUNG

Arbeiten über Carbamat-Insektizide begannen Ende der 40-iger Jahre und führten zur Entwicklung einiger bekannter Wirkstoffe, bei denen es sich fast ausschliesslich um Heterocyclen und aufgrund des beschrittenen Syntheseverfahrens ausnahmslos um N-Dimethylcarbamate handelte. In der zweiten Hälfte der 50-iger Jahre wurde Carbaryl (Sevin), das wohl bekannteste Carbamat-Insektizid entwickelt. Mit diesem wie auch den meisten später entwickelten Wirkstoffen erfolgte der Übergang zu aromatischen Verbindungen und vor allem zu den wesentlich wirksameren N-Monomethylverbindungen, welche die früheren Substanzen fast völlig verdrängten. Da der Trend heute zu den weniger persistenten Verbindungen geht, dürfte dieser Insektizidgruppe eine grosse Zukunft bevorstehen.

Die Carbamate stellen einigermaßen kräftige Cholinesterase-Hemmer dar, hemmen daneben jedoch auch wahrscheinlich ausnahmslos die Aliesterasen der Insekten¹. Trotz ihrer allgemein guten Anticholinesterase-Wirkung konnte keine generelle Korrelation zwischen der Cholinesterase-Hemmung und der insektiziden Wirkung festgestellt werden: Verbindungen mit sehr guten Anticholinesterase-Eigenschaften waren gegenüber Stubenfliegen praktisch ungiftig und solche mit geringer Hemmwirkung zeigten starke Toxizität². Der Grund für diese Diskrepanzen lässt sich nicht eindeutig angeben; er könnte einerseits in einem verstärkten Stoffwechsel der starken Antiesterase-Substanzen zu suchen sein, andererseits darin liegen, dass der Wirkstoff den Wirkungsort nicht erreicht. Da die Cholinesterasen—selbst von nahe verwandten Arten—ziemlich unterschiedlich durch einen Wirkstoff gehemmt werden, wie mit Organophosphaten gezeigt wurde³, besteht auch die Möglichkeit, dass die Diskrepanzen zwischen Cholinesterase-Hemmung und Toxizität auf Unterschieden in der Hemmbarkeit der Enzyme beruhen, da für den Esterase-Test seinerzeit eine Enzympräparation aus Zitteraalen (*Gymnotus electricus*) verwendet wurde². Trotz dieser Widersprüche besteht in der allgemeinen Lehrmeinung kein Zweifel daran, dass die Carbamate durch eine Hemmung der Acetylcholinesterase wirken.

Die Esterase-Hemmung kann bei Carbamaten ebenso wie bei Phosphorsäureestern zum recht empfindlichen dünn-schichtchromatographisch-enzymatischen Nachweis ausgenutzt werden, dennoch wurde von dieser Möglichkeit nur bei den Organophosphaten in grösserem Umfange Gebrauch gemacht. Aus der Gruppe der Carbamat-Insektizide hingegen wurden höchstens einige der bekanntesten in Untersuchungen über Methoden zum dünn-schichtchromatographisch-enzymatischen Nachweis von Phosphorsäureestern eingeschlossen⁴⁻⁸. Lediglich eine Arbeit befasste sich intensiver mit dem dünn-schichtchromatographisch-enzymatischen Nachweis einiger besonders verbreiteter Carbamat-Insektizide⁹. Vorliegende Arbeit soll auf diesem Gebiet eine Lücke schliessen und einerseits die Nachweisgrenzen von insektiziden Carbamaten nach verschiedenen Vorbehandlungen, andererseits Möglichkeiten für ihre dünn-schichtchromatographische Trennung untersuchen.

MATERIAL UND METHODEN

Reagenzien

Alle verwendeten Lösungsmittel und Chemikalien waren analysenrein und stammten von der Firma Merck, Darmstadt. Zur Plattenbeschichtung wurde Kieselgel G nach Stahl mit ca. 13% CaSO_4 und einer mittleren Korngrösse von 10–40 μ genommen.

Enzym- und Substratlösung

Die Herstellung der Enzympräparation und Substratlösung erfolgte nach ACKERMANN¹⁰, wurde jedoch, wie an anderer Stelle beschrieben¹¹, modifiziert. Insgesamt wird das Enzym etwa 1:40 verdünnt.

Insektizidlösungen und Dünnschichtchromatographie

Die untersuchten Wirkstoffe in analytischer Standardqualität (Tabelle I) wurden in Aceton gelöst, auf handgegossene Kieselgel G-Platten¹¹ aufgetragen und in verschiedenen Systemen (Tabelle II) chromatographiert.

TABELLE I

NAME UND STRUKTUR DER UNTERSUCHTEN CARBAMAT-INSEKTIZIDE

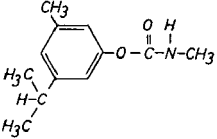
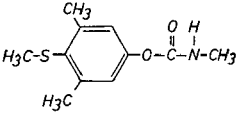
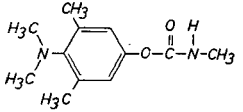
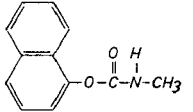
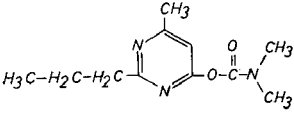
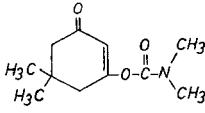
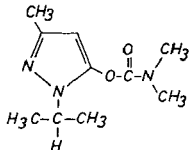
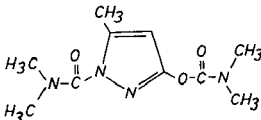
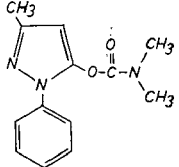
Trivial-Name	Chemische Bezeichnung	Strukturformel
Minacide (Promecarb)	3-Methyl-5-isopropylphenyl-N-methylcarbamate	
Methiocarb (Mesurol)	4-(Methylthio)-3,5-xylyl-N-methylcarbamate	
Zectran	4-(Dimethylamino)-3,5-xylyl-N-methylcarbamate	
Carbaryl (Sevin)	1-Naphthyl-N-methylcarbamate	
Pyramat	2-n-Propyl-4-methylpyrimidyl-(6)-N,N-dimethylcarbamate	
Dimetan	5,5-Dimethyl-1-oxocyclohex-2-enyl-(3)-N,N-Dimethylcarbamate	
Isofan	1-Isopropyl-3-methylpyrazolyl-(5)-N,N-dimethylcarbamate	
Dimetilan	2-Dimethylcarbamyl-3-methylpyrazolyl-(5)-N,N-dimethylcarbamate	
Pyrolan	1-Phenyl-3-methylpyrazolyl-(5)-N,N-dimethylcarbamate	

TABELLE II

VERWENDETE LAUFMITTELSYSTEME (v/v) ZUR TRENNUNG DER UNTERSUCHTEN CARBAMATE

Nr. Laufmittelsysteme

1	Cyclohexan
2	Äthylmethylketon
3	Benzol-Aceton (95:5)
4	Benzol-Aceton (66:34)
5	Benzol-Dichlormethan (30:120)
6	Benzol-Chloroform (30:120)
7	Chloroform-Acetonitril (20:10)
8	Chloroform-Wasser (untere Phase) (90:50)
9	Cyclohexan-Dioxan (70:30)
10	Cyclohexan-Äthyläther (10:90)
11	Cyclohexan-Aceton (80:20)
12	Cyclohexan-Aceton-Toluol (50:10:10)
13	Cyclohexan-Aceton-Toluol-Äthylacetat (20:20:10:10)

Durchführung des enzymatischen Hemmtestes

Die Platten wurden nach dem Entwickeln entweder sofort oder nach halbstündiger Bestrahlung mit ungefiltertem UV-Licht¹¹ zunächst leicht mit Puffer, anschliessend mit Enzymlösung besprüht und nach halbstündiger Inkubation bei 37° in der von ACKERMANN¹⁰ beschriebenen Weise weiterbehandelt. Im Falle der Brombehandlung werden die Platten nach dem Entwickeln mit einer gesättigten wässrigen Bromlösung besprüht und erst mit Puffer und Enzymlösung behandelt, wenn auf der Platte kein Bromgeruch mehr wahrzunehmen war und nochmals kurz mit Warmluft nachbehandelt wurde.

ERGEBNISSE UND DISKUSSION

Bei der hier angewandten Methode erscheinen die untersuchten Carbamate als helle Flecke auf violettem Untergrund. Zur Festlegung der unteren Nachweisgrenze der Insektizide wurden nur die aufgetragenen Mengen gewertet, die gerade noch sichtbare permanente Hemmflecke auf den DC-Platten hervorriefen. Die Ergebnisse in Tabelle III zeigen recht unterschiedliche Nachweisgrenzen, wobei Carbaryl mit 3 ng als stärkster und Methiocarb mit 400 ng als schwächster Esterase-Hemmer erscheint. Die relativ grossen Unterschiede in der Nachweisempfindlichkeit dürften sich weniger aus der allgemein schwächeren Antiesterase-Wirkung der entsprechenden Wirkstoffe als vielmehr aus der vielfach beobachteten unterschiedlichen Empfindlichkeit der Esterasen verschiedener Herkunft^{3,6,7} herleiten lassen. Sofern keine anderen Faktoren für eine Resistenz verantwortlich sind, dürften diese Unterschiede in der Empfindlichkeit der Acetylcholinesterase auch die Selektivität von Carbamaten bedingen.

Die hier ermittelte Grenzkonzentration für Carbaryl (3 ng) stimmt bei in etwa vergleichbarer Methode zum Teil recht gut (5 ng) (Lit. 5), zum Teil weniger gut (100 ng) (Lit. 9) mit anderen Arbeiten überein. Wie entscheidend die Methodik bei den verschiedenen Arbeiten ist, zeigt ein Vergleich zwischen Arbeiten von WINTERLIN *et al.*⁶ und MENN UND MCBAIN⁴, wo die Nachweisgrenzen für Carbaryl bei 25 ng bzw. 200 ng liegen, obwohl die gleiche Enzymquelle (Humanserum) benutzt wurde. Am empfind-

lichsten scheint jedoch der Nachweis mit Insektenhirn-Esterase zu sein, da Carbaryl mit Bienenhirn-Cholinesterase bis zu einer Konzentration von 1 pg nachzuweisen ist⁶. Allerdings dürfte sich diese Methode kaum für einen Routinenachweis eignen.

Auch für einige andere untersuchte Wirkstoffe liegen Vergleichszahlen aus anderen Arbeiten vor. Methiocarb (Mesurol) schneidet gegenüber den Werten von WALES *et al.*⁹ (100 ng) wesentlich schlechter ab, während Zectran gegenüber jenen Werten (500 ng) erheblich empfindlicher nachgewiesen wurde. Obwohl die Ergebnisse von MENN UND MCBAIN⁴ aufgrund der verschiedenen Methodik nicht unmittelbar mit den hier gefundenen Grenzkonzentrationen vergleichbar sind, erscheint ein Vergleich dennoch interessant. Auch hier zeigt sich erneut, dass die Nachweisgrenze für Methiocarb (200 ng) im Vergleich mit den hier gefundenen 400 ng bei MENN UND MCBAIN erheblich günstiger liegt, während vorliegende Arbeit Zectran und Carbaryl (beide 200 ng) erheblich empfindlicher nachweist (Tabelle III). Nimmt man die für

TABELLE III

UNTERE NACHWEISGRENZEN VON NEUN CARBAMAT-INSEKTIZIDEN NACH VERSCHIEDENEN VORBEHANDLUNGEN INFOLGE HEMMUNG DER RINDERLEBER-ESTERASE

Nachweisgrenze in ng; Laufmittelsystem Benzol-Aceton (95:5); () Flecke etwa 5 min sichtbar.

Wirkstoff	Ohne Vorbehandlung	Nach Brombehandlung	Nach UV-Bestrahlung
Minacide	6 (4)	6 (4)	80
Methiocarb	400 (200)	700 (300)	800
Zectran	80 (60)	500 (400)	1000
Carbaryl	3 (1)	0.9 (0.3)	60
Pyramat	200 (100)	400 (200)	900
Dimetan	80 (40)	60 (50)	100
Isolan	10 (8)	50 (30)	900
Dimetilan	60 (20)	40 (30)	900
Pyrolan	40 (30)	40 (20)	600

kurze Zeit erscheinenden und im Laufe der fortschreitenden Ausfärbung der Platte wieder verschwindenden Flecke, so gestaltet sich der Nachweis zum Teil noch erheblich empfindlicher (Tabelle III).

Allgemein ist festzustellen, dass der dünnschichtchromatographisch-enzymatische Nachweis durch Arbeiten mit stark verdünntem Enzym erheblich empfindlicher gestaltet werden kann. Die hier mitgeteilten Ergebnisse sind mit mittleren Verdünnungen des Enzyms erhalten worden. In diesem Zusammenhang wäre es eventuell günstiger, wenn man sich allgemein darauf einigen könnte, statt der bisher üblichen Verdünnungen den verwendeten Enzymgehalt in Einheiten pro ml anzugeben.

Nach Behandlung der Wirkstoffe mit Bromwasser zeigt sich lediglich bei Carbaryl, Dimetan und Dimetilan eine Verbesserung der Nachweisempfindlichkeit, während Minacide und Pyrolan nicht beeinflusst werden. Alle übrigen untersuchten Wirkstoffe zeigen zum Teil eine drastische Verschlechterung der Nachweisempfindlichkeit (Tabelle III). In den Fällen, wo ein Vergleich der hier erhaltenen Ergebnisse mit denen anderer Autoren möglich ist, stimmen sie grössenordnungsmässig weitgehend überein. WALES *et al.*⁹ finden für Carbaryl eine Verbesserung um den Faktor 10 und können Methiocarb und Zectran nach Brombehandlung nicht mehr nachweisen,

während hier für Carbaryl etwa eine Verbesserung um den Faktor 3 und für Methiocarb und Zectran eine Verschlechterung um den Faktor 1.75 bzw. 6.25 festzustellen ist. Interessant ist, dass mit Humanplasma-Esterase und Bienenhirn-Esterase nach Brombehandlung kein Carbaryl mehr nachgewiesen wurde⁶, obwohl vorliegende Ergebnisse und die von MENDOZA *et al.*⁷ und WALES *et al.*⁹ eine Verbesserung der Nachweisempfindlichkeit zeigen.

Eine Bestrahlung der Wirkstoffe mit ungefiltertem UV-Licht nach dem Entwickeln führt, wie aus Tabelle III hervorgeht, zu einer erheblichen Verschlechterung der Nachweisempfindlichkeit. Dieses Ergebnis stimmt—zumindest teilweise—mit dem von MENDOZA *et al.*⁸ überein, die mit Rinderleber-Esterase nach Brombehandlung 1 ng Carbaryl nachweisen konnten, während nach UV-Bestrahlung dieser Nachweis nicht mehr möglich war. Mit einem Enzymextrakt aus Schaf-, Schweine- oder Affenleber hingegen war dieser Nachweis noch möglich, so dass auch hier wieder Unterschiede in der Empfindlichkeit bei den Enzymen verschiedener Herkunft deutlich zutage treten. Damit verhalten sich die Carbamat-Insektizide beim Nachweis mit Rinderleber-Esterase völlig anders als beispielsweise die Phosphorsäureester¹⁰ und Chlorkohlenwasserstoffe¹¹, die durch die UV-Bestrahlung in zum Teil kräftige Esterase-Hemmer übergehen.

Eine intensive UV-Bestrahlung der Wirkstoffe dürfte unter anderem zu einer Hydroxylierung oder Epoxid-Bildung führen. Es hat sich jedoch gezeigt, dass einige hydroxylierte Metaboliten erhebliche Anticholinesterase-Aktivität besitzen¹², dass eine Hydroxylierung also nicht unbedingt die Hemmwirkung zerstören muss, wenn sie sie zweifelsohne auch vielfach vermindert. Sicher ist, dass Carbamate einen durch Licht katalysierten Abbau erleiden¹³. Eine Bestrahlung von sechs Methylcarbamaten mit Sonnenlicht und UV führte zu zahlreichen unbekannten Abbauprodukten, von denen viele ebenfalls Anticholinesterase-Aktivität zeigten¹³. Eine ältere Arbeit über Zectran weist ebenfalls eine Photozersetzung nach, wobei es zu erheblicher Toxizitätsabnahme kam¹⁴. Welche Photozersetzungsprodukte entstanden, wurde hier nicht untersucht. Nach den vorliegenden Ergebnissen scheinen jedoch Carbaryl und Minacide am stabilsten zu sein oder in relativ starke Antiesterase-Substanzen überzugehen.

Neben dem reinen Nachweis der Carbamat-Insektizide und der Untersuchung des Einflusses von Brom und UV auf denselben sollte versucht werden, die Wirkstoffe dünn-schichtchromatographisch zu trennen. Die in Tabelle IV wiedergegebenen hR_F -Werte stellen Mittelwerte aus grösseren Versuchsreihen dar. Allgemein kann man mittlere Schwankungen der hR_F -Werte beobachten. Diese sind wahrscheinlich auf Witterungseinflüsse zurückzuführen, da die Arbeiten in normalen Laborräumen ohne jede Klimatisierung durchgeführt wurden. Nimmt man jedoch einen Wirkstoff (z.B. Minacide) als Bezugssubstanz, so halten sich die Schwankungen in wesentlich engeren Grenzen. Auffallend ist, dass bei Carbaryl, Zectran, Isolan und in geringerem Masse auch bei Minacide oft ein schwacher Nebenfleck auftrat. Ob es sich bei dieser Antiesterase-Substanz um eine Verunreinigung des Wirkstoffes handelt, konnte nicht festgestellt werden. Wie aus Tabelle IV weiter hervorgeht, ist mit den dreizehn intensiver untersuchten Laufmitteln eine Trennung und Identifizierung einzelner Wirkstoffe durchaus möglich, sofern bekannt ist, um welche es sich handelt. Für die Analyse eines Wirkstoffgemisches unbekannter Zusammensetzung mit eindimensionaler Chromatographie eignet sich jedoch kaum eines der Laufmittel, da stets eine Reihe

TABELLE IV

 hR_F -WERTE DER UNTERSUCHTEN CARBAMAT-INSEKTIZIDE IN VERSCHIEDENEN LAUFMITTELSYSTEMEN (AUFTRAGMENGE 1 μ g)

Carbamat-Insektizide	Laufmittel												
	1	2	3	4	5	6	7	8	9	10	11	12	13
Minacide	0	98	39	85	30	30	95	25	59	80 (69)	39 (31)	33 (23)	79
Methiocarb	0	98	31	79	9.2	10.8	90	7.7	52	72	31	24	74
Zectran	0	98	37	85 (78)	15 (27)	22 (3.8)	95 (65)	20 (0)	58 (39)	79	39 (31)	32 (22)	80 (73)
Carbaryl	0	98	32 (8.5)	79 (66)	23	22 (5.4)	92 (79)	17 (0)	48 (22)	67 (38)	30 (15)	24 (5.4)	73 (61)
Pyramat	0	85	12	69	1.5	5.4	73	1.5	54	39	35	24	68
Dimetan	0	92	18	73	2.3	10	84	3.1	49	49	32	22	69
Isolan	0	91	19 (9.2)	72 (61)	3.1	6.9	76 (68)	2.3	49 (39)	51 (26)	34 (25)	25 (15)	68 (58)
Dimetilan	0	82	9.2	62	1.5	5.4	68	1.5	35	19	20	12	55
Pyrolan	0	98	30	84	4.6	11.6	89	5.4	55	65	37	30	76

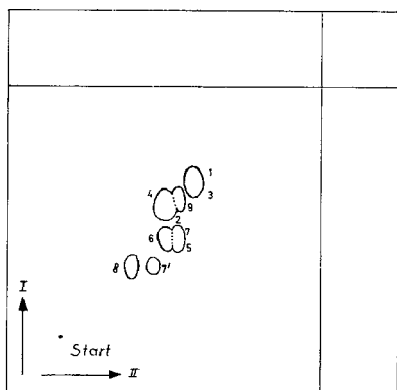


Fig. 1. Zweidimensionale Dünnschichtchromatographie der untersuchten Carbamate. Laufmittel: (I) Benzol-Aceton (90:10); (II) Cyclohexan-Aceton (75:25).

von Wirkstoffen ähnliche R_F -Werte aufweist. Lediglich die zweidimensionale Chromatographie mit beispielsweise Laufmittel 3 und 5 oder 3 und 11 führt zu einer gewissen Auftrennung der Wirkstoffe, doch wurden auch hier einige Substanzen nicht getrennt. Abbildung I zeigt den Versuch einer zweidimensionalen Chromatographie der Wirkstoffe mit den modifizierten Laufmittelsystemen 3 und 11.

Zusammenfassend lässt sich feststellen, dass der Nachweis mit Rinderleber-Esterase zu recht zufriedenstellenden Ergebnissen führt und nur zwei der untersuchten Wirkstoffe in ihrer Nachweisempfindlichkeit aus dem Rahmen fallen. UV-Bestrahlung führt zu einer kräftigen Verminderung der Nachweisempfindlichkeit, während sie von Brom recht unterschiedlich beeinflusst wird. Eine chromatographische Identifizierung der Wirkstoffe stösst mit den untersuchten Laufmitteln auf gewisse Schwierigkeiten, da eine Reihe von Substanzen eindimensional nicht zu trennen ist. Bei zweidimensionaler Chromatographie finden sich erste Ansätze zu einer Auftrennung der Wirkstoffe, doch sind die Ergebnisse noch nicht voll befriedigend.

DANK

Mein besonderer Dank gilt Fräulein I. BLEICH für die sorgfältige Mitarbeit bei der Durchführung der Versuche.

ZUSAMMENFASSUNG

Die DC-Enzymhemmungs-Methode wird zum Nachweis einiger Carbamat-Insektizide angewandt. Unter Normalbedingungen beträgt die untere Nachweisgrenze: Minacide 6 ng; Methiocarb 400 ng; Zectran 80 ng; Carbaryl 3 ng; Pyramat 200 ng; Dimetan 80 ng; Isolan 10 ng; Dimetilan 60 ng und Pyrolan 40 ng. Nach Brombehandlung zeigen einige Carbamate (Carbaryl, Dimetan und Dimetilan) eine stärkere Hemmung der Rinderleber-Esterase, während die anderen keinen Unterschied zeigten oder in schwächere Inhibitoren übergingen. Nach UV-Bestrahlung verlieren alle untersuchten Carbamate den grössten Teil ihrer Antiesterase-Aktivität.

Die Ergebnisse bei Trennversuchen der Carbamate in dreizehn Laufmittelsystemen waren unbefriedigend.

LITERATUR

- 1 F. W. PLAPP UND W. S. BIGLEY, *J. Econ. Entomol.*, 54 (1961) 793.
- 2 J. E. CASIDA, K. B. AUGUSTINSSON UND G. JONSSON, *J. Econ. Entomol.*, 53 (1960) 205.
- 3 S. D. MURPHY, R. R. LAUWERGS UND K. L. CHEEVER, *Toxicol. Appl. Pharmacol.*, 12 (1968) 22.
- 4 J. J. MENN UND J. B. MCBAIN, *Nature*, 209 (1966) 1351.
- 5 C. E. MENDOZA, P. J. WALES, H. A. MCLEOD UND W. P. MCKINLEY, *Analyst*, 93 (1968) 34.
- 6 W. WINTERLIN, G. WALKER UND H. FRANK, *J. Agr. Food Chem.*, 16 (1968) 809.
- 7 C. E. MENDOZA, D. L. GRANT, B. BRACELAND UND K. A. MCCULLY, *Analyst*, 94 (1969) 805.
- 8 C. E. MENDOZA, P. J. WALES, D. L. GRANT UND K. A. MCCULLY, *J. Agr. Food Chem.*, 17 (1969) 1196.
- 9 P. J. WALES, H. A. MCLEOD UND W. P. MCKINLEY, *J. Assoc. Offic. Anal. Chemists*, 51 (1968) 1239.
- 10 H. ACKERMANN, *J. Chromatog.*, 36 (1968) 309.
- 11 F. GEIKE, *J. Chromatog.*, 44 (1969) 95.
- 12 H. W. DOROUGH UND J. E. CASIDA, *J. Agr. Food Chem.*, 12 (1964) 244.
- 13 D. G. CROSBY, E. LEITIS UND W. L. WINTERLIN, *J. Agr. Food Chem.*, 13 (1965) 204.
- 14 E. E. KENAGA, A. E. DOTY UND J. L. HARDY, *J. Econ. Entomol.*, 55 (1962) 466.

J. Chromatog., 53 (1970) 269-277

CHROM. 4961

THE SEPARATION OF FREE DICARBOXYLIC ACID PORPHYRINS USING THIN-LAYER AND PAPER CHROMATOGRAPHY

R. V. BELCHER, S. G. SMITH, R. MAHLER AND J. CAMPBELL

Tenovus Institute for Cancer Research, Welsh National School of Medicine, Heath, Cardiff, S. Wales (Great Britain)

(Received August 4th, 1970)

SUMMARY

Mixtures of protoporphyrin, deuteroporphyrin, haematoporphyrin, pemttoporphyrin and mesoporphyrin can be separated as free acids on talc thin-layer chromatography plates by developing them with a mixture of ethanol–2,6-lutidine–water (30:3:67) in tanks containing an atmosphere saturated with ammonia vapour. Monoacrylic monopropionic deuteroporphyrin (“S/411” porphyrin) can be separated from coproporphyrin using this system. The same mixture of two-carboxyl porphyrins can also be separated on Whatman No. 1 chromatography paper by developing with pyridine–0.2 *M* sodium borate buffer pH 8.6 (1:9) by either ascending or descending techniques.

INTRODUCTION

During current investigations of porphyrin extracts from various tissues¹ it became apparent that chromatographic separation and identification of component porphyrins without prior esterification was desirable because of the known labile nature of some two-carboxyl porphyrins to esterification procedures².

Existing chromatographic methods for separating free (unesterified) porphyrins depend on the number of carboxyl groups. The lutidine methods of NICHOLAS AND RIMINGTON³ and ERIKSEN⁴, using paper, separate free porphyrins in this manner. Uroporphyrin (eight carboxyl groups) remains near the base line and protoporphyrin (two carboxyl groups) runs near to the solvent front. Porphyrins possessing seven to three carboxyl groups occupy intermediate positions on the chromatogram. Separation of coproporphyrin (four carboxyl groups) I and III isomers is also possible by these methods.

Other systems using paper (PC) and talc thin-layer chromatography (TLC)^{5,6} separate free porphyrins in the reverse order, with uroporphyrin running near to the solvent front and two-carboxyl porphyrins remaining together near the base line.

A column method employing Sephadex dextran gels and borate buffers has been described by RIMINGTON AND BELCHER⁷, which separates free porphyrins depending on differences of adsorptive properties rather than the number of carboxyl groups

thus making possible the separation of some two-carboxyl porphyrins from each other.

Techniques using porphyrin methyl esters on paper or thin layers usually do not separate two-carboxyl porphyrins. However, a convenient TLC method described by HENDERSON AND MORTON⁸ will separate some two-carboxyl porphyrin esters. Also a two-dimensional method⁹ employing two solvent systems and reversed phase will separate at least six dicarboxylic porphyrin esters. A quick method of separating haematoporphyrin dimethyl ester from other dicarboxylic porphyrin esters is described also by CHU *et al.*¹⁰, which is useful for investigating porphyrins suspected of containing hydroxyl substituents by observing increased R_F values after acetylation¹¹.

The methods described below enable identification and preparative separation of haematoporphyrin (haemato), deuteroporphyrin (deutero), mesoporphyrin (meso), pemptoporphyrin (pempto) and protoporphyrin (proto), in addition to coproporphyrin (copro) and monoacrylic monopropionic deuteroporphyrin ("S/411"), all without prior esterification.

MATERIALS AND METHODS

All solvents used were of "Analar" quality except for 2,6-lutidine, which was supplied as laboratory reagent grade. Talc (fine powder purified by acids) was obtained from B.D.H. Ltd.

Pempto ester was kindly supplied by Professor A. H. JACKSON, University College, Cardiff and "S/411" ester, isolated from calf meconium, was a gift from Dr. D. NICHOLSON, Kings College Hospital Medical School, London. The esters were converted to the free acids by treating with 25% w/v HCl at room temperature in the dark for 14 and 72 h, respectively, with subsequent recovery into ether for application to chromatograms. The prolonged hydrolysis period required for the "S/411" ester is due to the known stability to normal hydrolysis procedures of the acrylic ester substituent¹.

Proto was obtained from the dimethyl ester by hydrolysing with 25% w/v HCl for 5 h at room temperature and recovering the free porphyrin by precipitation at the isoelectric point (approx. pH 3.9). Proto and other porphyrins used were obtained from the laboratory stock.

Talc plates (20 × 20 cm) were prepared by thoroughly shaking a mixture of 40 g of talc and 70 ml methanol and spreading over five glass plates to give a thickness of 0.25 mm using the "Shandon" thin-layer apparatus. The plates were allowed to dry at room temperature for 20 min before use. Chromatograms were prepared by applying porphyrins dissolved in 2 *N* ammonia and spread in bands 1–2 cm long and about 2 cm from the bottom of the plate. The optimum range of application to maintain consistently good separations was 0.1–20 µg per band. The chromatograms were developed in glass tanks (solvent ascending) with an atmosphere previously saturated for at least 1 h with ammonia vapour by placing two small beakers containing concentrated (s.g. 0.880) ammonium hydroxide at the bottom of the tanks and also a filter paper lining soaked in concentrated ammonia–water (1:1). The plates were placed in 200 ml of developing mixture containing 30% ethanol, 3% 2,6-lutidine and 67% water and allowed to develop in the tank for at least 2 h at a temperature range of 20–25°. For convenience, plates could be left to develop overnight giving an improved

separation of the two-carboxyl porphyrins. After drying the plate with a hair drier or allowing to dry at room temperature, the bands were eluted after observing their red fluorescence under UV light, by extracting the talc scrapings with 3 ml of 20% acetic acid-ether. The dissolved porphyrin was extracted from the ether into 1 ml of 1.5 *N* HCl and the Soret peaks determined using an Optica CF4R recording spectrophotometer.

Sheets of Whatman No. 1 chromatography paper (20 × 23 cm) were spotted 2 cm from the shortest edge with the previously described porphyrin solutions. Individual spots were not allowed to spread more than 0.5 cm diameter and if repeated application of sample to a spot was required a hair drier was used to dry the spot before further additions were made. The useful limits of loading were found to be 0.5–7 µg per spot. The papers were rolled into a cylinder and the edges stapled together to enable the chromatograms to stand freely in the tanks. Cylindrical glass tanks (13 × 28 cm) were allowed to equilibrate for 30 min before use with 20 ml of 0.880 ammonia placed at the bottom. The tanks were also lined with filter paper soaked in concentrated ammonia. The paper was conveniently soaked in water to enable the tanks to be lined, and concentrated ammonia was sprayed on to the paper *in situ* using a pasteur pipette.

Twenty millilitres of developing mixture containing pyridine and 0.2 *M* sodium borate buffer pH 8.6 (1:9) were placed in a suitably sized Petri dish placed at the bottom of the tanks and the chromatograms were developed with the mixture for at least 4 h at 20–25°. The chromatograms could also be developed overnight. After drying at 40° for 15 min the positions of the spots were marked after observing their red fluorescence under UV light.

This method was readily adapted for descending chromatography by preparing tanks as for the ascending technique and using larger volumes of developing solvent in the trough. A suitably sized tank to hold Whatman No. 1 paper 57 × 19 cm was a glass "Shandon" 300 Chromotank (55 × 20 × 35 cm). The papers were spotted on a base-line drawn 12 cm from the short edge. Development took at least 16 h at 20–25° and chromatograms could be left overnight allowing the solvent front to run off the end of the paper. Descending chromatograms could be more heavily loaded with upper limits of approx. 12 µg per spot.

RESULTS

Thin-layer chromatography

A mixture of two-carboxyl porphyrins consisting of haemato, deuterio, meso,

TABLE I

TLC SEPARATION OF TWO-CARBOXYL PORPHYRINS SHOWING RELATIONSHIP OF R_F VALUE TO HCl NUMBER

<i>Porphyrin</i>	R_F value	<i>HCl No.</i>
Haemato	0.35	0.10
Deuterio	0.32	0.30
Meso	0.25	0.50
Proto	0.19	2.50
Pempto	0.28	—

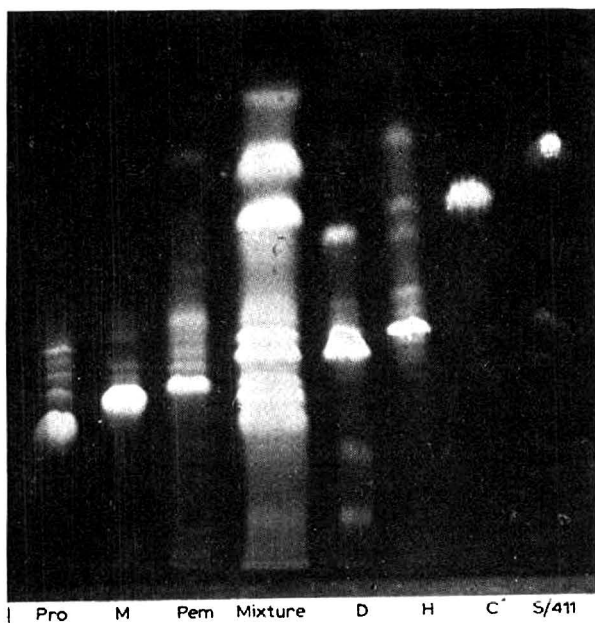


Fig. 1. Photograph taken under UV light of a typical TLC separation of porphyrins, Pro = proto, M = meso, Pem = pempto, D = deuterio, H = haemato, C = copro.

proto, and pempto separated according to their HCl numbers², with the possible exception of pempto, whose HCl number is not published. Table I shows that the most water-soluble (low HCl No.) porphyrins have the highest R_F values.

"S/411" porphyrin separates well from copro (R_F values 0.7 and 0.58, respectively) and since both porphyrins are tetracarboxylic and occur naturally in bile and certain tissues, a convenient method for separation and identification is important. Fig. 1 shows a typical separation with a 2-h development time. The faint bands that accompany the major components are due either to trace impurities or to artefacts. The results shown in Table II were obtained by determination of the Soret maxima after elution of marker and the appropriate component porphyrin separated from the

TABLE II

COMPARISON OF SORET MAXIMA OF PORPHYRIN MARKERS AND APPROPRIATE COMPONENTS OF MIXTURE AFTER TLC SEPARATION

Porphyrin	Soret (m μ) of marker	Soret (m μ) of porphyrin from mixture
Haemato	403	403
Deuterio	400	400
Meso	401-402	402
Proto	409	409
Pempto	404	404
S/411	410	411
Copro	403	403

TABLE III

COMPARISON OF R_F VALUES BY THREE METHODS OF TWO-CARBOXYL PORPHYRIN SEPARATION

<i>Porphyrin</i>	R_F (TLC)	R_F (<i>Paper,</i> <i>ascending</i>)	R_H^a (<i>Paper,</i> <i>descending</i>)
Haemato	0.35	0.53	1.0
Deutero	0.32	0.33	0.62
Meso	0.25	0.21	0.36
Pempto	0.28	0.21	0.36
Proto	0.19	0.09	0.10

^a R_H = position of spots relative to haemato.

mixture. The comparative values are sufficiently close to indicate good separation of bands with very little mutual contamination.

Paper chromatography

Table III shows the results of the separation of a mixture of porphyrins. It will be seen from the R_F values that the ascending and descending paper techniques give better separation of spots than the TLC technique. Consequently, the paper techniques are usually preferred for the identification of porphyrins. Unfortunately copro does not separate from the "S/411" porphyrin, and meso from pempto using the paper techniques.

Copro and "S/411" (R_F 0.87) run well above the two-carboxyl porphyrins when using the ascending method and do not interfere with their separation. Uroporphyrin runs with the solvent front.

DISCUSSION

The presence of ammonia in the tank atmosphere was essential for both TLC and PC. Mobilities and resolution were greatly depressed when ammonia was omitted⁴. Originally the TLC plates were prepared using Silica Gel G but because of unavoidable and extensive streaking of bands this medium was abandoned.

The use of borate buffer in the developing solvent prevented streaking of spots on paper runs. The effectiveness is probably due to the formation of a complex between the borate ion and the hydroxyl groups of the cellulose thus producing a de-adsorption effect. The pH of the buffer was found not to be critical. The usefulness of borate buffers in preventing streaking has been utilised for Sephadex column separation of free porphyrins⁷.

Although the TLC method separates a greater number of porphyrins (particularly copro and "S/411") the two-carboxyl porphyrins tend to "crowd" together, thus occasionally making individual identification difficult. The PC methods give spacing of the two-carboxyl porphyrins, making identification comparatively easy. Therefore, a combination of TLC and PC will give an excellent and comprehensive method of investigating mixtures of porphyrins eluted from two- or four-carboxyl porphyrin bands produced on 2,6-lutidine-water silica gel TLC plates¹² or directly from extracts of tissues.

Proto, pempto, deuterio and copro were readily detected in faecal extracts using the combination of TLC and PC. The "S/411" porphyrin was easily detected in ether extracts of dog bile contaminated with bile pigments. These did not interfere with the separation because they occupied positions between the two-carboxyl bands as small discrete areas. Other impurities ran diffusely near the solvent front.

ACKNOWLEDGEMENTS

We are grateful to Miss P. MARTIN and Mr. B. JONES of the departments of Medical Illustration and Photography, Dental Hospital, Heath, Cardiff for the preparation of the figures and photographs.

The generous support of the Abbotshill Trust is greatly appreciated.

REFERENCES

- 1 S. G. SMITH, R. V. BELCHER AND R. MAHLER, *Biochem. J.*, 114, No. 4 (1969) 88p.
 - 2 J. E. FALK, *Porphyrins and Metalloporphyrins*, Vol. 2, Elsevier, Amsterdam, 1964.
 - 3 R. E. H. NICHOLAS AND C. RIMINGTON, *Scand. J. Clin. Lab. Invest.*, 1 (1949) 12.
 - 4 L. ERIKSEN, *Scand. J. Clin. Lab. Invest.*, 10 (1958) 319.
 - 5 T. K. WITH, *Scand. J. Clin. Lab. Invest.*, 9 (1957) 395.
 - 6 T. K. WITH, *Clin. Biochem.*, 1 (1967) 30.
 - 7 C. RIMINGTON AND R. V. BELCHER, *J. Chromatog.*, 28 (1967) 112.
 - 8 R. W. HENDERSON AND T. C. MORTON, *J. Chromatog.*, 27 (1967) 180.
 - 9 T. C. CHU AND E. J. CHU, *J. Biol. Chem.*, 208 (1954) 537.
 - 10 T. C. CHU, A. A. GREEN AND E. J. CHU, *J. Biol. Chem.*, 190 (1951) 643.
 - 11 J. BARRETT, *Nature*, 183 (1959) 1185.
 - 12 R. V. BELCHER, S. G. SMITH AND R. MAHLER, *Clin. Chim. Acta*, 25 (1969) 45.
- J. Chromatog.*, 53 (1970) 279-284

CHROM. 5003

DEVELOPMENT AND COMPARISON OF THIN-LAYER CHROMATOGRAPHIC AND GAS-LIQUID CHROMATOGRAPHIC METHODS FOR MEASUREMENT OF METHIMAZOLE IN RAT URINE

J. B. STENLAKE, W. D. WILLIAMS AND G. G. SKELLERN

Drug Metabolism Unit, Department of Pharmaceutical Chemistry, School of Pharmaceutical Sciences, University of Strathclyde, Glasgow (Great Britain)

(Received July 28th, 1970)

SUMMARY

Thin-layer chromatographic and gas-liquid chromatographic methods have been developed for the measurement of methimazole in rat urine. Of the two methods, gas-liquid chromatography is the more sensitive, but because of the instability of the derivative which is used, replicate measurements must be made on the same day. The densitometric method is less sensitive because of interference by endogenous matter, but is more rapid and hence better suited to routine use.

INTRODUCTION

Little is known of the metabolism in humans of the antithyroid drugs carbimazole and methimazole, but recent studies by ALEXANDER *et al.*¹, have shown that [³⁵S]carbimazole is metabolised with release of [³⁵S]sulphate. Carbimazole is also known to be readily hydrolysed in acid and alkaline media to methimazole, and is believed to owe its anti-thyroid activity to the formation of methimazole *in vivo*². We have now confirmed that carbimazole is converted to methimazole in the presence of plasma *in vitro*. In seeking, therefore, to establish quantitative methods for determination of the distribution and fate of carbimazole when administered to human patients, we have focused attention firstly on methods for the detection and determination of methimazole.

Both infrared absorption³ and titrimetric procedures^{4,5} for the determination of methimazole are generally applicable only to relatively pure materials and could in no way be adapted to the very small quantity of methimazole expected in an extract of a biological fluid. The determination of thioimidazoles and thiopyrimidines colorimetrically using 2,6-dichloroquinonechlorimide^{6,7} although potentially applicable to measurements on biological extracts has been applied only to relatively pure methimazole. The sensitivity of the reaction is about 10 µg and we have, therefore, examined the use of this reagent for the development of spots, and for the quantitative determination of methimazole in urine extracts after chromatography on thin-layer plates.

Gas-liquid chromatography (GLC) is often the method of choice for the determination of drugs in low concentrations in blood and urine. CLARKE⁸ has reported that methimazole can be eluted from SE-30 columns, but this method proved unsatisfactory in our hands. We have found, also, that the methimazole peak shows considerable tailing on Apiezon L columns. We have, therefore, extended our studies of gas chromatographic methods to include alternative column packings, and methods based on the chemical modification of methimazole on the column.

EXPERIMENTAL

Materials and apparatus

Solvents. The solvents used were of A.R. grade or were re-distilled: methimazole (Nicholas Research); 2,6-dichloro-*p*-benzoquinone-4-chlorimine (DCQC), methyl iodide re-distilled, and *n*-tetradecane (B.D.H. Laboratory reagents).

Densitometric measurements. These were performed on a Chromoscan recording and integrating densitometer with a thin-layer attachment (Joyce, Loeb & Co. Ltd.). Operating conditions as follows. Chromoscan: aperture 10 × 0.5 mm, cam D, gain 5, optical wedge 0–0.5 O.D., light source 12 V, 100 W quartz iodine lamp. Thin-layer attachment: filter 465 mμ, aperture 10 × 1 mm, specimen expansion ratio 1:1, light source 12 V, 100 W standard tungsten projection lamp. The reflectance method of scanning was used.

Thin-layer chromatography. The plates (0.25 mm) were prepared from Merck Silica Gel G with zinc silicate (1%) as a phosphor. Plates (20 × 20 cm) were activated for 30 min at 110°, and stored at 30°. The developing solvent was the organic phase of a well-shaken mixture of chloroform-methanol-water (160:40:25), which gave *R_F* values of 0.44–0.46 for methimazole when freshly prepared. The detection reagent was 2,6-dichloroquinonechlorimide solution 0.4% in ethanol⁶.

Gas-liquid chromatography. GLC was performed on a Perkin-Elmer F11 with glass columns (6 ft. × 4 mm I.D.) packed with either Carbowax 20M (10%) plus potassium hydroxide (5%) on Chromosorb W (100–120 mesh), hereafter called column A; or Apiezon L grease (10%) plus potassium hydroxide (5%) on Chromosorb W (100–120 mesh), hereafter called column B; column temperature 180°; nitrogen flow rate 31 ml/min.

Methods

Animals, dosing and extraction of methimazole. Six male Sprague-Dawley rats (approx. 250 g) were used. Five of the rats were injected intraperitoneally with methimazole (2.17 mg) in water (0.5 ml). The sixth rat was used as control. The animals were kept in separate metabolism cages and no restriction was placed on food and water supplies. Total urines were collected over a period of 12 h and each made up to 20 ml with de-ionised water. Diluted urine (9.8 ml) was transferred to a separator (100 ml), saturated with sodium chloride and extracted with chloroform (3 × 50 ml).

Densitometric determination. Standard solutions of methimazole in chloroform were made, such that a volume (20 μl) contained 0.3, 0.4, 0.5, 0.6 and 0.7 μg for application to the plate. Samples were applied with a microliter pipette (Marburg; 10 μl; Eppendorf, Hamburg, G.F.R.).

The chloroform extracts obtained (above) were adjusted to appropriate volumes,

so that 20–30 μl of the extracts contained a suitable amount of methimazole for application to the plate.

Five standards plus three samples of the chloroform extract were applied to the plate approximately 2 cm from the edge of the plate, 2 cm apart and with a resultant diameter of the spot no greater than 5 mm. Plates were developed, dried at room temperature, sprayed with McALLISTER's reagent, and allowed to stand for 10 min. The entire width of the spots was scanned perpendicular to the solvent flow. For reflectance scanning, a piece of thick white filter paper was placed underneath the plate⁹.

Gas-liquid chromatographic determination. Column A: Methimazole (0.2, 0.4, 0.6, 0.8 mg) was dissolved in chloroform (1 ml). Each solution (1 μl) was injected onto the column, and after 5 min a subsequent injection (1 μl) of methyl iodide in acetone solution (0.1 ml/ml) made using a different syringe from that used for the methimazole injection. A calibration curve was plotted.

The peak of the derivative formed on column appeared at the retention time for S-methylmethimazole (3.2 min).

Column B: S-Methylmethimazole standards were prepared as follows. Methimazole (0.25, 0.5, 0.75, 1.0 mg) was dissolved in chloroform, methyl iodide (0.2 ml) added, and the solution left for 2 min. The volatile components were removed in a stream of nitrogen to dryness and methanol containing internal standard (*n*-tetradecane, 0.1 mg/ml) was added to each flask. Injections (1 μl) onto column B of each concentration were made to obtain the calibration curve.

Urine extracts. The chloroform extracts used for the densitometric determinations were evaporated to dryness in a stream of nitrogen, and methylated as de-

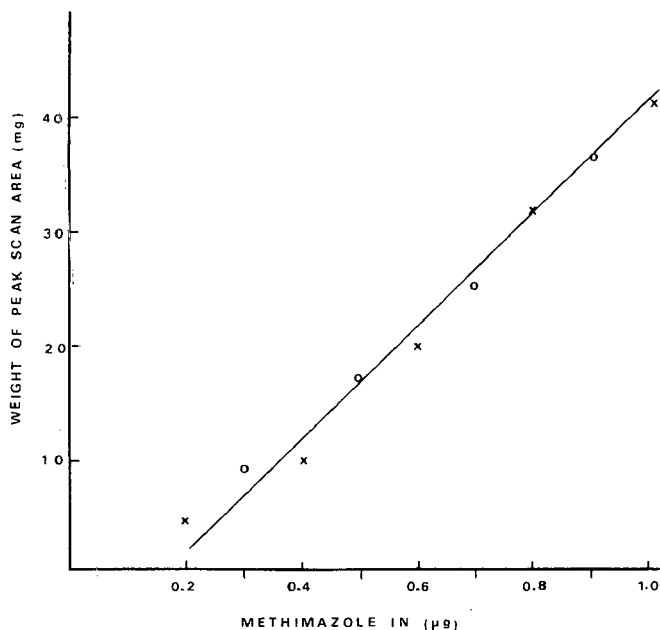


Fig. 1. Standard curve for pure methimazole added directly to plate (x—x—x) and recovered from urine (O—O—O).

scribed for the S-methylmethimazole standards. Methanol (100–200 μ l according to expected drug concentration and containing *n*-tetradecane) was added to each residue, and injections (1 μ l) made onto column B.

A chloroform extract of urine from the control was methylated by the same procedure, the residue was dissolved in methanol (100 μ l) and examined by GLC. No peak appeared at the retention time for internal standard (5.4 min) or for S-methylmethimazole (2.0 min).

RESULTS AND DISCUSSION

Densitometric determination. A typical standard curve for pure methimazole in solution is shown in Fig. 1. Direct correlation between peak height and concentration was not possible. Other workers^{9–11} used various methods of area measurement to correlate with the concentration of drug. We have used two methods (a) weight of peak scan area, and (b) area as defined by peak height \times width at half altitude⁹.

Table I shows the amounts of methimazole found in the urine extracts obtained using these methods, with a standard curve constructed for each plate. The overall

TABLE I

COMPARISON OF DENSITOMETRIC AND GAS-LIQUID CHROMATOGRAPHIC METHODS FOR THE MEASUREMENT OF METHIMAZOLE CONTENT OF DILUTED URINE SAMPLES

Rat	Methimazole content (μ g \pm S.D.)		
	Densitometric method		GLC method
	By area	By weight	
1	29 \pm 2.2	30 \pm 2.2	29 \pm 1.2 ^a
2	165 \pm 5.4	168 \pm 6.5	165 \pm 5.6 ^b
3	97 \pm 5.1	98 \pm 4.8	94 \pm 2.4 ^b
4	76 \pm 3.6	76 \pm 3.7	
5	154 \pm 8.8	154 \pm 8.4	153 \pm 4.4 ^a

^a Calculated on the basis of six replicate experiments.

^b Calculated on the basis of five replicate experiments.

mean and standard deviation are shown for the whole set of results. There is good agreement between the results obtained by weight and by area determination and, as there is no significant difference between the means (Student's *t* test), measurement of area was adopted for routine use since it is less time consuming.

For quantitative work with solutions of methimazole, McALLISTER⁶ found that the sensitivity of the colour reaction was about 10 μ g. By contrast the present densitometric method is capable of detecting 0.1 μ g methimazole on the thin-layer plate. Further work⁷ with DCQC showed that this reagent gave quantitative results with ether extracts of urine containing propylthiouracil but the lower limit of sensitivity was 20 μ g. Thiourea, however, also reacts with DCQC⁶. It could, therefore, interfere in the colorimetric assay when drugs such as propylthiouracil and methylthiouracil are used, since it has been reported¹² that methylthiouracil breaks down to thiourea in the rat. The densitometric method, however, is free of interference by both break-

down products and endogenous materials, since 100% recovery was obtained in recovery experiments from urine (Fig. 1). The complex formed is yellow and is attributed to an S-substituted derivative¹³. Other reagents¹⁴ were no more sensitive to methimazole than DCQC.

DALLAS⁹, and SHELLARD AND ALAM¹⁵ reported that the thickness of the layer on the plate, time of development and positioning of drug spot in the densitometer were important factors affecting the precision of densitometric methods. In our experience, calibration curves also showed variations from plate to plate substantiating that layer thickness affected reproducibility between plates. On the other hand, by virtue of the procedure adopted, time of development of the plate with respect to the nature of the solvent and distance travelled by the solvent were reasonably constant. The initial application of the sample was found to be fairly critical and the spot size was kept to 5 mm in diameter. This on development gave a symmetrical spot.

Conditions for measurement of the yellow coloured complex after uniform spraying were found to be important. The maximum yellow colour was obtained in 10 min against a white background. Although the background appeared to the naked eye to be satisfactory, it was found when scanning the plate that the pen did not always return to the original baseline. Thus, in all measurements the area of the peak was determined from its preceding baseline¹⁵.

Gas-liquid chromatographic determination. Preliminary work showed that whereas methimazole is retained on column A, subsequent injection with methyl

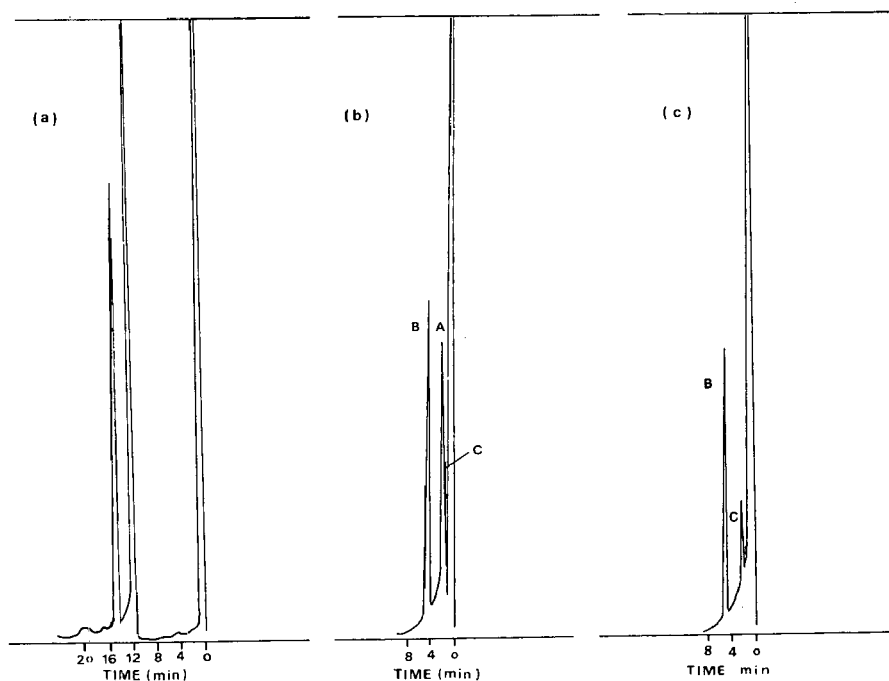


Fig. 2. (a) Methimazole in chloroform injected onto column A followed by methyl iodide at about 12 min. (b) Methimazole recovered from rats and converted to S-methylmethimazole (A); (B), internal standard and (C) endogenous material. (c) Control extract containing internal standard (B).

iodide in acetone gives a derivative peak (Fig. 2a). This was attributed to formation of the S-methyl derivative and confirmed when authentic S-methylmethimazole was injected on the same column and found to have the same retention time. A quantitative procedure was, therefore, developed using this observation, since most endogenous materials in biological extracts were removed from the column prior to derivative formation. Although a quantitative relationship could be obtained for on-column methylation of methimazole, it was not satisfactory with low concentrations in chloroform extracts of urine, since under these conditions a broad solvent peak often masked the S-methylmethimazole peak when methyl iodide was injected.

Column B was found to be satisfactory, and a linear relationship between the S-methylmethimazole peak height and concentration was obtained (Fig. 3). The derivative, however, was not formed *in situ* and it was necessary to pre-treat extracts with methyl iodide prior to injection. Column B gave the chromatogram for extracts containing drug and control as shown in Fig. 2b and 2c respectively.

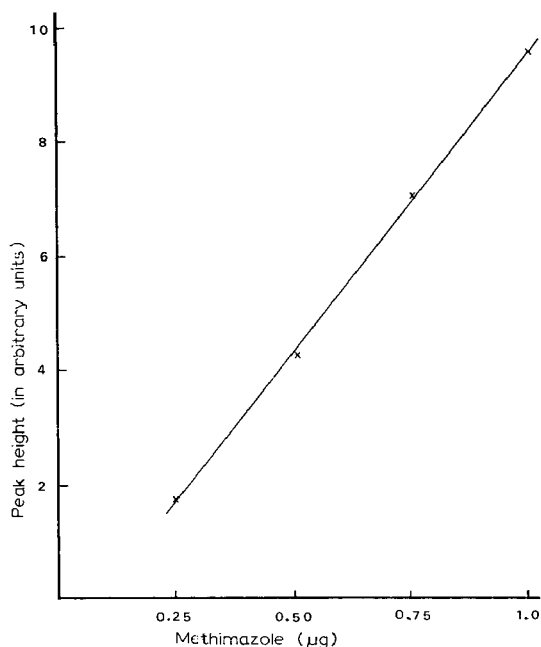


Fig. 3. Calibration curve for S-methylmethimazole by GLC.

Preliminary work with the methylation of methimazole showed that the reaction time was critical. A 10 min reaction time did not give as great a response as a 2 min reaction time and this was contrary to the observations of earlier workers. Solutions of S-methylmethimazole are, in fact, unstable if not stored below 0° . Thus, the whole procedure for a given urine extract was completed in one day.

Comparison of methods. Comparison of the densitometric and gas chromatographic results by Student's *t* test showed that there was no significant difference between the results of these two methods. The standard deviation, however, is less with the gas chromatographic method.

Although, therefore, the densitometric method has more variables than those

TABLE II

12 h EXCRETION OF METHIMAZOLE IN RAT URINE AS DETERMINED BY DENSITOMETRIC AND GAS-LIQUID CHROMATOGRAPHIC METHODS

Rat	Percentage recovery of administered dose (i.p.)	
	Densitometric method	GLC method
1	2.8	2.7
2	15.5	15.2
3	9.1	8.7
4	7.0	—
5	14.4	14.1

for the gas chromatographic method, it is more rapid and hence better suited to routine use. It is, however, less sensitive than the gas chromatographic method because of the possibility of overloading the plate with an excess of endogenous material when drug concentrations are low. The main disadvantage of the more sensitive gas chromatographic method is the instability of S-methylmethimazole, so that replicate measurements must always be made on the same day.

Table II shows the 12 h excretion of methimazole in the rat urine, expressed as a percentage of the dose administered (i.p.).

ACKNOWLEDGEMENTS

The authors wish to thank Dr. W. D. ALEXANDER for helpful co-operation, Mr. BRIAN MARCHANT (Western Infirmary, Glasgow) for performing the animal experiments and collecting urine samples, and Nicholas Research Ltd. for samples of methimazole. The work was carried out during the tenure of a Medical Research Council Scholarship by one of us (G.G.S.), and was supported by a grant from the Nuffield Foundation.

REFERENCES

- 1 W. D. ALEXANDER, V. EVANS, A. MACAULAY, T. F. GALLAGHER AND J. LONDONO, *Brit. Med. J.*, 2 (1969) 290.
- 2 A. LAWSON, C. RIMINGTON AND C. E. SEARLE, *Lancet*, 261 (1951) 619.
- 3 A. HAYDEN AND W. L. BRANNON, *J. Assoc. Offic. Agr. Chemist*, 48 (1965) 616.
- 4 J. BLÁŽEK, J. KRÁČMÁR AND Z. STEJSKAL, *Ceskoslov. Farm.*, 6 (1957) 441; *C.A.*, 54 (1960) 9204c.
- 5 I. BAYER AND G. POSGAY, *Acta Pharm. Hung.*, 31, *Suppl.* (1961) 43; *C.A.*, 56 (1962) 7431f.
- 6 R. A. MCALLISTER, *J. Pharm. Pharmacol.*, 3 (1951) 506.
- 7 R. A. MCALLISTER, *J. Clin. Pathol.*, 4 (1952) 432.
- 8 E. G. C. CLARKE (Editor), *Isolation and Identification of Drugs*, Pharmaceutical Press, London, 1969, 413.
- 9 M. S. J. DALLAS, *J. Chromatog.*, 33 (1968) 337.
- 10 B. L. WUCHU, F. S. MIKA, M. J. SOLOMON AND F. A. CRANE, *J. Pharm. Sci.*, 58 (1969) 1073.
- 11 J. G. HEATHCOTE AND C. HAWORTH, *Biochem. J.*, 114 (1969) 667.
- 12 M. F. MERKULOV, Materialy 8-oi (Vos'moi), *Nauchn. Konf. Po. Farmakol.*, Moscow, Sb. (1963) 26; *C.A.*, 60 (1964) 15004h.
- 13 C. E. SEARLE, *J. Appl. Chem.*, 5 (1955) 313.
- 14 F. FEIGEL, D. GOLDSTEIN AND E. K. LIBERGOTT, *Anal. Chim. Acta*, 47 (1969) 553.
- 15 E. J. SHELLARD AND M. Z. ALAM, *J. Chromatog.*, 33 (1968) 347.

CHROM. 4981

A COMPUTERISED SCANNER FOR BIDIMENSIONAL RADIOCHROMATOGRAMS

E. B. CHAIN, A. E. LOWE AND K. R. L. MANSFORD*

MRC Metabolic Reactions Research Unit, Department of Biochemistry, Imperial College of Science and Technology, London S.W.7 (Great Britain)

(Received August 6th, 1970)

SUMMARY

A computerised automatic scanner for the quantitative evaluation of paper radiochromatograms is described. In this instrument the paper chromatogram is held in a frame, vertically moveable, between two gas flow counters.

The scanning operation is performed by moving the counters horizontally across the paper radiochromatograms, discontinuously exploring unit areas for programmed time periods, the period depending on the level of radioactivity.

At the end of each line, the counters are made to return to their position of origin and simultaneously the radiochromatogram is moved vertically upwards to the next line of exploration. The coordinate positions, radioactive counts and time for each unit area are recorded on paper tape. Control and read-out of the coordinate positions is effected photo-electrically, employing perforated code plates.

A battery of up to ten scanners can be used simultaneously. The scanners are arranged in a time sharing system so that a single tape punch is used for all machines. The punch tape is processed using a programme which gives, for each machine, number map representation of the radioactive spots on the chromatogram, together with automatically computed spot totals of absolute radioactivity. Mechanical construction details and schematic electronic circuits are presented together with performance data.

INTRODUCTION

An automatic scanner for the quantitative evaluation of radiochromatograms was developed by one of the authors and his colleagues: CHAIN *et al.*¹ and FRANK *et al.*². This has been extensively used for studying the metabolic fate of radioactive metabolites in isolated tissues in different physiological and pathological conditions and in the presence of biodynamically active substances. The present paper describes a computerised modification of this scanner, which has been in routine use in this department for over four years.

* Present address: Nutritional Research Centre, Beecham Research Laboratories, Walton Oaks, Tadworth, Surrey, Great Britain.

The original apparatus consisted of an electric typewriter, the numeric keys of which were actuated by a series of solenoids; the radiochromatogram was fastened by Scotch tape to a sheet of blank paper inserted into the carriage of the typewriter and drawn by the movements of the typewriter carriage between two end-window collimated Geiger counters mounted at the rear of the typewriter. In this way "unit square" areas of radiochromatogram were exposed for counting. The counting period depended on the intensity of the radiation, *i.e.* for a short time in the case of the background radiation, and a longer time if the number of counts per unit time exceeded a threshold value. The number of counts collected in the Geiger counters was divided by ten electronically and registered by a 4-decade deatron scaler. At the end of the counting period, determined by an electronic timer, the count was read into the electric typewriter via the solenoids and printed on the blank sheet in the carriage, in a position corresponding to that of the counted area on the chromatogram. In printing out, the typewriter carriage moved the chromatogram automatically to the adjacent position. When the whole line was explored it returned to its original position, simultaneously turning the roll so that the blank paper sheet (and with it the chromatogram) was moved to the next line. Hence the electric typewriter had the dual function of moving the radiochromatogram between the Geiger counters and recording the distribution of radioactivity.

In order to eliminate manual computation of spot totals and correction factors a computerised version of the scanners has been built in which the data from each unit area scanned is recorded on punched paper tape.

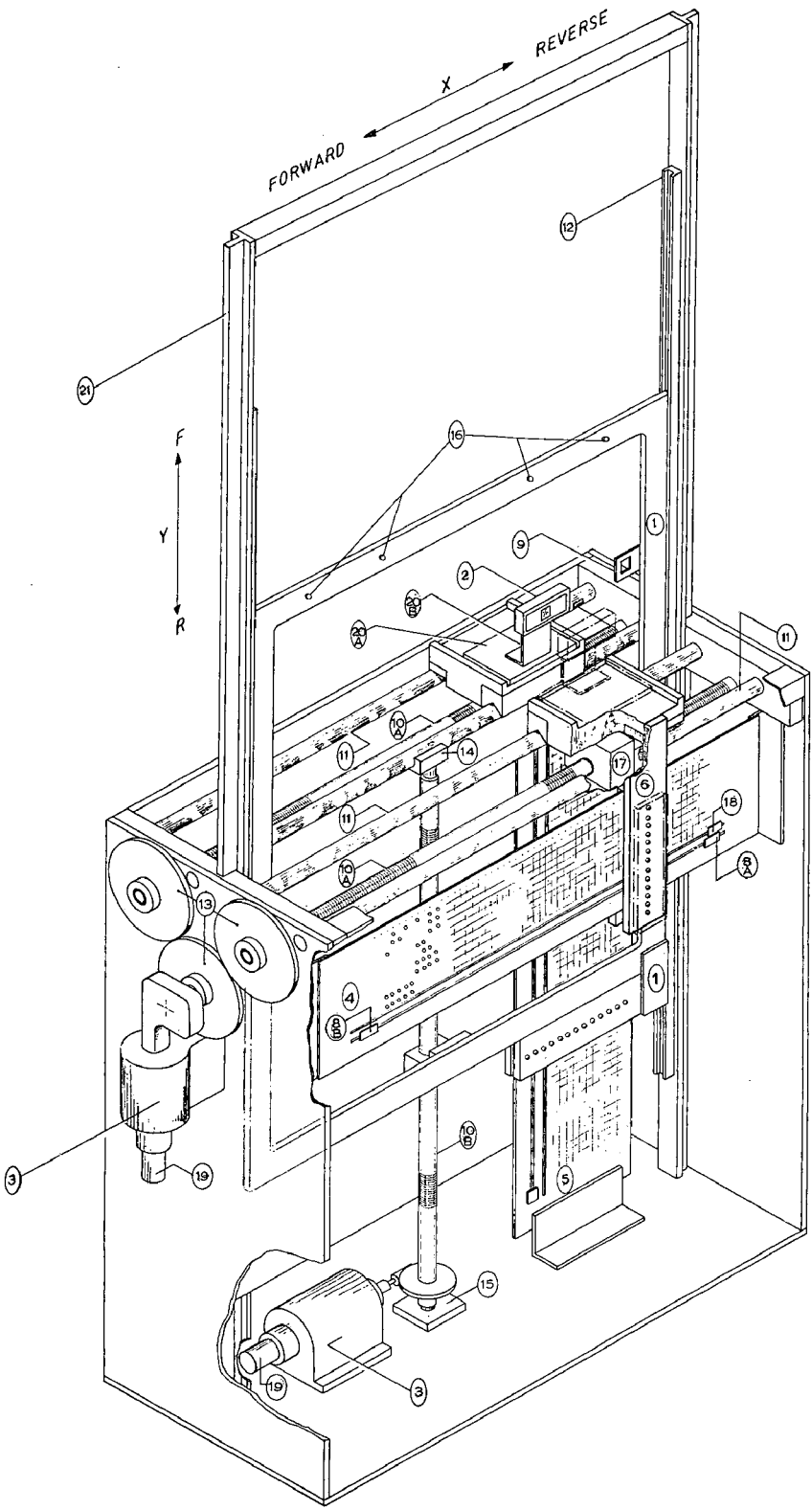
The present paper describes the computerised scanner which has been in routine use in this department for over four years.

GENERAL DESCRIPTION OF THE COMPUTERISED SCANNER

In the new model the dual function of the typewriter had to be regrettably abandoned. The scanning function is now carried out by specially constructed stands (Fig. 1) in which the radiochromatograms, held in frames (1, Fig. 1), can be moved vertically between the two gas flow counters (2, Fig. 1). The counters are moved horizontally across the radiochromatogram discontinuously exploring unit areas. After the end of one line has been reached, the counters are made to return to their original position, and simultaneously the frame is moved upwards so that the next line can be explored by the counters. Both the horizontal movement of the counters and the vertical movement of the frame are driven by two motors (3, Fig. 1). These motors are started and stopped as explained on p. 297 and are servo-controlled so that their running speeds in both forward and reverse directions are defined.

Indexing and read-out of the positions to be explored, both in the horizontal

Fig. 1. Main scanner assembly. 1 = Sliding aluminium frame; 2 = Geiger-Muller counter; 3 = motors; 4 = indexing and coding plate (horizontal direction); 5 = indexing and coding plate (vertical direction); 6 = plastic photocell-lamp holder (horizontal movement); 7 = plastic photocell-lamp holder (vertical movement); 8 A and B = sliding reversing stops; 9 = radioactive standard; 10A = horizontal lead screws; 10B = vertical lead screw; 11 = chromium plated guide rails; 12 = nylon channel for sliding frame; 13 = gear wheels for horizontal drive; 14 = top support bearing for vertical screw; 15 = bottom support bearing for vertical screw; 16 = pegs for suspending chromatogram; 17 = running nut for horizontal lead screw; 18 = sliding stop for "short time" control; 19 = tachometers; 20 A and B = sliding support bracket assembly for Geiger-Muller counter; 21 = aluminium support member.



and vertical directions, is controlled by a series of parallel rows of holes, cut in two aluminium coding (programming) plates, one (4, Fig. 1) for the horizontal movement of the Geiger counters, the other (5, Fig. 1) for the vertical movement of the radio-chromatogram.

These plates also contain slots fitted with moveable stops which define the end points of the scan and (in the horizontal direction) can modify the counting period (see p. 307). The sensing device for programming and reading out the scanning positions (Fig. 2) consists of a series of photo-cells and lamps which follow the scanning move-

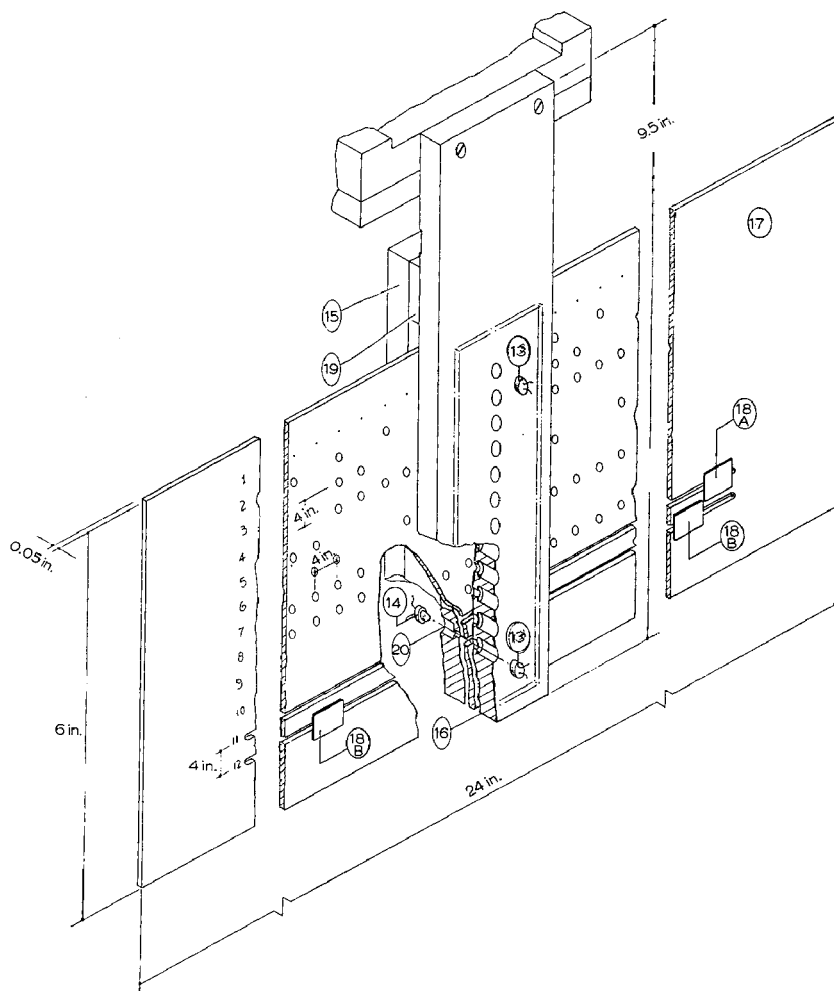


Fig. 2. Lines of holes and slots numbered 1 to 12 perform the following functions: 1 = Indexing; 2-5 = units position in binary coded decimal (B, C, D.); 6 = units parity; 7-9 = tens position in B, C, D. (8 × 10 is omitted); 10 = tens parity; 11 = carries sliding stop (18A) for "short time" counting; 12 = carries sliding stops for reversing motor; 13 = photocell; 14 = lamp; 15 and 16 = plastic strips housing lamps and photocells; 17 = perforated aluminium plate; 18A = sliding stop for "short time" counting; 18B = sliding stops for reversing motors; 19 = spacer; 20 = hole for lamp.

ment (13 and 14, Fig. 2) mounted opposite each other in holes drilled into two plastic strips (15 and 16, Fig. 2) with the fixed perforated aluminium coding plate (17, Fig. 2) located between them; one photocell-lamp pair is mounted at a position corresponding to that of each line of holes and slots in the aluminium coding plates. The aluminium plate thus masks the photocells from their respective light sources, except where the position of the holes and slots allows the light to reach the photocells.

One such sensing device is attached to one of the saddles of the counters for horizontal exploration and indexing (6, Fig. 1) and the other is attached to the lower bar of the radiochromatogram frame, for vertical exploration and indexing (7, Fig. 1).

The small holes on the first horizontal line of the coding plate (line 1, Fig. 2) determine the positions where the counters stop for horizontal exploration. This occurs when motor I is stopped by a signal due to the illumination of the topmost photocell.

Motor I is started by a timing pulse, and stops a few seconds later as the top photocell comes into line with the next small hole. The succeeding timing pulse (10 sec later) starts the counting period, which is set at two values, *viz.* a short one for counting the background activity and the radioactive standard (9, Fig. 1) and a multiple of this value for counting radioactivity intensities exceeding the set threshold for background activity.

After the completion of the counting period a tape punch records the data relevant to the area counted if the set threshold has been exceeded (otherwise it is not activated) and simultaneously the timer sets motor I in motion again, which runs until the counters are moved to the position of the next small hole in the coding plate, when it is stopped once more as described above. These periodic horizontal movements of the counters are repeated until the end of the line is reached.

The two ends of the exploration line are marked by two small brass stops (8A and B, Fig. 1), which can be moved in their slot to any desired position. When the sensing device has been transported to the position of the terminal brass stop (8B, Fig. 1), the light reaching the appropriate photocell is obstructed. This causes the photocell to emit a signal to motor I, which then reverses and returns the counters and the sensing system just beyond the point of origin, this position being marked by an appropriately placed brass stop at the end of the slot (8A, Fig. 1). Once this position is reached by the sensing system, motor I is again reversed by a signal from the same photocell, and the exploration of the next horizontal line begins. This is reached by an upward movement of the radiochromatogram frame. Motor II effects this movement and is started by a time pulse which reaches it during the return excursion of the counters. Motor II is stopped in the same way as motor I.

The vertical positions of the frame (determining the positions of the horizontal exploration lines) are thus programmed by the first row of holes in the vertical coding plate (5, Fig. 1).

On arriving at the last vertical position, when scanning is completed, motor II is reversed by the same light beam obstruction mechanism as for motor I. However, a switch is provided which enables the operator to postpone the return of the frame to a convenient time (S_3 in Fig. 4).

A system has been devised which allows the simultaneous use of up to ten scanners. This is based on time sharing, utilising a master clock and a common tape punch.

The tape punch records the following:

- (1) A code identifying the scanning machine (one digit).
- (2) The position of the explored area, *i.e.* its X and Y co-ordinates (four digits).
- (3) The number of counts (four digits).
- (4) The time period of counting (two digits).

The information on the paper tape, suitably programmed, is processed by the computer. The programme involves:

- (1) Separating the data from each scanning machine.
- (2) Presenting the figures as "number maps" of the distribution of radioactivity, corresponding to the positions of the radioactive spots on the radiochromatograms. The figures express counts per 10 sec per unit area scanned.

(3) Summing the total radioactivity of each spot with appropriate correction for overlapping and correcting at the same time for background, counting efficiency, decay time (if appropriate) and daily instrument variations; the latter are assessed by means of a fixed radioactive standard (9, Fig. 1), which is counted at the beginning of each line.

(4) Expressing the final data as d.p.m. for each spot. The output from the computer appears as shown in Fig. 11.

CONSTRUCTIONAL DETAILS

The most important requirement for the scanning assembly is reliable, reproducible and uninterrupted operation over prolonged periods, with the minimum of maintenance and service. In both the mechanical and electronic aspects of the design special attention was given to this requirement. The following description of the various components of the apparatus reports only those details critical for this purpose. Details of mechanical construction and electronic circuits are available on request.

Mechanical

Stand for counters and radiochromatogram frame. The supporting frame-work is made of stock size aluminium alloy sheet and bars, except for the leadscrews (10A and B, Fig. 1) and guide rails (11, Fig. 1) on which the counters are moved. Its construction is evident from Fig. 1. The stand consists of a base plate on which motor II, moving the radiochromatogram frame by the vertical lead screw, is mounted, and two side plates, on one of which motor I with the gear system driving the counter saddles is mounted. The two sides are connected by two aluminium bars, four guide rails and two leadscrews. Each of the two side plates carries a vertical T-section aluminium bar (21, Fig. 1) to which a nylon rail is sealed, in which the radiochromatogram frame slides (12, Fig. 1); the two vertical T-section bars are connected by a cross bar for stability. The leadscrews are turned from mild steel bars to the desired pitch (12 t.p.i.); the guide rails are made of hard chrome-surfaced mild steel bars. The gear assembly for moving the counter saddles (13, Fig. 1) consists of two mild steel gears attached to the end of the horizontal leadscrews, meshing with a Tufnol hard fibre gear (ratio of gears 1:1:1), mounted on the gear box (ratio 17:1) shaft of motor I. The vertical leadscrew, identical with the horizontal ones is mounted in bearing blocks, one located at the underside of one of the counter guide rails (14, Fig. 1) and

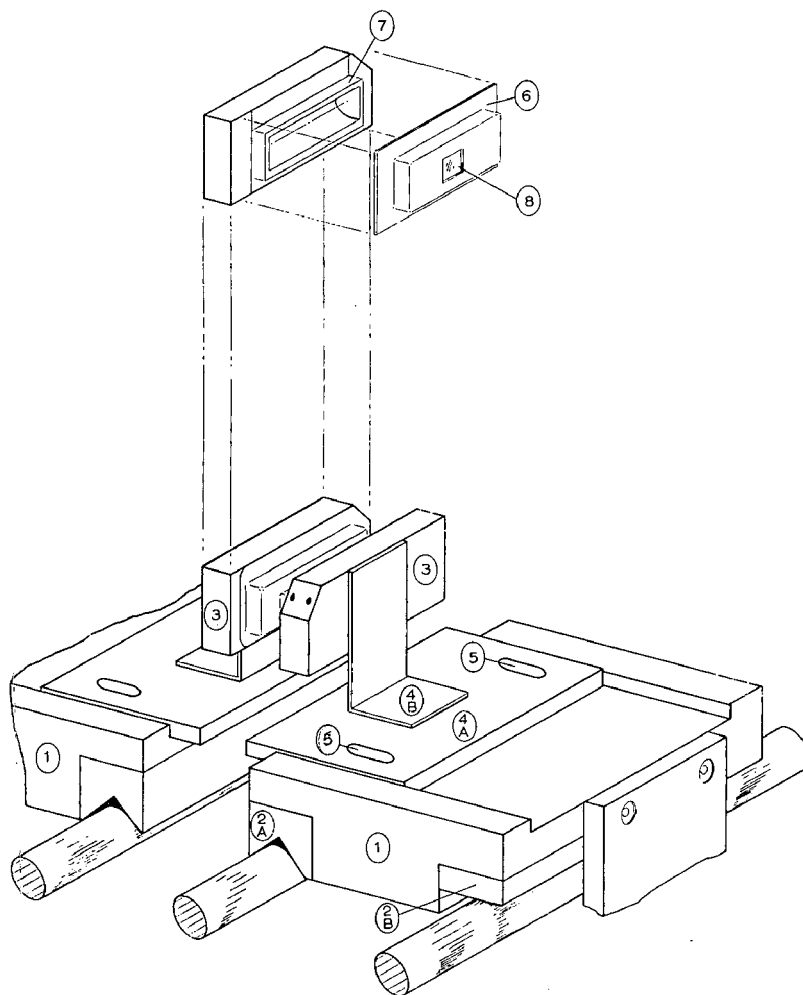


Fig. 3. Geiger-Muller counters and saddles. 1 = aluminium saddle; 2A and B = saddle bearing pads; 3 = Geiger-Muller flow counters; 4A = sliding plate; 4B = brass support bracket; 5 = screw slots; 6 = push-on cover for Geiger-Muller counter; 7 = Geiger-Muller counter boss; 8 = collimating aperture (1 cm^2).

the other on the plate (15, Fig. 1). It is driven by a worm and wheel (ratio 17:1) of Tuf-nol and steel, respectively, by motor II.

Frame for suspending the radiochromatograms. The radiochromatograms are suspended from an inner aluminium frame (1, Fig. 1) sliding in the nylon runners and thus moving the paper vertically between the two counters. Nylon was chosen because it is self-lubricating and ensures smooth movement. The set of the frame in the nylon slides must be accurate, the total freedom of movement not exceeding 0.2 mm.

Four asymmetrically spaced pegs (16, Fig. 1) are fitted in the top bar of the frame from which the radiochromatograms, punched in appropriate places at the top, are suspended; a special punch for perforating the chromatograms was constructed. The

chromatograms are then secured to the frames by spring clips. In this way reproducibility of positioning is assured. The maximal dimensions of radiochromatograms which can be scanned are 40×40 cm. A holder for a radioactive standard (9, Fig. 1) is screwed to the right-hand vertical T-section bar of the outer frame.

Saddles for carrying counters. The saddles (1, Fig. 3) for carrying the counters consist of aluminium blocks which have nylon runners sealed, with Araldite, to recesses cut into their undersides; they slide on the runners on the guide rails. One of the runners is V-shaped (2A, Fig. 3) the other is flat (2B, Fig. 3); they provide the high degree of stability and alignment (both horizontally and vertically) of the saddles during their travel along the guide rails, which is one of the most important requirements for the reproducible functioning of the scanner. Travel of the saddles along the guide rails is effected by the horizontal leadscrews (10A, Fig. 1), running in bronze leadscrew nuts (17, Fig. 1) bolted to the underside of the saddle.

The two counters (3, Fig. 3) are mounted on an angle plate (4A and B, Fig. 3), which slides into slots machined into the top faces of the saddles, to give the desired distance of 5 mm between the counters; at this position they are firmly locked by means of a screw passing into the saddle body through small elongated holes (5, Fig. 3) cut into the angle plate. The pair of counter saddles must retain their relative positions to within 0.2 mm to ensure reproducible scanning.

As the counter, bolted to the photocell-lamp sensing device, always approaches a given counting position from the same direction, and this positioning does not depend on any parts subject to wear, a constant amount of backlash is immaterial. However, differential backlash in the gears or leadscrews between different points of the traverse of the counter saddles, due to unequal wear, could lead to a displacement of one counter relative to the other. In practice, the wear has proved to be negligible.

Indexing and read-out of scanning positions

Photocell-lamp sensing devices. The indexing and read-out systems are electrically separate from each other, but for convenience both are mounted in one unit.

The photocell-lamp assemblies are mounted in housings (15 and 16, Fig. 2) made of black plastic strips bolted together at one end with a spacer (19, Fig. 2) to allow a sufficiently wide gap for the aluminium coding plate to be located between them. A series of holes (lines 1-12, Fig. 2) in alignment with the positions of the horizontal rows of holes drilled into the aluminium coding plate, is bored through each of the strips for housing photocells and lamps (20, Fig. 2), the photocells in one strip, and the lamps in the other. The lamps and photocells are thus opposite to each other, with the aluminium coding plate between them. Both photocells and lamps are held firmly in position by soldering to a printed circuit strip screwed to the outer faces of the plastic strips.

Coding plates. Two rectangular coding plates of identical dimensions and construction are used. One (4, Fig. 1), for coding in the horizontal direction, is screwed at its shorter ends to brackets at the inner face of the two side plates; the other (5, Fig. 1), for coding in the vertical direction, is secured at its lower end to a bracket at the base of the main frame, and at its upper end to a bracket fixed to the end plate.

The plates are made of 18 s.w.g. aluminium. A series of ten parallel longitudinal rows of holes are drilled (lines 1-10, Fig. 2) into each plate, the top row of holes (line 1, Fig. 2) being of smaller diameter than the others. Below the bottom row of holes, two

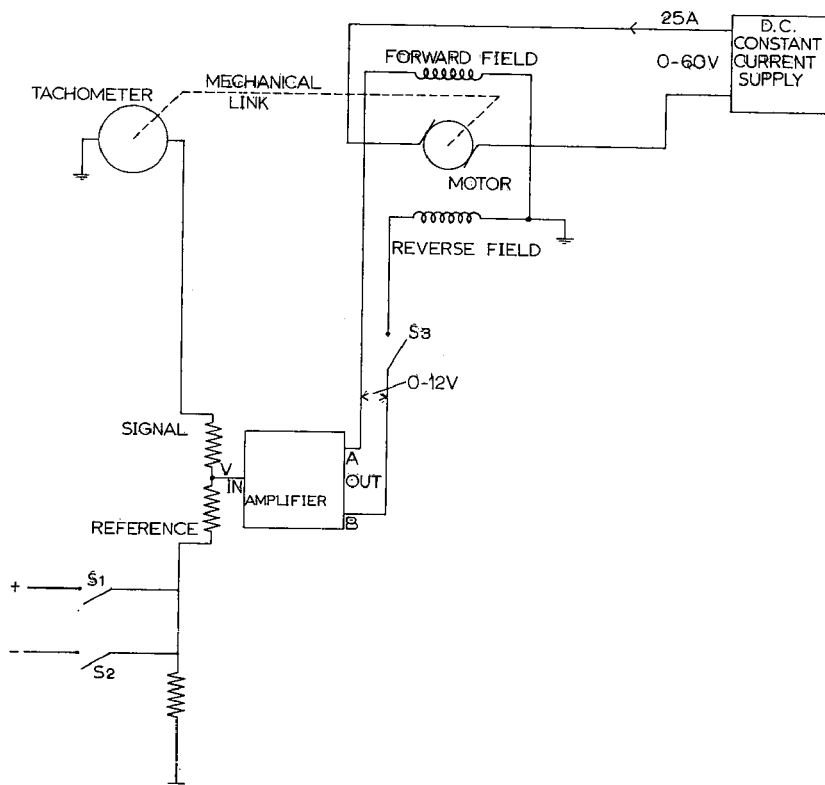


Fig. 4. Servo controlled motors. Amplifier output "A" energised if ref +ve to signal, and output "B" if ref -ve to signal. S_1 and S_2 = movement program switches. S_3 on motor II circuit only (for inhibiting return of frame).

slots (lines 11 and 12, Fig. 2) are cut into the plates, in which small rectangular sliding brass stops are fitted which can be moved to any desired position. One of these slots serves for fixing the limits of traverse in the horizontal or vertical direction. The other slot, used in the horizontal coding plate only (18, Fig. 1), serves to limit the counting time of the radioactive standard to the shorter counting period.

The diameter of the top row of holes was chosen to be small enough to give reproducible and accurate indexing of the scanning positions, yet large enough to prevent blockage by dust particles. A diameter of 0.75 mm was found to be optimal.

The remaining nine rows of holes (lines 2-9, Fig. 2) used to read out the positions of the explored areas had the larger diameter of 5 mm to obviate the need for amplifiers for the corresponding photocells.

The photocell-lamp assemblies must be correctly set with respect to the coding plates over the full traverse, both horizontally and vertically, to an accuracy better than one third of a small-hole diameter. This tolerance is critical for the functioning of the indexing system.

Motors. As motors I and II have to transport the counters and radiochromatogram frame in both directions they must be capable of reversing.

It is essential for the accuracy and reproducibility of positioning that the motors

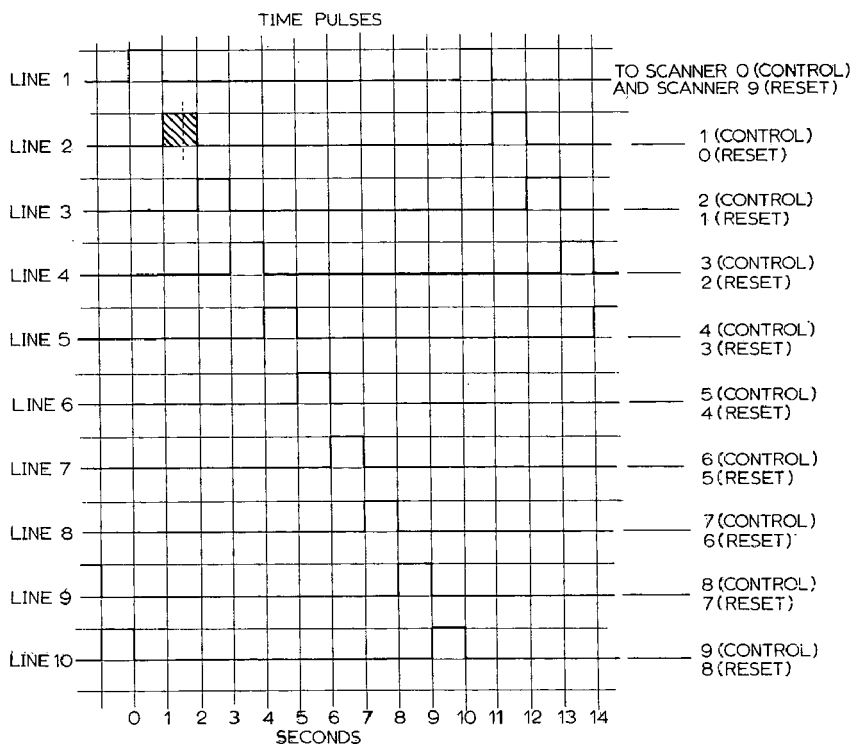


Fig. 5. Shaded area corresponds to state shown in Fig. 10.

stop immediately upon receiving the signal to do so from the appropriate photocells, *i.e.* as soon as the counters and the radiochromatogram frame have reached the indexed positions. Failure of the motors to stop immediately would lead to overshoot. An effective braking system to stop the motors is therefore required and this is provided by the servo system illustrated in Fig. 4. This system is designed so that the motors can rotate at two speeds, a slower one for the forward movements, to reduce the inertia momentum, and a faster one for the return movements, to save time. The slow speed is set so that the counters and frame travel at a rate of approximately 1 cm per 6 sec.

230 V series wound 1/20 h.p. universal motors of standard pattern (3, Fig. 1) with attached tachometer (19, Fig. 1) are used. The pair of field coils are electrically separated, one coil being used for each direction of rotation; the power for the field coils is supplied by d.c. amplifiers with a maximum output of 12 V. The armature is fed from a separate supply which holds the armature current constant to about 0.25 A over a voltage range of 0–60 V. Much less than the full torque is developed by the motors under these conditions but it is adequate for the purpose. The tachometer consists of a small 24-V d.c. motor in which the normal brushes are replaced by silver carbon brushes.

According to the polarity (S_1 and S_2 , Fig. 4) of the reference voltage one or other of the field coils of the motor is energised by the amplifier.

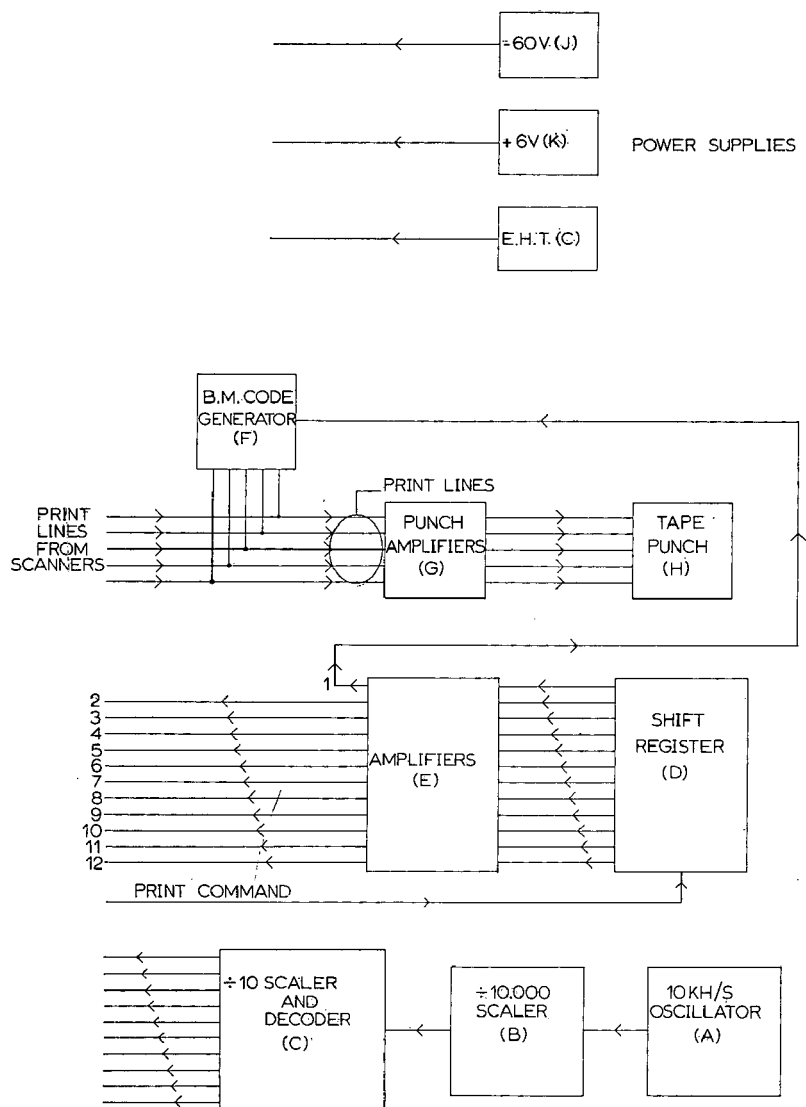


Fig. 6. Central module.

In consequence, the motor and with it the tachometer, rotates in the appropriate direction. The voltage generated by the tachometer is fed to the amplifier input so as to oppose the reference voltage. The system therefore tends to a steady state, where the tachometer voltage is nearly equal and opposite to the reference voltage; consequently, the motor speed and direction are governed by the reference voltage. Two suitable reference voltages of opposite polarity are routed to the amplifier by the programming system.

When the reference voltage drops to zero, *i.e.* the motor is required to stop, the amplifier momentarily attempts to reverse the direction of rotation of the motor; this provides a powerful braking action.

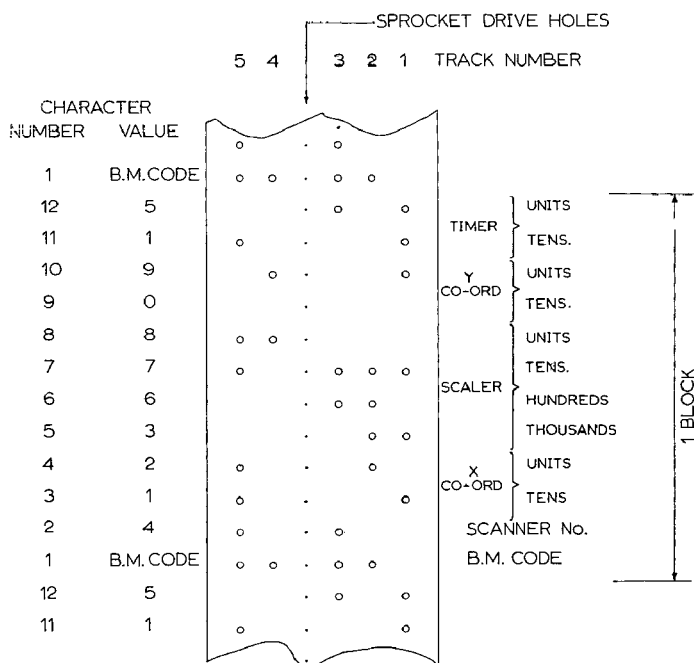


Fig. 7. Punch code and block layout.

The amplifier is designed so that unless the reference voltage exceeds a pre-determined level (of approximately 10 mV) there is no output. After this level is exceeded, the output power rises rapidly with increasing input voltage until full output is obtained. In this way the system has a fast response, with no danger of spurious rotation.

Time sharing and print out system

As was pointed out above, one tape punch serves a number of scanners; the system must therefore ensure the complete absence of mutual interference, especially during print-out.

The simplest method is to use a "time-sharing" system (Fig. 5).

Each scanner is controlled by a pulse 1 sec in duration, repeated every 10 sec. The print-out takes place during the first 0.6 sec of the pulse. All control and print-out functions of the scanner depend on this time pulse, but "reset" of the circuits (after each counting period) is activated by another 1-sec pulse.

By "staggering" the time pulses to the separate scanners it is impossible for more than one machine to be printing out at the same time (provided not more than ten scanners are used). As resetting does not involve use of the punch, one scanner may 'borrow' the control pulse from another for this purpose.

The time clock consists of a 10 KH/S oscillator (A, Fig. 6) 'counted down' by a scaler to 1 p.p.s. (B, Fig. 6). The 1-p.p.s. signal is fed to a divide by ten scaler and decoder (C, Fig. 6). The latter has ten outputs on which 1-sec wide pulses appear sequentially, *i.e.* each line carries 1-sec wide pulses separated by 10 sec (Fig. 5).

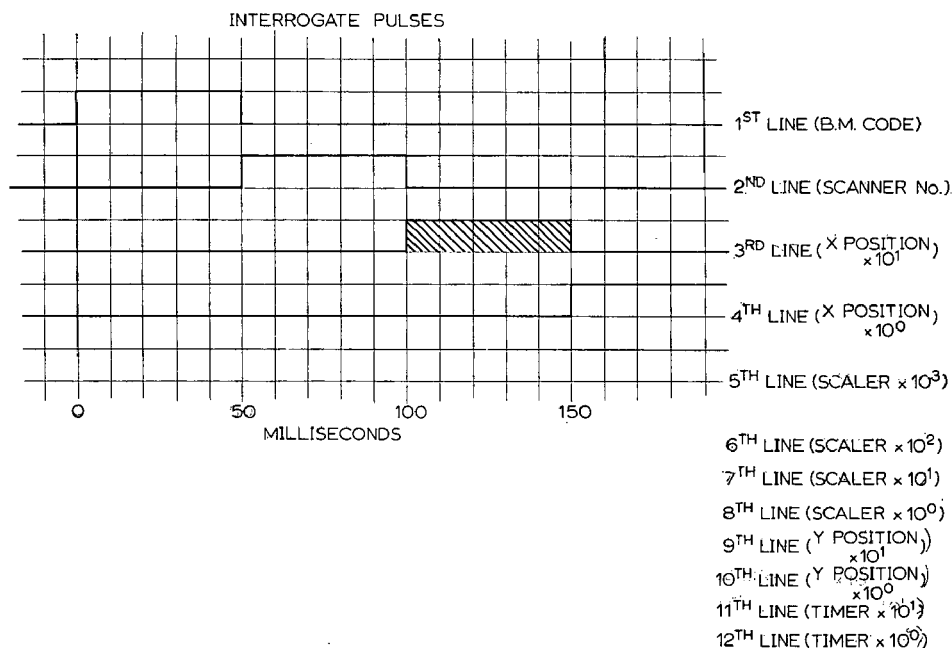


Fig. 8. Shaded area corresponds to state shown in Fig. 10.

The scanner data consist of a set of digits which must appear in a specified order on the tape (see Fig. 7). Each digit is represented by a single unique combination of holes across the tape (called a character). The first four tracks encode the digits in binary coded decimal form, the fifth is required to give correct parity*.

On each occasion when a print-out is required, the scanner concerned must be interrogated and its stored information transferred character by character to the

* The "parity" system has been devised by computer engineers as a sensitive monitor of the correct operation of digital systems.

Inspection of the punch tape (Fig. 7) shows that every character is represented by an even number of holes. Considering only numeric characters, the first four tracks represent the number in binary coded decimal form; the fifth track is punched only when the total number of holes would otherwise be odd. This hole is known as the parity "bit".

How the parity bit is generated and used for detecting scanning errors, becomes evident from a consideration of the arrangement of holes in the aluminium coding plates (Fig. 2). It will be seen that the number of large holes in each row which lie on lines 2-6 (coding the units position number in binary coded decimal form), taken together, always consists of an even number of holes, the holes lying on line 6 being drilled to make this so. (Lines 2-5 are the binary coded decimal numbers.)

Suppose that (due to lamp failure or some other cause) the photocell which registers line 4 (= the number 4) fails to read when required, then, for instance, position 5 (photocells 4 and 2) would "read" electrically as position 1 (photocell 2 only) and the error would not be readily detected. However, with the parity bit the total number of photocells activated is odd instead of even and this is obvious by inspection of the tape when the photocell states are printed out.

It will be appreciated that only a rare coincidence of failures will result in an erroneous character being punched with correct parity.

The last four lines of holes (lines 7-10) on the coding plate perform the same function for the tens position numbers.

Electronically generated parity bits are used for the scaler decades.

then carries these timing pulses along with the other supplies to the relevant scanner by means of a single multiway connector.

The E.H.T. is fed to the machines via a separate ring of co-axial cable. A 10 position switch is fitted to each scanner for adjusting the E.H.T. voltage to the flow counters.

Scanner circuits

The block diagram (Fig. 9) shows the general layout of the circuits of each individual scanner.

The programming and control of the motors has already been described. The time programmer (A, Fig. 9) has the additional functions of (a) stopping, starting and resetting the scalers which record the number of counts (C, Fig. 9) and the elapsed time (B, Fig. 9) for a counting period; and (b) passing a pulse (print command pulse) to the central module to start the shift register when a print out (see above) is required.

For each scanner the logic circuits are all reset to their zero or starting states by the reset pulse. This occurs 9 sec after the control pulse (Fig. 5). The motors have by this time come to rest and the cycle of operations therefore recommences in response to the next control pulse, which occurs at the following second.

The radioactive standard is counted using the shorter (background) counting period (see p. 296). This is achieved by means of a sliding stop (18, Fig. 1) in a slot of the horizontal coding plate which masks the light from a photocell as for the excursion control. This stop masks the photocell only for the first two positions of each horizontal scan and gives rise to a signal which overrides the multiplier setting, *i.e.* making it equal to 1, so that print-out in this case occurs after the shorter counting period.

The nine lines of large holes on each aluminium plate code the light signals to nine photocells. These provide for the horizontal or vertical position co-ordinate read-out. Lines 2-6 (Fig. 2) below the small holes code the units and their parity and the remaining four lines, lines 7-10 (Fig. 2), code the tens and their parity. Two-decimal characters are required for each co-ordinate, but as the co-ordinate number never reaches 8×10 , no line of holes is provided for this tens digit. As the holes are large, no amplifiers are needed for these photocells.

All the scaler decades which have to be "read out" are identical and are in standard binary coded decimal form (1, 2, 4, 8) plus parity.

Faults usually result in incorrect parities appearing on the data tape. These are detected by the computer during processing and are listed in the computer print-out.

A divide by 10 pre-scaler (D, Fig. 9) is used before the main counting scaler. This is necessary as a maximum count store of 99999 is required but only the first four decades are considered significant for read-out.

Print-out system

The following information is recorded on the tape (see Fig. 4):

- | | |
|--|---|
| (1) The scanner number | one character, a number between 0 and 9 |
| (2) The horizontal co-ordinate | two characters, a number between 1 and 44 |
| (3) The number of counts in the scaler | four characters, a number between 0 and 9,999 |
| (4) The vertical co-ordinate | two characters, a number between 1 and 44 |
| (5) The time of counting in 10-sec units | two characters, a number between 1 and 99 |

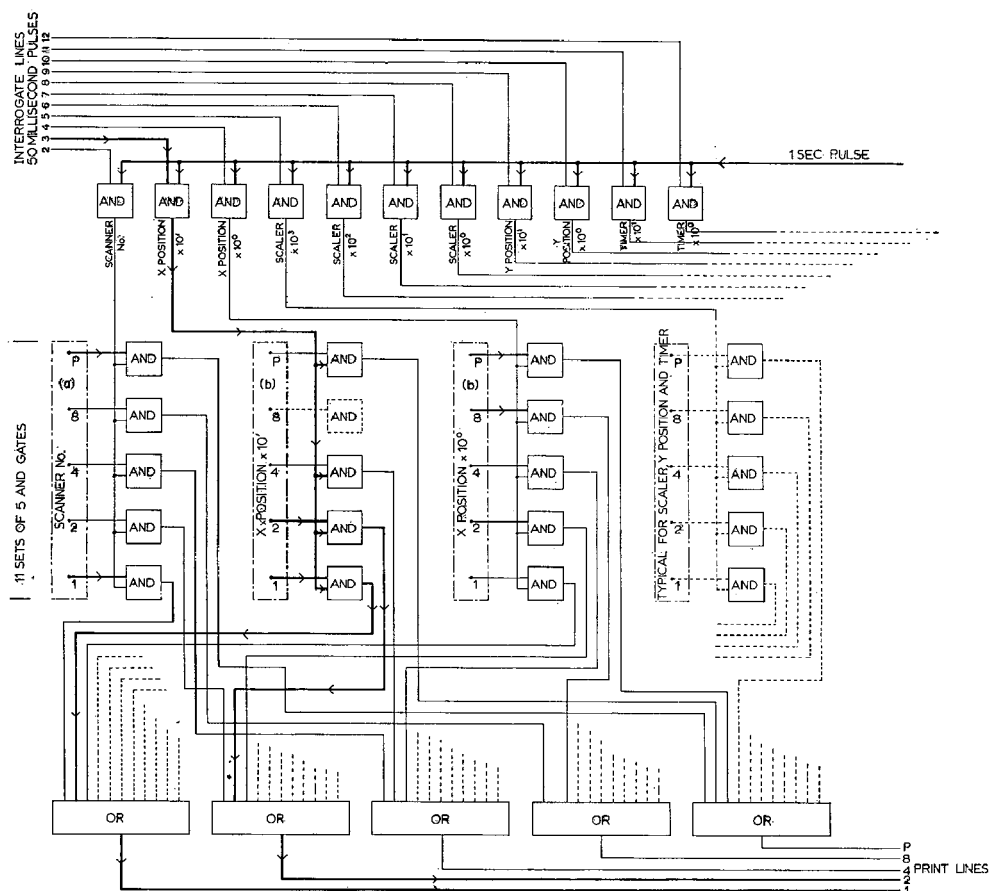


Fig. 10. Part of print matrix circuit. Heavy line shows electrical state during print out of scanner No. 1 at position 3×10^4 (to be followed by 8×10^6).

In addition each group of the above data must be separated from the next. This is done by a character (not a number code), called a Begin Message (B.M.) code. Thus there are a total of twelve characters, of which the first is the B.M. code, in each block of data. The data must be punched in the order shown. To print each character an "interrogating" pulse is needed on a separate line.

The first shift register pulse of the twelve "interrogates" the B.M. code which is invariant and is therefore not wired to the scanners; logic similar to that described below is incorporated into the central module for punching the B.M. code (F, Fig. 6).

The remaining eleven interrogating pulses are fed by the ring circuit into all the scanners, but as explained only the scanner which has commanded the shift register through its time programmer (A, Fig. 9) is interrogated by these pulses.

Logic circuits of print-out system

Part of the print matrix circuit is shown schematically in Fig. 10 to illustrate the working of the logic circuits of the print-out system. The blocks which have AND or OR printed in them operate as follows: Blocks may have any number of inputs,

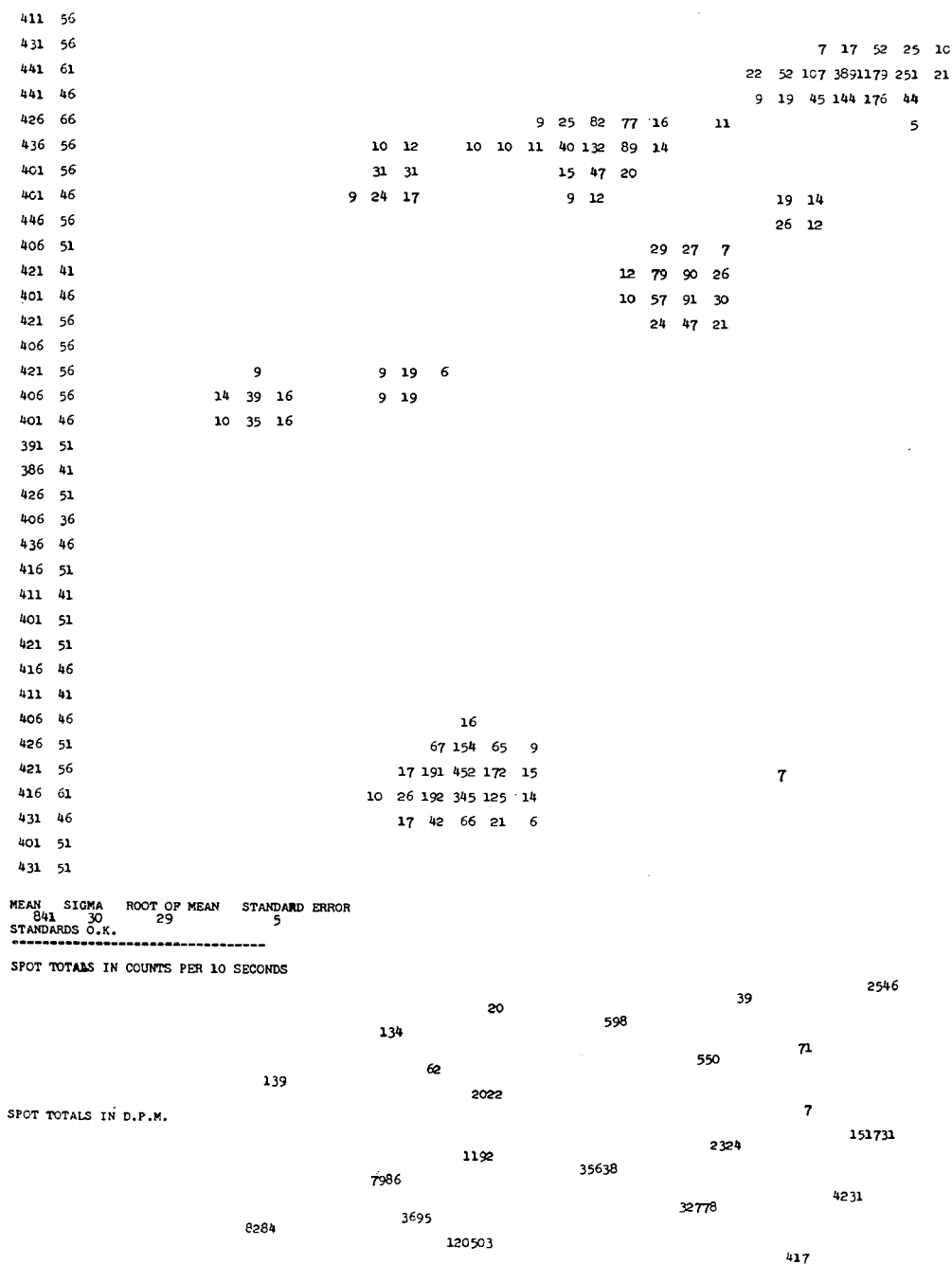


Fig. 11. Typical "number map" of a chromatogram of metabolites of [U-¹⁴C]glucose phosphate in rat brain cortex.

but only one output (signals flow towards the input and away from the output). In the AND gate a signal appears at the output (which is then in the "ON" state), only when all the inputs are energised, otherwise its output is zero or "OFF". In the OR gate, a signal appears at the output when one or more of the inputs is energised.

In both cases all signals, input or output, can have only one magnitude, *i.e.* the system recognises only two electrical states, "on" or "off".

The 1-sec control pulse energises one input of all the eleven "AND" gates. During the time this 1-sec pulse is present at these inputs, interrogation pulses from the shift register arrive at the other inputs of these gates and the outputs of the eleven "AND" gates are therefore each energised serially for 50 m sec.

These pulses then appear at one of the inputs of each set in turn, of five "AND" gates (four gates encode the number 1, 2, 4 and 8 and the fifth encodes the parity bit; see print-out system) connected to (a) the scanner number generator (one character), (b) the photocells (four characters), (c) the timer (two characters), and (d) the scalars (four characters), *i.e.* eleven sets of five gates in all. If any of the other inputs of these gates are energised by the above circuits (a), (b), (c) and (d) to which they are connected, a signal is passed to one of five "OR" gates which energise the appropriate print line, causing a hole to be punched in the corresponding track of the tape.

The "OR" gates are necessary as the outputs of "AND" gates may not be directly interconnected.

All the circuit construction is based on Mullard Series I circuit blocks on plug-in boards; discrete components are used only where necessary.

It will be realised that the horizontal co-ordinates are read out whilst the photocells are moving with respect to the coding plate. This movement, however, is small compared to the diameter of the light beam and does not effect the read-out.

COMPUTERISATION

From the information on the tape (see print out) and the background count of the detectors (which is known and punch coded on to a "leader" tape attached to the beginning of the main tape) the computer is programmed to print out a chromatogram map and spot totals for each scanner from which information has been punched into the tape. Fig. 11 is a typical example.

A storage programme is also available so that the results from any chromatogram which is unfinished, when the tape is removed for processing other completed chromatograms, can be stored at the computer centre on magnetic tape until the remainder of the information arrives.

The first two columns of figures down the lefthand side of Fig. 11 relate to the fixed radioactive standard (9, Fig. 1). In the first column the figures represent the counts emanating from 1 cm² of the standard, corresponding to the area of the detector window. In the second column the detectors have moved one indexing space and therefore are exposed to only a part of the standard. The first column is automatically checked for counting statistics and the result appears in the computer print out as "standards O.K." (or "not O.K.") immediately beneath the "map". The variation of the ratio (figure in first column)/(figure in second column) gives an indication of the accuracy of positioning. This is occasionally checked manually.

The main "map" appears to the right of the standards, and a set of spot totals

appears below the map. Up to this point all figures represent actual counts per 10 sec.

Below this first set of spot totals the corrected totals are printed in disintegration per min (d.p.m.). These are calculated as follows:

$$\text{d.p.m.} = C_{10} \times \frac{K}{S}$$

where d.p.m. is the required spot total in disintegrations per minute of the material on the chromatogram, C_{10} is the corresponding total in counts per 10 sec minus background, K is an experimentally derived value for counter efficiency in the conditions under which the chromatograms are prepared and measured, and S is the mean value of the standard in counts per 10 sec for the particular chromatogram.

Most of the cost of the data processing by the computer is allocated to the print-out (which includes the blank spaces) and is therefore a very large proportion of the total cost. A considerable reduction of the cost can be achieved by suppressing the number map and confining the print-out to the computed spot totals.

An alternative method for producing number maps without the computation of the spot totals involves the use of a reader-writer to which an additional programmer has been fitted. The lay-out of the data on the tape has been chosen with this end in view. This facility has the further advantage of providing a ready means of checking the performance of the scanners; this is desirable since one of the inherent disadvantages of a computerised system is that many faults are impossible to detect until the data have been processed.

DETECTORS OF RADIOACTIVITY

For the detection of radioactivity emanating from the chromatograms, gas flow counters were chosen as the most suitable devices, rather than sealed off end window counters as, due to their thicker windows, they have a much lower efficiency. Standard Tracerlab gas flow counters with specially designed windows were used. In front of each counter is fitted a collimating plate of material opaque to ^{14}C radiation, into which a square aperture has been cut. The dimension of this aperture corresponds to the spacing between the small holes in the horizontal and vertical coding plates. The collimators of a pair of detectors are mounted opposite to each other (within 1 mm). The distance between the collimators must remain constant to 0.2 mm during the travel of the counters.

The design of these collimated windows is shown in Fig. 3. A rectangular flanged metal cap (6, Fig. 3) is made, on a press tool, to be a push fit over the front of the flow counter (7, Fig. 3). The cap, when fitted, should be free from movement. Both brass and stainless steel caps have been made and used successfully.

An aperture (1 cm \times 1 cm) (8, Fig. 3) is cut centrally in the cap and a piece of Melinex (ICI Plastics) film, somewhat larger than the aperture, is fixed with Araldite to its inside surface so as to cover the aperture, thus forming a window. It is important that the Araldite does not spread to the area of the window.

The film used (thickness 0.00015 in. corresponding to 0.5 mg/cm²) is unmetallised. The commercially available 0.1 mg/cm² windows used with most flow detectors were rejected as being too expensive and too liable to damage.

The use of gas flow counters as against sealed off types doubles the counting efficiency and thus reduces the scanning time (for the same sensitivity of scanning) by half. The flow counters have an unshielded background of only 30 c.p.m. per pair.

These counters are run in the Geiger region on argon-2% isobutane at a flow rate of approx. 70 ml/min instead of the helium-isobutane mixture as recommended by the manufacturers.

The supply of gas for a large number of flow counters is very expensive if bought ready mixed in cylinders. The following system has therefore been adopted. Bulk supplies of argon and isobutane, stored in separate cylinders, are fed to a commercial gas mixer (G.N. Platon Ltd.), set to give a mixture of 98% argon and 2% isobutane. The gas leaves the mixer at a pressure which varies between 10 and 30 p.s.i. and is reduced to 5 p.s.i. by a standard reducer valve. A "T" piece then routes the gas to two "Camping Gaz" reducer valves (20-cm water gauge). Conveniently the thread of the "Camping Gaz" valves is such as to permit the use of standard $\frac{1}{4}$ in. B.S.P. fittings.

The outputs of these valves are connected to the ends of a loop of soft rubber tubing (2 cm O.D. \times 5 mm wall) which is laid out around the group of scanners. The loop is fed from both ends in order to minimise the pressure drop throughout the system.

Connections are made to the individual scanners by inserting surgical needle tubing (1.5-mm diameter) through the wall of the rubber tube. Each needle is connected to a "T" piece, each arm of which is connected to a gas flow counter by small-bore rubber tubing. In each of those latter connections a length (20-30 cm) of small-bore (0.5 mm) stainless steel tubing is included. By pushing lengths of stainless steel wire into the steel tubes the effective bores can be reduced still further so as to give the required flow rate to the counters. This adjustment is empirical.

Should a needle be withdrawn or a leak develop from any other cause, the large diameter tube can be patched with an ordinary cycle repair kit.

All tubes are thoroughly water washed and dried before use. On first putting into service, or after prolonged shut-down, the system takes several hours to deliver the correct mixture to the counters, but it is very reliable and stable thereafter. It has proved itself to be a cheap and flexible gas distribution system with the great advantage that all its components are readily obtainable.

Reliability

Over a period of four years the wear of the moving parts has been negligible and the critical tolerances with regard to the positions of the photocell-lamp sensing device and the saddle movements have not been exceeded. The only servicing necessary has been occasional cleaning and oiling of the gears and leadscrews.

The main cause of malfunction of the scanners has been the fact that the life of the filament lamps was only a small fraction of that stated by the manufacturers. We have recently replaced the filament lamps with two 8 in. fluorescent tubes; these work satisfactorily and have a much longer life. The next common source of failures has been the gas flow counters, especially after interruption of the gas supply. However, the proper functioning of the gas flow counters can be restored by washing them with *n*-propanol.

Faults in the circuitry have been extremely rare and mainly confined to power transistors. No trouble has ever been experienced with the circuit blocks or the large

TABLE I

REPRODUCIBILITY OF THE SCANNING OF A RADIOCHROMATOGRAM CONTAINING SPOTS OF DIFFERENT INTENSITIES

Chromatograms were prepared from [U-¹⁴C]glucose (200 d.p.m./ μ l and run overnight in butanol-acetic acid-water, 40:11:25). Each chromatogram was scanned on four separate occasions on each scanning machine. Data from computer output are already corrected in the programme for efficiency of counter and variations in counting a fixed radioactive standard of [¹⁴C]polymethyl-methacrylate.

	Spot			
	5 μ l (1000 d.p.m.)	10 μ l (2000 d.p.m.)	20 μ l (4000 d.p.m.)	Mean d.p.m./10 μ l (calc. 2000 d.p.m.)
Scanner 00	970 \pm 120	2090 \pm 245	4160 \pm 390	2063
Scanner 01	962 \pm 128	2120 \pm 238	4092 \pm 372	2050
Scanner 02	1071 \pm 150	2006 \pm 211	4185 \pm 450	2075
Scanner 03	922 \pm 150	1996 \pm 201	3902 \pm 386	1948
Scanner 04	1054 \pm 175	1896 \pm 260	3858 \pm 410	1939
Scanner 05	986 \pm 145	1910 \pm 198	4011 \pm 401	1973
Mean value \pm s.e.m.	994 \pm 137	2003 \pm 225	4034 \pm 401	2008

number of gold plated connectors. The "Addo" tape punch requires servicing at intervals of a few months.

Performance

Reproducibility of counting and print out operations. This was tested in a manner similar to that described for the earlier scanner² by measuring and recording both background radiation as well as fixed reference standards of different intensities. For this purpose [¹⁴C]polymethyl-methacrylate sheets of known emission rates were obtained from the Radiochemical Centre (Amersham). The standard deviation of the observed counts did not differ from that calculated statistically. The fixed standard (9, Fig. 1) on each scanner provides a day-to-day check on this aspect of the reproducibility.

Reproducibility of scanning. For testing the reproducibility of the scanning operations standard chromatograms were prepared from [U-¹⁴C]glucose as described in Table I. Each chromatogram was then scanned on four separate occasions on each scanning machine. The counts recorded on the scanners were automatically corrected in the computer programme for the efficiency of the particular detectors as judged by the counts recorded from the fixed standard. The results shown in Table I indicate that the standard deviation of a single measurement of a radioactive spot total is only slightly in excess of that expected from the statistically calculated value. The figures shown in Table I were obtained with an initial counting period of 40 sec and the multipliers set to four (*i.e.* 160 sec) and with a counter efficiency of approximately 11%. Therefore an area of 1 cm² of ¹⁴C radioactivity of as little as 250 d.p.m. would give a total count of 73 in this period with an expected error of 20% whilst one with 10,000 d.p.m. would have an expected error of 5%.

The performance of the scanners indicates that the observed error is not significantly in excess of the expected error and therefore both the mechanical and electrical functions are satisfactory.

Although weakly radioactive spots cannot be measured accurately unless the counting period is prolonged, the background of the gas flow counters is so constant that the threshold can be set to $1.5 \times$ background and areas twice the background can be detected in a counting period of 4×40 sec. This corresponds to levels of radioactivity which require seven days exposure on Kodirex X-ray film for recognition by autoradiography.

ACKNOWLEDGEMENTS

The authors wish to express their thanks and appreciation to the members of the Mechanical and Electronics Workshop of this Department, in particular to Messrs. R. C. ADAMS, I. KAYE, and A. R. SMITH, for their enterprise and skill, to Mrs. B. SHEARER, of the Centre for Computing and Automation of Imperial College, for developing the computer programmes, and to Professor B. MCA. SAYERS, of the Electrical Engineering Department of Imperial College, for his helpful criticisms in reading the typescript.

REFERENCES

- 1 E. B. CHAIN, M. FRANK, F. POCCHIARI, C. ROSSI, F. UGOLINI AND G. UGOLINI, *Selected Sci. Papers Inst. Super. Sanita*, 1 (1956) 241.
 - 2 M. FRANK, E. B. CHAIN, F. POCCHIARI AND C. ROSSI, *Selected Sci. Papers Inst. Super. Sanita*, 2 (1959) 75.
- J. Chromatog.*, 53 (1970) 293-314

CHROM. 4987

ISOTACHOPHORESIS

ELECTROPHORETIC ANALYSIS IN CAPILLARIES

F. M. EVERAERTS AND TH. P. E. M. VERHEGGEN

Department of Instrumental Analysis, Eindhoven University of Technology, Eindhoven (The Netherlands)

(Received August 4th, 1970)

SUMMARY

The aim of this paper is to give more details about the equipment used for isotachophoretic analysis. More accurate values, quantitatively as well as qualitatively, can be obtained by thermostating the system where the thermal detector is mounted. Mobilities of the different ion species are also strongly influenced by shifts in temperature. Therefore an electric diagram is given for an aluminum thermostat in which the capillary is mounted. A secondary effect, but also an important one, is that shorter times for analysis can be obtained because higher currents can be used by the increased heat transfer. Some electric diagrams are given for differentiating electronically, which makes balancing of thermocouples^{1,2} unnecessary. Detailed designs are given for injection blocs and electrode compartments.

INTRODUCTION

The principles for isotachophoretic analysis (displacement electrophoresis) have been described by EVERAERTS¹ and MARTIN AND EVERAERTS².

The apparatus basically consists of a capillary mounted between two electrode compartments, the anode and cathode compartment respectively. For the separation of anions the capillary is filled with a salt of an anion more mobile than any in the sample and a cation with buffering capacity (leading electrolyte). The anode compartment contains a solution of the buffering cation. The cathode compartment contains a solution of an anion less mobile than any in the sample (terminator). The sample must be introduced between the terminator and the leading electrolyte.

A constant current is passed between the electrodes. The anions in the sample move initially at different speeds until they are separated in order of their mobility. Then all anions in the apparatus move down in the capillary tube at the same speed (isotachophoresis), assuming the capillary to be of constant bore. The boundary between each successive pair of ions is more or less sharp^{1,2}.

Since each zone has a particular potential gradient, it has also a particular rate of heat generation per unit length and a particular temperature. Thus it will be possible

to follow the separation by means of fixed thermocouples on the outside of the capillary tube.

The temperature of each zone gives the information about the ion species in that zone. The length of each zone gives the possibility of calculating the amount of each ion species with the equation of Kohlrausch¹. The length of each zone is preferably measured from the distance between the peaks of the record provided by a differential thermocouple, measuring the difference in temperature along a short length of the tube, or by differentiating electronically the integral signal provided by the integral thermocouple.

The aim here is to provide experimental details and also to explain the reasons for some particular choices. If a capillary tube, surrounded by air, is freely supported in a thermostat and heat is produced in it by an electric current, it will lose this heat by transferring it to the air and by the low temperatures of the tube a negligible part is lost by radiation. Excessive heat production will result in bubble formation. If the detector is thermal (by a set of thermocouples) no extreme cooling by cold air or thermostated liquid can be used.

Future work in developing other detectors to be used in this field will therefore be very important both for the accuracy of the results and for the speed of the analysis. The current used actually is limited by the dimensions of the capillary, the temperature of the surrounding air and the overall heat-transfer coefficient. During an analysis, a stationary condition will be obtained inside the thermostated compartment, containing the capillary tube. This stationary condition depends on the amount and species of the intermediate ions, the terminator chosen, the current used, the dimensions of the capillary, the overall heat-transfer coefficient, the temperature of the surrounding air and the heat flow to the thermostat. The time for reaching this new steady state is given by the capacity of the thermostated system to dissipate the heat produced in it.

The reference junction of the integral thermocouple (ref. 1), however, will have the temperature of the thermostat. This still means that the temperature of a well-defined zone can differ from experiment to experiment because the air temperature is not constant. The temperature of a zone is used as a characteristic for each ion species. If all steady states now would give the same air temperature inside the thermostat, the zone temperatures should be the same from experiment to experiment. But the temperature is, as said above, also dependent on the terminator used and the amount and species of intermediate ions. Therefore accurate values can not be expected. A new type of thermostat has been developed. The reference junction of the thermocouple must never be mounted free in the air but must be embedded in a heat sink (isolator type) in the aluminum thermostat (see below). The thermal contact of the capillary tube with the metal thermostat must be made as good as possible.

MATERIALS AND METHODS

Description of the apparatus (Fig. 1)

A teflon capillary tube (O.D. 0.75 mm, I.D. 0.45 mm) is embedded in a groove of an aluminum bloc (Fig. 2). The capillary is wound around the aluminum block in the form of a helix. Gaps between the capillary and the aluminum bloc are carefully filled with a heat sink compound (Al_2O_3 powder with silicone oil). Because the heat

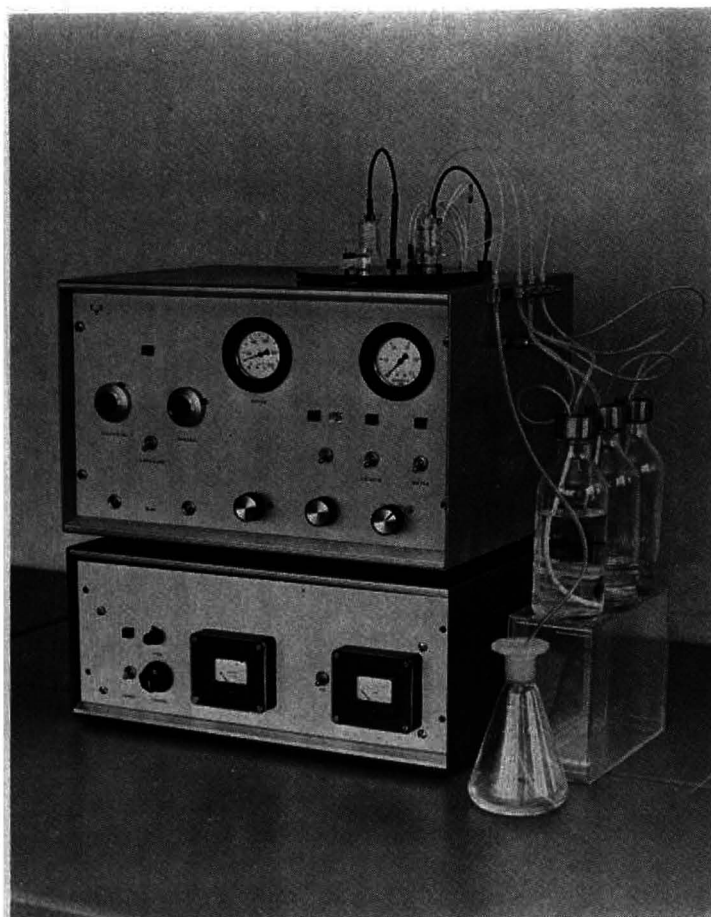


Fig. 1. Apparatus used for the isotachopheretic experiments.

produced in the capillary is so quickly transferred to the aluminum bloc, a compartment (Fig. 2E) is created where the thermocouples are mounted to be sure that there will still be a signal to detect. The reference junctions of the thermocouples have the temperature of the aluminum bloc because a certain amount of heat sink compound is smeared out on the junction, providing for the thermal contact with the aluminum bloc. The teflon capillary tube and the heat sink compound are fixed by a thin layer of shellac (Krylon). For cooling of the aluminum bloc thermostated water (0.1° accurate) is used. A temperature sensor (Pt-resistance $100\ \Omega$) is mounted in the neighborhood of the detector compartment. Here also gaps are filled with the heat sink compound. In the center of the aluminum bloc a load is mounted (60 watt). Pt-resistance and load are connected to the temperature controll unit (see Fig. 11). Rubber O-rings and Devcon material (metal glue) are employed to prevent contact of water, circulating inside the aluminum bloc, with the electric circuits.

Injection bloc and compartment for the terminal electrolyte

The capillary tube protruding from the thermostat is on one side connected

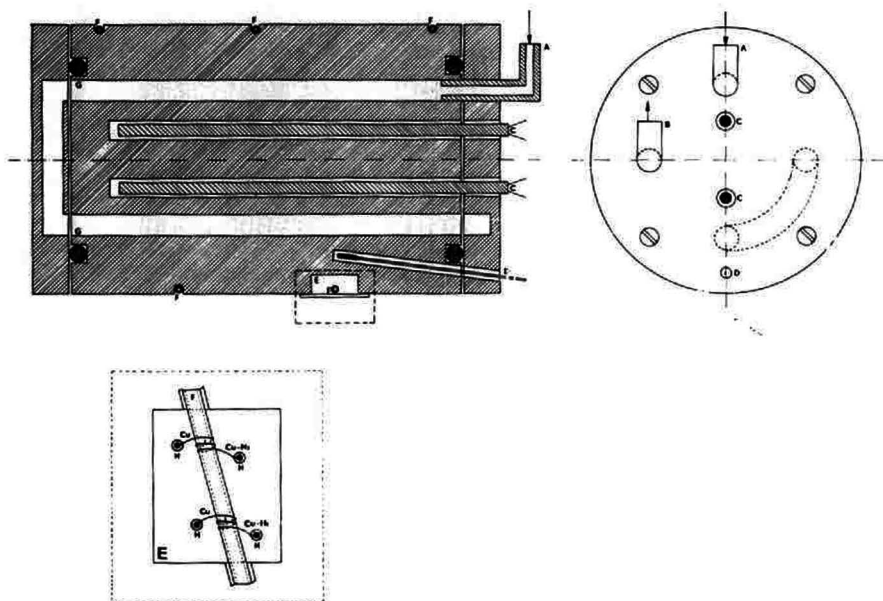


Fig. 2. Aluminum thermostat. A = input thermostated water; B = output thermostated water; C = loads; D = Pt resistance; E = detector compartment; F = capillary tube; G = rubber O-rings; H = thermocouples.

with the injection bloc (Figs. 3 and 4). All parts are made of perspex. Special care must be taken to make all holes in this injection bloc as smooth as possible. Scratches in it can give disturbances during an analysis by adhering impurities, difficult to remove. Holes in the perspex must therefore be made by very sharp tools, used for perspex exclusively. For lubrication no alcohol or glycerine but ordinary petroleum is recommended. Care must be taken too that no dead volumes are present because, in rinsing the system, these are difficult to clean. Thus a new source of errors is prevented. The capillary tube is connected with the injection bloc without the use of a cement. The inside diameter of the piece of perspex (Fig. 3.4) is the same as the outside diameter of the capillary tube (Fig. 3.7).

By stretching the teflon capillary first over a length of 2 cm, it can be brought into the hole of the piece of perspex mentioned above. Then the capillary tube can be brought into this piece such that it fills the hole entirely. The waste part of teflon can be cut off with a sharp knife. So constructed, only fitting the capillary over a length of about 1.5 cm, no leakage occurs even if the rinsing water is pressed through the capillary at 4 atm. A bolt (Fig. 3.6) will press the capillary tube and piece (Fig. 3.4) together in the perspex injection bloc (Fig. 3.1). The surfaces of contact are smooth and by the elasticity of the perspex no leakage occurs. No packing ring has been employed. In the injection bloc (Fig. 3.1) a hole is drilled providing the contact of the plunger compartment with the capillary tube. A septum (Fig. 3.3), fitted in the injection bloc with a bolt (Fig. 3.2), gives the possibility of injection with an ordinary syringe (Hamilton 1- μ l syringe). The compartment for the terminal electrolyte (Fig. 3.12) is blocked with a plunger (Fig. 3.15) during rinsing, filling and sampling. To

prevent any leakage the plunger is covered with a piece of teflon. By injecting the sample some of the leading electrolyte will be displaced into the plunger compartment. This will be sucked into the drain (Fig. 3.14) by a pump if the connection is made between the compartment filled with the terminal electrolyte and the capillary hole

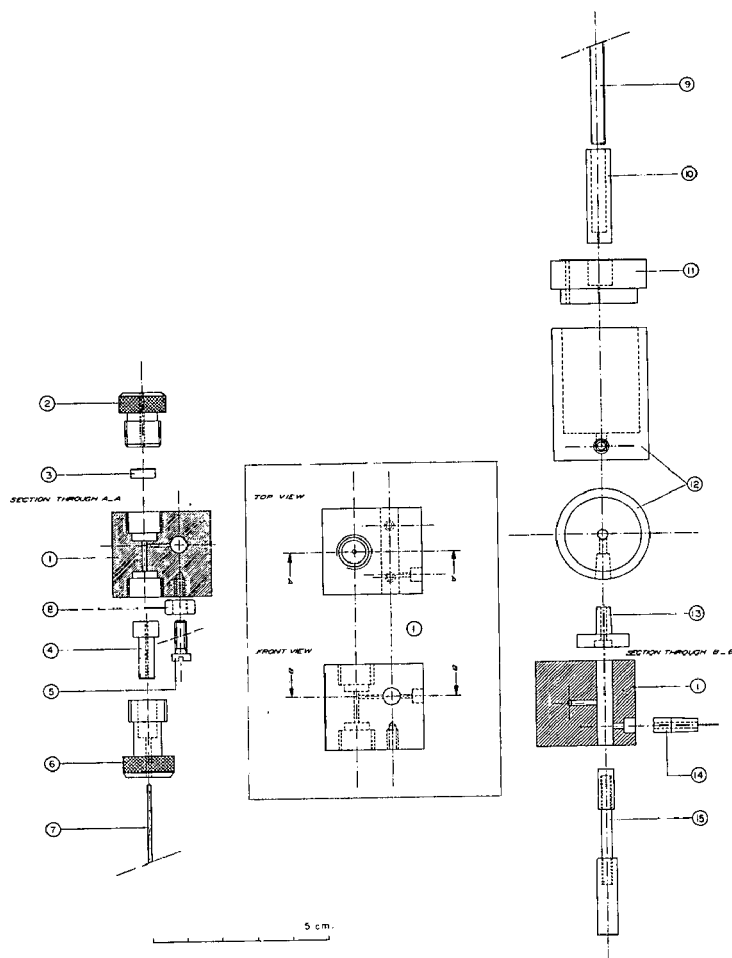


Fig. 3. Injection bloc and compartment for the terminal electrolyte. 1 = injection bloc; 2 = bolt for fitting septum; 3 = septum; 4 = piece of perspex for fitting capillary tube; 5 = screw for mounting injection bloc; 6 = bolt for fitting piece 4 and capillary tube; 7 = capillary tube; 8 = rubber O-ring; 9 = high tension cable; 10 = piece of perspex for mounting high tension cable; 11 = cover of electrode compartment; 12 = electrode compartment; 13 = connection of electrode compartment with plunger compartment; 14 = connection towards drain; 15 = teflon-covered plunger.

in the injection bloc. If the sample should be injected after this connection has been made, some of the leading electrolyte will also be introduced into the plunger compartment, now filled with the terminal electrolyte. The potential gradient in this compartment is very low because the dimensions are large in comparison with the

capillary holes. It will take quite a long time before this leading electrolyte electrically has moved back into the capillary part of the injection bloc. A certain eluting effect will be the result. An electrode, made of Pt wire, is connected to the high tension cable (Fig. 3.9). Piece 13 of Fig. 3 is glued to the injection bloc with chloroform, providing the contact with the compartment of the terminal electrolyte. Thus this compartment can easily be taken off to be rinsed.

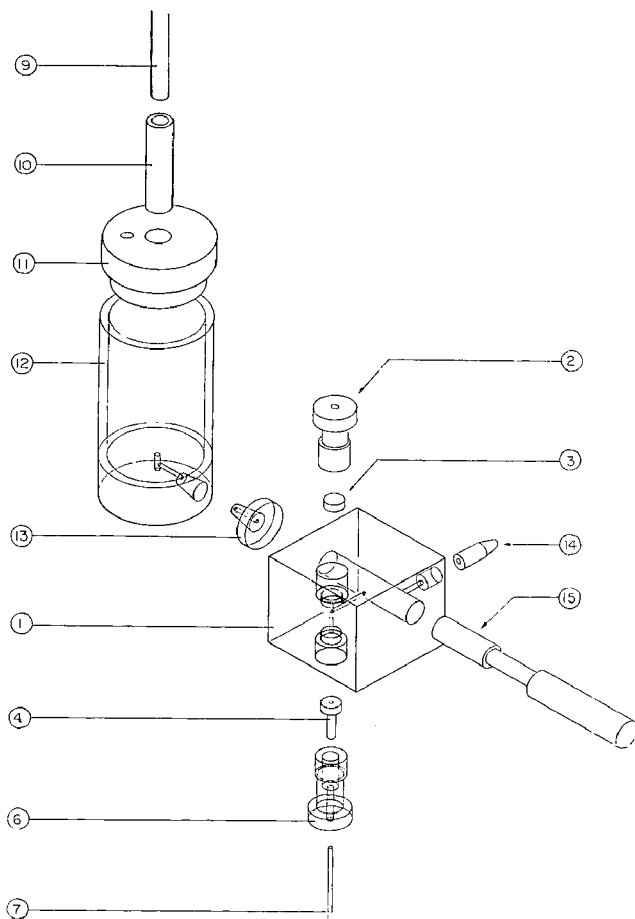


Fig. 4. Injection bloc and compartment for the terminal electrolyte. For further explanation see text and Fig. 3.

Counter-electrode compartment

The capillary protruding from the aluminum thermostat is at the other side connected with an electrode compartment in the same way as described above. The electrode compartment shown in Fig. 5 contains a semi-permeable membrane (Fig. 5.8) made of cellulose acetate. The electrode, made of Pt wire, is separated from the inside of the capillary tube by this membrane.

The use of a semi-permeable membrane has several advantages. First of all the

system is mechanically closed at one side. This decreases the electroendosmotic flow to such an extent that for the separation of small ions no polymer need to be used. For the stabilization of the zones of bigger molecules, such as proteins, a polymer is still needed. Differences in level between the two compartments do not give a hydrostatic flow of liquid. The capillary can be rinsed (Fig. 5.1) or filled with fresh electrolyte without disturbing the solution of the electrode compartment. If during an analysis products are formed at the Pt electrode, the electrode compartment can be continuously

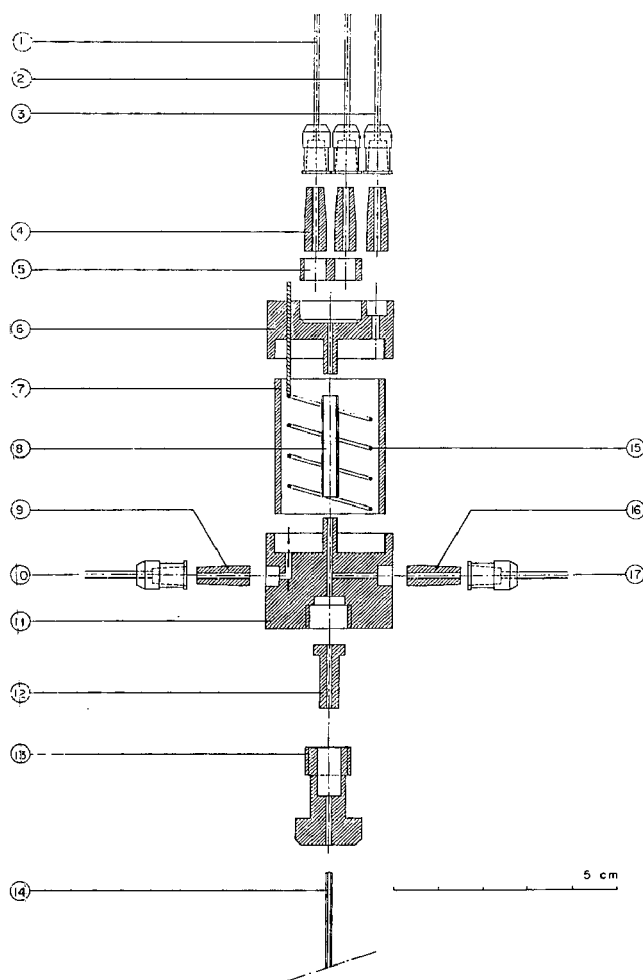


Fig. 5. Counter electrode. 1 = teflon tube, connected with water reservoir; 2 = teflon tube, connected with electrolyte reservoir; 3 = teflon tube, connected with drain; 4 = pieces of perspex used for connection; 5 = pieces of perspex used for connection; 6 = cover of electrode compartment; 7 = electrode compartment; 8 = membrane; 9 = perspex piece used for connection; 10 = teflon tube, connected with the electrolyte reservoir; 11 = bottom of the electrode compartment; 12 = piece of perspex used for fitting the capillary tube; 13 = bolt for fitting piece 12 and capillary tube; 14 = capillary tube; 15 = Pt electrode; 16 = piece of perspex used for connection; 17 = teflon tube, connected with the electrolyte reservoir of the counterflow equipment.

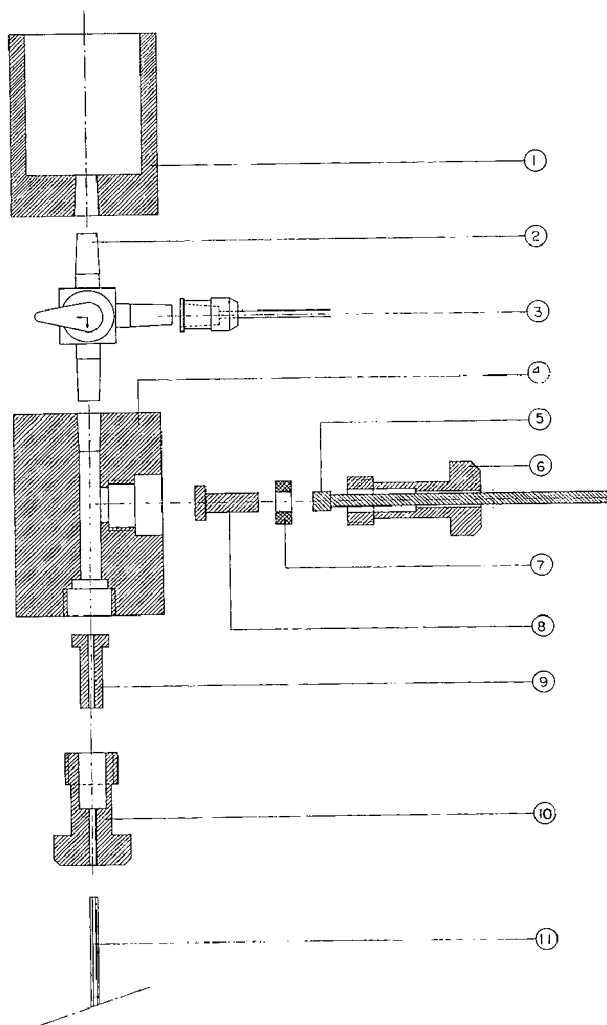


Fig. 6. Counter electrode. 1 = reservoir; 2 = tefton-lined valve; 3 = connection towards the counterflow equipment; 4 = electrode compartment; 5 = high tension cable; 6 = bolt for fitting the electrode; 7 = rubber O-ring; 8 = Ag electrode; 9 = piece of perspex used for fitting the capillary tube; 10 = bolt for fitting piece 9 and the capillary tube; 11 = capillary tube.

rinsed through the connections 3 and 10 of Fig. 5. The pH shift due to this membrane is regarded as a disadvantage³. After treatment with alcoholic potassium hydroxide the cellulose acetate membrane can be transformed into a more porous cellulose membrane. The membranes of cellulose acetate were made by rolling a sheet of cellulose acetate (0.2 mm thick) on a glass rod. By dipping it in acetone and washing it with streaming water a membrane is formed. The thickness of the membrane is about 0.5 mm. It was glued on the parts 6 and 11 of Fig. 5 with araldite (CIBA).

Pieces 16 and 17 of Fig. 5 are constructed for the possibility of using the equipment for counterflow analysis. All pieces of Fig. 5, apart from the membrane, are

joined without using cement or chloroform. The membrane is mechanically very strong, so one can work with it for years, if not too acidic (pH 1) solutions are used.

The tubing of Fig. 5.1 and Fig. 5.2 must be made of nonelastic material. This tubing is connected with a teflon-lined Hamilton valve (2 mm i). After rinsing the capillary tube or filling it with fresh electrolyte a pressure still remains. If the tubing is made of elastic material a counterflow of electrolyte during the analysis will be the result. This causes non-reproducible results and sometimes even leading electrolyte and sample leak into the plunger compartment. Apart from a possible loss of sample it will rise to an error as mentioned under *Injection bloc and compartment for the terminal electrolyte*. If electrode compartments with non-gassing electrodes are wanted, special arrangements can be made. Fig. 6 shows a possibility.

Besides the advantage of the elimination of a pH shift, due to the membrane, and under special conditions the possible prevention or stimulation of electrode reactions, it has also many disadvantages. By rinsing the capillary tube products formed at the electrode must first be removed. The water for rinsing and the electrolyte for filling the capillary tube pass the electrode compartment.

If the electrode compartment is not carefully rinsed after each experiment,

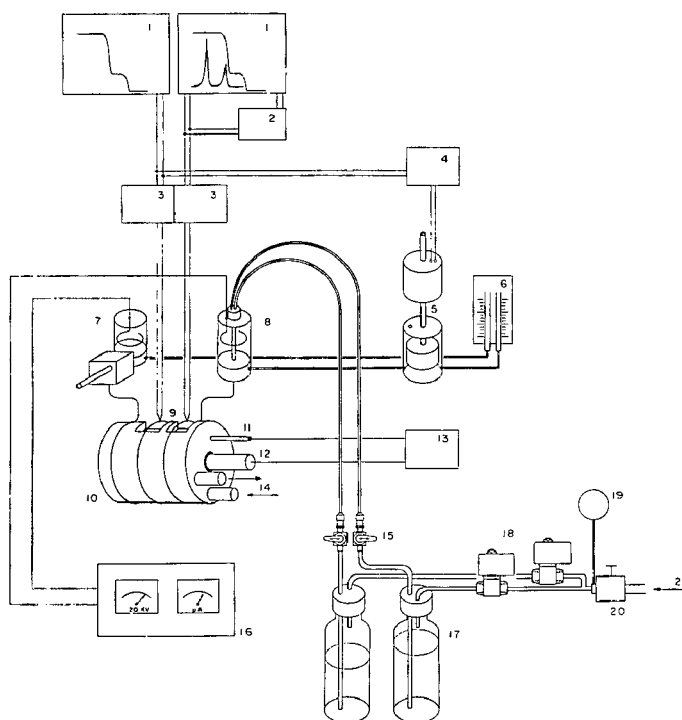


Fig. 7. Bloc diagram of the isotachopheresis equipment. 1 = recorders; 2 = differentiator; 3 = Knick amplifiers, type A; 4 = regulator for the counterflow; 5 = equipment for the counterflow; 6 = level control; 7 = injection bloc; 8 = counter electrode; 9 = thermocouples; 10 = Al bloc with capillary tube; 11 = Pt sensor; 12 = load; 13 = regulator for thermostating; 14 = thermostated water; 15 = teflon-lined valves; 16 = current stabilized power supply; 17 = reservoirs; 18 = magnetic valves; 19 = manometer; 20 = pressure regulator; 21 = air (2 atm).

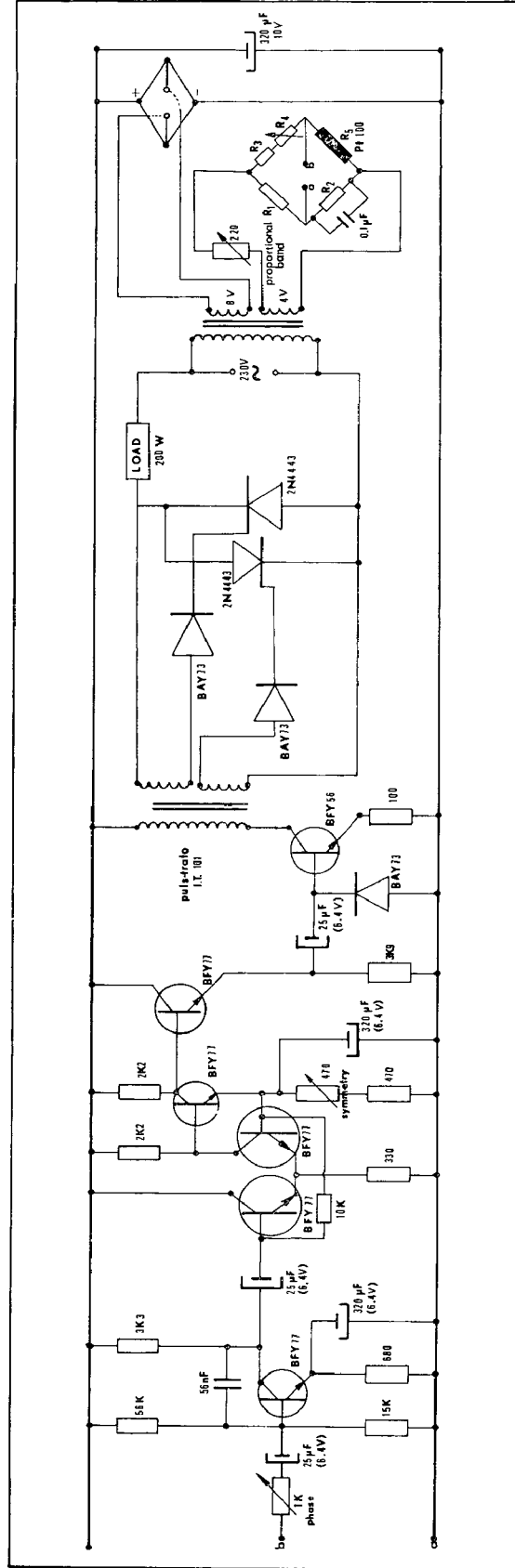


Fig. 8. Proportional temperature regulator. For further explanation see text.

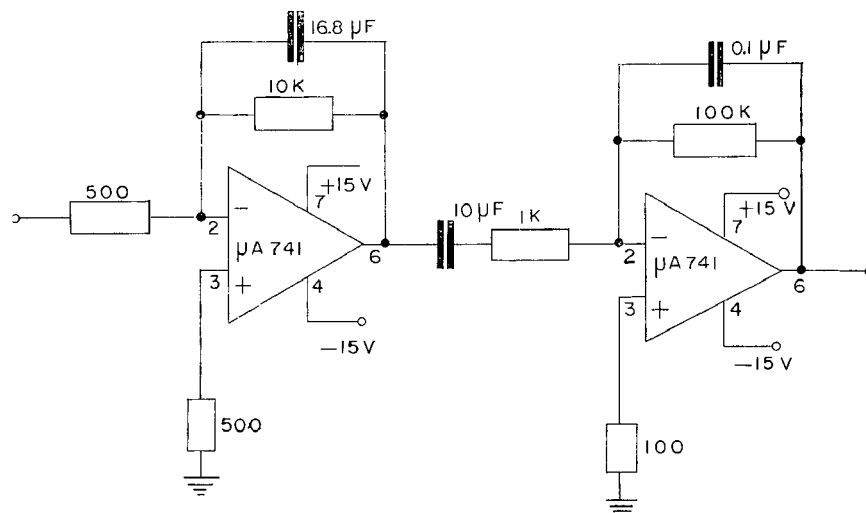


Fig. 9. Differentiator. For further explanation see text.

this too can give disturbances. Another disadvantage is that the electrode must be regenerated after each experiment to prevent formation of gas. Sometimes the pH changes slightly during the analysis, despite all precautions. The perspex reservoir (Fig. 6.1) is constructed because in the tubing (Fig. 6.3) gas bubbles may be present. If these enter the electrode compartment (Fig. 6.4) it will be very difficult to remove them. To make the tubing gas free, the first electrolyte containing the gas bubbles is expelled into this reservoir. The diameter of the boring of this compartment must be as small as possible, otherwise too much electrolyte is needed for each experiment.

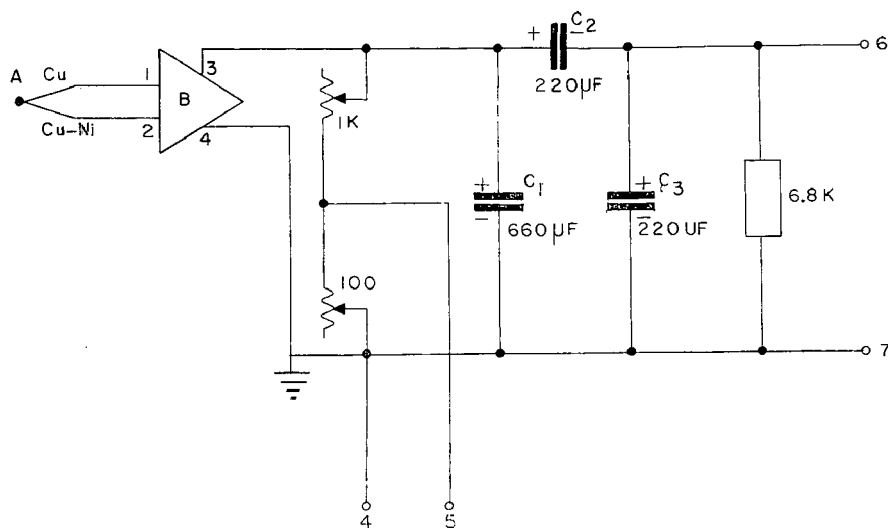


Fig. 10. Differentiator. For further explanation see text.

This diameter must be smaller than the diameter of the non-gassing electrode, to be sure that this electrode fits in the perspex electrode compartment. The diameter of the boring must not be too small; otherwise the contact surface of electrode and liquid is too small. The tap (Fig. 6.2) is also a teflon-lined Hamilton valve with a 90° connection.

Fig. 7 shows a block diagram of the isotachopheresis equipment. The apparatus for counterflow is described^{3,6}. The level control unit (Fig. 7.6) must only be used if the analysis is done in an open system such as analysis with counterflow of electrolyte.

More practical data can be found in refs. 7, 8 and 10.

The temperature control unit

The proportional temperature controller⁴ used in the thermostat is based on the relatively high temperature coefficient of a Pt resistor. Used is a Pt resistor of 100 Ω (0°). This Pt resistor forms an a.c. bridge (R_5) together with the resistors R_1 , R_2 , R_3 and R_4 . The temperature coefficients of all resistors in the a.c. bridge, apart from the resistor R_5 , must be as small as possible. The smaller the values are, the more accurate the thermostat control will be. Of course one of the resistors of the a.c. bridge is a variable one, to allow for balancing the a.c. bridge. If the bridge is unbalanced, a signal, being the result of the unbalanced condition, will be fed to a preamplifier. The phase of this preamplified signal is dependent on the polarity of the unbalance of the bridge. The preamplifier generates a sinusoidal voltage and by a limiter this signal will be transformed into a symmetrical square wave.

By the very high amplification of the preamplifier and the limiter, the amplitude of the bridge voltage is transformed into a phase shifted square wave. The leading edge of this square wave is amplified and triggers two antiparallely connected thyristors. These thyristors control the amount of heat dissipated in a load, mounted in the direct neighborhood of the Pt resistor (Fig. 2).

If the bridge approaches its balanced condition, the output voltage of the bridge decreases. Due to this the phase shift of the thyristor trigger pulse will be reduced. The thyristor will trigger later and the heat produced in the load decreases too. A steady state will be the result.

The temperature can be selected by the variable resistor R_4 of the a.c. bridge, according to the formula:

$$T = 2.59 \{R_4 - 0.5835\}^{\circ}\text{C}, (\text{temp. coef. } R_5 = 0.003916)$$

The table in Fig. 8 gives some suggestions. A R-C filter in front of the input of the preamplifier corrects the phase of the trigger pulse. The proportional band (system gain) can be changed by varying the a.c. voltage over the bridge. Uncorrect temperature regulation may result if the temperature coefficients of the resistors of the a.c. bridge are poor, leading to instabilities, if the thermal resistance between the load and the Pt resistor is large, or if the heat capacity of the object to be thermostated is too large.

Differentiator

Qualitative information is obtained from the signal given by the integral thermocouple. The quantitative information however is more easily and with more accuracy obtained from the signal of a differential thermocouple^{1,2}. Alternatively the

differential can be taken electronically from the signal of an integral thermocouple. The difficulty in balancing a differential thermocouple as described^{1,2} can be anticipated.

The frequency of the signals, however, is very low (5–20 Hz). Therefore a special arrangement must be made. Figs. 9 and 10 show possible electric circuits for differentiating⁵. The use of a Knick amplifier, type A, creates too much noise for using it in combination with the circuit of Fig. 9. Better results with respect to the signal-to-noise ratio are found with the circuit of Fig. 10.

Tantalum capacitors are used because they diminish the signal-to-noise ratio to negligible proportions. Fig. 11 shows two electropherograms of identical mixtures. The electropherogram on the left-hand side (A) is made with the differentiator of Fig. 10. The electropherogram on the right-hand side (B) is made with a differential thermocouple, but this thermocouple is badly balanced².

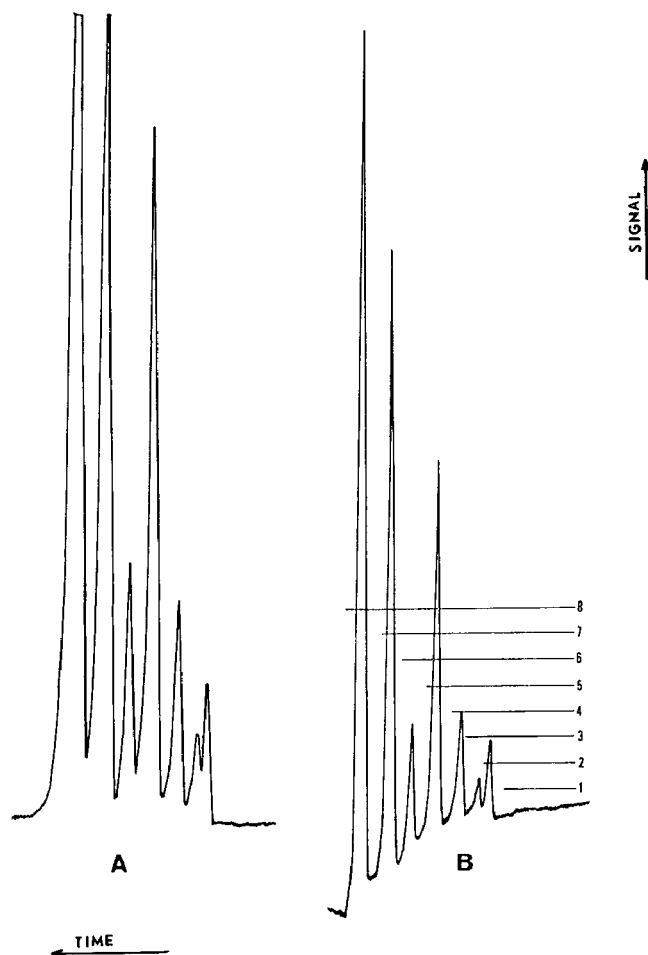


Fig. 11. Electropherogram obtained from a differentiator (A) and from a differential thermocouple (B), badly balanced. 1 = chloride; 2 = sulfate; 3 = oxalate; 4 = formate; 5 = citrate; 6 = adipate; 7 = acetate; 8 = glutamate.

The conditions for the analysis were as follows. The leading electrolyte was histidine (0.01 *M*) and histidine · HCl (0.01 *M*). The terminal electrolyte was glutamic acid (0.01 *M*). Injected was a mixture of sulfate, oxalate, formate, citrate, adipate and acetate. A stabilized current of 70 μ A was used. The initial voltage was about 4 kV and the final voltage was 20 kV. The system was thermostated at 18°. The velocity of the recorder paper was 30 cm/h (electropherogram A) and 12 in./h (electropherogram B). Fig. 11 shows clearly that the peaks obtained from the differential thermocouple are smaller than those made by the differentiator. Making the signal quicker by a factor 3 means enlarging the noise by a factor 7 (ref. 5). The use of a differential thermocouple still has an advantage. If a hot zone travels in the opposite direction, the integral thermocouple registers this zone in the normal way and a positive peak is the result by using a differentiator. By the use of a differential thermocouple a negative peak or dip will be seen. The same effect can be obtained if two integral thermocouples, close together, are used.

REFERENCES

- 1 F. M. EVERAERTS, *Thesis*, Eindhoven University of Technology, 1968.
 - 2 A. J. P. MARTIN AND F. M. EVERAERTS, *Proc. Roy. Soc. (London)*, Ser. A, 316 (1970) 493.
 - 3 F. M. EVERAERTS, J. VACÍK, T. P. E. M. VERHEGGEN AND J. ZUSKA, *J. Chromatog.*, 49 (1970) 262.
 - 4 A. H. M. T. WEYDEN, Private communication, Elisabeth Hospital, Tilburg, 1970.
 - 5 J. G. H. M. JONKERS, Private communication, Eindhoven University of Technology, 1970.
 - 6 J. VACÍK AND J. ZUSKA, *Chem. Listy*, in press.
 - 7 H. HAGLUND, *Sci. Tools*, 17 (1970) 2.
 - 8 F. M. EVERAERTS AND T. P. E. M. VERHEGGEN, *Sci. Tools*, 17 (1970) 17.
 - 9 A. J. P. MARTIN AND F. M. EVERAERTS, *Proc. Roy. Soc. (London)*, Ser. A, in press.
- J. Chromatog.*, 53 (1970) 315-328

CHROM. 4950

THE APPLICATION OF THIN-LAYER ELECTROPHORESIS AND CHROMATO-ELECTROPHORESIS ON SEPHADEX G-25 TO THE ANALYSIS OF AMINO ACID AND PEPTIDE COMPOSITION OF BIOLOGICAL FLUIDS

A. KLEIN, J. CHUDZIK AND M. SARNECKA-KELLER

Laboratory of Animal Biochemistry, Institute of Molecular Biology, Jagiellonian University, Kraków (Poland)

(Received July 27th, 1970)

SUMMARY

Some examples of the application of thin-layer electrophoresis on Sephadex G-25 and of the use of this technique with paper chromatography to the examination of amino acid and peptide composition of urine and blood plasma are given. Thin-layer electrophoresis appears to be a very convenient method for a preliminary rapid analysis, especially of urine. In most cases the deproteinization and desalting of samples are not required, and the procedure can be completed with photodensitometric analysis. The chromatoelectrophoresis is a more tedious and time-consuming method, but it enables the demonstration of variations in the level of individual amino acids and other ninhydrin-positive substances.

INTRODUCTION

In 1968 we reported the successful separation of artificial mixtures of amino acids and low-molecular-weight peptides by means of thin-layer electrophoresis and chromatoelectrophoresis on Sephadex G-25 (ref. 1). In this paper we describe the results of the application of the same methods to the analysis of amino acids and peptides present in urine and blood plasma of human or mammalian origin.

EXPERIMENTAL

Materials

The analyses were carried out on citrated blood plasma or 24-h samples of urine. The volume of the samples applied depended on the level of total nonprotein α -amino nitrogen present in the biological fluid under study. This was estimated in deproteinized urine or blood plasma with ninhydrin according to ROSEN². In all experiments Sephadex G-25 fine (Pharmacia, Uppsala, Sweden) was used, the same portion being repeatedly regenerated by the procedure given in the previous paper¹.

Methods

Thin-layer electrophoresis. The technique of thin-layer electrophoresis was the same as previously described¹ with only slight modifications. The size of glass plates was 6×36 cm and the time of electrophoresis 4 h. Samples of normal and pathological human urine were mostly used for analysis without any initial treatment. Mouse urine, especially from males, was deproteinized with 96% ethanol, the ratio of urine and alcohol being 1:4. The same method was also applied to the deproteinization of plasma.

Chromatoelectrophoresis. The use of descending paper chromatography with thin-layer electrophoresis on Sephadex G-25 was carried out in the same way as described for standard mixtures¹. The solvent system *n*-butanol-acetic acid-water (144:13:43) used in the chromatographic procedure was the only modification applied in these experiments. Glass plates, 24×36 in size, were used in most cases. In a few experiments the distance of development in paper chromatography was twice as long as usual. In these cases, after the development of the chromatograms, the paper strips were cut in two, and for each half a separate glass plate of the same size as before was employed. The samples of urine and blood plasma were deproteinized and desalted with Dowex 50 X8. The elution of the amphoteric substances from the ion exchanger was carried out with aqueous 2 *N* NH₃ which was then removed by evaporation under reduced pressure at room temperature. In some experiments a different deproteinization method was employed for blood plasma. The sample was evaporated to dryness under reduced pressure at *ca.* 25°, treated 3 times with 5 volumes of acetone containing 5% 6 *N* HCl, and the acetonic extracts were centrifuged and HCl removed by evaporation to dryness several times with water under the former conditions. In each comparative series of analysis, the same procedure of deproteinization and desalting was always used.

Staining and quantitation of the spots. After drying the plates in air at room temperature, the spots were dyed by carefully spraying the gel surface with a 2% acetone solution of ninhydrin. The color was developed at room temperature or at 60°. In some cases replicas were made on Whatman No. 1 paper strips and dyed with ninhydrin. A visual evaluation of the color intensity of the ninhydrin-positive spots obtained in the course of electrophoretic separation was checked by photo-densitometric analysis. For this purpose photo replicas of the electropherograms were made on a Fotopan DIA-T film, and measurements were carried out with photodensitometer VEB (Medizinische Gerätefabrik, Berlin, G.F.R.).

Elution of fractions from thin-layer electropherograms and analysis of the peptide-bound amino acids. The electrophoretic fractions revealing the differences in the amount or in quantitative proportion of the ninhydrin-positive substances were investigated with respect to peptide-bound amino acids. According to the pictures obtained on the paper replica stained with ninhydrin, the corresponding part of gel was carefully removed from glass plates, eluted with twice distilled water, and the pooled eluates were evaporated under reduced pressure to the proper volume. The substances with free α -amino groups were transformed into DNP-derivatives according to the method of SANGER³. The DNP-amino acids were extracted with ether, and DNP-peptides left in the water fraction were hydrolyzed in sealed tubes with 6 *N* HCl at 100° for 24 h. The HCl was removed under reduced pressure, and amino acids were analyzed by descending paper chromatography on Whatman No. 1 paper

strips using the solvent system *n*-butanol-acetic acid-water (143:13:43) and with ninhydrin as developing reagent.

RESULTS

Some examples from our investigations are given here to demonstrate the usefulness of thin-layer electrophoresis and chromatoelectrophoresis with Sephadex G-25 as supporting medium for examination of the amino acid and peptide composition of biological fluids.

Fig. 1 presents the patterns of ninhydrin-positive spots obtained during the

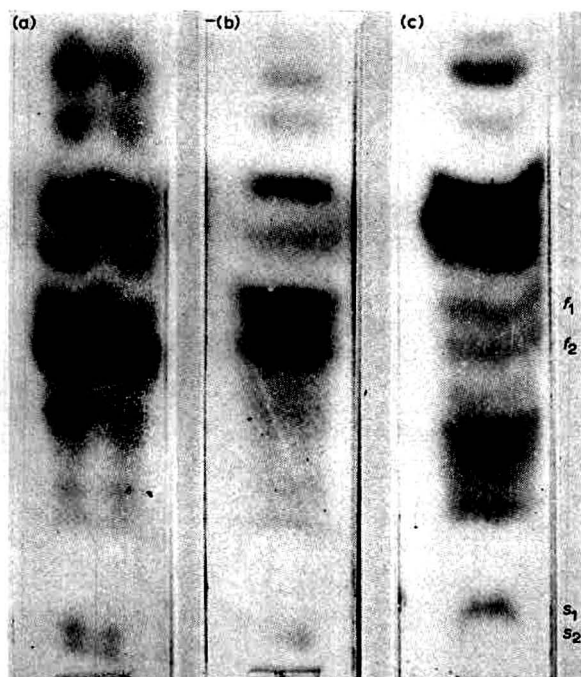


Fig. 1. The pattern of thin-layer Sephadex G-25 electrophoresis of the ninhydrin-positive substances present in 100 μ l of urine from male mice hemizygous for the sex-linked lethal Mosaic (Ms) mutation. (a) Mice 10 days old; (b) mice 18 days old; (c) mice 6 months old. The sample of urine was deproteinized with ethanol. s_1 and s_2 = non-amino acid substances; f_1 and f_2 = fractions with various levels of constituents.

thin-layer electrophoresis on Sephadex G-25 of the urine of male mice hemizygous for the sex-linked lethal Mosaic (Ms) mutation⁴. Three groups of mice, 10 days, 18 days and 6 months old, were considered. The patterns (a, b and c) are similar in qualitative composition, but there is a striking difference in the two electrophoretic fractions (f_1 and f_2), the quantities of which decreased gradually with the age of immature animals. The main components of fraction f_1 were identified as serine, valine and leucine while fraction f_2 contains methionine, glutamic acid and glutamine. We suspect that the exogenous amino acids are especially responsible for the differences observed, and this hypothesis will be checked in a further investigation.

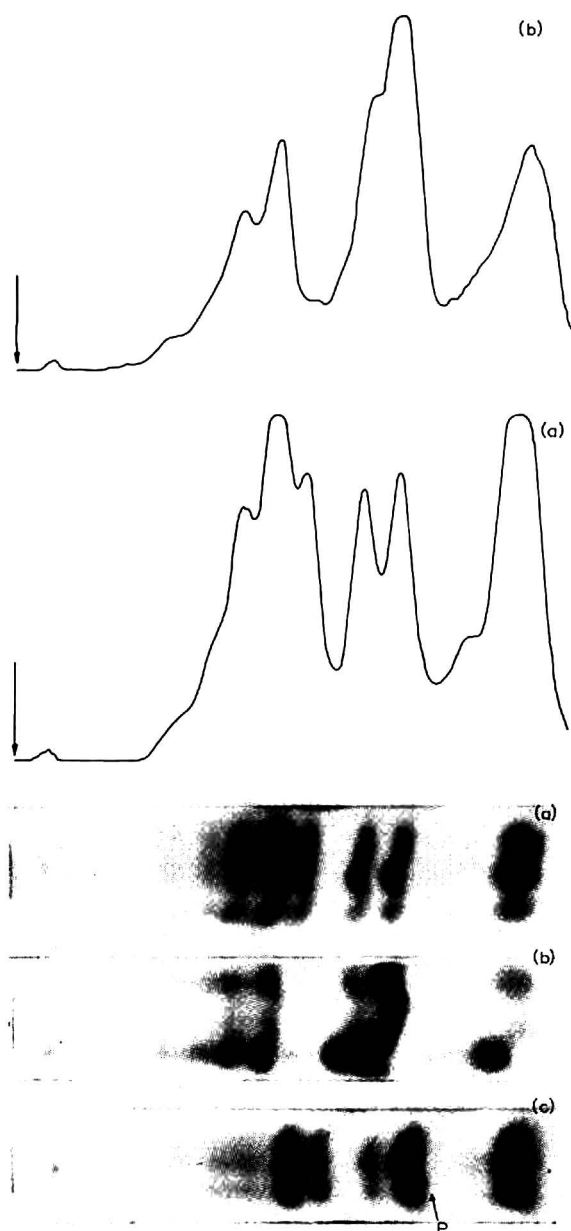


Fig. 2. The patterns of thin-layer Sephadex G-25 electrophoresis of urinary ninhydrin-positive substances and their corresponding photodensitograms. Urine is not deproteinized. Each sample analyzed corresponds to 100 μ l of urine. (a) Urine of normal human adults; (b) collagenic urine of a patient suffering from lupus erythematosus disseminatus; (c) collagenic urine of a patient suffering from periarteritis. P — abnormal peptide absent in normal urine.

Fig. 2 shows the thin-layer electropherogram on Sephadex G-25 of ninhydrin-positive substances present in normal adult human urine (a) in comparison with the corresponding electropherograms of two cases of collagenosis (b, c). In this figure



Fig. 3. The paper chromatograms of amino acids present in hydrolysates of a DNP-peptide. (a) Glycine electrophoretic fraction of periarthritis urine; (b) corresponding fraction of normal urine.

the photodensitograms of one normal and one of two pathological cases are also given as examples of the quantitation of the fractions. Besides the various proportions of the electrophoretic fractions in collagenic urine as compared with the normal one, the electrophoretic separation revealed one additional spot in the urine of the patient suffering from periarthritis nodosa. This substance shows the electrophoretic migration rate slightly greater than glycine but can be easily differentiated from this amino acid by its pink color with ninhydrin. After eluting the part of the gel containing this substance together with glycine, the fraction obtained was investigated with

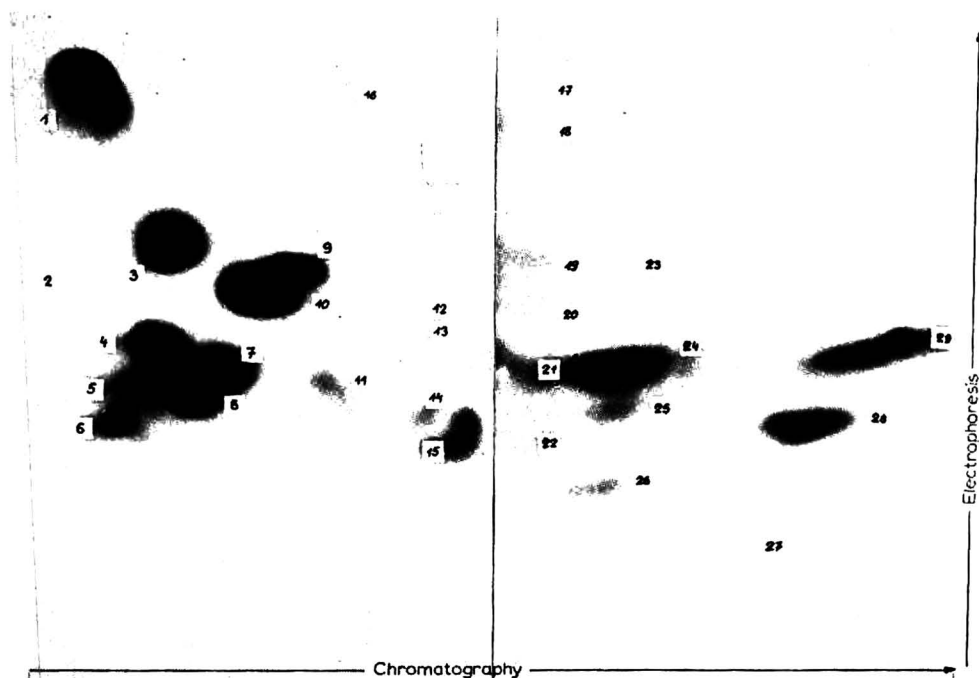


Fig. 4. The chromatoelectrophoretic pattern of ninhydrin-positive substances present in bovine blood plasma. Plasma deproteinized with Dowex 50 X8. The sample analyzed corresponds to a 170 μ l volume of blood plasma. The distance of chromatographic development is ca. 40 cm; the electrophoresis is carried out on two plates each 24 \times 36 cm. (1) His + Lys + Arg; (2) Cysteine; (3) Gly; (4) Ser; (5) GluNH₂; (6) Asp; (7) Thr; (8) Glu; (9) unidentified; (10) Ala; (11) Pro; (12) α -aminobutyric acid; (13) β -aminoisobutyric acid; (14) unidentified; (15) Tyr; (16) γ -amino butyric acid; (17-23) unidentified; (24) Val; (25) Met; (26) Try; (27) unidentified; (28) Phe; (29) Leu + Ile.

respect to peptide-bound amino acids. Simultaneously the same procedure was applied to the glycine fraction of normal human urine. In Fig. 3 the comparison of the paper chromatograms obtained from hydrolysates of both fractions previously devoid of free amino acids are presented. It is evident that the abnormal substance is a peptide composed chiefly of glycine, alanine and tyrosine.

The electrophoretic separation demonstrated the presence of two non-amino acid compounds (s_1 and s_2) in all samples of urine of different origin examined (see Fig. 1). Their migration rates are slower than that of taurine, and this is probably the consequence of their strong acidic nature. It was found that at least one of them contains a sugar residue.

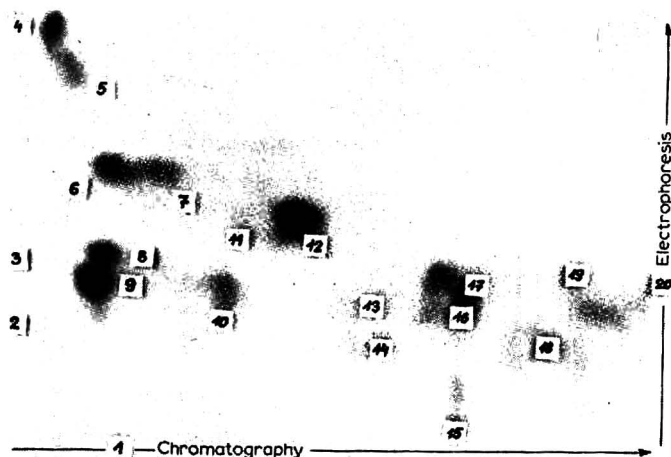


Fig. 5. The chromatoelectrophoretic pattern of ninhydrin-positive substances present in blood plasma of outbred male mice (wild genotype) 18 days old. The plasma deproteinized with acetone. The sample analyzed corresponds to 150 μ l volume of plasma. The distance of chromatographic development is ca. 20 cm; electrophoresis was carried out on a plate 24 \times 36 cm in size. (1) Tau; (2) unidentified; (3) Cystine; (4) Lys + His; (5) Arg; (6) Gly; (7) unidentified; (8) Ser; (9) GluNH₂; (10) Glu; (11) unidentified; (12) Ala; (13) unidentified; (14) Tyr; (15) Try; (16) Met; (17) Val; (18) Phe; (19) Ileu; (20) Leu.

Fig. 4 shows the chromatoelectrophoretic pattern of the ninhydrin-positive substances present in bovine plasma. Besides 19 spots corresponding to the three isomers of aminobutyric acid and to the amino acids that are the normal constituents of proteins, 10 unidentified substances were found. Some of them are probably low-molecular-weight peptides. The comparison of this pattern with those presented in Figs. 5 and 6 reveals the similarities and differences in the level of amino acids and some other ninhydrin-positive substances of bovine and mouse blood plasma. However, it should be noted here that the absence of taurine from bovine plasma is the consequence of only applying Dowex 50 X8 to deproteinization of the sample analyzed. The great number of unidentified spots observed on the chromatoelectropherogram of bovine blood plasma may also result from a longer chromatographic development.

Figs. 5 and 6 give a comparison of the composition of ninhydrin-positive substances of blood plasma originating from outbred male mice with the corresponding sample taken from male mice carrying the lethal Ms mutation. The most characteristic

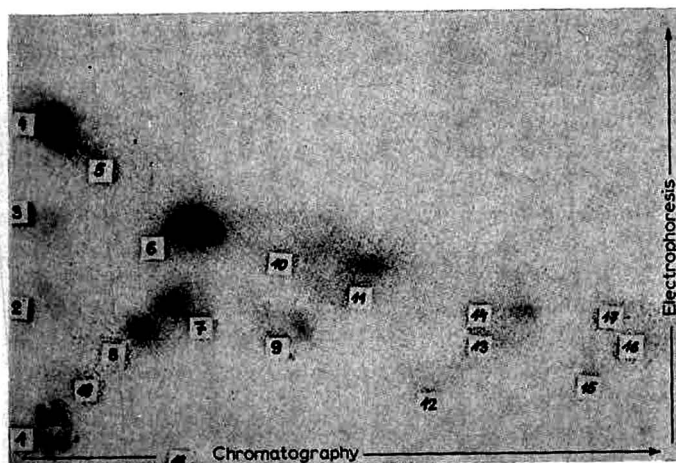


Fig. 6. The chromatoelectrophoretic pattern of ninhydrin-positive substances present in blood plasma of 18-day-old male mice hemizygous for the sex-linked lethal Mosaic(Ms) mutation. The deproteinization, volume of sample and conditions of chromatographic and electrophoretic separation are the same as those given in Fig. 5. (1) Unidentified; (2) Cystine; (3) Cysteine; (4) Lys + His; (5) Arg; (6) Gly; (7) Ser; (8) GluNH₂; (9) Glu; (10) unidentified; (11) Ala; (12) Tyr; (13) Met; (14) Val; (15) Phe; (16) Leu; (17) Ile; (18) Tau; (19) Asp.

feature of the last sample is the absence of tryptophan as well as a lower level of some other amino acids.

DISCUSSION

The results given in this paper showed that Sephadex G-25 (fine) is a good supporting medium for thin-layer electrophoresis of ninhydrin-positive substances present in biological fluids. The regeneration of the gel is very simple, and the patterns obtained are reproducible. It should be noted here that our attempts to apply Sephadex G-25 to thin-layer chromatography of the same substances were unsuccessful. Also the thin-layer electrophoresis carried out under the same conditions on Sephadex G-10 (fine) as well as on Bio-Gel P-2 have completely failed.

Thin-layer electrophoresis on Sephadex G-25 (fine) combined with photodensitometric analysis is especially useful in examining the amino acid and peptide composition of human urine with physiological level of proteins. In pathological cases connected with proteinuria or in some mammalian urine with normally high levels of proteins, *e.g.* in rats⁶ and in mice⁶, a very simple method of deproteinization with alcohol is sufficient. Thin-layer electrophoresis can be recommended for rough but rapid analysis of the amino acid and peptide composition of the urine. For this purpose the paper replicas should be made and the ninhydrin-positive spots developed on them at 60° for 10 min. After making the replica the plate can be used for performing a different color test or for a ninhydrin test developed at room temperature for 24–48 h because only in this way is it possible to obtain the gel surface suitable for taking the photographs of the pattern obtained.

The electrophoretic fractions can be very easily eluted by water and be further investigated as was the case in our examination of collagenic urine.

The chromatoelectrophoresis is undoubtedly more complicated and time consuming and therefore cannot be used in routine analyses. However like the other two-dimensional separation methods it is very precise and makes it possible to demonstrate the differences in individual amino acids. It can be also extended to the other ninhydrin-positive substances as amines, amino alcohols and low-molecular-weight peptides.

While employing the thin-layer electrophoresis on Sephadex G-25 we found, among others, the relationship between the urinary amino acid and peptide excretion and the age of mice. Also an abnormal peptide was demonstrated in the urine of the patient with periarteritis. Unfortunately owing to the scarcity of this disease we have only been able to examine one case. Although the results are very interesting they cannot be generalized and are reported here as an illustration of the efficiency of the method employed.

By means of chromatoelectrophoresis the variations in the composition of ninhydrin-positive substances of blood plasma of various species of mammals, and even different genotypes of the same species, were found. The details of the differences involving the amino acid and peptide composition in urine and blood plasma between Ms mutant and control mice are given in separate papers^{7,8}.

REFERENCES

- 1 J. CHUDZIK AND A. KLEIN, *J. Chromatog.*, 36 (1968) 262.
- 2 H. ROSEN, *Arch. Biochem. Biophys.*, 67 (1957) 10.
- 3 F. SANGER, *Biochem. J.*, 39 (1945) 507.
- 4 H. KRZANOWSKA, *Mouse News Letter*, 35 (1966) 35.
- 5 A. K. ROY, O. W. NEUHAUS AND CH. R. HARMISSON, *Biochim. Biophys. Acta*, 127 (1956) 72.
- 6 L. F. WICKS, *Proc. Soc. Exper. Biol. Med.*, 48 (1941) 395.
- 7 A. KLEIN AND J. STYRNA, *Acta Biol. Cracov. ser. Zool.*, in press.
- 8 A. KLEIN AND K. SITARZ, *Acta Biol. Cracov. ser. Zool.*, in press.

J. Chromatog., 53 (1970) 329-336

CHROM. 4946

ELECTROPHORESIS AND THIN-LAYER CHROMATOGRAPHY OF
ORGANIC BASE POLYTHIONATES

QUALITATIVE ANALYSIS

V. V. SMOLYANINOV

Institute of Protein Research, Academy of Sciences of the U.S.S.R., Moscow Region, Poustchino (U.S.S.R.)

(Received July 23rd, 1970)

SUMMARY

Methods of qualitative analysis of organic base polythionates are described.

Paper electrophoresis in the 0.05 *M* triethylammonium bicarbonate buffer with a pH of 7.5 permits the analysis of polythionates of organic and inorganic bases. In this case, large amounts of colloidal sulphur and halogens do not interfere with the determination of higher polythionic acids. However, we failed to separate decyl-quinolinium tetrathionate by electrophoresis.

Thin-layer chromatography on a layer of Kieselgel G + 10% of Dowex 50 W-X8 in the K⁺ form + 2% of potassium acetate makes it possible to analyse any polythionates, independent of the solubility and structure of the initial base, and the results of the separation of organic and inorganic polythionates agree well.

INTRODUCTION

Methods for the qualitative analysis of organic base polythionates and reaction mixtures by paper electrophoresis and thin-layer chromatography are described in this paper.

ELECTROPHORESIS

The study of the reactions involved in the formation of organic base tetra- and pentathionates during acidification of thiosulphate is greatly hindered by the absence of physico-chemical methods of analysis.

Current methods of analysing potassium or sodium polythionates^{1,2} when applied to the separation of organic polythionates give unsatisfactory results.

The purpose of the present paper is to develop a method of analysis of organic base polythionates³⁻⁵ and reaction mixtures.

Separation was carried out on FN-II paper with a "Labor" Model OE-202 vertical electrophoresis apparatus.

The following aqueous solutions were investigated as buffers: 0.05 *M* ammonium carbonate brought to pH 9.0 with ammonia; 0.05 *M* ammonium bicarbonate solution; 0.05 *M* sodium sulphate solution and 0.05 *M* triethylammonium bicarbonate solution, pH 7.5. The best separation was obtained by using the 0.05 *M* triethylammonium bicarbonate buffer.

Sodium sulphide and thiosulphate; potassium trithionate, potassium diethylnonylammonium and trioctylammonium tetrathionates; potassium and sodium pentathionates; potassium hexathionate; triethylnonylammonium chloride; decylquinolinium bromide; triethylbutylammonium iodide; trioctylammonium, diethylnonylammonium and triisoamylammonium polythionates were employed as markers and materials for investigation.

The material studied and markers were applied to the starting line in the form of 0.1 *M* solutions in methanol or water in a quantity varying from 1.0 μ l to 15 μ l in 2 cm length strips with 1 cm intervals; this constituted from $0.1 \cdot 10^{-6}$ mole to $1.5 \cdot 10^{-6}$ mole of material. The maximum sensitivity of detection of the polythionates was about $0.5 \cdot 10^{-8}$ mole or, depending on the molecular weight of the polythionate investigated, from 10 to 2 μ g.

TABLE I

DISTANCES OF POLYTHIONIC ACID, HALOGEN, THIOSULPHATE AND SULPHIDE IONS FROM THE STARTING LINE AT DIFFERENT PERIODS OF TIME

Time	Ion									
	<i>Cl</i> ⁻	<i>Br</i> ⁻	<i>I</i> ⁻	<i>S</i> ₂ <i>O</i> ₃ ²⁻	<i>S</i> ²⁻	<i>S</i> ₃ <i>O</i> ₆ ²⁻	<i>S</i> ₄ <i>O</i> ₆ ²⁻	<i>S</i> ₅ <i>O</i> ₆ ²⁻	<i>S</i> ₆ <i>O</i> ₆ ²⁻	<i>S</i> ₇ <i>O</i> ₆ ²⁻
1 h	203	203	197	200	202	193	165	147	136	113
1 h 30 min	332	330	325	320	318	292	251	232	208	191
1 h 45 min	372 ^a	370 ^a	370 ^a	360	368	318	290	270	256	246

^a Spots are located at the bottom of the sheet.

At different periods of time the ionic mobility of the polythionic acids and halogen ions, together with thiosulphate and sulphide was studied at an electrical field intensity equal to 20 V/cm. Distances covered in mm by the given ions from the starting line are reported in Table I.

The increase in temperature and the degree to which the paper is soaked with buffer solution has a decided influence on the ionic mobility, a different distance being covered by the same material on the same sheet as a result of some irregularity of spraying and heterogeneity of the paper, but the relative ionic mobility is in good accordance (Table II). The mobility of the *S*₄*O*₆²⁻ ion was taken as a unit for calculation.

After drying, the electropherograms were examined under BUV-15 bactericide lamps with a UVS-1 light filter, and the spots of the polythionates were marked beginning from tetrathionic acid and higher, and then the electropherograms were developed in a 0.1 *M* ammonia solution of silver nitrate; in this case *S*²⁻, *S*₂*O*₃²⁻, *S*₃*O*₆²⁻, *S*₄*O*₆²⁻ and higher polythionates produced brown spots, and the *S*₅*O*₆²⁻ was seen in the form of a black-and-brown spot. Among the halogens only the *I*⁻ ion is immediately discerned in the form of a yellow spot, but after a short exposure to an

TABLE II

RELATIVE IONIC MOBILITIES

Colloidal sulphur, present in some solutions, remained on the start.

Time	Ion									
	Cl^-	Br^-	I^-	$S_2O_3^{2-}$	S^{2-}	$S_3O_6^{2-}$	$S_4O_6^{2-}$	$S_5O_6^{2-}$	$S_6O_6^{2-}$	$S_7O_6^{2-}$
1 h	1.23	1.23	1.19	1.21	1.22	1.17	1.00	0.98	0.82	0.68
1 h 30 min	1.32	1.31	1.29	1.27	1.27	1.16	1.00	0.92	0.83	0.76
1 h 45 min	1.28	1.28	1.28	1.24	1.25	1.10	1.00	0.93	0.88	0.85

intense light the Cl^- and Br^- ions become dark violet and the I^- ion is seen as a violet spot. The electropherograms not developed with silver solution can be preserved for several months and the intensity of spots does not change, probably due to the decomposition of the polythionates to thiosulphate and sulphur, but those developed with silver solution become completely black in the course of a few days.

As is evident from Tables I and II, the ionic mobility of the Cl^- , Br^- , I^- ions practically coincides with that of a thiosulphuric acid ion, but halogen ions are located at a greater distance from the polythionic acid ions and were not used as markers in the subsequent operations. The sulphite ion which may be present in organic polythionates is not observed in either ultraviolet light or upon spraying with the ammoniacal silver nitrate solution.

The formation of polythionic acids during acidification of thiosulphate in the presence of organic bases occurs very rapidly, in practice, taking from a fraction of a second to 1–2 min; at the same time if 20 ml of dilute hydrochloric acid (1:4) are added to a solution of 7.4 g of sodium thiosulphate ($Na_2S_2O_3 \cdot 5H_2O$) in 25 ml of water the main components of the reaction mixture are thiosulphuric and trithionic acids.

TABLE III

EXPERIMENTAL RESULTS OF ELECTROPHORESIS OF A REACTION MIXTURE

Time	Point No.	Ions					
		$S_7O_6^{2-}$	$S_6O_6^{2-}$	$S_5O_6^{2-}$	$S_4O_6^{2-}$	$S_3O_6^{2-}$	$S_2O_3^{2-}$
0 min	1						m ^a
1 min	2				+ ^b	m	m
4 min	3				+	m	m
11 min	4			+	+	m	m
20 min	5			+	+	m	m
26 min	6			+	+	m	m
32 min	7		+	+	+	m	m
39 min	8		+	+	+	m	m
43 min	9		+	+	+	m	m
67 min	10		+	+	+	m	m
80 min	11		+	+	+	m	m
48 h	12	+	+	+	+	m	m
72 h	13	+	+	+	+	m	m
96 h	14	+	+	+	+	m	m

^a m is the main reaction product.

^b + = present in the reaction mixture.

Polythionic acids are formed within several minutes, the heptathionic acid only after 48 h.

Table III shows the experimental results obtained by electrophoresis of the reaction mixture.

The zero point was taken immediately after mixing the solution, the supernatant liquid being used for the analysis. A small amount of colloidal sulphur did not hinder the determination as it remained on the start. The quantity of the substance applied to the start constituted about $1 \cdot 10^{-5}$ mole, the quantity of thiosulphuric and tri-thionic acids in solution being essentially greater than necessary for their good separation and, moreover, the solution contained a high concentration of chloride ions.

THIN-LAYER CHROMATOGRAPHY

SEILER⁶ and SEILER AND ERLLENMEYER⁷ developed methods of analysis for halogen and sulphur compounds on silica gel in the form of their potassium and sodium salts and used solvent systems containing dioxane and ammonia. POLLARD *et al.*², in paper chromatography studies, noted that several spots are formed during polythionate analysis in the presence of several cations.

The distinct separation of anions is only possible in the presence of potassium or sodium ions, and in this case the sorbent or solvent system must not interact with them chemically.

Silica gel containing ion-exchange resin in the K^+ form and fixed with gypsum was used for the anion analysis.

Chromatographic separation was carried out on glass plates (100 × 200 and 200 × 200 mm) with a Kieselgel G sorbent layer + 10% of the ion-exchange resin Dowex 50 W-X8 (200–400 mesh) in the K^+ form + 2% of potassium acetate.

A 300 μ thick sorbent layer from an aqueous suspension was applied with an automatic applicator. 60 × 60 mm glass plates with the sorbent layer coated by hand were used for selecting the layer composition and the solvent system. On standard plates the chromatograms were developed in combined C- and BN-cells; on the non-standard ones—in the glass tanks with ground caps.

The use of a solvent system containing dioxane led to the formation of additional spots, as dioxane is rather quickly oxidised, and peroxides contributed to the formation of polythionates; for example, pure sodium thiosulphate gave several spots on the chromatogram.

The presence of ammonia in the solvent system led to the formation of twice as many spots, which suggests the displacement of anions in the form of ammonium salts and initial base salt. Cation-exchange resin in the K^+ form and potassium acetate, for the formation of a large excess of potassium ions during separation, were introduced into the sorbent layer in order to transform the organic base polythionates completely into potassium salts.

Acetate ions do not affect the separation and are not coloured during development.

In order to obtain an even front which is not discoloured with admixtures eluted from the layer by solvents, the plates were first washed up to their upper edge with the following solvent system: *tert.*-butanol–acetone–water (19:75:6).

Chromatograms were developed in a *tert.*-butanol–acetone–water (18:70:12)

system. The solvent used for a 200×200 mm plate was 15 ml, for a 100×200 mm one it was 9 ml; separation time was 30–40 min. 0.1 *M* solutions of the substances being investigated, in water or methanol, were applied as 2–3 mm diameter spots in a quantity up to $1 \mu\text{l} \cdot 1 \cdot 10^{-7}$ mole. Maximum detection sensitivity of anions constituted $1 \cdot 10^{-9}$ mole or from 1.0 to 0.2 μg .

If more than $0.5 \cdot 10^{-6}$ mole of the substance was applied the separation was unsatisfactory. The starting line (2 cm from the edge of the plate) and a start–front distance equal to 10 cm were chosen experimentally and gave the most distinct separation.

After drying the chromatograms were developed by spraying them with a 0.1 *M* ammonia solution of silver nitrate; they were also sprayed with an 0.1% solution of Bromcresol Green in 50% ethanol in order to determine SO_3^{2-} and $\text{S}_2\text{O}_8^{2-}$ ions. The luminophore L-36 was introduced into the sorbent layer for detecting $\text{S}_4\text{O}_6^{2-}$, $\text{S}_5\text{O}_6^{2-}$, $\text{S}_6\text{O}_6^{2-}$, $\text{S}_7\text{O}_6^{2-}$ ions without spraying. In this case polythionic acid ions are observed in the form of dark spots against a light background in ultraviolet light.

During the development by a silver salt solution S^{2-} , $\text{S}_2\text{O}_3^{2-}$, $\text{S}_3\text{O}_6^{2-}$, $\text{S}_4\text{O}_6^{2-}$, $\text{S}_5\text{O}_6^{2-}$, $\text{S}_6\text{O}_6^{2-}$, $\text{S}_7\text{O}_6^{2-}$ gave brown colourations; after exposure to the light halogen ions are seen as violet spots; SO_3^{2-} and $\text{S}_2\text{O}_8^{2-}$ ions produced yellow spots on a blue background after spraying with a solution of Bromcresol Green. The R_F values of the various anions are listed in Table IV.

TABLE IV

 R_F VALUES OF DIFFERENT ANIONS

Start- front dis- tance (cm)	R_F value													
	SO_3^{2-}	$\text{S}_2\text{O}_8^{2-}$	S^{2-}	$\text{S}_2\text{O}_3^{2-}$	Cl^-	Br^-	I^-	$\text{S}_3\text{O}_6^{2-}$	$\text{S}_4\text{O}_6^{2-}$	$\text{S}_5\text{O}_6^{2-}$	$\text{S}_6\text{O}_6^{2-}$	$\text{S}_7\text{O}_6^{2-}$	S_8	
5.0	—	—	o	o	0.23	0.52	0.69	0.17	0.38	0.56	0.85	—	1.0	
7.5	—	—	o	o	0.30	0.54	0.69	0.19	0.45	0.57	0.72	0.82	1.0	
10.0	0.18	0.30	o	o	0.30	0.55	0.72	0.23	0.48	0.63	0.73	0.81	1.0	
14.5	—	—	o	o	0.26	0.54	0.77	0.19	0.50	0.63	0.75	0.81	1.0	

Considerable diffusion of the higher polythionic acid spots took place with long start–front distances and detection sensitivity decreased sharply.

From Table IV it can be seen that S^{2-} and $\text{S}_2\text{O}_3^{2-}$ ions remain on the starting line, the Cl^- ion occupies an intermediate position between $\text{S}_3\text{O}_6^{2-}$ and $\text{S}_4\text{O}_6^{2-}$, the Br^- ion is between $\text{S}_4\text{O}_6^{2-}$ and $\text{S}_5\text{O}_6^{2-}$, the I^- ion practically coincides with the $\text{S}_6\text{O}_6^{2-}$ ion, colloidal sulphur present in polythionates forms a very diffused spot and is located mainly on the front line.

A high concentration of halogen, and especially I^- and Br^- ions, hinders the analysis of reaction mixtures owing to a complete overlapping of the polythionic acid spots.

Organic base polythionates and halides completely exchanged organic ions for K^+ ions on the ion-exchange resin. In this case even such slightly water-soluble polythionates as trioctylammonium and triisoamylammonium were completely converted into potassium salts.

THE COMPARISON OF METHODS OF ANALYSIS

A comparison of the methods of analysing organic base polythionates by paper electrophoresis and thin-layer chromatography is given in Table V.

It can be seen from Table V that the quantity of substance used for chromatography is 10 times less and the maximum detection sensitivity is 5 times higher as compared with that for electrophoresis. Time of analysis is 2–3 times shorter. But electrophoresis permits the separation of reaction mixtures with a high content of halides, thiosulphate and sulphide from polythionic acids, and even the measurement of their relative contents. In this case the large amount of colloidal sulphur which separates at the moment of reaction does not hinder the determination at all.

TABLE V

COMPARISON OF METHODS OF ANALYSIS

	<i>Electrophoresis</i>	<i>Thin-layer chromatography</i>
Time of analysis	1.5–2 h	30–40 min
Quantity of applied substance (moles)	$0.1 \cdot 10^{-6}$ – $1.5 \cdot 10^{-6}$	$0.1 \cdot 10^{-7}$ – $1 \cdot 10^{-7}$
Maximum detection sensitivity (moles)	$0.5 \cdot 10^{-8}$	$1 \cdot 10^{-9}$
Arrangement of anions:		
Start	colloidal sulphur	$S_2O_3^{2-}$, S^{2-}
	$S_7O_6^{2-}$	$S_3O_6^{2-}$
	$S_6O_6^{2-}$	Cl^-
	$S_5O_6^{2-}$	$S_4O_6^{2-}$
	$S_4O_6^{2-}$	Br^-
	$S_3O_6^{2-}$	$S_6O_6^{2-}$
	$S_2O_3^{2-}$, S^{2-}	$S_6O_6^{2-}$, I^-
	Cl^- , Br^- , I^-	$S_7O_6^{2-}$
Front	—	colloidal sulphur

However, it was not possible to achieve a distinct separation during analysis of N-alkylquinolinium polythionates by electrophoresis; for example, pure decylquinolinium tetrathionate gave a smeared spot which stretched from the start to the $S_4O_6^{2-}$ ion level.

Regardless of the nature of the organic base and the length and number of alkyl chains, organic base polythionates easily exchange an organic ion for a potassium ion, and ion-exchange adsorption–partition thin-layer chromatography makes it possible to determine their qualitative and quantitative composition.

The simultaneous application of these two methods of analysing organic and inorganic base polythionates provides the possibility of estimating the composition of the substances obtained more precisely and controlling the degree of purity, stability, and speed of formation of polythionic acids during thiosulphate acidification.

0.1 M sodium tetrathionate solution used as a marker contained about 90% of the original substance after a month while the rest was penta- and trithionic acids; the solution containing sodium thiosulphate, trithionate and tetrathionate gradually changed into a solution containing mainly sodium tri- and tetrathionate. Organic base polythionate solutions in methanol did not display visible changes in composition even after a year's storage.

CONCLUSIONS

1. A method of qualitative analysis of organic base polythionates by paper electrophoresis is described.

2. It was shown that polythionic acids produced during the acidification of thiosulphate are formed more slowly than in the presence of organic bases.

3. A technique for the analysis of organic and inorganic base polythionates and reaction mixtures by thin-layer chromatography has been worked out.

REFERENCES

- 1 H. W. WOOD, *J. Photogr. Sci.*, 2 (1954) 154.
- 2 F. H. POLLARD, G. NICKLESS AND R. B. GLOVER, *J. Chromatog.*, 15 (1964) 518.
- 3 N. P. VOLYNSKII, *Zh. Obshch. Khim. (U.S.S.R.)*, 29 (1959) 2114.
- 4 N. P. VOLYNSKII AND V. V. SMOLYANINOV, *Zh. Obshch. Khim. (U.S.S.R.)*, 33 (1963) 1456.
- 5 N. P. VOLYNSKII, *Zh. Obshch. Khim. (U.S.S.R.)*, 35 (1965) 167.
- 6 H. SEILER, *Helv. Chim. Acta*, 44 (1961) 1753.
- 7 H. SEILER AND H. ERLNMEYER, *Helv. Chim. Acta*, 47 (1964) 264.

J. Chromatog., 53 (1970)*337-343

CHROM. 4953

METAL ION SEPARATIONS IN THIOCYANATE MEDIA USING A LIQUID ANION EXCHANGER*

E. E. KAMINSKI** AND J. S. FRITZ***

Department of Chemistry, Iowa State University, Ames, Iowa 50010 (U.S.A.)

(Received July 28th, 1970)

SUMMARY

The liquid ion exchanger investigated, Alamine 336, may be used to effect numerous separations of metal ions in thiocyanate media. Some separations have been quantitatively demonstrated while others are suggested by the analogous behavior of metal ions in their particular extraction group. Under the mild conditions used in this study, *i.e.* room temperature and pressure, 10–30% (v/v) solution of exchanger in toluene, thiocyanate and acid concentrations less than 1.0 *M*, the physical handling of the amine was no problem. Phase separations were quick and clean for the solvent extraction work and there was no problem of extractant bleeding from the support in the reversed-phase column work.

INTRODUCTION

The use of liquid ion exchangers for the extraction of metal ions from thiocyanate media has been reported previously. MOORE¹ investigated the extraction of yttrium(III) from 7–8 *M* thiocyanate solutions into a xylene solution of methyl-diethylamine (MDOA). SHEPPARD² examined the extraction behavior of americium, curium, berkelium, californium and einsteinium between aqueous 5 *M* ammonium thiocyanate and a xylene solution of tri-*n*-octylamine (TOA). HUFF³ applied the liquid extraction data of MOORE⁴ and GERONTOPULOS *et al.*⁵ to column partition chromatographic studies of americium, yttrium and rare earths using Aliquat 336 as the sorbed liquid and aqueous eluents of 0.1 *M* to 0.4 *M* ammonium thiocyanate.

Several papers concerned with the extraction of cobalt from thiocyanate solution utilized Aliquat 336 in benzene⁶ and triisooctylamine (TIOA) in carbon tetrachloride⁷ for the spectrophotometric determination of cobalt(II) in the colored organic phase. WATANABE AND AKATSUKA⁸ used TOA dissolved in various diluents to study the extraction of cobalt(II) from aqueous thiocyanate solutions.

* Work was performed in the Ames Laboratory of the U.S. Atomic Energy Commission. Contribution No. 2788.

** Present address: Analytical Research Department, Abbott Laboratories, North Chicago, Ill., U.S.A.

*** To whom reprint requests should be addressed.

BRINKMAN *et al.*⁹ used five different liquid ion exchangers impregnated on paper and thin-layer adsorbents to study the behavior of copper(II), cadmium(II), lead(II), cobalt(II), manganese(II) and silver(I) in 0–10 *M* thiocyanate solutions. PRZESZLAKOWSKI¹⁰ used paper chromatography to study the extraction of a large number of metal ions between aqueous ammonium thiocyanate–hydrochloric acid mixtures and TOA, TIOA and tri-*n*-butylamine.

The purpose of this work is to investigate the analytical potential of a weak base liquid ion exchanger, Alamine 336, for the solvent extraction and reversed-phase column chromatographic separation of metal ions in thiocyanate media. Much of the quantitative work in the literature has been directed toward the lanthanide and actinide metals using fairly concentrated thiocyanate solutions. Thiocyanic acid is a strong acid and thiocyanate ion forms complexes with numerous metal ions^{11,12}, so it should be possible to perform separations with Alamine 336 using mild conditions, *i.e.* dilute solutions of thiocyanate (<1.0 *M*) and acid (~ 0.5 *M*).

APPARATUS AND CHEMICALS

A Perkin-Elmer Model 290 atomic absorption spectrophotometer equipped with a Perkin-Elmer combination cobalt, chromium, copper, manganese and nickel hollow cathode lamp was used for the atomic absorption analysis of cobalt, copper and nickel. An air–acetylene flame was used throughout.

Commercial Alamine 336 (tricapryl tertiary amine) was obtained from General Mills, Inc., and used without further purification. The company gives a typical analysis as showing 95% tertiary amine content, 1% secondary amine content, 0.2% primary amine content and 0.0% water.

The column support, Chromosorb W (non-acid washed, 80–100 mesh), was obtained from Johns-Manville Products Corporation and was washed successively with 6 *M* hydrochloric acid, distilled water, acetone and oven dried at 110° before use.

The reagent grade chloride, nitrate or oxide salt of the metal was diluted to a final acid concentration of 0.5 *M* unless hydrolysis was a problem. Gallium and indium solutions were prepared from the 99.99% pure metal. Synthetic sample mixtures for column separation studies were prepared by mixing given volumes of standardized metal ion solution and eluent (acidic solutions of potassium thiocyanate were prepared immediately before use). The sample volume added to the column was either 1 or 2 ml.

EXPERIMENTAL

Alamine 336 (R_3N) was diluted with toluene and converted to the thiocyanate form ($R_3NH^+SCN^-$) by equilibrating three times with an equal volume of a solution 1.0 *M* in potassium thiocyanate and 0.5 *M* in hydrochloric acid followed by a water wash. A 20% (v/v) solution of R_3N in toluene is 0.4 *M* (ref. 13).

Solvent extraction batch distribution ratios were determined by equilibrating equal volumes of organic and aqueous phases. Aliquots of the aqueous phase were taken and the metal ion concentration determined using an appropriate analytical method. The amount of metal ion in the organic phase was determined by material balance.

The reversed-phase column chromatographic columns were prepared by dissolving x ml of Alamine 336 in ether and then continuously slurrying with y g of support in an open vessel until no ether fumes were present (the maximum load is approximately 20 ml/17.5 g). The dry coated support was slurried in a solution 1.0 M in potassium thiocyanate and 0.5 M in hydrochloric acid, then poured into a column and allowed to settle via gravity flow.

Conditions for determination of copper(II), cobalt(II) and nickel(II) by atomic absorption are those recommended by the Perkin-Elmer Co.

RESULTS AND DISCUSSION

Distribution data were determined for 29 metal ions between an aqueous phase of 0.063 M KSCN–0.5 M HCl and an organic phase of 20% (v/v) $R_3NH^+SCN^-$

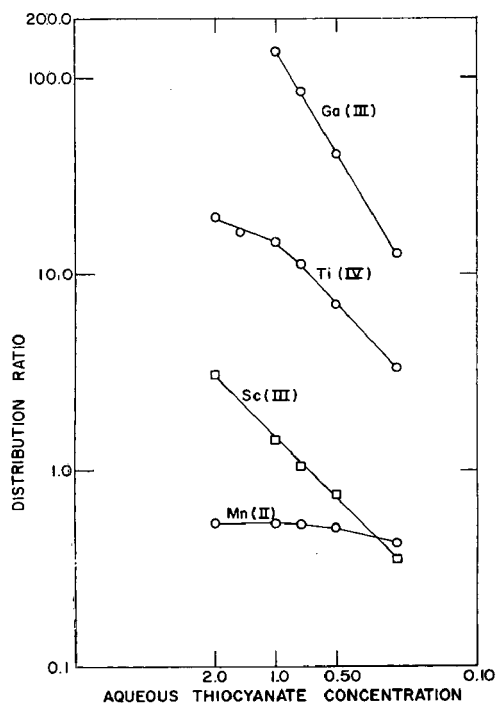


Fig. 1. Distribution ratio as a function of thiocyanate concentration.

in toluene. A 5-min equilibration period was used mainly for convenience because a series of gallium(III) extractions performed using initial aqueous solutions of 0.5 M HCl, 0.30 M KSCN–0.5 M HCl and 0.70 M KSCN–0.5 M HCl indicated that equilibrium was attained within 60 sec.

The volume distribution ratio, D_v , was calculated as follows:

$$D_v = \frac{\text{total concentration of metal ion in organic phase}}{\text{total concentration of metal ion in aqueous phase}}$$

The extraction data indicate that the metal ions studied may be divided into three distinct groups:

Group 1—Low extraction, $D_v < 0.10$. Ions included are Al(III), Ba(II), Ca(II), Eu(III), La(III), Lu(III), Mg(II), Ni(II), Pb(II), Sr(II), Th(IV), Y(III).

Group 2—High extraction, $D_v > 30.0$. Ions included are Bi(III), Cd(II), Co(II), Cu(II), Fe(III), Hg(II), In(III), Pd(II), Sn(IV), U(VI), Zn(II), Mo(VI).

Group 3—Intermediate extraction, $D_v = 0.2-2.0$. Ions included are Ga(III), Hf(IV), Mn(II), Sc(III), Ti(IV), Zr(IV).

The effect of increasing aqueous thiocyanate concentration on the distribution ratios of four intermediate extraction group ions is shown in Fig. 1. Two ions from the low percentage extraction group, thorium(IV) and nickel(II), were included in this study of increasing thiocyanate concentration. Their behavior is quite different from the intermediate extraction group ions, with the exception of manganese(II), because their extraction does not increase significantly over the entire thiocyanate concentration range studied. At 1.0 *M* thiocyanate the distribution ratios for nickel and thorium are still less than 0.03. Thus the possibility exists for column separations involving an ion or ions from each extraction group simply by controlling the thiocyanate concentration of the eluent.

Separations

The magnitude of the distribution data suggests that it should be possible to extract any combination of ions in Group 2 from any combination of ions in Group 1. Two practical applications of this concept were the removal of interfering metal ions from water prior to the determination of hardness via the method of FRITZ *et al.*¹⁴, and the quantitative separation of cobalt and nickel.

Water hardness

Traces of dissolved iron, copper, cobalt and certain other metal ions may

TABLE I

REMOVAL OF Fe(III), Cu(II) AND Co(II) FROM HARD WATER SAMPLES

Column: 1.0 cm × 6.0 cm of Alamine 336 impregnated Chromosorb W.

No.	Sample	Flow rate	Titration results	
			Initial hardness (p.p.m.)	Hardness found (p.p.m.)
1	20 p.p.m. Fe(III), 20 p.p.m. Cu(II) and 10 p.p.m. Co(II) as CaCO ₃	80 ml at 4 ml/min 150 ml at 12 ml/min	93.0	93.0
2	Same as 1	100 ml at 9 ml/min	93.0	91.8
3	20 p.p.m. Cu(II), 20 p.p.m. Fe(III) and 2 p.p.m. Co(II) as CaCO ₃	400 ml at 9 ml/min	110.3	109.9 ^a 109.9 ^b 109.9 ^c

^a First 150 ml.

^b Second 150 ml.

^c 300-400 ml fraction.

interfere with water hardness titrations by reducing the sharpness of the end point or completely preventing a color change. Cyanide masks these metals if their concentration is not too great, but its use is hazardous.

The solvent extraction separation procedure involved extraction of 200 ml of hard water, containing 50 p.p.m. each of Fe(III), Co(II), and Cu(II) as CaCO_3 , with 200 ml of 20% (v/v) exchanger and then 20 ml of a 20% (v/v) solution of Alamine 336 in toluene. Titrations of aliquots of the aqueous phase indicated an average hardness of 111.7 p.p.m., which corresponds favorably to the initial hardness of 110.3 p.p.m.

This separation problem was also attempted using a column procedure which would be more suitable for handling large volumes of water on a continuous basis. Table I lists the conditions and results of three such separations. In all cases the indicator change at the equivalence point was excellent and a comparison of total initial hardness and total hardness found indicates within experimental error no calcium or magnesium was lost during extraction. These separations are fast and the conditions used are mild. The water sample is not pretreated in any manner except to adjust the pH below 1.0 for the solvent extraction procedure.

Preparation of cobalt-free nickel salts

The very favorable separation factor between Group I and Group 2 metal ions, plus the fact that metal ions may be extracted from acidic aqueous solutions without direct addition of a complexing agent to the aqueous phase, makes Alamine 336-thiocyanate potentially useful for larger-scale separations such as the purification of metal salts. Although many possibilities exist the removal of small amounts of cobalt(II) from nickel(II) salts was selected for further study. Batch extraction

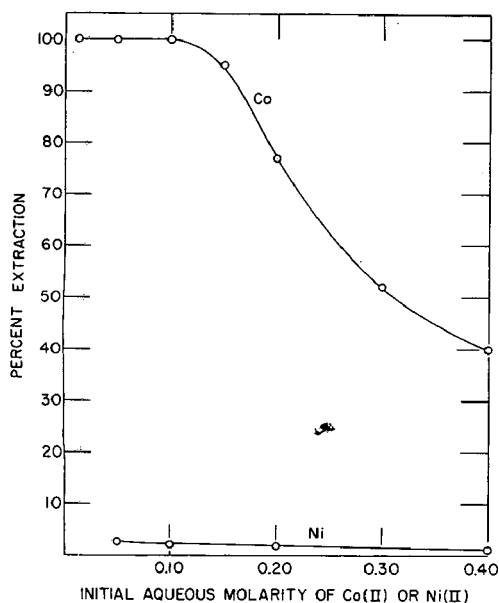


Fig. 2. Percent extraction of Co(II) or Ni(II) from 0.1 M HNO_3 into an equal volume of 0.6 M $\text{R}_3\text{NH}^+\text{SCN}^-$ in toluene (i.e. 9 mmoles).

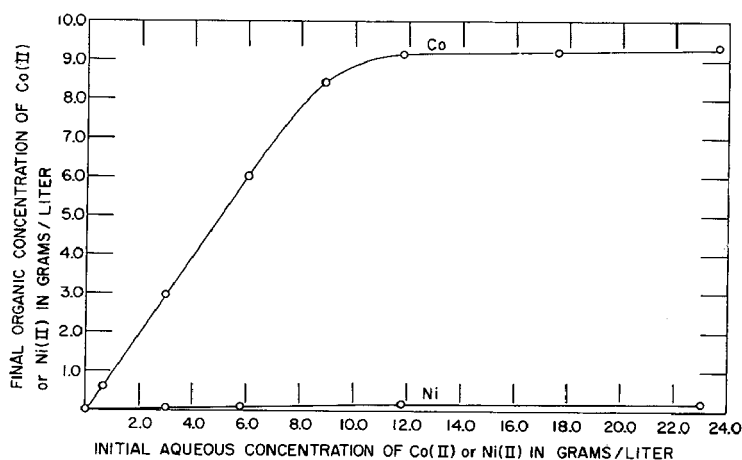


Fig. 3. Loading study for the extraction of Co(II) or Ni(II) from 0.1 M HNO_3 into an equal volume of 0.6 M $\text{R}_3\text{NH}^+\text{SCN}^-$ in toluene (*i.e.* 9.0 mmoles).

with $\text{R}_3\text{NH}^+\text{SCN}^-$ in toluene was used, although the use of a reversed-phase chromatographic column might be advantageous in some instances.

Figs. 2-4 show the results of a loading study performed by extracting increasing concentrations of cobalt(II) and nickel(II) individually with no thiocyanate initially present in the aqueous phase. Two extractions were also performed on nickel-cobalt mixtures with concentration ratios of 0.27 M /0.055 M and 0.27 M /0.027 M . The

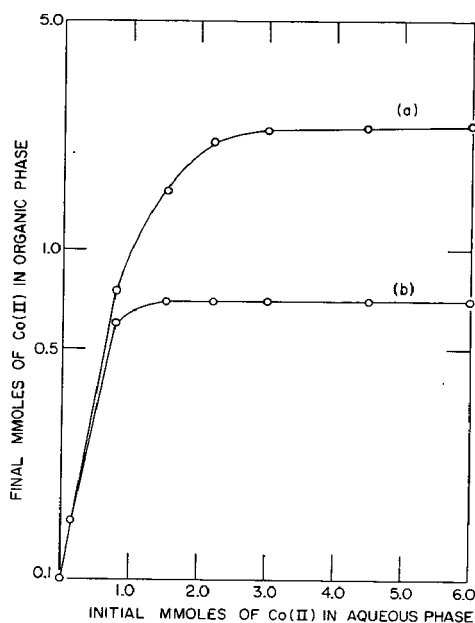
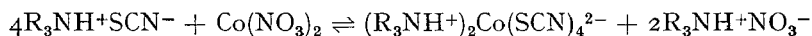


Fig. 4. Limiting loading curve for the extraction of Co(II) from 0.1 M nitric acid into (a) 9.0 mmoles of 30% (v/v) solution of $\text{R}_3\text{NH}^+\text{SCN}^-$ in toluene and (b) 3.0 mmoles of 10% (v/v) solution of $\text{R}_3\text{NH}^+\text{SCN}^-$ in toluene.

cobalt extraction was still complete while the nickel extraction actually decreased.

Fig. 2 indicates that a small amount of nickel is extracted for conditions under which cobalt is 100% extracted. Essentially all of this nickel may be recovered (cobalt-free) with two washings of dilute acid. Although there is no thiocyanate originally present in the aqueous phase, some partitioning occurs when equilibrium is attained between the organic and aqueous phases. The matrix element solution now contains thiocyanate ion, which may be undesirable. This is a minor problem because the aqueous thiocyanate can be removed by anion exchange or destroyed by boiling with nitric acid. When the organic phase becomes heavily loaded, the cobalt may be back-extracted with two washings of 1-M sulfuric acid, which converts much of the exchanger to the sulfate form, necessitating a reconversion before use.

Using Fig. 4 the cobalt to amine ratio for the extraction may be determined by the limiting loading method¹⁵. For the 30% solution the limiting cobalt/amine ratio is $2.34/9.0 = 1/3.85$. For the 10% solution the limiting cobalt/amine ratio = $0.70/3.0 = 1/4.28$. These results indicate a cobalt/amine ratio of 1/4. However, only one half the exchanger capacity was utilized because there was no thiocyanate initially present in the aqueous phase. Therefore, the equation for extraction may be written as:



Column separations

A series of nickel-copper and nickel-cobalt separations were achieved for concentration ratios ranging from 1/100 to 1000/1. These separations were performed to illustrate further the speed and ease with which ions from Groups 1 and 2 may be separated. The column was only 1.0 cm \times 9.0 cm and the nickel was washed through at a flow rate of 1.0 ml/min with 25 ml of 0.1 M HNO₃ while the cobalt or copper was stripped with 25 ml of methanol at a flow rate of \sim 3–5 ml/min.

Separations of this type can be very advantageous for the isolation of trace constituents from matrix elements which interfere with the analysis of the minor component. A pragmatic example of this concept occurred in the atomic absorption analysis of nickel in NBS standard sample 124d. This sample consists of the following elements and percentage composition:

Cu—83.60%	Ni—0.99%	P —0.02%
Pb—5.20%	Fe—0.18%	As—0.02%
Zn—5.06%	Sb—0.17%	S —0.093%
Sn—4.56%	Ag—0.02%	

A direct analysis of the sample resulted in only a 91.0% recovery of nickel. The error was traced to the presence of copper, which decreases the absorbance of nickel if present in concentration ratios greater than 5/1. The ratio for this sample was $83.6/0.99 = 84/1$. After the copper (as well as Zn, Sn and Fe) was removed by passing the sample through a 2.0 cm \times 9.0 cm reversed-phase column of Alamine 336–thiocyanate, the analysis for nickel showed 99.9% recovery.

Methanol is used to strip the highly sorbed metal ions and the Alamine 336 from the column. The presence of the liquid ion exchanger can be tolerated in the atomic absorption analysis of metal ions. However, the effect of the amine on the

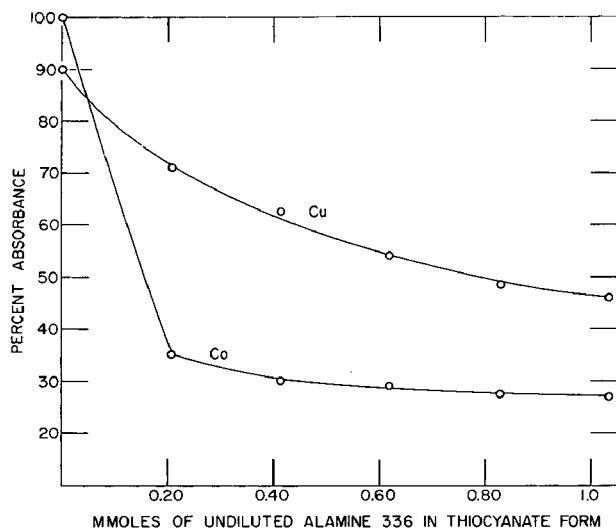


Fig. 5. Effect of $R_3NH^+SCN^-$ concentration on the atomic absorption determination of a methanolic 20 p.p.m. Co(II) solution or 20 p.p.m. Cu(II) solution. An air-acetylene flame was used.

absorbance of the metal ion should be investigated. It was found here and in cases cited by HARTLAGE¹⁶ that certain amines will decrease the absorbance of metal ions. Fig. 5 shows the effect of $R_3NH^+SCN^-$ on the absorbance of methanolic solutions of copper and cobalt. HARTLAGE has shown that the interference may be overcome by using a nitrous oxide-acetylene flame, but there was also a decrease in sensitivity. The amine was no problem here because its concentration was always sufficient for the analysis to be performed on the flat portion of the curve (Fig. 5). The average recovery for fourteen Cu determinations by the non-aqueous atomic absorption method was $99.9 \pm 2.28\%$ and the average recovery for six Co determinations was $100.9 \pm 3.02\%$.

ACKNOWLEDGEMENTS

The authors express their appreciation to J. P. SICKAFOOSE for his assistance in the water hardness titrations.

REFERENCES

- 1 F. L. MOORE, *National Academy of Sciences, Nuclear Science Series*, NAS-NS-3101, 1960.
- 2 J. C. SHEPPARD, *Hamford Laboratories Operation*, AEC Rept., HW-5195B, 1957.
- 3 E. A. HUFF, *J. Chromatog.*, 27 (1967) 229.
- 4 F. L. MOORE, *Anal. Chem.*, 36 (1964) 2158.
- 5 TH. P. GERONTOPULOS, L. RIGALI AND P. G. BARBAR, *Radiochim. Acta*, 4 (1965) 75.
- 6 A. M. WILSON AND O. K. MCFARLAND, *Anal. Chem.*, 35 (1963) 302.
- 7 A. R. SELMER-OLSEN, *Anal. Chim. Acta*, 31 (1964) 33.
- 8 H. WATANABE AND K. AKATSUKA, *Anal. Chim. Acta*, 38 (1967) 547.
- 9 U. A. TH. BRINKMAN, G. DE VRIES AND E. VAN DALEN, *J. Chromatog.*, 23 (1966) 287.
- 10 S. PRZESZLAKOWSKI, *Chim. Anal. (Warsaw)*, 12 (1967) 57.

- 11 G. GOLDSTEIN, *Equilibrium Distribution of Metal-Ion Complexes*, U.S. Atomic Energy Commission Rept. ORNL-3620 (Oak Ridge National Laboratory), 1964.
- 12 A. RINGBOM, *Complexation in Analytical Chemistry*, Interscience, New York, 1963.
- 13 J. S. FRITZ AND R. K. GILLETTE, *Anal. Chem.*, 40 (1968) 1777.
- 14 J. S. FRITZ, J. P. SICKAFOOSE AND M. A. SCHMITT, *Anal. Chem.*, 41 (1969) 1954.
- 15 K. A. ALLEN, *J. Am. Chem. Soc.*, 80 (1958) 4133.
- 16 F. R. HARTLAGE, JR., *Anal. Chim. Acta* 39 (1967) 273.

J. Chromatog., 53 (1970) 345-353

Notes

CHROM. 4955

A simple device for the selection of fractions in gas chromatography

The sampling of separate components after their separation in a chromatographic column for the purpose of identification by chemical and physical methods is of great importance in gas chromatography. Studies of IR spectra of separated components have a particular application.

At present the selection of fractions of separated components is principally used in preparative chromatography. The selection of fractions in analytical chromatography by formerly suggested methods is difficult because of small volumes of the samples analysed.

Many different types of traps for fraction selection are described in the literature. It was suggested that sealed glass tubes with a narrow end¹, U-tubes², thin hollow steel needles³, polyethylene capillaries⁴, and other devices be used as traps. The condensation of fractions can also be carried out in a tube filled with potassium bromide⁵ or directly on a tablet of this material⁶ prepared for taking IR spectra.

Various types of connecting systems including distribution combs with a number of taps, glass or metal ground joints, etc., are used for joining the traps. Such systems cause losses and impurity in the components. Furthermore, the complete condensation of samples in traps is not always achieved; the number of selected components is generally limited.

In this paper a new simple and reliable device is proposed⁷. It allows practically any number of components in a mixture to be collected quantitatively. The apparatus may be applied to both preparative and analytical chromatography.

Apparatus and procedure

The main feature of the proposed device is that the samples of components

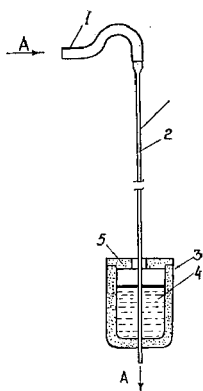


Fig. 1. Schematic layout of the device for fraction selection. 1 = flexible hose; 2 = capillary; 3 = vessel of heat-insulating material; 4 = cooling agent; 5 = lid; A = input and output of carrier gas.

separated in a chromatographic column are in a series condensed in a capillary tube passed through a cooling cell, rather than selected into separate samplers. The selected samples remain on the walls of the capillary in a liquid or solid state, depending on the physical properties of the components and on the temperature of the cooling agent. After condensing one of the samples, the tube is moved over a certain distance, and then the condensation of the following fraction occurs. One of the modifications of the proposed apparatus is shown in Fig. 1.

The total flow of carrier gas passed through the heat conductivity detector or its portion selected before the flame-ionization detector is involved in fractionation. The carrier gas from the detector passes through a flexible hose of silicone rubber (1) and enters a thin-walled capillary tube (2). The length of the tube is directly proportional to the number of components in the mixture; the choice of its diameter depends upon the quantity of the mixture introduced for the separation: the less the sample, the smaller the diameter. The condensed fraction is distributed in a thin layer on the inner walls of the capillary. Filling the total cross section of the capillary with the separated substance is impermissible here, otherwise the flow of the carrier gas will be disturbed. The cooling agent (4) (liquid N_2 , solid CO_2 and its various mixtures, etc.) is placed into a plastic foam condenser (3). The capillary is passed through the bottom of the condenser (3). The thin plastic foam bottom or the walls of the vessel are easily pierced by the capillary tube. In this case no leakage of liquefied gas is observed. The condensation of the components occurs in the cooled capillary part. Completeness of their condensation depends upon the temperature of the cooling agent in the vessel.

The condensation of the first component being completed (control on the potentiometer of the chromatograph), the capillary tube (2) is passed through the condenser (3) over the length exceeding the layer thickness of the cooling agent (4). The piece of the capillary with liquid or solid fraction is broken off and sealed at both ends. In doing so, it is a good practice to hold the capillary tube with special pincers of heat-insulating material to prevent evaporation of the fraction due to heating. A small notch can be made on the capillary before breaking it off. Fractions of the second and subsequent components are selected in the similar way.

For the purpose of decreasing the evaporation velocity of the liquefied gases, the vessel (3) is closed with a lid (5). While sampling high-boiling substances, it is advisable to heat the capillary above the condenser approximately to the chromatographic column temperature in order to prevent their condensation on the walls of the capillary. This heating can be ensured by means of a ventilator with air heating ("Fan" type). The temperature in the capillary zone is controlled by a thermometer. When operating on sufficiently volatile components, no condensation on the walls of the capillary is observed before the cooling zone.

The fractions of substances under study selected into sealed capillaries by the above method can be kept without any changes for a long period of time. For the identification of these components it is possible to use the IR spectroscopy, elementary analysis, chemical reactions as well as repeated chromatography by various methods.

In order to obtain a sufficient number of components for identification, one may consecutively accumulate the samples while performing several chromatographic analyses of the mixture.

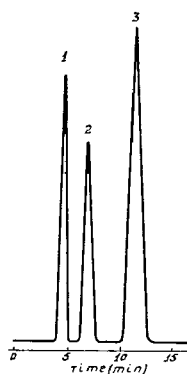


Fig. 2. Example of chromatographic separation of a model mixture with a simultaneous selection of fractions. 1 = acetone; 2 = methyl ethyl ketone; 3 = chloroform.

Experimental

The experimental investigation was carried out on HL-4 analytical laboratory chromatographs with a heat conductivity detector and on LHM-7a chromatographs containing heat conductivity and flame-ionization detectors. As an example, we provide the results of the separation of a model mixture of three components: acetone, methyl ethyl ketone, and chloroform.

The chromatographic separation was performed in a column (180×0.6 cm) containing 10% of polyethyleneglycol 15 000 on Celite-545 (30–60 mesh) at the column and detector temperature 110° ; the carrier gas (N_2) flow was 50 ml/min. The chromatogram of the model mixture separation obtained at the simultaneous selection of fractions of the separated components is shown in Fig. 2.

Glass capillaries of different inner diameters (0.5–2.0 mm) connected through a flexible hose with the heated yield of carrier gas were used for the preparative selection of the components under investigation. Such a capillary was passed through a vessel of plastic foam (I.D. 85 mm, height 55 mm, wall thickness 20 mm) containing liquid N_2 (boiling point = -195.8°).

The model mixture to be investigated was introduced into the evaporation cell of the chromatograph with the help of a microsyringe which was weighed before and after introducing the sample. The yield of the components was controlled by a poten-

TABLE I

FRACTIONATION OF THE MODEL MIXTURE

Component	Composition of the model mixture (%)	Introduced into the chromatograph (g)	Weight of the filled capillary (g)	Weight of the empty capillary (g)	Weight of the component in the capillary (g)	Losses of the component (g)
Acetone	26.17	0.0025	0.1275	0.1255	0.0020	0.0005
Methyl ethyl ketone	24.63	0.0024	0.3339	0.3318	0.0021	0.0003
Chloroform	49.20	0.0046	0.2839	0.2800	0.0039	0.0007

tiometer. At the moment the yield of chromatographic peak ended, the capillary with the solid sample was moved out of the cooling cell, broken off, sealed and weighed on an analytical balance with an accuracy of 0.0001 g. The absolute weight contents of the capillary was estimated by the difference in weights of the filled and empty capillary.

The data on the fractionation balance of the model mixture are illustrated in Table I. The data obtained show a high efficiency of sampling separated components by the method described.

The selected components were identified in IR spectra with a Zeiss (Jena) UR-20 spectrometer. The substances were removed from sections of the capillary with an indifferent solvent (CCl_4). To obtain a quantity of substance sufficient to take spectra, five parallel analyses of the model mixture with the selection of the separated components were performed.

The techniques described have been used for solving a number of analytical problems⁸, in particular when identifying the components formed in pyrolytic gas-liquid chromatography of polysaccharide mixtures and their technical products.

Simplicity and reliability of the proposed method allow it to be recommended for a wide application to analytical and preparative gas chromatography. It is advisable that chromatographs produced by industry be provided with arrangements for sampling based on the described method.

*Department of Chemical Technology of Wood,
The Kirov Byelorussian Institute of Technology,
Minsk (U.S.S.R.)
Institute of Physics, The Byelorussian Academy of Sciences,
Minsk (U.S.S.R.)*

YU. I. KHOL'KIN
G. S. GRIDYUSHKO

A. K. POTAPOVICH

- 1 H. E. BELLIS AND E. J. SLOWINSKY, *J. Chem. Phys.*, 25 (1956) 794.
- 2 J. HASLAM, A. R. JEFFS AND H. A. WILLS, *Analyst*, 86 (1961) 44.
- 3 R. A. EDWARDS AND I. S. FAGERSON, *Anal. Chem.*, 37 (1965) 1630.
- 4 W. S. MOLNAR AND V. A. YARBOROUGH, *Appl. Spectroscopy*, 12 (1958) 143.
- 5 H. W. LEGGON, *Anal. Chem.*, 33 (1961) 1295.
- 6 K. H. KUBESZKA, *Naturwiss.*, 52 (1965) 429.
- 7 YU. I. KHOL'KIN, A. K. POTAPOVICH AND G. S. GRIDYUSHKO, *Pat. U.S.S.R.*, No. 247606, 23.4.68-22.4.69.
- 8 YU. I. KHOL'KIN, *Chromatography in Chemistry of Wood*, Zesnaja Prom., Moscow, 1968.

Received July 28th, 1970

CHROM. 4991

An automatic device for injection of gas samples into a gas chromatograph

A study of the occurrence of gaseous hydrocarbon compounds in the soil atmosphere¹ has involved the analysis of a large number of samples by gas chromatography. To make more efficient use of the chromatograph, and reduce the time spent on manual operation, an automatic device for the injection of gas samples has been constructed.

Description of apparatus

The injection apparatus is shown in Fig. 1. Sixteen samples can be accommodated in glass syringes fitted with 22-gauge needles; the syringes are lubricated with a grease made from mannitol, glycerol and starch², which does not absorb hydrocarbon

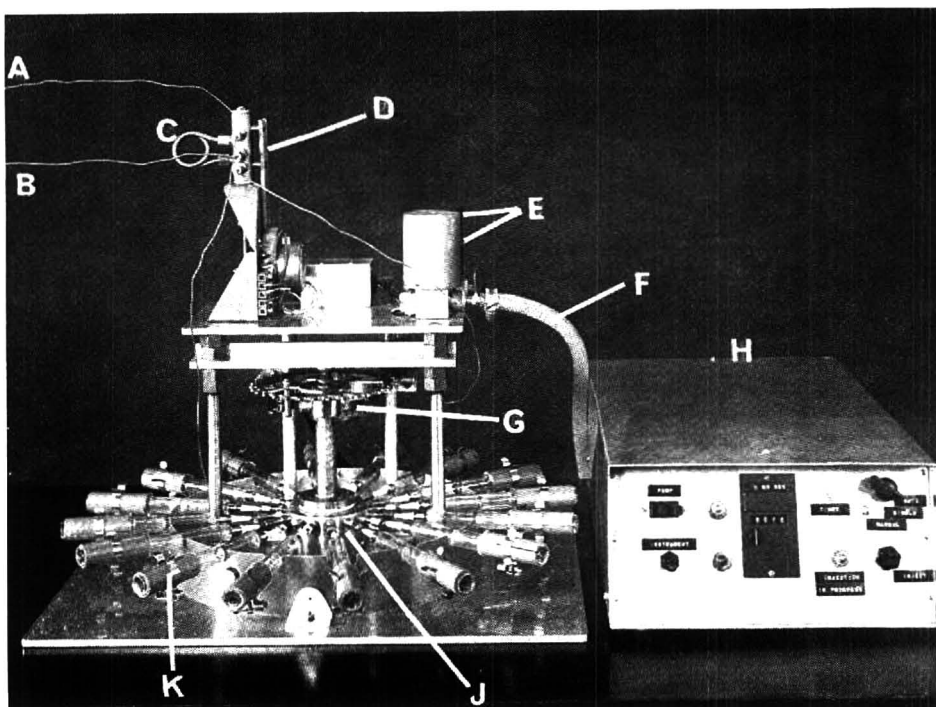


Fig. 1. Automatic gas-injection apparatus. Key: A = 1.6 mm (1/16 in.) O.D. carrier gas tube from chromatograph; B = tube carrying sample + carrier gas to chromatograph; C = sample loop; D = automatic sampling valve; E = solenoid valves; F = tube to vacuum pump; G = rotary valve drive motor; H = control unit; J = rotary valve; K = syringe collar.

gases to any significant extent. The needles are inserted through rubber septa in the inlet ports of a specially designed rotary valve (Fig. 2). The rotary valve is operated by an arm attached to the shaft of a synchronous motor turning at 1 r.p.m. The arm engages with a 32-tooth cycle sprocket attached to the valve rotor; thus each revolution of the arm turns the valve through 1/32 revolution. Each syringe, in turn, is connected

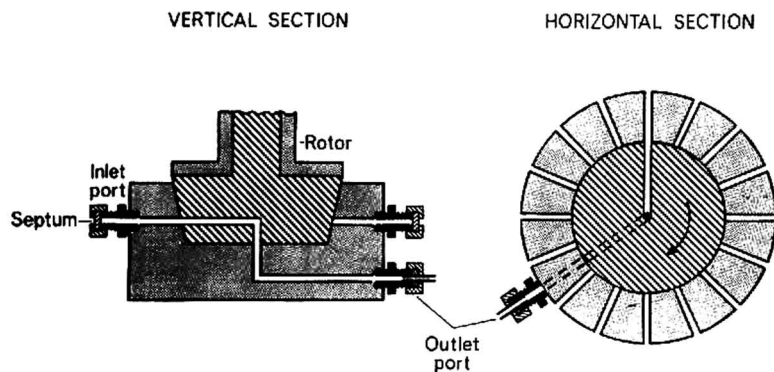


Fig. 2. Rotary valve of automatic gas-injection apparatus. The tapered end of the rotor is made of PTFE, and is fixed to a brass shaft; the body of the valve is brass. The sixteen inlet ports (not shown in the horizontal section) are made from Simplifix stainless steel couplings for 1.6 mm O.D. tubing, and fitted with latex rubber septa 1 mm thick.

by way of the outlet port of the rotary valve, and a 50-cm length of 1.6 mm O.D. stainless steel tubing, to the sample loop of a motor-operated gas sampling valve (Field Instrument Co., Richmond, Surrey, Great Britain), the loop having previously been evacuated and then sealed off from the pump by the closure of a solenoid-operated valve (Edwards High Vacuum Ltd., Crawley, Sussex, Great Britain, Type D11103). The gas connections are shown in Fig. 3.

Collars made from rigid PVC tubing are fitted to the syringe plungers to prevent them being forced in by atmospheric pressure when the syringes are connected to the evacuated sample loop, so that the total gas-filled volume, and the proportion of the sample which flows into the sample loop, remain constant. 5-ml syringes and a 2-ml loop have been used routinely, but any convenient combination of syringe and loop

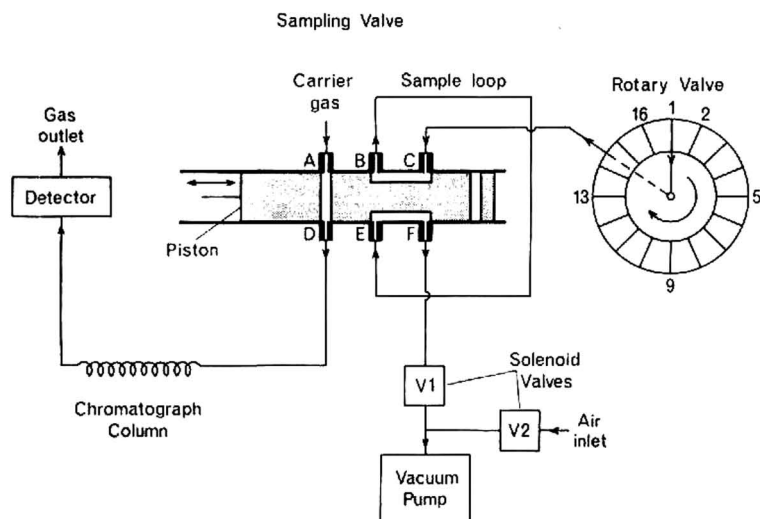


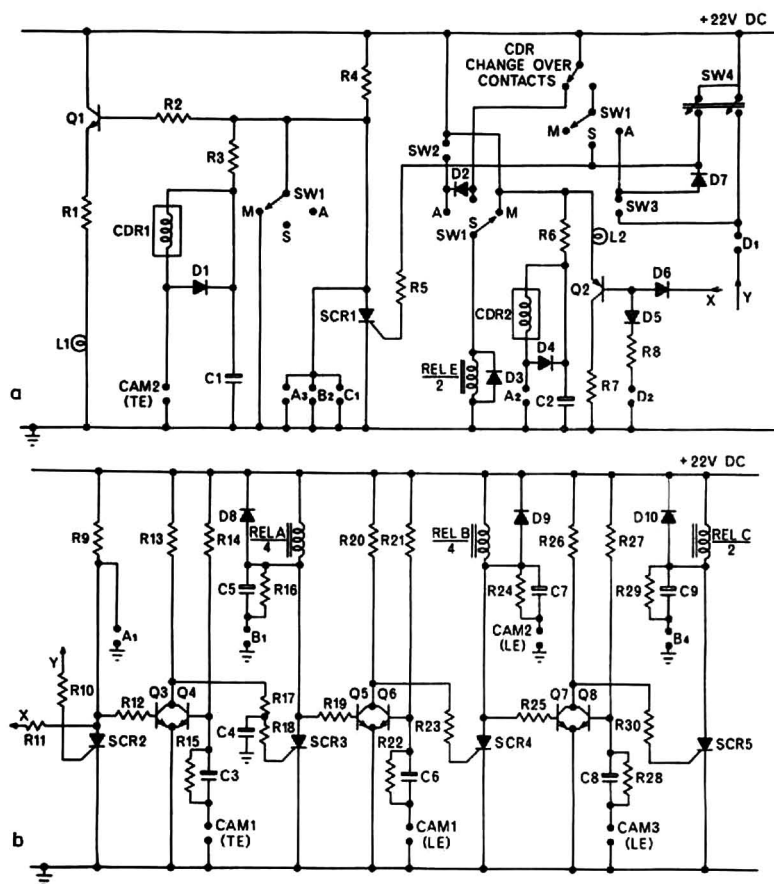
Fig. 3. Connections for the transfer of gas between components of the automatic injection apparatus and the gas chromatograph.

volumes may be employed. The gas in the sample loop is automatically injected into the chromatograph.

A 3-cam timing motor (2 r.p.m.) in the control unit produces a series of signals to initiate each operation, and to operate the countdown register of the timer which determines the interval between successive injections. The control circuits are shown in Fig. 4.

The sequence of operations is determined by the settings of the cams of the timing motor. All output signals are generated by the closure of the cam-operated microswitch contacts. When the instrument is in the "stand-by" condition, all relay contacts and microswitches are open, with the exception of B₄, D₁, SW₂ and SW₃, which are closed. After the "inject" switch SW₄ has been operated the cam sequence is as follows: (1) Cam 1 trailing edge sets relay A; the closing of contacts A₄ operates solenoid valve V₁, which opens. (2) Cam 1 leading edge sets relay B, which, through contacts B₃, closes the circuit to relay D. Contacts D₃ start the motor of the rotary valve. Relay B (contacts B₁) also resets relay A. (3) Cam 3 leading edge sets relay C (contacts C₂) to start the motor of the sampling valve. (4) Cam 2 leading edge resets relays B and C. (5) Cam 2 trailing edge operates the count-down register.

Both the rotary and sampling valve motors continue to rotate until the micro-



(continued on p. 361)

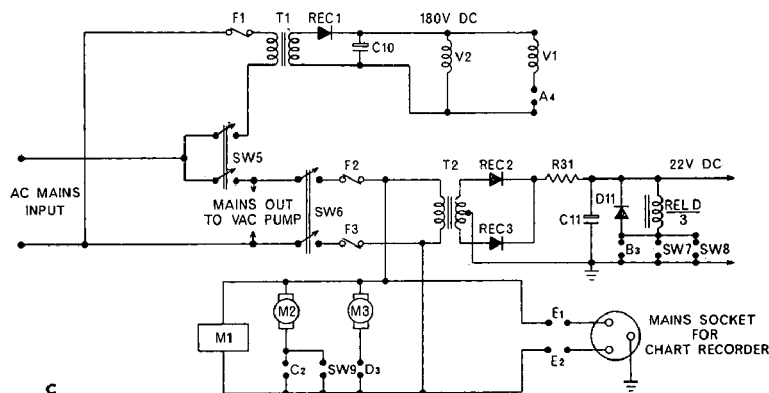


Fig. 4. Circuit diagrams of the control unit. Key: SW1 = auto/manual mode switch; SW2, SW3 = "last sample" microswitches; SW4 = "inject" switch; SW5 = vacuum pump on/off switch; SW6 = control unit on/off switch; SW7 = "push to make-push to break" switch operated by rotary valve motor. M1 = 3-cam timing motor; M2 = rotary valve motor; M3 = sampling valve motor. CDR1 = count-down register coil; CDR2 = count-down register reset coil. LE = leading edge of cam; TE = trailing edge of cam. Components: R1, R7 = 330 Ω ; R2, R17, R18, R23, R30 = 5.6 k Ω ; R3, R15, R28 = 8.2 k Ω ; R4, R9, R13, R20, R26 = 3.3 k Ω ; R5, R8, R10, R11 = 6.8 k Ω ; R6 = 2.7 k Ω ; R12, R14, R19, R21, R25, R27 = 22 k Ω ; R16 = 27 k Ω ; R22 = 82 k Ω ; R24, R29 = 100 k Ω ; R31 = 10 Ω . C1, C11 = 500 μ F; C2 = 1000 μ F; C3, C6, C8 = 50 μ F; C4 = 2 μ F; C5 = 10 μ F; C7, C9 = 1 μ F; C10 = 60 μ F. D1, D3, D4, D8, D9, D10, D11 = CV2290; D2, D5, D6, D7 = OA10. SCR 1, 2, 3, 4, 5 = TAG100 (Transistor AG). REC1 = 10D4 (Int. Rectifier); REC2, REC3 = 10D1 (Int. Rectifier). SW4 = DPST-loaded switch. CDR = Sodeco countdown register Type TCeF4PE. M1 = timing motor, Magnetic Devices Ltd. Model 8303B3/30S/3C6A/230-50; M2 = synchronous motor, Crouzet Type 395, 1 r.p.m.

switches operated by their shafts (SW8 and SW9, respectively), and switch SW7 on the rotary valve, have all returned to the "off" condition. The rotary valve motor thus makes two revolutions before coming to rest.

When the 3-position switch on the control unit (Fig. 1) is set to the "manual" position, a sample is injected only when the "inject" switch is operated, and the timer does not function; when set to "automatic", the apparatus will continue to operate until the sample in position 16 has been injected; if the unit is switched from "automatic" to "single sample" operation, only one further injection will be made.

The apparatus is switched off, after injection of the sixteenth sample, by microswitches operated by an arm attached to the rotating sprocket. This arm may be easily removed if it is desired to allow the rotary valve to operate for more than one complete revolution.

Sequence of operations

The rotary valve is at the intermediate position between inlet ports 16 and 1 (Fig. 3). The sampling valve is in the "fill" position (sample loop connected to ports C and F). The count-down register is set to give an appropriate time interval between injections. The solenoid valves V1 and V2 are closed, and the vacuum pump switched on.

The solenoid valve V1 is opened and the sample loop evacuated.

After 30 sec, V1 is closed, the rotary valve is turned to port 1, and the sample gas flows into the loop.

After a further 15 sec, the sampling valve is moved to the "inject" position (sample loop connected to ports A and D) and the sample in the loop is swept into the column by the carrier gas. The sampling valve is then returned to the "fill" position. The timer is reset at the beginning of the injection procedure.

The rotary valve is turned to the next intermediate position, between inlet ports 1 and 2.

When the count-down register of the timer reaches zero, valve V1 is opened, and the sequence is repeated.

After sixteen cycles (*i.e.* when the rotary valve has completed one revolution) the chart recorder is automatically switched off. When the control unit and the vacuum pump are switched off, or in the event of a mains power failure, valve V2 is opened to admit air to the pump.

Reproducibility of injections

In Table I the results are shown of two series of analyses, each involving sixteen successive injections of the same standard mixture of hydrocarbons in nitrogen. The standard deviations varied from 1.55 to 2.0% of the mean peak heights; these figures

TABLE I

REPRODUCIBILITY OF RESULTS OBTAINED BY AUTOMATIC INJECTION OF SIXTEEN SAMPLES OF A STANDARD MIXTURE OF GASES INTO A GAS CHROMATOGRAPH

Gas	Concentration (p.p.m.)	Peak height (% full-scale deflection)			
		Series No. 1 (12.5.70)		Series No. 2 (14.5.70)	
		Mean	S.D.	Mean	S.D.
Methane	6.1	46.34	0.77	46.45	0.78
Ethane	5.9	58.82	1.09	59.04	0.99
Ethylene	5.8	48.58	0.97	48.74	0.92
Propane	6.9	48.13	0.80	48.49	0.75
Propylene	7.9	31.45	0.55	31.53	0.51

indicate the upper limit of the errors associated with the injection process, because they also include any errors associated with sampling, and variations in chromatograph response and syringe volume.

The authors wish to thank Mr. P. M. LAY, Head of the Electronics Section of the Letcombe Laboratory, for his advice on the design of the apparatus, and Mr. F. W. HEPBURN for workshop assistance.

*Agricultural Research Council, Letcombe Laboratory,
Wantage, Berks. (Great Britain)*

K. A. SMITH
W. HARRIS

1 K. A. SMITH AND R. S. RUSSELL, *Nature*, 222 (1969) 769.

2 P. G. JEFFERY AND P. J. KIPPING, *Gas Analysis by Gas Chromatography*, Pergamon, Oxford, 1964, p. 191.

Received August 10th, 1970

J. Chromatog., 53 (1970) 358-362

CHROM. 4980

Direct gas chromatographic estimation of lower alcohols, acetaldehyde, acetone and diacetyl in milk products

Data pertaining to the lower alcohols, aldehyde and ketone, their occurrence and concentration in milk and milk products are often mentioned in connection with the study of fermentation, flavour structure, stability of quality of milk products during storage, etc.

The determination of the above compounds is discussed in numerous papers. Practically all of these methods are based on two principal operations: isolation of the compounds from the samples (distillation, extraction) and then determination mostly by GLC. The isolation usually involves some loss especially of the easily volatile compounds. Direct GLC analysis of these compounds without processing the sample prior to its injection onto the column is difficult because the water content and other accompanying components in the sample and still other factors lower and affect the quality of chromatographic analysis. These problems are usual with liquid-solid column packing.

Uncoated porous polyaromatic materials as column packing are very suitable for direct determination of water, alcohols, glycols, certain gases, hydrocarbons and volatile acids¹. Porous polyaromatic materials were used to advantage for direct GLC determination of the lower alcohols, volatile acids, etc., in microbial fermentation media and in rumen fluid²⁻⁴. Remarkable results were achieved by BAKER *et al.*⁵ in determination of lower alcohols, acetone and acetaldehyde in blood by direct GLC analysis of untreated samples by using Porapak Q as column packing. Also in milk serum and in aqueous extracts of cheese, Polypack-2 in direct GLC determination of water-soluble fatty acids was used⁶.

The results achieved in using porous polyaromatic materials in GLC for direct determination of some compounds prompted us to apply this materials also for direct GLC determination especially of the non-acidic fermentation products in milk and milk products.

Experimental

Apparatus and column. Fractovap Model GB (Carlo Erba, Milan) with FID was used. The glass column (160 cm long, I.D. 4 mm) was filled with 80-100 mesh Porapak Q and Porapak P (1:1). The column temperature was 105° and the inlet and detector were maintained at 125°. Nitrogen as carrier gas (1.5 kp/cm²) was used. In the inlet part of the column, a removable glass tube (or glass beads) was installed providing protection against pollution of the chromatographic column with accompanying substances of sample.

Procedure. Methanol, acetaldehyde, acetone, ethanol, isopropanol, *n*-propanol and isobutanol were used for preparation of the standard solution. Anhydrous acetonitrile (b.p. 81-82°) as the internal standard was used. Standard curves were plotted for the substances covering the wide concentrations required for the material analysed.

For the determination of volatiles in milk and liquid milk products (or milk products homogenised with water), samples were adjusted to pH 7.5-8.0 (ref. 7).

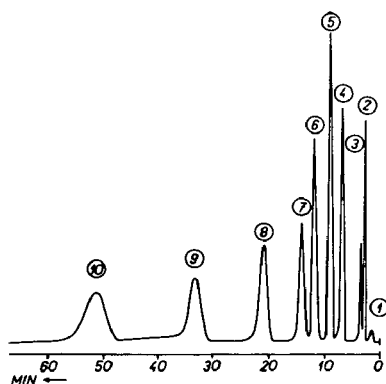


Fig. 1. Chromatogram of a standard solution with acetonitrile as internal standard. 1 = water; 2 = methanol; 3 = acetaldehyde; 4 = ethanol; 5 = acetonitrile; 6 = acetone; 7 = isopropanol; 8 = *n*-propanol; 9 = diacetyl; 10 = isobutanol.

Internal standard (0.05–0.40%) was used in addition depending on the levels of volatiles anticipated or encountered. In all determinations 5–10 μ l of the standard solution or sample were injected directly into the gas chromatograph.

Standard curves were plotted from a water or milk solution of the standards. The ratio of each peak area to that of the internal standard acetonitrile was determined and plotted against the concentration ratio.

Results and discussion

Excellent separation of methanol, acetaldehyde, ethanol, acetone, isopropanol, *n*-propanol, diacetyl, isobutanol and acetonitrile was obtained by using a Porapak Q and Porapak P mixture as column packing (see Fig. 1).

Comparing the separation quality using Porapak Q or Porapak P separately and then their mixture, it can be seen that the separation of the tested compounds and the situation of the internal standard improved and the time of analysis got

TABLE I

RELATIVE RETENTION TIMES OF MILK PRODUCTS VOLATILES AS COMPARED TO ACETONITRILE ON PORAPAK Q, PORAPAK P AND THEIR MIXTURE

Compound	Relative retention times		
	Porapak Q	Porapak P	Mixture (1:1)
Methanol	0.30	0.22	0.31
Acetaldehyde	0.38	0.28	0.40
Ethanol	0.82	0.53	0.75
Acetonitrile	1.00	1.00	1.00
Acetone	1.46	0.93	1.31
Isopropanol	1.86	0.91	1.57
<i>n</i> -Propanol	2.73	1.47	2.36
Diacetyl	4.32	2.41	3.75
Isobutanol	7.01	2.93	5.74

TABLE II

RECOVERY OF VOLATILE COMPOUNDS FROM MILK

<i>Compound</i>	<i>Sample number</i>	<i>Present (mg)</i>	<i>Found (mg)</i>	<i>Recovered (%)</i>
Methanol	1	23.5	21.6	91.8
	2	10.8	11.3	105.0
	3	15.6	15.1	96.8
	4	7.8	7.6	97.5
Ethanol	1	131.3	121.6	92.6
	2	204.6	188.3	92.0
	3	69.7	68.5	98.3
<i>n</i> -Propanol	1	14.7	14.3	97.6
	2	23.4	24.6	105.4
	3	14.2	13.4	94.4
	4	12.8	12.9	100.9
	5	31.6	33.2	105.1
Isopropanol	1	13.3	12.4	93.3
	2	34.1	33.1	97.1
	3	13.8	13.9	100.6
	4	21.9	23.0	105.2
Acetone	1	15.3	16.1	105.3
	2	13.4	14.3	106.9
	3	28.4	27.1	95.5
	4	17.4	16.0	92.0
Acetaldehyde	1	20.5	20.0	97.6
	2	98.2	89.9	91.5
	3	101.7	99.0	97.4
	4	58.1	56.1	96.6
	5	80.3	73.2	91.2
Diacetyl	1	30.4	29.6	97.3
	2	32.3	32.6	100.8
	3	66.4	67.3	101.3

TABLE III

PRECISION OF SIMULTANEOUS DETERMINATIONS OF VOLATILE COMPOUNDS IN YOGHURT CULTURE

	<i>Methanol(?) (mg%)</i>	<i>Acetaldehyde (mg%)</i>	<i>Ethanol (mg%)</i>	<i>Acetone (mg%)</i>
	0.65	4.39	7.71	0.50
	0.64	3.99	7.94	0.44
	0.63	4.30	8.05	0.53
	0.53	4.20	7.14	0.42
	0.62	4.41	7.51	0.48
	0.65	4.18	7.71	0.41
	0.61	3.69	7.40	0.37
	0.49	3.87	7.01	—
	0.58	3.69	6.99	—
	0.53	3.68	6.99	—
Mean	0.59	4.04	7.44	0.45
Standard deviations (\pm)	0.06	0.29	0.40	0.05
Coefficient of variation (%)	10.1	7.2	5.4	11.1

TABLE IV

VOLATILE COMPOUNDS IN SOME MILK PRODUCTS

Milk product	Volatile compounds (mg %)						
	Methanol (?)	Acetaldehyde	Ethanol	Acetone	Isopropanol	n-Propanol	Diacetyl
Milk (cowy flavour)	—	0.61	3.33	79.54	—	—	—
Kefir culture	0.22	0.64	712.54	—	0.02	0.07	0.08
Cream culture	0.42	0.46	2.86	0.11	—	0.04	0.51
Yoghurt culture	—	1.55	0.91	—	0.15	—	—

shorter using the mixture (see Table I). The standard curves were linear in the whole range of the concentrations tested.

Precision of the method described was determined by the recovery percentage of the compounds added to analysed samples of milk. Results are given in Table II. Isobutanol was not evaluated because we did not find it in detectable concentration in any of our materials tested. Precision of simultaneous determinations of volatiles in a yoghurt culture by using the described method is presented in Table III. Using this method we also tested some of fermented milk products. The results are given in Table IV. The typical chromatogram of volatile compounds of kefir culture is presented in Fig. 2.

The modification of the inlet part of the column (removable glass tube or glass beads) increases the lifetime of the column. It is recommended to clean (changing the removable tube or beads) this inlet part of column after about 25–30 injections.

Previous gas chromatographic methods for the determination of volatile compounds in milk and milk products required specimen processing— isolation of volatile compounds from the tested material—prior to their analysis by GLC. By this method no processing is required prior to the injection. This is accomplished by the use of polyaromatic materials as column packing and a modified glass inlet part of the column

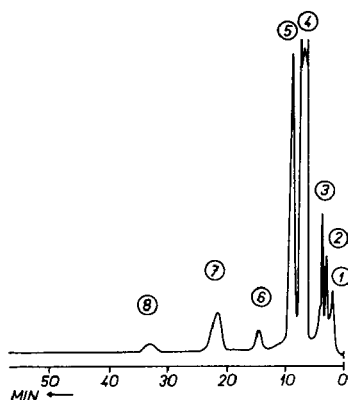


Fig. 2. Chromatogram of kefir culture. 1 = water, attenuation $10^2/1$; 2 = methanol, attenuation $10^2/1$; 3 = acetaldehyde, attenuation $10^2/1$; 4 = ethanol, attenuation $10^2/256$; 5 = acetonitrile, attenuation $10^2/64$; 6 = isopropanol, attenuation $10/1$; 7 = n-propanol, attenuation $10/1$; 8 = diacetyl, attenuation $10/1$.

trapping the milk and milk product nonvolatile substances and protecting the column. The application of this method is limited by the lower boundary of concentrations of the analysed compounds occurring in the sample. It depends on the sensibility of the apparatus used. In our case for example even 0.08 mg% diacetyl, 0.04 mg% *n*-propanol, 0.02 mg% isopropanol and 0.1 mg% acetone could be determined.

The work suggests the use of this method also for the determination of other compounds as described and shows the possibility of its application to other materials than milk products. For this purpose it is necessary to change the analytical conditions and to use respectively some other combination of column packing polymer materials.

*Department of Biotechnology,
Slovak Polytechnical University,
Bratislava (Czechoslovakia)*

V. PALO
H. ILKOVÁ

- 1 O. L. HOLLIS, *Anal. Chem.*, 32 (1966) 309.
- 2 M. ROGOSA AND L. L. LOVE, *Appl. Microbiology*, 16 (1968) 285.
- 3 L. DOOMS, D. DECLERCK AND H. VERACHTERT, *J. Chromatog.*, 42 (1969) 349.
- 4 D. W. KELLOGG, *J. Dairy Sci.*, 52 (1969) 1690.
- 5 R. N. BAKER, A. L. ALENTY AND J. F. ZACK, *J. Chromatog. Sci.*, 7 (1969) 312.
- 6 R. A. LEDFORD, *J. Dairy Sci.*, 52 (1969) 949.
- 7 H. W. DOELLE, *J. Microbiology Serology*, 32 (1966) 373.

Received July 15th, 1970

J. Chromatog., 53 (1970) 363-367

CHROM. 5005

The determination of picloram in fescue by gas-liquid chromatography*

Several residue methods for the determination of picloram (4-amino-3,5,6-trichloropicolinic acid) in soil and a variety of crops employ extraction with aqueous base and electron capture gas-liquid chromatography (GLC) of the methyl ester or the pyrolysis product of this herbicide. Recently we have reported a method for the determination of picloram in soil, which uses a closed-tube decarboxylation¹.

Picloram is extensively used to eradicate brush and other broad-leaved plants on grazing ranges². We therefore decided to apply our method to the analysis of fescue. However, several serious analytical difficulties became apparent.

Basic extracts of fescue caused emulsions of considerable stability. The formerly used silica gel column failed to separate larger amounts of co-extractants from the

* Contribution from the Experiment Station Chemical Laboratories, Journal Series No. 6060. Approved by the director. This study was supported by Public Health Service Research Grant FD-00262, formerly CC-00314 and by Grant No. 12-14-100-9146 (34) of the Crops Research Division, Agricultural Research Service, United States Department of Agriculture.

decarboxylated picloram and there was danger of its loss in the prior and subsequent evaporation steps. Finally, the yield of decarboxylated product decreased as the culture tubes were used repeatedly in this investigation.

To cope with these problems, an organic extraction system, an alumina column, and two "keepers" were introduced. A special study traced the inconsistencies in decarboxylation efficiency to the catalytic activity of the tube walls, which could be reduced by acid treatment and silylation. (In our work on soil, decarboxylation tubes had repeated prior exposure to silylation reagents which—unrealized then—contributed to the success of the method.)

Experimental

Pretreatment of glassware. Screw cap culture tubes (16 × 75 mm) for the decarboxylation of picloram were soaked in *aqua regia* overnight and thoroughly rinsed with distilled water. After drying, the tubes were filled with a 10% solution of trimethylchlorosilane (TMCS) or dimethyldichlorosilane (DMCS) in toluene, capped and allowed to stand for 48 h. Then the tubes were rinsed with a few small portions of toluene and filled with methanol. After standing for about 30 min, the methanol was discarded and the tubes were rinsed with several portions of acetone and dried.

Sample preparation. The fescue was frozen in liquid nitrogen and finely chopped in a blender. Care was taken to maintain the sample in a frozen state by keeping a small amount of dry ice in the blender. The chopped fescue was stored in a deep freeze and samples were weighed out and spiked as needed. Picloram was added to 2 g fescue samples in 22 × 150 mm tubes with 19/38 ground glass tops in 0.1 ml or less of acetone. The solvent was allowed to evaporate and the samples were thoroughly mixed.

Extraction and partitioning. The samples were shaken for 3 min on a Vortex mixer with three 15 ml portions of acetonitrile–ammonia (95:5) and filtered through a plug of glass wool into a 100 ml round bottom flask. The extract was taken to dryness on a rotary evaporator, and transferred to a 125 ml separatory funnel with 50 ml of 0.1 N KOH. This solution was shaken with two 25 ml portions of ethyl acetate. After separation, the ethyl acetate fractions were discarded and the aqueous solution remaining in the separatory funnel was acidified with 10 ml of 1 N HCl. Two 25 ml portions of ethyl acetate were used to extract the acidic solution. The combined ethyl acetate layers were taken to dryness on a rotary evaporator and the residue transferred to a 16 × 75 mm screw cap culture tube (previously treated with *aqua regia* and TMCS) with several small portions of ethyl acetate, and evaporated to dryness under a gentle stream of nitrogen.

Decarboxylation. One ml of acetonitrile containing 5 μ l of 12 N HCl was added to culture tubes containing samples and standards and capped tightly. The tubes were placed in a 150° oil bath for 30 min. After this time, the tubes were removed, cooled in a beaker of water and opened. Ten μ l of ethylene glycol were added to each tube and the solutions carefully evaporated just to dryness under a gentle stream of nitrogen. Two ml of hexane were added to each tube.

Column clean-up. A column of basic alumina (Brockman activity grade I) was prepared by adding a hexane slurry of alumina to a disposable Pasteur pipet plugged with a small amount of glass wool. The column was washed with 10 ml of hexane and one half (1 ml) of the sample was placed on the column. The column was then washed with 5 ml of benzene, the benzene discarded, and the decarboxylated picloram was

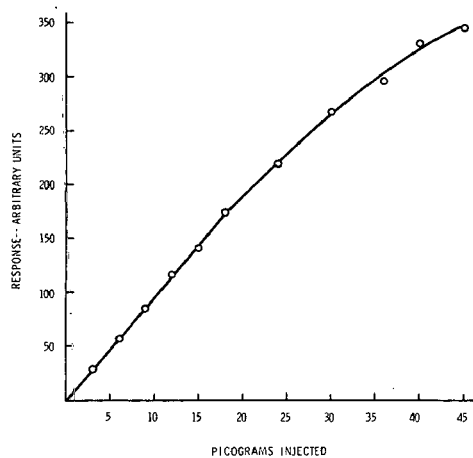


Fig. 1. Standard curve for decarboxylated picloram. Column: 3.5% OV-17 + 4.5% QF-1 on 80/100-mesh, Chromosorb W-HP, 1.8 m \times 4 mm I.D. Pyrex. Oven temperature: 200°. N_2 flow rate: 40 ml/min. Micro Tek model MT-220, Ni-63 detector, pulse mode, 60 V, 250 μ sec rate, 6 μ sec width.

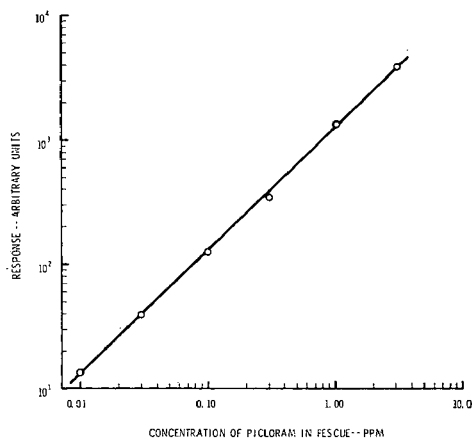
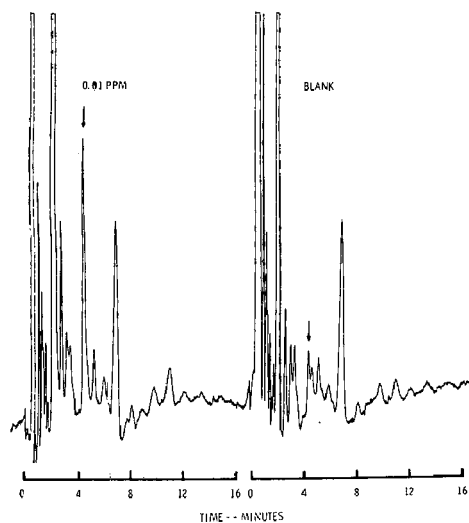


Fig. 2. Chromatograms of a fescue sample spiked with 0.01 p.p.m. picloram, and of a blank. Column: 3.5% OV-17 + 4.5% QF-1 on 80/100 mesh Chromosorb W-HP, 1.8 m \times 4 mm I.D. Pyrex. Oven temperature: 200°. N_2 flow rate 40 ml/min. Micro Tek model MT-220, Ni-63 detector, pulse mode, 60 V, 250 μ sec rate, 6 μ sec width.

Fig. 3. Calibration curve for the extraction of picloram from fescue. Column: 3.5% OV-17 + 4.5% QF-1 on 80/100 mesh, Chromosorb W-HP, 1.8 m \times 4 mm I.D. Pyrex. Oven temperature: 200°. N_2 flow rate: 40 ml/min. Micro Tek model MT-220, Ni-63 detector, pulse mode, 60 V, 250 μ sec rate, 6 μ sec width.

eluted from the column with 15 ml of 5% ethyl ether in benzene. This solution was adjusted to contain a concentration of picloram suitable for injection into the gas chromatograph (see below). If this meant concentrating the solution, 10 μ l of tetradecane were added prior to evaporation under a stream of nitrogen.

Gas-liquid chromatography. At the time of this work, the linear range of our ^{63}Ni electron capture detector was between 3 and 18 pg of decarboxylated picloram injected (Fig. 1). The various fescue samples were adjusted to a final volume such that a 5 μ l injection would produce a peak for decarboxylated picloram within this linear range of the detector. Representative chromatograms of a blank and of a 10 p.p.b. sample are shown in Fig. 2. A calibration curve for fescue samples spiked with 10 to 3000 p.p.b. picloram is shown in Fig. 3.

Results and discussion

Our original method for the determination of picloram¹ was developed for soil—the use of grass as a substrate therefore required extensive modification. Emulsion problems encountered when fresh crop samples were extracted with aqueous base could be circumvented by using a basic acetonitrile solution for extraction. Much of the interfering coextracted material was subsequently eliminated in the regular partitioning step³. The remaining interferences were further reduced by chromatography on alumina. As a result, relatively “clean” chromatograms could be obtained from fescue samples containing as little as 10 p.p.b. picloram.

Deactivation of the culture tubes used for decarboxylation was found to aid greatly the long-term reproducibility of results. Apparently, traces of metals and/or active sites in the glass caused decomposition. In line with this assumption, a 30 min decarboxylation time gave a better yield than the previously reported 15 min, provided deactivated tubes were used.

Ethylene glycol and tetradecane, the two “keepers” employed in the method, helped to minimize losses of decarboxylated picloram during evaporation. Neither of these compounds interfered with the final analysis by GLC.

The described method offers an alternate—and confirmatory—route to the determination of picloram residues in fescue and possibly other plant materials. It shows a wide linear range down to picloram concentrations of 10 p.p.b. and is thus well suited for residue analysis.

The authors are pleased to acknowledge the competent technical assistance of Mr. ERNEST LEAKE and want to thank Dow Chemical Co., Midland, Mich., U.S.A., for several samples of analytical grade Tordon.

*University of Missouri,
Columbia, Mo. 65201 (U.S.A.)*

ROBERT F. MOSEMAN*
WALTER A. AUE**

1 R. F. MOSEMAN AND W. A. AUE, *J. Chromatog.*, 49 (1970) 432.

2 M. E. GETZENDANER, J. L. HERMAN AND B. VAN GIESSEN, *J. Agr. Food Chem.*, 17 (1969) 1251.

3 J. S. LEAHY AND T. TAYLOR, *Analyst*, 92 (1967) 371.

Received August 21st, 1970

* Data in this paper taken from doctoral thesis.

** To whom reprint requests should be directed.

CHROM. 5017

The gas chromatographic determination of nitrosamines at the picogram level by conversion to their corresponding nitramines

We have had occasion to examine the response to a series of nitrosamine standards in hexane of flame ionisation and electron capture detectors fitted to a gas chromatograph. After initial analysis the solutions were inadvertently allowed to stand in direct sunlight for several hours. When these standards were reinjected we found that the peak associated with nitrosamine response had decreased slightly in size and a second peak of longer retention time had appeared in every case. The response of this new species to electron capture was some 200 times greater than its response to flame ionisation.

An examination of each new species using gas chromatography-mass spectrometry showed in every case that its molecular weight was 16 mass units higher than that of the original nitrosamine. High resolution mass spectrometry confirmed that this was due to an extra oxygen atom in the molecule. It therefore seemed possible that the new species could be the corresponding nitramine.

We have now prepared a series of nitramines from their corresponding nitrosamines using a modification of the oxidation technique proposed by EMMONS¹ and have examined their gas chromatographic properties.

Experimental

Reagent. Peroxytrifluoroacetic acid (PTFA). Place 4-5 ml of redistilled methylene chloride in a 10 ml volumetric flask and carefully add 0.4 ml 85-90% w/w hydrogen peroxide by pipette. Slowly add by pipette 2.5 ml redistilled trifluoroacetic anhydride, swirl gently and allow to stand in an ice bath for 5 min. Allow the contents of the flask to attain room temperature, then dilute to volume with redistilled methylene chloride. Prepare fresh reagent every day.

Oxidation technique. Place a 1 ml aliquot of a solution of nitrosamine in methylene chloride in a stoppered test tube. Add 0.1 ml PTFA reagent, mix by swirling and allow to stand for 3½ h. Add 2 drops of distilled water, shake gently and leave for 1 min. Add excess calcium carbonate by spatula (0.25 g). When effervescence ceases add 0.25 g powdered anhydrous sodium sulphate, shake gently and allow to settle. Examine the solution by electron capture gas chromatography.

Results and discussion

Using this technique we have determined the efficiency of conversion, retention times and the relative response to nitrosamine of a flame ionisation detector and to the corresponding nitramine by an electron capture detector.

Efficiency of conversion. This was studied for 50 µg amounts of nitrosamine and the efficiency of conversion was calculated by comparing peak areas for nitrosamine and corresponding nitramine by flame ionisation gas chromatography. A mean of five determinations is reported in each case.

Retention times. These were studied on a 5 ft. PEG 20 M column run isothermally at 140°.

Relative responses. The response in terms of both peak heights and peak areas

TABLE I

THE EFFICIENCY OF CONVERSION OF NITROSAMINE TO NITRAMINE

<i>Nitrosamine</i>	<i>Conversion (%)</i>
Dimethyl	86
Methyl ethyl	85.5
Diethyl	84.5
Methyl-isopropyl	76
Di-isopropyl	72
Di- <i>n</i> -propyl	84
Di-isobutyl	82.5
Di- <i>n</i> -butyl	83
N-Nitrosopiperidine	25
N-Nitrosopyrrolidine	85

TABLE II

RETENTION TIMES OF NITROSAMINES AND CORRESPONDING NITRAMINES

<i>Nitrosamine</i>	<i>Retention time (min)</i>	<i>Retention time of corresponding nitramine (min)</i>
Dimethyl	4.0	9.8
Methyl ethyl	4.9	11.25
Diethyl	5.5	12.4
Methyl isopropyl	5.8	12.65
Di-isopropyl	7.15	15.05
Di- <i>n</i> -propyl	9.5	20.5
Di-isobutyl	10.45	20.65
Di- <i>n</i> -butyl	20.2	42.9
N-Nitrosopiperidine	22.5	39.6
N-Nitrosopyrrolidine	25.25	57.65

TABLE III

INCREASE IN SENSITIVITY OBTAINED USING EC DETECTION OF NITRAMINES

<i>Original nitrosamine</i>	<i>Increase in sensitivity for nitramine</i>	
	<i>By peak areas</i>	<i>By peak heights</i>
Dimethyl	1150	545
Methyl ethyl	620	372
Diethyl	438	215
Methyl isopropyl	243	141
Di-isopropyl	119	65
Di- <i>n</i> -propyl	245	125
Di-isobutyl	215	110
Di- <i>n</i> -butyl	205	91
N-Nitrosopiperidine	183	102
N-Nitrosopyrrolidine	255	98

of nitrosamines by flame ionisation detection and of the corresponding nitramines by electron capture detection were determined. Increases in sensitivity of between 100 fold and 1100 fold, depending on the particular nitrosamine studied, were obtained for nitramines using electron capture as shown in Table III.

The smaller increase in sensitivity obtained from peak heights is a reflection of the increased retention time of the nitramines.

It would therefore seem that the technique of oxidation of nitrosamines to their corresponding nitramines, coupled with the use of electron capture GLC, offers a means of improving the sensitivity of detection of the former by several orders of magnitude and of thus achieving the detection levels required for biological purposes.

Addendum

After preparing this communication we learned from Dr. N. P. Sen of the Food and Drug Directorate, Ottawa that he has submitted a paper based on the same basic idea to the *Journal of Chromatography* (51 (1970) 301).

*Unilever Research Laboratory,
Colworth/Welwyn,
Colworth House,
Sharnbrook, Beds. (Great Britain)*

J. ALTHORPE
D. A. GODDARD
D. J. SISSONS
G. M. TELLING

I. W. D. EMMONS, *J. Am. Chem. Soc.*, 76, (1964) 3468.

Received August 31st, 1970

J. Chromatog., 53 (1970) 371-373

CHROM. 4960

Experience with an electrolytic "ninhydrin reactor"

A commercial unit for electrically producing a hydrindantin-ninhydrin reagent for automated amino acid analyzers was very recently marketed (Sondell Scientific Instruments, Inc., Palo Alto, Calif., U.S.A.)*. The device uses a nickel-platinum couple and offers many worthwhile advantages. Claims include improved color yields yet with substantial savings in materials and time by using one-fifth the usual ninhydrin concentration and by eliminating waste through improved stability of ninhydrin stock solution. Absence of tin salts and precipitates reportedly eliminates cuvette clean-ups and costly coil plugging, decreases baseline noise and analyzer down-time, and minimizes calibration runs. The reactor is "...designed to function with any amino acid analyzer" and, assuming appropriate adapters and fitting are at hand, is "...simple to install and operate".

This note is to share experience with other potential users who also may find that eliminating all the interferences which inactivate the unit is easier said than done.

* Mention of trademark or company names is for information purposes and does not constitute preferential endorsement by the U.S. Department of Agriculture.

J. Chromatog., 53 (1970) 373-374

Attaining base-line stability, or consistent or improved color yield has yet to be achieved in this laboratory despite solicitous help from the maker. To be sure, sulfur, metallic, or other contaminants which "passivate" the nickel-slug electrodes must be scrupulously eliminated from the system. Specially purified ninhydrin and methyl cellosolve appear essential, as well as metal-free water and buffer salts. Also, any trace of residual tin salts from the old ninhydrin system must be removed and the nickel electrodes must be activated with an acid flush.

The acid clean-up and activation (or "depassivation") step unsuspectingly proved a major key to repeated failure of our unit. As with most analyzers, the ninhydrin-line components of our apparatus were specified as wholly pyrex-type glass, teflon, or chemically resistant stainless steel. Costly experience showed that some pump fittings, pressure gauge and back-pressure valve components were not sufficiently acid resistant. We call especial attention here to a small spring in the supposedly all stainless steel back-pressure device used on some analyzers such as the Phoenix for surge control and proper operation of the ninhydrin mini-pump. When finally located as a major contaminant source, the spring was badly corroded and magnetic, indicating poor quality stainless, if stainless steel at all. Other metal parts showed discoloration and tarnish. Any flaws in such metallic parts obviously lead to progressively rapid corrosion and inactivation of the "ninhydrin reactor" nickel electrodes, and in time to failure of the parts themselves.

Clearly, unless all parts are nonmetallic or of proved noncorrosive metals, strong acid flushes through the ninhydrin (and other) pumps, gauges and lines should be avoided. It is better that the nickel slugs of the ninhydrin reactor be activated by flushing 1 *N* or 6 *N* HCl through the reactor only (*e.g.* by using a hand syringe) rather than by overnight pumping of acid washes.

*Soil and Water Conservation Research Division,
Agricultural Research Service, U.S. Department
of Agriculture, in cooperation with the Oregon Agricultural
Experiment Station, c/o Department of Soils,
Oregon State University, Corvallis, Oreg. (U.S.A.)*

J. L. YOUNG
M. YAMAMOTO

Received August 4th, 1970

J. Chromatog., 53 (1970) 373-374

CHROM. 4983

The examination of volatile oils by combined gas-liquid chromatography/thin-layer chromatography

The resolution of volatile oil components can be a particularly difficult task and as more sophisticated methods are applied, the complexity becomes more apparent. In the use of gas-liquid chromatography (GLC) for the quantitative analysis of components in volatile oils it is necessary to have an independent check on the resolution of the component of interest and it is for this particular application that our combined GLC/thin-layer chromatography (TLC) technique has mainly been developed.

The principle of using GLC to effect further resolution of components separated by TLC is widely used and there are numerous literature references to this application. Similarly the use of TLC to effect further resolution of components separated by GLC is fairly well established and was described by JANÁK in 1963¹ in relation to the separation of components in coal tar. Subsequent extensions of this work were published^{2,3}, but in each case, the necessary movement of the TLC plate was achieved by an independent drive mechanism. In the last paper of this series, the authors describe a logarithmic drive so the eluted homologous components from an isothermally operated GLC appeared in a linear fashion on the TLC plate.

A similar method was described by KAISER⁴, in which the linearity of homologous components was achieved by temperature programming the GLC equipment. This paper also described the addition of a cooling device for the more efficient trapping of components on to the TLC plate. MINYARD *et al.*^{5,6} used a combination technique to form derivatives directly on the TLC plate before final elution and they used a manual movement of the TLC plate. CURTIUS AND MÜLLER⁷ applied the technique to steroid analysis and used an independent drive for the TLC plate. CASU AND CAVALLOTTI in 1962 described a method for the formation of derivatives from a GLC effluent on a TLC plate driven by a gear train from a potentiometric recorder, and no attempt was made to use the separation abilities of a TLC plate, which was used only as a means of trapping components and subsequently converting them into recognisable derivatives.

The concept of splitting the effluent from a GLC analysis and leading a portion of it to a TLC plate has the basic merit of simplicity, but automating the procedure seems to have been a more difficult task. It is evidently desirable to be able to move the TLC plate continuously and subsequently to be able to match the spots developed on the TLC plate with the peaks produced by the gas chromatograph on the recorder. It has been found that these requirements can be very easily achieved by using the chart paper from a potentiometric recorder as the driving mechanism for the TLC plate. The recorder is equipped with a smooth, flat shelf extending at least 40 cm at an angle of 45° from the point of emergence of the chart paper. The chart is allowed to run over the sloping shelf and the TLC plate is fixed to the paper with a small piece of adhesive tape. The open capillary end of a heated stream splitter is suitably positioned over the TLC plate at a distance of 2 mm from the surface. The heated transfer line in our apparatus gives a 98:2 split ratio, and a line temperature of 150° is satisfactory for most volatile oil applications, although it has been found necessary to increase this to 180° or 200° for oils containing phenols or sesquiterpene alcohols. The

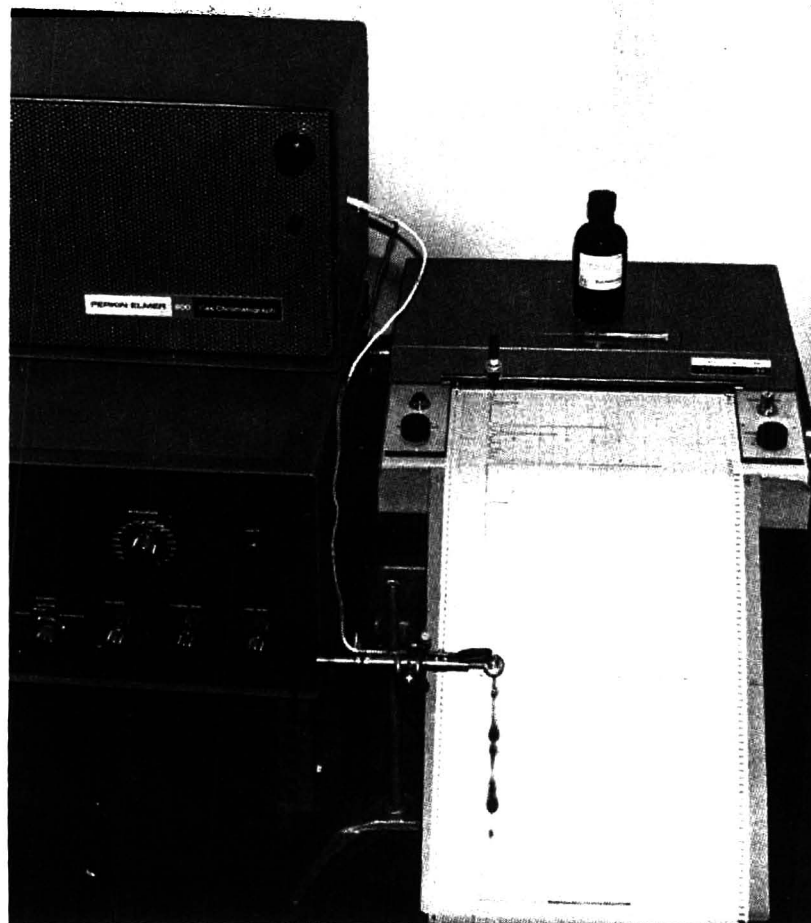


Fig. 1. A general view of the combined GLC/TLC arrangement.

transfer line is heated electrically by means of a separate power supply, using the stainless steel capillary itself as the resistance element. The maximum electrical requirements are 8 A, 12 V, and in our original experiments the transfer line was bolted directly to the stream splitter inside the gas chromatograph and the electrical connections were made using the outer end of the line and an earth return through the chassis of the chromatograph. The power supply was 0-12 V a.c. supplied from a Variac transformer. This was found to be satisfactory for a short time, but noise was gradually developed on the recorder and this was attributed to the gradual breakdown of the capacitors in the input filter circuit due to a.c. being picked up by the detector. The power supply was then rectified using four silicone diodes and a smoothing capacitor, which reduced the problem but did not eliminate it entirely. Using this rectified supply, the transfer line was then electrically isolated from the gas chromatograph by making the connection to the stream splitter with a short length of PTFE tubing. This entirely eliminated the problem and the arrangement has now worked

satisfactorily for several months. When the recorder chart is set in motion, the TLC plate moves with it and the trapped spots are thus kept in perfect phase with the peaks drawn by the recorder. The general arrangement is shown in Fig. 1. At the end of the run, the TLC plate is removed from the chart paper and eluted with a suitable solvent system. The separated components are detected with spray reagents, which may be specific in nature, thereby converting the TLC system into a specific detector. Alternatively, a specific reagent may be used before the TLC plate is eluted. Particular applications of this method are the formation of 2,4-dinitrophenylhydrazones with ketones and aldehydes and 2,4-dinitrobenzoates with alcohols. However, when the technique is applied to volatile oils, preparation of derivatives is not always feasible, because many terpenoid components do not readily form derivatives. Two well known examples are camphor and fenchone, which only form DNP derivatives with difficulty. When dealing with volatile oil components on a TLC plate, the R_F values can be a good guide to the nature of the components, and the colours which they form on condensation with vanillin or other aromatic aldehydes can also be helpful.

The TLC plate, duly developed by one or other of the foregoing methods, is then placed alongside the GLC tracing in such a way that the spots correspond to the peaks. In the case of volatile oils the correlation is usually self evident but the start points

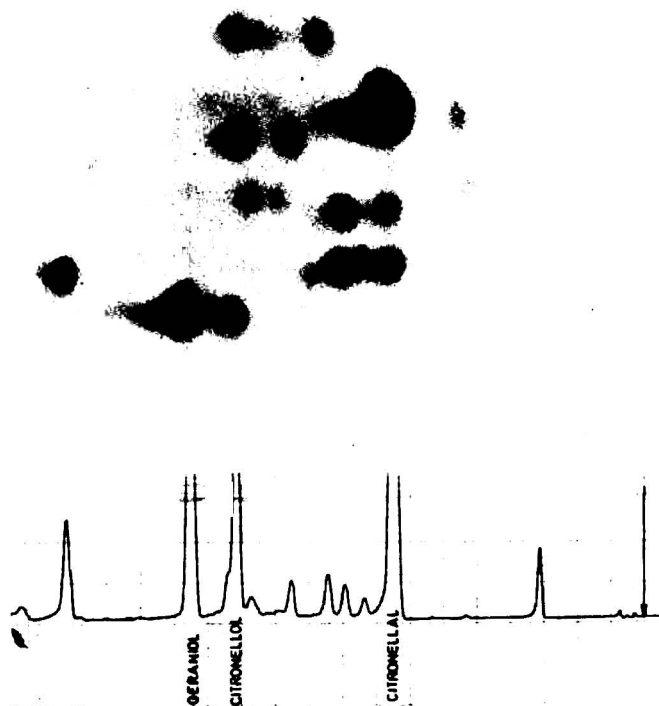


Fig. 2. An examination of citronella oil (Java type) by combined GLC/TLC. Sample applied, 1 μ l. Conditions for GLC: 6-ft. PEG 20 M column; temperature 75°–225°, 3.3°/min. Conditions for TLC: adsorbent, Silica Gel Hk; solvent, 5% ethyl acetate-methylene chloride.

of the GLC and TLC are best marked, so that no doubt can occur. Examination of the spots on the TLC plate will show whether the GLC peaks represent pure compounds and, if not, can often give information as to the nature of the accompanying compounds.

As an example of the results which may be obtained, our work on citronella oil has shown that the GLC peaks assigned to citronellal and citronellol contain more than one compound although the geraniol peak appears to be specific (see Fig. 2). Samples of pure citronellal and citronellol, when examined under the same conditions, each give a single TLC spot and it was therefore concluded that the interfering compounds in the citronella oil were not artefacts but genuine components of the oil.

Although the GLC was run under programmed temperature conditions it is apparent that this column (6 ft. \times $\frac{1}{8}$ in. Carbowax 20M 15% on Chromosorb W, 80/100 mesh) would be satisfactory for the determination of geraniol in citronella oil under isothermal conditions.

We feel that the general principles of a combined GLC/TLC technique have wide application and the simplicity of the arrangement allows results to be obtained very rapidly.

The author wishes to thank the Directors of Bush Boake Allen Ltd., for permission to publish this work.

*Research Department, Bush Boake Allen Ltd.,
London N.1 (Great Britain)*

A. M. HUMPHREY

1 J. JANÁK, *J. Gas Chromatog.*, 1 (1963) 20.

2 J. JANÁK, *J. Chromatog.*, 15 (1964) 15.

3 J. JANÁK, I. KLIMES AND K. HÁNA, *J. Chromatog.*, 18 (1965) 270.

4 R. KAISER, *Z. Anal. Chem.*, 205 (1964) 284.

5 J. H. TUMLINSON, J. P. MINYARD, P. A. HEDIN AND A. C. THOMPSON, *J. Chromatog.*, 29 (1967) 80.

6 J. P. MINYARD, J. H. TUMLINSON, A. C. THOMPSON AND P. A. HEDIN, *J. Chromatog.*, 29 (1967) 88.

7 H. C. CURTIUS AND M. MÜLLER, *J. Chromatog.*, 32 (1968) 222.

8 B. CASU AND L. CAVALLOTTI, *Anal. Chem.*, 34 (1962) 1514.

Received August 7th, 1970

J. Chromatog., 53 (1970) 375-378

CHROM. 5028

Comments on the use of Blue Dextran in gel chromatography

Blue Dextran is a high-molecular-weight dextran fraction carrying a covalently linked chromophore. This polymer (Blue Dextran 2000) is reported by the manufacturers (Pharmacia Fine Chemicals, Inc.) to be excluded from all grades of Sephadex and has been recommended for checking the packing of gel columns¹ and for the determination of void volumes during calibration². A recent report by WHITE AND JENCKS³ that Blue Dextran binds certain proteins prompts the author to report some of his experiences with this material.

In a recent experiment a column (100 × 5 cm) was packed with Sephadex G-200 which had been swelled according to the method recommended by the manufacturers⁴ in 50 mM Tris-HCl buffer pH 7.5–0.1 M NaCl. After pumping the column in an ascending direction for two days with the same buffer, a sample (10 ml) of Blue Dextran solution (10 mg/ml), which had been stored at room temperature for about six months was applied to the bottom of the column. An unusual phenomenon was observed, whereby the Blue Dextran failed to pass through the column. Despite pumping the column with several bed-volumes of buffer, all the Blue Dextran remained apparently bound to the gel within one in. of the bottom flow adapter. Communication with the suppliers yielded the information that this phenomenon had been reported before and generally took place when "aged" solutions of the chromogenic material were used.

After being assured that this would not interfere with chromatography on the column⁵, a sample of a partially purified enzyme preparation (sweet-corn R-enzyme⁶) was applied to the column and elution continued. 185 fractions were collected, by which time we knew from previous experiments the activity should have been eluted, and the fractions assayed for enzymic activity. None was found, despite the fact that protein had been eluted (Fig. 1). On the basis that the only possible explanation for

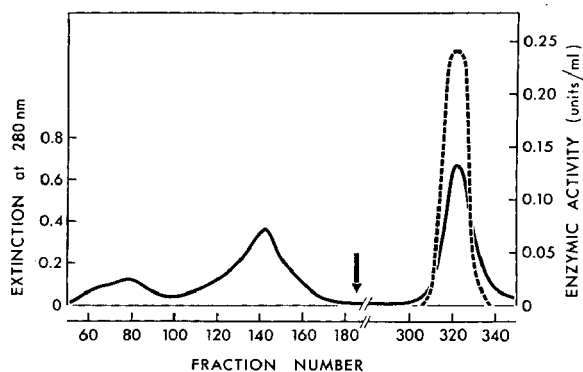


Fig. 1. Elution profile of a sweet-corn R-enzyme preparation chromatographed on Sephadex G-200 in the presence of Blue Dextran. The continuous line shows the distribution of protein in the fractions as measured by the extinction at 280 nm. The broken line shows the distribution of enzymic activity determined using pullulan as substrate⁶. Elution was carried out initially with 50 mM Tris-HCl buffer 7.5–0.1 M NaCl; at the point indicated by the arrow the NaCl concentration was increased to 0.5 M. The fractions were of volume 12 ml.

this was the presence of the Blue Dextran on the column, possibly acting as an ion-exchanger and binding the enzyme, the sodium chloride concentration in the eluting buffer was then increased to 0.5 *M*. A Uvicord connected in the outflow from the column showed a peak of protein which started to appear after another 120 fractions had been collected (Fig. 1). Assay for enzymic activity showed that the enzyme was in this protein peak; the recovery of activity was 100%. The Blue Dextran, however, remained bound to the Sephadex and the contaminated gel was then discarded.

It is difficult to explain the mechanism of adsorption of the Blue Dextran to the Sephadex. It is, however, clear that the Blue Dextran was able to bind proteins applied to the column and that the binding was inhibited at increased salt concentration. This suggests an ion-exchange type of mechanism, possibly through the sulfonic acid groups in the dye.

The important practical point which emerges from this is that extreme caution must be exercised when gel columns, on which Blue Dextran has been run, are used for chromatography of proteins. Accumulation of Blue Dextran is frequently noticed at the bottom (or top) of gel beds and also in the fine nylon mesh of sample applicators and flow adapters (despite filtration of the Blue Dextran solutions). The possibility of artefactual results is obvious from the experience described.

This problem has been overcome by discontinuing the use of Blue Dextran. Void volumes of columns are now determined in this Laboratory by use of proteins of sufficiently high molecular weight to be excluded from the gels. Column packings are checked using a solution of myoglobin. This latter protein is also useful for checking the packing of Biogel columns on which adsorption effects have been noticed when Blue Dextran is used, especially when the eluting buffer is of low ionic strength.

A possible application of this phenomenon is to enzyme purification, and we are investigating this possibility. Such an application of Blue Dextran, in a slightly different manner, has been suggested by WHITE AND JENCKS³.

I wish to thank Dr. W. J. WHELAN for encouragement and helpful discussion. I also thank Mr. JOHN REILAND of Pharmacia Fine Chemicals, Inc., for advice.

This work was supported by a grant from the National Science Foundation (GB8342).

*Department of Biochemistry,
University of Miami School of Medicine,
P.O. Box 875, Miami, Fla. 33152 (U.S.A.)*

J. J. MARSHALL

1 *Technical Data Sheet No. 8*, Pharmacia Fine Chemicals, Inc., Piscataway, N.J., U.S.A.

2 P. ANDREWS, *Biochem. J.*, 96 (1965) 595.

3 H. D. WHITE AND W. P. JENCKS, *Abstract No. 43 (Division of Biological Chemistry)*, 160th *Am. Chem. Soc. Mtg.*, Chicago, Ill., U.S.A., September 1970.

4 *Sephadex-gel filtration in theory and practice*, Pharmacia Fine Chemicals, Inc., Piscataway, N.J., U.S.A.

5 J. REILAND (Pharmacia Fine Chemicals, Inc.), personal communication.

6 E. Y. C. LEE, J. J. MARSHALL AND W. J. WHELAN, *Arch. Biochem. Biophys.*, submitted for publication.

Received September 7th, 1970

CHROM. 4943

The retardation of certain proteins during chromatography on tanned gelatin

Chromium-formalin tanned gelatin, the medium introduced by POLSON AND KATZ¹ for molecular exclusion chromatography, has the advantage that it is mechanically strong. This property makes it possible to maintain high flow rates over a large number of chromatographic runs, thereby making tanned gelatin ideally suited to preparative chromatography.

During a series of investigations in this laboratory an attempt was made to calibrate a tanned gelatin column, using the procedure of LAURENT AND KILLANDER² and ANDREWS^{3,4}, in order to use elution data as a rough guide to the molecular weight of protein fractions. It was observed, however, that certain proteins are retarded during chromatography on tanned gelatin and this paper reports on a preliminary investigation of this phenomenon.

Experimental

Unfractionated acid process pigskin gelatin (Gelrite type A, 275 bloom, Canada Packers Ltd., 60 Paton Road, Toronto 4, Canada) was made up at the required concentration in distilled water and tanned with Kromex chrome tanning salt (Chrome Chemicals (Pty) Ltd., Merebank Durban) as described by POLSON AND KATZ¹. The tanned cubes were fragmented in a Waring blender into granules which were packed into a column (4 × 45 cm) and washed with 0.14 *M* NaCl until the effluent was free of chromium. The 0.14 *M* NaCl was then replaced by formalin tanning solution, pH 9.0 (ref. 1), which was run through the column until formalin could be detected in the effluent. At this stage the gelatin was extruded from the column, suspended in formalin tanning solution, adjusted to pH 9.0 with 5 *N* NaOH and maintained at this pH for 2 h by the addition of further NaOH, prior to being set aside for 24 h at 4°. After this period the granules were repacked into the column, washed free of formalin with 0.14 *M* NaCl and equilibrated with buffer. The granules were then extruded from the column, homogenised for 3 to 5 min in a Waring blender to yield finer fragments and finally, after temperature equilibration, were packed into a jacketed analytical column (1.75 × 125 cm). After packing the column was equilibrated with at least two column volumes of buffer before use.

The analytical column was packed and operated at 6–8°, except where the effect of running the column at 40° was investigated. In this case the gel was extruded from the column, equilibrated to 40° and repacked into the column, which was maintained at this temperature.

Protein mixtures, containing 5 mg of each protein species, were applied to the column in 1 ml of buffer. As a reference the mixture in successive chromatographic runs always had one component in common with the mixture used in the preceding run. The proteins used as standards were chymotrypsinogen A, trypsinogen, horse heart cytochrome C (grade II), horse skeletal muscle myoglobin (1 × cryst.), egg white lysozyme chloride (grade I) and yeast hexokinase (grade II) (Miles-Seravac Laboratories, Epping Industria, Cape Town); soybean trypsin inhibitor (Koch-Light Laboratories, Colnbrook, Bucks., Great Britain); bovine albumin (Cohn frac-

tion V) and bovine γ -globulins (Cohn fraction II) (Sigma Chemical Co., Mo., U.S.A.). Non-protein standards were Blue Dextran 2000 (Pharmacia, Uppsala, Sweden) and L-tryptophan (Sigma Chemical Co.).

Except where stated otherwise, the buffer system used consisted of 0.01 *M* Tris, pH 7.6 containing 0.15 *M* NaCl and 0.2% NaN_3 . The effluent from the column was monitored at 280 nm in a Beckman DB spectrophotometer, equipped with a flow-through cell.

Results

Standard curves, based upon the theory of LAURENT AND KILLANDER² and according to the method of ANDREWS^{3,4}, relating elution volumes to molecular weights, are presented in Figs. 1 and 2, respectively. From these curves it is apparent that the proteins lysozyme, chymotrypsinogen A, trypsinogen and soybean trypsin inhibitor are retarded, relative to the other proteins tested, during chromatography on tanned gelatin under these conditions.

This retardation is an undesirable effect with regard to the estimation of molecular weights from elution volumes and therefore possible methods of eliminating the effect were investigated. Chymotrypsinogen A was selected for further study using an 8% chromium-formalin tanned gel. In successive experiments the effects of the following changes to the eluting buffer were investigated: (i) increasing the concentration of NaCl to 1.5 *M*, (ii) addition of 2-mercaptoethanol (1×10^{-3} *M*), and (iii) addition of EDTA (0.01 *M*). In each case the column was equilibrated with the

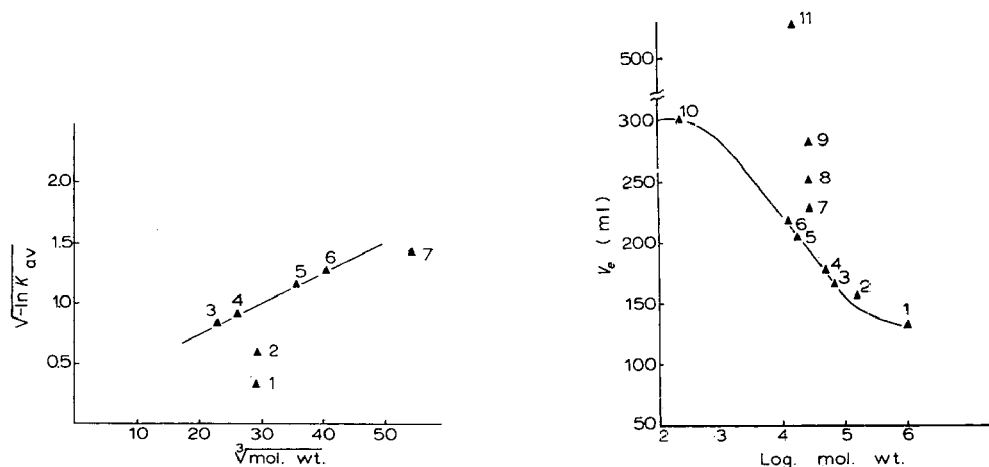


Fig. 1. Relationship between K_{av} (apparent) and molecular weight (mol. wt.) of a number of standard proteins chromatographed on 4% chromium-formalin tanned gelatin. No values are shown for lysozyme as this is eluted at a volume greater than V_{max} and the K_{av} value is thus meaningless. 1 = Chymotrypsinogen A; 2 = soybean trypsin inhibitor; 3 = cytochrome C; 4 = myoglobin; 5 = hexokinase; 6 = bovine serum albumin; 7 = γ -globulin.

Fig. 2. Relationship between the elution volume (V_e) and the molecular weight (mol. wt.) of a number of standard proteins chromatographed on 4% chromium-formalin tanned gelatin. 1 = Blue Dextran; 2 = γ -globulin; 3 = bovine serum albumin; 4 = hexokinase; 5 = myoglobin; 6 = cytochrome C; 7 = trypsinogen; 8 = soybean trypsin inhibitor; 9 = chymotrypsinogen A; 10 = tryptophan; 11 = lysozyme.

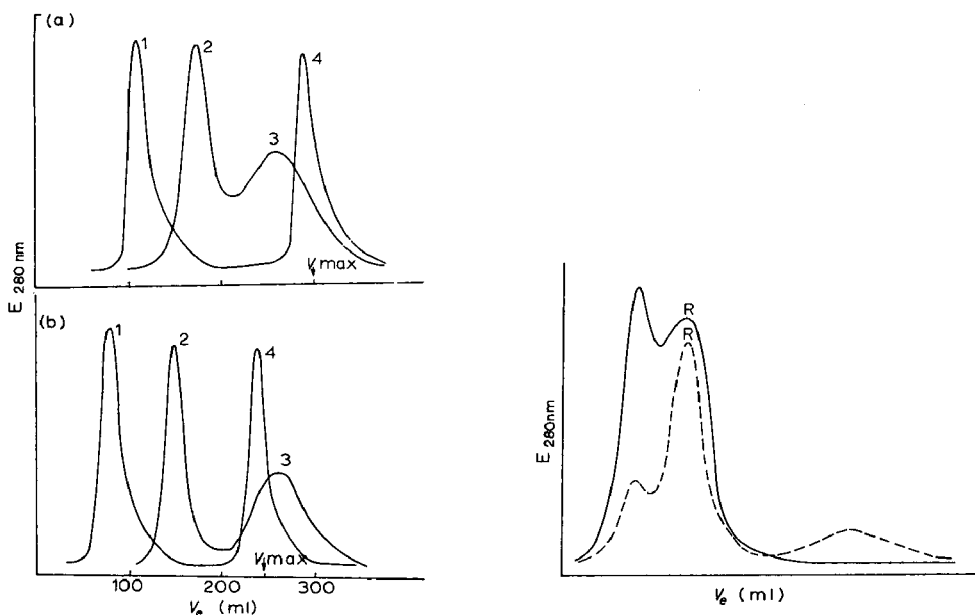


Fig. 3. The effect of a change in the operating temperature ($a = 8^\circ$, $b = 40^\circ$) upon the chromatography of chymotrypsinogen A on 8% chromium-formalin tanned gelatin. 1 = Blue Dextran; 2 = cytochrome C; 3 = chymotrypsinogen A; 4 = tryptophan.

Fig. 4. The effect of high urea concentrations upon the chromatography of chymotrypsinogen A on 8% chromium-formalin tanned gelatin. ---, 6 *M* urea; —, 8 *M* urea. R = cytochrome C reference peak.

new buffer before addition of the sample. As none of these agents reduced the retardation of the protein, it was concluded that retardation is probably not due to ion-exchange, sulphhydryl interactions or co-ordinate bonding with the chromium. Furthermore, an indication that hydrophobic interactions are not operative is provided by the amino acid tryptophan, which is eluted at a volume corresponding to the calculated V_{\max} of the column.

The effect of an increase in temperature from 8° to 40° and the effect of the addition of urea at two different concentrations were also investigated (Figs. 3 and 4). It is apparent from Fig. 3 that an increase in temperature from 8° to 40° causes the gel to shrink (as manifested by the decrease in V_{\max}) although it does not affect the elution volume of chymotrypsinogen A. In the presence of 6 or 8 *M* urea, the gel completely lost its mechanical resilience, becoming soft and easily compacted. At the same time, in 6 *M* urea, the retardation effect was apparently reduced, resulting in the chymotrypsinogen A being distributed into two peaks while, in 8 *M* urea, the retardation effect was apparently completely eliminated as the chymotrypsinogen A was eluted as a single peak which lay in front of the cytochrome C reference peak.

Discussion

It is commonly accepted that the structure of gelatin results from the collapse of the more ordered hydrogen-bonded triple-helical structure of collagen. In the model of HARRINGTON AND VON HIPPEL⁵, gelation of a hot solution of gelatin by

cooling is thought to be due to the reformation of poly-L-proline II type helices along regions of the individual peptide chains. These are thought to associate subsequently to regenerate local regions of triple helix, stabilised by interchain hydrogen bonds. An overall randomly ramified structure, composed of regions of triple helix linked together by single polypeptide chains (presumably in the poly-L-proline II configuration) is thought to result.

The possible role of hydrogen bonds in the stabilisation of the structure of tanned gelatin gels is indicated by the loss of gel strength occasioned by high concentrations of urea. Furthermore, as the retardation of chymotrypsinogen A is eliminated by high concentrations of urea, it may be concluded that retardation during chromatography, in the absence of urea, is either due to hydrogen bond interactions between the gel and the sample protein, or that it is a consequence of some unique three-dimensional aspect of the gel structure. That the Stokes' radius of chymotrypsinogen A is not markedly affected by high urea concentration is indicated by the chromatographic data of OLSON AND LIENER⁶.

In the model outlined above, the regions comprised of single polypeptide chains would be particularly rich in potential (unpaired) hydrogen bonding groups which, during chromatography, could pair in a dynamic manner with complementary groups on the sample protein and thus cause its retardation. The degree of retardation experienced by a given protein would thus be a function of the number of potential hydrogen bonding groups arrayed upon its surface. It should be noted, however, that in the case of agarose, gelling is also commonly ascribed to intermolecular hydrogen bonding but agarose has not been found to retard proteins during chromatography in buffers of adequate ionic strength.

Although no conclusive explanation can be offered the observation that certain proteins are retarded during chromatography on tanned gelatin has the consequence that the molecular weights of proteins cannot be estimated confidently from their elution volumes on columns of this material. This does not detract from the usefulness of tanned gelatin as a separating agent, however (for example tanned gelatin would appear to be particularly suitable for the isolation of lysozyme), and, in view of its high strength and low cost, tanned gelatin should find widespread application, particularly in preparative chromatography.

Natal Agricultural Research Institute,
Private Bag 9021, Pietermaritzburg
(South Africa)

C. DENNISON

- 1 A. POLSON AND W. KATZ, *Biochem. J.*, **108** (1968) 641.
- 2 T. C. LAURENT AND J. KILLANDER, *J. Chromatog.*, **14** (1964) 317.
- 3 P. ANDREWS, *Biochem. J.*, **91** (1964) 222.
- 4 P. ANDREWS, *Biochem. J.*, **96** (1965) 595.
- 5 W. F. HARRINGTON AND P. H. VON HIPPEL, *Advan. Protein Chem.*, **16** (1961) 1.
- 6 M. O. J. OLSON AND I. E. LIENER, *Biochemistry*, **6** (1967) 3801.

Received July 21st, 1970

J. Chromatog., **53** (1970) 381-384

CHROM. 4990

Gelchromatographie strukturisomerer Peptide an Sephadex G-10

Über die "reversible Adsorption" von aromatischen und heterocyclischen Verbindungen an Dextransgelen in Abhängigkeit von der Art der Gelmatrix und des Elutionsmittels ist von zahlreichen Arbeitskreisen berichtet worden¹⁻⁴. In einer vorangegangenen Mitteilung beschrieben wir das unterschiedliche Verhalten strukturisomerer Phenylalaninpeptide bei der Gelchromatographie an Sephadex G-15 (Lit. 5). Wir haben diese Untersuchungen an Sephadex G-10 fortgesetzt.

Methodik

Für die Versuche wurde ein Chromatographierohr mit den Abmessungen 105×1.2 cm bis zu einer Höhe von 102 cm mit in 0.2 *M* Essigsäure gequollenem Sephadex G-10 (Lot No. 8986) gefüllt. Die Versuche wurden mit folgenden Elutionsmitteln in der angegebenen Reihenfolge durchgeführt: (A) 0.2 *M* Essigsäure; (B) 0.2 *M* Essigsäure mit 0.5 *M* NaCl; (C) 0.2 *M* Essigsäure mit 1.0 *M* NaCl; (D) 0.2 *M* Essigsäure mit 0.1 *M* Phenol; (E) 0.01 *M* NaOH; (F) 0.01 *M* NaOH mit 0.5 *M* NaCl; (G) 0.2 *M* Essigsäure, nachdem die Säule mit dest. Wasser neutral gewaschen und anschliessend mit 300 ml 1 *M* Pyridinlösung behandelt worden war⁶. Das verbleibende Pyridin wurde dann mit 0.2 *M* Essigsäure von der Säule eluiert. Es wurden jeweils 1 μ Mol Aminosäure oder Peptid in 0.5 ml Elutionsmittel gelöst und auf die Säule gegeben. Das Eluat wurde in 1-ml Fraktionen aufgefangen. Die Elutionsgeschwindigkeit betrug 20 ml/Std. Die einzelnen Fraktionen wurden mit 2,4,6-Trinitrobenzolsulfonsäure bzw. Ninhydrin (Prolin und Pro-Gly) umgesetzt und die Extinktionen bei 420 nm gemessen. Die Berechnung der K_{av} -Werte erfolgte nach der Gleichung von LAURENT UND KILLANDER⁷

$$K_{av} = \frac{V_e - V_0}{V_t - V_0}$$

Das mit der entsprechenden Mengen Wasser ausgemessene Gesamtvolumen V_t betrug 110 ml. Das äussere Volumen V_0 wurde mittels Rinderserumalbumin zu 41 ml bestimmt. Die für die Versuche verwendeten Peptide wurden nach bekannten Methoden synthetisiert und sind aus der Tabelle I zu ersehen.

Diskussion

Die strukturisomeren Phenylalanin- und Leucinpeptide zeigten in 0.2 *M* Essigsäure unterschiedliche Affinitäten zur Gelphase, wobei die Peptide mit N-terminalem Glycin stärker adsorbiert wurden als die Peptide mit C-terminalem Glycin. Durch Salzzugabe zum Elutionsmittel (System B und C) wurden diese Affinitätsunterschiede besonders deutlich. Dabei wurden die Peptide Gly-Phe, Phe-Gly, Gly-Gly-Phe, Gly-Ala, Ala-Gly, Gly-Leu, Leu-Gly und Gly-Pro später von der Säule eluiert als die entsprechenden Aminosäuren Glycin, Phenylalanin, Alanin, Leucin und Prolin. Diesen Effekt beobachteten wir schon bei unseren Untersuchungen an Sephadex G-15 (Lit. 5). Der Versuch, eine "aromatische Sättigung" des Gels durch Phenolzusatz

TABELLE I

K_{av}-WERTE VON AMINOSÄUREN UND PEPTIDEN AN SEPHADEX G-10

Säulenparameter, 102 × 1.2 cm; Gesamtvolumen (*V_t*), 110 ml; Ausschlussvolumen (*V₀*), 41 ml.
 Elutionsmittel: (A) 0.2 *M* Essigsäure; (B) 0.2 *M* Essigsäure mit 0.5 *M* NaCl; (C) 0.2 *M* Essigsäure mit 1.0 *M* NaCl; (D) 0.2 *M* Essigsäure mit 0.1 *M* Phenol; (E) 0.01 *M* NaOH; (F) 0.01 *M* NaOH mit 0.5 *M* NaCl; (G) 0.2 *M* Essigsäure, nachdem die Säule mit 1 *M* Pyridin gewaschen wurde.

	Elutionsmittel						
	A	B	C	D	E	F	G
Glycin	0.30	0.32	0.36	0.28	0.17	0.24	0.25
Phenylalanin	0.54	0.76	0.98	0.54	0.26	0.53	0.46
Gly-Phe	0.55	1.10	1.43	0.55	0.19	0.43	0.33
Phe-Gly	0.43	0.82	1.03	0.42	0.22	0.47	0.28
Gly-Gly-Phe	0.49	0.89	1.10	0.48	0.15	0.33	0.27
Phe-Gly-Gly	0.29	0.36	0.39	0.26	0.12	0.25	0.25
Alanin	0.27	0.33	0.34	0.25	0.15	0.23	0.23
Gly-Ala	0.25	0.38	0.42	0.24	0.11	0.22	0.17
Ala-Gly	0.25	0.36	0.39	0.23	0.09	0.22	0.15
Leucin	0.29	0.36	0.43	0.29	0.15	0.28	0.25
Gly-Leu	0.31	0.57	0.65	0.31	0.11	0.23	0.18
Leu-Gly	0.25	0.37	0.45	0.26	0.11	0.26	0.17
Prolin	0.24	0.27	0.30	0.25	0.16	0.26	0.18
Gly-Pro	0.23	0.35	0.37	0.24	0.09	0.21	0.17
Pro-Gly	0.23	0.31	0.35	0.23	0.11	0.23	0.18

zum Elutionsmittel zu erreichen, scheiterte ebenso wie der Versuch dieses mittels Na-salicylat zu erzielen⁸.

Erwartungsgemäss wurden die Aminosäuren und Peptide in 0.01 *M* NaOH von der Gelphase ausgeschlossen. Durch Salzzugabe wurden die Verbindungen jedoch wieder unterschiedlich stark adsorbiert. Dabei fiel auf, dass Phe-Gly stärker als Gly-Phe retardiert wurde. Nach den Versuchen mit den Elutionsmitteln A–F überprüften wir die Eigenschaften der Säule. Diese hatten sich offensichtlich nicht geändert, denn für alle Aminosäuren und Peptide wurden in 0.2 *M* Essigsäure dieselben *K_{av}*-Werte gefunden wie zu Beginn der Versuchsreihen. Nach dem Waschen der Säule mit Pyridinlösung jedoch wurden alle Verbindungen mit 0.2 *M* Essigsäure deutlich früher von der Säule eluiert als zuvor. Diese von EAKER UND PORATH gemachte Beobachtung können wir für Sephadex G-10 (Lot No. 8986) bestätigen. Dagegen konnten wir diesen Effekt bei unseren Arbeiten mit Sephadex G-15 (Lot No. 9190) nicht beobachten⁵.

Staatsliches Institut für Immunpräparate und Nährmedien,
 112 Berlin-Weissensee (D.D.R.)

P. ZISKA

- 1 B. GELOTTE, *J. Chromatog.*, 3 (1960) 330.
- 2 J.-C. JANSON, *J. Chromatog.*, 28 (1967) 12.
- 3 R. K. BRETHAUER UND A. M. GOLICHOWSKI, *Biochim. Biophys. Acta*, 155 (1967) 549.
- 4 J. PORATH, *Nature*, 218 (1968) 834.
- 5 P. ZISKA, *J. Chromatog.*, 48 (1970) 544.
- 6 D. EAKER UND J. PORATH, *Separation Sci.*, 2 (1967) 507.
- 7 T. C. LAURENT UND J. KILLANDER, *J. Chromatog.*, 14 (1964) 317.
- 8 J. PORATH, *Biochim. Biophys. Acta*, 39 (1960) 193.

Eingegangen am 11. August 1970

CHROM. 4999

Schnell-Transfer Dünnschichtchromatographie-Infrarotspektroskopie

Zur Charakterisierung chromatographisch getrennter μg -Mengen ist die IR-Spektroskopie in ihrer Ultramikrotechnik¹ sehr vorteilhaft. Da sich eine direkte Kopplung ausschliesst, muss der Zwischenschritt in Form eines mechanischen Transfers durchgeführt werden.

Neben den bisher bekannten Verfahren^{2,3} zur DC-IR-Kombination hat sich in unseren Laboratorien die nachstehend beschriebene Methode am besten bewährt:

In ein beiderseitig trichterförmig erweitertes Glasröhrchen (Fig. 1.1) von 60–80 mm Länge und einem Innendurchmesser von 1–2 mm stopft man etwa 10 mm von einem Ende einen Quarzwattebausch (c). Das andere Ende des Röhrchens verbindet man mit einer Wasserstrahlpumpe (d) und saugt die losgeschabte Substanzzone (a) von der DC-Platte (b) staubsaugerartig ein. Dann dreht man es um 180° (Fig. 1.2)

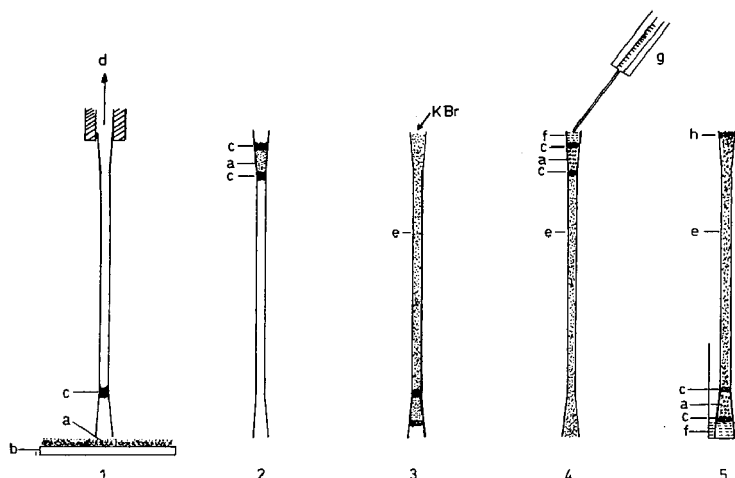


Fig. 1. Herstellung und Handhabung einer KBr-Mikrotransfersäule. Einzelheiten 1–5 im Text. a = DC-Fleck; b = DC-Platte; c = Quarzwolle; d = zur Wasserstrahlpumpe; e = KBr zur Spektroskopie; f = Elutionsmittel; g = Mikroliterspritze; h = mit Substanz angereicherte KBr-Zone.

und löst die Verbindung zur Wasserstrahlpumpe. Auf die so eingesaugte Substanzzone (a) stopft man einen Quarzwattebausch (c).—Liegen jedoch sauerstoffempfindliche Substanzen vor, so ist von diesem "Staubsaugerprinzip" abzuraten. In diesem Falle fülle man die losgeschabte Substanzzone mit einem Mikrospatel in das Röhrchen (Fig. 1.2).—Danach dreht man es abermals um 180° und füllt es mit fein gepulvertem Kaliumbromid "zur Spektroskopie" (e) auf. Durch leichtes Klopfen erreicht man, dass eine kleine saugfähige Kaliumbromidsäule entsteht (Fig. 1.3). Nun drückt man mit dem Mikrospatel die obere Kaliumbromidschicht etwas fest, so dass beim anschliessenden Drehen um 180° das Kaliumbromid nicht herausrieselt. Dann gibt man mit einer 100-Mikroliterspritze (g) ca. 20–50 μl Elutionsmittel in den noch freien, trichterförmig erweiterten Raum (f), so dass dieser gerade gefüllt ist (Fig. 1.4). Die zu transferierende

Substanz wandert in der Kaliumbromidsäule abwärts. Noch bevor das Elutionsmittel völlig eingesaugt ist, wird das Röhrchen um 180° gedreht und in ein mit $100\ \mu\text{l}$ Elutionsmittel gefülltes, kleines Tablettenröhrchen ($5 \times 20\ \text{mm}$) gestellt. Das Lösungsmittel steigt nach oben, transportiert die gelöste Substanz und verdampft am oberen Ende. Auf diese Weise sammelt sich nach und nach die Substanz im obersten Teil der Kaliumbromidsäule (Fig. 1.5h). Bei Bedarf ist mit einer Mikroliterspritze das Elutionsmittel im Tablettenröhrchen nachzufüllen. Nachdem das Elutionsmittel verdampft ist, bereitet man aus der obersten KBr-Zone (ca. 4 mg) einen Mikropressling ($\varnothing\ 1.5\ \text{mm}$). Hierzu ist der Gerätezusatz "Ultramikropressform" der Firma Perkin-Elmer, Überlingen vorteilhaft.

Zum Einarbeiten stelle man sich eine 0.1% Lösung von 4-Dimethylaminoazobenzol (Buttergelb) in Tetrachlorkohlenstoff her und trage hiervon $10\ \mu\text{l}$ auf eine übliche Kieselgel G-Schicht auf. Diesen Farbfleck transferiere man in der beschriebenen Art mit Dichlormethan als Elutionsmittel und verfolge den Vorgang visuell.

Da je nach Substanz und Lösungsmittel die Elutionszeit mehrere Stunden betragen kann und sich so die hygroskopische Eigenschaft des Kaliumbromids ungünstig auswirkt (zu intensive OH-Valenz und Deformationsschwingungsbanden, die Anlass

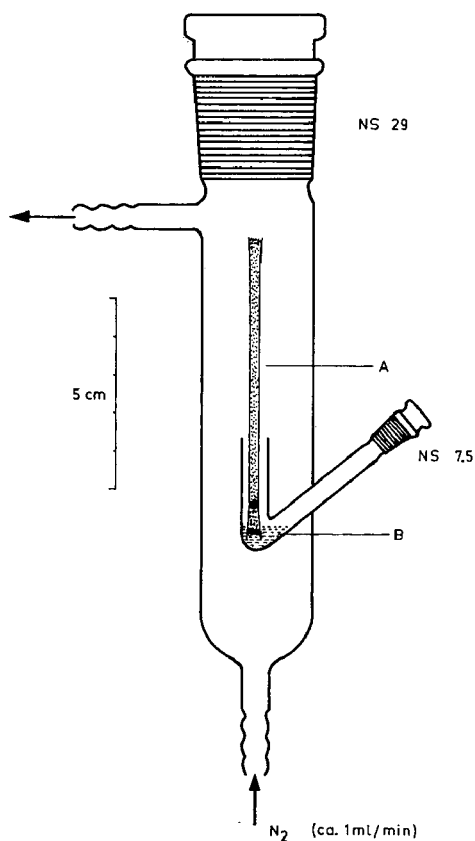


Fig. 2. Vorrichtung zur Elution und Verdampfung in einem Inertgasstrom. A = Mikrotransfer-säule; B = Elutionsmittel.

zu Fehlinterpretationen sein können), führt man die Elution und das anschliessende Verdunsten am besten in einem trockenen Stickstoffstrom durch. Die hierzu notwendige Glasapparatur ist nach der Fig. 2 leicht vom Glasbläser herstellbar. Ein weiterer Vorteil dieser Vorrichtung ist der Schutz labiler Substanzen vor Oxydation.

*Institut für Pharmakognosie
und Analytische Phytochemie der Universität
des Saarlandes, 66 Saarbrücken (B.R.D.)*

EGON STAHL
WERNER SCHILD

1 P. KROHMER UND G. KEMMER, *Z. Anal. Chem.*, 243 (1968) 80.

2 G. SZÉKELY, *J. Chromatog.*, 48 (1970) 313.

3 R. AMOS, *J. Chromatog.*, 48 (1970) 343.

Eingegangen am 17. August 1970

J. Chromatog., 53 (1970) 387-389

CHROM. 5011

Manganous chloride spray reagent for cholesterol and bile acids on thin-layer chromatograms

Cholesterol reacts with a variety of chemical substances to give colored products. KRITCHEVSKY¹ has summarized some of these color reactions of cholesterol. But the spray detection of cholesterol in thin-layer chromatography (TLC) has been accomplished by means of antimony trichloride², phosphomolybdic acid³, anisaldehyde-sulfuric acid⁴ and ferric chloride⁵. Antimony trichloride has its disadvantage due to its toxicity and reactivity with water to form insoluble precipitates. Phosphomolybdic acid and anisaldehyde-sulfuric acid gives a colored background and cannot clearly distinguish the cholesterol from the bile acids. All these difficulties may be overcome by the use of this manganous chloride spray reagent for the detection of cholesterol and bile acids on thin-layer chromatograms.

Materials and methods

Cholesterol and bile acids are obtained from Applied Science Laboratories, Pa., and manganous chloride from Allied Chemicals, General Chemical Division, N.Y. DuPont concentrated sulfuric acid is used. The samples are applied to Silica Gel F-254 of 0.25 mm thickness as supplied by Brinkmann Instruments, Westbury, N.Y., and detected without chromatography. The spray reagent is prepared by dissolving 50 mg of $\text{MnCl}_2 \cdot 4\text{H}_2\text{O}$ in 15 ml of water and 0.5 ml of concentrated sulfuric acid. After the reagent has been sprayed on the thin-layer plate, it is placed in an oven at 100-110° for 10-15 min and the color is noted. Five to ten micrograms of each in ethanol is sufficient for color detection.

Results and discussion

The color reactions of cholesterol and bile acids are shown in Table I. The

J. Chromatog., 53 (1970) 389-390

TABLE I

COLOR REACTIONS OF CHOLESTEROL AND BILE ACIDS ON THIN-LAYER CHROMATOGRAM (10 μ g)The thin-layer plate is sprayed with manganous chloride spray reagent ($\text{MnCl}_2 \cdot 4\text{H}_2\text{O}$, 50 mg; water, 15 ml and concentrated sulfuric acid, 0.5 ml).

<i>Compound</i>	<i>Color</i>
Cholesterol	Pink
Cholic acid	Deep yellow
Chenodeoxycholic acid	Greyish green
Deoxycholic acid	Yellow
Hyodeoxycholic acid	Tan
Lithocholic acid	Light pink

color of cholesterol begins to fade and the bile acid colors deepen after 5 min. On longer exposure to air, all the characteristic color disappears. So, the cholesterol color should be noted after removing the plate from the oven and the bile acids after 5 min from then. There is no background color and so the resulting color stands out clearly from the white background. This method allows as little as 1 μ g of cholesterol and 2 μ g of bile acids to be detected and the reagent is very simply to prepare. It is always suggested to prepare ones' own color standards.

This work was supported by the National Institutes of Health, Public Health Service Grant AM 11315 and the Begole Brownell Research Grant 30554.

*Department of General Surgery,
University of Michigan Medical Center,
Ann Arbor, Mich. 48104 (U.S.A.)*

SATINDRA K. GOSWAMI
CHARLES F. FREY

- 1 D. KRITCHEVSKY, *Cholesterol*, Wiley, New York, 1958, p. 235.
- 2 J. M. BOBBITT, *Thin-layer Chromatography*, Reinhold, New York, 1963, p. 169.
- 3 D. KRITCHEVSKY AND M. R. KIRK, *Arch. Biochem. Biophys.*, 35 (1952) 346.
- 4 N. J. DESOUZA AND W. R. NES, *J. Lipid Res.*, 10 (1969) 240.
- 5 R. R. LOWRY, *J. Lipid Res.*, 9 (1968) 397.

Received June 29th, 1970

J. Chromatog., 53 (1970) 389-390

CHROM. 4956

Empfindlicher Nachweis von Östrogenen mit einem automatischen Leitfähigkeitsdetektor für die Dünnschicht-Chromatographie

Die Messung der elektrischen Leitfähigkeit zum selektiven Nachweis dissozierender Substanzen wurde schon verwendet, das Dünnschicht-Chromatogramm von Indikatorfarbstoffen und Aminosäuren zu registrieren¹. In der vorliegenden Arbeit soll die Anwendbarkeit dieser Methode zum empfindlichen Nachweis von Steroid-Östrogenen erprobt werden. Dabei wurden Östrogen-Reinsubstanzen sowie Harnextrakte untersucht.

Wir verwendeten eine modifizierte BN-Kammer², wie sie in Fig. 5 der Arbeit von CREMER *et al.*¹ dargestellt ist. Auf einer 5×20 cm Dünnschichtplatte wurde an den beiden Längsrändern das Adsorbens in einer Breite von 5 mm entfernt, um zwei Glasstäbe zur Einhaltung des Abstandes von 1 mm zur Deckplatte aufzulegen. In die Schicht wurden zwei Bahnen von 1 cm Breite eingeritzt. Auf jede dieser Bahnen konnten durch Löcher in der Deckplatte ein Paar Platinelektroden auf die Schicht gepresst werden. Die Elektroden (Durchmesser 0.8 mm, Abstand 1 mm) waren vertikal leicht verschiebbar in Teflonstopfen eingepasst. In einem Abstand von 2, 4 und 6 cm wurden in die Deckplatte weitere Teflonstopfen eingeschliffen, durch deren Bohrungen die Proben mit einer 1- μ l Hamilton-Spritze aufgetragen werden konnten. Das Fließmittel wurde mit einer Filterpapierbrücke eingeführt und verdunstete beim Austritt aus der "zweidimensionalen Säule", die auf diese Weise kontinuierlich durchflossen wurde.

Nach der Probenaufgabe wurden die einzelnen Komponenten eines Substanzgemisches auf der Säule getrennt und durchwanderten nacheinander den Raum zwischen den Messelektroden. Die Widerstände der beiden Elektrodenpaare wurden mit Hilfe einer Wheatstoneschen Brücke abgeglichen. An das Brückeninstrument

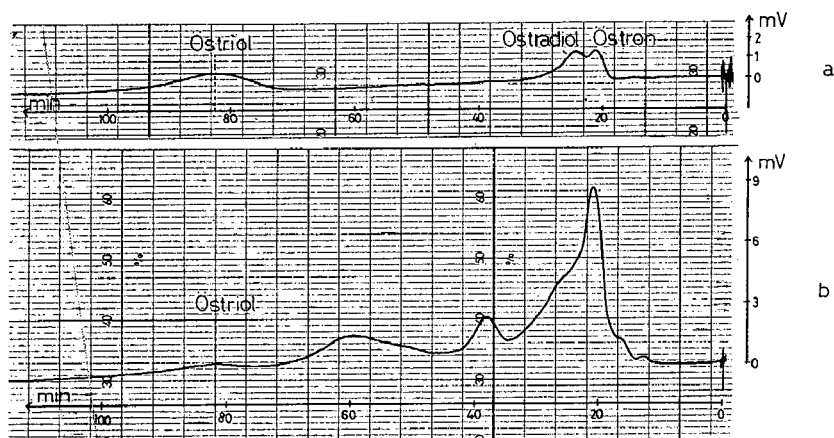


Fig. 1. Dünnschicht: Kieselgel H. Abstand Probenaufgabe-Elektroden ("Säulenlänge"): 6 cm. Fließmittel: Methylisobutylketon, wasser-gesättigt. Widerstände der beiden Elektrodenpaare: 80 M Ω . Probe: (a) je 0.3 μ g Östron, Östradiol-17 β und Östriol (0.3 μ l einer 0.1-%igen Lösung der drei Östrogene im Fließmittel); (b) 0.3 μ l aus 0.5-ml Harnextrakt A.

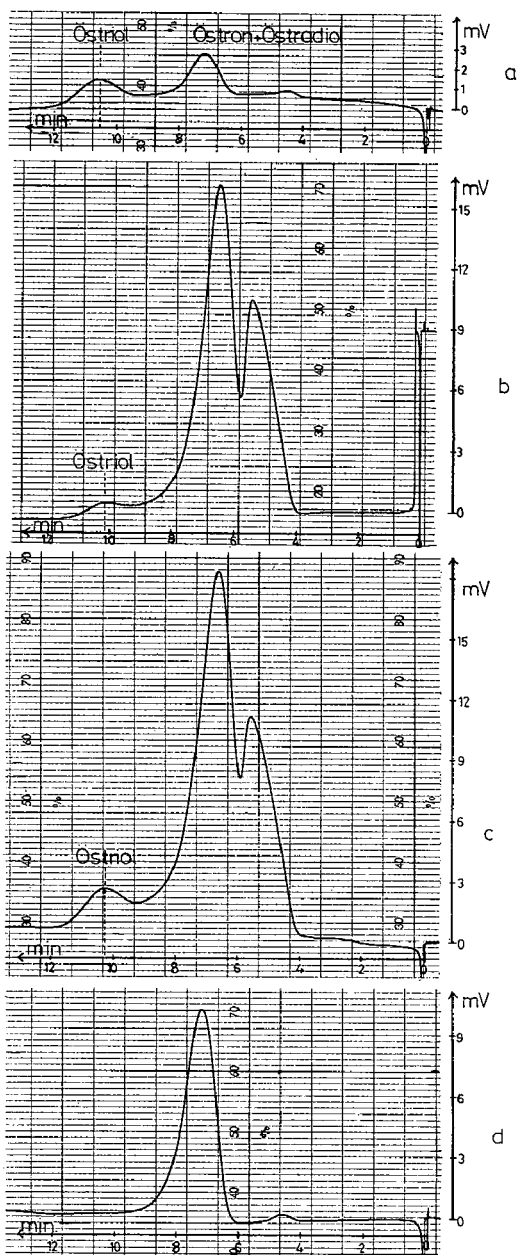


Fig. 2. Dünnschicht: Kieselgel-H. Abstand Probenaufgabe-Elektroden ("Säulenlänge"): 4 cm. Fließmittel: Aceton. Widerstände der beiden Elektrodenpaare: 7 M Ω . Probe: (a) je 20 ng Östron, Östradiol-17 β und Östrol (0.1 μ l einer 0.02-%igen Lösung der drei Östrogene im Fließmittel); (b) 0.1 μ l aus 1 ml Harnextrakt A; (c) = (b) + (a); (d) 0.1 μ l aus 1 ml Harnextrakt B.

(Keithley Elektrometer 602) war ein Kompensationsschreiber angeschlossen. Die Brückenspannung ΔU ist bei symmetrischer Brücke der relativen Widerstandsänderung $\Delta R/R$ proportional³:

$$\Delta U = \frac{U}{4} \cdot \frac{\Delta R}{R}$$

wobei U = Spannung der Gleichstromquelle (4.5 V).

Als Fliessmittel wurden Ketone verwendet. Sie haben relativ hohe Dipolmomente (Aceton: 2.9 Debye) und Dielektrizitätskonstanten (Aceton: 20.7) und begünstigen so die Dissoziation der Östrogene mit ihren phenolischen OH-Gruppen.

Wir haben zwei verschiedene Harne untersucht*. Harnextrakt A stammt von einer Frau im 8. Monat der Schwangerschaft, Harnextrakt B ist eine entsprechende Probe eines weiblichen Normalharns. Fig. 1a zeigt die Auftrennung der drei Östrogene Östron, Östradiol-17 β und Östriol mit Methyisobutylketon, wasser-gesättigt, als Fliessmittel. Fig. 1b zeigt das Chromatogramm der Trennung des Harnextraktes A. Die übrigen im Harn vorkommenden phenolischen Verbindungen treten in einer sehr viel grösseren Menge auf als das Östriol und verdecken die in sehr geringen Mengen vorhandenen Östrogene Östron und Östradiol, konnten aber von Östriol gut getrennt werden. Der Östriolpeak erscheint in diesem Falle erst bei etwa 80 min und ist dementsprechend stark verbreitert.

Mit Aceton als Fliessmittel (Fig. 2a) wurden zwar Östron und Östradiol-17 β

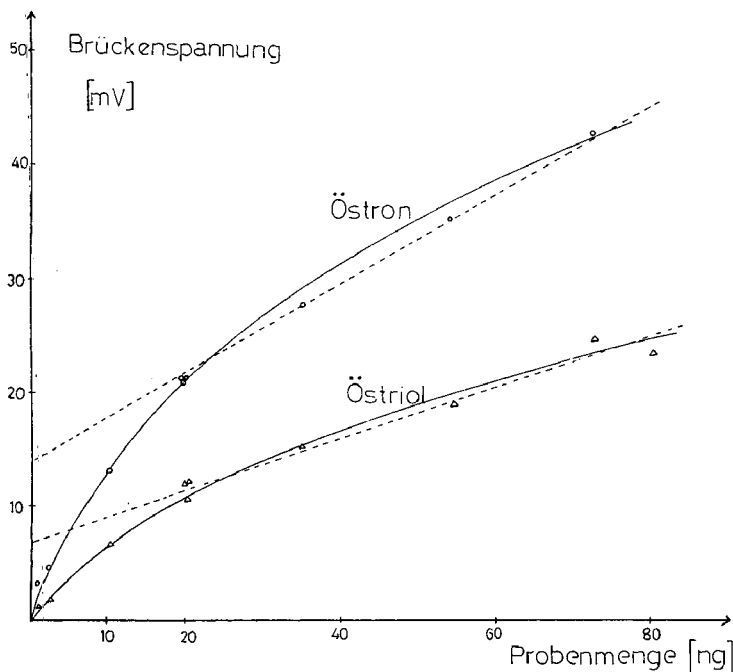


Fig. 3. Abhängigkeit der Brückenspannung ΔU (mV) von der Probenmenge (ng) von Östron und Östriol.

* Herr Dr. H. GLEISPACH, Universitäts-Kinderklinik, Innsbruck, stellte mir in dankenswerter Weise Harnextrakte zur Verfügung. Die 1/30 Menge des 24-h Harns wurde mit Salzsäure hydrolysiert. Der Ätherextrakt wurde mit alkalischen Puffern gewaschen, eingedampft und mit dem jeweiligen Fliessmittel aufgenommen.

nicht aufgetrennt, der Östriolpeak aber dafür schon bei 10.5 min erhalten. Die Analysen können mit diesem Fließmittel sehr schnell ausgeführt werden. Das Chromatogramm in Fig. 2b zeigt wieder die Auftrennung des Harnextraktes A. In Fig. 2c wurde dem Harn A Östriol zugesetzt und eine Vergrößerung des Peaks bei 10.3 min registriert. In Fig. 2d wurde der Harnextrakt B aufgetrennt. Die phenolischen Verbindungen treten hier in geringeren Mengen auf, der Östriolpeak fehlt ganz.

In Fig. 3 wurden die Höhen der Peaks (in mV-Brückenspannung) gegen die Probenmenge (in ng) für Östron und Östriol aufgetragen. Als Fließmittel wurde Aceton verwendet, der Abstand Probenaufgabe-Elektroden betrug hier 4 cm. Die Brückenspannung ist nicht proportional der aufgegebenen Probenmenge. Die Abhängigkeit kann aber im Bereich von 20–80 ng durch eine Gerade dargestellt werden.

Das Fließmittel strömte kontinuierlich durch die Dünnschicht, sodass die Apparatur tagelang in Betrieb war. Ausserdem konnten ohne weiteres über dreissig Proben auf einer Platte bestimmt werden.

Mit der bisherigen einfachen Versuchsanordnung erreichten wir für die Östrogene eine Nachweisgrenze von 1 ng. Durch weitere Verfeinerung der Methode, namentlich durch Thermostatisierung, könnte man die Nachweisgrenze noch weiter senken. Bisher arbeitete man meist im μg -Bereich, durch fluorimetrische Auswertung ist auch ein Nachweis im ng-Bereich möglich, worüber auch OERTEL UND PENZES⁴ jüngst berichteten. Auf Dünnschichtplatten konnten wir bisher 0.2 ng an Östrogenen gut nachweisen⁵.

*Physikalisch-Chemisches Institut der Universität
Innsbruck, Innsbruck (Österreich)*

H. NAU

1 E. CREMER, TH. KRAUS UND H. NAU, *Z. Anal. Chem.*, 245 (1969) 37.

2 M. BRENNER UND A. NIEDERWIESER, *Experientia*, 17 (1961) 237.

3 R. KAISER, *Gas-Chromatographie*, Akademische Verlagsgesellschaft, Leipzig, 1960, S. 102.

4 G. W. OERTEL UND L. PENZES, *Vortrag auf der Tagung Biochemische Analytik 70, München*, 1970.

5 E. CREMER, F. DEUTSCHER, P. FILL UND H. NAU, *J. Chromatog.*, 48 (1970) 132.

Eingegangen am 3. August, 1970

J. Chromatog., 53 (1970) 391–394

CHROM. 4976

Dünnschichtchromatographie von Sulfonsäureestern

Das Auffinden geeigneter chromatographischer Verfahren war Voraussetzung für die Aufklärung der bei der Sulfonierung von α -Olefinen mit Schwefeltrioxid¹ entstehenden Reaktionsprodukte. Der wasserlösliche Anteil des Sulfonierungsgemisches konnte mit Erfolg papierchromatographisch aufgetrennt werden². Für die wasserunlöslichen Verbindungen, die ein Gemisch von 1,3- und 1,4-Alkansultonen mit offenkettigen Sulfonsäureestern darstellen³, wurde die im Folgenden beschriebene Methode gefunden.

Experimentelles

Die Trennung von Sulfonsäureestern, wie sie in den Sulfonierungsprodukten der α -Olefine vorliegen, gelingt dünnschichtchromatographisch auf Kieselgel G (Merck; Schichtdicke 0.25 mm, Substanzmenge 20 μ g). Als Laufmittel wird ein Äther-Benzin (Sdp. 60–70°)-Gemisch (8:2) benutzt. Zur Detektion der Verbindungen werden die Platten mit einer 0.2%igen alkoholischen Lösung von 2,7-Dichlorfluorescein besprüht und im UV-Licht betrachtet. Dabei treten gelb gefärbte Flecken auf gelbgrünem Grund auf.

Ergebnisse

Die verschiedenartigen Sulfonsäureester, die bei der Sulfonierung von α -Olefinen mit Schwefeltrioxid neben Sulfonsäuren gebildet werden, konnten bisher nicht vollständig aufgetrennt und identifiziert werden. Nur die relativ leicht kristallisierenden höhermolekularen 1,3-Alkansultone⁴ und einige 1,4-Alkansultone^{3,5} sind aus dem Sulfoniergemisch isoliert worden. Mit Hilfe der Dünnschichtchromatographie gelingt es nun, wie in Fig. 1 am Beispiel des wasserunlöslichen Teils einer Dodecen-(1)-Sulfonierung gezeigt wird, sowohl 1,3-Sultone und 1,4-Sultone nebeneinander zu unterscheiden als auch weitere Sulfonsäureester nachzuweisen.

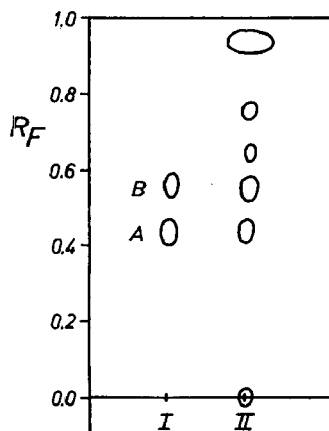


Fig. 1. Dünnschichtchromatographie von Sulfonsäureestern. (I) Sultone: A = Dodecan-1,3-sulton und B = Dodecan-1,4-sulton; (II) wasserunlöslicher Anteil einer Dodecen-(1)-Sulfonierung.

Die n -Alkansultone der Kettenlängen C_{10} bis C_{16} ergeben bei der Chromatographie keinen wesentlichen Unterschied im R_F -Wert. So ist es dünn-schichtchromatographisch möglich, sämtliche 1,3- und 1,4-Sultone im Kettenlängenbereich C_{10} – C_{16} in je einem Fleck zu vereinigen und beide Flecken voneinander getrennt zu erhalten, auch wenn die Konzentration bedeutend erhöht wird. Das ist vorteilhaft für die Analyse von Sulfonierungsprodukten technischer Gemische von Olefinen mit verschiedenen Kettenlängen. Hierbei erfolgt die Trennung der Sultone nach ihrer Ringgröße. Der Fleck, der in Fig. 1 in Frontnähe erscheint, entspricht einem Gemisch von überwiegend Dodecensulfonsäuredodecylester mit wenig Dodecen³. Drei Sulfonsäure-alkylester: Dodecansulfonsäure-1-dodecylester (I), Dodecansulfonsäure-*sec.*-dodecylester (II) und Dodecensulfonsäure-*sec.*-dodecylester (III), die durch Umsetzung von Sulfonsäurechloriden mit den entsprechenden Alkoholen gewonnen wurden³, ergeben den gleichen Fleck in Frontnähe wie die Sulfonierungsprodukte ohne eine Differenzierung ihrer R_F -Werte. Bemerkenswert ist jedoch, dass die beiden Ester sekundärer Alkohole (II und III) im Gegensatz zu dem Sulfonsäureester des primären (I) eine hydrolytische Zersetzung auf der Kieselgelplatte erleiden können, die sich durch das Auftreten eines zusätzlichen Flecks am Start (Sulfonsäuren) bemerkbar macht. Diese Zersetzung der Ester findet nur beim Lagern der mit Substanz beladenen DC-Platte an der Luft statt, jedoch nicht, wenn die Platte sofort nach Auftragen der Substanzen in die mit dem Laufmitteldampf gesättigte Entwicklungskammer gestellt wird. Der bei den Sulfonierungsprodukten in Fig. 1 am Start erscheinende Fleck beruht ebenfalls auf einer Sulfonsäureesterzersetzung.

Die zwei in Fig. 1 zwischen den Flecken für Dodecensulfonsäuredodecylester und 1,4-Sulton erscheinenden Flecke werden auf Grund der IR-Spektren entsprechender säulenchromatographischer Fraktionen und der Eigenschaften (GC, PC, DC, IR) der Hydrolyseprodukte der wasserunlöslichen Sulfonierungsanteile als Dodecendisulfonsäure-didodecylester und Sultondodecansulfonsäuredodecylester angesehen³.

*Institut für Fettchemie der Deutschen Akademie der
Wissenschaften zu Berlin, Berlin-Adlershof (D.D.R.)*

Fritz PÜSCHEL
DIETRICH PRESCHER

- 1 F. PÜSCHEL, *Tenside (München)*, 3 (1966) 71.
- 2 F. PÜSCHEL UND D. PRESCHER, *J. Chromatog.*, 32 (1968) 337.
- 3 D. PRESCHER, *Dissertation*, Humboldt-Universität, Berlin, 1970.
- 4 F. PÜSCHEL UND C. KAISER, *Chem. Ber.*, 98 (1965) 735.
- 5 D. M. MARQUIS, S. H. SHARMAN, R. HOUSE UND W. A. SWEENEY, *J. Am. Oil Chemists' Soc.*, 43 (1966) 607.

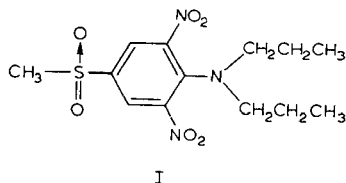
Eingegangen am 9. April 1970; geänderte Fassung am 5. August 1970

J. Chromatog., 53 (1970) 395–396

CHROM. 495I

Separation of Planavin® herbicide and some related compounds by two-dimensional thin-layer chromatography

The herbicide, 4-(methylsulfonyl)-2,6-dinitro-N,N-dipropylaniline (I), is marketed under the brandname Planavin® herbicide as a selective pre-emergent herbicide for use on agronomic crops. It is active against a great variety of annual grasses and broadleaf weeds¹.



In conjunction with metabolic studies of I in plant and soil systems it was necessary to investigate the chromatographic behavior of this compound, certain related compounds, and possible metabolite or breakdown products. Optimum separation of I and eleven related compounds was obtained using two-dimensional

TABLE I

COLORS AND R_F VALUES OF SELECTED COMPOUNDS IN FOUR SOLVENT SYSTEMS

Solvent systems: (A) hexane-ethyl acetate-tetrahydrofuran (66:30:4); (B) benzene-acetonitrile (3:2); (C) hexane-acetone (3:2); (D) benzene-methanol (9:1).

No.	Compound	Color	Solvent system				
			A (once)	A (twice)	B	C	D
1	2-(Methylsulfonyl)-4,6-dinitro-N,N-dipropylaniline	Yellow	0.44	0.63	0.69	0.48	0.64
2	4-(Methylsulfonyl)-2,6-dinitro-N,N-dipropylaniline ^a	Bright yellow	0.41	0.60	0.67	0.45	0.62
3	4-(Methylsulfonyl)-2,6-dinitro-N-propylaniline	Bright yellow	0.30	0.48	0.65	0.40	0.59
4	4-(Methylsulfonyl)-2-nitro-N,N-dipropylaniline	Bright yellow	0.23	0.37	0.64	0.40	0.56
5	5-(Methylsulfonyl)-3-nitro-N ² ,N ² -dipropyl- <i>o</i> -phenylenediamine	Yellow	0.19	0.30	0.62	0.36	0.48
6	4-(Methylsulfonyl)-2,6-dinitroaniline	Pale yellow	0.18	0.30	0.61	0.32	0.52
7	5-(Methylsulfonyl)-N ² ,N ² -dipropyl-1,2,3-benzenetriamine	Colorless	0.15	0.25	0.56	0.32	0.43
8	5-(Methylsulfonyl)-3-nitro-N ² ,N ² -propyl- <i>o</i> -phenylenediamine	Orange	0.04	0.09	0.56	0.27	0.31
9	4-(Methylsulfonyl)-2-nitroaniline	Yellow	0.04	0.09	0.51	0.21	0.25
10	5-(Methylsulfonyl)-3-nitro- <i>o</i> -phenylenediamine	Brown	0.02	0.04	0.40	0.15	0.36
11	4-(Methylsulfonyl)-2-nitrophenol	Yellow	0.02	0.04	0.09	0.05	0.10
12	4-(Methylsulfonyl)-2,6-dinitrophenol	Bright yellow	0.00	0.00	0.09	0.06	0.02

^a Marketed under brandname Planavin® herbicide.

thin-layer chromatography on Silica Gel F₂₅₄ precoated plates (Merck) developing twice with a mixture of hexane-ethyl acetate-tetrahydrofuran (66:30:4) in one direction and once with benzene-acetonitrile (3:2) in the perpendicular direction.

The compounds were detected either as colored spots or as blue absorbing areas when the chromatograms were exposed to short-wavelength (254 mμ) UV irradiation.

Experimental

Thin-layer plates (20 × 20 cm) precoated with 0.25 mm silica gel F₂₅₄ (E. Merck AG, Darmstadt, G.F.R., distributed by Brinkman Instruments, Inc., Westbury, N.Y., U.S.A.) were used for the work in this study. The layers were dried but not activated.

Two micrograms of I and each of the eleven compounds (Table I) in methylene chloride solution were applied at a point 2 cm from the bottom of the silica gel layer and developed in one of the following solvent systems: (A) hexane-ethyl acetate-tetrahydrofuran (66:30:4); (B) benzene-acetonitrile (3:2); (C) hexane-acetone (3:2); (D) benzene-methanol (9:1). The chromatograms were dried at room temperature in a forced air hood.

For two-dimensional chromatography, a mixture of 2–5 μg of each of the twelve compounds was spotted 2 cm from the left-hand edge and 2 cm from the bottom of the plate, and developed twice in solvent A, then turned 90° and developed in solvent B. The chromatography tanks were lined with filter paper to insure saturation.

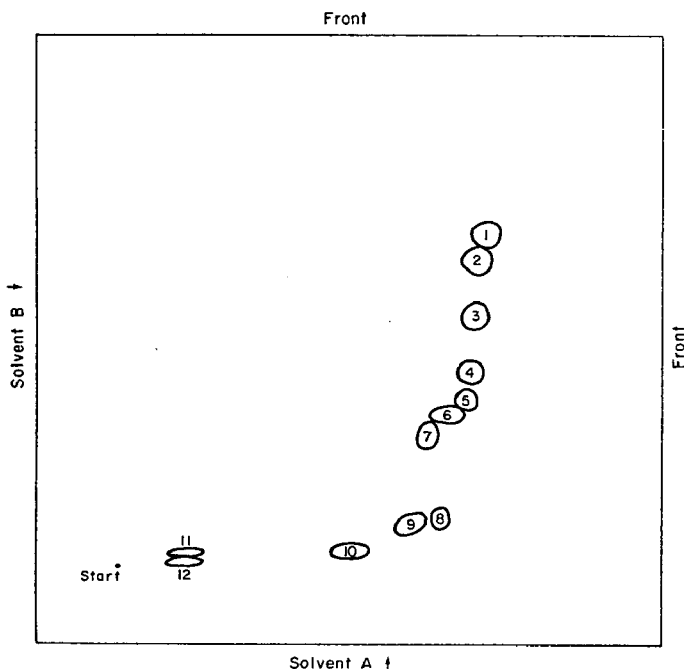


Fig. 1. Two-dimensional thin-layer chromatogram of Planavin® herbicide and eleven related compounds. Solvent systems: (A) hexane-ethyl acetate-tetrahydrofuran (66:30:4) (twice); (B) benzene-acetonitrile (3:2). Compounds: see Table I for identification.

Results and discussion

Table I shows the colors of the twelve compounds, and their approximate R_F values in the four solvent systems used. The detection limit with UV light or the unaided eye was about 0.5 μg or less for compounds 2, 3, 6, 8, 9, 10 and 11, and about 1.0 μg or less for the compounds 1, 4, 5, 7, and 12.

Fig. 1 illustrates the results of the separation obtained using the two-dimensional technique. When radioactive Planavin® herbicide was used, the separated compounds were isolated or eluted and the radioactivity quantified using liquid scintillation counting or scanning methods. In instances where the concentration was below the visible detection limits, the radioactive spots were located by exposing the chromatogram to X-ray film for a specified time, after which the film was developed. The areas were then located and eluted for quantification.

The author is indebted to R. D. SKILES and K. D. ZWAHLEN, who prepared the compounds used in this study, and to T. D. HOEWING and N. H. POONAWALLA for technical assistance.

Shell Development Company, Biological Sciences
Research Center, Modesto, Calif. 95352 (U.S.A.)

W. B. BURTON

1 W. J. HUGHES AND R. H. SCHIEFERSTEIN, *Proc. Ann. Mtg. Southern Weed Conf.*, 19th, 1966, p. 170.

Received July 31st, 1970

J. Chromatog., 53 (1970) 397-399

CHROM. 4947

The separation of plant glycosides and aglycones using thin-layer chromatography and electrophoresis

Thin-layer chromatographic techniques have been used previously to investigate the phenolic glycosides¹⁻⁴ and their hydrolysed aglycones⁵ present in plants. In a taxonomic study of the distribution of these compounds in the genus *Coprosma* (Rubiaceae), it became apparent that such chromatography was inadequate. One-dimensional separations failed to separate all the compounds present and two-dimensional separations were difficult to analyse because of the increased spot sizes and concomitant lack of definition (a difficulty also with paper chromatography).

Since a number of methods have been developed to separate organic mixtures by thin-layer electrophoresis⁶ it was decided to investigate this technique for these phenolic compounds. Its principal advantage over chromatography is the speed of separation of any ionized compounds formed, thereby decreasing zone distortion and increasing definition.

Materials and methods

Extraction. Leaves from both freshly collected and herbarium specimens of

J. Chromatog., 53 (1970) 399-402

Coprosma species and hybrids were analysed. Unhydrolysed glycosidic extracts were prepared by soaking 1 g fresh weight or 0.5 g dry weight of leaves for 24 h in 5 ml of 1% hydrochloric acid in methanol (all solvents were analytical reagent grade, and proportions v/v or v/v/v). The leaf debris was then removed and the extract stored at 4° until required. To prepare samples of hydrolysed aglycones, 1 g fresh weight or 0.2 g dry weight of leaves was immersed in 7 ml of 2 N HCl. This was heated in a boiling water bath for 30 min, cooled, and the debris centrifuged off. To the supernatant was added 0.4 ml of isoamyl alcohol, and this mixture was shaken vigorously for 30 sec. The two layers were then allowed to separate, the alcohol layer pipetted off the top, and stored at 4°.

Chromatography. Shandon equipment was used to prepare the thin-layer plates and for chromatographic separations. For five 20 × 20 cm plates, 15 g of cellulose powder MN300 (Macherey, Nagel & Co) was dispersed in 90 ml distilled water using a Virtis "45" homogeniser, and spread to a wet depth of 0.25 mm. The layer was dried at 60° overnight. Using Microcap pipettes (Drummond Scientific Co.), 5–10 µl quantities of the extracts were applied 3 cm from the edge of the plate (and for two-dimensional separations, 5 cm from the cathodic end). After drying, 1 µl of catechol (50 mg/10 ml ethanol) was added as a reference compound.

A number of solvents were tested for their ability to separate the compounds in the leaf extracts. They were: acetic acid–hydrochloric acid–water (30:3:10), formic acid–hydrochloric acid–water (10:1:3), amyl alcohol–acetic acid–water (AAW, 2:1:1), AAW (10:6:5), *n*-butanol–acetic acid–water (BAW, 4:1:5, top phase), BAW (6:1:2), BAW (8:1:2), isopropanol–ethyl acetate–water (7:1:2), 40% aq. acetic acid, and 6% aq. acetic acid. Only 6% aq. acetic acid gave an even distribution of both glycosides and aglycones over the length of the solvent run.

After the chromatogram had been thoroughly dried by a hot-air fan and left to stand overnight, new margins were scribed through the layer, 1.5 cm under the origin and 1 cm below the solvent front. These were made to reduce electrophoretic distortions near the original edges.

Electrophoresis. Thin-layer electrophoresis was carried out using the equipment and techniques described by BIELESKI⁷. The buffers tested were (1) pH 5: 675 ml of 95% ethanol, 206 ml of water, 32 g of boric acid, 16 g of sodium acetate, adjusted to pH 5 with glacial acetic acid; (2) pH 5.3: 25 ml of pyridine, 8 ml of acetic acid, made up to 2.5 l with distilled water; (3) pH 8.04: phosphate buffer; (4) pH 10: 6 g of boric acid, 3 g of sodium hydroxide, made up to 2 l with distilled water; (5) pH 9.2: 38.1 g of borax (disodium tetraborate) dissolved in 2.5 l of distilled water.

The buffer was sprayed evenly onto the thin layer taking care not to spray directly the origin or the line of chromatographically separated compounds. The surface was then blotted with clean filter paper so that it appeared matte under reflected light, thus giving an even depth of buffer over the layer. To prevent evaporation, the plate was then immediately immersed in the coolant of the electrophoresis tank with the origin at the cathode. Wicks of Miracloth (Calbiochem) covered with dialysis tubing were placed so that one end dipped into the buffer, the other being laid carefully upon the layer with a 1-cm overlap. Glass rods held these in position. A potential difference of 1000 V was then applied to the system for 20 min. After electrophoresis, the plate was carefully removed from the coolant and dried with a hot-air fan.

Detection. Both glycosides and aglycones were visualised with short-wave UV light followed by a spray of diazotised benzidine⁸. The distance moved by each compound in both dimensions was calculated with respect to catechol, *i.e.*

$$R_{\text{cat}} = \frac{\text{distance moved by spot}}{\text{distance moved by catechol}} \times 100$$

Results and discussion

Movement in buffer 1 was very slow and extensive heating occurred as the resistance of the system increased. Some of the compounds appeared to be insoluble in buffers 2 and 3 as indicated by their diffusion from the origin with no electrophoretic movement, and buffer 4 was unstable, bubbles of gas arising from the layer during the course of the run. The heat produced by these four buffers at this potential also tended to dry the layer so that the wick-layer contact dried out and electrical arcing carbonised the layer, destroying the contact. By contrast, the borax buffer (5) maintained a relatively steady current with therefore negligible coolant heating, and gave excellent separations. These are achieved after 17–20 min at 1000 V and 20° (*i.e.* approximately 55 V cm⁻¹ length, 1.1 mA cm⁻¹ width, 0.06 W cm⁻² or 4.8 cal sec⁻¹). Furthermore, if buffer polarity is reversed after each run, at least 25 separations can be made without

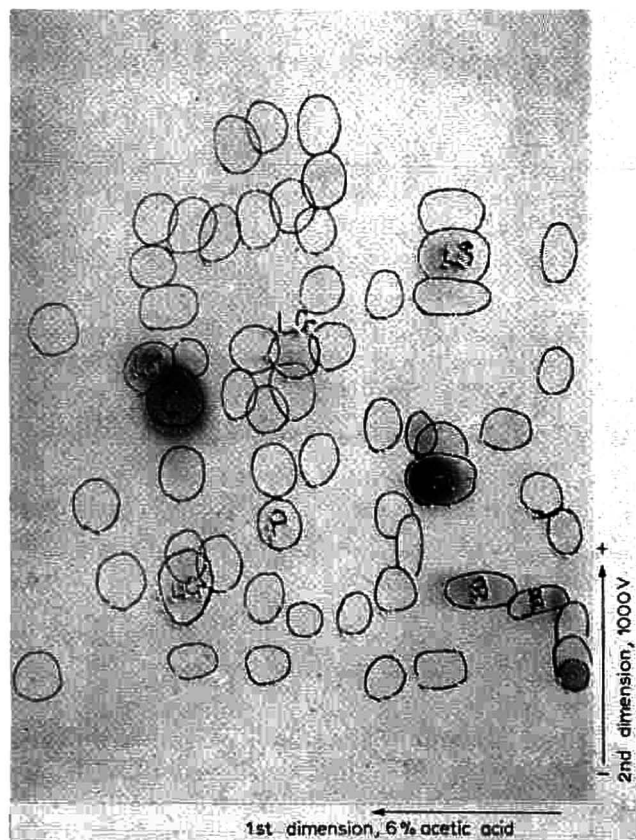


Fig. 1. A two-dimensional separation of the aglycones present in the leaves of a specimen of *Coprosma spathulata* (after UV inspection and spraying with diazotised benzidine). C = catechol.

having to renew the buffer. Residual borax cannot be removed from the thin layer so the chromatographic separation must be performed first. The majority of glycosides and aglycones act as anions under these conditions. A typical separation is shown in Fig. 1.

The aglycones were found to be more amenable to chemotaxonomic analysis than the glycosides. Leaves gathered in different seasons, of different ages, from differing light intensities, and—as most species of the genus *Coprosma* are dioecious—from different sexes, showed much less variation of the aglycone components than of the glycosides. The latter proved to be especially variable quantitatively. Also, under UV light, yellow glycosides at high concentration effectively quenched those compounds with similar R_{cat} values which were less fluorescent. Thus some glycosides were very difficult to detect.

In the final analysis of 115 *Coprosma* specimens representing some 45 species, a total of 192 aglycones were recognised from the two-dimensional patterns of these individuals. It was apparent that specimens collected in the 1880's were relatively no different from later acquisitions of the same species (as has been noted previously for the genera *Lotus*² and *Artemisia*⁹, and the family Rosaceae¹⁰). However, the final numerotaxonomic analysis utilised all an individual's spots or attributes, whether present in all or only one of the specimens of a species. This study is in the process of preparation for press.

Botany Department, University of Auckland,
Auckland 1 (New Zealand)

CEDRIC E. MAY*
J. M. A. BROWN

- 1 S. BOSE AND S. FROST, *Hereditas*, 58 (1967) 145.
- 2 W. F. GRANT AND J. M. WHETTER, *J. Chromatog.*, 21 (1966) 247.
- 3 S. B. GUPTA, *J. Chromatog.*, 36 (1968) 258.
- 4 H. JAWORSKA AND N. NYBOM, *Hereditas*, 57 (1967) 159.
- 5 K. BRUNSBURG, *Botan. Notiser*, 118 (1965) 377.
- 6 V. STEFANOVICH, *J. Chromatog.*, 31 (1967) 466.
- 7 R. L. BIELESKI, *Anal. Biochem.*, 12 (1965) 230.
- 8 D. E. HATHWAY, in I. SMITH (Editor), *Chromatographic and Electrophoretic Techniques*, Vol. 1, Heinemann, London, 1960, p. 324.
- 9 H. R. HOLBO AND H. N. MAZINGO, *Am. J. Botany*, 52 (1965) 970.
- 10 E. C. BATE-SMITH, *Phytochemistry*, 4 (1965) 535.

Received July 24th, 1970

* Present address: Botany School, University of New South Wales, Sydney 2033, Australia.

CHROM. 5002

A thin-layer chromatographic limit test for the detection of anhydrotetracycline and 4-*epi*-anhydrotetracycline in tetracycline

Following the publication of reports¹⁻⁵ in the literature of the Fanconi-type syndrome associated with the ingestion of degraded tetracycline, which principally implicated the degradation products anhydrotetracycline and 4-*epi*-anhydrotetracycline, a large number of chromatographic procedures concerned with the separation and identification of tetracyclines has appeared. Recently the *British Pharmacopoeia*⁶ published a thin-layer chromatographic (TLC) limit test for the detection of anhydrotetracycline, 4-*epi*-anhydrotetracycline and 4-*epi*-tetracycline in tetracycline which appears to be based principally on the procedure reported by ASCIONE *et al.*⁷ Such a system is particularly useful both for quality control of raw material and for the stability evaluation of aged tetracycline proprietary products. In our hands, however, the B.P. procedure proved tedious, the results variable and, in particular, the limits of detection appeared to be optimistic.

SIMMONS *et al.*⁸ described a quantitative method involving TLC separation, elution and spectrophotometric assay of the separated tetracycline compounds. Using the TLC separation procedure described by these workers as a basis, we have been able to develop a simple and reproducible limit test for the detection of anhydrotetracycline and 4-*epi*-anhydrotetracycline in tetracycline hydrochloride raw materials and in proprietary products containing tetracycline hydrochloride.

Experimental

Preparation of plates. Rapidly mix 30 g of microgranular cellulose (Whatman)* with 75 ml distilled water in a pestle and mortar. Apply a 0.5-mm layer of homogenous slurry to five clean glass plates (20 × 20 cm) using a suitable TLC spreader. Air-dry the plates at room temperature for 10 min and then heat in an oven at 90° for 30 min.

Preparation of standard solutions. Weigh accurately 15.0 mg of anhydrotetracycline hydrochloride A.S.** and 15.0 mg of 4-*epi*-anhydrotetracycline hydrochloride A.S.** into a 25-ml volumetric flask, dissolve in and dilute to volume with a solvent mixture consisting of absolute methanol (analytical grade)–1.0 *N* hydrochloric acid (analytical grade) (95:5).

Into each of five labelled 10-ml volumetric flasks weigh accurately 100 mg of tetracycline hydrochloride U.S.P. reference standard, into these flasks pipette aliquots of the anhydrotetracycline hydrochloride–4-*epi*-anhydrotetracycline hydrochloride solution as indicated in Table I. Then dissolve in and dilute to volume with methanol–1.0 *N* hydrochloric acid (95:5) solvent mixture.

Preparation of test solutions. 100 mg of the sample of tetracycline hydrochloride to be tested is accurately weighed into a 10-ml volumetric flask and dissolved in and diluted to volume with the methanol–1.0 *N* hydrochloric acid (95:5) solvent mixture.

Application of solution aliquots to the chromatoplate. Manually apply 20- μ l aliquots of test solution and standard solutions to the chromatoplate as indicated in Table II.

* W. & R. Balston Ltd., Great Britain.

** Authentic specimens available from the British Pharmacopoeia Commission, 8 Bulstrode Street, London, W.1, Great Britain.

TABLE I

VOLUMES OF ANHYDROTETRACYCLINE HYDROCHLORIDE-4-*epi*-ANHYDROTETRACYCLINE HYDROCHLORIDE SOLUTION REQUIRED IN THE PREPARATION OF THE STANDARD SOLUTION

Flask No.	Mixture (ml)
1	0.25
2	0.50
3	1.00
4	2.00
5	4.00

Chromatography. Spray the plate uniformly with 10 ml of buffer solution (0.1 *M* disodium EDTA-0.1% ammonium chloride). Immediately develop the chromatoplate in a chromatographic chamber containing 100 ml of buffer-saturated chloroform (analytical grade). After development for a distance of 16 cm (*ca.* 45-min duration), the chromatoplate is removed and air-dried in a stream of cool air. The chromatoplate is then exposed for 2 min in a second chamber to an atmosphere saturated with ammonia.

The chromatoplate is then examined under an enclosed short-wave UV lamp. The intensities of the zones of anhydrotetracycline hydrochloride and 4-*epi*-anhydrotetracycline hydrochloride separated in the sample being tested are then visually compared with the intensities of the zones of the standards and the anhydrotetracycline

TABLE II

SEQUENCE OF APPLICATION OF STANDARD AND SAMPLE SOLUTIONS TO THE CHROMATOPLATE

Solution	Equivalent % contents of anhydrotetracycline hydrochloride and of 4- <i>epi</i> -anhydrotetracycline hydrochloride in the tetracycline hydrochloride sample being tested
Standard solution 1	0.15
Standard solution 2	0.30
Sample solution	—
Standard solution 3	0.6
Sample solution	—
Standard solution 4	1.2
Standard solution 5	2.4

hydrochloride and 4-*epi*-anhydrotetracycline hydrochloride contents of the sample thus deduced.

R_F values. The *R_F* ranges of the three compounds are as follows: tetracycline hydrochloride (band), 0 to 0.25; anhydrotetracycline hydrochloride, 0.93; 4-*epi*-anhydrotetracycline hydrochloride, 0.48.

Results

Using the procedure described, recent and 18-month-aged samples of tetra-

TABLE III

ANHYDROTETRACYCLINE HYDROCHLORIDE CONTENT OF SAMPLES OF PROPRIETARY TETRACYCLINE HYDROCHLORIDE PRODUCTS EXAMINED

Product	Age (months)	% AT content in sample
A	48	0.5
A	26	0.5
A	23	0.5
A	13	0.5
A	3	0.25
B	13	3.0
B	12	2.0
C	12	0.25-0.50
D	12	0.25-0.50
E	—	0.25
F	12	0.25

cycline hydrochloride were examined; 4-*epi*-anhydrotetracycline hydrochloride (4-EAT) could not be detected in any of the samples, 0.25% of anhydrotetracycline hydrochloride (AT) was detected in the 18-month samples.

The procedure was also applied to samples of proprietary tetracycline hydrochloride products. No 4-EAT could be detected. The AT content is given in Table III.

*Armour Pharmaceutical Company Ltd.,
Hampden Park, Eastbourne (Great Britain)*

P. B. LLOYD
CAROL C. CORNFORD

- 1 J. M. GROSS, *Ann. Intern. Med.*, 58 (1963) 523.
- 2 L. I. EHRLICH AND H. S. STEIN, *Pediatrics*, 31 (1963) 339.
- 3 A. T. MENNIE, *Lancet*, II (1963) 840.
- 4 G. W. FRIMPTER, *J. Am. Med. Assoc.*, 184 (1963) 111.
- 5 S. R. SULKOWSKI AND J. R. HASERICK, *J. Am. Med. Assoc.*, 189 (1964) 152.
- 6 *British Pharmacopoeia* 1968, 1969 Addendum, p. 77.
- 7 P. P. ASCIONE, J. B. ZAGAR AND G. P. CHREKIAN, *J. Pharm. Sci.*, 56 (1967) 1393.
- 8 D. L. SIMMONS, R. J. RANZ, H. S. L. WOO AND P. PICOTTE, *J. Chromatog.*, 43 (1969) 141.

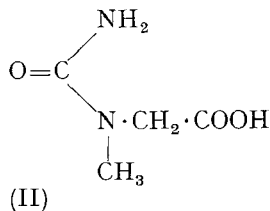
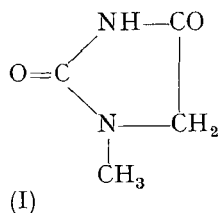
Received August 6th, 1970

J. Chromatog., 53 (1970) 403-405

CHROM. 5001

Paper chromatography of 3-methylhydantoic acid and 1-methylhydantoin, possible intermediates of microbial degradation of creatine and creatinine

As is generally known, creatine and creatinine are normal constituents of meat. 1-Methylhydantoin (I) is a product of the bacterial desimination^{1,2} of creatinine. The formation of this substance in whale meat, which was caused by the deterioration of freshness of the meat, has been reported in the previous paper³. 3-Methylhydantoic acid (II) is a possible intermediate of creatine decomposition, but its microbial formation has not been reported so far.



To further study the freshness of meat³, either a paper chromatographic (PC) or a thin-layer chromatographic (TLC) technique, which permits the complete separation of the above four compounds and causes a specific color formation, is needed. The present paper describes a PC technique which is applicable.

Materials

3-Methylhydantoic acid was synthesized by the method of GAEBLER⁴ (Found: C, 36.16; H, 6.22; N, 21.41. Calculated for $\text{C}_4\text{H}_8\text{O}_3\text{N}_2$: C, 36.36; H, 6.10; N, 21.20). It melted at 142.5° with decomposition. The 1-methylhydantoin which had been isolated from deteriorated whale meat and identified in the previous work³ was used as a material for the present experiments. Creatine and creatinine were purchased from commercial sources. These materials were paper chromatographically pure. Appropriate quantities of these materials were dissolved in water and chromatographed by the procedure described below. All solvents used were of JIS special grade.

Procedure

PC was carried out by the one-dimensional ascending technique, using Toyo-Roshi No. 51 paper which is similar to Whatman No. 1 and one of the following three solvent systems: (a) *n*-butanol-pyridine-water (20:30:15); (b) *n*-butanol-pyridine-water (20:30:20); and (c) isopropanol-pyridine-water (20:30:15). After the solvent front had travelled 12–23 cm from the starting line, the sheet was thoroughly air-dried at room temperature and then heated for 1 h in an oven at 110° . The sheet was then sprayed with Jaffé's reagent which was prepared by mixing a 1.3% ethanolic solution of picric acid with 1/5 volume of 10% NaOH (refs. 5 and 6).

Results and discussion

Of a wide variety of solvent systems tested, the three systems mentioned above gave the most satisfactory results (Fig. 1).

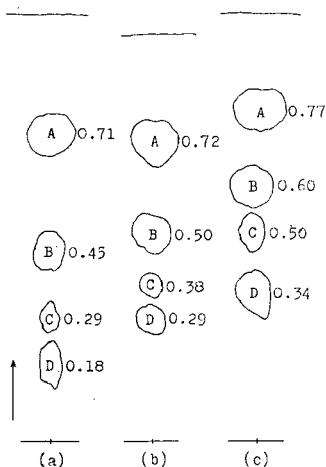


Fig. 1. Resolution patterns obtained with solvent systems a, b and c. A = 1-methylhydantoin; B = creatinine; C = 3-methylhydantoic acid; D = creatine. The numeral close to each spot shows the R_F value of the spot.

Creatinine and 1-methylhydantoin⁴ give positive reactions with Jaffé's reagent, but creatine and 3-methylhydantoic acid do not. It is possible, however, to convert creatine to creatinine on paper chromatograms by heating the chromatograms at 110° before spraying^{5,6}. A preliminary experiment showed that 3-methylhydantoic acid, similarly as creatine, could be converted to 1-methylhydantoin by heating the chromatograms for 1 h at 110°. The above four substances which had been heated on chromatograms at 110°, therefore, all reacted with the reagent and appeared as orange spots against a yellow background. Creatine and creatinine appeared immediately after spraying, but methylhydantoic acid and methylhydantoin appeared very slowly, often 10–20 min later. Such behavior of the last two is significant for their identification. The color intensities of the spots of the last two reached their maxima usually after the sprayed sheets had been kept in the dark overnight.

In water solution, methylhydantoic acid changed to methylhydantoin spontaneously. The change was already appreciable 2 days after solution and almost complete after about a month, as ascertained by PC. Sample solutions containing methylhydantoic acid, therefore, should be prepared just before spotting.

Acetoacetic and pyruvic acids, which may occur in meat, also give weakly positive Jaffé reactions. Acetoacetic acid, however, is readily destroyed by heating the chromatograms at 110° and does not interfere with the detection of the four substances. Pyruvic acid, as described in the previous paper³, was not found in extracts from whale meat of different degrees of freshness when the extracts were examined by silica gel TLC with Jaffé's reagent. It seems likely, therefore, that when meat extracts are examined for the above four substances by the present technique, it is practically unnecessary to take account of the presence of the two acids.

Methylhydantoin can also be detected by the chlorine–starch method⁷ and by the ferricyanide–nitroprusside method¹. These methods, however, are not suitable for the present purpose because they also reveal many other substances interfering with the detection of the four substances.

Creatine was added to an aqueous extract solution prepared from whale meat and its aerobic and anaerobic decompositions were surveyed by using the present technique. The formation of 1-methylhydantoin from creatine was observed in an anaerobic experiment, but that of 3-methylhydantoic acid has not been ascertained yet. A detailed report on this subject will be published elsewhere.

*Faculty of Pharmaceutical Sciences,
Science University of Tokyo,
Ichigayafunagawara-machi, Shinjuku-ku, Tokyo (Japan)*

TADASHI NAKAI
SHIZUO UCHIJIMA
MIDORI KOYAMA

- 1 J. SZULMAJSTER, *J. Bacteriol.*, **75** (1958) 633.
- 2 J. SZULMAJSTER, *Biochim. Biophys. Acta*, **30** (1958) 154.
- 3 T. NAKAI, S. SATO AND N. TSUJIGADO, *J. Food Hyg. Soc. Japan*, **10** (1969) 82 (in Japanese).
- 4 O. H. GAEBLER, *J. Biol. Chem.*, **69** (1926) 613.
- 5 R. J. WILLIAMS, *Texas Univ. Publ.*, **4**, No. 5109 (1951) 205.
- 6 R. J. BLOCK, E. L. DURRUM AND G. ZWEIG, *A Manual of Paper Chromatography and Paper Electrophoresis*, 2nd Ed., Academic Press, New York, 1958, p. 349.
- 7 Y. KOAZE, *Bull. Agr. Chem. Soc. Japan*, **22** (1958) 238.

Received July 28th, 1970

J. Chromatog., **53** (1970) 406-408

CHROM. 5016

A rapid chromatographic procedure for the detection of some diuretics in pharmaceuticals and biological fluids

Although a few procedures for the determination of non-mercurial diuretic drugs have been developed by either paper chromatography, UV or visible spectroscopy, most methods lack rapidity, sensitivity and specificity¹⁻⁵.

PILSBURY AND JACKSON² described a procedure for the extraction and the identification of some thiadiazines in tablets and biological fluids by paper chromatography and UV spectroscopy. They used 1,2-naphthoquinone-4-sulphonate as detecting agent, while NEIDLEIN *et al.*⁶ coloured several diuretics with sodium pentacyanoaminoferrate. By using thin-layer chromatography (TLC), DUCHÊNE AND LAPIÈRE⁷ identified some diuretics by UV (254 nm).

In order to evaluate a rapid method for the screening of some of these drugs in pharmaceuticals and in urine from patients under medication, we developed a new TLC technique and a new extraction method.

Experimental

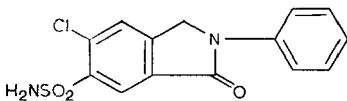
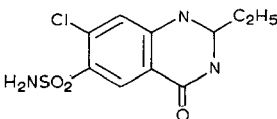
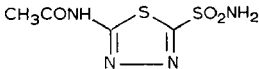
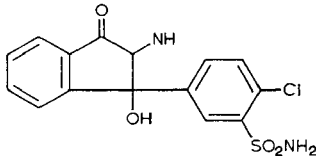
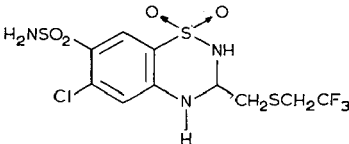
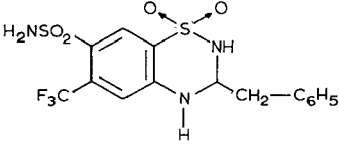
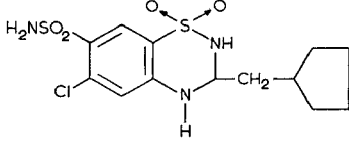
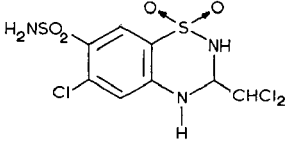
Apparatus and reagents. The following material was used.

- (1) Desaga TLC set and chromatoplates.
- (2) Precoated plates: Merck Alufolien Silica Gel F₂₅₄, 20 × 20 cm, layer thickness 0.25 mm; Macherey, Nagel & Co. MN-Polyamide TLC 6 UV₂₅₄, 20 × 20 cm; Macherey Nagel & Co. MN-Polyamide TLC 11 UV₂₅₄, 20 × 20 cm.

J. Chromatog., **53** (1970) 408-412

TABLE I

STRUCTURES AND CHEMICAL NAMES OF DIURETICS

No.	Name	Chemical name	Formula
1	Clorexolone	6-chloro-2-cyclohexyl-3-oxo-5-isindoline-sulphonamide	
2	Quinethazone	7-chloro-2-ethyl-1,2,3,4-tetrahydro-4-oxo-6-quinazoline-sulphonamide	
3	Acetazolamide	5-acetamido-1,3,4-thiadiazole-2-sulphonamide	
4	Chlorthalidone	2-chloro-5-(1-hydroxy-3-oxo-1-isindolinyl)-benzenesulphonamide	
5	Epithiazide	6-chloro-3,4-dihydro-3-[(2,2,2-trifluoroethyl)thio]-methyl}-2H-1,2,4-benzothiadiazine-7-sulphonamide-1,1-dioxide	
6	Bendroflumethiazide	3-benzyl-3,4-dihydro-6-(trifluoromethyl)-2H-1,2,4-benzothiadiazine-7-sulphonamide-1,1-dioxide	
7	Cyclopenthiazide	6-chloro-3-(cyclopentylmethyl)-3,4-dihydro-2H-1,2,4-benzothiadiazine-7-sulphonamide-1,1-dioxide	
8	Trichlormethiazide	6-chloro-3-(dichloromethyl)-3,4-dihydro-2H-1,2,4-benzothiadiazine-7-sulphonamide-1,1-dioxide	

(3) Aluminium Oxide GF₂₅₄ Merck for TLC.

(4) Stock solutions of 1 mg per ml in acetone were made of each studied diuretic (Table I).

(5) NQS reagent²: (a) 1 N sodium hydroxide; (b) A saturated solution of sodium 1,2-naphthoquinone-4-sulphonate in ethanol-water (1:1). By use, spray (a) followed by (b).

(6) Diazotisation and coupling reagent: After diazotisation in nitrous oxide vapours (obtained by reaction of copper curlings in nitric acid) coupling with 0.5% α -naphthylethylenediamine hydrochloride in ethanol.

(7) Fearons' reagent⁶: (A) 1% of sodium pentacyanoferrate in water; (B) 20% of sodium hydroxide in water. Before use mix 15 ml of (A), 5 ml of (B) and 1 drop of 30% hydrogen peroxide.

Thin-layer chromatography. From each compound we spotted 10 μ g on a thin-layer plate. We eluted in saturated chromatotanks at room temperature to give a solvent front rise of 15 cm. As elution mixture, we tried different solvent systems of changing polarity (Table II).

Two-dimensional TLC with a mixture of *n*-hexane-acetone-diethylamine (4:4:2) as first solvent and a less polar solution of chloroform-methanol and diethylamine as second solvent (Table II, F and G of Fig. 1) was most successful. We also tried Aluminium Oxide GF₂₅₄ and polyamide as adsorbents for the thin-layer chromatographic separation of the studied diuretics, but unsuccessfully. After the plates were eluted and dried at 100°, the drugs could be located by UV-light (254 nm) without prior treatment; a detection limit of 2–5 μ g was obtained.

TABLE II

R_F VALUES ($\times 100$) OF THE STUDIED DIURETICS ON SILICA GEL PLATES WITH DIFFERENT SOLVENTS
Solvent systems: (A) ethyl acetate-benzene (8:2) (ref. 1); (B) ethyl acetate-benzene-ammonia, 25%-methanol (80:20:1:10); (C) ethyl acetate-benzene-ammonia, 25%-methanol (60:40:2:8); (D) ethyl acetate-benzene-ammonia, 25%-methanol (50:40:2:10); (E) *n*-hexane-acetone-diethylamine (60:30:10); (F) *n*-hexane-acetone-diethylamine (40:40:20); (G) chloroform-methanol-diethylamine (80:15:5).

Diuretic No.	Solvent systems						
	A	B	C	D	E	F	G
1				70	21	61	91
2				27	6.5	32	49
3				3	0	2	22
4				30	12	55	58
5	67	70	30	41	5	24	46
6	70	75	40	68	10	46	75
7	78	82	43	62	18	70	76
8	69	43	5	17	1	7	40

As spray reagents three chemicals were tested: sodium 1,2-naphthoquinone-4-sulphonate, α -naphthylethylenediamine and sodium pentacyanoaminoferrate. From our experiments we concluded sodium 1,2-naphthoquinone-4-sulphonate to be the most satisfactory. Stable weak orange spots appear within 15 min and became more

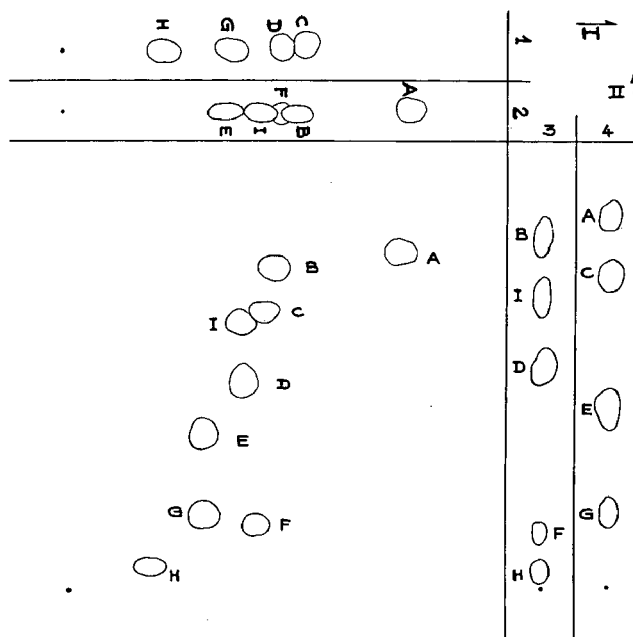


Fig. 1. Two-dimensional chromatography of the studied diuretics. Solvent systems: (I) chloroform-methanol-diethylamine (80:15:5); (II) *n*-hexane-acetone-Diethylamine (40:40:20). A = Clorexolone, B = Cyclopenthiazide, C = Bendroflumethiazide, D = Quinethazone, E = Epithiazide, F = Impurity spot from quinethazone, G = Trichlormethiazide, H = Acetazolamide, I = Chlorthalidone.

pronounced after storing in the dark for one or two days. The sensitivity limit was 5 μ g for each drug.

Extraction of the diuretics from tablets or from urine. 30 ml of urine were deproteinised with 5 ml of 10% of lead acetate and acidified with diluted hydrochloric acid (pH 2-3) after which the mixture was filtered through glass-wool.

The tablet was ground in a mortar with 20 ml of distilled water, acidified with diluted hydrochloric acid (pH 2-3) and the mixture was filtered through glass-wool.

The filtrate was extracted with 60 ml of ethyl acetate by shaking in a separatory funnel for 5 min. The aqueous layer was discarded while the ethyl acetate extract was washed twice with 25 ml of a freshly prepared saturated sodium bicarbonate solution. After separation, the ethyl acetate phase was washed twice with 10 ml of sodium hydroxide 0.25 *N*. Separately, the bicarbonate as well as the sodium hydroxide washings were reacidified with concentrated hydrochloric acid and both were extracted again with 30 ml of ethyl acetate. The separated ethyl acetate extracts were dried over anhydrous sodium sulphate and evaporated in a rotavapor at 20°.

The two residues were dissolved in 0.2 ml of acetone and separately spotted on a thin-layer chromatographic Silica Gel GF₂₅₄ plate for identification (Table III).

Conclusions

From the results of the Tables II and III, the TLC determination of the studied diuretics is best performed on Silica Gel GF₂₅₄ plates by two-dimensional chromato-

TABLE III

RESULTS OF THE URINE EXTRACTS AFTER INGESTION AND PASSAGE THROUGH THE BODY OF SOME THIADIAZINES

Diuretic No.	Oral dose (mg)	Time (h) after intake		
		1	2	3
5	4	+	+	++
6	3	+	+	++
7	0.5	—	—	+
8	4	+	++	+++

graphy by combination of systems F and G. For general use, the NQS spray reagent is preferred.

Because the extraction procedure of PILSBURY AND JACKSON² is rather time consuming, we tried to develop a shorter method. This method provided a good qualitative and semi-quantitative analysis as well as a rapid and sufficient clean-up of urine samples.

This screening may be important to the clinical and toxicological chemist, since some diuretics are frequently used in the treatment of barbiturate poisoning in order to increase their excretion, so they may interfere in the determination of barbiturates and salicylates.

Two different ethyl acetate extracts are observed due to the different acidity of the studied compounds. Therefore, the thiazides were preferentially extracted at higher pH than the sulphonamide derivatives.

*Department of Analytical Chemistry and Bromatology,
University of Leuven (Belgium)*

R. MAES
M. GIJBELS
L. LARUELLE

1 E. ADAM AND C. L. LAPIÈRE, *J. Pharm. Belg.*, 19 (1964) 79.

2 V. B. PILSBURY AND J. V. JACKSON, *J. Pharm. Pharmacol.*, 18 (1966) 713.

3 E. F. SALIM, A. HAUSSELER AND J. B. VAUGHAN, *J. Pharm. Sci.*, 57 (1968) 640.

4 H. SHEPPARD, T. F. MOWLES AND A. J. PLUMMER, *J. Am. Pharm. Assoc. Sci. Ed.*, 49 (1960) 722.

5 J. BERNEJO, *Galencia Acta (Madrid)*, 14 (1961) 255.

6 R. NEIDLEIN, H. KRÜLL AND M. MEYL, *Deut. Apotheke-Ztg.*, 105 (1965) 481.

7 M. DUCHÊNE AND C. L. LAPIÈRE, *J. Pharm. Belg.*, 20 (1965) 275.

First received June 9th, 1970, revised manuscript received August 31st, 1970

J. Chromatog., 53 (1970) 408-412

CHROM. 5007

Differentiation of phenothiazine derivatives by locating agent on thin-layer chromatographic plates*

There are many different phenothiazine-type drugs which may be encountered in toxicological analyses. Although a number of comprehensive articles dealing with the paper or thin-layer chromatographic behavior of phenothiazines have appeared in the literature¹⁻³, the authors felt a need for a fast and simple screening technique which would give the analytical toxicologist some clues as to which particular phenothiazine drug may be involved, so that its identity could be confirmed by additional specific tests. The following presentation describes an attempt to develop a single chromatographic system (one developing solvent and one locating agent) which could be routinely used for this purpose.

Experimental

The plates (20 × 20 cm or microscope slides) were prepared in the usual manner using Silica Gel GF as the adsorbent. The reference phenothiazines were spotted as alcoholic solutions of their salts. Development was carried out at room temperature, and a 15 cm running distance was used with the 20 × 20 cm plates. Following the development, the dried plates (or slides) were sprayed with a locating agent, and after drying at room temperature the identification of the phenothiazines was based on the different colours developed as well as on the relative R_F values. The compositions of the developing solvent and of the spray reagent are given as follows:

Developing solvent: ethyl acetate, 90 ml; acetone, 45 ml; ammonium hydroxide in ethanol (1:1), 4 ml.

Spray reagent: 10% phosphomolybdic acid (aqueous solution), 40 ml; 2.5% ferric chloride in ethanol, 10 ml; 6 *N* hydrochloric acid, 20 ml; distilled water, 20 ml.

The chromatographic behaviour of the 19 phenothiazine derivatives studied is summarised in Table I.

Discussion

The sensitivity of this technique was found to range between 5 and 10 µg for the compounds studied. Spotting of lesser amounts, in some cases, produced colours which were too weak to differentiate. The developed colours were found to be stable for several days.

If the presence of phenothiazine sulphoxides is anticipated, spraying the developed chromatogram with sulphuric acid will demonstrate their presence, and may give additional analytical information to enable the differentiation. A spray reagent consisting of concentrated sulphuric acid (125 ml), ethanol (50 ml) and distilled water (75 ml), works quite well. Following this treatment, it is necessary to wait for at least 10 min before examining the chromatogram. The R_F values of the sulphoxides are lower than those of the corresponding parent compounds.

The technique has been successfully applied in toxicological analyses for phenothiazines. Following a positive general test for the presence of a phenothiazine,

* Presented at the Fifth International Meeting of Forensic Sciences, June 5-11th, 1969, Toronto, Canada.

TABLE I

CHROMATOGRAPHIC DATA OF 19 PHENOTHIAZINE DERIVATIVES

No.	Compound	R_F value	Colour developed
1	Ethopropazine (Parsitan)	0.90	Greenish-brown
2	Levomepromazine (Nozinan)	0.87	Blue (intense)
3	Trimeprazine (Temaril)	0.85	Red
4	Triflupromazine (Vesprin)	0.79	Yellowish-brown
5	Thiopropazate (Dartal)	0.78	Reddish-violet
6	Chlorpromazine (Largactil)	0.72	Reddish-violet (plum)
7	Mepazine (Pacatal)	0.66	Reddish-brown
8	Promethazine (Phenergan)	0.65	Reddish-brown (light)
9	Thioridazine (Mellaril)	0.64	Turquoise
10	Aminopromazine (Lispamol)	0.60	Beige
11	Promazine (Sparine)	0.55	Reddish-brown (deep)
12	Acetylpromazine (Plegicil)	0.49	Orange-red
13	Trifluoperazine (Stelazine)	0.44	Yellowish-brown (tan)
14	Methdilazine (Tacaryl)	0.38	Reddish-brown
15	Thiethylperazine (Torecan)	0.38	Turquoise
16	Prochlorperazine (Compazine)	0.37	Reddish-violet
17	Fluphenazine (Prolixan)	0.35	Yellowish-brown
18	Perphenazine (Trilafon)	0.30	Reddish-violet
19	Thiopropazine (Majeptil)	0.23	Pink

such as a UV absorption curve, or the bromination-acidulation reaction⁴, extracts of suitable biological materials, prepared according to the method of CURRY⁵, were dissolved in as little ethanol as possible, and spotted with a mixture of phenothiazine drugs as the reference. Microplates were found very useful for screening, since the development takes only about 10 min. However, best separation of the different phenothiazines was accomplished on the 20 × 20 cm plates. In fatal cases, the drugs were detected in stomach contents, liver tissue and blood. In a case involving a patient receiving therapeutic doses of chlorpromazine, the chromatographic pattern of the urine extract gave a clear indication of the parent compound as well as its metabolites.

The technique makes it possible to achieve an adequate measure of differentiation between most of the commonly encountered phenothiazine derivatives, and has been found useful as a screening procedure in routine toxicological analyses.

*The Centre of Forensic Sciences,
Department of Justice,
8 Jarvis Street, Toronto, Ontario, Canada*

C. KORCZAK-FABIERKIEWICZ
G. CIMBURA*

1 I. ZINGALES, *J. Chromatog.*, 31 (1967) 405.

2 J. VEČERKOVÁ, M. SULCOVÁ AND K. KÁČL, *J. Chromatog.*, 7 (1962) 527.

3 H. VON EBERHARDT, *Arzneimittel-Forsch.*, 13 (1963) 804.

4 G. H. W. LUCAS AND C. FABIERKIEWICZ, *J. Forensic Sci.*, 8, No. 3 (1963) 462.

5 A. S. CURRY, *Poison Detection in Human Organs*, 2nd Ed., Charles C. Thomas, Springfield, 1969.

First received July 15th, 1970; revised manuscript received August 24th, 1970

* Head, Toxicology Section, The Centre of Forensic Sciences, Toronto, Canada.

CHROM. 5014

Some pH control problems in gradient elution ion-exchange chromatography*

Buffered eluent solutions are often used in ion-exchange chromatography to minimize pH instabilities and to avoid adverse effects on the liquid-resin equilibria or on the chemical forms of the species being separated. However, in gradient elution chromatography, where the eluent changes from a dilute buffer solution to a highly concentrated buffer as the run progresses, the initial buffering capacity may be insufficient to maintain the system pH within desired limits. As a result, the column and eluate pH may vary with time although the eluent pH is constant.

This problem of pH control during the early stages of gradient elution chromatography has been examined on a high-pressure anion-exchange chromatograph developed at the Oak Ridge National Laboratory for the determination of ultraviolet (UV)-absorbing constituent of body fluids¹⁻³.

This report describes the results of tests designed to define the mechanisms relating operating parameters to eluate pH and discusses methods for minimizing the adverse effects of insufficient pH buffering.

Experimental

A Mark II model of the UV-analyzer previously described³ was adapted with a 0.5 cc flow cell for continuous monitoring of the eluate pH. With that analyzer the sample is introduced into a flowing stream of 0.015 *N* acetate buffer (ammonium acetate-acetic acid) at pH 4.4 and pumped at 100–200 atmospheres pressure through a 150 cm × 0.62 cm anion-exchange column. During the course of elution the concentration of acetate buffer is gradually increased from 0.015 *N* to 6.0 *N*, with no change in pH. The eluate pH was recorded from normal runs with and without a urine sample and also with different operating conditions to demonstrate the effects of sample constituents and abrupt buffer concentration changes.

Normal analytical runs. During the course of normal analyses the buffer concentration in the liquid phase entering the column is changed from 0.015 *N* to 6.0 *N* as shown in Fig. 1. Over 100 chromatographic peaks are produced from a urine sample. During such an analysis the eluate pH has significant variations as shown in Fig. 2. A comparison of pH and chromatographic recordings from this and repeated analyses shows that two undesirable features of the chromatograms were found to coincide with pH excursions. The first undesirable chromatographic feature was the variability in size and position of peaks, including that for creatinine, which elute in the first hour (Fig. 1). The second was the variability in position and relative broadness of as many as 15 peaks, including hypoxanthine, xanthine, and tryptophan peaks, eluting in the 3 to 11 h region.

Run without sample. In the absence of a sample, the eluate pH (Fig. 2) shows only two major pH excursions. The first excursion is a broad rise beginning at 2 h where the eluent buffer concentration is about 0.3 *N*; it reaches a maximum at about 11 h where the buffer concentration is about 1.0 *N*; and it ends near 22 h with the

* Research sponsored by the National Institute of General Medical Sciences.

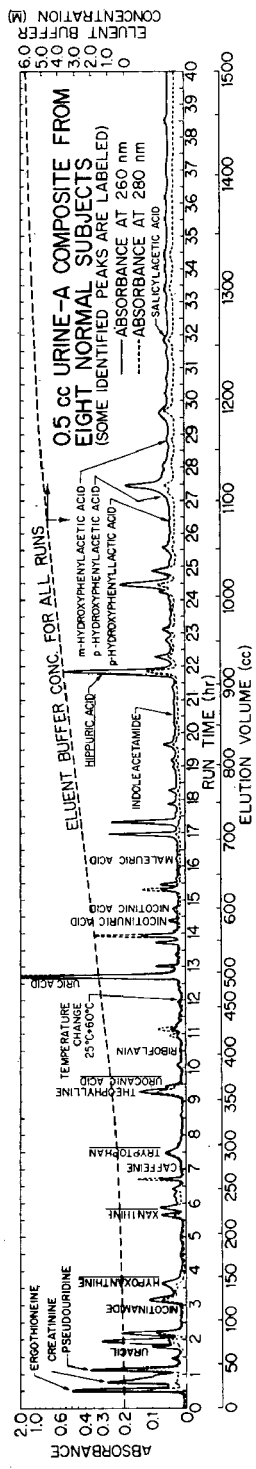
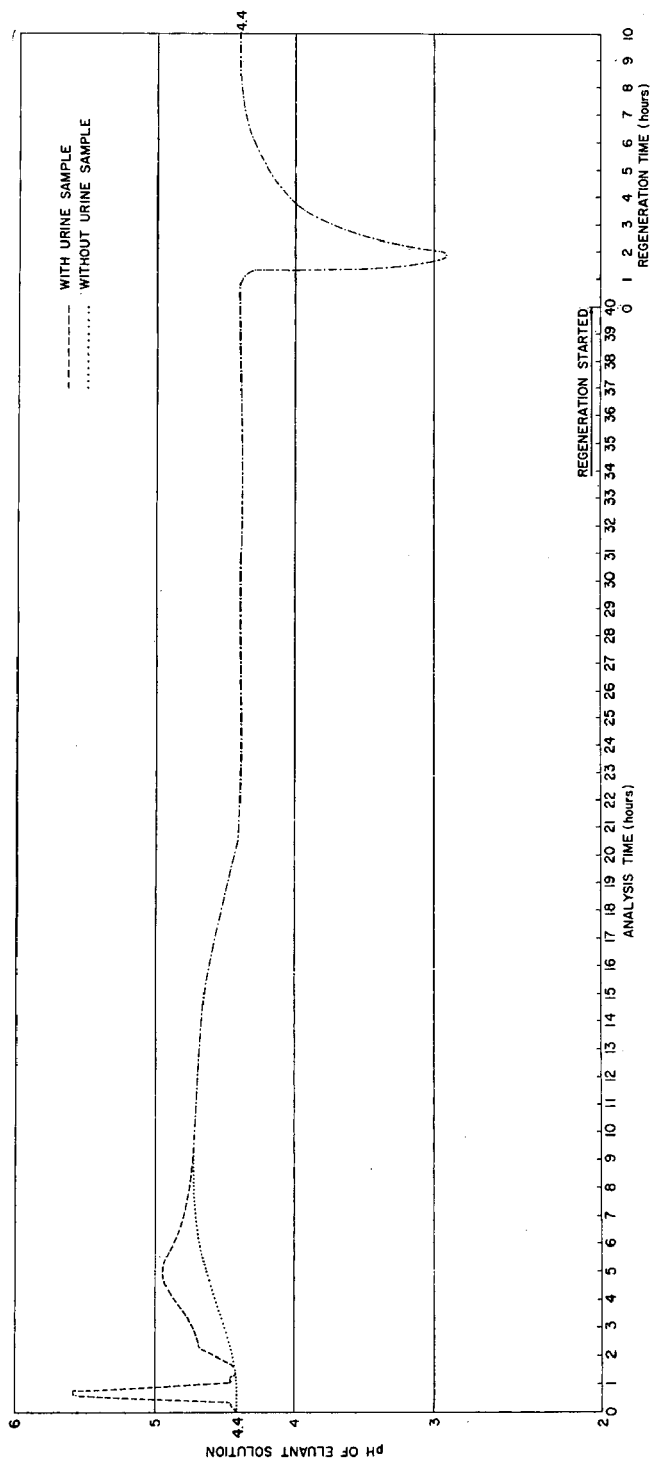


Fig. 1. The eluent buffer gradient and a representative chromatogram.



TYPICAL pH RECORDINGS

Fig. 2. A comparison of the eluate pH recordings with and without a sample.

buffer concentration about 2.5 *N*. The second pH excursion is the large dip immediately following the change from a feed concentration of 6.0 *N* to 0.015 *N* at the end of the run where regeneration is begun.

An abrupt increase in buffer concentration. Operating the system with step changes in eluent buffer concentration shows that eluate pH excursions occur after such changes. For example, after an abrupt change in eluent buffer concentration from 0.015 *N* to 6.0 *N* a rapid increase in eluate pH from 4.40 to 5.65 occurs.

Discussion

Buffer concentration changes. The experimental eluate pH excursions associated with changes in eluent buffer concentration appear to be a sharp decrease following an abrupt drop in buffer concentration, a sharp rise following an abrupt increase in buffer concentration, and a broad peak following an initial gradual increase in concentration (Fig. 2). The direction of these changes are consistent with current ideas of the nature of the chemical equilibria^{4,5}. That is, at each point along the anion-exchange column an equilibrium exists between the acetate and hydroxyl ions in the liquid and at the active sites of the resin. To satisfy the anion-exchange resin equilibrium with the acetate ion, a net transfer of acetate ion from the liquid to resin phase occurs with a corresponding transfer of hydroxyl ion to the liquid phase when the concentration of buffer is increased in the liquid phase. This results in the acid present in the buffer being neutralized. Conversely the opposite exchange occurs when the buffer concentration is decreased. Thus, in this anion-exchange system it is to be expected that an increase in eluent buffer concentration will cause a temporary increase in eluate pH and a decrease in eluent buffer concentration will cause a temporary decrease in eluate pH.

The broad pH peak starting at 2 h in a normal analysis is therefore most important since it is caused by an increase in buffer concentration from about 0.3 to 1.0 *N* and is associated with erratic chromatographic peak positions and broadening of peaks. While this pH variation could be reduced in magnitude by starting the elution at a higher buffer concentration, such a change would be counterproductive because of undesirable crowding of peaks from basic and neutral compounds which elute early. Another possible solution would be to impose a declining pH gradient upon the increasing concentration gradient; this, however, greatly alters the order of peak elution and appears to cause broadening of peaks in the latter half of the chromatogram. Some improvement appears possible through reducing the slope of the concentration gradient.

Sample constituents. The eluate pH peaks that occurred with the urine sample but were absent in the run without sample (Fig. 2) appear related to eluted sample constituents. Where the acetate concentration of the sample differs from the 0.015 *N* buffer the effect will be as discussed above. In the area of the chromatogram where the dilute 0.015 *N* buffer was used, ions more strongly retained by the resin, like chloride ions, will displace the acetate ion and thereby affect the liquid-resin equilibria. Other constituents of body fluid samples are pH buffers and affect the pH of the eluate as they elute. The first large pH peak in the runs with a urine sample, rising from pH 4.4 to 5.9, appears due to the additive effect of each of these mechanisms. The smaller pH peaks which follow are associated with the arrival in the eluate of buffering compounds such as urea and amino acids.

The best way to reduce the magnitude of the pH excursions due to sample constituents is by using smaller samples. That may be possible with the development of more sensitive photometric systems.

Conclusions

The excursions in pH caused by concentration gradient elution of a buffer and by eluted sample constituents have been demonstrated for anion-exchange chromatography and have been shown to be predictable in direction. Consideration of the mechanisms affecting the eluate pH are helpful in making system and operational changes designed to mitigate the adverse effects of pH excursions.

Oak Ridge National Laboratory,
Oak Ridge, Tenn. 37830 (U.S.A.)*

SIDNEY KATZ

- 1 C. D. SCOTT, J. E. ATTRILL AND N. G. ANDERSON, *Proc. Soc. Exptl. Biol. Med.*, 125 (1967) 181.
- 2 C. D. SCOTT, *Clin. Chem.*, 14 (1968) 521.
- 3 C. D. SCOTT, R. L. JOLLEY AND W. F. JOHNSON, *Am. J. Clin. Pathol.*, 53 (1970) 701.
- 4 M. HONDA, *J. Am. Chem. Soc.*, (1951) 2943.
- 5 F. HELFFERICH, *Ion Exchange*, McGraw-Hill, New York, N.Y., 1962, pp. 79-90.

Received September 1st, 1970

* Operated for the U.S. Atomic Energy Commission by the Union Carbide Corporation.

Book Reviews

CHROM. 4975

An Introduction to Ion Exchange, by R. PATTERSON, Heyden, London, 1970, 105 pp., price 50 sh., \$6.00

This introductory paper back volume embraces a vast topic in seven chapters and one thermodynamic appendix. Each chapter, except the first, carries some journal or book reference support. For a 1970 production item, very few of these references are as recent as might be expected.

The introductory chapter summarises some of the basic terminology of ion exchange. The next chapter gives a good account of the various types of orthodox ion-exchanger materials. However, the macroreticular ion exchangers are not mentioned. Chapter three deals with the Donnan membrane potential, selectivity and distribution coefficients, and the importance of resin swelling, while the kinetic aspects of ion exchange follow in chapter four. The fifth chapter largely features the electrical properties of ion-exchanger membranes. Column techniques and the "new" inorganic ion exchangers are outlined in the final two chapters.

This well produced book offers a substantial introduction to ion exchange and can be thoroughly recommended, but the price for a short paper back is too high.

G. J. MOODY

*University of Wales, Institute of Science
and Technology, Cardiff (Great Britain)*

Column Chromatography, edited by E. KOVÁTS, Sauerländer AG, Aarau, 1970, 285 pp., price Sw. Fr. 56.00.

This supplement to *Chimia (Aarau)* contains all the papers presented at a symposium held in Lausanne in 1969 under the auspices of GAMS, together with the subsequent discussions.

Teoria y Practica de la Chromatografia en Fase Gaseosa, by L. GASCO, Ediciones J.E.N., Madrid, 1970, 549 pp., price 715 pesetas.

This comprehensive text on gas chromatography is perhaps the first to be published in Spanish. It appears to give adequate coverage of all significant aspects of the technique and is up to date.

J. Chromatog., 53 (1970) 420

CHROM. 5019

PRESSURE DEPENDENCE OF THE COEFFICIENTS OF MASS-TRANSFER RESISTANCE IN GAS CHROMATOGRAPHY

J. NOVÁK, S. WIČAR AND P. BOČEK

Institute of Instrumental Analytical Chemistry, Czechoslovak Academy of Science, Brno (Czechoslovakia)

(Received August 31st, 1970)

SUMMARY

The liquid and gas-phase mass-transfer resistance coefficients have been evaluated from HETP *versus* carrier gas flow velocity (\bar{u}) measurements carried out at different absolute column pressure (\bar{P}) levels. The C_s coefficients in the liquid-phase mass-transfer term ($C_s\bar{u}$), as obtained by measuring the HETP increments of a constant $\bar{P}\bar{u}$, were increasing upon raising the pressure level, while the respective C_m coefficients in the gas-phase mass-transfer term ($C_m\bar{P}\bar{u}$) displayed a decrease. Both C_s and C_m coefficients decreased with increasing carrier gas flow velocity. The above situation indicates that the liquid and gas-phase mass-transfer terms are dependent on each other.

INTRODUCTION

The rate theory expressed by either $\bar{H} = A + B/\bar{P}\bar{u} + C_m\bar{P}\bar{u} + C_s\bar{u}$ or by $\bar{H} = [1/(1/A + 1/C_m\bar{P}\bar{u}) + B/\bar{P}\bar{u} + C_s\bar{u}]$ (where the symbols have the usual meaning), predicts that the coefficients of mass-transfer resistance, C_m and C_s , are independent both of each other and of \bar{P} and \bar{u} . However, PERRETT AND PURNELL¹ found the C_m term to be generally dependent on the inhomogeneity of the liquid phase film. On the other hand, SAHA AND GIDDINGS² found a dependence between the C_s coefficient and the diameter of the support particle. Thus, the mobile-phase mass-transfer resistance coefficient seems to be a function of a parameter typical for the liquid-phase mass-transfer resistance coefficient, the latter being, in turn, dependent on a parameter controlling the mass transfer in the mobile phase.

This indicates that there is some kind of interdependence between the coefficients C_m and C_s ; a theoretical substantiation of this concept has been presented in another paper³. The present paper is to demonstrate a phenomenon that appears to be associated with the above situation — a dependence of the coefficients C_s and C_m on the absolute column pressure and on the mobile phase flow velocity. This phenomenon was disclosed by virtue of obtaining systematically inconsistent results in the isolation of the C_s and C_m coefficients from HETP *versus* carrier gas flow velocity measurements carried out at various levels of the mean absolute column pressure on packed columns⁴.

CALCULATION OF THE C_s AND C_m COEFFICIENTS

A computer program for the least square fitting of the equation $\bar{H} = A + B/\bar{P}\bar{u} + C_m\bar{P}\bar{u} + C_s\bar{u}$ to the experimental data obtained at different column pressures failed; frequently negative values were obtained for the C_m coefficients, though a large number of precisely measured data had been processed. Therefore, we employed the graphical method of GIDDINGS AND SCHETTLER⁵ of measuring the \bar{H}/f_1 increments of a constant X .

This method was originally proposed for processing HETP *versus* column outlet flow velocity data obtained either with various kinds of carrier gas or at different levels of the column outlet pressure, with a given carrier gas. As we disposed of a lot of HETP *versus* average flow velocity data obtained on columns of different lengths at various levels of either constant column outlet pressure or constant column inlet pressure and related to the mean column pressure, we have modified the original formulation of the method to make it suitable for readily processing the above kind of data.

The original version⁵ has been based on the relation

$$\frac{\bar{H}}{f_1}(X) = \bar{H}_m(X) + C_s X D_m' f_2 / P_o f_1 \quad (1)$$

where \bar{H} is the apparent plate height, \bar{H}_m is the sum of the mobile phase terms, X stands for $u_o P_o / D_m'$ where u_o is the carrier gas velocity at the column outlet, P_o and D_m' are the column outlet pressure and the solute diffusion coefficient in the gas phase at a unit pressure, respectively. f_1 is the decompression factor given by $f_1 = (9/8)(P^4 - 1)(P^2 - 1)/(P^3 - 1)^2$ where P is the column inlet-to-outlet pressure ratio, and f_2 is the well-known James-Martin factor.

Since $P_o u_o = \bar{P}\bar{u}$, $\bar{D}_m \bar{P} = D_m' P'$, and $u_o = \bar{u}/f_2$, where \bar{P} and P' are the mean column pressure and a unit pressure, respectively, and \bar{D}_m is the solute diffusion coefficient in the mobile phase at the mean column pressure, one can write with reference to the fundamental GIDDINGS' papers⁶

$$\bar{H} = \left(A + \frac{2\gamma D_m' P'}{\bar{P}\bar{u}} + \frac{\omega d_p^2}{D_m' P'} \bar{P}\bar{u} \right) f_1 + C_s \bar{u} \quad (2)$$

Hence, eqn. 1 may be rearranged to read

$$\frac{\bar{H}}{f_1}(X) = \bar{H}_m(X) + C_s X D_m' / \bar{P} f_1 \quad (3)$$

where X is given by $\bar{P}\bar{u}/D_m'$, which is obviously equivalent to the above $P_o u_o / D_m'$. The product $\bar{P} f_1$ may be expressed with the aid of STERNBERG AND POULSON'S⁷ form of f_1 , $(P_i^2 + P_o^2)/2(\bar{P})^2$, where P_i is the column inlet pressure.

Following the originally proposed procedure, C_s may be expressed by

$$C_s = A \left[\frac{\bar{H}}{f_1}(X) \right] / X A (D_m' / \bar{P} f_1) \quad (4)$$

where the Δ 's designate the differences between the respective items, obtained by measurement for a given X at two different values of \bar{P} or D_m' . In our case, the kind of carrier gas (H_2) remained unchanged and the mean column pressure was varied by changing parametrically either the outlet or the inlet column pressure, or, in one case, by changing the column length. Therefore, we chose $X = \bar{P}\bar{u}$, which renders

$$\frac{\bar{H}}{f_1}(X) = \bar{H}_m(X) + C_s X / \bar{P}f_1$$

and

$$C_s = \Delta \left[\frac{\bar{H}}{f_1}(X) \right] / X \Delta(1/\bar{P}f_1) \quad (5)$$

The C_m coefficient ($\omega d_p^2 / D_m' P'$) was calculated from

$$C_m = \left[\frac{\bar{H}}{f_1}(X) - (C_s X / \bar{P}f_1) \right] / X \quad (6)$$

provided the respective experimental data have been obtained in a flow region dominated by the mass-transfer terms.

EXPERIMENTAL

The measurements were carried out on 3- and 0.75-m-long columns of 3 mm I.D., made of stainless-steel and packed with two sorts of packing — 25 and 3 wt. % of dinonyl phthalate on Chromosorb P 60/80 mesh. A Becker Multigraph 409 (Becker, Delft, The Netherlands) was employed in its version with thermal conductivity detection, adapted for work under controlled column outlet pressure. Hydrogen was used as the carrier gas.

With the high and the low liquid load packing, pentane and hexane were used as the solutes, respectively, the samples being introduced in the form of about 40 μ l of the solute vapors diluted in hydrogen containing traces of air. A Zimmermann syringe was employed (Zimmermann, G. D. R.). In all cases the column as well as the injection port and the detector were kept at 40°. The chromatograms were recorded by a Servogor RE 512 recorder (Goerz Electro G.m.b.H., Austria). A more detailed description of the experimental conditions has been given in a previous paper⁴.

RESULTS AND DISCUSSION

The results of the measurements were processed by plotting against the flow velocity the C_s and C_m values obtained for different levels of the mean column pressure. The above plots were complemented by the corresponding \bar{P} versus flow velocity data.

The C_s and C_m versus \bar{u} curves in Fig. 1 were obtained from the \bar{H}/f_1 versus $\bar{P}\bar{u}$ data measured with the 25% liquid load packing on the 0.75-m column operated at constant outlet pressures of 1 and 3 atm (columns a and c, respectively) and on the 3-m column operated at an outlet pressure of 1 atm (column b). As for the mean

column pressure levels, the longer column (b) was chosen as a reference one (cf. the \bar{P} versus \bar{u} curves in Fig. 1), i.e., the data for the $C_s(a,b)$ and $C_m(a,b)$ curves were obtained from the \bar{H}/f_1 and $1/\bar{P}f_1$ versus $\bar{P}\bar{u}$ measurements carried out on columns a and b, while the $C_s(b,c)$ and $C_m(b,c)$ correspond, analogously, to the measurements on columns b and c. The individual \bar{H}/f_1 and $1/\bar{P}f_1$ increments were read out in steps given by the experimental points on the \bar{H}/f_1 and $1/\bar{P}f_1$ versus $\bar{P}\bar{u}$ curves for the reference column; the flow velocities incidental to the individual C coefficients were determined from the respective $\bar{P}\bar{u}$ and \bar{P} data.

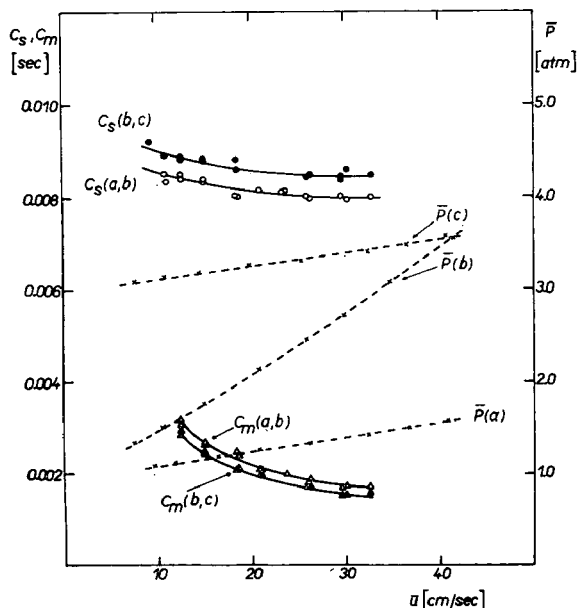


Fig. 1. Flow velocity dependence of the coefficients C_s and C_m at two different absolute column pressure (\bar{P}) levels (constant column outlet pressure operation). a and c, 0.75-m-long column operated at 1 and 3 atm outlet pressure, respectively. b, 3-m-long column operated at 1 atm outlet pressure; column packing, 25 wt.% dinonyl phthalate on Chromosorb P 60/80 mesh at 40°; solute, pentane.

When accepting the arithmetic means of the absolute pressures in columns a and b and in columns b and c as approximate levels incidental to the corresponding C coefficients, one may infer from Fig. 1 that an increase in the absolute column pressure by about 1 atm leads to an increase in the C_s coefficient by about 0.0004 sec, while the C_m coefficient decreases by about 0.0002 sec under the same circumstances. Both the C_s and C_m coefficients show a pronounced decrease upon rising the flow velocity. As an increase in the flow velocity has associated with it an increase of the mean column pressure in this mode of column operation, the above situation indicates that the C_s coefficient decreases with increasing flow velocity.

The fall-off of the decrease of the C_s coefficients with increasing flow velocity may be explained by the counteracting effect of increasing column pressure; this account is supported by the results obtained on columns operated at constant inlet pressures and variable outlet pressure (cf. Fig. 2) where the increasing flow velocity leads to a fall of the column pressure.

Fig. 2 represents the results obtained with the same packing as mentioned in the previous case, but only with the 0.75-m-long column operated at three different inlet pressures, namely, 3.0, 3.6, and 5.5 atm (columns d, e, and f, respectively). The results were processed in the same way as described with Fig. 1; the reference results were those obtained on the column operated at 3.6 atm inlet pressure.

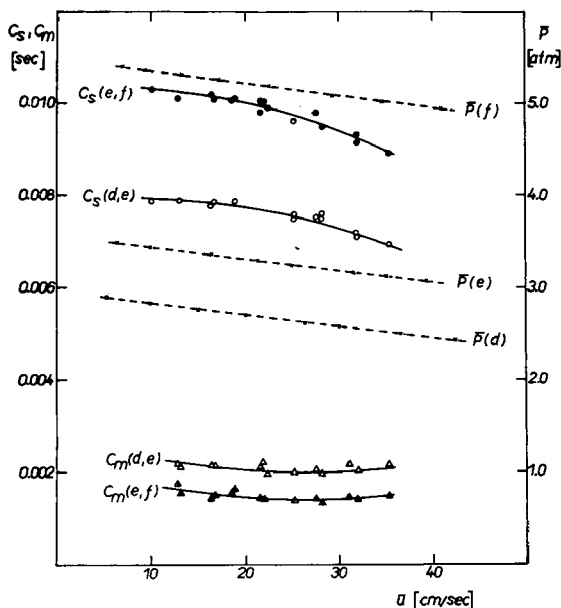


Fig. 2. Flow velocity dependence of the coefficients C_s and C_m at two different absolute column pressure (\bar{P}) levels (constant column inlet pressure operation). d, e and f, 0.75-m-long column operated at 3.0, 3.6, and 5.5 atm inlet pressure, respectively; column packing, 25 wt.% dinonyl phthalate on Chromosorb P 60/80 mesh at 40°; solute, pentane.

In this case, the pressure effects on both the C_s and C_m coefficients are higher than in the preceding case. Using again the above concept on the column pressure levels, a pressure increase by about 1.25 atm results in an increase of the C_s coefficients by about 0.002 sec and in a decrease of the C_m coefficients by about 0.0006 sec. The higher effect of the column pressure in this case may be due to the fact that all the measurements at the constant column inlet pressures have been carried out in a region of appreciably higher pressures (2.5–5.5 atm) as compared with those obtained at the constant outlet pressures (1–3.5 atm).

Contrary to the case with the constant column outlet pressures, the decrease of the C_s coefficients grows steeper upon raising flow velocity.

The relationship between the courses of the C_m curves obtained from the measurements under the constant outlet and the constant inlet pressures indicate that also the C_m coefficients show a decrease with increasing flow velocity. However, the present results are not apt for isolating the net flow-velocity contribution to the change of the C_s and C_m coefficients.

Fig. 3 shows the C_s and C_m versus \bar{u} curves obtained from the data measured with the low liquid load packing on the 0.75-m-long column operated at constant

column outlet pressures of 1 and 3 atm (column g and h, respectively). These results are supplemented by the results obtained with the same column and within approximately the same column pressure region, but with the high liquid load packing (Fig. 4). Apart from the obvious difference between the respective C_s coefficients, the comparison of the C_m curves in Figs. 3 and 4 shows an increase of the C_m coefficients upon the increase in the stationary liquid loading as described earlier by others¹, despite having injected pentane in this case.

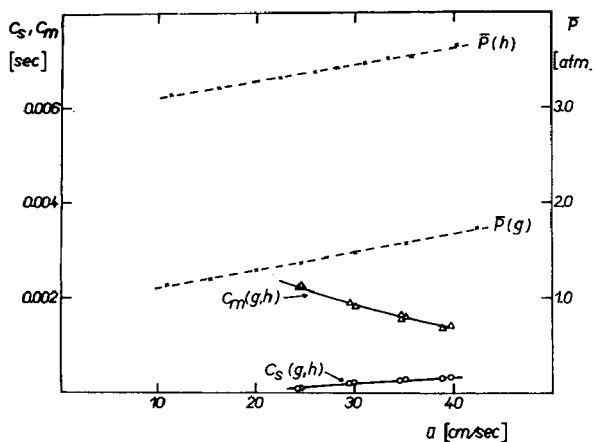


Fig. 3. Flow velocity dependence of the coefficients C_s and C_m (constant column outlet pressure operation). g and h, 0.75-m-long column operated at 1 and 3 atm outlet pressure, respectively; column packing, 3 wt.% dinonyl phthalate on Chromosorb P 60/80 mesh at 40°; solute, hexane.

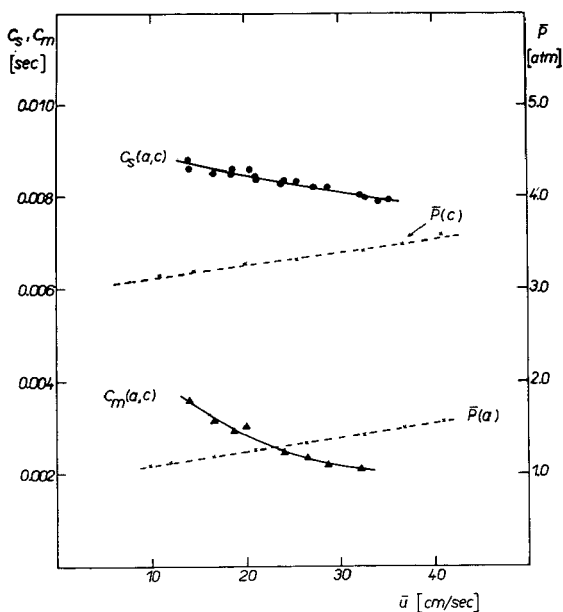


Fig. 4. Flow velocity dependence of the coefficients C_s and C_m (constant column outlet pressure operation). a and c, 0.75-m-long column operated at 1 and 3 atm outlet pressure, respectively; column packing, 25 wt.% dinonyl phthalate on Chromosorb P 60/80 mesh at 40°; solute, pentane.

CONCLUSIONS

The coefficients of the resistance to mass transfer in the liquid and in the gaseous phase appear to be functions of the column pressure and the mobile phase flow velocity. The liquid-phase mass-transfer resistance coefficient, as determined from the HETP, \bar{P} , \bar{u} measurements by conventional methods, increases with increasing mean column pressure, while the gas-phase mass-transfer coefficient (defined by $C_m = \omega d_p^2 / D_m' P'$, ref. 6), determined from the same measurements, decreases with increasing column pressure. Both the C_s and C_m coefficients decrease with increasing carrier gas flow velocity.

It follows from the pressure and flow velocity dependences of the coefficients C_s and C_m that the sum of the gas phase contributions to the HETP is not invariable with the position along the column and that the local liquid phase contribution, $C_s u$, rises not as steeply with increasing distance from the column inlet as it would be given by the growth of the flow velocity in a column operated at a constant outlet pressure. This indicates that it is hardly possible to separate accurately the coefficients C_m and C_s by the conventional methods, despite carrying out the corrections for the gas decompression effects^{5,8}.

The pressure dependence of the C_s coefficient may also play some role in the dependence of the HETP on the column length and the column pressure, especially with high liquid load packings. One can expect a less pronounced decrease of the minimum HETP and a more expressive rise of the steepness of the ascending branch of the HETP *versus* \bar{u} curve upon increasing the column length or the column pressure than it would be encountered if the C_s coefficient were a constant independent of pressure, with columns operated at a constant outlet pressure. Nevertheless, it has followed from a previous paper⁴ that these effects are practically insignificant under current conditions.

As it is hardly imaginable that the C_s coefficient might be directly affected by the pressure, it may be assumed that the pressure dependence of the mass transfer in the liquid phase is rooted actually in the pressure dependence of the mass transfer in the gaseous phase, *i.e.*, that the gas and liquid-phase mass-transfer terms are coupled with each other (*cf.* ref.3).

REFERENCES

- 1 R. H. PERRETT AND J. H. PURNELL, *Anal. Chem.*, 35 (1963) 431.
- 2 W. C. SAHA AND J. C. GIDDINGS, *Anal. Chem.*, 37 (1965) 830.
- 3 S. WIČAR AND J. NOVÁK, *J. Chromatog.*, 53 (1970) 429.
- 4 J. NOVÁK AND P. BOČEK, *J. Chromatog.*, 52 (1970) 1.
- 5 J. C. GIDDINGS AND P. D. SCHETTLER, *Anal. Chem.*, 36 (1964) 1483.
- 6 J. C. GIDDINGS, *Anal. Chem.*, 35 (1963) 35.
- 7 J. C. STERNBERG AND R. E. POULSON, *Anal. Chem.*, 36 (1964) 58.
- 8 J. C. GIDDINGS, S. L. SEAGER, L. R. STUCKI AND G. H. STEWART, *Anal. Chem.*, 32 (1960) 867.

J. Chromatog., 53 (1970) 421-427

CHROM. 5020

NONADDITIVITY OF THE GAS AND LIQUID PHASE MASS-TRANSFER RESISTANCES IN GAS CHROMATOGRAPHY

S. WIČAR AND J. NOVÁK

Institute of Instrumental Analytical Chemistry, Czechoslovak Academy of Sciences, Brno (Czechoslovakia)

(Received August 31st, 1970)

SUMMARY

The results of a number of papers dealing with the isolation of the 'C' terms of the VAN DEEMTER equation and with the interpretation of the respective results led, in many cases, to discrepancies that could not be explained satisfactorily in virtue of the classical VAN DEEMTER or GOLAY's equations. Abandoning the principle of the independence of the processes controlling the interphase mass transfer in a chromatographic column led to a modified HETP equation, the qualitative predictions of which are in very good agreement with the experimental results.

INTRODUCTION

The very useful concept of the additivity of the partial resistances to the mass transfer between two phases, representing one of the basic presuppositions in WHITMAN's film theory¹, was applied to gas-liquid chromatography (GLC) as early as in the pioneer papers by LAPIDUS AND AMUNDSON² and by VAN DEEMTER *et al.*^{3,4}. The analytical substantiation of the above concept was later⁵ seen in the results of GOLAY's solution of the equation of the solute mass balance in a capillary column⁶.

From the viewpoint of the stochastic theories on the growth of the variance of the chromatographic zone (*c.f. e.g.* GIDDINGS⁷), the presupposition of the above additivity is equivalent to an assumption on the independence between the processes taking place in the mass transfer within both phases in the chromatographic column.

The existence of a number of papers dealing with the isolation of the 'C' terms in the Van Deemter equation has been a practical consequence of the conviction about the applicability of the above additivity principle. To this effect, changes have been utilized of the HETP brought about by changes in the retentive capacity⁸, by changes in the column length at a constant column inlet or column outlet pressure⁹, by changes of the pressure within the column of a given length, or by varying the kind of carrier gas¹⁰⁻¹⁵. As long as the authors of the individual papers limited themselves to finding such pairs of the C_G and C_L values that complied with the measured HETP and flow velocity values, their efforts were always successful. However, the attempts at a further qualitative or even quantitative interpretation of the values obtained often

led to paradox results. For instance, PERRETT AND PURNELL¹⁶ found a very significant dependence of the gas-phase mass-transfer term (C_G) on the loading of the support by the stationary phase (within a range of 0.5–20 wt. % the value of the C_G term arose about 80 %). Further, in the paper by GIDDINGS *et al.*⁹ devoted, besides other objectives, to the correlation of the data measured on columns of different lengths in terms of the equation $\hat{H} = (B'/P_2 u_2 + C'_G P_2 u_2) f_1 + C_L u_2 f_2$, one can notice a significant decrease of the C_L coefficient with decreasing column length (mean column pressure). Similar difficulties were encountered also by HAZELDEAN AND SCOTT¹⁵ in testing the GOLAY⁶ and KHAN¹⁷ equations by working with nylon capillaries at various absolute pressures. SAHA AND GIDDINGS¹⁸ found a correlation between the diameter of the column packing particles and the C_L coefficient. Finally, NOVÁK *et al.*¹⁹ ascertained an expressive growth of the C_L coefficient upon raising the absolute column pressure, while the C'_G coefficient ($C_G = C'_G P$) was decreasing at the same time.

THEORETICAL

The simplest analytical model for describing the mass transfer between the phases in the chromatographic column is indubitably an idealized capillary column with the walls coated by a homogeneous film of the stationary phase. In such a column, one may define two continuous concentration fields of the solute in both phases. When neglecting the longitudinal diffusion and, further, assuming the axial symmetry of the concentration fields and laminar flow, it is then possible to write for the solute mass balance in the phases

$$\frac{\partial c}{\partial t} = D_G \left(\frac{\partial^2 c}{\partial r^2} + \frac{1}{r} \frac{\partial c}{\partial r} \right) - 2u_0 \left(1 - \frac{r^2}{a^2} \right) \frac{\partial c}{\partial z} \quad (1)$$

and

$$\frac{\partial c'}{\partial t} = D_L \left(\frac{\partial^2 c'}{\partial r^2} + \frac{1}{r} \frac{\partial c'}{\partial r} \right) \quad (2)$$

The initial conditions may be formulated by the equations

$$c(0, r, z) = c'(0, r, z) = 0 \quad (3)$$

The boundary condition determining the concentration signal at the column inlet in a case of elution analysis can be expressed by

$$c(t, r, 0) = c_0 \delta(t) \quad (4)$$

The boundary condition (eqn. 4) has to be further supplemented by four equations, describing the radial concentration distribution at the outlets. One of these equations follows from the above postulated symmetry of the concentration field in the mobile phase,

$$\frac{\partial c}{\partial r}(t, 0, z) = 0 \quad (5)$$

the second one from the impermeability of the capillary wall for the solute

$$\frac{\partial c'}{\partial r}(t, a_1, z) = 0 \quad (6)$$

and the remaining two boundary conditions describe the properties of both concentration fields at the phase interface. Let us suppose instantaneous equilibration at the interface, then

$$c'(t, a, z) = kc(t, a, z) \quad (7)$$

Further, let us suppose that there may occur no solute accumulation at the interface, then

$$\frac{D_G v_L}{D_L v_G} \frac{\partial c}{\partial r}(t, a, z) = \frac{\partial c'}{\partial r}(t, a, z) \quad (8)$$

The radial concentration distribution complying with conditions 5–8 is shown schematically in Fig. 1.

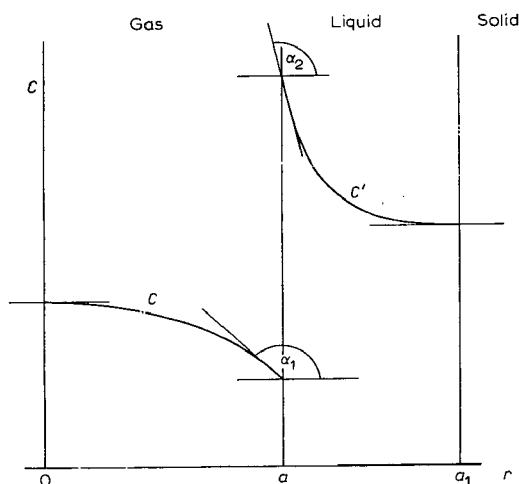


Fig. 1. Scheme of the radial concentration distribution in an idealized capillary column. $\operatorname{tg} \alpha_2 / \operatorname{tg} \alpha_1 = D_G v_L / D_L v_G$.

The system of eqns. 1–8 may be simplified, at least formally, by introducing the following substitutions:

$$C = c/c_0 \quad C' = c'/c_0 \quad (9, 10)$$

$$T = tu_0/l \quad L = z/l \quad R = r/a \quad Q = r/d_f \quad (11-14)$$

$$\beta = D_G l / u_0 a^2 \quad \gamma = D_L l / u_0 d_f^2 \quad \delta = D_G / D_L \quad (15-17)$$

$$\xi = a/d_f \doteq 2v_G/v_L \quad (18)$$

This results in a system of dimensionless equations

$$\frac{\partial C}{\partial T} = \beta \left(\frac{\partial^2 C}{\partial R^2} + \frac{1}{R} \frac{\partial C}{\partial R} \right) - 2(1 - R^2) \frac{\partial C}{\partial L} \quad (1a)$$

$$\frac{\partial C'}{\partial T} = \gamma \left(\frac{\partial^2 C'}{\partial Q^2} + \frac{1}{Q} \frac{\partial C'}{\partial Q} \right) \quad (2a)$$

$$C(0, R, L) = C'(0, Q, L) = 0 \quad (3a)$$

$$C(T, R, 0) = \delta(T) \quad (4a)$$

$$\frac{\partial C}{\partial R}(T, 0, L) = 0 \quad (5a)$$

$$\frac{\partial C'}{\partial Q}(T, \xi + 1, L) = 0 \quad (6a)$$

$$C'(T, \xi, L) = kC(T, 1, L) \quad (7a)$$

$$\frac{\delta \xi}{2} \frac{\partial C}{\partial R}(T, 1, L) = \frac{\partial C'}{\partial Q}(T, \xi, L) \quad (8a)$$

$$T \geq 0, \quad 0 \leq R \leq 1, \quad \xi \leq Q \leq \xi + 1, \quad 0 \leq L \leq 1$$

The analytical solution of the parabolic system 1a–8a has not yet been found. However, it may easily be proved by applying the theory of physical similarity (*cf.* WIČAR²⁰) to the capillary columns obeying the system 1a–8a that the number of the theoretical plates of the idealized capillary column is a function of all the variable parameters occurring in the system 1a–8a except the functions C and C' themselves and the variables T , R , Q , and L . Hence, there holds

$$N = N(\beta, \gamma, \delta, k, \xi) \quad (19)$$

The individual criterions and simplexes occurring in the above symbolic equation have different roles; the values of β and γ characterize the maximum attainable mass-transfer rates, under given conditions, in the individual phases. For the gaseous phase and for the criterion β , the above statement may be documented for instance by the results of TAYLOR²¹ and ARIS²². On the other hand, the quantities δ , k , and ξ , occurring in the boundary conditions, signify obviously certain limitations for the above maximum values.

From this viewpoint, the condition 8a is particularly important; if no solute accumulation is to occur at the phase interface, the rates of the mass fluxes in both phases must be mutually coordinated. Therefore, any limitation in the possibilities of the mass transfer in the stationary phase (a decrease of the γ value caused, for instance, by increasing the d_f) will inevitably also induce a decrease in the mass-transfer rate in the mobile phase, regardless the fact that the β value itself remains unchanged. Similarly, a decrease of the β value brings about a decrease in the mass transfer in the stationary phase with the γ value remaining unchanged.

When introducing the presupposition of quasi-ideality (long-time approximation) of the chromatographic process into our consideration, which presupposition is common in the theory of gas chromatography, one may look for a direct relation between the values of β , γ , and the variance of the concentration band caused by a finite rate of the interphase mass transfer.

The classical GOLAY theory which leads, in its consequences, to the mutual independence of the mass-transfer processes taking place in both phases expresses the final variance by the sum of the partial variances:

$$H = F_1(k)l/\beta + F_2(k)l/\gamma = \sigma_G^2/l + \sigma_L^2/l \quad (20)$$

Hence, one may easily derive for the individual variances:

$$\sigma_G^2 = \frac{F_1(k)a^2l}{D_G} u_0, \quad \sigma_L^2 = \frac{F_2(k)d_f^2l}{D_L} u_0 \quad (21)$$

Now, let us assume, in compliance with eqn. 8a, that the processes effective in the mass transfer in both phases are interdependent; employing the elementary theory of probability, one may easily find a combination law for the resultant variance*:

$$H = \sigma^2/l = \sigma_G^2/l + \sigma_L^2/l + 2\rho_{GL}\sqrt{\sigma_G\sigma_L/l} =$$

$$= F_1(k) \frac{a^2}{D_G} u_0 + F_2(k) \frac{d_f^2}{D_L} u_0 + 2\rho_{GL} u_0 \sqrt{F_1(k)F_2(k)} \frac{a^2 d_f^2}{D_G D_L} \quad (22)$$

In accordance with eqn. 19, the correlation coefficient ρ_{GL} may be regarded as an undefined function of exclusively the quantities k , δ , and ξ , i.e.,

$$\rho_{GL} = \rho_{GL}(k, \delta, \xi) \quad (23)$$

Without the knowledge of the solution of the system of eqns. 1a-8a, the actual shape of the function ρ_{GL} expressed by eqn. 23 may be obtained only experimentally. Eqn. 22 may be written, referring to the conventional formal notation, to read:

$$H = (C_G + C_L + 2\rho_{GL}\sqrt{C_G C_L})u_0 \quad (24)$$

or, after introducing the mean pressure and the mean flow velocity to respect, at least approximately, the mobile phase compressibility,

$$\hat{H} = (C_L + C_G' \bar{P} + 2\rho_{GL}(\bar{P})\sqrt{C_L C_G' \bar{P}})\bar{u} \quad (25)$$

DISCUSSION AND CONCLUSIONS

First, let us go into the two fundamental phenomenological theories of gas-liquid chromatography, VAN DEEMTER's theory and the GOLAY theory of the capillary column, and investigate the effect of that critical step in them which leads to the principle of the additivity of the partial resistances.

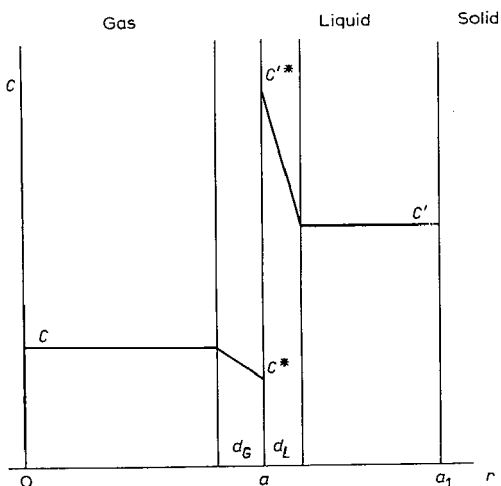


Fig. 2. Radial concentration distribution according to the film theory. d_G, d_L = effective thicknesses of the gas and liquid diffusion films, respectively.

* A similar procedure has been used by JONES²³ for combining the variances produced in the stationary and mobile part of the gaseous phase.

The VAN DEEMTER theory assumes the radial concentration distribution in accordance with the film theory (Fig. 2). The concentrations c^* and c'^* at the phase interface are colligated with each other by the relation $c'^* = kc^*$; there holds for both partial mass-transfer coefficients

$$1/K_{0G} = 1/K_G + 1/kK_L \quad (26)$$

Hence, the presupposition of the additivity of the partial resistances to mass transfer in both phases has been introduced in the very description of the model of the mass transfer at the interface.

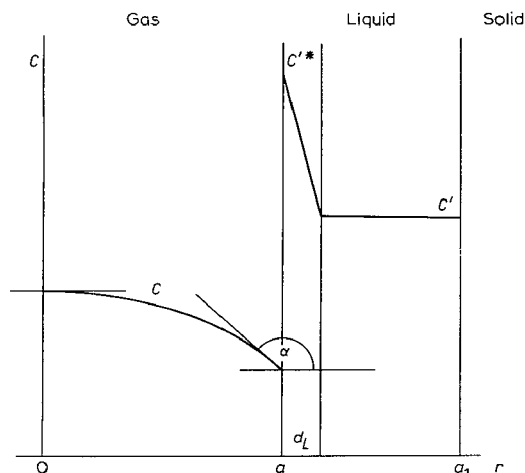


Fig. 3. Radial concentration distribution according to GOLAY's theory. d_L = effective thickness of the liquid diffusion film, $\tan \alpha = (K_L a / 2 D_G) (c' - c'^*)$.

The GOLAY model is substantially more involved; the radial concentration distribution presupposed in this model is shown schematically in Fig. 3. A hybrid model is apparently at stake here — the rate of the mass transfer in the mobile phase obeys the equation of diffusion while the rate of the mass transfer in the liquid phase is described, similarly as in VAN DEEMTER's model, by means of the partial mass-transfer coefficient K_L . At the phase interface, two boundary conditions apply. One of them colligates the concentrations in the mobile and in the stationary phases at the interface by the relation $c'^* = kc^*$, the other one describes the mass fluxes at the interface by the Fourier relation

$$2 \frac{D_G}{a} \frac{\partial c}{\partial r}(t, a, z) = K_L [c' - kc(t, a, z)] \quad (27)$$

which is analogous to the condition described by eqn. 8. Hence, the exact solution of the GOLAY model would have to lead to an interdependence between both partial processes in the mass transfer. The resultant independence of C_G and C_L is a consequence of the simplification of the model during the solution. The decisive step is undoubtedly the substitution of eqn. 21 into eqn. 17a (in GOLAY's notation) which implies the concentration field in the mobile phase to be independent of the rate of the mass transfer in the stationary phase.

The concept of the mutual dependence of the mass transfer in both phases may easily be applied also to packed columns. Let us turn back to eqn. 22, supplemented now by the terms accounting for the variances due to longitudinal and eddy diffusion,

$$\hat{H} = A + B'/\bar{P}\bar{u} + C_G'\bar{P}\bar{u} + C_L\bar{u} + 2\rho_{GL}(\bar{P})\sqrt{C_L C_G'\bar{P}}\bar{u} \quad (28)$$

and compare it with the classical VAN DEEMTER equation

$$\hat{H} = A + B'/\bar{P}\bar{u} + C_G'\bar{P}\bar{u} + C_L\bar{u} \quad (29)$$

Both equations may be divided by the average velocity of the mobile phase, \bar{u} :

$$\hat{H}/\bar{u} = A/\bar{u} + B'/\bar{P}\bar{u}^2 + C_G'\bar{P} + C_L + 2\rho_{GL}(\bar{P})\sqrt{C_L C_G'\bar{P}} \quad (28a)$$

$$\hat{H}/\bar{u} = A/\bar{u} + B'/\bar{P}\bar{u}^2 + C_G'\bar{P} + C_L \quad (29a)$$

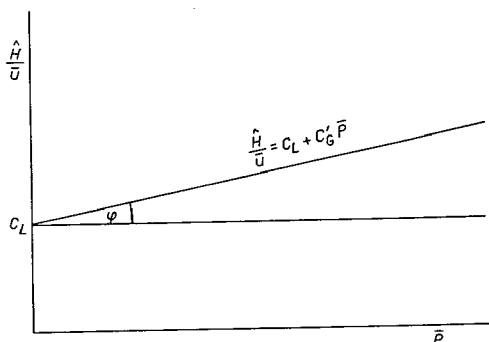


Fig. 4. Scheme of the isolation of the C_L and C_G' coefficients according to the classical concepts (eqn. 29a).

In a region of higher flow velocities of the mobile phase, where the plate height is dominated by the rate of the interphase solute-transfer, the two first members of the right-hand sides in eqns. 28a and 29a may be neglected to a good approximation. In compliance with the classical eqn. 29, one could easily isolate the C_L and C_G' coefficient by plotting the ratio \hat{H}/\bar{u} against the mean column pressure \bar{P} (cf. Fig. 4). On the other hand, eqn. 28a, when neglecting the dependence of ρ_{GL} on \bar{P} (for instance by introducing the mean value, $\overline{\rho_{GL}}$, within the given interval of the mean pressure \bar{P}), renders the curves resulting from the composition of the straight lines $\hat{H}/\bar{u} = C_G'\bar{P} + C_L$ and the parabolas $\hat{H}/\bar{u} = 2\overline{\rho_{GL}}\sqrt{C_L C_G'\bar{P}}$ (Fig. 5).

The endeavour to express the C_G' and C_L values from the measured data by the classical relation 29 is equivalent to the seeking for the tangent or secant to the curves given by eqn. 28a. Therefore, the C_G' and C_L coefficients obtained from HETP *versus* flow velocity data in virtue of the conventional concepts represent some apparent values, $(C_G')_{app}$ and $(C_L)_{app}$. Hence, when calculating with the tangent and neglecting the first two members of the right-hand side of eqn. 28a, one obtains

$$(C_L)_{app} = C_L + \overline{\rho_{GL}}\sqrt{C_L C_G'\bar{P}_0} \quad (30)$$

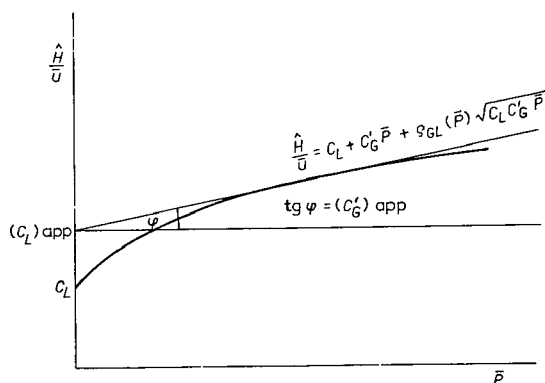


Fig. 5. Scheme of the isolation of the apparent C_L and C_G coefficients according to the concept of the interdependence between the gas and liquid mass-transfer terms.

where \bar{P}_0 stands for the mean pressure determining the position of the tangent on the curve given by eqn. 28a.

Hence, the obtained apparent value of C_L , $(C_L)_{app}$, increases, on a given column, with increasing mean pressure \bar{P}_0 and with increasing C'_G (increasing gas phase diffusion coefficient), which is in conformity with the experimental experience. To illustrate the above account, Fig. 6 shows the plots of \hat{H}/\bar{u} against \bar{P} for octane with hydrogen, nitrogen, and argon as the carrier gases. The column was 190 cm long, packed with 10 wt. % of Apiezon L on Chezasorb (an equivalent of Chromosorb P) of the particle diameter 0.08–0.1 mm and kept at a temperature of 100°.

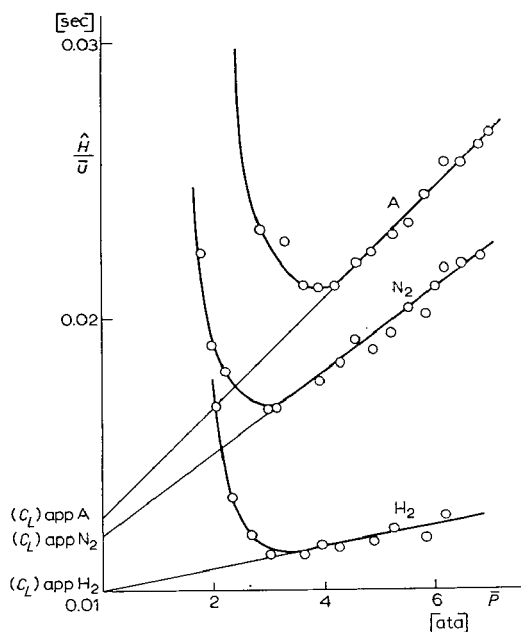


Fig. 6. Plot of \hat{H}/\bar{u} versus \bar{P} for octane chromatographed with A, N₂, and H₂ carrier gases, illustrating the dependence of the apparent C_L on the gas phase diffusion coefficient.

The slopes of the tangents to the curves, rendering the apparent values of C_G' , $(C_G')_{\text{app}}$, are given by the relation

$$(C_G')_{\text{app}} = C_G' + \overline{\rho_{GL}} \sqrt{C_L C_G' / \bar{P}_0} \quad (31)$$

Thus, the measured value of $(C_G')_{\text{app}}$ rises with increasing values of C_L , in compliance with the papers by PURNELL AND PERRETT¹⁶, and decreases with increasing P_0 , as found by NOVÁK *et al.*¹⁹.

LIST OF SYMBOLS

- c = solute concentration in the mobile phase, expressed by the mass of solute in a unit volume of the empty column
- c' = solute concentration in the stationary phase, expressed in the same units as quoted with c
- D_G = diffusion coefficient of the solute in the mobile phase
- D_L = diffusion coefficient of the solute in the stationary phase
- u_0 = mobile phase forward flow velocity averaged over the void cross-sectional area of the column
- $\delta(t)$ = Dirac's delta function
- a = distance of the gas-liquid interface from the capillary axis
- a_1 = internal radius of the capillary tube
- k = partition ratio
- v_G = volume of the gaseous phase per unit volume of the empty column
- v_L = volume of the liquid phase per unit volume of the empty column
- d_f = (effective) thickness of the stationary liquid layer
- $F_1(k) = (1 + 6k + 11k^2)/24(1 + k)^2$
- $F_2(k) = k^3/6(1 + k)^2$
- t, r, z = time, radius, and distance coordinates

REFERENCES

- 1 W. G. WHITMAN, *Chem. Metal. Eng.*, 29 (1923) 147.
- 2 L. LAPIDUS AND N. R. AMUNDSON, *J. Phys. Chem.*, 56 (1952) 984.
- 3 J. J. VAN DEEMTER, F. J. ZUIDERWEG AND A. KLINKENBERG, *Chem. Eng. Sci.*, 5 (1956) 271.
- 4 J. J. VAN DEEMTER, *2nd Informal Symp., GC Disc. Group, Cambridge, Sept. 1957*.
- 5 J. C. GIDDINGS, *Dynamics of Chromatography*, Part. I, M. Dekker, New York, 1965, p. 176.
- 6 M. J. E. GOLAY, in D. H. DESTY (Editor), *Gas Chromatography 1958*, Butterworths, London, 1958, p. 36.
- 7 J. C. GIDDINGS, *J. Chem. Educ.*, 35 (1958) 588.
- 8 S. DAL NOGARE AND J. CHIU, *Anal. Chem.*, 34 (1962) 890.
- 9 J. C. GIDDINGS, S. L. SEAGER, L. R. STUCKI AND G. H. STEWART, *J. Clin. Anal. Chem.*, 32 (1960) 867.
- 10 R. H. PERRETT AND J. H. PURNELL, *Anal. Chem.*, 34 (1962) 1336.
- 11 R. H. PERRETT, *Anal. Chem.*, 37 (1965) 1346.
- 12 D. D. DE FORD, R. J. LOYD AND B. D. AYERS, *Anal. Chem.*, 35 (1963) 426.
- 13 J. C. GIDDINGS AND P. D. SCHETTLE, *Anal. Chem.*, 36 (1964) 1483.
- 14 J. C. STERNBERG AND R. E. POULSON, *Anal. Chem.*, 36 (1964) 58.
- 15 G. S. F. HAZELDEAN AND R. P. W. SCOTT, *J. Inst. Petrol.*, 48 (1962) 380.
- 16 R. H. PERRETT AND J. H. PURNELL, *Anal. Chem.*, 35 (1963) 430.
- 17 M. A. KHAN, in M. VAN SWAAY (Editor), *Gas Chromatography 1962*, Butterworths, London, 1962, p. 3.

- 18 W. C. SAHA AND J. C. GIDDINGS, *Anal. Chem.*, 37 (1965) 830.
- 19 J. NOVÁK, S. WIČAR AND P. BOČEK, *J. Chromatog.*, 53 (1970) 421.
- 20 S. WIČAR, in E. KOVATS (Editor), *5th Intern. Symp. on Separation Methods, Column Chromatography, Lausanne, 1969*.
- 21 G. TAYLOR, *Proc. Roy. Soc. (London)*, A 219 (1953) 186.
- 22 A. ARIS, *Proc. Roy. Soc. (London)*, Z 235 (1956) 67.
- 23 W. JONES, *Anal. Chem.*, 33 (1961) 829.

J. Chromatog., 53 (1970) 429-438

CHROM. 4998

THE EFFECT OF CARRIER GAS NONIDEALITY AND ADSORPTION ON THE NET RETENTION VOLUME IN GAS-SOLID CHROMATOGRAPHY

J. J. CZUBRYT*, H. D. GESSER AND E. BOCK

The University of Manitoba, Department of Chemistry, Winnipeg (Canada)

(First received May 11th, 1970; revised manuscript received August 11th, 1970)

SUMMARY

The effect of carrier gas nonideality and adsorption on the net retention volume has been considered and certain approximate relationships are developed. These in turn are applied to the net retention volumes of methane obtained on a 200-ft. (1/8 in. O.D.) Porapak S column at 0°C where He, Ar and CO₂ were employed as carrier gases. In all cases it was found that the effect of carrier gas nonideality on the net retention volume was much smaller than that arising from carrier gas adsorption. The relative degree of adsorption was found to be in the expected order, that is, He < Ar < CO₂. The adsorption of all three gases was found to be governed by a single pseudo adsorption isotherm of the form $\theta = k\bar{P}^n/(1 + k\bar{P}^n)$. All indications are that due to the uncertainty in the nature of the carrier gas adsorption isotherms, gas-solid chromatography is not a suitable method in the determination of the B_{12} terms.

INTRODUCTION

Since our previous report¹, dealing with the separation of CH₄-CD₄ mixtures on a Porapak S column using helium as a carrier gas, other carrier gases were employed in order to try and enhance this separation. Our preliminary experiments, carried out at constant temperature and flow rate, showed that the effect of carrier gases such as N₂, Ar, and CO₂ was to decrease dramatically both the retention times and the separation efficiency. This is illustrated in Fig. 1. In every case the heavy methane is eluted before the lighter one.

BROOKMAN *et al.*² have pointed out that if gas viscosity and compressibility are considered, then differential retention times are to be expected as one changes carrier gases and that the order would be in the same direction as the carrier gas viscosity. According to Fig. 1, the retention time order is $t(\text{He}) > t(\text{Ar}) > t(\text{N}_2) > t(\text{CO}_2)$ whereas the viscosity order for the gases is $\text{Ar} > \text{He} > \text{N}_2 > \text{CO}_2$ (ref. 3).

Rough calculations showed that neither this discrepancy nor the large decrease in the retention times could be accounted for by carrier gas nonideality alone. With the aid of an electron capture detector (used as a helium detector) it was found that N₂, Ar, and CO₂ could be separated on the same column under similar conditions. Un-

* Holder of the National Research Council of Canada Studentship 1966-1968.

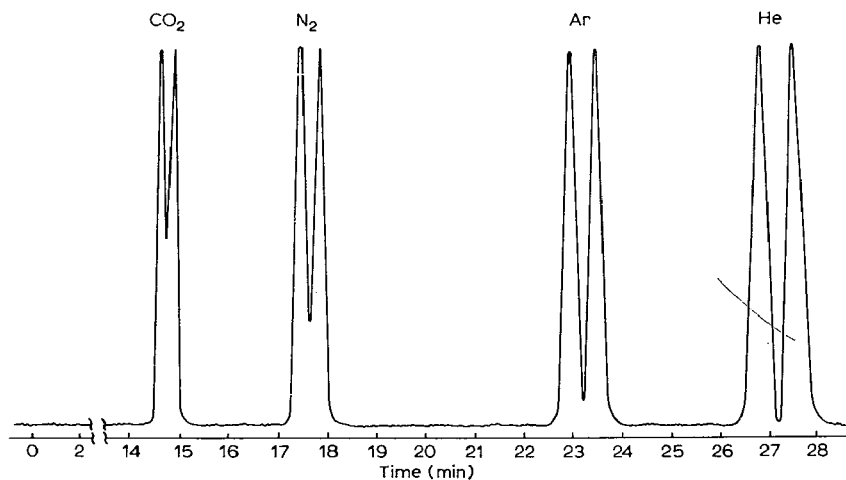


Fig. 1. Elution of $\text{CH}_4\text{-CD}_4$ mixtures with various carrier gases. Column, 80 ft. (1/8 in. O.D.) Porapak S (50–80 mesh); flow rate, $20 \text{ cm}^3/\text{min}$; temperature, $0 \pm 1/2^\circ\text{C}$.

doubtedly this differential interaction between these gases and the packing material must also exist when these gases assume the role of a carrier gas. In the presence of an adsorbing carrier gas there will be competition between the solute and the carrier gas molecules for the active sites on which partitioning takes place, and consequently a reduction of both the retention times and the separation efficiency can be expected. The order of elution is now a function of carrier gas viscosity (and compressibility) and the degree of interaction between the carrier gas and the surface.

A study was initiated to determine the nature and degree of interaction between the carrier gas and the packing. The three carrier gases He, Ar, and CO_2 were chosen for this study since they exhibit a different degree of nonideality and a progressively stronger interaction with the packing.

THEORETICAL

The fundamental quantity in gas chromatography which relates the operating parameters to the thermodynamic properties is the net retention volume (V_N). For a gas–solid chromatography (GSC) system this relationship can be written as

$$V_N = KS \quad (1)$$

where K and S are respectively the distribution coefficient and the surface area on which partitioning can take place. The net retention volume in turn can be calculated by means of the following expression

$$V_N = t_R F_o j - V_M \quad (2)$$

where t_R , F_o , j , and V_M are the elution time of the solute, the flow rate at the column outlet, the Martin–James compressibility factor, and the column void accessible to the mobile phase respectively. Eqn. 2 is only valid under ideal gas conditions. In practice, however, one deals with real gases and eqn. 2 serves only as an approximation, the

degree of which depends on the nonideality of the carrier gas and the operating pressure. The relationship expressed by eqn. 1 on the other hand is independent of the nature of the carrier gas or the pressure, but the magnitude of V_N certainly is.

The effect of pressure and the nature of the carrier gas on the net retention volume or the partition coefficient in gas-liquid chromatography (GLC) has been explored theoretically and/or experimentally by a number of workers⁶⁻¹⁶, but virtually no work of this type has been done in the field of GSC. LOCKE¹⁷ has considered this problem theoretically and has proposed several expressions relating the distribution coefficient to pressure and the carrier gas nonideality. Unfortunately these expressions are of limited use. In the first place he only considers two basic adsorption isotherms (linear and Langmuir). What is more important is the number of errors contained in these expressions. One of these has been pointed out by YOUNG¹⁸ and refers to LOCKE's case III. Further perusal of these expressions reveals that for one reason or another the seven of the remaining nine expressions are also in error, namely cases II, IV, V, VI, VII, IX, and X.

Our approach to this problem is basically that used by LOCKE. Here it is also assumed that the solute samples are very small and consequently that their adsorption isotherms are linear.

In a very short section of column under pressure P where S is the available surface area of the packing material and V is the column void accessible to the mobile phase, the expression for the local distribution coefficient is defined as follows:

$$K = \frac{N_a V}{N_g S} \quad (3)$$

where N_a and N_g refer to the number of moles of solute adsorbed on the surface and in the mobile phase respectively. Following LOCKE, N_a can be expressed in terms of fugacity of the solute f by

$$N_a = k S f \quad (4)$$

where S has the same meaning as above and k is the solute adsorption constant. Now, the relationship between fugacity, f , the partial pressure p , and the local carrier gas pressure P is given by^{19, 20},

$$\ln f = \ln p + \frac{P}{RT} [B_{22} - (1-y)^2(B_{11} - 2B_{12} + B_{22})] \quad (5)$$

where y is the mole fraction of the solute in the gas phase and B_{11} and B_{22} are the second virial coefficients of the pure carrier gas and the pure solute, respectively. B_{12} is the second virial cross coefficient, which is a measure of the interaction between the two types of molecules and is related to B_{11} and B_{22} by the following expression²¹,

$$B_m = (1-y)^2 B_{11} + 2y(1-y)B_{12} + y^2 B_{22} \quad (6)$$

where B_m is the second virial coefficient of the mixture and in the limit as $y \rightarrow 0$ becomes equal to B_{11} . In the present system, where we are dealing with infinitely dilute mixtures, we can express N_g (eqn. 3) as

$$N_g = \frac{pV}{RT + B_{11}P} \quad (7)$$

After substituting this and eqn. 4 into eqn. 3 and taking natural logarithms we get

$$\ln K = \ln kRT + \ln \frac{f}{p} + \ln \left(1 + \frac{B_{11}P}{RT} \right) \quad (8)$$

Since normally $B_{11}P/RT \ll 1$, then the third term of the r.h.s. can be approximated by $B_{11}P/RT$. In the limit as $y \rightarrow 0$, eqn. 5 becomes

$$\ln \frac{f}{p} = (2B_{12} - B_{11}) \frac{P}{RT} \quad (9)$$

Substituting this into eqn. 8 we get

$$\ln K = \ln kRT + \frac{2B_{12}}{RT} P \quad (10)$$

It has been pointed out by DESTY *et al.*⁷ that fugacity of the solute varies with pressure according to

$$\left(\frac{\partial \ln f}{\partial P} \right)_T = \frac{v}{RT} \quad (11)$$

where v is the molar volume of the solute which may be approximated to the molar volume of the pure solute (V_0). Integregation between limits between $P = P$ and $P = 0$ gives

$$\ln f(P = 0) = \ln f(P = P) - \frac{V_0 P}{RT} \quad (12)$$

Following DESTY *et al.* and correcting eqn. 10 to the standard state, we obtain the desired expression

$$\ln K = \ln kRT + (2B_{12} - V_0) \frac{P}{RT} \quad (13)$$

or

$$\ln K = \ln K_0 + (2B_{12} - V_0) \frac{P}{RT} \quad (14)$$

where

$$K_0 = K(P = 0) = kRT \quad (15)$$

The relationship between K and P thus obtained for a GSC system is found to be identical to that of GLC systems when similar approximations are involved (here reference is made to GLC systems where factors such as carrier gas solubility, liquid phase compressibility etc. are ignored). This is expected if one considers that in both cases correction is being made for the effect of carrier gas nonideality and pressure on the fugacity of the solute in the mobile phase and consequently on K .

Eqn. 14 represents the distribution coefficient at any point in the column where the carrier gas pressure is P . The quantity of interest, however, is a particular value of K which is experimentally representative of the entire column (the mean value of K). In the field of GLC a number of above cited workers have chosen the representative value of K (or V_N) as that which is obtained at the mean column pressure \bar{P} defined as

$$\bar{P} = P_0/\bar{j} = P_0 J_2^3 \quad (16)$$

where P_o is the column outlet pressure and as before j is the Martin-James compressibility factor. EVERETT⁸ questioned the use of \bar{P} and has shown that a more representative value of pressure should be

$$P = P_o J_3^4 \quad (17)$$

where

$$J_n^m = \frac{n \left[\left(\frac{P_i}{P_o} \right)^m - 1 \right]}{m \left[\left(\frac{P_i}{P_o} \right)^n - 1 \right]} \quad (18)$$

and P_i is the column inlet pressure. In view of what has been said above, this can be extended to the GSC system and our final expression becomes

$$\ln K = \ln K_0 + (2B_{12} - V_0) \frac{P_o J_3^4}{RT} \quad (19)$$

where K of eqn. 19 no longer symbolizes the local value, but the column mean.

The carrier gas can further influence the magnitude of V_N in a GSC system by competing with the solute molecules for the active sites. This competition process leads to an effective loss of available surface area to the solute. If we define S as the available surface area and S_0 as the total surface area (no carrier gas adsorption) of the entire column, then the mean value of the fraction of the surface covered by the carrier gas is

$$\theta = 1 - \frac{S}{S_0} \quad (20)$$

It should be pointed out at this time that θ is only an apparent fraction since under ordinary conditions (no chemisorption) the solute molecules can displace the adsorbed carrier gas and the ease with which this can be done will be related to the relative magnitudes of the adsorption constants of the solute and the carrier gas. When the adsorption constant of the carrier gas becomes much greater than that of the solute, the θ (apparent) will approach θ (true).

Eqns. 1, 19 and 20 can be combined to give

$$V_N = K_0 S_0 (1 - \theta) \exp [(2B_{12} - V_0) P_o J_3^4] \quad (21)$$

In the limit as $P \rightarrow 0$ (and consequently $\theta \rightarrow 0$), $K_0 S_0$ represents the net retention volume at zero pressure ($V_N(0)$). Making this substitution and rearrangement of eqn. 21 gives

$$\frac{V_N}{\exp [(2B_{12} - V_0) P_o J_3^4]} = V_N(0) (1 - \theta) = V_N^* \quad (22)$$

and consequently θ can be expressed as

$$\theta = 1 - \frac{V_N^*}{V_N(0)} \quad (23)$$

Eqn. 23 allows one to determine the mean apparent value of θ in terms of the corrected net retention volume V_N^* of some suitable solute. Unfortunately, eqn. 23 does not

allow for the determination of the nature of the adsorption isotherm of the carrier gas since in no way is it related to the proper pressure variable. To clarify this it must be realized that for any region of the column the local value of θ (θ_L) will be

$$\theta_L = f(P) \quad (24)$$

Thus, if we assume the carrier gas to behave ideally so that $f = P$ and that it has a linear adsorption isotherm, then

$$\theta_L = kP \quad (25)$$

In order to find the mean value of θ the following integration must be performed

$$\frac{\int \theta_L dx}{\int dx} = \frac{\int kP dx}{\int dx} = \bar{\theta}_L \quad (26)$$

But since²²

$$\frac{x}{L} = \frac{P_i^2 - P_o^2}{P_i^2 - P_o^2} \quad (27)$$

where x is the distance along the column where the pressure is P , and L is the total length of the column, and consequently

$$dx = \frac{-2LP dP}{P_i^2 - P_o^2} \quad (28)$$

then eqn. 26 becomes

$$\bar{\theta}_L = \frac{k \int P^2 dP}{\int P dP} = \theta \quad (29)$$

and upon integration this gives

$$\theta = k \frac{2}{3} \left(\frac{P_i^3 - P_o^3}{P_i^2 - P_o^2} \right) = k\bar{P} \quad (30)$$

Eqn. 30 shows that for this particular case \bar{P} is the proper pressure variable. Should the adsorption isotherm have been Langmuir then

$$\theta = \frac{k \int \frac{P^2 dP}{1 + kP}}{\int P dP} \quad (31)$$

and consequently \bar{P} would no longer serve as the proper pressure variable, that is

$$\theta \neq \frac{k\bar{P}}{1 + k\bar{P}} \quad (32)$$

It follows that for every different carrier gas adsorption isotherm, θ will be a new function of P_i and P_o and consequently $f(\bar{P})$ cannot be substituted for $f(P)$. This means then that although it is possible to determine θ from GSC data, it is not possible to determine the nature of the adsorption isotherm and as a result the B_{12} terms cannot be obtained from GSC system unless the exact carrier gas adsorption isotherm is known in advance. The situation becomes more complex if one considers θ_L as a function of fugacity.

V_N and consequently V_N^* must be calculated from the working parameters. It has been already pointed out that eqn. 2 is inadequate for systems using real carrier gases, particularly at elevated pressures. A more accurate expression can be arrived at by:

(a) Assuming that the carrier gas is governed by the following equation of state

$$PV = RT + B_{11}P \quad (33)$$

(b) By keeping a mass balance in the column (*i.e.* mass inflow = mass outflow). The final expression for V_N is

$$V_N = t_R F_o \left(\frac{P_o}{\bar{P}} \right) \left(\frac{1 + b\bar{P}}{1 + bP_o} \right) - V_M \quad (34)$$

where

$$b = \frac{B_{11}}{RT} \quad (35)$$

and \bar{P} is the mean column pressure derived for a nonideal gas by MARTIRE AND LOCKE²³ and has the form

$$\bar{P} = \frac{\frac{1}{3}(a^3 - 1) - \frac{b}{4}(a^3 P_i - P_o)}{\frac{1}{2P_o}(a^2 - 1) - \frac{b}{3}(a^3 - 1)} \quad (36)$$

where

$$a = \frac{P_i}{P_o} \quad (37)$$

The ratio P_o/\bar{P} has the same significance as the Martin-James compressibility factor. Under ideal gas conditions where $B_{11} = 0$, eqn. 34 reduces to eqn. 2.

EXPERIMENTAL

The packing material used in this study was 50-80 mesh Porapak S. Out of 100 random particles, the average particle diameter was measured to be 0.20 ± 0.02 mm by means of a Unitron (U-11) microscope having a micrometer scale in the eyepiece. A photomicrograph showed these particles to be smooth and generally quite spherical.

The packing material was first washed in tetrahydrofuran (THF) dried at 100°C, and degassed under vacuum while the temperature was slowly raised to 200°C and maintained there for about 5 min after which the heat was turned off. The cooled packing material was then added to a 10 % trimethylchlorosilane in benzene solution and after 20 min, the packing was filtered and washed with methyl alcohol and then dried at 100°C, under vacuum for three days.

The copper tubing (1/8 in. O.D. and 0.065 in. I.D.) was washed with acetone, THF, and methyl alcohol and then dried at room temperature by passing nitrogen gas through it.

The final 200-ft. column was made up of four 50-ft. sections which were packed

separately. The ends of each section were terminated with approximately 1/16 in.-thick plug of G.E. Foametal. To prevent the plug from falling out, the ends of the copper tubing were gently filed towards the tube axis so as to form a slight lip over the plug. The four sections were joined together with Swagelok unions which were filled with the packing material. The final column was coiled on a length (~ 12 in.) of 4-in.-diameter brass pipe.

A Seiscor Model VIII high pressure and helium purge modified sampling valve having a sample volume of $0.5 \mu\text{l}$ was used throughout the study. In all experiments the sample pressure was below atmospheric and gave an effective sample size of $0.12 \mu\text{l}$ at S.T.P.

Most experiments were carried out at 0°C in a stirred and ice-filled bath or a temperature-controlled oil bath ($\pm 1/2^\circ\text{C}$).

The inlet pressure was measured with a 0–200 p.s.i. Marsh Master gauge which had an accuracy of better than 0.5 % of the pressure reading. The outlet pressure was measured with a mercury manometer to within ± 0.1 cm. Both pressures were measured before and after each experiment.

All gases except hydrogen were passed through a stainless steel enclosed Cu–CuO furnace maintained at about 850°C and through a molecular sieve (5A) trap.

Flow rate measurements were made by the method described elsewhere²⁴. On the average the reproducibility was better than 0.01 %.

A 1-mV, 11-in. chart, 1-sec response Bristol recorder was used throughout. The chart drive motor was connected in parallel to a Lab-Chrom timer which served as a check on the accuracy of the chart advance.

A Beckman G.C.4 flame ionization detector was used in experiments where methane was the only constituent in the sample. In experiments involving other gases an Aerograph (250 mCi tritium source) electron capture detector was used in a "helium detector" mode. The voltage to the detectors was supplied by Keithley 240 power supply and the current through the detectors was measured by a Keithley 410 electrometer.

Further details of the precautions taken and experimental procedure are described elsewhere²⁵.

RESULTS AND DISCUSSION

Before the experimental data are presented, the manner in which V_N^* were calculated will be discussed.

The net retention volume was calculated by means of eqn. 34, which requires that V_M be known. V_M is normally determined from the elution time of a non-sorbing solute, but in the present system the normal calibrating gases (air, methane) are known to interact quite strongly with the packing material. Of the several avenues open to overcome this problem, the following procedure was followed to determine V_M . Using helium as the carrier gas and an electron capture detector (used as helium detector) the corrected retention volume (V_R^0) of hydrogen was determined at several temperatures. It was found that there was a significant decrease in V_R^0 with increasing temperature, suggesting that hydrogen could not be regarded as non-sorbing solute. Unfortunately the limited temperature range covered did not allow extrapolation of V_R^0 vs. $1/T$ plot to $1/T = 0$, where $V_R^0 = V_M$ without an introduction of a large error.

Since $\log(V_R^0 - V_M)$ is a linear function of $1/T$ (ref. 26), this relationship was applied and $\log(V_R^0 - X)$ was plotted against $1/T$. The value of X was increased by 0.5 cc until a straight-line relationship was obtained. This particular value of X was chosen as V_M and was used in all the calculations.

The $B_{11}(T)$ values for He and Ar were calculated from a Beattie-Bridgeman type equation which has the form²⁷

$$\frac{B_{11}}{V^*} = 0.461 - 1.158 \left(\frac{T^*}{T} \right) - 0.503 \left(\frac{T^*}{T} \right)^3 \quad (38)$$

where T^* and V^* are the characteristic temperature and volume, respectively. The values of T^* and V^* were obtained from the same source as eqn. 38.

$B_{11}(T)$ for CO_2 was calculated from eqn. 39 and the available tables²⁸.

$$B_{11}(T) = b_0 B_{11}^*(T^*) \quad (39)$$

where B_{11}^* , T^* and b_0 are the reduced second virial coefficient, the reduced temperature (as defined in ref. 28) and the steric parameter, respectively.

The second virial cross coefficients were calculated from an equation similar to that of eqn. 38 (ref. 27), that is

$$\frac{B_{12}}{V_{12}^*} = 0.461 - 1.158 \left(\frac{T_{12}^*}{T} \right) - 0.503 \left(\frac{T_{12}^*}{T} \right)^3 \quad (40)$$

where

$$T_{12}^* = (T_1^* \cdot T_2^*)^{1/2} \quad (41)$$

and

$$V_{12}^* = 1/2[(V_1^*)^{1/3} + (V_2^*)^{1/3}] \quad (42)$$

where as before subscripts 1 and 2 refer to the carrier gas and the solute.

According to eqn. 22, carrier gas adsorption is signaled by a decrease in V_N^* as the column pressure is increased. From what has been said before, the exact relationship between V_N^* and pressure cannot be determined unless the carrier gas adsorption isotherm is known. The trend, however, can be shown by plotting V_N^* against some suitable pressure variable which is related to P_i and P_o . For the present purpose we have chosen \bar{P} (MARTIRE AND LOCKE's expression) as it best describes the condition of the column and most probably will be closer to the true pressure variable than pressure variables such as $[(P_i + P_o)]/2$ or P_i/P_o . Such plots of $V_N^*(\text{CH}_4)$ vs. \bar{P} (mean column pressure) for He, Ar, and CO_2 are shown in Fig. 2. The helium plot shows that although helium gas is generally considered as being ideal, it does measurably interact with this surface even at 273°K. This plot is of considerable importance in that, unlike the other two, it allows extrapolation to the $P = 0$ region and consequently the determination of $V_N(0)$.

The unexpected minimum followed by a relative increase in V_N^* with increasing pressure is only observed in the helium plot. As it is indicated by the dark circles, this region is quite reproducible. The two experiments were performed independently, that is, they were interspersed by the Ar and CO_2 experiments. Consequently, this result is not an artifact of the working system and has to be accepted as genuine. The reason for this trend will be discussed elsewhere since it is related to other factors. It is suffi-

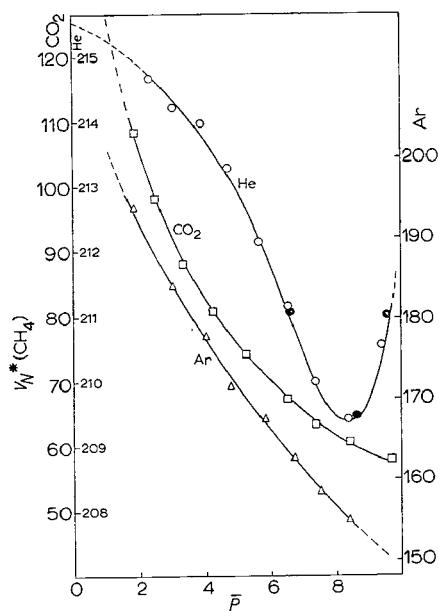


Fig. 2. $V_N^*(\text{CH}_4)$ as a function of \bar{P} for He (\circ and \bullet), Ar (\triangle), and CO_2 (\square). Carrier gas at $0 \pm 1/2^\circ\text{C}$.

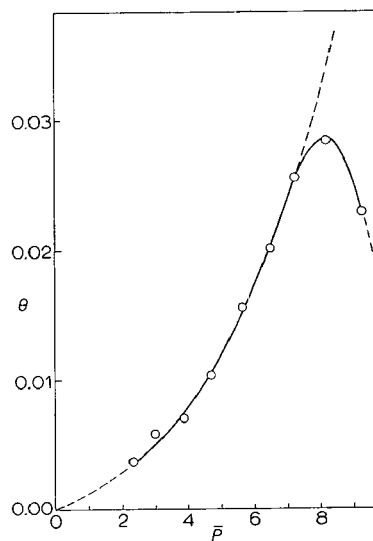


Fig. 3. θ (He) as a function of \bar{P} .

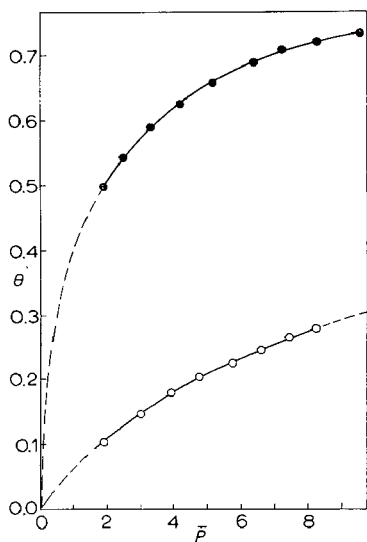


Fig. 4. θ (Ar, \circ) and θ (CO_2 , \bullet) as a function of \bar{P} .

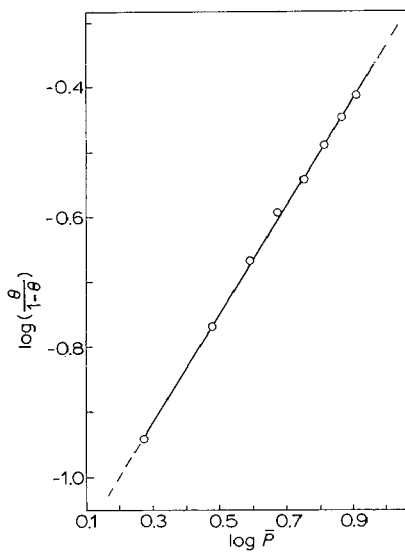


Fig. 5. $\log \{\theta/(1 - \theta)\}$ vs. $\log \bar{P}$ for Ar.

cient to say at the present time that this anomalous effect is a by-product of a secondary flow mechanism in which only helium can participate. Fig. 2 shows that at constant \bar{P} the magnitude of V_N^* is in the opposite direction to the anticipated order of carrier gas interaction; this of course is expected if V_N^* is related to $(1-\theta)$.

The degree of interaction of the carrier is perhaps more meaningful in terms of θ . A plot of θ vs. \bar{P} for helium is shown in Fig. 3, whereas those for Ar and CO_2 are shown in Fig. 4. It may be mentioned again that in the helium plot the results at the highest \bar{P} become meaningless if the above comment is not considered. Fig. 4 shows that in the case of Ar almost 30 % of the surface is apparently covered at $\bar{P} \approx 8.5$ atm whereas in the case of CO_2 coverage is about 75 % at the same \bar{P} . The actual values are probably somewhat higher.

It was found that for all three gases θ could be related to the variable \bar{P} through the following expression

$$\log \left(\frac{\theta}{1-\theta} \right) = A + n \log \bar{P} \quad (43)$$

In all cases the fit was quite good, as it is illustrated by Fig. 5, where $\log\{\theta/(1-\theta)\}$ is plotted against $\log \bar{P}$ for Ar. After taking antilogs and rearrangement, eqn. 43 becomes

$$\theta = \frac{k\bar{P}^n}{1 + k\bar{P}^n} \quad (44)$$

This pseudo adsorption isotherm is neither Langmuir nor Freundlich, it is a combination of both. It has the property of reducing to the Freundlich form at low pressures, and exhibits the characteristic Langmuir plateau at high pressures. It, in fact, becomes the Langmuir adsorption isotherm when $n = 1$.

This equation has been used advantageously²⁹⁻³¹ and is preferred to the Freundlich or Langmuir equation in many cases.

The k and the n constants for the three carrier gases are given in Table I.

TABLE I

ADSORPTION PARAMETERS FOR THE CARRIER GASES IN TERMS OF CH_4 AS SOLUTE AT 273°K

	k	n
He	8.158×10^{-4}	1.7010
Ar	6.890×10^{-2}	0.8191
CO_2	6.523×10^{-1}	0.6438

According to SIPS³² the maximum value that n can have is ± 1 , but for physically real systems this can only be 1. According to Table I, n for helium is greater than 1 (1.7). This is probably in part an artifact from the choice of the pressure variable.

A comparison was made to determine the validity of these pseudo adsorption isotherms. For each working pressure of each gas, θ was calculated by two different methods. In the first case θ was calculated from eqn. 44. In the second case θ was calculated by assuming the relationship of eqn. 44 to hold but in the place of \bar{P} the local value of P was substituted as a different segment of the column was considered (at

intervals of 1 in.). The resulting θ 's were then summed and divided by the total number of contributions (2,400). The expressions used to relate x (column distance) and θ were eqn. 44, 45 and 46.

$$P = \frac{yb}{2} + \left[2y + \left(\frac{yb}{2} \right)^2 \right]^{1/2} \quad (45)$$

and

$$y = \frac{x}{L} \left(\frac{P_i^2}{2 + bP_i} - \frac{P_o^2}{2 + bP_o} \right) + \frac{P_o^2}{2 + bP_o} \quad (46)$$

where as before b is given by eqn. 35.

The expressions for P and y were derived from Darcy's Law, in which allowance is made for gas imperfections. If we relate θ_1 and θ_2 to the first case and the second case, respectively, then the percent deviation is expressed as

$$\frac{\theta_1 - \theta_2}{\theta_1} \times 100 = \% \text{ deviation} \quad (47)$$

This relationship for all the three gases is given in Fig. 6. In the case of He, these deviations are positive and some ten times larger than Ar and CO₂, in which cases they are negative and have an average value of about -1.5%. On first inspection it appears that at least for the Ar and the CO₂ case the adsorption isotherm may be well approximated by eqn. 44. Approximations of this magnitude cannot be made, however, if the GSC system is being used as a tool in determining the B_{12} terms as suggested by LOCKE. In support of this an example is drawn from the present study. For the argon experiment ($\bar{P} = 4.77$) the % deviation is about -1.6%. Utilizing θ_2 rather than θ_1 to determine V_N^* from $V_N(0)$, and consequently the B_{12} term, it is found that there is a difference of some 67% between the two values.

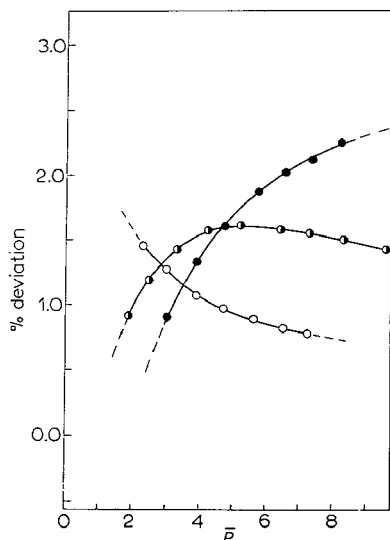


Fig. 6. $\{(\theta_1 - \theta_2)/\theta_1\} \times 100$ as a function of \bar{P} . \circ , He ($10 \times \circ$); \bullet , CO₂ ($-1 \times \bullet$); \bullet , Ar ($-1 \times \bullet$).

In conclusion, it appears that GSC is not suitable for the determination of the B_{12} terms unless the exact expression for the carrier gas adsorption isotherm is known precisely but not from static systems where only the pure carrier gas is involved, but in terms of θ (apparent) where the relative adsorption of the solute and the carrier gas are taken into account. Such would be perhaps a fruitless task considering the effort involved and comparing this to the relative case offered by GLC.

ACKNOWLEDGEMENT

We wish to thank the National Research Council of Canada for the financial support of this work.

REFERENCES

- 1 J. J. CZUBRYT AND H. D. GESSER, *J. Gas Chromatog.*, 6 (1968) 41.
- 2 D. J. BROOKMAN, G. L. HARGROVE AND D. T. SAWYER, *Anal. Chem.*, 39 (1967) 1196.
- 3 E. A. MOELWYN-HUGHES, *Physical Chemistry*, Pergamon, London, 1961, p. 160.
- 4 L. R. SNYDER, *Principles of Adsorption Chromatography*, Marcel Dekker, New York, 1968, p. 246.
- 5 C. HORVATH, in L. S. ETTRE AND A. ZLATKIS (Editors), *The Practice of Gas Chromatography*, Interscience, New York, 1967, p. 140.
- 6 D. H. EVERETT AND C. T. H. STODDART, *Trans. Faraday Soc.*, 57 (1961) 746.
- 7 D. H. DESTY, A. GOLDFUP, G. R. LUCKHURST AND T. W. SWANTON, in M. VAN SWAAY (Editor), *Gas Chromatography 1962*, Butterworth, London, 1962, p. 67.
- 8 D. H. EVERETT, *Trans. Faraday Soc.*, 61 (1965) 1637.
- 9 A. J. B. CRUICKSHANK, M. L. WINDSOR AND C. L. YOUNG, *Proc. Roy. Soc. (London)*, Ser. A., 295 (1966) 259.
- 10 A. J. B. CRUICKSHANK, M. L. WINDSOR AND C. L. YOUNG, *Proc. Roy. Soc. (London)*, Ser. A., 295 (1966) 271.
- 11 S. T. SIE, W. VAN BEERSUM AND G. W. A. RIJENDERS, *Separation Sci.*, 1 (1966) 459.
- 12 B. W. GAINNEY AND C. L. YOUNG, *Trans. Faraday Soc.*, 64 (1968) 349.
- 13 R. L. PESCOCK AND M. L. WINDSOR, *Anal. Chem.*, 40 (1968) 1238.
- 14 D. C. LOCKE AND W. W. BRANDT, in L. FOWLER (Editor), *Gas Chromatography*, Academic Press, New York, 1963, p. 55.
- 15 E. M. DANTZLER, C. M. KNOBLER AND M. L. WINDSOR, *J. Chromatog.*, 32 (1968) 433.
- 16 A. J. B. CRUICKSHANK, B. W. GAINNEY, C. P. HICKS, T. M. LETCHER, R. W. MOODY AND C. L. YOUNG, *Trans. Faraday Soc.*, 65 (1969) 1014.
- 17 D. C. LOCKE, *J. Phys. Chem.*, 69 (1965) 3768.
- 18 C. L. YOUNG, *Chromatog. Rev.*, 10 (1968) 129.
- 19 E. A. GUGGENHEIM, *Thermodynamics*, North-Holland, Amsterdam, 1967, p. 177.
- 20 E. A. GUGGENHEIM, *Mixtures*, Clarendon, Oxford, 1952, p. 153.
- 21 J. E. LENNARD-JONES AND W. R. COOK, *Proc. Roy. Soc. (London)*, Ser. A, 115 (1927) 334.
- 22 A. J. M. KEULEMANS, in C. G. VERVER (Editor), *Gas Chromatography*, Reinhold, New York, 1960, p. 142.
- 23 D. E. MARTIRE AND D. C. LOCKE, *Anal. Chem.*, 37 (1965) 144.
- 24 J. J. CZUBRYT AND H. D. GESSER, *J. Gas Chromatog.*, 6 (1968) 528.
- 25 J. J. CZUBRYT, *Ph. D. Thesis*, University of Manitoba, Winnipeg, Canada, 1968.
- 26 S. DAL NOGARE AND R. S. JOUVET, JR., *Gas-Liquid Chromatography*, Interscience, New York, 1962, p. 78.
- 27 E. A. GUGGENHEIM AND M. L. MCGLASHAN, *Proc. Roy. Soc. (London)*, Ser. A, 206 (1951) 448.
- 28 D. F. EGGERS, JR., N. W. GREGORY, C. D. HALSEY, JR. AND B. S. RABINOVITCH, *Physical Chemistry*, Wiley, New York, 1964, p. 330.
- 29 H. BRADLEY, *Trans. Faraday Soc.*, 31 (1935) 1652.
- 30 R. A. KOBLE AND T. E. CORRIGAN, *Ind. Eng. Chem.*, 44 (1952) 383.
- 31 E. O. WIGG AND S. B. SMITH, *J. Phys. Colloid Chem.*, 55 (1951) 27.
- 32 R. SIPS, *J. Chem. Phys.*, 16 (1948) 490.

CHROM. 5051

FLOW OF He, Ar, AND CO₂ THROUGH A 200 ft. $\frac{1}{8}$ in. O.D. PORAPAK S (50-80 MESH) COLUMN AT 273° K

J. J. CZUBRYT* AND H. D. GESSER

Department of Chemistry, University of Manitoba, Winnipeg (Canada)

(Received August 11th, 1970)

SUMMARY

The flow of He, Ar, and CO₂ through a 200 ft. $\frac{1}{8}$ in. O.D. Porapak S (50-80 mesh) column has been studied at 273° K. It was found that the gas flow cannot be completely described in terms of the existing relationships. Certain mechanisms must be postulated in order to explain some of the anomalies found in this study.

INTRODUCTION

In the previous article dealing with the effect of carrier gas nonideality and adsorption on the net retention volume of a solute¹, it was found that in the experiments using helium as a carrier gas, the experimental data at the highest pressures employed was inconsistent with the proposed mechanism of carrier gas adsorption. Without evidence this discrepancy was attributed to a secondary flow mechanism in which only helium can participate. It is the intent of this article to provide experimental evidence to support this view as well as to explore the question of carrier gas flow through this type of column (described in ref. 1) in terms of the existing theories and/or empirical relationships.

Due to compressibility, the carrier gas will experience acceleration as it travels down the column and consequently its velocity will increase with the distance. Texts treating fluid motion often describe the velocity profile by the Navier-Stokes equation^{2,3}. Solution of this equation leads to the correct description of gas flow but as GIDDINGS⁴ points out the intractable nature of this equation is beyond exact treatment for such complex flow space geometries as those found in a gas chromatographic column.

The flow of gas through a porous media is more practically described by an empirical relationship proposed by Darcy⁵. In terms of the apparent gas velocity u_a (using CARMAN's notation⁵) Darcy's Law states that for a flow of gas in the x direction

$$u_a = - \left(\frac{B_o}{\eta} \right) \frac{dP}{dx} \quad (1)$$

where B_o is the specific permeability coefficient and η is the gas viscosity, and u_a is defined as⁵,

$$u_a = Q/At \quad (2)$$

* Holder of the National Research Council of Canada Studentship 1967-1968.

where Q , A and t are the volume of gas, the cross-sectional area of the porous media and the time, respectively. It has been pointed out on several occasions^{4,6,7} that u_a is not the true velocity of the gas since the actual cross-sectional area of a porous media such as the gas chromatographic column through which gas can flow is $A\varepsilon$ where ε is the porosity of the media. Applying this correction to eqn. 1 and remembering that

$$F = uA\varepsilon \quad (3)$$

eqn. 1 can be expressed in terms of the flow rate (F) as follows

$$F = - \left(\frac{B_o A}{\eta} \right) \frac{dP}{dx} \quad (4)$$

For a gas chromatographic column where the carrier gas may be considered as ideal it can be shown that

$$F = \frac{F_o P_o}{P} \quad (5)$$

where F and F_o are the flow rates at points where the pressure is P and P_o respectively, the latter of which is the outlet pressure. Substitution of eqn. 5 into eqn. 4 and upon rearrangement we get

$$F_o P_o dx = - \left(\frac{B_o A}{\eta} \right) P dP \quad (6)$$

Integration between the limits of $x = 0$ and $x = L$ where the column pressures are P_i and P_o respectively followed by rearrangement gives

$$F_o = \left(\frac{B_o A}{2\eta L P_o} \right) (P_i^2 - P_o^2) \quad (7)$$

If the carrier gas is nonideal and can be approximated by the following equation of state

$$n = \frac{PV}{RT + B_{11}P} \quad (8)$$

then eqn. 6 will become

$$\frac{F_o P_o dx}{RT + B_{11}P_o} = - \left(\frac{B_o A}{\eta} \right) \left(\frac{P dP}{RT + B_{11}P} \right) \quad (9)$$

Integration between the same limits as above leads to

$$\frac{F_o}{1 + bP_o} = \left(\frac{B_o A}{\eta b^2} \right) [b(P_i - P_o) + \ln(1 + bP_o) - \ln(1 + bP_i)] \quad (10)$$

where b is merely the ratio B_{11}/RT . The \ln terms are of the form $\ln(1 + x)$ and can be approximated by

$$\ln(1 + x) = \frac{2x}{2 + x} \quad (11)$$

This form of approximation is very good in that even for x having a value of 0.5 which is much higher than normally encountered, the difference between the actual value of

$\ln(1 + x)$ and the approximation is only -1.35% . After making this approximation in eqn. 10 and algebraic rearrangement, the final expression becomes:

$$F_o = \left(\frac{B_o A}{\eta L P_o} \right) \left[(1 + b P_o) \left(\frac{P_i^2}{2 + b P_i} - \frac{P_o^2}{2 + b P_o} \right) \right] \quad (12)$$

In the limit when the carrier gas is ideal (*i.e.* $b = 0$), eqn. 12 reduces to eqn. 7.

The specific permeability (B_o) has the units of cm^2 but can also be expressed in Darcy units where 1 Darcy = $9.87 \times 10^{-9} \text{ cm}^2$. It is related to the porosity (ϵ) which in turn is related to the nature of the packing material and column construction. The relating equation is the Kozeny-Carman eqn.⁵ which has the form

$$B_o = \frac{d_p^2 \cdot \epsilon^3}{36k(1 - \epsilon)^2} \quad (13)$$

where d_p is the diameter of a sphere with the same specific surface as the particle so that for a spherical nonporous particles, d_p will be that of the particle diameter. k is a constant but it appears that for normal granular packed columns there are two distinct values of k that are in use.

In some publications the accepted value of k is 5.0 (refs. 4-6, 8, 9). Using this value eqn. 13 becomes

$$B_o = \frac{d_p^2 \cdot \epsilon^3}{180(1 - \epsilon)^2} \quad (14)$$

In other publications^{7, 10-14} the accepted value of k is very close to 4.17 thus making eqn. 13 become

$$B_o = \frac{d_p^2 \cdot \epsilon^3}{150(1 - \epsilon)^2} \quad (15)$$

Now, eqn. 15 has been referred to as the Blake-Kozeny equation^{6, 10, 11} whereas eqn. 14 has been referred to as the Kozeny-Carman equation^{4-6, 9}. On occasions eqn. 15 has been called the Kozeny-Carman equation¹³ as well as the Ergun equation⁹. It is not clear which of the two equations is the correct one since it appears that there exists sufficient experimental data to support them both^{5, 10, 13}.

For a GC column porosity can be defined as the fraction of the total volume which is accessible to the mobile phase, that is

$$\text{porosity} = \frac{V_M}{V_T} = \frac{V_M}{\pi r^2 L} \quad (16)$$

For porous materials V_M will contain it in the inter and the intraparticle volumes and consequently the porosity as defined by eqn. 16 is the total porosity or ϵ_T . The free space which is chiefly responsible for gas transport is the interparticle void. It follows then that the porosity contained in eqn. 14 or 15 is the interparticle porosity (ϵ).

The two porosities can be related as follows:

$$\epsilon_T = \epsilon + \Delta \quad (17)$$

where Δ is the porosity arising from the porous nature of the material. For nonporous materials such as glass beads Δ vanishes and the two porosities become identical. The

interparticle porosity can range from 0.35 to 0.9, but for a fairly well packed column the value is very close to 0.4 (ref. 4). The value of 0.9 is encountered in unusual situations such as the aerogel columns¹⁵.

Darcy's Law is applicable only to relatively low gas velocities, that is, in the region of laminar flow. As the gas velocity is increased the laminar flow becomes unstable and gives way to a flow of an erratic pattern which is generally known as turbulent flow. With the onset of turbulence there is an apparent decrease in permeability with increasing flow rate, that is higher pressure differences are required than that expressed by eqn. 7 or eqn. 12. The deviations are too large to be accounted for by the carrier gas nonideality (eqn. 12) or by the increase in viscosity, and can be explained by the loss of the gas kinetic energy through heat dissipation in the numerous eddies and cross-currents of turbulent flow. To account for this a quadratic velocity term is added to Darcy's relationship^{4,5}, that is

$$\frac{-dP}{dx} = au + bu^2 \quad (18)$$

The degree of turbulence can be estimated by a velocity dependant dimensionless term known as the Reynolds number (R_e), which has the form^{4,7}

$$R_e = \frac{\rho u d_p}{\eta} \quad (19)$$

where ρ is the specific gravity of the gas. It should be pointed out that the product ρu will be constant throughout the entire column. According to GIDDINGS⁴, turbulence develops gradually from a minor to a dominant role as R_e increases from 1 to 100. He further states that the departure from Darcy's Law when $R_e > 1$ constitutes evidence that turbulence is occurring, and at $R_e \simeq 1$ turbulence can be expected in only a few of the largest channels. GUIOCHON⁷ on the other hand contends that the flow must be laminar at $R_e \sim 1$ and that Darcy's Law extends to $R_e = 10$ to 15. BIRD *et al.*¹⁰ mention that for $\varepsilon < 0.5$ the Blake-Kozeny equation (which by their notation contains the integrated form of Darcy's Law) is valid up to $R_e/(1-\varepsilon) < 10$, or, if $\varepsilon \simeq 0.4$ then $R_e < 6$.

GUIOCHON points out that use can be made of Ergun's equation for calculating the permeability coefficient in the turbulent region. Using the present notation this relationship can be expressed as follows

$$\frac{1}{k} = \frac{150(1-\varepsilon)^2}{d_p^2 \varepsilon^2} + \frac{1.75 \rho u_o (1-\varepsilon)}{d_p \eta \varepsilon} \quad (20)$$

where k is a velocity dependent permeability coefficient and u_o is the column outlet velocity. By dividing both sides of eqn. 20 by ε and remembering that the resulting first term on the right hand side is actually $1/B_o$, eqn. 20 can be rewritten to give

$$\frac{1}{k\varepsilon} = \frac{1}{B} = \frac{1}{B_o} + \frac{1.75 \rho u_o (1-\varepsilon)}{d_p \eta \varepsilon^2} \quad (21)$$

At relatively low pressures, the density can be approximated by

$$\rho = \frac{P_o M}{RT \times 10^3} \quad (22)$$

Substituting this relationship and the one expressed by eqn. 3 into eqn. 21, eqn. 21 reduces to

$$\frac{1}{B} = \frac{1}{B_0} + Y \left(\frac{M}{\eta} \right) F_0 \quad (23)$$

where

$$Y = \frac{1.75 P_0 (1 - \varepsilon)}{RT A d_p \varepsilon^3 \times 10^3} \quad (24)$$

At constant P_0 , Y is a constant which is independent of the nature of the carrier gas. F_0 in eqn. 23 is expressed in cc/sec.

EXPERIMENTAL

The experimental apparatus and procedure has been described elsewhere¹. All experiments were carried out at 273° K.

RESULTS AND DISCUSSION

The experiments from which the data is extracted will be designated by the carrier gas used. For example Ar I, Ar II and Ar III refer to three distinct experiments using argon as the carrier gas.

For simplicity of notation eqn. 12 can be rewritten to read

$$F_0 = \chi \phi \quad (25)$$

where

$$\chi = \frac{BA}{\eta} \quad (26)$$

and

$$\phi = \frac{1}{P_0} (1 + bP_0) \left(\frac{P_i^2}{2 + bP_i} - \frac{P_0^2}{2 + bP_0} \right) \quad (27)$$

The method for calculating the B_{11} terms used in eqn. 12 or 27 was already described in ref. 1.

According to eqn. 25 and eqn. 26 the relationship between F_0 and ϕ will be linear in the laminar flow region where B is constant. With the onset of turbulence where there is an apparent decrease in B , there will be a progressive decrease in the slope as ϕ increases and as the result a nonlinear departure from Darcy's Law will be observed. To test this relationship F_0 (cc/min) was plotted against ϕ (atm) for three different carrier gases, namely, He, Ar, and CO₂. Figs. 1, 2 and 3 refer to He I, Ar (II and III) and CO₂ I, respectively. The helium plot shows a linear relationship throughout the entire experimental range. If for the present it can be assumed that $\varepsilon = 0.4$, then it appears that Darcy's Law is valid for the gas velocity range from 0 to about 120 cm/sec. This is quite consistent with the results obtained by HARGROVE AND SAWYER¹⁶ for helium gas flowing through a glass bead column. They observed a linear relationship between F_0 and ϕ (ideal gas) up to F_0 of approx. 550 cc/min or in terms of gas velocity up to about 290 cm/sec.

In the case of Ar and CO₂ a straight line could be drawn through only four or five points. If it can be assumed that Darcy's Law is valid for this region, extrapolation of this line to cover the entire experimental range serves to indicate the deviation from this law. Since the line is extrapolated from the laminar flow region, its slope can serve to evaluate χ_0 and in turn B_0 . This is done below.

$$\begin{aligned}\chi_0(\text{He}) &= 0.55 \text{ cc/min atm} \\ \chi_0(\text{Ar}) &= 0.51 \text{ cc/min atm} \\ \chi_0(\text{CO}_2) &= 0.68 \text{ cc/min atm}\end{aligned}$$

In order to convert these values to B_0 , the following constants were used:

$$\begin{aligned}1 \text{ atm} &= 1.0133 \times 10^6 \text{ dynes/cm}^2 \\ L &= 6096 \text{ cm} \\ A &= 2.14 \times 10^{-2} \text{ cm}^2 \\ \eta(\text{He}, 273) &= 1.887 \times 10^{-4} \text{ g/cm} \cdot \text{sec (ref. 17)} \\ \eta(\text{Ar}, 273) &= 2.104 \times 10^{-4} \text{ g/cm} \cdot \text{sec (ref. 17)} \\ \eta(\text{CO}_2, 273) &= 1.380 \times 10^{-4} \text{ g/cm} \cdot \text{sec (ref. 17)}\end{aligned}$$

The corresponding B_0 values were calculated to be:

$$\begin{aligned}B_0(\text{He}) &= 4.88 \times 10^{-7} \text{ cm}^2 \\ B_0(\text{Ar}) &= 5.05 \times 10^{-7} \text{ cm}^2 \\ B_0(\text{CO}_2) &= 4.40 \times 10^{-7} \text{ cm}^2\end{aligned}$$

The average value to B_0 was calculated to be:

$$\bar{B}_0 = (4.78 \pm 0.25) \times 10^{-7} \text{ cm}^2$$

The linearity in Fig. 1 implies the constancy of B and/or χ . To test this the ratio F_0/ϕ was calculated for all the points. It was found that χ was not constant but varied in a regular manner *i.e.* it decreased with increasing ϕ and/or F_0 . Although no

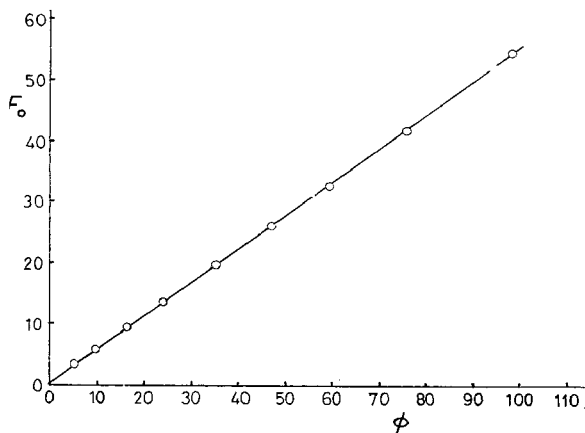


Fig. 1. F_0 as a function of ϕ for He I.

present theory warrants it, it was found that χ could be plotted against \bar{P} (the mean column pressure as defined by MARTIRE AND LOCKE¹⁸) to give a straight line fit. It was somewhat surprising to find this relationship to hold also for Ar and CO₂. Such plots

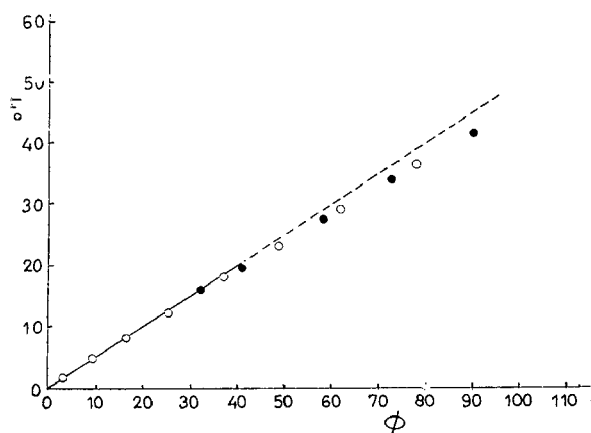


Fig. 2. F_o as a function of ϕ for Ar(II and III). \circ = Ar II; \bullet = Ar III.

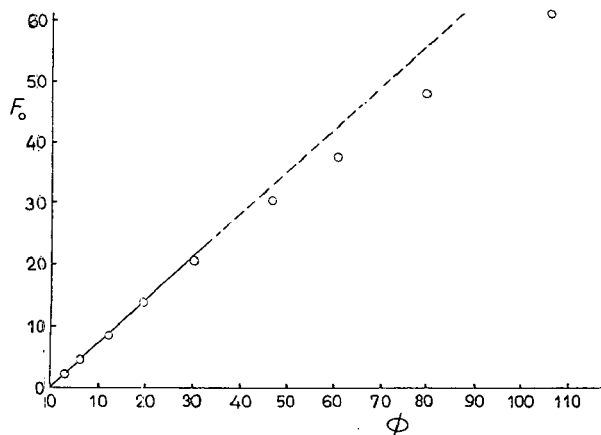


Fig. 3. F_o as a function of ϕ for CO₂ I.

are shown in Figs. 4–6 for He (I and II), Ar (II and III) and CO₂ I, respectively. In all three cases the relationship between χ and \bar{P} was found to be

$$\chi = \chi_o - m\bar{P} \quad (28)$$

or more specifically from the least squares analysis the following three expressions were obtained:

$$\chi(\text{He}) = 0.602 - 0.00666 \bar{P} \quad (29)$$

$$\chi(\text{Ar}) = 0.531 - 0.00794 \bar{P} \quad (30)$$

$$\chi(\text{CO}_2) = 0.809 - 0.0247 \bar{P} \quad (31)$$

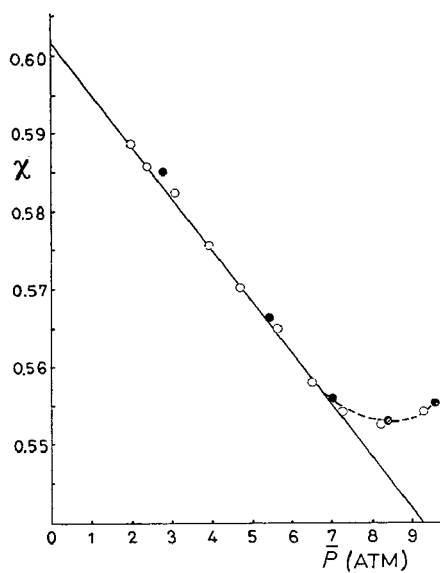


Fig. 4. χ as a function of \bar{P} for helium carrier gas. \circ = He I; \bullet = He II.

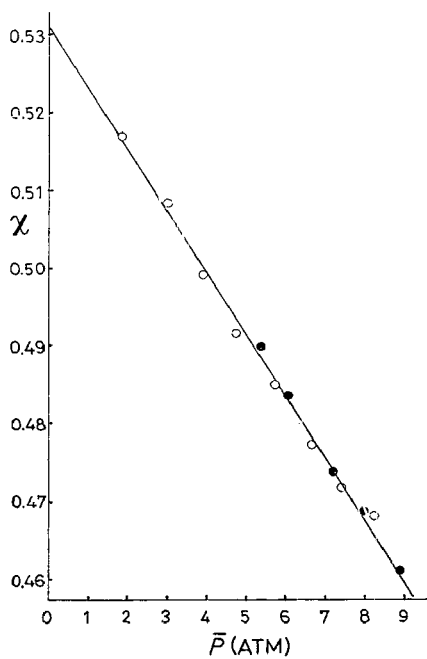


Fig. 5. χ as a function of \bar{P} for Ar(II and III). \circ = Ar II; \bullet = Ar III.

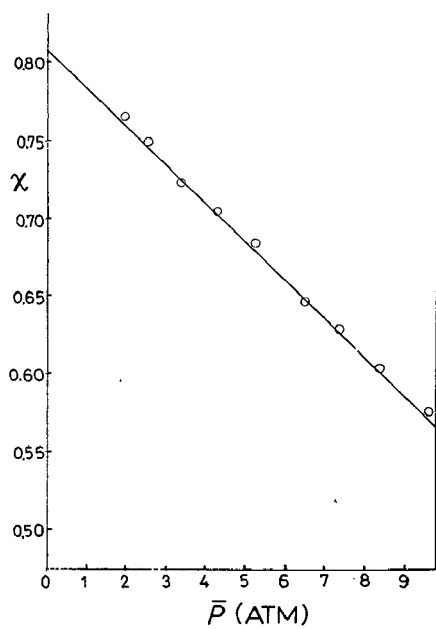


Fig. 6. χ as a function of \bar{P} for CO_2 I.

From the χ_0 values (χ at $\bar{P} = 0$ or very low flow rates where Darcy's Law is definitely valid) the following B_0 values were obtained.

$$\begin{aligned} B_0(\text{He}) &= 5.32 \times 10^{-7} \text{ cm}^2 \\ B_0(\text{Ar}) &= 5.24 \times 10^{-7} \text{ cm}^2 \\ B_0(\text{CO}_2) &= 5.23 \times 10^{-7} \text{ cm}^2 \end{aligned}$$

The average B_0 was found to be

$$\bar{B}_0 = (5.26 \pm 0.04) \times 10^{-7} \text{ cm}^2$$

The value is somewhat higher than that obtained from the slopes and has a spread of only 0.76 % compared to 5.23 %.

Perhaps the most unusual feature of Figs. 4-6 is the minima found in Fig. 4. Repeated experiments consistently showed the presence of this minima (this is shown in Fig. 4 by only one of the several repeated experiments, He II). The presence of this minima suggests that either the mechanism responsible for decreasing χ (or B) with mean column pressure begins to break down at elevated helium \bar{P} or that a secondary mechanism working in the opposite direction becomes effective at \bar{P} of about 7 atm. This deviation from the "normal" trend is coincidental with that observed in the V_N^* (net retention volume corrected for carrier gas nonideality) vs. \bar{P} , and θ (apparent fraction of surface covered by the carrier gas) vs. \bar{P} plots contained in the previous article¹. Since χ is not directly related to V_N^* (and in turn θ), then the first suggested reason for the presence of the minima must be dismissed. More clearly, in its simplest form V_N^* is a function of F_0 , t_R , and j and at constant pressure drop across the column the effect of changing χ will be only to alter F_0 and t_R , but these vary in such a way so as to keep V_N^* constant.

The secondary mechanism which is probably responsible for the coincidental departure must be such as to affect both χ and V_N^* (or θ) simultaneously. It must be remembered that the anomalous effect is observed only in the helium case, indicating that only helium can participate in this type of mechanism. If it can be assumed that helium being of the right size and/or having the property such that at elevated pressure drops certain channels become permeable to it then the flow through the column will be somewhat greater than that predicted by eqns. 28 and 12 combined. Since F_0 is the total flow measured at the column outlet, then from the definition of χ there will be an increase in χ (above that predicted by eqn. 29) proportional to the magnitude of the secondary flow.

If we define F_n and F_s as the normal interparticle flow and the secondary flow respectively, and if for the present we assume gas ideality, then essentially the net retention volume was calculated in ref. 1 by:

$$V_N = t_R j (F_n + F_s) - V_M \quad (32)$$

where as in ref. 1 V_M is the column volume accessible to the carrier gas and $(F_n + F_s)$ is merely F_0 . Now, since methane like Ar and CO₂ cannot participate in the secondary flow then it is incorrect to use F_0 in the calculation of V_N . The correct expression for V_N should be

$$V_N = F_n t_R j - V_M \quad (33)$$

and consequently V_N as calculated by eqn. 32 is larger than the true value by $F_s t_R j$.

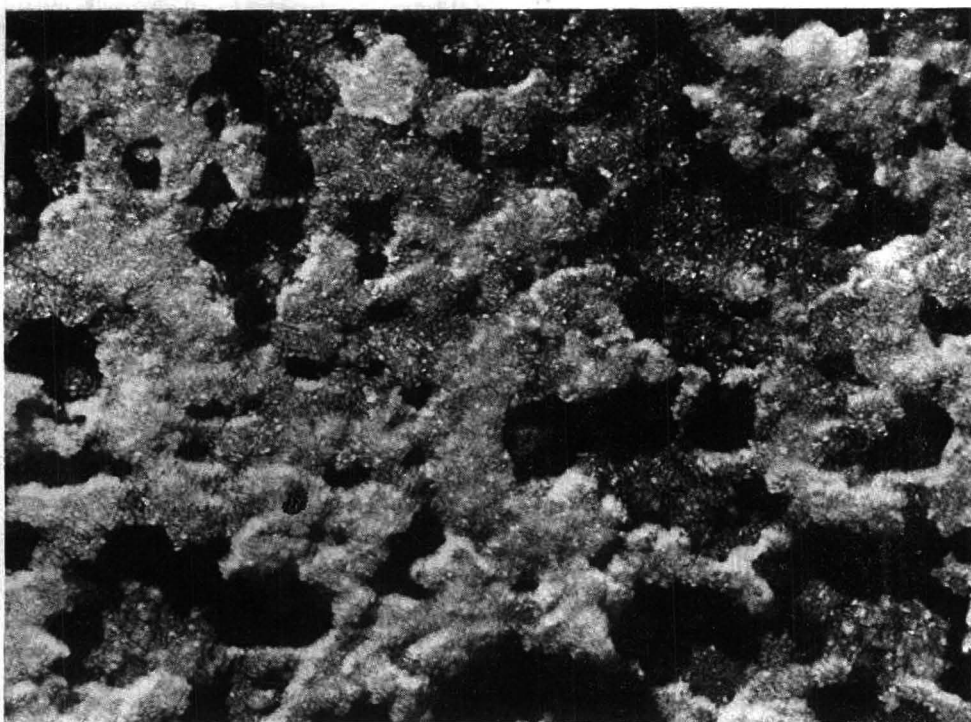
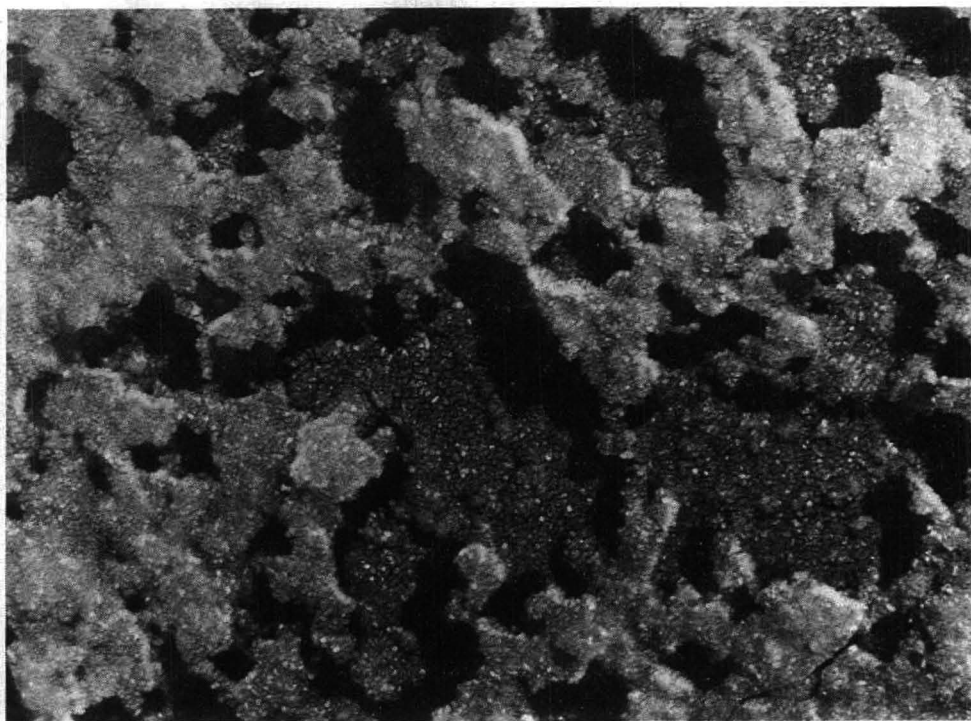


Fig. 7. Electronmicrographs of Porapak S.

Since F_s is expected to increase with increasing pressure drop, so will this difference. This is what is observed experimentally.

The secondary flow mechanism seems to satisfy, at least qualitatively, the experimental data. The limited range of this anomalous effect and the experimental scatter make a quantitative discussion fruitless. More can and will be said when the experimental range is extended to much higher \bar{P} .

The interparticle porosity was calculated from eqn. 14 (constant factor of 1/180) and eqn. 15 (constant factor at 1/150) using $B_0 = 5.26 \times 10^{-7}$ cm² and $d_p = 0.02$ cm and was found to be 0.427 and 0.410, respectively. The total porosity was calculated from eqn. 16. V_M and $V_T (\pi r^2 L)$ were found to be 89.5 and 130.5 cc, respectively, thus making $\varepsilon_T = 0.685$. Comparing this to the average of the interparticle porosity ($\varepsilon = 0.419$) shows that although the particles appear to be smooth and spherical under low magnification ($\sim 30\times$) they are indeed quite porous ($\Delta \simeq 0.267$). In fact the particle porosity is calculated to be about 0.47 which means that at least 47 % of the particle is empty space. This is in good agreement with the electronmicrographs shown in Fig. 7.

In order to test whether the present experimental data is governed by the Ergun relationship, $1/B$ was plotted against F_0 . These plots are shown in Figs. 8–10 for He I, Ar II and CO₂ I, respectively. Included in each figure is the plot of eqn. 23 as well as the Reynolds number.

As can be seen in all three figures there is very little (if any) resemblance between the experimental curves and those dictated by the Ergun equation. All three figures show that the permeability coefficient decreases at a much faster rate than that predicted by eqn. 23, this being particularly true for the low flow rate region. In the case of Ar and CO₂, however, the slopes of the experimental curves do decrease and begin to approach those of the Ergun equation as the flow is increased. This may also be true in the helium case but the undue increase in permeability masks this.

One feature common to all three figures is the break in the curve at F_0 of about

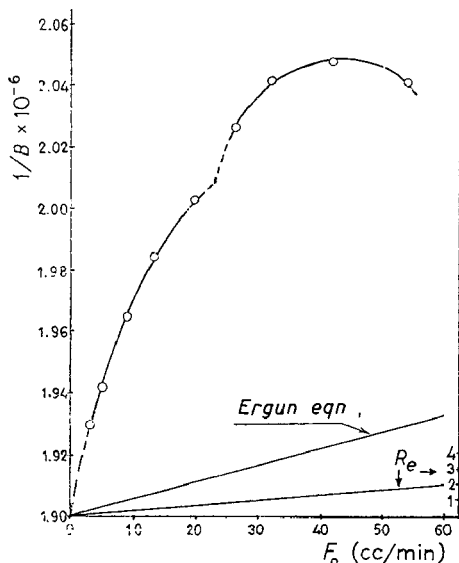
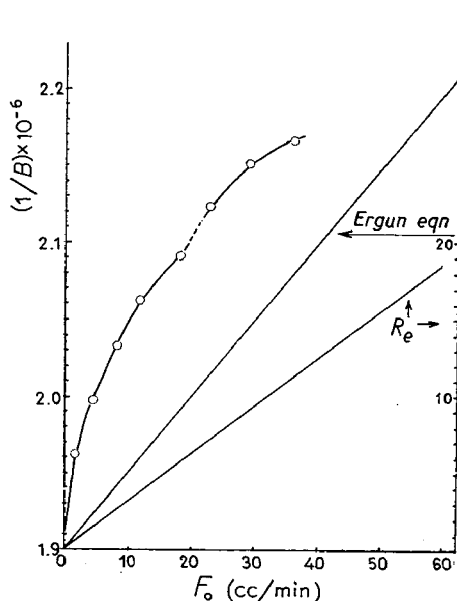
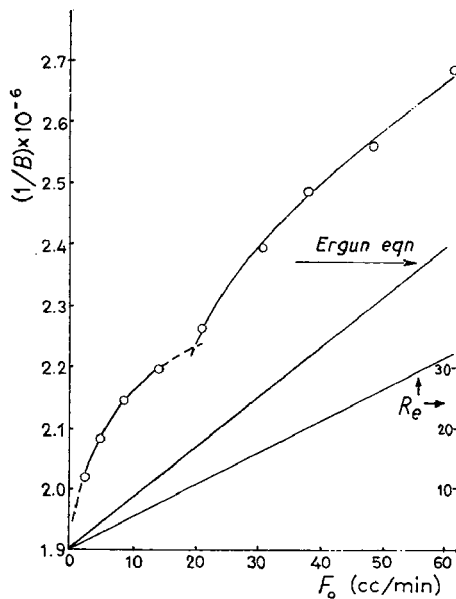


Fig. 8. $1/B$ as a function of F_0 for He I.

Fig. 9. $1/B$ as a function of F_o for Ar II.Fig. 10. $1/B$ as a function of F_o for CO_2 I.

20 cc/min. This cascading variation may be the result of flow induced decrease of inter-particle porosity in the individual sections of the column (it must be remembered that the resulting 200 ft. column is made up of four terminated 50 ft. sections). This is not unreasonable if one considers that in the vicinity of $\epsilon = 0.4$ a 1% change in the inter-particle porosity alters the permeability by some 5%. From the three figures it would appear (if the mechanism is valid) that only two of the four sections are affected and these would necessarily be those closest to the column outlet where the gas velocity is the greatest.

All the experiments that have been carried out are grouped as follows. The first group contains He I, Ar II, Ar III and CO_2 I (these experiments have already been discussed) and the second group contains experiments Ar I, CO_2 II, CO_2 III and CO_2 IV. The basic difference between the two groups is the way in which the working inlet pressures were approached. In the first group an experiment was carried out by starting at the highest operating inlet pressure. After the completion of a run the pressure regulating valve was turned down by a suitable amount and the pressure was allowed to fall relatively slowly to the next highest operating pressure. All subsequent operating pressures were approached in the same way.

Experiment Ar I and CO_2 IV were carried out starting at the lowest inlet pressure and incrementally increasing it to highest value. Under these conditions the alteration of the pressure regulating valve resulted in a sudden inrush of gas into the column and as a result the column experienced a pressure pulse before it reached a steady state.

In experiment CO_2 II, the inlet pressure was first allowed to fall to about 4 p.s.i. above the atmospheric (4 p.s.i. + P_o), after which it was raised to the first operating

pressure (19.25 p.s.i. + P_0). After sufficient equilibrium time (~ 16 h) the first experiment was performed. The subsequent experiments were carried out as in Ar I and CO₂ IV.

The only difference between experiments CO₂ II and CO₂ III is that in experiment CO₂ III the inlet pressure was first allowed to fall to approximately (16 p.s.i. + P_0) after which it was raised to the first operating pressure (20.2 p.s.i. + P_0).

The results of the second group of experiments are summarised by plotting χ vs. \bar{P} in Fig. 11 (Ar) and Fig. 12 (CO₂). For comparison Fig. 5 and Fig. 6 are also reproduced in Fig. 11 and Fig. 12, respectively. Comparing the results of the first group to those of the second group shows that the relationship between χ and \bar{P} is not only dependent on whether the inlet pressure is altered in an increasing or decreasing direction but it also depends on the initial starting conditions (comparison of CO₂ II, CO₂ III and CO₂ IV).

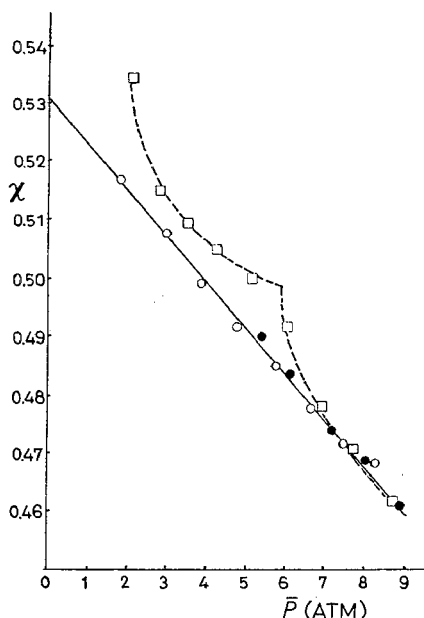


Fig. 11. χ as a function of \bar{P} for Ar I and Ar(II and III). \square = Ar I; \circ = Ar II; \bullet = Ar III.

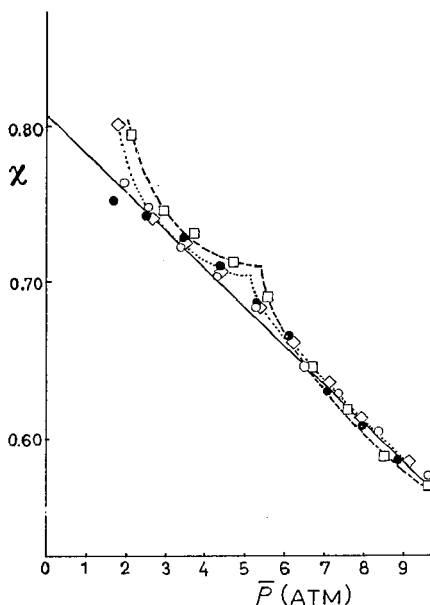


Fig. 12. χ as a function of \bar{P} for CO₂ I, CO₂ II, CO₂ III and CO₂ IV. \circ = CO₂ I; \bullet = CO₂ II; \diamond = CO₂ III; \square = CO₂ IV.

The experiments Ar I, Ar II, CO₂ II, CO₂ III, CO₂ IV and Ar III were performed in the order written. Considering this and the fact that the experiments are reproducible leads to the conclusion that the column behaves as if though it possessed a permeability hysteresis. The term hysteresis serves here only to describe the fact that a different set of results are obtained by changing the direction in which the inlet pressure is altered. This hysteresis effect is not only found in the permeability study but it also appears in the plate height study. This is illustrated in Fig. 13 where \hat{H}/f_2 is plotted against $u_0 P_0$ for the Ar I, Ar II, and Ar IV experiments where CH₄ was the

solute. A similar effect is also found for the CO_2 case but the inclusion of such a plot would be of no additional interest.

In both Figs. 11 and 12 the break in the curve is unmistakable. In both cases this break occurs at a \bar{P} value close to 6 atm which corresponds to F_0 of about 20 cc/min. In the first group of experiments the break in the curve was found in the $1/B$ vs. F_0 plot whereas in the second group of experiments this is found in the χ vs. \bar{P} plot.

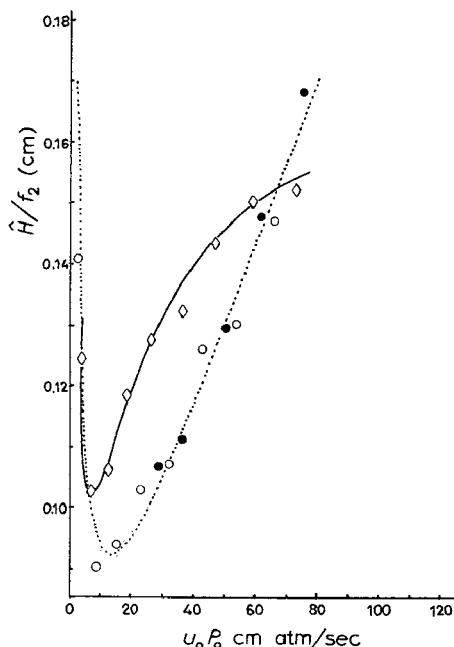


Fig. 13. Plot of \hat{H}/f_2 as a function of $u_0 P_0$ for Ar I and Ar(II and III). \diamond = Ar I; \circ = Ar II; \bullet = Ar III.

Finally a common $1/B$ vs. F_0 plot for Ar and for CO_2 (not included) reveals that for either carrier gas although the individual experimental plots are non linear they do tend to approach a common straight line whose slope is somewhat similar to that predicted by the Ergun equation. The experimental scatter about this central line is not from experimental uncertainty for each point consists of about six flow rate measurements each with the reproducibility of better than $\pm 0.01\%$. The experimental line is vertically displaced from the Ergun equation in the direction of higher $1/B$ suggesting that extrapolation from the high F_0 region leads to a lower column permeability. This is in accord with the particle shift (compacting) proposal.

ACKNOWLEDGEMENTS

We wish to thank the National Research Council of Canada for the financial assistance. We would also like to thank Dr. P. K. ISAAC for the electron photomicrographs of Porapak S cross sections.

REFERENCES

- 1 J. J. CZUBRYT, H. D. GESSER AND E. BOCK, *J. Chromatog.*, 53 (1970) 439
- 2 L. PRANDTL, *Essentials of Fluid Dynamics*, Blackie, Glasgow, 1954, p. 102
- 3 Fluid Motion Memoirs: *Laminar Boundry Layers*, Rosenhead, Oxford (Clarendon Press), 1963, p. 121.
- 4 J. C. GIDDINGS, *Dynamics of Chromatography*, Part I, Marcel Dekker, New York, 1965, pp. 199-224.
- 5 P. C. CARMAN, *Flow of Gases Through Porous Media*, Butterworths, London, 1956.
- 6 H. PURNELL, *Gas Chromatography*, Wiley, New York, 1962, pp. 60-66.
- 7 G. GUIOCHON, *Chromatog. Rev.*, 8 (1966) 1
- 8 J. BOHEMAN AND J. H. PURNELL, *J. Chem. Soc.*, (1961) 360.
- 9 S. DAL NOGARE AND R. S. JUVET, JR., *Gas-Liquid Chromatography*, Interscience, New York, 1962, p. 134.
- 10 R. B. BIRD, W. E. STEWART AND E. N. LIGHTFOOT, *Transport Phenomena*, Wiley, New York, 1960, p. 199.
- 11 D. A. WHITE, *Chem. Eng. Sci.*, 22 (1967) 669.
- 12 T. SEELY, *J. Polymer Sci.*, 5 (1967) 3029.
- 13 W. L. McCABE AND J. C. SMITH, *Unit Operations of Chemical Engineering*, McGraw-Hill, New York, 1967, p. 161.
- 14 J. C. REISCH, C. H. ROBINSON AND T. D. WHEELLOCK, in N. BRENNER, J. E. CALLEN AND M. D. WEISS (Editors), *Gas Chromatography*, Academic Press, New York, 1962, p. 91.
- 15 J. HALASZ AND H. D. GERLACH, *Anal. Chem.*, 38 (1966) 281.
- 16 G. L. HARGROVE AND D. T. SAWYER, *Anal. Chem.*, 39 (1967) 9115.
- 17 E. A. MOELWYN-HUGHES, *Physical Chemistry*, Pergamon Press, London, 1961, p. 610.
- 18 D. E. MARTIRE AND D. C. LOCKE, *Anal. Chem.*, 37 (1965) 144.

J. Chromatog., 53 (1970) 453-467

CHROM. 5004

PEAK BROADENING IN PAPER CHROMATOGRAPHY AND RELATED TECHNIQUES

VII. THE CONTRIBUTION OF THE MACROSCOPIC MOBILE PHASE VELOCITY PROFILE TO PEAK BROADENING IN PAPER AND THIN-LAYER CHROMATOGRAPHY

C. L. DE LIGNY AND W. VAN DE MEENT

Laboratory for Analytical Chemistry, State University, Croesestraat 77 A, Utrecht (The Netherlands)

(Received July 28th, 1970)

SUMMARY

The contribution of the macroscopic mobile phase velocity profile in a paper or thin-layer strip to longitudinal dispersion in chromatography was investigated. For this purpose the dependence of the plate height on the breadth of the paper or thin-layer strip, scanned by the densitometer, was determined using Whatman W2 paper and Camag D cellulose powder. As longitudinal dispersion depends on transversal (convective and diffusive) dispersion, the latter was determined for both chromatographic techniques.

INTRODUCTION

Longitudinal dispersion in chromatography can be described by the equation:

$$H = \frac{\sigma^2}{\mu} = B \frac{\bar{1}}{\bar{u}} + C_M \bar{u} + C_S \bar{u} + C_F(u) \bar{u} + C_E(u) \bar{u} \quad (1)$$

where

H = height equivalent to a theoretical plate,

σ = standard deviation of the solute distribution in the medium used for chromatography,

μ = distance travelled by the solute,

\bar{u} = mean flow rate of the eluent.

The terms B , C_M , C_S , $C_F(u)$ and $C_E(u)$ are concerned with longitudinal diffusion, resistance to attainment of the partition equilibrium in the mobile and in the stationary phase, the macroscopic mobile phase velocity profile and eddy diffusion, respectively.

DE LIGNY AND BAX¹ showed that peak broadening in paper chromatography at

low liquid velocity ($0.0005 \text{ cm} \cdot \text{sec}^{-1}$) is exclusively caused by longitudinal diffusion, both in the mobile and the stationary phases. At higher liquid velocities (up to $0.002 \text{ cm} \cdot \text{sec}^{-1}$) DE LIGNY AND REMIJNSE² demonstrated, in addition, the occurrence of slow attainment of the partition equilibrium. The slow mass transfer between the mobile and the stationary phase appeared to be caused mainly by slowness of diffusion in the mobile phase³. For thin-layer chromatography similar results were obtained⁴. A contribution of the mobile phase velocity profile (or, possibly, the $C_S \bar{u}$ and $C_E(u) \bar{u}$ terms) was found only in paper chromatography³.

The various terms in the right-hand side of Eqn. 1 can be specified as follows for paper and thin-layer chromatography³⁻⁵:

$$B \frac{\bar{1}}{u} = \frac{\sigma^2_{\text{diff}}}{\mu} = \frac{2\gamma_M D_M R_F t + 2\gamma_S D_S (1 - R_F) t}{\mu} \quad (2)$$

$$C_M \bar{u} = 0.01(1 - R_F)^2 \frac{d_p^2}{D_M} \bar{u} \quad (3)$$

$$C_S \bar{u} = \frac{2}{3} R_F (1 - R_F) \frac{d_f^2}{D_S} \bar{u} \quad (4)$$

$$C_F(u) \bar{u} = \frac{2\kappa L^2}{\lambda_R d_p \bar{u} + \gamma_M D_M + \gamma_S D_S (1 - R_F)/R_F} \bar{u} \quad (5)$$

$$C_E(u) \bar{u} = \frac{2\kappa' d_p^2}{\lambda_R d_p \bar{u} + \gamma_M D_M + \gamma_S D_S (1 - R_F)/R_F} \bar{u} \quad (6)$$

where:

γ = tortuosity factor,

D = diffusion coefficient,

R_F = ratio of the distances travelled by the solute and by the eluent,

t = elution time,

d_p = diameter of the support particles,

d_f = thickness of the layer of stationary fluid on the support particles,

$\kappa, \kappa', \lambda_R$ = dimensionless constants, depending on the dynamics of flow,

L = dimension, characteristic for the flow profile (breadth of the paper or thin-layer strip scanned by the densitometer, or mean distance between maxima or minima in the flow profile, whichever is the smaller).

$$\bar{u} = \frac{0.4 k}{l_f - l_0} \ln \frac{l_f}{l_0}$$

$$k = \frac{l_f^2 - l_0^2}{t}$$

l_f = distance from the surface of the eluent in the tank to the solvent front,

l_0 = distance from the surface of the eluent in the tank to the starting point.

Transversal dispersion can be described by⁵:

$$\sigma^2_{\text{tr, chrom}} = \sigma^2_{\text{tr, conv}} + \sigma^2_{\text{tr, diff}} = 2(\lambda_R d_p \bar{u} + \gamma_M D_M + \gamma_S D_S (1 - R_F)/R_F) t \quad (7)$$

The first term between brackets represents convective dispersion, the other one diffusive dispersion. According to Eqn. 5, the contribution of the flow profile term can be assessed in a straightforward way by determining the plate height H as a function of the breadth L of the paper or thin-layer strip scanned by the densitometer. As the contributions of the $B \cdot \overline{1/u}$ and $C_M \bar{u}$ terms can be calculated from previous work^{3,4}, the contribution of the $C_S \bar{u}$ and $C_E(u) \bar{u}$ terms (if different from zero) can then be estimated from the extrapolated value of H at $L = 0$. When the transversal dispersion is also measured, the value of κ can be determined from Eqns. 5 and 7. Further, the value of λ_R can be obtained as estimates of d_p , γ , D and R_F have been made previously^{1,3,4}.

EXPERIMENTAL

Chemicals

L-Valine, Whatman W 2 paper, Camag D cellulose powder, were used.

Procedure

(a) *Determination of H as a function of L .* The chromatograms were obtained and stained as described earlier⁶. Then each band was divided in parts with a length equal to the slit length used in the densitometer. The travelled distance, μ , and the variance originating from the chromatographic transport, σ^2 , were determined for each part*.

(b) *Determination of transversal dispersion.* The variance, originating from transversal convective and diffusive dispersion, $\sigma_{tr,chrom}^2$, was determined by applying the bands parallel to the elution direction and eluting, staining and scanning them as described earlier (ref. 6)*. The variance, originating from transversal diffusive dispersion in paper chromatography, $\sigma_{tr,diff}^2$, was determined by applying the bands parallel to the elution direction, leaving them to diffuse for a certain time, staining and scanning them as described earlier (ref. 1)*. The corresponding variance in thin-layer chromatography was calculated from the known values of γ , D and R_F ** . The variance, originating from transversal convective dispersion, $\sigma_{tr,conv}^2$, can then be calculated by difference.

Calculations

As described in the foregoing section under (a), each eluted and stained band was divided in q parts of length a , so that $q \cdot a = b$, where a is the applied slit length of the densitometer and b is the total length of the band. The variance, σ^2 , and the position of the maximum, μ , of the solute distribution were determined for each part. On the score of the unevenness of flow over the distance b , each part of the band has its own particular value of σ^2 and of μ . So, the result of the measurements on one band is:

$$\mu_1, \mu_2 \dots \mu_i \dots \mu_q$$

$$\sigma_1^2, \sigma_2^2 \dots \sigma_i^2 \dots \sigma_q^2$$

* All variances were corrected for the variance originating from the application procedure and the equilibration period.

** This is not warranted in the case of paper chromatography, in view of the possibility that the tortuosity factors parallel and perpendicular to the machine direction are different.

TABLE I

TRANSVERSAL DISPERSION IN PAPER CHROMATOGRAPHY; CALCULATION OF λ_R

$\sigma_{tr, diff}^2$ (mm^2)	t (sec)	$\gamma M D_M +$ $\gamma S D_S(1-R_F)/R_F$ ($mm^2 \cdot sec^{-1}$)	$\sigma_{tr, chrom}^2$ (mm^2)	t (sec)	$\lambda_R d_p \bar{u} + \gamma M D_M +$ $\gamma S D_S(1-R_F)/R_F$ ($mm^2 \cdot sec^{-1}$)	\bar{u} ($mm \cdot sec^{-1}$)	$\lambda_R d_p$ (mm)	d_p (mm) (ref. 3)	λ_R
4.88	16 020	1.52×10^{-4}	8.39	13 720	3.06×10^{-4}	1.13×10^{-4}	75.3×10^{-4}	0.0150	
7.26	15 720	2.31	9.14	14 430	3.17	1.24	71.6	0.0173	
5.63	15 480	1.82	7.50	14 090	2.66	0.73	74.7	0.0098	
5.66	14 040	2.02	8.78	13 690	3.21	1.28	71.8	0.0178	
5.57	14 100	1.98							
Mean ^a		$(1.93 \pm 0.28) \times 10^{-4}$						0.0150 ± 0.0041	0.016 ± 0.008

^a Accuracy is given throughout this paper as the 90% probability interval.

TABLE II

TRANSVERSAL DISPERSION IN THIN-LAYER CHROMATOGRAPHY; CALCULATION OF λ_R

$\gamma M D_M +$ $\gamma S D_S(1-R_F)/R_F$ ($mm^2 \cdot sec^{-1}$)	$\sigma_{tr, chrom}^2$ (mm^2)	t (sec)	$\lambda_R d_p \bar{u} + \gamma M D_M +$ $\gamma S D_S(1-R_F)/R_F$ ($mm^2 \cdot sec^{-1}$)	\bar{u} ($mm \cdot sec^{-1}$)	$\lambda_R d_p$ (mm)	d_p (mm) (ref. 4)	λ_R
	3.00	7800	1.92×10^{-4}	151×10^{-4}	0.0041		
	2.51	7800	1.61	151	0.0020		
	2.61	7800	1.67	149	0.0024		
	2.49	7800	1.60	147	0.0020		
	2.61	7800	1.67	146	0.0025		
$(1.30 \pm 0.13) \times 10^{-4}$					0.0026 ± 0.0008	0.32 ± 0.02	0.008 ± 0.003

Now we introduce σ_p^2 for the variance of a composite part of the band, composed of p neighbouring strips (breadth equal to $L = p \cdot a$; $p = 1, 2, 3 \dots q$). μ_p is the mean distance travelled by the solute in the part of the band of length L . It follows from the principle of the additivity of independent variances that the total variance of the solute distribution in the considered composite part of the band is equal to the sum of the variance within a single strip and the variance between strips:

$$\sigma_p^2 = \frac{1}{p} \sum_{i=1}^p \sigma_i^2 + \frac{1}{p} \sum_{i=1}^p (\mu_i - \mu_p)^2 \quad (8)$$

where:

$$\mu_p = \frac{1}{p} \sum_{i=1}^p \mu_i$$

Further:

$$H_p = \frac{\sigma_p^2}{\mu_p} = \frac{1}{p\mu_p} \sum_{i=1}^p \{\sigma_i^2 + (\mu_i - \mu_p)^2\} = c + dL^2 \quad (9)$$

where:

$$c = B \frac{1}{u} + C_M \bar{u} + C_S \bar{u} + C_E(u) \bar{u} \quad (10)$$

and:

$$d = \frac{2\kappa}{\lambda_R d_p \bar{u} + \gamma_M D_M + \gamma_S D_S (1 - R_F)/R_F} \bar{u} \quad (11)$$

RESULTS

The values of μ_p at various values of p (or L) are shown in Fig. 1. The data on transversal dispersion are shown in Tables I and II.

DISCUSSION

We observe in Fig. 1 that H hardly increases further when L exceeds 6 mm. Therefore, to estimate c and d in Eqn. 9, straight lines were drawn through the points corresponding to the smallest two L values. Furthermore, lines parallel to the abscissa were drawn through the remaining points. The points of intersection with the sloping lines give approximately the distance between maxima or minima in the macroscopic flow velocity profile. The mean values of this distance are 9 and 8 mm in paper and thin-layer chromatography, respectively.

From the difference between the H values at $L = 0$ and $L > 9$, respectively 8 mm, the (maximum) value of the $C_F(u)\bar{u}$ term follows, that is observed in practice. For paper and thin-layer chromatography, this term amounts to 0.01 and 0.001 mm, respectively. Previously⁴, it was found that in paper chromatography $C_F(u)\bar{u} + C_E(u)\bar{u} + C_S\bar{u} = 0.07 \pm 0.03$ mm (using a densitometer slit length L of 6 mm). It follows from these data that $C_E(u)\bar{u} + C_S\bar{u} = 0.06 \pm 0.03$ mm.

From the slopes of the graphs in Fig. 1 and \bar{u} , the values of

$$\frac{\kappa}{\lambda_R d_p \bar{u} + \gamma_M D_M + \gamma_S D_S (1 - R_F)/R_F}$$

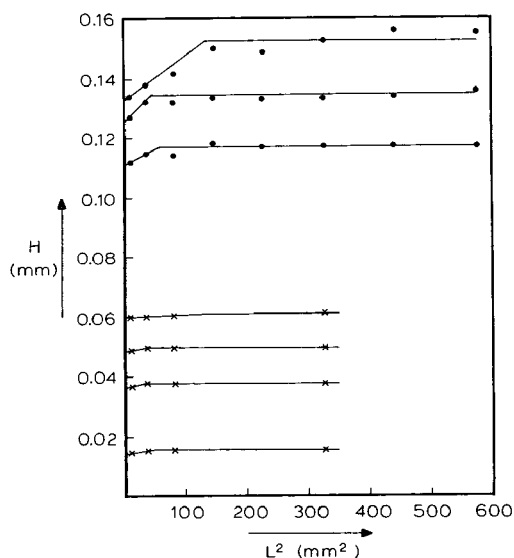


Fig. 1. Plate height H as a function of the breadth L of the paper or thin-layer strip scanned by the densitometer. ●, paper chromatography; ×, thin-layer chromatography.

TABLE III

CALCULATION OF κ IN PAPER CHROMATOGRAPHY

$\frac{\Delta H}{\Delta L^2}$ (mm ⁻¹)	\bar{u} (mm·sec ⁻¹)	κ $\lambda_R \bar{d}_p \bar{u} + \gamma_M D_M + \gamma_S D_S (1 - R_F) / R_F$ (mm ⁻² ·sec)	κ
1.89×10^{-4}	164×10^{-4}	57.6×10^{-4}	2.50×10^{-6}
0.96	169	28.5	1.26
1.59	190	41.9	2.08
Mean			$(1.9 \pm 0.8) \cdot 10^{-6}$

TABLE IV

CALCULATION OF κ IN THIN-LAYER CHROMATOGRAPHY

$\frac{\Delta H}{\Delta L^2}$ (mm ⁻¹)	\bar{u} (mm·sec ⁻¹)	κ $\lambda_R \bar{d}_p \bar{u} + \gamma_M D_M + \gamma_S D_S (1 - R_F) / R_F$ (mm ⁻² ·sec)	κ
0.259×10^{-4}	134×10^{-4}	9.6×10^{-4}	1.26×10^{-7}
0.074	134	2.8	0.36
0.222	135	8.2	1.07
0.259	135	9.6	1.25
Mean			$(1.0 \pm 0.5) \times 10^{-7}$

can be found. From the values of λ_R given in Tables I and II and the known values of D (ref. 1) d_p , γ , R_F (refs. 3, 4) and \bar{u} the denominator can be calculated, so that κ is obtained (Tables III and IV). κ equals $2 \cdot 10^{-6}$ and $1 \cdot 10^{-7}$ for paper and thin-layer chromatography, respectively. These values are of the same magnitude as expected from the values found for packed columns*

The value of $\gamma_M D_M + \gamma_S D_S (1 - R_F)/R_F$ found for transversal diffusive dispersion in paper chromatography $((1.93 \pm 0.19) \times 10^{-4} \text{ mm}^2 \cdot \text{sec}^{-1})$ (Table I) is in good accord with the value that is calculated using the γ values for longitudinal diffusive dispersion⁴ $((2.05 \pm 0.40) \times 10^{-4} \text{ mm}^2 \cdot \text{sec}^{-1})$. So, the tortuosity factors parallel and perpendicular to the machine direction appear to be equal, *a posteriori*.

The values found for λ_R , 0.016 and 0.008 for paper and thin-layer chromatography, respectively, are about an order of magnitude smaller than the values holding for packed columns (ref. 5)**.

CONCLUSIONS

As a result of our investigations in the field of peak broadening in paper and thin-layer chromatography, the various parameters determining this phenomenon can be specified as given in Table V, for Whatman W2 paper and Camag D cellulose powder.

TABLE V

PARAMETERS DETERMINING PLATE HEIGHT IN PAPER AND THIN-LAYER CHROMATOGRAPHY

Parameter	Dimension	Whatman W2 paper	Camag D cellulose powder
γ_M		0.60 ± 0.12	0.42 ± 0.29
γ_S		0.03 ± 0.02	0.02 ± 0.08
d_p	mm	0.91 ± 0.36	0.32 ± 0.02
$C_S \bar{u} + C_E(u) \bar{u}$	mm	0.06 ± 0.03	negligible
λ_R		0.016 ± 0.008	0.008 ± 0.003
κ		$(1.9 \pm 0.8) \times 10^{-6}$	$(1.0 \pm 0.5) \times 10^{-7}$

REFERENCES

- 1 C. L. DE LIGNY AND D. BAX, *Z. Anal. Chem.*, 205 (1964) 333.
- 2 C. L. DE LIGNY AND A. G. REMIJNSE, *Rec. Trav. Chim.*, 86 (1967) 410.
- 3 C. L. DE LIGNY AND A. G. REMIJNSE, *J. Chromatog.*, 35 (1968) 257.
- 4 C. L. DE LIGNY AND A. G. REMIJNSE, *J. Chromatog.*, 33 (1968) 242.
- 5 C. L. DE LIGNY, *J. Chromatog.*, 49 (1970) 393.
- 6 C. L. DE LIGNY AND A. G. REMIJNSE, *Rec. Trav. Chim.*, 86 (1967) 421.

* If (see ref. 5, Eqn. 16 and Fig. 4) in the calculation of the expected value of $\kappa'/\rho^2 + \kappa \simeq \kappa, \rho$ is calculated from the distance between maxima or minima in the mobile phase flow profile (~ 8 mm) and the real fiber diameter of the paper or the real diameter of the cellulose powder particles (~ 0.01 mm).

** However, if the real paper fiber diameter or the real diameter of the cellulose powder particles as given by the manufacturer^{3,4} are used in the calculation of λ_R , rather than the effective d_p values calculated from the $C_M \bar{u}$ term, values are found at least as large as the λ_R values holding for packed columns.

CHROM. 5073

A STUDY OF THE STRONTIUM AND BARIUM HALIDES AS COLUMN PACKINGS IN GAS-SOLID CHROMATOGRAPHY

ROBERT L. GROB, ROBERT J. GONDEK* AND THOMAS A. SCALES**

Chemistry Department, Villanova University, Villanova, Pa. 19085 (U.S.A.)

(Received July 20th, 1970)

SUMMARY

The halide salts (chloride, bromide, iodide) of strontium and barium have been investigated as column packings in gas-solid chromatography. Various groups of organic compounds have been studied, their heats of adsorption calculated and models presented to explain their behavior on these columns. Sample size required to produce overloading generally increased with increasing anion size in the packing. Retention volumes generally followed boiling points; two compounds having the same boiling point a greater adjusted retention volume was noted for the more polar compound. Chain branching reduced retention volume. Adjusted retention volume increased as size of anion in packing increased.

INTRODUCTION

The most exhaustive work in gas-solid chromatography (GSC) has been carried out using charcoal, alumina and silica gel. Since 1960, however, considerable attention has been focused on the use of inorganic salts either in eutectic mixtures adsorbed on a solid support or as a pure salt adsorbed on a solid support¹⁻⁷. In particular SOLOMON^{6,7} carried out a comprehensive study which included the use of alkaline earth salts and alkali metal halides, carbonates and sulfates which gave an indication of the versatility of inorganic salts in gas chromatography for separating many organic systems. In 1964, ALTENEAU AND ROGERS⁸ published their work on the use of the nitrate and sulfate salts of the ammonia and pyridine complexes of copper. Further an extensive study of the alkali chlorides and nitrates, using a variety of organic adsorbates, was done by GROB *et al.*⁹.

More recent work in the area of GSC represented an extensive investigation into specific interactions affecting retention, thermodynamics and separation efficiencies, and correlations of aromatic substituent effects¹⁰⁻¹⁴. These studies led to a thermodynamic gas chromatographic retention index for organic molecules.

Because of the great potential selectivity of solids, GSC is especially desirable for the separation of isomers and high molecular weight compounds^{6,7}. This selectivity,

* Present address: Applied Physics Laboratory, Sun Oil Company, Newtown Square, Pa., U.S.A.

** Present address: Research and Development Laboratory, ARCO Chemical Company, Philadelphia, Pa., U.S.A.

coupled with high column temperatures permissible prompted the present research dealing with an evaluation of the adsorptive properties of the barium and strontium halides (chloride, bromide and iodide) as column packings in GSC.

EXPERIMENTAL

Column preparation

The alkaline earth halides, with the exception of strontium iodide, were dehydrated in a muffle furnace at 400° using a nitrogen purge. Strontium iodide was dehydrated at 325° because higher temperatures results in slight decomposition and discoloration. After cooling in a vacuum desiccator, the halides were transferred to a dry box where they were ground with a mortar and pestle, sieved to 60/80 mesh, and packed into 6-ft. glass columns (O.D. 0.25 in., I.D. 0.23 in.) using vacuum and gentle tapping. 1/4 in. plugs of glass wool were used in both ends of the glass tubing. Silicon rubber plugs were then inserted into both ends of the packed columns. The columns were transferred directly to the chromatograph oven and conditioned for 24 h at 300° with a helium flow rate of 100 ml/min. It was often necessary to re-sieve and repack the columns after conditioning due to the formation of gas pockets within the column packings. Apparently the barium and strontium halides are very brittle and easily produce fines and pack tighter once carrier gas is passed through the column.

Sample syringes

One and ten microliter Hamilton syringes were used for all sampling.

Recorder

The recorder was a Leeds and Northrup Speedomax H with a 1 mV chart span.

Gas chromatograph

A modified Nester-Faust Anakro IA gas chromatograph equipped with a thermal conductivity detector was employed throughout the entire investigation. The gas chromatograph was modified to increase sensitivity of response and temperature control.

Inorganic salt packings

Barium and strontium chloride were obtained from Baker Chemical Co., Phillipsburg, N. J. and were Baker Analyzed quality. Barium bromide, strontium iodide and strontium bromide were obtained from Rocky Mountain Research Company, Denver, Colo. Barium iodide was acquired from the Fisher Scientific Company, Pittsburgh, Pa. The latter four halides were reagent grade. All of the salts were purchased as the di-hydrate.

Samples

All organic chemicals used for this investigation were supplied by Chemical Service Inc., Media, Pa. and were chromatographic grade.

Experimental conditions

The retention time for each sample was obtained in triplicate on each column at

temperatures of 170, 200, and 250° for the barium halides and 150, 200 and 250° for the strontium halides. Only those values which were reproducible within ± 0.1 sec were considered acceptable. The injection port temperature was 250° and the detector temperature was 360°. Carrier gas flow for the strontium halide columns was 40 ml/min and that for the barium halide columns was 60 ml/min. 0.1 μ l samples were used throughout the investigation.

RESULTS AND DISCUSSION

The samples used throughout this investigation can be classified into three main groups, *i.e.*, alcohols, carboxylic acids, and isomeric aromatic compounds. Heats of adsorption for the above compounds have been tabulated in Table I and Table II. Table III shows a selected group of aromatic compounds along with their adjusted retention volumes and heats of adsorption on the barium chloride column.

Alcohols

The alcohols shown in Table I are listed in order of increasing boiling point. Certain trends are immediately obvious. In all cases, as one proceeds from the chloride to the bromide to the iodide column for a specific cation, the heat of adsorption ($-\Delta H_a$) increases. It can be seen from the data for the C₁ to C₅ straight chain alcohols, that adsorption is not merely a function of boiling point as one might anticipate. It appears that dipole moment and possibly the formation of weak hydrogen-like bonds would best explain our results. The inversion of the methanol and ethanol

TABLE I

HEATS OF ADSORPTION FOR ALCOHOL AND CARBOXYLIC ACID SAMPLES(kcal/mole)^a

Sample	b.p.(°C)	Dipole moment	Column					
			SrCl ₂	SrBr ₂	SrI ₂	BaCl ₂	BaBr ₂	BaI ₂
<i>Alcohols</i>								
Methyl	64.6	1.68	0.78	1.26	6.22	6.71	7.80	a
Ethyl	78.5	1.71	1.51	3.69	8.59	4.81	5.21	a
Propyl	97.0	1.66	1.27	1.39	4.98	1.53	a ^b	a
n-Butyl	117.0	1.67	2.73	3.41	7.53	2.80	a	a
n-Amyl	138.0	1.73	3.53	4.12	8.52	2.81	a	a
Isopropyl	82.0	1.59	1.21	1.26	4.67	1.36	10.17	a
Isobutyl	108.0	1.64	1.79	2.86	7.52	1.23	a	a
sec.-Butyl	99.0	N.A. ^c	1.72	3.60	5.45	0.82	a	a
tert.-Butyl	82.8	N.A.	1.66	1.80	3.10	0.58	a	a
Isoamyl	131.5	N.A.	3.35	3.65	6.29	1.76	a	a
tert.-Amyl	102.0	N.A.	1.95	3.63	5.49	0.94	a	a
<i>Acids</i>								
Formic	100.7	1.52 ^d	0.28	2.22	a	2.70	3.61	a
Acetic	118.1	1.69	0.43	2.39	a	2.81	a	a
Propionic	141.0	1.76	1.22	2.95	a	5.61	a	a
Butyric	162.5	N.A.	2.21	3.36	a	7.03	a	a
Isobutyric	154.0	N.A.	1.21	2.39	a	4.22	a	a
Valeric	182.5	N.A.	a	a	a	7.36	a	a

^a All results are negative.

^b a = unable to calculate due to rounded peak tops and excessive tailing.

^c N.A. = not available.

^d Dipole moment = 1 for dimer at 150°.

TABLE II

HEATS OF ADSORPTION FOR AROMATIC SAMPLES(kcal/mole)^a

Sample	<i>b.p.</i> (°C)	Dipole moment	Column					
			SrCl ₂	SrBr ₂	SrI ₂	BaCl ₂	BaBr ₂	BaI ₂
Benzene	80.0	0.00	0.92	1.71	2.19	0.00	0.10	5.03
Toluene	110.6	0.37	1.46	2.80	4.15	0.00	2.13	6.56
Mesitylene	164.0	0.00	3.13	5.56	7.29	2.80	6.92	a ^b
<i>o</i> -Xylene	144.4	0.62	2.28	2.67	7.16	1.11	5.62	8.92
<i>m</i> -Xylene	139.8	N.A. ^c	2.06	2.91	6.22	N.A.	N.A.	N.A.
<i>p</i> -Xylene	138.4	0.00	2.56	2.60	9.26	1.76	5.65	8.79
Cl-Benzene	131.0	1.70	1.33	2.03	2.49	2.11	6.46	6.55
Br-Benzene	155.5	1.70	1.95	3.59	3.81	2.81	6.50	6.56
I-Benzene	188.6	1.70	3.13	5.59	6.64	8.43	12.58	12.64
Cumene	151.5	0.65	1.98	3.74	4.48	2.81	7.34	10.62
<i>p</i> -Cymene	177.0	N.A.	2.68	3.80	6.25	2.80	8.00	a
<i>o</i> -Cl-Toluene	158.0	1.57	1.80	2.80	5.02	2.62	4.21	9.31
<i>m</i> -Cl-Toluene	161.0	N.A.	2.48	3.09	4.32	2.68	4.25	9.94
<i>p</i> -Cl-Toluene	167.0	2.21	2.19	2.24	4.29	2.81	4.28	9.95
<i>o</i> -Br-Toluene	181.8	N.A.	N.A.	N.A.	N.A.	2.70	4.16	9.34
<i>m</i> -Br-Toluene	183.7	N.A.	N.A.	N.A.	N.A.	2.73	4.19	9.64
<i>p</i> -Br-Toluene	184.0	N.A.	N.A.	N.A.	N.A.	2.77	4.23	9.74
<i>m</i> -DiCl-benzene	172.0	1.68	N.A.	N.A.	N.A.	1.07	2.62	5.62
<i>o</i> -DiCl-benzene	181.0	2.51	1.96	2.16	a	4.23	6.56	9.96

^a All results are negative.^b a = Unable to calculate due to rounded peak tops and excessive tailing.^c N.A. = not available.

TABLE III

ADJUSTED RETENTION VOLUMES AND HEATS OF ADSORPTION FOR SELECTED AROMATIC COMPOUNDS ON BARIUM CHLORIDE AT 250°, 200°, 170°

Compound	<i>b.p.</i> (°C)	Adjusted retention volume (ml)			Heat of adsorption (kcal/mole) ^a
		250°C	200°C	170°C	
<i>o</i> -Toluidine	199.8	1.2	3.0	13.5	5.57
<i>m</i> -Toluidine	203.0	1.8	4.9	18.3	6.09
<i>o</i> -Cl Aniline	208.8	1.6	2.3	16.9	2.23
<i>o</i> -NO ₂ Toluene	222.3	1.7	2.6	17.3	2.59
Nitrobenzene	210.9	4.6	8.0	30.2	3.37
<i>o</i> -Anisidine	225.0	3.4	8.6	31.0	6.83
<i>m</i> -Nitrotoluene	231.0	2.0	3.3	15.8	3.06

^a All results are negative.

heats of adsorption on the barium halide columns seems to be a combined results of the increased electropositive character of the larger barium ion and the difference in polarity between methanol and ethanol. It also could be attributed to the solubility differences of the barium and strontium halides in methanol and ethanol. Anhydrous SrCl₂ is sparingly soluble in methanol, whereas BaCl₂ is moderately soluble. The bromide and iodide of barium and strontium are readily soluble in methanol¹⁵.

Chain branching appears to have a significant effect on the heat of adsorption.

The data for the normal and branched alcohols support this observation. Increased branching usually results in an increase in the heat of adsorption. This increase in adsorption is partly due to the change in structure resulting from the increasing number of alkyl groups in the α - and β -positions to the hydroxyl group. These alkyl groups would effectively orient the hydroxyl group in reference to the solid surface seen by the molecule. This can be seen by comparison of the alcohol structures in Table IV.

Carboxylic acids

The heats of adsorption for the carboxylic acids increase as the boiling point increases and, as in the case of the alcohols, branching of the acids results in affecting the heat of adsorption. The absence of any anomalous results for formic and acetic acids, which might compare with the heat of adsorption for methanol and ethanol indicates the possibility of gas phase dimer formation. The carboxylic acids were eluted from strontium and barium iodide and barium bromide columns only under the most severe conditions. The resulting peaks were characterized by rounded tops and excessive tailing. Calculations of heats of adsorption for these samples were not possible.

Aromatic samples

The aromatic samples in Table II exhibit a variety of different interactions. As one adds electron releasing groups to the ring, the heat of adsorption increases. This increase also corresponds to the increase in boiling point, but appears unrelated to the change in gas phase dipole moment. The electron releasing methyl group in the series benzene, toluene, *m*-xylene, and mesitylene increases the π -electron density in the ring and consequently allows for successively greater adsorption.

Consideration of the halogenated benzenes, which have the same gas phase dipole moments, show that their heats of adsorption increase in a trend corresponding to their boiling points. They also follow the trend of charge transfer stabilities between Ag^+ with benzene and halobenzenes¹⁶. The halogen atom is an electron withdrawing group and decreases the electron density in the ring. As a result of this decrease in π -electron density the halobenzenes are not as strongly adsorbed as the alkyl substituted aromatics of comparable boiling point. A comparison of the heats of adsorption for cumene (b.p. 151.5°) and bromobenzene (b.p. 155.5°) on both the strontium and barium halide columns, and toluene (b.p. 110.6°) and chlorobenzene (b.p. 132.0°) on the strontium halide columns supports this observation. This data appears to be in good agreement with similar results published by ALTENEAU AND ROGERS⁸ and BROOKMAN AND SAWYER¹⁰. Fig. 1 shows a plot of ΔH_a versus boiling point for the halobenzenes. With the exception of the barium bromide column there is a gradual increase in heat of adsorption progressing from benzene to chlorobenzene to bromobenzene. One then notes a big increase in ΔH_a from bromobenzene to iodobenzene. This same type of trend is noted with the relative charge transfer stabilities of the Ag^+ with the same four compounds¹⁶.

Combining the electron withdrawing halogen and the electron releasing alkyl groups should yield a heat of adsorption somewhat lower than that obtained for a dialkyl substituted aromatic of comparable boiling point. This is found to be true when one considers the heat of adsorption for *p*-chlorotoluene (b.p. 162.4°) compared to *p*-xylene (b.p. 138.4°) on the strontium halide columns, and *p*-bromotoluene (b.p.

TABLE IV

EFFECT OF SUBSTITUENTS

Compound	Substituent				$-\Delta H_a$		
	α	β	b.p.	μ	SrCl ₂	SrBr ₂	SrI ₂
$\begin{array}{c} \text{H} \\ \\ \text{CH}_3-\text{C}-\text{H} \\ \\ \text{OH} \end{array}$	—	—	78.5	1.71	1.51	3.69	8.59
$\begin{array}{c} \text{H} \\ \\ \text{CH}_3-\text{C}-\text{CH}_3 \\ \\ \text{OH} \end{array}$	1	—	82.0	1.59	1.21	1.26	4.67
$\begin{array}{c} \text{CH}_3 \\ \\ \text{CH}_3-\text{C}-\text{CH}_3 \\ \\ \text{OH} \end{array}$	2	—	82.8	—	1.66	1.80	3.10
$\begin{array}{c} \text{CH}_3 \\ \diagdown \\ \text{CH}_2-\text{CH}_2 \\ \diagup \quad \\ \quad \text{OH} \end{array}$	—	1	97.0	1.66	1.27	1.37	4.98
$\begin{array}{c} \text{CH}_3 \quad \text{CH}_3 \\ \diagdown \quad \\ \text{CH}_2-\text{CH} \\ \diagup \quad \\ \quad \text{OH} \end{array}$	1	1	99.0	—	1.72	3.60	5.45
$\begin{array}{c} \text{CH}_3 \quad \text{CH}_3 \\ \diagdown \quad \\ \text{CH}_2-\text{C}-\text{CH}_3 \\ \\ \text{OH} \end{array}$	2	1	102	—	1.95	3.63	5.49
$\begin{array}{c} \text{CH}_3-\text{CH}_2 \\ \\ \text{OH} \end{array}$	—	—	78.5	1.71	1.51	3.69	8.59
$\begin{array}{c} \text{CH}_3 \\ \diagdown \\ \text{CH}_2-\text{CH}_2 \\ \\ \text{OH} \end{array}$	—	1	97.0	1.66	1.27	1.37	4.98
$\begin{array}{c} \text{CH}_3 \quad \text{H} \\ \diagdown \quad \\ \text{C}-\text{CH}_2 \\ \diagup \quad \\ \text{CH}_3 \quad \text{OH} \end{array}$	—	2	108	1.64	1.79	2.86	7.52

TABLE IV (continued)

Compound	Substituent				$-\Delta H_a$		
	α	β	b.p.	μ	SrCl ₂	SrBr ₂	SrI ₂
$\begin{array}{c} \text{CH}_3\text{---CH}_2 \\ \\ \text{OH} \end{array}$	—	—	78.5	1.71	1.51	3.69	8.59
$\begin{array}{c} \text{CH}_3 \\ \diagdown \\ \text{CH}_2\text{---CH}_3 \\ \\ \text{OH} \end{array}$	—	1	97.0	1.66	1.27	1.39	4.98
$\begin{array}{c} \text{CH}_3 \\ \\ \text{CH}_3\text{---CH} \\ \\ \text{OH} \end{array}$	1	—	82.0	1.59	1.21	1.26	4.67
$\begin{array}{c} \text{CH}_3 \quad \text{CH}_3 \\ \diagdown \quad / \\ \text{CH}_2\text{---CH} \\ \\ \text{OH} \end{array}$	1	1	99.0	—	1.72	3.60	5.45
$\begin{array}{c} \text{CH}_3 \\ \\ \text{CH}_3\text{---C---CH}_3 \\ \\ \text{OH} \end{array}$	2	—	82.8	—	1.66	1.80	3.10
$\begin{array}{c} \text{CH}_3 \quad \text{CH}_3 \\ \diagdown \quad / \\ \text{CH}_2\text{---C---CH}_3 \\ \\ \text{OH} \end{array}$	2	1	102.0	—	1.95	3.63	5.49

184°) compared to *p*-cymene (b.p. 177°) on the barium halide columns. The apparent deviation of *p*-chlorotoluene and *p*-xylene on barium chloride and iodide from the trend postulated above is possibly attributable to the increased ionic radius and electropositive character of the barium ion.

The dichlorobenzenes in Table II were studied briefly. The *ortho* isomer is adsorbed to a much greater extent than the *meta* isomer. This increase corresponds to both boiling point and gas phase dipole moment increase. The magnitude of the difference in heat of adsorption between the *ortho* and *meta* isomers, however, is surprising. It was earlier stated that the halogen withdraws electrons, decreases π -electron density and thus decreases adsorption. In the case of the *meta* isomer this explanation still appears valid. For the *ortho* isomer, it seems that the positioning of the electron withdrawing groups on two adjacent carbons increases the electron density in that region to such a great extent as to result in a significantly large increase in heat of adsorption over the *meta* isomer.

Fig. 2 illustrates the marked effect of going from chloride to iodide salts when utilizing the barium halides as packings. Very little separation occurs on the barium

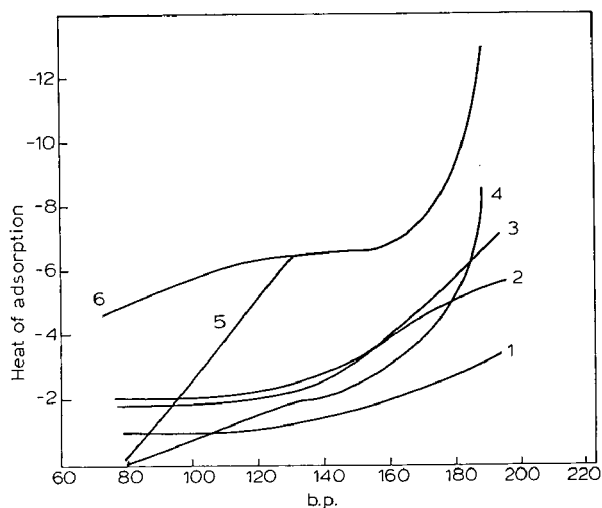


Fig. 1. Variation in ΔH_a vs. b.p. for halobenzenes. Boiling points: benzene, 80.0°; chlorobenzene 132.0°; bromobenzene 155.5°; iodobenzene 188.6°. Curve No.: 1 = SrCl_2 column; 2 = SrBr_2 column; 3 = SrI_2 column; 4 = BaCl_2 column; 5 = BaBr_2 column; 6 = BaI_2 column.

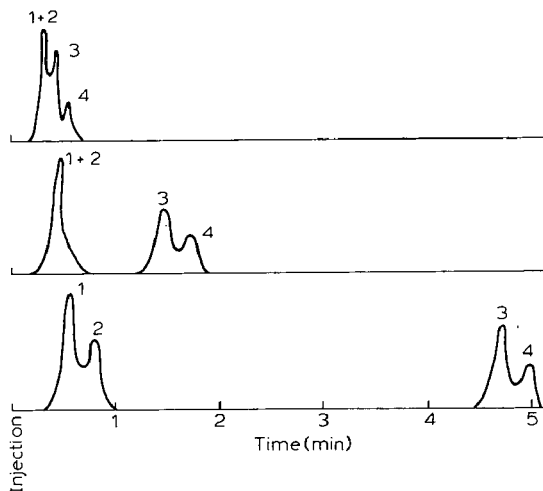


Fig. 2. Separation of various compounds on the barium halide columns. Conditions: temperature, 200°; flow rate, 60 ml/min; sample size, 1.0 μl . Compounds: 1 = hexane; 2 = bromocyclohexane; 3 = cumene; 4 = 1,2,4-trichlorobenzene.

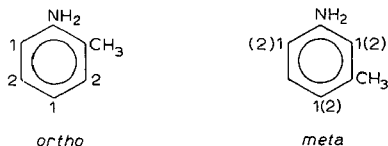
chloride column, whereas a separation of pairs occurs on the barium bromide column. However, a peak is obtained for each component on the barium iodide column.

Special aromatic samples (nitrogen substituted benzenes)

Due to the high boiling points of these isomers, a complete set of data was only obtained with the barium chloride column. All other columns produced peaks with rounded tops and excessive tailing.

The nitrogen substituted benzenes produced an interesting array of data. Table III listed the adjusted retention volumes and heats of adsorption for these compounds on the barium chloride column.

If one looks at the data for *o*- and *m*-toluidines, one can see that *m*-toluidine possesses a larger heat of adsorption and larger adjusted retention volume than those given for *o*-toluidine. This can probably be explained by an increase in boiling point and also by a greater increase in electron density. This increased electron density in *m*-toluidine may be explained by the structures below.



(1) Refers to increased electron density due to NH_2

(2) Refers to increased electron density due to CH_3

From attempts to chemically substitute an aromatic ring system of this type, we know that substitution would predominate *ortho* and *para* to the strongest electron releasing group, *i.e.*, to the amino group. In the *ortho* isomer there is increased electron density in four unsubstituted ring positions. In this structure there are two areas of high electron density and two of less electron density. The *meta* isomer has three areas of extremely high electron density and one of low electron density. In the *meta* product, the two releasing groups supplement each other to produce areas of great density⁹. This should explain the increased adsorption of the *meta* product. The above explanation was based upon the fact that in *o*- and *m*-toluidine one has a strong activating amino group and a weakly activating methyl group. These groups donate electron density into the ring and are *ortho* and *para* directors.

It is also possible that steric effects cause a decrease in adjusted retention volumes and heats of adsorption for the *ortho* isomer because nitrogen's electrons may be partially blocked from the column packing whereas this condition should not arise in the *meta* isomer.

When the methyl group in *o*-toluidine is replaced with a chloride group, as in *o*-chloroaniline, the adjusted retention volumes and heats of adsorption decrease. This is expected since the chloride group is electron withdrawing.

If one now compares *o*-nitrotoluene to nitrobenzene, a decrease in adjusted retention volume and heat of adsorption is seen even though the boiling point has increased twelve degrees. Since the nitro group withdraws electrons from the ring, an activating group placed in the *ortho* position would decrease adsorption.

Looking at *o*-nitrotoluene and *m*-nitrotoluene, one sees an increase in adjusted retention volume and heats of adsorption. This is probably due to the nine degrees increase in boiling point and also to an increase in dipole moment from *o*- to *m*-nitrotoluene.

o-Anisidine has a higher heat of adsorption than that reported for *o*-toluidine. This may be due to a large boiling point increase and/or the presence of the weakly activating methyl group being replaced with a strong activating methoxy group. This increased electron donating effect should produce a larger heat of adsorption and an increase in adjusted retention volume.

It is also possible that an interaction between the electrons of nitrogen and oxygen (in NO_2) and the column packing cation were partially responsible for some of the above trends.

Some generalities can be drawn for the nitrogen substituted benzenes. Boiling point, in most cases, determines elution order. The heats of adsorption trends could have been produced by the sum of three effects: (1) interaction with the electrons of oxygen and nitrogen and the column packing, (2) interaction between the electrons of the aromatic nucleus and the cation, (3) increases in boiling point. It was noted that electron releasing groups enhance adsorption and electron withdrawing groups decrease adsorption.

REFERENCES

- 1 W. W. HANNEMAN, C. F. SPENCER AND J. F. JOHNSON, *Anal. Chem.*, 32 (1960) 1386.
- 2 R. S. JUVET AND F. M. WACHI, *Anal. Chem.*, 36 (1964) 2368.
- 3 J. A. FAVRE AND L. D. KALLENBACH, *Anal. Chem.*, 36 (1964) 631.
- 4 C. S. G. PHILLIPS AND P. L. TIMMS, *Anal. Chem.*, 35 (1963) 505.
- 5 J. ISSORI AND L. CHAPUT, *Chem. Anal.*, 41 (1961) 313.
- 6 P. W. SOLOMON, *Anal. Chem.*, 36 (1964) 476.
- 7 P. W. SOLOMON, *Atomic Energy Commun. Res. Rept.*, No. IDO-16912, March, 1963.
- 8 A. G. ALTENEAU AND L. B. ROGERS, *Anal. Chem.*, 36 (1964) 1726.
- 9 R. L. GROB, G. W. WEINERT AND J. W. DRELICH, *J. Chromatog.*, 30 (1967) 305.
- 10 D. J. BROOKMAN AND D. T. SAWYER, *Anal. Chem.*, 40 (1968) 106.
- 11 D. J. BROOKMAN AND D. T. SAWYER, *Anal. Chem.*, 40 (1968) 1368.
- 12 D. J. BROOKMAN AND D. T. SAWYER, *Anal. Chem.*, 40 (1968) 1847.
- 13 D. J. BROOKMAN AND D. T. SAWYER, *Anal. Chem.*, 40 (1968) 2013.
- 14 G. L. HARGROVE AND D. T. SAWYER, *Anal. Chem.*, 40 (1968) 409.
- 15 J. R. PARTINGTON, *General and Inorganic Chemistry*, MacMillan, London, 1966, p. 379.
- 16 L. J. ANDREWS AND R. M. KIEFER, *J. Am. Chem. Soc.*, 74 (1952) 4500.

J. Chromatog., 53 (1970) 477-486

CHROM. 5031

SURFACE-BONDED SILICONES FROM VOLATILE MONOMERS
FOR CHROMATOGRAPHY*

CORAZON R. HASTINGS** AND WALTER A. AUE***

University of Missouri, Columbia, Mo. 65201 (U.S.A.)

AND

JOSEPH M. AUGL

Naval Ordnance Laboratories, Silver Spring, Md. 20910 (U.S.A.)

(First received May 19th, 1970; revised manuscript received August 8th, 1970)

SUMMARY

In an earlier report¹² we have described a multistage process which produces silicones polymerized on, and chemically bonded to, chromatographic supports. While only monomers of low volatility could be used at that time, we have now modified the process to accommodate highly volatile starting materials. Di- and trifunctional compounds of different polarity could be partially hydrolyzed in solution and subsequently polymerized in fluidized bed. The resulting phases were characterized by gas-liquid chromatography in terms of column bleed, solute retention and resolution; by liquid phase extractability, by thermogravimetric analysis, and C, H analysis. Most of the phases showed virtually complete surface bonding and bleed comparable to chromatography-grade SE-30. Resolution and retention time of various solutes appeared related to liquid phase cross-linking and substituent carbon chain length. Plate numbers generally improved, and retention times increased, through secondary heat treatments. The developed phases have been utilized in typical gas-liquid chromatographic separations.

INTRODUCTION

The modification of solid surfaces by chemical or physical bonding of organic substances is a subject which bridges traditional areas of research. It is of considerable importance in the industrial areas of protective coatings and reinforced plastics and the academic fields of surface chemistry and chromatography.

For most applications, stable chemical bonding would represent the ideal solu-

* Contribution from the Missouri Agricultural Experiment Station. Journal Series No. 6005. Approved by the director. This research was supported by PHS grant No. FD-00262-03 (former CC-00314), and NSF grant GP 18616. Initial experiments were presented at the 5th Midwest Regional Meeting of the ACS, Kansas City, Mo., October, 1969.

** Postdoctoral fellow.

*** To whom correspondence should be directed.

tion, but it is usually hard to achieve. The question: chemical bonding — yes or no? has been asked in many instances. Numerous studies on the nature of glass-resin interfaces are a case in point (*e.g.* refs. 1, 2, 3).

In the area of chromatographic techniques, two directions of research can generally be distinguished. The first, the older and predominant one, concerns the modification of surfaces vaguely in the range of an incomplete monomolecular layer. The purpose of these investigations is manifold: physicochemical characterization of surfaces, gas-solid chromatographic separation, surface deactivation for subsequent use in gas-liquid chromatography (GLC) and the like. A review listing works in some of these areas has recently appeared⁶. Of perhaps special importance in the context of this paper are results by the groups of OTTENSTEIN, PURNELL, KISELEV, KREJCI, and others (compare ref. 7).

The second field, younger and of considerable recent prominence, concerns the modification of surfaces with liquid layers of greater thickness, similar to regular GLC phases, but chemically bonded to the surface. These materials are designed for use in partition chromatography with either gas or liquid used as mobile phase. The "brushes" of HALASZ AND SEBASTIAN^{8,16,17} are the best-known example. Another surface-bonded carbon-based polymer was reported by MOORE AND DAVISON⁹.

The first attempt in chemically bonding silicone liquid phases to solid supports was carried out by ABEL *et al.*¹⁰, who polymerized hexadecyltrichlorosilane on Celite. GROB¹¹ tried similar procedures for glass capillaries.

In our first study on surface-bonded silicones, we used a variety of di- and tri-chlorosilanes, neat and in mixture, to produce liquid phases on diatomaceous earth or silica gel supports, and glass or porous silica beads. Some of these phases were virtually non-removable by exhaustive extraction and showed good chromatographic performance in terms of thermal stability, HETP and peak symmetry of polar compounds¹². Liquid phase loading can reach 40 % and such materials can also be used for the collection of air pollutants¹³.

Recently, KIRKLAND AND DESTEFANO¹⁴ of DuPont and FILBERT AND EATON¹⁵ of Corning reported on the polymerization of silanes on "controlled surface porosity support" and "controlled-pore glass particles", respectively. Modification of porous glass for GC was also studied by WOLF AND HEYER¹⁸. AL-TAIAR *et al.*⁷ mixed silicon-tetrachloride with silicone monomers, hydrolized and ground the resulting material for use in a gas chromatograph-mass spectrometer unit.

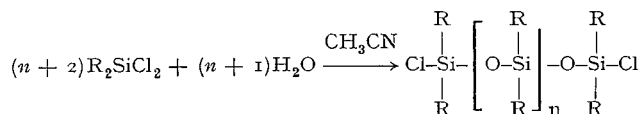
In this present study, we used Chromosorb G exclusively as a support and investigated the effects of silicone monomer structure. In previous work¹², we had used only monomers of relatively low volatility to produce the desired coatings. Both in industrial usage and chromatographic applications, however, silicones derived from highly volatile monomers dominate. We considered it therefore highly desirable to investigate such compounds as starting materials for chromatographic phases.

The most important step in our synthesis of surface-bonded silicones is the polymerization in fluidized bed¹². The amount of monomer lost from the coated particles to the carrier gas is negligible with compounds such as octadecyltrichlorosilane. With compounds of high vapor pressure, however, serious if not complete loss can result.

The situation is aggravated by the particular conditions which are desirable in the polymerization process. In general, the rate of water addition should be low and the temperature of the gas as high as proves compatible with other process

variables. Unfortunately, both of these conditions result in increased monomer loss.

Rather than to cool the reactor, recycle the carrier gas, or otherwise modify the fluidized bed polymerization, we decided to add a partial hydrolysis step to the process. In this step, water is added slowly to the halosilane solution in amounts sufficient to combine a small number of monomer units, for instance:



where $n = 2$ in this paper.

Of course, the exact nature and distribution of the resulting compounds are unknown. The preferred products would be straight polysiloxane chains devoid of silanol groups. There is some reason to assume¹⁹ that the reaction conditions chosen favor the formation of the desired structures.

Through partial hydrolysis, a decrease in volatility is achieved which permits the subsequent polymerization to be conducted in a fluidized bed at elevated temperature.

We have selected series of di- and trifunctional chlorosilanes according to high volatility and commercial availability, and not just according to expected GLC performance. Methyltrichlorosilane, for instance, could hardly be expected to yield a superior chromatographic phase. Dimethyldichlorosilane, on the other hand, is the monomer from which such common GLC phases as SE-30, DC-200, OV-1, OV-101, etc., are derived. In comparing the products formed from different monomers, it was important for us to notice any consistent change related to chemical structure, as for instance, in the methyl-ethyl-propyl-butyl series of trichlorosilanes.

There are quite a number of analytical techniques which can be mustered to characterize the produced materials. We have chosen criteria closely related to gas chromatographic performance, a main field of use for silicone coatings. Thus, we conducted (1) GLC bleed experiments, (2) plate height measurements, (3) exhaustive extraction, (4) chromatographies of test mixtures, (5) thermogravimetric characterization and (6) C, H analysis of the developed phases.

EXPERIMENTAL

(A) Synthesis of chromatographic phases

(1) *Treatment of the solid support.* Chromosorb G, 60/80 mesh, "non-acid washed" (Johns-Manville), is covered with conc. HCl and kept under gentle reflux for 24 h, decanting and replacing the acid once, approximately at half-time. After washing the diatomaceous earth with distilled water to neutrality, the remaining water is removed by several rinses with anhydrous acetone, followed by evaporation of the acetone in vacuum at 65°. The resulting material can be stored in a tightly stoppered bottle.

For the so-called "initial reaction"¹², 30.0 g of the acid-treated Chromosorb is poured into a solution of 10 ml methyltrichlorosilane (MTCS) in toluene (sufficient to cover the Chromosorb) and the mixture refluxed for 4 h under exclusion of atmospheric moisture. The excess MTCS and the toluene are evaporated in vacuum on

a 65° waterbath (this particular temperature is incidental) and the solid support is now ready for reaction with the partially polymerized halosilane.

(2) *Partial monomer hydrolysis*. To a magnetically stirred solution of halosilane(s) in 50 ml acetonitrile, a solution of water in 30 ml acetonitrile is added dropwise at room temperature and the mixture allowed to stand for 30 min. Permitting only a minimum of contact time with the atmosphere, the pretreated solid support (see above) is poured into the solution of partially hydrolyzed monomer and the solvent removed by rotary evaporation on a 65° waterbath.

For all reactions, the amount of halosilane is calculated to yield a 10.0% "theoretical load", defined as one hundred times the weight of the polymer divided by the weight of Chromosorb + polymer. Three moles of water are used for four moles of halosilane. To preserve the integrity of this ratio, the acetonitrile is dried prior to the reaction over calcium sulfate. Typical amounts calculated for this procedure are shown in Table I.

(3) *Polymerization*. The dried materials are polymerized in a fluidized bed of air at 100–110°, with approximately 6–8 ml of water introduced per hour. Most polymerizations are complete after 30 h as indicated by a pH higher than 6. This measurement is made on a sample taken from the fluidized bed and suspended in a small amount of distilled water.

(B) Characterization of chromatographic phases

(1) *Extraction*. All polymerized materials were extracted exhaustively in a Goldfisch Extractor (Fischer Scientific Company, St. Louis, Mo.) with benzene for 16 h, to determine the loss caused by extraction of non-surface bonded polymer. This loss was added to the "actual load" (*i.e.* the percentage of polymer on the extracted phases, as determined by C, H analysis) to calculate the "initial load" (*i.e.* the percentage of polymer before extraction) in Table III.

The residual, surface-bonded material was used for all chromatographic and other tests.

(2) *Column efficiency, performance, and bleed rate*. The exhaustively extracted chromatographic materials, and 10% GC grade GE-SE-30 coated on acid-washed Chromosorb G, 60/80 mesh, were packed into 0.5 m × 4 mm I.D. pyrex columns (Perkin-Elmer model 800). These columns were subjected to the following consecutive

TABLE I
PARTIAL MONOMER HYDROLYSIS

Monomer	g monomer	g water
CH ₃ SiCl ₃	7.522	0.679
C ₂ H ₅ SiCl ₃	6.731	0.556
C ₃ H ₇ SiCl ₃	6.222	0.473
C ₄ H ₉ SiCl ₃	5.827	0.411
CH ₃ (H)SiCl ₂	7.666	0.900
(CH ₃) ₂ SiCl ₂	5.808	0.607
(C ₂ H ₅) ₂ SiCl ₂	5.131	0.441
(CH ₃) ₂ SiCl ₂	4.014	0.559
+	+	
CH ₃ SiCl ₃ (3:1 molar ratio)	1.549	

procedures: (a) Bring column temperature from ambient to 250° at a rate of 10°/min and then condition 16 h at 250° with a N₂ flow of 13 ml/min. (b) Chromatograph two test mixtures containing several types of organic structures; some of them typical

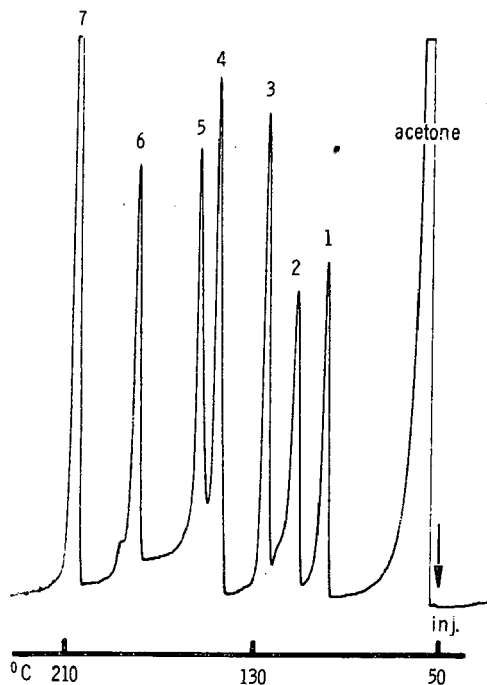


Fig. 1. Column, $[\text{CH}_3(\text{H})\text{SiO}]_n$ (3.65 w % $(\text{CH}_3\text{SiO}_{3/2})_n$, see text) on 60/80 Chromosorb G, 0.5 m \times 4 mm I.D. glass (Perkin-Elmer model 800). Initial temperature, 50°, 10°/min; N₂ flow rate, 13 ml/min. 1 = phenol; 2 = di-*n*-butylamine; 3 = ethylaniline; 4 = octanoic acid; 5 = *p*-toluic acid; 6 = dodecyl alcohol; 7 = methyl myristate.

TABLE II

EFFECT OF HEAT TREATMENT ON COLUMN EFFICIENCY

Monomer	% actual load ^a	HETP-250 ^b	HETP-350	HETP-400 (cm)
CH_3SiCl_3	9.4	5.14	9.62	5.65
$\text{C}_2\text{H}_5\text{SiCl}_3$	6.5	0.14	0.08	0.08
$\text{C}_3\text{H}_7\text{SiCl}_3$	6.5	0.07	0.08	0.04
$\text{C}_4\text{H}_9\text{SiCl}_3$	5.4	0.07	0.05	0.05
$\text{CH}_3(\text{H})\text{SiCl}_2$	7.9	0.21	0.13	0.11
$(\text{CH}_3)_2\text{SiCl}_2$	4.4	0.16	0.11	0.10
$(\text{C}_2\text{H}_5)_2\text{SiCl}_2$	0.4	0.68	0.57	0.63
$(\text{CH}_3)_2\text{SiCl}_2$ + CH_3SiCl_3 (3:1 molar ratio)	6.3	0.24	0.23	0.21
SE-30	9.6	0.11	0.10	0.10

^a The polymer load of the extracted phases as determined by C, H analysis.

^b All HETP values were measured at 6.5 ml/min N₂ and 190° with hexadecane.

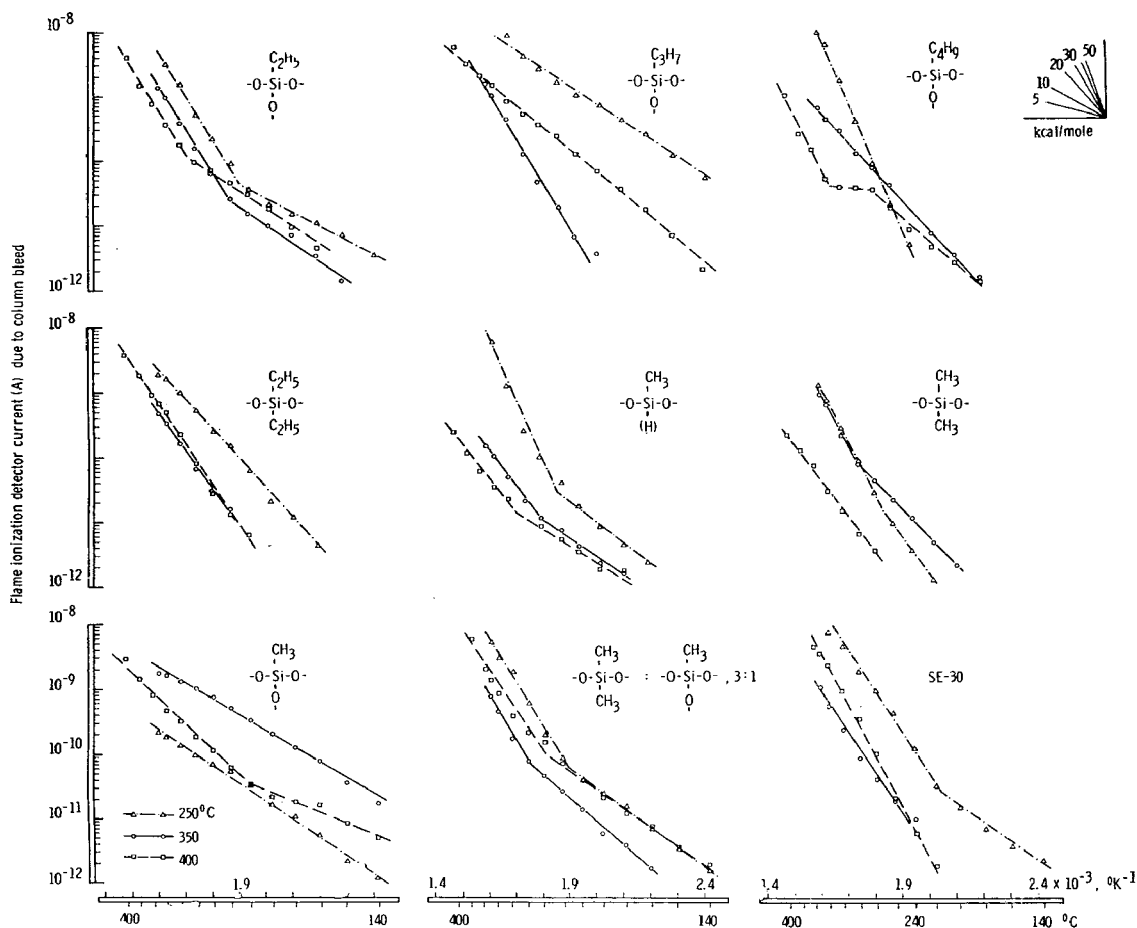


Fig. 2. Plot of log column bleed vs. $1/T$.

problem compounds such as phenols, acids, and amines. (A characteristic chromatogram is shown in Fig. 1, taken from step g below.) (c) Chromatograph a solution of hexadecane in pentane at 190° and a N_2 flow of 6.5 ml/min to obtain the HETP after the 250° heat treatment, called "HETP-250" in Table II; and the hexadecane retention time shown in Fig. 8. (d) Temperature-program (starting at the highest sensitivity and attenuating as required) at $4^\circ/\text{min}$ from 50° to 350° and a N_2 flow of 6.5 ml/min, to determine the bleed rate after the 250° heat treatment, called "250" in the bleed diagram (Fig. 2). (e) Repeat steps b and c (to check for a possible deterioration of the liquid phase). (f) Condition at 350° for 3 h at a N_2 flow of 13 ml/min, and repeat steps b, c, and d, to determine performance, column efficiency, and bleed rate (called "HETP-350" in Table II, and "350" in Fig. 2, respectively). (g) Condition at 400° for 1 h at a N_2 flow of 13 ml/min, and repeat steps b, c, and d, except that the column bleed is measured up to 400° . ("HETP-400" and "400".)

(3) *Other GLC tests.* After the column efficiency and bleed rate studies as described above, the columns were used to chromatograph a mixture of equal weights

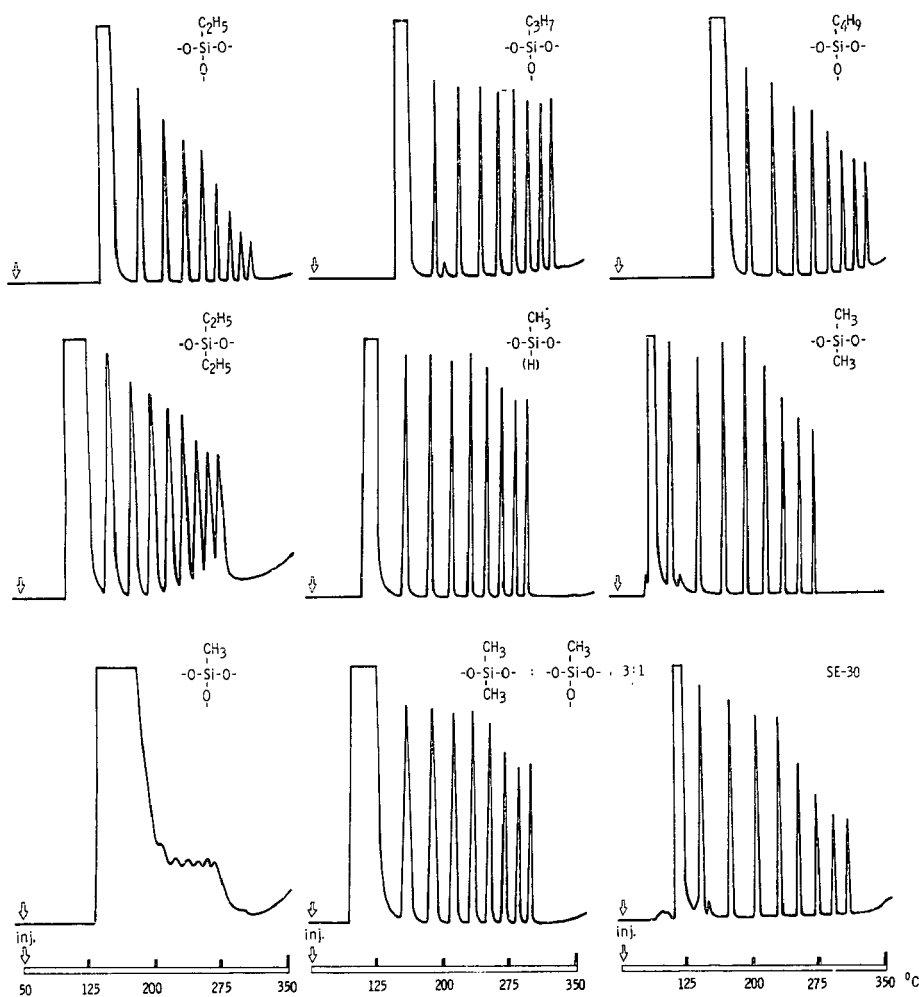


Fig. 3. Chromatogram of equal weights C_{10} through C_{24} even-numbered hydrocarbons. Column, $0.5 \text{ m} \times 4 \text{ mm}$ I.D. glass (Perkin-Elmer model 800). Initial temperature, 50° , $12^\circ/\text{min}$; N_2 flow rate, 6.5 ml/min .

of even-numbered hydrocarbons in ethylbenzene solution from C_{10} to C_{24} (Fig. 3).

Further, some of these packed columns were tested with a mixture of equal volumes of *n*-alcohols comprising ethanol, 1-butanol, 1-hexanol, 1-octanol, 2-octanol, 1-decanol, and 1-dodecanol (Fig. 4).

The Van Deemter plots of four supported-bonded columns and the standard GE-SE-30 columns were measured at 190° using $0.2 \mu\text{l}$ injections of 1% hexadecane in pentane (Fig. 5).

A portion of the exhaustively extracted mixed phase from dichlorodimethylsilane (DMCS) and MTCS was used to pack a $1.1 \text{ m} \times 4 \text{ mm}$ I.D. pyrex column (MicroTek model MT-220). It was conditioned at 250° for 30 h, deactivated with several injections of $10 \mu\text{l}$ bis(trimethylsilyl)trifluoroacetamide (BSTFA) at 190° , and

again conditioned at 320° for 15 h. This column was then used to separate picogram amounts of chlorinated hydrocarbon insecticides using the Mikro Tek Ni-63 electron capture detector (Fig. 6).

(4) *Thermogravimetric analysis.* Portions of the initial, exhaustively extracted phases (paragraph B1, above), were dried for 16 h at 100° in oil pump vacuum and analyzed in vacuum on a Mettler thermobalance. Part of the same dried phases were

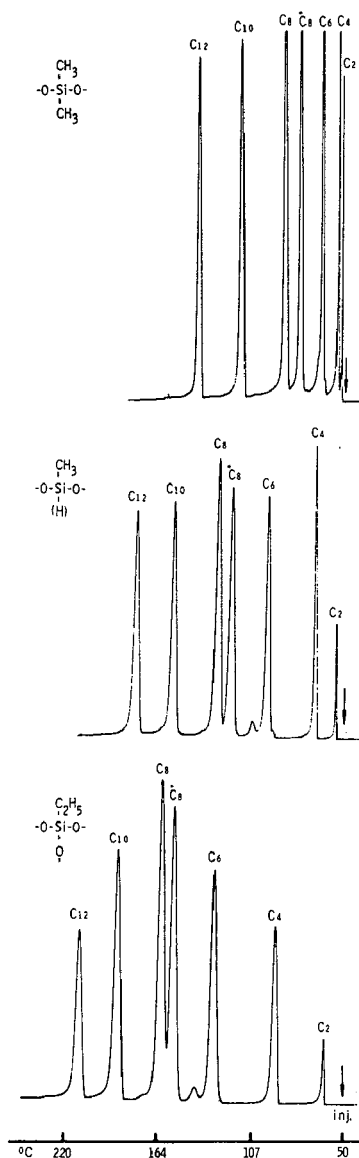


Fig. 4. Chromatogram of equal volume *n*-alkanol (1)s. Column, 0.5 m × 4 mm I.D. glass (Perkin-Elmer model 800). Initial temperature, 50°, 10°/min; N₂ flow rate, 13 ml/min. *2-octanol.

sent for C, H determination to Dr. F. KASLER at the University of Maryland (Table III).

RESULTS AND DISCUSSION

This study was designed primarily to show the feasibility of using silicone monomers of high volatility in an earlier described process¹², which yields support-bonded

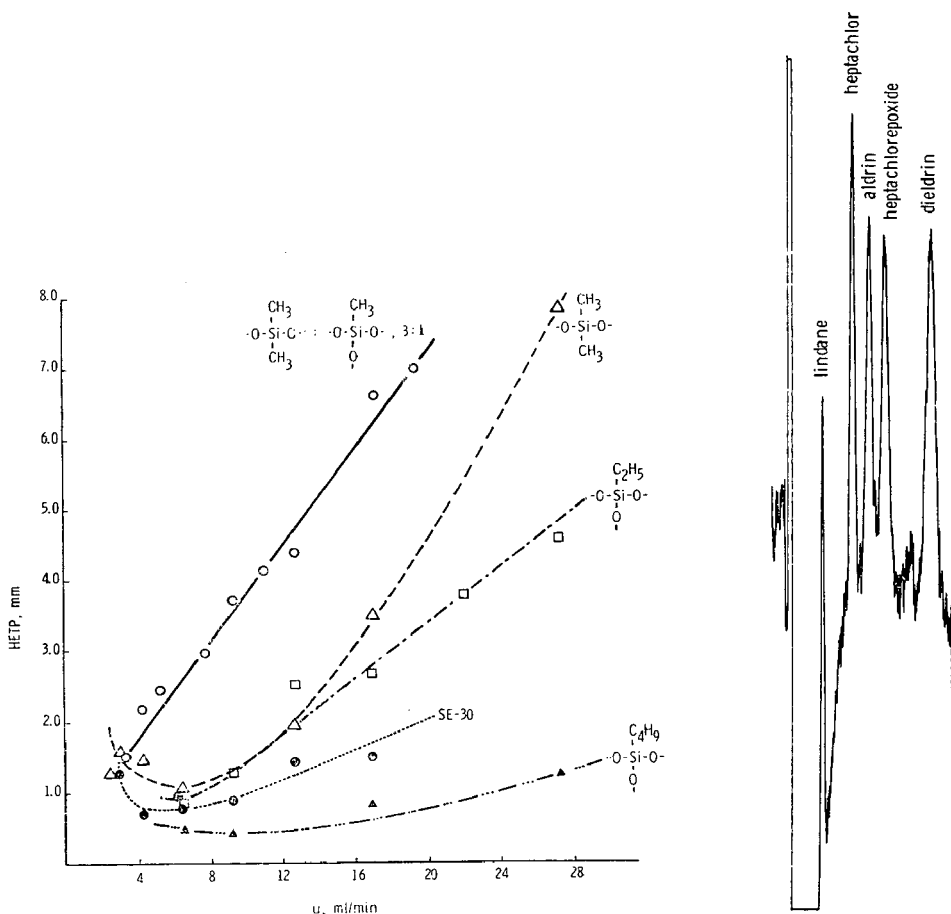


Fig. 5. GLC column efficiency (Van Deemter plot). 190°, hexadecane.

Fig. 6. Chromatogram of picogram amounts of chlorinated hydrocarbon insecticides. Column, 6.3 wt. % $[\text{3}(\text{CH}_3)_2\text{SiO} + \text{CH}_3\text{SiO}_{3/2}]_n$ on 60/80 Chromosorb G, 1.1 m \times 4 mm I.D. glass. Oven temperature, 190°; N_2 flow rate, 33 ml/min. MicroTek model MT-220, Ni-63 detector, RF mode, 60 V, 240 μsec interval, 6 μsec width. Injected amounts, Dieldrin 2×10^{-12} g, all others 1×10^{-12} g.

liquid phases for chromatography. To avoid monomer losses in the heated fluidized bed, a partial hydrolysis was conducted prior to the polymerization, yielding still reactive products of much reduced volatility, *i.e.*, chlorosiloxanes of one structure or another.

TABLE III
THERMO-GRAVIMETRIC ANALYSIS OF EXTRACTED PHASES

Monomer	% initial load ^{a,c}	% actual load ^b	Microanalysis ^d % found		TGA		
			C	H	Before heat treatment		After heat treatment
					% loss	Loss start (°C)	Half-life (°C) ^e
CH ₃ SiCl ₃	9.44	9.4	1.65	0.43	1.1	225	>760
C ₂ H ₅ SiCl ₃	6.55	6.5	1.94	0.40	4.0	225	530
C ₃ H ₇ SiCl ₃	6.55	6.5	2.49	0.48	2.7	275	520
C ₄ H ₉ SiCl ₃	5.60	5.4	2.16	0.48	3.0	235	505
CH ₃ (H)SiCl ₂ ^f	7.93	7.9 (3.65) ^g	1.64 (0.60)	0.50 (0.16)	5.5	240	375
(CH ₃) ₂ SiCl ₂	5.06	4.4	1.43	0.36	4.1	300	560
(C ₂ H ₅) ₂ SiCl ₂	1.87	0.4	0.10	0.05	N.D.	—	—
(CH ₃) ₂ SiCl ₂							
+ CH ₃ SiCl ₃ (3:1 molar ratio)	7.20	6.3	1.73	0.41	4.8	275	610
SE30		9.6 ^h	2.99	0.78	9.6	325	615

^a Polymer load before extraction, calculated from C, H analyses and extraction losses.

^b Polymer load after extraction, calculated from C, H analyses.

^c The last digit is not significant, but was included to precisely yield the extraction loss, when the "actual load" is subtracted from the "initial load".

^d Extracted, non-heat treated phases.

^e Middle (≈ inflection point) of final S-shaped decomposition curve.

^f Data in parentheses are measured after the heat treatment.

^g Calculated for (CH₃SiO_{3/2}) (see text).

^h Not-extracted, of course.

ⁱ N.D. = none detectable.

The chlorosiloxanes could then be used in a 30-h 100° fluidized bed polymerization. Rather than to optimize the process conditions for each monomer, the same conditions were used for all of them. This was done to provide a basis for comparing the resulting materials and predict the characteristics of products from various monomer mixtures. One such mixture, DMCS + MTCS in a 3:1 molar ratio, was included in this study.

Polymer load

The quantity of polymer coated on, and bonded to, the solid support was judged by exhaustive extraction, thermogravimetric analysis (TGA) in vacuum and C, H analysis. The results summarized in Table III show that only negligible amounts of the polymer could be extracted in most cases. These exhaustive extractions with benzene, conducted for 16 h in a Goldfish apparatus, are roughly equivalent to soxhlet extractions four times as long. Under these conditions, limiting values of extractable material are reached¹².

The TGA and especially the C, H analysis showed that losses did occur, presumably in the fluidized-bed reaction. These losses were of tolerable magnitude (within the exploratory framework of this study at least), except in the case of the diethyldichlorosilane-based material. Clearly, lower polymerization temperatures — and perhaps an optimization of the partial hydrolysis step — would tend to reduce these losses.

It is readily apparent from Table III that TGA yields only a rough approximation on the amount of polymer present. The values are lower than those derived from C, H analysis, indicating non-volatile residues. On the other hand, the only non-support-bonded phase investigated in this study proved completely volatile in TGA. (Whether this method is indeed capable of differentiating between coated and support-bonded phases, could be ascertained only through further comparisons.) In the polymer derived from MTCS, the 760° temperature limitation of the thermobalance did not permit to scan the full temperature range of decomposition (Fig. 7). Consequently, only 1.1 % from a 9.4 % load show up as volatile (Table III).

The values for “% actual load” in the same table represent the means of the weight % of polymer values calculated from the % carbon and % hydrogen content. In most cases, these values were similar. If the amount of C and H introduced by the initial treatment with MTCS is considered negligible, the C/H ratio should be the same as in the monomer. This was the case within the apparent experimental error in all cases except methyldichlorosilane. The C/H weight ratio for $(\text{CH}_3\text{HSiO})_n$ is 3.0; for $(\text{CH}_3\text{Si}-\text{O}-)_n$ 4.0. The experimental value was 3.28, indicating partial oxidation. After the heat treatments, this ratio was again measured. It had changed to 3.75, close to the trifunctional polymer derived from MTCS.

In the case of this and other monomers, the criterion for inclusion in this study was their high volatility and commercial availability rather than their anticipated chromatographic performance. Therefore, it was surprising that some phases, for instance the above mentioned $(\text{CH}_3\text{HSiO})_n$, performed rather well in the chromatographic tests (Figs. 1, 3, and 4). It is interesting to note that the TGA of this heat-treated material showed no detectable weight loss (Table III, Fig. 7).

The polymer derived from DMCS, of course, possesses characteristics similar to

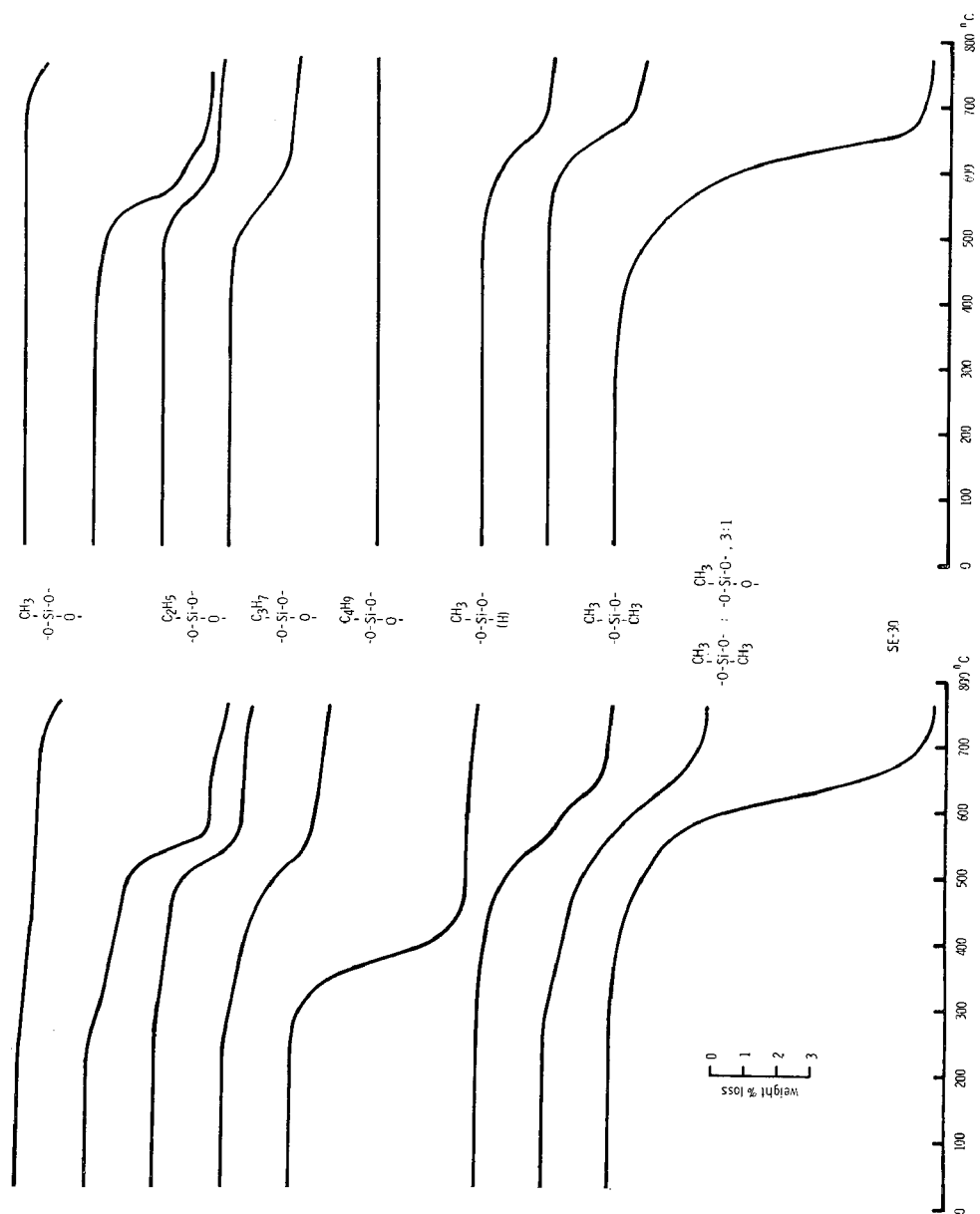


Fig. 7. TGA in vacuum of support-bonded liquid phases and SE-30. Formulas given concue with the left-hand side curves.

the dimethylpolysiloxane liquid phases rampant in the realm of GLC. One of these dimethylpolysiloxanes (General Electric's SE-30 GC-grade) was used as the standard phase for comparisons through various methods of testing. In the exhaustive extractions, for example, a load of 9.6 % SE-30 could be extracted, leaving a support which showed the same chromatographic behavior as uncoated Chromosorb G. (A small amount of SE-30 evidently stuck to the fluted flask used in the rotary evaporation coating technique and was thus lost to the phase, as shown by C, H analysis noted in Table III.)

In contrast, only a very small amount of the surface-bonded polymer derived from DMCS could be removed by extraction (Table III) and the remaining material showed typical GLC characteristics. Since DMCS would not be expected to yield a completely insoluble polymer, the conclusion is apparent that actual chemical bonding exists between the polymer and the solid surface.

The same reasoning does not necessarily apply to all of the phases synthesized in this study. One could imagine highly cross-linked, completely insoluble polymers being formed from trifunctional monomers, which would give the erroneous impression of complete surface-bonding in the exhaustive extraction tests. However, this seems improbable and we believe that the "% actual load" in Table III describes accurately the amount of surface-bonded polymer. This belief is supported by several earlier experiments, which involved polymers synthesized from trifunctional chlorosilanes in fluidized bed under similar conditions. These monomers, however, were coated on untreated supports and the resulting polymers proved largely or even completely extractable.

The various treatments and tests described under EXPERIMENTAL followed the same exact schedule for each one of the phases. They were designed to answer several questions: How well would a phase perform with various test compounds? Would its behavior change with successive heat treatments? Would it stand up to relatively high temperatures and how was the amount of bleed obtained in temperature programming going to be affected?

Heat-treatment

Commercial silicones are heat-treated (cured) after hydrolysis, resulting in the formation of chains from cyclic structures, an increase in molecular weight, cross-linking, etc. Surface-bonded phases, on the other hand, are "cured" *in situ operandi*, i.e., in the chromatographic column during conditioning and ensuing operations.

Besides removing some of the volatile fractions of "regular" polymers, (as distinguished from support-bonded varieties), conditioning is believed to provide a more even coating of the support through local polymer flow or distillation. At the same time, silicones are subject to molecular rearrangements at higher temperatures. These rearrangements are the only obvious mechanism by which support-bonded phases can attain the slightly different coating characteristics which subsequently influence chromatographic performance. Curing can also be expected to change the diffusion coefficients of chromatographed substances and consequently their mass transfer resistance terms.

Column bleed and thermal decomposition

In this study, the method used to determine column bleed is a modified (and

abbreviated) version of the commonly employed one. Instead of selecting various temperatures and recording the column bleed at isothermal conditions at a steady state, we temperature-programmed the column and made bleed measurements in a "dynamic" state. This appears justified when several columns are compared at exactly alike conditions of carrier gas flow, program rate, etc. It gives a better picture of the column bleed to be expected in a temperature-programmed run than the steady state measurements. More important for us, however, this approach provided an exactly reproducible step (in terms of column history) in the succession of treatments and tests, and furthermore, greatly reduced time requirements.

Very little is known about the mechanism or the composition of GLC bleed from silicone liquid phases. The gas chromatographer is generally not too interested to know whether the bleed he experiences results from volatile fractions originally present in the silicone, or from thermal rearrangement resulting in volatile siloxanes, or from oxidative rupture of Si-C bonds by traces of oxygen in the carrier gas.

In this study, a hydrogen flame detector (FID) was used for its sensitivity and ruggedness. Since it essentially monitors combustible carbon, the amount of bleed measured is not exactly proportional to the loss of polymer incurred in comparing different phases. For example, the FID will respond stronger to bleed from $(C_4H_9SiO_{3/2})_n$ than from $(CH_3SiO_{3/2})_n$ on an equal weight basis. It is also known to respond in an irregular manner to silicon-containing compounds²⁰. We have made no effort to correct for these effects, since the chemical composition of the bleed was not determined.

The bleed curves, plotted as usual in $\log A$ vs. $1/T$, are shown in Fig. 2. General Electric's SE-30 GC grade, a phase of low bleed, was included to allow comparisons. The three curves for each phase correspond to measurements after the 250°, 350°, and 400° heat treatments. We want to stress the point that such curves were not exactly reproducible. This was apparently due to the fact that several polymerization variables, and the heat treatments themselves, influenced the polymer structure and consequently the bleed behavior. This touch of irreproducibility is paralleled by the behavior of different batches of normal GLC phases, which any gas chromatographer can attest to.

The bleed curves in Fig. 2 generally show the expected reduction in bleed after heat treatments of increasing temperature. Where the 400° curve is higher than the 350° one, it appears likely that significant thermal rearrangement to more volatile fragments (decomposition) has occurred in the 400° heat treatment.

The polymer derived from MTCS behaves irregularly in bleed as well as in chromatographic characteristics. Its bleed curves, on the whole, are noticeably flatter than those of the other materials, indicating that chemical decomposition is less prevalent (as compared to volatilization). Indeed, the TGA curves of this material show that the final decomposition started at 680° and had not reached the inflection point of the S-curve at the temperature limit of the thermobalance. At this limit (760°), only a small fraction of the material had decomposed (Table III, Fig. 7). Therefore, the bleed plotted in Fig. 2 is obviously due to a small amount of volatile materials. While the surface-bonded polymer could be expected to be virtually devoid of bleed after suitable further conditioning, its chromatographic properties leave everything to be desired (Fig. 3). Viewed as an organic structure, however, its thermal stability is remarkable.

Some of the bleed curves apparently contain breaks. For instance, the materials conditioned at 250° show these breaks in a range between 220 and 260°; several of them show a break exactly at 250°. It may be interesting to speculate on the reasons for these breaks and their connection with conditioning and the above mentioned causes of column bleed. For purposes of comparison, we have included an angular scale of the slopes representing the apparent Arrhenius activation energies. Certainly the steeper parts of the curves are indicative of chemical reactions. We would like to stress, however, that our measurements were done in a dynamic system and are not directly amenable to the usual physicochemical treatment.

Furthermore, the different "actual loads" (Table III), and possible effects of silicone on the FID, render comparisons of different materials in regard to their bleed levels as semiquantitative at best. It has been our experience that support-bonded phases improve considerably more than regular phases with extended conditioning. Regular phases, of course, were heat-cured before reaching the consumer and are therefore less affected by such treatment. Since this study was directed toward the synthesis and comparison of polymers rather than their applications for the best possible chromatography, all polymers were treated alike. For optimal GLC, however, each phase should be conditioned according to its particular characteristics. It may be appropriate to note, furthermore, that chromatographic bleed curves *per se* may only tell part of the story and should be interpreted with due caution.

The amount of bleed, which can be expected from silicone liquid phases in GLC, is of great importance in several types of analysis, for instance in temperature-programmed trace analysis, in the use of certain detectors such as the Ni-63 electron capture detector, in the ever more popular gas chromatography-mass spectrometry combination, etc. Yet, there is but scant documented knowledge on this subject available and the choice of a column and its further treatment retain the flavor of an art.

In comparison with the GE-SE-30 GC-grade, which is noted for its thermal stability, the support-bonded phases showed bleed rates of comparable magnitude. $[(\text{CH}_3)_2\text{SiO}]_n$ was generally lower than SE-30. This is also evident for the TGA decomposition after the phases had been subjected to the various tests. The inflection points of the S-curves lie at 630° (support-bonded material) and 615° (SE-30). The C_1 to C_4 series of trifunctional compounds did not show any great differences in bleed. Thermal stability as measured by TGA half-life decreases with the increasing length of substituent hydrocarbon chains (>760, 615, 555, and 545; for C_1 through C_4). This decrease becomes small, however, as the chain length increases. Support-bonded $[\text{C}_{18}\text{H}_{37}\text{SiO}_{3/2}]_n$, for instance has a half-life temperature of 510° (ref. 21).

Cross-linking does not seem to reduce bleed (DMCS + MTCS *vs.* DMCS derived polymers) under the conditions of the experiment. Under the much harsher conditions of the much less sensitive TGA, however, the cross-linked polymer begins to show a small advantage. The middle (\approx inflection point) of the S-curve lies at 630° for the difunctional polymer and at 640° for the mixed polymer. In comparison, this temperature for the trifunctional methyl polymer is higher than 760° (Fig. 7, Table III). The chromatographic efficiency of the purely difunctional $[(\text{CH}_3)_2\text{SiO}]_n$, however, is much better and this polymer would be the phase of choice for many applications.

No deliberate effort has been made to determine the life-expectancy of support-bonded columns. Judged from our limited experience in working with them for longer

periods of time, their life-expectancy should be comparable if not superior to regular GLC coatings of similar structure.

If comparisons between TGA in vacuum, and bleed experiments under nitrogen, are permissible, it would appear that the polymers up to 400° rearranged and lost some material, but did not lose their essential structure necessary for efficient GLC. On the contrary, GLC efficiency increased. This is borne out by the HETP values (Table II) and especially the analysis of test mixtures, which showed various degrees of improvement. Only one particular test (the analysis of alcohols on $\text{RSiO}_{3/2}$) showed some deterioration after the 400° heat treatment. From the viewpoints of both chromatography and polymer chemistry, the half-life temperatures found by TGA in vacuum are relatively high. In a nitrogen or helium environment, this stability would yet increase.

It is interesting to compare the TGA curves before and after the phases had gone through the various heat treatments. The final decomposition (the S-curve) remains similar, although shifting slightly to higher temperatures. There is present, however, a fraction which is lost at considerably lower temperatures. This fraction apparently accounted for most of the measured GLC bleed. A comparison of the two sides of Fig. 7 shows an all but complete disappearance of these less stable parts of the polymer caused by the heat treatments. Besides providing an instructive illustration to the effects of column conditioning, the TGA suggests that some further reduction in GLC bleed could still be achieved through additional conditioning.

A special case in thermal stability is $(\text{CH}_3\text{HSiO})_n$. The polymer decomposes at the lowest temperatures of all the phases (Fig. 7, left side). Once it has gone through the heat-treatments, no weight loss is recorded anymore by TGA (Fig. 7, right side). The phase, however, showed reasonable GLC properties (Figs. 1 and 3). Therefore, a C, H analysis was again made and indicated a load of 3.65 %. This load was calculated as $(\text{CH}_3\text{SiO}_{3/2})_n$ because of its 3.75 C/H weight ratio. It should have shown up clearly in the TGA. Further studies to investigate the properties of the two most stable polymers, namely those derived from CH_3SiCl_3 and $\text{CH}_3(\text{H})\text{SiCl}_2$, are under way.

Column efficiency

Fig. 3 shows the chromatograms of a mixture of even-numbered *n*-hydrocarbons. The best performing phases were $[(\text{CH}_3)_2\text{SiO}]_n$, (CH_3HSiO) and the propyl and butyl derivatives of the trifunctional series. $[(\text{C}_2\text{H}_5)_2\text{SiO}]_n$ effected a relatively poor resolution, possibly caused by its low load. $(\text{CH}_3\text{SiO}_{3/2})$ was the worst of all GLC phases; it is indeed questionable whether it still possessed properties of a liquid on the support. (The differences in height of the hydrocarbon peaks in the chromatograms are not significant; they resulted from different speeds of syringe withdrawal after injection by two operators.)

These hydrocarbon analyses illustrate GLC performance in terms of resolution, retention temperature and bleed. All variables such as carrier gas flow, column length, etc., were kept constant to permit comparison of different phases. In the ethyl-propyl-butyl series of trifunctional polymers, for instance, the resolution as well as the retention temperatures increase. This is obviously due to the increased interactions between the test compound hexadecane and the hydrocarbon substituents. The rise in baseline, as the final temperature of 350° is approached, visually demonstrates typical bleed levels.

In a mixture such as DMCS + MTCS, the trifunctional monomer serves to demonstrate the effects of cross-linking. Although the mixed polymer is still a satisfactory phase for some purposes, the HETP has risen from 0.10 cm for the pure $[(\text{CH}_3)_2\text{SiO}]_n$ to 0.21 cm through the addition of $\text{CH}_3\text{SiO}_{3/2}$ units (Table II). Trifunctionality is an apparent disadvantage in the lower members of the series (methyl, ethyl), but gives good results from propyl up. One of the best support-bonded phases ever synthesized ($(n\text{-C}_{18}\text{H}_{37}\text{SiO}_{3/2})_n$, see ref. 12) is a member of this series.

The HETP measurements have been performed at the same conditions (especially the same carrier gas flow) for all columns. Consequently, they do not represent minima in the Van Deemter curve; although the chosen gas velocity was close to the optimum one for most columns (compare Fig. 5).

In these measurements, a pronounced dependence of the retention time of the test compound hexadecane on the structure and the thermal history of the column was noted. Fig. 8 gives a graphic presentation of retention times as related to prior heat treatments. The polymers derived from difunctional monomers showed no appreciable changes. Heat treatment of the trifunctional ones, however, caused marked increases in retention time. These polymers cause longer retention times even before heat treatment, apparently due to the length of their substituent hydrocarbon chains. It appears likely, although by no means proven, that further cross-linking is the predominant effect brought about by the rearrangement of silicones under thermal stress.

Methyl, propyl, and butyl form a consistent trifunctional series; ethyl deviates somewhat from the pattern. $(\text{CH}_3\text{HSiO})_n$ does not conform to the pattern for difunctional polymers; this is in agreement with the conclusion, based on C, H analysis, that most of the Si-H bonds have been broken. The polymer would thus approach the characteristics of one derived from a trifunctional monomer.

Cross-linking, in this context, is a multi-faceted term. It could involve condensation of some residual silanol groups, rearrangements to higher molecular weight structures and/or the formation of three-dimensional networks.

It is interesting to note the increase in retention time and the decrease in HETP resulting from the heat treatments. Although the HETP depends on many factors, it can be assumed that the formation of a dense, three-dimensional network would have certainly increased the HETP considerably because of its effect on the diffusion coefficient of hexadecane in the stationary phase. Such was not the case. A closer examination of the problem alluded to would need to involve a better characterization of the liquid phases before and after heat treatments in terms of molecular weight, viscosity, etc. However, the presence of chemical bonding between the liquid phase and the support does not allow the use of some common analytical methods.

Where the extent of cross-linking is increased, the viscosity of the liquid phase increases and the diffusion coefficients decrease (for a detailed discussion of the subject, see ref. 22). Therefore, the slope of the Van Deemter plot at high flows $[8/\pi^2(1-R)R \cdot d^2/D_s]$ can be used to estimate relative diffusion rates in comparing different phases at similar conditions.

The liquid film thickness d is roughly proportional to the weight % load and $(1-R)R$ can be easily calculated from the chromatograms. Fig. 5 shows the Van Deemter plots of several support-bonded phases and SE-30. From this plot, relative diffusion rates can be obtained. If the standard phase SE-30 is arbitrarily assigned a value of 100, the diffusion rates for $(\text{C}_4\text{H}_9\text{SiO}_{3/2})_n$, $(\text{C}_2\text{H}_5\text{SiO}_{3/2})_n$, $[(\text{CH}_3)_2\text{SiO}]_n$ and

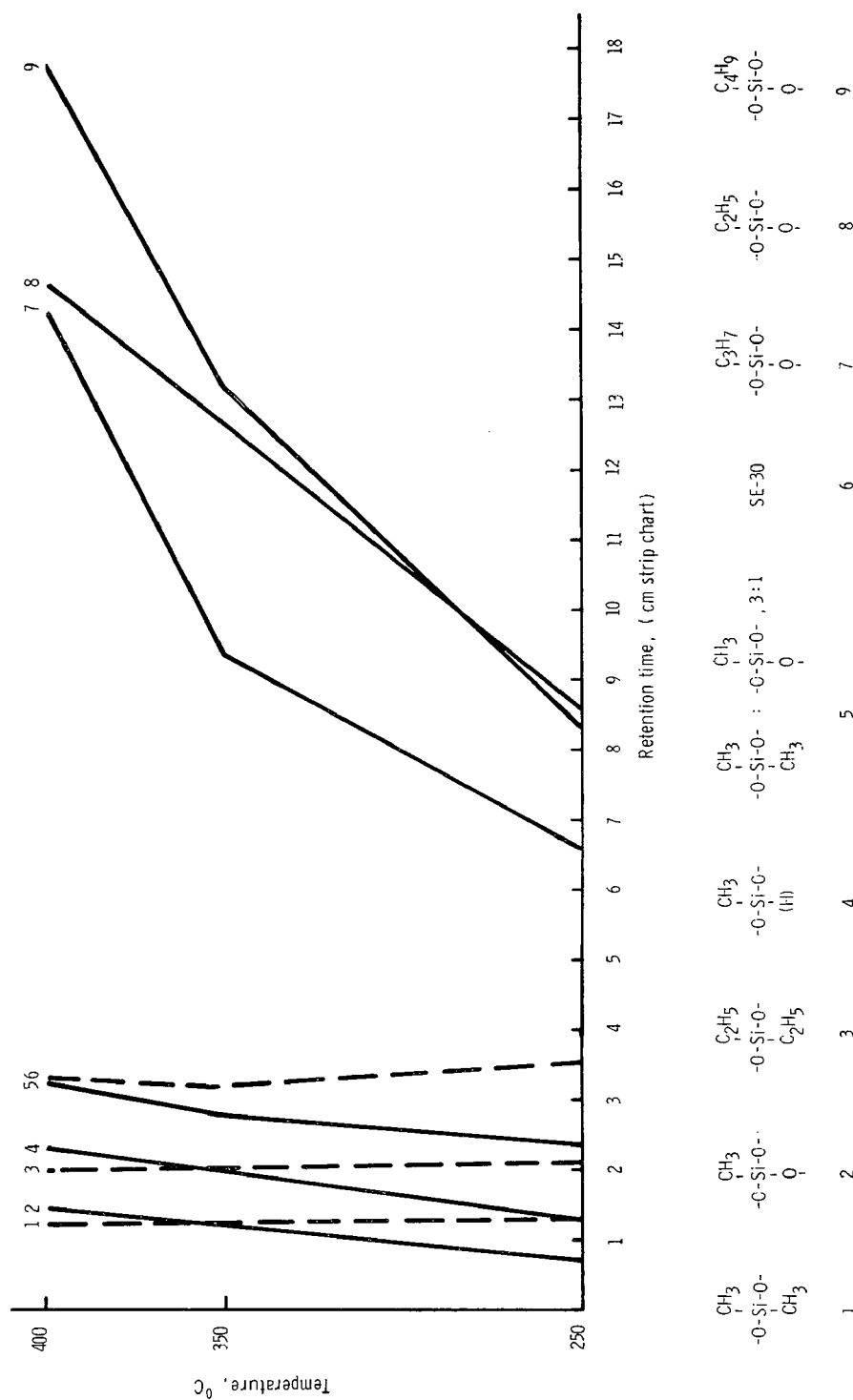


Fig. 8. Retention time of hexadecane as a function of heat treatments. Column, 0.50 m \times 74 mm I.D., glass, 190°; N_2 flow rate, 6.5 ml/min. Dotted line, difunctional polymers; full line, trifunctional polymers.

$[3(\text{CH}_3)_2\text{SiO} + \text{CH}_3\text{SiO}_{3/2}]_n$ are 32.3, 8.3, 25.6, and 17.3, respectively. In this regard, SE-30 shows a distinctive advantage over all support-bonded phases including its counterpart $[(\text{CH}_3)_2\text{SiO}]_n$. Nothing is known about the "molecular weight" of the latter phase, nor about the extent of cross-linking caused by impurities, nor about the number of chemical bonds between liquid phase and Chromosorb surface. The last effect is, of course, peculiar to support-bonded phases. It should tend to increase the viscosity, decrease diffusion and raise the HETP.

Some or most of the characterized properties of support-bonded liquid phases from volatile monomers may well be similar to those of commercial silicones. A comparison with these products, however, is beyond the scope of this present study.

Chromatographic applications

The test mixtures, which were chromatographed after each heat treatment as described under EXPERIMENTAL, showed that adequate chromatography could be obtained from most phases. The performance (= separation and symmetry of peaks) improved somewhat with each heat treatment. The only exception found was the chromatography of *n*-alcohols (C_2 to C_{12}) which deteriorated on $(\text{C}_3\text{H}_7\text{SiO}_{3/2})_n$ and $(\text{C}_4\text{H}_9\text{SiO}_{3/2})_n$ after the 400° heat treatment. Fig. 1 shows a representative test mixture, Fig. 4 the above-mentioned alcohol mixture on three different phases. In the latter analysis, the change in retention time (temperature) was quite noticeable; this effect was strongly enhanced with the propyl and butylsilicones which caused extremely high retention temperatures of the alcohols. This provides yet another example for the contrast between di- and trifunctional polymers discussed above.

A number of applications appeared possible, of which we chose one related to other work in our laboratories. Several phases performed well with chlorinated hydrocarbon insecticides. Fig. 6 shows a sample chromatogram from a Ni-63 EC detector at high sensitivity. The amounts present, 1×10^{-12} g each of Lindane, Heptachlor, Aldrin and Heptachlorepoxyde, and 2×10^{-12} g of Dieldrin, are close to the minimum detectable limits imposed by the detector (*p,p'*-DDT had been included, but failed to show up at these extremely low levels). The chromatogram indicates that support-bonded phases can be well used in trace analysis.

Some phases have also been successfully used in exploratory liquid-liquid chromatography; this study will be described in a later paper.

ACKNOWLEDGEMENTS

We are glad to acknowledge the competent technical assistance of Mr. KEITH FLACK from Dr. C. W. GEHRKE's group and of Mr. TAKESHI O'HARA.

REFERENCES

- 1 T. E. WHITE, *The Society of the Plastics Industry, 20th Annual Meeting, Chicago, Ill., 1965*.
- 2 N. M. TRIVISONNO, L. H. LEE AND S. M. SKINNER, *Ind. Eng. Chem.*, 50 (1958) 912.
- 3 L. P. BIEFELD AND T. E. PHILIPPS, *Ind. Eng. Chem.*, 45 (1953) 1281.
- 4 W. R. SUPINA, R. S. HENLY AND R. F. KRUPPA, *J. Am. Oil Chemists' Soc.*, 43 (1966) 202A.
- 5 D. M. OTTENSTEIN, *J. Gas Chromatog.*, 6 (1968) 129.
- 6 R. S. JUVET, JR. AND S. P. CRAM, *Anal. Chem. Ann. Rev.*, 42 (1970) IR.
- 7 A. H. AL-TAIAR, J. R. LINDSAY SMITH AND D. J. WADDINGTON, *Anal. Chem.*, 42 (1970) 935.
- 8 I. HALASZ AND I. SEBASTIAN, *Angew. Chem. Intern. Ed. Engl.*, 8 (1969) 453.

- 9 D. J. MOORE AND V. L. DAVISON, *J. Am. Oil Chemists' Soc.*, 44 (1967) 362A.
- 10 E. W. ABEL, F. H. POLLARD, P. C. UDEN AND G. NICKLESS, *J. Chromatog.*, 22 (1966) 23.
- 11 K. GROB, *Helv. Chim. Acta*, 51 (1968) 718.
- 12 W. A. AUE AND C. R. HASTINGS, *J. Chromatog.*, 42 (1969) 319.
- 13 W. A. AUE, C. R. HASTINGS, S.-F. TSAI AND P. M. TELI, *Proc., 4th Intern. Conf. Trace Substances in Environmental Health*, University of Missouri, Columbia, 1970, in press.
- 14 J. J. KIRKLAND AND J. J. DEStEFANO, *J. Chromatog. Sci.*, 8 (1970) 309.
- 15 A. M. FILBERT AND D. L. EATON, *Joint ACS-CIC Conference, Toronto, Canada, May 1970*.
- 16 J. N. LITTLE, W. A. DARK, P. W. FARLINGER AND K. J. BOMBAUGH, *1970 Pittsburgh Conference, Cleveland, Ohio, February 1970*.
- 17 *Durapak*, promotional literature, Waters Associates, Framingham, Mass.
- 18 F. WOLF AND W. HEYER, *J. Chromatog.*, 35 (1968) 489.
- 19 K. A. ANDRIANOV, *Metalorganic polymers*, Interscience, New York, 1965, p. 129.
- 20 D. FRITZ, G. GARZO, T. SZEKELLY AND F. TILL, *Acta. Chim. Acad. Sci. Hung.*, 45 (1965) 301.
- 21 J. M. AUGL AND W. A. AUE, unpublished material.
- 22 H. FUJITA, in J. CRANK AND J. S. PARK, (Editors), *Diffusion in Polymers*, Academic Press, London and New York, 1968, p. 86.

J. Chromatog., 53 (1970) 487-506

CHROM. 5022

COLUMN SEPARATIONS DESIGNED PRECISELY WITH THE AID OF THIN-LAYER CHROMATOGRAPHY

A. G. NETTING

School of Botany, University of New South Wales, Kensington, N.S.W. (Australia)

(Received August 17th, 1970)

SUMMARY

The use of thin-layer silica gel as a column adsorbent has been investigated. It was found that excellent separations of a plant wax could be obtained with quantitative recovery. Further, by the prior use of thin-layer chromatography on the same adsorbent it was possible to predict the course of the separation knowing only the elution volume of the first peak and the point at which solvents were changed. Thus thin-layer chromatography may be used to design column separations.

INTRODUCTION

The components of plant waxes have been isolated by column chromatography on Florisil, preparative thin-layer chromatography (TLC) on silica gel, or a combination of these two methods^{1,2}. Florisil does not separate adequately the least polar components. Preparative TLC is suitable only for small amounts of wax and up to 40 % of some components can be lost, apparently by irreversible binding to the dried thin-layer. Since excellent resolution of plant wax components can be obtained by TLC on silica gel³ it seemed that the use of this material in columns could be profitably investigated. In this paper it is shown that the properties of silica gel are the same in thin-layers and columns.

EXPERIMENTAL

Materials and methods

A diagram of the apparatus is given in Fig. 1.

Boiling Tube. Before entering the column the solvent is passed through a boiling tube to remove air which might otherwise come out of solution in the low-pressure side of the pump. The tube, which is internally ground to prevent "bumping", is coiled with "Eureka" resistance wire and heated by the circuit shown in Fig. 1.

Pump. Since thin-layer silica gel has a very small particle size (10–40 μ) the flow rate of solvents is restricted. However, a reasonable and constant flow rate (approx. 0.2 ml/min) can be attained with a pump (Beckman Model 746).

Pressure equalising U-tube. The pump used has a piston action and thus the

pressure equalising U-tube (Fig. 1a) is introduced between the pump and the column to ensure constant head pressure on the column.

Fittings. The use of stainless steel swagelock fittings with teflon ferrules (Duff & McIntosh, Sydney, Ltd.) and teflon tubing (Polypenco TFE, AWG 20; The Polymer

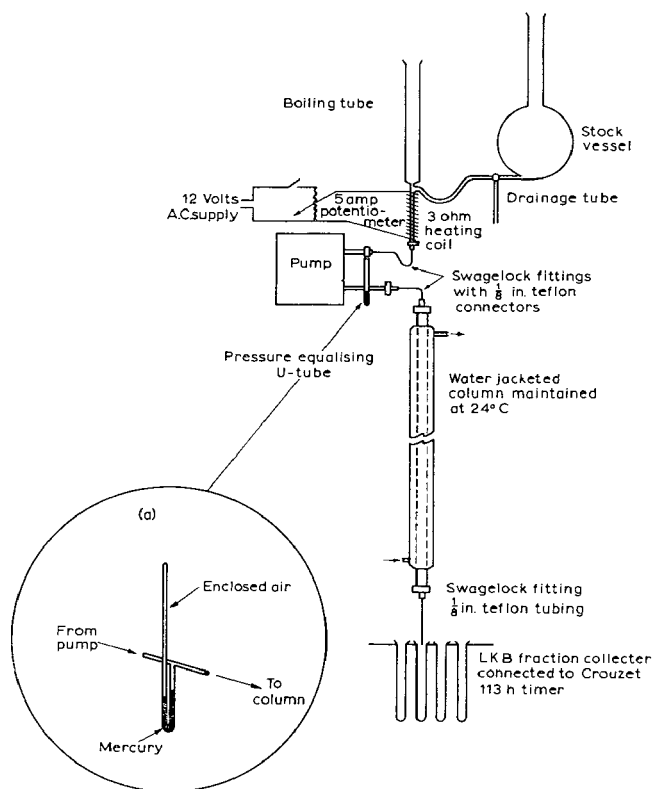


Fig. 1. Diagram of apparatus.

Corporation of Pennsylvania) provide flexible connections free from leaks. The swagelock fitting on the base of the column provides a seat for a filter paper pad to support the adsorbent and the narrow bore teflon tubing on the outlet reduces evaporation of the solvent thus eliminating deposition of solutes on the column tip.

Column. The column was 140 cm long with an I.D. of 1.3 cm. As considerable amounts of heat can be released by the adsorption of some solutes and solvents the column was water jacketed and maintained at constant temperature of 24° using a Colora Ultra-thermostat.

Adsorbent preparation. Five 20 × 20 cm glass plates were spread with silica gel (Merck, Kieselgel H) to a depth of 1 mm using Shandon equipment. These were activated by heating for 30 min at 110° and then washed with carbon tetrachloride by ascending chromatography to remove organic impurities. Following the removal of the top 1 in. of silica gel the plates were air-dried and reactivated. The remaining silica gel was then weighed.

TCL of standards. Thin-layer plates 0.3 mm thick were prepared from the same

batch of silica gel as that used to prepare the column adsorbent. These were then activated and washed in exactly the same way as the plates used for adsorbent preparation. Samples of gl_6 wax and its components ($4 \mu\text{l}$ of a 1 % solution in CHCl_3) were then spotted onto the plates. One plate was run, to a pre-marked line, in each of the following solvents: carbon tetrachloride, benzene and ethyl acetate. The spots were detected as previously described¹ and the R_F value of each component determined.

Packing the column. Sufficient carbon tetrachloride was added to the silica gel to make a thin slurry which was then boiled to remove dissolved air. Aliquots were packed in the column under pressure from the pump. The flow rate at the tip of the column was determined after packing was complete.

Sample preparation. Wax was extracted from a non-glaucous mutant of kale (*Brassica oleracea*) known as gl_6 , by dipping the leaves in boiling petrol ether (60–80°) for 20 sec. The solid wax was obtained following filtration and evaporation of the petrol ether under oxygen-free nitrogen. This wax contains fatty acids and although these can be eluted from silica gel by acetic acid, this procedure was not adopted because acetic acid attacks the swagelock fittings. Therefore, prior to chromatography on silica gel the wax was chromatographed on a Florisil column (60–100 mesh, acetone washed to remove an oily residue and reactivated). All components of the wax except the fatty acids were eluted with ethyl acetate. This eluent was dried, reweighed and less than 0.1 % of the adsorbent weight dissolved in a minimum volume of carbon tetrachloride and added to the silica gel column. The apparatus was then filled with boiled carbon tetrachloride and the elution commenced. The fatty acids were eluted from the Florisil column by 4 % acetic acid in ether⁴.

Solvents. All the chromatography solvents were distilled and dried before use. Solvents were changed at the appropriate times by removing all the old solvent from the head of the column, rinsing the apparatus and refilling with the new solvent.

Collection of fractions. An LKB fraction collector connected to a Crouzet 113H timer set at 50.5 min was used.

Conditions Flow rate, 0.21 ml/min; weight of activated adsorbent, 60.4 g; fatty acid free sample weight, 51.3 mg, timer setting, 50.5 min; volume of fractions, 10.6 ml; volume of solvents, carbon tetrachloride 693 ml, benzene 288 ml, ethyl acetate 291 ml.

Analysis of fractions. The test tubes were placed in a 50° water bath and their contents evaporated to dryness under a stream of oxygen-free nitrogen. When evaporation was complete each tube was visually inspected for wax. An appropriate volume of chloroform (visually estimated, 0.1–5 ml) was added to each tube and the tube warmed to dissolve the wax. Using Microcap pipettes (Drummond Scientific Co.) $4 \mu\text{l}$ from each tube were applied to a Silica Gel G plate. The plates were developed and the spots detected and then the intensity of each spot was estimated on an arbitrary, approximately linear scale (1, 2 or 3). Tubes containing the same components were pooled and chloroform solutions of each component forced through a millipore filter, in a Sweeney syringe, to remove silica gel particles. Following drying under vacuum overnight, each component was weighed. The scale given on the ordinate of Fig. 2 was arrived at for each tube by the following formula:

$$\frac{\text{vol. CHCl}_3 \times \text{spot intensity}}{\Sigma(\text{vol. CHCl}_3 \times \text{spot intensity})} \times \text{total mass of component}$$

where the summation is over all tubes containing the component in question.

THEORETICAL CONSIDERATIONS

JOHNSON⁵ derives the following three equations of general applicability to chromatographic systems:

For a complete column (*i.e.* a thin-layer plate):

$$R_F = \frac{B}{B + 1}$$

For a flowing column:

$$\frac{V}{v} = \frac{B + 1}{B}$$

and

$$B = K \cdot \frac{v}{w}$$

Where

B = effective distribution coefficient;

K = distribution coefficient;

V = volume of solvent required to elute peak;

v = volume of mobile phase;

w = weight of adsorbent.

Since the adsorbents for the column and the plates were prepared in the same way we may assume that the values of K are the same.

Thus for a column:

$$B_c = K\rho_c$$

where, by definition:

$$\rho_c = \frac{v_c}{w_c}$$

and for a plate:

$$B_p = K\rho_p$$

where, by definition:

$$\rho_p = \frac{v_p}{w_p}$$

$$\therefore R_F = \frac{K\rho_p}{K\rho_p + 1}$$

and

$$\frac{v}{V} = \frac{K\rho_c}{K\rho_c + 1}$$

$$\therefore K = \frac{R_F}{\rho_p - R_F\rho_p} = \frac{v}{V\rho_c - v\rho_c}$$

$$\therefore V = \frac{v(R_F\rho_c - R_F\rho_p + \rho_p)}{R_F\rho_c} \quad (1)$$

The experimental data gained to date indicates that under the conditions used:

$$\rho_p = \rho_c$$

In which case eqn. 1 reduces to:

$$V = \frac{v}{R_F} \quad (2)$$

Thus, knowing the elution volume of the first peak and the R_F of components on thin-layers one can calculate the elution volume of all other peaks eluted by the first solvent. However, it is advisable to check that $\rho_p = \rho_c$. This can be done using the experimentally determined elution volume of the second peak:

From above

$$R_{F1} = \frac{K_1 \rho_p}{K_1 \rho_p + 1} \quad R_{F2} = \frac{K_2 \rho_p}{K_2 \rho_p + 1}$$

$$\therefore \frac{K_1}{K_2} = \frac{R_{F1}(1 - R_{F2})}{R_{F2}(1 - R_{F1})}$$

where the subscripts 1 and 2 refer to components 1 and 2 and

$$V_1 = \frac{v(K_1 \rho_c + 1)}{K_1 \rho_c}, \quad V_2 = \frac{v(K_2 \rho_c + 1)}{K_2 \rho_c}$$

$$\therefore \frac{K_1}{K_2} = \frac{V_2 - v}{V_1 - v}$$

$$\therefore \frac{V_2 - v}{V_1 - v} = \frac{R_{F1}(1 - R_{F2})}{R_{F2}(1 - R_{F1})}$$

From which

$$v = \frac{V_2 - V_1 \cdot \frac{R_{F1}(1 - R_{F2})}{R_{F2}(1 - R_{F1})}}{1 - \frac{R_{F1}(1 - R_{F2})}{R_{F2}(1 - R_{F1})}} \quad (3)$$

If v calculated by eqn. 3 does not turn out to be equal to the value obtained by eqn. 2, ρ_p/ρ_c can be calculated from eqn. 1 using the value for v obtained from eqn. 3.

The elution volumes of components eluted by the second and third solvents can be calculated from the equations derived below.

Let a be the volume through which a component has been displaced when the second solvent is applied to the top of the column. Let b be the total displacement volume of this component when the solvent front of the second solvent overtakes it. Then, since R_F is the displacement volume of the solute divided by the displacement volume of the solvent front,

$$\frac{b - a}{b} = R_{F1}$$

where the subscript refers to the first solvent.

$$\therefore b = \frac{a}{1 - R_{F_I}}$$

Also,

$$\frac{a}{V_I} = R_{F_I}$$

where V_I is total volume of solvent I added to the column.

$$\therefore b = \frac{R_{F_I} V_I}{1 - R_{F_I}}$$

The elution volume in solvent II can now be found since after solvent II overtakes the component, the remainder of the column is equivalent to a short column loaded at the top with the component and with solvent II as eluent. Thus, the effective column volume in solvent II is:

$$v - \frac{R_{F_I} V_I}{1 - R_{F_I}}$$

From eqn. 2 the elution volume for this partial column is:

$$\frac{1}{R_{F_{II}}} \left(v - \frac{V_I R_{F_I}}{1 - R_{F_I}} \right)$$

thus the total elution volume is:

$$V_I + \frac{R_{F_I} V_I}{1 - R_{F_I}} + \frac{1}{R_{F_{II}}} \left(v - \frac{V_I R_{F_I}}{1 - R_{F_I}} \right) \quad (4)$$

By an extension of this line of reasoning it can be shown that the elution volume of a component eluted by solvent III is:

$$V_I + \frac{R_{F_I} V_I}{1 - R_{F_I}} + V_{II} + \frac{R_{F_{II}} V_{II}}{1 - R_{F_{II}}} + \frac{1}{R_{F_{III}}} \left[v - \left(\frac{R_{F_I} V_I}{1 - R_{F_I}} + \frac{R_{F_{II}} V_{II}}{1 - R_{F_{II}}} \right) \right] \quad (5)$$

Note that the derivations of eqns. 4 and 5 assume that $\rho_p = \rho_c$. If this is not

TABLE I

R_F VALUES FROM THIN-LAYER PLATES

Compound	Solvent		
	Carbon tetrachloride	Benzene ^a	Ethyl acetate ^a
Hydrocarbons	0.82	—	—
Esters	0.37	—	—
Ketones	0.26	—	—
Aldehydes	0.23	—	—
Secondary alcohols	0.078	0.34	—
Unknown	0.054	0.27	—
Primary alcohols	0.024	0.12	0.65

^a Values not listed are not required for this experiment.

the case the R_F values obtained from the thin-layers will have to be modified using eqn. 1 to obtain an R_F value that can be applied to the column.

RESULTS AND CALCULATIONS

Table I gives the R_F values obtained from the thin-layer plates. An elution diagram for the column separation is given in Fig. 2.

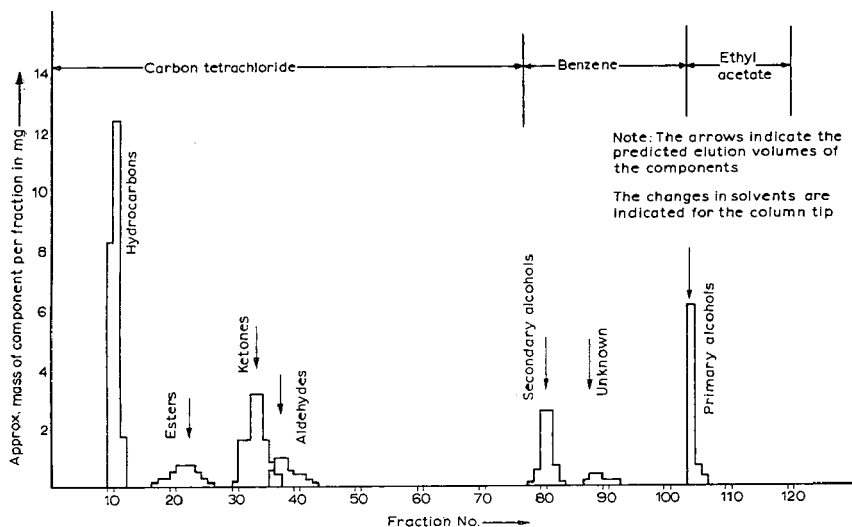


Fig. 2. Column separation of gl_6 wax on thin-layer silica gel.

Calculations

Elution volume of hydrocarbons (see Fig. 2): $10\frac{1}{2}$ tubes = 111 ml. From eqn. 2, $v = 111 \times 0.82 = 91$ ml. Elution volume of esters: end of tube 22 = 254 ml. Checking v from eqn. 3:

$$v = \frac{254 - \frac{111 \times 0.82 \times 0.63}{0.37 \times 0.18}}{1 - \frac{0.82 \times 0.63}{0.37 \times 0.18}} = 91 \text{ ml.}$$

Thus, $\rho_p = \rho_c$.

Using eqn. 2 the elution volumes of esters, ketones and aldehydes can be calculated. These values are given in Table II. The elution volumes of the secondary alcohols and the unknown were calculated using eqn. 4, and the elution volume of primary alcohols by eqn. 5. These values are also given in Table II. The experimental values determined from Fig. 2 have been included for comparative purposes.

DISCUSSION

The experimental and calculated values given in Table II are in good agreement, the maximum error being about 1%. Since the experimental values were found by

attempting to estimate the position of the peaks in 10.6 ml fractions, a better agreement could hardly be expected. This emphasises that the assumptions underlying the calculations are correct. Thus K , the distribution coefficient, is not dependent on the chromatographic system and in the column K is not affected by the passage of previous solvents.

TABLE II

COMPARISON OF CALCULATED AND EXPERIMENTAL VALUES FOR ELUTION VOLUMES

<i>Component</i>	<i>Elution volume (ml)</i>	
	<i>Calculated</i>	<i>Experimental</i>
Hydrocarbons	—	111
Esters	246	254
Ketones	350	350
Aldehydes	396	392
Secondary alcohols	847	848
Unknown	924	934
Primary alcohols	1091	1098

The separation illustrated in Fig. 2 took nearly four days to complete. Although this may be considered a disadvantage, it is not serious since once the procedure is commenced it requires little maintenance. All that has to be done is to observe the elution volume of the first peak so that the elution volumes of the other peaks can be calculated. By calculation, one can then find which times for solvent changes can be used which still allow satisfactory separations. In general a solvent should be changed just after the elution of a component with an R_F of about 0.25 on TLC in that solvent. If an accurate determination of the complete elution of such a peak is required so that the optimal time for the change of solvents is known, the R_F value for the trailing edge of the spot on TLC should be measured and substituted in either eqn. 2 or eqn. 4.

Fig. 2 shows that there was a slight overlap between the ketone and aldehyde peaks. The same overlap was found on TLC. Practically this is of little importance since the two components may be readily separated on a Florisil column after mild oxidation.

TABLE III

ANALYSIS OF g^I_6 WAX

<i>Components</i>	<i>Mass (mg)</i>	<i>Adjusted mass (mg)</i>	<i>Composition (%)</i>
Hydrocarbons	22.2	22.2	39.7
Esters	3.7	3.7	6.6
Ketones	11.1	11.1	19.8
Aldehydes	2.5	2.5	4.5
Secondary alcohols	6.3	6.3	11.2
Unknown	1.4	1.4	2.5
Primary alcohols	7.0	4.1	7.3
Fatty acids	5.2	4.7	8.4
Total	59.4	56.0	100.0

Table III gives the percentage composition of gl_6 wax. It will be noted that the masses of the primary alcohols and fatty acids have been adjusted. The reasons for this are as follows. 56.0 mg of wax were applied to the Florisil column and 5.2 mg of fatty acids and 51.3 mg of other components were eluted from it, giving a total recovery of 56.5 mg. Florisil contains about 0.5 % Na_2SO_4 which can be eluted by acetic acid. The excess 0.5 mg recovered is thus assigned to Na_2SO_4 contaminating the fatty acid fraction. The mass of the primary alcohols was adjusted because although 51.3 mg were applied to the silica gel column a total of 54.2 mg was recovered. It was assumed for the purposes of calculating percentage composition that the excess 2.9 mg was due to a contaminant that was discovered in the primary alcohol fraction. This is a yellow oily substance and appears to be a contaminant on the silica gel. Thus the wash with carbon tetrachloride was inadequate. However, the problem can be overcome by washing with ethyl acetate instead of carbon tetrachloride.

Although precautions were taken to ensure that the resolved components were free of solvents and silica gel particles, it may be that part of the excess 2.9 mg assigned to the contaminant came from other sources. Nevertheless recovery from a silica gel column is quantitative; a fact that gives this procedure a decided advantage over preparative TLC.

It should be pointed out that it is not yet clear whether the procedure given here can be applied directly to solvent mixtures. This is because the column separates solvent mixtures as can be seen by applying a mixture of carbon tetrachloride and benzene and watching the boundary form. This also appears to occur on thin-layer plates, and thus accounts for the excellent separations given by solvent mixtures in TLC. The least polar component of the solvent mixture will move to the front and resolve the least polar solutes. The more polar components of the solvent will travel only a small distance up the plate and thus separate the more polar solutes at the bottom of the plate. A case in point is the hexane-ether-acetic acid mixture (70:30:2) used to analyse barley wax⁶.

The results reported here show that there is no essential difference between TLC and column chromatography. Therefore one can design a column separation rapidly and quantitatively without actually packing a column. It seems pertinent to ask at this point why it is that column separations are so often inferior to thin-layer separations. Various authors (*e.g.* ref. 7) have emphasised the importance of a small particle size, but this is often sacrificed so that a high flow rate can be used. A small particle size gives an efficient use of the adsorbent because the void volume is small and the surface area is large. With difficult separations the efficient use of the adsorbent determines whether or not the separation can be made. If the separation is to be made, reduced flow rate must be accepted and inconvenience minimised by the use of automated equipment. Time saving faster flow rates can only be employed when the separation is easily made.

A future publication will give a more detailed analysis of gl_6 wax, and will examine the composition of the fractions isolated by the procedure reported in this paper.

ACKNOWLEDGEMENTS

The author is grateful to Prof. H. N. BARBER, Drs. R. S. VICKERY and M. J. MACEY, and Mr. C. E. MAY for helpful discussion and advice.

REFERENCES

- 1 H. N. BARBER AND A. G. NETTING, *Phytochemistry*, 7 (1968) 2089.
- 2 M. J. K. MACEY AND H. N. BARBER, *Phytochemistry*, 9 (1970) 13.
- 3 S. J. PURDY AND E. V. TRUTER, *Proc. Roy. Soc. (London)*, B 158 (1963) 536.
- 4 K. K. CARROLL, *J. Am. Oil Chemists' Soc.*, 40 (1963) 413.
- 5 M. J. JOHNSON, in W. W. UMBREIT, R. H. BURRIS AND J. F. STAUFFER (Editors), *Manometric Techniques*, Burgess, 1957, Chap. 15.
- 6 U. LUNDQVIST, P. VON WETTSTEIN-KNOWLES AND D. VON WETTSTEIN, *Hereditas*, 59 (1968) 473.
- 7 J. HIRSCH AND E. H. AHRENS, *J. Biol. Chem.*, 233 (1958) 311.

J. Chromatog., 53 (1970) 507-516

CHROM. 5042

DETERMINATION OF CREATININE IN SOUPS AND SOUP PREPARATIONS BY ION-EXCHANGE CHROMATOGRAPHY

II. AUTOMATIC APPARATUS

A. CARISANO, M. RIVA AND A. BONECCHI

Research Laboratories of Star Food Co. Ltd., 20041 Agrate Brianza (Italy)

(Received September 11th, 1970)

SUMMARY

An automatic apparatus for the determination of creatinine in soups and soup preparations by cation-exchange chromatography and the continuous UV spectrophotometric monitoring of the effluent is described. The data obtained in the analysis of a soup preparation for sixty consecutive days showed a small scatter. The recovery of creatinine amounted to $99.52 \pm 1.80\%$ of the most probable value. The main features of the apparatus are described in detail.

INTRODUCTION

A previous article¹ dealt with a method for the determination of creatinine in soups and soup preparations by separating this compound from interfering substances on a column packed with a cation-exchange resin and by subjecting the effluent to continuous UV spectrophotometric analysis. This was a discontinuous method because all the operations in it, including the sample introduction, were carried out manually. This method has now been fully automated, and the apparatus developed is described below.

APPARATUS

The automatic analyser shown in Fig. 1 is composed of the following main parts:

- (I) 4-l bottle A containing 0.4 M sodium acetate buffer ($\text{pH } 4.35 \pm 0.01$);
- (II) pump P for passing the buffer solution to column C at a rate of 77 ml/h;
- (III) column C packed with a cation-exchange resin;
- (IV) a sample-introducing device (patent pending) connected to column C;
- (V) thermostat (not shown) which keeps the water circulating in the water jacket of the column at 56.5° ;
- (VI) UV spectrophotometer linearized between 0 and 1000 optical density units, fitted with photomultiplier and a 300- μl quartz flow cell;

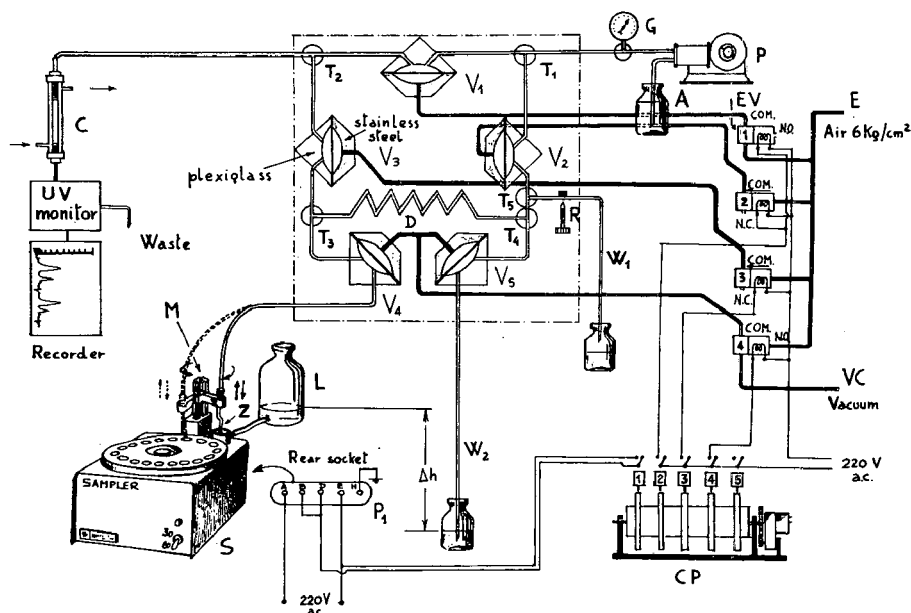


Fig. 1. Scheme of the automated analytical system for the determination of creatinine. For key, see text.

(VII) potentiometric recorder with a suitable sensitivity and a response time of about 1 sec (full scale). (For easy measurement of the peak areas, the deflection should be at least 25 cm.)

Fig. 2 shows the chromatographic column C with all its accessories. This column has an I.D. of 0.57 cm, an O.D. of 1.03 cm, and a total length of 22 cm. The resin (Aminex A₅*; height 11 cm) is kept firmly in place by a small PVC piston at the top and bottom. The end of each piston is fitted with a porous teflon disk (pore size 8 μ), which permits the eluent to flow through, while retaining the resin particles. The lower piston is supported by a ferrule while the upper piston can move, since the ferrule contains a spring, exerting a pressure of at least 7 kg/cm² on the piston head. The tightness of the pistons against the walls of the glass column is ensured by silicone rubber O-rings. Polyethylene tubing (I.D. 1 mm; O.D. 2 mm) is used for all connections, namely the pneumatic connections for the actuation of the diaphragm valves and the tubes carrying the buffer.

Sample-introduction device

Fig. 1 shows that the sampling system, whose parts are enclosed by a dash-dot line, is between pump P and the chromatographic column C. Other parts shown are as follows: (1) eluent reservoir A; (2) washing liquid reservoir L; (3) sample dispenser S; (4) compressed air inlet (6 kg/cm²) E; (5) five small diaphragm valves V₁–V₅ actuated by compressed air; (6) 4 pneumatic electro-valves EV₁–EV₄, which directly control the diaphragm valves; (7) cyclic programmer with a rotating drum CP, actuating the electro-valves EV₁–EV₄; (8) water pump VC generating vacuum. The whole system is

* Bio-Rad Labs., Richmond, Calif., U.S.A.

controlled by the programmer via microswitches 1-4, connected to the valves EV and to sample dispenser S. A more detailed picture of the part inside the dash-dot line also includes the following components: (1) metering channel D (0.5 ml); (2) three-way joints T_1 - T_5 ; (3) micrometric screw clamp R on the discharge tube W_1 . The micro-valves, the sample dispenser, and the programmer will be described before discussing the operation of the system.

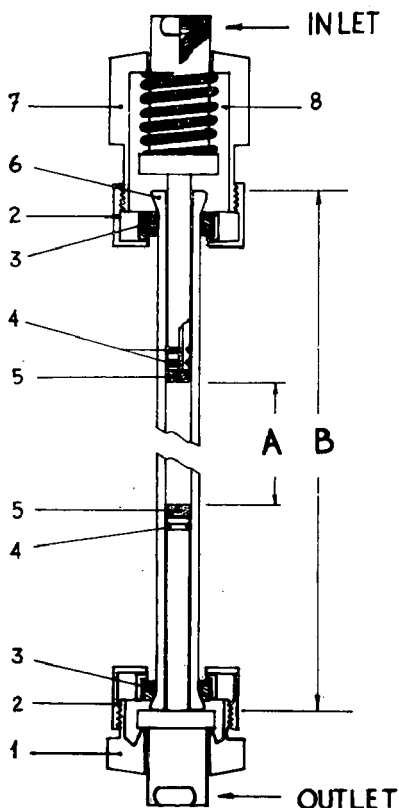


Fig. 2. Chromatographic column and its accessories (A = 11 cm; B = 22 cm). (1) Male ferrule made of PVC; (2) Female ferrule made of stainless-steel; (3) Teflon washer; (4) Silicone rubber O-rings; (5) Porous teflon disks (thickness 3 mm); (6) Glass column; (7) Male ferrule made of PVC, housing the spring; (8) Spring.

Diaphragm micro-valves

The diaphragm micro-valves deserve a brief description, although they have been used before in various automatic devices. They score because there is no mechanical friction here between the moving parts that effect closure, the dead space is negligible, and the operation is rapid, reliable, and easy to actuate by compressed air, regulated by electro-valves. As can be seen in Fig. 1, each diaphragm valve consists of a lens-shaped cavity, divided along the longer axis by an elastic membrane (coupled silicone and Viton). This membrane ensures perfect insulation between the analytical circuit and the control circuit. The transparent plexiglass top of the valve houses the

tubes for the liquid, while the stainless-steel bottom houses the membrane-command tube. When this part is pressurized, the membrane is deformed, and the flow of the liquid is stopped. When the pressure is discontinued and/or partial vacuum is created, the membrane is deformed in the opposite direction, and the valve is kept open. Four units with two independent command circuits are housed in a block, and the connection of two such blocks gives the five functions needed for operating the system shown in Fig. 1. The two blocks in our apparatus were made by Carlo Erba* after our design.

Sample dispenser

The sample dispenser device S (type CLA 1510), made by Carlo Erba, essentially consists of a rotating disk that can accommodate 40 sample holders. A mobile device M is mounted at a fixed point over the disk. This device introduces a suction tube into the sample holders. This operation alternates with the introduction of the same tube into the washing liquid reservoir at point Z. A positioning motor and a small timing motor perform the operations in the required sequence. The independent cyclic arrangement of the commercial apparatus was modified; a momentary closure of switch 1 of the general programmer (Fig. 1) now starts the process, while the end is brought about automatically by the positioning motor as soon as the suction tube is introduced into the washing liquid (point Z). The modification was done in accordance with the circuit shown in Fig. 1, and the power supply (220-V a.c.) is now introduced not in the normal cable (which remains unused) but through connector P₁ on the back of the sample dispenser. This modification is essential to ensure the synchronized operation of the various parts.

Programmer

The programmer is of the drum type and is fitted with a motor and a reduction gear that perform one complete revolution every 35 min. The command sections of the microswitches 1–5 are made of a moulded plastic and can be easily replaced. It is therefore possible to set up any program for each channel (the phase during the calibration being then varied). Four channels were used in the apparatus described here. The programmer was chosen from the Carlo Erba's fractomatic range of process-control gas chromatographs.

Operation

Pump P passes the eluent from bottle A into column C via devices T₁, V₁ and T₂. The eluate leaving the column is subjected to continuous UV spectrophotometric monitoring at 240 mμ and is then discarded. Therefore diaphragm valve V₁ is open while diaphragm valves V₂ and V₃ are closed. Furthermore, the sample to be introduced is already in the metering channel D, and hence V₄ and V₅ are closed as well. The suction tube is placed into the washing liquid L at point Z. This is the condition that prevails for the longer time during each analytical cycle; therefore the pneumatic connections between valves V₁–V₅ and electro-valves EV₁–EV₄ are so arranged as to obtain the required functions with all the solenoids non-activated. The microswitches 1–4 of the programmer are open, and the sampler is therefore not energized.

* Carlo Erba S.p.a., Scientific Apparatus Division, 20090 Rodano, Italy.

When the sample is to be introduced, the programmer closes the micro-switch 2, and valves EV_1 and EV_2 are simultaneously energized, which makes valve V_1 close and valve V_2 open. The eluent is discharged into tube W_1 via the constriction R, which is regulated to keep the route $P-T_1-V_2-T_5-W_1$ under a pressure of 1.5 kg/cm². The closure of V_1 decreases the pressure and the flow rate in the column, and these changes favour the imminent reception of the sample. After some seconds, the programmer closes micro-switches 3; EV_3 is energized, and micro-valve V_3 opens to permit the sample to enter the column. The sample is pushed along by the eluent, part of which is split off at W_1 in order to keep the pressure and the rate of introduction low.

When the sample has been transferred into the column, the programmer de-energizes valve EV_3 , which makes valve V_3 close. After a few seconds, micro-switch 2 opens, and both EV_1 and EV_2 are de-energized, whereby the initial state, with V_1 open and V_2 closed, is re-established. The analytical phase then begins.

During this phase, the line of the metering channel D is rinsed, and then the next sample is fed into it. This sample is introduced into the column when the previous analytical phase is over. In this way, the programmer closes the micro-switch 4, thus energizing valve EV_4 . Valves V_4 and V_5 then open on account of a lack of command pressure. To ensure a perfect opening of the inlet and outlet, the membrane is brought back with the aid of vacuum. Owing to the level difference between the washing liquid in the reservoir L and the discharge point W_2 , the washing liquid starts flowing spontaneously at this moment along the route $Z-V_4-T_3-D-T_4-V_5-W_2$. Simultaneously with the closure of the micro-switch 4, the programmer closes micro-switch 1, and the sample dispenser is thus energized for 80 sec. The mobile attachment then removes the suction tube from the washing position and places it into a sample holder on the disk. A small amount of air is sucked in during the transit, and this air plug serves to separate the washing liquid from the sample. Thus begins the spontaneous flow of the sample which lasts for 40 sec and fills up the whole system of the metering channel D (part is discarded into W_2). Before the sample (ca. 3 ml) in the holder is exhausted, the programmer de-energizes valve EV_4 , thus causing V_4 and V_5 to close. The sample is thus detained in the metering channel D. As described before, the internal mechanism of the sample dispenser stops the operation of the mobile suction unit when this is inserted into the washing liquid and when the sample-holder disk advances by one step, offering the next sample for suction.

To stop the whole operation, a dummy sample holder is introduced into the disk after the last sample. On starting the suction phase at this dummy sample holder, the mobile unit closes a low-voltage circuit which is connected to an auxiliary relay and can terminate the power supply to the whole system or can put it in stand-by position. Table I shows the operative positions of the four programmer-controlled micro-switches, and the state of the four electro-valves, which regulate the five micro-valves V_1-V_5 of the analytical circuit.

RESULTS AND DISCUSSION

In view of the geometry of the chromatographic system (which is optimized for the separation of creatinine from interfering substances) and in view of the fact that at least 0.5-ml samples are needed for accurate automatic sampling, the sample must be introduced slowly and at a low pressure, as in manual operation with open columns.

TABLE I

ROUTINE SCHEDULE

O = Open; C = Closed.

Time (sec)	Micro-switch on programmer				Micro-valve				
	1	2	3	4	V ₁	V ₂	V ₃	V ₄	V ₅
0	O	C	O	O	C	O	C	C	C
10	O	C	C	O	C	O	O	C	C
208	O	C	O	O	C	O	C	C	C
222	O	O	O	O	O	C	C	C	C
1905	C	O	O	O	O	C	C	C	C
1912	C	O	O	C	O	C	C	O	O
1985	O	O	O	C	O	C	C	O	O
2002	O	O	O	O	O	C	C	C	C
2100	O	C	O	O	C	O	C	C	C

In this way, the sample is deposited correctly on the first theoretical plate of the column, and the maximum resolving power is thus ensured. The system described above satisfies these requirements in a cyclic and automatic manner.

Special care was taken to make the micro-valve V_1 close and the micro-valve V_2 open some seconds before micro-valve V_3 , thus lowering the analytical-circuit pressure of 4–5 kg/cm² by at least 1 kg/cm² in the V_1 – T_2 – C section. The latter is then temporarily isolated from the pump and is connected only to the discharge route. The pressure in the section P – T_1 – V_2 – T_5 is reduced to 1.5 kg/cm², since at this pressure the eluent overcomes the calibrated resistance R and is discharged along W_1 . It is only at this moment that the delayed opening of V_3 permits the slow introduction of the sample, waiting in the T_4 – D – T_3 section, onto the first theoretical plate of the column. After a sufficient time, microvalve V_3 closes a few seconds before micro-valve V_1 opens, and thus the pressure in the column C decreases from 1.5 kg/cm² to zero.

The conditions of manual sample introduction were carefully reproduced in this manner because distorted and ill-resolved peaks had been obtained in preliminary experiments with the automatic system when the samples were introduced into the column fast and at the usual (high) pressure prevailing in the system. Such sample introduction evidently causes a marked reduction in the efficiency and the resolving power of the column.

To promote an even better collection of the sample on the first plate, the sample was dissolved in a buffer more acidic than the eluent. We used for this 1 mM solution of cytosine in 0.3 *M* acetic acid, adjusted to pH 3.70 with 40% NaOH (used previously in the manual method). The sample was prepared and treated exactly as before¹ and then it was dissolved in exactly 5 ml of the 1 mM cytosine solution. Whenever necessary the sample was filtered through a Whatman No. 42 paper, an aliquot was placed in a *ca.* 3-ml plastic holder, and the latter was introduced into the sample holder disk.

In this fully automated system, the samples prepared during the day can be analyzed during the night. 24 samples can be analyzed between 6 p.m. and 8 a.m.

Since an internal standard (creatinine) is used, the creatinine values can be found from the ratio between the creatinine peak area (or height) and the cytosine peak area (or height). The evaporation of the sample does not influence this ratio, so the samples can be left uncovered on the plate. The filtration of the samples before the analysis

removes mucilaginous substances which may clog up the column, and so the resin can be used for several months without regeneration. When eventually a pressure of 5.5–6 kg/cm² on the gauge G (see Fig. 1) is needed to make the eluent flow, the column is dismantled, and the resin is poured into a beaker and regenerated. This is done by washing it in turn with hot 6 N HNO₃, distilled water, hot 4 N HCl, and 2 N NaOH. The resin, thus obtained in the Na⁺ form, is washed repeatedly with distilled water and then replaced into the column, ready for further analysis. When analyzing an average of 12 samples a day, we used a column for about three months before regenerating the resin. The automatic system had the same precision and accuracy as the manual system. The reproducibility of the results was excellent. The creatinine content of a soup preparation was found to be 0.51–0.57% (mean 0.537%) by HADORN'S method^{2,3}, and 0.54–0.57% (mean 0.552%) by the automated method, these analyses being carried out simultaneously for 60 consecutive days. On the basis of the data for the meat extract used, the most probable creatinine content of this soup preparation was 0.555%.

REFERENCES

- 1 A. CARISANO, A. BONECCHI AND M. RIVA, *J. Chromatog.*, 45 (1969) 264.
- 2 H. HADORN, *Mitt. Lebensm. Hyg.*, 37 (1946) 342.
- 3 *Analytical Methods for the Soup Industry*, Association of Swiss Soup Manufacturers, Berne, May 1st, 1961.

J. Chromatog., 53 (1970) 517–523

CHROM. 5008

USE OF OLEFIN- Ag^+ COMPLEXES FOR CHROMATOGRAPHIC SEPARATIONS OF HIGHER OLEFINS IN LIQUID-SOLID SYSTEMS*

J. JANÁK, Z. JAGARIĆ** AND M. DRESSLER

Institute of Instrumental Analytical Chemistry, Czechoslovak Academy of Sciences, Brno (Czechoslovakia)

(Received August 25th, 1970)

SUMMARY

The selectivity effect caused by the formation of olefin-silver ion complexes in systems of propanol-water- AgNO_3 /porous polymers (like Porapak Q) were studied under static and dynamic conditions.

Liquid as well as thin-layer chromatographic separations of higher olefins from mixtures with other hydrocarbons are possible with a selectivity equivalent to seven carbon atoms when comparing the chromatographic retention of *n*-paraffin and *n*-olefin (heptane, tetradecene) under conditions used.

INTRODUCTION

Olefins form unstable π -complexes with Ag^+ . The bond between the olefinic ligand and the metal ion is formed¹ by donation of electrons from the double bond to the vacant s-orbital of Ag^+ and then donation of d-electrons from the metal ion to the antibonding orbitals of the olefin. Because the symmetry is not correct for interaction, the two bonds are distinct. Stability of π -complexes is therefore, low, formation depending a great deal on the steric hindrance of a double bond. This fact has been utilized in gas chromatography (GC) by BRADFORD *et al.*² for selective separation of isomeric butenes; they used glycol saturated with AgNO_3 as a stationary phase at 0°. GIL-AV *et al.*³ gave a survey of positive results on the separation of cyclic olefins having a four- to seven-membered ring by GC on columns containing AgNO_3 solutions at temperatures up to 50°. However, the optimum working conditions of this type of chromatographic system are within the temperature range 0–30°. The complex stability at temperatures exceeding 50–60° drops to a value that is no longer significant for the separation. Further, the stability of AgNO_3 solutions in the organic solvents used is poor even at room temperature and chromatographic columns only retain their original properties for a few minutes. Therefore, only very volatile olefins can be separated in this way. In addition, on account of reasons mentioned above, this

* This work has been carried out during the stay of Z. JAGARIĆ in the UNESCO Longterm Postgradual Course in Modern Method of Analytical Chemistry (UNALCO) 1969/1970 in the Institute of Instrumental Analytical Chemistry.

** Present address: Organsko Kemijska Industrija, Zagreb, Yugoslavia.

method is suitable only for research work and fails in common analytical practice. However, the very separation of higher olefins from paraffinic, cyclic, and aromatic hydrocarbons is important from an analytical point of view.

To solve this problem we utilized the high sorption affinity of porous polyhydrocarbons (styrene-ethylvinylbenzene copolymers, type Porapak) to hydrocarbons; this has lately led to successful separations in liquid-solid systems^{4,5}. Using a complex forming solution as mobile phase, a change in partition coefficients of paraffin (aromatic compound)-olefin pairs can be expected also with higher olefins. Since olefins should be eluted before the corresponding paraffins, the separation should be more rapid unlike the experiments of BRADFORD *et al.*² and GIL-AV *et al.*³ in which olefins were retained more than paraffins. The method may not be limited due to the low stability of AgNO₃ solutions because Ag⁺ solutions remain only a short time in the column. We carried out static and dynamic measurements of the partition stage of model hydrocarbons (paraffin-olefin-aromatic compounds) using the system Porapak Q-AgNO₃ in propanol containing various quantities of water. Our results are promising.

EXPERIMENTAL AND RESULTS

Static measurements

The established equilibria of some hydrocarbons were measured in the system Porapak Q/AgNO₃-propanol-water, expressed by adsorbed* hydrocarbons on Porapak Q. *n*-Nonane, *n*-decene and benzene (pure products of BDH, London) were used as a model mixture. Porapak Q (100-120 mesh, batch. No. 558, Waters Associates Inc., Framingham, Mass., U.S.A.) and a mixture of *n*-propanol (Lachema N.E., Brno, Czechoslovakia), water and AgNO₃ were used as sorbent and solvent, respectively. The concentration of AgNO₃ and the propanol-water ratio were changed when necessary.

The mixture of hydrocarbons was dissolved in a known amount of the solvent; then a known amount of sorbent was added and the decrease in concentration of the solution was determined. The quantity of adsorbed hydrocarbons was determined by GC from the ratios of the chromatographic peak heights of hydrocarbons obtained before adding Porapak and after establishing equilibrium. The complex of an olefinic hydrocarbon with silver is unstable and a temperature above 100° in the injection chamber allows complete complex breakdown.

Dynamic measurements

A dark glass column (43 cm long and 0.3 cm I.D.) was used for liquid chromatography and Teflon tubing was used for all connections to prevent the reduction of AgNO₃. The concentration of AgNO₃ was 0.08 g/ml of mobile liquid in all cases. Porapak Q (150-200 mesh, batch No. 413) served as the column packing. Since the paraffins and olefins used give no adequate signals when using conventional liquid chromatographic detectors⁶, the column effluent composition was followed by GC (data in chromatograms mean GC peak heights according to ref. 7).

Fig. 1 illustrates the effect of the concentration of AgNO₃ on the adsorption of *n*-nonane, *n*-decene, and benzene. The propanol-water ratio was kept constant (2:1).

* The term adsorption is used in this paper but it is unclear whether the process is ad- or absorption, or both.

The quantity of adsorbed hydrocarbon does not change within the concentration range of AgNO_3 examined (0–0.10 g/ml) in the case of nonane as well as of benzene. However, in the case of olefin the fraction of adsorbed decene changes with the concentration of silver salt in the solvent. With the increasing AgNO_3 concentration the quantity of olefin adsorbed on Porapak Q decreases. The fraction of adsorbed decene is less than that of nonane but still higher than that of benzene in the concentration range 0.015–0.045 g/ml. The quantity of decene adsorbed at still higher concentrations of silver salt is the least of all model mixture compounds; the quantity within a concentration range of about 0.060 up to 0.100 g/ml remains constant.

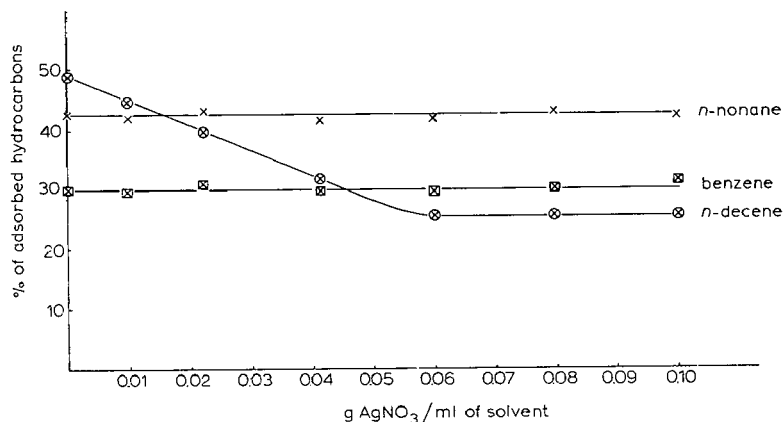


Fig. 1. Effect of the AgNO_3 concentration in the solvent on hydrocarbon adsorption on Porapak Q. 0.2 g of Porapak Q, 5 ml of propanol–water (2:1), 0.1 % hydrocarbon solution in a given mixture.

The effect of the propanol–water ratio on adsorption equilibria of hydrocarbons is given in Table I. The concentration of AgNO_3 was 0.10 g/ml; the quantity of adsorbed hydrocarbons was always measured before and after adding AgNO_3 for each mixture again. The quantity of adsorbed hydrocarbons on Porapak Q increases with increasing water content for all three compounds investigated as expected. With nonane and benzene there are no concentration changes after adding silver salt to the solvent mixture. With decene the quantity of adsorbed hydrocarbon decreases regularly

TABLE I

INFLUENCE OF RATIO OF PROPANOL–WATER ON THE ADSORPTION OF MODEL HYDROCARBONS

Propanol– water ratio	AgNO_3 (g/ml)	Fraction of adsorbed hydrocarbons on Porapak			C_9/C_{10}
		C_9	Benzene	C_{10}	
1:2	0.0	95.3	71.5	97.5	0.98
1:2	0.1	95.5	71.4	89.3	1.07
1:1	0.0	68.2	49.5	72.0	0.94
1:1	0.1	68.0	49.7	40.4	1.68
2:1	0.0	42.4	31.2	48.9	0.87
2:1	0.1	42.2	31.0	25.6	1.65

again. The adsorption selectivity which is represented by the ratio C_9/C_{10} increases with increasing water content up to a propanol–water ratio of 1:1; C_9/C_{10} ratio tends to be constant for the mixtures 1:1 and 2:1.

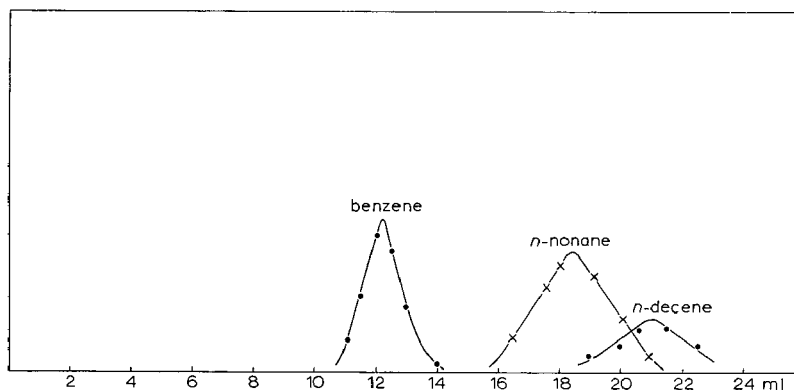


Fig. 2. Liquid chromatogram of a model mixture. Solvent: mixture of *n*-propanol–water (2:1); flow rate: 0.3 ml/min.

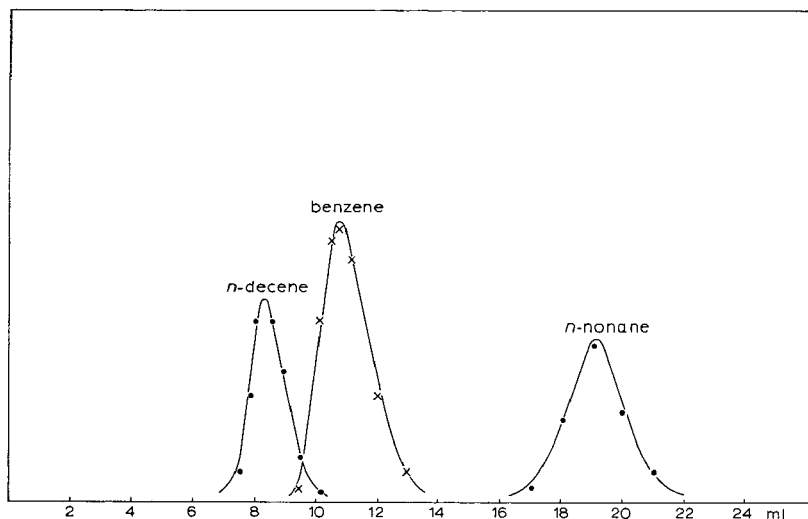


Fig. 3. Liquid chromatogram of a model mixture — the effect of AgNO_3 . Solvent: mixture of *n*-propanol–water (2:1), and AgNO_3 (0.08 g/ml); flow rate: 0.24 ml/min.

The chromatogram of a model mixture containing *n*-nonane, *n*-decene, and benzene eluted with propanol–water (2:1) is shown in Fig. 2. The retention sequence is the following: benzene, *n*-nonane, *n*-decene. The effect of complex formation on the retention behavior of hydrocarbons mentioned is evident from Fig. 3. The retention sequence is principally changed; decene forming a silver complex has the lowest retention volume. Thus the results confirm the data obtained by static equilibrium measurements.

Fig. 4 shows the chromatogram of the hydrocarbon mixture which consists of

n-heptane, *n*-nonane, *n*-dodecene, and *n*-tetradecene separated under the same conditions as given in Fig. 3. It is evident that the effect of the complex formed is so high that the tetradecene peak overlaps the peak of heptane so that the selectivity effect achieves 7 carbon atoms.

The effect of the ratio of propanol-water on the retention of model compounds is evident from Fig. 5. Higher relative propanol content shifts the adsorption equilibrium of all hydrocarbons in favor of the mobile phase which is manifested by more rapid elution.

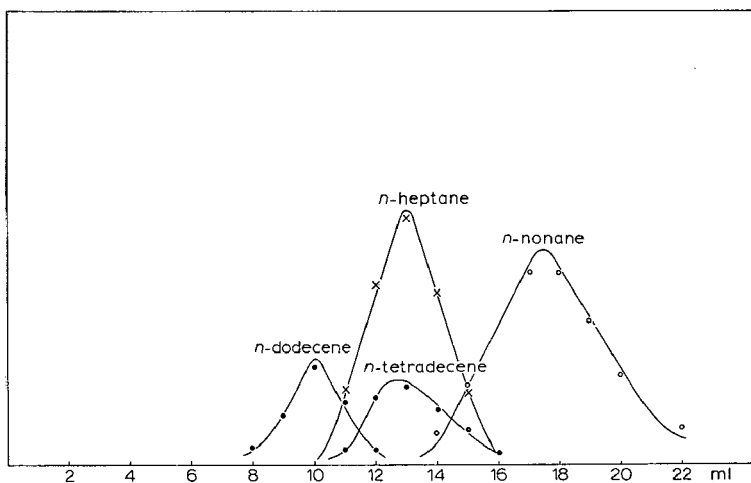


Fig. 4. Liquid chromatogram of a more complex mixture. Solvent: mixture of *n*-propanol-water (2:1), and AgNO_3 (0.08 g/ml); flow rate: 0.25 ml/min.

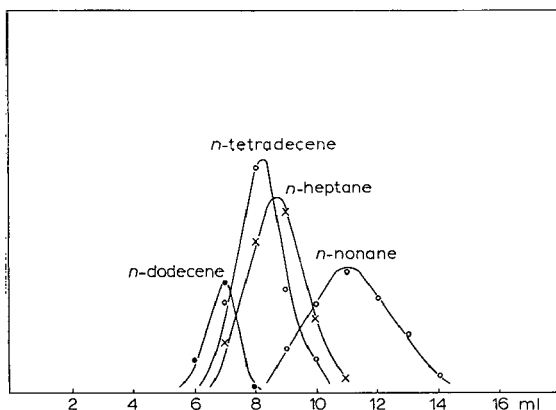


Fig. 5. Effect of an increased water content on retention of model compounds. Solvent: mixture of *n*-propanol-water (3:1), and AgNO_3 (0.08 g/ml); flow rate: 0.27 ml/min.

CONCLUSIONS

The π -complex formation of olefinic hydrocarbons and silver ions in liquid mobile phase produces a change of their retention volumes. This allows the separation

of olefins from the mixture containing other hydrocarbons by liquid chromatography and/or thin-layer chromatography. The olefin elution is more rapid in the system mentioned, as compared with systems in which the mobile liquid does not contain Ag^+ while the retention of aromatic and paraffinic hydrocarbons does not change. The selective effect is considerable; a shift equivalent to the effect of 7 carbon atoms has been found.

REFERENCES

- 1 M. J. S. DEWAR, *Bull. Soc. Chim.*, 18 (1951) C 79.
- 2 B. W. BRADFORD, D. HARVEY AND D. E. CHALKLEY, *J. Inst. Petrol.*, 41 (1955) 80.
- 3 E. GIL-AV AND J. HERLING, in G. PARISSAKIS (Editor), *Chromatographie et Méthodes de Séparation Immédiate*, Part I, Union Chim. Hellènes, Athens, 1966, p. 167.
- 4 J. JANÁK, *Chem. Ind. (London)*, (1967) 1137.
- 5 J. JANÁK, *J. Chromatog.*, 48 (1970) 288.
- 6 J. F. K. HUBER, *J. Chromatog. Sci.*, 7 (1969) 172.
- 7 V. R. ALISHOEV, V. G. BEREZKIN AND V. S. TATARINSKII, *Zavod. Lab.*, 34 (1968) 148.

J. Chromatog., 53 (1970) 525-530

CHROM. 4997

CHROMATOGRAPHIC PURIFICATION OF CYTOPLASMIC RIBOSOMES
FROM PEA PLANTS

C. KLIFFEN

Institute of Phytopathological Research, Wageningen (The Netherlands)

(Received August 17th, 1970)

SUMMARY

A chromatographic procedure was developed for the purification of ribosomes. Young pea plants were ground in a solvent containing polyethylene glycol, magnesium acetate, sucrose, and tris(hydroxymethyl)aminomethane-acetic acid buffer (pH 7). The slurry was poured onto a column of cellulose and sand and the impurities washed out using a solvent containing magnesium acetate, sucrose, and tris(hydroxymethyl)aminomethane-acetic acid buffer (pH 7). The ribosomes were eluted by omitting magnesium acetate from the developing solvent. The effluent was centrifuged at $40000 \times g$ for 10 min. To achieve a higher degree of purification and concentration of the ribosomes, the chromatographic procedure was repeated with the supernatant. The solvent used for the grinding medium was used to eliminate more undesirable components from the eluate containing the ribosomes. This method completely separates chloroplasts and most of the other unwanted impurities from the ribosomes. The final preparation contained highly purified ribosomes, as evidenced by ultraviolet spectra, sedimentation constants and electron micrographs.

INTRODUCTION

A chromatographic procedure was developed by VENEKAMP AND MOSCH¹ for the purification of a number of rod-shaped plant viruses. After addition of a solution containing polyethylene glycol (PEG) to homogenates of freshly infected leaves, the viruses and chloroplasts were retained by cellulose adsorbents. Impurities were washed out with a similar solution. The virus was eluted by decreasing the PEG content of the developing solvent.

VENEKAMP *et al.*² reported the purification of some spherical viruses by the use of a similar procedure. These viruses have a size comparable to that of ribosomes. An attempt was therefore made to isolate ribosomes from plant material by employing the same procedures used for virus isolation. This method has several advantages besides its simplicity, such as the high purity that can be attained³ and the complete recovery of the isolated viruses¹. According to VENEKAMP AND MOSCH⁴ these results may be due to the stabilizing effect of polyethylene glycol. This phenomenon had already been mentioned by ALBERTSSON⁵ and ALBERTSSON AND BALTSCHIEFFSKY⁶.

MATERIALS AND METHODS

Plant material

Pea plants, *Pisum sativum* L. var. Rondo, were grown to a height of 5 to 10 cm. The upper parts including the first unfolded leaves were harvested.

Chromatographic columns

For the first column, 200 g of white sand (50 mesh) and 12 g of cellulose (Whatman fibrous powder, CF11) were mixed to form a homogeneous slurry in 100 ml of an aqueous solution containing 10 % PEG 6000 (Carbowax 6000, Carbide and Carbon Chemicals Co., U.S.A.), 0.4 *M* sucrose, 0.004 *M* magnesium acetate, and 0.005 *M* tris(hydroxymethyl)aminomethane-acetic acid buffer (pH 7). This was poured into a chromatographic column 6 cm in diameter. The second column (diameter 3 cm) consisted of 10 g of cellulose powder, suspended in the above-mentioned solvent. The chromatographic columns used in these studies were cooled by attached mantles with alcohol circulated in them at 4°.

Purification

Fresh plant material (25 g) was homogenized for 30 sec in a Waring Blendor with 100 ml of 0.005 *M* tris(hydroxymethyl)aminomethane-acetic acid buffer (pH 7) containing 10 % PEG, 0.4 *M* sucrose and 0.004 *M* magnesium acetate. The homogenate was mixed with 200 g of white sand and 12 g of cellulose powder to form a slurry. This mixture was applied to the first column and washed with 900 ml of a solvent containing 0.4 *M* sucrose, 0.004 *M* magnesium acetate and 0.005 *M* tris(hydroxymethyl)aminomethane-acetic acid buffer (pH 7). The initial effluent was turbid and had a yellowish-brown color. Next the solvent was modified by eliminating magnesium acetate. After 150 ml of the modified solution passed through the column, a subsequent quantity of 250 ml of this solution eluted UV-absorbing material. The effluent was centrifuged in a Sorvall refrigerated centrifuge RC-2 at $40\,000 \times g$ for 10 min.

PEG and magnesium acetate were added to the supernatant to give final concentrations of 10 % and 0.004 *M*, respectively. This solution was then passed through the second column. This column was then washed with 100 ml of 10 % PEG, 0.4 *M* sucrose, 0.004 *M* magnesium acetate, and 0.005 *M* tris(hydroxymethyl)aminomethane-acetic acid buffer (pH 7). Finally, 100 ml of a similar solvent minus PEG was passed through the column. To concentrate the ribosome fraction the last effluent was made 10 % with respect to PEG and the mixture centrifuged at $40\,000 \times g$ for 30 min. The precipitate was resuspended in 15 ml of water and the resulting suspension was stirred carefully for 1 h followed by centrifugation at $40\,000 \times g$ for 10 min. The supernatant contained the cytoplasmic ribosomes.

The flow rate of the first column was 4 ml/min and that of the second column was 3 ml/min. The presence of UV-absorbing substances in the effluents was detected using an automatic recording LKB-Uvicord absorption meter at 254 nm.

RESULTS

The chromatographic effluents showed strong absorbance at 254 nm as indicated in Fig. 1. The first solvent containing 0.4 *M* sucrose, 0.004 *M* magnesium acetate, and

0.005 *M* tris(hydroxymethyl)aminomethane-acetic acid buffer (pH 7) eluted a large amount of yellowish-brown colored and UV-absorbing material. The effluent by the second solution containing 0.4 *M* sucrose and 0.005 *M* tris(hydroxymethyl)aminomethane-acetic acid buffer (pH 7) was pale green and turbid.

The initial effluent from the second column had a slight UV-absorption. The solution containing 0.4 *M* sucrose, 0.004 *M* magnesium acetate, and 0.005 *M* tris(hydroxy-

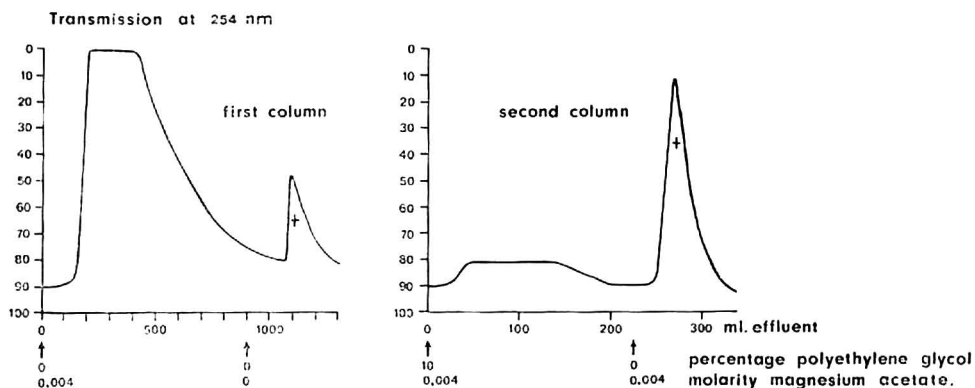


Fig. 1. Fractionation of ribosomes and other UV-absorbing substances from pea plant homogenates on cellulose columns. Column 1 (6 × 6 cm) is a mixture of 200 g of white sand (50 mesh) and 12 g of cellulose. Column 2 (3 × 6 cm) consists of 10 g of cellulose. Composition of the solvents: 0.4 *M* sucrose, 0.005 *M* tris(hydroxymethyl)aminomethane-acetic acid buffer (pH 7) and percentages of PEG and magnesium acetate as indicated by the arrows. Absorption of the effluents was recorded by the LKB Uvicord absorption meter at 254 nm. Presence of ribosomes is indicated by plus sign (+).

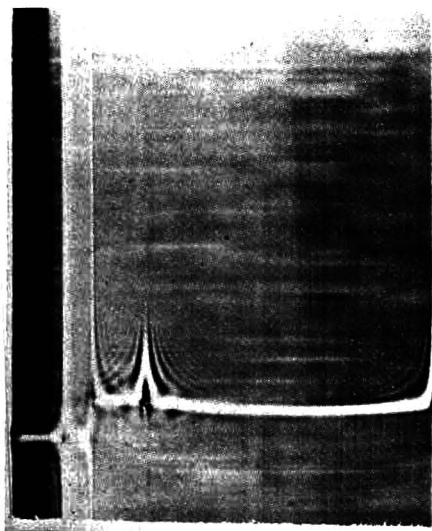


Fig. 2. Ultracentrifugal pattern of ribosomes isolated from homogenates of pea plants by means of chromatography on cellulose. Solvent constituents removed by centrifugation. Ribosomes dissolved in water.

methyl)aminomethane-acetic acid buffer (pH 7) eluted a large quantity of UV-absorbing substances from the second column. According to the studies described below, this effluent contained the ribosomes.

The absorption spectrum of the final preparation recorded by a combination of a Beckman UV spectrophotometer DB-G and a Sargent recorder Model SRLG, was characteristic of ribosomes. The maximum absorption was at 258 nm and the minimum absorption was at 238 nm. The ratio of these absorptions was 1.5.

The sedimenting behavior was studied with the aid of the Spinco analytical ultracentrifuge Model E. The pattern is given in Fig. 2. A sedimentation constant of 80 S was obtained based on the method of MARKHAM⁷.

Electron microscopic studies of the final preparation failed to show the presence of impurities. The electron micrograph in Fig. 3 represents a portion of the pattern on the grid and is considered to be a representative field. The ribosomes were well separated from each other. An average diameter of 25 nm was found.

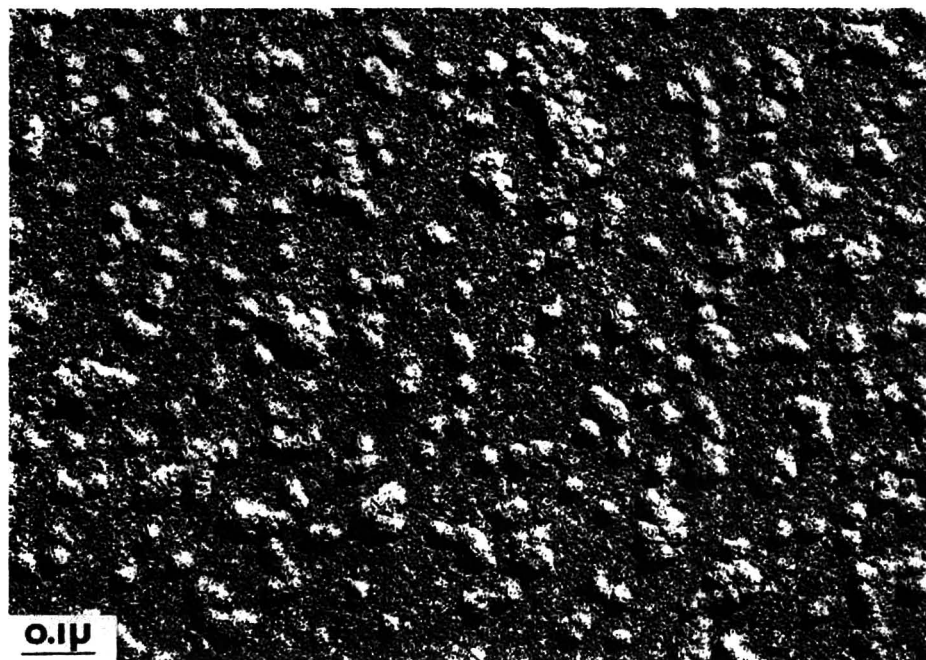


Fig. 3. Electron micrograph of ribosomes purified by chromatography on cellulose. Solvent constituents removed by centrifugation. Ribosomes dissolved in water. (Photograph: Technical and Physical Engineering Research Service, T.F.D.L., Wageningen).

DISCUSSION

This paper presents a procedure for the purification of ribosomes from young pea plants.

The packing material used for the columns is essentially cellulose because of its high capacity for adsorbing cell components. The column is especially efficient in ad-

sorbing chloroplasts and their fragments. Direct application of the plant homogenate on a cellulose column resulted in an immediate clogging of the system and hence the solvent flow was completely inhibited. The plant homogenate was mixed with white sand which reduced clogging. When the homogenate was mixed with white sand and cellulose, and at the same time the column cellulose was mixed with white sand, the solvent flow rate could be adjusted to 4 ml or more per min. The diameter of the column determined the flow rate also.

The stabilization of ribosomes by magnesium ions has been reported by many workers. BARKER AND RIEBER⁸ described this effect on ribosomes from peas. ARGLEBE AND HALL⁹ mentioned the same effect on ribosomes from bean plants. Consequently magnesium ions were added to the homogenate and to the solvents used in the procedures reported in this paper.

Ts'o¹⁰ and Hsiao¹¹ reported that low concentrations of ions and a pH of 7 reduced the dissociation of the ribosomes. A buffer system of 0.005 *M* tris(hydroxymethyl)aminomethane-acetic acid (pH 7) seemed to be suitable.

Sucrose at a concentration of 0.4 *M* produced an osmotic protection of the chloroplasts and mitochondria (see for example LYTTLETON¹²). This may be of importance in reducing the interactions between the breakdown products of these organelles and the ribosomes.

VENEKAMP AND MOSCH¹³ reported that a solvent containing large amounts of PEG (8 percent or more) was necessary for adsorption of spherical virus particles similar in size to ribosomes. Here these particles are considered to behave like small virus particles. The presence of PEG is only necessary during the application of the homogenate on the column. Perhaps due to the effect of magnesium ions on the ribosomes and the presence of plant material in the column, elution with a solvent containing magnesium ions and no PEG removed undesirable components from the column while a solvent without magnesium ions eluted the ribosomes.

Removal of enzymes may have eliminated degradation of ribosomes during the purification procedure. This may partly account for a high recovery of ribosomes in the final preparation.

Using the first column the ribosomes could be purified in a short time, but UV-absorbing materials were tailing throughout the elution schedule. The purity of the ribosomes depended on the amount of the first solvent percolated through the column. Tailing did not occur during percolation through the second column.

The difference in the behavior of ribosomes in the first and in the second columns with respect to magnesium ions is likely due to the occurrence of various substances in the homogenate applied onto the first column. VENEKAMP AND MOSCH¹ described a similar effect in chromatographic virus purification. According to VENEKAMP *et al.*³ protoplasmic membranes may be responsible for this phenomenon.

Cooling of the columns may have reduced enzymatic degradation of ribosomes.

The ribosome-carrying effluent from the second column is opaque but the color is pale-green. The final treatment of this effluent yielded a ratio of the absorption maximum and minimum similar to values found previously (see for example LYTTLETON¹²).

Three pieces of evidence suggest that this procedure yields pure cytoplasmic ribosomes. First, the UV absorption spectrum of the final preparation showed a maximum at 258 nm and a minimum at 238 nm; the ratio of these absorptions was 1.5.

Second, the sedimentation constant of the particles in this preparation was 80 S, consistent with the value reported among others by BARKER AND RIEBER⁸. Third, the electron micrograph represented a portion of the pattern on the grids and therefore was considered to be a representative field with particles, well separated from each other. The value for the diameter (25 nm) of the particles agrees with that reported for example by BONNER¹⁴. The absorption and sedimentation values of the preparations reported here suggest the absence of polysomes.

ACKNOWLEDGEMENTS

The author is indebted to DR. G. W. MILLER and his colleagues (Huxley College of Environmental Studies, Western Washington State College) for their critical reading of this manuscript and the corrections in the text.

REFERENCES

- 1 J. H. VENEKAMP AND W. H. M. MOSCH, *Virology*, **23** (1964) 394.
- 2 J. H. VENEKAMP, W. H. M. MOSCH AND K. E. ERKELENS-NANNINGA, *Phytopathology*, **54** (1964) 608.
- 3 J. H. VENEKAMP, W. H. M. MOSCH AND J. P. W. NOORDINK, *Viruses of Plants*, Proc., Wageningen (The Netherlands), 1965, p. 108.
- 4 J. H. VENEKAMP AND W. H. M. MOSCH, *Virology*, **22** (1964) 503.
- 5 P.-Å. ALBERTSSON, *Partition of Cell Particles and Macromolecules*, Almquist & Wiksells, Uppsala, 1960, p. 148.
- 6 P.-Å. ALBERTSSON AND H. BALTSCHIEFFSKY, *Biochem. Biophys. Res. Commun.*, **12** (1963) 14.
- 7 R. MARKHAM, *Biochem. J.*, **77** (1960) 516.
- 8 G. R. BARKER AND M. RIEBER, *Biochem. J.*, **105** (1967) 1195.
- 9 C. ARGLEBE AND T. C. HALL, *Plant and Cell Physiol.*, **10** (1969) 171.
- 10 P. O. P. TS'O, *Microsomal Particles and Protein Synthesis*, Pergamon Press, London, New York, Paris and Los Angeles, 1958, p. 156.
- 11 T. C. HSIAO, *Biochim. Biophys. Acta*, **91** (1964) 598.
- 12 J. W. LYTILETON, *Biochim. Biophys. Acta*, **154** (1968) 145.
- 13 J. H. VENEKAMP AND W. H. M. MOSCH, *Neth. J. Plant Pathol.*, **70** (1964) 85.
- 14 J. BONNER, *Plant Biochemistry*, Academic Press, New York and London, 1965, Ch. 3.

J. Chromatog., **53** (1970) 531-536

CHROM. 5030

ZUR IDENTIFIZIERUNG UND BESTIMMUNG VON STEROLEN

TH. KARTNIG UND G. MIKULA

Institut für Pharmakognosie der Universität Graz, Graz (Österreich)

(Eingegangen am 9. Juni 1970)

SUMMARY

The identification and quantitative determination of sterols

A method for the separation of free sterols by thin-layer chromatography is described using magnesium oxide as adsorbent and cyclohexane-diethyl ether-acetic acid as the solvent system. When using other solvent systems the naturally occurring palmitic and stearic acid esters of these sterols could also be separated on magnesium oxide. The quantitative estimation of sterols separated by precipitation with digitonin followed by thin-layer chromatography on magnesium oxide is carried out by UV-spectrophotometric measurement in concentrated sulphuric acid. The application of this method is demonstrated by the identification and quantitative determination of the sterols of some vegetable oils.

EINLEITUNG

Die Untersuchung von pflanzlichem und tierischem Material auf Sterole ist nicht nur von wissenschaftlichem, sondern auch von praktischem Interesse. Da entsprechend der Bedeutung der Sterolforschung auch die Zahl der einschlägigen Veröffentlichungen sehr gross ist, soll hier nicht näher darauf eingegangen werden, sondern lediglich auf die Arbeiten von PEEREBOOM UND ROOS¹ sowie SEHER UND HOMBERG² hingewiesen werden, in denen umfassende Zusammenstellungen der neueren, einschlägigen Literatur, insbesondere der Bestimmung von Sterolen, gebracht werden.

Die Sterole, die frei oder gebunden vorliegen können, finden sich im Untersuchungsmaterial sehr oft als Gemische. Die Auftrennung solcher Sterolgemische erfolgt heute vorwiegend papier- oder dünnschichtchromatographisch, wobei häufig auf imprägnierten Schichten gearbeitet wird (Verteilungschromatographie) oder Umsetzungsprodukte der Sterole (Acetate, Bromide) getrennt werden. Über die Auftrennung freier Sterole auf nicht-imprägnierten Schichten (Adsorptionsschichtchromatographie) wurden nach SEHER UND HOMBERG² noch keine befriedigenden Ergebnisse berichtet. SEHER UND HOMBERG selbst gelingt die Auftrennung der Sterole durch die Chromatographie der acetylierten Produkte auf $\text{MgO-Al}_2\text{O}_3\text{-CaSO}_4$ -Schichten.

EIGENE UNTERSUCHUNGEN

Bei unseren Untersuchungen über die Brauchbarkeit des MgO als Sorptionsmittel in der DC von Pflanzeninhaltsstoffen³⁻⁵ zeigte es sich, dass bei der Benützung

entsprechender Fließmittel auch freie Sterole und deren natürlich vorkommende Ester (z.B. Palmitate, Stearate) auf MgO-Schichten getrennt werden können. Darüber sei im folgenden berichtet.

Abtrennung der Sterole

Die Abtrennung der Gesamtsterole aus dem Untersuchungsmaterial erfolgt nach der bei PEEREBOOM UND ROOS¹ angegebenen Vorschrift durch Fällern mit Digintonin nach vorangegangener Verseifung. Die Spaltung der Digitonide wird mittels Pyridin⁶ durchgeführt. Die letztlich in chloroformiger Lösung vorliegenden Sterole werden von uns wie folgt aufgetrennt.

Auftrennung der Sterole mittels DC

Sorptionsmittel

Als Sorptionsmittel verwenden wir MgO (Handelspräparat Merck, "MgO für die DC"), das unmittelbar vor dem Einschlännen (15 g MgO + 68 ml H₂O) durch Sieb VI gebürstet wird. Die Beschichtung erfolgt wie üblich. Trocknung bei 130° durch 30 min. Die Platten sind über einem Trocknungsmittel unbeschränkt haltbar.

Fließmittelgemische

Von ca. 30 versuchten Fließmittelgemischen (FG) erwiesen sich die folgenden als am besten geeignet:

FG (a), Cyclohexan-Diäthyläther-Eisessig (20:79.5:0.5);

FG (b), Cyclohexan-Diäthyläther-Eisessig (50:49.5:0.5);

FG (c), Petroläther (40–60°)-Eisessig (99.9:0.1);

FG (d), Petroläther (40–60°)-Aceton (98:2);

FG (e), Tetrachlorkohlenstoff.

Die Entwicklung der Chromatogramme erfolgt bei Zimmertemperatur und normaler Kammersättigung. Die Laufstrecke beträgt 15 cm, die Laufzeit etwa 30 min.

Detektionsmittel

Vanillin-Schwefelsäure. 3 % Vanillin in H₂SO₄ konz.: Nach dem Besprühen ca. 10 min auf 120° erhitzen. Rot-violette Flecken auf hellem Grund. Nachweisgrenze ca. 5 µg.

Alkalische Permanganatlösung. 0.1 M KMnO₄-Lösung + gleiche Teile 10 %ige, wässrige NaOH: Nach dem Besprühen ca. 10 min auf 120° erhitzen. Helle Flecken auf violettem Grund. Nachweisgrenze ca. 10 µg.

Wasser. Nach vorsichtigem Besprühen erscheinen helle Flecken auf dunklerem Grund. Nachweisgrenze ca. 20 µg.

Für die quantitativen Bestimmungen verwenden wir Wasser als Detektionsmittel, das es uns ermöglicht, auch die Bahnen, deren Flecken abgeschabt werden, zu besprühen.

Quantitative Bestimmung der Sterole

ZAFFARONI⁷ und neuerdings LEVORATO⁸ haben darauf hingewiesen, dass Adrenocorticosteroide in konzentrierter Schwefelsäure im UV-Bereich absorbieren. Eigene Untersuchungen⁹ ergaben, dass auch Sterole, Steroidglykoside und triterpenoide Verbindungen in konzentrierter Schwefelsäure spezifische Absorptionsbanden im UV-Bereich aufweisen und durch Messung der Absorption quantitativ bestimmt werden

können. Die spektrophotometrische Messung wird so durchgeführt, dass die abgeschabte Zone des Chromatogrammes in einem Reagensglas in 0.2 ml konz. HCl gelöst und sodann mit 3 ml konz. H_2SO_4 versetzt und gut durchgerührt wird. Man erwärmt durch 15 min auf 60° (oder lässt 2 h 30 min bei Zimmertemperatur stehen), kühlt ab und misst die völlig klare Flüssigkeit bei der entsprechenden Wellenlänge (für Sterole 318 nm) gegen 0.2 ml HCl konz. + 3 ml H_2SO_4 konz., worin eine entsprechende Menge MgO gelöst wurde. Ein allfälliger Niederschlag von $MgSO_4$ wird abzentrifugiert.

Sollen die Sterole ohne vorherige Trennung mittels DC gemessen werden, so bringt man die Substanz oder deren Lösung in ein Reagensglas, dampft das Lösungsmittel ab und verfährt weiter wie oben angegeben.

Die Erfassungsgrenze dieser Messmethode beträgt für Sterole ca. 5 μg , die Standardabweichung $\pm 1.4\%$.

ERGEBNISSE UND DISKUSSION

Qualitative Auftrennung von Sterolen und Sterolestern mit Hilfe der Fließmittelgemische a–e

Bei Verwendung der FG (a) und (b) können die untersuchten Sterole mit Ausnahme des Campesterol, das bislang in nur wenigen Ölen nachgewiesen werden konnte, auch im freien Zustand zufriedenstellend aufgetrennt werden. Durch Verlängerung der Laufstrecke auf 25 cm und Verwendung des FG (a) gelingt auch die Auftrennung der kritischen Paare Campesterol (73), Cholesterol (78) und β -Sitosterol (66). Die Auftrennung der Sterole in Form der natürlich vorkommenden Palmitate und Stearate gelingt mit den FG (c–e), wird jedoch sinnvoll nur dort angewendet werden, wo eine Abtrennung über die Digitonide nicht nötig ist (Tabelle I, Fig. 1).

TABELLE I

$R_F \times 100$ WERTE VON STEROLEN UND STEROLESTERN

Verbindung	Fließmittel				
	a	b	c	d	e
Cholesterol	86	51	—	—	—
Stigmasterol	80	41	—	—	—
β -Sitosterol	94	60	—	—	—
Ergosterol	61	27	—	—	—
Campesterol	90	55	—	—	—
Lunisterol	10	15	—	—	—
Lanosterol	100	75	—	—	—
Cholesterolacetat	—	—	57	100	—
Stigmasterolacetat	—	—	45	83	—
β -Sitosterolacetat	—	—	68	100	—
Ergosterolacetat	—	—	21	53	—
Cholesterolpalmitat	—	—	—	86	80
Stigmasterolpalmitat	—	—	—	66	70
β -Sitosterolpalmitat	—	—	—	95	96
Ergosterolpalmitat	—	—	—	43	55
Cholesterolstearat	—	—	—	76	78
Stigmasterolstearat	—	—	—	55	60
β -Sitosterolstearat	—	—	—	93	92
Ergosterolstearat	—	—	—	38	48

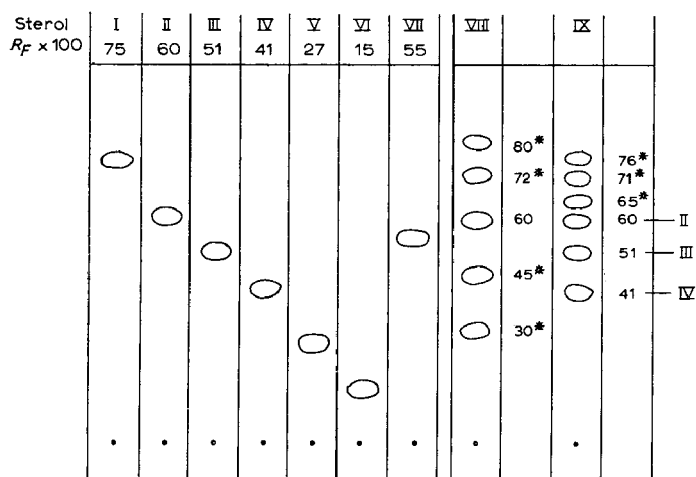


Fig. 1. Auftrennung von Sterolen und Sterolgemischen mit FG (b). Sorptionsmittel, MgO; Laufstrecke, 15 cm. I = Lanosterol, II = β -Sitosterol, III = Cholesterol, IV = Stigmasterol, V = Ergosterol, VI = Lumisterol, VII = Campesterol, VIII = Oleum Olivae, IX = Oleum Arachidis und Oleum Ricini (Sterole identisch). * Nicht identifizierbares Sterol.

Quantitative Bestimmung der Sterole

Die quantitative Bestimmung der isolierten Sterole erfolgt durch die oben beschriebene spektralphotometrische Messung in konzentrierter Schwefelsäure mit grosser Genauigkeit. Die günstigste Menge sowohl zur DC Auftrennung wie auch zur spektroskopischen Messung liegt zwischen 40 und 100 μg pro Sterol. Die Standardabweichung der Gesamtbestimmung liegt bei $\pm 2.5\%$. In Tabelle II und Fig. 2 sind die Extinktionswerte und Eichkurven einiger Sterole und Sterolester als Beispiele geführt.

Der Vorteil der beschriebenen Bestimmung, deren Erfassungsgrenze (ca. 20 μg)

TABELLE II

EXTINKTIONEN DER EICHKURVEN EINIGER STEROLE UND ESTER
 $\lambda = 318 \text{ nm}$.

Verbindung	Extinktion für		
	50 μg	75 μg	100 μg
Cholesterol	0.305	0.450	0.600
Stigmasterol	0.370	0.550	0.740
β -Sitosterol	0.370	0.550	0.740
Cholesterolacetat	0.255	0.375	0.500
Stigmasterolacetat	0.275	0.400	0.540
β -Sitosterolacetat	0.250	0.370	0.490
Cholesterolpalmitat	0.210	0.310	0.420
Stigmasterolpalmitat	0.210	0.320	0.425
β -Sitosterolpalmitat	0.190	0.280	0.375
Cholesterolstearat	0.200	0.285	0.380
Stigmasterolstearat	0.200	0.300	0.410
β -Sitosterolstearat	0.170	0.260	0.350

und Genauigkeit (Standardabweichung $\pm 2.5\%$) zufriedenstellend scheinen, liegt durch die Auftrennung der Sterole auf MgO darin, dass sich das Sorptionsmittel der abgeschabten Zone im Salzsäure-Schwefelsäuregemisch völlig löst und somit das gesamte in der Beschichtung (MgO) vorhandene Sterol zur Umsetzung und Messung gelangt. Diesbezügliche Versuche mit eingewogenen Reinsubstanzen und von der DC abgeschabten Flecken ergaben identische Extinktionswerte.

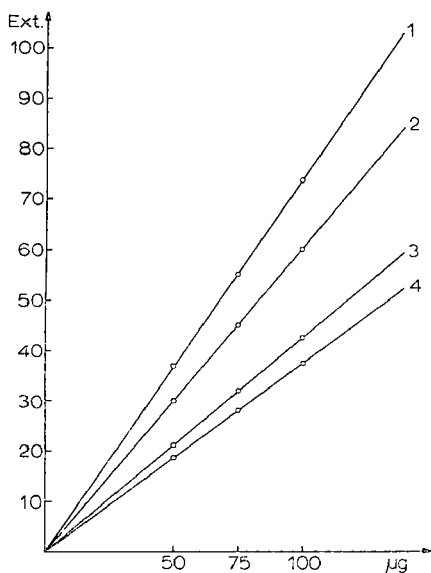


Fig. 2. Eichkurven einiger Sterole und Sterolester. UV-Spektroskopische Messung in konz. H_2SO_4 bei 318 nm. 1 = β -Sito- und Stigmasterol, 2 = Cholesterol, 3 = β -Sito- und Stigmasterolpalmitat, 4 = Cholesterolpalmitat.

ANWENDUNGSBEISPIELE

Als Anwendungsbeispiele der vorgestellten Methode bestimmten wir die Sterolgehalte einiger im ÖAB 9 angeführter Öle. Die Chromatogramme der über die Digtonidfällung erhaltenen Sterolgemische des *Oleum Olivae*, *Oleum Arachidis* und *Oleum Ricini* zeigen neben vier bekannten Sterolen die Flecken von 3 bzw. 4 weiteren, nicht identifizierbaren Sterolen (siehe Fig. 1), wobei die Zusammensetzung der Sterolfraction des *Oleum Arachidis* und *Oleum Ricini* praktisch gleich ist. Die in Kolonne 1 der Tabelle III angeführten Gesamtsterolgehalte sind gleichzeitig die Sterolgehalte nach der Methode von PEEREBOOM UND ROOS¹.

In allen drei untersuchten Ölen erwiesen sich sowohl bei den frei vorliegenden wie auch bei den gebunden vorliegenden Sterolen die qualitative wie auch die quantitative Zusammensetzung dieser beiden Fraktionen praktisch als gleich.

DANK

Herrn Prof. Dr. J. W. COPIUS PEEREBOOM danken wir die grosszügige Überlassung hochreiner Sterole. Ebenso gilt unser Dank Herrn Prof. Dr. A. SEHER für die Überlassung von Campesterol.

TABELLE III
BESTIMMUNG DER STEROLGEHALTE EINIGER ÖLE DES ÖAB 9

	Gesamtsterole (mg %)	Sterole		Qualitative Zusammensetzung des Sterolgemisches	Quantitative Zusammensetzung des Sterolgemisches		
		frei (mg %)	gebunden (mg %)		Gesamtsterole	Sterole frei	Sterole gebunden
Oleum Olivae	12.94	3.12	9.82	β -Sitosterol 4 weitere Sterole (nicht identifizierbar)	78.4 % β -Sitosterol 21.6 % restl. Sterole	78.0 % β -Sitosterol 22.0 % restl. Sterole	78.5 % β -Sitosterol 21.4 % restl. Sterole
Oleum Arachidis	28.00	15.56	12.44	β -Sitosterol Stigmasterol Cholesterol 3 weitere Sterole (nicht identifizierbar)	50.0 % β -Sitosterol 27.7 % Stigmasterol 13.8 % Cholesterol 8.5 % restl. Sterole	50.0 % β -Sitosterol 27.8 % Stigmasterol 13.8 % Cholesterol 8.4 % restl. Sterole	50.0 % β -Sitosterol 27.7 % Stigmasterol 13.8 % Cholesterol 8.5 % restl. Sterole
Oleum Ricini	24.46	21.32	3.14	β -Sitosterol Stigmasterol Cholesterol 3 weitere Sterole (nicht identifizierbar)	48.0 % β -Sitosterol 31.3 % Stigmasterol 16.6 % Cholesterol 5.1 % restl. Sterole	48.0 % β -Sitosterol 30.7 % Stigmasterol 16.1 % Cholesterol 5.2 % restl. Sterole	48.0 % β -Sitosterol 31.2 % Stigmasterol 16.5 % Cholesterol 5.3 % restl. Sterole

ZUSAMMENFASSUNG

Es wird eine Methode zur dünn-schichtchromatographischen Trennung freier Sterole beschrieben, wobei Magnesiumoxid als Sorptionsmittel und das System Cyclohexan-Diäthyläther-Eisessig (20:79.5:0.5) als Fließmittelgemisch benützt werden. Bei Verwendung weiterer Fließmittelgemische können auch die natürlich vorkommenden Palmitinsäure- und Stearinsäureester der Sterole auf Magnesiumoxid getrennt werden. Die quantitative Bestimmung der über Digitonidfällung und Dünn-schichtchromatographie auf Magnesiumoxid aufgetrennten Sterole (sieben Substanzen) erfolgt durch UV-spektroskopische Messung in konzentrierter Schwefelsäure. Als Anwendungsbeispiele wird der Sterolgehalt einiger Öle bestimmt.

LITERATUR

- 1 J. W. COPIUS PEEREBOOM UND J. B. ROOS, *Fette, Seifen, Anstrichmittel*, 62 (1960) 91.
- 2 A. SEHER UND E. HOMBERG, *Fette, Seifen, Anstrichmittel*, 70 (1968) 481.
- 3 TH. KARTNIG, A. HIERMANN UND G. MIKULA, *Pharm. Zentralhalle*, 108 (1969) 177.
- 4 TH. KARTNIG UND G. MIKULA, *Pharm. Zentralhalle*, 108 (1969) 457.
- 5 TH. KARTNIG UND G. MIKULA, *Zentr. Pharm.*, 109 (1970) 251.
- 6 H. DAM UND R. SCHOENHEIMER, *Z. Physiol. Chem.*, 215 (1933) 59.
- 7 A. ZAFFARONI, *J. Am. Chem. Soc.*, 72 (1950) 3828.
- 8 C. LEVORATO, *Il Farmaco, Ed. Prat.*, 24 (1969) 227.
- 9 TH. KARTNIG UND G. MIKULA, *Arch. Pharm.*, 303 (1970) 767.

J. Chromatog., 53 (1970) 537-543

CHROM. 4921

ÜBER DIE CHROMATOGRAPHISCHE ANALYSE VON TOXINEN
AUS *AMANITA PHALLOIDES*

VLADIMÍR PALYZA UND VÁCLAV KULHÁNEK

Institut für Medizinische Chemie der Universität in Brünn, Brno (Tschechoslowakei)

(Eingegangen am 6. Juli 1970)

SUMMARY

Chromatographic analysis of toxins from Amanita phalloides

A review of the recent literature and a comparison of the various methods served as the basis for the development of a rapid procedure in which commercially prepared Silufol plates (150 × 150 mm, 0.1 mm silica gel layer) were used together with a methyl ethyl ketone-methanol (1:1) system for the successful thin-layer chromatographic separation of amanita toxins. By observing the recommended parameters the following R_F values for separate toxins were obtained: α -amanitin = 0.65 ± 0.06 ($n = 249$), β -amanitin = 0.47 ± 0.06 ($n = 85$), γ -amanitin = 0.75 ± 0.05 ($n = 27$), phalloidin = 0.55 ± 0.02 ($n = 10$). In addition, it was possible to identify two spots which showed a phallotoxin character with R_F values of 0.20 ± 0.02 ($n = 14$) and 0.47 ± 0.06 ($n = 7$), respectively. The detection was made by cinnamaldehyde-HCl (sensitivity 1–2 μg of α -amanitine) and by Pauly's reagent; some stable diazotates were also examined experimentally.

EINLEITUNG

Das Bedürfnis des Nachweises toxischer Polypeptiden in verschiedenen verarbeiteten Extrakten aus *Amanita phalloides* und die Bemühung, bei menschlichen Vergiftungen Pilzreste zu identifizieren, führte uns zum chromatographischen Studium der Amanita-Toxine.

Unser Ziel war die Ausarbeitung einer schnellen, arbeitsmässig anspruchslosen, aber dabei doch verlässlichen Methodik.

Eine Übersicht der bisherigen chromatographischen Verfahren zur Trennung von Amanita-Toxinen gibt die Tabelle I.

Nach SULLIVAN und Mitarbeitern⁶ haben die älteren Methoden^{1–4}, gewisse Mängel und ihre Verwendung bei Pilzextrakten erfordert erhebliche Erfahrung, um einem Fehlschluss zu verhindern. Die Auftragung grosser Mengen konzentrierter methanolischen Extrakten, wie BLOCK und Mitarbeitern³ empfohlen haben, gab oft gestreifte und schiefe Chromatogramme, vielleicht durch die Anwesenheit begleitender Lipide verursacht. Die von WIELAND *et al.*¹ benutzte Lösungsmittelmischung bildet eine Emulsion, die vor der Verwendung zentrifugiert sein muss und weder diese, noch das modifizierte System nach BLOCK *et al.*³ geben reproduzierbare Ergebnisse. Die R_F -Werte der Amanitine schwanken stark mit der Grösse der aufgetragener Menge,

TABELLE I

ÜBERSICHT VON CHROMATOGRAPHISCHEN METHODEN ZUR TRENNUNG VON AMANITA-TOXINEN

Abkürzungen: PHD = Phalloidin, PHN = Phalloin, AMA = Amanitin.

Abchnitt im Text	Autor	Literatur	Träger- material	Trägerregelung	Chromatographie- art
A	TH. WIELAND G. SCHMIDT L. WIRTH	1	Papier Schleicher & Schüll 2043 b	—	zweidimen- sional ↑ ↓
	TH. WIELAND CH. DUDENŠING	2	Papier Schleicher & Schüll 2043 b	Impregnation durch 0.05 M Boratpuffer (pH = 8.6)	eindimensional ↑
B	S. S. BLOCK R. L. STEPHENS A. BARRETO W. A. MURRILL	3	Papier Schleicher & Schüll 2043 b oder Whatman No. 1	Die Streifen etwa 2.5 × 25 cm oder 35 cm lang	eindimensional ↑
	S. S. BLOCK R. L. STEPHENS W. A. MURRILL	4	Cellulosesäule	5 g Papier Whatman No. 1 standard zermalm und mit Azeton durchgewaschen	Säulenchroma- tographie ↓
C	G. SULLIVAN L. R. BRADY V. E. TYLER, JR.	6	Kieselgel G, Schichtdicke 0.2 mm	30 g Kieselgel G + 60 ml Wasser; 20 × 20 cm; Aktivation 90 Min. bei 105°	eindimensional ↑
	H. P. RAAEN	9	Kieselgel G, Schichtdicke 0.2 mm	Dasselbe und weiter die Kieselgelschichtregelung auf die Streifen für einzelne Proben	eindimensional ↑
D	P. E. KAMP W. M. DE WIT	10	Cellulose L (Merck)	—	zweidimensional ↑ ↑

ausserdem wurden mit frisch vorbereiteten Lösungsmittelmischungen andere Ergebnisse erzielt, als mit den einige Tage alten Lösungsmitteln.

Die von SULLIVAN *et al.*⁶ erarbeitete Dünnschichtchromatographie sollte die oben erwähnten Mängel der vorgehenden Verfahren vermeiden.

BENEDICT *et al.*⁷ haben durch Chromatographie nach SULLIVAN *et al.*⁶ in Fermentationsprodukten von *Galerina marginata* (*Pholiota marginata* Batsch) Amanitine nachgewiesen, als Vergleichversuch hat ein methanolischer Extrakt aus pulvergetrocknem *Amanita phalloides* gedient. Sie haben hier andere R_F -Werte gefunden. Tabelle II gibt die R_F -Werte der Dünnschichtchromatographie. Dabei wurde die Amanitin-Identität durch andere chromatographische Methoden mit denselben Ergebnissen für die beiden Muster beglaubigt.

Lösungsmittel	Auftragungs- menge	Trennungs- zeit	R _F -Werte	Bemerkungen
Die obere Phase der getrennten Emulsion: Methyläthylketon–Azeton– Wasser (20:2:5) (B) Äthylformiat–Azeton– Wasser (100:145:40)	etwa 10 µl	↑ 3 Std. Lösungs- mittel B ↓ 2 Std. Lösungs- mittel A	PHD = 0.50 α-AMA = 0.41 β-AMA = 0.24 PHN = 0.6–0.65	R _F -Werte gelten für eindimensionale Chroma- tographie im System A
Die obere Phase der getrennten Emulsion: Methyläthylketon– Azeton–Wasser (20:2:8)	etwa 10 µl		PHD = 0.17 α-AMA = 0.17 β-AMA = 0.05 γ-AMA = 0.28	Durch die Papierimpregna- tion wurden die verschie- denen R _F -Werte für PHD und γ-AMA erreicht, die anders zusammen- fließen würden
Methyläthylketon– Azeton–Wasser– <i>n</i> -Butanol (20:6:5:1)	etwa 300 µl	40 Min. oder 2 Std.	nicht angeführt α-AMA = 0.43 β-AMA = 0.17	Anwendung der Methode: P. CATALFOMO UND V. E. TYLER, JR. ⁵
Methanol–Methyläthyl- keton (1:1)	etwa 5–100 µl		α-AMA = 0.46 β-AMA = 0.23	Anwendung der Methode: BENEDICT <i>et al.</i> ⁷ TYLER <i>et al.</i> ⁸
	wiederholt 2 µl		(Lösungsmittelüber- fluss: β < α < γ)	
(A) Methyläthylketon– Azeton–Wasser (30:3:5) (B) Methyläthylketon– Azeton–Wasser– <i>n</i> -Butanol (20:6:5:1)	5–20 µl		nicht angeführt	

TYLER *et al.*⁸ erforschten mit dieser Methode die Anwesenheit von *Amanita*-Toxinen in den amerikanischen giftigen Knollenpilzen *A. phalloides*, *A. verna*, *A. virosa* und *A. bisporigera*, Durchschnittliche R_F-Werte sind auch in der Tabelle II angegeben.

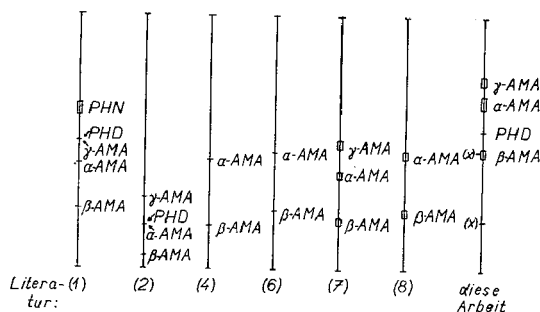
RAAEN⁹ bewirkte einige Verbesserungen an SULLIVAN's⁶ Verfahren, und zwar vor allem durch die Formung der Kieselgelschichten: durch Rillen verteilte sie die Platte in Streifen für die Trennung der einzelnen Proben. Die Streifen wurden im unteren Teil von beiden Seiten durch runde Einschnitte verengt. Die so gemachten Chromatogramme geben schärfer gefärbte Flecken, wie man durch Vergleichen einer farbigen Beilage in der Originalarbeit beurteilen kann. Für die Chromatographie wurden hier die nach SULLIVAN *et al.*⁶ zubereiteten Platten benutzt. Kommerzielle

TABELLE II

 R_F -WERTE DER DÜNNSCHICHTCHROMATOGRAPHIE

	Sullivan <i>et al.</i> ⁶	Benedict <i>et al.</i> ⁷		Tyler <i>et al.</i> ⁸
		<i>A. phalloides</i>	<i>G. marginata</i>	
α -AMA	0.46	0.38	0.36	0.44–0.47
β -AMA	0.23	0.20	0.18	0.21–0.24
γ -AMA	—	0.51	0.48	—

Fertigplatten gaben keine befriedigende Ergebnisse. RAAEN⁹ hat die dünn-schicht-chromatographische Methode nach SULLIVAN *et al.*⁶ eingehend kritisiert und betonte, dass die R_F -Werte der einzelnen Amanitine nicht konstant waren, sondern mit der Form, dem Aktivationsgrad und dem Alter der chromatographischen Platten schwankten. Auch die Menge des extrahierten Materials im getesteten Teil beeinflusst die R_F -Werte. Eine schematische Übersicht von allen erwähnten R_F -Werten zeigt die Fig. 1.

Fig. 1. Schematische Übersicht von allen erwähnten R_F -Werten.

VORBEREITUNG VON PILZEXTRAKTEN

Die Autoren benutzten folgendes Verfahren zu Vorbereitung von Pilzextrakten.

(A) Die Probe war ein methanolischer Pilzextrakt, im Vakuum getrocknet¹. Im Niederschlag wurde die Peptidfraktion von Salzen (vorwiegend KCl) durch Pyridin getrennt, das Pyridin-Supernatant wurde verdampft und aus dem Residuum eine wässrige oder methanolische Lösung hergestellt, so dass die Konzentration für jede Komponente ungefähr 1/2 % war.

(B) Der kleingehackte, unzerquetschte Pilz wurde mit Methanol bedeckt, das Gemisch wurde zum Sieden gebracht und weiterhin einige Minuten unter Rühren und Zerquetschen des Pilzgewebes erwärmt^{3, 4}. Vom extrahierten Gewebe wurde alle Flüssigkeit entfernt, der verbliebene methanolische Extrakt bis zum Trocknen verdampft, wieder in Methanol gelöst und ungelöste Teile durch Zentrifugieren getrennt. Die so gewonnene möglichst hoch konzentrierte methanolische Lösung wurde chromatographiert. Wenn dieses Verfahren für die Trennung (nicht nur für einfache Detektion) von Toxinen benutzt werden soll, empfehlen einige Autoren³ folgende Massnahmen: (i) Pilzgewebe im Methanol 1 Std. oder auch länger extrahieren, (ii) den methanolischen

Extrakt verdampfen, die Trockensubstanz wieder in Methanol lösen. Dieser Schritt muss dreimal, bis zum Erreichen der Peptidkoagulation, wiederholt werden; (iii) einen Papierstreifen von ungefähr 35 cm Länge benutzen und das Chromatogramm 2 Std. entwickeln.

(C) Als Muster dienten methanolische Extrakte aus Pilzen, entweder roh oder wie folgt zubereitet⁶: das Pilzgewebe, 4 g, wurde mit Methanol (100 ml) im Soxhlet-Apparat extrahiert. Der Extrakt wurde bis 10° abgekühlt und von den Niederschlags-Resten durch Zentrifugieren getrennt. Reines Supernat wurde ungefähr bis zu 20 ml auf dem Glühlampenverdampfer eingeengt, nochmals bis 10° abgekühlt und zentrifugiert. Die reine Flüssigkeit, wozu vor Ablauf der Präzipitation eine kleine Menge Wasser gegeben wurde, wurde dekantiert. Nach der Zentrifugation wurde die wässrige-methanolische Flüssigkeit bis zum Trocknen verdampft und der Rest wieder in Methanol gelöst (in 4 ml). Mit so gereinigten Extrakten wurden bessere Erfolge erreicht als mit den durch vorhergehende Verfahren vorbereiteten Extrakte (B) nach BLOCK *et al.*³. RAAEN⁹ hat konzentrierte methanolische Extrakte aus pulver-trocknem *A. phalloides* durch Extraktion im Soxhlet und durch Verdampfen des Methanols aus dem Extrakt hergestellt.

(D) KAMP *et al.*¹⁰ haben zur Bereitung der Probe für die Chromatographie das Verfahren nach WIELAND *et al.*¹¹ benutzt: Frische Fruchtkörper wurden in Methanol extrahiert und nach einigen Tagen zerquetscht. Der Extrakt wurde filtriert und in Vakuum bis Sirupkonsistenz verdampft. Durch Zugabe von 5–10 Methanolvolumen formte sich ein reichlicher Niederschlag von KCl und anderen Salzen, die durch Filtrieren entfernt wurden. Das Methanol wurde nochmals verdampft, der Rest in Wasser gelöst, dazu wurden dann Pb-Azetat gegeben — solange es zum Niederschlag kam, nicht länger. Das Pb-freie Filtrat wurde mit Ammoniumsulfat gesättigt. So wurde der Hauptteil von Toxinen ausgefällt. Die Toxine wurden auf dem Filter aufgefangen und davon mit kleinen Methanolportionen ausgewaschen. Das Endvolumen wurde so eingestellt, dass 1 ml Extrakt 10 g vom Ausgangsmaterial entsprach.

EMPFINDLICHKEITSGRENZEN

Die Empfindlichkeitsgrenzen bei der Dünnschichtchromatographie können nach TYLER *et al.*⁸ zufolge der Gesamtmenge von Amanitinen und des Volumens vom aufgetragenen Muster schwanken. Doch mit Sicherheit können etwa 0.3 µg reines α- oder β-Amanitins nachgewiesen werden. Mit der Dünnschichtchromatographie auf Cellulose¹⁰ lassen sich 1–2 µg α-Amanitins nachweisen.

BLOCK *et al.* beobachteten³, dass die Papierchromatographie die Identifikation von Toxinen in weniger als 0.1 g frischen Pilzgewebes möglich macht (was ungefähr 8 µg α- und 5 µg β-Amanitins entspricht). Über die Empfindlichkeit der Papierchromatographie nach WIELAND *et al.*¹ siehe weiter bei den Reagenzien.

DIE REAGENZIEN ZUR TOXINDETEKTION

Eine Übersicht geben WIELAND *et al.*¹. Wie man aus der Tabelle III ersehen kann, verhält sich Phalloidin in einigen Fällen anders als die Amanitine. Die Differenz wird durch unterschiedliche Struktur bedingt (auf dem Indolkern von Tryptophan besitzen die Amanitine an der Stelle 6 eine Hydroxylgruppe, das Phalloidin nicht).

TABELLE III

ÜBERSICHT VON REAGENZIEN ZUR AMANITA-TOXIN DETEKTION

Reagens (nach):	Farbe		Literatur
	Phalloidin	Amanitine	
(a) Folin-Denis	blau	blau	1
(b) Millon	gelbbraun	gelbbraun	
(c) Tollens	—	schwarz	
(d) Pauly	gelb	rot	
(e) KI-Stärke unter Verwen- dung von Cl ₂ -Gas	graublau	graublau	
(f) Zimtaldehyd-HCl-Gas	hellblau	violett	10
(g) Emerson (Modifikation nach Eisdorfer, Post)	—	purpurbraun	

Von den angeführten Reagenzien haben das System Zimtaldehyd-HCl^{1-10, 12} und die Reaktion mit Pauly's Reagens^{1, 5, 6, 8} praktische Anwendung erreicht. Zimtaldehyd haben alle Autoren deshalb benutzt, weil ungiftige Begleitstoffe mit diesem Reagens rotbraune, ockerfarbene und gelbe Flecken geben, die man gut von der blauen oder violetten Farbe des Phalloidins oder der Amanitine unterscheiden kann.

Die Reaktion mit Zimtaldehyd in gasförmigem Chlorwasserstoff genügt auch für den Beweis von Phalloidin, wenn bei der Reaktion eine hohe Konzentration von Chlorwasserstoff gewährleistet ist. Das Phalloidin gibt eine gelbbraune Farbe, die sich ausserhalb der HCl-Atmosphäre vorübergehend in hellblau ändert, jedoch bald verschwindet. Die Amanitine färben sich im HCl-Gas violett, ausserhalb der HCl-Atmosphäre verschwindet die Farbe ebenfalls langsam. In einem Flecken mit einem Durchmesser von etwa 1 cm auf dem Papier kann man noch 1 µg Amanitin und 10 µg Phalloidin nachweisen.

Zur Reaktion mit Pauly's Reagens (= diazotierte Sulfanilsäure) verwenden wir nur frisch bereitetes Reagens. Mit Amanitinen entstehen rote Flecken, mit Phalloidin tritt nur bei höheren Konzentrationen eine nicht sehr empfindliche Gelbreaktion ein. SULLIVAN *et al.*⁶ haben beschrieben, dass auf Dünnschicht die mit Pauly's Reagens gefärbten Amanitin-Flecken rosafarbig sind und dass diese Reaktion ungefähr 10 mal empfindlicher ist als die Reaktion mit dem System Zimtaldehyd-HCl.

Toxikologischen Nachweis mit Hilfe der Papierchromatographie nach WIELAND *et al.*¹ haben ABUL-HAJ *et al.*¹² nach Verarbeitung von 400 g Lebergewebe eines Verstorbenen gegeben. Die Anwesenheit von α- und γ-Amanitin wird als umstritten angeführt; soweit es den Autoren bekannt ist, wurden Amanita-Toxine in Menschen-gewebe nach tödlicher Vergiftung das erste Mal identifiziert.

VERSUCHSTEIL

Wir haben die in der Einleitung angeführte chromatographische Methoden sowohl auf Papier, als auch mit Hilfe der Dünnschichtmethode geprüft. Die Dünnschichtchromatographie hat sich bei uns am besten bewährt. Die Plattenvorbereitung mit der Aktivierung ist langwierig, deshalb beschränkten wir uns schliesslich auf die Benützung von Fertigplatten.

Kieselgelplatten

Von den Fertigplatten haben wir uns nach der Erprobung der Platten "DC Alufolien Kieselgel F 254 Merck" und "Silufol", resp. "Silufol UV 254" für die beiden letzt genannten entschieden. Die Platten "Silufol" haben nämlich eine genügend feste Kieselgel-Schicht, die während ihrer Formierung nicht loskommt. (Die Platten "Silufol" erzeugt in der ČSSR die Firma "Kavalier", in der B.R.D. die Firma "Serva-Feinbiochemica" u. Co. GmbH, Heidelberg.)

Plattengestaltung

Zuerst haben wir die nicht formierten Platten benutzt, später haben wir verschiedene Formungsweisen geprüft, von welchen sich die auf der Fig. 2. dargestellte Streifenform bestens bewährt hat.

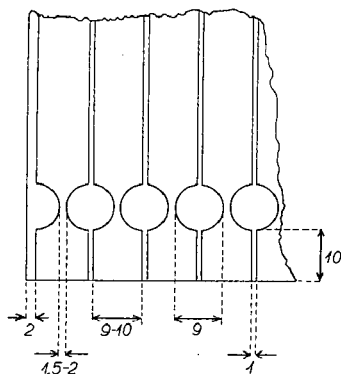


Fig. 2. Der untere linke Rand der Regelungsplatte.

Die angegebene Anordnung stimmt, was den Abstand des aufgetragenen Musters vom unteren Rand, die Fleckenbreite und das Eintauchen der Platte in das Lösungsmittelsystem anbelangt, mit der Firmenanweisung der Silufol-Platten überein. Die eigentliche Gestaltung führt man mit Hilfe eines Korkbohrers durch: die Streifen graviert man mit der Spitze, deren angeschliffene Fläche 1 mm breit ist. Von den runden Flächen entfernt man durch Abkratzen und folgendes Absaugen mit einem weichem PVC-Schlauch das Kieselgel völlig, bis die spiegelglatte Aluminiumfolie zum Vorschein kommt. Bei der Streifengravierung ist darauf zu achten, dass die Aluminiumfolie nicht auf die Papierschicht durchreißt. Um den "Randeffekt", der ein ungleichmäßiges Aufsteigen des Laufmittels in verschiedenen Plattenteilen verursacht, zu verhindern, muss man auch mindestens 2 mm von der Kieselgelschicht auf jedem senkrechten Plattenrand abkratzen.

Die Probenauftragung

Die Proben trägt man üblicherweise auf, und zwar an der schmalsten Stelle des Streifens oder ein wenig darunter. Wir haben die halbsteife Polyäthylenpipette benutzt, bei welcher das Volumen der durch die Kapillarität angesaugten Proben 5 μ l (die Hälfte der Pipette) bis 10 μ l (die volle Pipette) betrug.

Waschen der Pipette vor Auftragung. Vor der Auftragung einer neuen Probe wurde die Pipette nacheinander mit Wasser und weiter mit Methanol (Lösung even-

tueller Toxispuren) durchgewaschen und schliesslich mit Azeton unter Absaugen durch eine Wasserstrahlpumpe getrocknet.

Lösungsmittelsystem zur Entwicklung

Wir haben einige Lösungsmittelgemische geprüft, von denen bewährte sich das System Methyläthylketon–Methanol (1:1) für "Silufol" am besten. Zur Chromatographie muss man doppelt destillierte Lösungsmittel benutzen. Massgebend ist die Reinheit des Methyläthylketons (Siedepunkt 79.6°). Da es mit 21.4 g % Wasser ein Azeotrop bildet, ist es nötig, vor der Destillation mit CaCl_2 zu trocknen. Methyläthylketon ist bei direktem Tageslicht nicht stabil. Deshalb haben wir das System in den Kammern täglich frisch zubereitet und das Methyläthylketon in dichtverschlossenen Flaschen im Dunkel gelagert.

Die Entwicklungszeit für die Platten "Silufol" 150 × 150 mm (Schichtdicke des Kieselgels mit dem Stärkeverbindungsglied 0.1 mm) bei Temperaturen von 19–22° und dem Volumen der Kammer war 40–50 Min.

Die Detektion

Zimtaldehyd–HCl. Die 1 %-ige Lösung des Zimtaldehyds im Methanol wurde jeweils frisch zubereitet. Als (*trans*-)Zimtaldehyd (= Phenylakrolein) wurde einerseits unser eigenes Erzeugnis (aus dem Benzaldehyd und Azetaldehyd bei Anwesenheit von NaOH mit Hilfe der Reaktion nach Claisen und Schmidt) und andererseits ein Erzeugnis der englischen Firma Halewood Chemical Ltd. ohne wesentliche Unterschiede benutzt.

Nach Eintrocknen der methanolischen Lösung wurde die Platte in eine Kammer, die konzentrierte HCl enthielt, eingelegt. Die vertikale Einstellung der Platte über dem HCl-Dampf, wie sie bisher angewendet wurde, hat sich bei uns wegen der sinkenden Konzentration der HCl-Dämpfen im oberen Teil der Kammer nicht bewährt. Deshalb benutzten wir eine Glaswanne mit konzentrierter, täglich frischer HCl, in die das Chromatogramm horizontal, die Kieselgelschicht nach unten, auf 4 Verdampfschalen mit rundem Boden eingelegt wurde. (Beinahe Punktkontakt mit dem Chromatogramm.) Die Färbung des Chromatogramms in der durch eine Glasplatte zugedeckten Kammer wurde mit Hilfe eines unter dem Kammergrund aufgestellten Spiegels beobachtet.

Die Anfärbung der Flecken ist gewöhnlich in 5 Min. erreicht. Die Chromatogramme haben wir den HCl-Dämpfen regelmässig 15 Min. ausgesetzt, nicht länger (nach RAAEN⁹ soll das Farbintensitätsmaximum nicht später als nach 20–30 Min. erreicht werden). Das Nachzeichnen der Farbflecken muss man unmittelbar nach dem Herausnehmen des Chromatogramms aus der HCl durchführen, weil die Flecken allmählich verschwinden (die intensivsten bleiben jedoch selbst nach einigen Stunden sichtbar).

Pauly's Reagens (diazotierte Sulfanilsäure). Wir haben mit Erfolg das folgende modifizierte Reagens benutzt: 0.9 Sulfanilsäure wurde durch Erwärmung in 9 ml konz. Salzsäure gelöst und auf 100 ml ergänzt. Weitere Lösungen waren: 4.5 % NaNO_2 und 10 % Na_2CO_3 . Vor der Verwendung wurden die ersten zwei Lösungen im gleichen Verhältniss gemischt und bis zu 0°–+5° abgekühlt. Dieses Gemisch wurde kurz vor der Verwendung mit einer gleichen Menge abgekühlter Sodalösung gemischt. Nach dem Aufspritzen haben sich auf den Platten rote Flecke verschiedener Intensität ge-

formt, selbst an den Stellen, wo die Detektion mit Zimtaldehyd-HCl fast nicht sichtbar war. Die Flecken sind relativ beständig, erst nach einigen Tagen verbleicht die rote Farbe etwas.

Tollen's Reagens. Die Detektion durch einige Verfahren¹³ war weniger erfolgreich, gute Erfolge gab das Verfahren nach PRICE *et al.*¹⁴: das Chromatogramm bespritzt man mit 5 ml 1 % AgNO_3 in Methanol, zu dem man 0.4 ml konzentriertes NH_4OH gibt. Nach UV-Bestrahlung aus einer Entfernung von 10 cm waren die Flecken bis zu 3 Min. sichtbar.

Detektion durch stabile Diazotate. Orientierend haben wir 17 Muster von stabilen Diazotaten geprüft und aus ihnen 8 entnommen, mit denen man die Toxindetektion durchführen konnte: *p*-Nitrobenzendiazoaminochlorid (Firma Bayer), Naphthanyl-Blau-Diazosalz (Firma Gurr), Echtrot-GG-Salz, Echtrot TR, Echtrot RC, Echtrot B, Echtrot GG und Echtblau B. Ungefähr 1–2 mg des stabilen Diazotats in 5 ml Wasser wurden zum Bespritzen des Chromatogramms benutzt. Eine folgende Bespritzung wurde mit 0.1 *N* NaOH unternommen. (Die Verwendung von Ammoniakdämpfe auch bei beträchtlicher Verdünnung hat sich wegen der diffusen Färbung des Chromatograms nicht bewährt.)

Alle durch die angewendeten Detektionsweisen gefundenen Flecken waren identisch mit den durch Zimtaldehyd-HCl entstandenen Flecken, nur bei Tollen's Reagens entstehen durch unspezifische Reduktion noch weitere Flecken.

Mustervorbereitung für die Chromatographie: Standard

Für die Gabe des reinen kristallischen α -Amanitins und Phalloidins sind wir Herrn Prof. Dr. THEODOR WIELAND (Max-Planck-Institut, Chemische Abteilung, Heidelberg, B.R.D.) zu Dank verpflichtet.

Die Extrakte aus *Amanita phalloides* wurden auf verschiedene Weise hergestellt: nach WIELAND *et al.*¹¹, später mit unseren verschiedenen Verfahren, von denen das definitive an einer anderen Stelle beschrieben wird¹⁵. (Das Prinzip: Extraktion des Pilzgewebes durch Methanol, Destillation, Verdünnung durch Wasser, Lipidstoffausschüttlung durch Chloroform, Zugabe von wasserfreiem Na_2SO_4 , Toxinverdrängung durch $(\text{NH}_4)_2\text{SO}_4$, Isopropanolausschüttlung und Lösung des getrockneten Restes im Methanol.) Kleine Pilzmengen verarbeiten wir auf folgende Weise: den frischen Pilz homogenisieren wir mit Wasser, kochen ihn 10–20 Min. und filtrieren. Das kalte Filtrat schütteln wir mit Chloroform aus. Auf 100 ml der abkochten Menge geben wir 40 g wasserfreien Na_2SO_4 und nach Auflösen 20 g $(\text{NH}_4)_2\text{SO}_4$, zu. Sobald durch milde Erwärmung auch dieses Salz gelöst wurde, schütteln wir dreimal mit durch wasserfreiem Na_2SO_4 getrockneten Isopropanol aus, und nach Filtrieren verdampfen wir auf dem Wasserbad bis zum Trocknen. Den Rest lösen wir in einer kleinen Menge Methanols auf und chromatographieren.

Parallel wurden Muster aus anderen Pilzen hergestellt.

ERGEBNISSE

Die erreichten Ergebnisse dokumentieren wir durch Farbenphotographien der Chromatogramme und eine anschliessende Tabelle IV der R_F -Werte.

Die Art und die Qualität der Platten machen keinen grossen Unterschied und auch die Aktivierung, oder umgekehrt das Belassen der Platten an der Luft äussert sich nicht wesentlich.

TABELLE IV

R_F-WERTE VON AMANITA-TOXINEN BEI CHROMATOGRAPHIE AUF "SILUFOL"

Abkürzungen: PHD = Phalloidin; AMA = Amanitin. Die in der Säule "Andere (X)" erwähnte blaue Farbe ist mit Zimtaldehyd-HCl-Detektion gewonnen.

<i>Muster</i>	<i>Vorbereitung:</i> (<i>Literatur</i>)	α -AMA	β -AMA	γ -AMA	PHD
α -AMA	Standard (Geschenk von Herrn Prof. Dr. TH. WIELAND)	0.64 ± 0.06	—	—	—
PHD	Standard (Geschenk von Herrn Prof. Dr. TH. WIELAND)	—	—	—	0.55 ± 0.02
<i>A. phalloides</i> Ernte 1968 frischer Pilz	nach WIELAND ¹¹	0.65 ± 0.05	0.47 ± 0.08	0.76 ± 0.05	
<i>A. phalloides</i> Ernte 1969, frischer Pilz	unsere Methode ¹⁵	0.64 ± 0.05	0.48 ± 0.04	0.78 ± 0.04	—
<i>A. virosa</i> Ernte 1963 und 1969 getrockneter Pilz	unsere Methode ¹⁵	0.69 ± 0.06	—		
<i>A. phalloides</i> Ernte 1968 frischer Pilz	Modifikation unseres Verfahrens ^a , siehe Bemerkung ^b	0.65 ± 0.06	0.45 ± 0.05	0.74 ± 0.06	—
<i>A. phalloides</i> Ernte 1968 frischer Pilz	Modifikation unseres Verfahrens ^a , siehe Bemerkung ^c	0.66 ± 0.07	—	—	—
Gesamtwerte:	—	0.65 ± 0.06	0.47 ± 0.06	0.75 ± 0.05	0.55 ± 0.02

^a Modifikation unseres Verfahrens: nach Entfernung von Lipidstoffen durch Chloroform wurde der toxinhaltige wässrige Teil zur Sirupkonsistenz auf dem Vakuumrotationsverdampfer eingengt und mit wasserfreiem Na₂SO₄ getrocknet. Folgende enthaltene Trockensubstanzen wurden gelagert und endlich auf verschiedene Weise extrahiert.

^b Die Extraktion der Trockensubstanz Toxine-Na₂SO₄ durch Methanol unter Hitze, Pyridin-Doppel-extraktion von Rückstand.

^c Die Extraktion der Trockensubstanz Toxine-Na₂SO₄ durch verschiedene Lösungsmittel unter Hitze und auch unter Kühlung (12 Gruppen von verschiedenartig vorbereiteten Mustern).

Von beträchtlicher Bedeutung für die Trennungsqualität ist die Plattengestaltung (einschliesslich der Randmodifikation) und eine einwandfreie Lösungsmittelreinheit. Die Lösungsmittel muss man immer doppelt destillieren und unter Standardbedingungen getrennt lagern, am besten im Kühlschrank (Kühle, Dunkelheit).

Die Reproduzierbarkeit der *R_F*-Werte der einzelnen Toxine ist verhältnismässig gut. Schlechte Resultate werden vor allem durch wesentlich unterschiedliche Musterkonzentrationen, durch die Menge von Nebenstoffen und Verunreinigungen und auch durch ihr gegenseitiges Verhältniss erhalten.

Aus unserer statistischen Ausarbeitung der *R_F*-Werte geht hervor, dass die

Andere (X)	n					Plattenzahl				
	α -AMA	β -AMA	γ -AMA	PHD	X	α -AMA	β -AMA	γ -AMA	PHD	X
—	41	—	—	—	—	15	—	—	—	—
—	—	—	—	10	—	—	—	—	3	—
0.47 \pm 0.06 blau	26	20	10	—	7	22	17	9	—	7
0.20 \pm 0.02 blau	39	37	4	—	14	13	12	4	—	7
—	4	—		—	—	3	—		—	—
—	46	28	13	—	—	24	12	9	—	—
—	93	—	—	—	—	58	—	—	—	—
0.47 \pm 0.06 0.20 \pm 0.02	249	85	27	10	$\frac{7}{14}$	135	41	22	3	14

Trennungsfaktoren reproduzierbar sind, unter Vorbehalt möglicher Schwankung in der angewandten Breite.

Das Vergleichen mit einem Standard (reiner Stoff oder Standardextrakt) ist deshalb immer ratsam, besonderes bei der Einführung der Methode.

Grundsätzlich kann man sagen, dass der Chromatographische Nachweis von *A. phalloides* Toxinen auf den Nachweis von Amanitine eingestellt wird. Er ist zweifellos weit empfindlicher und zuverlässiger als der Phallotoxin Nachweis. Farbe und Form der Flecken bei den Amanitinen ist viel charakteristischer. In unserer Anordnung gibt α -Amanitin einen sehr kompakten Flecken, die typische Form des β -Amanitin-

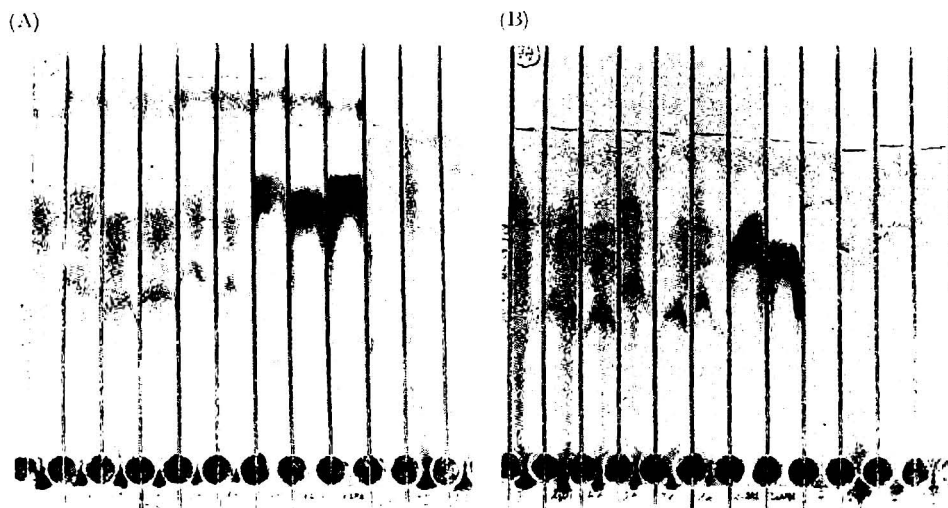


Fig. 3. Photographie von Chromatogrammen. (A) Detektion: Zimtaldehyd-HCl, etwa 15 Min. ausserhalb der HCl-Atmosphäre. 6 Streifen von links: etwa 0, 5, 4, 3, 2 und 1 μ l von dem mit unserer Methode¹⁵ vorbereiteten *A. phalloides*-Extrakt. 1 μ l entspricht hier ungefähr 2 μ g Phalloidin, 1,6 μ g α -Amanitin und 1 μ g β -Amanitin. Weitere drei Streifen: α -Amanitin-Standardlösung 5, 10 und 15 μ g. Drei letzte Streifen: negative Reaktionen. (B) Detektion: Pauly's-Reagens. 6 Streifen von links und die zwei weiteren Streifen, wie bei (A). Weitere Streifen: negative Reaktionen. Auf den Platten waren die Kieselgelrandzonen nicht entfernt ("Randeffekt" beim ersten Chromatogramm).

Fleckens ist das Hufeisen, mit der Konvexität zur Chromatogrammfront gerichtet.

Wir haben eine deutliche Toxinabnahme (vor allem von Phalloidin) in älteren getrockneten Präparaten von *A. phalloides* und auch in einige Jahre alten *A. virosa*-Trockenpräparaten, wo auch β -Amanitin nicht erfasst wurde, festgestellt. (Für die Gabe getrockneter Pilzkörper von *A. virosa* — Pilzernte 1963 — danken wir auf diesen Weg Herrn PhMr KAREL VONEŠ, Apotheke Měříň.) Die Beständigkeit der Toxine ist also nicht unbegrenzt und zeigt sich ausser im schon erwähnten Altern der Trockensubstanz auch beim längeren Sieden in Pyridin. Die Extrakterstellung mit Hilfe von Pyridin empfehlen wir nicht. Zur Toxinabnahme kommt es auch durch langfristiges Stehen von Pyridinextrakten. (Wir haben mit wasserfreiem, doppelt destilliertem Pyridin gearbeitet.)

Die Toxinabnahme haben wir auf den Einfluss der Oxydation bezogen und probeweise die Wirkung des Wasserstoffsuperoxyds als Oxydationsmittel bei der Neutralreaktion geprüft. Schon nach kurzer Einwirkung des 2 % H_2O_2 (die Endkonzentration) wurde das Verschwinden des blauen Fleckens mit $R_F = 0.20$ aus der Phalloxinengruppe beobachtet. $Na_2S_2O_3$ in einer Endkonzentration von ca. 5 % hatte keinen Einfluss auf die Fleckenintensität noch in Normalextrakten, noch in den Extrakten nach Peroxyd-Behandlung. Mit Hilfe der Dünnschichtchromatographie in der erwähnten Anordnung ist es uns nicht gelungen Flecken mit R_F und Farbcharakteristik ähnlich der der Amanita-Toxine, in irgendeinem anderen Knollenpilz nachzuweisen. (Es wurden *A. muscaria*, *A. pantherina* und vor allem die verwandte *A. citrina* geprüft.)

Den Toxinbeweis im Pilz *A. phalloides* erachten wir deshalb als zuverlässig, vorteilhaft und verhältnismässig schnell. Die Ausnutzung von fertigen dünn-

chromatographischen Platten erleichtert die Arbeit sehr. Durch ihre Gestaltung (einschliesslich der Randmodifikation) kann man eine gute Trennung mit ziemlich gut reproduzierbaren R_F -Werten erreichen.

Die Dünnschichtchromatographie gewährt eine verhältnismässig schnelle und zuverlässige Auskunft über das Vorkommen von zyklischen Polypeptiden der Amanitin- und Phalloidin-Typen, unter gewissen Voraussetzungen:

(1) Der Extrakt muss aus frischen Pilzen gewonnen und standardmässig durch Isopropanol Ausschüttlung gereinigt werden.

(2) Im Gegensatz zu RAAEN⁹ benutzen wir handelsübliche chromatographische Platten "Silufol", die sich zu diesem Zwecke ausgezeichnet bewährt haben und die man nicht vor der Verwendung aktivieren muss.

(3) Die Platten gestalten wir einschliesslich der Randmodifikation.

(4) Die bewegliche Phase muss immer frisch aus gereinigten Lösungsmitteln zubereitet werden.

(5) Die Platte ordnen wir bei der Zimtaldehyd-HCl-Detektion immer horizontal mit der Kieselgelschicht zum Spiegel der konz. HCl an.

(6) Für die sichere Identifizierung auf jeder Platte benutzen wir zur Vergleichung Standardextrakt aus *A. phalloides*.

(7) Die zuverlässigste Detektionsart ist mit Zimtaldehyd-HCl, die es erlaubt, ungefähr 1–2 μg des α -Amanitins zu entdecken; die Phallotoxin-Detektion ist viel weniger empfindlich und zuverlässig.

DANK

Wir danken herzlich Frau Dr. med. HEDDA und Herrn Dr. med. NORBERT RÖMHILD aus Leipzig für die sorgfältige Korrektur der deutschen Übersetzung.

ZUSAMMENFASSUNG

Vergleich einiger Methoden und bisheriger Erfahrungen bildeten eine Basis für die Ausarbeitung schneller Verfahren, die mit Hilfe der formierten Fertigplatten "Silufol" (150 × 150 mm, 0.1 mm Kieselgelschicht) und des Systems Methyläthylketon-Methanol (1:1) eine erfolgreiche dünnschichtchromatographische Trennung von Amanita-Toxinen erlauben. Bei Einhaltung der empfohlenen Massnahmen gelten die folgenden R_F -Werte für die einzelnen Toxine: α -Amanitin: 0.65 ± 0.06 ($n = 249$), β -Amanitin 0.47 ± 0.06 ($n = 85$), γ -Amanitin 0.75 ± 0.05 ($n = 27$), Phalloidin 0.55 ± 0.02 ($n = 10$). Ausserdem war es möglich zwei Flecken mit Phallotoxin-Charakter zu identifizieren. Ihre R_F -Werte betrugen 0.20 ± 0.02 ($n = 14$) und 0.47 ± 0.06 ($n = 7$). Die Detektion wurde mit Zimtaldehyd-HCl (Empfindlichkeit von 1–2 μg α -Amanitin) und Pauly's Reagens durchgeführt; versuchsweise wurden auch einige stabile Diazotate geprüft.

LITERATUR

- 1 TH. WIELAND, G. SCHMIDT UND L. WIRTH, *Ann. Chem.*, 577 (1952) 215.
- 2 TH. WIELAND UND CH. DUDENSING, *Ann. Chem.*, 600 (1956) 156.
- 3 S. S. BLOCK, R. L. STEPHENS, A. BARRETO UND W. A. MURRILL, *Science*, 121 (1955) 505.
- 4 S. S. BLOCK, R. L. STEPHENS UND W. A. MURRILL, *J. Agr. Food Chem.*, 3 (1955) 584.

- 5 P. CATALFOMO UND V. E. TYLER, JR., *J. Pharm. Sci.*, 50 (1961) 689.
- 6 G. SULLIVAN, L. R. BRADY UND V. E. TYLER, JR., *J. Pharm. Sci.*, 54 (1965) 921.
- 7 R. G. BENEDICT, V. E. TYLER, JR., R. L. BRADY UND L. J. WEBER, *J. Bacteriol.*, 91 (1966) 1380.
- 8 V. E. TYLER, JR., R. G. BENEDICT, R. L. BRADY UND J. E. ROBBERS, *J. Pharm. Sci.*, 55 (1966) 590.
- 9 H. P. RAAEN, *J. Chromatog.*, 38 (1968) 403.
- 10 P. E. KAMP UND W. M. DE WIT, *Pharm. Weekblad*, 103 (1968) 813.
- 11 TH. WIELAND UND O. WIELAND, *Pharmacol. Rev.*, 11 (1959) 87.
- 12 S. K. ABUL-HAJ, R. A. EWALD UND L. KAZYAK, *New Engl. J. Med.*, 269 (1963) 223.
- 13 *Anfärbereagentien für Dünnschicht- und Papier-Chromatographie*, E. Merck A.G., Darmstadt, 1968.
- 14 T. D. PRICE UND L. S. DIETRICH, *Chromatog. Methods*, 1 (1956) 4.
- 15 V. KULHÁNEK UND V. PALYZA, in Vorbereitung.

J. Chromatog., 53 (1970) 545-558

CHROM. 5043

DISC ELECTROPHORESIS: AVOIDING ARTIFACTS CAUSED BY PERSULFATE

E. E. KING *

Crops Research Division, Agricultural Research Service, United States Department of Agriculture, State College, Miss. 39762 (U.S.A.)

(Received September 14th, 1970)

SUMMARY

Artifacts of separation and inactivation of enzymes in polyacrylamide disc electrophoresis may be avoided by substituting riboflavin for persulfate, or by incorporating an antioxidant into stacking gels and samples. Polymerization with riboflavin results in gels having poor resolution and reproducibility. Addition of an antioxidant to stacking gels and samples is the more reliable alternative for general use.

INTRODUCTION

Polyacrylamide gels for electrophoresis are generally prepared with ammonium persulfate as the polymerization catalyst. It has been shown that the use of persulfate leads to artifacts in separation patterns and inactivation of enzymes¹⁻³. Pre-runs of separating gels without sample have been proposed to remove residual persulfate³, but this technique affords no more protection against artifact and enzyme inactivation than does a riboflavin-polymerized stacking gel as employed in the standard disc electrophoresis procedure. The mobility of persulfate in alkaline gels is greater than that of the Bromphenol Blue tracking dye⁴. Therefore if a riboflavin-polymerized stacking gel is interposed between sample and separating gel, protein should never encounter persulfate. By the time protein has migrated into the separating gel, persulfate will have migrated ahead of it and will remain ahead throughout the run. Nevertheless, inactivation of enolase and multiple bands from a single protein species have been detected with these conditions¹. These effects are therefore likely caused by nonionic by-products of the polymerization reaction in the separating gel instead of by persulfate *per se*.

Polymerization of separating gels with riboflavin instead of persulfate has been suggested to avoid the difficulties caused by persulfate^{1,2}, as has incorporation of an antioxidant into the sample, stacking gel, or both¹. Either of these methods should prevent separation artifacts and enzyme inactivation due to residual persulfate or nonionic oxidizers. A comparison of these two methods is the subject of this report.

* Address correspondence to: E. E. King, P. O. Box 5367, State College, Miss. 39762, U.S.A.

EXPERIMENTAL

Materials and methods

Formulations and techniques of disc electrophoresis were those of DAVIS⁵ except that no sample gel was used. Samples were prepared in 5 % sucrose and layered beneath the tank buffer onto the stacking gels. Gels were prepared in glass tubes 75 × 5 mm I.D. Photolysis of riboflavin was accomplished with two 15 W cool white fluorescent lamps. Twelve gels at a time were run at room temperature; electrode buffers were used only once. Constant current of 1 mA per tube was applied until the Bromphenol Blue tracking dye entered the separating gel; current was then increased to 2 mA per tube for the remainder of the run. Low current was used to test the resolving capabilities of experimental gel formulations by maximizing any lack of resolution caused by diffusion of protein within gels.

At the completion of each electrophoretic run, gels were removed from the glass tubes, cut off at the tracking dye front, fixed for 30 min in cold 15 % trichloroacetic acid (TCA) and stained overnight with Coomassie Blue in 10 % TCA as described by CHRAMBACH *et al.*⁶ Excess dye was removed by rinsing with 10 % TCA.

Migration of protein bands was measured on a fluorescent light box by using a metric rule and hand lens; accuracy of measurement was ± 0.25 mm. Results are expressed as relative mobilities (R_M), the ratio of protein migration to tracking dye migration. Mean R_M values shown in Fig. 1 are based on values obtained from six to eight gels representing two separate electrophoretic runs. Diagrammatic representations of gels are used to present mean R_M values and to overcome the limitations of photography which are particularly noticeable with faint bands.

Sample material was a partially purified, salt-free lyophilized preparation from bovine pancreas marketed by Worthington Biochemical Corp., Freehold, N. J. under the designation protease*. 300 μ g of sample in 25 μ l of 5 % sucrose was applied to each gel. Electrophoresis in 7 % acrylamide persulfate-polymerized gels in the DAVIS⁵ system yields thirteen bands (Fig. 1a) which are diverse in size, staining intensity, and R_M . This pattern is the standard with which all others were compared; two such gels were included in each electrophoretic run as controls.

Experimental variables

Preliminary experiments showed that riboflavin concentration has a marked effect on gel strength and porosity. High concentrations of riboflavin produce soft, porous gels which are seldom removed from the glass tubes without damage. R_M values of proteins are greater in riboflavin-polymerized gels than in persulfate-polymerized gels of the same acrylamide concentration. One of the problems then became that of producing a riboflavin-polymerized separating gel with physical strength and sieving characteristics similar to the standard persulfate-polymerized gel. To attempt this, the concentrations of riboflavin, N,N'-methylenebisacrylamide (bis) and acrylamide were varied.

BRACKENRIDGE AND BACHELARD⁷ show that porosity of riboflavin-polymerized gels is reduced by increasing polymerization time to 1 h or more. DAVIS⁵, however, warns that extended polymerization times are likely to produce gel inhomogeneities,

* Mention of a specific trade name is made for purposes of identification only, and does not imply endorsement by the United States Department of Agriculture.

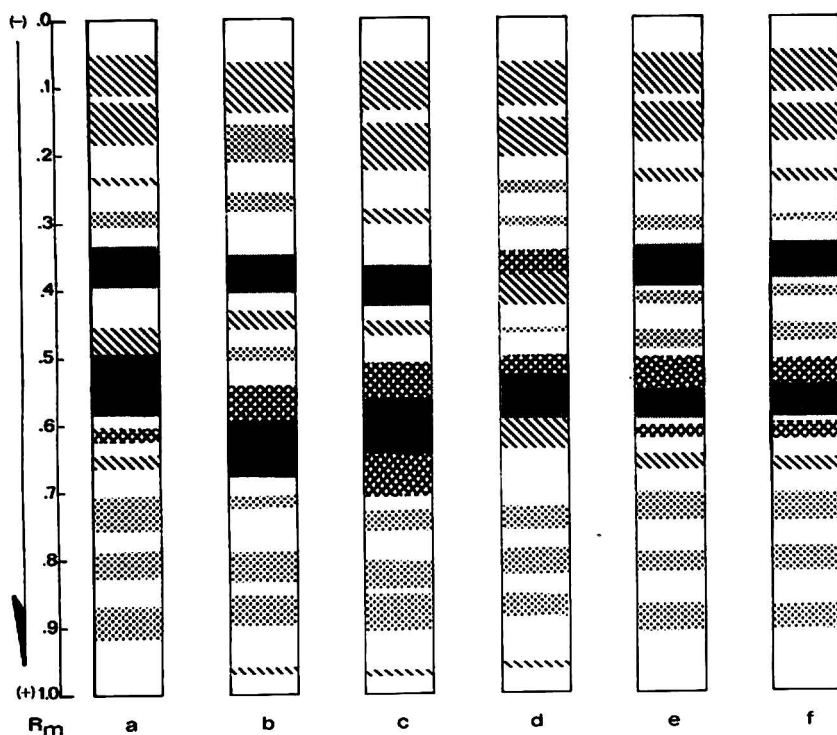


Fig. 1. Protein separation patterns in standard and experimental gel formulations. (a) 7% acrylamide, 0.184% bis, polymerized with persulfate; (b) 7% acrylamide, 0.184% bis, polymerized with riboflavin; (c) 7% acrylamide, 0.5% bis, polymerized with riboflavin; (d) 8.25% acrylamide, 0.184% bis, polymerized with riboflavin; (e) as (a) with 2.5 mM 2-mercaptoethanol in stacking gel and sample. (f) as (a) with 2.5 mM dithiothreitol in stacking gel and sample. Arrow indicates direction of current flow.

giving rise to localized zones of decreased resolution. Therefore, the effect of varying riboflavin concentration was studied using the standard 30 min polymerization time. To find the lowest concentration that would accomplish polymerization, riboflavin concentration was varied from 2×10^{-3} to 2.5×10^{-5} % using a separating gel of 7% acrylamide and 0.184% bis as employed in the DAVIS⁵ disc technique.

There is conflict in the literature concerning the influence that bis concentration has on the porosity or sieving characteristics of a gel^{8,9}. To determine the effect of varying bis concentrations on gel strength and the separation pattern of the heterogeneous sample, bis concentration was varied from 0.184% to 0.875% (2.6 to 12.5% expressed as percent of monomer concentration). Acrylamide and riboflavin concentrations were constant at 7% and 5×10^{-5} % respectively.

Acrylamide concentration, the parameter most influential on pore size, was varied from 7 to 9.75%. Bis and riboflavin concentrations were constant at 0.184% and 5×10^{-5} % respectively.

Dithiothreitol and 2-mercaptoethanol were incorporated into sample solutions and stacking gels used with 7% acrylamide persulfate-polymerized separating gels. Both antioxidants were employed at concentrations of 2.5 mM and 5.0 mM.

RESULTS

Gels polymerized with riboflavin

Of the riboflavin concentrations tested, $5 \times 10^{-5}\%$ was most suitable. Higher concentrations produced soft, weak gels; lower concentrations resulted in incomplete polymerization during the thirty min exposure to light. Although $5 \times 10^{-5}\%$ riboflavin produced gels with physical strength approaching that of persulfate-polymerized gels of equivalent acrylamide concentration, protein separation patterns were dissimilar (Fig. 1a,b). Fewer bands were apparent, R_M values were greater, and bands were wider and less distinct in the riboflavin-polymerized gels.

Increasing the bis concentration from the usual 0.184%, produced gels with good physical strength, but also with decreased transparency. Gels with bis concentrations greater than 0.5% were white and opaque; only the most intense bands were visible. Bis concentration of 0.5% yielded the same number of bands as the standard persulfate-polymerized gel, but in a different pattern (Fig. 1a,c). R_M values were generally greater, and it is difficult to identify many bands with those in the standard gel.

Riboflavin-polymerized gels were prepared in which the bis concentration was constant at 0.184% and acrylamide concentration was increased from 7 to 9.75%. In terms of general pattern similarity and R_M comparability, 8.25% gels are closest to the standard 7% persulfate-polymerized gel, although differences are present (Fig. 1a,d). Though many bands have comparable R_M values, some bands cannot be positively identified with any in the standard gel, and one band present in the standard gel (R_M 0.65–0.67) is not visible in the riboflavin-polymerized gel.

Reproducibility of R_M values between riboflavin-polymerized gels of similar acrylamide concentration in the same electrophoretic run was poor, and even poorer between gels in separate runs. Bands in these gels were often badly distorted and indistinct (Fig. 2), whereas this was seldom the case with gels polymerized with persulfate.

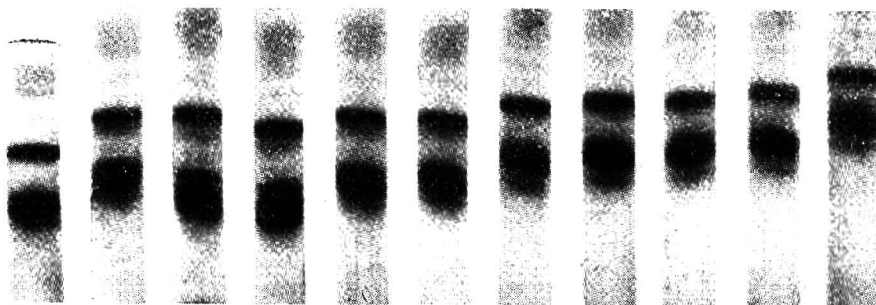


Fig. 2. Protein band distortion in gels polymerized with riboflavin. Gel on extreme left polymerized with persulfate, others contain various concentrations of acrylamide polymerized with riboflavin. All gels were from the same electrophoretic run.

Antioxidants in stacking gel and sample

Addition of dithiothreitol or 2-mercaptoethanol to stacking gels and sample solutions in conjunction with persulfate polymerization of separating gels produced separation patterns nearly identical with those in the standard gel (Fig. 1a,e,f). The poor resolution and distortion of bands characteristic of riboflavin-polymerized gels was missing, and reproducibility was good. There were no apparent differences in

separation patterns between 2.5 mM and 5 mM concentrations of either antioxidant.

The only detectable differences in protein separation patterns between the standard gel (Fig. 1a) and gels containing antioxidants (Fig. 1e,f) were in the regions of R_M 0.33–0.43 and 0.45–0.50. In the first region two bands exist in the gels with antioxidant *versus* one in the standard gel; in the second region, resolution of a band was markedly improved in the gels containing antioxidant over that in the standard gel.

DISCUSSION

Results of this investigation show that it is possible to produce a riboflavin-polymerized separating gel which approximates the standard persulfate-polymerized gel in terms of gross mechanical properties and sieving characteristics. There are differences between the two types of gels in terms of separation patterns, quality of resolution and reproducibility.

Differences in separation patterns are a logical result, since the major objection to the use of ammonium persulfate^{1–3,7} is that separation artifacts are produced by the adverse action of the persulfate ion or its reaction products upon sensitive proteins. BREWER¹ and MITCHELL³ have shown that such oxidation may produce multiple bands from a single protein species; FANTES and FURMINGER² report decreased staining intensity with Amido Black and band absence. The differences between separation patterns of persulfate- and riboflavin-polymerized gels in this study may represent similar circumstances, the pattern in the riboflavin-polymerized gel being the more realistic.

A comparison of the pattern in the 8.25 % acrylamide riboflavin-polymerized gel (Fig. 1d) with those in the gels containing antioxidants (Fig. 1e,f) tends to substantiate this view. Aside from generally increased resolution in the gels containing antioxidant, differences in the separation patterns are few. The areas of marked difference are the regions of R_M 0.60–0.70 and 0.95–0.97, where patterns in the gels containing antioxidant resemble the standard gel rather than the riboflavin-polymerized gel.

CONCLUSION

The band distortion, poor resolution, and inadequate reproducibility associated with riboflavin polymerization preclude its recommendation as a routine substitute for persulfate polymerization. Instead, the use of persulfate-polymerized separating gels with the addition of a suitable antioxidant such as dithiothreitol or 2-mercaptoethanol to stacking gels and sample material is recommended. Resolution and reproducibility are at least equal to that of the standard persulfate procedure, and the risk of artifacts due to oxidation is minimized.

REFERENCES

- 1 J. M. BREWER, *Science*, 156 (1967) 256.
- 2 K. H. FANTES AND I. G. S. FURMINGER, *Nature*, 215 (1967) 750.
- 3 W. M. MITCHELL, *Biochim. Biophys. Acta*, 147 (1967) 171.
- 4 A. BENNICK, *Anal. Biochem.*, 26 (1968) 453.
- 5 B. J. DAVIS, *Ann. N. Y. Acad. Sci.*, 121 (1964) 404.
- 6 A. CHRAMBACH, R. A. REISFELD, M. WYCOFF AND J. ZACCARI, *Anal. Biochem.*, 20 (1967) 150.
- 7 C. J. BRACKENRIDGE AND H. S. BACHELARD, *J. Chromatog.*, 41 (1969) 242.
- 8 J. L. HEDRICK AND A. J. SMITH, *Arch. Biochem. Biophys.*, 126 (1968) 155.
- 9 M. L. WHITE, *J. Phys. Chem.*, 64 (1960) 1563.

Notes

CHROM. 5029

Dosage par chromatographie en phase gazeuse des tranquillisants carbamates

La littérature sur la recherche et le dosage des carbamates par chromatographie en phase gazeuse est relativement réduite. Quelques auteurs se sont attachés à l'étude des carbamates simples et N-substitués utilisés comme herbicides¹⁻³; d'autres à l'occasion de mises au point générales⁴⁻⁶ ou particulières⁷ ont envisagé principalement le problème du méprobamate. Il n'existe cependant à notre connaissance guère de travaux abordant simultanément la recherche et/ou le dosage des trois tranquillisants carbamates courants que sont le carbamate de méthylpentynol (Oblivon C[®]), l'hexapropymate (Mérixax[®]) et le méprobamate.

Expérimentation

Nous avons réalisé notre recherche sur un appareil Varian-Aerograph 1840-3 équipé d'un détecteur FID et d'une colonne métallique de 5 ft.; comme phase stationnaire, nous avons choisi le SE-30 à 3 %. Les solutions de base étaient à la concentration de 5 µg/µl dans le chloroforme. A la suite d'une étude antérieure, l'amobarbital a été pris comme étalon interne. Nous avons opéré d'une part en isotherme à des températures variant entre 60 et 200° et d'autre part en programmation linéaire de température de 65-200° à raison de 6 et de 8°/min.

Résultats et discussion

Les conditions opératoires finalement retenues sont reprises dans les Tableaux I et II.

TABLEAU I

CONDITIONS OPÉRATOIRES RETENUES POUR LE DOSAGE PAR CHROMATOGRAPHIE EN PHASE GAZEUSE DU CARBAMATE DE MÉTHYLPENTYNOL ET DE L'HEXAPROPYMATÉ.

Appareil, Varian Aerograph 1840-3; détecteur, ionisation flamme; colonne, métallique 5 ft.; phase stationnaire, SE-30, 3 %. Temp.: injecteur, 155°; colonne, programmation 65-200°; détecteur, 205°. Gaz vecteur, N₂, 30 p.s.i.

Vitesse de programmation	Carbamate-méthylpentynol		Hexapropymate		Amobarbital		Rapport surfaces pics de mêmes concentrations	
	<i>t_R</i> ^a	<i>t_R</i> relatif	<i>t_R</i> ^a	<i>t_R</i> relatif	<i>t_R</i> ^a	<i>t_R</i> relatif		
							Carbamate méthylpentynol/amobarbital ^a	Hexapropymate/amobarbital ^a
6°/min	3'42"	1.00	10'26"	2.82	16'01"	4.33	0.45	0.98
8°/min	3'06"	1.00	8'59"	2.89	13'08"	4.24		

^a Valeurs moyennes sur 10 essais.

TABLEAU II

CONDITIONS OPÉRATOIRES RETENUES POUR LE DOSAGE PAR CHROMATOGRAPHIE EN PHASE GAZEUSE DU MÉPROBAMATE

Appareil, Varian Aerograph 1840-3; détecteur, ionisation flamme; colonne, métallique, 5 ft.; phase stationnaire, SE-30, 3 %. Temp.: injecteur, 190°; colonne, 155°; détecteur, 180°. Gaz vecteur, N₂; 30 p.s.i.

<i>Méprobamate</i>		<i>Amobarbital</i>		<i>Rapport surfaces pics de même concentration</i>
<i>t_R</i>	<i>t_R relatif</i>	<i>t_R</i>	<i>t_R relatif</i>	
<i>Méprobamate/amobarbital^a</i>				
2'01	1.00	4'51''	2.40	0.15

^a Valeurs moyennes sur 10 essais.

Le carbamate de méthylpentynol et l'hexapropymate sont aisément différenciés et dosés sur SE-30 en programmation linéaire de température de 65 à 200° à raison de 6 ou de 8°/min. Cette dernière option, donnant des résultats plus rapides, a été retenue pour l'application en toxicologie clinique (Tableau I). La limite de détection est de l'ordre de 5 ng pour le carbamate de méthylpentynol et de l'ordre du ng pour l'hexapropymate. Dans ces conditions, le méprobamate se décompose et donne généralement deux pics présentant des *t_R* proches de celui caractérisant l'amobarbital. Pour le méprobamate, il est donc nécessaire d'avoir recours à une autre technique. Celle que nous avons retenue prévoit une chromatographie sur SE-30 à 155° (Tableau II). A cette température, le carbamate de méthylpentynol et l'hexapropymate ont des *t_R* inférieurs à la minute et, aux sensibilités nécessaires pour le méprobamate, leur pic disparaît pratiquement dans celui du solvant. La limite de détection pour le méprobamate est de l'ordre de 0.1 µg.

Préalablement au dosage par chromatographie en phase gazeuse, le ou les tranquillisants carbamates en présence peuvent être caractérisés par chromatographie sur couche mince de gel de silice^{8,9}.

L'application aux milieux biologiques ainsi qu'une étude portant sur la séparation de l'hexapropymate et de ses métabolites feront l'objet d'une note ultérieure.

Laboratoire de Toxicologie Clinique et Médico-Légale,
Faculté de Médecine, Université de Liège,
151, Boulevard de la Constitution, B-4000, Liège (Belgique)

A. NOIRFALISE*

- 1 W. L. ZIELINSKI, JR. ET L. FISHBEIN, *J. Gas Chromatog.*, 3 (1965) 260.
- 2 W. L. ZIELINSKI, JR. ET L. FISHBEIN, *J. Gas Chromatog.*, 3 (1965) 333.
- 3 L. WHEELER ET A. STROTHER, *J. Chromatog.*, 45 (1969) 362.
- 4 M. K. LINTURI-LAURILA, *Acta Chem. Scand.*, 18 (1964) 415.
- 5 N. C. JAIN, *Microchem. J.*, 12 (1967) 256.
- 6 H. V. STREET, *J. Chromatog.*, 41 (1969) 358.
- 7 R. K. MADDOCK, JR. ET H. A. BLOOMER, *Clin. Chem.*, 13 (1967) 333.
- 8 A. NOIRFALISE, *J. Chromatog.*, 20 (1965) 61.
- 9 A. NOIRFALISE, *Thèse Doctorat en Sci. Pharm.*, Liège (1968).

Reçu le 11 juin 1970

* Avec la collaboration technique de J. VAN ROY.

CHROM. 4996

Pyrolysis-gas chromatography of polyene antifungal antibiotics: the nature of candicidin, levorin and trichomycin

The polyene antifungal antibiotics are labile substances which possess a macrocyclic skeleton containing a conjugated system of up to seven double bonds, together with other substituents¹. The highest antifungal activity is exhibited by the heptaene compounds. These are also the most complex chemically, with molecular weights in the range 900–1300, and most difficult to purify, and their complete structures are as yet unknown. Three heptaene preparations, candicidin from *Streptomyces griseus*, levorin from *S. levoris* and trichomycin from *S. hachijoensis*, isolated respectively in U.S.A., U.S.S.R. and Japan, have each been separated into several components by counter-current distribution^{2–4}. Studies based on such separations, together with other chromatographic and spectroscopic evidence and biological potency data, suggest that the major components in levorin and candicidin may be identical² and those in trichomycin and candicidin may be the same³. KALÁSZ *et al.*³ were also unable to differentiate between an antibiotic S-515 from *S. levoris* and candicidin and concluded that they are identical. S-515 may be considered as a levorin sample. Exhaustive comparison of the three substances is hampered by their degradation during prolonged handling. Detailed, but incomplete, proposals for chemical structure have only been published for trichomycin A (ref. 5).

BRODASKY⁶ demonstrated the application of pyrolysis-gas chromatography, a fingerprinting technique established in the field of polymer chemistry⁷, to differentiation and characterisation of some antibiotics. His results also indicated the sensitivity of the pyrolysis chromatograms (pyrograms) to small changes in structure and stereochemistry. We have, therefore, investigated the behaviour of some polyene antibiotics after low- and high-temperature pyrolysis with the particular object of studying the identity of candicidin, levorin and trichomycin. This paper describes our results.

Materials and methods

Antibiotics. The W.H.O. 1st International Standards of nystatin and amphotericin B were used. Candicidin was provided by S.B. Penick and Co., New York (Batch No. 8461-NJF-1); one sample (Batch No. 684-NKF-1) was obtained through Pharmax Ltd., Dartford. Levorin, including samples of five separate production batches for which all the data in Table I were supplied, was generously donated by Dr. W. O. KUHLEBAKH, Leningrad. Trichomycin (Lot No. 0016431) was given by Fujisawa Pharmaceutical Co. Ltd., Osaka. As far as possible all the samples were stored at -20° and in the dark to prevent decomposition. Solutions (about 10 mg/ml) were prepared in dimethylformamide or water immediately before use. The solubility of some samples in water was increased by addition of a trace of sodium hydroxide solution.

Pyrolysis. (a) Low temperature. The solution (6 μ l containing about 60 μ g antibiotic) was applied to the tip of a solids injector (Scientific Glass Engineering Pty. Ltd., London N.20) and the solvent evaporated. The solid residue was held in the injection block of the gas chromatograph for 10 sec at $380^{\circ} \pm 10^{\circ}$, then the needle withdrawn. Glass liners fitted in the block were changed when contaminated.

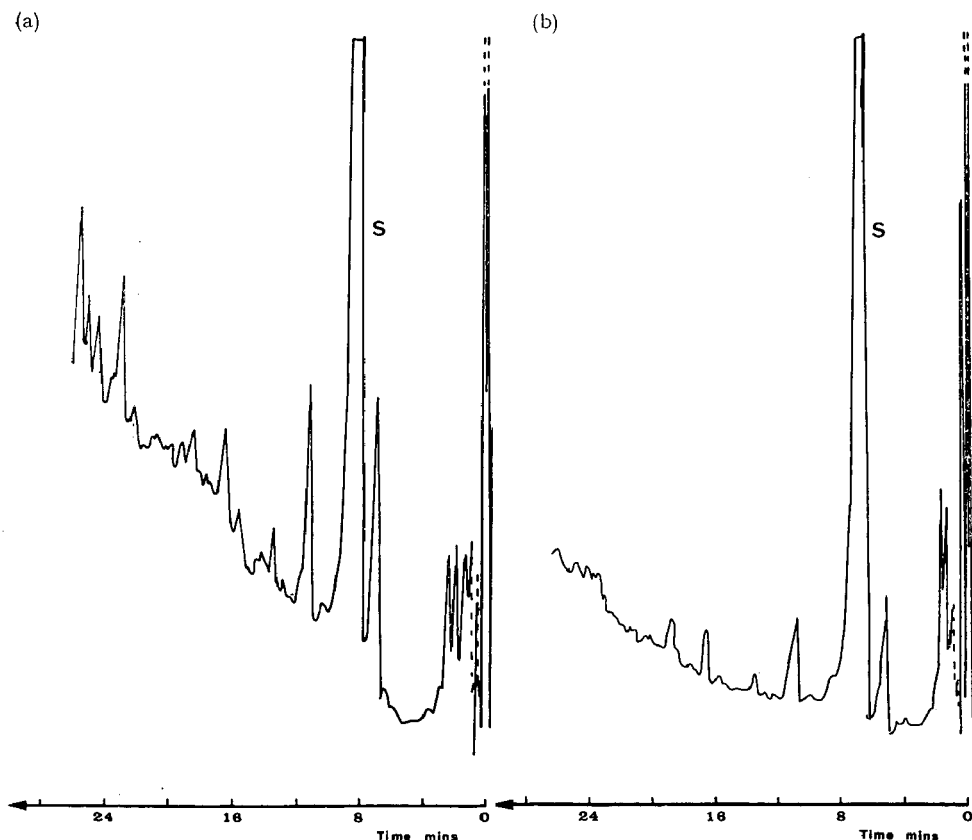


Fig. 1. Chromatograms of (a) nystatin and (b) amphotericin B after heating for 10 sec at 380°. Solid obtained by evaporation from dimethylformamide solution. Column: 1 m \times 2.2 mm I.D. stainless steel containing 5 % FFAP on Chromosorb G AW-DMCS. Nitrogen carrier at 15 ml/min. Programme: 4 min at 75°, then 6°/min to 200°, then isothermal.

(b) High temperature. The solution was coated on the filament of a pyrolyser unit (Bodenseewerk Perkin-Elmer and Co., GmBH, Überlingen/See) and solvent evaporated. The unit was fitted to the chromatograph injection block and current applied so that the solid was heated for 10 sec at about 900°.

Gas chromatography. Gas chromatography was performed with a Perkin-Elmer F11 instrument equipped with a flame ionisation detector. Nitrogen was used as carrier gas at 15 ml/min. Several stationary phases were investigated and best results obtained with a 1 m \times 2.2 mm I.D. stainless steel column packed with 5 % FFAP on Chromosorb G AW-DMCS. Pyrolysis products were separated by a temperature programme of 4 min at 75°, then increasing at 6°/min to 200°. The total run was about 30 min.

Results and discussion

Preliminary experiments indicated the usefulness of FFAP, a modified Carbowax 20M, as liquid phase for the separation of pyrolysis products, in accord with the

findings of BRODASKY⁶. We also found that low-temperature pyrolysis generally resulted in more intense and characteristic chromatograms than pyrolysis at high temperature.

Figs. 1-3 reproduce chromatograms obtained with the five antibiotics studied, after pyrolysis for 10 sec at 380°. Slight differences in retention time of peaks for the different samples reflect small variations in experimental conditions, such as temperature and carrier gas flow, over several months.

Fig. 1 shows that nystatin and amphotericin B give pyrograms which differentiate the two substances. The large peak, S, arises from traces of solvent, dimethylformamide, occluded in the solid during evaporation of the sample before pyrolysis.

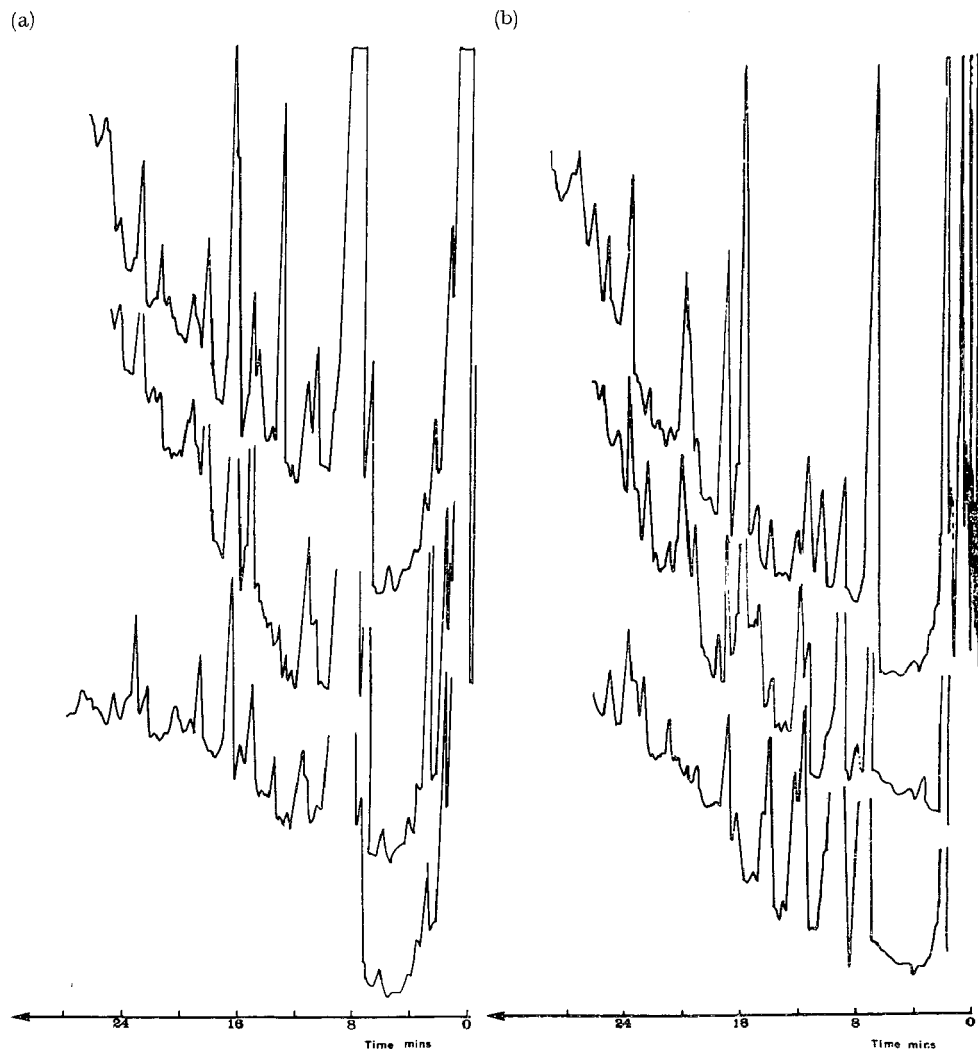


Fig. 2. Chromatograms of levorin (upper), candicidin (middle) and trichomycin (lower) after heating for 10 sec at 380°. Conditions as in Fig. 1. Solid obtained by evaporation from (a) dimethylformamide solution and (b) aqueous solution.

Its identity is confirmed by the behaviour of dimethylformamide under the same programming conditions. Although their complete structures are unknown, both nystatin⁸ and amphotericin B⁹ contain 38-membered lactone rings with the same substituents at some positions. Common peaks in the two pyrograms probably arise from fragments derived from identical regions in the two molecules.

Fig. 2 shows pyrograms from samples of candicidin, levorin and trichomycin: all differ from those in Fig. 1. They derive from solid obtained by evaporation (a)

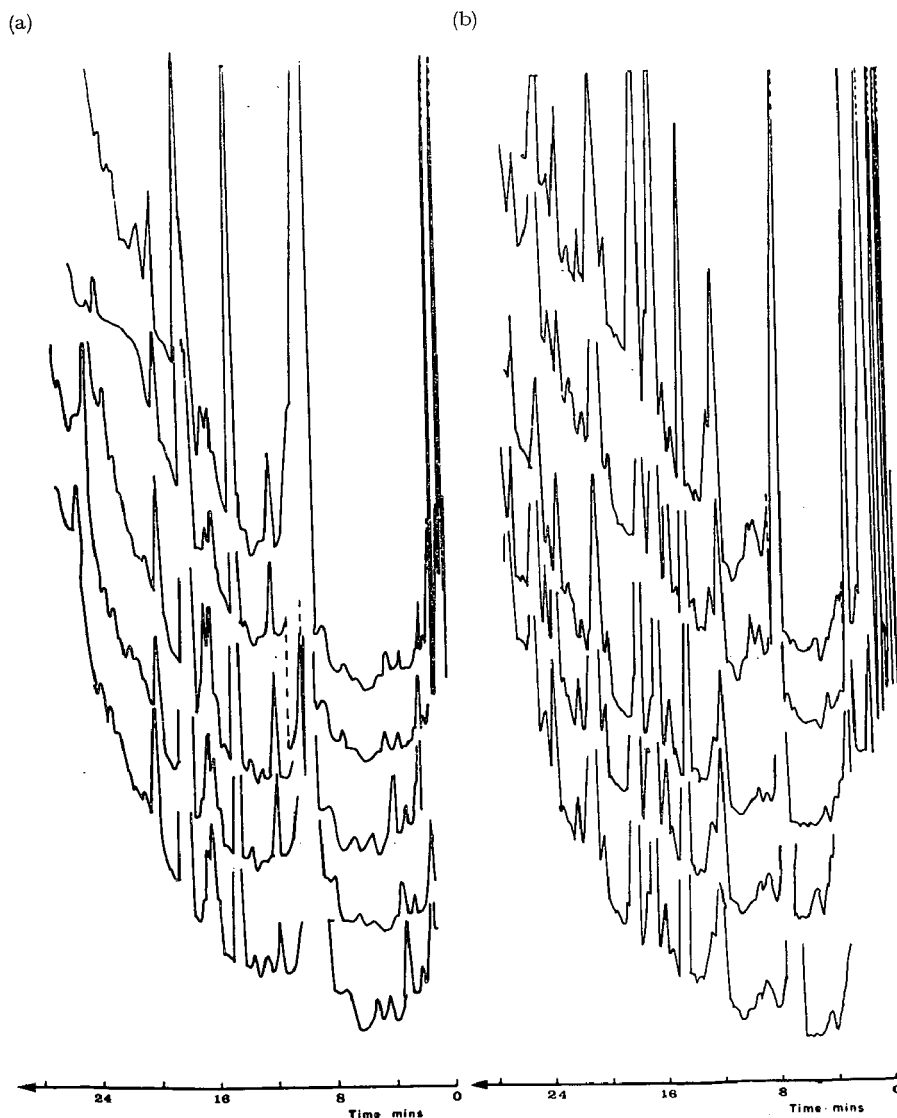


Fig. 3. Chromatograms of five samples of levorin after heating for 10 sec at 380°. Conditions as in Fig. 1. Solid obtained by evaporation from solution in (a) dimethylformamide and (b) water to which a trace of sodium hydroxide was added. Batch number (from top): (a) 10869, 12669, 16069, 11869, and 11169, and (b) 11869, 11169, 12669, 16069, and 10869.

from dimethylformamide solution and (b) from aqueous solution. In contrast to the results in Fig. 1, the patterns obtained from candididin and levorin are in almost complete agreement. Since more than 35 peaks can be distinguished and their relative intensities are similar, this is good evidence for close structural identity of the two antibiotics.

The pyrograms from trichomycin contain essentially the same peaks but show greater quantitative differences: larger volumes of trichomycin solution in dimethylformamide were needed to give traces comparable in intensity with those from 6 μ l solutions of the other preparations.

Pyrograms from solutions left exposed to air and light for up to four days showed changes in the relative intensities of a few peaks, compared with those from fresh solutions, but were basically unaltered.

Candididin, levorin and trichomycin eliminate *p*-aminoacetophenone when treated with alkali^{1,3,4}. Pyrograms from these substances, but not nystatin or amphotericin B, contain a peak corresponding to that from *p*-aminoacetophenone. This peak is observed after about 50 min on temperature-programmed analyses but is more conveniently obtained in approximately 25 min by isothermal analysis at 200°.

All five antibiotics examined contain one residue of the amino-sugar, mycosamine. No authentic sample of this was available but pyrograms obtained with glucosamine and galactosamine indicate that such molecules give rise to a number of fragments and no single, major, peak can be considered diagnostic. This is consistent with lower stability and less specific cleavage of a sugar unit compared with an aromatic one and may be likened to the fragmentation patterns of similar molecules observed by mass spectrometry.

Fig. 3 shows pyrograms obtained with five batches of levorin and are from solid after evaporation of (a) a dimethylformamide solution, and (b) an aqueous solution to which a trace of sodium hydroxide was added (to increase the solubility of the samples). Control experiments with candididin and trichomycin showed that addition of alkali resulted in more intense pyrograms without affecting their composition.

At least thirty peaks are common to the traces in Fig. 3 although minor differences exist between the samples, for example small peaks are not always present. Each pyrogram contains the same four major peaks but their relative intensities vary. The pyrograms also differ according to the solvent originally used but this difference is constant between the samples.

Chromatograms obtained after pyrolysis of samples at 900° for 10 sec confirmed the results described above. They were weaker and contained fewer peaks, presumably reflecting greater thermal breakdown, but were otherwise essentially the same.

It is known that the components of the levorin A complex vary in their biological activities¹⁰ and that variations in composition occur between levorin samples obtained from different strains of *S. levoris*¹¹. Quantitative changes in the pyrograms in Fig. 3 probably reflect small changes in composition from sample to sample. The relationship between the pyrogram of a sample and its biological potency is, however, complex whereas that between UV absorption and potency appears, from Table I, to be qualitatively simple. The intensity of UV absorption may be considered as an indication of the heptaene content of the sample.

The pyrograms in Fig. 1 differentiate nystatin and amphotericin B from each other and from the other three antibiotics (Fig. 2). This distinction is supported by

TABLE I

SOME ANALYTICAL DATA SUPPLIED FOR SAMPLES OF LEVORIN

	Batch No.				
	10 869	11 169	11 869	12 669	16 069
Biological activity, units/mg	42 100	33 600	40 800	37 800	37 200
Specific absorption					
at 342 nm	418	300	389	337	325
at 360 nm	520	415	470	455	447
at 380 nm	702	560	680	630	620
at 402 nm	605	480	570	538	524

such chemical evidence as is available. On the other hand, the pyrograms from candidin, levorin and trichomycin (Fig. 2) all contain similar peaks although those from trichomycin are quantitatively less like the others. The differences between candidin and levorin are no greater than those between the five levorin samples (Fig. 3).

These observations can be explained on the basis that all the samples used to obtain Figs. 2 and 3 are mixtures with similar, if not identical, components. Small quantitative differences in composition of the levorin samples give rise to the observed variations in biological potency (Table I) and in the pyrograms (Fig. 3). Fig. 2 suggests a similar difference between levorin and candidin and a more pronounced difference between these and trichomycin, although the main component may be identical in all three. This conclusion supports and extends the chromatographic and other evidence cited in the introduction.

We are grateful to the suppliers of the antibiotics used in this study, especially to Dr. W. O. KUHLEBAKH, Director of the Research Institute for Antibiotics, Leningrad, for samples of production batches of levorin; and to J. W. LIGHTBOWN for helpful discussion.

National Institute for Medical Research,
Mill Hill, London N.W.7 (Great Britain)

HILARY J. BURROWS
D. H. CALAM*

- 1 W. O. OROSHNIK AND A. D. MEBANE, *Fortschr. Chem. Org. Naturstoffe*, 21 (1963) 17.
- 2 R. BOSSHARDT AND H. BICKEL, *Experientia*, 24 (1968) 422.
- 3 H. KALÁSZ, J. GYIMESI, A. USHERT, K. MAGYAR AND I. HORVATH, *Acta Chim. Acad. Sci. Hung.*, 51 (1967) 431.
- 4 V. A. TSYGANOV AND E. P. YAKOVLEVA, *Antibiotiki*, 14 (1969) 387.
- 5 H. NAKANO, *J. Antibiotics (Tokyo)*, 14A (1961) 72.
- 6 T. F. BRODASKY, *J. Gas Chromatog.*, 7 (1967) 311.
- 7 N. B. COUPE, C. E. R. JONES AND S. G. PERRY, *J. Chromatog.*, 47 (1970) 291.
- 8 D. G. MANWARING, R. W. RICKARDS AND B. T. GOLDING, *Tetrahedron Letters*, (1969) 5319.
- 9 A. C. COPE, U. AXEN, E. P. BURROWS AND J. WEINLICH, *J. Am. Chem. Soc.*, 88 (1966) 4228.
- 10 V. A. TSYGANOV AND E. P. YAKOVLEVA, *Antibiotiki*, 14 (1969) 635.
- 11 V. A. TSYGANOV AND E. P. YAKOVLEVA, *Antibiotiki*, 14 (1969) 505.

Received August 17th, 1970

* To whom correspondence should be addressed.

The selectivity of polyacrylamide gels for sugars

Employing the usual techniques of gel permeation chromatography, it was shown¹ that polyacrylamide gels allow the separation of the cellohexaose. The separation is based mainly on molecular size but interactions between solute and the gel matrix become progressively more important with increasing molecular weight.

The present work was undertaken to investigate the extent to which the structure of the monomeric sugar influences the distribution coefficient, K_D , in this type of gel.

Experimental

Column preparation. The column was packed with polyacrylamide P-2, 200–400 mesh (Bio-Rad Laboratories, Richmond, Calif.). An accurately weighed quantity of dry gel was allowed to swell in distilled water for 24 h. The slurry was de-gassed under high vacuum and the column packed under gravity with continual addition of slurry to avoid defects in layering. Subsequent to preparation, the column was washed until a constant value of refractive index was obtained for the eluent. The final column dimensions are summarized in Table I. The pressure head (Mariotte flask) was adjusted to provide a flow rate of about 2 ml/h at which it was judged that equilibrium conditions on the column would be approximated. The column was thermostated to $25 \pm 0.1^\circ$.

TABLE I

DIMENSION OF THE COLUMN (POLYACRYLAMIDE P-2)

Column height: ~ 60 cm; cross-sectional area: 0.785 cm^2 ; flow rate: 2 ml/h; sample volume: 0.1 ml; sample concentration: 1 mg/ml.

Settled bed volume	47.7 ml
Void volume (Blue dextran) V_0	17.1 ml
Internal volume ^a V_I	28.7 ml
Wt. of dry gel	~ 15 g

^a Determined as the ordinate intercept of a plot of $(V_e - V_0)$ vs. molecular weight for the celloextrin series; this value agreed closely with that obtained from the elution of NaCl.

Sample application and detection. The sample solution (0.1 ml containing 0.1 mg solute) was applied to the gel surface with a micropipette in a layer 1 mm deep. The solution was allowed to enter the bed, was washed with successive portions of solvent and the column was connected to the constant head device. The eluent was collected and the volume recorded to within ± 0.02 ml at regular intervals. A Waters Associates Model R4 differential, automatically recording refractometer was operated at $\times 8$ attenuation. Under these conditions 90 % full-scale deflection was obtained at the sample maximum. The dead volume between the end of the column and the refractive index cell was approximately 0.3 ml.

Results and discussion

Table II lists distribution coefficients for a number of common sugars (reproducibility in K_D is ± 0.002). Comparison of the figures for mannose and rhamnose (6-deoxy-L-mannose) shows that replacement of the primary hydroxyl at C₆ with H results in a lower K_D value. The reactions of the 6-deoxy-aldohexoses are known to be the same as those of the corresponding aldohexose except where the primary hydroxyl group is involved in the latter. Consequently, this means that the carbinol group plays a significant part in the interaction between solute and gel matrix, as the order would be reversed if molar volumes predominate.

TABLE II

K_D VALUES FOR SOME SUGARS ON POLYACRYLAMIDE P-2 WITH DEIONIZED WATER AS ELUENT

Compound	K_D^a
D-Glucose	0.921
L-Glucose	0.920
Mannose	0.930
Rhamnose	0.879
Glucuronic acid	0.415
Galactose	0.917
Fructose	0.929
Xylose	0.931
Sucrose	0.854
Raffinose	0.750
Stachyose	0.715

$$^a K_D = \frac{V_e - V_0}{V_t - V_0}$$

V_0 = void volume

V_t = total solvent volume in column

V_e = elution volume for a given solute.

The K_D values for glucose and glucuronic acid show that replacement of the carbinol group with a carboxyl group leads to a striking reduction in K_D . The probable explanation is ionic exclusion² due to coulombic interactions between the solute and the small number of residual carboxyl groups present in the gel. One would also expect a Donnan effect at low sample concentrations causing a reduced concentration in the internal volume of the gel; this in turn would cause earlier elution of the charged solute compared with the neutral counterpart.

D- and L-glucose have identical K_D values, as observed by MARSDEN³ for a number of enantiomers on Sephadex gels. The similar K_D values for glucose and galactose show that the configuration of the hydroxyls at the C₄ position (erection from the equatorial to the axial position) is unimportant. This is understandable as the group will be equally accessible sterically in either position. However, erection of the hydroxyl at the C₂ position as in mannose leads to a small but significant increase in K_D compared with the value for glucose.

Fructose, having predominantly the pyranose form in free solution but the furanose form when linked to other sugars, has the same K_D value as mannose. It would appear to be immaterial whether the carbinol group is situated at C₂ or C₅ unless

the differing configurations at C₃ counterbalance a possible effect; erection of the hydroxyl at C₃ should lead to an increase in K_D .

It is open to speculation whether the differences in K_D arise mainly from the relative abilities of the solutes to fit into the water lattice or whether they are primarily a function of the accessibility of the hydroxyls to the gel. KABAYAMA AND PATTERSON⁴ suggest that β -D-glucose, having all hydroxyls equatorially displaced, can fit into the water lattice with unstrained hydrogen bonds. This would lead to a higher affinity for the water phase than the gel phase. Alternatively, one might reason that axial hydroxyls facilitate interaction with the gel.

On the basis of molar volumes, one would expect xylose to elute at a greater volume than glucose, as observed. The data for the cellodextrins and xylodextrins⁵ (up to the heptamers) fall on a common line in a plot of K_D as a function of molecular weight.

The significance of the structure of the group at C₅ in the pyranose ring may be inferred from the K_D values for methyl alcohol, formic acid and formamide (Table III).

TABLE III

K_D VALUES FOR SOME SIMPLE COMPOUNDS ON POLYACRYLAMIDE P-2 WITH DEIONIZED WATER AS ELUENT

Compound	K_D
Formic acid	0.674
Formamide	0.939
Methanol	0.839
<i>n</i> -Propanol	0.820
Isopropanol	0.777

Formic acid and formamide are respectively accelerated and retarded in relation to methanol by charge effects owing to the residual carboxyl groups in the gel. These differences should be eliminated if an electrolyte solution is used as the eluent. Methanol has a higher K_D value than *n*-propanol in correspondence with the molar volumes. However, MARSDEN³ has observed with Sephadex gels that the increasing hydrophobicity of *n*-alcohols of longer chain length leads to a progressive retardation on elution, which outweighs the molecular size effect. That a greater weight is to be allotted to the affinity of a given alcohol for water (or conversely for the gel matrix) rather than molar volume is shown by the lower K_D value for isopropanol than *n*-propanol; the former is the more hydrophilic.

The series glucose-sucrose-raffinose-stachyose separate linearly in a plot of chain length *versus* K_D as observed for the cellodextrins glucose-cellotetraose¹. The plots are in fact superimposable. This is not unexpected as galactose, glucose and fructose have similar K_D values.

This work forms part of a research program financially supported by the Swedish Forest Products Research Laboratory, Billeruds AB, Mo och Domsjö AB, Stora

Kopparbergs Bergslags AB, Svenska Cellulosa AB and Uddeholms AB. This support is gratefully acknowledged.

*Institute of Physical Chemistry, University of Uppsala,
Box 532, S-751 21 Uppsala 1 (Sweden)*

W. BROWN

- 1 W. BROWN, *J. Chromatog.*, 52 (1970) 273.
- 2 P. A. NEDDERMEYER AND L. B. RODGERS, *Anal. Chem.*, 40 (1968) 755.
- 3 N. V. B. MARSDEN, *Ann. N.Y. Acad. Sci.*, 125 (1965) 478.
- 4 M. A. KABAYAMA AND D. PATTERSON, *Can. J. Chem.*, 36 (1958) 563.
- 5 W. BROWN, unpublished results.

Received September 3rd, 1970.

J. Chromatog., 53 (1970) 572-575

CHROM. 5015

The isolation, separation and determination of isopropylnoradrenaline and its O-methyl derivative in blood serum and tissue homogenate

The assay procedure was essentially that of COHEN AND GOLDENBERG¹ commonly applied for the estimation of epinephrine and norepinephrine using the final evaluation of the isoproterenol and O-methylisoproterenol in the form of corresponding adrenolutines. For the estimation in serum the procedure of KAHANE AND VESTERGAARD² was modified, and for the determination of the isoproterenol level in tissue homogenates the original procedure of BERTLER *et al.*³ was applied. The final part of the analytical procedure was the chromatographic separation of isoproterenol and its O-methyl derivative from adrenalin and noradrenalin. For this purpose tandem chromatography on cellulosophosphate and carboxymethylcellulose was used.

Experimental

Isolation of isoproterenol and the corresponding O-methyl derivative from plasma. A 15-ml plasma sample was incubated with 0.5 g of aluminium oxide under vigorous shaking for 3 min. The suspension of aluminium oxide was spun off at $700 \times g$, and the sediment was resuspended in an equal volume of double-distilled water and spun off again. The whole procedure was repeated twice. In the last phase the resuspended mixture of aluminium oxide (containing adsorbed catecholamines including isoproterenol and O-methylisoproterenol) were poured into a small column (0.8×15 cm) and eluted with distilled water; the eluate was discarded. The catecholamine mixture was eluted with 5 ml of 0.4 M acetic acid. The eluate was taken to dryness and repurified by chromatography on a Dowex 50 X2 column. The ion-exchange column was prepared as follows. A column (1.2×4 cm) was filled with swollen ion exchanger

J. Chromatog., 53 (1970) 575-577

(minus 400 mesh) and introduced into the ammonia cycle by subsequent washing with the following series of solvents:

- (1) 10 ml of 2 *N* hydrochloric acid;
- (2) 5 ml deionized water;
- (3) 10 ml of 1 *M* ammonium acetate, pH adjusted to 6.0 by dropwise addition of glacial acetic acid;
- (4) 5 ml of deionized water.

The dissolved sample from the first purification step was applied to the Dowex 50 column and the column was eluted twice with 8 ml of 0.4 *N* acetic acid. Before the subsequent run, the column was regenerated by washing in the same series of solvents as indicated above. The eluate from the Dowex column was evaporated to dryness, dried in a desiccator overnight, dissolved in 0.5 ml of 0.05 *M* ammonium acetate, the pH value of which had been adjusted before to 6.1 by addition of glacial acetic acid. This sample was subjected to the final chromatographic separation as described below.

Isolation of isoproterenol and the corresponding O-methyl derivative in a heart tissue homogenate. Pooled hearts of five albino rats were homogenized in 30 ml of 0.4 *M* perchloric acid. The homogenate was spun off and the sediment reextracted under identical conditions. Pooled extracts were stored overnight at -20° . The next morning, the pH of this sample was adjusted by 5 *N* potassium carbonate to 4.0 and the precipitate of potassium perchlorate was spun off at a temperature not exceeding 0° . The precipitate was quickly washed on a Buechner funnel and both the supernatant and the washings were used for the further assay. An aliquot containing 150–500 μg of catecholamines each was applied to the Dowex 50 column (see previous paragraph), and catecholamines were eluted by 8 ml of 1 *N* hydrochloric acid. The flow rate in the Dowex column did not exceed 0.25 ml/min. The eluate was, as in the case of plasma samples, evaporated to dryness and prepared for further analysis by dissolving it in 0.5 ml 0.05 *M* ammonium acetate (pH 6.1).

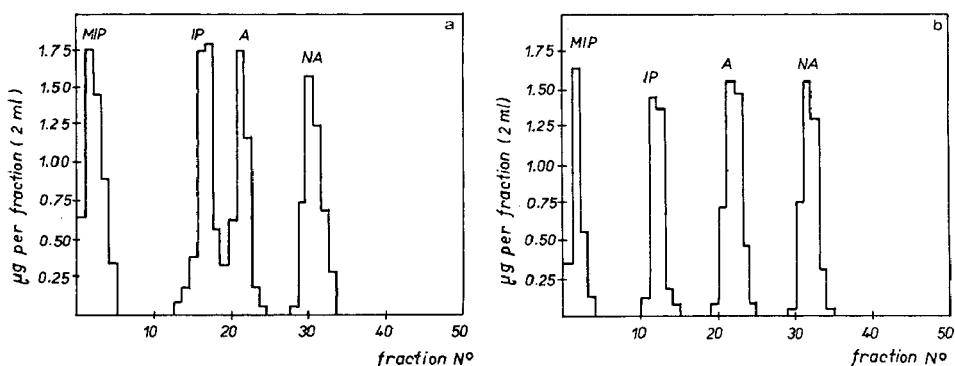


Fig. 1. The chromatographic profile of the mixture of O-methylisopropylnoradrenaline (MIP), isopropylnoradrenaline (IP), adrenaline (A) and noradrenaline (NA) on cellulosophosphate (a) and on the tandem system of cellulosophosphate and carboxymethylcellulose (b). For experimental details see text.

Separation of isopropylnoradrenaline and the corresponding O-methyl derivative using a tandem chromatographic procedure on cellulosophosphate and carboxymethyl-cellulose. For the separation of both catecholamines from epinephrine and norepinephrine two columns 0.6×40 cm combined in series were used. These columns were filled up to 35 cm with cellulosophosphate Whatman CP 11 (Column No I) and carboxymethyl cellulose Whatman CM 32 (Column No II). Columns were eluted by a linear gradient of ammonium acetate buffer with a concentration change from 0.05 to 0.25 *M*. The pH of the buffer was adjusted previously to 6.1; flow rate on both columns was less than 0.8 ml/min. Fractions of 2 ml were collected. Columns were loaded with 0.5 ml of a sample obtained after either purification procedure. The elution of the column was stopped after 100 ml of the eluant had passed through the system. Under these conditions *O*-methylisopropylnoradrenaline is eluted in fractions No. 3-7, isopropylnoradrenaline in fractions No. 10-15 (see Fig. 1).

Oxidation of isopropylnoradrenaline and its O-methyl derivative to the corresponding lutines. Combined fractions 3-7 and 10-15 were evaporated to a final volume of 0.2 ml, diluted to 1 ml with borate buffer (0.66 *M*, pH 7) and the following reagents were added subsequently: 0.05 ml of 0.02 % $\text{CuCl}_2 \cdot 2\text{H}_2\text{O}$ and 0.05 ml of 0.25 % potassium ferricyanide. The reaction was stopped after 3 min by adding 0.05 ml of 10 % BAL in 25 % formaldehyde. After 10-20 sec 0.2 ml of 10 *N* NaOH was added, and after another 5 min 0.15 ml of glacial acetic acid was pipetted into the sample. The reaction mixture was vigorously mixed and subjected to fluorimetric evaluation.

*Physiological Institute, Czechoslovak Academy of Science,
Prague (Czechoslovakia)*

ZDENĚK DEYL
JIŘÍ PILNÝ

*Research Institute of Food Industry of the Czech
Agricultural Academy, Prague (Czechoslovakia)*

JAN ROSMUS

1 G. COHEN AND M. GOLDENBERG, *J. Neurochem.* 2 (1957) 58; *ibid.*, 2 (1957) 71.

2 P. KAHANE AND P. VESTERGAARD, *J. Lab. Clin. Med.*, 70 (1963) 333.

3 A. BERTLER, A. CARLSEN AND E. ROSENGREN, *Acta Physiol. Scand.*, 44 (1958) 273.

Received August 31st, 1970

J. Chromatog., 53 (1970) 575-577

CHROM. 5027

Separation and determination of cobalamins on an SP-Sephadex column

In a previous paper¹ we have described the separation of a mixture of methylcobalamin, cobamamide, cyanocobalamin and hydroxocobalamin by means of successive chromatograms carried out on CM-cellulose and Dowex 50 W-X2 columns. The present note describes a simple method of separating the above derivatives of vitamin

J. Chromatog., 53 (1970) 577-579

B₁₂ using a single ion-exchange column of SP-Sephadex. The proposed method is also used for the quantitative determination of cobalamins.

Experimental

Apparatus and materials. The following apparatus was employed: a Beckman DU-2 spectrophotometer; a Fractomat Y-3 with photoelectric cell for the automatic collection of fractions; a Photocrom twin-ray spectrophotometer and a Sargent S.R. recorder for the analysis of effluents and a Beckman 746 peristaltic pump (1–10 ml/min). SP-Sephadex C-25 (Na⁺) was obtained from Pharmacia, Uppsala, Sweden. Cobalamins: cyanocobalamin USP, methylcobalamin and cobamamide were obtained by partial synthesis in the Research Laboratories of Alfa Farmaceutici S.p.A. by DR. VITALE and DR. GUERRA. Commercial hydroxocobalamin was spectrophotometrically and chromatographically pure.

Preparation of the resin and the column. SP-Sephadex was dispersed in a beaker with a 0.05 *M* sodium acetate buffer (pH 5.0) by means of an electromagnetic shaker and then poured into the chromatographic column (diameter 0.9 cm) until it reached a height of 20 cm after settling. It was repeatedly washed with distilled water to remove excess ions, and the eluate was checked for spectrophotometric purity in the wavelength range 260–400 nm.

Elution. 2 ml of a solution containing 50 µg/ml of each cobalamin were placed at the top of the column containing the cationic Sephadex. First, elution was carried out with 40 ml of distilled water and then with 70 ml of 0.05 *M* CH₃COONa–CH₃COOH buffer (pH 5.0), 2-ml fractions being collected. The rate of elution was maintained at a constant value of 0.4 ml/min.

Cyano- and methylcobalamin were eluted separately with distilled water, while cobamamide and hydroxocobalamin remained fixed at the top of the resin. They can be separated by increasing the ionic force of the eluent. Each 2-ml fraction was read against a blank of the same eluent at the wavelength corresponding to the absorption peak typical of each cobalamin (Table I). All the operations were conducted in dim red light to avoid photolytic degradation of the cobalamins.

Results

Fig. 1 shows the separation of the cobalamins on SP-Sephadex which proves particularly suitable for the quantitative determination of labile substances.

Quantitative determination. Table I shows the percentages of the four cobalamins recovered, the wavelengths at which the spectrophotometric readings of the single

TABLE I

% RECOVERY OF COBALAMINS SEPARATED ON COLUMN OF SP-SEPHADEX C-25 (Na⁺)

Cobalamin	% Recovery ± S.D. ^a	λ_{max}	$\epsilon \times 10^{-3}$
Cyanocobalamin	103 ± 1.2	361	28.056 (ref. 2)
Methylcobalamin	96.6 ± 0.5	340	14.002 (ref. 3)
Hydroxocobalamin	99.2 ± 0.8	351	25.985 (ref. 4)
Cobamamide	97.2 ± 1.7	338	12.636 (ref. 5)

^a Standard deviation based on 8 determinations.

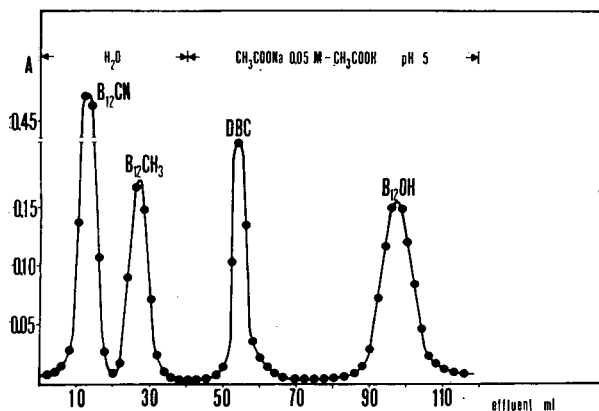


Fig. 1. Chromatographic separation of cyanocobalamin ($B_{12}CN$), methylcobalamin ($B_{12}CH_3$), hydroxocobalamin ($B_{12}OH$) and cobamamide (DBC) on a 0.9×20 cm column. $B_{12}CN$ and $B_{12}CH_3$ eluted with distilled water at flow rate of 24 ml/h. DBC and $B_{12}OH$ eluted with 0.05 M acetate buffer (pH 5.0). The volume of each fraction is 2 ml. Absorbance measurements at the absorption of each cobalamin.

fractions were carried out and the molar absorption values used to calculate the amounts recovered.

Discussion

The chromatogram in Fig. 1 shows good separation of the cobalamins which were eluted in symmetrical peaks with very few ml of eluent. Cyanocobalamin is neutral and is therefore the first to be eluted with distilled water separately from methylcobalamin, which, presumably on account of the inductive effect of the methylic group imparting a very slight basicity to the molecule, is delayed.

The molecule of adenine and the hydroxyl group bonded to the cobalt atom impart a certain basicity to cobamamide and hydroxocobalamin. With distilled water they remain at the top of the column and their elution is only possible by increasing the ionic force of the eluent.

Since cobamamide and hydroxocobalamin have different basicities it is not necessary to adopt a gradient of concentration and/or pH.

The data reported in Table I show that the technique used is satisfactory from a quantitative point of view as well, errors being of the order of $\pm 5\%$.

The method described is easily performed and requires about 4 h.

*Alfa Farmaceutici S.p.A., Research Laboratories,
Analytical Chemistry Laboratory,
Bologna (Italy)*

G. TORTOLANI
P. BIANCHINI
V. MANTOVANI

- 1 G. TORTOLANI, P. BIANCHINI AND V. MANTOVANI, *Farmaco, Ed. Prat.*, 25 (1970) 772.
- 2 R. STROHECKER AND H. M. HENNING, *Vitamin Assay*, Verlag Chemie, (1966) 152.
- 3 J. A. HILL, J. M. PRATT AND E. R. J. P. WILLIAMS, *J. Chem. Soc.*, (1964) 5149.
- 4 E. LESTER SMITH, J. L. MARTIN, R. J. GREGORY AND W. H. C. SHAW, *Analyst*, 87 (1962) 183.
- 5 G. FABRIZIO, F. SALMIERI, L. CASILLI AND J. ROLOVICH, *Boll. Chim. Farm.*, 105 (1966) 898.

Received September 3rd, 1970

Some aspects of fractionation of DNA on an IR-120 Al³⁺ column

II. Effect of the physical state of DNA on chromatographic profiles

Native DNA consists of two right-handed helical complementary polynucleotide chains of opposite polarity coiled around the common axis. Hydrogen bonds between the two bases of the complementary chains stabilise such an orderly structure. Deformation of such a structure into a disorderly state by breaking down hydrogen bonds leads to denaturation of DNA. In apurinic acid, all adenine and guanine species are quantitatively removed from a polynucleotide chain without any dislocation of pyrimidines in the macromolecule. Degradation of DNA by splitting up of the phosphodiester linkage gives rise to partially depolymerised DNA. Mononucleotides are the building blocks of DNA polymer, and it is obvious from this that differently treated DNA molecules possess different physicochemical characteristics. Thus it was worthwhile to investigate if the physical state of DNA has any effect on the chromatographic behaviour, using an IR-120 Al³⁺ column.

With the tool developed, IR-120 Al³⁺ column^{1,2}, studies are carried out on the chromatographic behaviour of denatured DNA, apurinic acid, partial and complete enzymic digest of DNA, and compared with the studies of native DNA on IR-120 Al³⁺ column.

Experimental

Deoxyribonucleic acid. Sodium salt of DNA, used in these experiments, was isolated from buffalo liver (Mammalia, Ruminantia) by the method of SEVAG *et al.*³. It was a white fibrous and fairly pure preparation². Its purity and nativity were examined by the usual methods⁴.

IR-120 Al³⁺ column. 10 g of a dry regenerated Amberlite IR-120 Na⁺ form of cation exchanger, sufficiently equilibrated with a 0.2 M aluminium chloride solution, gave an IR-120 Al³⁺ column. After percolating glycine-sodium hydroxide buffer (pH 8.6, 0.054 M) through the column until the pH of the influent and effluent were the same, it was used for chromatographic studies of differently treated DNA molecules.

Treatments. DNA was deliberately denatured by controlled heat treatment (96°, 15 min) and cooled suddenly to room temperature in an ice bath. Denaturation by this method is very specific and causes no side reactions such as hydrolysis or deamination. Apurinic acid was achieved by keeping DNA at pH 4.0 with perchloric acid at 27° for 24 h (ref. 5). Perchlorate ions were subsequently removed as potassium salt. A partial digest of DNA was obtained by incubating DNA with pancreatic deoxyribonuclease at 37° for 6 h. As an activator 0.001 M Mg²⁺ was added. DNA was reduced to mononucleotides by the combined action of pancreatic deoxyribonuclease and spleen phosphodiesterase at 37° for 48 h. 0.001 M Mg²⁺ was also added. The chromatographic behaviour of these DNA's treated specifically was studied and compared with native DNA as follows.

Procedure. A known amount of the treated DNA (not treated in the case of the native one) was chromatographed on an IR-120 Al³⁺ column (size 1 × 15 cm), and

TABLE I

CHROMATOGRAPHIC PROFILES OF DNA SUBJECTED TO DIFFERENT TREATMENTS ON AN IR-120 Al^{3+} COLUMN

State of DNA	Treatment	Retention (%)	Elution (%)	Profiles
Native	None	100	100	Typical seven fractions
Denatured	96° for 15 min	95	100	Typical seven fractions
Apurinised	pH 4.0, 27°, 24 h	25	100	One fraction only, 0.5 M saline elutable
Partial digest	DNAase I + 0.001 M Mg^{2+} , 37°, 6 h	55	100	One fraction only, 0.5 M saline elutable
Complete hydrolysate	DNAase I + Phosphodiesterase + 0.001 M Mg^{2+} , 37°, 48 h	0	—	—

the adsorbed DNA was eluted using 100 ml of each of the different eluting agents in the following sequence: 0.5 M, 1.0 M, 2.0 M saline; 1.0 %, 2.0 % EDTA, 1.0 M ammonium acetate, glass-distilled water and finally 0.1 M sodium hydroxide. The flow rate during adsorption and elution was 10–15 ml/h. The fractions, each 25 ml, were

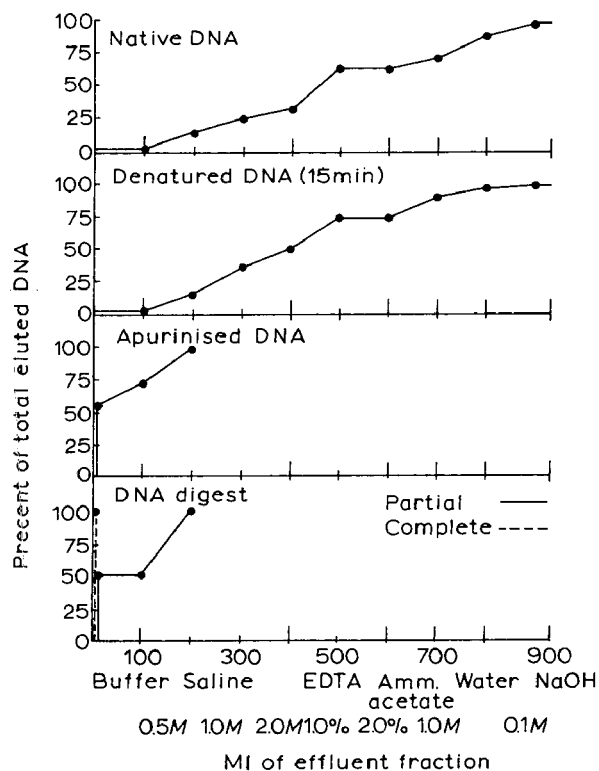


Fig. 1. Percent of total eluted buffalo liver DNA subjected to different treatments, chromatographed on an IR-120 Al^{3+} column.

analysed for their DNA content using the reaction of BURTON⁶. It was noted that DNA was fractionated on the IR-120 Al^{3+} column on the basis of its purine and pyrimidine composition².

The percent retention of DNA and percent elution of totally adsorbed DNA and the fractions obtained are given in Table I. The percent of total DNA eluted with different eluting agents is given in Fig. 1 and the profiles in Fig. 2.

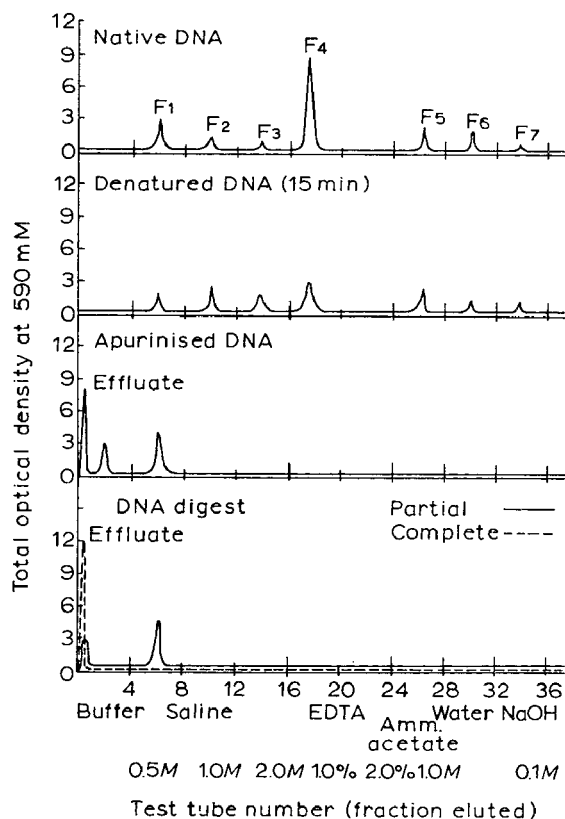


Fig. 2. Chromatographic elution profiles of buffalo liver DNA, subjected to different treatments, on an IR-120 Al^{3+} column.

Results and discussion

From Table I it is clear that the native DNA is 100 % adsorbable on an IR-120 Al^{3+} column and also is completely elutable in seven distinct fractions using different eluting agents². Denatured DNA was also found to be nearly 100 % retainable and gave a chromatographic profile similar to that of native DNA. However, the percent distribution of DNA eluted in the fractions varies in the two cases as can be seen in Figs. 1 and 2. HERSHEY *et al.*⁷ studied the effect of denaturation on the chromatographic behaviour using an MSAK column. It was observed that heat-sheared DNA has less affinity for the column, and hence it was easily elutable. Present results are comparable with those of HERSHEY *et al.*⁷ as seen by more elution due to saline and less due to 1.0 % EDTA. SKIDMORE *et al.*⁸, however, observed that the chromatographic

profiles of heat-treated DNA are different from those of unheated DNA on ECTEOLA-cellulose. BERNARDI⁹ noted that the degree of denaturation also changes the relative proportion of various fractions. Here it may be concluded that on the IR-120 Al³⁺ column, as on the protamine-coated Kieselguhr column¹⁰, native and denatured DNA cannot be distinguished.

Apurinic acid was found to be 25 % retainable and 100 % elutable in 0.5 M saline fraction alone, giving only one peak. The inability to retain 75 % DNA may not be due to the breakdown of the polynucleotide chain because, under the mild conditions used in the present experiments, the chances of scission of the polynucleotide chain are minimum¹¹.

The partial digest of DNA is 55 % retainable on the column and is easily and completely elutable in 0.5 M saline alone, giving one peak. This behaviour indicates a relatively low affinity for the column. The complete digest of DNA is completely nonretainable, indicating that mononucleotides have no affinity for the column. It is known that DNAase acts on DNA giving rise to oligo-, di-, tri-, and tetranucleotides¹². If this partial digest is simultaneously treated with spleen phosphodiesterase, mononucleotides are formed. It is possible that the retainability to oligonucleotides may be due to their partial macromolecular structure. Once, however, DNA is reduced to a mononucleotide state, the macromolecular structure is completely lost and, as a result, the mononucleotides are not retained on the column. KIT¹³ has also made similar observations using an ECTEOLA-cellulose column. BERNARDI⁹ also found that a DNAase digest of DNA is eluted earlier than intact DNA from a hydroxyapatite column, thus indicating that the depolymerised product has poor affinity and binding on the column and, therefore, requires a polymeric structure. BROWN AND WATSON¹⁴ have also pointed out that a finite structure of DNA is necessary for adsorption on histone coated with Kieselguhr.

Department of Zoology, University of Poona,
Poona-7 (India)

R. M. KOTHARI

- 1 R. M. KOTHARI, *Chromatog. Rev.*, 12 (1970) 127.
- 2 R. M. KOTHARI, *J. Chromatog.*, 52 (1970) 119.
- 3 M. G. SEVAG, D. B. LACKMAN AND J. SMOLENS, *J. Biol. Chem.*, 124 (1938) 425.
- 4 R. M. KOTHARI, *Ph. D. Thesis*, Poona, 1968.
- 5 G. SCHMIDT, *Methods Enzymol.*, 3 (1957) 757.
- 6 K. BURTON, *J. Biochem.*, 62 (1956) 315.
- 7 A. D. HERSHEY, E. GOLDBERG, E. BURGI AND L. INGRAHAM, *J. Mol. Biol.*, 6 (1963) 230.
- 8 W. D. SKIDMORE, R. K. MAIN AND J. J. COLE, *Biochim. Biophys. Acta*, 76 (1963) 534.
- 9 G. BERNARDI, *Nature*, 206 (1965) 779.
- 10 J. L. DE'MARE, N. REBEYROTTE, A. LEPRIEUR AND J. ROUSSAUX, *Biochim. Biophys. Acta*, 87 (1964) 165.
- 11 S. GREER AND S. ZAMENHOF, *J. Mol. Biol.*, 4 (1962) 123.
- 12 R. SINSHEIMER, *J. Biol. Chem.*, 208 (1954) 445.
- 13 S. KIT, *Arch. Biochem. Biophys.*, 87 (1960) 324.
- 14 G. L. BROWN AND M. WATSON, *Nature*, 172 (1953) 339.

Received July 24th, 1970

CHROM. 5040

Cation-exchange chromatography of nucleotides, nucleosides and nucleic bases

Various methods for the separation of nucleotides, nucleosides and nucleic bases have been reported using adsorption chromatography^{1,2} and anion-³⁻⁶ or cation-exchange⁷⁻¹⁰ column chromatography. BLATTNER AND ERICKSON⁷ rapidly separated nucleotides on an AG 50W X4 column using an ammonium formate elution buffer (pH 3.2). BONNELYCKE *et al.*⁸ reported a simultaneous analysis of purines, pyrimidines and amino acids using a modified amino acid analyzer.

In this note we report that nucleotides, nucleosides and nucleic bases were successfully separated on a cation-exchange resin (Aminex A-4) column using citrate and acetate buffers.

Materials and methods

A mixture* of nucleotides (5'-UMP, 5'-GMP, 5'-CMP and 5'-AMP), nucleosides (Guo, Ado, Ino and Urd) and nucleic bases (Ura, Gua, Ade, Cyt and Hyp) was used at a concentration of 0.25 μ mole/ml in 0.05 *M* hydrochloric acid. Twelve additional compounds (5'-IMP, 2'- and 3'-CMP, 2'- and 3'-UMP, 2'- and 3'-GMP, 2'- and 3'-AMP, ATP, ADP and Thy) were also dissolved in distilled water to a concentration of 5.0 μ mole/ml. All compounds were obtained from Kojin Co., Tokyo, and Sigma Chemical Co., St. Louis, Mo.

A Hitachi liquid chromatograph model 034 with a 2-mm flow cell and a three wavelength detection system was employed. In this experiment optical densities at 260, 270 and 280 *m* μ were measured and recorded on a three-point current recorder which prints one dot per 4 sec. A water-jacketed column contained 0.9 \times 50 cm of Aminex A-4 (Bio Rad Laboratories, Richmond, Calif.). A 1-ml aliquot of the authentic

TABLE I
COMPOSITION OF BUFFER SYSTEMS

Buffer	Autograd chamber ^a	Sodium citrate concn. (M)	Sodium acetate concn. (M)	pH	Sodium ion concn. (M) ^b
I		0.20		3.00	0.25
II	1		0.25	6.40	0.25
	2		0.50	6.40	0.50
	3		1.00	6.40	1.00
	4		1.00	6.40	1.00

^a Each chamber contained 50 ml of buffer solutions.

^b Adjusted with sodium chloride.

* The abbreviations used are: UMP, uridine monophosphate; GMP, guanosine monophosphate; CMP, cytidine monophosphate; AMP, adenosine monophosphate; Guo, guanosine; Ado, adenosine; Ino, inosine; Urd, uridine; Ura, uracil; Ade, adenine; Cyt, cytosine; Hyp, hypoxanthine; IMP, inosine monophosphate; ATP, adenosine 5'-triphosphate; ADP, adenosine 5'-diphosphate; Thy, thymine.

mixture was applied to the column bed equilibrated with citrate buffer (pH 3.0, buffer I). After using the first buffer for 40 min, the buffer selection valve was changed to a four-component gradient elution from a Technicon Autograd. The buffers were pumped out at a flow rate of 60 ml/h and the column was operated at 30° throughout the chromatography. The elution program and buffer compositions employed in this system are summarized in Table I.

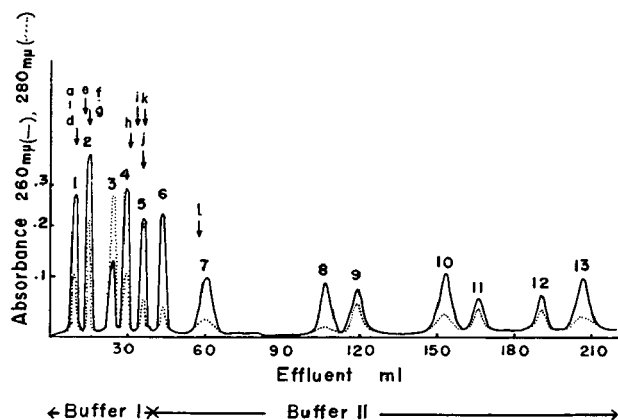


Fig. 1. Chromatogram of nucleotides, nucleosides and nucleic bases. 1 = 5'-UMP, 2 = 5'-GMP, 3 = 5'-CMP, 4 = Urd, 5 = 5'-AMP, 6 = Ura, 7 = Ino, 8 = Hyp, 9 = Guo, 10 = Ado, 11 = Cyt, 12 = Gua, 13 = Ade. a = 5'-IMP, b = 2'-UMP, c = 3'-UMP, d = ATP, e = ADP, f = 2'-GMP, g = 3'-GMP, h = 2'-AMP, i = 2'-CMP, j = 3'-CMP, k = 3'-AMP, l = Thy.

TABLE II

HW VALUES AND RETENTION VOLUMES AND THE COEFFICIENTS OF VARIATION

Compound	HW value ^a (0.25 μmole)	C.V. of HW value (%)	Retention volume ^a (ml)	C.V. of retention volume (%)
5'-UMP	1.31	2.3	9.1	0
5'-GMP	1.95	1.6	14.7	1.1
5'-CMP	2.50	1.9	24.5	0.9
Urd	2.51	2.0	29.9	0.7
5'-AMP	2.99	2.9	36.0	1.6
Ura	2.03	2.6	43.3	0.7
Ino	1.62	1.7	59.9	1.1
Hyp	1.58	2.0	107.0	0.6
Guo	2.52	0.9	118.6	0.8
Ado	3.90	1.5	153.3	0.9
Cyt	1.51	3.0	167.0	0.8
Gua	1.77	2.1	189.8	1.4
Ade	3.66 ^b	1.2	206.1	2.1

^a Average of 10 experiments.

^b Average of 5 experiments.

Results

A chromatogram of 13 nucleotides, nucleosides and nucleic bases is shown in Fig. 1, and the retention volumes of 12 additional compounds are indicated with

arrows. The total analysis time was 210 min. Each peak area on the chromatogram, obtained using 0.25 μ mole of the compound, was estimated at 260 m μ (except for CMP at 280 m μ) height-width (*HW*) method. The *HW* values, the retention volumes of each compound, and their coefficients of variation are given in Table II. Quantitative accuracy of this analysis was found to be within $\pm 3.0\%$, and the most suitable range of sample concentration was from 0.1 to 0.8 μ mole. Reproducibility of retention volumes of 13 compounds was obtained within $\pm 2.1\%$ as shown in Table II.

Discussion

By this procedure 13 nucleotides, nucleosides and nucleic bases were eluted with enough resolution for quantitative and qualitative analysis; however, some additional compounds were eluted so close together that not every compound could be found as a well-separated peak. In such cases, identification can be carried out by comparing the optical density obtained at three different wavelengths.

Careful preparation of the buffers was required for excellent separation, because the retention volumes of nucleotides were very sensitive to pH when buffers ranging from pH 2 to 4 are employed. Cyt and Ade were sensitive to the Na⁺ concentration of the buffers.

Sample solutions were freshly prepared every week to prevent the reduction of the peak area that was observed when the mixture was stored in a refrigerator for some weeks.

Department of Chemistry,
Faculty of Science, Kyoto University,
Kyoto (Japan)

FUMIKO MURAKAMI
SOUJI ROKUSHIKA
HIROYUKI HATANO

- 1 F. J. KULL AND M. SOODAK, *Anal. Biochem.*, 32 (1969) 10.
- 2 J. L. HOFFMAN, *Anal. Biochem.*, 33 (1970) 209.
- 3 M. HORI AND E. KONISHI, *J. Biochem.*, 56 (1964) 375.
- 4 N. G. ANDERSON, J. G. GREEN, M. L. BARBEN AND F. C. LADD, Sr., *Anal. Biochem.*, 6 (1963) 153.
- 5 T. SHIMIZU, H. UDA, H. MATUMIYA, K. MIYAUCHI AND S. GANNO, *Japan Analyst*, 18 (1969) 632.
- 6 T. ROSETT, J. G. SMITH, Jr., I. MATSUO, P. A. BAILEY, D. B. SMITH AND S. SURAKIAT, *J. Chromatog.*, 49 (1970) 308.
- 7 R. E. BLATTNER AND H. P. ERICKSON, *Anal. Biochem.*, 18 (1967) 220.
- 8 B. E. BONNELYCKE, K. DUS AND S. L. MILLER, *Anal. Biochem.*, 27 (1969) 262.
- 9 M. UZIEL, C. K. KOH AND W. E. COHN, *Anal. Biochem.*, 77 (1968) 25.
- 10 Z. ŽENÍŠEK, J. LAŠTOVKOVÁ AND J. VARHANÍK, *Sci. Tools*, 39 (1969) 16.

Received August 17th, 1970

J. Chromatog., 53 (1970) 584-586

CHROM. 5034

Chromatographic studies of some halogenated quinones

I. Thin-layer chromatography of some chlorinated derivatives of *p*-benzoquinone

Although a number of papers deal with the chromatographic behaviour of substituted quinones, with the exception of chloranil¹ there is no report in the literature with regard to TLC of chlorinated *p*-benzoquinones. Two papers^{2,3} have appeared on the separation and identification of some chlorinated derivatives of *p*-benzoquinone by paper chromatography. As can be concluded from the results of these authors, the R_F values of 2,6-dichloro-1,4-benzoquinone and 2,3,5-trichloro-1,4-benzoquinone are not very different, and therefore the methods used for separation of these compounds are not convenient.

The aim of our investigation was to find the most satisfactory developing system for separation of 2,6-dichloro-1,4-benzoquinone, 2,3,5-trichloro-1,4-benzoquinone and their mixtures with chloranil (2,3,5,6-tetrachloro-1,4-benzoquinone).

Experimental

Preparation of pure compounds. All chlorinated derivatives of *p*-benzoquinone were prepared by methods described in the literature (Table I). All compounds were purified by several crystallizations. Melting points of the pure compounds obtained are listed in the same table. A commercial sample of *p*-benzoquinone was also recrystallized. The samples of chlorinated *p*-benzoquinones were dissolved in anhydrous benzene. *p*-Benzoquinone was dissolved in abs. ethanol. 1 % solutions were spotted.

TABLE I

SOME CHLORINATED DERIVATIVES OF *p*-BENZOQUINONE

Compound	Melting point ^a (°C)	Reference
2-Chloro-1,4-benzoquinone	57.0	4
2,3-Dichloro-1,4-benzoquinone	98.0	5
2,5-Dichloro-1,4-benzoquinone	159.0	6
2,6-Dichloro-1,4-benzoquinone	119.0	7
2,3,5-Trichloro-1,4-benzoquinone	169.5	8
2,3,5,6-Tetrachloro-1,4-benzoquinone(chloranil)	289.5	9

^a = The melting points are corrected.

Mobile phases. All solvents were redistilled before use. All mixtures were allowed to reach the temperature at which the chromatograms were to be eluted. All solvents used were reagent grade.

Plate preparation. Plates 20 × 20 cm with thin layers were prepared using a Camag applicator.

Silica gel layers. A slurry was obtained by adding 80 ml of redistilled water to 35 g of Silica Gel DF 5 (Camag) with a UV indicator and after mixing them thoroughly,

this was immediately used to coat the plates with a layer 300 μ thick. The plates were dried for 30 min at room temperature and then heated for 24 h at 120° in an oven. The plates were then cooled and stored in a desiccator for at least 24 h before use.

Kieselguhr layers. In the same way a slurry was obtained by adding 100 ml of redistilled water to 50 g of Kieselguhr G (Merck). The plates were dried for 30 min at room temperature and then heated for 60 min at 110–120° in an oven. The plates were cooled and stored in a desiccator for at least 4 h before use. The impregnation of Kieselguhr thin layers was made in a chromatography chamber by allowing a solution of β -phenoxyethanol in benzene to ascend the plate by capillary action. Benzene was then allowed to evaporate into the air from the layer at room temperature.

Chromatographic procedure. Pure samples of chlorinated *p*-benzoquinones were applied at the starting line. After drying the spots at room temperature, the plates were placed in developing chambers saturated with solvents and developed by an ascending method, until the solvent front had travelled 15 cm beyond the original spots. The plates were removed from the chambers and, after marking the solvent front, allowed to dry in air. During the experiments the temperature was $24 \pm 0.5^\circ$.

Detection. All spots on silica gel layers were located in UV light (D_1), but the spots on kieselguhr were revealed using chemical detection (D_2). D_1 = UV light (254 nm) — quenching spots; D_2 = solution of 0.1 *N* AgNO₃ – 5 *N* NH₄OH (1:1) — dark brown spots.

Results and discussion

Many solvent combinations were examined for developing the chromatograms on Silica Gel DF 5 and Kieselguhr G; the best of these were found to be: S_1 = a 25 % solution of benzene in carbon tetrachloride; S_2 = a saturated solution of β -phenoxyethanol in *n*-hexane. The saturated solutions of β -phenoxyethanol in *n*-heptane and *n*-octane were also examined.

The R_F values of chlorinated *p*-benzoquinones in the solvent system used are given in Table II. A 25 % solution of benzene in carbon tetrachloride has been found to be the most satisfactory developing system both for identification and separation of these compounds on silica gel. The characteristic shades of chlorinated derivatives of *p*-benzoquinone in UV light provide a means for their quick and satisfactory identification. It was found that silica gel gave much better and reproducible R_F values than

TABLE II

R_F VALUES OF SOME CHLORINATED DERIVATIVES OF *p*-BENZOQUINONE

Compound	Silica Gel, S_1	Kiesel- guhr ^a , S_2
1,4-Benzoquinone	0.14	—
2-Chloro-1,4-benzoquinone	0.23	0.39
2,3-Dichloro-1,4-benzoquinone	0.30	0.52
2,5-Dichloro-1,4-benzoquinone	0.37	0.36
2,6-Dichloro-1,4-benzoquinone	0.40	0.41
2,3,5-Trichloro-1,4-benzoquinone	0.53	0.29
2,3,5,6-Tetrachloro-1,4-benzoquinone	0.73	0.24

^a = Impregnation: 4 % β -phenoxyethanol in benzene.

kieselguhr. The R_F values of 2,6-dichloro-1,4-benzoquinone, 2,3,5-trichloro-1,4-benzoquinone and chloranil obtained on silica gel layers are different and allow satisfactory identification and separation of these compounds.

Better separation of 2,6-dichloro-1,4-benzoquinone and 2,5-dichloro-1,4-benzoquinone was obtained on kieselguhr impregnated with solutions of β -phenoxyethanol in benzene, using its saturated solution in *n*-hexane as the mobile phase. The optimal separation of chlorinated *p*-benzoquinones on kieselguhr was obtained, when the concentration of β -phenoxyethanol in impregnation solution was 3.2 to 6.0 %.

Department of Organic Technology,
Institute for Chemical Technology,
Prague 6, Techická 1905 (Czechoslovakia)

P. ŠVEC
R. SEIFERT
M. ZBÍROVSKÝ

- 1 K. SUZUKI AND S. KATO, *Eisei Shinkenjo Kenkyu Hokoku*, 81 (1962) 51.
- 2 J. ELIÁŠEK AND A. JUNGWIRTH, *Collection Czech. Chem. Commun.*, 28 (1954) 2163.
- 3 T. SPROSTON, *Anal. Chem.*, 26 (1954) 552.
- 4 J. B. CONANT AND L. F. FIESER, *J. Am. Chem. Soc.*, 45 (1923) 2201.
- 5 A. ECKERT AND R. ENDLER, *J. Prakt. Chem.*, 104 (1922) 82.
- 6 S. LEVY AND G. SCHULTZ, *Ann. Chem.*, 210 (1881) 148.
- 7 J. GUARESCHI AND G. DACCOMO, *Chem. Ber.*, 18 (1885) 1170.
- 8 H. BILTZ AND W. GIESE, *Chem. Ber.*, 37 (1904) 4009.
- 9 A. SCHAEFFER AND D. SCHULZE, *Ger. (East) Pat.*, 12 224 (1956).

Received August 31th, 1970

J. Chromatog., 53 (1970) 587-589

CHROM 5032

A modified detection of triazine herbicide residues and their hydroxy-derivatives on thin-layer chromatograms

For the serial investigation of triazine herbicides, thin-layer chromatography (TLC) is the most suitable method at present. The detection of substances separated on the chromatogram has been tried by several methods described earlier in the literature. Among these chlorination and subsequent reaction with iodine starch proved to be the most sensitive¹. The use of chlorine gas and some other factors, however, make the widespread application of this method difficult. Therefore, based on this reaction, a method has been developed that, besides being sensitive, might be easily and safely applied. This method is also suggested for the detection of certain triazine transformation products, hydroxy derivatives in particular.

The chlorination of triazines was performed by submersion of the layer into a carbon tetrachloride solution containing chlorine instead of chlorine gas. The potassium iodide starch solvent was substituted by a potassium iodide-*o*-toluidine solution² which can be stored well.

J. Chromatog., 53 (1970) 589-591

Experimental

Chlorination solution. In equal volumes carbon tetrachloride, a 3 % solution of potassium permanganate, and a 12 % solution of hydrochloric acid are carefully but vigorously mixed. The separated tetrachloride phase is filtered through a dry filter paper. In a refrigerator the solution may be stored for some days.

Detection solution. 1 g of *o*-tolidine is dissolved in 10 ml of acetic acid and 4 g of potassium iodide in distilled water, respectively. The solutions are poured together and then filled up with water to 1 l. The solution will keep well for an unlimited time.

Thin-layer. The suspension is made of 25 g of silica gel (Merck) and 60 ml of water calculated for five 20 × 20 cm layers of 250 μ thickness. The layers are activated at 120° for 30 min and then cooled to room temperature.

Development is performed in the case of triazine herbicides with a solvent mixture of toluol and acetone (85:15) (ref. 1) and in the case of hydroxy derivatives with a solvent mixture of benzene-acetic acid-water (50:50:3). The plate which has been dried at room temperature is then placed in a vessel of suitable size, into which so much chlorination solution must be poured as to cover the plate. In the case of a 18 × 24 cm vessel, 250 ml of solution are needed. Then the vessel is covered with a glass plate and from time to time shaken in order to mix the solution. (The preparation of the solution and chlorination should be carried out in a hood.)

With this amount of solution two plates can be chlorinated in succession. Chlorination takes 3 and 6 min, respectively. Then the plate is removed and dried at room temperature for about 10 min. To guarantee that the removal of chlorine gas is adequate (in the case of chlorine being present in excess the background when sprayed also turns blue, thus rendering detection of the spots impossible), it is advisable to

TABLE I
THE SENSITIVITY OF SOME DETECTION METHODS

Detection method	Triazine herbicides (μg/spot)			Hydroxy derivatives (μg/spot)		
	Prometryne	Atrazine	Simazine	OH-propazine	OH-atrazine	OH-simazine
Dragendorff reagent ³	2	3	3	10	10	10
Iodine platinate ⁵	1	2	2	5	5	5
Silver nitrate 0.1 N aq. solution ^{1,5}	—	0.5	0.25	—	—	—
Brilliant-Green 0.5 % acetone solution + bromine vapour ⁴	2	2	3	3	3	3
Fluorescence quenching on MN UV ₂₅₄ silica gel (germicide fluorescent tube, Camag filter) ⁶⁻⁸	0.2	0.4	0.4	1	1	1
Chlorination (with a chlorine-containing carbon tetrachloride solution) + <i>o</i> -tolidine-potassium iodide solution	0.02	0.05	0.05	0.1	0.2	0.2

spray the edge of the layer with the agent, and if no discolouration appears to continue spraying the whole layer. On a white background triazines are visible as blue spots. Estimation must take place within 10 min.

Results

The present method has been compared with other known detection methods. The comparison has been carried out with three triazine herbicides and their hydroxy derivatives. The results are shown in Table I.

By modification of the chlorination method of DELLEY *et al.*¹, which is no doubt the most sensitive, the following advantages were obtained. By submerging the plate in the chlorine solution, the possibility of direct contact with chlorine gas is minimal. The chlorine solution is prepared in the laboratory, so difficulties connected with the handling of chlorine gas cylinders does not occur, and health hazards are also minimized. It has to be mentioned that the chlorination solution is not suitable for spraying. According to our observations Silica Gel H does not run off from the plate during submersion. By reaction with potassium iodide-*o*-tolidine subsequent to chlorination, we obtained the greatest possible sensitivity which can be generally obtained with a starch-containing agent. Subsequent to chlorination the detection with potassium iodide-*o*-tolidine can be combined with the informative fluorescence quenching method because the chlorination of triazines can also be carried out on MN UV₂₅₄ silica gel.

Thanks are due to Mrs. IRENE LEDER for her technical assistance.

*Institute of Nutrition, Department of Toxicological Chemistry,
Gyáli ut 3/a, Budapest IX (Hungary)*

S. KOUDELA

- 1 R. DELLEY, K. FRIEDRICH, B. KARLHUBER, G. SZÉKELY AND K. STAMMBACH, *Z. Anal. Chem.*, 228 (1967) 23.
- 2 K. MACEK AND J. VECERKOVA, *Pharmazie*, 20 (1965) 605.
- 3 H. G. HENKEL AND W. EBING, *J. Chromatog.*, 14 (1964) 283.
- 4 D. C. ABBOTT, S. A. BUNTING AND S. THOMSON, *Analyst*, 90 (1965) 35.
- 5 K. STAMMBACH, H. KILCHHER, K. FRIEDRICH, M. LARSEN AND G. SZÉKELY, *Weed Res.*, 4 (1964) 64.
- 6 R. W. FREI, N. S. NOMURA AND M. N. FRODYMA, *Mikrochim. Acta*, 6 (1967) 1099.
- 7 L. P. MANNER, *J. Chromatog.*, 21 (1966) 430.
- 8 S. KOUDELA, *Kísérlet. Orvostudomány*, 19 (1967) 331.

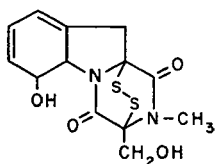
First received May 22nd, 1969; revised manuscript received August 25th, 1970

J. Chromatog., 53 (1970) 589-591

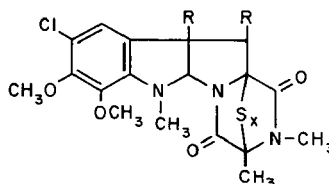
CHROM. 5013

Separation of polythiadioxopiperazine antibiotics by thin-layer chromatography

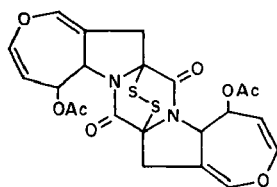
In recent years the number of 2,5-epipolythia-3,6-dioxopiperazine antibiotics has increased significantly due to isolation of new members of the series and by chemical transformations of the naturally-occurring compounds. By extensive chemical and/or X-ray crystallographic investigations the structure of gliotoxin¹ (I), sporidesmin^{2,3} (II, X = 2, R = OH) and dehydrogliotoxin⁴ (III, X = 2) was determined and other closely related compounds have since been isolated or synthesized^{3,5}. More recently several compounds related to acetyl aranotin⁶⁻⁸ (IV) have been described



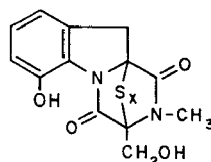
(I)



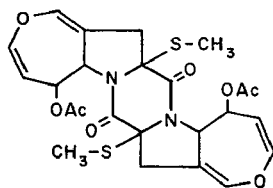
(II)



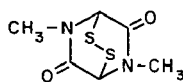
(IV)



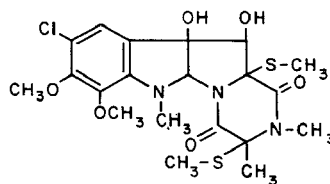
(III)



(V)



(VI)



(VII)

(i.e. V^{3,9}) and the synthesis of 1,4-dimethyl-2,5-piperazinedione (VI) has also been reported. Chetomin, another sulfur-containing natural product is also believed to contain the epipolythiadioxopiperazine moiety¹⁰. Most of the above compounds possess biological activity¹⁰⁻¹². This communication deals with the thin-layer chromato-

* Issued as NRCC No. 11496.

graphic behavior of fifteen of these sulfur-containing compounds. The separation of polysulfides (II, $X = 1, 2, 3, 4$, $R = OH$) and (III, $X = 1, 2, 3, 4$) differing only in the number of sulfur atoms in the 2,5 bridge is particularly noted.

Compounds

Gliotoxin (I) was isolated from the fungus *P. terlikowskii*⁴ and converted into dehydrogliotoxin (III, $X = 2$) as described⁴. Treatment of dehydrogliotoxin (III, $X = 2$) with triphenylphosphine¹³ gave (III, $X = 1$) and with hydrogen polysulfide gave (III, $X = 3$) and (III, $X = 4$). Sporidesmin (II, $X = 2$, $R = OH$) was isolated from *P. chartarum* and reaction with triphenylphosphine gave (II, $X = 1$, $R = OH$)³. Sporidesmin E¹⁴ (II, $X = 3$, $R = OH$), B (II, $X = 2$, $R = H$)¹⁵ and D (VII)¹⁶ were also isolated from the above fungus and the tetrasulfide (II, $X = 4$, $R = OH$) has also been isolated and prepared by treatment of (II, $X = 2$, $R = OH$) with hydrogen polysulfide¹⁷. Bisdethiodi(methylthio)-acetylaranotin (V) (BDA) and acetylaranotin (IV) were gifts of Eli Lilly Laboratories and the 1,4-dimethyl-2,5-piperazinedione (VI) was prepared by the method of TROWN¹⁸. Chetomin was obtained from *Chaetomium cochliodes*¹¹.

Chromatographic procedures

The solvent systems used and the R_F values for the compounds (I-VII) are given in Table I. Commercially available Merck Silica Gel F₂₅₄ plates (20 × 20 cm, thickness 0.25 mm) were used and 5 μ l of an 0.0002 % solution (in chloroform) was applied to the plate.

Detection

All compounds were visible under short wave UV light. When the chromato-

TABLE I
 R_F VALUES FOR EPIPOLYTHIADIOXOPIPERAZINE ANTIBIOTICS

Compound	Solvent system				
	Benzene-ethyl acetate (4:1)	Chloroform	Benzene-ether-acetic acid (70:30:1)	Hexane-tert.-butanol (9:1)	Chloroform-methanol (95:5)
I	0.15	0.06	0.20	0.09	0.50
II, $X = 1$, $R = OH$	0.32	0.06	0.31	0.17	0.53
II, $X = 2$, $R = OH$	0.38	0.09	0.39	0.17	0.57
II, $X = 3$, $R = OH$	0.36	0.07	0.39	0.24	0.54
II, $X = 4$, $R = OH$	0.21	0.03	0.25	0.24	0.49
II, $X = 2$, $R = H$	0.39	0.11	0.41	0.23	0.59
III, $X = 1$	0.25	0.11	0.26	0.15	0.47
III, $X = 2$	0.40	0.22	0.44	0.26	0.58
III, $X = 3$	0.35	0.15	0.43	0.25	0.55
III, $X = 4$	0.19	0.05	0.23	0.17	0.49
IV	0.30	0.15	0.32	0.11	0.65
V	0.20	0.11	0.23	0.09	0.65
VI	0.16	0.13	0.22	0.07	0.56
VII	0.19	0.04	0.24	0.01	0.55
Chetomin	0.05	0.01	0.09	0.01	0.51

grams were sprayed with neutral aqueous 5 % silver nitrate solution spots of black (or brown) silver sulfide were obtained where the sulfur compounds were located.

The results obtained (Table I) show that by judicious choice of solvent systems separation of most of these sulfur-containing compounds can be obtained. In the dehydrogliotoxin series (III, X = 1-4) all four polysulfides as well as gliotoxin (I) are clearly separated with the solvent system benzene-ethyl acetate (4 : 1). The mono- and tetrasulfides of sporidesmin (II, X = 1 and 4, R = OH) have different R_F in benzene-ethyl acetate (4:1) (R_F 0.32 and 0.21) and in benzene-ether-acetic acid (70:30:1) and (R_F 0.31 and 0.25), from the chromatographically similar di- and trisulfides (II, X = 2 and 3, R = OH). Separation of the latter two compounds is readily effected in hexane-*tert.*-butanol (9:1). The above solvent systems have all been used for the separation of large quantities of material (100-300 mg) by preparative thin-layer chromatography. Sporidesmin B (II, X = 2, R = H) is generally less polar and sporidesmin D (VII) more polar than the other members of the series in most of the solvent systems used. Chetomin and (VI) are the two most polar compounds and both BDA (V) acetylaranotin (VI) are readily separable in all five solvent systems. With chloroform as solvent the R_F values are low for a single elution however with repeated elution (four times) excellent separations of most of the structurally-similar polysulfides is obtained.

*Atlantic Regional Laboratory, National Research Council of Canada,
Halifax, Nova Scotia (Canada)*

R. RAHMAN
S. SAFE
A. TAYLOR

- 1 FRIDRICHSONS AND A. M. MATHIESON, *Acta Cryst.*, 23 (1967) 439.
- 2 J. FRIDRICHSONS AND A. M. MATHIESON, *Acta Cryst.*, 18 (1965) 1043.
- 3 S. SAFE AND A. TAYLOR, *J. Chem. Soc. (C)*, (1970) 432 and references cited.
- 4 G. LOWE, A. TAYLOR AND L. C. VINING, *J. Chem. Soc. (C)*, (1966) 1799.
- 5 K. C. MURDOCK AND R. B. ANGIER, *Chem. Commun.*, (1970) 55.
- 6 D. B. CONSULICH, N. R. NELSON AND J. H. VAN DEN HENDE, *J. Am. Chem. Soc.*, 90 (1968) 6519.
- 7 P. A. MILLER, P. W. TROWN, W. FULMOR, J. KARLINER AND G. MORTON, *Biochem. Biophys. Res. Commun.*, 33 (1968) 219.
- 8 R. NAGARAJAN, L. L. HUCKSTEP, D. H. LIVELY, D. C. DELONG, M. M. MARSH AND N. NEUSS, *J. Am. Chem. Soc.*, 90 (1968) 2980.
- 9 J. W. MONCRIEFF, *J. Am. Chem. Soc.*, 90 (1968) 6517.
- 10 A. TAYLOR, in R. I. MATELES AND G. N. WOGAN (Editors), *Biochemistry of Some Foodborne Microbial Toxins*, MIT press, 1967, p. 69 and references cited.
- 11 D. BREWER AND A. TAYLOR, *Can. J. Microbiol.*, 13 (1967) 1577 and references cited.
- 12 N. NEUSS, L. D. BOECK, D. R. BRANNON, J. C. CLINE, D. C. DELONG, M. GORMAN, L. L. HUCKSTEP, D. H. LIVELY, J. MABE, M. M. MARSH, B. B. MULLOY, R. NAGARAJAN, J. D. NELSON AND W. M. STARK, in *Antimicrobial Agent and Chemotherapy*, American Society for Microbiology, 1968, p. 213.
- 13 D. BREWER, R. RAHMAN, S. SAFE AND A. TAYLOR, *Chem. Commun.*, (1968) 1571.
- 14 R. RAHMAN, S. SAFE AND A. TAYLOR, *J. Chem. Soc. (C)*, (1969) 1665.
- 15 J. W. RONALDSON, A. TAYLOR, E. P. WHITE AND R. J. ABRAHAM, *J. Chem. Soc.*, (1963) 3172.
- 16 W. D. JAMIESON, R. RAHMAN AND A. TAYLOR, *J. Chem. Soc. (C)*, (1969) 1564.
- 17 S. SAFE AND A. TAYLOR, to be published.
- 18 P. W. TROWN, *Biochem. Biophys. Res. Commun.*, 33 (1968) 402.

Received August 28th, 1970

J. Chromatog., 53 (1970) 592-594

Phospholipid analysis on a micro scale

Usually, phospholipids are separated by two-dimensional thin-layer chromatography on 20×20 cm plates¹⁻⁴ and after digestion the phospholipid phosphorus is quantitatively determined with ammonium molybdate (modifications of the method of FISKE AND SUBBAROW⁵ and BARTLETT⁶).

Working with small amounts of membraneous material from various sources, it appeared desirable to develop a system which permits the analysis of phospholipids in the nanomole range. This was achieved by the use of two-dimensional thin-layer chromatography on 6×6 cm plates with an adsorbent of Silica Gel G plus calcium sulfate, followed by phospholipid phosphorus determination in a sample volume of 0.2 ml as described in this communication.

Experimental

The material was extracted according to FOLCH *et al.*⁷. The sample was then applied to 6×6 cm plates using a micropipet. The application point should not exceed 1.5 mm in height and 3 mm in width. The plates with the adsorbent composed of Silica Gel G (Merck, Darmstadt, G.F.R.) plus calcium sulfate (3:1) were activated at 120° for 20 min before use. As solvent systems we selected chloroform-methanol-acetic acid-water (30:10:0.4:1) or chloroform-methanol-water (30:10:0.5) in the first dimension and chloroform-methanol-28 % aq. ammonia (15:5:1) in the second. Development distance was about 5 cm in each dimension with 15 min air-drying in between. The spots were made visible under UV light by spraying with 0.05 % Rhodamine B in ethanol supplemented with 5 % Tinopal (Geigy AG, Frankfurt, G.F.R.) according to POPOV AND STEFANOV⁸. This reagent was found to be very sensitive for phospholipids⁹. The individual phospholipids then were carefully scraped from the plates and digested together with the adsorbent in small calibrated vials (I.D. 4 mm) in an electrically heated stove (Thermoblock with small bore holes, WTW, Weilheim, G.F.R.). Digestion and color development were performed essentially according to GERLACH AND DEUTICKE¹⁰ with 0.06 or 0.03 ml of digestion reagent, 0.3 or 0.15 ml of 1 % ammonium molybdate solution, and 0.02 or 0.01 ml of reduction reagent with an exact final volume of 0.4 or 0.2 ml (distilled water added when necessary) for the main or minor components of the sample, respectively. The optical density was determined in micro cuvettes at 650 or 820 nm.

Nuclear membranes of pig liver were prepared as described elsewhere¹¹. HeLa cells were grown in Roux bottles with Eagle's essential medium supplemented with 2 % fetal calf serum. Suspension cultures of the blue-green alga *Plectonema boryanum* were a gift from R. M. BROWN, Jr., Chapel Hill, N.C., U.S.A. Phosphatidylcholine, phosphatidylethanolamine, phosphatidylserine, phosphatidylinositol, lysophosphatidylcholine, sphingomyelin, and cardiolipin were purchased from Applied Science Lab. Inc., State College, Pa., U.S.A. Monogalactosyl diglyceride and digalactosyl diglyceride were gifts from G. UNSER, Freiburg, G.F.R.

Results and discussion

In Fig. 1 four representative two-dimensional chromatograms are presented

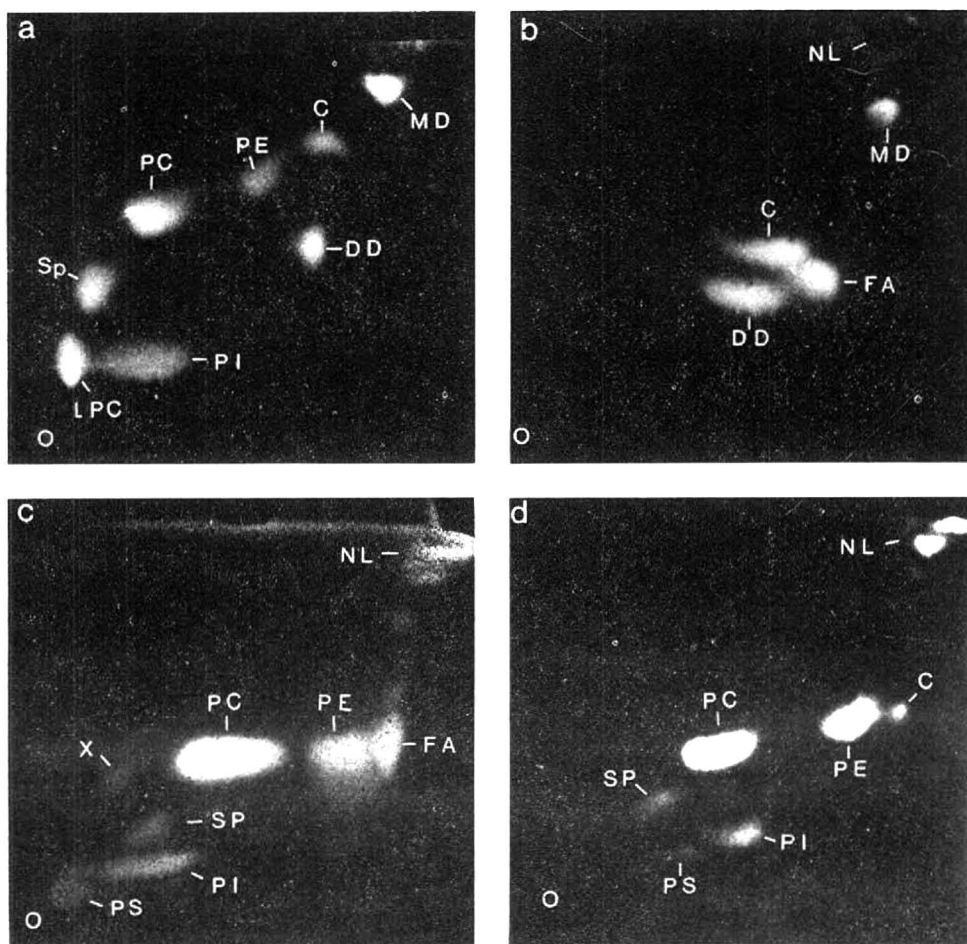


Fig. 1. Thin-layer chromatograms photographed under UV light. Original size. (a) Reference substances; (b) lipids of the blue-green alga *Plectonema boryanum*; (c) lipids of pig-liver nuclear membranes; (d) lipids of HeLa cells. Identification of components: PS = phosphatidylserine; LPC = lysophosphatidylcholine; PI = phosphatidylinositol; SP = sphingomyelin; PC = phosphatidylcholine; PE = phosphatidylethanolamine; C = cardiolipin; FA = fatty acids; DD = digalactosyl diglyceride; MD = monogalactosyl diglyceride; NL = neutral lipids; X = unknown; O = origin.

which demonstrate the usefulness of the method described. As generally can be observed, variations in temperature and humidity may cause small shifts of the spots. The separation and the sharpness of the spots is greatly enhanced by mixing Silica Gel G with calcium sulfate, compared with pure Silica Gel G layers. With the highly sensitive Rhodamine B-Tinopal spray less than 0.1 nmole phospholipid can be detected. This spray, however, cannot be used with the solvent mixtures of PARSONS AND PATTON⁴ which also give good separations in our system, since the sensitivity of this spray is diminished under acidic conditions.

In Figs. 1a and 1b the plastidal galactolipids monogalactosyl diglyceride and digalactosyl diglyceride are also chromatographed together with some phospholipids.

These glycolipids can be quantitatively estimated by the method of ROUGHAN AND BATT²².

The phospholipid composition of HeLa cells determined by a macro method and by the micro method described in this communication is listed in Table I. As can be seen, the results of both methods agree well, and the standard deviations are only slightly increased with the micro method.

TABLE I

PHOSPHOLIPIDS OF HeLa CELLS: COMPARISON OF THE RESULTS OF QUANTITATIVE ANALYSES AFTER THE MICRO METHOD AND A MACRO METHOD (% OF TOTAL PHOSPHOLIPID)

<i>Phospholipid</i>	<i>Micro method^a</i>	<i>Macro method^a</i>
Phosphatidylcholine	52.1 ± 1.9	51.0 ± 1.5
Phosphatidylethanolamine	23.5 ± 1.7	24.8 ± 1.6
Sphingomyelin	9.1 ± 2.4	8.7 ± 1.9
Phosphatidylinositol	7.0 ± 1.4	6.3 ± 1.3
Phosphatidylserine	5.7 ± 2.1	4.2 ± 1.4
Cardiolipin	3.3 ± 1.6	3.7 ± 1.3

^a Mean values ± S.D. of six analyses.

With our method less than 0.1 nmole phospholipid can be visualized on the thin-layer plates, and 0.5 nmole phospholipid can be measured quantitatively. Depending on the different content of individual phospholipids in biological material 30–50 nmole phospholipid are required for one analysis in order to also determine the minor compounds.

The investigations were supported by the Deutsche Forschungsgemeinschaft.

*Institut für Biologie II, Lehrstuhl für Zellbiologie,
78 Freiburg, Schänzlestrasse (G.F.R.)*

HANS KLEINIG
ULRIKA LEMPERT

- 1 W. D. SKIDMORE AND C. ENTENMAN, *J. Lipid Res.*, 3 (1962) 471.
- 2 D. ABRAMSON AND M. BLECHER, *J. Lipid Res.*, 5 (1964) 628.
- 3 G. ROUSER, A. N. STAKOTOS AND S. FLEISCHER, *Lipids*, 1 (1966) 85.
- 4 J. G. PARSONS AND S. PATTON, *J. Lipid Res.*, 8 (1967) 696.
- 5 C. H. FISKE AND Y. SUBBA ROW, *J. Biol. Chem.*, 66 (1925) 375.
- 6 G. R. BARTLETT, *J. Biol. Chem.*, 234 (1959) 466.
- 7 J. FOLCH, M. LEES AND G. H. SLOAN STANLEY, *J. Biol. Chem.*, 226 (1957) 497.
- 8 A. D. POPOV AND K. L. STEFANOV, *J. Chromatog.*, 37 (1968) 533.
- 9 H. KLEINIG, *J. Cell Biol.*, 46 (1970) 396.
- 10 E. GERLACH AND B. DEUTICKE, *Biochem. Z.*, 337 (1963) 477.
- 11 W. W. FRANKE, B. DEUMLING, B. ERMEN, E. JARASCH AND H. KLEINIG, *J. Cell Biol.*, 46 (1970) 379.
- 12 P. G. ROUGHAN AND R. D. BATT, *Anal. Biochem.*, 22 (1968) 74.

Received August 24th, 1970

CHROM. 5039

Separation of dansylated products of L-seryltyrosine and their identification

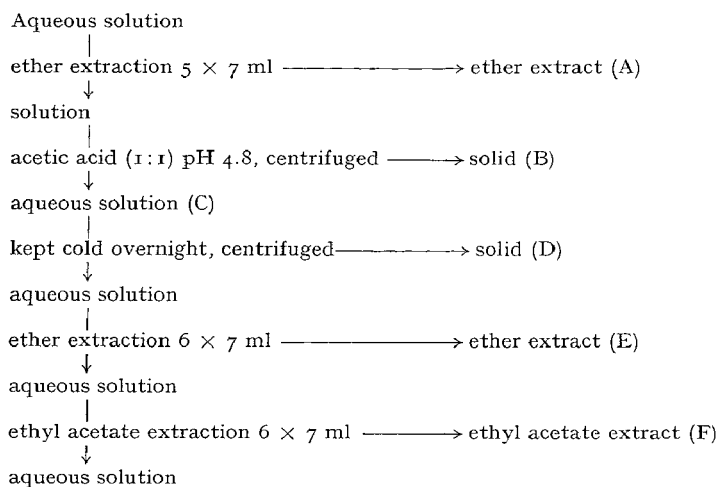
Dansyl chloride has been increasingly utilized in labeling proteins and peptides for the identification and characterization of N-terminal amino acids of those proteins and peptides¹ as it reacts with amino groups to form highly fluorescent derivatives which can be detected in extremely small amounts (10^{-3} – 10^{-4} μ mole). Dansyl derivatives of amino acids have been prepared as standards and a mixture of them was separated and identified by thin-layer chromatography (TLC)².

Confusing results may be obtained where compounds with two reactive places in the molecule are to be separated. Besides serine, tyrosine, threonine, cysteine, lysine, ornithine, arginine and histidine which present at least two spots upon dansylation, peptides offering the possibility of N- and O-dansyl derivatives are of particular interest.

The scope of the present work was to work out a method of separation and identification of the N-dansyl and N,O-didansyl derivatives of small molecular weight peptides. L-Seryltyrosine, which results from the chymotryptic digest of ACTH is of particular practical interest and was used as the model substance during this study.

Experimental

Dansyl chloride (206 mg) dissolved in acetone (6.5 ml) was added to a solution of seryltyrosine (90.3 mg, Cyclo Chemical Co.) in 5 % sodium bicarbonate solution (6 ml). The mixture was stirred at room temperature in the dark. After 1 h, some precipitate formed which was redissolved by the addition of acetone (5 ml) and water (5 ml). Then the extent of the reaction was checked by taking an aliquot (5 μ l) of the mixture and running it on a TLC plate (Silica Gel G) with solvent system I (chloroform-ethyl alcohol-acetic acid (60:40:2.5)). Four fluorescent spots were observed under UV light at R_F values of 0.4 (blue), 0.76 (yellow), 0.88 (yellow) and 1.0 (yellow). When the plate was sprayed with ninhydrin reagent, a purple spot appeared at the origin, indicating that the reaction was not yet complete. After 4 h, the acetone from half of the reaction mixture was evaporated under nitrogen; the aqueous residue was processed as described in the flow-sheet.



A small aliquot of each fraction was tested on TLC (Silica Gel G) using solvent system I; the R_F values of the fluorescent spots are given in Table I. Similar results were obtained on the other half of the reaction mixture after 22 h of reaction.

TABLE I

TLC OF THE FRACTIONS FROM THE AQUEOUS SOLUTION AFTER REACTION WITH DANSYL CHLORIDE

Fractions	R_F			
	1.0 (yellow)	0.43-0.44 (blue)	0.77-0.79 (yellow)	0.85-0.89 (yellow)
A	++	—	—	—
B ^a	—	—	—	++
C	—	++	++	+
D	—	++	+	+
E	—	++	++	+
F ^b	—	++	++	—

^a Several minor spots.

^b Two faint spots between the two reported.

Fraction A (yellow) and the blue fluorescent spot were identified as dansyl amine and dansyl acid respectively, by comparison with standards. The yellow material of R_F 0.77 and 0.85 in fractions B, C, D, E and F was purified by preparative TLC using a 0.5 mm thick Silica Gel H plate and solvent system II, consisting of chloroform-ethyl alcohol-acetic acid (85:15:1), as well as system I. Spots with an R_F value of 0.21 (designated X) and 0.46 (designated Y) in system II corresponded to R_F of 0.77 (X) and 0.85 (Y) in system I, respectively. The products were eluted with acetone, concentrated under nitrogen and dried *in vacuo* yielding glassy masses. It has been observed that fraction Y when treated with dilute sodium hydroxide solution for 24 h at room temperature gave fraction X and dansyl acid, identified by TLC with solvent system II. The nature of the mobilities and the results of this reaction indicate that the fractions X and Y are N-dansyl-seryltyrosine and N,O-didansyl-seryltyrosine respectively.

Further proof of their identities was obtained in the following manner. Fraction X was hydrolyzed with 6 N HCl in an atmosphere of nitrogen for 24 h. The solution was evaporated to dryness and the residual material was dissolved in methanol. TLC using solvent system II yielded two yellow fluorescent spots (R_F 0.23 and 0.79) and a ninhydrin spot (purple, R_F 0.0). The fluorescent spots corresponded exactly with those obtained by hydrolysis of dansyl-L-serine and the ninhydrin spot corresponded to L-tyrosine itself. The fast moving fluorescent material (R_F 0.79) was obtained from dansyl-L-serine during hydrolysis by β -elimination of the hydroxyl group. Fraction Y, in a similar way, was hydrolyzed and chromatographed. In system II, it gave three fluorescent spots of R_F 0.09, 0.23 and 0.79. The spot of R_F 0.09 corresponded to that obtained from hydrolyzed product of N-acetyl-O-dansyl-L-tyrosine. The other two spots of R_F 0.23 and 0.79 corresponded to those obtained from dansyl-L-serine hydrolysis. The material of R_F 0.09 was also ninhydrin positive.

Hence, it has been definitely established that the fractions X and Y are N-dansyl and N,O-didansyl seryltyrosine respectively. The fraction X was utilized as our standard in our ACTH work.

Our sincere thanks are due to Dr. W. R. SLAUNWHITE, Jr. for his valued advice and encouragement during the progress of the work.

*Medical Foundation of Buffalo,
Buffalo, N.Y. 14203 (U.S.A.)*

N. KUNDU
SUJATA ROY

- 1 B. S. HARTLEY AND V. MASSEY, *Biochim. Biophys. Acta*, 21 (1956) 58.
2 D. MORSE AND B. L. HORECKER, *Anal. Biochem.*, 16 (1966) 429.

First received May 4th, 1970; revised manuscript received August 11th, 1970

J. Chromatog., 53 (1970) 598-600

CHROM. 4905

Chromatography and 77°K luminescence of some hydrocarbons on thin layers of microcrystalline nylon-polytetrafluoroethylene (Aviamide-6-Fluoroglide 200)*

The separation, identification, and quantitative measurement of hydrocarbons is of particular interest in studies of air pollutants, tobacco-smoke components, and chemical carcinogenesis. Low-temperature luminescence has been shown to be a sensitive means to detect organic compounds on thin-layer chromatograms¹. This technique was used to evaluate new layer materials for thin-layer chromatography (TLC). The evaluation of particulate polytetrafluoroethylene as a layer material for TLC and its usefulness for separating metal ions have been described^{2,3}. A mixed layer that consists of the polytetrafluoroethylene Fluoroglide 200 and the new microcrystalline nylon Aviamide-6 has been found suitable for separating hydrocarbons.

Ten hydrocarbons (aromatic and heterocyclic) and a mixture that contained the ten were chromatographed on thin layers of Aviamide-6-Fluoroglide 200 (4:1) developed with *n*-propanol. The resulting chromatograms were observed with 254- and 366-nm UV light under liquid nitrogen (77°K). Eight of the ten hydrocarbons were resolved. Presumably, the separation is based on the differences in the solubilities of the hydrocarbons in *n*-propanol. The hydrocarbons show distinctive luminescent properties by which they can be identified; even the unresolved hydrocarbons were detectable in the presence of each other. The intensity of the phosphorescence of certain of the compounds is particularly striking and possibly may be a means to their sensitive quantitative measurement.

Materials

Fluoroglide 200, chromatography grade TWO218 from Chemplast, Inc., 150 Dey Road, Wayne, N.J. 07470.

* Research sponsored by the U.S. Atomic Energy Commission under contract with the Union Carbide Corporation.

Aviamide-6, from Chemical Research and Development Center, FMC Corporation, Box 8, Princeton, N.J. 08540. The *Aviamide-6* is available as an aqueous paste (40–45 % solids) and as a dry powder. The dry powder was found to be more satisfactory for TLC and was used in this work.

Hydrocarbons. The following hydrocarbons, from the sources indicated, were used:

Hydrocarbons	Source
<i>o</i> -Hydroxydiphenyl	Eastman Kodak Co.
Naphthalene	J. T. Baker Chemical Co. ("Baker's Analyzed")
Fluorene	V. F. RAAEN, ORNL Chemistry Division
Phenanthrene	Matheson, Coleman and Bell (reagent 3468)
Pyrene	Eastman Kodak Co.
Chrysene	Aldrich Chemical Co., Inc. (reagent 121971)
Anthracene	V. F. Raaen (scintillation grade; purified)
Fluoroanthene	Eastman Kodak Co.
Benzo- <i>e</i> -pyrene	Aldrich Chemical Co., Inc. (reagent 042071)
(1,2-benzopyrene)	
Benzo- <i>g,h,i</i> -perylene	Aldrich Chemical Co., Inc. (reagent 020981)
(1,12-benzoperylene)	

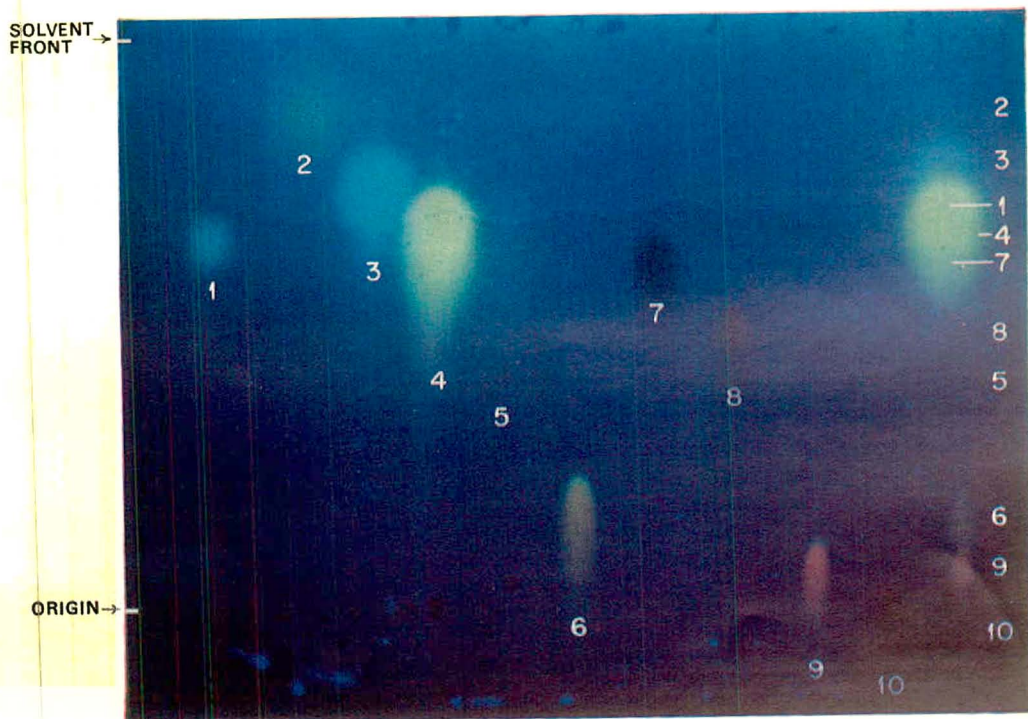


Fig. 1. Color photograph of chromatogram of hydrocarbons on *Aviamide-6*-Fluoroglide TWO218 (4:1) under liquid nitrogen (77°K) after excitation with 254-nm UV light. 1 = *o*-hydroxydiphenyl; 2 = naphthalene; 3 = fluorene; 4 = phenanthrene; 5 = pyrene; 6 = chrysene; 7 = anthracene; 8 = fluoroanthene; 9 = benzo-*e*-pyrene; 10 = benzo-*g,h,i*-perylene.

For each of the hydrocarbons, a benzene solution was prepared. Its concentration was $\sim 0.5 \mu\text{g/ml}$ except that of naphthalene, which was $\sim 5 \mu\text{g/ml}$. A benzene solution of a mixture of the hydrocarbons was also prepared that contained these same concentrations of the hydrocarbons. The other materials used either were reagent-grade chemicals or have been described earlier¹⁻³.

Procedures

Preparation of slurry. The slurry was prepared by adding 20.0 g of Aviamide-6 powder and 5.0 g of Fluoroglide 200 TWOz18 to 75 ml of *n*-propanol and mixing the components on an orbital sander for about 1 min. This amount of slurry was suitable for preparing two 8×8 in. chromatofilms.

Preparation of chromatofilms. The slurry was layered onto two 8×8 in. sheets of 0.0075-in.-thick Mylar film as follows. The sheets were placed on a plate-glass support. To establish layer thickness, a row of three microscope slides was placed flush with each of two parallel sides of each film sheet. The slurry was poured onto the films and was spread manually with a 1/4-in.-diam. glass rod. The layers were air-dried at room temperature until they were evenly opaque.

Preparation of chromatograms. Volumes of the benzene solutions of the hydrocarbons were spotted on the layers with 1- μl Lang-Levy type pipets. The chromatograms were developed at room temperature with *n*-propanol in a standard Desaga developing tank, saturated with *n*-propanol, to a distance of about 16 cm from the origin. They were removed from the chamber and were dried at ambient conditions.

TABLE I

RESPONSE OF CHROMATOGRAPHED HYDROCARBONS TO UV LIGHT^a

Hydrocarbon	Ambient temperature		77° K			
	Fluorescence		Fluorescence		Phosphorescence	
	254 nm	366 nm	254 nm	366 nm	254 nm ^b	366 nm
<i>o</i> -Hydroxy diphenyl	Brilliant violet	Violet	White	Pale violet	Pale yellow	Green white
Naphthalene	Dull purple	Dull purple	Purple (yellow ring)	Pale flesh	Deep yellow	Pale yellow
Fluorene	Orchid (yellow ring)	Dull orchid	White	Pale flesh	Blue	Pale yellow
Phenanthrene	Brilliant violet	Brilliant purple	Violet (yellow ring)	Violet	Bright yellow (Absorbs)	Brilliant yellow orange (Absorbs)
Pyrene	Brilliant white	Brilliant white	Brilliant white	Brilliant blue white		
Chrysene	Brilliant purple	Brilliant purple	Orchid	Orchid	Yellow	Yellow
Anthracene	Violet	Bright violet	Pale orchid	Pale orchid	(Absorbs)	(Absorbs)
Fluoranthene	Brilliant blue white	Brilliant blue white	Brilliant white	Brilliant white	Red orange	Orange
Benzo- <i>e</i> -pyrene	Brilliant orchid white	Brilliant orchid white	Violet	Pale purple	Orange	Orange
Benzo- <i>g,h,i</i> -perylene	Brilliant green white	Brilliant green white	Brilliant green white	Brilliant blue white	(Absorbs)	(Not detectable)

^a Under fluorescent room light, the chromatograms showed no spots, neither at ambient temperature nor at 77° K.

^b See Fig. 1.

Analysis and photography of chromatograms. The chromatograms were observed with fluorescent room light and with 254- and 366-nm UV light. The observations were made both at room temperature and under liquid nitrogen¹. To obtain an accurate record of the observation, the chromatograms were photographed under 254- and 366-nm UV light in air at room temperature and under liquid nitrogen¹. Both the fluorescence and phosphorescence were photographed. The techniques for observing the chromatograms under liquid nitrogen and for photographing them have been described earlier¹.

Results and discussion

Table I is a chart of the responses of the hydrocarbons to the various conditions under which the chromatograms were observed. Fig. 1 is a photograph of the phosphorescence of the compounds under liquid nitrogen after exposure to 254-nm UV light. Unfortunately, the total brilliance of the phosphorescence was not captured in the photograph.

The chromatographic properties of the layers were excellent. They adhered well to the Mylar film, spotted easily, and gave straight solvent fronts. It may be of interest to note that, in experiments separate from those described above, gradient layers of Aviamide-6-Fluoroglide 200 were evaluated, both in the horizontal and vertical orientations. Separations of the hydrocarbons were also effected on the gradient layers.

Observation of the low-temperature (77°K) luminescence of the hydrocarbons permits the detection of unresolved hydrocarbons in the presence of one another.

*Methodology Group, Analytical Chemistry Division,
Oak Ridge National Laboratory,
Oak Ridge, Tenn. 37830 (U.S.A.)*

HELEN P. RAAEN

1 L. J. CRIST AND H. P. RAAEN, *J. Chromatog.*, 39 (1969) 515.

2 H. P. RAAEN, *J. Chromatog.*, 44 (1969) 522.

3 H. P. RAAEN, *J. Chromatog.*, 53 (1970) 605.

Received June 29th, 1970

J. Chromatog., 53 (1970) 600-604

CHROM. 4904

Chromatography of metal ions on thin layers of polytetrafluoroethylene with di-(2-ethylhexyl)orthophosphoric acid*

The development of polytetrafluoroethylene layers for thin-layer chromatography (TLC) has already been described¹. The chromatography of some readily available radioisotopes of metal ions with the commonly used liquid cation exchanger di-(2-ethylhexyl)orthophosphoric acid (HDEHP) was selected to demonstrate the performance of the layers. The liquid ion exchanger HDEHP has been used extensively in the reversed-phase partition chromatography of inorganic substances². For reversed-phase TLC, it has been used with layers of silica gel³⁻⁵, polyvinyl chloride⁵, and Corvic (vinyl chloride-vinyl acetate co-polymer)⁶ to separate inorganic substances. On HDEHP-impregnated paper, some alkaloids and heterocyclic bases have been separated⁷. Also, HDEHP has been used as the mobile phase in the TLC of the rare-earth elements on layers of Silica Gel H (ref. 8). The chemistry and mechanism of extractions with HDEHP have been studied extensively⁹⁻¹⁶.

In this work, the radioisotopes of some 31 metal ions and of chloride ion were chromatographed on thin layers of 100 % polytetrafluoroethylene. The polytetrafluoroethylene was layered onto Mylar film from a slurry in methyl isobutyl ketone that contained nitric acid and a wetting agent. The chromatograms were developed with a methyl isobutyl ketone solution of HDEHP. The positions of the metal ions on the chromatograms were detected by autoradiography. The autoradiograms show the migration of numerous of the metal ions and indicate the suitability of the polytetrafluoroethylene layers for the separations.

Materials

The following materials were used: *Particulate polytetrafluoroethylene*, Fluoroglide 200 TWO218, from Chemplast, Inc., 150 Dey Road, Wayne, N.J. 07470. *Mylar polyester film*, 0.0075 in. thick \times 48 in. long, from Kensington Scientific Corp., P.O. Box 531, Berkeley, Calif. 94701. *Radioisotopes* were obtained from the ORNL Isotopes Division. The radioisotopes were in acid solution, usually nitric acid. When dilution of the original solution was required, nitric acid was used. *Di-(2-ethylhexyl)orthophosphoric acid (HDEHP)*, >99 % pure, was obtained from J. R. STOKELY, ORNL Analytical Chemistry Division, who obtained HDEHP from the Union Carbide Corporation and then purified it according to the procedure of SCHMITT AND BLAKE¹⁶. *Fluorochemical wetting agent FX-173*, from the Atlanta Branch, Industrial Chemical Division, 3M Company, 5925 Peachtree Industrial Blvd., Chamblee, Ga. *Methyl isobutyl ketone*, b.p. 114-116°, reagent grade, from Matheson, Coleman and Bell, Norwood, Ohio, was used without further purification. *Nitric acid*, C.P. reagent grade, from Allied Chemical, Morristown, N.J. *Special 1- μ l pipet*. For spotting the solutions of the radioisotopes onto the chromatofilm, special expendable micropipets were used. They were made as follows. A Drummond "Microcaps" type 1- μ l pipet was positioned with Silastic 731RTV adhesive/sealant (Dow Corning Corp., Midland, Mich.) in the end of a 4-in.-long \times 1/4-in.-O.D. glass tube. The other end of this tube was attached

* Research sponsored by the U.S. Atomic Energy Commission under contract with the Union Carbide Corporation.

to a short length of rubber tubing connected to the top half of a medicine dropper into which a 4- μ l micropipet was held by rubber tubing. This pipet control sufficiently restricted the expulsion pressure so that the contents of the 1- μ l pipet was deposited onto the chromatofilm without splattering of the radioisotope solution.

Procedures

Preparation of the polytetrafluoroethylene slurry

The slurry was prepared by dissolving 0.2 g of FX-173 in 72 ml of methyl isobutyl ketone, adding 0.8 ml of concentrated nitric acid, and then adding to the solution 24 g of Fluoroglide 200 TWO218. The mixture was shaken for about 30 sec on an orbital sander. This amount of slurry was sufficient to layer a 20 \times 20 cm area of Mylar film to microscope-slide thickness.

Preparation of chromatofilms

Eight strips of 1 \times 8 in. Mylar film (0.0075 in. thick) were placed side by side on a glass plate and were held to the plate by a thin film of acetone. The long sides of the outer strips were edged with microscope slides aligned end-to-end. The slurry was then poured onto the film strips and was spread manually by rolling a heavy glass rod back and forth along the microscope slides. The chromatofilms were dried for 1 h at the face of a laboratory hood, with the hood window lowered. When almost dry, they were marked with a stylus at the 3-cm (origin) and 13-cm (solvent-front) positions.

Preparation of chromatograms

Spotting. With an expendable micropipet, a 1- μ l portion of a radioisotope solution was spotted at the origin on each of the chromatostrips. The spot was allowed to dry in air until the area it covered became opaque.

Development. Each chromatofilm was developed in a sparge-gas bottle (chromatographic chamber) that contained 5 ml of 0.5 M HDEHP in methylisobutyl ketone. The bottle was covered with plastic film during the development. The chromatofilms were developed to a distance 10 cm from the origin; the duration of the development was about 1 h.

Drying. The chromatograms were removed from the chambers, dried in air at the face of the hood until they were opaque, and wrapped in clear 1/4-mil-thick Mylar film.

Preparation of autoradiograms

The chromatograms were autoradiographed by placing them face down in contact with Eastman Medical No-screen X-ray film. The assembly was then confined in a dark box¹⁷ for two to three days. After being thus exposed, the X-ray film was developed as specified by the manufacturer.

Results and discussion

The autoradiograms are shown in Figs. 1-4. They indicate the innumerable separations that are possible with the particular system and conditions chosen. Since the extractability of metal ions by HDEHP is known to be highly pH dependent, it is to be expected that a slight change in the acidity of the layer will cause a change in

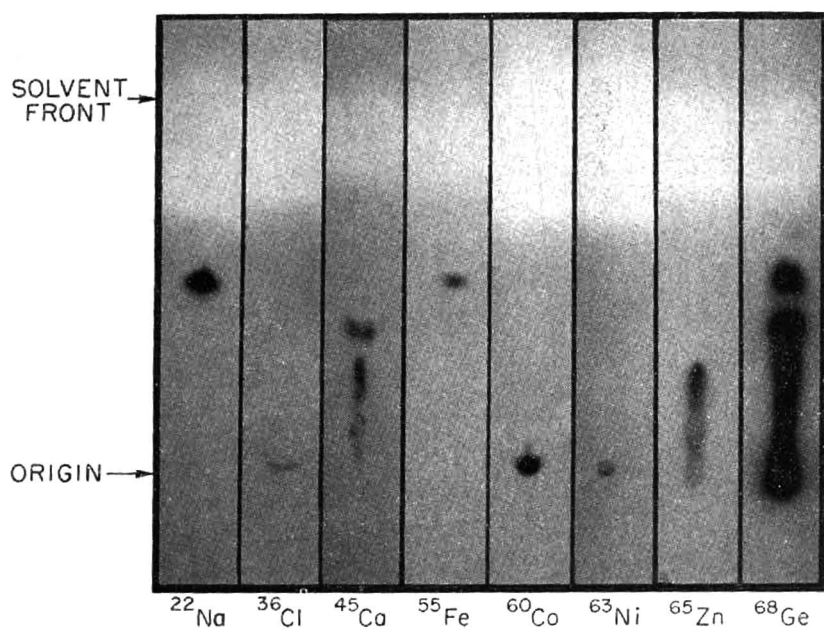


Fig. 1. Autoradiograms of chromatograms of ions of ^{22}Na , ^{36}Cl , ^{45}Ca , ^{55}Fe , ^{60}Co , ^{63}Ni , ^{65}Zn , and ^{68}Ge on Fluoroglide 200 TWO218 layers.

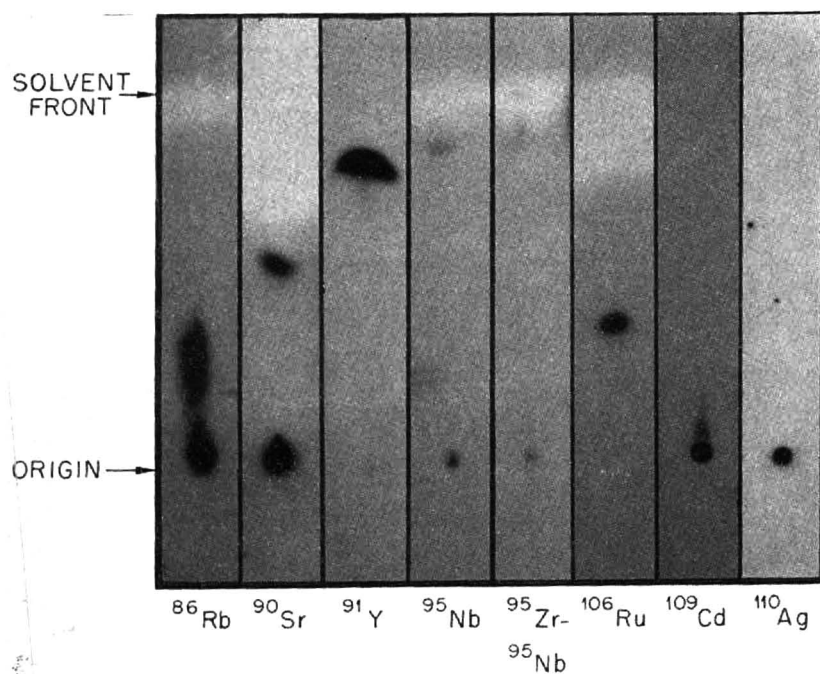


Fig. 2. Autoradiograms of chromatograms of ions of ^{86}Rb , ^{90}Sr , ^{91}Y , ^{95}Nb , ^{95}Zr - ^{95}Nb , ^{106}Ru , ^{109}Cd , and ^{110}Ag on Fluoroglide 200 TWO218 layers.

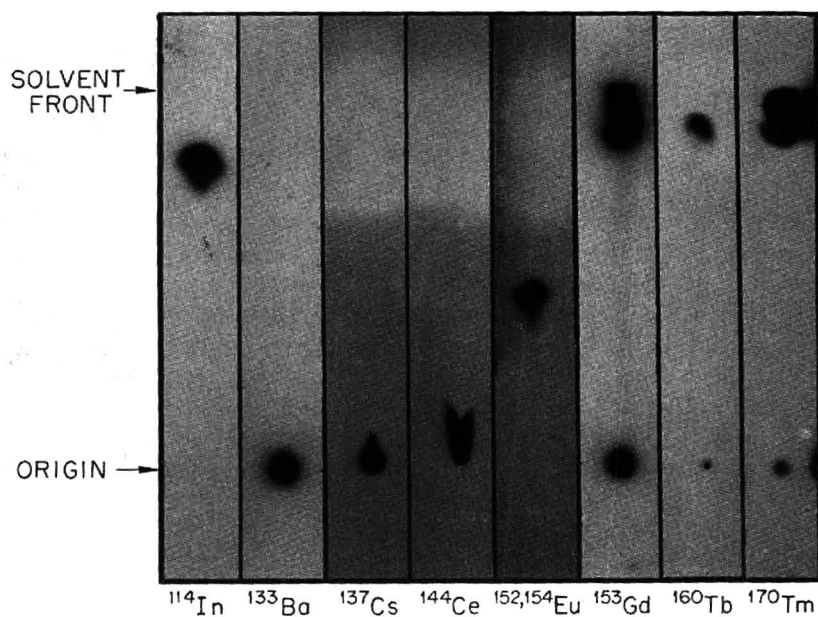


Fig. 3. Autoradiograms of chromatograms of ions of ^{114}In , ^{133}Ba , ^{137}Cs , ^{144}Ce , $^{152,154}\text{Eu}$, ^{153}Gd , ^{160}Tb , and ^{170}Tm on Fluoroglide 200 TWO218 layers.

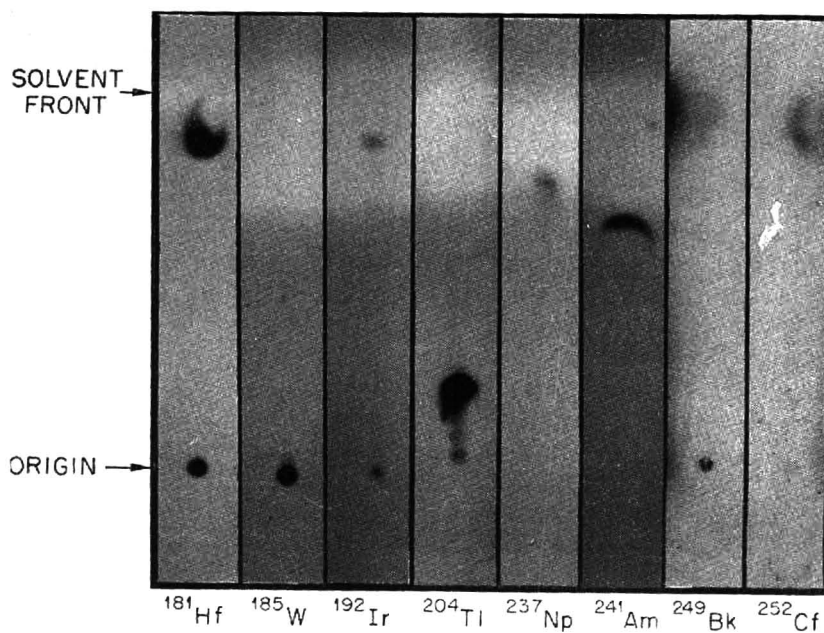


Fig. 4. Autoradiograms of chromatograms of ions of ^{181}Hf , ^{185}W , ^{192}Ir , ^{204}Tl , ^{237}Np , ^{241}Am , ^{249}Bk , and ^{252}Cf on Fluoroglide 200 TWO218 layers.

the positions of the ions. Also, if the HDEHP is located in the layer instead of in the developer, the order of migration of the resolved components can be reversed. This reversal was demonstrated experimentally with ^{55}Fe and ^{63}Ni . The polytetrafluoroethylene layers were thus shown to be suitable for either normal or reversed-phase TLC.

The results are in general agreement with those DANEELS *et al.*⁸ obtained on a silica gel layer, which they also developed with HDEHP in the mobile phase.

This work provides experimental evidence that layers of 100% polytetrafluoroethylene (no binder present) can be used for satisfactory TLC separations. Although the experiments were done with HDEHP as the liquid ion exchanger, the layers should be equally useful with numerous other ion exchangers, extractants, and chelating agents. When a fluorochemical wetting agent is included in the TLC system, reversed-phase TLC is possible. By means of the polytetrafluoroethylene layers, it should be possible to scale down those column chromatographic separations of both inorganic and organic compounds in which the support is polytetrafluoroethylene.

Methodology Group, Analytical Chemistry Division,
Oak Ridge National Laboratory,
Oak Ridge, Tenn. 37830 (U.S.A.)

HELEN P. RAAEN

- 1 H. P. RAAEN, *J. Chromatog.*, **44** (1969) 522.
- 2 H. ESCHRICH AND W. DRENT, *Bibliography on Applications of Reversed-Phase Partition Chromatography to Inorganic Chemistry and Analysis*, Eurochemic Technical Report No. 211, Nov. 1967.
- 3 H. HOLZAPFEL, LE VIET LAN AND G. WERNER, *J. Chromatog.*, **20** (1965) 580.
- 4 H. HOLZAPFEL, LE VIET LAN AND G. WERNER, *J. Chromatog.*, **24** (1966) 153.
- 5 T. B. PIERCE AND R. F. FLINT, *J. Chromatog.*, **24** (1966) 141.
- 6 T. B. PIERCE AND R. F. FLINT, *Anal. Chim. Acta*, **31** (1964) 595.
- 7 E. SOCZEWSKI AND M. ROJOWSKA, *J. Chromatog.*, **27** (1967) 206.
- 8 A. DANEELS, D. L. MASSART AND J. HOSTE, *J. Chromatog.*, **18** (1965) 144.
- 9 T. SATO, *J. Inorg. Nucl. Chem.*, **29**, No. 2 (1967) 555.
- 10 T. G. LENZ, *U. S. Atomic Energy Commission Report*, IS-T-138, Feb. 1967.
- 11 T. C. OWENS, *U. S. Atomic Energy Commission Report*, IS-T-188, Nov. 1967.
- 12 L. A. BRAY AND J. A. PARTRIDGE, *U. S. Atomic Energy Commission Report*, BNWL-SA-1447, Sept. 1968.
- 13 W. W. SCHULZ, *U. S. Atomic Energy Commission Report*, BNWL-759, July 1968.
- 14 J. W. RODDY, S. ARAI AND C. F. COLEMAN, paper presented at the 22nd International Congress of Pure and Applied Chemistry, Sydney, Australia, Aug. 20-27, 1969.
- 15 E. P. HORWITZ, C. A. A. BLOOMQUIST AND D. H. HENDERSON, *J. Inorg. Nucl. Chem.*, **31**, No. 4 (1969) 1149.
- 16 J. M. SCHMITT AND C. A. BLAKE, Jr., *U. S. Atomic Energy Commission Report*, ORNL-3548, Feb. 17, 1964.
- 17 H. P. RAAEN AND P. F. THOMASON, *Anal. Chem.*, **27** (1955) 936; esp. Fig. 1.

Received June 29th, 1970

J. Chromatog., **53** (1970) 605-609

Studies of thin-layer chromatography of inorganic salts

V. Resolution of the racemic trisethylenediaminecobalt(III) complex by means of thin-layer chromatography on silica gel

Since TSUCHIDA *et al.*¹ reported the partial resolution of racemic complexes using quartz powder, the technique of resolution by the use of asymmetric adsorbents has been widely adopted. KREBS AND RASCHE² have shown several examples of the resolution of racemic complexes using a starch column. FUJISAWA³ and others⁴ resolved racemic tyrosine-3-sulphonic acid by paper chromatography without using an optically active solvent. YOSHINO *et al.*⁵ resolved racemic complexes using common ion-exchange resins saturated with optically active substances. These methods are all based on the tendency of the optically active adsorbent to adsorb one enantiomer in preference to the other.

Recently YONEDA AND MIURA⁶ have succeeded in resolving the racemic $[\text{Co}(\text{en}_3)]^{3+}$ complex by means of electrophoresis. This method was based on the different degrees of ion-pair formation of the *d*- $[\text{Co}(\text{en}_3)]$ -*d*-tartrate and *l*- $[\text{Co}(\text{en}_3)]$ -*d*-tartrate systems in a solution containing aluminium ions. Against this, in studies on the thin-layer chromatography of inorganic salts⁷, it was found that the complex cation can be adsorbed on the negatively charged surface of silica gel and is eluted through ion-pair formation. Thus, the resolution obtained by electrophoresis suggests that resolution by means of thin-layer chromatography might be possible. The successful result obtained is described here.

Experimental

Material. Samples tested were *dl*- $[\text{Co}(\text{en}_3)]\text{Cl}_3 \cdot 3\text{H}_2\text{O}$, *d*- $[\text{Co}(\text{en}_3)]\text{Cl}(\textit{d}\text{-tartrate}) \cdot 5\text{H}_2\text{O}$ and *l*- $[\text{Co}(\text{en}_3)]\text{Cl}(\textit{l}\text{-tartrate}) \cdot 5\text{H}_2\text{O}$. These salts were dissolved in water to 1/50 *M*, and 2.5 μl of the solution was applied to the thin-layer.

Chromatography. As an adsorbent, Merck's Silica Gel H prepared for thin-layer chromatography was used without further purification. This was spread on glass plates of 20 cm length at a thickness of 0.25 mm.

Aqueous solutions containing sodium *d*-tartrate and aluminium chloride in various concentrations were used as a developer. Development was carried out at room temperature (20–22°). Sodium sulphide solution was sprayed for visualisation of the developed spot.

Results and discussion

When only sodium *d*-tartrate was used as the developer, the racemic form of the complex always appeared in one spot, irrespective of the concentration of the developer. This means that the resolution was not successful. However, when aluminium chloride was dissolved at a suitable concentration in the sodium *d*-tartrate solution, the racemic form was completely separated into two spots, as can be seen in Fig. 1C and D. This should be taken as a resolution, because the sample of the *d*-form alone showed a spot in the same position as the upper spot of the racemic form, and the *l*-form alone showed a spot corresponding to the lower spot of the racemic form.

In order to find required concentration of aluminium chloride for resolution, five developers each containing 0.3 *M* sodium *d*-tartrate and various concentrations of aluminium chloride were used. The composition of the developers is listed as follows;

- | | |
|-------------------------------------|--|
| (A) 0.05 <i>M</i> AlCl ₃ | } plus 0.3 <i>M</i> Na <i>d</i> -tartrate. |
| (B) 0.10 <i>M</i> AlCl ₃ | |
| (C) 0.15 <i>M</i> AlCl ₃ | |
| (D) 0.20 <i>M</i> AlCl ₃ | |
| (E) 0.30 <i>M</i> AlCl ₃ | |

The chromatograms using the above-listed developers are shown in Fig. 1. In this figure, the letters *r*, *d* and *l* represent the racemic and the *d*- and *l*-forms of the [Co(en)₃]³⁺ complex, respectively. From these chromatograms, it is easily seen that complete resolution was achieved in the case when 0.15 *M* or 0.20 *M* AlCl₃ and 0.30 *M* sodium *d*-tartrate was used as a developer. Resolution proved to be unsuccessful when the concentration of AlCl₃ is below 0.10 *M* and above 0.30 *M*.

In order to see the effect of the pH of the developer, various kinds of developers prepared by adding small amounts of sodium hydroxide solution to developer D were used. The result is shown in Table I. It is noteworthy that resolution was not achieved with a developer whose pH is above 4.

Lastly, we should like to refer to the role of the aluminium salt in the resolution. Suppose the complex is developed with an aqueous solution which contains only sodium *d*-tartrate. A small amount of the *d*- and *l*-forms of the complex cation is eluted by the *d*-tartrate anion through ion-pair formation. In the case where the developer is a dilute solution of sodium *d*-tartrate, the complex cation and the *d*-tartrate anion are both supposed to be highly hydrated. Therefore, the *d*-tartrate anion is

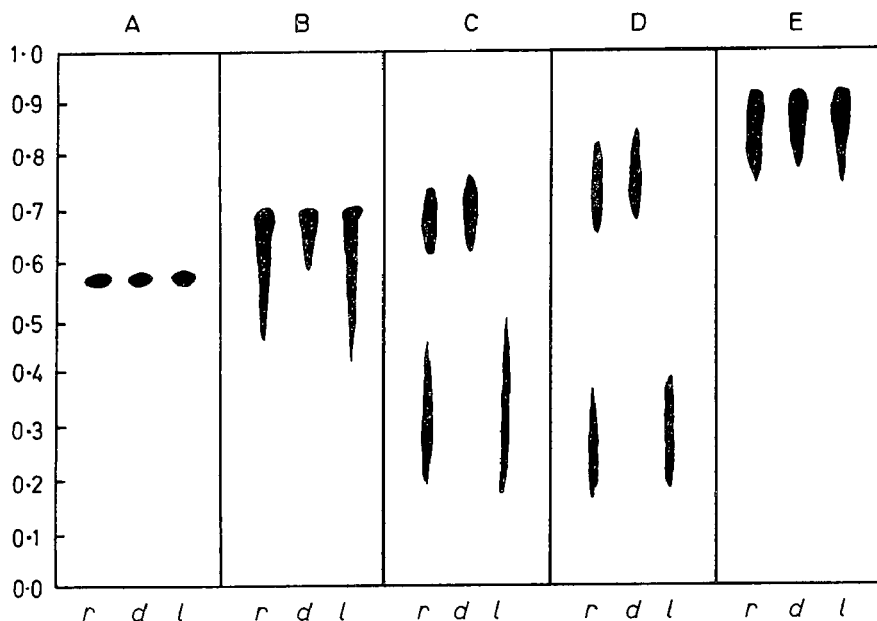


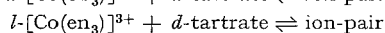
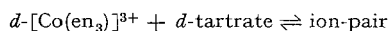
Fig. 1. Chromatograms of the *d*, *l* and racemic forms of [Co(en)₃]³⁺ developed with the mixed solutions of Na *d*-tartrate and AlCl₃.

TABLE I

EFFECT OF THE pH OF THE DEVELOPER UPON THE R_F VALUES

Sample	pH					
	2.5	3.0	4.0	5.0	6.0	7.0
Racemate	$\left\{ \begin{array}{l} 0.67 \\ 0.23 \end{array} \right.$	$\left\{ \begin{array}{l} 0.58 \\ 0.35 \end{array} \right.$	0.53	0.55	0.61	0.63
<i>d</i> -form	0.70	0.60	0.53	0.56	0.58	0.60
<i>l</i> -form	0.20	0.35	0.56	0.59	0.58	0.60

only affected by the electrostatic attraction of the tervalent complex cation and cannot detect the enantiomeric difference between the *d*- and *l*-forms of the complex cation. For the *d*-tartrate anion to be able to distinguish between the *d*- and *l*-forms of the complex, it is necessary to reduce the degree of hydration of each ion in solution. The use of a concentrated solution of sodium *d*-tartrate seems to satisfy this requirement. However, in such a case, although the number of hydrating water molecules per ion is actually decreased by the increase of the tartrate concentration, the existence of a large number of tartrate anions shifts the equilibria



nearly completely towards ion-pair formation. Therefore, both the *d*- and *l*-forms show large R_F values indistinguishable from each other. Thus, resolution by chromatography is not achieved in this case either.

Therefore, we have to reduce the degree of hydration of each ion without increasing the tartrate concentration. The addition of aluminium salt to the developer will do this, because the large hydration energy of the tervalent aluminium ion will cause dehydration of the complex cation. In this way, the *d*-tartrate anion can distinguish between the *d*- and *l*-forms of the complex cation in the poorly hydrated state.

Department of Chemistry,
Wakayama University, Masagocho,
Wakayama (Japan)

HAYAMI YONEDA*
TETSUO BABA**

- 1 R. TSUCHIDA, M. KOBAYASHI AND A. NAKAMURA, *Nippon Kagaku Zasshi*, 56 (1935) 1339; *Bull. Chem. Soc. Japan*, 11 (1936) 38.
- 2 H. KREBS AND R. RASCHE, *Z. Anorg. Allgem. Chem.*, 276 (1954) 236.
- 3 Y. FUJISAWA, *Osaka Shiritu Daigaku Igaku Zasshi*, 1 (1951) 7.
- 4 M. KOTAKE, T. SAKAN, N. NAKAMURA AND S. SENOH, *J. Am. Chem. Soc.*, 73 (1951) 2973.
- 5 Y. YOSHINO, H. SUGIYAMA, S. NOGAITO AND H. KINOSHITA, *Sci. Papers Coll. Gen. Educ. (Univ. Tokyo)*, 16 (1966) 57.
- 6 H. YONEDA AND T. MIURA, *Bull. Chem. Soc. Japan*, 43 (1970) 574.
- 7 T. BABA, H. YONEDA AND M. MUTO, *Bull. Soc. Chem. Japan*, 41 (1968) 1965.

Received July 8th, 1970

* Correspondence should be addressed to Chemistry Department A, The Technical University of Denmark, Lyngby, Denmark, where H. Y. will be staying until the end of May, 1971.

** On leave from the Minoshima High School, Arita-shi, Wakayama.

CHROM. 5025

Zirconium tellurate, an inorganic ion exchanger

In contrast to organic ion-exchange resins, inorganic ion-exchangers are highly stable under high temperatures and high doses of radiation. As a result, inorganic ion-exchangers have the potentiality of being used in the recovery of highly radioactive fission products. During the last decade different inorganic compounds, specially the zirconium salts, have been investigated as ion-exchange materials^{1,2}. Very little information is available regarding the ion-exchange properties of zirconium tellurate³. The composition and some ion-exchange properties of this compound are reported in this paper.

Experimental

Preparation. The sample was prepared by refluxing solutions of zirconyl chloride and sodium tellurate in 1.0 *M* hydrochloric acid. 400 ml of a 0.45 *M* sodium tellurate solution were placed in a refluxing assembly and refluxed for about 1 h before 330 ml of a 0.2 *M* zirconyl chloride solution were added dropwise at the rate of about 5 ml/min. There was instant precipitation as the two solutions were mixed. The system was refluxed for 40 h. The precipitate was separated by centrifugation and was washed with distilled water and dried at 50–60° until it broke into coarse particles. These particles were converted to the H⁺ form by treating with a 1.0 *N* hydrochloric acid solution until there was no Na⁺ in the effluent. The granules were again dried at 50–60° and sieved to different mesh sizes. The particles of mesh size 72–120 BSS were used in all the experiments unless otherwise mentioned.

Analysis. Analysis with respect to the ratio of Te/Zr was made in an indirect way by using known amounts of zirconium and tellurium while precipitating and then estimating the excess tellurium. Tellurium was determined by a gravimetric method⁴ involving reduction of the tellurate ion to the tellurium element. To study the thermogravimetric behaviour of the sample, thermograms were obtained using a Stanton Thermobalance.

Exchange capacity and pH titration. The total exchange capacity of the sample was determined by batch method in strongly alkaline solution. 1.0 g of the solid was first equilibrated with 25 ml of distilled water to which 25 ml of strong NaOH or KOH solution were added and equilibrated. The strength of NaOH in contact with the solid was 1.3 *N* and that of KOH was 0.63 *N*. The amount of H⁺ released was determined by estimating the amount of alkali neutralized. During this experiment and the pH titration described below, due precaution was taken to keep the system free from atmospheric carbon dioxide.

To study the mode of dissociation of the exchangeable H⁺ 1.0 g of the solid was equilibrated by shaking at room temperature (28°) with 50 ml of a 2.0 *M* NaCl solution and the equilibrium pH was recorded. After that a known amount of standard NaOH solution was added with time and the constant pH was recorded after each addition. The pH reading was taken to be constant when the variation was <0.01 pH scale per 30 min. It took several minutes to several hours to get equilibrium readings. A similar operation was repeated with KCl and KOH and also with LiCl and NaOH. This experiment was carried out with a Beckmann Electroscan TM30P. The electrode

system was earlier calibrated using standard buffer solutions, and the pH reading was corrected according to the calibration curve.

Results and discussion

Supernatant liquid of the ZrTe precipitate gave a negative test for zirconium but a positive test for tellurium. This indicates that during precipitation tellurium was in excess. According to the analysis the molar ratio of Te/Zr in the reported sample was found to be 1.13. Fig. 1 shows the thermogram of the zirconium tellurate in particle as well as powdered form. If the composition corresponding to the constant weight at the temperature 700–900° is assumed to be $\text{ZrO}_2 \cdot \text{TeO}_3$, then the calculated composition of the product reported in this paper becomes $\text{ZrO}_2 \cdot \text{TeO}_3 \cdot 5\text{H}_2\text{O}$ which is identical to the composition $\text{ZrOTeO}_4 \cdot 7\text{H}_2\text{O}$ reported by MONTIGNIE⁵. The excess two molecules of water in the latter case could be due to absorbed moisture.

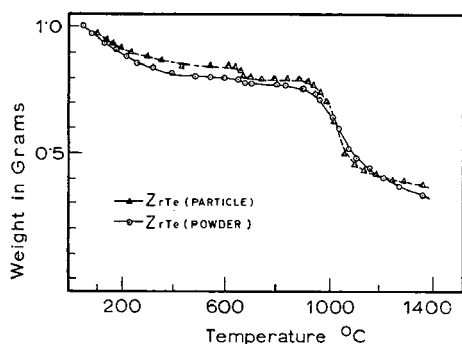


Fig. 1. Thermograms for ZrTe samples.

While the work reported in this paper was carried out ZSINKA *et al.*³ presented a report on zirconium tellurate inorganic ion exchanger and proposed its formula to be $\text{ZrO}(\text{HTeO}_4) \cdot n\text{H}_2\text{O}$ and concluded an analogy between phosphates and tellurates of zirconium. However, it is to be noted that the above formula cannot explain the electroneutrality of the compound if, as proposed by the authors, the univalent (HTeO_4^-) be functional group because the cationic ZrO group is supposed to be a divalent one and because it is not clear whether $n\text{H}_2\text{O}$ in any form has chemical bonding with the $\text{ZrO}(\text{HTeO}_4)$ matrix. They have considered the compound as a salt of *o*-telluric acid whose formula they have taken as $\text{H}_2\text{TeO}_4 \cdot 2\text{H}_2\text{O}$ but this is discarded by others⁶. The latest formula of the *o*-telluric acid is H_6TeO_6 and it forms monoclinic salts like KH_5TeO_6 and $\text{Li}_2\text{H}_4\text{TeO}_6$ and a few salts, Ag_6TeO_6 being one of them, in which more than two protons of the acid are replaced⁷.

Until recently all the zirconium phosphates would be generally represented as zirconyl phosphates¹. Recently using soluble zirconyl salt and phosphoric acid CLEARFIELD AND STYNE⁸ prepared gelatinous zirconium phosphate which on refluxing with an excess of phosphoric acid yielded crystalline zirconium phosphate and by X-ray and thermogravimetric analysis established the formula $\text{Zr}(\text{HPO}_4)_2 \cdot 2\text{H}_2\text{O}$.

Considering the above facts it is likely that the molecular formula of the compound reported in this paper is $\text{Zr}(\text{H}_2\text{TeO}_6) \cdot 4\text{H}_2\text{O}$. Based on this formula all the experimental results can be best explained. The formula is in agreement with observed

Te/Zr ratio of about 1. Approximately 18% weight loss at 100–500° indicates the splitting out of the equivalent of four moles of water. About 4.5% weight loss at 650–700° is likely the loss of one mole of water of constitution because of the condensation of $\text{Zr}(\text{H}_2\text{TeO}_6)$ to $\text{Zr}(\text{TeO}_5) \cdot \text{H}_2\text{O}$. The continuous weight loss starting at about 900° may be due to the decomposition of ZrTeO_5 into ZrO_2 and TeO_3 followed by evaporation of TeO_3 . The difference observed between the particle and the powder forms of the sample is likely due to excess adsorption of moisture by the powder.

According to the composition of the compound proposed above the total capacity should be 2 moles per mole and there should be two plateaus in the pH titration curves.

TABLE I

EXCHANGE CAPACITY AT ROOM TEMP. (28°)

Ions	Total capacity (mequiv/g)	Approx. capacity up to pH 12 ^a (mequiv/g)
Li^+	—	2.8
Na^+	4.7	2.8
K^+	4.4	2.6

^a Calculated from the titration curves.

The observed total capacities as shown in Table I are 4.4 and 4.7 mequiv./g which on calculation according to the proposed formula result in the capacities 1.8 and 1.9 mole/mole for K^+ and Na^+ , respectively. These values are quite in agreement with theoretical values. The pH titration curves shown in Fig. 2 have no sharp plateaux. Some difference in the titration curves may be due to different metal ions. The approximate capacities up to pH 12, as calculated from the titration curves, are 1.0 to 1.1 mole/mole for Li^+ , Na^+ and K^+ . These values are in agreement with those reported by ZSINKA *et al.*³. Thus it appears that in the pH range from 2.5 to 12 only about 50% of the H^+ are exchanged while the rest of the H^+ exchange only in strongly

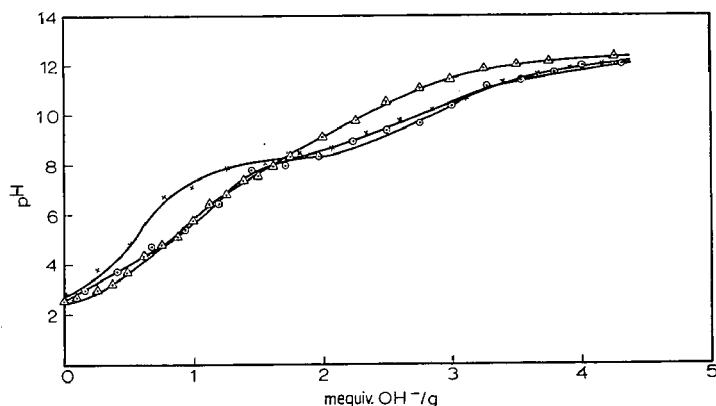


Fig. 2. Titration curves of Zr-tellurate with different salts and alkalis. ○, $\text{NaCl} + \text{NaOH}$; ×, $\text{LiCl} + \text{NaOH}$; △, $\text{KCl} + \text{KOH}$.

alkaline medium. Further investigations for evaluating the distribution of different ions, specially of those which constitute the fission products, are receiving attention.

One of us (M. K. RAHMAN) wishes to thank Dr. J. A. W. DALZIEL and Dr. J. BARRETT of the Chelsea College of Science and Technology, London, for making necessary arrangement for thermogravimetric analysis.

*Chemistry Division, Atomic Energy Centre, P.O. Box 164,
Ramna, Dacca (East Pakistan)*

M. K. RAHMAN
A. M. S. HUQ

- 1 C. B. AMPHLETT, *Inorganic Ion-Exchangers*, Elsevier, Amsterdam, 1964.
- 2 S. C. CHURMS, *The South African Industrial Chemist*, (a) Page 26, Feb. (1965), (b) Page 48, March (1965), (c) Page 68, April (1965), (d) Page 87, Sept. (1965), (e) Page 148, Nov. (1965).
- 3 L. ZSINKA AND L. ZSIRTES, *Proceedings Second Hungarian Conf. on Ion-Exchange, Balatonszeplak, Sept. 10-14, 1969*, Vol. II, 1969, p 627.
- 4 L. HILLEBRAND, G. F. F. LONDELL, H. A. BRIGHT AND J. HOFFMAN. *Applied Inorganic Analysis*, 2nd Ed., J. Wiley, 1953, p. 377.
- 5 E. MONTIGNIE, *Bull. Soc. Chim.*, 6 (1939) 672; *ibid.*, 13 (1946) 176.
- 6 K. W. BAGNALL, *The Chemistry of Selenium, Tellurium and Polonium*, Elsevier, Amsterdam, 1966, p. 67-69.
- 7 S. RAMAN, *Inorg. Chem.*, 3 (1964) 639.
- 8 A. CLEARFIELD AND J. A. STYNES, *J. Inorg. Nucl. Chem.*, 26 (1964) 117.

First received April 8th, 1970; revised manuscript received September 2nd, 1970.

J. Chromatog., 53 (1970) 613-616

CHROM. 5024

The use of Teflon film in quantitative analysis by enclosed-strip paper electrophoresis

The separation and determination of the valence states of iron

The enclosed-strip method of paper electrophoresis has been used widely as a qualitative tool for the identification of unknown compounds, for the separation of mixtures and for the study of complexes, but it seems rarely to have been applied to quantitative work, probably for the following reason. The insulating films most commonly used for enclosure of the paper strips consist of polyethylene or Mylar [poly(ethylene terephthalate)] and when wet papers are removed from the apparatus after electrophoresis, traces of the impregnating electrolytes often adhere as droplets to the films, making quantitative recovery of the experimental compounds difficult. It is now shown that the method is readily adaptable to quantitative analysis if a film of Teflon (polytetrafluoroethylene) is used as the insulating envelope. The hydrophobic nature of Teflon allows the paper strips to retain aqueous electrolytes completely when they are parted from the film after electrophoresis. Mixtures of iron(II)

J. Chromatog., 53 (1970) 616-619

and iron(III) were used to test the innovation and data are presented which show that, under the conditions to be described, the ionic species were recovered quantitatively from paper strips on which they were separated.

Experimental

Electrolyte. Sodium chloride solution (0.05 *M*).

Reagents. All reagents were of analytical grade or comparable purity. Aqueous solutions of 1,10-phenanthroline (0.25 % w/v), hydroquinone (1 %) and sodium citrate (25 %) were used for the colorimetric determination of iron¹. Two test solutions were prepared in 0.1 *N* sulphuric acid, (A) containing ferrous ammonium sulphate (3.27×10^{-2} *M*) and ferric ammonium sulphate (2.34×10^{-3} *M*), and (B) containing the same salts in 4.1×10^{-3} *M* and 1.71×10^{-2} *M* concentrations, respectively.

Apparatus. Paper electrophoresis was conducted in the enclosed-strip apparatus described previously² except that a film (5×10^{-3} in. thick) of Teflon (from Ludowici and Son Ltd., Lane Cove, N.S.W.) replaced polyethylene film as the insulating envelope. Whatman No. 4 paper was used in strips 13.5×61 cm with 45 cm under pressure and cooled. Mains water at 24° was circulated through the coils of the cooling plate.

A Unicam SP600 spectrophotometer was used for measurements of absorbance.

Procedure. The paper strip was wetted with electrolyte and blotted between sheets of blotting paper ("Devon Valley 431 Mill", from Australian Paper Manufacturers Ltd.). A rubber roller was pressed firmly on the blotter during rolling to remove excess electrolyte from the paper strip which was then placed on the opened Teflon envelope covering the cooling plate of the apparatus. The test solution (100 μ l) was applied immediately as a streak 10 cm long across the middle of the paper using a micropipette. 1 or 2 min was allowed for the complete absorption of the solution into the paper before covering it with a piece of Teflon film (14×45 cm). The envelope was closed, pressure applied to the assembly, and electrophoresis allowed to proceed at 22 V/cm for 15 min when less than 100 μ g of iron(III) had been applied to the paper. Up to 25 min was allowed for increasing quantities of iron(III) to a limit of 200 μ g.

The envelope was then opened and the Teflon cover peeled from the paper slowly enough to allow the paper to absorb the electrolyte completely from the surface of the film as it was removed. The paper itself was similarly withdrawn from the envelope surface upon which it rested. It was dried in an air-oven at 100° for 8 min and the separated iron(II) and iron(III) located as dark blue bands under a Hanovia "Chromatolite" UV lamp. Pieces (13.5×3 cm) containing the bands were cut from the pherogram and "paper blanks" of equal size were cut from the anode side of the starting-line. Each of the paper pieces was shredded into 4 mm strips and dropped into a 25 ml volumetric flask. (As a precaution against accidental contamination of papers with iron, new scissors and nickel-plated forceps were used to cut and transfer the paper strips³.) Hydrochloric acid (10 ml, 0.1 *N*) was then added with gentle shaking to extract the iron. Hydroquinone solution (1 ml), 2 ml phenanthroline reagent and 0.75 ml sodium citrate buffer were added and the mixtures shaken occasionally during the following hour¹. The mixtures were diluted to the mark with distilled water and a further addition of 0.25 ml water was made to compensate for the volume displaced by the paper in the flask. They were centrifuged at 2000 r.p.m. in covered tubes and

the optical densities of the clear supernatants measured in the spectrophotometer at 508 $m\mu$ against paper blanks prepared similarly. The transmittance of the paper blanks measured against reagent blanks was about 97 % (equivalent to 2 $\mu\text{g Fe}$). Determinations of the iron extracted from the papers were made by reference to a calibration curve prepared previously using standard solutions of ferrous ammonium sulphate.

Results and discussion

Electrophoresis of iron mixtures on papers impregnated with the sodium chloride electrolyte causes iron(II) to migrate freely as a compact cationic zone, possibly in the form of the complex ion, FeOH^+ , resulting from hydrolysis of the Fe(II) (ref. 4). This separates cleanly from the iron(III) which remains fixed on the cellulose fibres at the point of application, probably as the insoluble, microcrystalline species, $\beta\text{-FeOOH}$, known to form and precipitate from solutions containing iron(III) and sodium chloride⁵. Table I, containing typical results for test solutions (A) and (B),

TABLE I
QUANTITATIVE SEPARATION OF Fe^{2+} AND Fe^{3+}

Test solution (100 μl)	Amt. applied (μg)		Amt. found (μg)		Error (%)	
	Fe^{2+}	Fe^{3+}	Fe^{2+}	Fe^{3+}	Fe^{2+}	Fe^{3+}
A	183	26	185	27	+1.1	+3.9
A	183	26	182	26	-0.5	0
B	23	191	22	194	-4.3	+1.6
B	23	191	24	196	+4.3	+2.6

illustrates the quantitative nature of the separations of the valence states and of the recoveries of iron from papers after compression between the surfaces of the Teflon envelope. Mixtures of iron(II) and iron(III) were selected to demonstrate the usefulness of Teflon film for quantitative applications because of the ease and accuracy with which iron can be determined. It appears, however, that the modification is of general application for quantitative work because it has also been applied, with success, to the separation and quantitative recovery of organic compounds⁶. Valuable features of the enclosed-strip method of paper electrophoresis thus retained for quantitative studies include the reproducibility with which the experiments may be conducted, and this stems from the ease with which effective control may be exercised over the experimental conditions. Positive control of the temperature of the working area of the paper strip is achieved by pressing the insulating envelope containing it firmly against the metal cooling plate⁷. Adequate cooling of the enclosed strip ensures, in turn, that water and other volatile components are not lost from the impregnating electrolyte which is then maintained at constant pH and concentration throughout the experiment. Enclosure of the paper strip in this way also ensures that the electrophoresis is conducted in the absence of air and the method therefore lends itself to investigations of compounds sensitive to oxygen and carbon dioxide⁷. The quantitative accuracy of the above results is probably due, in part, to the fact that iron(II) was protected from atmospheric oxygen during the separations.

When iron (III) is present in low concentrations in the applied test solutions it precipitates rapidly on the neutral papers as described above, but in higher concentrations, it begins to move cationically during the initial stages of electrophoresis. The acidity of the test solutions is probably partly responsible for this mobility⁸, and it is not until the hydrogen ions migrate out of the band that the residual, slower-moving iron (III) is converted completely to the insoluble species. The effect is to broaden the bands of iron (III) and when quantities in excess of 150 μg are applied, it is often necessary to take larger areas of the pherograms for the determinations. The comparatively narrow, cationic bands of iron (II) are found approximately 4 cm from the starting line after electrophoresis for 15 min.

Regarding the preparation of the bands for spectrophotometry, the presence of Whatman No. 4 paper in solutions containing the colorimetric reagents does not interfere with the formation of the iron-phenanthroline complex, and the complex does not suffer preferential adsorption by the paper.

LINGREN *et al.*³ recently reported a quantitative study of separations of mixtures of iron (II) and iron (III) by simultaneous paper chromatography and electrophoresis conducted in dilute sulphuric acid as the electrolyte. Under these conditions, iron (III) was mobile on the paper support. The results indicate that, as a method for the separation and estimation of the valencies of iron, the present one is the more rapid and accurate of the two, and this may be owing to the conversion of iron (III), under the present conditions, to an insoluble species which remains fixed at or near the origin allowing more rapid and complete separation of the cationically mobile iron (II).

*Division of Nutritional Biochemistry, CSIRO, Kintore Avenue,
Adelaide, South Australia 5000 (Australia)*

J. L. FRAHN

- 1 E. B. SANDELL, *Colorimetric Determination of Traces of Metals*, 3rd ed., Interscience, New York, 1959, p. 541.
- 2 J. L. FRAHN AND J. A. MILLS, *Australian J. Chem.*, 17 (1964) 256.
- 3 W. E. LINGREN, G. R. REECK AND R. J. MARSON, *Anal. Chem.*, 40 (1968) 1585.
- 4 T. MOROZUMI AND F. A. POSEY, *Denki Kagaku*, 35 (1967) 633; *C.A.*, 68 (1968) 83727v.
- 5 R. SÖDERQUIST AND S. JANSSON, *Acta Chem. Scand.*, 20 (1966) 1417.
- 6 M. F. HOPGOOD, unpublished work.
- 7 J. L. FRAHN AND J. A. MILLS, *Anal. Biochem.*, 23 (1968) 546.
- 8 D. GROSS, *J. Chromatog.*, 10 (1963) 221.

First received August 18th, 1970; revised manuscript received September 4th, 1970

J. Chromatog., 53 (1970) 616-619

CHROM. 4962

Letter to the Editor

Dear Sir,

I should like to comment on a paper by R. A. DE ZEEUW *et al.* (*J. Chromatog.*, 47 (1970) 382) entitled *Improved separation in thin-layer chromatography using a single-component solvent in an unsaturated chamber.*

Therein several statements are made:

(1) "For the system under investigation, using a single-component solvent, unsaturated chambers generally yielded better separation [expressed as $(R_F)_{\max} - (R_F)_{\min}$] than did saturated chambers."

(2) "Although a possible explanation for the occurrence of improved separations when using multi-component solvents in unsaturated chambers has been given¹, an explanation is not yet available for single-component solvents."

(3) "In unsaturated chambers, solvent evaporation during the run will take place to a higher extent than in saturated chambers, which require an extra solvent supply from the solvent reservoir."

(4) "As a consequence of this solvent supplementation more solvent will be transported across the lower parts of the plate than across the higher parts, which, in turn, would be expected to result in a higher migration of the lower spots. Hence this "pushing up" would have an adverse effect on the separation and on the speed of the spots. However, the findings described here indicate that other factors must also be involved, ..."

(5) "In general it appeared that unsaturated chambers yielded lower a values (constant of the Galanos-Kopoulas equation) than did saturated chambers."

ad (1)

For judging "separation" of two compounds one should better refer to their resolution, $R_s = \Delta R_F / [2(\sigma_1 + \sigma_2)]$, taking into account also the band width, than only to ΔR_F .

To judge the improvement of separation in unsaturated chambers with respect to saturated ones, rather *distant spots with relatively elevated R_F values* must not be considered: Going from saturated to unsaturated their ΔR_F values may remain constant or decrease, as shown by examples III and IV in Fig. 1. When considering only the upper two spots in DE ZEEUW's table (with high R_F values), the ΔR_F values are less in favour of the unsaturated N-chamber (Table I). Also from a practical aspect *only the separation of neighbouring spots is of interest* (the separation of wide polarity range mixture, requiring gradients, is disregarded here).

The ΔR_F values of *closely adjacent pairs of spots* (e.g. II in Fig. 1) in almost all cases must increase when passing from a saturated to an unsaturated N-chamber, or to continuous TLC (see *ad*. 4).

Since much improved separation can be duplicated as well by continuous TLC (this is not exactly true for multi-component solvents), one should prefer the latter technique, which is easier to control.

TABLE I

ΔR_F saturated chamber	ΔR_F unsaturated chamber	ΔR_F saturated chamber	ΔR_F unsaturated chamber
0.12	0.17	0.17	0.15
0.14	0.16	0.16	0.18
0.11	0.13	0.12	0.24
0.11	0.10	0.13	0.15
0.11	0.02	0.16	0.13
0.13	0.24	0.18	0.14
0.10	0.15	0.09	0.26
0.08	0.21	0.09	0.12
0.15	0.16	0.11	0.08
		0.16	

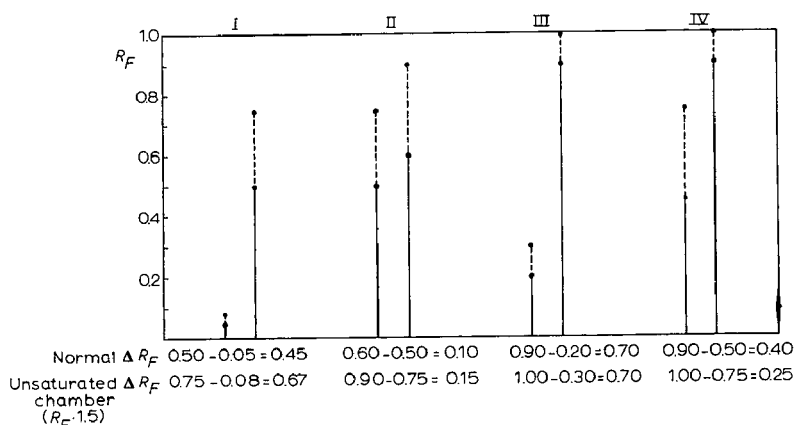


Fig. 1. ΔR_F of two spots in saturated N-chamber (solid line) and unsaturated N-chamber (or continuous TLC) (solid line + dotted line), assuming that the integral solvent flow in the latter one is 50 % higher. Schematic. For high R_F values ΔR_F may decrease in unsaturated chamber.

ad (2)

Both for single-component and multi-component solvents, improved separations in unsaturated N-chambers are essentially based upon the same effect: increased total amount of solvent transported through the layer, as shown in the literature^{2,3}. The mechanism postulated by DE ZEEUW for multi-component solvents¹ (gradient of decreasing activity in the sense of migration) has become untenable^{2,4-6}.

ad (3)

Solvent evaporation during the run only takes place in large-volume unsaturated chambers, so-called (unsaturated) N-chambers, but not in (small-volume) S-chambers that are (ideally) unsaturated as well. Thus, "unsaturated chamber" in this case must be specified further. Nevertheless R_F values (and hence ΔR_F) in S-chambers are (for single-component solvents) slightly higher than in saturated ones, all other conditions being constant. This is not due to solvent evaporation from the S-chamber (there is almost no evaporation because of the tiny volume) but to the absence of vapour pre-adsorption by the dry layer.

ad (4)

Even in unsaturated N-chambers, the saturation of the lower and medium zones of the trough starting from the bottom is almost accomplished within 15 min². Thus the solvent will evaporate only from the zones of the layer close to the front from a height at which the chamber is still rather unsaturated. Hence the entire solvent supplementation for loss by evaporation is transported up to the front integrally through all zones of the layer (except the parts close to the front). Therefore the same effect is achieved as in continuous ("flow-through") TLC (Fig. 2): Increased solvent transport (to the front) increases *proportionally* the migrating distances of all spots.

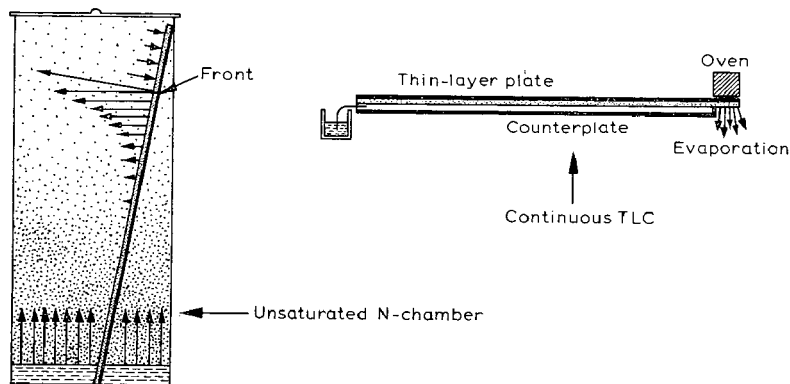


Fig. 2. Similarities of "unsaturated N-chamber" and continuous TLC. In each system integral solvent flow is increased by solvent evaporation from the upper parts of the layer.

Thus one makes a better use of the theoretical plates along the layer (= increase of the number of effective plates)! Result: proportional increase of all R_F values and improvement of resolution. Only a *simultaneous* evaporation of solvent from all wetted parts of the layer would have lifted superproportionally ("pushed up") the R_F value of the lower spot, as postulated by DE ZEEUW *et al.*, and reduced the distances of the extreme R_F values.

ad (5)

This is only due to the casual choice of a reference data set for a *saturated* chamber. If a set from an unsaturated N-chamber had been designed as a standard, the opposite would be true; then the a values from saturated chambers would be the lower ones. The constant a essentially corrects for differences of integral solvent flow between the two systems.

Euratom, I-21020 Ispra (Italy)

F. GEISS

- 1 R. A. DE ZEEUW, *Anal. Chem.*, 40 (1968) 915.
- 2 F. GEISS, S. SANDRONI AND H. SCHLITT, *J. Chromatog.*, 44 (1969) 290.
- 3 G. H. STEWART AND T. D. GIERCKE, *Separation Sci.*, 8 (1970) 129.
- 4 L. R. SNYDER AND D. L. SAUNDERS, *J. Chromatog.*, 44 (1969) 1.
- 5 A. NIEDERWIESER, *Chromatographia*, 2 (1969) 23.
- 6 A. NIEDERWIESER, *Chromatographia*, 2 (1969) 519.

Received June 15th, 1970

Author Index

- Althorpe, J., 371
Aue, W. A., 367, 487
Augl, J. M., 487
Baba, T., 610
Bates, T. W., 85
Bayer, H., 63
Belcher, R. V., 279
Belenkii, B. G., 3, 77
Benoit, H., 55
Berek, D., 55
Betts, T. J., 163
Bianchini, P., 577
Boček, P., 421
Bock, E., 439
Bogaert, M. G., 263
Bombaugh, K. J., 27
Bömer, B., 51
Bonecchi, A., 517
Breckler, P. N., 163
Brown, J. M. A., 399
Brown, W., 572
Bruner, F., 135
Burrows, H. J., 566
Burton, W. B., 397
Calam, D. H., 566
Campbell, J., 279
Carisano, A., 517
Cervenka, A., 85
Chain, E. B., 293
Chudzik, J., 329
Churáček, J., 69
Cimbura, G., 413
Clemence, M., 209
Cornford, C. C., 403
Craske, J. D., 253
Czubryt, J. J., 439, 453
De Ligny, C. L., 469
Dennison, C., 381
Deyl, Z., 575
Di Corcia, A., 135
Dousté-Blazy, L., 217
Dressler, M., 525
Edwards, R. A., 253
Entelis, S. G., 109, 117
Everaerts, F. M., 315
Evreinov, V. V., 109
Frahm, J. L., 616
Frey, C. F., 389
Fritz, D., 135
Fritz, J. S., 345
Ganetskii, M. B., 77
Gankina, E. S., 3
Gass, J., 209
Gehrke, C. W., 171, 195, 201
Geike, F., 269
Geiss, F., 620
Gesser, H. D., 439, 453
Gijbels, M., 408
Goddard, D. A., 371
Golynko, O. M., 77
Gondek, R. J., 477
Goswami, S. K., 389
Gridyushko, G. S., 354
Grob, R. L., 477
Grubisic-Gallot, Z., 55
Habboush, A. E., 143, 151
Harris, W., 358
Hastings, C. R., 487
Hatano, H., 584
Havel, Z., 233
Heitz, W., 37, 51
Holmström, A., 95
Humphrey, A. M., 375
Huq, A. M. S., 613
Ilková, H., 363
Jagarić, Z., 525
Janák, J., 525
Jandera, P., 69
Johnson, D. F., 225
Kaminski, E. E., 345
Kartnig, Th., 537
Katz, S., 415
Kern, W., 51
Khol'kin, Yu. I., 354
King, E. E., 559
Klein, A., 329
Kleinig, H., 595
Kliffen, C., 531
Korczak-Fabierkiewicz, C., 413
Koromaldi, E. V., 77
Korovina, G. V., 117
Kothari, R. M., 580
Koudela, S., 589
Koyama, M., 406
Kulhánek, V., 545
Kundu, N., 598
Lamontagne, N. S., 225
Landis, W. R., 125
Laruelle, L., 408
Leimer, K., 195, 201
Lempert, U., 595
Lloyd, P. B., 403
Lowe, A. E., 293
Maes, R., 408
Mahler, R., 279
Mansford, K. R. L., 293
Mantovani, V., 577
Marshall, J. J., 379
Maury, Y., 217
May, C. E., 399
Mikula, G., 537
Moerman, E. J., 263
Moseman, R. F., 367
Mostecký, J., 233

- Murakami, F., 584
 Nakai, T., 406
 Nau, H., 391
 Nefedov, P. P., 77
 Netting, A. G., 507
 Noirfalise, A., 564
 Novák, I., 55
 Novák, J., 421, 429
 Novikov, D. D., 117
 Oelert, H. H., 241
 Palo, V., 363
 Palyza, V., 545
 Perrine, T. D., 125
 Pilný, J., 575
 Popl, M., 233
 Potapovich, A. K., 354
 Prescher, D., 395
 Püschel, F., 395
 Raaen, H. P., 600, 605
 Rahman, M. K., 613
 Rahman, R., 592
 Randau, D., 63
 Riva, M., 517
 Roach, D., 171
 Rokushika, S., 584
 Romanov, A. K., 109
 Rosmus, J., 575
 Rosseel, M.-T., 263
 Roy, S., 598
 Safe, S., 592
 Sarnecka-Keller, M., 329
 Scales, T. A., 477
 Schild, W., 387
 Seifert, R., 587
 Sissons, D. J., 371
 Skellern, G. G., 285
 Smith, K. A., 358
 Smith, S. G., 279
 Smolyaninov, V. V., 337
 Souillard, C., 217
 Soula, G., 217
 Sörvik, E., 95
 Stahl, E., 387
 Stenlake, J. B., 285
 Švec, P., 587
 Taganov, N. G., 117
 Tameesh, A. H., 143, 151
 Tan, L., 209
 Taylor, A., 592
 Telling, G. M., 371
 Thomas, G., 125
 Tortolani, G., 577
 Uchijima, S., 406
 Van de Meent, W., 469
 Verheggen, Th. P. E. M., 315
 Vilenchik, L. Z., 77
 Vinogradova, R. G., 77
 Wičar, S., 421, 429
 Williams, W. D., 285
 Yamamoto, M., 373
 Yoneda, H., 610
 Young, J. L., 373
 Zbirovský, M., 587
 Zhdanov, S. P., 77
 Zhilzova, N. E., 77
 Ziska, P., 385
 Zumwalt, K. W., 171

Subject Index

- Acetaldehyde
Direct GC estimation of lower alcohols, —, acetone and diacetyl in milk products, 363
- Acetone
Direct GC estimation of lower alcohols, acetaldehyde, — and diacetyl in milk products, 363
- Adrenocortical steroids
Chromatography of — on silicic acid columns, 225
- Aglycones
The separation of plant glycosides and — using TLC and electrophoresis, 399
- Alcohols
Direct GC estimation of lower —, acetaldehyde, acetone and diacetyl in milk products, 363
- Alcohols
A study of the strontium and barium halides as column packings in GSC, 477
- Amanita phalloides*
Chromatographic analysis of toxins from —, 545
- Amanitin
Chromatographic analysis of toxins from *Amanita phalloides*, 545
- Amino acid
The application of thin-layer electrophoresis and chromatoelectrophoresis on Sephadex G-25 to the analysis of — and peptide composition of biological fluids, 329
- Amino acids
The effect of salts on the derivatisation and chromatography of —, 195
- Amino acids
Experience with an electrolytic "ninhydrin reactor", 373
- Amino acids
GLC of — in biological substances, 171
- Amino-acids
Trimethylsilylation of —. Effect of solvents on derivatisation using bis(trimethyl)trifluoroacetamide, 201
- Anhydrotetracycline
A TLC limit test for the detection of — and 4-*epi*-anhydrotetracycline in tetracycline, 403
- Anisoles
GLC of disubstituted benzene isomers. II. Separation and study of the halonitrobenzenes, — and toluenes, 151
- Antibiotics
Pyrolysis-GC of polyene antifungal —: the nature of candidin, levorin and trichomycin, 566
- Antibiotics
Separation of polythiadioxopiperazine — by TLC, 592
- Apparatus
An automatic device for injection of gas samples into a gas chromatograph, 358
- Apparatus
A computerised scanner for bidimensional radiochromatograms, 293
- Apparatus
Isotachophoresis. Electrophoretic analysis in capillaries, 315
- Apparatus
A multiple column gas chromatograph, 125
- Apparatus
Rapid transfer in TLC-IR spectroscopy, 387
- Apparatus
A simple device for the selection of fractions in GC, 354
- Aromatic compounds
A study of the strontium and barium halides as column packings in GSC, 477
- Benzene
GLC of disubstituted — isomers. I. Separation and study of the dichlorobenzenes, 143
- Benzene
GLC of disubstituted — isomers. II. Separation and study of the halonitrobenzenes, anisoles and toluenes, 151
- p*-Benzoquinone
Chromatographic studies of some halogenated quinones. I. TLC of some chlorinated derivatives of —, 587
- Bile acids
Manganous chloride spray reagent for cholesterol and — on thin-layer chromatograms, 389
- Candidin
Pyrolysis-GC of polyene antifungal antibiotics: the nature of —, levorin and trichomycin, 566
- Carbamate insecticides
TLC-enzymatic identification of carbamates. I. Identification of — with bovine liver esterase, 269
- Carbamate tranquilisers
Determination of — by GC, 564
- Carbimazole
Development and comparison of TLC and GLC methods for measurement of methimazole in rat urine, 285
- Carbohydrates
The selectivity of polyacrylamide gels for sugars, 572

Carboxylic acids

A study of the strontium and barium halides as column packings in GSC, 477

Cholesterol

GC analysis of fecal pollution sterols on a single combined packed column, 209

Cholesterol

Manganous chloride spray reagent for — and bile acids on thin-layer chromatograms, 389

Cobalamin

Separation and determination of — on an SP-Sephadex column, 577

Column chromatography

Column separations designed precisely with the aid of TLC, 507

Column packings

A study of the strontium and barium halides as — in GSC, 477

Coprostanol

GC analysis of fecal pollution sterols on a single combined packed column, 209

Coprostanone

GC analysis of fecal pollution sterols on a single combined packed column, 209

Creatine

PC of 3-methylhydantoic acid and 1-methylhydantoin, possible intermediates of microbial degradation of — and creatinine, 406

Creatinine

Determination of — in soups and soup preparations by ion-exchange chromatography. II. Automatic apparatus, 517

Creatinine

PC of 3-methylhydantoic acid and 1-methylhydantoin, possible intermediates of microbial degradation of creatine and —, 406

Creosote oils

Gradient elution adsorption chromatography of aromatic hydrocarbons, 233

Cytoplasmic ribosomes

chromatographic purification of — from pea plants, 531

Deuterium substituted compounds

The use of high efficiency packed columns for GSC. III. Separation of —, 135

Diacetyl

Direct GC estimation of lower alcohols, acetaldehyde, acetone and — in milk products, 363

Dicarboxylic acid porphyrins

The separation of free — using TLC and PC, 279

Dichlorobenzenes

GLC of disubstituted benzene isomers. I. Separation and study of the —, 143

N,N-Dimethyl-*p*-aminobenzeneazobenzoyl esters and amides

The separation of the coloured derivatives of some organic compounds using liquid chromatography in small-bore columns packed with ion-exchange resins, 69

Disc electrophoresis

—: avoiding artifacts caused by persulphate, 559

Diuretics

A rapid chromatographic procedure for the detection of some — in pharmaceuticals and biological fluids, 408

DNA

Some aspects of fractionation of — on an IR-120 Al³⁺ column. II. Effect of the physical state of — on chromatographic profiles, 580

Drugs

Development and comparison of TLC and GLC methods for measurement of methimazole in rat urine, 285

Drugs

Differentiation of phenothiazine derivatives by locating agent on TLC plates, 413

Drugs

A rapid chromatographic procedure for the detection of some diuretics in pharmaceuticals and biological fluids, 408

Electrophoresis

Disc —: avoiding artifacts caused by persulphate, 559

Enzymes

Disc electrophoresis: avoiding artifacts caused by persulphate, 559

Erythrocytes

Chromatographic study of steroids and methyl esters in nucleated —, 217

Fatty acid

CC of the bromo-mercuri-methoxy adducts of — methyl esters as a means of isolating polyenoic acids present in low concentrations, 253

Gas chromatograph

An automatic device for injection of gas samples into a —, 358

Gas chromatograph

A multiple column —, 125

Gas chromatography

Nonadditivity of the gas and liquid phase mass-transfer resistances in —, 429

Gas chromatography

Pressure dependence of the coefficients of mass-transfer resistance in —, 421

Gas chromatography

A simple device for the selection of fractions in —, 354

Gas chromatography

Surface-bonded silicones from volatile monomers for chromatography, 487

Gas-solid chromatography

The effect of carrier gas nonideality and adsorption on the net retention volume in —, 439

Gas-solid chromatography

Flow of He, Ar, and CO₂ through a 200 ft. 1/8 in. O.D. Porapak S (50–80 mesh) column at 273°K, 453

- Gas-solid chromatography
A study of the strontium and barium halides as column packings in —, 477
- Gel chromatography
Application of vinyl acetate gels, 63
- Gel chromatography
Comments on the use of Blue Dextran in —, 379
- Gel chromatography
Syntheses and properties of — materials, 37
- Gel permeation chromatography,
Preparation of monodisperse polyethylene oxides by — of discontinuous polymer-homologous series, 51
- Gel permeation chromatography
Recent developments in —: high speed and high resolution. Introductory lecture, 27
- Gel permeation chromatography
Shape of the chromatographic band for individual species and its influence on — results, 117
- Gel permeation chromatography
Surface area and volume of pores as characteristics of silica support for —, 55
- Glycerol nitrates
Quantitative analysis of — on thin-layer chromatograms. Comparison of colorimetry and densitometry, 263
- Glycosides
The separation of plant — and aglycones using TLC and electrophoresis, 399
- Halonitrobenzenes
GLC of disubstituted benzene isomers. II. Separation and study of the —, anisoles and toluenes, 151
- Herbicides
The determination of picloram in fescue by GLC, 367
- Herbicide
A modified detection of triazine — residues and their hydroxy derivatives on thin-layer chromatograms, 589
- Herbicide
Separation of Planavin® — and some related compounds by two-dimensional TLC, 397
- Hydrocarbons
Chromatography and 77°K luminescence of some — on thin layers of microcrystalline nylon-polytetrafluoroethylene (Aviamide-6-Fluoroglide 200), 600
- Hydrocarbons
Gel chromatographic separation characteristics of vinyl acetate gel for — and petroleum, 241
- Hydrocarbons
Gradient elution adsorption chromatography of aromatic —, 233
- Inorganic ions
Chromatography of metal ions on thin layers of polytetrafluoroethylene with di-(2-ethylhexyl)orthophosphoric acid, 605
- Inorganic ions
Metal ion separations in thiocyanate media using a liquid anion exchanger, 345
- Inorganic ions
The use of Teflon film in quantitative analysis by enclosed-strip paper electrophoresis. The separation and determination of the valence states of iron, 616
- Inorganic ions
Zirconium tellurate, an inorganic ion exchanger, 613
- Inorganic salts
Studies of TLC of —. V. Resolution of the racemic trisethylenediaminecobalt(III) complex by means of TLC on silica gel, 610
- Insecticides
TLC-enzymatic identification of carbamates. I. Identification of carbamate — with bovine liver esterase, 269
- Ion-exchange chromatography
Some pH control problems in gradient elution —, 415
- Iron
The use of Teflon film in quantitative analysis by enclosed-strip paper electrophoresis. The separation and determination of the valence states of —, 616
- Isotachophoresis
— Electrophoretic analysis in capillaries, 315
- Isotopic pairs
The use of high efficiency packed columns for gas-solid chromatography. III. Separation of deuterium substituted compounds, 135
- Levorin
Pyrolysis-GC of polyene antifungal antibiotics: the nature of candicidin, — and trichomycin, 566
- Lipids
CC of the bromo-mercuri-methoxy adducts of fatty acid methyl esters as a means of isolating polyenoic acids present in low concentrations, 253
- Lipids
Phospholipid analysis on a micro scale, 595
- Metal ions
Chromatography of — on thin layers of polytetrafluoroethylene with di-(2-ethylhexyl)orthophosphoric acid, 605
- Metal ion
— separation in thiocyanate media using a liquid anion exchanger, 345
- Metal ions
The use of Teflon film in quantitative analysis by enclosed-strip paper electrophoresis. The separation and determination of the valence states of iron, 616
- Methimazole
Development and comparison of TLC and GLC methods for measurement of — in rat urine, 285

- 3-Methylhydantoic acid
PC of — and 1-methylhydantoin, possible intermediates of microbial degradation of creatine and creatinine, 406
- 1-Methylhydantoin
PC of 3-methylhydantoic acid and —, possible intermediates of microbial degradation of creatine and creatinine, 406
- Ninhydrin reactor
Experience with an electrolytic —, 373
- Nitroglycerin
Quantitative analysis of glyceryl nitrates on thin-layer chromatograms. Comparison of colorimetry and densitometry, 263
- Nitrosamines
The GC determination of — at the picogram level by conversion to their corresponding nitrosamines, 371
- Noradrenaline
The isolation, separation and determination of isopropyl — and its O-methyl derivative in blood serum and tissue homogenate, 575
- Nucleic bases
Cation-exchange chromatography of nucleotides, nucleosides and —, 584
- Nucleosides
Cation-exchange chromatography of nucleotides, — and nucleic bases, 584
- Nucleotides
Cation-exchange chromatography of —, nucleosides and nucleic bases, 584
- Oestrogens
Sensitive detection of — using an automatic conductivity detector after TLC, 391
- Olefins
TLC of sulphonic acid esters, 395
- Olefins
Use of — Ag^+ complexes for chromatographic separations of higher — in liquid-solid systems, 525
- Oligomers
Calculation of the weight and number functions of molecular weight distribution for — from the gel permeation chromatography data, 109
- Paper chromatography
A computerised scanner for bidimensional radiochromatograms, 293
- Paper chromatography
Peak broadening in — and related techniques. VII. The contribution of the macroscopic mobile phase velocity profile to peak broadening in PC and TLC, 469
- Paper electrophoresis
The use of Teflon film in quantitative analysis by enclosed-strip —. The separation and determination of the valence states of iron, 616
- Peptide
The application of thin-layer electrophoresis and chromatoelectrophoresis on Sephadex G-25 to the analysis of amino acid and — composition of biological fluids, 329
- Peptides
Gel chromatography of structural-isomeric — on Sephadex G-10, 385
- Peptides
Separation of dansylated products of L-seryltyrosine and their identification, 598
- Pesticides
The determination of picloram in fescue by GLC, 367
- Pesticides
A modified detection of triazine herbicide residues and their hydroxy derivatives on thin-layer chromatograms, 589
- Pesticides
Separation of Planavin® herbicide and some related compounds by two-dimensional TLC, 397
- Pesticides
TLC-enzymatic identification of carbamates. I. Identification of carbamate insecticides with bovine liver esterase, 269
- Petroleum
Gel chromatographic separation characteristics of vinyl acetate gel for hydrocarbons and — 241
- Phalloidin
Chromatographic analysis of toxins from *Amanita phalloides*, 545
- Pharmaceuticals
A rapid chromatographic procedure for the detection of some diuretics in — and biological fluids, 408
- Phenothiazine
Differentiation of — derivatives by locating agent on TLC plates, 413
- Phospholipid
— analysis on a micro scale, 595
- Picloram
The determination of — in fescue by GLC, 367
- Piperazine
Separation of polythiadioxo — antibiotics by TLC, 592
- Planavin®
Separation of — herbicide and some related compounds by two-dimensional TLC, 397
- Polyethylene
Thermal degradation of — in a nitrogen atmosphere of low oxygen content. I. Changes in molecular weight distribution, 95
- Polyethylene oxides
Preparation of monodisperse — by gel permeation chromatography of discontinuous polymer-homologous series, 51
- Polymers
Application of porous glasses for gel chromatography of —, 77
- Polymers
Characterisation of polydisperse branched — by means of gel permeation chromatography, 85

Polymers

Syntheses and properties of — materials, 37

Polymers

TLC of —. Introductory lecture, 3

Polythiadioxopiperazine

Separation of — antibiotics by TLC, 592

Polythionates

Electrophoresis and TLC of organic base —, 337

Porphyrins

The separation of free dicarboxylic acid — using TLC and PC, 279

Proteins

The retardation of certain — during chromatography on tanned gelatin, 381

Quinones

Chromatographic studies of some halogenated —. I. TLC of some chlorinated derivatives of *p*-benzoquinone, 587

Ribosomes

Chromatographic purification of cytoplasmic — from pea plants, 531

Scanner

A computerised — for bidimensional radiochromatograms, 293

L-Seryltyrosine

Separation of dansylated products of — and their identification, 598

Silicones

Surface-bonded — from volatile monomers for chromatography, 487

Soups

Determination of creatinine in — and soup preparations by ion-exchange chromatography. II. Automatic apparatus, 517

Steroids

Chromatographic study of — and methyl esters in nucleated erythrocytes, 217

Steroids

Chromatography of adrenocortical — on silicic acid columns, 225

Steroids

GC analysis of fecal pollution sterols on a single combined packed column, 209

Steroids

The identification and quantitative determination of sterols, 537

Steroids

Manganous chloride spray reagent for cholesterol and bile acids on thin-layer chromatograms, 389

Steroids

Sensitive detection of oestrogens using an automatic conductivity detector after TLC, 391

Sterols

GC analysis of fecal pollution — on a single combined packed column, 209

Sterols

The identification and quantitative determination of —, 537

Sugars

The selectivity of polyacrylamide gels for —, 572

Sulphonic acid esters

TLC of —, 395

Terpenes

Relative retention time changes with temperature for the GC identification of volatile oil components, 163

Tetracycline

A TLC limit test for the detection of anhydrotetracycline and 4-*epi*-anhydrotetracycline in —, 403

Thin-layer chromatography

Peak broadening in PC and related techniques. VII. The contribution of the macroscopic mobile phase velocity profile to peak broadening in PC and —, 469

Thin-layer chromatography

Rapid transfer in — -IR spectroscopy, 387

Toluenes

GLC of disubstituted benzene isomers. II. Separation and study of the halonitrobenzenes, anisoles and —, 151

Toxins

Chromatographic analysis of — from *Amanita phalloides*, 545

Triazine herbicide

A modified detection of — residues and their hydroxy derivatives on thin-layer chromatograms, 589

Trichomycin

Pyrolysis-GC of polyene antifungal antibiotics: the nature of candicidin, levorin and —, 566

Trisethylenediaminecobalt (III) complex

Studies of TLC of inorganic salts. V. Resolution of the racemic — by means of TLC on silica gel, 610

Vinyl acetate gels

Application of —, 63

Vitamin B₁₂

Separation and determination of cobalamin on an SP-Sephadex column, 577

Volatile oils

The examination of — by combined GLC/TLC, 375

Volatile oil

Relative retention time changes with temperature for the GC identification of — components, 163

Zirconium tellurate

—, an inorganic ion exchanger, 613

Errata

J. Chromatog., 49 (1970) 469-472

Page 469, INTRODUCTION, line 13, and page 470, *Chromatographic plates*, line 1: "0.02 *M* sodium acetate" should read "0.03 *M* sodium acetate".

J. Chromatog., 50 (1970) 142-144

Page 143, Table III, line 4 under *Heptachlor epoxide*, "67" should read "97".

J. Chromatog., 52 (1970) 141-144

Page 141, *Theory*, line 9, "shelves¹" should read "shelves".

J. Chromatog., 52 (1970) 154-157.

Page 156, line 24, "identification of the methyl esters" should read "identification".

J. Chromatog., 53 (1970) 77-83.

Page 78, line 7, "NaDH" should read "NaOH".

J. Chromatog., 53 (1970) 630